Stereoselective Synthesis of α- and β-Functionalized Carbonyl Derivatives: Allylic Alkylation of Dialkyl Malonates, Total Synthesis of Hunterine A, and Progress Toward the Synthesis of Kuroshine A

Thesis by

Elliot Frederick Hicks

In Partial Fulfillment of the Requirements for

the Degree of

Doctor of Philosophy



CALIFORNIA INSTITUTE OF TECHNOLOGY

Pasadena, California

2025

(Defended June 2, 2025)

© 2025

Elliot Frederick Hicks
ORCID: 0009-0004-8965-0460

All rights reserved

ACKNOWLEDGEMENTS

The research presented in this thesis describes my academic endeavors over roughly five years at Caltech and in the Stoltz group. While it is written in scientific language to convey concepts, strategies, difficulties, and solutions (hopefully with some degree of rigor and correctness), it does not depict many of the aspects of this endeavor that have made it so personally transformative and meaningful. I've done my best to highlight all those who have made this journey possible.

I would like to first acknowledge my family for their unwavering support. It hasn't been easy to be across the country from one another, especially with the time commitments of work and grad school preventing us from spending a lot of time together. But the times we've been able get together have been all the more meaningful. Thanks mom, dad, and Emma.

In the same vein, I need to thank some of my closest friends prior to coming to Caltech, particularly Chirs Adusei-Poku, Josh and Jordy Fischbach, Spencer Rose, and Jon Whyte. I'm grateful for such a strong support network that keeps me grounded and reminds me of the things that are truly important.

I would never have ended up at Caltech without the incredible mentorship I received as an undergraduate at Emory. Professors Dennis Liotta and Huw Davies inspired me to study organic chemistry, and Prof. Davies was generous enough to allow me to work in his lab. In the Davies lab, Dr. Zachary Garlets was my first research mentor, and his guidance and teaching gave me a strong practical foundation that I was able to take with me to grad school. His willingness to drop everything and help with whatever it was I needed is a trait I've tried to mimic in my time in the Stoltz lab; I now fully appreciate how difficult that can

be. I also need to acknowledge Professors Jose Soria and Antonio Brathwaite (Dr. B) for their mentorship. Dr. B set me up for success with all the time he spent helping with recommendations, applications, and sharing wisdom during our many conversations about plans after Emory.

My time in the Stoltz group began on the 3rd floor of Church due to social distancing requirements that stretched our lab across campus. I feel lucky that my introduction to research in the group at that time was under the guidance of Nick Hafeman and Tyler Fulton, two exceptional chemists and even better friends. They have been role models whose work ethic, attention to detail, and willingness to help others have become the pillars of how I approach research. I wouldn't be half the chemist I am now without them helping me along when I first started. Thanks also to Kali Flesch who started at the same time working in this same lab space. I'm glad to have had such a good friend from the very beginning.

During my time at Caltech, I've had the great pleasure of collaborating with a number of people on various projects. Farbod Moghadam was a great project partner on the iridium chemistry and provided many laughs along the way. Zack Sercel and Alex Cusumano were also instrumental on that project. Kengo Inoue visited our lab from the University of Kobe and made some very valuable contributions to the hunterine A synthesis. He is one of the most talented chemists I've ever worked with. Leanne Fuentes Ruiz, who spent a summer in our lab through the WAVE Fellows program, was a joy to mentor and was very quick to learn a lot of lab techniques and helped push the aziridine investigation forward. Bryce Gaskins rotated with me and did a lot of the early-stage work on some of the aziridine chemistry. I'm excited to see all the things he accomplishes. Colin Regli visited our lab from

ETH Zurich and made some valuable contributions in our early-stage progress toward kuroshine A.

I also want to acknowledge all the people I've worked next to (and probably bumped elbows with) in Bay 2, some of whom have already been mentioned: Jay Barbor, Leanne Fuentes Ruiz, Ben Gross, Yutaro Hatano, Trevor Lohrey, Zack Sercel, Kim Sharp, and Hao Yu. I can confidently say I've learned something from everyone. I'm glad I'll get to continue working alongside Jay; Merck is lucky to have him. I also want to thank Ben and Hao for many conversations about chemistry and life, and for their great senses of humor that have made them so fun to work next to.

I also want to acknowledge Samir Rezgui, Kevin Gonzalez, Adrian Samkian, Christian Strong, and Adrian de Almenara. Samir and Kevin have been great friends I can go and talk to about anything and who will give me an honest answer. Setting up and working in an auxiliary lab space on the 3rd floor of Crellin with Samir, and all the long and meaningful conversations I've had with Kevin are things I'll always happily remember about my time at Caltech. Thanks to Christian for his sense of humor, thoughtful questions, and unflinching adherence to an 11:30 lunchtime. Thanks to Adrian ("student") de Almenara for his willingness to join Samir and me in Crellin and to Adrian ("teacher") Samkian for his many practical tips that have made me a better experimentalist.

Thanks as well to all other current members of the Stoltz lab who I haven't mentioned so far: Chloe Cerione, Ruby Chen, Johnathan Farhi, Elijah Gonzalez, Sara Siddiqui, Camila Suarez, Marva Tariq. It's been great getting to work with all of them.

I want to acknowledge all members of the current G5 cohort for being such a kind, intelligent, and motivated group of people. I feel fortunate to have been alongside them

during this journey. Specifically, I need to thank those I've interacted with on the 3rd floors of Schlinger and Church/Crellin: Emily Chen, Cedric Lozano, Jordan Thompson, Skylar Osler, and Stella Luo. I need to give a special thank you to Emily for being a fun, understanding, thoughtful, and constantly supportive partner. I've enjoyed the last (almost) two years the most, and she deserves all the credit for that.

I want to thank Hamilton Evans and Sadie Dutton for being great friends outside of lab. I'll always cherish watching Saturday morning Premier League, F1 races, and many Dodger games with both of them. Ham's undying enthusiasm for crazy trail runs and hikes has provided some great memories and amazing stories to tell. Nobody else would've been able to convince me to run/jog/hike across the Grand Canyon, let alone do it again–both ways–two years and one ankle surgery later.

I was fortunate during my last three years to have been a Resident Associate (RA) of Ricketts house. The students have always been a kind and unique bunch and I'm happy to have interacted with them at various events. I also want to thank the other members of the Student and Family Engagement Team I've had the pleasure of working with, especially my direct mentor as an RA, Mahlet Tesfaye.

At Caltech, we are fortunate to have a dedicated a knowledgeable group of people who maintain all the facilities and who are capable of providing invaluable expertise. Dr. Scott Virgil works tirelessly to keep the instruments in the catalysis center (and seemingly almost everywhere else on campus) up and running. His insights have helped me immensely during my studies. Dr. Michael Takase has provided me plenty of help with X-Ray crystallography and has never ceased to amaze me with his ability to get structures form some of the things I've brought to him. Dr. David VanderVelde has a vast knowledge of

everything NMR and has always been willing to answer whatever questions I've had. His dry humor has never failed to make me chuckle. Joe Drew has done a phenomenal job of maintaining the buildings and keeping the hoods pulling. With Dave and Joe retiring, the department has big shoes to fill. Thanks as well to Greg and Armando for all they do behind the scenes to keep our lab supplied. Additionally, I need to thank the entire CCE staff for everything they do to make things run smoothly, especially to Beth Marshall, Tomomi Kano, and Annette Luymes for all of their help getting things on the calendar over the years.

I want to sincerely thank all members of my committee. Professor Sarah Reisman has been a supportive chair of my committee, and I'm grateful to have had her thoughtful and creative input on my research. Sharing the 3rd floor of Schlinger with her lab has provided a lot of valuable additional knowledge. I had the pleasure of being a TA for Professor Max Robb's Chem 41a class, and I was delighted that he agreed to serve on my thesis committee. His insights and guidance have always been meaningful. Professor Linda Hsieh-Wilson has been a kind and supportive committee member, and I've enjoyed my interactions with her.

Last but certainly not least, I want to extend my utmost gratitude to Professor Brian Stoltz for welcoming me into his lab and making my Ph.D. research possible. I first met Brian at a conference at Emory in 2019. Although our conversation lasted at most five minutes, I was immediately struck by how laidback and down to earth he was. Moreover, we spent no more than 30 seconds talking about chemistry and instead we talked about our experiences abroad and common interest in sports. That interaction left a lasting impression on me that no doubt strongly influenced my desire to join his lab; it also proved to be one of many I can recount that perfectly depicts the caring person he is. Overall, his mentorship style provides all of us a unique opportunity to grow in a way that I don't think is possible in

any other environment. I'm grateful for the freedom he has given me to pursue my interests, and the ways in which he has supported me along the way both in and outside of the lab. I can confidently say I wouldn't want to be anyone other than the chemist and person I am now after five years in the Stoltz lab.

ABSTRACT

Research in the Stoltz group generally focuses on the synthesis of complex molecules enabled by the discovery and application of new synthetic methodologies. The majority of the research described in this thesis encompasses variations on this unifying central theme.

Chapter 1 focuses on the development of new asymmetric methodology for the synthesis of stereogenic all-carbon quaternary centers through the application of iridium catalysis. A key advance was the use of malonate nucleophiles and bis-alkyl substituted electrophiles, two inputs commonly employed in allylic alkylation chemistry that had yet to be utilized for the synthesis of quaternary carbon centers.

Chapter 2 describes the development and execution of a synthetic strategy for the asymmetric construction of a rearranged monoterpene indole alkaloid, hunterine A. Key to the assembly of this molecule were an enantioselective desymmetrization, aza-Cope/Mannich rearrangement, azide-alkene dipolar cycloaddition, and regioselective aziridine opening.

Chapter 3 details an investigation born out of an observation of a regioselective aziridine opening during the course of the synthesis of hunterine A. This research focuses on the synthesis of sterically unbiased fused bicyclic N-aryl aziridines and their reactivity in a variety of ring opening reactions.

Chapter 4 and Appendix 7 describe ongoing efforts toward the synthesis of Kuroshine A and other highly oxidized zoanthamine alkaloids. The synthetic strategies described focus on evaluating formation of the ABC ring system of the molecule via a masked *ortho*-benzoquinone cycloaddition.

PUBLISHED CONTENT AND CONTRIBUTIONS

1. Moghadam, F. A.[†]; Hicks. E. F[†].; Sercel, Z. P.; Cusumano, A. Q.; Bartberger, M. D.; Stoltz, B. M. Ir-Catalyzed Asymmetric Allylic Alkylation of Dialkyl Malonates Enabling the Construction of Enantioenriched All-Carbon Quaternary Centers. *J. Am. Chem. Soc.* **2022**, *144*, 7983–7987. DOI: 10.1021/jacs.2c02960

   E.F.H. participated in project design, experimental work, data acquisition and analysis, and manuscript preparation.

2. Hicks. E. F.; Inoue, K.; Stoltz, B. M. Enantioselective Total Synthesis of (−)-Hunterine A Enabled by a Desymmetrization/Rearrangement Strategy. *J. Am. Chem. Soc.* **2024**, *146*, 4340–4345. DOI: 10.1021/jacs.3c13590

   E.F.H. participated in project design, experimental work, data acquisition and analysis, and manuscript preparation.

3. Hicks. E. F.; Fuentes Ruiz, L. M.; Gaskins, B. E.; Takase, M. K.; Stoltz, B. M. Preparation and Regioselective Ring Opening Reactions of Fused Bicyclic N-Aryl Aziridines. *Manuscript Submitted*.

   E.F.H. participated in project design, experimental work, data acquisition and analysis, and manuscript preparation.

TABLE OF CONTENTS

Acknowledgements iii
Abstract ix
Published Content and Contributions x
Table of Contents xi
List of Figures xv
List of Schemes xxvi
List of Tables xxix
List of Abbreviations xxxiv

CHAPTER 1 ***1***
Iridium-Catalyzed Asymmetric Allylic Alkylation of Dialkyl Malonates

1.1 Introduction 1

1.2 Iridium-Catalyzed Allylic Alkylation 2

1.3 Regioselectivity of Iridium-Catalyzed Allylic Alkylation 5

1.4 Synthesis of All-Carbon Quaternary Centers via Iridium-Catalyzed Alkylation 7

1.5 Reaction Optimization 9

1.6 Role of Zinc Iodide 12

1.7 Temperature Dependence and Mechanistic Implications 13

1.8 Scope of Asymmetric Allylic Alkylation 15

1.9 Synthetic Utility of the Allylic Alkylation Products 21

1.10 Conclusion 22

1.11 Experimental Section 22

1.11.1 Materials and Methods 22

1.11.2 Experimental Procedures 24

1.11.2.1 General Procedure 1 for Iridium-Catalyzed Allylic Alkylation Reactions 24

1.11.2.2 Derivatizations of Products 47

1.11.2.3 Ligand Synthesis 54

1.11.2.4 General Procedure 2: Synthesis of Allylic Carbonate Electrophiles 55

1.11.3 Determination of Absolute Configuration of 32a via Vibrational Circular Dichroism (VCD) 70

1.11.3.1 Experimental Protocol 70

1.11.3.2 Computational Protocol 70

1.12 References and Notes 73

APPENDIX 1 ***79***

Spectra Relevant to Chapter 1

CHAPTER 2 ***160***

Enantioselective Total Synthesis of Hunterine A

2.1 Introduction 160

2.2 Rearranged Monoterpene Indole Alkaloids 162

2.3 Retrosynthetic Analysis 164

2.4 Synthesis of Hunterine A 166

2.5 Conclusion 187

2.6 Experimental Section 187

2.6.1 Materials and Methods 187

2.6.2 Experimental Procedures 24

2.7 References and Notes 250

APPENDIX 2 ***261***
Synthetic Summary for Chapter 2

APPENDIX 3 ***263***
Spectra Relevant to Chapter 2

APPENDIX 4 ***335***
X-Ray Crystallography Reports Relevant to Chapter 2

CHAPTER 3 ***409***
Preparation and Regioselective Ring Opening Reactions of Fused Bicyclic N-Aryl Aziridines

3.1 Introduction 409

3.2 Attempted Synthesis of Simplified Aziridines 411

3.3 Successful Synthesis and Ring Opening of Simplified Aziridines 412

3.4 Conclusion 422

3.5 Experimental Section 422

3.5.1 General Information 423

3.5.2 Safety 424

3.5.3 Experimental Procedures 424

3.6 References and Notes 457

APPENDIX 5 ***463***
Spectra Relevant to Chapter 3

APPENDIX 6 ***527***
X-Ray Crystallography Reports Relevant to Chapter 3

CHAPTER 4 ***577***
Progress Toward the Synthesis of Kuroshine A

4.1 Introduction 577

4.2 Synthesis of Zoanthamine Alkaloids 578

4.3 Retrosynthetic Analysis of Kuroshine A (**XX**) 584

4.4 Model System Evaluation of the Dearomative [4+2] Reaction 585

4.5 Synthetic Progress Toward a Fully Functionalized ABC Ring System 588

4.6 Conclusion 592

4.7 Experimental Section 592

4.7.1 Materials and Methods 592

4.7.2 Experimental Procedures 594

4.8 References and Notes 616

APPENDIX 7 ***624***
Spectra Relevant to Chapter 4

APPENDIX 8 ***656***
X-Ray Crystallography Reports Relevant to Chapter 4

APPENDIX 9 ***666***
Alternative Masked "A" Ring Strategies

APPENDIX 10 ***704***
Spectra Relevant to Appendix 9

APPENDIX 11 ***733***
Notebook Cross-References for New Compounds

ABOUT THE AUTHOR ***739***

LIST OF FIGURES

CHAPTER 1

Iridium-Catalyzed Asymmetric Allylic Alkylation of Dialkyl Malonates

Figure 1.1.1 *Construction of all-carbon quaternary centers via allylic alkylation..... 1*

Figure 1.11.3.1 *Experimental and computationally determined IR, VCD spectra of **32a** and overlayed experimentally and computationally determined IR, VCD spectra of **32a** 72*

Figure 1.2.1 *"Types" of Ir-catalyzed allylic alkylation reactions. 5*

APPENDIX 1

Spectra Relevant to Chapter 1

Figure A1.1 *^{1}H NMR (400 MHz, $CDCl_3$) of compound **32a** 80*

Figure A1.2 *Infrared spectrum (Thin Film, NaCl) of compound **32a** 81*

Figure A1.3 *^{13}C NMR (100 MHz, $CDCl_3$) of compound **32a** 81*

Figure A1.4 *^{1}H NMR (500 MHz, $CDCl_3$) of compound **33** 82*

Figure A1.5 *Infrared spectrum (Thin Film, NaCl) of compound **33** 83*

Figure A1.6 *^{13}C NMR (100 MHz, $CDCl_3$) of compound **33** 83*

Figure A1.7 *^{1}H NMR (500 MHz, $CDCl_3$) of compound **34** 84*

Figure A1.8 *Infrared spectrum (Thin Film, NaCl) of compound **34** 85*

Figure A1.9 *^{13}C NMR (100 MHz, $CDCl_3$) of compound **34** 85*

Figure A1.10 *^{1}H NMR (500 MHz, $CDCl_3$) of compound **35** 86*

Figure A1.11 *Infrared spectrum (Thin Film, NaCl) of compound **35** 87*

Figure A1.12 *^{13}C NMR (100 MHz, $CDCl_3$) of compound **35** 87*

Figure A1.13 *^{1}H NMR (400 MHz, $CDCl_3$) of compound **32b**. 88*

Figure A1.14 *Infrared spectrum (Thin Film, NaCl) of compound **32b** 89*

Figure A1.15 *^{13}C NMR (100 MHz, $CDCl_3$) of compound **32b** 89*

Figure A1.16 *^{1}H NMR (400 MHz, $CDCl_3$) of compound **32c**. 90*

Figure A1.17 *Infrared spectrum (Thin Film, NaCl) of compound **32c** 91*

Figure A1.18 *^{13}C NMR (100 MHz, $CDCl_3$) of compound **32c** 91*

Figure A1.19 *^{1}H NMR (400 MHz, $CDCl_3$) of compound **32d**. 92*

Figure A1.20 *Infrared spectrum (Thin Film, NaCl) of compound **32d** 93*

Figure A1.21 *^{13}C NMR (100 MHz, $CDCl_3$) of compound **32d** 93*

Figure A1.22 *^{1}H NMR (400 MHz, $CDCl_3$) of compound **32e**. 94*

Figure A1.23 *Infrared spectrum (Thin Film, NaCl) of compound **32e** 95*

Figure A1.24 *^{13}C NMR (100 MHz, $CDCl_3$) of compound **32e** 95*

Figure A1.25 *^{1}H NMR (400 MHz, $CDCl_3$) of compound **32f**. 96*

Figure A1.26 *Infrared spectrum (Thin Film, NaCl) of compound **32f** 97*

Figure A1.27 *^{13}C NMR (100 MHz, $CDCl_3$) of compound **32f** 97*

Figure A1.28 *^{1}H NMR (400 MHz, $CDCl_3$) of compound **32g**. 98*

Figure A1.29 *Infrared spectrum (Thin Film, NaCl) of compound **32g*** 99
Figure A1.30 *^{13}C NMR (100 MHz, $CDCl_3$) of compound **32g*** 99
Figure A1.31 *^{1}H NMR (400 MHz, $CDCl_3$) of compound **32h***. 100
Figure A1.32 *Infrared spectrum (Thin Film, NaCl) of compound **32h*** 101
Figure A1.33 *^{13}C NMR (100 MHz, $CDCl_3$) of compound **32h*** 101
Figure A1.34 *^{1}H NMR (400 MHz, $CDCl_3$) of compound **32i***. 102
Figure A1.35 *Infrared spectrum (Thin Film, NaCl) of compound **32i*** 103
Figure A1.36 *^{13}C NMR (100 MHz, $CDCl_3$) of compound **32i*** 103
Figure A1.37 *HSQC spectrum ($CDCl_3$) of compound **32i*** 104
Figure A1.38 *^{1}H NMR (500 MHz, $CDCl_3$) of compound **32j***. 105
Figure A1.39 *Infrared spectrum (Thin Film, NaCl) of compound **32j*** 106
Figure A1.40 *^{13}C NMR (100 MHz, $CDCl_3$) of compound **32j*** 106
Figure A1.41 *^{19}F NMR (282 MHz, $CDCl_3$) of compound **32j*** 107
Figure A1.42 *^{1}H NMR (500 MHz, $CDCl_3$) of compound **32k***. 108
Figure A1.43 *Infrared spectrum (Thin Film, NaCl) of compound **32k*** 109
Figure A1.44 *^{13}C NMR (100 MHz, $CDCl_3$) of compound **32k*** 109
Figure A1.45 *^{1}H NMR (400 MHz, $CDCl_3$) of compound **32l***. 110
Figure A1.46 *Infrared spectrum (Thin Film, NaCl) of compound **32l*** 111
Figure A1.47 *^{13}C NMR (100 MHz, $CDCl_3$) of compound **32l*** 111
Figure A1.48 *^{1}H NMR (500 MHz, $CDCl_3$) of compound **32m***. 112
Figure A1.49 *Infrared spectrum (Thin Film, NaCl) of compound **32m*** 113
Figure A1.50 *^{13}C NMR (100 MHz, $CDCl_3$) of compound **32m*** 113
Figure A1.51 *^{1}H NMR (400 MHz, $CDCl_3$) of compound **32n***. 114
Figure A1.52 *Infrared spectrum (Thin Film, NaCl) of compound **32n*** 115
Figure A1.53 *^{13}C NMR (100 MHz, $CDCl_3$) of compound **32n*** 115
Figure A1.54 *^{1}H NMR (500 MHz, $CDCl_3$) of compound **32p***. 116
Figure A1.55 *Infrared spectrum (Thin Film, NaCl) of compound **32n*** 117
Figure A1.56 *^{13}C NMR (100 MHz, $CDCl_3$) of compound **32n*** 117
Figure A1.57 *^{1}H NMR (400 MHz, $CDCl_3$) of compound **32q***. 118
Figure A1.58 *Infrared spectrum (Thin Film, NaCl) of compound **32q*** 119
Figure A1.59 *^{13}C NMR (100 MHz, $CDCl_3$) of compound **32q*** 119
Figure A1.60 *^{1}H NMR (400 MHz, $CDCl_3$) of compound **32s***. 120
Figure A1.61 *Infrared spectrum (Thin Film, NaCl) of compound **32s*** 121
Figure A1.62 *^{13}C NMR (100 MHz, $CDCl_3$) of compound **32s*** 121
Figure A1.63 *^{1}H NMR (400 MHz, $CDCl_3$) of compound **32t***. 122
Figure A1.64 *Infrared spectrum (Thin Film, NaCl) of compound **32t*** 123
Figure A1.65 *^{13}C NMR (100 MHz, $CDCl_3$) of compound **32t*** 123
Figure A1.66 *^{1}H NMR (400 MHz, $CDCl_3$) of compound **32u***. 124
Figure A1.67 *Infrared spectrum (Thin Film, NaCl) of compound **32u*** 125
Figure A1.68 *^{13}C NMR (100 MHz, $CDCl_3$) of compound **32u*** 125
Figure A1.69 *^{1}H NMR (500 MHz, $CDCl_3$) of compound **40***. 126
Figure A1.70 *Infrared spectrum (Thin Film, NaCl) of compound **40*** 127
Figure A1.71 *^{13}C NMR (100 MHz, $CDCl_3$) of compound **40*** 127
Figure A1.72 *^{1}H NMR (500 MHz, $CDCl_3$) of compound **41***. 128
Figure A1.73 *Infrared spectrum (Thin Film, NaCl) of compound **41*** 129

Figure A1.74 *^{13}C NMR (100 MHz, $CDCl_3$) of compound **41*** 129
Figure A1.75 *^{1}H NMR (500 MHz, $CDCl_3$) of compound **42***. 130
Figure A1.76 *Infrared spectrum (Thin Film, NaCl) of compound **42*** 131
Figure A1.77 *^{13}C NMR (100 MHz, $CDCl_3$) of compound **42*** 131
Figure A1.78 *^{1}H NMR (400 MHz, $CDCl_3$) of compound **43***. 132
Figure A1.79 *Infrared spectrum (Thin Film, NaCl) of compound **43*** 133
Figure A1.80 *^{13}C NMR (100 MHz, $CDCl_3$) of compound **43*** 133
Figure A1.81 *^{1}H NMR (400 MHz, $CDCl_3$) of compound **44***. 134
Figure A1.82 *Infrared spectrum (Thin Film, NaCl) of compound **44*** 135
Figure A1.83 *^{13}C NMR (100 MHz, $CDCl_3$) of compound **44*** 135
Figure A1.84 *^{1}H NMR (500 MHz, $CDCl_3$) of compound **45***. 136
Figure A1.85 *Infrared spectrum (Thin Film, NaCl) of compound **45*** 137
Figure A1.86 *^{13}C NMR (100 MHz, $CDCl_3$) of compound **45*** 137
Figure A1.87 *^{1}H NMR (400 MHz, $CDCl_3$) of compound **31g***. 138
Figure A1.88 *Infrared spectrum (Thin Film, NaCl) of compound **31g*** 139
Figure A1.89 *^{13}C NMR (100 MHz, $CDCl_3$) of compound **31g*** 139
Figure A1.90 *^{1}H NMR (400 MHz, $CDCl_3$) of compound **31h***. 140
Figure A1.91 *Infrared spectrum (Thin Film, NaCl) of compound **31h*** 141
Figure A1.92 *^{13}C NMR (100 MHz, $CDCl_3$) of compound **31h*** 141
Figure A1.93 *^{1}H NMR (500 MHz, $CDCl_3$) of compound **31k***. 142
Figure A1.94 *Infrared spectrum (Thin Film, NaCl) of compound **31k*** 143
Figure A1.95 *^{13}C NMR (100 MHz, $CDCl_3$) of compound **31k*** 143
Figure A1.96 *^{1}H NMR (400 MHz, $CDCl_3$) of compound **31l***. 144
Figure A1.97 *Infrared spectrum (Thin Film, NaCl) of compound **31l*** 145
Figure A1.98 *^{13}C NMR (100 MHz, $CDCl_3$) of compound **31l*** 145
Figure A1.99 *^{1}H NMR (400 MHz, $CDCl_3$) of compound **31m***. 146
Figure A1.100 *Infrared spectrum (Thin Film, NaCl) of compound **31m*** 147
Figure A1.101 *^{13}C NMR (100 MHz, $CDCl_3$) of compound **31m*** 147
Figure A1.102 *^{1}H NMR (400 MHz, $CDCl_3$) of compound **46n***. 148
Figure A1.103 *Infrared spectrum (Thin Film, NaCl) of compound **46n*** 149
Figure A1.104 *^{13}C NMR (100 MHz, $CDCl_3$) of compound **46n*** 149
Figure A1.105 *^{1}H NMR (400 MHz, $CDCl_3$) of compound **47n***. 150
Figure A1.106 *Infrared spectrum (Thin Film, NaCl) of compound **47n*** 151
Figure A1.107 *^{13}C NMR (100 MHz, $CDCl_3$) of compound **47n*** 151
Figure A1.108 *^{1}H NMR (400 MHz, $CDCl_3$) of compound **31n***. 152
Figure A1.109 *Infrared spectrum (Thin Film, NaCl) of compound **31n*** 153
Figure A1.110 *^{13}C NMR (100 MHz, $CDCl_3$) of compound **31n*** 153
Figure A1.111 *^{1}H NMR (400 MHz, $CDCl_3$) of compound **31p***. 154
Figure A1.112 *Infrared spectrum (Thin Film, NaCl) of compound **31p*** 155
Figure A1.113 *^{13}C NMR (100 MHz, $CDCl_3$) of compound **31p*** 155
Figure A1.114 *^{1}H NMR (400 MHz, $CDCl_3$) of compound **31q***. 154
Figure A1.115 *Infrared spectrum (Thin Film, NaCl) of compound **31q*** 157
Figure A1.116 *^{13}C NMR (100 MHz, $CDCl_3$) of compound **31p*** 157
Figure A1.117 *^{1}H NMR (500 MHz, $CDCl_3$) of compound **31q***. 158
Figure A1.118 *Infrared spectrum (Thin Film, NaCl) of compound **31q*** 159

Figure A1.119 *^{13}C NMR (100 MHz, $CDCl_3$) of compound **31p*** *159*

CHAPTER 2

Enantioselective Total Synthesis of Hunterine A

Figure 2.1.1 *Carbon skeletons of various MIA subfamilies* *160*
Figure 2.1.2 *MIAs and monoterpene bisindole alkaloids synthesized by the Stoltz laboratory*..... *161*
Figure 2.1.3 *Structure of Hunterine A.* *162*
Figure 2.2.1 *Aspidospermidine (non-rearranged) and rearranged aspidosperma MIAs* *164*
Figure 2.4.1 *Hypothesized differences in coordination and reactivity of different nucleophile classes*..... *176*

APPENDIX 3

Spectra Relevant to Chapter 2

Figure A3.1 *^{1}H NMR (500 MHz, $CDCl_3$) of compound **72*** *264*
Figure A3.2 *Infrared spectrum (Thin Film, NaCl) of compound **72*** *265*
Figure A3.3 *^{13}C NMR (125 MHz, $CDCl_3$) of compound **72*** *265*
Figure A3.4 *^{1}H NMR (500 MHz, $CDCl_3$) of compound **73*** *266*
Figure A3.5 *Infrared spectrum (Thin Film, NaCl) of compound **73*** *267*
Figure A3.6 *^{13}C NMR (125 MHz, $CDCl_3$) of compound **73*** *267*
Figure A3.7 *^{1}H NMR (400 MHz, $CDCl_3$) of compound **76*** *268*
Figure A3.8 *Infrared spectrum (Thin Film, NaCl) of compound **76*** *269*
Figure A3.9 *^{13}C NMR (100 MHz, $CDCl_3$) of compound **76*** *269*
Figure A3.10 *^{1}H NMR (500 MHz, $CDCl_3$) of compound **80*** *270*
Figure A3.11 *Infrared spectrum (Thin Film, NaCl) of compound **80*** *271*
Figure A3.12 *^{13}C NMR (125 MHz, $CDCl_3$) of compound **80*** *271*
Figure A3.13 *^{1}H NMR (500 MHz, $CDCl_3$) of compound **68*** *272*
Figure A3.14 *Infrared spectrum (Thin Film, NaCl) of compound **68*** *273*
Figure A3.15 *^{13}C NMR (125 MHz, $CDCl_3$) of compound **68*** *273*
Figure A3.16 *^{1}H NMR (500 MHz, $CDCl_3$) of compound **70*** *274*
Figure A3.17 *Infrared spectrum (Thin Film, NaCl) of compound **70*** *275*
Figure A3.18 *^{13}C NMR (125 MHz, $CDCl_3$) of compound **70*** *275*
Figure A3.19 *^{1}H NMR (400 MHz, $CDCl_3$) of compound **81*** *276*
Figure A3.20 *Infrared spectrum (Thin Film, NaCl) of compound **81*** *277*
Figure A3.21 *^{13}C NMR (100 MHz, $CDCl_3$) of compound **81*** *277*
Figure A3.22 *^{1}H NMR (500 MHz, $CDCl_3$) of compound **122*** *278*
Figure A3.23 *Infrared spectrum (Thin Film, NaCl) of compound **122*** *279*
Figure A3.24 *^{13}C NMR (125 MHz, $CDCl_3$) of compound **122*** *279*
Figure A3.25 *^{1}H NMR (400 MHz, $CDCl_3$) of compound **(Z)-82*** *280*

Figure A3.26 *Infrared spectrum (Thin Film, NaCl) of compound **(Z)-82*** 281
Figure A3.27 *^{13}C NMR (100 MHz, $CDCl_3$) of compound **(Z)-82*** 281
Figure A3.28 *^{1}H NMR (500 MHz, $CDCl_3$) of compound **83*** 282
Figure A3.29 *Infrared spectrum (Thin Film, NaCl) of compound **83*** 283
Figure A3.30 *^{13}C NMR (125 MHz, $CDCl_3$) of compound **83*** 283
Figure A3.31 *^{1}H NMR (400 MHz, $CDCl_3$) of compound **(Z)-86*** 284
Figure A3.32 *Infrared spectrum (Thin Film, NaCl) of compound **(Z)-86*** 285
Figure A3.33 *^{13}C NMR (100 MHz, $CDCl_3$) of compound **(Z)-86*** 285
Figure A3.34 *^{1}H NMR (400 MHz, $CDCl_3$) of compound **(E)-86*** 286
Figure A3.35 *Infrared spectrum (Thin Film, NaCl) of compound **(E)-86*** 287
Figure A3.36 *^{13}C NMR (100 MHz, $CDCl_3$) of compound **(E)-86*** 287
Figure A3.37 *^{1}H NMR (400 MHz, $CDCl_3$) of compound **87*** 288
Figure A3.38 *Infrared spectrum (Thin Film, NaCl) of compound **87*** 289
Figure A3.39 *^{13}C NMR (100 MHz, $CDCl_3$) of compound **87*** 289
Figure A3.40 *^{1}H NMR (400 MHz, $CDCl_3$) of compound **88*** 290
Figure A3.41 *Infrared spectrum (Thin Film, NaCl) of compound **88*** 291
Figure A3.42 *^{13}C NMR (100 MHz, $CDCl_3$) of compound **88*** 291
Figure A3.43 *^{1}H NMR (400 MHz, $CDCl_3$) of compound **67*** 292
Figure A3.44 *Infrared spectrum (Thin Film, NaCl) of compound **67*** 293
Figure A3.45 *^{13}C NMR (100 MHz, $CDCl_3$) of compound **67*** 293
Figure A3.46 *^{1}H NMR (600 MHz, $CDCl_3$) of compound **67b*** 294
Figure A3.47 *Infrared spectrum (Thin Film, NaCl) of compound **67b*** 295
Figure A3.48 *^{13}C NMR (150 MHz, $CDCl_3$) of compound **67b*** 295
Figure A3.49 *^{1}H NMR (600 MHz, $CDCl_3$) of compound **67c*** 296
Figure A3.50 *Infrared spectrum (Thin Film, NaCl) of compound **67c*** 297
Figure A3.51 *^{13}C NMR (150 MHz, $CDCl_3$) of compound **67c*** 297
Figure A3.52 *^{1}H NMR (600 MHz, $CDCl_3$) of compound **67d*** 298
Figure A3.53 *Infrared spectrum (Thin Film, NaCl) of compound **67d*** 299
Figure A3.54 *^{13}C NMR (150 MHz, $CDCl_3$) of compound **67d*** 299
Figure A3.55 *^{1}H NMR (400 MHz, $CDCl_3$) of compound **92*** 300
Figure A3.56 *Infrared spectrum (Thin Film, NaCl) of compound **92*** 301
Figure A3.57 *^{13}C NMR (100 MHz, $CDCl_3$) of compound **92*** 301
Figure A3.58 *^{1}H NMR (400 MHz, $CDCl_3$) of compound **93*** 302
Figure A3.59 *Infrared spectrum (Thin Film, NaCl) of compound **93*** 303
Figure A3.60 *^{13}C NMR (100 MHz, $CDCl_3$) of compound **93*** 303
Figure A3.61 *^{1}H NMR (400 MHz, $CDCl_3$) of compound **97*** 304
Figure A3.62 *Infrared spectrum (Thin Film, NaCl) of compound **97*** 305
Figure A3.63 *^{13}C NMR (100 MHz, $CDCl_3$) of compound **97*** 305
Figure A3.64 *^{1}H NMR (500 MHz, $CDCl_3$) of compound **101*** 306
Figure A3.65 *Infrared spectrum (Thin Film, NaCl) of compound **101*** 307
Figure A3.66 *^{13}C NMR (125 MHz, $CDCl_3$) of compound **101*** 307
Figure A3.67 *^{1}H NMR (400 MHz, $CDCl_3$) of compound **103*** 308
Figure A3.68 *Infrared spectrum (Thin Film, NaCl) of compound **103*** 309
Figure A3.69 *^{13}C NMR (100 MHz, $CDCl_3$) of compound **103*** 309
Figure A3.70 *^{1}H NMR (400 MHz, $CDCl_3$) of compound **104*** 310

Figure A3.71 *Infrared spectrum (Thin Film, NaCl) of compound **104*** 311
Figure A3.72 *^{13}C NMR (100 MHz, $CDCl_3$) of compound **104*** 311
Figure A3.73 *^{1}H NMR (500 MHz, $CDCl_3$) of compound **105*** 312
Figure A3.74 *Infrared spectrum (Thin Film, NaCl) of compound **105*** 313
Figure A3.75 *^{13}C NMR (125 MHz, $CDCl_3$) of compound **105*** 313
Figure A3.76 *^{1}H NMR (400 MHz, $CDCl_3$) of compound **106*** 314
Figure A3.77 *Infrared spectrum (Thin Film, NaCl) of compound **106*** 315
Figure A3.78 *^{13}C NMR (100 MHz, $CDCl_3$) of compound **106*** 315
Figure A3.79 *^{1}H NMR (400 MHz, C_6D_6) of compound **107*** 316
Figure A3.80 *Infrared spectrum (Thin Film, NaCl) of compound **107*** 317
Figure A3.81 *^{13}C NMR (100 MHz, C_6D_6) of compound **107*** 317
Figure A3.82 *^{1}H NMR (600 MHz, C_6D_6) of compound **48*** 318
Figure A3.83 *^{1}H NMR (600 MHz, C_6D_6) of compound **112*** 319
Figure A3.84 *Infrared spectrum (Thin Film, NaCl) of compound **112*** 320
Figure A3.85 *^{13}C NMR (100 MHz, C_6D_6) of compound **112*** 320
Figure A3.86 *^{1}H NMR (600 MHz, C_6D_6) of compound **64*** 321
Figure A3.87 *Infrared spectrum (Thin Film, NaCl) of compound **64*** 322
Figure A3.88 *^{13}C NMR (125 MHz, C_6D_6) of compound **64*** 322
Figure A3.89 *Stacked ^{13}C NMR (C_6D_6) of compounsd **64**, **116**, and **117*** 323
Figure A3.90 *^{1}H NMR (400 MHz, C_6D_6) of compound **116*** 324
Figure A3.91 *Infrared spectrum (Thin Film, NaCl) of compound **116*** 325
Figure A3.92 *^{13}C NMR (100 MHz, C_6D_6) of compound **116*** 325
Figure A3.93 *HSQC Spectrum (C_6D_6) of compound **116*** 326
Figure A3.94 *^{1}H NMR (400 MHz, C_6D_6) of compound **117*** 327
Figure A3.95 *Infrared spectrum (Thin Film, NaCl) of compound **117*** 328
Figure A3.96 *^{13}C NMR (100 MHz, C_6D_6) of compound **117*** 328
Figure A3.97 *HSQC Spectrum (C_6D_6) of compound **117*** 329
Figure A3.98 *^{1}H NMR (600 MHz, CD_3OD) of compound **53*** 330
Figure A3.99 *Infrared spectrum (Thin Film, NaCl) of compound **53*** 331
Figure A3.100 *^{13}C NMR (125 MHz, , CD_3OD) of compound **53*** 331
Figure A3.101 *Overlaid ^{1}H NMR (600 and 400 MHz, CD_3OD) of synthetic and natural **53*** 332
Figure A3.102 *Overlaid ^{13}C NMR (100 MHz, CD_3OD) of synthetic and natural **53*** 333
Figure A3.103 *^{1}H NMR (400 MHz, C_6D_6) of compound **118*** 334

APPENDIX 4

X-Ray Crystallography Reports Relevant to Chapter 2

Figure A4.2.1 *X-Ray Coordinate of Compound **(Z)-82** (V23277)* 337
Figure A4.3.1 *X-Ray Coordinate of Lactam **87** (V23031)* 361
Figure A4.4.1 *X-Ray Coordinate for **97b** (V23134)* 370
Figure A4.5.1 *X-Ray Coordinate for **116** (V23324)* 380

Figure A4.6.1 *X-Ray Coordinate of **117** (V23195)* *390*
Figure A4.7.1 *X-Ray Coordinate of **53*** *400*

CHAPTER 3

Synthesis and Regioselective Ring Opening Reactions of Fused Bicyclic N-Aryl Aziridines

Figure 3.3.1 *Conformational analysis of aziridines and identification of a relationship between lone pair conjugation and N1–C1 bond length* *420*

APPENDIX 5

Spectra Relevant to Chapter 3

Figure A5.1 *^{1}H NMR (600 MHz, $CDCl_3$) of compound **144*** *464*
Figure A5.2 *^{1}H NMR (400 MHz, $CDCl_3$) of compound **145*** *465*
Figure A5.3 *Infrared spectrum (Thin Film, NaCl) of compound **145*** *466*
Figure A5.4 *^{13}C NMR (100 MHz, $CDCl_3$) of compound **145*** *466*
Figure A5.5 *^{1}H NMR (500 MHz, $CDCl_3$) of compound **146*** *467*
Figure A5.6 *Infrared spectrum (Thin Film, NaCl) of compound **146*** *468*
Figure A5.7 *^{13}C NMR (125 MHz, $CDCl_3$) of compound **146*** *468*
Figure A5.8 *^{1}H NMR (400 MHz, $CDCl_3$) of compound **149*** *469*
Figure A5.9 *Infrared spectrum (Thin Film, NaCl) of compound **149*** *470*
Figure A5.10 *^{13}C NMR (100 MHz, $CDCl_3$) of compound **149*** *470*
Figure A5.11 *^{11}B NMR (128 MHz, $CDCl_3$) of compound **149*** *471*
Figure A5.8 *^{1}H NMR (400 MHz, $CDCl_3$) of compound **150*** *472*
Figure A5.9 *Infrared spectrum (Thin Film, NaCl) of compound **150*** *473*
Figure A5.10 *^{13}C NMR (100 MHz, $CDCl_3$) of compound **150*** *473*
Figure A5.11 *^{11}B NMR (128 MHz, $CDCl_3$) of compound **150*** *474*
Figure A5.16 *^{1}H NMR (500 MHz, $CDCl_3$) of compound **151*** *475*
Figure A5.17 *Infrared spectrum (Thin Film, NaCl) of compound **151*** *476*
Figure A5.18 *^{13}C NMR (125 MHz, $CDCl_3$) of compound **151*** *476*
Figure A5.19 *^{1}H NMR (500 MHz, $CDCl_3$) of compound **152*** *477*
Figure A5.20 *Infrared spectrum (Thin Film, NaCl) of compound **152*** *478*
Figure A5.21 *^{13}C NMR (125 MHz, $CDCl_3$) of compound **152*** *478*
Figure A5.22 *^{1}H NMR (400 MHz, C_6D_6) of compound **155*** *479*
Figure A5.23 *Infrared spectrum (Thin Film, NaCl) of compound **155*** *480*
Figure A5.24 *^{13}C NMR (100 MHz, C_6D_6) of compound **155*** *480*
Figure A5.25 *^{1}H NMR (400 MHz, C_6D_6) of compound **155*** *481*
Figure A5.26 *Infrared spectrum (Thin Film, NaCl) of compound **155*** *482*
Figure A5.27 *^{13}C NMR (100 MHz, C_6D_6) of compound **155*** *482*
Figure A5.28 *^{1}H NMR (400 MHz, C_6D_6) of compound **156*** *483*
Figure A5.29 *Infrared spectrum (Thin Film, NaCl) of compound **156*** *484*

Figure A5.30 *^{13}C NMR (100 MHz, C_6D_6) of compound **156*** 484
Figure A5.31 *^{1}H NMR (400 MHz, C_6D_6) of compound **157*** 485
Figure A5.32 *Infrared spectrum (Thin Film, NaCl) of compound **157*** 486
Figure A5.33 *^{13}C NMR (100 MHz, C_6D_6) of compound **157*** 486
Figure A5.34 *^{1}H NMR (400 MHz, C_6D_6) of compound **158*** 487
Figure A5.35 *Infrared spectrum (Thin Film, NaCl) of compound **158*** 488
Figure A5.36 *^{13}C NMR (100 MHz, C_6D_6) of compound **158*** 488
Figure A5.37 *^{1}H NMR (400 MHz, C_6D_6) of compound **159*** 490
Figure A5.38 *Infrared spectrum (Thin Film, NaCl) of compound **159*** 491
Figure A5.39 *^{13}C NMR (100 MHz, C_6D_6) of compound **159*** 491
Figure A5.40 *COSY spectrum (C_6D_6) of compound **159*** 492
Figure A5.41 *HSQC spectrum (C_6D_6) of compound **159*** 493
Figure A5.42 *HMBC spectrum (C_6D_6) of compound **159*** 494
Figure A5.43 *^{1}H NMR (400 MHz, C_6D_6) of compound **166*** 495
Figure A5.44 *Infrared spectrum (Thin Film, NaCl) of compound **166*** 496
Figure A5.45 *^{13}C NMR (100 MHz, C_6D_6) of compound **166*** 496
Figure A5.46 *^{1}H NMR (400 MHz, $CDCl_3$) of compound **160*** 498
Figure A5.47 *Infrared spectrum (Thin Film, NaCl) of compound **160*** 499
Figure A5.48 *^{13}C NMR (100 MHz, $CDCl_3$) of compound **160*** 499
Figure A5.49 *COSY spectrum ($CDCl_3$) of compound **160*** 500
Figure A5.50 *HSQC spectrum ($CDCl_3$) of compound **160*** 501
Figure A5.51 *HMBC spectrum ($CDCl_3$) of compound **160*** 502
Figure A5.52 *^{1}H NMR (400 MHz, C_6D_6) of compound **161*** 504
Figure A5.53 *Infrared spectrum (Thin Film, NaCl) of compound **161*** 505
Figure A5.54 *^{13}C NMR (100 MHz, C_6D_6) of compound **161*** 505
Figure A5.55 *COSY spectrum (C_6D_6) of compound **161*** 506
Figure A5.56 *HSQC spectrum (C_6D_6) of compound **161*** 507
Figure A5.57 *HMBC spectrum (C_6D_6) of compound **161*** 508
Figure A5.58 *^{1}H NMR (400 MHz, C_6D_6) of compound **162*** 510
Figure A5.59 *Infrared spectrum (Thin Film, NaCl) of compound **162*** 511
Figure A5.60 *^{13}C NMR (100 MHz, C_6D_6) of compound **162*** 511
Figure A5.61 *COSY spectrum (C_6D_6) of compound **162*** 512
Figure A5.62 *HSQC spectrum (C_6D_6) of compound **162*** 513
Figure A5.63 *HMBC spectrum (C_6D_6) of compound **162*** 514
Figure A5.64 *^{1}H NMR (400 MHz, C_6D_6) of compound **163*** 516
Figure A5.65 *Infrared spectrum (Thin Film, NaCl) of compound **163*** 517
Figure A5.66 *^{13}C NMR (100 MHz, C_6D_6) of compound **163*** 517
Figure A5.67 *COSY spectrum (C_6D_6) of compound **163*** 518
Figure A5.68 *HSQC spectrum (C_6D_6) of compound **163*** 519
Figure A5.69 *HMBC spectrum (C_6D_6) of compound **163*** 520
Figure A5.70 *^{1}H NMR (400 MHz, C_6D_6) of compound **164*** 522
Figure A5.71 *Infrared spectrum (Thin Film, NaCl) of compound **164*** 523
Figure A5.72 *^{13}C NMR (100 MHz, C_6D_6) of compound **164*** 523
Figure A5.73 *COSY spectrum (C_6D_6) of compound **164*** 524
Figure A5.74 *HSQC spectrum (C_6D_6) of compound **164*** 525

Figure A5.75 *HMBC spectrum (C_6D_6) of compound **164*** 526

APPENDIX 6

X-Ray Crystallography Reports Relevant to Chapter 3

Figure A6.2.1 *X-Ray Coordinate of Compound **155*** 529
Figure A6.3.1 *X-Ray Coordinate of Compound **156*** 537
Figure A6.4.1 *X-Ray Coordinate of Compound **157*** 545
Figure A6.5.1 *X-Ray Coordinate of Compound **158*** 557
Figure A6.6.1 *X-Ray Coordinate of Compound **160*** 569

CHAPTER 4

Progress Toward the Synthesis of Kuroshine A

Figure 4.1.1 *Zoanthamine alkaloids and highly oxidized subfamily of "kuroshines"* 578
Figure 4.3.1 *Retrosynthetic analysis of **172*** 584
Figure 4.4.1 *Rationalization of the MOB cycloaddition stereochemical outcome through transition state analysis* 587
Figure 4.5.1 *Strategies to mask the A ring methyl enone* 588

APPENDIX 7

Spectra Relevant to Chapter 4

Figure A7.1 *^{1}H NMR (400 MHz, $CDCl_3$) of compound **205*** 625
Figure A7.2 *Infrared spectrum (Thin Film, NaCl) of compound **205*** 626
Figure A7.3 *^{13}C NMR (100 MHz, $CDCl_3$) of compound **205*** 626
Figure A7.4 *^{1}H NMR (400 MHz, $CDCl_3$) of compound **207*** 627
Figure A7.5 *Infrared spectrum (Thin Film, NaCl) of compound **207*** 628
Figure A7.6 *^{13}C NMR (100 MHz, $CDCl_3$) of compound **207*** 628
Figure A7.7 *^{1}H NMR (400 MHz, $CDCl_3$) of compound **208*** 629
Figure A7.8 *Infrared spectrum (Thin Film, NaCl) of compound **208*** 630
Figure A7.9 *^{13}C NMR (100 MHz, $CDCl_3$) of compound **208*** 630
Figure A7.10 *^{1}H NMR (400 MHz, $CDCl_3$) of compound **234*** 631
Figure A7.11 *Infrared spectrum (Thin Film, NaCl) of compound **234*** 632
Figure A7.12 *^{13}C NMR (100 MHz, $CDCl_3$) of compound **234*** 632
Figure A7.13 *^{1}H NMR (400 MHz, $CDCl_3$) of compound **209*** 633
Figure A7.14 *Infrared spectrum (Thin Film, NaCl) of compound **209*** 634
Figure A7.15 *^{13}C NMR (100 MHz, $CDCl_3$) of compound **209*** 634
Figure A7.16 *^{1}H NMR (400 MHz, $CDCl_3$) of compound **210*** 635
Figure A7.17 *Infrared spectrum (Thin Film, NaCl) of compound **210*** 636

Figure A7.18 *^{13}C NMR (100 MHz, $CDCl_3$) of compound **210*** 636
Figure A7.19 *^{1}H NMR (400 MHz, $CDCl_3$) of compound **211*** 637
Figure A7.20 *Infrared spectrum (Thin Film, NaCl) of compound **211*** 638
Figure A7.21 *^{13}C NMR (100 MHz, $CDCl_3$) of compound **211*** 638
Figure A7.22 *^{1}H NMR (500 MHz, $CDCl_3$) of compound **217*** 639
Figure A7.23 *^{1}H NMR (500 MHz, $CDCl_3$) of compound **219*** 640
Figure A7.24 *^{1}H NMR (500 MHz, $CDCl_3$) of compound **220*** 641
Figure A7.25 *^{1}H NMR (400 MHz, $CDCl_3$) of compound **221*** 642
Figure A7.26 *Infrared spectrum (Thin Film, NaCl) of compound **221*** 643
Figure A7.27 *^{13}C NMR (100 MHz, $CDCl_3$) of compound **221*** 643
Figure A7.28 *^{1}H NMR (400 MHz, $CDCl_3$) of compound **225*** 644
Figure A7.29 *Infrared spectrum (Thin Film, NaCl) of compound **225*** 645
Figure A7.30 *^{13}C NMR (100 MHz, $CDCl_3$) of compound **225*** 645
Figure A7.31 *^{1}H NMR (400 MHz, $CDCl_3$) of compound **226*** 646
Figure A7.32 *Infrared spectrum (Thin Film, NaCl) of compound **226*** 647
Figure A7.33 *^{13}C NMR (100 MHz, $CDCl_3$) of compound **226*** 647
Figure A7.34 *^{1}H NMR (500 MHz, C_6D_6) of compound **227*** 648
Figure A7.35 *Infrared spectrum (Thin Film, NaCl) of compound **227*** 649
Figure A7.36 *^{13}C NMR (125 MHz, C_6D_6) of compound **227*** 649
Figure A7.37 *^{1}H NMR (500 MHz, $CDCl_3$) of compound **228*** 650
Figure A7.38 *Infrared spectrum (Thin Film, NaCl) of compound **228*** 651
Figure A7.39 *^{13}C NMR (125 MHz, $CDCl_3$) of compound **228*** 651
Figure A7.40 *^{1}H NMR (500 MHz, $CDCl_3$) of compound **230*** 652
Figure A7.41 *Infrared spectrum (Thin Film, NaCl) of compound **230*** 653
Figure A7.42 *^{13}C NMR (125 MHz, $CDCl_3$) of compound **230*** 653
Figure A7.43 *^{1}H NMR (500 MHz, $CDCl_3$) of compound **231*** 654
Figure A7.44 *Infrared spectrum (Thin Film, NaCl) of compound **231*** 655
Figure A7.45 *^{13}C NMR (125 MHz, $CDCl_3$) of compound **231*** 655

APPENDIX 8

X-Ray Crystallography Reports Relevant to Chapter 4

Figure A8.2.1 *X-Ray coordinate of compound **211*** 658

APPENDIX 9

Alternative Masked "A" Ring Strategies

Figure A9.2.1 *Initial retrosynthesis masking the A ring enone as a tertiary allylic alcohol* 667
Figure A9.3.1 *Revised synthetic approach to preserve A ring oxidation level* 671

APPENDIX 10

Spectra Relevant to Appendix 9

Figure A10.1 *^{1}H NMR (500 MHz, $CDCl_3$) of compound **240*** *705*
Figure A10.2 *^{1}H NMR (500 MHz, $CDCl_3$) of compound **241*** *706*
Figure A10.3 *^{1}H NMR (500 MHz, $CDCl_3$) of compound **242*** *707*
Figure A10.4 *^{1}H NMR (500 MHz, $CDCl_3$) of compound **243*** *708*
Figure A10.5 *^{1}H NMR (500 MHz, $CDCl_3$) of compound **244*** *709*
Figure A10.6 *^{1}H NMR (500 MHz, $CDCl_3$) of compound **245*** *710*
Figure A10.7 *^{1}H NMR (500 MHz, C_6D_6) of compound **247** (major)* *711*
Figure A10.8 *^{1}H NMR (500 MHz, C_6D_6) of compound **247** (minor)* *712*
Figure A10.9 *^{1}H NMR (500 MHz, C_6D_6) of compound **268*** *713*
Figure A10.10 *^{1}H NMR (500 MHz, $CDCl_3$) of compound **248*** *714*
Figure A10.11 *^{1}H NMR (500 MHz, $CDCl_3$) of compound **249*** *715*
Figure A10.12 *^{1}H NMR (500 MHz, $CDCl_3$) of compound **250a*** *716*
Figure A10.13 *^{1}H NMR (500 MHz, $CDCl_3$) of compound **250b*** *717*
Figure A10.14 *^{1}H NMR (500 MHz, $CDCl_3$) of compound **251b*** *718*
Figure A10.15 *^{1}H NMR (500 MHz, $CDCl_3$) of compound **251a*** *719*
Figure A10.16 *^{1}H NMR (500 MHz, $CDCl_3$) of compound **252*** *720*
Figure A10.17 *^{1}H NMR (500 MHz, $CDCl_3$) of compound **253*** *721*
Figure A10.18 *^{1}H NMR (600 MHz, C_6D_6) of compound **269** (diast. 1)* *722*
Figure A10.19 *^{1}H NMR (600 MHz, C_6D_6) of compound **269** (diast. 2)* *723*
Figure A10.20 *^{1}H NMR (500 MHz, $CDCl_3$) of compound **254*** *724*
Figure A10.21 *^{1}H NMR (500 MHz, C_6D_6) of compound **256*** *725*
Figure A10.22 *^{1}H NMR (500 MHz, C_6D_6) of compound **257*** *726*
Figure A10.23 *^{1}H NMR (600 MHz, C_6D_6) of compound **258*** *727*
Figure A10.24 *^{1}H NMR (600 MHz, C_6D_6) of compound **259*** *728*
Figure A10.25 *^{1}H NMR (500 MHz, $CDCl_3$) of compound **262*** *729*
Figure A10.26 *^{1}H NMR (500 MHz, $CDCl_3$) of compound **270*** *730*
Figure A10.27 *^{1}H NMR (500 MHz, $CDCl_3$) of compound **264*** *731*
Figure A10.28 *^{1}H NMR (500 MHz, C_6D_6) of compound **266*** *732*

LIST OF SCHEMES

CHAPTER 1

Iridium-Catalyzed Asymmetric Allylic Alkylation of Dialkyl Malonates

Scheme 1.2.1 *Regioselectivity trends in transition metal-catalyzed allylic alkylation of all-carbon quaternary centers via allylic alkylation* *2*

Scheme 1.2.2 *A. Initial report by Takeuchi. B. Enantioselective reports by Helmchen.* *3*

Scheme 1.2.3 *General catalytic cycle of iridium-catalyzed allylic alkylation reactions* *4*

Scheme 1.3.1 *A. Correlations between C–Ir bond length and regioselectivity. B. Kinetic experiments by Hartwig.* *7*

Scheme 1.4.1 *Construction of all-carbon quaternary centers via Ir-catalyzed allylic alkylation reported by the Stoltz group. A. Use of substituted B-ketoester nucleophiles. B. Use of MAC nucleophiles. C. Use of substituted malononitriles. D. Proposed use of malonate nucleophiles* *9*

Scheme 1.6.1 *Control experiments and mechanistic probes* *12*

Scheme 1.7.1 *Control experiments and mechanistic probes* *14*

Scheme 1.7.2 *A. Temperature dependence and results with isomeric allylic carbonate electrophiles. B. Lack of equilibration leads to lack of enantioenrichment.* *15*

Scheme 1.8.1 *Nucleophile scope* *16*

Scheme 1.8.2 *Electrophile scope and use of a drug-like molecule* *18*

Scheme 1.8.3 *Limitations of the allylic alkylation reaction* *19*

Scheme 1.8.4 *Success of alkyl-alkyl electrophiles* *20*

Scheme 1.9.1 *Product diversification* *21*

Scheme 1.9.2 ***:*** *Formal total synthesis of sporochnols A–C* *22*

CHAPTER 2

Enantioselective Total Synthesis of Hunterine A

Scheme 2.2.1 *Biosynthesis of Aspidosperma MIAs* *163*

Scheme 2.3.1 *A. Retrosynthetic Analysis of* ***53****. B. Strategies for C7 quaternary center formation. C. Possibilities for desymmetrization and use of keto-alcohol* ***70****.* *165*

Scheme 2.3.1 *Construction of racemic keto alcohol* ***70*** *and optimization of the 1,4-addition* *167*

Scheme 2.4.2 *Construction of bicyclic diketone* ***68*** *168*

Scheme 2.4.3 *Optimization of the reductive desymmetrization and determination of absolute stereochemistry.* *170*

Scheme 2.4.4 *CIDT reported by Lisnyak and failed CIDT of bicyclic ketones* ***70*** *and* ***83****.* *171*

Scheme 2.4.5 *Oxime formation, separation, and recycling* *172*

Scheme 2.4.6 *Beckmann rearrangement and synthesis of aminoketone* ***67*** *173*

Scheme 2.4.7 *A) Synthesis of vinyl iodide nucleophile containing aryl triazene. B) Successful addition to ketone **83**. C) Failed addition to aminoketones **67b–d**.* *174*
Scheme 2.4.8 *Successful 1,2-addition using chloride nucleophile and subsequent aza-Cope/Mannich reaction.*. *175*
Scheme 2.4.9 *Synthesis of dianion nucleophile precursors **103** and **105*** *177*
Scheme 2.4.10 *Optimization of the dianion 1,2-addition* *178*
Scheme 2.4.11 *Undesired condensation following aza-Cope/Mannich reaction and synthesis of (–)-aspidospermidine.* *180*
Scheme 2.4.12 *Formation of aryl azide prior to aza-Cope/Mannich and avoidance of a potential undesired aza-Cope rearrangement* *180*
Scheme 2.4.13 *Optimization of the [3+2] cycloaddition* *182*
Scheme 2.4.14 *Rationalization of diastereoselectivity and one-pot aza-Cope/Mannich, [3+2] cycloaddition* *184*
Scheme 2.4.15 *Completion of the synthesis of hunterine A* *185*
Scheme 2.4.16 *Nitrogen pyramidality and differences in reactivity of triazoline diastereomers.* *186*

CHAPTER 3

Synthesis and Regioselective Ring Opening Reactions of Fused Bicyclic N-Aryl Aziridines

Scheme 3.1.1 *Ring opening reactions of fused bicyclic aziridines* *409*
Scheme 3.1.2 *Ring opening reactions of fused bicyclic N-aryl aziridines* *410*
Scheme 3.1.3 *Proposed simplified bicyclic N-aryl aziridine for systematic study of ring opening* *411*
Scheme 3.2.1 *Initial attempts to synthesize simplified bicyclic N-aryl aziridines* *412*
Scheme 3.3.1 *Successful synthesis of fused bicyclic N-aryl aziridines* *414*
Scheme 3.3.2 *Ring opening of fused bicyclic N-aryl aziridines* *416*
Scheme 3.3.3 *Failed ring opening without strong activation* *417*
Scheme 3.3.4 *Ring opening of triazolines and formation of imine/enamine byproducts* *418*
Scheme 3.3.5 *Possible factors influencing regioselective attack* *422*

CHAPTER 4

Progress Toward the Synthesis of Kuroshine A

Scheme 4.2.1 *Proposed biosynthesis of **169** and oxidation leading to **172**, **173**, and **174*** *579*
Scheme 4.2.2 *Total syntheses of **171** and **170** by Miyashita and coworkers* *580*
Scheme 4.2.3 *Total synthesis of **171** by Kobayashi and coworkers* *581*

Scheme 4.2.4 *Total synthesis of **171** and attempted synthesis of **194** by Gao and coworkers* *582*
Scheme 4.2.4 *Efficient total synthesis of **171** by Sun and coworkers* *583*
Scheme 4.4.1 *Successful synthesis of the ABC ring system using a model system* *586*
Scheme 4.5.1 *Synthesis of chiral cyclohexenone derivative through known procedures* *589*
Scheme 4.5.2 *Synthesis of aryl bromide coupling partner* *589*
Scheme 4.5.3 *Conjugate addition/alkylation and further manipulation* *591*
Scheme 4.5.4 *Installation of the dieneophile* *592*

APPENDIX 9

Alternative Masked "A" Ring Strategies

Scheme A9.2.1 *Synthesis of substituted arene **244*** *668*
Scheme A9.2.2 *Elaboration of arene **244**, failed deprotection, and formation of A ring enone* *669*
Scheme A9.2.3 *Failed cycloaddition of MOB **258** and potential decomposition pathway* *670*
Scheme A9.3.1 *Revised synthetic approach to avoid allylic alcohol and preserve A ring oxidation* *671*

LIST OF TABLES

CHAPTER 1

Iridium-Catalyzed Asymmetric Allylic Alkylation of Dialkyl Malonates

Table 1.5.1 *Initial evaluation of phosphoramidite ligands* *10*
Table 1.5.2 *π -σ-π equilibration*..... *14*

APPENDIX 4

X-Ray Crystallography Reports Relevant to Chapter 2

Table A4.2.1 *Crystal Data and Structure Refinement for* ***(Z)-82*** *337*
Table A4.2.2 *Atomic coordinates (x 10^4) and equivalent isotropic displacement parameters ($Å^2$x 10^3) for* ***(Z)-82*** *(V23277). U(eq) is defined as one third of the trace of the orthogonalized U^{ij} tensor*..... *338*
Table A4.2.3 *Bond lengths [Å] and angles [°] for* ***(Z)-82*** *(V23277)* *341*
Table A4.2.4 *Anisotropic displacement parameters ($Å^2$x 10^3) for* ***(Z)-82*** *(V23277). The anisotropic displacement factor exponent takes the form: $-2p^2[h^2 a^{*2}U^{11} + ... + 2\ h\ k\ a^*\ b^*\ U^{12}]$*..... *349*
Table A4.2.5 *Hydrogen coordinates (x 10^4) and isotropic displacement parameters ($Å^2$x 10^3) for* ***(Z)-82*** *(V23277).* *352*
Table A4.2.6 *Torsion angles [°] for* ***(Z)-82*** *(V23277)* *355*
Table A4.2.7 . *Hydrogen bonds for* ***(Z)-82*** *(V23277) [Å and °].* *358*

Table A4.3.1 *Crystal Data and Structure Refinement of* ***87*** *(V23031)* *361*
Table A4.3.2 *Atomic coordinates (x 10^4) and equivalent isotropic displacement parameters ($Å^2$x 10^3) for* ***87*** *(V23031). U(eq) is defined as one third of the trace of the orthogonalized U^{ij} tensor.*..... *362*
Table A4.3.3 *Bond lengths [Å] and angles [°] for* ***87*** *(V23031)* *363*
Table A4.3.4 *Anisotropic displacement parameters ($Å^2$x 10^3) for* ***87*** *(V23031). The anisotropic displacement factor exponent takes the form: $-2p^2[\ h^2 a^{*2}U^{11} + ...\ + 2\ h\ k\ a^*\ b^*\ U^{12}\ ]$*..... *365*
Table A4.3.5 *Hydrogen coordinates (x 10^4) and isotropic displacement parameters ($Å^2$x 10^3) for* ***87*** *(V23031)*..... *366*
Table A4.3.6 *Torsion angles [°] for* ***87*** *(V23031)* *367*
Table A4.3.7 *Hydrogen bonds for* ***87*** *(V23031) [Å and °]* *368*

Table A4.4.1 *Crystal data and structure refinement for* ***97b*** *(V23134)* *370*
Table A4.4.2 *Atomic coordinates (x 10^4) and equivalent isotropic displacement parameters ($Å^2$x 10^3) for V23134. U(eq) is defined as one third of the trace of the orthogonalized Uij tensor*..... *371*

Table A4.4.3 *Bond lengths [Å] and angles [°] for **97b** (V23134)* *372*
Table A4.4.4 *Anisotropic displacement parameters ($Å^2$x 10^3) for **97b** (V23134). The anisotropic displacement factor exponent takes the form: $-2p^2[h^2 a^{*2}U^{11} + ... + 2 h k a^* b^* U^{12}]$.* *375*
Table A4.4.5 *Hydrogen coordinates (x 104) and isotropic displacement parameters ($Å^2$x 10^3) for **97b** (V23134)* *376*
Table A4.4.6 *Torsion angles [°] for **97b** (V23134)* *377*
Table A4.4.7 *Hydrogen bonds for **97b** (V23134) [Å and °]* *378*

Table A4.5.1 *Crystal data and structure refinement for **116** (V23324)* *380*
Table A4.5.2 *Atomic coordinates (x 10^4) and equivalent isotropic displacement parameters ($Å^2$x 10^3) for V23324. U(eq) is defined as one third of the trace of the orthogonalized Uij tensor* *381*
Table A4.5.3 *Bond lengths [Å] and angles [°] for **97b** (V23324)* *382*
Table A4.5.4 *Anisotropic displacement parameters ($Å^2$x 10^3) for **116** V23324. The anisotropic displacement factor exponent takes the form: $-2p^2[h^2 a^{*2}U^{11} + ... + 2 h k a^* b^* U^{12}]$* *385*
Table A4.5.5 *Hydrogen coordinates (x 10^4) and isotropic displacement parameters ($Å^2$x 10^3) for **116** (V23324)* *386*
Table A4.5.6 *Torsion angles [°] for **116** (V23324)* *387*

Table A4.6.1 *Crystal data and structure refinement for **117** (V23195)* *390*
Table A4.6.2 *Atomic coordinates (x 10^4) and equivalent isotropic displacement parameters ($Å^2$x 10^3) for **117** (V23195). U(eq) is defined as one third of the trace of the orthogonalized U^{ij} tensor.* *391*
Table A4.6.3 *Bond lengths [Å] and angles [°] for **117** (V23195).* *392*
Table A4.6.4 *Anisotropic displacement parameters ($Å^2$x 10^3) for **117** (V23195). The anisotropic displacement factor exponent takes the form: $-2p^2[h^2 a^{*2}U^{11} + ... + 2 h k a^* b^* U^{12}]$* *393*
Table A4.6.5 *Hydrogen coordinates (x 10^4) and isotropic displacement parameters ($Å^2$x 10^3) for **117** (V23195)* *396*
Table A4.6.6 *Torsion angles [°] for **177** (V23195)* *397*

Table A4.7.1 *Crystal data and structure refinement for **53** (V23353)* *400*
Table A4.7.2 *Atomic coordinates (x 10^4) and equivalent isotropic displacement parameters ($Å^2$x 10^3) for **53** (V23353). U(eq) is defined as one third of the trace of the orthogonalized U^{ij} tensor* *401*
Table A4.7.3 *Bond lengths [Å] and angles [°] for **53** (V23353)* *402*
Table A4.7.4 *Anisotropic displacement parameters ($Å^2$x 10^3) for **53** (V23353). The anisotropic displacement factor exponent takes the form: $-2p^2[h^2 a^{*2}U^{11} + ... + 2 h k a^* b^* U^{12}]$* *405*

Table A4.7.5 *Hydrogen coordinates (x 10^4) and isotropic displacement parameters ($Å^2$x 10^3) for **53** (V23353)* *406*
Table A4.7.6 *Torsion angles [°] for **53** (V23353).* *407*
Table A4.7.7 *Hydrogen bonds for **53** [Å and °]* *408*

APPENDIX 5

Spectra Relevant to Chapter 3

Table A5.1 *2D NMR Correlations for **159*** *488*
Table A5.2 *2D NMR Correlations for **160*** *497*
Table A5.3 *2D NMR Correlations for **161*** *503*
Table A5.4 *2D NMR Correlations for **162*** *509*
Table A5.5 *2D NMR Correlations for **163*** *515*
Table A5.6 *2D NMR Correlations for **164*** *521*

APPENDIX 6

X-Ray Crystallography Reports Relevant to Chapter 3

Table A6.2.1 *Crystal data and structure refinement for **155*** *529*
Table A6.2.2 *Atomic coordinates (x 10^4) and equivalent isotropic displacement parameters ($Å^2$x 10^3) for **155**. U(eq) is defined as one third of the trace of the orthogonalized U^{ij} tensor* *530*
Table A6.2.3 *Bond lengths [Å] and angles [°] for **155*** *531*
Table A6.2.4 *Anisotropic displacement parameters ($Å^2$x 10^3) for **155**. The anisotropic displacement factor exponent takes the form: $-2p^2[h^2 a^{*2}U^{11} + ... + 2 h k a^* b^* U^{12}]$* *533*
Table A6.2.5 *Hydrogen coordinates (x 10^4) and isotropic displacement parameters ($Å^2$x 10^3) for **155*** *533*
Table A6.2.6 *Torsion angles [°] for **155*** *534*

Table A6.3.1 *Crystal data and structure refinement for **156*** *537*
Table A6.3.2 *Atomic coordinates (x 10^4) and equivalent isotropic displacement parameters ($Å^2$x 10^3) for **155**. U(eq) is defined as one third of the trace of the orthogonalized U^{ij} tensor* *538*
Table A6.3.3 *Crystal data and structure refinement for **156*** *539*
Table A6.3.4 *Anisotropic displacement parameters ($Å^2$x 10^3) for **156**. The anisotropic displacement factor exponent takes the form: $-2p^2[h^2 a^{*2}U^{11} + ... + 2 h k a^* b^* U^{12}]$* *541*

Table A6.3.5 *Hydrogen coordinates x 10^4) and isotropic displacement parameters ($Å^2$x 10^3) for* ***156*** *542*

Table A6.3.6 *Hydrogen coordinates x 10^4) and isotropic displacement parameters ($Å^2$x 10^3) for* ***156*** *543*

Table A6.4.1 *Crystal data and structure refinement for* ***157*** *545*

Table A6.4.2 *Atomic coordinates (x 10^4) and equivalent isotropic displacement parameters ($Å^2$x 10^3) for* ***157****. U(eq) is defined as one third of the trace of the orthogonalized U^{ij} tensor* *546*

Table A6.4.3 *Bond lengths [Å] and angles [°] for* ***157*** *547*

Table A6.4.4 *Anisotropic displacement parameters ($Å^2$x 10^3) for* ***157****. The anisotropic displacement factor exponent takes the form: $-2p^2[h^2 a^{*2}U^{11} + ... + 2 h k a^* b^* U^{12}]$* *551*

Table A6.4.5 *Hydrogen coordinates (x 10^4) and isotropic displacement parameters ($Å^2$x 10^3) for* ***157*** *552*

Table A6.4.6 *Torsion angles [°] for* ***157*** *554*

Table A6.5.1 *Crystal data and structure refinement for* ***158*** *557*

Table A6.5.2 *Atomic coordinates (x 10^4) and equivalent isotropic displacement parameters ($Å^2$x 10^3) for* ***158****. U(eq) is defined as one third of the trace of the orthogonalized U^{ij} tensor.* *558*

Table A6.5.3 *Bond lengths [Å] and angles [°] for* ***158****.* *559*

Table A6.5.4 *Anisotropic displacement parameters ($Å^2$x 10^3) for* ***158****. The anisotropic displacement factor exponent takes the form: $-2p^2[h^2 a^{*2}U^{11} + ... + 2 h k a^* b^* U^{12}]$* *563*

Table A6.5.5 *Hydrogen coordinates (x 10^4) and isotropic displacement parameters ($Å^2$x 10^3)for* ***158****.* *563*

Table A6.5.6 *Torsion angles [°] for* ***158*** *563*

Table A6.6.1 *Crystal data and structure refinement for* ***160*** *569*

Table A6.6.2 *Atomic coordinates (x 10^4) and equivalent isotropic displacement parameters ($Å^2$x 10^3) for* ***160****. U(eq) is defined as one third of the trace of the orthogonalized U^{ij} tensor* *570*

Table A6.6.3 *Bond lengths [Å] and angles [°] for* ***160*** *571*

Table A6.6.4 *Anisotropic displacement parameters ($Å^2$x 10^3) for* ***160****. The anisotropic displacement factor exponent takes the form: $-2p^2[h^2 a^{*2}U^{11} + ... + 2 h k a^* b^* U^{12}]$* *573*

Table A6.6.5 *Hydrogen coordinates (x 10^4) and isotropic displacement parameters ($Å^2$x 10^3) for* ***160****.* *574*

Table A6.6.6 *Torsion angles [°] for* ***160*** *575*

Table A6.6.7 *Hydrogen bonds for **160** [Å and °].....576*

CHAPTER 4

Progress Toward the Synthesis of Kuroshine A

Table 4.5.1 *Optimization of the ortho-phenol bromination.....590*

APPENDIX 8

X-Ray Crystallography Reports Relevant to Chapter 4

Table A8.2.1 *Crystal data and structure refinement for **211**.....658*
Table A8.2.2 *Atomic coordinates (x 10^4) and equivalent isotropic displacement parameters (Å^{2}x 10^3) for V24053. U(eq) is defined as one third of the trace of the orthogonalized U^{ij} tensor.....659*
Table A8.2.3 *Bond lengths [Å] and angles [°] for **211**.....660*
Table A8.2.4 *Anisotropic displacement parameters (Å^{2}x 10^3) for **211**. The anisotropic displacement factor exponent takes the form: $-2p^2[h^2 a^{*2}U^{11} + ... + 2 h k a^* b^* U^{12}]$.....662*
Table A8.2.5 *Hydrogen coordinates (x 10^4) and isotropic displacement parameters (Å^{2}x 10^3) for **211**.....663*
Table A8.2.6 *Torsion angles [°] for **211**.....664*

APPENDIX 11

Notebook Cross-References for New Compounds

Table A11.1 *Notebook cross-reference for Chapter 1.....734*
Table A11.2 *Notebook cross-reference for Chapter 2.....735*
Table A11.3 *Notebook cross-reference for Chapter 3.....736*
Table A11.4 *Notebook cross-reference for Chapter 4.....737*
Table A11.5 *Notebook cross-reference for Appendix 9.....738*

LIST OF ABBREVIATIONS

μ	micro
$[\alpha]_D^{23}$	specific rotation at wavelength of sodium D line
[H]	reduction
[O]	oxidation
°C	degrees Celsius
Å	Ångstrom
Ac	acetyl
AcOH	acetic acid
APCI	atmospheric pressure chemical ionization
app	apparent
aq	aqueous
Ar	aryl
atm	atmosphere
Bn	benzyl
BHT	butylated hydroxytoluene
Boc	*tert*-butyloxycarbonyl
bp	boiling point
br	broad
c	concentration for specific rotation measurements
calc'd	calculated
cat	catalytic
cm^{-1}	wavenumber (s)
COD	1,5-cyclooctadiene
cont'd	continued
CSA	camphorsulfonic acid
d	doublet
D	deuterium
DBU	1,8-diazabicyclo[5.4.0] undec-7-ene
DCE	1,2-dichloroethane
DIBAL–H	diisobutylaluminum hydride
DIPEA	*N,N*-diisoprobylethylamine
DMAP	4-dimethylaminophyridine
DMF	dimethylformamide
DMP	Dess–Martin periodinane
DMS	dimethylsulfide
DMSO	dimethyl sulfoxide
DNPH	2,4-dinitrophenylhydrazine
DPEN	diphenylethylenediamine
dr	diastereomeric ratio
ee	enantiomeric excess

EI	electron impact
equiv	equivalent(s)
ESI	electrospray ionization
Et	ethyl
EtOAc	Ethyl acetate
EWG	electron withdrawing group
FAB	fast atom bombardment
FD	field desorption (ionization)
FI	field ionization
g	gram(s)
h	hour(s)
HMDS	1,1,1,3,3,3-hexamethyl Disilazane
HMPA	hexamethylphosphoramide
HPLC	high-performance liquid chromatography
HRMS	high-resolution mass Spectrometry
Hz	hertz
i-Bu	*iso*-butyl
i.e.	that is (Latin id est)
imid.	Imidazole
IPA	2-propanol
IR	infrared (spectroscopy)
J	NMR coupling constant
K	Kelvin
kcal	kilocalorie
KHMDS	potassium Hexametyldisilazide
L	liter; ligand
LC–MS	liquid chromatography mass spectrometry
LDA	lithium diisopropylamide
LG	leaving group
LHMDS	lithium Hexamethyldisilazide
m	multiplet; milli
M	metal; molar; molecular ion
m	meta
m/z	mass to charge ratio
*m*CPBA	*meta*-Chloroperoxybenzoic acid
Me	methyl
MEM	2-methyoxyethoxymethyl
mg	milligram(s)
MHz	megahertz
min	minute(s)
mol	mole(s)
Ms	methanesulfonyl (mesyl)
mp	melting point

MS	molecular sieves
n	nano
N	normal
n-Bu	(*normal*) butyl
NBS	*N*-bromosuccinimide
TBD	1,5,6-triazabicyclo [4.4.0]dec-5-ene
NMO	*N*-methylmorpholine *N*-oxide
NMR	nuclear magnetic resonance
Nu	nucleophile
o	ortho
p	para
Pd/C	palladium on carbon
PG	protecting group
Ph	phenyl
pH	hydrogen ion concentration in aqueous solution
PIDA	(bis(acetoxyl)iodo)benzene
ppm	parts per million
PPTS	pyridinium *p*-toluenesulfonic acid
Pr	propyl
PTSA	*para*-toluenesulfonic acid
Py	pyridine
q	quartet
R	any atom or functional group
Ref.	reference
s	singlet
sat. or satd.	saturated
SFC	supercritical fluid Chromatography
Su	succinimide
t	triplet
t-Bu	*tert* (*tertiary*) butyl
TBAF	tetrabutylammonium fluoride
TBDPS	*tert*-butyldiphenylsilyl
TBS	*tert*-butyldimethylsilyl
Teoc	(trimethylsilyl)ethoxy carbonyl
TES	triethylsilyl
Tf	trifluoromethanesulfonyl (triflyl)
TFE	2,2,2-trifluoroethanol
THF	tetrahydrofuran
TLC	thin-layer chromatography
TMG	1,1,3,3-tetramethyl guanidine

TMS	trimethylsilyl	UV	ultraviolet
TOF	time-of-flight	v/v	volume to volume
TPAP	tetrapropylammonium perruthenate	w/v	weight to volume
		w/w	weight to weight
t_R	retention time		
		X	anionic ligand; electronegative element
Ts	*p*-toluenesulfonyl (tosyl)		

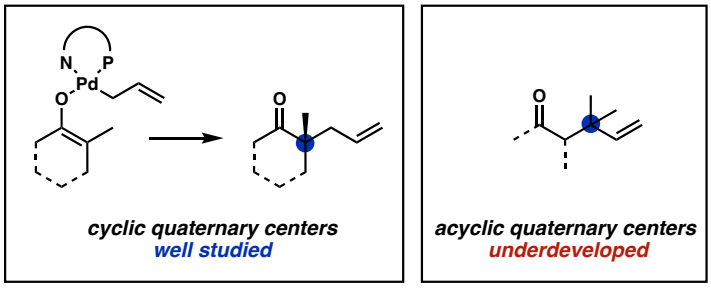
CHAPTER 1

Iridium-Catalyzed Asymmetric Allylic Alkylation of Dialkyl Malonates[†]

1.1 INTRODUCTION

The construction of all-carbon quaternary stereocenters is an important problem in synthetic organic chemistry and one that is central to the focus of research in our laboratory. In the last ten to twenty years, our group has focused on developing new technologies for the synthesis of all-carbon quaternary stereocenters.[1] Many of these approaches utilize cyclic prochiral enolates and palladium catalysis (Scheme 1.1.1). However, despite many of these advances, the construction of *acyclic* all-carbon quaternary stereocenters still remains a significant challenge (Scheme 1.1.1).[2] In recent years, powerful technologies for the construction of such stereogenic centers via iridium- and palladium-catalyzed allylic alkylation reactions have emerged to meet this challenge.[3,4] Ongoing efforts in this area of chemical research have inspired us to study the underdeveloped area of iridium-catalyzed allylic alkylation as a means to synthesize acyclic all-carbon quaternary stereogenic centers.

Scheme 1.1.1. *Construction of all-carbon quaternary centers via allylic alkylation.*

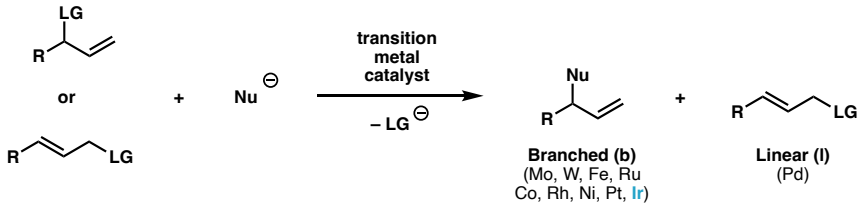


1.2 IRIDIUM-CATALYZED ALLYLIC ALKYLATION

[†]This research was performed in collaboration with Farbod A. Moghadam, Zachary P. Sercel, and Alexander Q. Cusumano. Portions of this chapter have been reproduced with permission from Moghadam, F. A.; Hicks, E. F.; Sercel, Z. P.; Cusumano, A. Q.; Bartberger, M. D.; Stoltz, B. M. *J. Am. Chem. Soc.* **2022**, *144*, 7983–7987. © 2022 American Chemical Society.

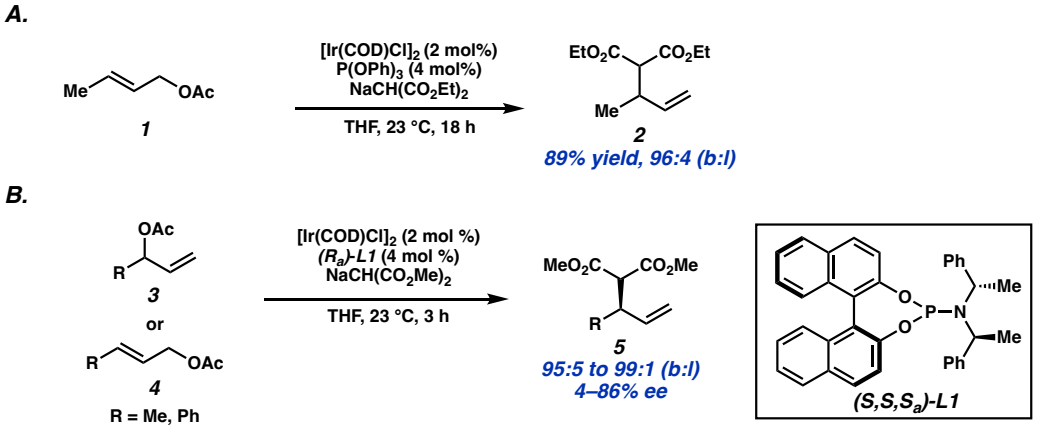
Our interest in iridium-catalyzed allylic alkylation stems from the highly regioselective nature of these transformations that favors the formation of more substituted (branched) products. Moreover, it has been well established that iridium-catalyzed allylic alkylation reactions exhibit drastically different regioselectivities than their palladium counterparts that generally favor formation of the less-substituted, linear products (Scheme 1.2.1).[5]

Scheme 1.2.1. *Regioselectivity trends in transition metal-catalyzed allylic alkylation.*



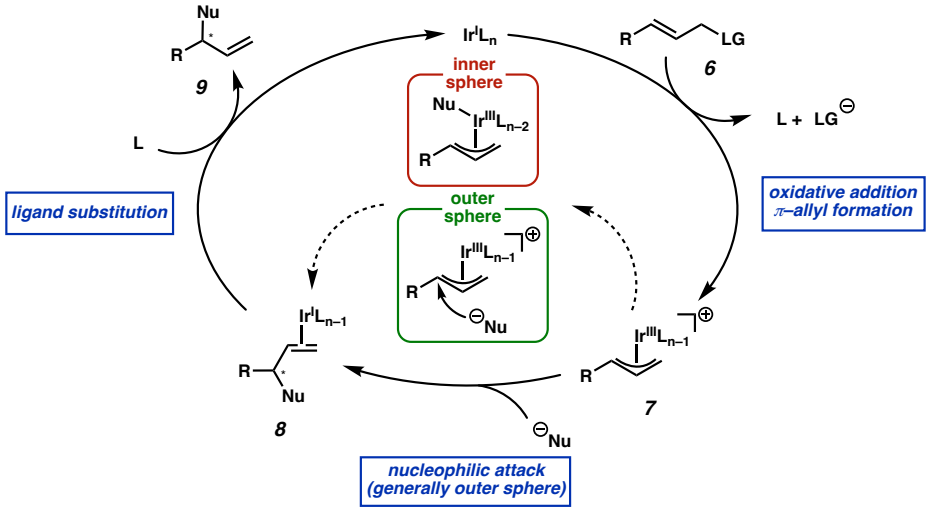
The first report of an iridium catalyzed allylic alkylation was disclosed by Takeuchi in 1997 (Scheme 1.2.2, A), demonstrating that when the sodium salt of diethyl malonate reacted with allylic acetate **1** in the presence of $[Ir(COD)Cl]_2$ and triphenylphosphite, the corresponding branched allylic alkylation product was observed.[6] Soon after, Helmchen reported the first enantioselective variants of this chemistry utilizing phosphinooxazoline and later phosphoramidite ligands (Scheme 1.2.2, B).[7,8]

Scheme 1.2.2. *A. Initial report by Takeuchi. B. Enantioselective reports by Helmchen.*



Iridium catalyzed allylic alkylation reactions generally proceed through a mechanism involving oxidative addition, nucleophilic attack, and ligand substitution.[3] As outlined in Scheme 1.2.3 an iridium (I) catalyst undergoes oxidative addition into an allylic electrophile and forms an iridium (III) allyl species. X-ray crystallographic structures of the π-allyl intermediates suggest that the allyl group is bound as shown in the η^3 mode.[9–11] Nucleophilic attack on the allyliridium (III) species (**7**) results in the formation of **8**. The nature of the nucleophilic attack is generally believed to be an "outer sphere" process in which the nucleophile is not bound to the metal, which constitutes a mechanism that is distinct from more traditional reductive elimination processes. Finally, ligand substitution completes the cycle and liberates the product.

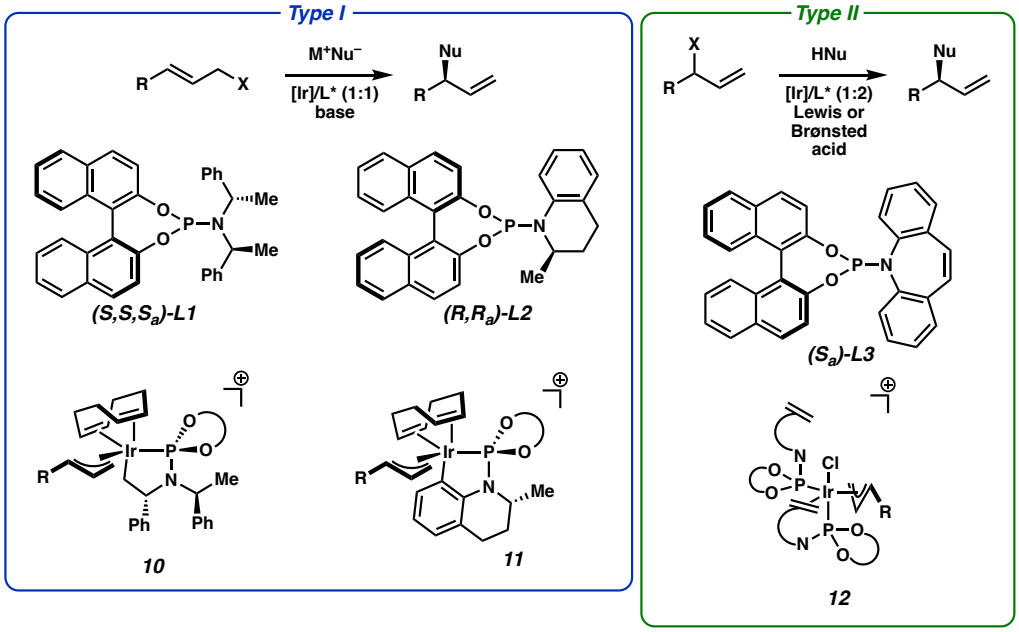
Scheme 1.2.3. *General catalytic cycle of iridium-catalyzed allylic alkylation reactions.*



It should be noted that since these initial reports, phosphoramidite ligands have proven to be privileged in the iridium catalyzed allylic alkylation reaction manifold both in terms of enantioinduction and regioselectivity. Detailed mechanistic studies of transformations using phosphoramidite ligands has partitioned these reactions into two "Types" based on the phosphoramidite ligand structure and iridium/ligand stoichiometry (Scheme 1.2.4).[12] Type I transformations use ligands of the type **L1** or **L2**, are performed under basic conditions, and use a ligand/iridium stoichiometry of 1:1. Mechanistic studies of Type I reactions revealed that under the basic reactions conditions a catalytically competent iridacycle is formed (**10**, **11**), suggesting that these iridacycles are the active catalytic species in Type I transformations. Type II transformations use ligand **L3** with a ligand/iridium stoichiometry of 2:1. The active species in these transformations is complex **12**. Typically, these transformations are performed under acidic conditions, and are less water sensitive than their Type I counterparts. It should also be noted that Krische allylation reactions, Ir-catalyzed allylations of carbonyl compounds[13,14] via σ-allyliridium intermediates are

mechanistically distinct from the allylic substitution processes discussed herein, and are therefore not included in the classification of "Types" of allylic alkylation reactions.

Scheme 1.2.4. *"Types" of Ir-catalyzed allylic alkylation reactions.*



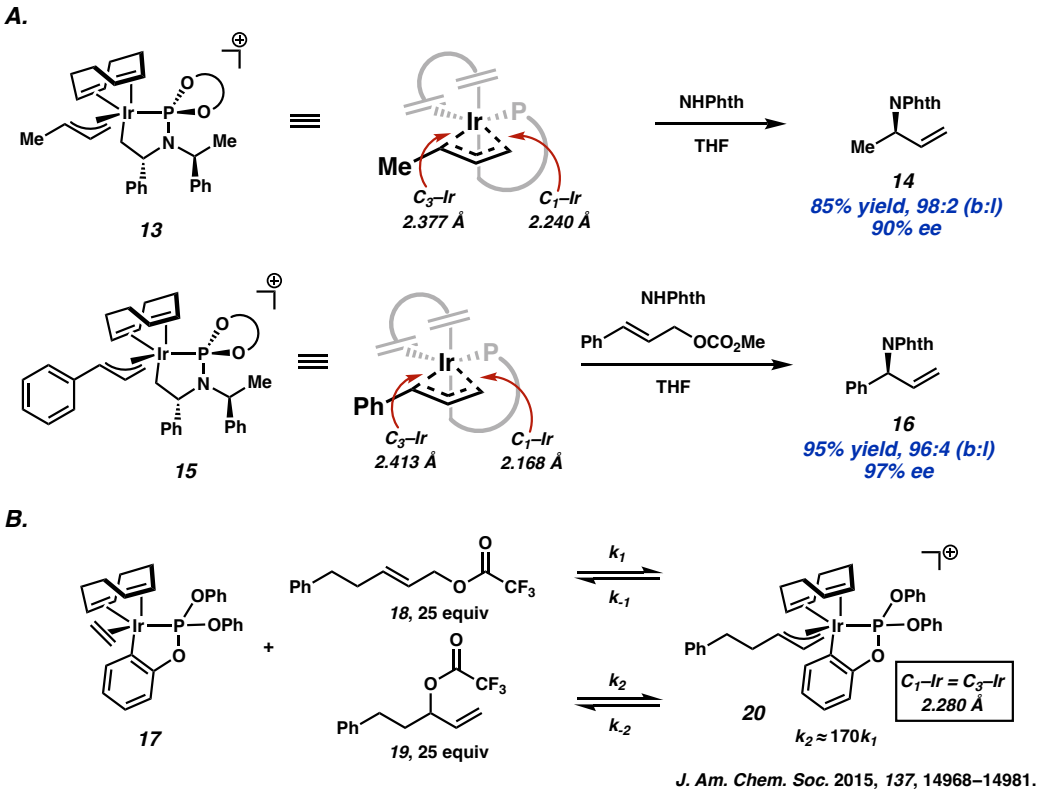
1.3 REGIOSELECTIVITY OF IRIDIUM-CATALYZED ALLYLIC ALKYLATION

The origin of the exquisite regioselectivities obtained in these transformations has been the subject of considerable investigation. Although to date a general explanation for the observed regioselectivities has not been uncovered, several studies have provided insight into the potential factors governing this exclusive regioselectivity. For example, Hartwig and coworkers have demonstrated that the site of reactivity of crotyl-iridium(III) complex **13** can be directly correlated with differences in the Ir–C bond lengths of the two allyl termini (Scheme 1.3.1, A).[15] The crystal structure of the complex reveals that the Ir–C1 bond length is 2.240 Å, while the Ir–C3 bond length is 2.377 Å. Hartwig and coworkers subsequently showed that these complexes are catalytically competent, and that nucleophiles preferentially attack the allyliridium species at C3, leading to the formation of branched products.

Helmchen and coworkers later systematically studied amination reactions of a variety of related allyliridium complexes (**15**, Scheme 1.3.1, A). Although they do not comment extensively on the origin of regioselectivity for these reactions, they note that in cases where R^1 = H and R^2 = CH_3 or Ph, the bond C–Ir bond length at the more substituted terminus (C3) is longer, and, therefore, it is possible that nucleophiles add preferentially to the site bearing the longer, weaker C–Ir bond.[16]

Contrary to this trend, Hartwig and coworkers studied the reaction originally reported by Takeuchi and coworkers both experimentally and computationally (Scheme 1.3.1, B).[17] Synthesis of the catalytically competent allyliridium complexes revealed that the C–Ir bond lengths at the two termini were both 2.28 Å, suggesting that bond length alone is not a sufficient explanation for the observed regioselectivity. In an attempt to further understand the regioselectivity of the transformation, they then performed a kinetic experiment. By measuring the rates of oxidative addition of the Ir(cod)($P(OPh)_3$) complexes into both branched and linear allylic trifluoroacetates **18** and **19**, they determined that the rate of oxidative addition into the branched isomer was ~170 times faster than oxidative addition into the linear isomer (k_2 = 170 k_1). Invoking the principle of microscopic reversibility, they reasoned that nucleophilic attack to form the branched isomer should be kinetically more facile, which is in agreement with the experimentally observed outcomes, although it does not explain the fundamental origin of this regioselectivity. Taken together, the studies by Helmchen and Hartwig indicate that a general explanation for the observed regioselectivity in iridium-catalyzed asymmetric allylic alkylation reactions has not yet been developed.

Scheme 1.3.1. *A. Correlations between C–Ir bond length and regioselectivity. B. Kinetic experiments by Hartwig.*



J. Am. Chem. Soc. 2015, *137*, 14968–14981.

1.4 SYNTHESIS OF ALL-CARBON QUATERNARY CENTERS VIA IRIDIUM-CATALYZED ALKYLATION

Although a general explanation for the exquisite branched selectivity of iridium catalyzed asymmetric allylic alkylation reactions remains ambiguous, since the initial discovery of this transformation many groups have reported numerous iridium-catalyzed allylic alkylation processes utilizing a variety of both carbon and heteroatom (N, O, S) nucleophiles.[3] Despite these advances, the construction of all-carbon quaternary centers remains an underexplored chemical space in the context of iridium-catalyzed allylic alkylation, and few such transformations have been reported. Given the natural propensity for iridium-catalyzed allylic alkylation reactions to form sterically congested, branched

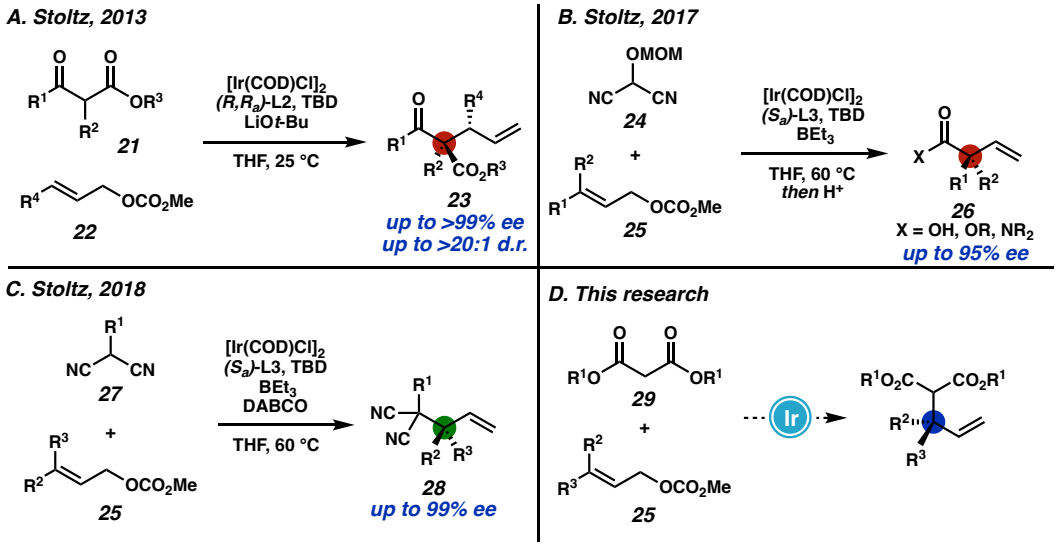
products, in the past decade our group has endeavored to study these catalytic systems and utilize them for the synthesis of molecules containing all-carbon quaternary centers.

This type of transformation was first disclosed by our group in 2013, in which substituted β-ketoester nucleophiles were reacted with allylic carbonate electrophiles in the presence of an iridium catalyst derived from TBD (1,5,7-triazabicyclo[4.4.0]dec-5-ene), **L2**, and $[Ir(cod)Cl]_2$ (Scheme 1.4.1, A).[18] Both the diastereo- and enantioselectivity of the reaction was high for almost all substrates. The all-carbon quaternary center in these examples is formed as result of using a trisubstituted nucleophile. Alternatively, our group was then interested in the possibility of forming all-carbon quaternary centers derived from prochiral trisubstituted electrophiles. To that end, in 2017 we disclosed that trisubstituted electrophiles (**25**) were competent in iridium catalyzed allylic alkylation reactions (Scheme 1.4.1, B).[19] Due to the more difficult oxidative addition of the iridium catalyst into the trisubstituted electrophile, an additional Lewis acid was necessary to activate the carbonate leaving group and facilitate this process. The masked acyl cyanide nucleophiles allowed for conversion to the corresponding carboxylic acids and an overall synthesis of α-quaternary carbonyl compounds.

Building upon this report, in 2018 our group disclosed a further extension of this chemistry using both trisubstituted electrophiles and trisubstituted nucleophiles for the synthesis of vicinal quaternary products in which one all-carbon quaternary center is derived from the nucleophile while the other is derived from the electrophile (Scheme 1.4.1, C).[20] It should also be noted that more recently Carreira and coworkers disclosed an additional methodology for the synthesis of vicinal quaternary products via iridium catalysis, in their case using silyl ketene acetal nucleophiles and branched allylic alcohol electrophiles.[21]

Together, the ability to synthesize vicinal quaternary centers using iridium catalysis serves to highlight the power of this catalytic system to construct highly sterically congested motifs with excellent regio- and stereoselectivity.

Scheme 1.4.1. *Construction of all-carbon quaternary centers via Ir-catalyzed allylic alkylation reported by the Stoltz group. A. Use of substituted B-ketoester nucleophiles. B. Use of MAC nucleophiles. C. Use of substituted malononitriles. D. Proposed use of malonate nucleophiles.*

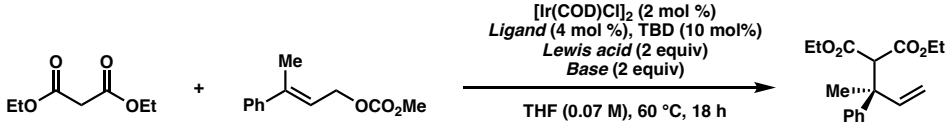


Inspired by these efforts, we aimed to further expand this technology and make use of other classes of nucleophiles. We noted that while malonate nucleophiles have been frequently employed in iridium-catalyzed allylic alkylation reactions, prior to this study they had not been used in reactions involving the formation of an all-carbon quaternary centers (Scheme 1.4.1, D).[22] Additionally, this transformation would allow access to β-quaternary carboxylic acids that are complementary stereochemical motifs to the α-quaternary acids previously accessed by our group through this technology.

1.5 REACTION OPTIMIZATION

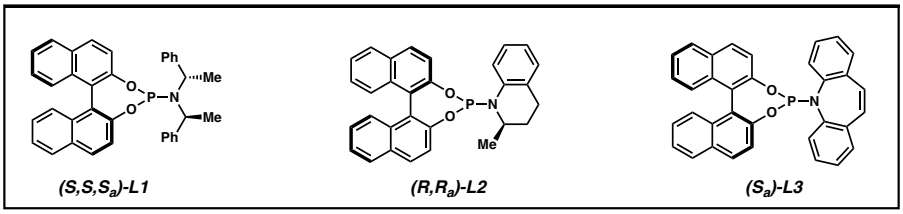
As a starting point for our investigation, we imagined leveraging similar conditions to those previously exploited by our group (Table 1.5.1). Given that this transformation would use a trisubstituted allylic carbonate electrophile, we hypothesized that the Lewis acid would have a considerable effect on the reaction outcome. Employing the same catalyst system as had previously been disclosed by our group, $[Ir(cod)Cl]_2$, TBD, **L3**, with LiOt-Bu as the base, and BEt_3 as the Lewis acid, we were encouraged to observe the formation a small amount of desired product (**32a**). The use of other phosphoramidite ligands (**L1**, **L2**) did not lead to the formation of any amount of the desired quaternary product.

Table 1.5.1. *Initial evaluation of phosphoramidite ligands.*



30 *31a* *32a*

Entry	Ligand	Base	Lewis Acid	NMR Yield
1a	*(S_a)-L3*	LiO*t*-Bu	BEt_3	23%
1b	*(R,R_a)-L2*	LiO*t*-Bu	BEt_3	0%
1c	*(S,S,S_a)-L1*	LiO*t*-Bu	BEt_3	0%



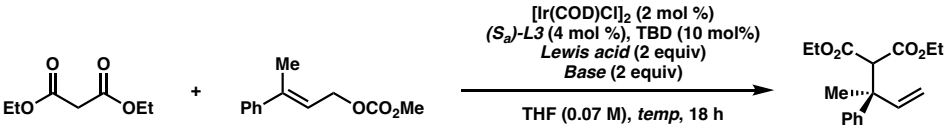
(S,S,S_a)-L1 *(R,R_a)-L2* *(S_a)-L3*

***all reactions performed on 0.05 mmol scale. [Ir], ligand, TBD, pre-stirred prior to addition of other reagents 1:1 stoichiometry of 30 and 31. TBD = 1,5,7-triazabicyclo[4.4.0]dec-5-ene**

With the optimal ligand in hand, our focus turned to evaluating other reaction parameters. Other Lewis acids, such as $Yb(OTf)_3$, CPh_3BF_4, $ZrCl_4$, $Sc(OTf)_3$, $La(OiPr)_3$, did not lead to any improvement in yield (Table 1.5.2, entries 2–6). ZnI_2, however, proved to be a more effective promoter of the reaction than any other Lewis acid, and its employment improved the yield of the reaction to 50%. Notably this was accompanied by complete consumption of allylic carbonate. The marked increase in yield prompted us to turn our

attention to other reaction parameters. To that end, evaluation of other bases revealed that hexamethydisilazide bases were superior to the previously employed LiO*t*-Bu (Table 2, entries 8–10). Use of LiHMDS caused a dramatic increase in yield to 71% isolated yield and 75% ee. While KHMDS was considerably less effective likely due to insolubility of the potassium diethyl malonate nucleophile, the reaction utilizing NaHMDS proved more successful and delivered the product in 86% yield and 89% ee. Further improvement of the enantioselectivity was possible by lowering the temperature of the reaction to an ambient 21 °C; in this case the product was isolated in 83% yield and 97% ee. Any further deviations from these conditions proved to be detrimental. For example, other ethereal solvents led to dramatic decreases in yield due to issues with solubility, and leaving groups other than carbonate were equally ineffective.

Table 1.5.2. *Reaction optimization.*



30 *31a* *32a*

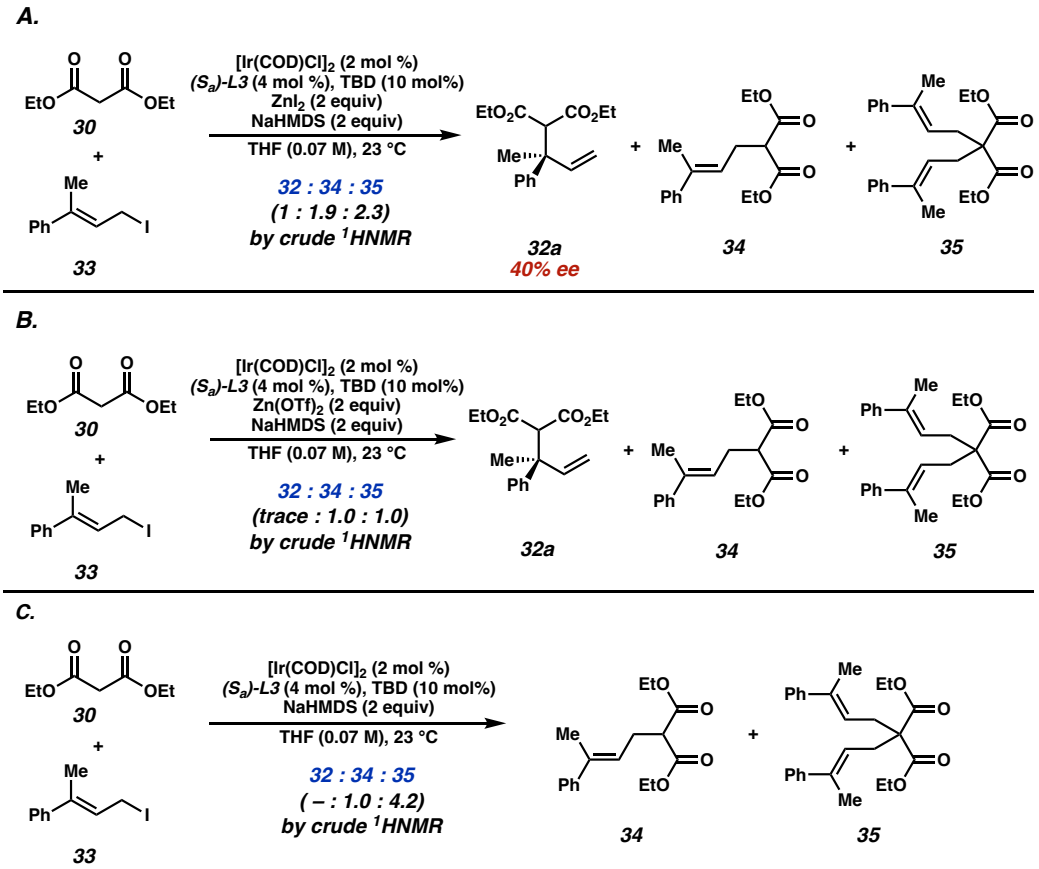
Entry	Base	Lewis Acid	temp (°C)	% NMR yield (isolated)	% ee
1	LiO*t*-Bu	BEt_3	60	23	n.d.
2	LiO*t*-Bu	$Yb(OTf)_3$	60	14	n.d.
3	LiO*t*-Bu	CPh_3BF_4	60	0	n.d.
4	LiO*t*-Bu	$ZrCl_4$	60	trace	n.d.
5	LiO*t*-Bu	$Sc(OTf)_3$	60	0	n.d.
6	LiO*t*-Bu	$La(O\textit{i}\text{-}Pr)_3$	60	0	n.d.
7	LiO*t*-Bu	ZnI_2	60	50	n.d.
8	LiHMDs	ZnI_2	60	92 (71)	75
9	NaHMDS	ZnI_2	60	95 (71)	83
9	KHMDS	ZnI_2	60	28	83
10	NaHMDS	ZnI_2	40	87 (75)	90
11**	NaHMDS	ZnI_2	23	90 (83)	97
12	NaHMDS	$Zn(OTf)_2$	23	0	–
13	NaHMDS	$ZnBr_2$	23	13	n.d.
14	NaHMDS	$Zn(OAc)_2$	23	86	79

*all reactions performed on 0.05 mmol scale. [Ir], ligand, TBD, pre-stirred prior to addition of other reagents
**THF (0.17 M)

1.6 ROLE OF ZINC IODIDE

In an attempt to understand the unique efficacy of ZnI_2, a series of control experiments were performed. Evaluation of other Zn (II) salts led, in almost all cases, to poor yields (<20%), with the exception of the reaction using $Zn(OAc)_2$ (Table 1.5.2, entries 12–14), in which case the product was isolated in 86% yield but only 79% ee. Attempts to generate ZnI_2 in situ were equally unsuccessful. It seemed possible that ZnI_2 played a key role in assisting with the in situ formation of a linear allylic iodide. To test this, the extremely unstable allylic iodide **33** was synthesized[23] via an Appel reaction and immediately subjected to different reaction conditions (Scheme 1.6.1).

Scheme 1.6.1. *Control experiments and mechanistic probes.*

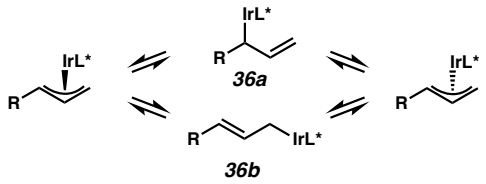


Subjecting this electrophile to otherwise identical reaction conditions led to the formation of **32a** but in extremely low enantiomeric excess (40%). Additionally, other background allylations occurred to give **34** and **35**, products not observed under the normal reaction conditions. Changing the zinc source to zinc triflate in an attempt to decouple the effects of the cation and anion, only background allylation reactions occurred with no formation of branched product (Scheme 1.6.1, B). These results are comparable to the result obtained in the absence of zinc (Scheme 1.6.1, C). Together, these results indicate that the role of ZnI_2 is not as a promoter of allylic iodide formation. If this were the operative mechanism it would be expected that the use of the allylic iodide and any Zn(II) salt would similar results. On the basis of these experiments, we ruled out the possibility of the allylic iodide being an important intermediate in this process and concluded that the role of ZnI_2 may be more complex than initially hypothesized.

1.7 TEMPERATURE DEPENDENCE AND MECHANISTIC IMPLICATIONS

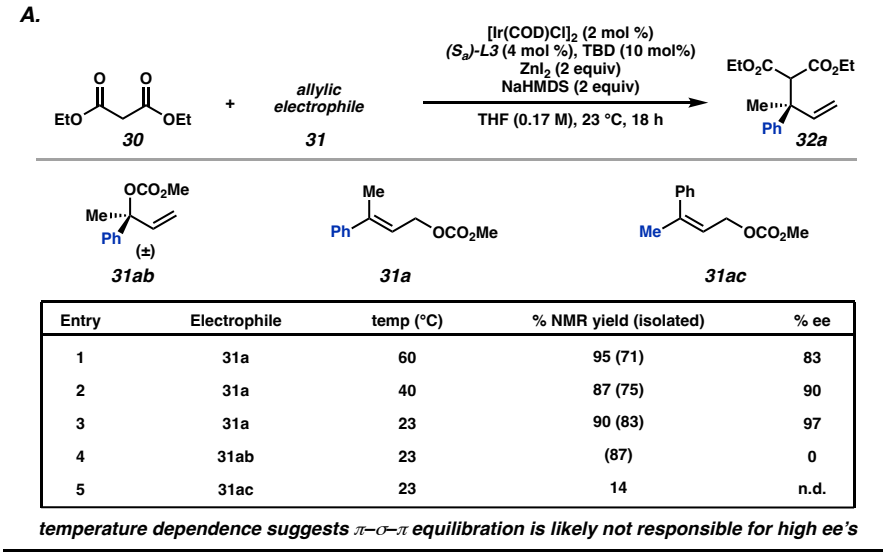
Another unique feature of this transformation is the relationship between enantioselectivity and temperature. For many allylic alkylation processes, particularly those catalyzed by iridium, increased temperatures often lead to improved enantioselectivity.[24,25] The origin of this effect is a function of the reaction mechanism, specifically, that nucleophilic attack on the π-allyl species is, usually enantiodetermining. Studies have demonstrated that after undergoing oxidative addition, the iridium π-allyl complex is able to equilibrate between the possible diastereomers via the σ-bound allyl complexes **36a** and **36b** to ultimately arrive at the more thermodynamically stable diastereomer of the iridium π-allyl complex (Scheme 1.7.1). Because this is thermodynamically driven, increased reaction temperature accelerates the process and leads to improved enantioselectivity.

Scheme 1.7.1. *π -σ-π equilibration.*



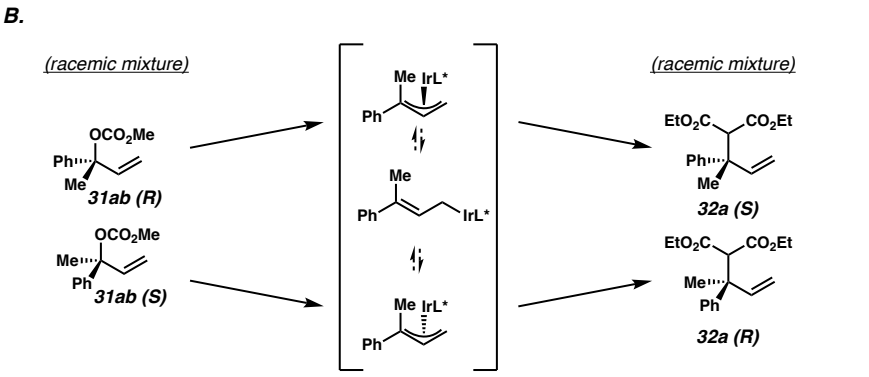
In the transformation developed in this study, the enantioselectivity improves with decreased temperature (results shown again in Scheme 1.7.2, A), opposite the trend commonly observed for these reactions. To probe this further, other isomers of the starting allylic carbonate were subjected to this transformation. The *Z*-isomer of the starting material (**31ac**) performed very poorly, possibly due to a slower oxidative addition process. The branched isomer (**31ab**) provided the desired branched product in very high yield, however as a racemate. This indicates that in the case of the branched electrophile, there appears to be no equilibration of the possible π-allyl complexes (Scheme 1.7.2, B). If any equilibration between different complexes were occurring, one would expect to at least observe a small amount of product enantioenrichment. Taken together these results suggest that oxidative addition may be enantiodetermining.

Scheme 1.7.2. *A. Temperature dependence and results with isomeric allylic carbonate electrophiles. B. Lack of equilibration leads to lack of enantioenrichment.*



Entry	Electrophile	temp (°C)	% NMR yield (isolated)	% ee
1	31a	60	95 (71)	83
2	31a	40	87 (75)	90
3	31a	23	90 (83)	97
4	31ab	23	(87)	0
5	31ac	23	14	n.d.

temperature dependence suggests π–σ–π equilibration is likely not responsible for high ee's



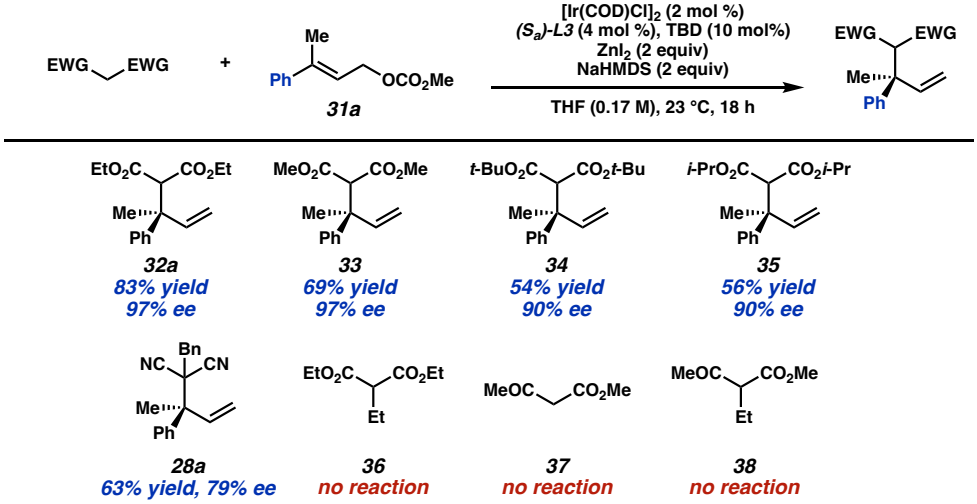
lack of enantioenrichment suggests equilibration does not occur

1.8 SCOPE OF THE ASYMMETRIC ALLYLIC ALKYLATION

Having both evaluated the reaction parameters and probed several nuances of this transformation, we then turned our attention to investigating the use of other substrates in this reaction. Other malonate nucleophiles such as dimethyl malonate performed well, in this case affording the product in slightly diminished yield (Scheme 1.8.1, **33**). Di-*iso*-propyl and di-*tert*-butyl malonate were also competent, although both suffered from diminished product yield and enantiomeric excess (**33**, **34**). Structurally related nucleophiles tended to suffer from a lack of reactivity. For example, employing substituted malonate nucleophiles (**36**)

yielded none of the vicinal quaternary product. Likewise, ketoesters (**37**) and substituted ketoesters (**38**) did not undergo the desired transformation in isolable amounts. Interestingly, substituted malononitriles could be employed under these conditions, although the enantioenrichment of **28a** was a greatly diminished 79% in comparison to our group's prior report (Scheme 1.4.1, C). As such, the optimal conditions were uniquely effective for malonate nucleophiles. With this in mind, other allylic carbonate electrophiles were then evaluated.

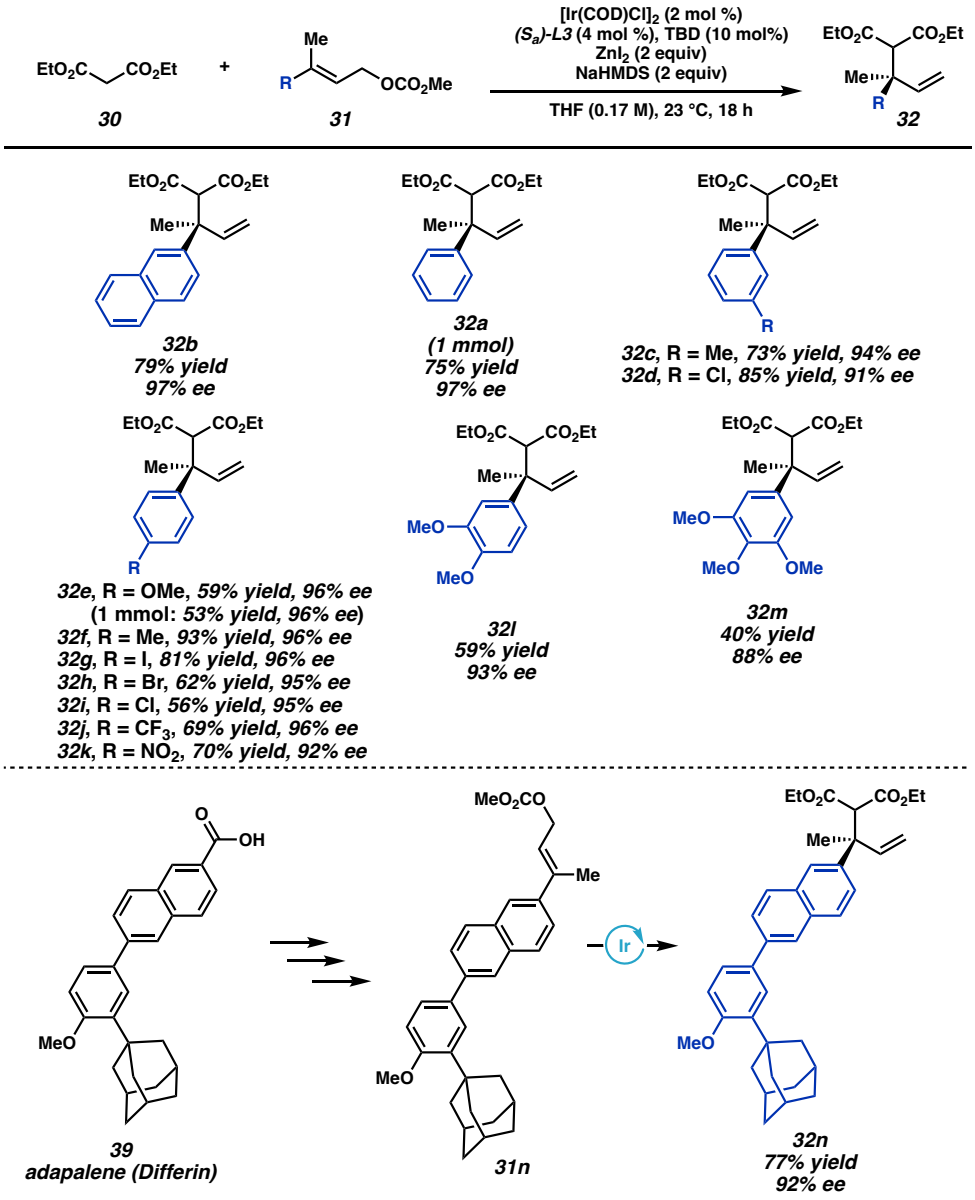
Scheme 1.8.1. *Nucleophile scope.*



A variety of structurally similar aryl electrophiles were well tolerated in this transformation (Scheme 1.8.2). The reaction employing the naphthyl electrophile proceeded smoothly to give the corresponding product **32b** in 79% yield and 97% ee. The reaction could also be scaled to 1 mmol without significant deviation in yield or enantioselectivity (**32a**). Reactions of *meta*- and *para*-substituted electrophiles (**31c–k)** proceeded smoothly to deliver the corresponding quaternary products (**32c–k**). Of these, the reaction of the 4-methyl aryl electrophile afforded the desired product **32f** in 93% yield, the highest observed for any substrate with an equally high enantiomeric excess of 96%. Also of note was that aryl

bromides and iodides were well tolerated (**32g**, **32h**). Increased electron richness of the aryl groups trended to diminish product yield, though enantioselectivity remained relatively high, as illustrated by the 4-methoxy (**32e**), 3,4-dimethoxy (**32l**), and 3,4,5-trimethoxy (**32m**) series of products. We were also interested in more structurally complex aryl electrophiles. To this end, the drug molecule adapalene (**39**),[26] a topical retinoid and active ingredient in a leading acne treatment, was converted to the corresponding trisubstituted methyl carbonate electrophile (**31n**). Subjection of electrophile **31n** to the standard iridium conditions afforded the corresponding product **32n** in 77% yield and 96% ee (Scheme 1.8.2).

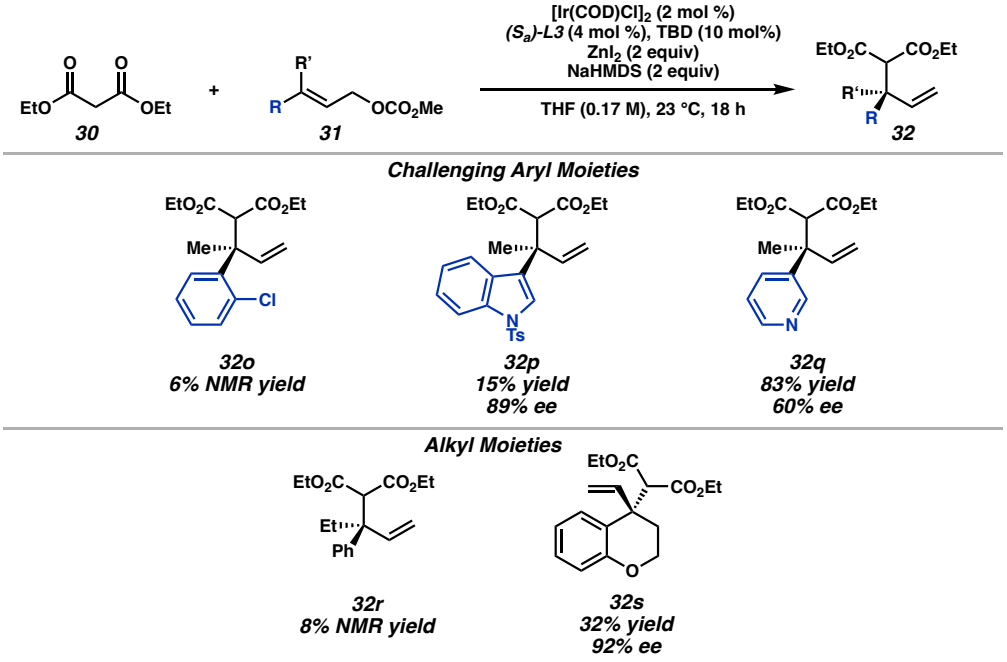
Scheme 1.8.2. *Electrophile scope and use of a drug-like molecule.*



Some limitations were encountered when using aryl electrophiles (Scheme 1.8.3). The reaction of the pyridyl substrate was poorly enantioselective, giving **32q** in 83% yield and 60% ee. Substitution at the *ortho*-position was not tolerated and is clearly illustrated by the 6% NMR yield obtained of **32o**. The issue of 2-substituted aryl moieties may also contribute to the low 15% yield of the indole product (**32p**), although gratifyingly the product was afforded in highly enantioenriched form. Substitution of R' with an ethyl group instead

of methyl almost entirely eliminated reactivity (**32r**). Intriguingly, the cyclic product **32s**, which contains substitution other than methyl at R' and 2-substitution, was formed with moderate success. This result is intriguing in that the cyclic electrophile (**31s**) is conformationally restricted and presumably reacts more readily than the electrophiles in either of the two isolated cases.

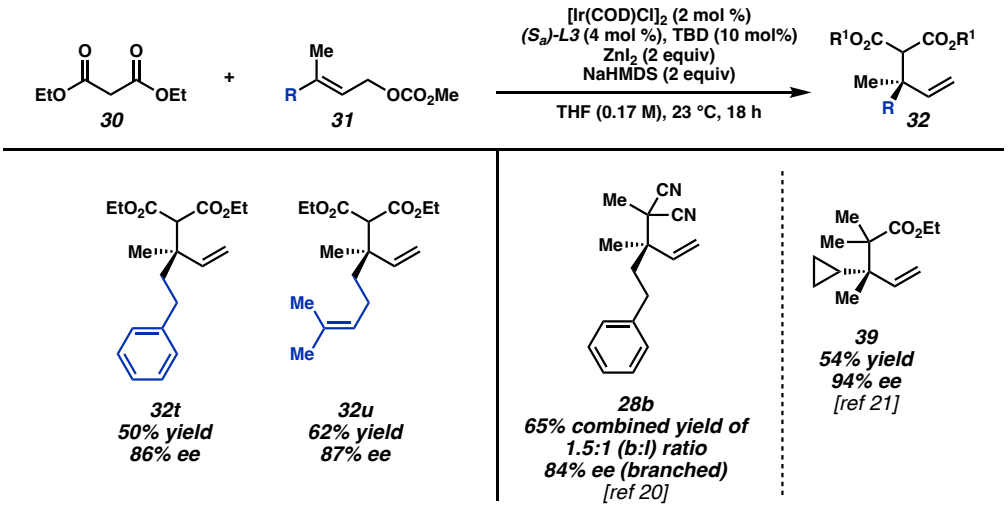
Scheme 1.8.3. *Limitations of the allylic alkylation reaction.*



One of the more significant discoveries made during the substrate scope evaluation was that alkyl electrophiles could also be utilized to afford enantioenriched products. Conversion of the geranyl electrophile to the corresponding branched malonate product proceeded smoothly, furnishing the desired product **32u** in 87% ee (Scheme 1.8.4). Product **32u** was disclosed in the original Takeuchi report from 1997[6] as a racemic mixture. The reaction employing the phenethyl substrate also proceeded smoothly, generating **32t** in 86% ee. This development is significant due to the stereochemical challenges associated with this

electrophile class, as the catalyst must differentiate between a methyl group and alkyl chain to afford an enantioenriched product.

Scheme 1.8.4. *Success of alkyl-alkyl electrophiles.*

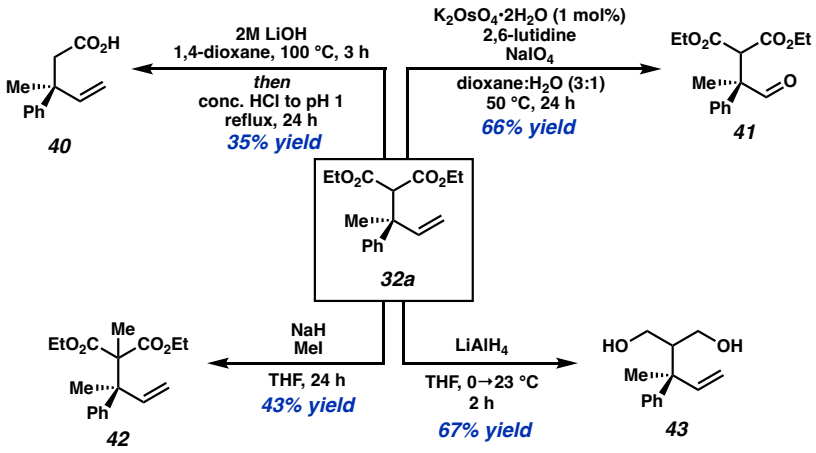


The challenges associated with the alkyl-alkyl electrophile class have largely precluded their use in the synthesis of acyclic all-carbon quaternary centers with synthetically useful levels of enantioenrichment. Our group previously reported the use of the same phenethyl electrophile giving rise to **28b** as a 1.5:1 mixture of branched and linear constitutional isomers, although the enantioselectivity associated with forming the branched product was reasonably high (84%).[20] To the best of our knowledge, the only other example of the use of an electrophile in this class was reported by Carreira and coworkers, in which they employ a cyclopropyl allenylic electrophile to afford the corresponding product (**39**) in high enantiomeric excess.[21] In short, these electrophiles are challenging with respect to the stereochemical outcome of the reaction, and the compatibility of this class with the developed transformation presents a significant advance with respect to prior technologies.

1.9 SYNTHETIC UTILITY OF THE ALLYLIC ALKYLATION PRODUCTS

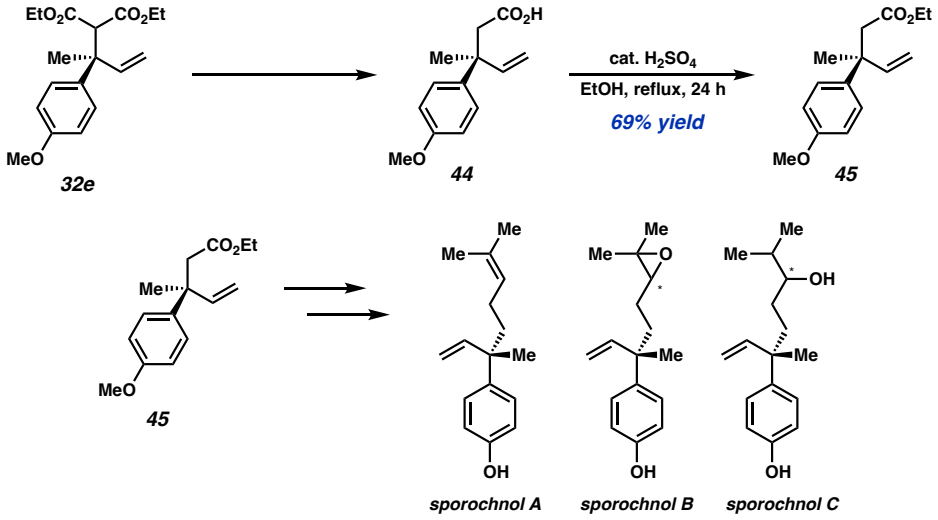
Finally, we were able to diversify the alkylation products in a number of ways to highlight their synthetic utility (Scheme 1.9.1). Hydrolysis and decarboxylation formed acid **40** in 35% yield. Lemieux-Johnson oxidation of the alkene provided aldehyde **41** in 66% yield. Methylation yielded the vicinal quaternary product **42** in 43% yield. Exhaustive reduction of the ester moieties gave the corresponding 1,3-diol (**43**) in 67% yield**.**

Scheme 1.9.1. *Product diversification.*



Decarboxylation of the 4-methoxy malonate product **32e** delivered corresponding β-quaternary acid **43** (Scheme 1.9.2). This acid could then be subjected to Fischer esterification with ethanol to form the corresponding ethyl ester **44**. Ethyl ester **44** is a known intermediate in the synthesis of sporochnols A–C, natural products isolated from the marine algae *Sporochnus bolleanus* that act as chemical defense agents.[27] Intermediate **44** was previously accessed as a racemate in the total synthesis of these molecules.[28] By intercepting the ethyl ester intermediate in enantioenriched form we achieved a formal enantioselective total synthesis of this class of natural products.

Scheme 1.9.2: *Formal total synthesis of sporochnols A–C.*



1.10 CONCLUSION

In conclusion, we have developed an asymmetric iridium catalyzed allylic alkylation of malonate nucleophiles to deliver products bearing all-carbon quaternary centers. The transformation has demonstrated reasonable generality with respect to most allylic carbonate electrophiles. Several malonate derivatives are also compatible as nucleophiles. A key finding in this study was that alkyl electrophiles perform well in this reaction and deliver the corresponding products with reasonable levels of enantioselectivity. We have also demonstrated several ways in which the allylic alkylation products can be transformed, including one example in which one product could be elaborated to intercept an intermediate from a previously racemic total synthesis. Future studies will investigate the use of additional classes of nucleophiles, particularly those bearing additional substitution in hope of generating increasingly dense functionality and stereochemical complexity.

1.11 EXPERIMENTAL SECTION

1.11.1 MATERIALS AND METHODS

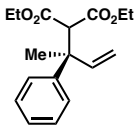
Unless otherwise stated, reactions were performed in flame-dried glassware under an argon or nitrogen atmosphere using dry, deoxygenated solvents. Solvents were dried by passage through an activated alumina column under argon.[29] Reaction progress was monitored by thin-layer chromatography (TLC) or Agilent 1290 UHPLC-MS. TLC was performed using E. Merck silica gel 60 F254 precoated glass plates (0.25 mm) and visualized by UV fluorescence quenching, *p*-anisaldehyde, or $KMnO_4$ staining. Silicycle Silia*Flash*® P60 Academic Silica gel (particle size 40–63 μm) was used for flash chromatography. ^1H NMR spectra were recorded on Varian Inova 500 MHz and Bruker 400 MHz spectrometers and are reported relative to residual $CHCl_3$ (δ 7.26 ppm). ^{13}C NMR spectra were recorded on a Varian Inova 500 MHz spectrometer (125 MHz) and Bruker 400 MHz spectrometers (100 MHz) and are reported relative to $CDCl_3$ (δ 77.16 ppm). Data for ^1H NMR are reported as follows: chemical shift (δ ppm) (multiplicity, coupling constant (Hz), integration). Multiplicities are reported as follows: s = singlet, d = doublet, t = triplet, q = quartet, p = pentet, sept = septuplet, m = multiplet, br s = broad singlet, br d = broad doublet. Data for ^{13}C NMR are reported in terms of chemical shifts (δ ppm). IR spectra were obtained by use of a Perkin Elmer Spectrum BXII spectrometer using thin films deposited on NaCl plates and reported in frequency of absorption (cm^{-1}). Optical rotations were measured with a Jasco P-2000 polarimeter operating on the sodium D-line (589 nm), using a 100 mm path-length cell. Analytical SFC was performed with a Mettler SFC supercritical CO_2 analytical chromatography system utilizing Chiralpak (AD-H, AS-H or IC) or Chiralcel (OD-H, OJ-H, or OB-H) columns (4.6 mm x 25 cm) obtained from Daicel Chemical Industries, Ltd. Analytical chiral HPLC was performed with an Agilent 1100 Series HPLC utilizing Chiralpak (IH) or Chiralcel (OD-H) columns (4.6 mm x 25 cm) both obtained from Daicel

Chemical Industries, Ltd. High resolution mass spectra (HRMS) were obtained from the Caltech Mass Spectral Facility using a JEOL JMS-600H High Resolution Mass Spectrometer in field ionization (FI+) or field desorption (FD+) mode, or an Agilent 6230 Series TOF with an Agilent Jet Stream ion source in electrospray ionization (ESI+) mode. Reagents were purchased from commercial sources and used as received unless otherwise stated.

1.11.2 EXPERIMENTAL PROCEDURES

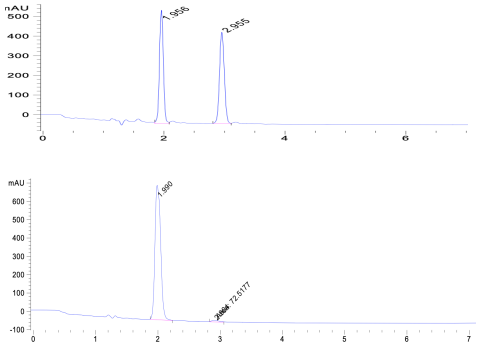
1.11.2.1 General Procedure 1 for Iridium-Catalyzed Allylic Alkylation Reactions

In a nitrogen-filled glovebox, a catalyst solution $[Ir(COD)Cl]_2$ (6.5 mg/mL), ***(S_a)-L3*** (10 mg/mL), and TBD (7 mg/mL) in THF was stirred for 20 min at 25 °C. In separate vials, solutions of *(E)*-allylic carbonate (0.5 mmol/mL) and of malonate nucleophile (0.5 mmol/mL) were prepared in THF. During that time, the reaction vial was charged with ZnI_2 (63.8 mg, 0.2 mmol, 2.0 equiv) and NaHMDS (36.7 mg, 0.2 mmol, 2.0 equiv). 0.2 mL of the nucleophile solution (0.1 mmol, 1.0 equiv) was added to the reaction vial and stirred for 5 min, followed by 0.2 mL of catalyst solution, and finally 0.2 mL of allylic carbonate solution (0.1 mmol, 1.0 equiv). The vial was sealed with a Teflon-lined cap, removed from the glovebox, and stirred at 21 °C in a metal heating block for 18 h unless noted otherwise. After 18 h, 3 mL 0.5 M HCl was added to the crude reaction mixture, which was then extracted three times with ethyl acetate, dried over $MgSO_4$, concentrated, and purified by silica gel flash chromatography to provide the desired alkylation product.

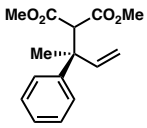


Diethyl (*R*)-2-(2-phenylbut-3-en-2-yl)malonate (32a)

Prepared according to general procedure 1 using carbonate **31a** (20.6 mg, 0.1 mmol) and diethyl malonate (16.0 mg, 0.1 mmol) with by preparative TLC (10% EtOAc in hexanes) to provide a colorless oil (24.1 mg, 83% yield, 97% ee). Prepared on 1.0 mmol scale according to general procedure 1 using carbonate 31a (206.1 mg, 1.0 mmol) and diethyl malonate (160.2 mg, 1.0 mmol) with purification by silica gel chromatography (10% EtOAc in hexanes) to provide a light orange oil (217 mg, 75% yield, 97% ee); ^{1}H NMR (500 MHz, $CDCl_3$) δ 7.35 – 7.26 (m, 4H), 7.21 – 7.17 (m, 1H), 6.59 (dd, *J* = 17.5, 10.8 Hz, 1H), 5.25 (dd, *J* = 10.8, 1.0 Hz, 1H), 5.12 (dd, *J* = 17.5, 1.0 Hz, 1H), 4.10 – 4.00 (m, 5H), 1.68 (s, 3H), 1.13 (td, *J* = 7.1, 5.4 Hz, 6H); ^{13}C NMR (100 MHz, $CDCl_3$) δ 167.7, 145.6, 128.2, 126.3, 114.4, 61.1, 61.0, 60.9, 46.3, 23.6, 14.0, 13.9; IR (Neat Film, NaCl) 3055, 2981, 1755, 1731, 1599, 1493, 1444, 1413, 1368, 1320, 1268, 1230, 1133, 1096, 1037, 919, 761, 700 cm^{-1}; HRMS (FI+) *m/z* calc'd for $C_{17}H_{22}O_4$: 290.1513, found 290.1527; $[\alpha]_D^{25}$ –7.4 (*c* 1.0, $CHCl_3$); SFC Conditions: 5% MeOH, 2.5 mL/min, Chiralcel OJ-H column, λ = 210 nm, t_R (min): major = 1.99, minor = 2.90.

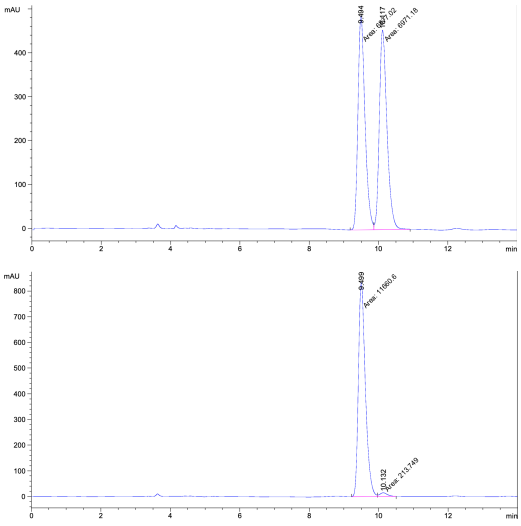


Peak #	RetTime [min]	Type	Width [min]	Area [mAU*s]	Height [mAU]	Area %
1	1.990	BB	0.1022	4662.24561	733.34625	98.4684
2	2.904	MM	0.1309	72.51768	9.23042	1.5316

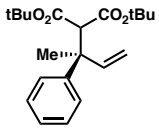


Dimethyl (*R*)-2-(2-phenylbut-3-en-2-yl)malonate (33)

Prepared according to general procedure 1 using carbonate **31a** (20.6 mg, 0.1 mmol) and dimethyl malonate (13.2 mg, 0.1 mmol) with purification by preparative TLC (10% EtOAc in hexanes) to provdie a colorless oil (18.0 mg, 69% yield, 97% ee); ^{1}H NMR (500 MHz, $CDCl_3$) δ 7.35 – 7.27 (m, 4H), 7.20 (ddt, *J* = 7.1, 6.1, 1.9 Hz, 1H), 6.58 (dd, *J* = 17.5, 10.8 Hz, 1H), 5.26 (dd, *J* = 10.8, 1.0 Hz, 1H), 5.12 (dd, *J* = 17.5, 1.0 Hz, 1H), 4.08 (s, 1H), 3.59 (d, *J* = 1.1 Hz, 6H), 1.67 (s, 3H); ^{13}C NMR (100 MHz, $CDCl_3$) δ 168.2, 168.2, 145.5, 142.7, 128.4, 126.6, 126.3, 114.6, 60.9, 52.3, 52.2, 46.4, 23.7; IR (Neat Film, NaCl) 2951, 1758, 1735, 1433, 1321, 1231, 1133, 1029, 925 cm^{-1}; HRMS (FI+) *m/z* calc'd for $C_{15}H_{18}O_4$: 262.1110 found 262.1214; $[\alpha]_D^{25}$ +15.8 (*c* 1.0, $CHCl_3$); HPLC Conditions: 2% IPA, 1.0 mL/min, Chiralcel OD-H column, λ = 210 nm, t_R (min): major = 9.50, minor = 10.13.

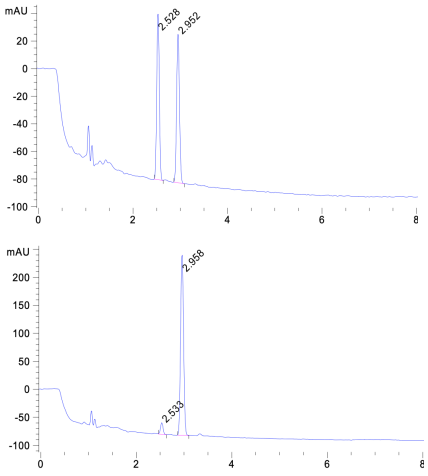


Peak #	RetTime [min]	Type	Width [min]	Area mAU *s	Height [mAU]	Area %
1	9.499	MF	0.2329	1.16606e4	834.39954	98.1999
2	10.132	FM	0.2497	213.74857	14.26826	1.8001

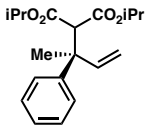


Di-*tert*-butyl (*R*)-2-(2-phenylbut-3-en-2-yl)malonate (34)

Prepared according to general procedure 1 using carbonate **31a** (20.6 mg, 0.1 mmol) and di-*tert*-butyl malonate (21.6 mg, 0.1 mmol) with purification by preparative TLC (5% EtOAc in hexanes) to provide a colorless oil (18.6 mg, 54% yield, 90% ee); ^{1}H NMR (500 MHz, $CDCl_3$) δ 7.33 – 7.27 (m, 4H), 7.22 – 7.14 (m, 1H), 6.58 (dd, *J* = 17.5, 10.8 Hz, 1H), 5.25 (dd, *J* = 10.7, 1.2 Hz, 1H), 5.11 (dd, *J* = 17.6, 1.2 Hz, 1H), 3.87 (s, 1H), 1.65 (s, 3H), 1.34 (s, 9H), 1.29 (s, 9H); ^{13}C NMR (100 MHz, $CDCl_3$) δ 167.3, 167.3, 146.4, 143.1, 128.2, 126.4, 126.3, 114.3, 81.7, 81.5, 62.7, 46.3, 27.9, 27.8, 24.1; IR (Neat Film, NaCl) 2976, 1727, 1455, 1392, 1367, 1317, 1246, 1123, 972, 914, 845, 746, 699, 668 cm^{-1}; HRMS (FI+) *m/z* calc'd for $C_{21}H_{30}O_4$: 346.2139 found 346.2151; $[\alpha]_D^{25}$ –6.5 (*c* 1.0, $CHCl_3$); SFC Conditions: 5% IPA, 2.5 mL/min, Chiralpak AD-H column, λ = 210 nm, t_R (min): minor = 2.53, major = 2.95.

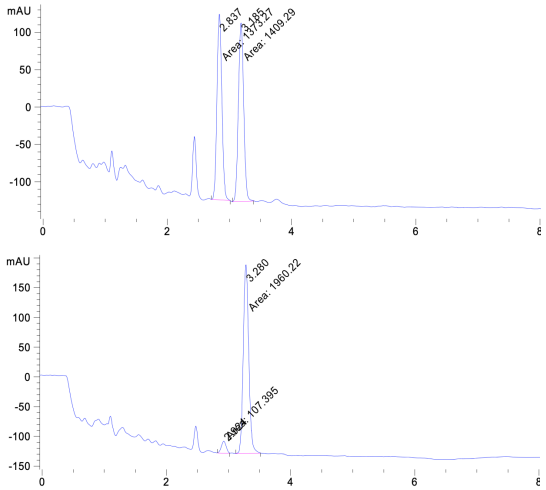


Peak #	RetTime [min]	Type	Width [min]	Area [mAU*s]	Height [mAU]	Area %
1	2.533	BB	0.0577	77.51880	20.70369	5.2601
2	2.958	BB	0.0684	1396.19421	322.89331	94.7399

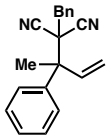


Diisopropyl (*R*)-2-(2-phenylbut-3-en-2-yl)malonate (35)

Prepared according to general procedure 1 using carbonate **31a** (20.6 mg, 0.1 mmol) and diisopropyl malonate (18.8 mg, 0.1 mmol). Purification by preparative TLC (10% EtOAc in hexanes) provided a colorless oil (17.9 mg, 56% yield, 90% ee); ^{1}H NMR (500 MHz, $CDCl_3$) δ 7.34 – 7.26 (m, 4H), 7.18 (ddt, *J* = 7.7, 6.6, 1.4 Hz, 1H), 6.59 (dd, *J* = 17.5, 10.8 Hz, 1H), 5.25 (dd, *J* = 10.8, 1.1 Hz, 1H), 5.11 (dd, *J* = 17.5, 1.1 Hz, 1H), 4.91 (dp, *J* = 10.6, 6.2 Hz, 2H), 3.99 (s, 1H), 1.67 (s, 3H), 1.18 – 1.06 (m, 12H); ^{13}C NMR (100 MHz, $CDCl_3$) δ 167.4, 146.0, 142.9, 128.3, 126.4, 126.4, 114.5, 68.8, 68.6, 61.3, 46.3, 24.0, 21.7, 21.7, 21.5. IR (Neat Film, NaCl) 2980, 2938, 1754, 1728, 1446, 1374, 1315, 1276, 1232, 1140, 1102, 1028, 913 cm^{-1}; HRMS (FI+) *m/z* calc'd for $C_{19}H_{26}O_4$: 318.1826, found 318.1843; $[\alpha]_D^{25}$ +12.0 (*c* 1.0, $CHCl_3$); SFC Conditions: 5% IPA, 2.5 mL/min, Chiralpak IC column, λ = 210 nm, t_R (min): minor = 2.92, major = 3.28.

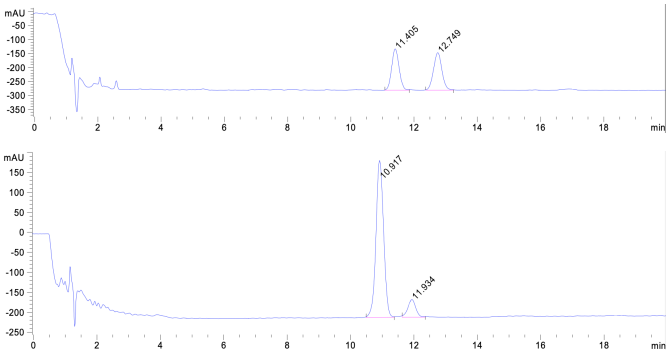


Peak #	RetTime [min]	Type	Width [min]	Area [mAU*s]	Height [mAU]	Area %
1	2.924	MM	0.0886	107.39502	20.21061	5.1942
2	3.280	MM	0.1027	1960.21631	317.97314	94.8058

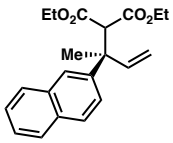


2-Benzyl-2-(2-phenylbut-3-en-2-yl)malononitrile (28a)

Prepared according to general procedure 1 using carbonate **31a** (20.6 mg, 0.1 mmol) and benzyl malononitrile (15.6 mg, 0.1 mmol) with purification by preparative TLC (10% EtOAc in hexanes) afforded a colorless oil (83% yield, 79% ee); ^{1}H NMR (400 MHz, $CDCl_3$) δ 7.68 – 7.60 (m, 2H), 7.48 – 7.29 (m, 8H), 6.64 (dd, *J* = 17.3, 10.9 Hz, 1H), 5.60 (d, *J* = 11.0 Hz, 1H), 5.46 (d, *J* = 17.3 Hz, 1H), 3.01 (d, *J* = 13.5 Hz, 1H), 2.94 (d, *J* = 13.4 Hz, 1H), 1.93 (s, 3H). All characterization data matched those reported in the literature.[20]

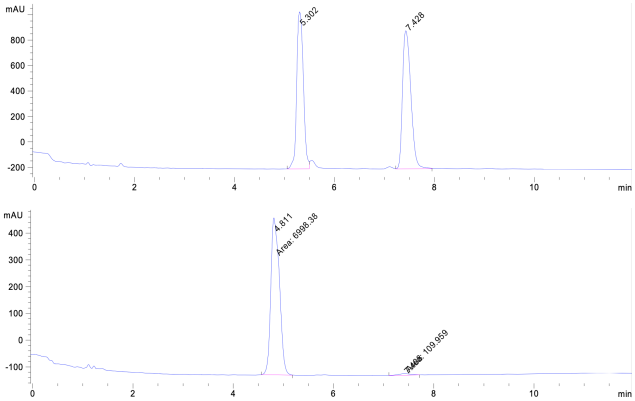


Peak #	RetTime [min]	Type	Width [min]	Area [mAU*s]	Height [mAU]	Area %
1	10.917	BB	0.2590	6559.89062	392.39392	89.5775
2	11.934	BB	0.2621	763.25513	44.05166	10.4225

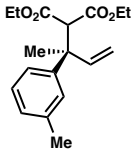


Diethyl (*R*)-2-(2-(naphthalen-2-yl)but-3-en-2-yl)malonate (32b)

Prepared according to general procedure 1 using carbonate **31b** (25.6 mg, 0.1 mmol) and diethyl malonate (16.0 mg, 0.1 mmol) with purification by preparative TLC (10% EtOAc in hexanes) to provide a colorless oil (26.8 mg, 79% yield, 97% ee); ^{1}H NMR (400 MHz, $CDCl_3$) δ 7.90 – 7.68 (m, 4H), 7.46 (dtd, *J* = 14.5, 7.9, 3.6 Hz, 3H), 6.69 (dd, *J* = 17.5, 10.8 Hz, 1H), 5.32 (dd, *J* = 10.9, 1.0 Hz, 1H), 5.17 (dd, *J* = 17.6, 1.0 Hz, 1H), 4.18 (s, 1H), 4.04 (qd, *J* = 7.1, 2.1 Hz, 4H), 1.78 (s, 3H), 1.08 (td, *J* = 7.1, 4.8 Hz, 6H); ^{13}C NMR (100 MHz, $CDCl_3$) δ 167.8, 167.8, 143.0, 142.8, 133.4, 132.1, 128.2, 127.9, 127.5, 126.1, 125.9, 125.2, 124.8, 114.8, 61.3, 61.2, 60.8, 46.6, 23.8, 14.0, 14.0; IR (Neat Film, NaCl) 2977, 1754, 1728, 1367, 1314, 1229, 1131, 1034, 921, 749, cm^{-1}; HRMS (FI+) *m/z* calc'd for $C_{21}H_{24}O_4$: 340.1669 found 340.1695; $[\alpha]_D^{25}$ +18.5 (*c* 1.0, $CHCl_3$); SFC Conditions: 5% MeOH, 2.5 mL/min, Chiralcel OJ-H column, λ = 210 nm, t_R (min): minor = 5.21, major = 5.92.

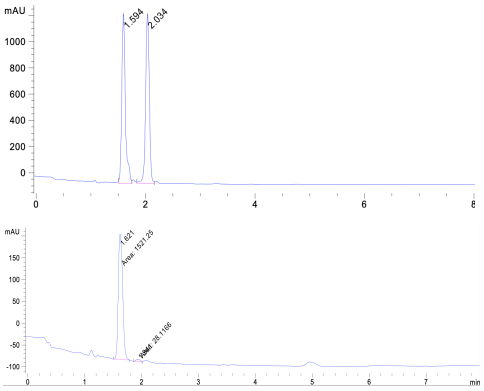


Peak #	RetTime [min]	Type	Width [min]	Area [mAU*s]	Height [mAU]	Area %
1	4.811	MM	0.1988	6998.37939	586.80725	98.4531
2	7.408	MM	0.3068	109.95891	5.97275	1.5469

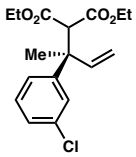


Diethyl (*R*)-2-(2-(*m*-tolyl)but-3-en-2-yl)malonate (32c)

Prepared according to general procedure A using carbonate **31c** (22.0 mg, 0.1 mmol) and diethyl malonate (16.0 mg, 0.1 mmol) with purification by preparative TLC (10% EtOAc in hexanes) to provide a colorless oil (22.3 mg, 73% yield, 94% ee); ^{1}H NMR (400 MHz, $CDCl_3$) δ 7.13 – 7.02 (m, 3H), 6.94 – 6.91 (m, 1H), 6.51 (dd, *J* = 17.5, 10.9 Hz, 1H), 5.17 (dd, *J* = 10.9, 1.1 Hz, 1H), 5.04 (dd, *J* = 17.6, 1.1 Hz, 1H), 4.06 – 3.91 (m, 5H), 2.25 (s, 3H), 1.58 (s, 3H), 1.05 (td, *J* = 7.1, 5.2 Hz, 6H); ^{13}C NMR (100 MHz, $CDCl_3$) δ 167.7, 145.6, 142.8, 137.6, 128.1, 127.1, 127.0, 123.2, 114.3, 61.1, 61.0, 60.9, 46.2, 23.7, 21.7, 14.0, 13.9; IR (Neat Film, NaCl) 2981, 1757, 1730, 1605, 1447, 1367, 1321, 1224, 1132, 1097, 1038, 924, 705 cm^{-1}; HRMS (FI+) *m/z* calc'd for $C_{18}H_{24}O_4$: 304.1669 found 304.1669; $[\alpha]_D^{25}$ –4.9 (*c* 1.0, $CHCl_3$); SFC Conditions: 5% MeOH, 2.5 mL/min, Chiralcel OJ-H column, λ = 210 nm, t_R (min): major = 1.62, minor = 1.94.

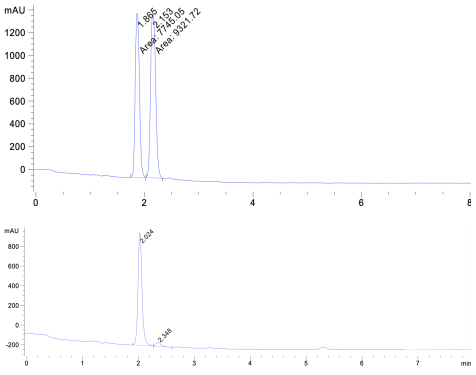


Peak #	RetTime [min]	Type	Width [min]	Area [mAU*s]	Height [mAU]	Area %
1	1.621	MM	0.0879	1521.25269	288.32150	98.1853
2	1.941	MM	0.0876	28.11655	5.35145	1.8147

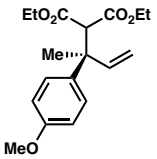


Diethyl (*R*)-2-(2-(3-chlorophenyl)but-3-en-2-yl)malonate (32d)

Prepared according to general procedure A using carbonate **31d** (24.0 mg, 0.1 mmol) and diethyl malonate (16.0 mg, 0.1 mmol) with purification by preparative TLC (10% EtOAc in hexanes) to provide a colorless oil (27.6 mg, 85% yield, 91% ee); ^{1}H NMR (400 MHz, $CDCl_3$) δ 7.26 – 7.23 (m, 1H), 7.17 – 7.08 (m, 3H), 6.46 (dd, *J* = 17.5, 10.9 Hz, 1H), 5.21 (dd, *J* = 10.9, 0.9 Hz, 1H), 5.05 (dd, *J* = 17.5, 0.9 Hz, 1H), 4.07 – 3.95 (m, 4H), 3.92 (s, 1H), 1.58 (s, 3H), 1.07 (td, *J* = 7.1, 3.5 Hz, 7H); ^{13}C NMR (100 MHz, $CDCl_3$) δ 167.6, 167.5, 148.0, 142.1, 134.3, 129.6, 126.9, 126.7, 124.6, 115.2, 61.4, 61.3, 60.8, 46.3, 23.8, 14.1, 14.0; IR (Neat Film, NaCl) 2981, 2937, 1755, 1730, 1593, 1571, 1465, 1445, 1415, 1367, 1322, 1267, 1232, 1134, 1097, 1037, 924, 861, 785, 740 cm^{-1}; HRMS (FI+) *m/z* calc'd for $C_{17}H_{21}O_4Cl$: 324.1123 found 324.1136; $[\alpha]_D^{25}$ –1.0 (*c* 1.0, $CHCl_3$); SFC Conditions: 2% MeOH, 2.5 mL/min, Chiralcel OJ-H column, λ = 210 nm, t_R (min): major = 2.02, minor = 2.35.

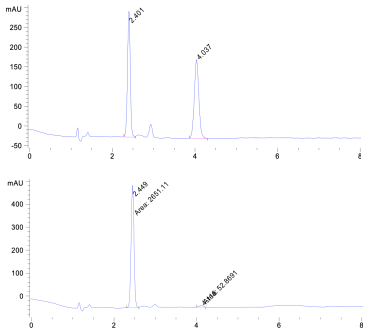


Peak #	RetTime [min]	Type	Width [min]	Area [mAU*s]	Height [mAU]	Area %
1	2.024	BV	0.0788	5787.72168	1147.99402	95.7894
2	2.348	VV	0.0868	254.41066	43.14692	4.2106

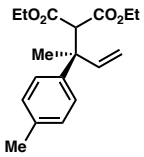


Diethyl (*R*)-2-(2-(4-methoxyphenyl)but-3-en-2-yl)malonate (32e)

Prepared according to general procedure A using carbonate **31e** (23.6 mg, 0.1 mmol) and diethyl malonate (16.0 mg, 0.1 mmol). Purification by preparative TLC (10% EtOAc in hexanes) provided a colorless oil (17.9 mg, 56% yield, 96% ee). Prepared by the general procedure using carbonate **31e** (236.3 mg, 1.0 mmol) and diethyl malonate (160.2 mg, 1.0 mmol). Purification by column chromatography (10% EtOAc in hexanes) provided a light orange oil (166.4 mg, 52% yield, 96% ee); ^{1}H NMR (400 MHz, $CDCl_3$) δ 7.24 (d, *J* = 9.0 Hz, 3H), 6.82 (d, *J* = 9.0 Hz, 2H), 6.55 (dd, *J* = 17.5, 10.8 Hz, 1H), 5.22 (dd, *J* = 10.8, 1.0 Hz, 1H), 5.08 (dd, *J* = 17.5, 1.0 Hz, 1H), 4.05 (qd, *J* = 7.1, 5.3 Hz, 4H), 3.98 (s, 1H), 3.78 (s, 3H), 1.65 (s, 3H), 1.13 (td, *J* = 7.1, 3.1 Hz, 6H); ^{13}C NMR (100 MHz, $CDCl_3$) δ 167.7, 167.7, 158.0, 143.0, 137.5, 127.4, 114.0, 113.5, 61.1, 61.0, 61.0, 55.2, 45.7, 23.6, 14.0, 14.0; IR (Neat Film, NaCl) 2981, 1709, 1621, 1368, 1280, 1231, 1168, 1042, 854, 816, 750 cm^{-1}; HRMS (FI+) *m/z* calc'd for $C_{18}H_{24}O_5$: 320.1618, found 320.1635; $[\alpha]_D^{25}$ +1.6 (*c* 0.5, $CHCl_3$); SFC Conditions: 10% IPA, 2.5 mL/min, Chiralpak OJ-H column, λ = 210 nm, t_R (min): major = 2.45, minor = 4.12.

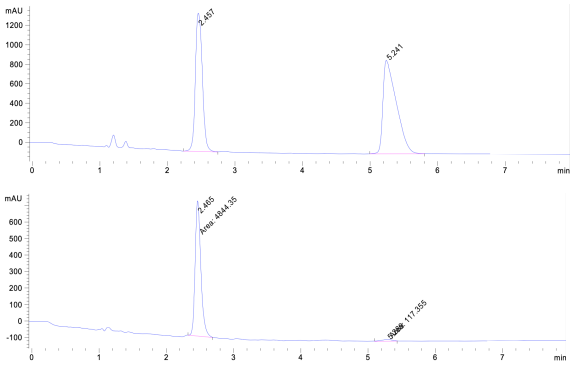


Peak #	RetTime [min]	Type	Width [min]	Area [mAU*s]	Height [mAU]	Area %
1	2.449	MM	0.0827	2651.10791	534.46008	98.0448
2	4.118	MM	0.1196	52.86905	7.36877	1.9552

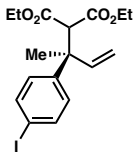


Diethyl (*R*)-2-(2-(*p*-tolyl)but-3-en-2-yl)malonate (32f)

Prepared according to general procedure 1 using carbonate **31f** (22.0 mg, 0.1 mmol) and diethyl malonate (16.0 mg, 0.1 mmol) with purification by preparative TLC (10% EtOAc in hexanes) to provide a colorless oil (28.3 mg, 93% yield, 96% ee); ^{1}H NMR (400 MHz, $CDCl_3$) δ 7.21 (d, *J* = 8.3 Hz, 2H), 7.12 – 7.07 (m, 2H), 6.57 (dd, *J* = 17.5, 10.8 Hz, 1H), 5.23 (dd, *J* = 10.9, 1.0 Hz, 1H), 5.10 (dd, *J* = 17.6, 1.1 Hz, 1H), 4.06 (qd, *J* = 7.1, 1.4 Hz, 4H), 4.02 (s, 1H), 2.30 (s, 3H), 1.65 (s, 3H), 1.13 (t, *J* = 7.1 Hz, 6H); ^{13}C NMR (100 MHz, $CDCl_3$) δ 167.9, 167.8, 143.0, 142.7, 136.0, 129.0, 126.2, 114.2, 61.2, 61.1, 61.0, 46.0, 23.7, 21.0, 14.1, 14.0; IR (Neat Film, NaCl) 2980, 1757, 1729, 1691, 1444, 1367, 1316, 1228, 1132, 1038, 922, 817 cm^{-1}; HRMS (FI+) *m/z* calc'd for $C_{18}H_{24}O_4$: 304.1667 found 304.1686; $[\alpha]_D^{25}$ –1.1 (*c* 1.0, $CHCl_3$); SFC Conditions: 2% MeOH, 2.5 mL/min, Chiralcel OJ-H column, λ = 210 nm, t_R (min): major = 2.47, minor = 5.29.

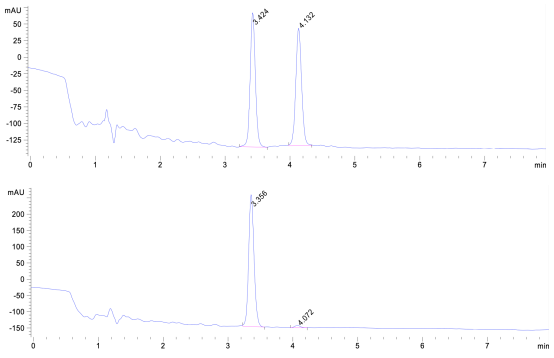


Peak #	RetTime [min]	Type	Width [min]	Area [mAU*s]	Height [mAU]	Area %
1	2.465	MM	0.0983	4844.34570	821.30530	97.6348
2	5.289	MM	0.1854	117.35537	10.55191	2.3652

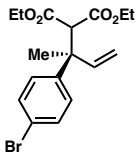


Diethyl (*R*)-2-(2-(4-iodophenyl)but-3-en-2-yl)malonate (32g)

Prepared according to general procedure 1 using carbonate **31g** (33.2 mg, 0.1 mmol) and diethyl malonate (16.0 mg, 0.1 mmol) with purification by preparative TLC (10% EtOAc in hexanes) to afford a light yellow oil (33.7 mg, 81% yield, 96% ee); ^{1}H NMR (400 MHz, $CDCl_3$) δ 7.60 (d, *J* = 8.6 Hz, 2H), 7.07 (d, *J* = 8.7 Hz, 2H), 6.52 (dd, *J* = 17.5, 10.8 Hz, 1H), 5.25 (dd, *J* = 10.8, 0.9 Hz, 1H), 5.10 (dd, *J* = 17.6, 0.9 Hz, 1H), 4.06 (q, *J* = 7.1 Hz, 4H), 3.97 (s, 1H), 1.63 (s, 3H), 1.14 (td, *J* = 7.1, 1.3 Hz, 6H).; ^{13}C NMR (100 MHz, $CDCl_3$) δ ^{13}C NMR (100 MHz, $CDCl_3$) δ 167.3, 167.2, 145.3, 141.9, 137.0, 128.3, 114.7, 91.8, 61.1, 61.0, 60.4, 45.8, 23.4, 13.8, 13.7; IR (Neat Film, NaCl) 2980, 1755, 1730, 1486, 1465, 1412, 1392, 1367, 1322, 1264, 1231, 1133, 1095, 1078, 1037, 1003, 923, 860, 822 cm^{-1}; HRMS (FI+) *m/z* calc'd for $C_{29}H_{30}O_4I$: 416.0479, found 416.0472; $[\alpha]_D^{25}$ +12.9 (*c* 1.0, $CHCl_3$); SFC Conditions: 5% IPA, 2.5 mL/min, Chiralpak OJ-H column, λ = 210 nm, t_R (min): major = 3.36, major = 4.07.

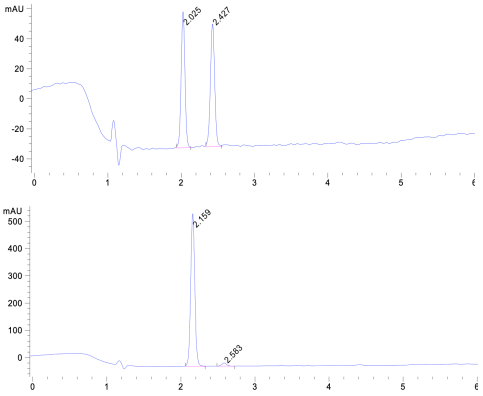


Peak #	RetTime [min]	Type	Width [min]	Area [mAU*s]	Height [mAU]	Area %
1	3.356	BB	0.0893	2337.94263	405.50409	98.3082
2	4.072	BB	0.0901	40.23287	6.89535	1.6918

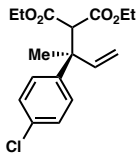


Diethyl (*R*)-2-(2-(4-bromophenyl)but-3-en-2-yl)malonate (32h)

Prepared according to general procedure 1 using carbonate **31h** (28.5 mg, 0.1 mmol) and diethyl malonate (16.0 mg, 0.1 mmol) with purification by preparative TLC (10% EtOAc in hexanes) to provide a pale yellow oil (22.7 mg, 62% yield, 95% ee); ^{1}H NMR (400 MHz, $CDCl_3$) δ 7.41 (d, *J* = 8.7 Hz, 2H), 7.20 (d, *J* = 8.7 Hz, 2H), 6.53 (dd, *J* = 17.5, 10.8 Hz, 1H), 5.26 (dd, *J* = 10.8, 0.9 Hz, 1H), 5.10 (dd, *J* = 17.5, 0.9 Hz, 1H), 4.06 (q, *J* = 7.1 Hz, 4H), 3.97 (s, 1H), 1.64 (s, 3H), 1.14 (td, *J* = 7.1, 1.3 Hz, 6H); ^{13}C NMR (100 MHz, $CDCl_3$) δ 167.6, 167.6, 144.9, 142.3, 131.4, 128.3, 120.6, 115.0, 61.4, 61.3, 60.8, 46.1, 23.8, 14.1, 14.1; IR (Neat Film, NaCl) 2981, 1755, 1731, 1488, 1394, 1367, 1321, 1268, 1229, 1133, 1095, 1081, 1038, 1008, 925, 812 cm^{-1}; HRMS (FI+) *m/z* calc'd for $C_{17}H_{21}O_4Br$: 368.0617, found 368.0638; $[\alpha]_D^{25}$ +4.5 (*c* 1.0, $CHCl_3$); SFC Conditions: 10% MeOH, 2.5 mL/min, Chiralpak OJ-H column, λ = 210 nm, t_R (min): major = 2.16, minor = 2.58.

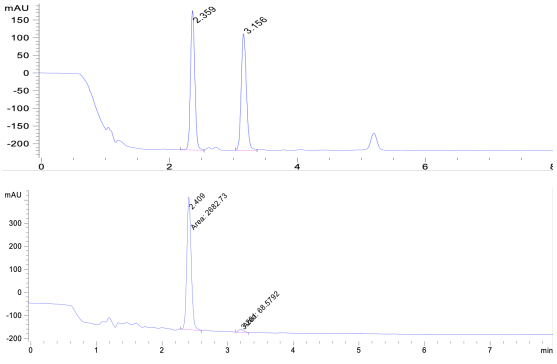


Peak #	RetTime [min]	Type	Width [min]	Area [mAU*s]	Height [mAU]	Area %
1	2.159	BB	0.0613	2173.74390	560.06818	97.5552
2	2.583	BB	0.0693	54.47504	11.93149	2.4448

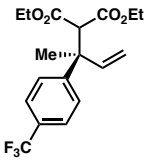


Diethyl (*R*)-2-(2-(4-chlorophenyl)but-3-en-2-yl)malonate (32i)

Prepared according to general procedure 1 using carbonate **31i** (12.0 mg, 0.05 mmol) and diethyl malonate (8.0 mg, 0.05 mmol) with purification by preparative TLC (10% EtOAc in hexanes) provided a light yellow oil (9.0 mg, 56% yield, 95% ee); ^{1}H NMR (500 MHz, $CDCl_3$) δ 7.26 (m, 4H), 6.54 (dd, *J* = 17.5, 10.8 Hz, 1H), 5.26 (dd, *J* = 10.8, 0.9 Hz, 1H), 5.11 (dd, *J* = 17.5, 0.9 Hz, 1H), 4.07 (q, *J* = 7.1 Hz, 4H), 3.98 (s, 1H), 1.65 (s, 3H), 1.15 (td, *J* = 7.1, 1.7 Hz, 6H). The aromatic protons are tightly spaced underneath the residual chloroform signal (see HSQC spectrum); ^{13}C NMR (100 MHz, $CDCl_3$) δ 167.6, 167.6, 144.3, 142.4, 132.4, 128.4, 127.9, 115.0, 61.4, 61.3, 60.9, 46.0, 23.9, 14.1, 14.1; IR (Neat Film, NaCl) 2980, 1755, 1730, 1486, 1392, 1367, 1322, 1231, 1132, 1037, 1003, 923, 822 cm^{-1}; HRMS (FI+) *m/z* calc'd for $C_{17}H_{21}O_4Cl$: 324.1123, found 324.1142; $[\alpha]_D^{25}$ +4.2 (*c* 0.5, $CHCl_3$); SFC Conditions: 10% IPA, 2.5 mL/min, Chiralcel OJ-H column, λ = 210 nm, t_R (min): major = 2.41, minor = 3.20.

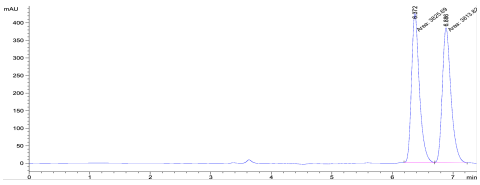


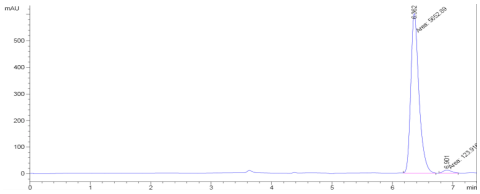
Peak #	RetTime [min]	Type	Width [min]	Area [mAU*s]	Height [mAU]	Area %
1	2.409	MM	0.0776	2682.73145	576.25537	97.5074
2	3.201	MM	0.0892	68.57921	12.81879	2.4926



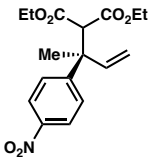
Diethyl (*R*)-2-(2-(4-(trifluoromethyl)phenyl)but-3-en-2-yl)malonate (32j)

Prepared according to general procedure 1 using carbonate **31j** (27.4 mg, 0.1 mmol) and diethyl malonate (16.0 mg, 0.1 mmol) with purification by preparative TLC (10% EtOAc in hexanes) to provide a pale yellow oil (24.6 mg, 69% yield, 96% ee); ^{1}H NMR (500 MHz, $CDCl_3$) δ 7.57 – 7.52 (m, 2H), 7.48 – 7.42 (m, 2H), 6.57 (dd, J = 17.5, 10.8 Hz, 1H), 5.30 (dd, J = 10.9, 0.8 Hz, 1H), 5.14 (dd, J = 17.5, 0.8 Hz, 1H), 4.10 – 4.04 (m, 4H), 4.04 (s, 1H), 1.68 (s, 3H), 1.14 (td, J = 7.1, 5.3 Hz, 6H); ^{13}C NMR (100 MHz, $CDCl_3$) δ 167.4, 167.4, 149.8, 149.8, 141.9, 129.2, 128.9, 128.5, 128.2, 126.7, 125.2, 125.2, 125.1, 125.1, 115.3, 61.3, 61.2, 60.6, 46.3, 23.8, 13.9, 13.9, the splitting pattern between 128–129 ppm is caused by ^{19}F and also present in the parent carbonate; ^{19}F NMR (282 MHz, $CDCl_3$) δ -62.5; IR (Neat Film, NaCl) 2983, 1756, 1731, 1617, 1447, 1414, 1369, 1328, 1232, 1169, 1125, 1080, 1056, 1037, 1014, 925, 843, 675 cm^{-1}; HRMS (FI+) *m/z* calc'd for $C_{18}H_{21}O_4F_3$: 358.1387, found 358.1403; $[\alpha]_D^{25}$ –5.6 (*c* 0.5, $CHCl_3$); HPLC Conditions: 2% IPA, 1.0 mL/min, Chiralcel OD-H column, λ = 210 nm, t_R (min): major = 6.36, minor = 6.90.



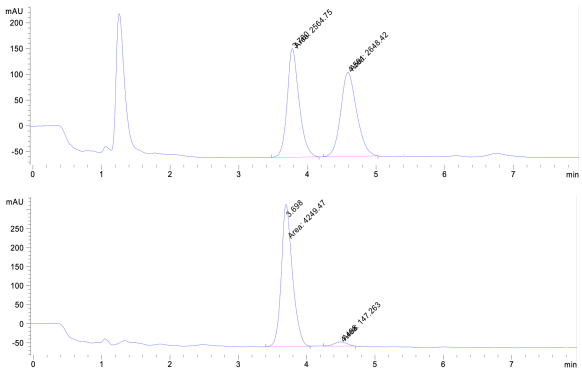


Peak #	RetTime [min]	Type	Width [min]	Area mAU *s	Height [mAU]	Area %
1	6.362	MM	0.1566	5652.89453	601.51556	97.8549
2	6.901	MM	0.1663	123.91565	12.41713	2.1451

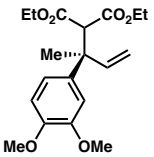


Diethyl (*R*)-2-(2-(4-nitrophenyl)but-3-en-2-yl)malonate (32k)

Prepared according to general procedure 1 using carbonate **31k** (25.1 mg, 0.1 mmol) and diethyl malonate (16.0 mg, 0.1 mmol) with purification by preparative TLC (10% EtOAc in hexanes) to provide a pale yellow oil (23.6 mg, 70% yield, 92% ee); ^{1}H NMR (500 MHz, $CDCl_3$) δ 8.15 (d, *J* = 9.0 Hz, 2H), 7.50 (d, *J* = 8.9 Hz, 2H), 6.56 (dd, *J* = 17.5, 10.8 Hz, 1H), 5.34 (dd, *J* = 10.8, 0.7 Hz, 1H), 5.16 (dd, *J* = 17.5, 0.7 Hz, 1H), 4.14 – 4.01 (m, 5H), 1.68 (s, 3H), 1.16 (dt, *J* = 8.3, 7.1 Hz, 6H); ^{13}C NMR (100 MHz, $CDCl_3$) δ 167.4, 167.3, 153.6, 146.5, 141.4, 127.4, 123.6, 116.0, 61.6, 61.5, 60.7, 46.6, 24.1, 14.1, 14.1; IR (Neat Film, NaCl) 2981, 1731, 1595, 1520, 1347, 1367, 1347, 1231, 1135, 1038, 931, 851, 698 cm^{-1}; HRMS (FI+) *m/z* calc'd for $C_{17}H_{21}NO_6$: 335.1363, found 335.1375; $[\alpha]_D^{25}$ +9.5 (*c* 0.5, $CHCl_3$); SFC Conditions: 5% IPA, 2.5 mL/min, Chiralcel OB-H column, λ = 210 nm, t_R (min): major = 3.70, minor = 4.50.

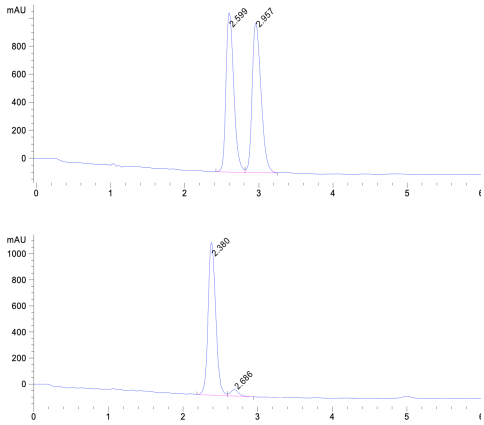


Peak #	RetTime [min]	Type	Width [min]	Area [mAU*s]	Height [mAU]	Area %
1	3.698	MM	0.1892	4249.46777	374.28323	96.6506
2	4.498	MM	0.2219	147.26280	11.06176	3.3494

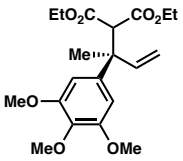


Diethyl (*R*)-2-(2-(3,4-dimethoxyphenyl)but-3-en-2-yl)malonate (32l)

Prepared according to general procedure 1 using carbonate **31l** (26.6 mg, 0.1 mmol) and diethyl malonate (16.0 mg, 0.1 mmol) with purification by preparative TLC (10% EtOAc in hexanes) provided a colorless oil (20.5 mg, 59% yield, 93% ee); ^{1}H NMR (400 MHz, $CDCl_3$) δ 6.88 – 6.83 (m, 2H), 6.80 – 6.76 (m, 1H), 6.56 (dd, *J* = 17.5, 10.8 Hz, 1H), 5.23 (dd, *J* = 10.8, 1.0 Hz, 1H), 5.10 (dd, *J* = 17.5, 1.1 Hz, 1H), 4.05 (qd, *J* = 7.1, 1.5 Hz, 4H), 3.99 (s, 1H), 3.85 (d, *J* = 5.1 Hz, 6H), 1.65 (s, 3H), 1.13 (td, *J* = 7.1, 0.9 Hz, 6H); ^{13}C NMR (100 MHz, $CDCl_3$) δ 167.8, 167.8, 148.6, 147.6, 143.0, 138.2, 118.6, 114.3, 110.8, 110.2, 61.2, 61.1, 61.1, 56.0, 55.9, 46.1, 24.0, 14.1, 14.1; IR (Neat Film, NaCl) 2980, 1756, 1730, 1588, 1518, 1460, 1412, 1366, 1322, 1258, 1149, 1029, 922, 866 cm^{-1}; HRMS (FI+) *m/z* calc'd for $C_{19}H_{26}O_6$: 350.1724 found 350.1730; $[\alpha]_D^{25}$ +2.6 (*c* 1.0, $CHCl_3$); SFC Conditions: 2% MeOH, 2.5 mL/min, Chiralpak OJ-H column, λ = 210 nm, t_R (min): major = 2.38, major = 2.69.

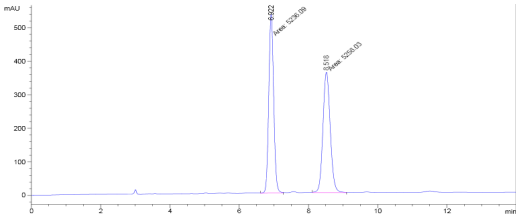


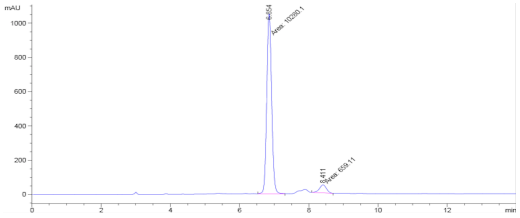
Peak #	RetTime [min]	Type	Width [min]	Area [mAU*s]	Height [mAU]	Area %
1	2.380	VV	0.1127	8309.95898	1172.47168	95.8458
2	2.686	VB	0.1071	360.17776	50.56734	4.1542



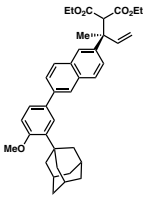
Diethyl (*R*)-2-(2-(3,4,5-trimethoxyphenyl)but-3-en-2-yl)malonate (32m)

Prepared according to general procedure A using carbonate **32m** (29.6 mg, 0.1 mmol) and diethyl malonate (16.0 mg, 0.1 mmol) with purification by preparative TLC (20% EtOAc in hexanes) to provide a light orange oil (15.0 mg, 40% yield, 88% ee); ^{1}H NMR (500 MHz, $CDCl_3$) δ 6.58 (dd, *J* = 17.5, 10.8 Hz, 1H), 6.53 (s, 2H), 5.27 (dd, *J* = 10.9, 1.0 Hz, 1H), 5.14 (dd, *J* = 17.6, 1.1 Hz, 1H), 4.13 – 4.03 (m, 4H), 4.01 (s, 1H), 3.84 (s, 6H), 3.81 (s, 3H), 1.66 (s, 3H), 1.15 (dt, *J* = 11.3, 7.1 Hz, 6H); ^{13}C NMR (100 MHz, $CDCl_3$) δ 167.8, 167.7, 152.9, 142.5, 141.5, 136.7, 114.7, 103.9, 61.4, 61.2, 61.1, 60.9, 56.2, 46.7, 24.2, 14.1, 14.1; IR (Neat Film, NaCl) 2979, 1730, 1586, 1512, 1456, 1413, 1367, 1321, 1231, 1125, 1036 cm^{-1}; HRMS (FI+) *m/z* calc'd for $C_{20}H_{28}O_7$: 380.1829 found 380.1855; $[\alpha]_D^{25}$ +1.7 (*c* 0.5, $CHCl_3$); HPLC Conditions: 5% IPA, 1.0 mL/min, Chiralcel OD-H column, λ = 210 nm, t_R (min): major = 6.85, minor = 8.41.



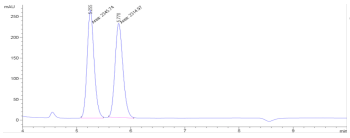


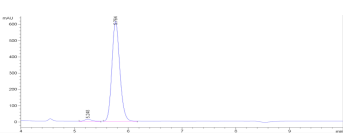
Peak #	RetTime [min]	Type	Width [min]	Area mAU *s	Height [mAU]	Area %
1	6.854	MM	0.1629	1.02801e4	1052.01624	93.9748
2	8.411	MM	0.2360	659.11011	46.55566	6.0252



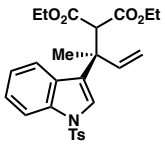
Diethyl 2-((2*R*)-2-(6-(3-((1*S*,3*S*)-adamantan-1-yl)-4-methoxyphenyl)naphthalen-2-yl)but-3-en-2-yl)malonate (32n)

Prepared according to general procedure A using carbonate **31n** (49.6 mg, 0.1 mmol) and diethyl malonate (16.0 mg, 0.1 mmol) with purification by preparative TLC (10% EtOAc in hexanes) to provide a colorless oil which slowly solidified on standing to a white amorphous solid (44.7 mg, 77% yield, 92% ee); ^{1}H NMR (400 MHz, $CDCl_3$) δ 7.95 (d, *J* = 1.8 Hz, 1H), 7.84 (dd, *J* = 8.7, 3.3 Hz, 2H), 7.79 (d, *J* = 2.0 Hz, 1H), 7.73 (dd, *J* = 8.5, 1.8 Hz, 1H), 7.60 (d, *J* = 2.3 Hz, 1H), 7.56 – 7.49 (m, 2H), 6.99 (d, *J* = 8.5 Hz, 1H), 6.72 (dd, *J* = 17.5, 10.8 Hz, 1H), 5.34 (dd, *J* = 10.9, 1.0 Hz, 1H), 5.19 (dd, *J* = 17.6, 1.1 Hz, 1H), 4.20 (s, 1H), 4.06 (qd, *J* = 7.1, 3.3 Hz, 4H), 3.90 (s, 3H), 2.23 – 2.19 (m, 6H), 2.18 (s, 1H), 2.15 – 2.09 (m, 4H), 1.85 – 1.79 (m, 8H), 1.11 (td, *J* = 7.1, 5.5 Hz, 6H); ^{13}C NMR (100 MHz, $CDCl_3$) δ 167.8, 167.8, 158.6, 142.8, 142.6, 138.9, 138.9, 133.2, 132.5, 132.1, 128.5, 128.0, 125.9, 125.6, 125.1, 124.9, 124.5, 114.8, 112.2, 61.2, 61.1, 60.8, 55.2, 46.6, 40.7, 37.3, 37.2, 31.0, 29.2, 23.7, 14.0, 14.0; IR (Neat Film, NaCl) 2904, 1755, 1731, 1603, 1462, 1368, 1235, 1133, 1031, 883, 810 cm^{-1}; HRMS (FI+) *m/z* calc'd for $C_{38}H_{34}O_5$: 580.3183 found 580.3188;); $[\alpha]_D^{25}$ +23.2 (*c* 1.0, $CHCl_3$); HPLC Conditions: 10% IPA, 1.0 mL/min, Chiralcel OB-H column, λ = 210 nm, t_R (min): minor = 5.25, major = 5.76.



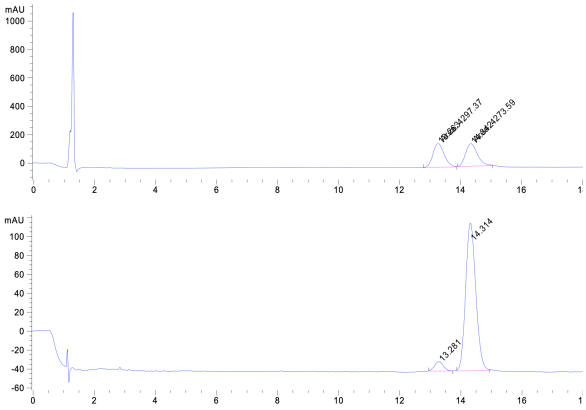


Peak #	RetTime [min]	Type	Width [min]	Area mAU *s	Height [mAU]	Area %
1	5.248	BB	0.1489	129.75508	12.95858	2.0203
2	5.764	BB	0.1576	6292.72559	613.15375	97.9797

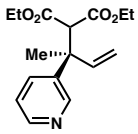


Diethyl (*R*)-2-(2-(1-tosyl-1H-indol-3-yl)but-3-en-2-yl)malonate (32p)

Prepared according to general procedure 1 using carbonate **31p** (39.9 mg, 0.1 mmol) and diethyl malonate (16.0 mg, 0.1 mmol) with purification by preparative TLC (100% CH_2Cl_2) to provide a light yellow oil (7.1 mg, 15% yield, 89% ee); ^{1}H NMR (500 MHz, $CDCl_3$) δ 7.95 (dt, *J* = 8.4, 0.9 Hz, 1H), 7.76 – 7.70 (m, 2H), 7.59 (dt, *J* = 7.9, 1.0 Hz, 1H), 7.43 (s, 1H), 7.28 – 7.17 (m, 4H), 6.54 (dd, *J* = 17.4, 10.7 Hz, 1H), 5.20 (dd, *J* = 10.7, 0.9 Hz, 1H), 5.03 (dd, *J* = 17.4, 0.9 Hz, 1H), 4.20 (s, 1H), 4.07 – 3.96 (m, 2H), 3.89 – 3.74 (m, 2H), 2.34 (s, 3H), 1.80 (s, 3H), 1.05 (t, *J* = 7.1 Hz, 3H), 0.86 (t, *J* = 7.1 Hz, 3H); ^{13}C NMR (100 MHz, $CDCl_3$) δ 167.5, 167.3, 144.9, 141.2, 135.8, 135.3, 129.9, 128.9, 127.0, 126.6, 124.4, 124.4, 122.9, 122.1, 115.2, 114.0, 61.2, 61.0, 58.6, 43.3, 22.4, 21.7, 14.0, 13.7; IR (Neat Film, NaCl) 2982, 1731, 1446, 1369, 1298, 1225, 1174, 1136, 1091, 1037, 959, 809, 753, 687 cm^{-1}; HRMS (ESI +) *m/z* calc'd for $C_{26}H_{29}NO_6S$ $[M+NH_4]^+$: 501.2054 found 501.2077; $[\alpha]_D^{25}$ +10.4 (*c* 0.3, $CHCl_3$); SFC Conditions: 10% IPA, 2.5 mL/min, Chiralpak IC column, λ = 210 nm, t_R (min): minor = 13.28, major = 14.31.

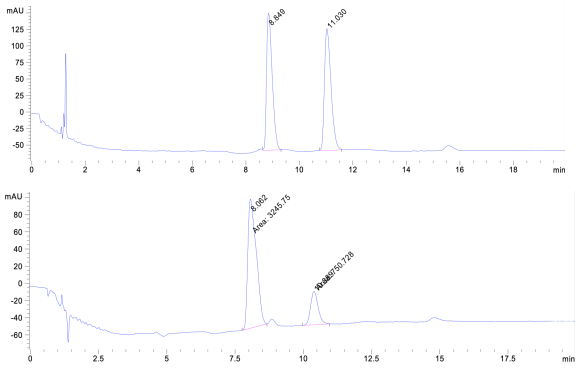


Peak #	RetTime [min]	Type	Width [min]	Area [mAU*s]	Height [mAU]	Area %
1	13.281	BB	0.2555	203.75606	10.09447	5.3448
2	14.314	BB	0.3637	3608.45264	156.11813	94.6552

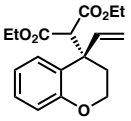


Diethyl (*R*)-2-(2-(pyridin-3-yl)but-3-en-2-yl)malonate (32q)

Prepared according to general procedure 1 using carbonate **31q** (20.7 mg, 0.1 mmol) and diethyl malonate (16.0 mg, 0.1 mmol) with purification by preparative TLC (10% EtOAc in hexanes) provided a colorless oil (24.3 mg, 83% yield, 63% ee); ^{1}H NMR (400 MHz, $CDCl_3$) δ 7.90 – 7.68 (m, 4H), 7.46 (dtd, *J* = 14.5, 7.9, 3.6 Hz, 3H), 6.69 (dd, *J* = 17.5, 10.8 Hz, 1H), 5.32 (dd, *J* = 10.9, 1.0 Hz, 1H), 5.17 (dd, *J* = 17.6, 1.0 Hz, 1H), 4.18 (s, 1H), 4.04 (qd, *J* = 7.1, 2.1 Hz, 4H), 1.78 (s, 3H), 1.08 (td, *J* = 7.1, 4.8 Hz, 6H); ^{13}C NMR (100 MHz, $CDCl_3$) δ ^{13}C NMR (100 MHz, $CDCl_3$) δ 167.4, 167.3, 148.2, 147.5, 141.6, 141.5, 135.3, 123.4, 115.7, 61.5, 61.5, 60.5, 45.1, 23.7, 14.1, 14.0; $[\alpha]_D^{25}$ –0.6 (*c* 1.0, $CHCl_3$) SFC Conditions: 5% MeOH, 2.5 mL/min, Chiralpak IC column, λ = 210 nm, t_R (min): major = 8.06, minor = 10.39.

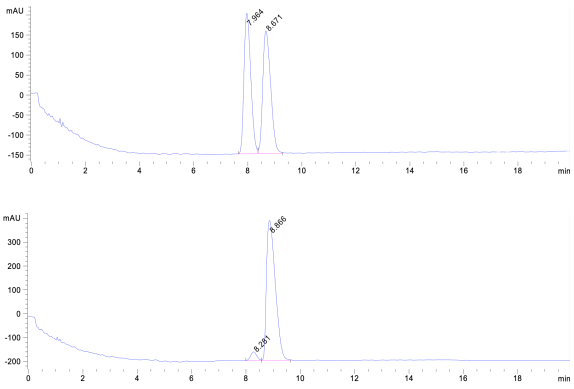


Peak #	RetTime [min]	Type	Width [min]	Area [mAU*s]	Height [mAU]	Area %
1	8.062	MM	0.3594	3245.74902	150.52498	81.2153
2	10.389	MM	0.3217	750.72809	38.89208	18.7847

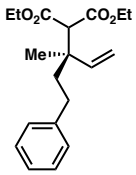


Diethyl (*R*)-2-(2-(naphthalen-2-yl)but-3-en-2-yl)malonate (32s)

Prepared according to general procedure 1 using carbonate **31s** (23.4 mg, 0.1 mmol) and diethyl malonate (16.0 mg, 0.1 mmol) with purification by preparative TLC (10% EtOAc in hexanes) to provide a colorless oil (10.1 mg, 32% yield, 92% ee); ^{1}H NMR (400 MHz, $CDCl_3$) δ 7.13 – 7.07 (m, 2H), 6.88 – 6.78 (m, 2H), 6.22 (ddd, *J* = 17.1, 10.5, 1.7 Hz, 1H), 5.24 (ddd, *J* = 10.5, 2.1, 1.0 Hz, 1H), 4.76 (ddd, *J* = 17.1, 2.0, 0.9 Hz, 1H), 4.23 (tdd, *J* = 7.1, 5.2, 1.8 Hz, 3H), 4.08 (d, *J* = 1.7 Hz, 1H), 4.01 – 3.87 (m, 3H), 2.91 (dddd, *J* = 14.2, 12.4, 4.0, 1.7 Hz, 1H), 2.03 (ddt, *J* = 14.1, 3.1, 1.9 Hz, 1H), 1.28 (td, *J* = 7.1, 1.7 Hz, 3H), 0.97 (td, *J* = 7.1, 1.7 Hz, 3H); ^{13}C NMR (100 MHz, $CDCl_3$) δ 167.8, 167.3, 155.6, 143.3, 128.6, 128.2, 123.6, 120.1, 117.6, 117.4, 62.6, 61.6, 61.2, 59.2, 43.3, 29.0, 14.2, 13.8; IR (Neat Film, NaCl) 2981, 1749, 1732, 1489, 1449, 1366, 1304, 1226, 1169, 1031, 931 cm^{-1}; HRMS (FD+) *m/z* calc'd for $C_{18}H_{22}O_5$ $[M]^+$: 318.1462 found 318.1469; $[\alpha]_D^{25}$ +2.5 (*c* 0.5, $CHCl_3$); SFC Conditions: 2% MeOH, 2.5 mL/min, Chiralpak IC column, λ = 210 nm, t_R (min): minor = 8.28, major = 8.87.

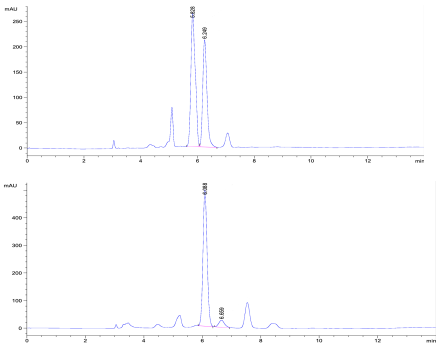


Peak #	RetTime [min]	Type	Width [min]	Area [mAU*s]	Height [mAU]	Area %
1	8.281	BV	0.2319	558.66656	36.22104	4.0546
2	8.866	VB	0.3546	1.32198e4	587.27740	95.9454

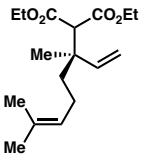


Diethyl (*R*)-2-(3-methyl-5-phenylpent-1-en-3-yl)malonate (32t)

Prepared according to general procedure 1 using carbonate **31t** (23.4 mg, 0.1 mmol) and diethyl malonate (16.0 mg, 0.1 mmol) with purification by preparative TLC (5% EtOAc in hexanes, eluted twice) to provide a colorless oil. An unidentified impurity persisted despite extensive attempts to further purify the title compound. This impurity did not affect product assignment or assignment of enantiomers, but as a result, the yield is reported by NMR relative to an internal (CH_2Br_2) standard (50% yield by ^{1}H NMR, 86% ee); ^{1}H NMR (400 MHz, $CDCl_3$) δ 7.32 – 7.16 (m, 5H), 6.12 – 6.01 (m, 1H), 5.17 (dt, *J* = 10.8, 0.9 Hz, 1H), 5.08 (dt, *J* = 17.5, 0.9 Hz, 1H), 4.25 – 4.09 (m, 4H), 3.47 (s, 1H), 2.60 – 2.50 (m, 2H), 1.96 – 1.76 (m, 2H), 1.35 (s, 3H), 1.25 (tdd, *J* = 7.1, 3.5, 0.8 Hz, 6H); ^{13}C NMR (100 MHz, $CDCl_3$) δ 168.0, 167.9, 143.1, 142.6, 128.5, 128.5, 128.4, 128.4, 125.9, 125.9, 114.2, 61.2, 61.1, 60.1, 42.3, 41.4, 30.6, 20.1, 14.3, 14.2; IR (Neat Film, NaCl) 2970, 1729, 1470, 1167, 1040, 851 cm^{-1}; HRMS (FI+) *m/z* calc'd for $C_{19}H_{26}O_4$: 318.1826 found 318.1846; $[\alpha]_D^{25}$ +1.3 (*c* 0.5, $CHCl_3$); HPLC Conditions: 0.07% IPA, 1.0 mL/min, Chiralpak IH column, λ = 210 nm, t_R (min): major = 6.09, minor = 6.66.

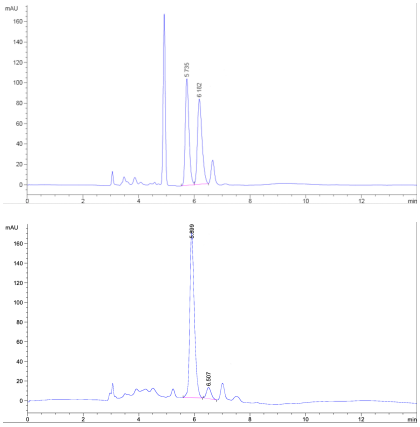


Peak #	RetTime [min]	Type	Width [min]	Area mAU *s	Height [mAU]	Area %
1	6.088	MM	0.1635	4858.69092	495.35336	93.1809
2	6.659	MM	0.2294	355.56625	25.83048	6.8191



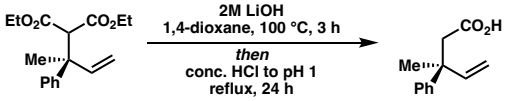
Diethyl (*R*)-2-(3,7-dimethylocta-1,6-dien-3-yl)malonate (32u)

Prepared according to general procedure A using carbonate **31u** (21.2 mg, 0.1 mmol) and diethyl malonate (16.0 mg, 0.1 mmol). Purification by preparative TLC (5% EtOAc in hexanes, eluted twice) provided a colorless oil. An unidentified impurity persisted despite extensive attempts to further purify the title compound. This impurity did not affect product assignment or assignment of enantiomers, but as a result, the yield is reported by NMR relative to an internal (CH_2Br_2) standard (63% yield by ^{1}H NMR, 87% ee); ^{1}H NMR (400 MHz, $CDCl_3$) δ 5.99 (dd, *J* = 17.5, 10.9 Hz, 1H), 5.14 – 4.95 (m, 3H), 4.16 (dq, *J* = 8.5, 7.1 Hz, 4H), 3.41 (s, 1H), 1.94 – 1.85 (m, 2H), 1.66 (d, *J* = 1.4 Hz, 3H), 1.57 (d, *J* = 1.2 Hz, 4H), 1.32 – 1.18 (m, 10H); ^{13}C NMR (100 MHz, $CDCl_3$) δ 168.0, 168.0, 143.3, 131.7, 124.3, 113.8, 61.1, 61.1, 60.2, 42.2, 39.3, 25.8, 22.8, 20.0, 17.7, 14.3, 14.2; IR (Neat Film, NaCl) 2985, 1982, 1755, 1736, 1444, 1166, 1035, 912, 681 cm^{-1}; HRMS (FI+) *m/z* calc'd for $C_{17}H_{28}O_4$: 296.1982 found 296.2001; $[\alpha]_D^{25}$ +1.1 (*c* 1.0, $CHCl_3$); HPLC Conditions: 0.06% IPA, 1.0 mL/min, Chiralpak IH column, λ = 210 nm, t_R (min): major = 5.90, minor = 6.50.



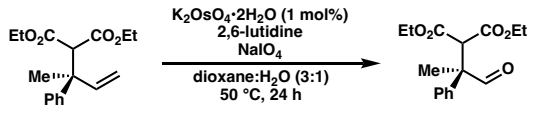
Peak #	RetTime [min]	Type	Width [min]	Area mAU *s	Height [mAU]	Area %
1	5.899	MM	0.1884	1901.37109	168.21719	93.4025
2	6.507	MM	0.1957	134.30399	11.43600	6.5975

1.11.2.2 Derivatizations of products



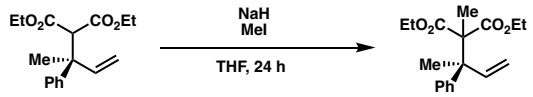
Carboxylic acid 40

To a round bottom flask with stir bar and reflux condenser was added malonate product **32a** (145 mg, 0.5 mmol, 1.0 equiv) in dioxane (2.5 mL). 2 N aq. LiOH (0.75 mL) was added, and the mixture was heated to reflux. After 3h, TLC analysis indicated full consumption of the starting material. The solution was allowed to cool to room temperature, then concentrated HCl was added until the solution reached a pH of 1. The reaction mixture was then heated to reflux and periodically monitored by LC/MS. After 36h, although full conversion of the diacid to the decarboxylated product was not entirely complete, ethyl acetate was added, and the layers were partitioned and extracted three times with ethyl acetate (5 mL). The combined organic layers were washed with brine, dried over $MgSO_4$, and concentrated under reduced pressure. The crude reaction mixture was purified by silica gel chromatography (20% EtOAc, 1% AcOH in hexanes) to afford a yellow oil (33.0 mg, 35% yield); $[\alpha]_D^{25}$ –4.5 (*c* 1.0, $CHCl_3$); ^{1}H NMR (500 MHz, $CDCl_3$) δ 7.34 – 7.29 (m, 4H), 7.21 (ddt, *J* = 6.1, 5.4, 2.6 Hz, 1H), 6.15 (dd, *J* = 17.4, 10.7 Hz, 1H), 5.16 (dd, *J* = 10.6, 0.9 Hz, 1H), 5.09 (dd, *J* = 17.4, 0.9 Hz, 1H), [2.83, 2.82] (ABq, 2H, J_{AB} = 14.5 Hz), 1.57 (s, 3H); ^{13}C NMR (100 MHz, $CDCl_3$) δ 177.0, 145.9, 145.2, 128.4, 126.5, 126.4, 112.9, 45.4, 43.4, 25.6. HRMS (FI+) *m/z* calc'd for $C_{12}H_{14}O_2$: 190.0984, found 190.0988.



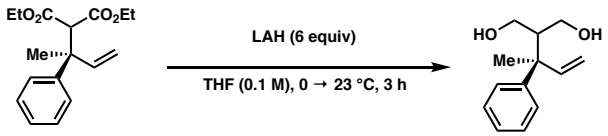
Quaternary aldehyde 41

To a flame-dried 1 Dr vial with stir bar was added the malonate product **32a** (29.0 mg, 0.1 mmol, 1.0 equiv) and K_2OsO_4•$2H_2O$ (0.4 mg, 0.001 mmol, 1 mol %). 2,6 lutidine (21.4 mg, 0.2 mmol, 2.0 equiv) was added as a solution in dioxane:H_2O (1.0 mL). To the stirring mixture was then added $NaIO_4$ (86 mg, 0.4 mmol, 4.0 equiv). The reaction vial was then heated to 50 °C for 24 h. After 24 h, the starting material had been consumed by TLC. The reaction mixture was cooled to room temperature and filtered through a pad of celite, eluting with dichloromethane (10 mL) and EtOAc (5 mL). Water was then added, and the layers were separated and extracted three times with dichloromethane. The combined organic layers were washed with brine, then dried over $MgSO_4$ and concentrated under reduced pressure. The crude mixture was purified by silica gel flash chromatography (10% EtOAc in hexanes) to afford the product as a colorless oil (19.0 mg, 67% yield); $[\alpha]_D^{25}$ +0.5 (*c* 1.0, $CHCl_3$); ^{1}H NMR (500 MHz, $CDCl_3$) δ 9.55 (s, 1H), 7.38 – 7.27 (m, 5H), 4.35 (s, 1H), 4.19 (qd, *J* = 7.2, 2.7 Hz, 2H), 3.96 (q, *J* = 7.1 Hz, 2H), 1.88 (s, 3H), 1.25 (t, *J* = 7.1 Hz, 3H), 0.99 (t, *J* = 7.1 Hz, 3H); ^{13}C NMR (100 MHz, $CDCl_3$) δ 199.1, 167.6, 167.5, 136.7, 129.0, 128.1, 127.6, 61.8, 61.4, 57.3, 54.6, 16.0, 14.1, 13.9; IR (Neat Film, NaCl) 2982, 1728, 1446, 1368, 1310, 1232, 1164, 1078, 1029 cm^{-1}; HRMS (ESI+); *m/z* calc'd for $C_{16}H_{20}O_5Na$ $[M+Na]^+$: 315.1209, found 315.1203.



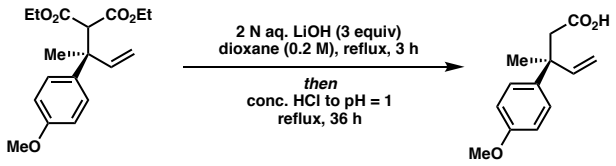
Vicinal quaternary product 42

Sodium hydride (60 % dispersion in mineral oil, 0.12 mmol) was added to a 1 Dr vial. The vessel was purged and backfilled three times with nitrogen. THF (0.25 mL) was added and the suspension was cooled to 0°C. Malonate **32a** (29.0 mg, 0.1 mmol, 1.0 equiv) was added as a solution in THF (0.25 mL). The solution was allowed to warm to 23°C over the course of one hour. Methyl iodide (0.2 mmol) in THF (0.5 mL) was then added dropwise to the stirred solution. After 24 hours the crude reaction mixture was diluted with ethyl acetate, then water was added and the mixture was stirred for 10 minutes. The layers were separated and extracted three times with EtOAc (20 mL). The combined organic layers were washed with brine, dried over $MgSO_4$, and concentrated under reduced pressure. The crude residue was purified by silica gel flash chromatography (2% to 10% EtOAc in hexanes; 2% increments, 50 mL each) to afford a colorless oil (13.0 mg, 43% yield); $[\alpha]_D^{25}$ +15.0 (*c* 1.0, $CHCl_3$); ^{1}H NMR (500 MHz, $CDCl_3$) δ 7.45 – 7.39 (m, 2H), 7.25 – 7.16 (m, 2H), 6.90 (dd, *J* = 17.5, 11.0 Hz, 1H), 5.21 (dd, *J* = 11.0, 1.1 Hz, 1H), 5.02 (dd, *J* = 17.5, 1.2 Hz, 1H), 4.12 – 4.02 (m, 4H), 1.72 (s, 3H), 1.49 (s, 3H), 1.17 (dt, *J* = 14.5, 7.1 Hz, 6H); ^{13}C NMR (100 MHz, $CDCl_3$) δ 171.4, 171.4, 144.6, 144.2, 128.9, 127.4, 126.5, 114.4, 61.3, 61.2, 61.1, 49.1, 23.2, 19.8, 14.0, 14.0; IR (Neat Film, NaCl) 2981, 1729, 1445, 1381, 1254, 1026, 917, 753, 702 cm^{-1}; HRMS (FI+) *m/z* calc'd for $C_{18}H_{24}O_4$: 304.1669, found 304.1683.



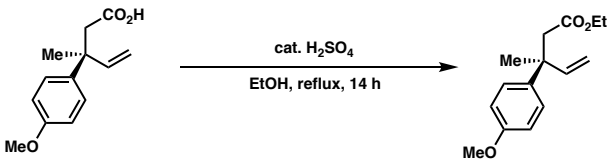
Diol 43

LAH (0.6 mmol, 6.0 equiv) was added to a flame dried 1 Dr vial fitted with septum. The vial was cooled to 0 °C and 0.5 mL THF was added. Malonate **32a** (29.0 mg, 0.1 mmol, 1.0 equiv) was dissolved in 0.5 mL THF and added to the stirred LAH suspension. After stirring for 3 h, the reaction was cooled to 0 °C. 0.5 mL EtOAc was added to quench the reaction, which was then diluted with Et_2O followed by addition of a twofold excess of saturated potassium sodium tartrate. The layers were partitioned, the aqueous layer was extracted three times with ethyl acetate (10 mL), washed with brine, dried over $MgSO_4$, and concentrated under reduced pressure. The crude mixture was purified by preparative TLC (50 % EtOAc in hexanes) affording a colorless oil (13.8 mg, 67%); $[\alpha]_D^{25}$ +4.4 (*c* 1.0, $CHCl_3$); ^{1}H NMR (400 MHz, $CDCl_3$) δ 7.36 – 7.29 (m, 4H), 7.20 (ddt, *J* = 6.6, 5.6, 2.3 Hz, 1H), 6.13 (dd, *J* = 17.5, 10.8 Hz, 1H), 5.19 (dd, *J* = 10.8, 1.0 Hz, 1H), 5.11 (dd, *J* = 17.5, 1.0 Hz, 1H), 3.85 (ddd, *J* = 10.7, 3.3, 1.4 Hz, 1H), 3.77 – 3.64 (m, 3H), 2.61 (br s, 1H), 2.51 (br s, 1H), 2.40 (tdd, *J* = 8.6, 4.1, 3.2 Hz, 1H), 1.37 (s, 3H; ^{13}C NMR (100 MHz, $CDCl_3$) δ 146.5, 144.3, 128.6, 126.4, 126.3, 113.6, 64.9, 64.9, 50.1, 45.4, 21.7; IR (Neat Film, NaCl) 3304 (br), 2935, 1599, 1444, 1066, 1009, 919, 763, 730, 702 cm^{-1}; HRMS (FI+) *m/z* calc'd for $C_{13}H_{18}O_2$: 206.1301, found 206.1315.



Carboxylic acid 44

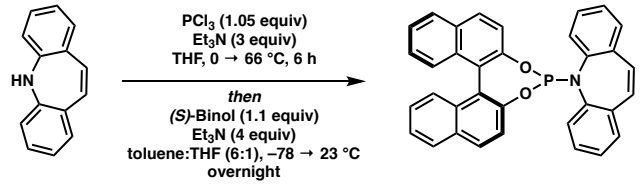
To a round bottom flask with stir bar and reflux condenser was added malonate **32e** (246 mg, 0.77 mmol) in dioxane (3 mL). 2 N aq. LiOH (1.15 mL) was added, and the mixture was heated to reflux. After 3h, TLC analysis indicated full consumption of the starting material. The solution was allowed to cool to room temperature, then concentrated HCl was added until the solution reached a pH of 1. The reaction mixture was then heated to reflux and periodically monitored by LC/MS until consumption of the diacid was observed. After 36h, ethyl acetate was added, the layers were partitioned and extracted three times with ethyl acetate. The combined organic layers were washed with brine, dried over $MgSO_4$, and concentrated under reduced pressure. The crude product was re-dissolved in a minimal amount of ethyl acetate (0.1 mL), 2 M K_2CO_3 (5 mL) was added and the solution was stirred vigorously for 2h. The layers were separated and concentrated HCl was added until the solution reached a pH of 1. The aqueous layer was extracted four times with ethyl acetate (5 mL). The combined organic layers were washed with brine, dried over $MgSO_4$, and concentrated to afford an oil that solidified to an off-white amorphous solid (110 mg, 65% yield); $[\alpha]_D^{25}$ –5.5 (*c* 0.5, $CHCl_3$); ^{1}H NMR (400 MHz, $CDCl_3$) δ 7.26 – 7.22 (m, 2H), 6.89 – 6.79 (m, 2H), 6.12 (dd, *J* = 17.4, 10.7 Hz, 1H), 5.22 – 5.01 (m, 2H), 3.79 (s, 3H), [2.81, 2.78] (ABq, 2H, J_{AB} = 14.3 Hz), 1.55 (s, 3H); ^{13}C NMR (100 MHz, $CDCl_3$) δ 176.8, 158.1, 145.6, 137.9, 127.5, 113.7, 112.5, 55.3, 45.5, 42.8, 25.7; IR (Neat Film, NaCl) 2929, 1706, 1609, 1581, 1512, 1462, 1413, 1294, 1248, 1182, 1163, 1034, 921, 827 cm^{-1}; HRMS (FI+) *m/z* calc'd for $C_{13}H_{16}O_3$: 220.1094, found 220.1108.



Ethyl ester 45

To a flame-dried round bottom 5 mL flask with stir bar and reflux condenser was added the β-quaternary acid **44** (20 mg, 0.09 mmol) in ethanol (1 mL). Catalytic H_2SO_4 (0.05 mL) was added, and the mixture was heated to reflux. After 14h, TLC and LC/MS analysis indicated full consumption of the starting material. The solution was allowed to cool to room temperature, then neutralized with $NaHCO_3$, extracted 3x with ethyl acetate, washed with brine, dried over $MgSO_4$, and concentrated under reduced pressure. The product was purified by preparative TLC (20% ethyl acetate in hexanes) affording a colorless oil (15.3 mg, 69% yield); $[\alpha]_D^{25}$ –6.9 (*c* 0.5, $CHCl_3$); ^{1}H NMR (500 MHz, $CDCl_3$) δ 7.25 – 7.22 (m, 2H), 6.87 – 6.81 (m, 2H), 6.13 (dd, *J* = 17.4, 10.7 Hz, 1H), 5.15 – 5.02 (m, 2H), 4.00 (q, *J* = 7.1 Hz, 2H), 3.79 (s, 3H), [2.77, 2.72] (ABq, 2H, J_{AB} = 13.9 Hz), 1.55 (s, 3H), 1.12 (t, *J* = 7.1 Hz, 3H); ^{13}C NMR (100 MHz, $CDCl_3$) δ 171.5, 158.0, 146.0, 138.2, 127.6, 113.6, 112.1, 60.2, 55.4, 46.0, 43.0, 25.7, 14.3; IR (Neat Film, NaCl) 2976, 2834, 1733, 1609, 1512, 1462, 1366, 1296, 1251, 1183, 1034, 911, 861, 831 cm^{-1}; HRMS (FI+) *m/z* calc'd for $C_{15}H_{20}O_3$: 248.1407, found 248.1424.

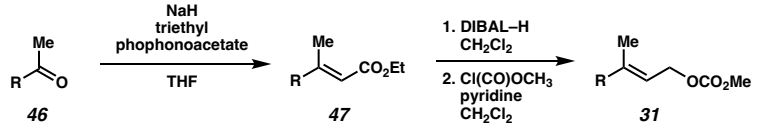
1.11.2.3 Ligand Synthesis



Phosphoramidite Ligand *(S_a)*-L3

The ligand was prepared according to a modified procedure disclosed by You and coworkers;[30] A flame-dried 250 mL 3-necked round bottomed flask equipped with a reflux condenser and addition funnel was charged with PCl_3 (504 mg (0.32 mL), 3.68 mmol, 1.05 equiv) and THF (5 mL). The solution was cooled to 0 ºC. Iminostilbene (676 mg, 3.0 mmol, 1 equiv) and Et_3N (1.06 g (1.46 mL), 10.5 mmol, 3 equiv) in THF (12 mL) were added dropwise. After the addition was complete, the solution was warmed to 23 °C then heated to reflux for 6 h. After TLC indicated consumption of the amine, the solution was cooled to –78 °C. A solution of *(S)*-Binol (1.10 g, 3.85 mmol, 1.1 equiv) and Et_3N (1.42 g (1.95 mL), 14 mmol, 4 equiv) in THF (10 mL) in toluene (60 mL) was added dropwise. After addition the solution was allowed to warm to 23 °C and stir overnight. The solution was then filtered over celite and silica eluting with ethyl acetate. The crude reaction mixture was concentrated and purified by silica gel chromatography (25% → 50% toluene in hexanes) to afford the desired ligand as a white solid (600 mg, 34% yield); ^{1}H NMR (500 MHz, $CDCl_3$) δ 7.98 (d, J = 8.8 Hz, 1H), 7.90 (d, J = 8.2 Hz, 1H), 7.78 – 7.73 (m, 1H), 7.61 (d, J = 8.8 Hz, 1H), 7.45 – 7.32 (m, 3H), 7.30 – 7.07 (m, 9H), 7.02 – 6.89 (m, 3H), 6.84 (d, J = 8.8 Hz, 1H), 6.53 (td, J = 7.6, 1.6 Hz, 1H). All characterization data matched those reported in the literature.[31]

1.11.2.4 General procedure 2: Synthesis of allylic carbonate electrophiles



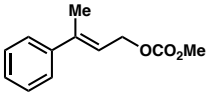
Horner–Wadsworth–Emmons Olefination: To a flame-dried round bottom flask was added NaH (60% dispersion in mineral oil, 1.5 equiv). The flask was purged and backfilled three times with nitrogen. Then THF (0.4 M) was added, and the resulting gray suspension was cooled to 0 °C and stirred. To the cooled suspension was added neat triethyl phosphonoacetate (1.5 equiv) dropwise, causing rapid gas evolution, and stirred for 30 minutes, during which time the solution became clear. The solution was allowed to warm to 21 °C then heated to 40 °C using a metal heating block or oil bath. A solution of ketone (1.0 equiv, 1.0 M in THF) was added slowly to the reaction mixture and allowed to stir overnight. After stirring for ~20h, the mixture was cooled to 0 °C, diluted with Et_2O and quenched with water. The layers were separated and extracted three times with EtOAc (75 mL). The combined organic layers were washed with brine, dried over $MgSO_4$, and concentrated under reduced pressure. The crude residue showed the desired (*E*)-alkene product in ratios ranging from 2:1 to 10:1 depending on the substrate. These geometric isomers were separated by silica gel flash column chromatography to afford the desired (*E*)-products (**47**).

Diisobutyl aluminum hydride reduction: To a flame-dried round bottom flask was added the (*E*)-alkene (1.0 equiv) and CH_2Cl_2 (0.25 M), and the solution was cooled to –78 °C. DIBAL (3 equiv) was added neat dropwise. The solution was stirred at –78 °C for 1h, before warming to room temperature and stirring for an additional hour. Upon completion as determined by TLC analysis, the reaction was quenched with EtOAc and diluted twofold with Et_2O. A large excess of a saturated Rochelle's salt solution was added and allowed to

stir until two clear layers had formed. The layers were separated and extracted three times with Et_2O (75 mL). The combined organic layers were washed with brine, dried over $MgSO_4$, and concentrated under reduced pressure. The crude allylic alcohol products were used directly in the subsequent step without further purification.

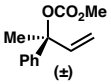
Carbonate formation: To a flame-dried round bottom flask was added crude allylic alcohol (1.0 equiv) followed by dichloromethane (0.25 M) and pyridine (9.0 equiv), and the resulting mixture stirred at 0 °C for 5 min. Methyl chloroformate (3 equiv) was added dropwise (neat). The reaction mixture was then allowed to stir and gradually reach 23 °C overnight. After stirring for 20h the crude reaction mixture was diluted with and equal volume of Et_2O and quenched with 1N HCl (8 equiv). The layers were separated, and the aqueous layer was extracted three times with EtOAc (70 mL). The combined organic layers were washed with brine, dried over $MgSO_4$, and concentrated under reduced pressure. The crude product was purified by silica gel flash chromatography to afford the desired allylic carbonate.

For known allylic carbonates, only ^1H NMR data is presented. For new carbonates, yields reported refer to the formation of the allylic carbonate from the corresponding ester unless otherwise stated, and ^1H NMR data for the intermediate ester **47** is for previously reported compounds.



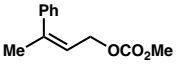
(*E*)-methyl (3-phenylbut-2-en-1-yl) carbonate (31a)

Prepared according to general procedure 2. ^{1}H NMR (500 MHz, $CDCl_3$) δ 7.41 (dd, *J* = 7.7, 1.7 Hz, 2H), 7.33 (t, *J* = 7.5 Hz, 2H), 7.28 (d, *J* = 7.2 Hz, 1H), 5.93 (td, *J* = 7.0, 1.5 Hz, 1H), 4.86 (d, *J* = 7.0 Hz, 2H), 3.81 (s, 3H), 2.14 (s, 3H). All characterization data matched those reported in the literature.[32]



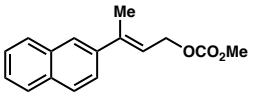
Methyl (2-phenylbut-3-en-2-yl) carbonate (31ab)

Prepared according to a literature procedure[33] from 2-phenylbut-3-en-2-ol and used without purification. ^{1}H NMR (400 MHz, $CDCl_3$) δ 7.42 – 7.27 (m, 5H), 6.29 (dd, *J* = 17.4, 10.8 Hz, 1H), 5.37 – 5.25 (m, 2H), 3.70 (s, 3H), 1.92 (s, 3H). The compound has a propensity to undergo [3,3]-sigmatropic rearrangement on silica gel and at temperatures >30 °C and should be handled cautiously.



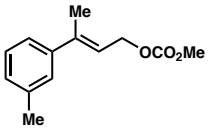
(*Z*)-methyl (3-phenylbut-2-en-1-yl) carbonate (31ac)

Prepared according to general procedure 2 using minor (*Z*) isomer separated after Horner-Wadsworth-Emmons olefination for the preparation of **31a**. ^{1}H NMR (500 MHz, $CDCl_3$) δ 7.38 – 7.33 (m, 2H), 7.31 – 7.27 (m, 1H), 7.20 – 7.16 (m, 2H), 5.70 (td, *J* = 7.3, 1.6 Hz, 1H), 4.56 (dt, *J* = 7.2, 1.1 Hz, 2H), 3.77 (d, *J* = 0.8 Hz, 3H), 2.11 (t, *J* = 1.3 Hz, 3H). All characterization data matched those reported in the literature.[19]



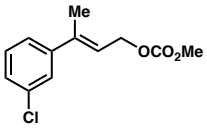
(*E*)-methyl (3-(naphthalen-2-yl)but-2-en-1-yl) carbonate (31b)

Prepared according to general procedure 2. ^{1}H NMR (400 MHz, $CDCl_3$) δ 7.90 – 7.76 (m, 4H), 7.58 (dd, *J* = 8.6, 1.9 Hz, 1H), 7.51 – 7.43 (m, 2H), 6.08 (tq, *J* = 7.0, 1.3 Hz, 1H), 4.92 (dt, *J* = 7.0, 0.7 Hz, 2H), 3.82 (s, 3H), 2.24 (dt, *J* = 1.4, 0.7 Hz, 3H). All characterization data matched those reported in the literature.[19]



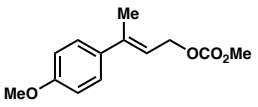
(*E*)-methyl (3-(*m*-tolyl)but-2-en-1-yl) carbonate (31c)

Prepared according to general procedure 2. ^{1}H NMR (400 MHz, $CDCl_3$) δ 7.25 – 7.18 (m, 3H), 7.11 – 7.08 (m, 1H), 5.95 – 5.86 (m, 1H), 4.85 (dq, *J* = 7.0, 0.7 Hz, 2H), 3.80 (s, 3H), 2.36 (d, *J* = 0.8 Hz, 3H), 2.12 (dt, *J* = 1.3, 0.7 Hz, 3H). All characterization data matched those reported in the literature.[34]



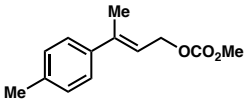
(*E*)-3-(3-chlorophenyl)but-2-en-1-yl methyl carbonate (31d)

Prepared according to general procedure 2. ^{1}H NMR (400 MHz, $CDCl_3$) δ 7.38 (q, *J* = 1.5 Hz, 1H), 7.29 – 7.23 (m, 3H), 5.92 (tq, *J* = 7.0, 1.4 Hz, 1H), 4.84 (dq, *J* = 6.9, 0.9 Hz, 2H), 3.81 (s, 3H), 2.10 (dt, *J* = 1.4, 0.8 Hz, 3H). All characterization data matched those reported in the literature.[20]



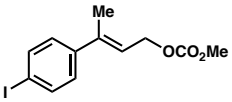
(*E*)-3-(4-methoxyphenyl)but-2-en-1-yl methyl carbonate (31e)

Prepared according to general procedure 2. ^{1}H NMR (500 MHz, $CDCl_3$) δ 7.38 – 7.30 (m, 2H), 6.89 – 6.83 (m, 2H), 5.87 (t, *J* = 7.1 Hz, 1H), 4.84 (d, *J* = 7.1 Hz, 2H), 3.82 (s, 3H), 3.80 (s, 3H), 2.11 (s, 3H). All characterization data matched those reported in the literature.[20]



(*E*)-methyl (3-(*p*-tolyl)but-2-en-1-yl) carbonate (31f)

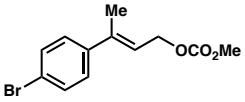
Prepared according to general procedure 2. ^{1}H NMR (400 MHz, $CDCl_3$) δ 7.35 – 7.27 (m, 2H), 7.18 – 7.09 (m, 2H), 5.90 (tq, *J* = 7.1, 1.3 Hz, 1H), 4.84 (dd, *J* = 7.1, 0.8 Hz, 2H), 3.80 (s, 3H), 2.34 (s, 3H), 2.11 (dd, *J* = 1.4, 0.8 Hz, 3H). All characterization data matched those reported in the literature.[34]



(*E*)-3-(4-iodophenyl)but-2-en-1-yl methyl carbonate (31g)

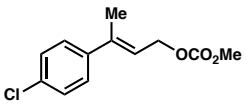
Prepared according to general procedure 2. Purified by silica gel column chromatography (10% EtOAc in hexanes) to provide the title compound as a yellow solid (165 mg, 57% yield). ^{1}H NMR (400 MHz, $CDCl_3$) δ 7.65 (d, J = 8.5 Hz, 2H), 7.14 (d, J = 8.5 Hz, 2H), 5.91 (tq, J = 6.9, 1.4 Hz, 1H), 4.83 (dd, J = 6.9, 0.9 Hz, 2H), 3.80 (s, 3H), 2.09 (dt, J = 1.5, 0.7 Hz, 3H); ^{13}C NMR (100 MHz, $CDCl_3$) δ 155.9, 142.0, 140.1, 137.5, 127.9, 121.4, 93.3, 64.9, 55.0, 16.2; IR (Neat Film, NaCl) 2955, 1744, 1687, 1582, 1483, 1442, 1392, 1262, 1125,

1073, 1004, 945, 849, 818, 793, 742 cm^{-1}; HRMS (FI+) *m/z* calc'd for $C_{12}H_{13}O_3I$: 331.9904, found 331.9922. Data for intermediate (*E*)-ester **47e** matched those previously reported;[35] ^1H NMR (500 MHz, $CDCl_3$) δ 7.70 (d, *J* = 8.2 Hz, 2H), 7.21 (d, *J* = 8.2 Hz, 2H), 6.11 (s, 1H), 4.22 (q, *J* = 7.1 Hz, 2H), 2.54 (d, *J* = 1.4 Hz, 3H), 1.32 (t, *J* = 7.1 Hz, 3H).



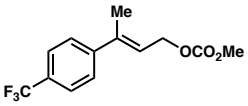
(*E*)-3-(4-bromophenyl)but-2-en-1-yl methyl carbonate (31h)

Prepared according to general procedure 2. Purified with a short silica plug eluting with 5% EtOAc in hexanes to provide the title compound as a white amorphous solid (1.04 g, 50% yield); ^1H NMR (500 MHz, $CDCl_3$) δ 7.48 – 7.42 (m, 2H), 7.30 – 7.24 (m, 2H), 5.91 (td, *J* = 6.7, 3.3 Hz, 1H), 4.84 (d, *J* = 6.9 Hz, 2H), 3.81 (d, *J* = 1.3 Hz, 3H), 2.11 (s, 3H); ^{13}C NMR (100 MHz, $CDCl_3$) δ 156.0, 141.4, 140.0, 131.5, 127.7, 121.8, 121.4, 64.9, 55.0, 16.3; IR (Neat Film, NaCl) 2954, 1744, 1442, 1262, 940, 791 cm^{-1}; HRMS (FI+) *m/z* calc'd for $C_{12}H_{13}O_3$: 284.0042, found 284.0056. Data for intermediate (*E*)-ester **47h** matched those previously reported;[36] ^1H NMR (500 MHz, $CDCl_3$) δ 7.50 (d, *J* = 8.4 Hz, 2H), 7.34 (d, *J* = 8.3 Hz, 2H), 6.11 (s, 1H), 4.22 (q, *J* = 7.1 Hz, 2H), 2.55 (s, 3H), 1.32 (t, *J* = 7.1 Hz, 3H).



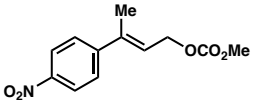
(*E*)-3-(4-chlorophenyl)but-2-en-1-yl methyl carbonate (31i)

Prepared according to general procedure 2. ^{1}H NMR (500 MHz, $CDCl_3$) δ 7.36 – 7.28 (m, 4H), 5.91 (dd, *J* = 7.8, 6.1 Hz, 1H), 4.84 (d, *J* = 7.0 Hz, 2H), 3.81 (s, 3H), 2.11 (s, 3H). All characterization data matched those reported in the literature.[34]



(*E*)-methyl (3-(4-(trifluoromethyl)phenyl)but-2-en-1-yl) carbonate (31j)

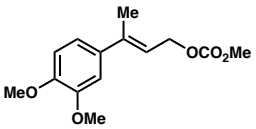
Prepared according to general procedure 2. ^{1}H NMR (400 MHz, $CDCl_3$) δ 7.62 – 7.54 (m, 2H), 7.53 – 7.45 (m, 2H), 6.02 – 5.93 (m, 1H), 4.86 (dd, *J* = 6.8, 0.9 Hz, 2H), 3.81 (s, 3H), 2.14 (dt, *J* = 1.5, 0.8 Hz, 3H). All characterization data matched those reported in the literature.[34]



(*E*)-methyl (3-(4-nitrophenyl)but-2-en-1-yl) carbonate (31k)

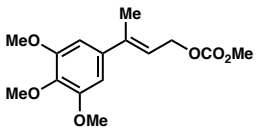
Prepared according to general procedure 2. Purified by column chromatography (5% EtOAc in hexanes) to provide the title compound product as a light orange amorphous solid (195.3 mg, 39% yield); ^{1}H NMR (500 MHz, $CDCl_3$) δ 8.19 (d, *J* = 8.7 Hz, 2H), 7.54 (d, *J* = 8.8 Hz, 2H), 6.05 (dd, *J* = 7.5, 5.9 Hz, 1H), 4.88 (d, *J* = 6.7 Hz, 2H), 3.82 (s, 3H), 2.17 (s, 3H); ^{13}C NMR (100 MHz, $CDCl_3$) δ 155.9, 148.9, 147.3, 138.9, 126.8, 124.6, 123.8, 64.7, 55.1, 16.4; IR (Neat Film, NaCl) 2961, 1742, 1592, 1515, 1438, 1345, 1271, 968, 860, 792, 744 cm^{-1};

HRMS (FI+) *m/z* calc'd for $C_{12}H_{13}NO_5$: 251.0788, found 251.0796. Data for intermediate (*E*)-ester **47k** matched those previously reported;[37] ^{1}H NMR (500 MHz, $CDCl_3$) δ 8.23 (d, *J* = 8.8 Hz, 2H), 7.61 (d, *J* = 8.8 Hz, 2H), 6.18 (q, *J* = 1.4 Hz, 1H), 4.24 (q, *J* = 7.1 Hz, 3H), 2.59 (d, *J* = 1.4 Hz, 2H), 1.34 (t, *J* = 7.1 Hz, 3H).



(*E*)-3-(3,4-dimethoxyphenyl)but-2-en-1-yl methyl carbonate (31l)

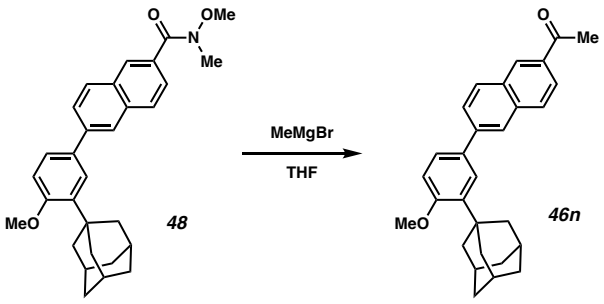
Prepared according to general procedure 2. Purification by silica gel chromatography (10% EtOAc in hexanes) afforded the title compound as a colorless oil (224 mg, 84% yield); ^{1}H NMR (400 MHz, $CDCl_3$) δ 7.01 – 6.92 (m, 2H), 6.83 (d, *J* = 8.3 Hz, 2H), 5.88 (ddt, *J* = 7.1, 5.7, 1.3 Hz, 1H), 4.85 (dq, *J* = 7.1, 0.7 Hz, 2H), 3.90 (s, 3H), 3.89 (s, 3H), 3.80 (s, 3H), 2.14 – 2.10 (m, 3H); ^{13}C NMR (100 MHz, $CDCl_3$) δ 156.0, 149.0, 148.8, 140.9, 135.4, 119.4, 118.5, 110.9, 109.3, 65.2, 56.1, 56.1, 55.0, 16.5; (Neat Film, NaCl) 2954, 2856, 1746, 1601, 1583, 1517, 1444, 1416, 1376, 1340, 1255, 1174, 1149, 1026, 944, 905, 860, 792, 767 cm^{-1}; HRMS (FI+) *m/z* calc'd for $C_{14}H_{18}O_5$: 266.1149, found 266.1173. Data for intermediate (*E*)-ester **47l** matched those previously reported;[36] ^{1}H NMR (400 MHz, $CDCl_3$) δ 7.10 (dd, *J* = 8.4, 2.2 Hz, 1H), 7.01 (d, *J* = 2.2 Hz, 1H), 6.86 (d, *J* = 8.4 Hz, 1H), 6.11 (q, *J* = 1.3 Hz, 1H), 4.22 (q, *J* = 7.1 Hz, 2H), 3.91 (d, *J* = 4.6 Hz, 6H), 2.57 (d, *J* = 1.3 Hz, 3H), 1.32 (t, *J* = 7.1 Hz, 3H).



(*E*)-methyl (3-(3,4,5-trimethoxyphenyl)but-2-en-1-yl) carbonate (31m)

Prepared according to general procedure 2. Purification by silica gel chromatography (10 → 20% EtOAc in hexanes) afforded the title compound as a colorless oil (692 mg, 39% yield); ^{1}H NMR (400 MHz, $CDCl_3$) δ 6.60 (s, 2H), 5.87 (tq, *J* = 7.0, 1.4 Hz, 1H), 4.84 (dd, *J* = 7.0, 0.9 Hz, 2H), 3.87 (s, 6H), 3.85 (s, 3H), 3.80 (s, 3H), 2.11 (dd, *J* = 1.4, 0.7 Hz, 3H); ^{13}C NMR (100 MHz, $CDCl_3$) δ 155.8, 153.0, 141.1, 138.4, 137.8, 120.5, 103.3, 64.9, 60.9, 56.2, 54.9, 16.6. IR (Neat Film, NaCl) 3478, 2968, 1500, 2160, 2020, 1954, 1754, 1584, 1412, 1253, 1122, 943, 794 cm^{-1}; HRMS (FI+) *m/z* calc'd for $C_{15}H_{20}O_6$: 296.1254, found 296.1277.

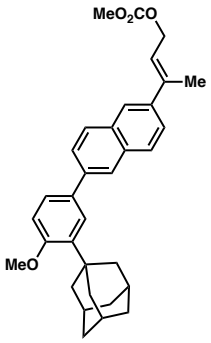
Data for intermediate (*E*)-ester **47m** matched those previously reported;[38] ^{1}H NMR (400 MHz, $CDCl_3$) δ 6.68 (s, 2H), 6.10 (d, *J* = 1.3 Hz, 1H), 4.22 (q, *J* = 7.1 Hz, 2H), 3.89 (s, 6H), 3.87 (s, 3H), 2.56 (d, *J* = 1.3 Hz, 3H), 1.33 (t, *J* = 7.1 Hz, 3H).



Ketone 46n

To a flame-dried flask was added Weinreb amide **48** (prepared according to the procedure of Lu and coworkers[39]) (1.83 g, 4.02 mmol, 1.0 equiv). The reaction vessel was purged and backfilled. THF (20 mL) was added and the solution was stirred and cooled to 0 °C. MeMgBr

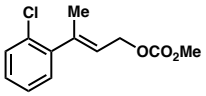
(3.0 M in Et_2O, 2.0 mL, 6.03 mmol, 1.5 equiv) was added dropwise to the stirred solution. The solution was stirred at 0 °C for 40 min. Then saturated aqueous NH_4Cl was added. CH_2Cl_2 was added, the layers were partitioned, and the aqueous layer was extracted four times with CH_2Cl_2. The combined extracts were dried over Na_2SO_4 and concentrated. The title compound was afforded relatively cleanly by NMR and was used without further purification (1.40 g, 85% yield). ^{1}H NMR (400 MHz, $CDCl_3$) δ 8.48 (d, *J* = 1.7 Hz, 1H), 8.08 – 7.97 (m, 3H), 7.93 (d, *J* = 8.7 Hz, 1H), 7.81 (dd, *J* = 8.5, 1.8 Hz, 1H), 7.61 (d, *J* = 2.4 Hz, 1H), 7.55 (dd, *J* = 8.4, 2.4 Hz, 1H), 7.00 (d, *J* = 8.4 Hz, 1H), 3.91 (s, 3H), 2.74 (s, 3H), 2.19 (d, *J* = 3.1 Hz, 6H), 2.15 – 2.08 (m, 3H), 1.81 (t, *J* = 3.1 Hz, 6H). ^{13}C NMR (100 MHz, $CDCl_3$) δ 198.2, 159.1, 141.8, 139.2, 136.2, 134.2, 132.6, 131.4, 130.1, 130.1, 128.6, 126.7, 126.1, 125.9, 124.9, 124.4, 112.2, 55.3, 40.7, 37.3, 37.3, 29.2, 26.8; IR (neat film, NaCl) 2901, 2845, 1676, 1624, 1472, 1285, 1237, 1138, 1029, 878, 819; HMRS (FD+) *m/z* calc'd for $C_{29}H_{30}O_2$: 410.2240, found 410.2259.



(*E*)-3-(6-(3-((1*s*,3*s*)-adamantan-1-yl)-4-methoxyphenyl)naphthalen-2-yl)but-2-en-1-yl methyl carbonate (31n)

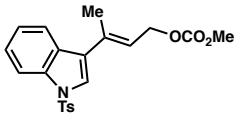
Prepared according to general procedure 2 from ketone **46n**. Purification by silica gel chromatography (15% EtOAc in hexanes) afforded the title compound as an amorphous

white solid (557 mg, 90% yield); ^{1}H NMR (400 MHz, $CDCl_3$) δ 7.96 (d, *J* = 1.8 Hz, 1H), 7.90 – 7.80 (m, 3H), 7.73 (dd, *J* = 8.4, 1.8 Hz, 1H), 7.59 (td, *J* = 4.1, 1.8 Hz, 2H), 7.53 (dd, *J* = 8.4, 2.3 Hz, 1H), 6.99 (d, *J* = 8.5 Hz, 1H), 6.11 (tt, *J* = 5.6, 1.3 Hz, 1H), 4.93 (dd, *J* = 7.0, 0.9 Hz, 2H), 3.90 (s, 3H), 3.83 (s, 3H), 2.25 (d, *J* = 1.3 Hz, 3H), 2.19 (d, *J* = 3.0 Hz, 6H), 2.10 (t, *J* = 3.3 Hz, 3H), 1.81 (d, *J* = 2.8 Hz, 6H). ^{13}C NMR (100 MHz, $CDCl_3$) δ 158.6, 155.9, 140.8, 139.1, 139.1, 138.9, 133.2, 133.1, 132.1, 128.6, 128.0, 126.1, 125.9, 125.6, 124.6, 124.5, 124.4, 121.0, 112.1, 65.1, 55.2, 54.9, 40.6, 37.2, 37.2, 29.1, 16.3; IR (neat film, NaCl) 2903, 1746, 1443, 1266, 948, 813; HMRS (FD+) *m/z* calc'd for $C_{33}H_{36}O_4$: 496.2608, found 496.2634. Intermediate (*E*)-ethyl ester **47n** was afforded after Horner–Wadsworth–Emmons olefination according to general procedure 2 and purification by silica gel chromatography (0 → 100% EtOAc in hexanes) as a white powder (619 mg, 38% yield).). ^{1}H NMR (400 MHz, $CDCl_3$) δ 8.00 – 7.94 (m, 2H), 7.89 (dd, *J* = 11.7, 8.6 Hz, 2H), 7.76 (dd, *J* = 8.5, 1.8 Hz, 1H), 7.66 – 7.57 (m, 2H), 7.54 (dd, *J* = 8.4, 2.4 Hz, 1H), 7.00 (d, *J* = 8.5 Hz, 1H), 6.32 (q, *J* = 1.3 Hz, 1H), 4.25 (q, *J* = 7.1 Hz, 2H), 3.91 (s, 3H), 2.71 (d, *J* = 1.3 Hz, 3H), 2.19 (d, *J* = 3.1 Hz, 6H), 2.11 (br t, *J* = 3.2 Hz, 3H), 1.81 (d, *J* = 3.2 Hz, 6H), 1.35 (t, *J* = 7.1 Hz, 3H). ^{13}C NMR (100 MHz, $CDCl_3$) δ 167.1, 158.9, 155.4, 140.0, 139.1, 139.0, 134.0, 133.0, 132.0, 129.0, 128.4, 126.4, 126.0, 125.9, 125.7, 124.8, 124.4, 117.4, 112.2, 60.0, 55.3, 40.8, 37.3, 37.3, 29.3, 18.0, 14.5; IR (neat film, NaCl) 2904, 2848, 1710, 1620, 1475, 1367, 1341, 1265, 1238, 1156, 1041, 873, 812, 737, 660; HMRS (FD+) *m/z* calc'd for $C_{33}H_{36}O_3$: 480.2659, found 480.2668.



(*E*)-3-(2-chlorophenyl)but-2-en-1-yl methyl carbonate (2r)

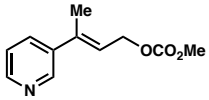
Prepared according to general procedure 2. ^{1}H NMR (400 MHz, $CDCl_3$) δ 7.40 – 7.27 (m, 5H), 5.78 (t, *J* = 7.0 Hz, 1H), 4.85 (d, *J* = 7.1 Hz, 2H), 3.80 (s, 3H), 2.64 – 2.53 (m, 2H), 1.55 (s, 1H), 1.00 (t, *J* = 7.5 Hz, 3H). All characterization data matched those reported in the literature.[34]



(*E*)-methyl (3-(1-tosyl-1*H*-indol-3-yl)but-2-en-1-yl) carbonate (31p)

Prepared according to general procedure 2 with the following modified reduction procedure: To a flame dried 40 mL vial was added lithium aluminum hydride. The vial was cooled to 0 °C and THF (3.0 mL) was added. Ethyl (*E*)-3-(1-tosyl-1*H*-indol-3-yl)but-2-enoate (as prepared according to the Horner–Wadsworth–Emmons olefination procedure) (520 mg, 1.36 mmol, 1.0 equiv) was dissolved in THF (2.0 mL), and this solution was slowly added to the stirring lithium aluminum hydride suspension using additional THF (0.4 mL) to complete the transfer. After 20 minutes, saturated aqueous NH_4Cl (10 mL) was slowly added at 0 °C. Then saturated aqueous sodium potassium tartrate (100 mL) was added and stirred at 23 °C. The layers were separated and extracted three times with EtOAc (50 mL), dried over Na_2SO_4, and concentrated under reduced pressure. The crude allylic alcohol was converted to the corresponding carbonate following the carbonate formation procedure in general procedure 2. Purification by silica gel chromatography (35% EtOAc in hexanes) afforded the title compound as a colorless oil (278 mg, 51% yield). ^{1}H NMR (400 MHz,

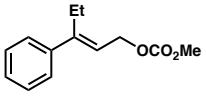
$CDCl_3$) δ 8.00 (dt, *J* = 8.3, 0.9 Hz, 1H), 7.80 – 7.70 (m, 3H), 7.32 (ddd, *J* = 8.4, 7.2, 1.3 Hz, 1H), 7.32 – 7.17 (m, 3H), 6.13 (ddt, *J* = 8.4, 7.1, 1.4 Hz, 1H), 4.89 (dd, *J* = 7.0, 0.8 Hz, 2H), 3.80 (s, 3H), 2.33 (s, 3H), 2.19 – 2.11 (m, 3H). ^{13}C NMR (100 MHz, $CDCl_3$) δ 155.9, 145.2, 135.6, 135.2, 133.8, 130.1, 128.7, 126.9, 125.0, 124.8, 123.8, 123.6, 121.6, 121.3, 113.9, 64.6, 55.0, 21.7, 17.1. IR (neat film, NaCl) 3136, 2956, 1748, 1648, 1596, 1446, 1372, 1268, 1176, 1140, 1092, 1055, 940, 812, 792, 747, 703, 669, 622, 603 cm^{-1}; HRMS (ESI+) *m/z* calc'd for $C_{21}H_{21}NO_5S$ $[M+H]^+$: 400.1140, found 400.1204. Data for intermediate (*E*)-ester **47p** matched those previously reported;[40] ^{1}H NMR (400 MHz, $CDCl_3$) δ 8.04 – 7.97 (m, 1H), 7.84 – 7.73 (m, 5H), 7.40 – 7.27 (m, 2H), 7.24 (dq, *J* = 1.3, 0.7 Hz, 1H), 6.33 (d, *J* = 1.3 Hz, 1H), 4.23 (q, *J* = 7.2 Hz, 2H), 2.61 (d, *J* = 1.3 Hz, 3H), 2.35 (s, 3H), 1.32 (t, *J* = 7.1 Hz, 3H).



(*E*)-methyl (3-(pyridin-3-yl)but-2-en-1-yl) carbonate (31q)

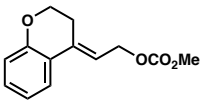
Prepared according to general procedure 2. Purification by silica gel chromatography (0 → 100% EtOAc in hexanes) afforded the title compound as a colorless oil (564 mg, 30% yield). ^{1}H NMR (400 MHz, $CDCl_3$) δ 8.66 – 8.60 (m, 1H), 8.48 (dd, *J* = 4.8, 1.6 Hz, 1H), 7.65 (ddd, *J* = 8.0, 2.3, 1.6 Hz, 1H), 7.22 (ddd, *J* = 8.0, 4.8, 0.9 Hz, 1H), 5.92 (tq, *J* = 6.9, 1.5 Hz, 1H), 4.83 (dd, *J* = 6.8, 0.9 Hz, 2H), 3.77 (s, 3H), 2.11 (dt, *J* = 1.5, 0.7 Hz, 3H). ^{13}C NMR (100 MHz, $CDCl_3$) δ 155.8, 148.9, 147.4, 138.0, 137.8, 133.2, 123.2, 122.5, 64.6, 54.9, 16.1. IR (neat film, NaCl) 2957, 1748, 1568, 1444, 1415, 1378, 1327, 1263, 1129, 1022, 944, 792, 711, 624; HRMS (ESI+) *m/z* calc'd for $C_{11}H_{13}NO_3$ $[M+H]^+$: 208.0968, found 208.0972. Data for intermediate (*E*)-ester **47q** matched those previously reported;[38]

^{1}H NMR (400 MHz, $CDCl_3$) δ 8.73 (dd, *J* = 2.5, 0.9 Hz, 1H), 8.59 (dd, *J* = 4.8, 1.6 Hz, 1H), 7.75 (ddd, *J* = 8.0, 2.4, 1.6 Hz, 1H), 7.31 (ddd, *J* = 8.0, 4.8, 0.9 Hz, 1H), 6.14 (q, *J* = 1.4 Hz, 1H), 4.23 (q, *J* = 7.1 Hz, 2H), 2.58 (d, *J* = 1.4 Hz, 3H), 1.32 (t, *J* = 7.1 Hz, 3H).



(*E*)-methyl (3-phenylpent-2-en-1-yl) carbonate (31r)

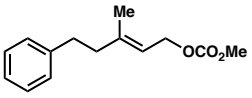
Prepared according to general procedure 2. ^{1}H NMR (400 MHz, $CDCl_3$) δ 7.40 – 7.30 (m, 1H), 7.24 – 7.15 (m, 3H), 5.59 (ddt, *J* = 6.9, 5.4, 1.5 Hz, 1H), 4.83 (dq, *J* = 6.9, 0.8 Hz, 2H), 3.81 (s, 3H), 2.07 (dt, *J* = 1.5, 0.8 Hz, 3H). All characterization data matched those reported in the literature.[34]



(*E*)-2-(chroman-4-ylidene)ethyl methyl carbonate (31s)

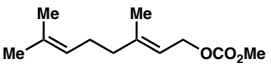
Prepared according to general procedure 2. Purified by column chromatography (10% EtOAc in hexanes) to provide the title compound as a colorless oil (514 mg, 80% yield); ^{1}H NMR (500 MHz, $CDCl_3$) δ 7.58 (dd, *J* = 8.0, 1.6 Hz, 1H), 7.21 (ddd, *J* = 8.5, 7.2, 1.6 Hz, 1H), 6.93 (ddd, *J* = 8.3, 7.2, 1.3 Hz, 1H), 6.88 (dd, *J* = 8.2, 1.2 Hz, 1H), 6.20 (tt, *J* = 7.3, 1.7 Hz, 1H), 4.87 (d, *J* = 7.3 Hz, 2H), 4.29 – 4.24 (m, 2H), 3.83 (s, 3H), 2.83 – 2.77 (m, 2H); ^{13}C NMR (100 MHz, $CDCl_3$) δ 156.0, 155.1, 134.7, 129.9, 124.4, 121.5, 121.0, 117.8, 114.3, 66.0, 64.0, 55.0, 26.0; IR (Neat Film, NaCl) 2957, 1744, 1650, 1605, 1575,

1484, 1454, 1375, 1351, 1264, 1119, 1051, 939 cm^{-1}; HRMS (FD+) *m/z* calc'd for $C_{13}H_{14}O_4$: 234.0887, found 234.0888. Data for intermediate (*E*)-ester **47s** matched those previously reported;[41] ^1H NMR (500 MHz, $CDCl_3$) δ 7.61 (dd, *J* = 8.0, 1.6 Hz, 1H), 7.30 – 7.25 (m, 1H), 7.00 – 6.81 (m, 2H), 6.35 (t, *J* = 1.7 Hz, 1H), 4.32 – 4.13 (m, 4H), 3.40 (ddd, *J* = 7.2, 5.5, 1.8 Hz, 2H), 1.33 (t, *J* = 7.1 Hz, 3H).



(*E*)-methyl (3-methyl-5-phenylpent-2-en-1-yl) carbonate (31t)

Prepared according to general procedure 2. ^1H NMR (400 MHz, $CDCl_3$) δ 7.31 – 7.26 (m, 2H), 7.22 – 7.15 (m, 3H), 5.40 (tq, *J* = 7.1, 1.3 Hz, 1H), 4.69 – 4.62 (m, 2H), 3.78 (s, 3H), 2.78 – 2.69 (m, 2H), 2.39 – 2.30 (m, 2H), 1.78 – 1.76 (m, 3H). All characterization data matched those reported in the literature.[34]



(*E*)-3,7-dimethylocta-2,6-dien-1-yl methyl carbonate (31u)

Prepared according to carbonate formation procedure in general procedure 2 from geraniol. ^1H NMR (400 MHz, $CDCl_3$) δ 5.37 (ddq, *J* = 7.2, 5.7, 1.3 Hz, 1H), 5.07 (dddd, *J* = 6.8, 5.4, 2.9, 1.4 Hz, 1H), 4.65 (dq, *J* = 7.2, 0.7 Hz, 2H), 3.77 (s, 3H), 2.15 – 1.99 (m, 4H), 1.73 – 1.71 (m, 3H), 1.68 (q, *J* = 1.3 Hz, 3H), 1.60 (d, *J* = 1.3 Hz, 3H). All characterization data matched those reported in the literature.[42]

1.11.3 Determination of Absolute Configuration of 32a via Vibrational Circular Dichroism (VCD)

1.11.3.1. Experimental Protocol

A solution of **32a** (50 mg/mL) in $CDCl_3$ was loaded into a front-loading SL-4 cell (International Crystal Laboratories) possessing BaF_2 windows and a 100 mm path length. Infrared (IR) and VCD spectra were acquired on a BioTools ChiralIR-2X VCD spectrometer as a set of 24 one-hour blocks (24 blocks, 3120 scans per block) in dual PEM mode. A 15-minute acquisition of neat (+)-α-pinene control yielded a VCD spectrum in agreement with literature spectra. IR and VCD spectra were background corrected using a 30-minute block IR acquisition of the empty instrument chamber under gentle N_2 purge, and were solvent corrected using a 16-hour (16 blocks, 3120 scans per block) IR/VCD acquisition of $CDCl_3$ in the same 100 μm BaF2 cell. The reported spectra represent the result of block averaging.

1.11.3.2. Computational Protocol

The arbitrarily chosen *(S)* enantiomer of compound **32a** was subjected to an exhaustive initial molecular mechanics-based conformational search (OPLS_2005 force field, $CHCl_3$ solvent, 10.0 kcal/mol cutoff, "Enhanced" torsional sampling) as implemented in MacroModel program.[43] The resulting ensemble containing 202 conformers was iteratively refined using the CENSO program of the Grimme group, interfaced to the Orca program of Neese, et. al. The refinement procedure includes the following steps:

1. Single point calculations with the B97-3c method. To these electronic energies are added thermochemical contributions calculated at the GFN2-xTB semi-empirical level of theory. 174 conformers remain within an energy window of 4.0 kcal/mol.

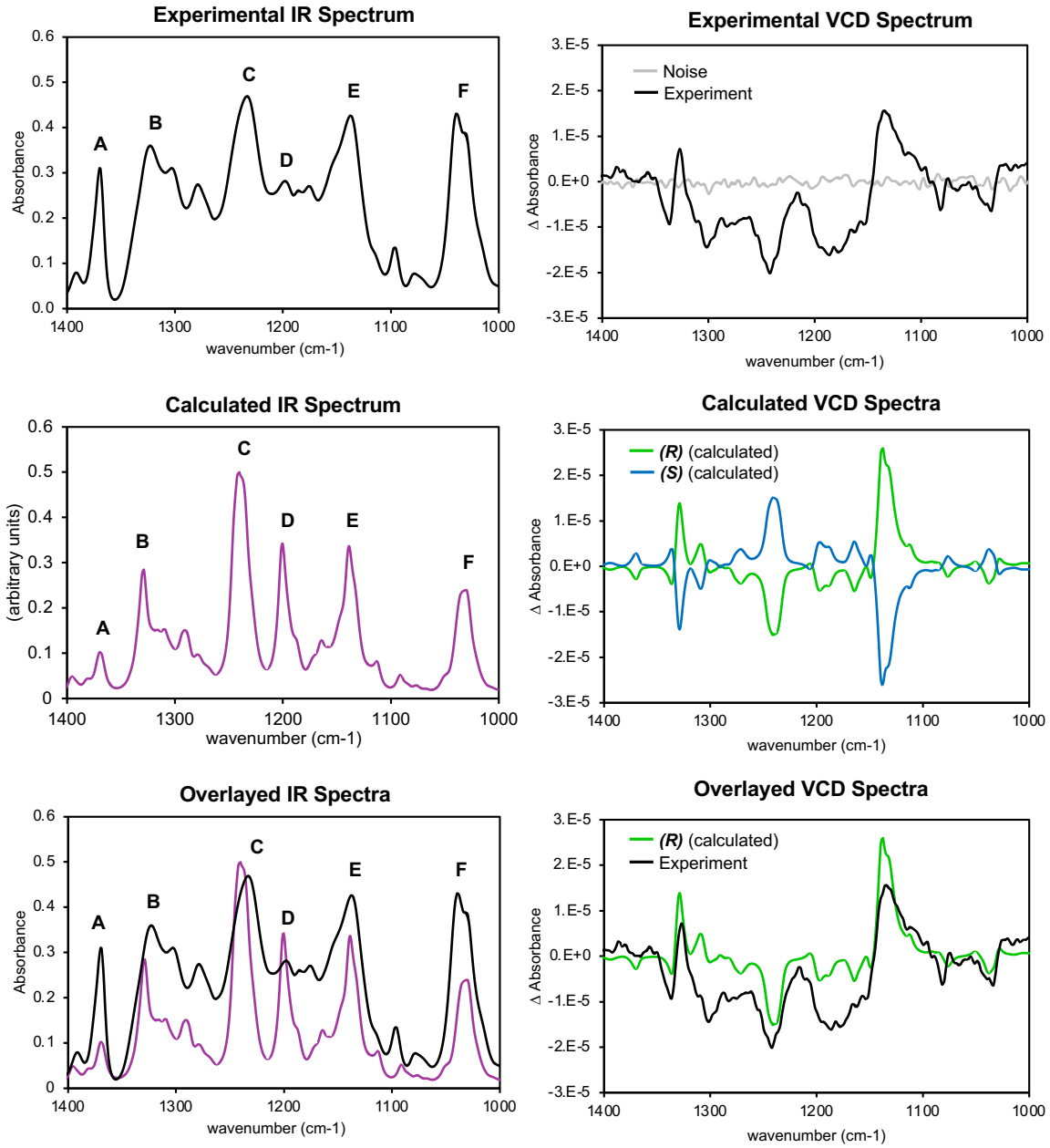
2. The conformer geometries are then optimized at the B97-3c level of theory employing a batchwise optimization procedure searching for parallel potential energy surfaces (default parameters in CENSO). 99 unique conformers remain.
3. Free energies are derived from adding thermochemical contributions calculated at the GFN2-xTB level of theory to the final electronic energies (B97-3c) from the optimizations. The 76 lowest energy conformers account for 99% of the Boltzmann population of conformers at 298.15 K (see table below).

ΔG (kcal/mol)	# conformers	Sum(Boltzmann_Pop)
0.0 – 0.5	17	64%
0.0 – 1.0	26	78%
0.0 – 1.5	46	93%
0.0 – 2.0	56	96%
0.0 – 2.5	**76**	**99%**
0.0 – 3.0	92	>99%
0.0 – 3.5	95	>99%
0.0 – 4.0	96	>99%
0.0 – 4.5	99	100%

The 76 lowest energy conformers are subsequently optimized using the B3PW91 functional, cc-pVTZ(-f) basis, and implicit PBF solvation model for chloroform using the Jaguar program.[44] Harmonic frequencies computed at the B3PW91/cc-pVTZ(-f)/PBF(chloroform) level were scaled by 0.98. The resultant 55 structurally unique conformers possessing all positive Hessian eigenvalues were Boltzmann weighted by relative free energy at 298.15 K. The predicted IR and VCD frequencies and intensities of the retained conformers were convolved using Lorentzian line shapes (γ = 4 cm^{-1}) and summed using the respective Boltzmann weights to yield the final predicted IR and VCD spectra of the *(S)* enantiomer of **32a**. The predicted VCD of the corresponding *(R)* enantiomer was generated by inversion of sign. From the reasonable agreement between the predicted and measured IR and VCD

spectra in the useful range (1000–1400 cm^{-1}, see below), the absolute configuration of **32a** was assigned as *(R)*.

Figure 1.11.3.1. *Experimental and computationally determined IR, VCD spectra of* ***32a*** *and overlayed experimentally and computationally determined IR, VCD spectra of* ***32a***.



1.11.3 References and Notes

(1) Liu, Y.; Han, S.-J.; Liu, W.-B.; Stoltz, B. M. Catalytic Enantioselective Construction of Quaternary Stereocenters: Assembly of Key Building Blocks for the Synthesis of Biologically Active Molecules. *Acc. Chem. Res.* **2015**, *48*, 740–751.

(2) Feng, J.; Holmes, M.; Krische, M. J. Acyclic Quaternary Carbon Stereocenters via Enantioselective Transition Metal Catalysis. *Chem. Rev.* **2017**, *117*, 12564–12580.

(3) Cheng, Q.; Tu, H.-F.; Zheng, C.; Qu, J.-P.; Helmchen, G.; You, S.-L. Iridium-Catalyzed Asymmetric Allylic Substitution Reactions. *Chem. Rev.* **2019**, *119*, 1855–1969.

(4) Pàmies, O.; Margalef, J.; Cañellas, S.; James, J.; Judge, E.; Guiry, P. J.; Moberg, C.; Bäckvall, J.-E.; Pfaltz, A.; Pericàs, M. A.; Diéguez, M. Recent Advances in Enantioselective Pd-Catalyzed Allylic Substitution: From Design to Applications. *Chem. Rev.* **2021**, *121*, 4373–4505.

(5) Hethcox, J. C.; Shockley, S. E.; Stoltz, B. M. Iridium-Catalyzed Diastereo-, Enantio-, and Regioselective Allylic Alkylation with Prochiral Enolates. *ACS Catal.* **2016**, *6*, 6207–6213.

(6) Takeuchi, R.; Kashio, M. Highly Selective Allylic Alkylation with a Carbon Nucleophile at the More Substituted Allylic Terminus Catalyzed by an Iridium Complex: An Efficient Method for Constructing Quaternary Carbon Centers. *Angew. Chem. Int. Ed.* **1997**, *36*, 263–265.

(7) Bartels, B.; García-Yebra, C.; Helmchen, G. Asymmetric IrI-Catalysed Allylic Alkylation Of Monosubstituted Allylic Acetates With Phosphorus Amidites As Ligands. *Eur. J. Org. Chem.* **2003**, *2003*, 1097–1103.

(8) Janssen, J. P.; Helmchen, G. First Enantioselective Alkylations of Monosubstituted Allylic Acetates Catalyzed by Chiral Iridium Complexes. *Tetrahedron Lett.* **1997**, *38*, 8025–8026.

(9) Rössler, S. L.; Petrone, D. A.; Carreira, E. M. Iridium-Catalyzed Asymmetric Synthesis of Functionally Rich Molecules Enabled by (Phosphoramidite,Olefin) Ligands. *Acc. Chem. Res.* **2019**, *52*, 2657–2672.

(10) Hartwig, J. F.; Stanley, L. M. Mechanistically Driven Development of Iridium Catalysts for Asymmetric Allylic Substitution. *Acc. Chem. Res.* **2010**, *43*, 1461–1475.

(11) Liu, W.-B.; Zheng, C.; Zhuo, C.-X.; Dai, L.-X.; You, S.-L. Iridium-Catalyzed Allylic Alkylation Reaction with N-Aryl Phosphoramidite Ligands: Scope and Mechanistic Studies. *J. Am. Chem. Soc.* **2012**, *134*, 4812–4821.

(12) Qu, J.; Helmchen, G. Applications of Iridium-Catalyzed Asymmetric Allylic Substitution Reactions in Target-Oriented Synthesis. *Acc. Chem. Res.* **2017**, *50*, 2539–2555.

(13) Ketcham, J. M.; Shin, I.; Montgomery, T. P.; Krische, M. J. Catalytic Enantioselective C–H Functionalization of Alcohols by Redox-Triggered Carbonyl Addition: Borrowing Hydrogen, Returning Carbon. *Angew. Chem. Int. Ed.* **2014**, *53*, 9142–9150.

(14) Kim, S. W.; Zhang, W.; Krische, M. J. Catalytic Enantioselective Carbonyl Allylation and Propargylation via Alcohol-Mediated Hydrogen Transfer: Merging the Chemistry of Grignard and Sabatier. *Acc. Chem. Res.* **2017**, *50*, 2371–2380.

(15) Madrahimov, S. T.; Hartwig, J. F. Origins of Enantioselectivity during Allylic Substitution Reactions Catalyzed by Metallacyclic Iridium Complexes. *J. Am. Chem. Soc.* **2012**, *134*, 8136–8147.

(16) Raskatov, J. A.; Spiess, S.; Gnamm, C.; Brödner, K.; Rominger, F.; Helmchen, G. Ir-Catalysed Asymmetric Allylic Substitutions with Cyclometalated (Phosphoramidite)Ir Complexes—Resting States, Catalytically Active (π-Allyl)Ir Complexes and Computational Exploration. *Chem. – Eur. J.* **2010**, *16*, 6601–6615.

(17) Madrahimov, S. T.; Li, Q.; Sharma, A.; Hartwig, J. F. Origins of Regioselectivity in Iridium Catalyzed Allylic Substitution. *J. Am. Chem. Soc.* **2015**, *137*, 14968–14981.

(18) Liu, W.-B.; Reeves, C. M.; Stoltz, B. M. Enantio-, Diastereo-, and Regioselective Iridium-Catalyzed Asymmetric Allylic Alkylation of Acyclic β-Ketoesters. *J. Am. Chem. Soc.* **2013**, *135*, 17298–17301.

(19) Shockley, S. E.; Hethcox, J. C.; Stoltz, B. M. Enantioselective Synthesis of Acyclic α-Quaternary Carboxylic Acid Derivatives through Iridium-Catalyzed Allylic Alkylation. *Angew. Chem. Int. Ed.* **2017**, *56*, 11545–11548.

(20) Hethcox, J. C.; Shockley, S. E.; Stoltz, B. M. Enantioselective Synthesis of Vicinal All-Carbon Quaternary Centers via Iridium-Catalyzed Allylic Alkylation. *Angew. Chem. Int. Ed.* **2018**, *57*, 8664–8667.

(21) Isomura, M.; Petrone, D. A.; Carreira, E. M. Construction of Vicinal Quaternary Centers via Iridium-Catalyzed Asymmetric Allenylic Alkylation of Racemic Tertiary Alcohols. *J. Am. Chem. Soc.* **2021**, *143*, 3323–3329.

(22) Onodera, G.; Watabe, K.; Matsubara, M.; Oda, K.; Kezuka, S.; Takeuchi, R. Iridium-Catalyzed Enantioselective Allylic Alkylation Using Chiral Phosphoramidite Ligand Bearing an Amide Moiety. *Adv. Synth. Catal.* **2008**, *350*, 2725–2732.

(23) Pinna, G. A.; Cignarella, G.; Loriga, G.; Murineddu, G.; Mussinu, J.-M.; Ruiu, S.; Fadda, P.; Fratta, W. *N*-3(9)-Arylpropenyl-*N*-9(3)-Propionyl-3,9-

Diazabicyclo[3.3.1]Nonanes as μ-Opioid Receptor Agonists. Effects on μ-Affinity of Arylalkenyl Chain Modifications. *Bioorg. Med. Chem.* **2002**, *10*, 1929–1937.

(24) Helmchen, G.; Kazmaier, U.; Förster, S. Enantioselective Allylic Substitutions with Carbon Nucleophiles. In *Asymmetric Carbon–Carbon Bond-Forming Reactions;* Iwao, O., Ed.; Catalytic Asymmetric Synthesis; John Wiley & Sons, Hoboken, New Jersey; 3rd Edition, pp 497–641.

(25) Hartwig, J. F.; Pouy, M. J. Iridium-Catalyzed Allylic Substitution. In *Iridium Catalysis*; Andersson, P. G., Ed.; Topics in Organometallic Chemistry; Springer Berlin Heidelberg: Berlin, Heidelberg, 2011; Vol. 34, pp 169–208.

(26) Rusu, A.; Tanase, C.; Pascu, G.-A.; Todoran, N. Recent Advances Regarding the Therapeutic Potential of Adapalene. *Pharmaceuticals* **2020**, *13*, 217.

(27) Fadel, A.; Vandromme, L. Total Synthesis of (−)-Sporochnol A, the Fish Deterrent, from a Chiral Malonate. *Tetrahedron Asymmetry* **1999**, *10*, 1153–1162.

(28) Srikrishna, A.; Satyanarayana, G.; Prasad, M. R. Synthetic Approaches to Sporochnols A–C. *Synth. Commun.* **2005**, *35*, 1687–1698.

(29) Pangborn, A. B.; Giardello, M. A.; Grubbs, R. H.; Rosen, R. K.; Timmers, F. J. Safe and Convenient Procedure for Solvent Purification. *Organometallics* **1996**, *15*, 1518–1520.

(30) Liu, W.-B.; Zheng, C.; Zhuo, C.-X.; Dai, L.-X.; You, S.-L. Iridium-Catalyzed Allylic Alkylation Reaction with N-Aryl Phosphoramidite Ligands: Scope and Mechanistic Studies. *J. Am. Chem. Soc.* **2012**, *134*, 4812–4821.

(31) Hamilton, J. Iridium-Catalyzed Enantioselective Allylic Vinylation with Potassium Alkenyltrifluoroborates. *Org. Synth.* **2015**, *92*, 1–12.

(32) Matsubara, R.; Jamison, T. F. Nickel-Catalyzed Allylic Substitution of Simple Alkenes. *J. Am. Chem. Soc.* **2010**, *132*, 6880–6881.

(33) Evans, P. A.; Oliver, S.; Chae, J. Rhodium-Catalyzed Allylic Substitution with an Acyl Anion Equivalent: Stereospecific Construction of Acyclic Quaternary Carbon Stereogenic Centers. *J. Am. Chem. Soc.* **2012**, *134*, 19314–19317.

(34) Guzman-Martinez, A.; Hoveyda, A. H. Enantioselective Synthesis of Allylboronates Bearing a Tertiary or Quaternary B-Substituted Stereogenic Carbon by NHC-Cu-Catalyzed Substitution Reactions. *J. Am. Chem. Soc.* **2010**, *132*, 10634–10637.

(35) Sauerberg, P.; Bury, P. S.; Mogensen, J. P.; Deussen, H.-J.; Pettersson, I.; Fleckner, J.; Nehlin, J.; Frederiksen, K. S.; Albrektsen, T.; Din, N.; Svensson, L. A.; Ynddal, L.; Wulff, E. M.; Jeppesen, L. Large Dimeric Ligands with Favorable Pharmacokinetic Properties and Peroxisome Proliferator-Activated Receptor Agonist Activity in Vitro and in Vivo. *J. Med. Chem.* **2003**, *46*, 4883–4894.

(36) Meiß, R.; Kumar, K.; Waldmann, H. Divergent Gold(I)-Catalyzed Skeletal Rearrangements of 1,7-Enynes. *Chem. – Eur. J.* **2015**, *21*, 13526–13530.

(37) Ando, K.; Yamada, K. Highly E-Selective Solvent-Free Horner–Wadsworth–Emmons Reaction Catalyzed by DBU. *Green Chem.* **2011**, *13*, 1143–1146.

(38) Metternich, J. B.; Gilmour, R. A Bio-Inspired, Catalytic E → Z Isomerization of Activated Olefins. *J. Am. Chem. Soc.* **2015**, *137*, 11254–11257.

(39) Dong, X.; Ma, P.; Zhang, T.; Jalani, H. B.; Li, G.; Lu, H. Iridium-Catalyzed C–H Amination of Weinreb Amides: A Facile Pathway toward Anilines and Quinazolin-2,4-Diones. *J. Org. Chem.* **2020**, *85*, 13096–13107.

(40) Link, A.; Zhou, Y.; Buchwald, S. L. CuH-Catalyzed Asymmetric Reductive Amidation of α,β-Unsaturated Carboxylic Acids. *Org. Lett.* **2020**, *22*, 5666–5670.

(41) Lei, J.; Liu, X.; Zhang, S.; Jiang, S.; Huang, M.; Wu, X.; Zhu, Q. Copper-Catalyzed Trifluoromethylation of Trisubstituted Allylic and Homoallylic Alcohols. *Chem. – Eur. J.* **2015**, *21*, 6700–6703.

(42) Chen, Y.; Song, X.; Gao, L.; Song, Z. Intramolecular Sakurai Allylation of Geminal Bis(Silyl) Enamide with Indolenine. A Diastereoselective Cyclization To Form Functionalized Hexahydropyrido[3,4-b]Indole. *Org. Lett.* **2021**, *23*, 124–128.

(43) *Schrödinger Release 2021-4*. Schrödinger.

(44) Bochevarov, A. D.; Harder, E.; Hughes, T. F.; Greenwood, J. R.; Braden, D. A.; Philipp, D. M.; Rinaldo, D.; Halls, M. D.; Zhang, J.; Friesner, R. A. Jaguar: A High-Performance Quantum Chemistry Software Program with Strengths in Life and Materials Sciences. *Int. J. Quantum Chem.* **2013**, *113*, 2110–2142.

APPENDIX 1

Spectra Relevant to Chapter 1:

Iridium Catalyzed Asymmetric Allylic Alkylation of Dialkyl Malonates

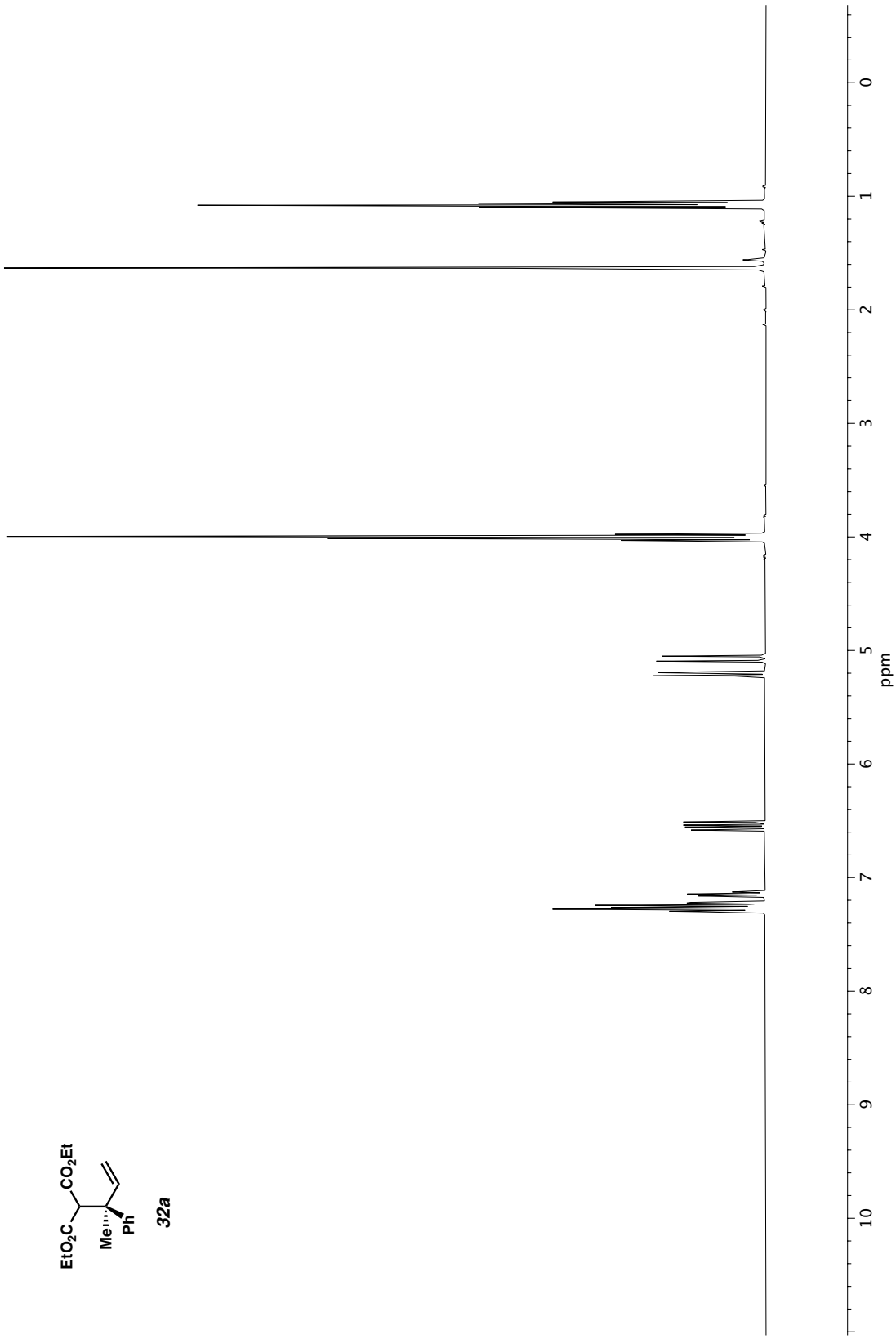


Figure A1.1 *^1H NMR (400 MHz, $CDCl_3$) of compound* ***32a***.

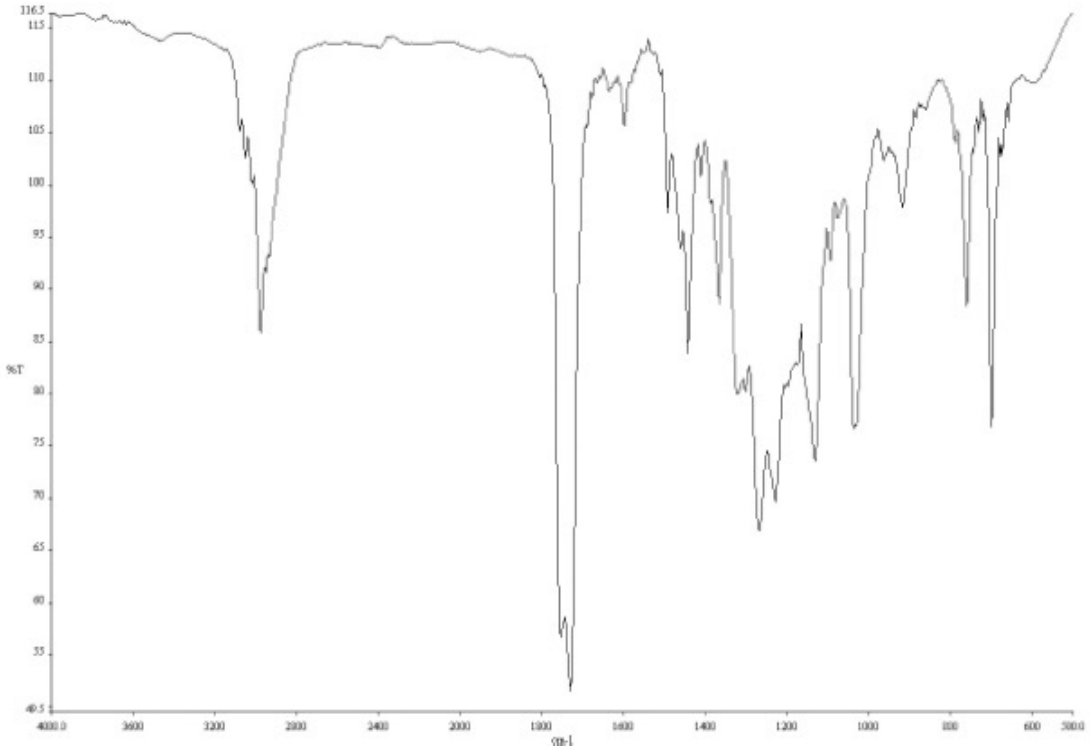


Figure A1.2 *Infrared spectrum (Thin Film, NaCl) of compound* ***32a***.

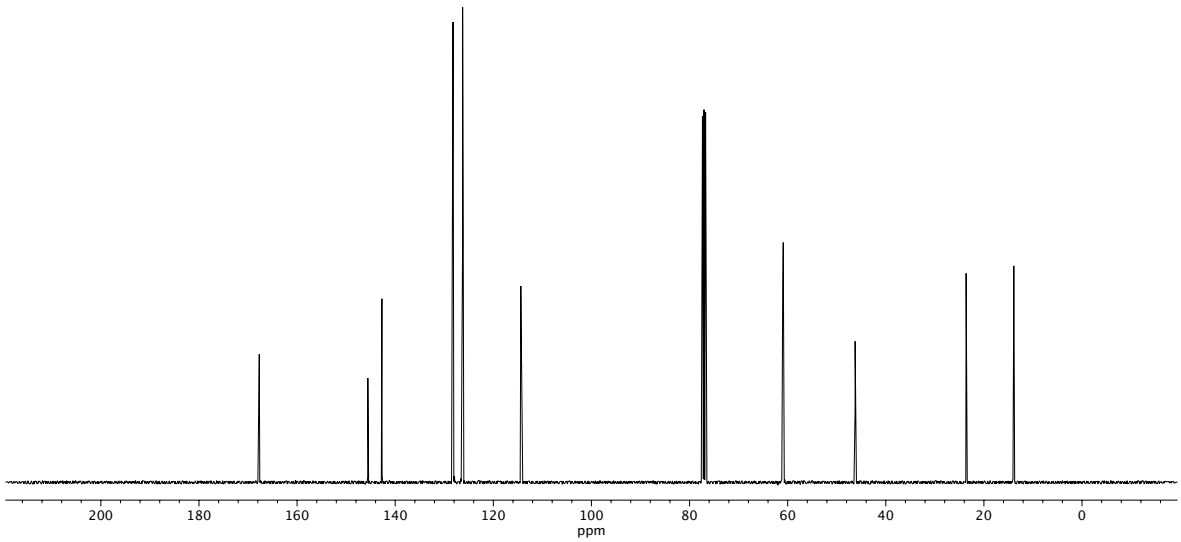


Figure A1.3 *^{13}C NMR (100 MHz, $CDCl_3$) of compound* ***32a***.

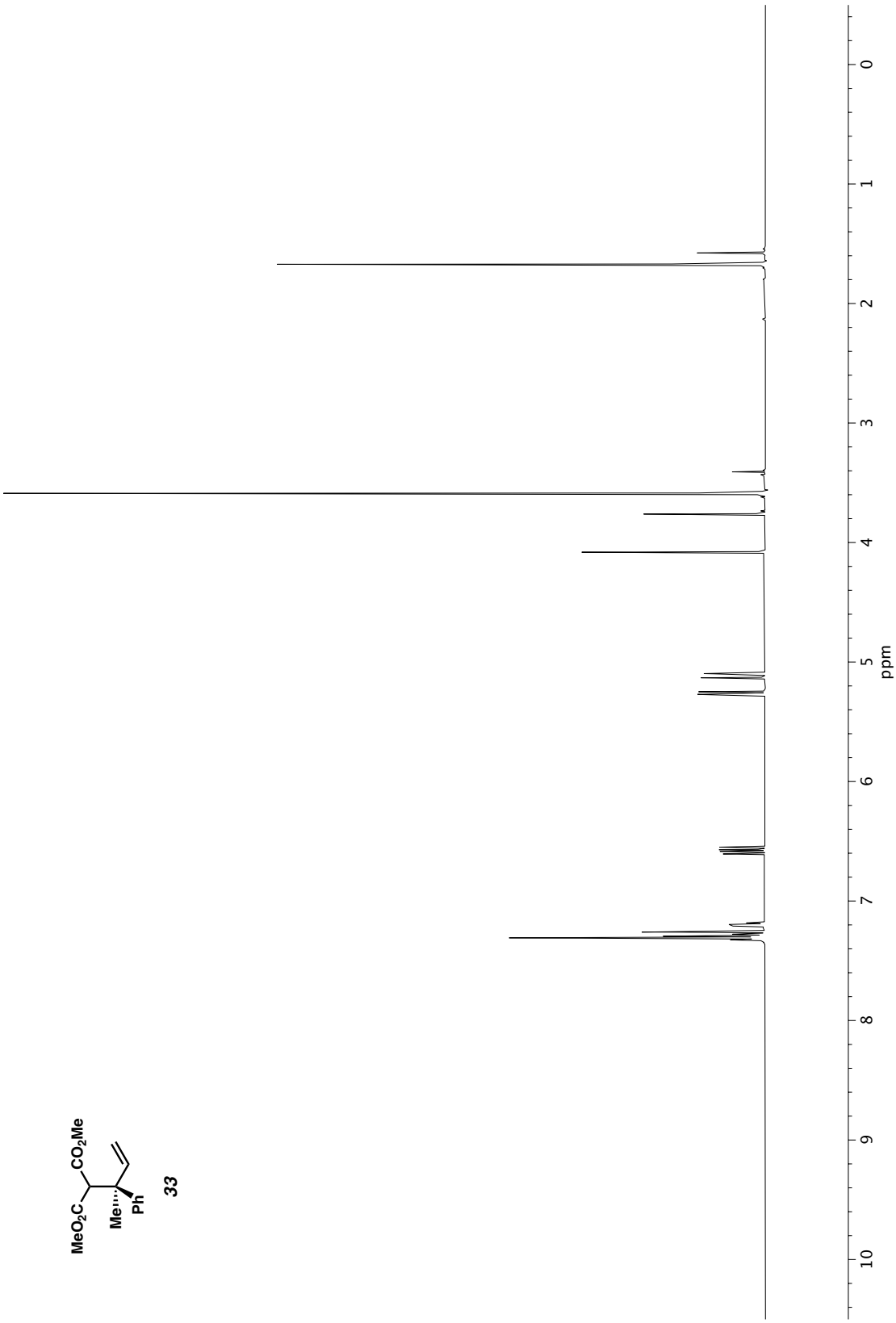


Figure A1.4 *^1H NMR (500 MHz, $CDCl_3$) of compound* ***33***.

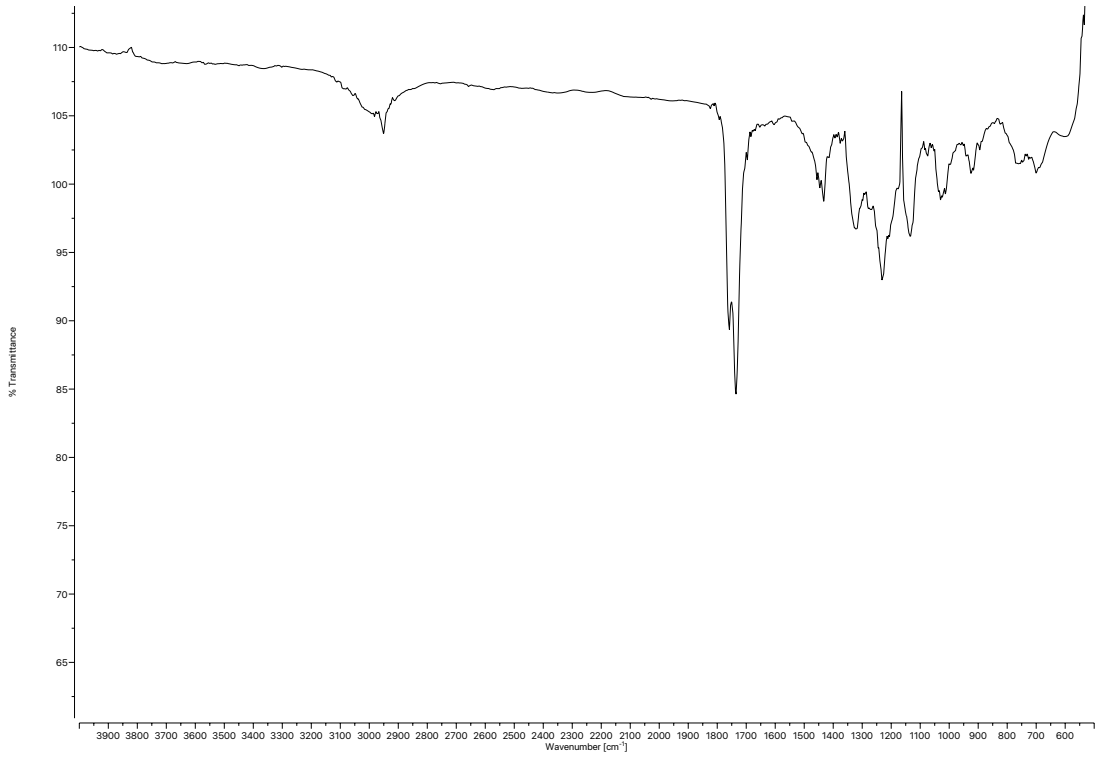


Figure A1.5 *Infrared spectrum (Thin Film, NaCl) of compound* ***33***.

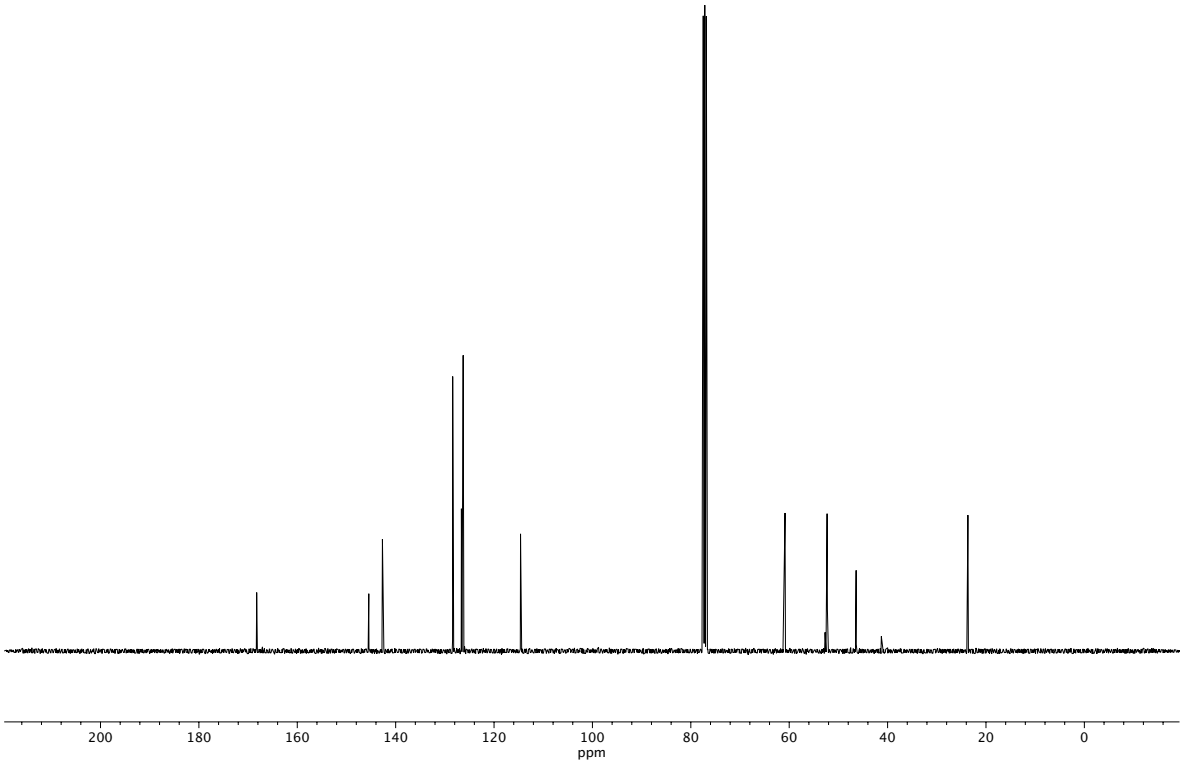


Figure A1.6 *^{13}C NMR (100 MHz, $CDCl_3$) of compound* ***33***.

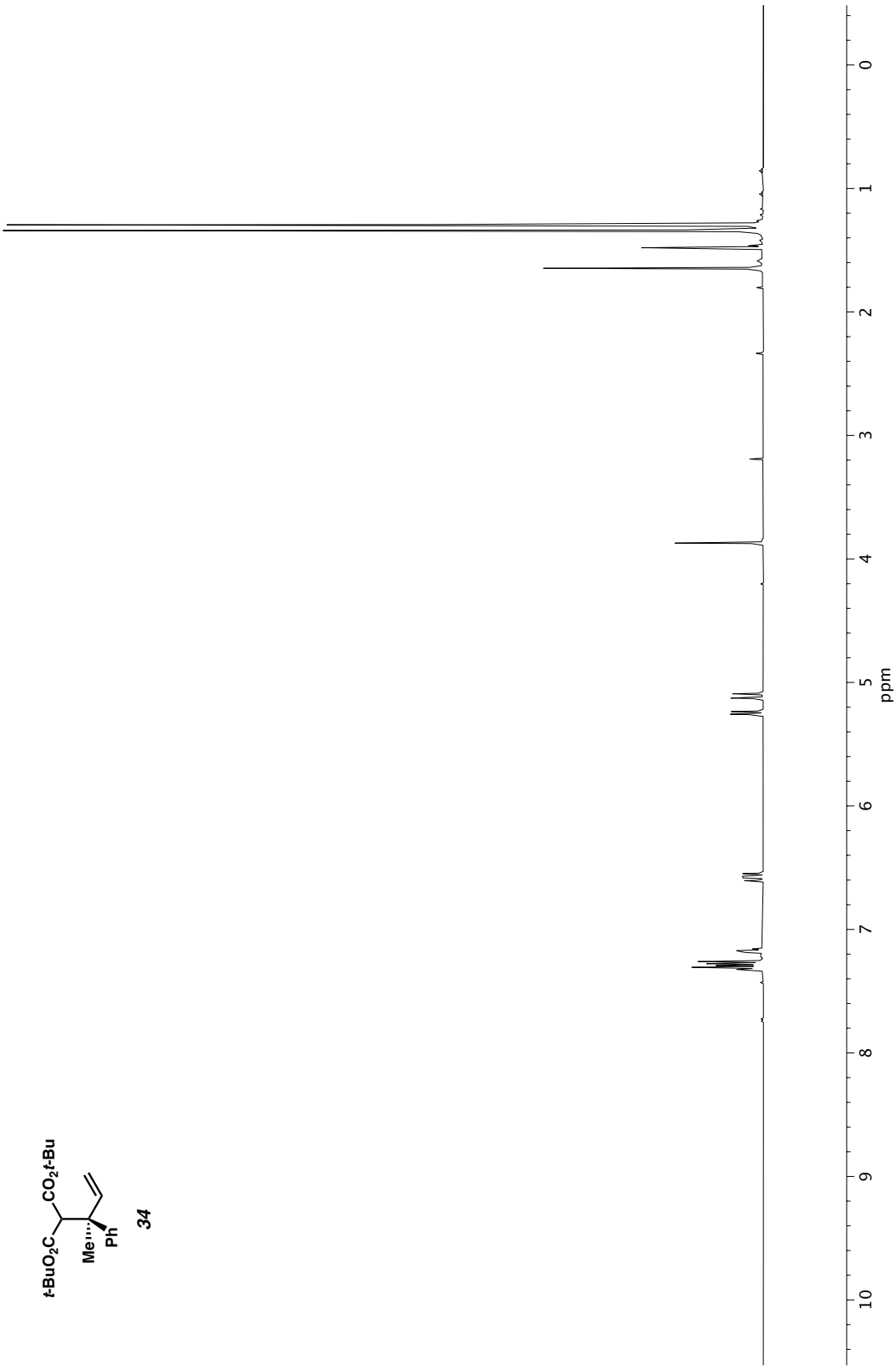


Figure A1.7 *^1H NMR (500 MHz, $CDCl_3$) of compound **34**.*

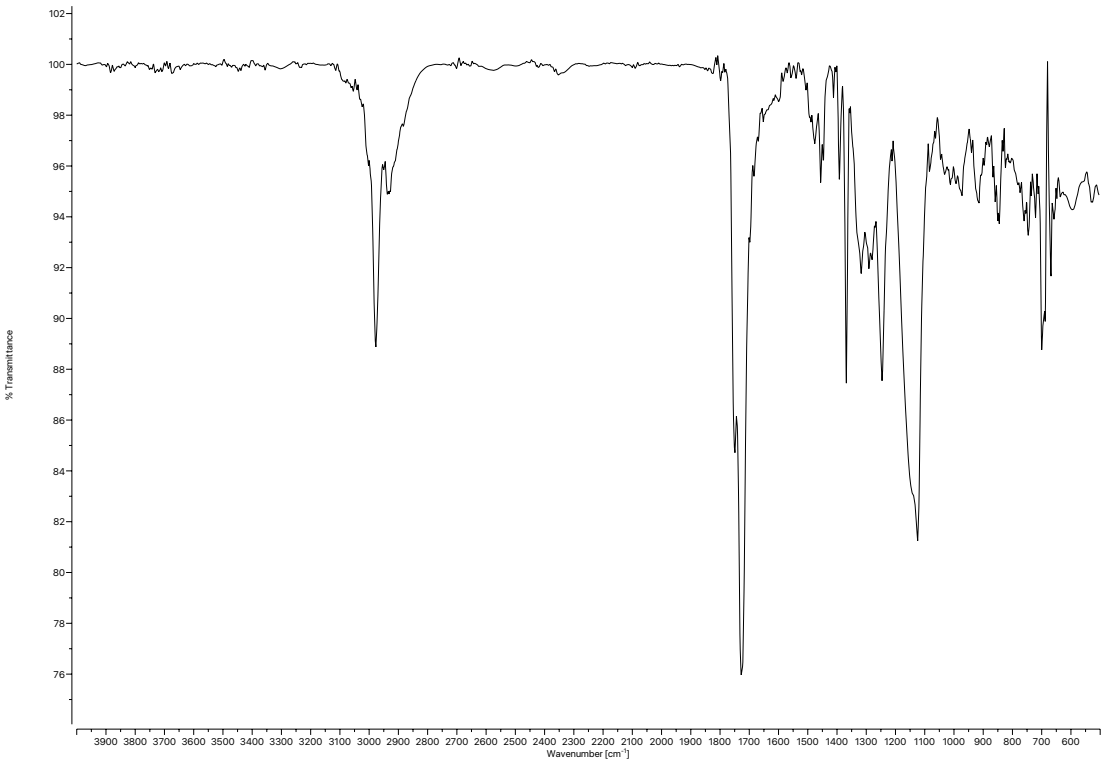


Figure A1.8 *Infrared spectrum (Thin Film, NaCl) of compound* ***34****.*

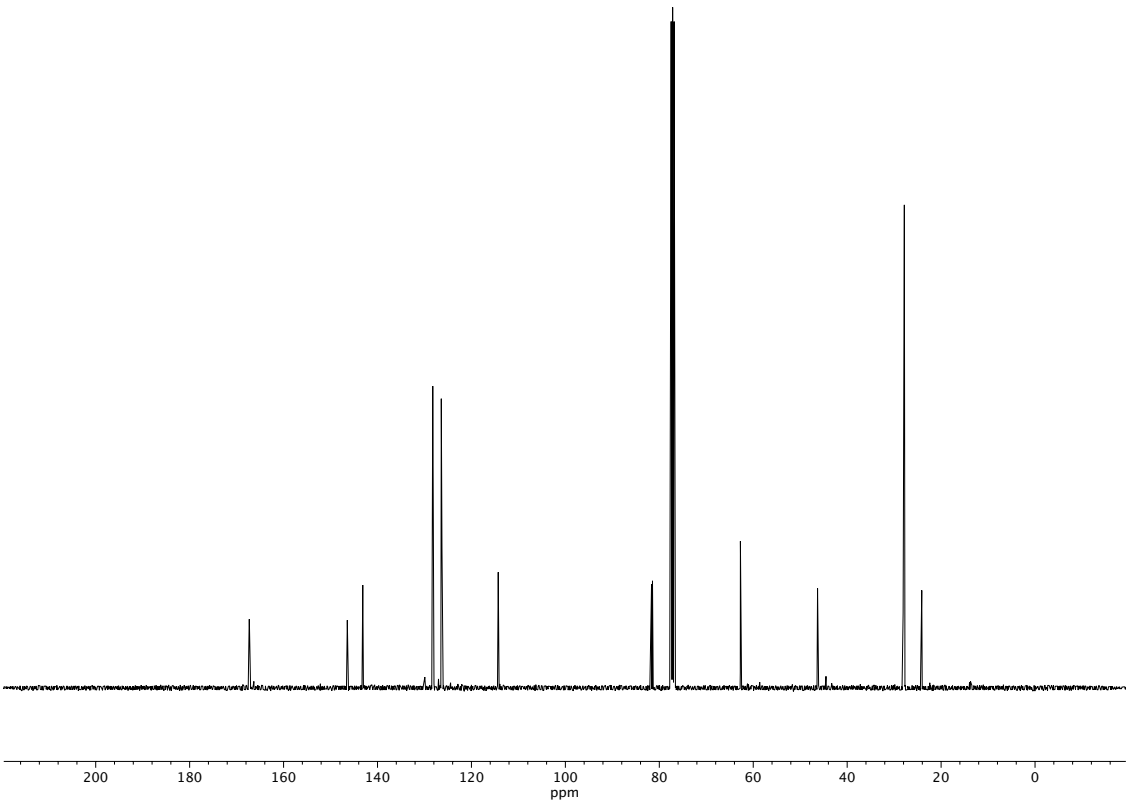


Figure A1.9 *^{13}C NMR (100 MHz, $CDCl_3$) of compound* ***34****.*

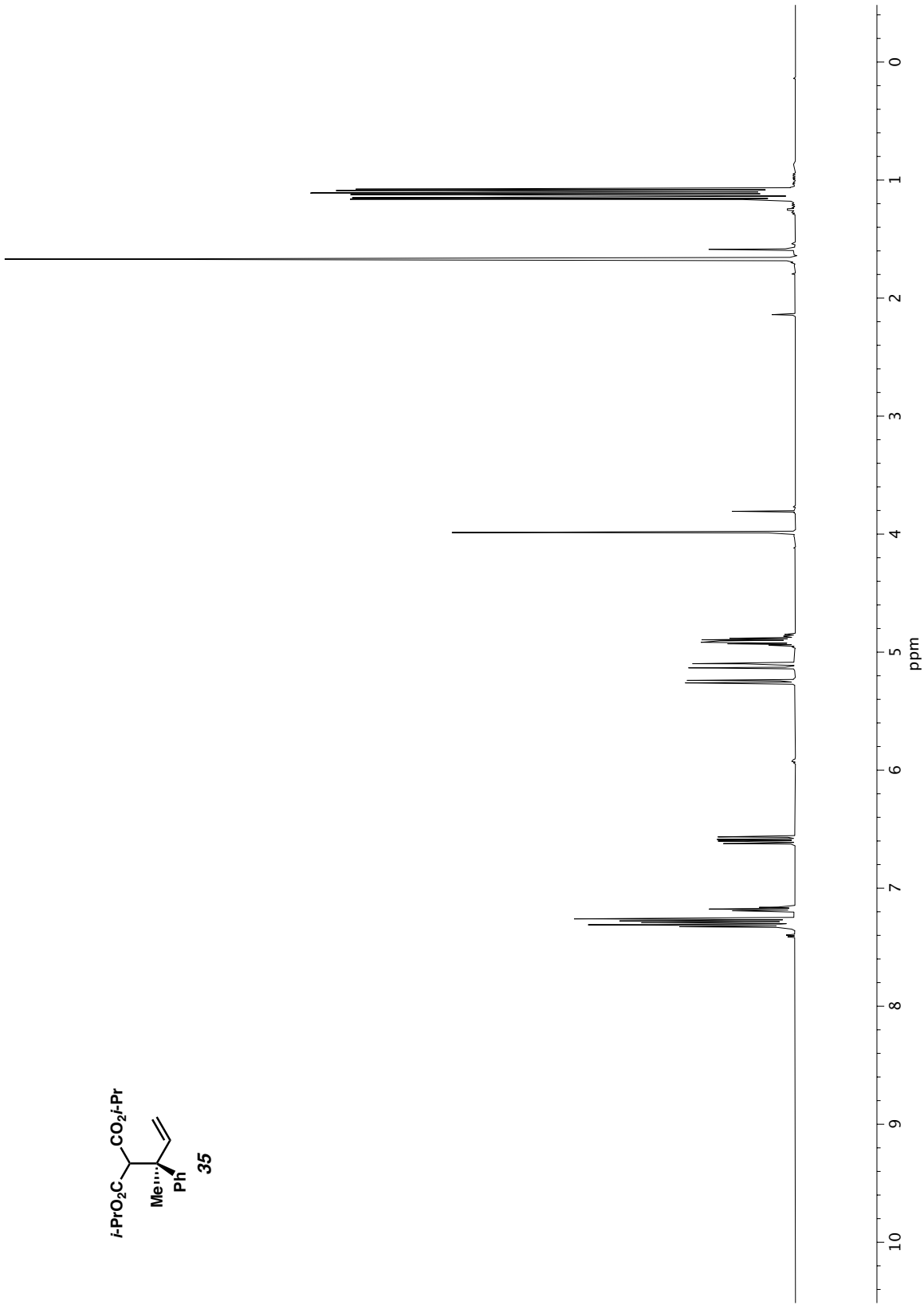


Figure A1.10 *^{1}H NMR (500 MHz, $CDCl_3$) of compound **35**.*

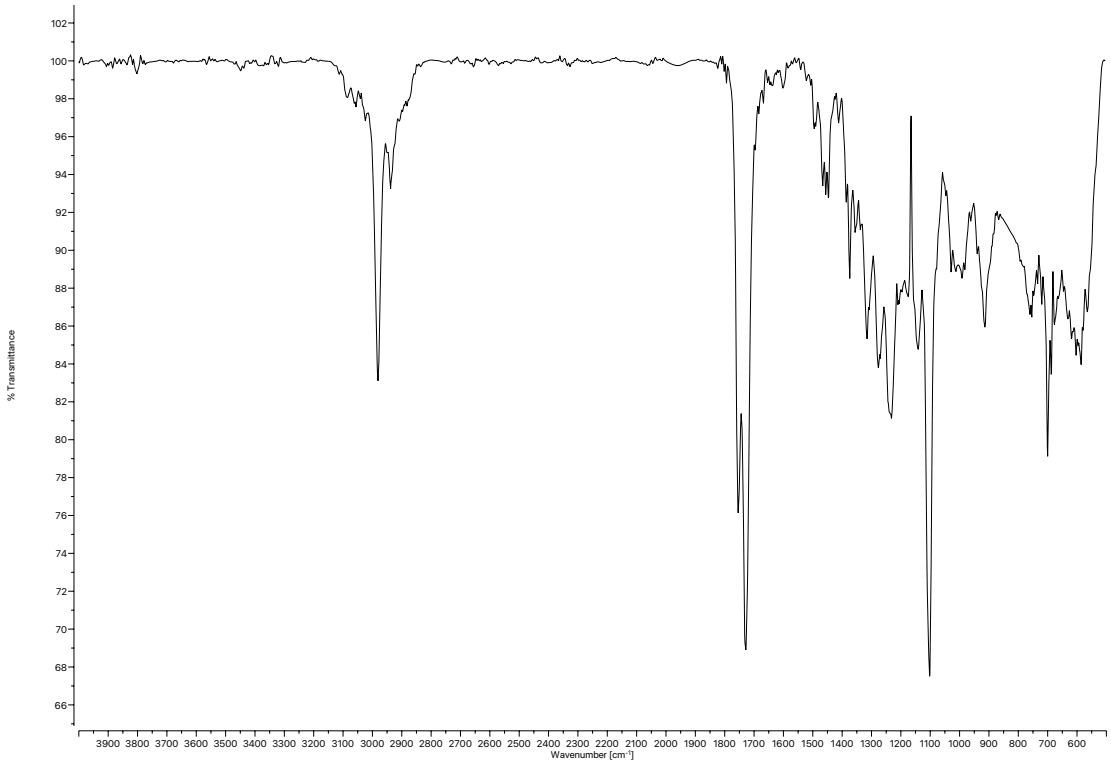


Figure A1.11 *Infrared spectrum (Thin Film, NaCl) of compound* ***35***.

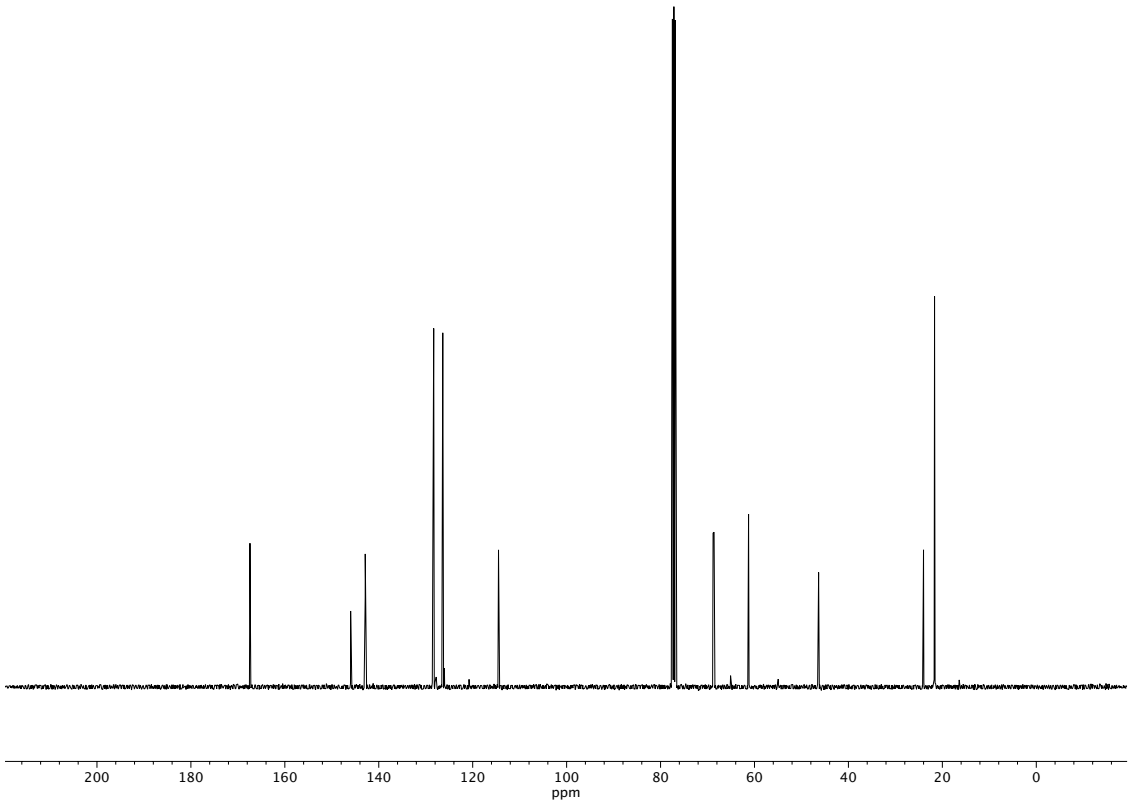


Figure A1.12 *^{13}C NMR (100 MHz, $CDCl_3$) of compound* ***35***.

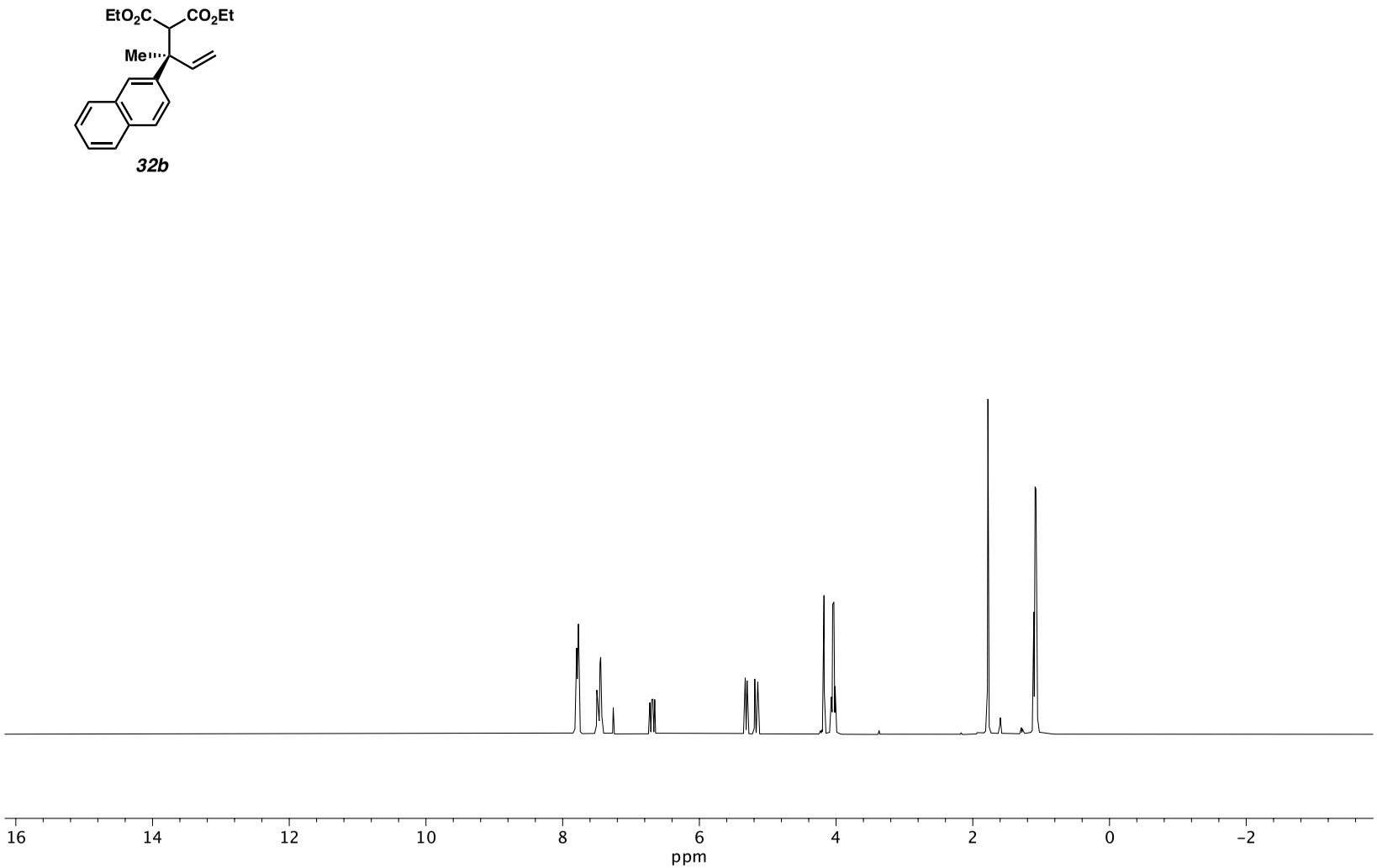


Figure A1.13 *^{1}H NMR (400 MHz, $CDCl_3$) of compound* ***32b****.*

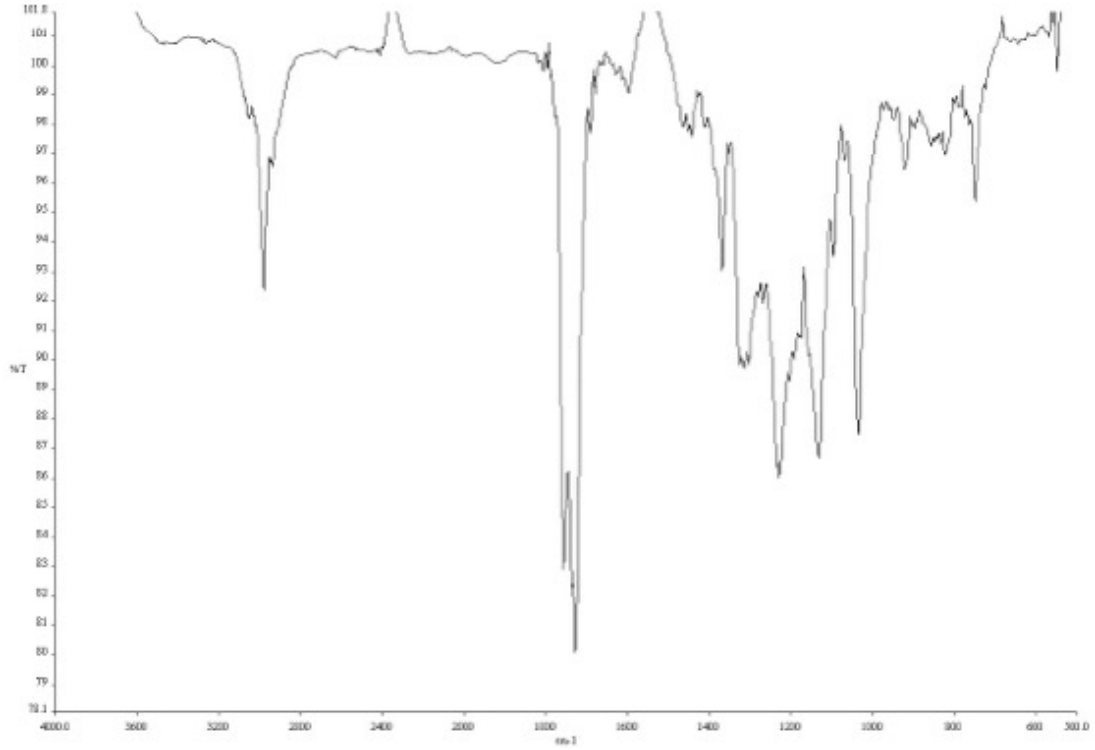


Figure A1.14 *Infrared spectrum (Thin Film, NaCl) of compound* ***32b****.*

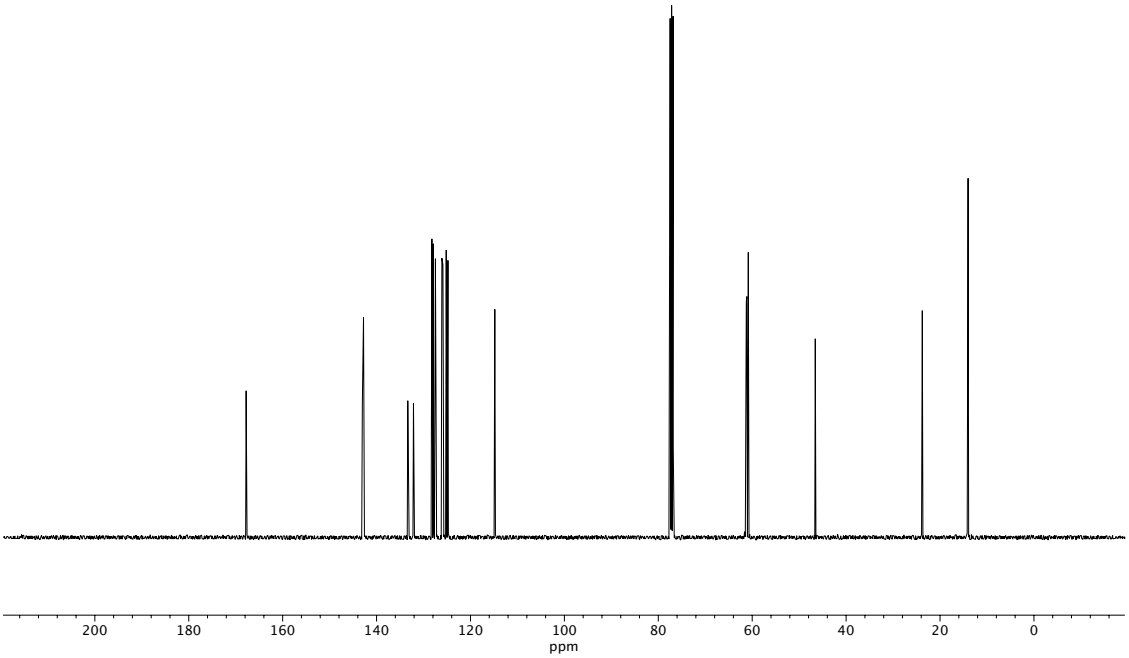


Figure A1.15 *^{13}C NMR (100 MHz, $CDCl_3$) of compound* ***32b****.*

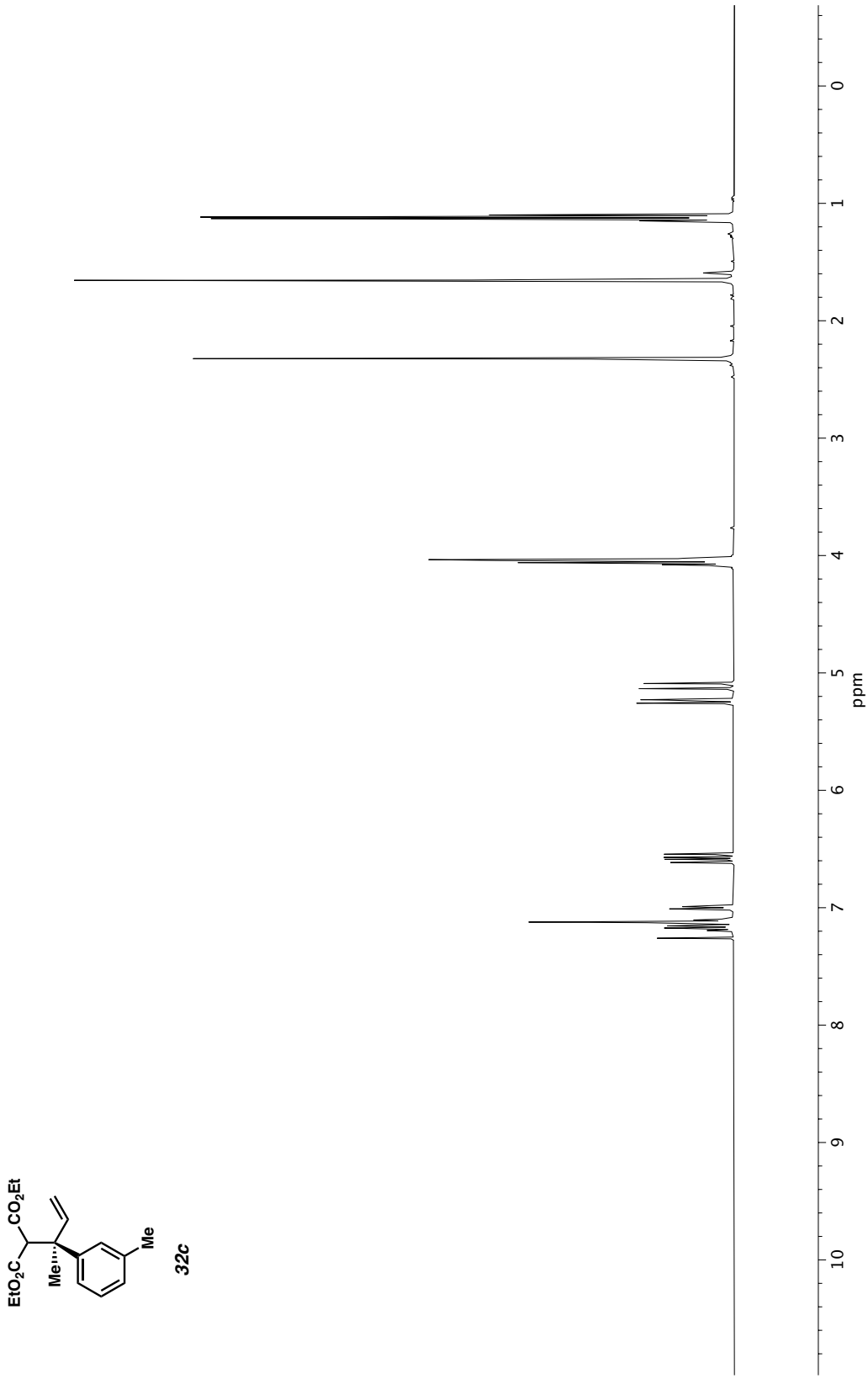


Figure A1.16 *^{1}H NMR (400 MHz, $CDCl_3$) of compound* ***32c****.*

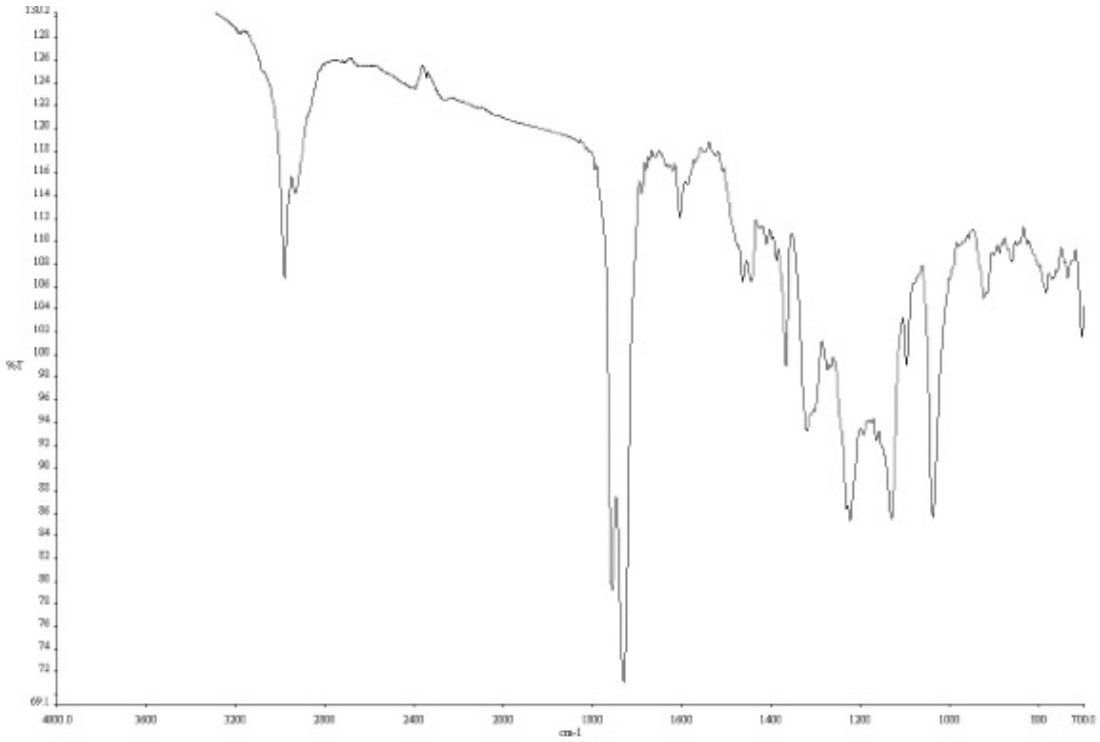


Figure A1.17 *Infrared spectrum (Thin Film, NaCl) of compound* ***32c****.*

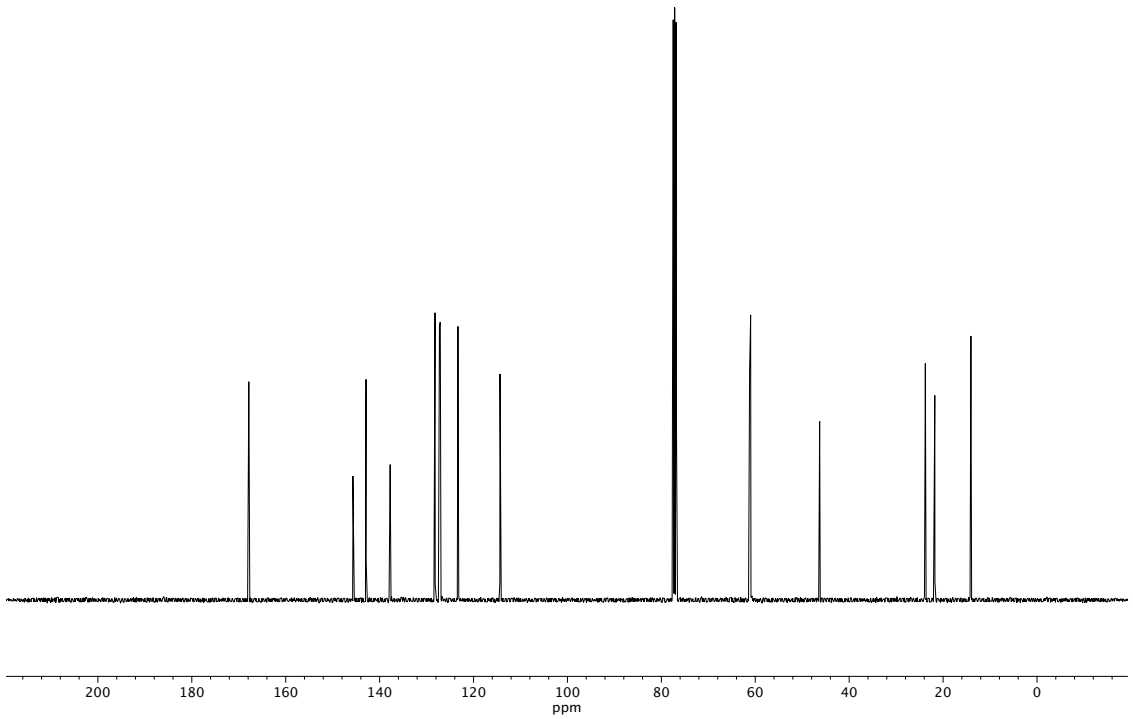


Figure A1.18 *^{13}C NMR (100 MHz, $CDCl_3$) of compound* ***32c****.*

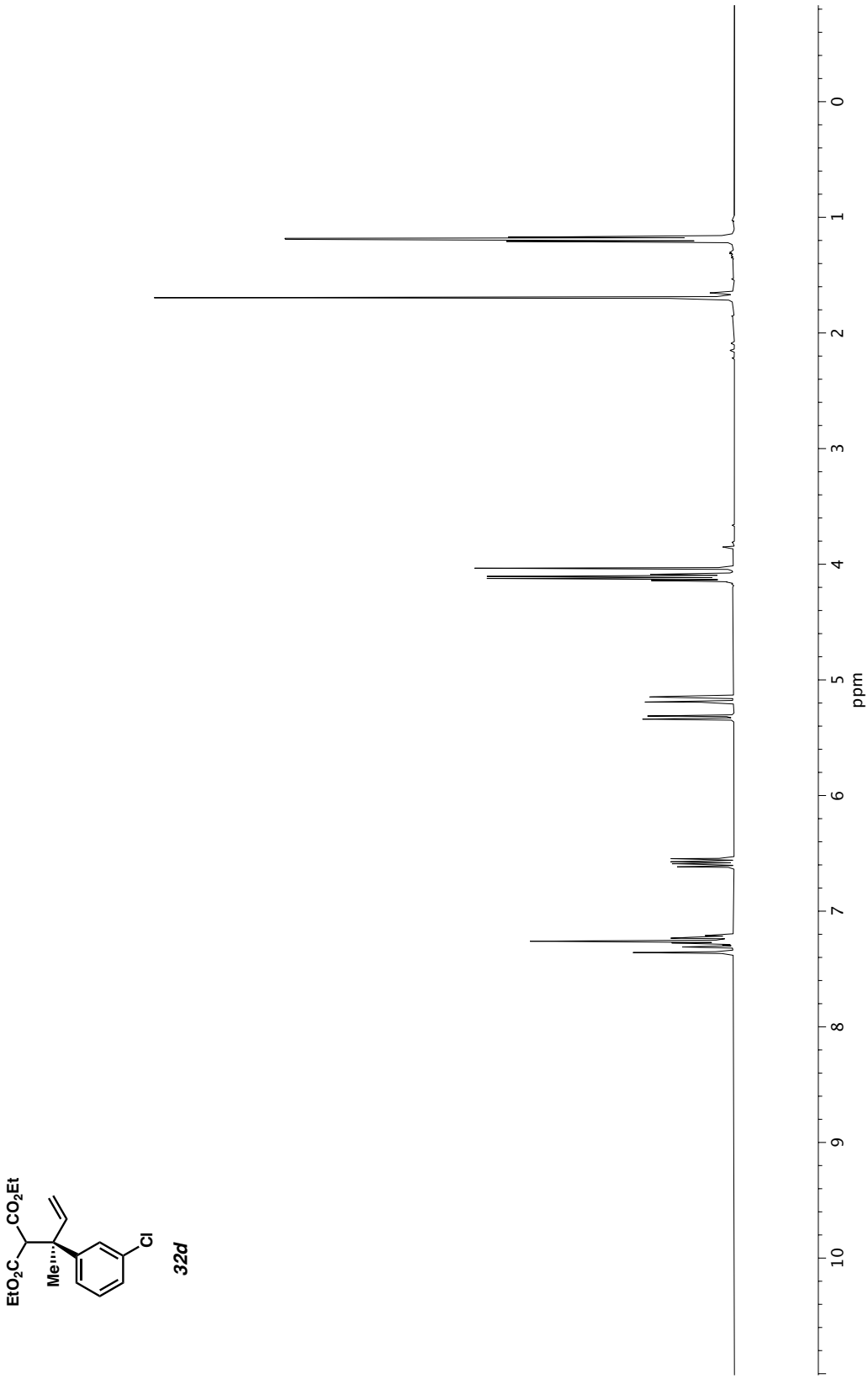


Figure A1.19 *^1H NMR (400 MHz, $CDCl_3$) of compound* ***32d****.*

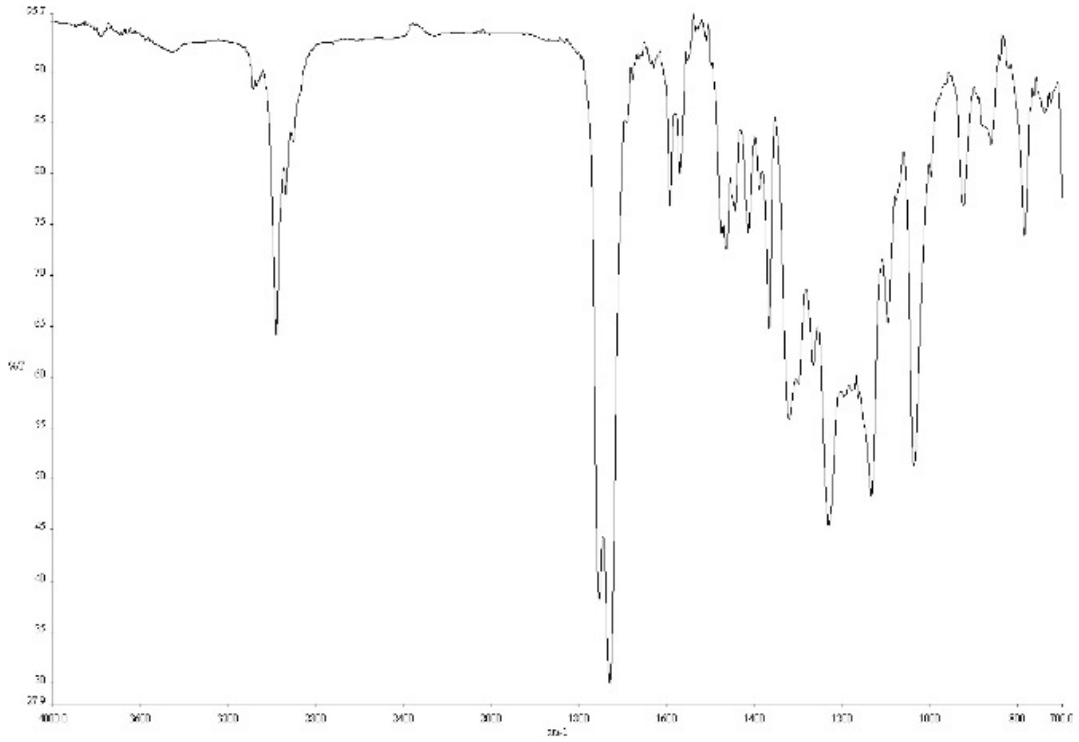


Figure A1.20 *Infrared spectrum (Thin Film, NaCl) of compound* ***32d****.*

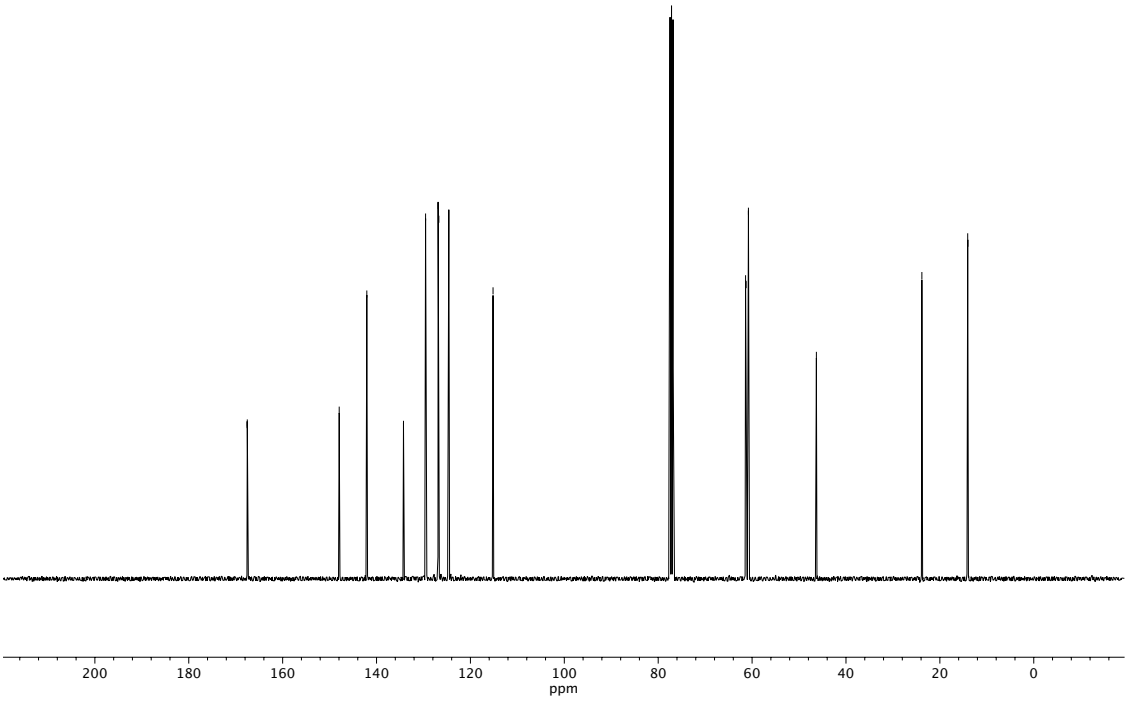


Figure A1.21 *^{13}C NMR (100 MHz, $CDCl_3$) of compound* ***32d****.*

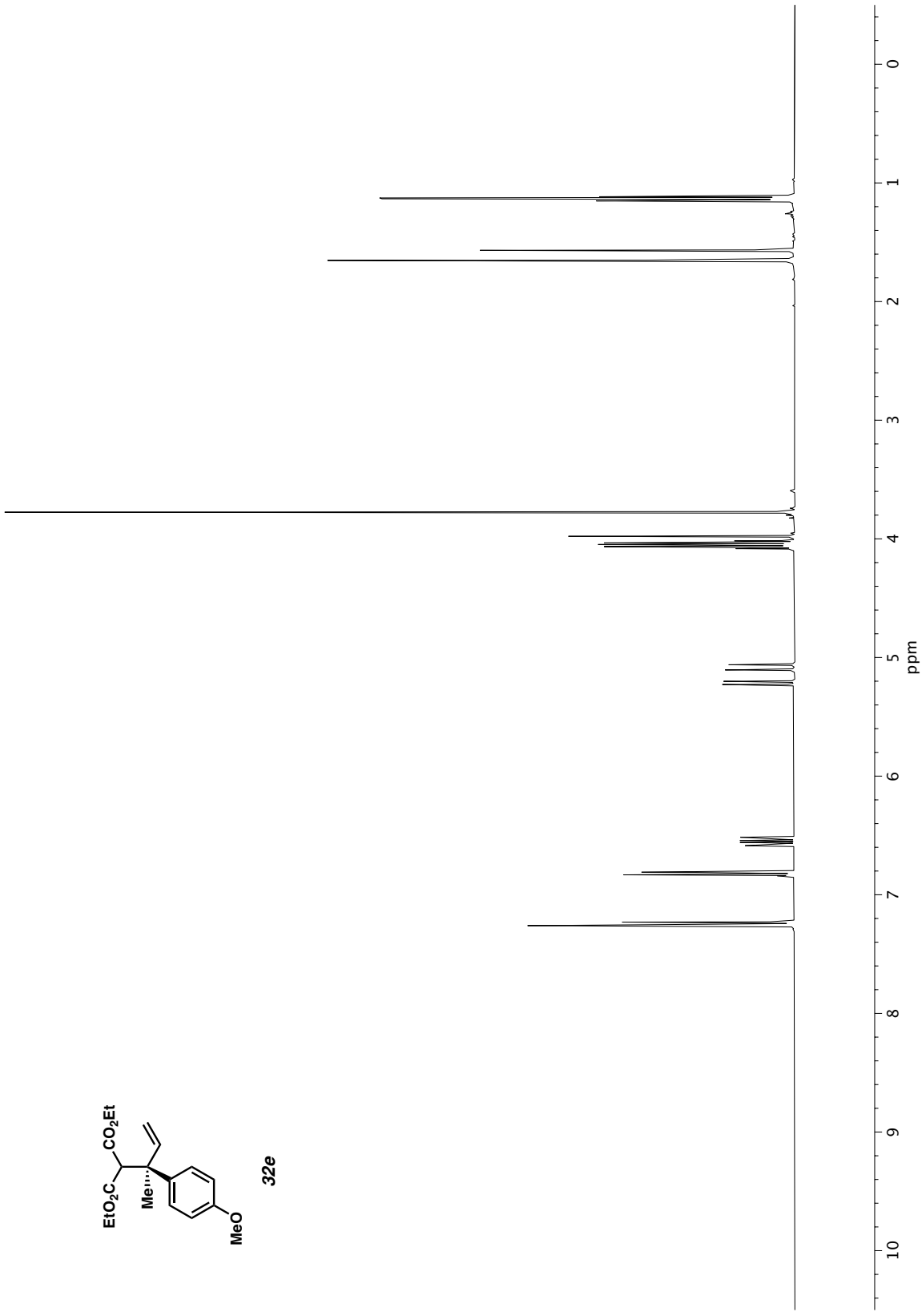


Figure A1.22 *^1H NMR (400 MHz, $CDCl_3$) of compound* ***32e***.

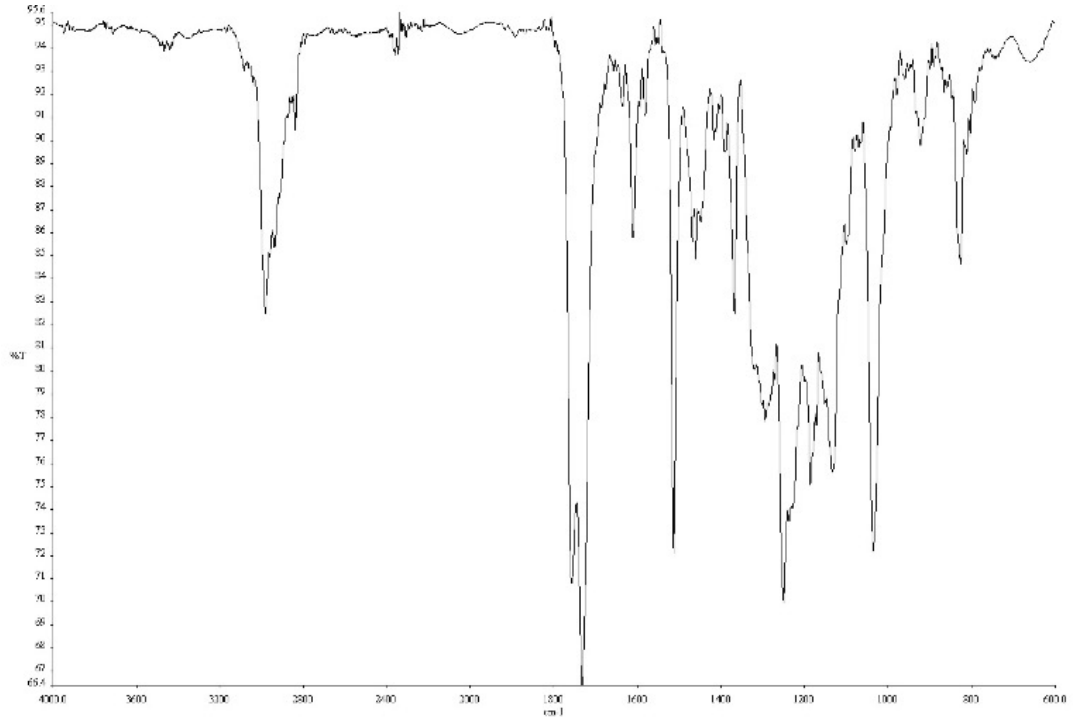


Figure A1.23 *Infrared spectrum (Thin Film, NaCl) of compound* ***32e****.*

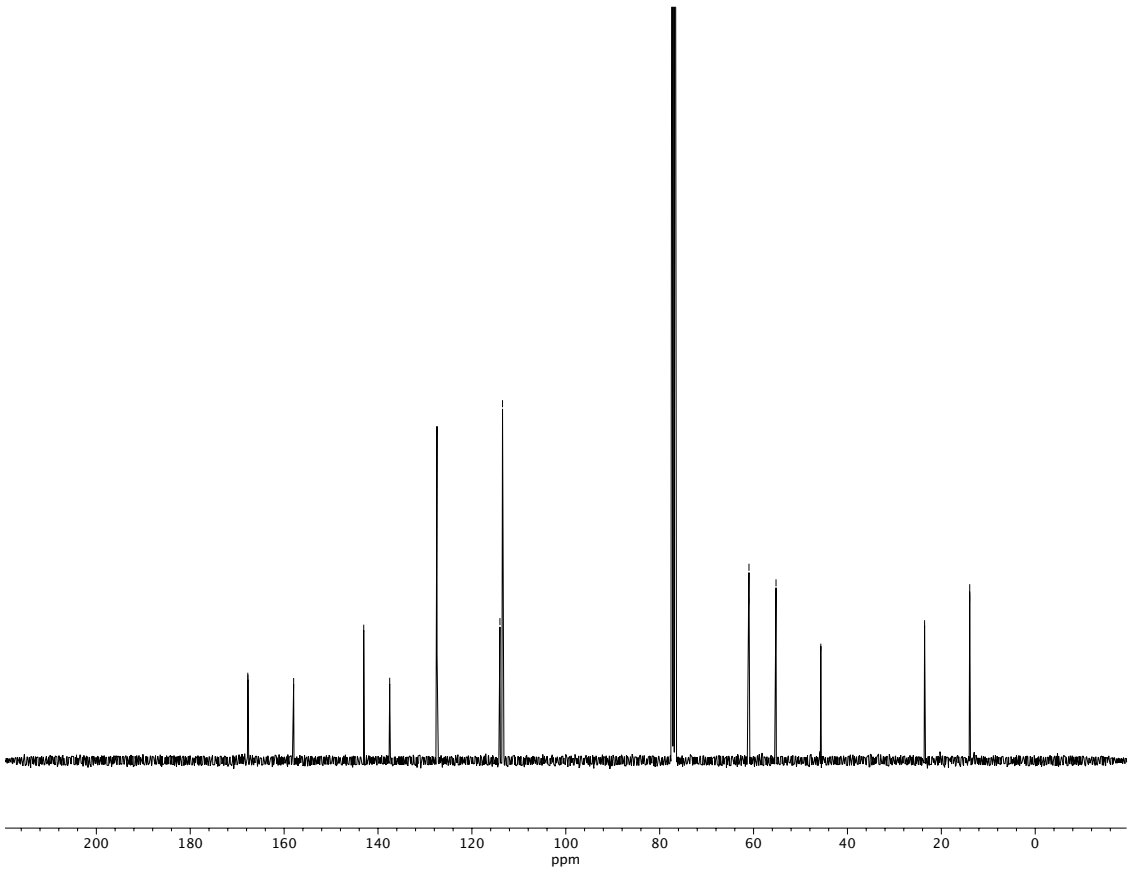


Figure A1.24 *^{13}C NMR (100 MHz, $CDCl_3$) of compound* ***32e****.*

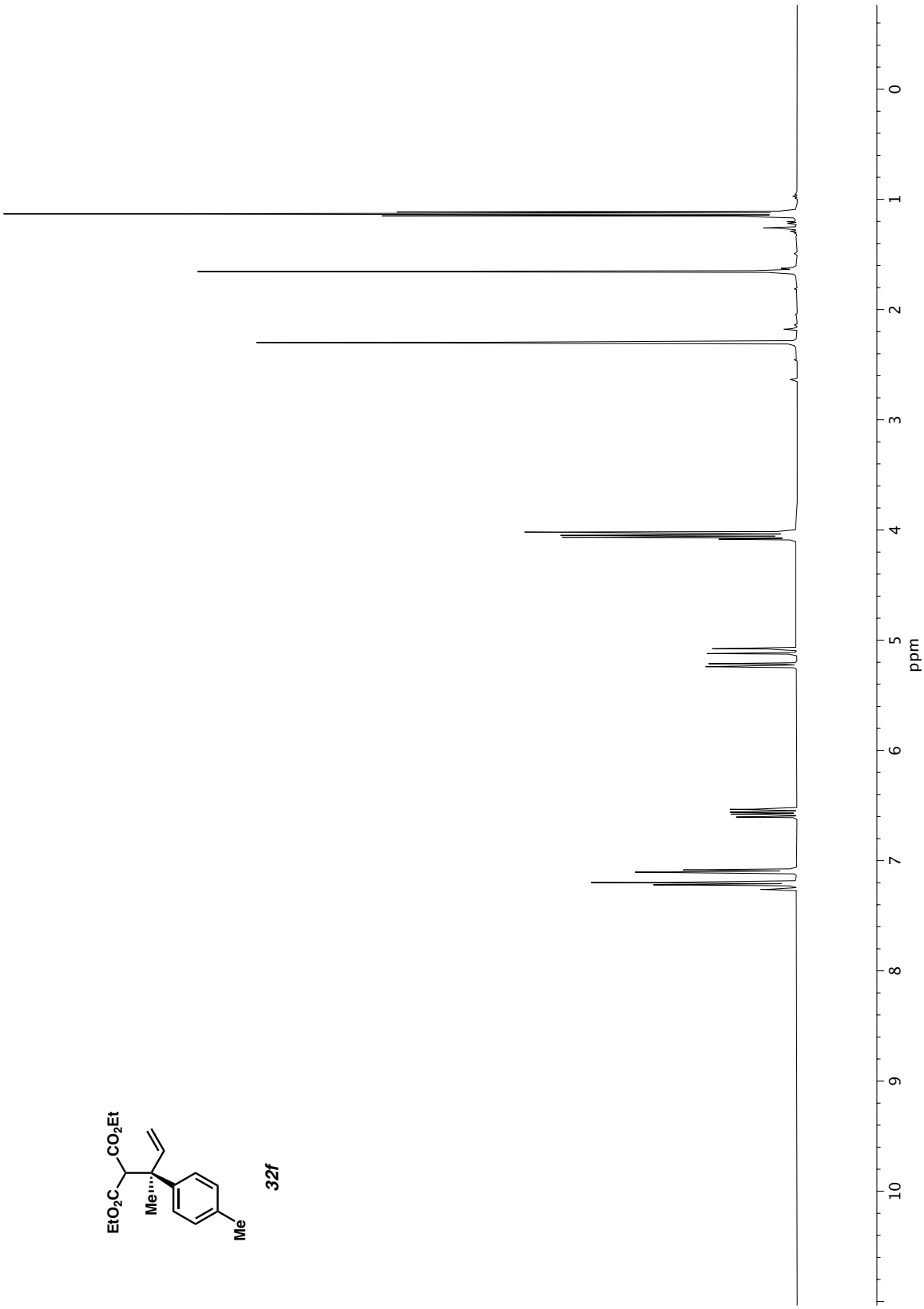


Figure A1.25 *^{1}H NMR (400 MHz, $CDCl_3$) of compound* ***32f****.*

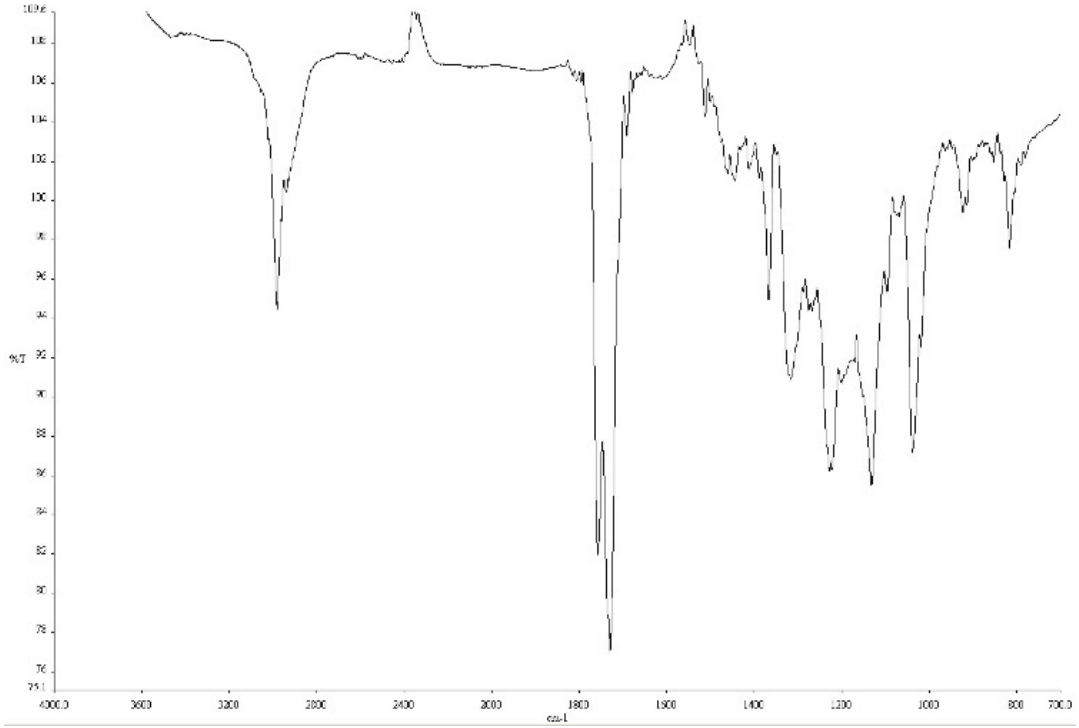


Figure A1.26 *Infrared spectrum (Thin Film, NaCl) of compound* ***32f****.*

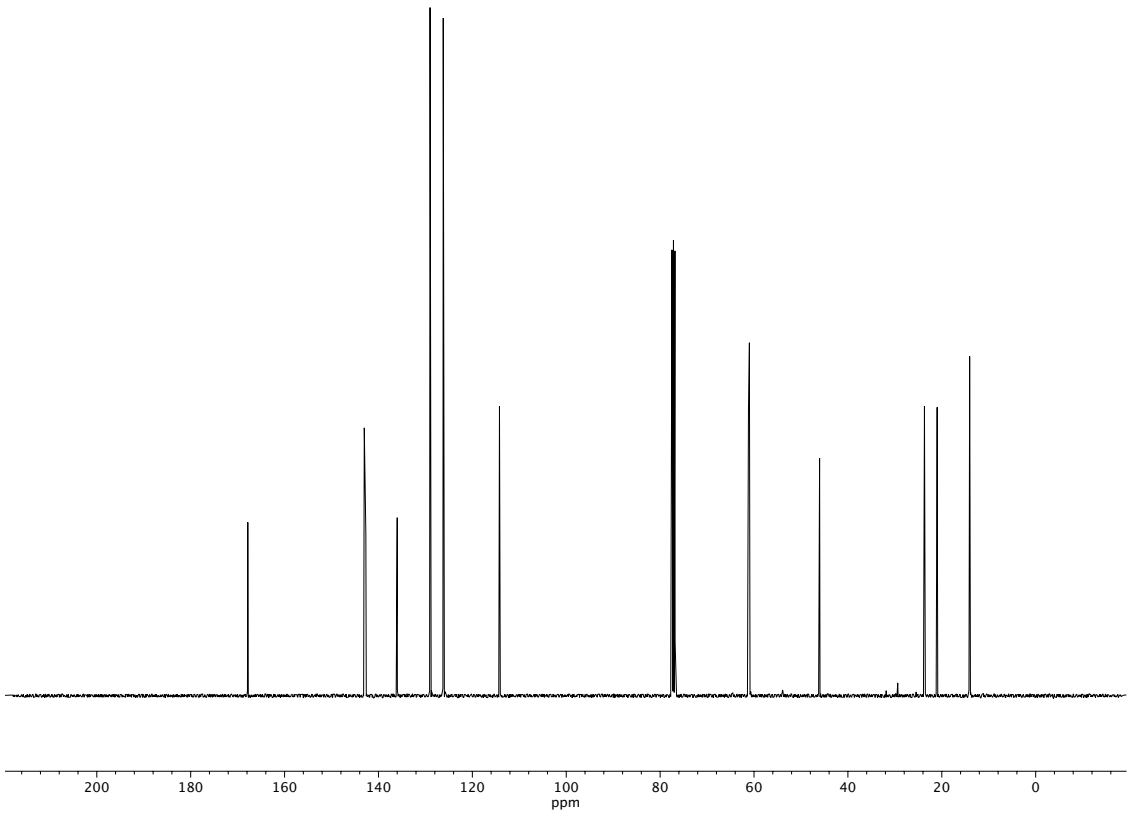


Figure A1.27 *^{13}C NMR (100 MHz, $CDCl_3$) of compound* ***32f****.*

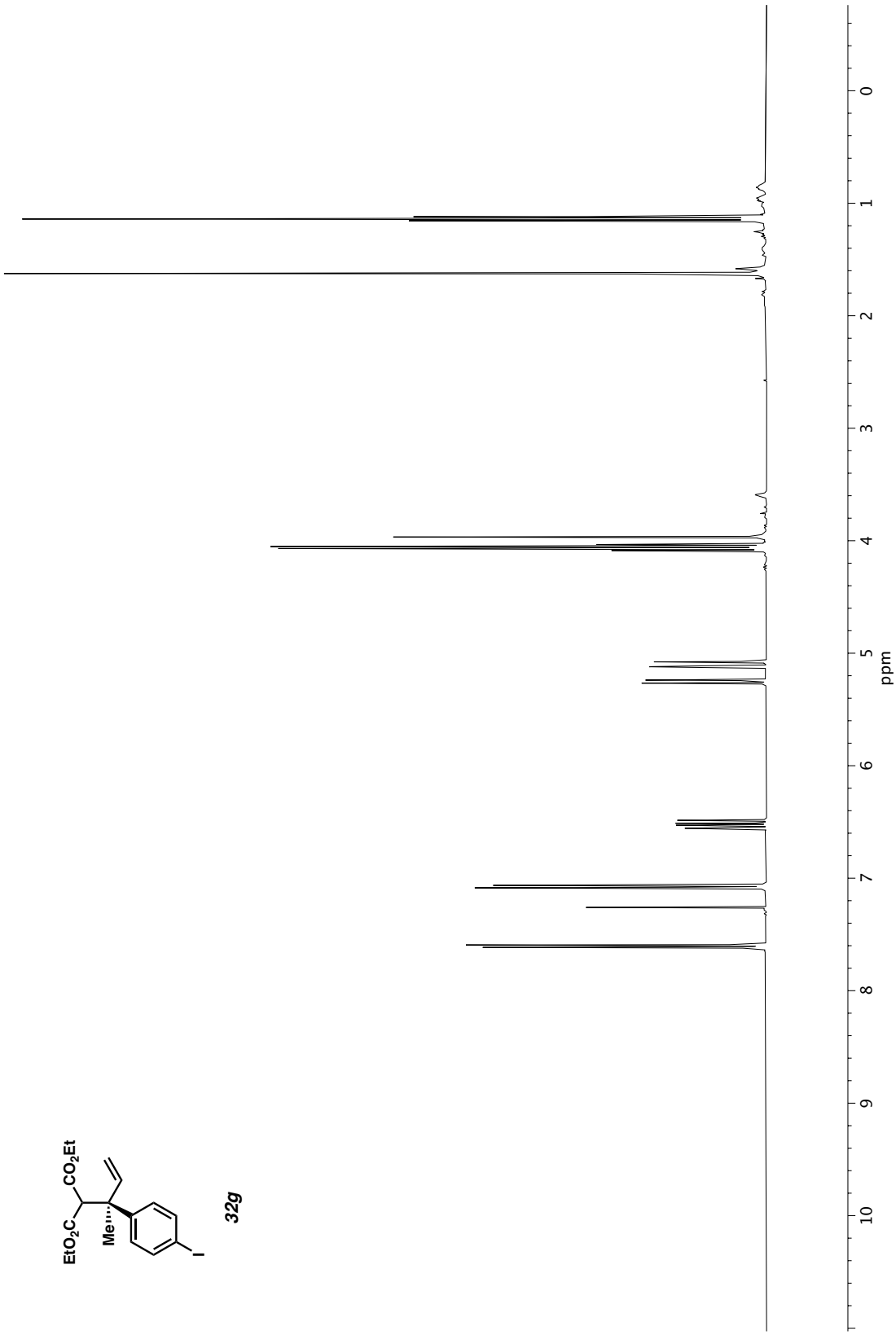


Figure A1.28 *^{1}H NMR (400 MHz, $CDCl_3$) of compound* ***32g****.*

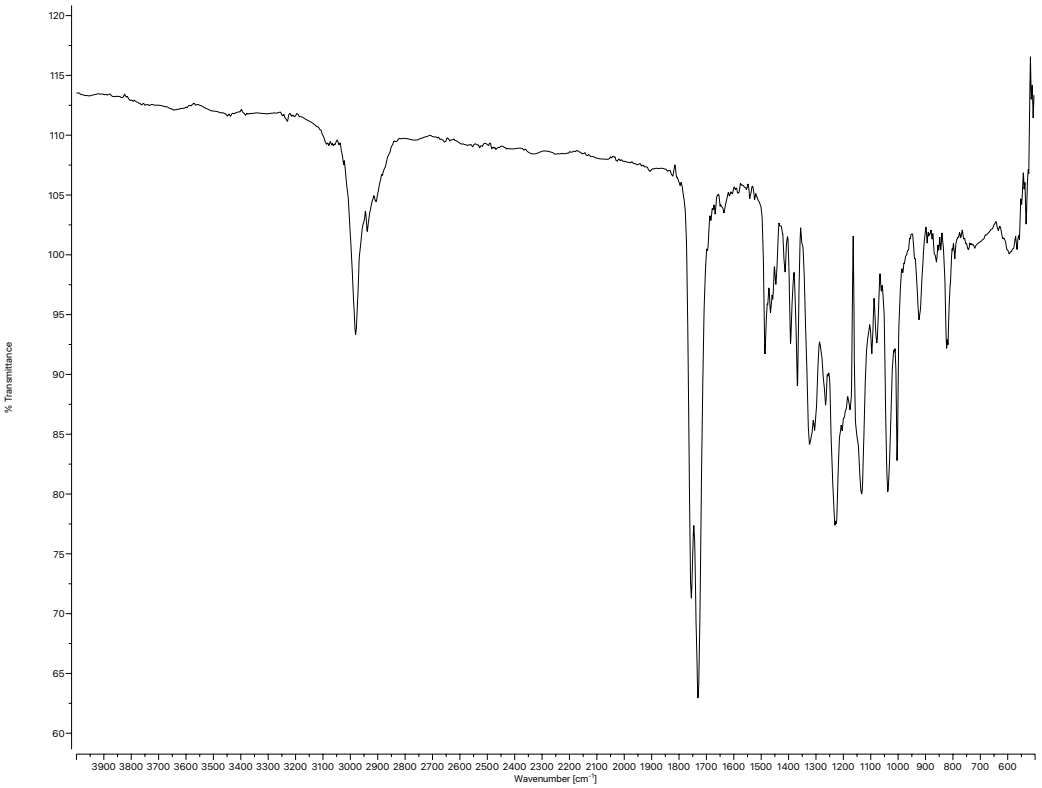


Figure A1.29 *Infrared spectrum (Thin Film, NaCl) of compound* ***32g***.

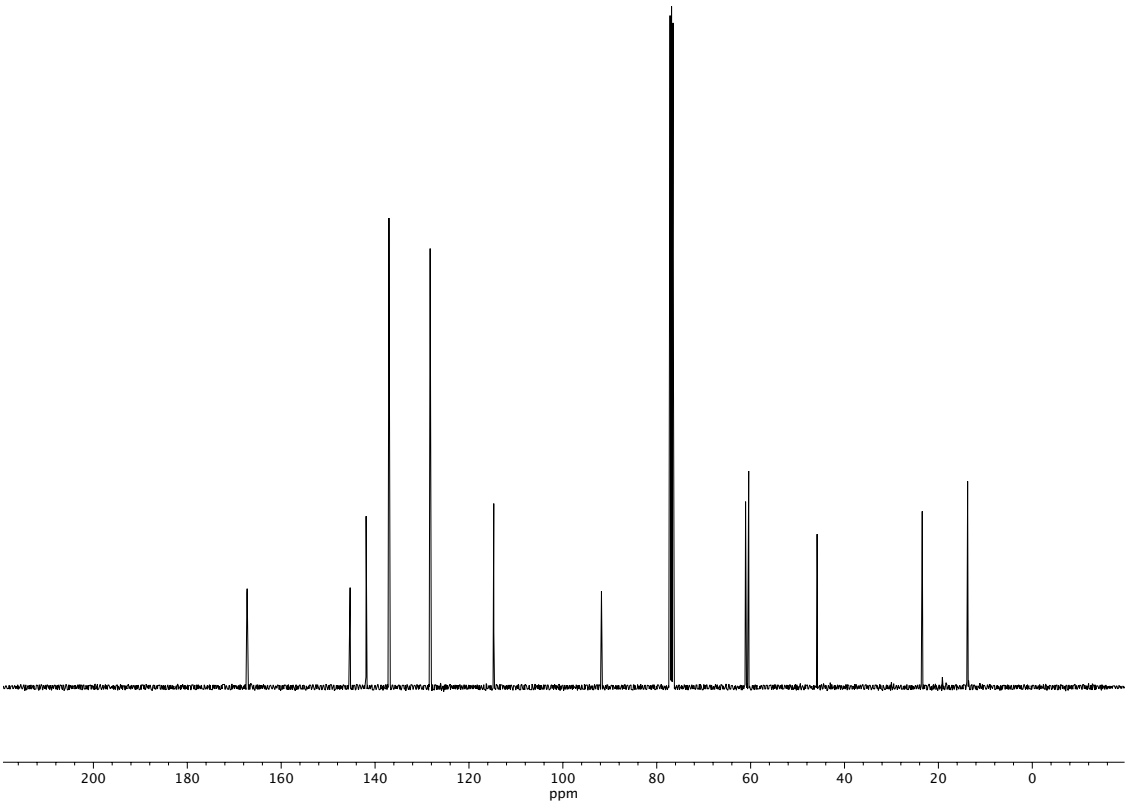


Figure A1.30 *^{13}C NMR (100 MHz, $CDCl_3$) of compound* ***32g***.

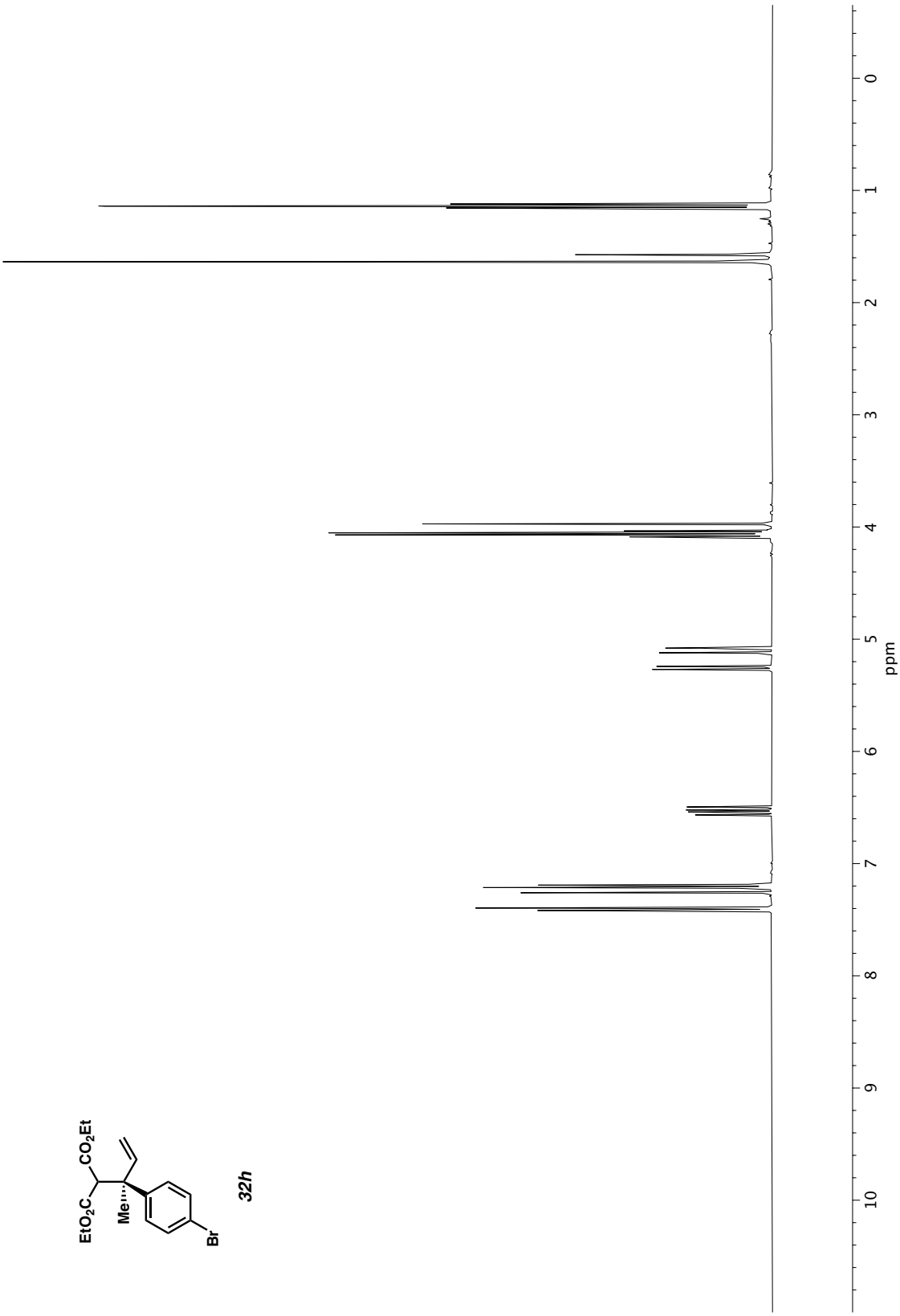


Figure A1.31 *^{1}H NMR (400 MHz, $CDCl_3$) of compound* ***32h****.*

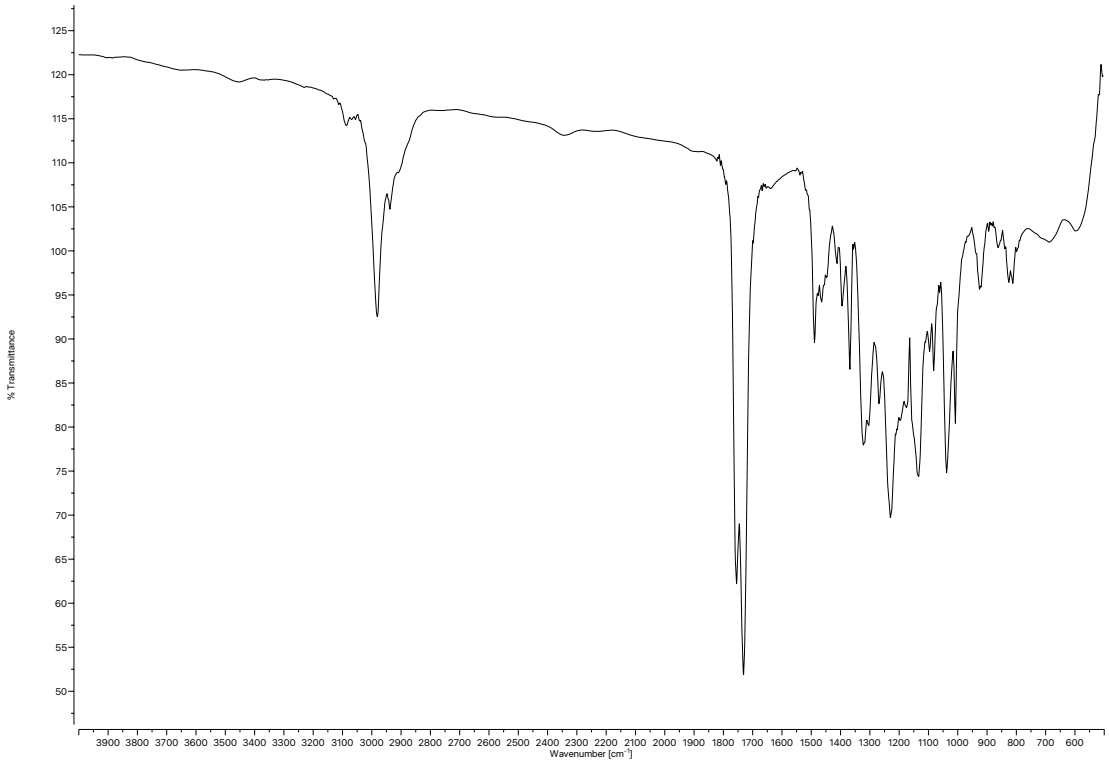


Figure A1.32 *Infrared spectrum (Thin Film, NaCl) of compound* ***32h****.*

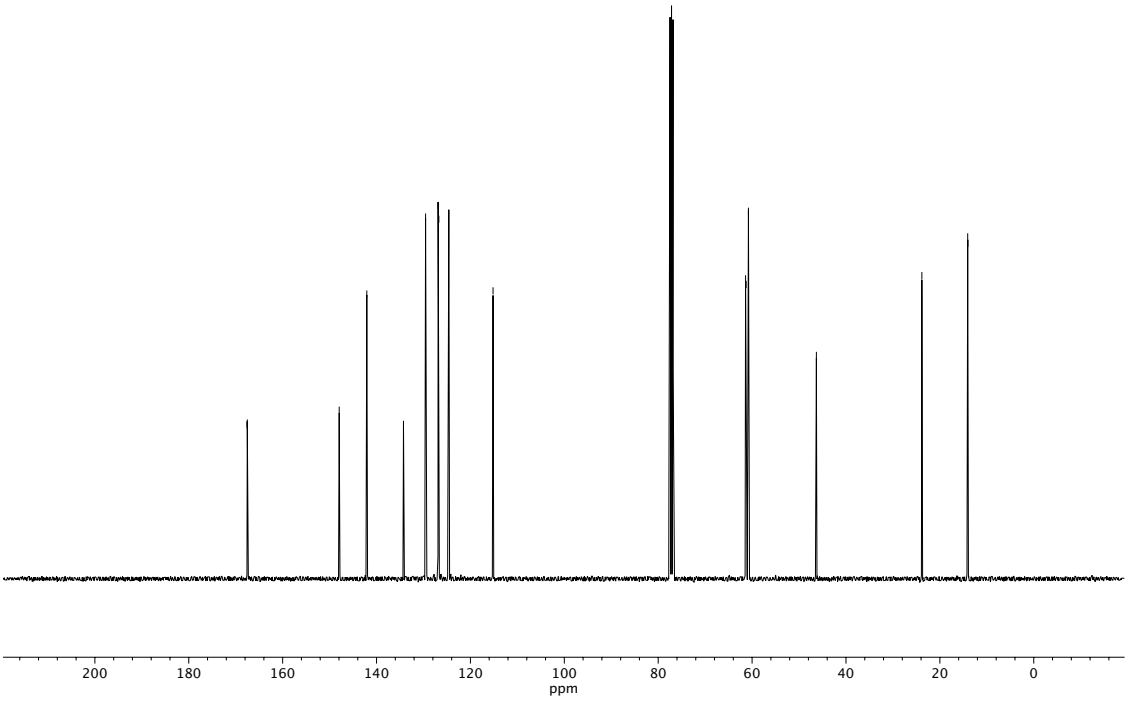


Figure A1.33 *^{13}C NMR (100 MHz, $CDCl_3$) of compound* ***32h****.*

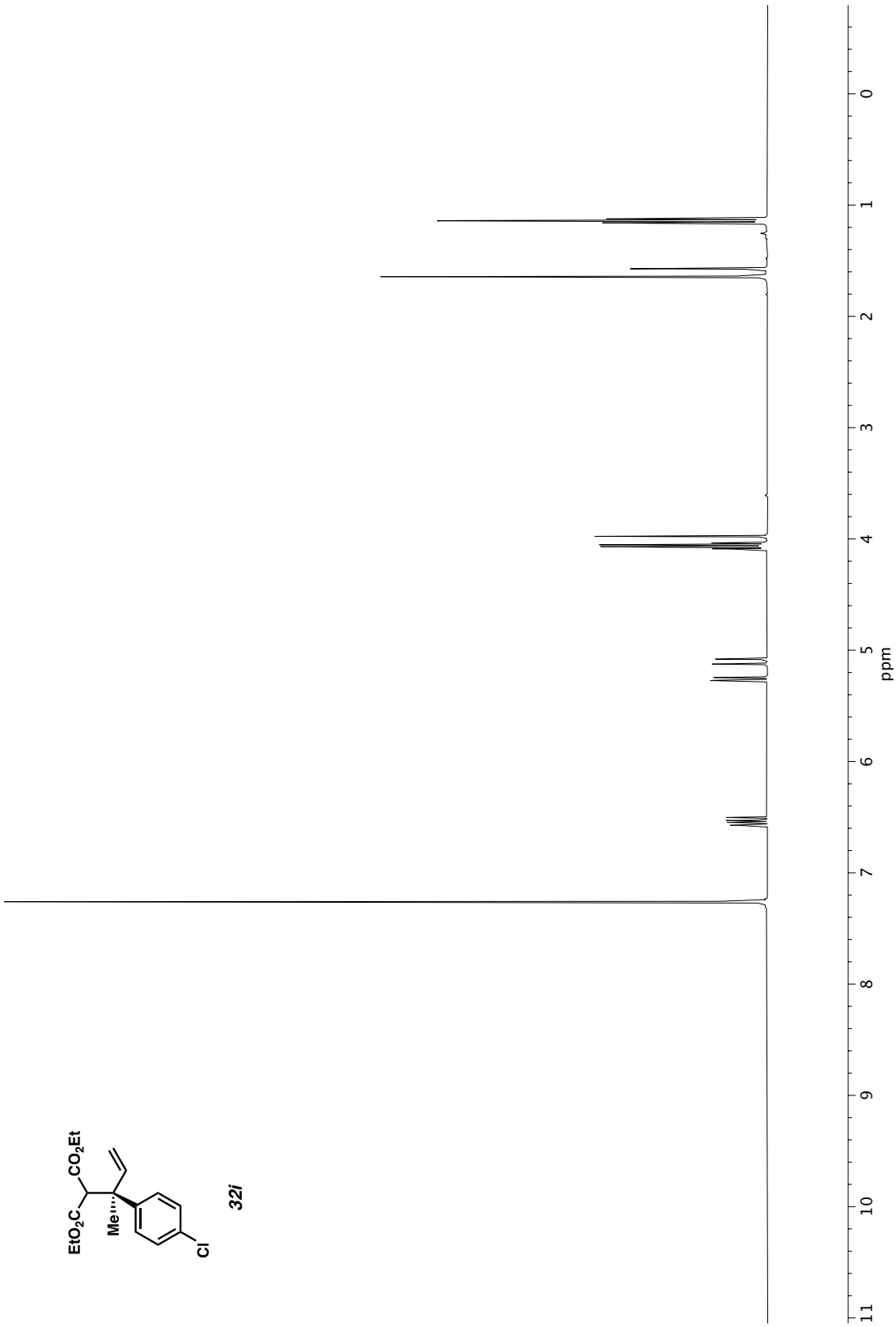


Figure A1.34 *^{1}H NMR (400 MHz, $CDCl_3$) of compound* ***32i****.*

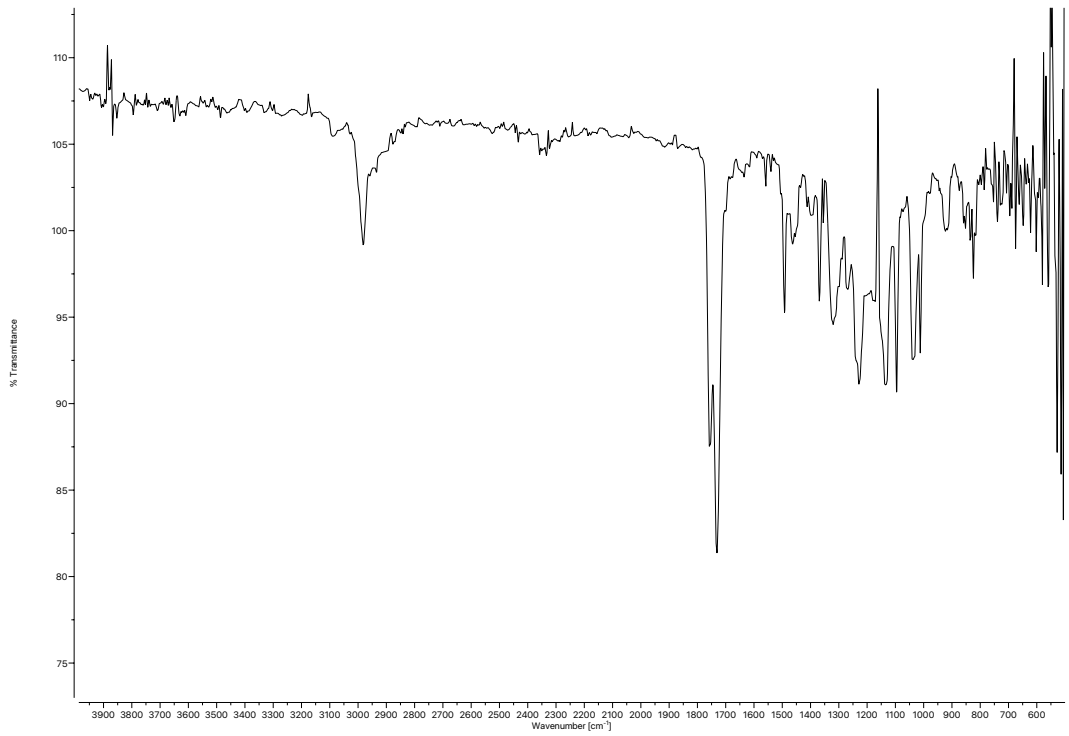


Figure A1.35 *Infrared spectrum (Thin Film, NaCl) of compound* ***32i****.*

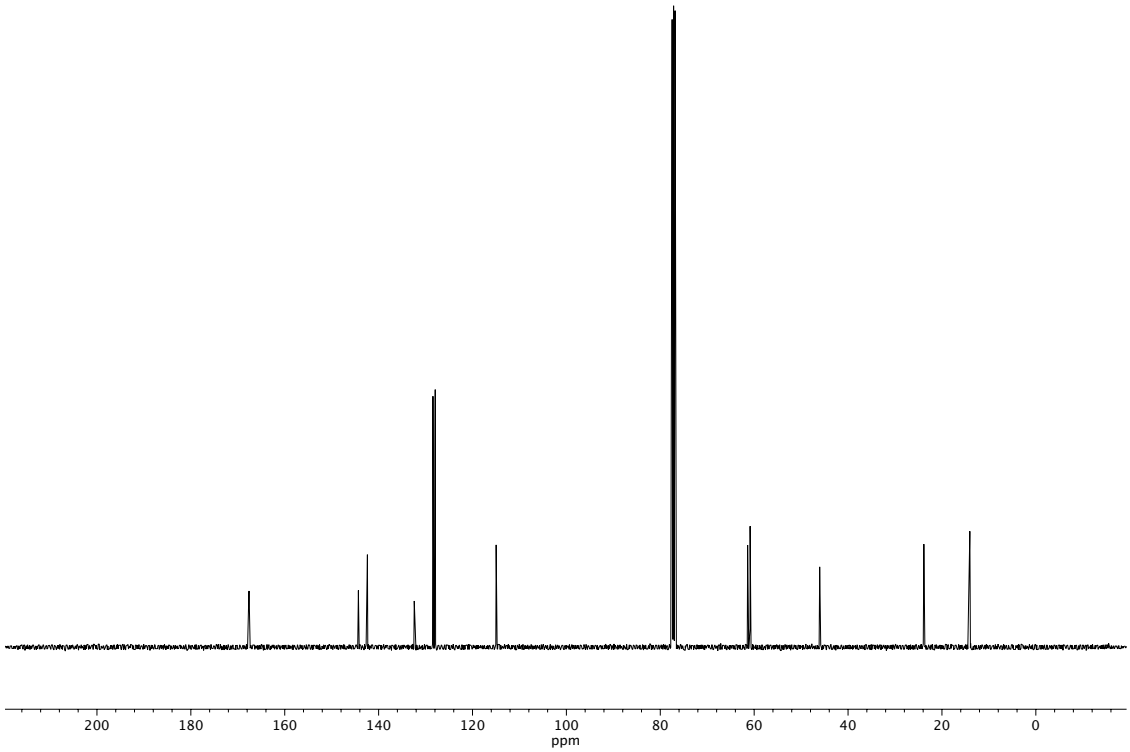


Figure A1.36 *^{13}C NMR (100 MHz, $CDCl_3$) of compound* ***32i****.*

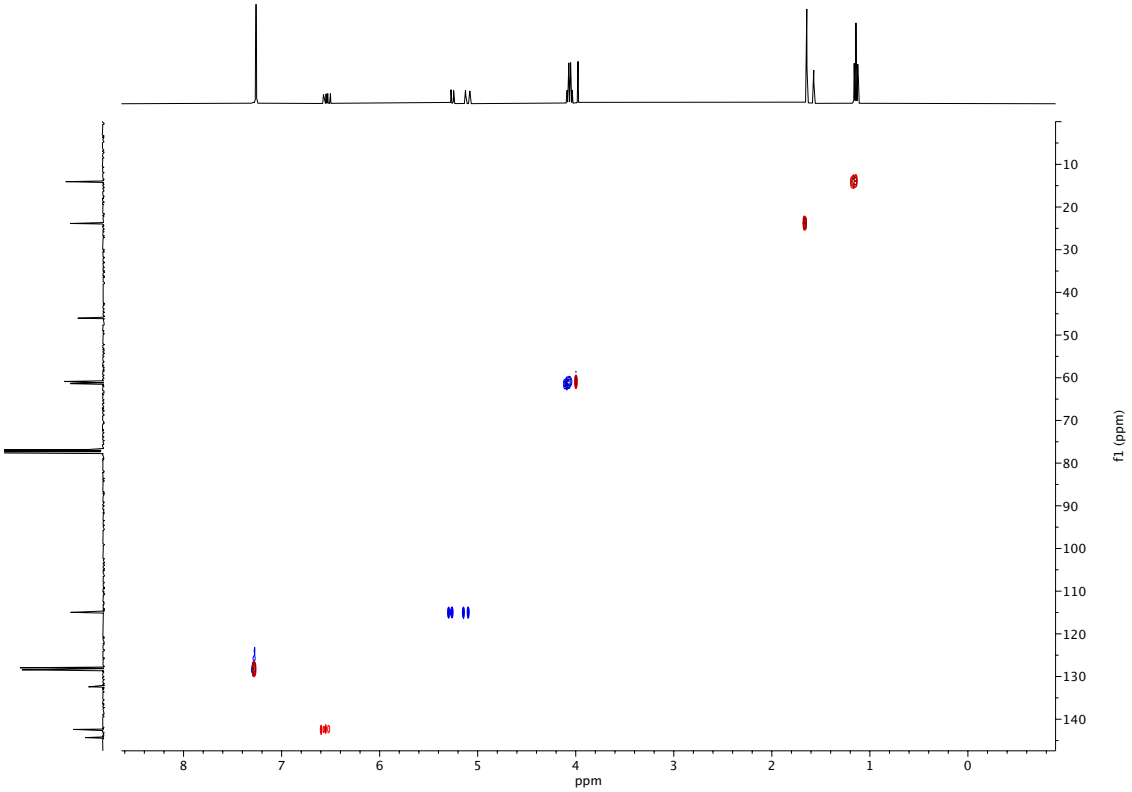


Figure A1.37 *HSQC Spectrum ($CDCl_3$) of compound* ***32i***.

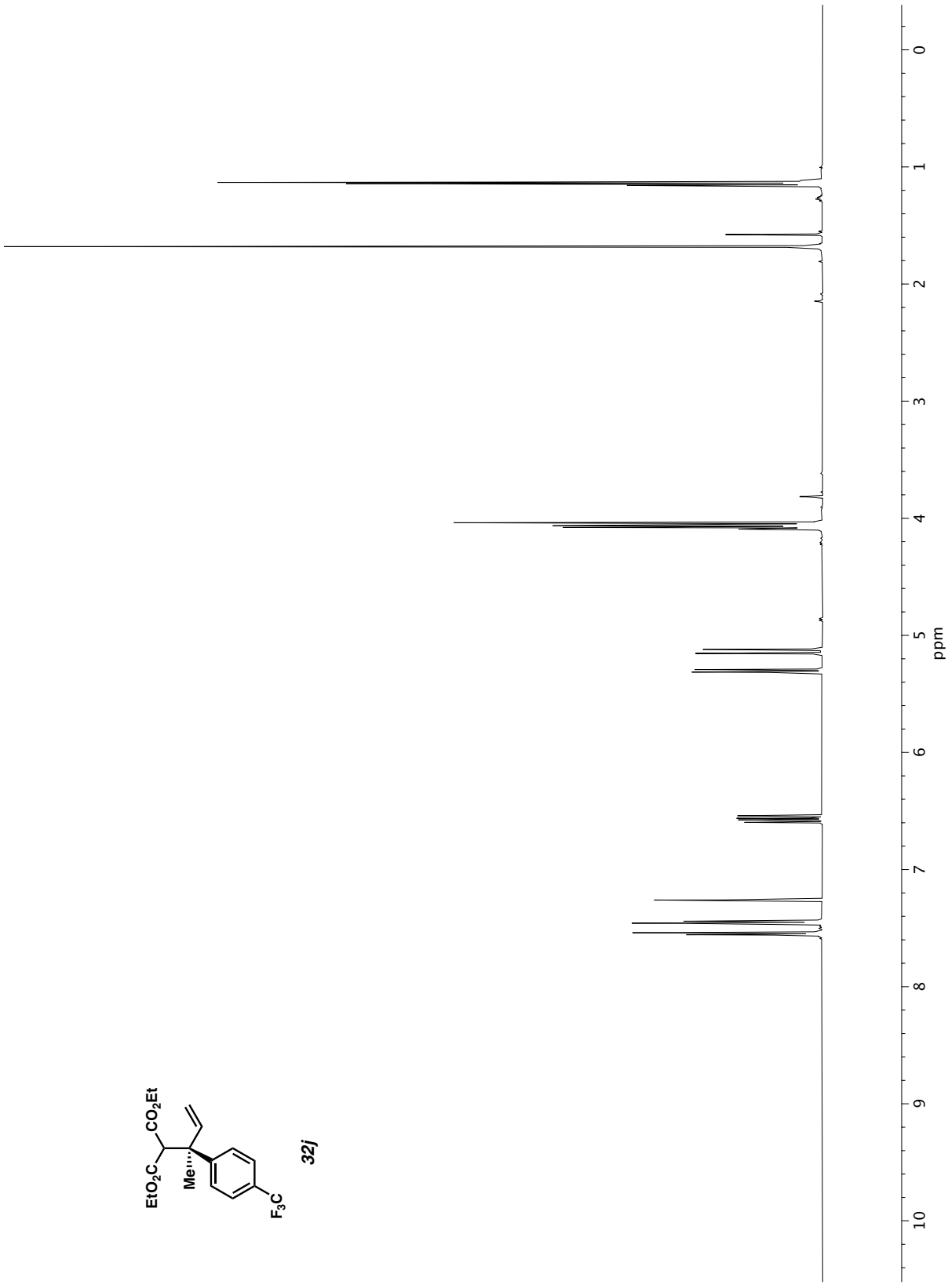


Figure A1.38 *^{1}H NMR (500 MHz, $CDCl_3$) of compound* ***32j***.

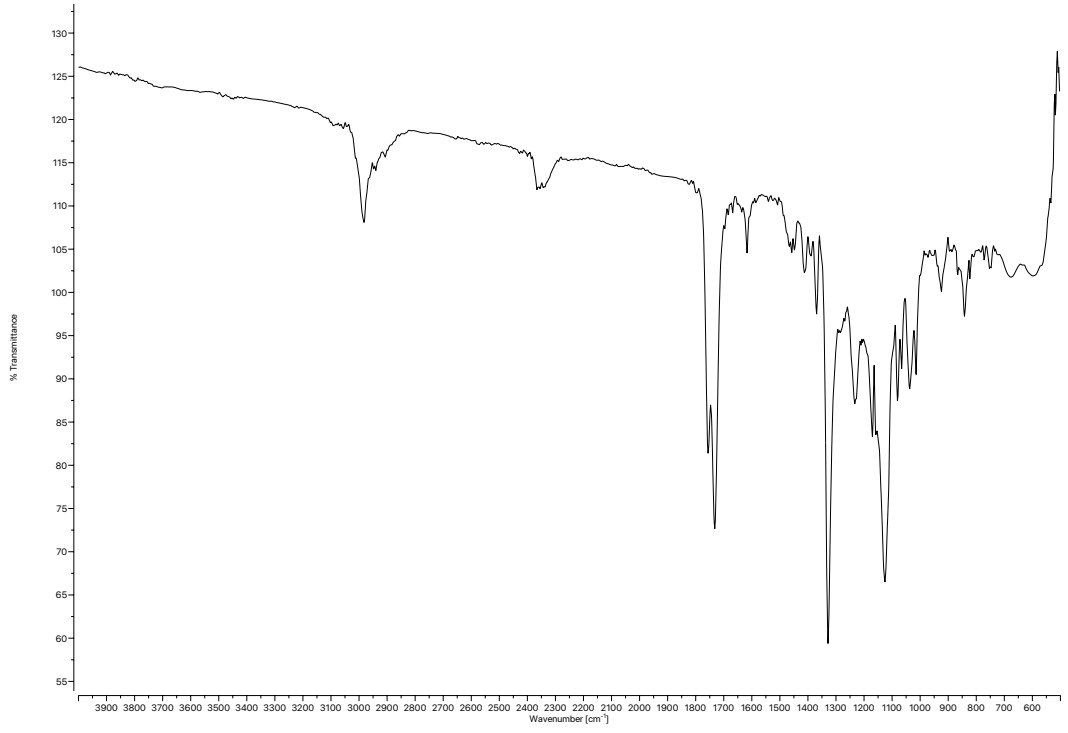


Figure A1.39 *Infrared spectrum (Thin Film, NaCl) of compound* ***32j****.*

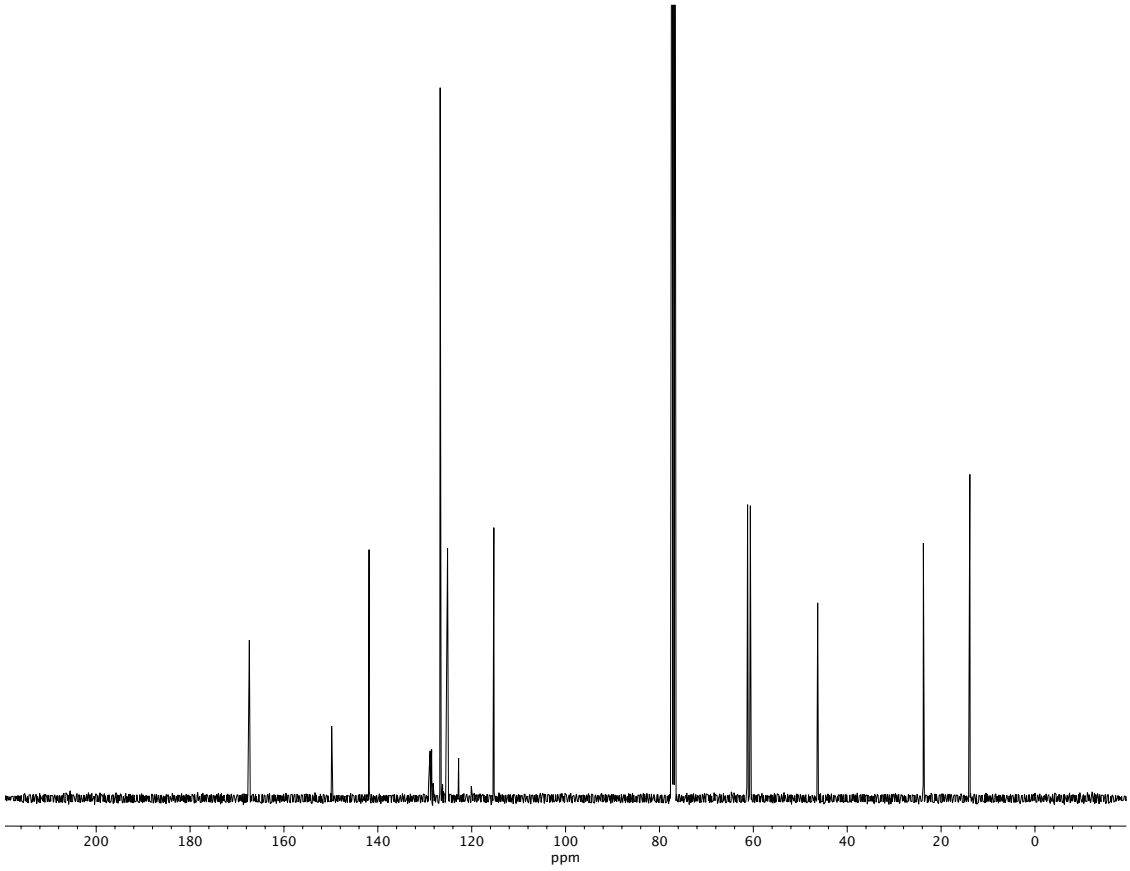


Figure A1.40 *^{13}C NMR (100 MHz, $CDCl_3$) of compound* ***32j****.*

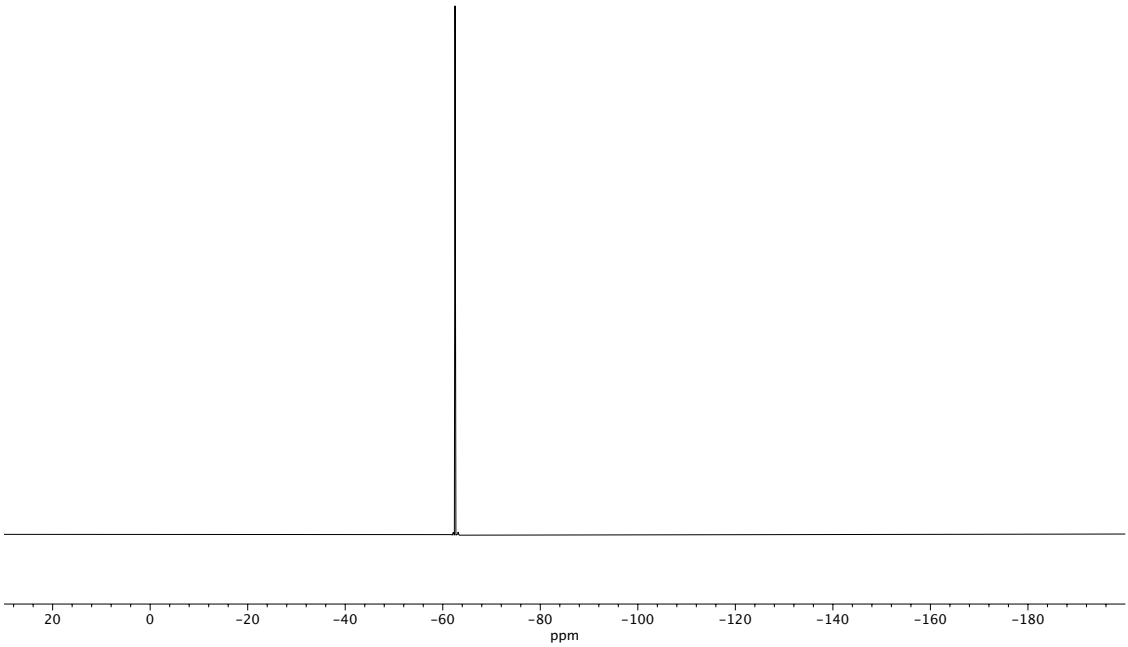


Figure A1.41 *^{19}F NMR (282 MHz, $CDCl_3$) of compound* ***32j****.*

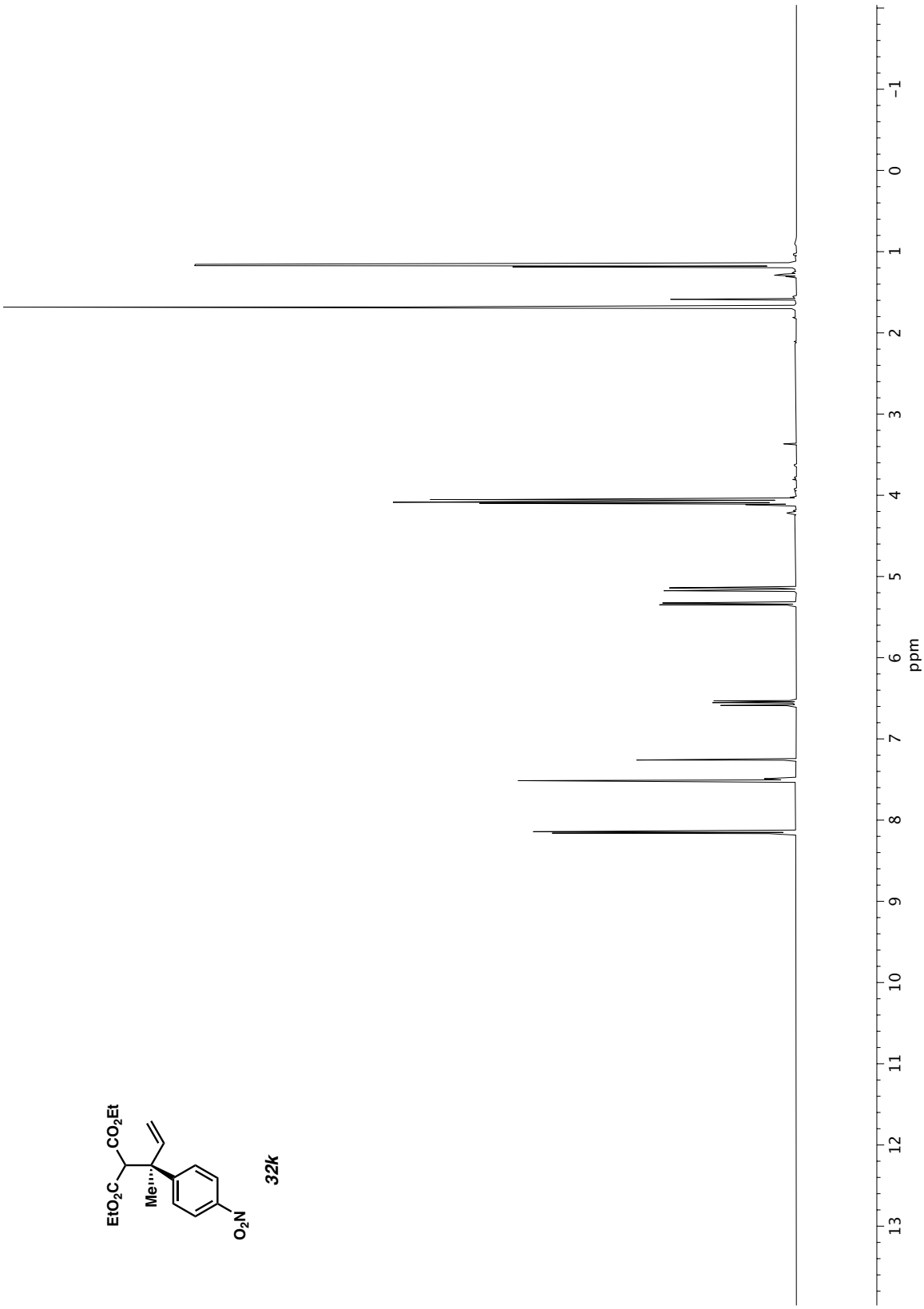


Figure A1.42 *^{1}H NMR (500 MHz, $CDCl_3$) of compound* ***32k****.*

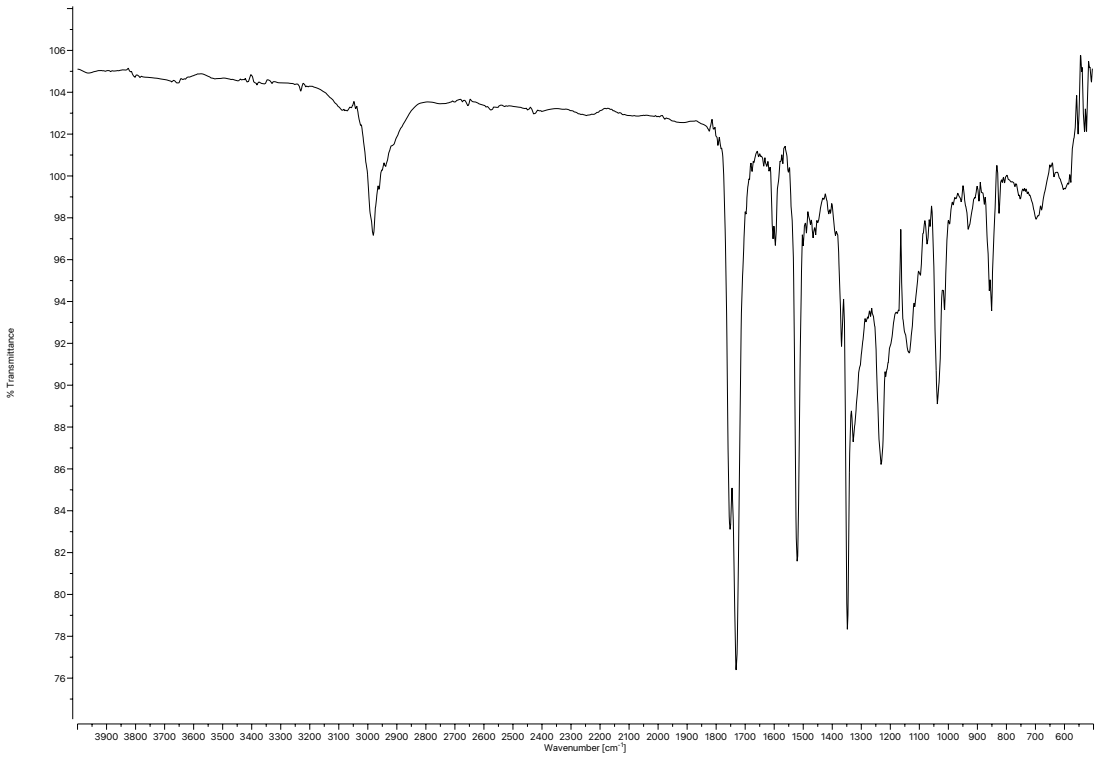


Figure A1.43 *Infrared spectrum (Thin Film, NaCl) of compound* ***32k***.

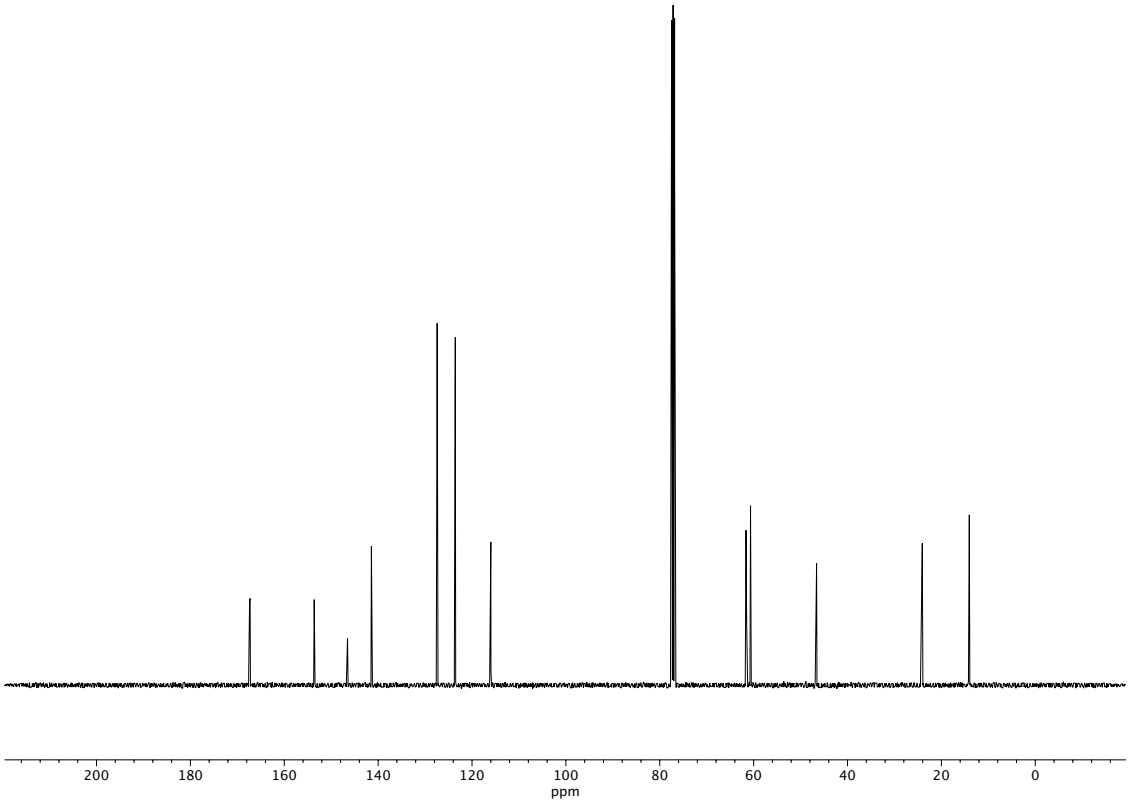


Figure A1.44 *^{13}C NMR (100 MHz, $CDCl_3$) of compound* ***32k***.

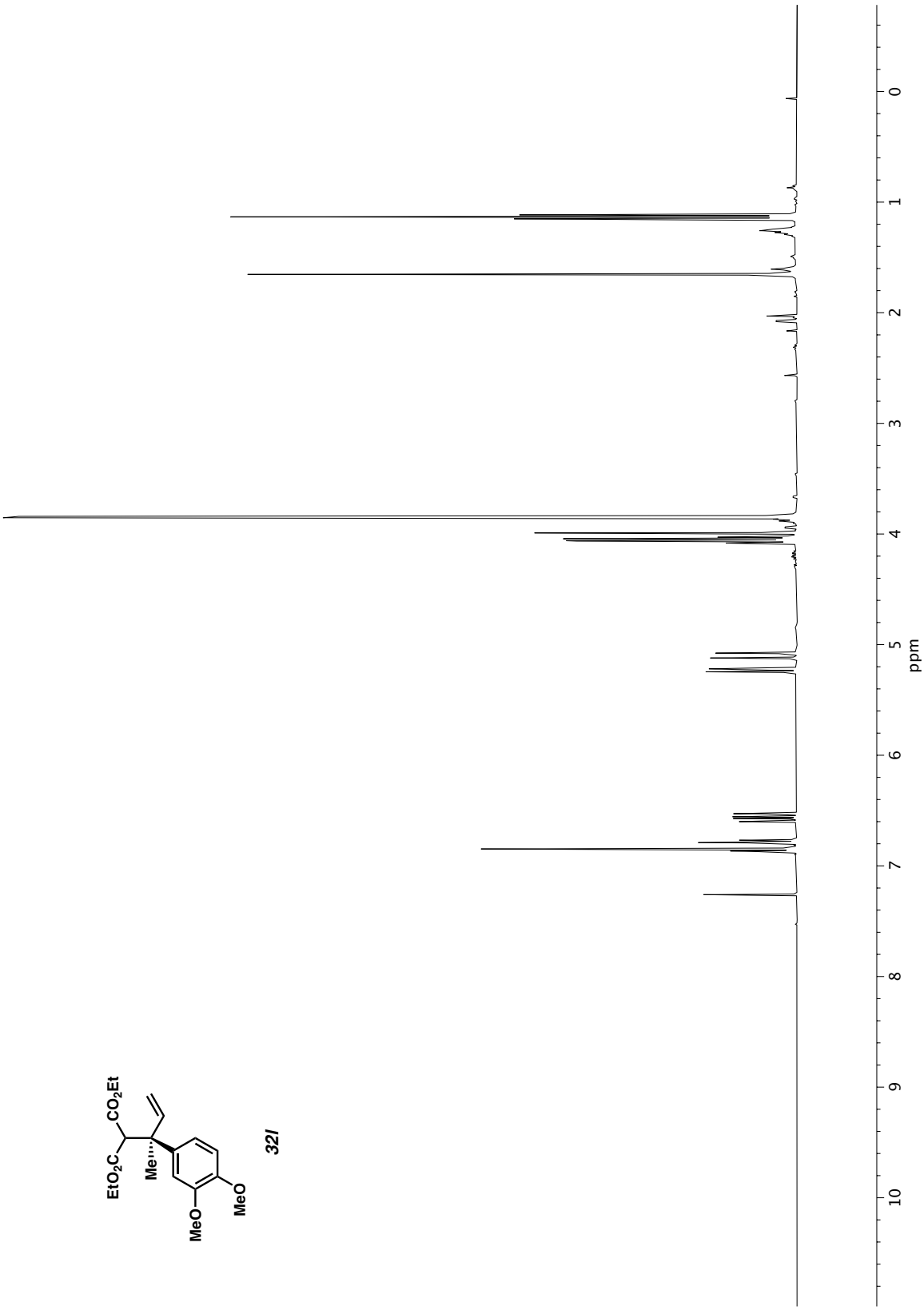


Figure A1.45 *^{1}H NMR (400 MHz, $CDCl_3$) of compound* ***32l****.*

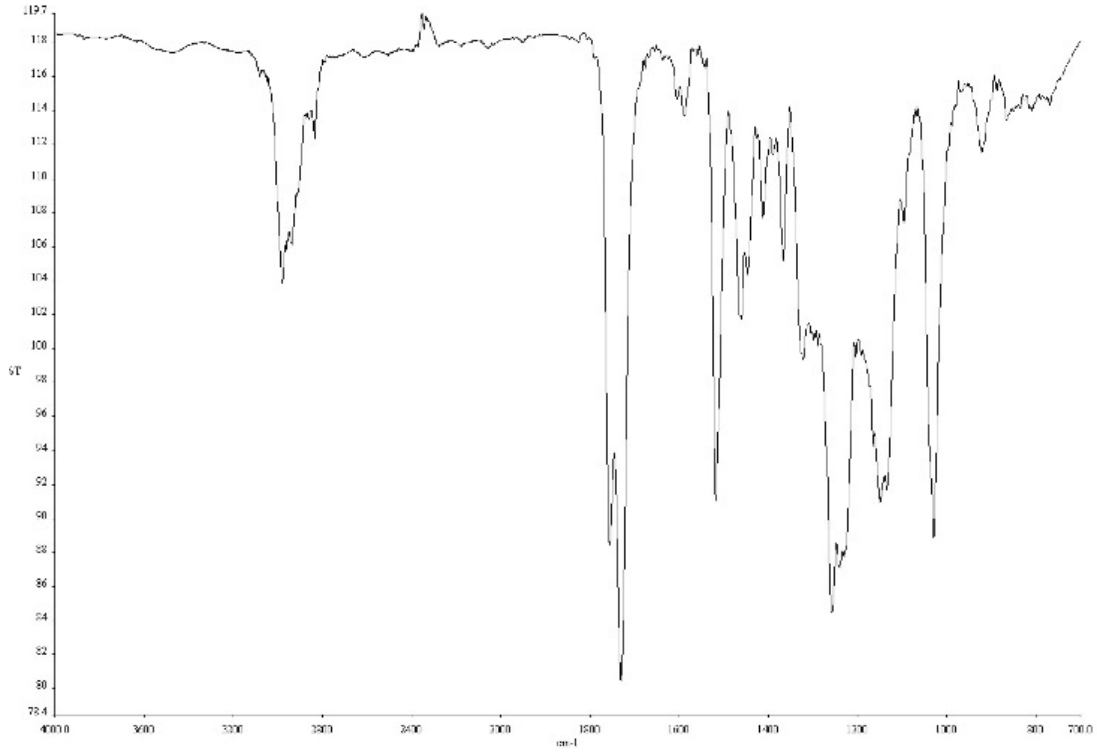


Figure A1.46 *Infrared spectrum (Thin Film, NaCl) of compound* ***32l****.*

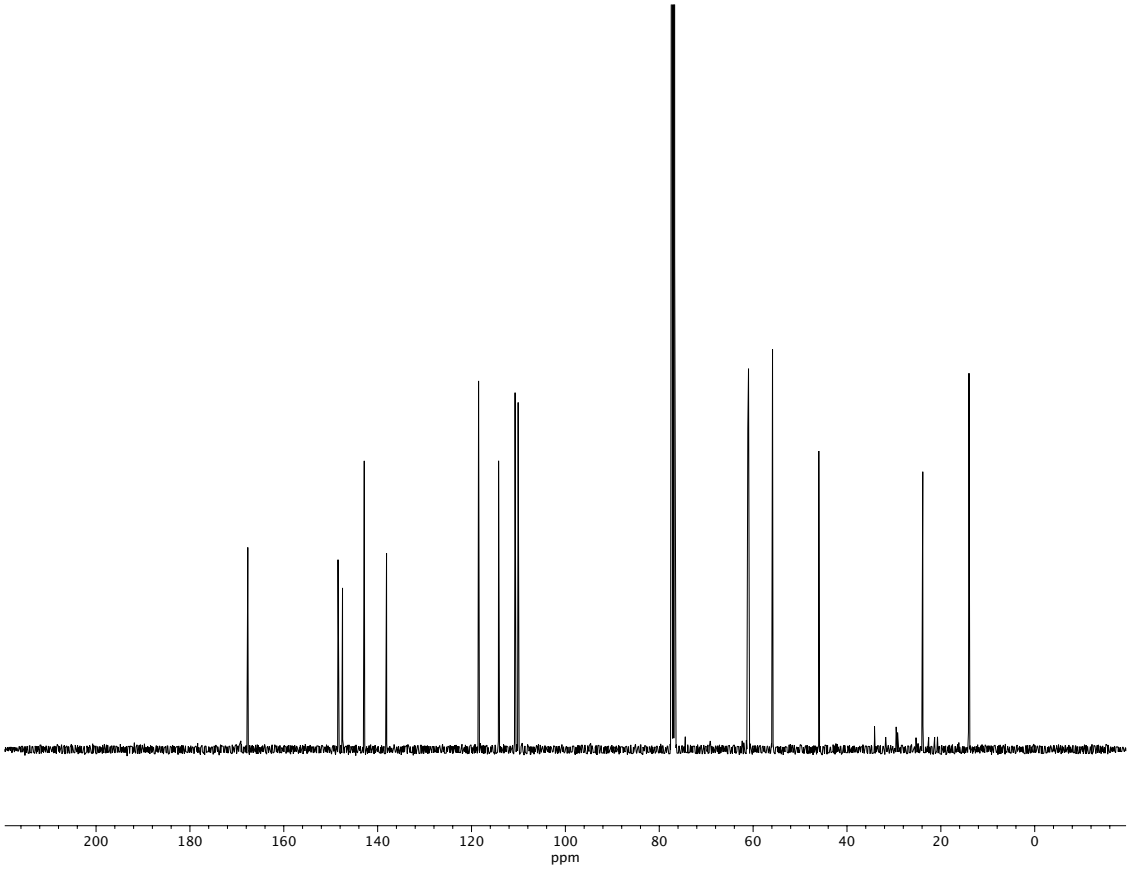


Figure A1.47 *^{13}C NMR (100 MHz, $CDCl_3$) of compound* ***32l****.*

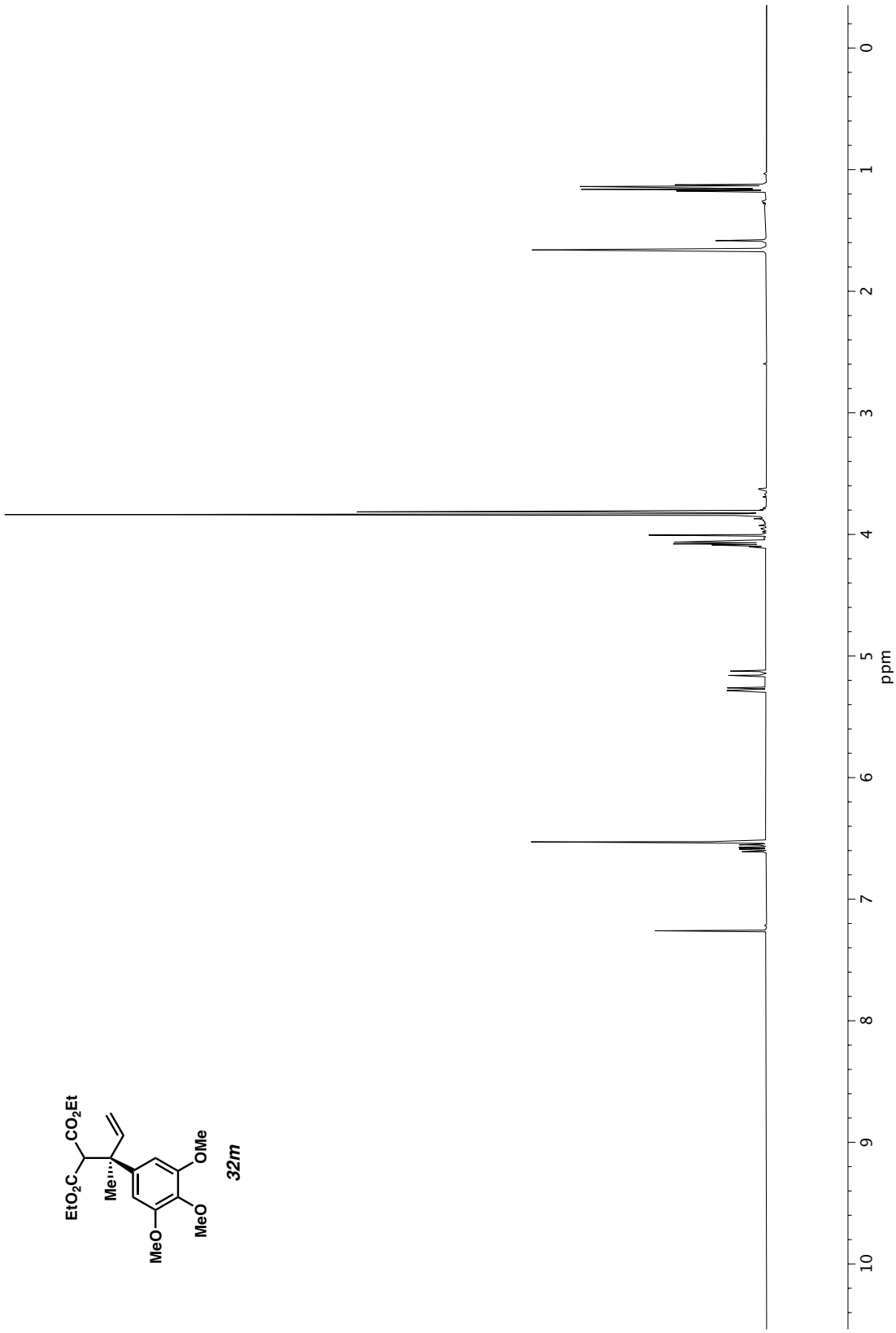


Figure A1.48 *^1H NMR (500 MHz, $CDCl_3$) of compound* ***32m****.*

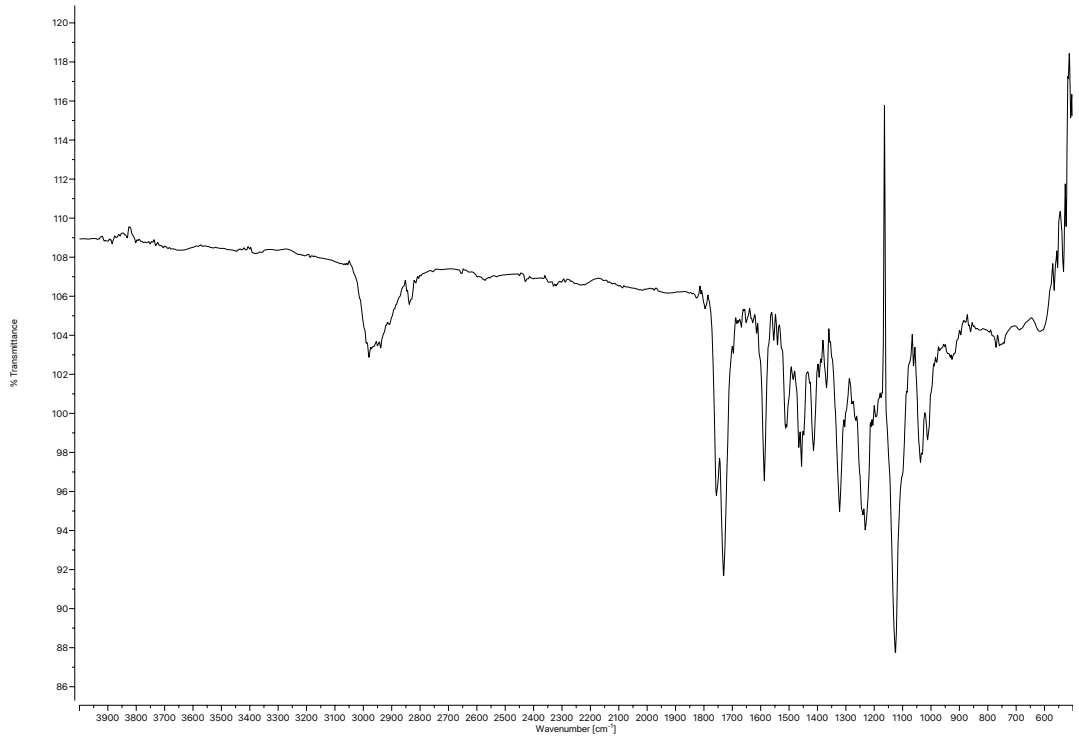


Figure A1.49 *Infrared spectrum (Thin Film, NaCl) of compound* ***32m***.

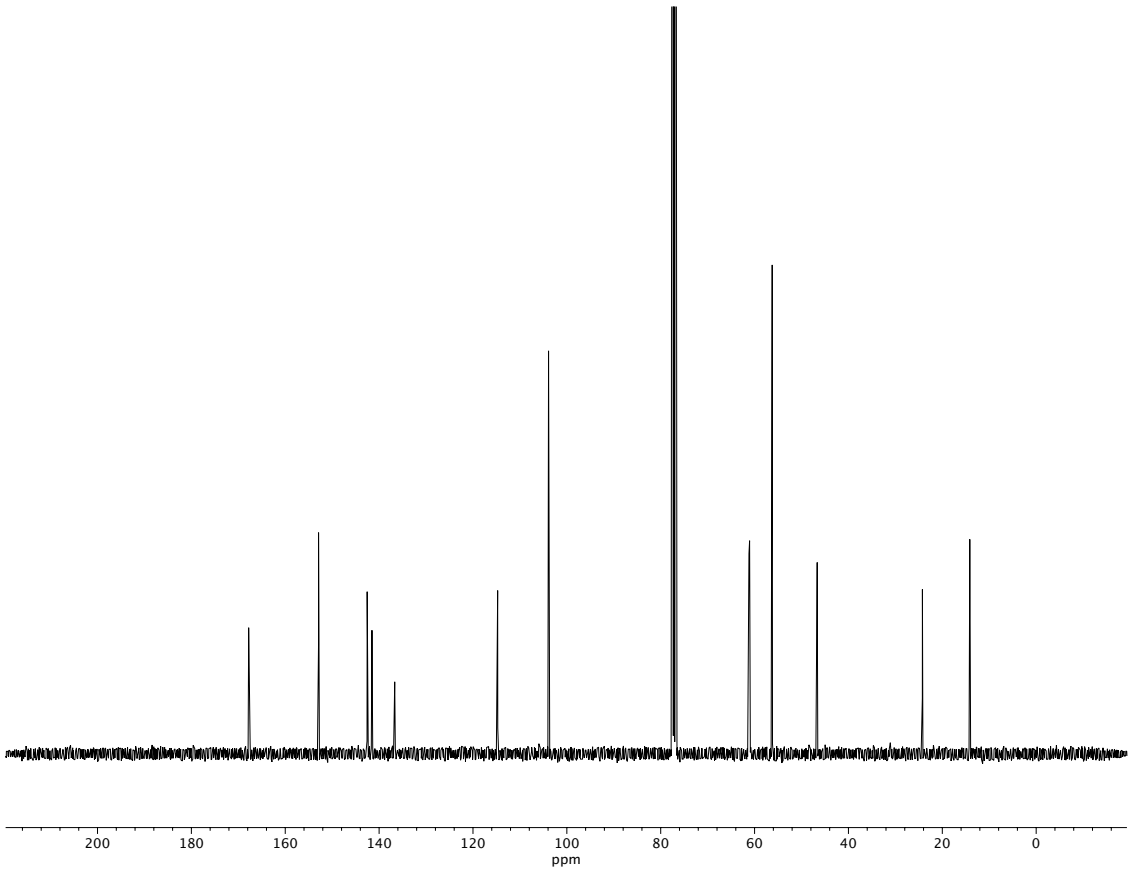


Figure A1.50 *^{13}C NMR (100 MHz, $CDCl_3$) of compound* ***32m***.

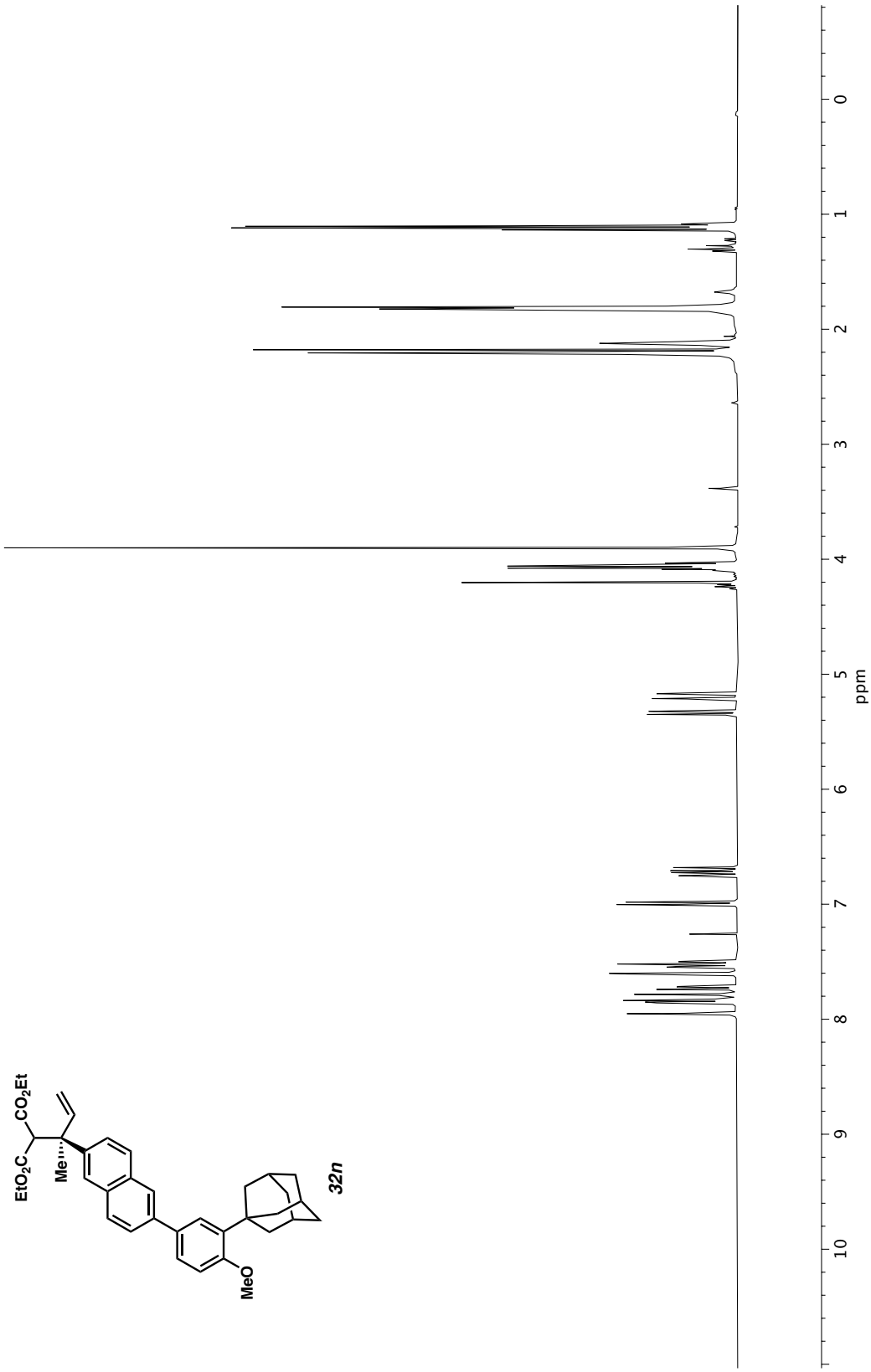


Figure A1.51 *^{1}H NMR (400 MHz, $CDCl_3$) of compound* ***32n***.

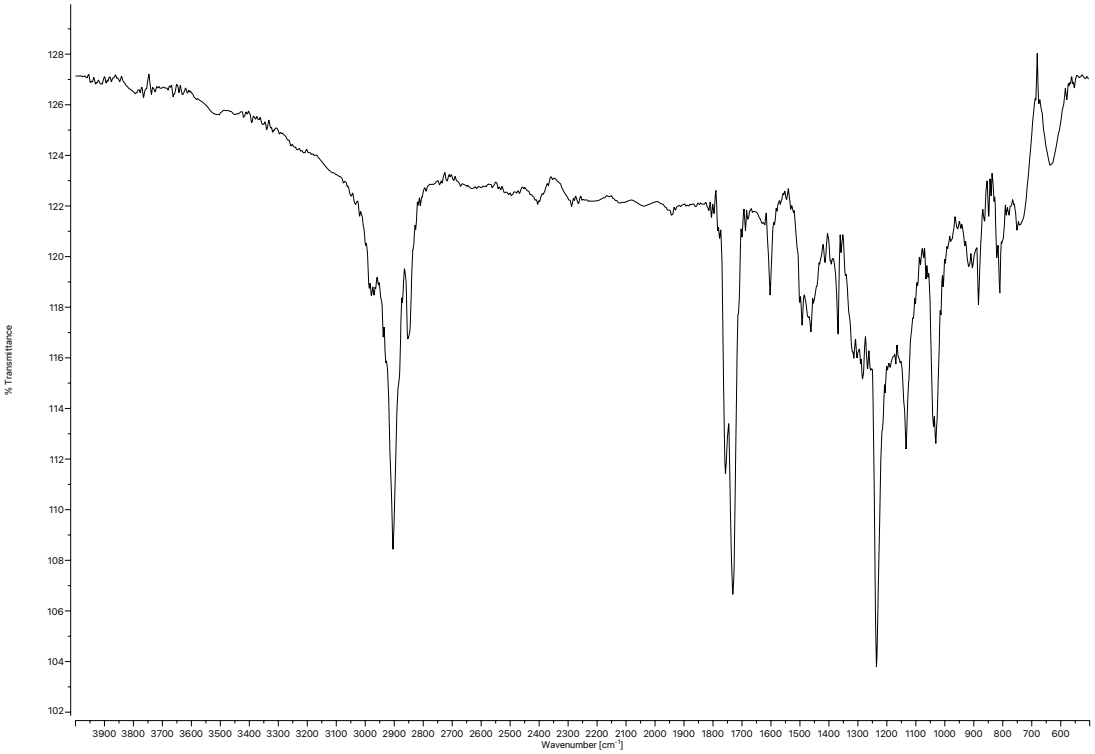


Figure A1.52 *Infrared spectrum (Thin Film, NaCl) of compound* ***32n***.

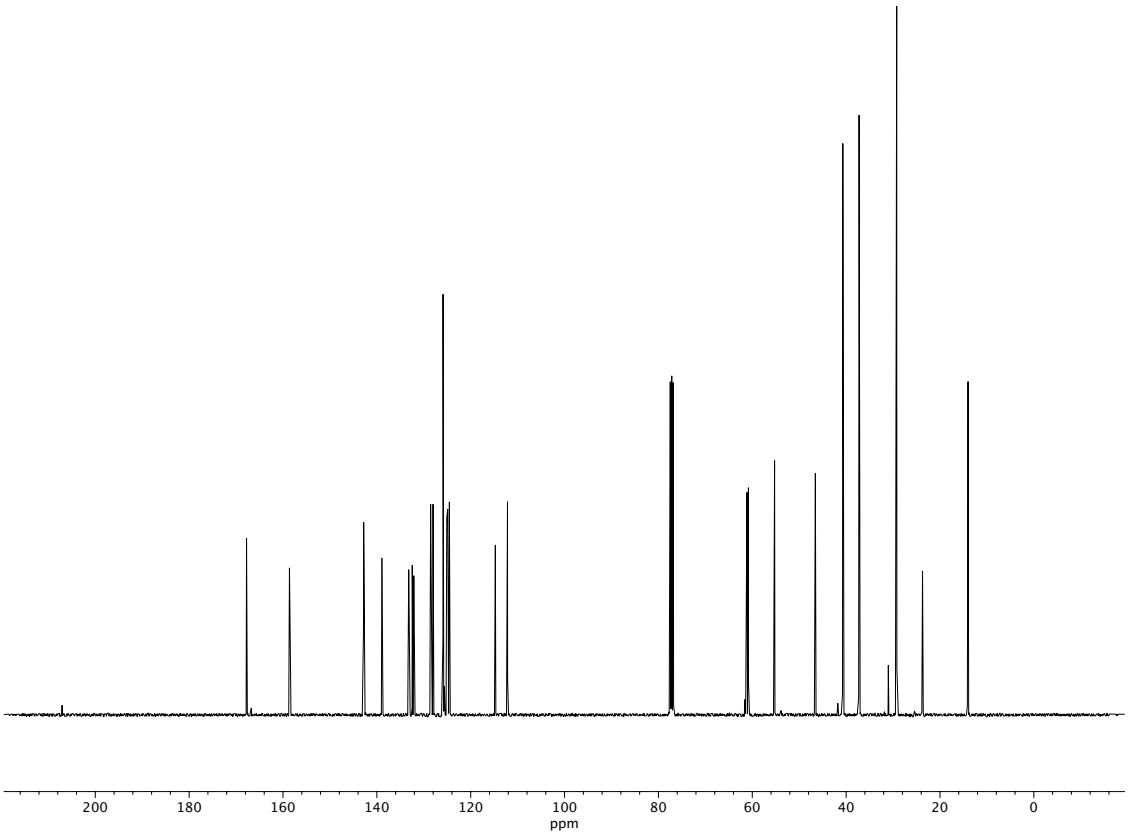


Figure A1.53 *^{13}C NMR (100 MHz, $CDCl_3$) of compound* ***32n***.

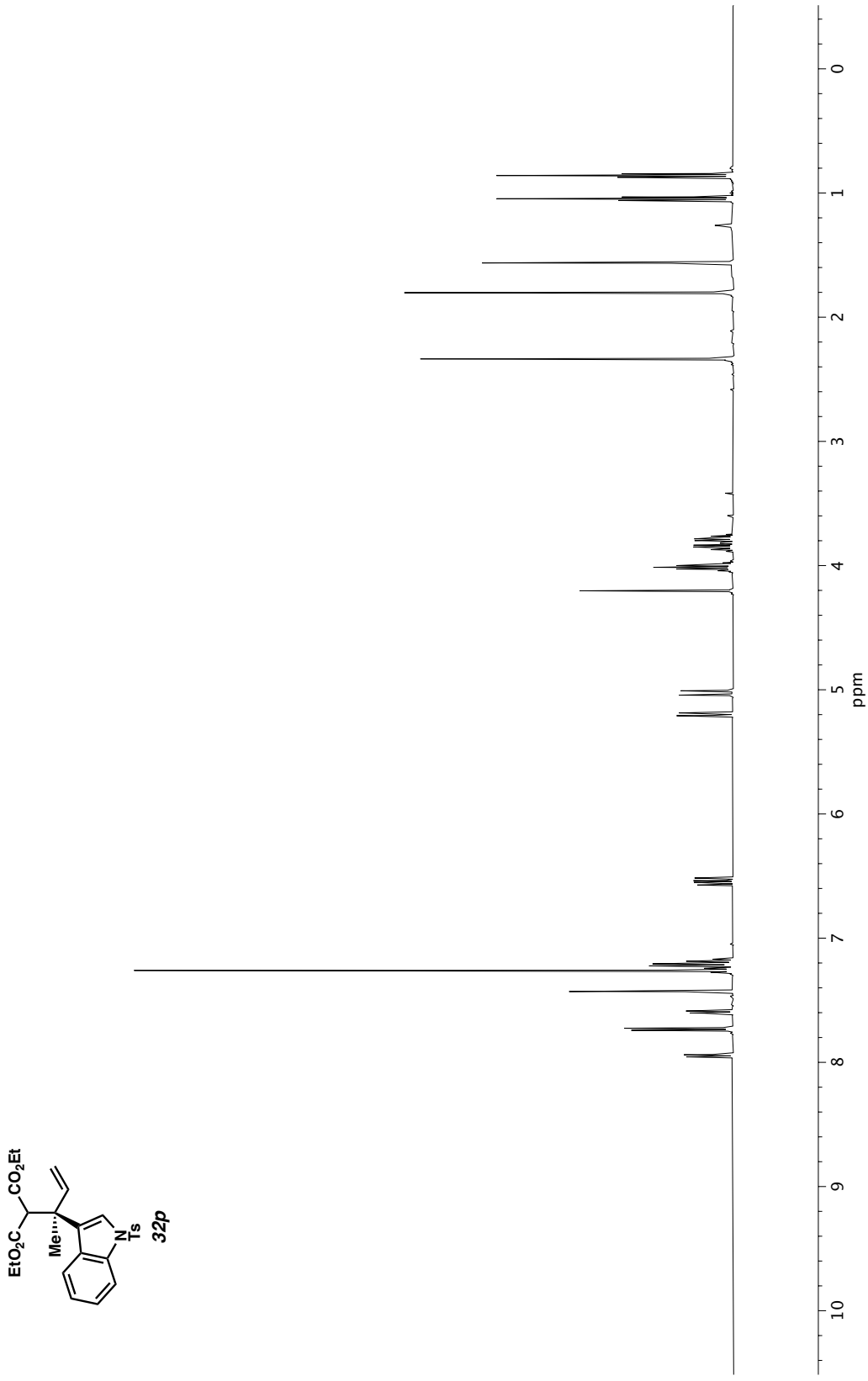


Figure A1.54 *^1H NMR (500 MHz, $CDCl_3$) of compound* ***32p***.

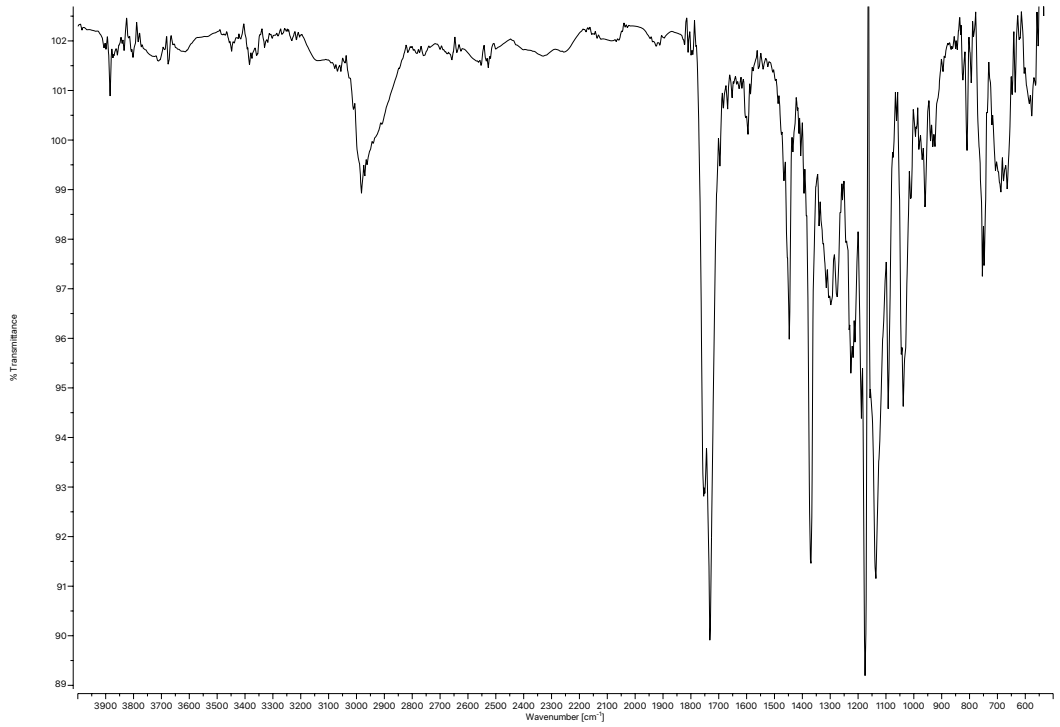


Figure A1.55 *Infrared spectrum (Thin Film, NaCl) of compound* ***32p***.

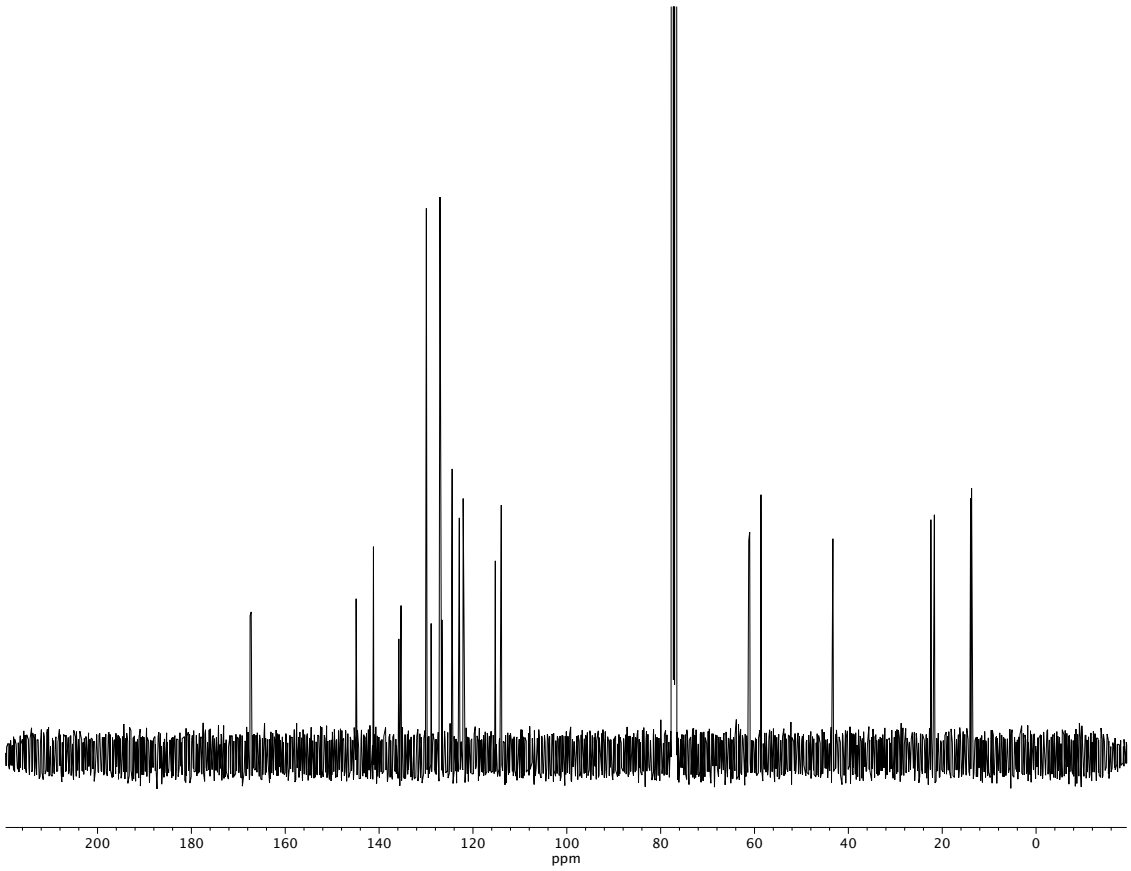


Figure A1.56 *^{13}C NMR (100 MHz, $CDCl_3$) of compound* ***32p***.

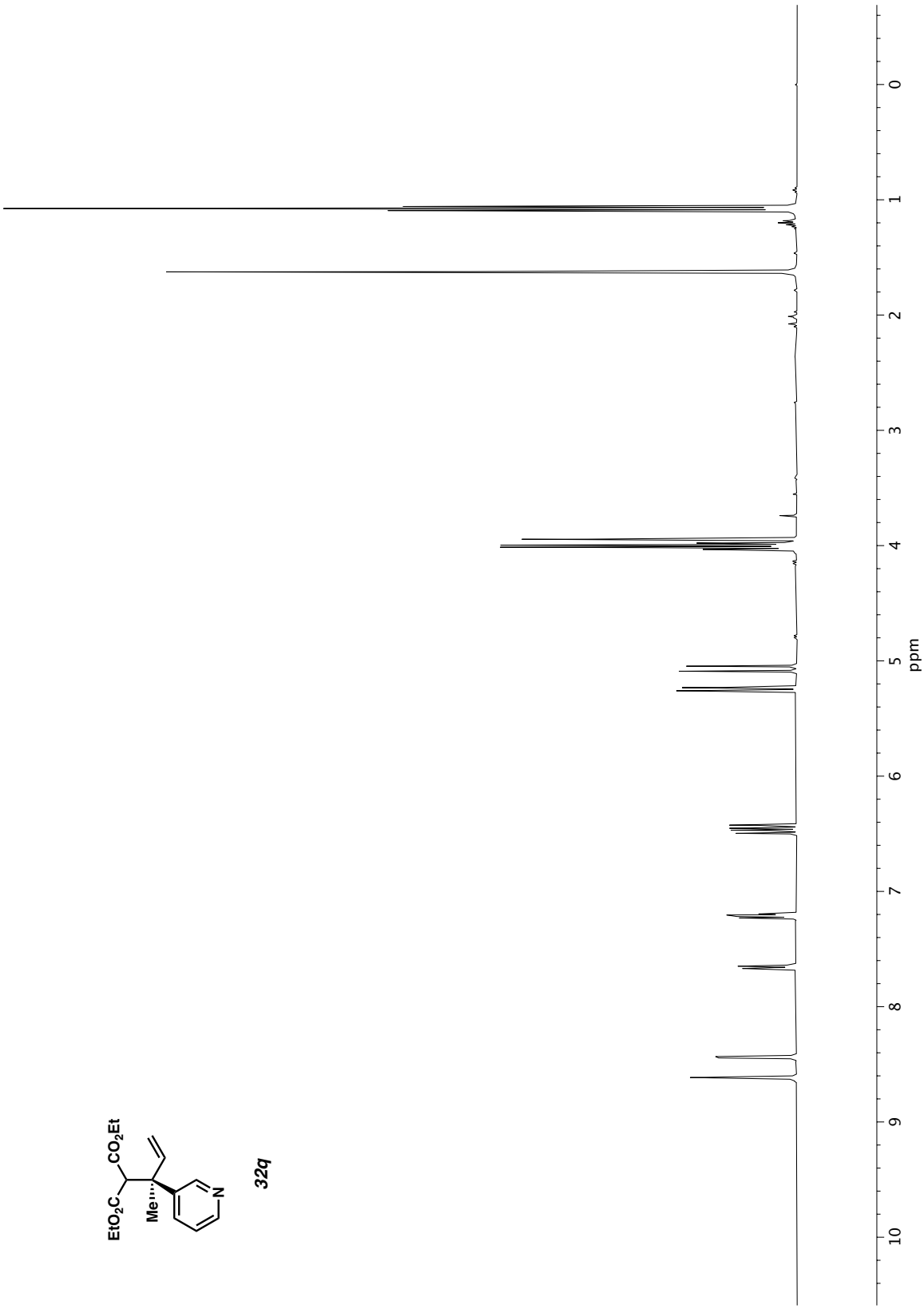


Figure A1.57 *^1H NMR (400 MHz, $CDCl_3$) of compound* ***32q***.

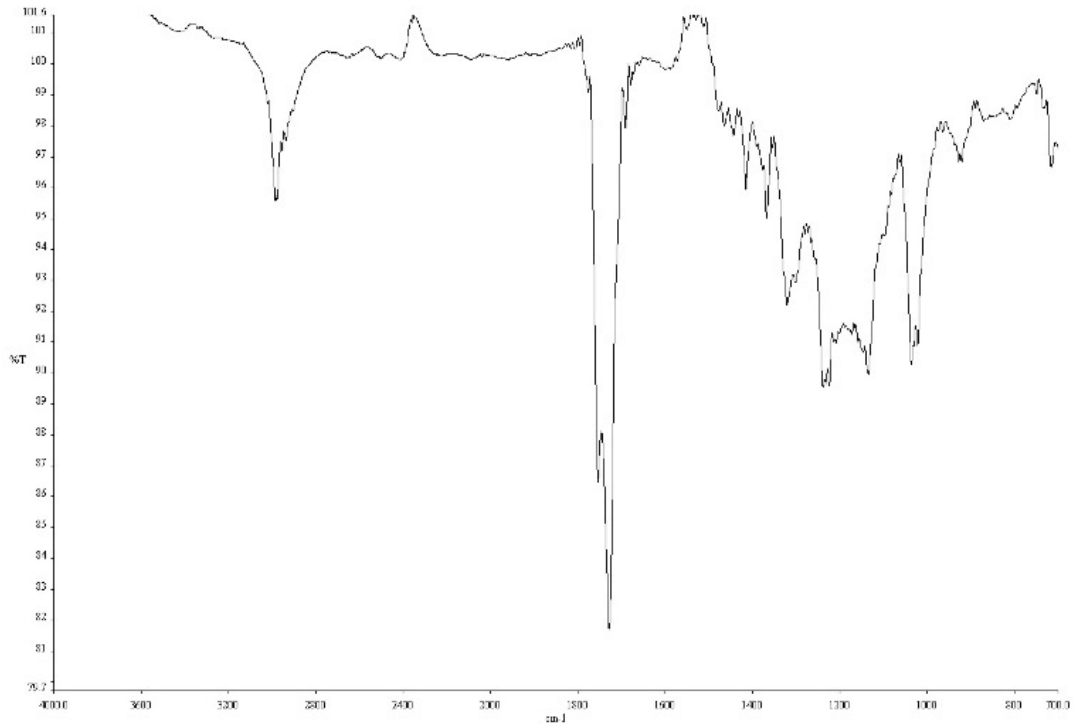


Figure A1.58 *Infrared spectrum (Thin Film, NaCl) of compound* ***32q***.

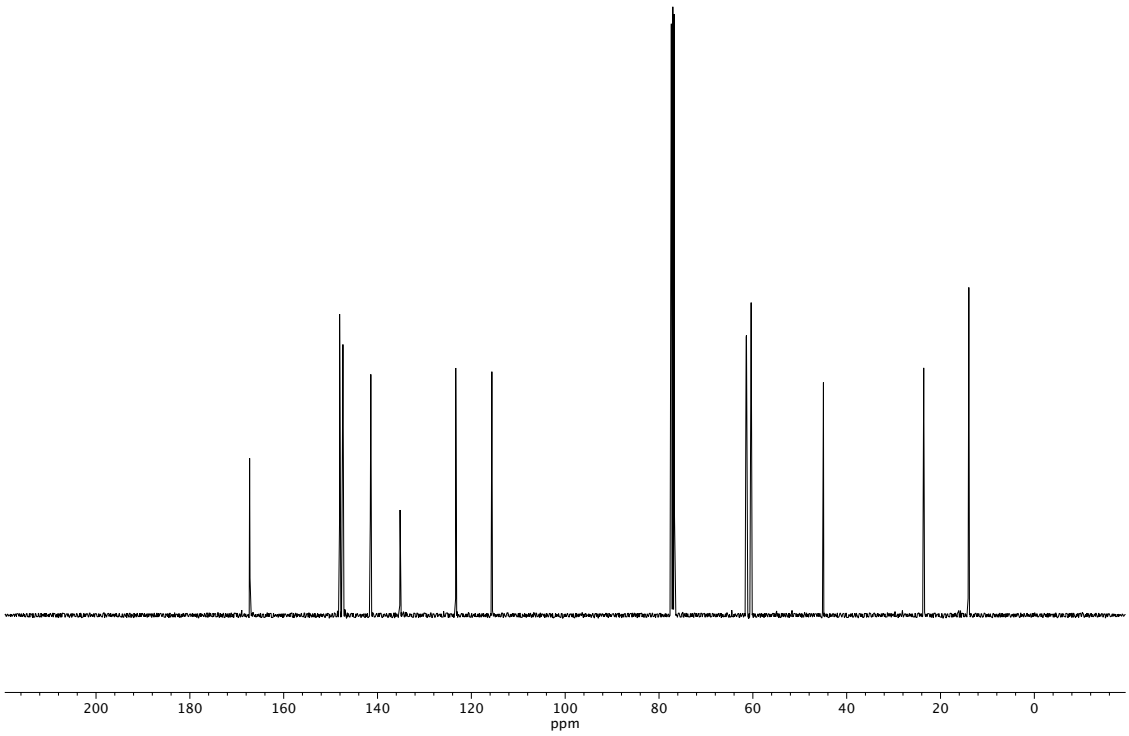


Figure A1.59 *^{13}C NMR (100 MHz, $CDCl_3$) of compound* ***32q***.

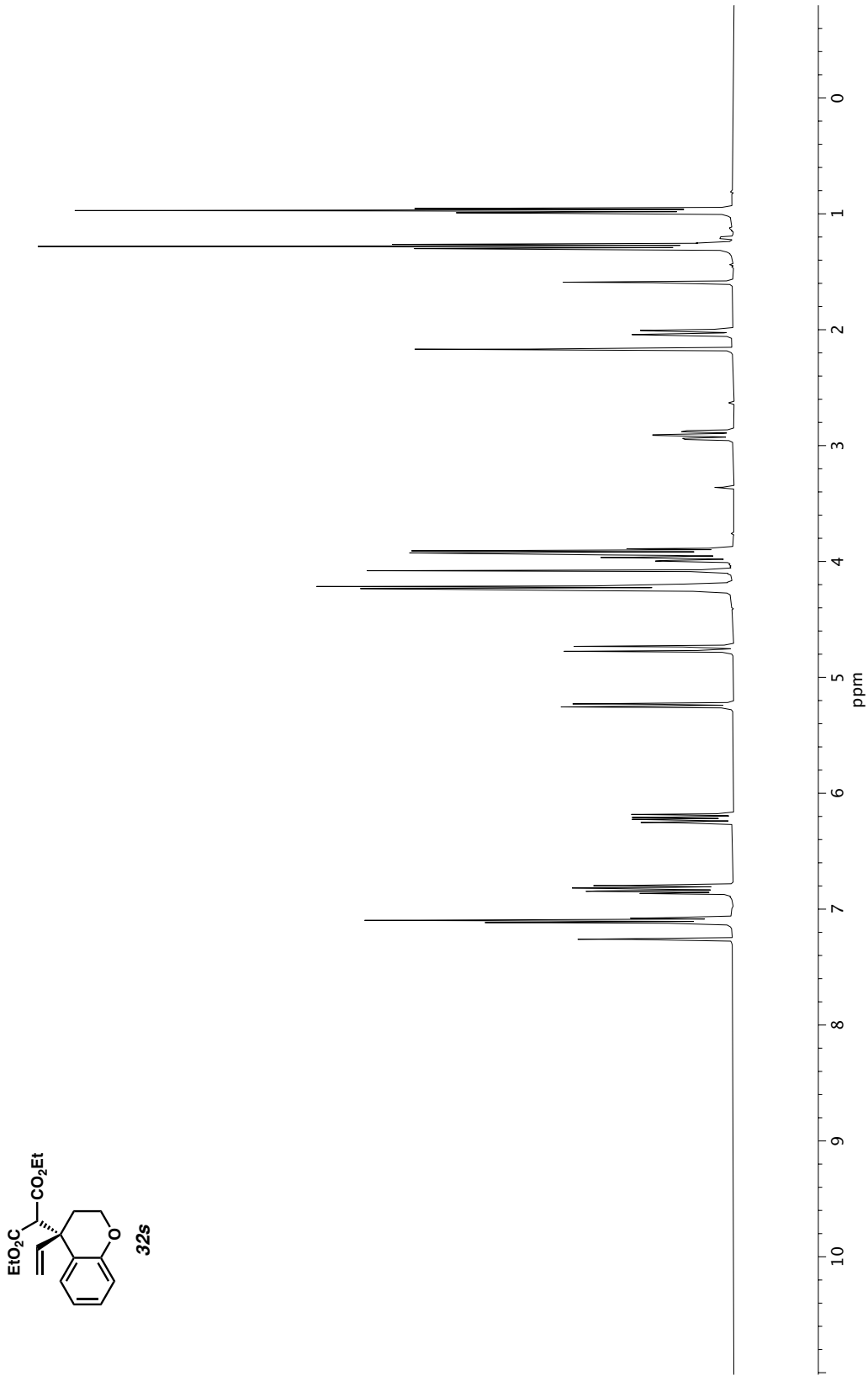


Figure A1.60 *^{1}H NMR (400 MHz, $CDCl_3$) of compound* ***32s****.*

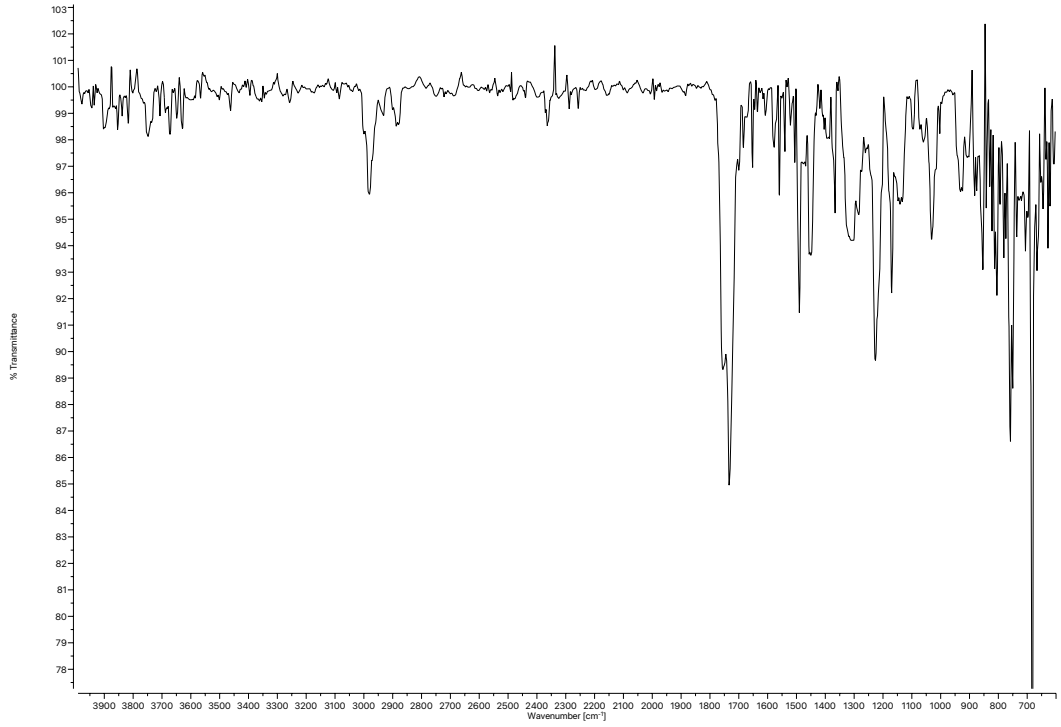


Figure A1.61 *Infrared spectrum (Thin Film, NaCl) of compound* ***32s***.

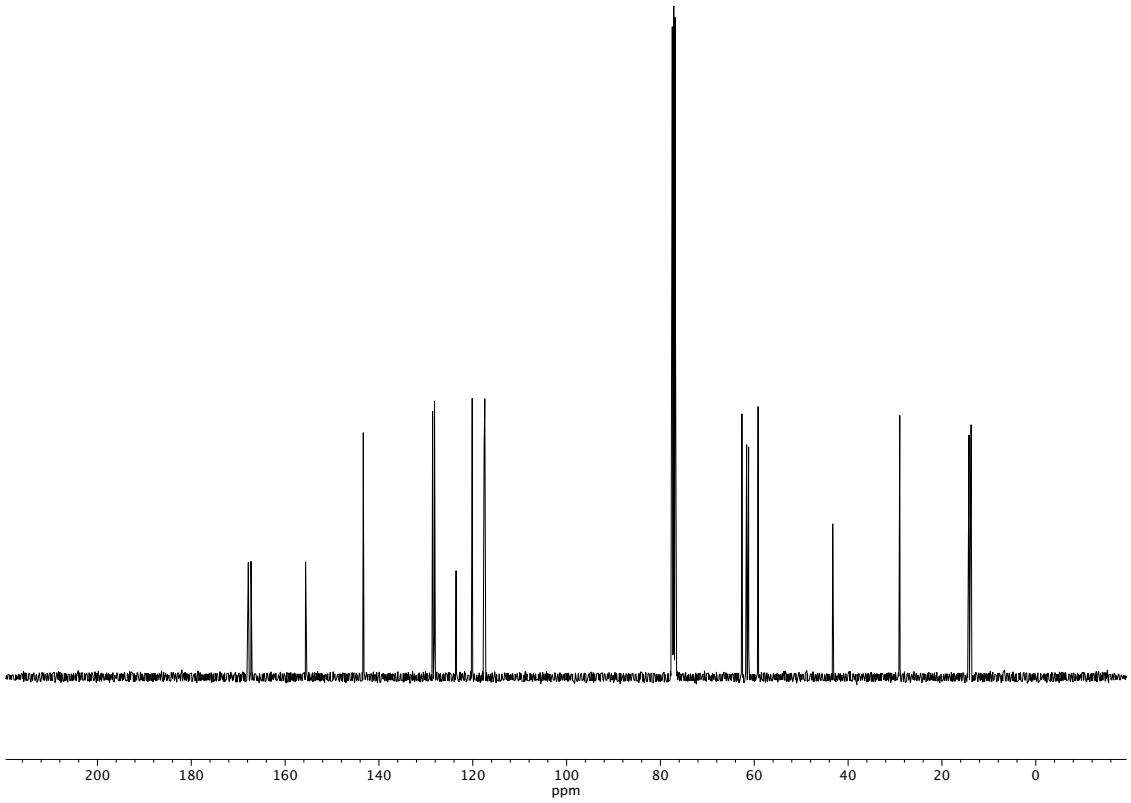


Figure A1.62 *^{13}C NMR (100 MHz, $CDCl_3$) of compound* ***32s***.

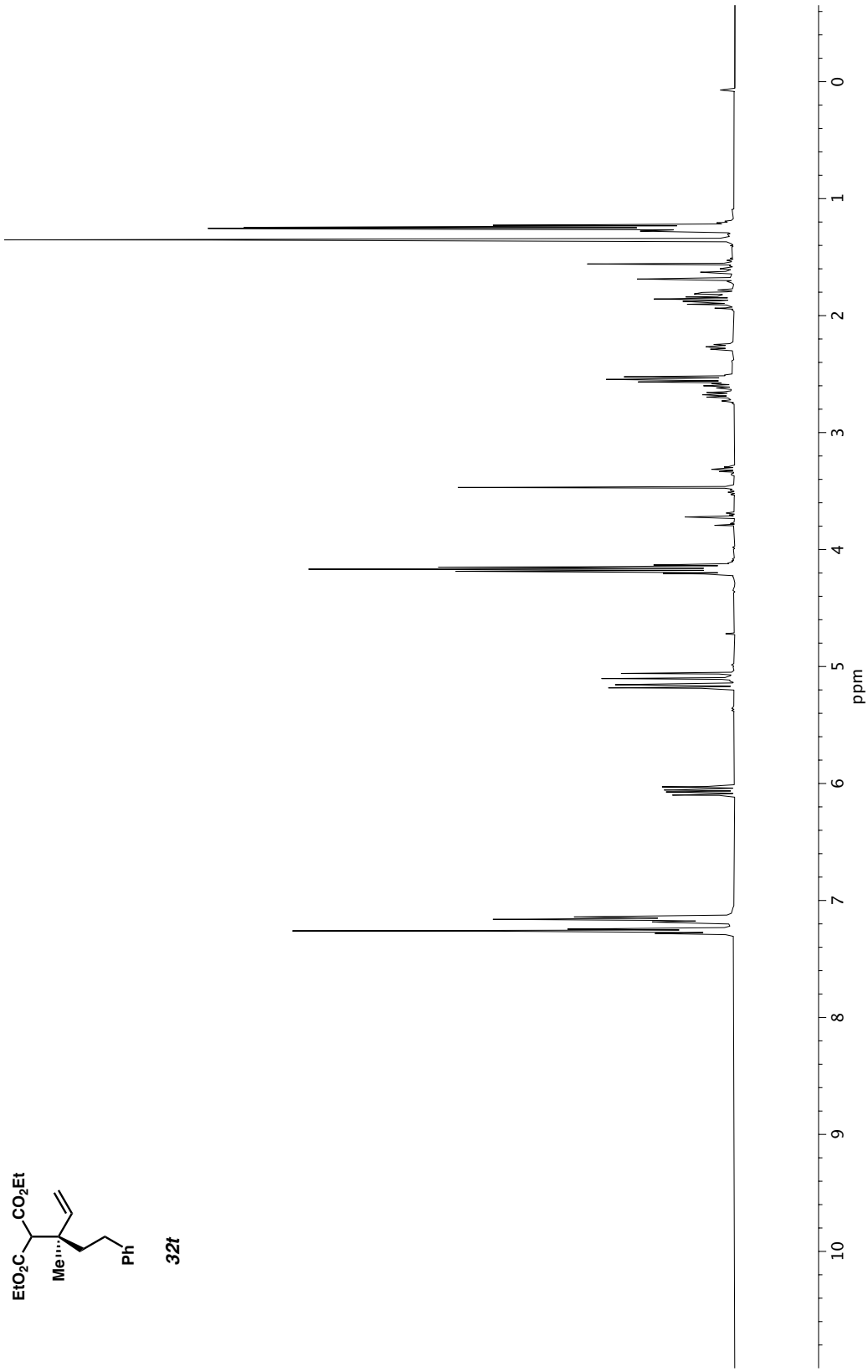


Figure A1.63 *^1H NMR (400 MHz, $CDCl_3$) of compound* ***32t****.*

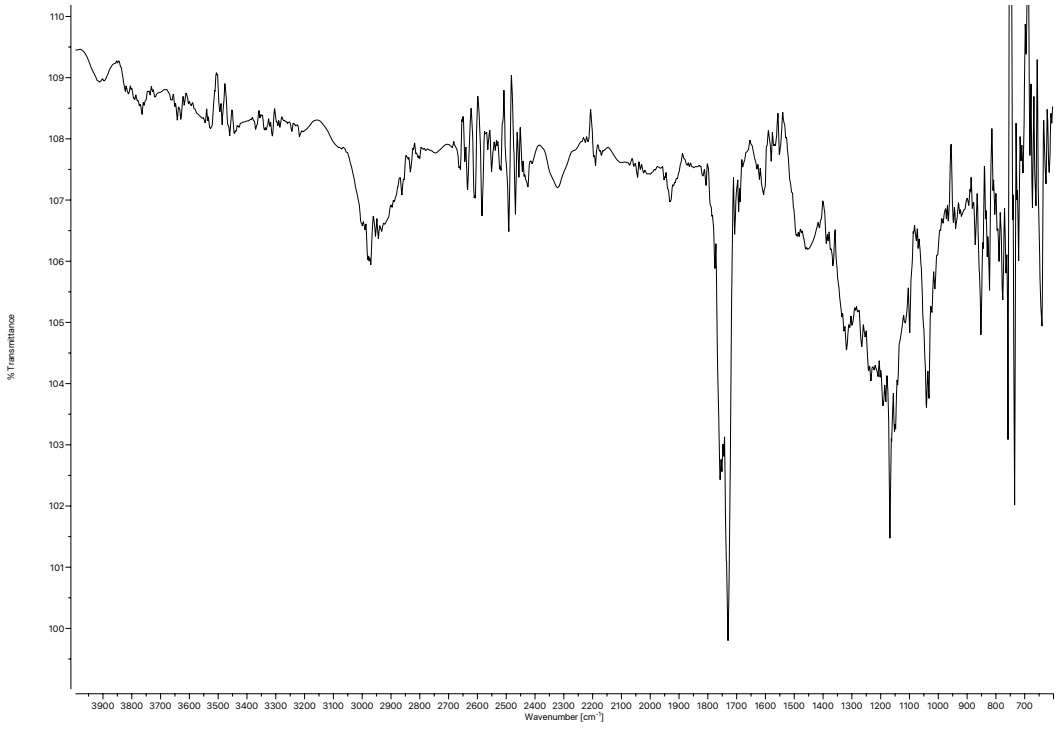


Figure A1.64 *Infrared spectrum (Thin Film, NaCl) of compound* ***32t****.*

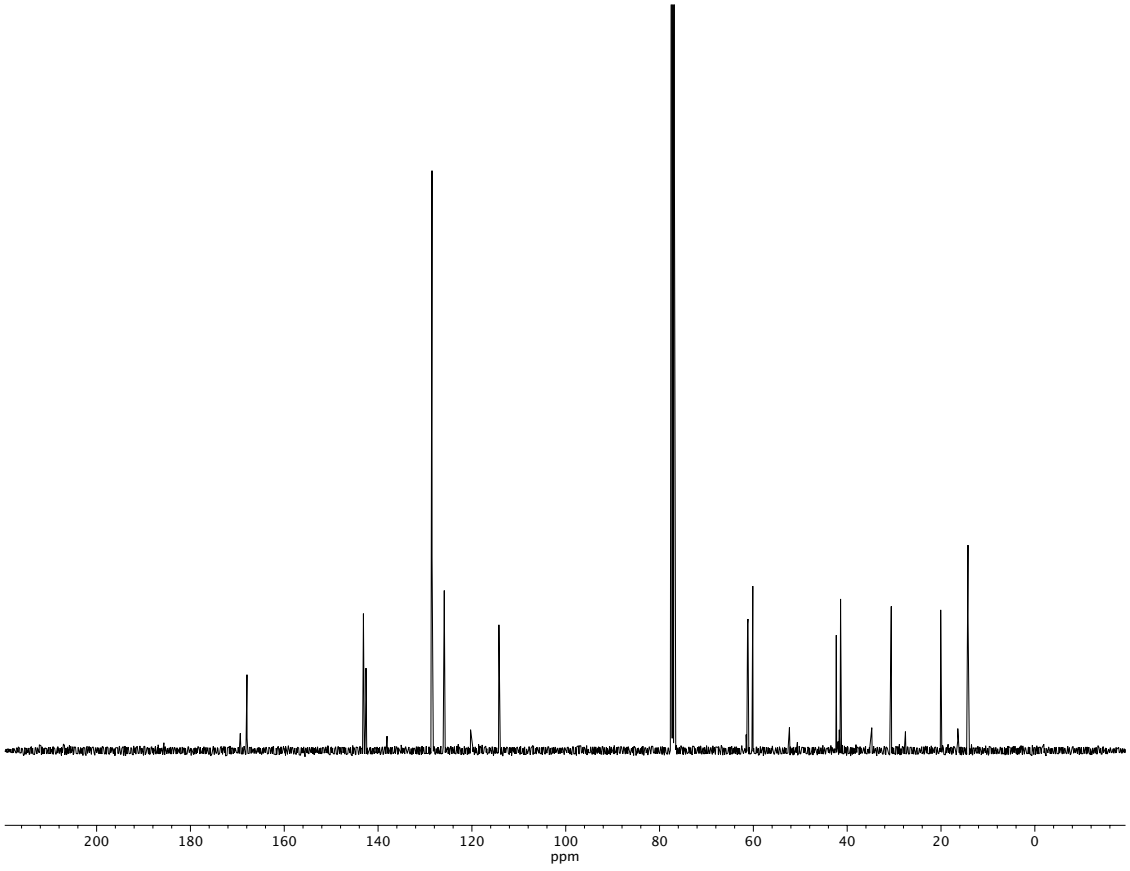
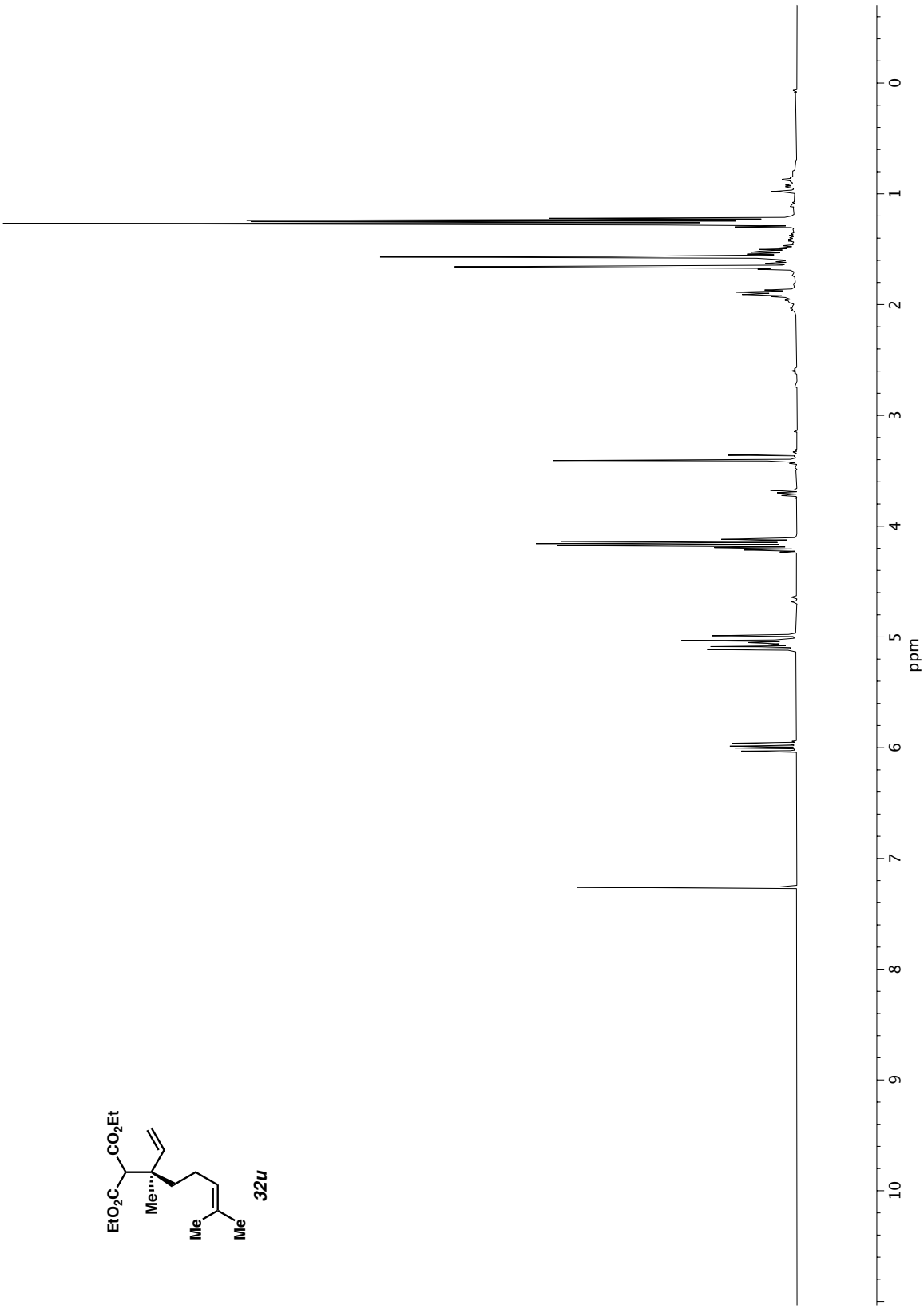


Figure A1.65 *^{13}C NMR (100 MHz, $CDCl_3$) of compound* ***32t****.*



32u

Figure A1.66 *^1H NMR (400 MHz, $CDCl_3$) of compound* ***32u***.

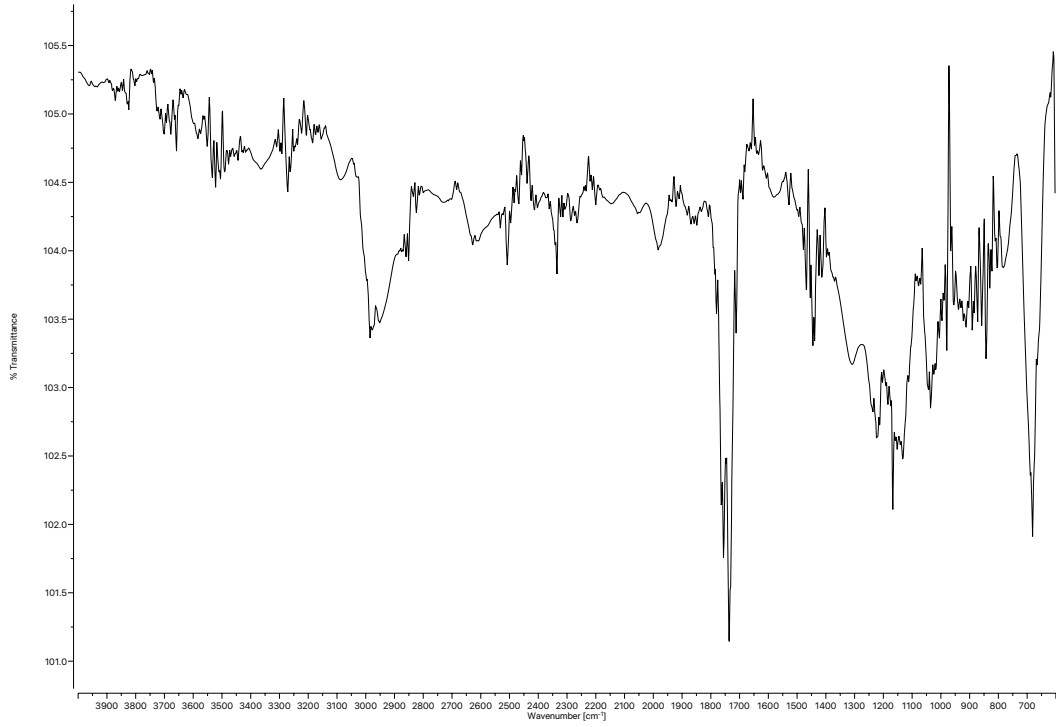


Figure A1.67 *Infrared spectrum (Thin Film, NaCl) of compound* ***32u***.

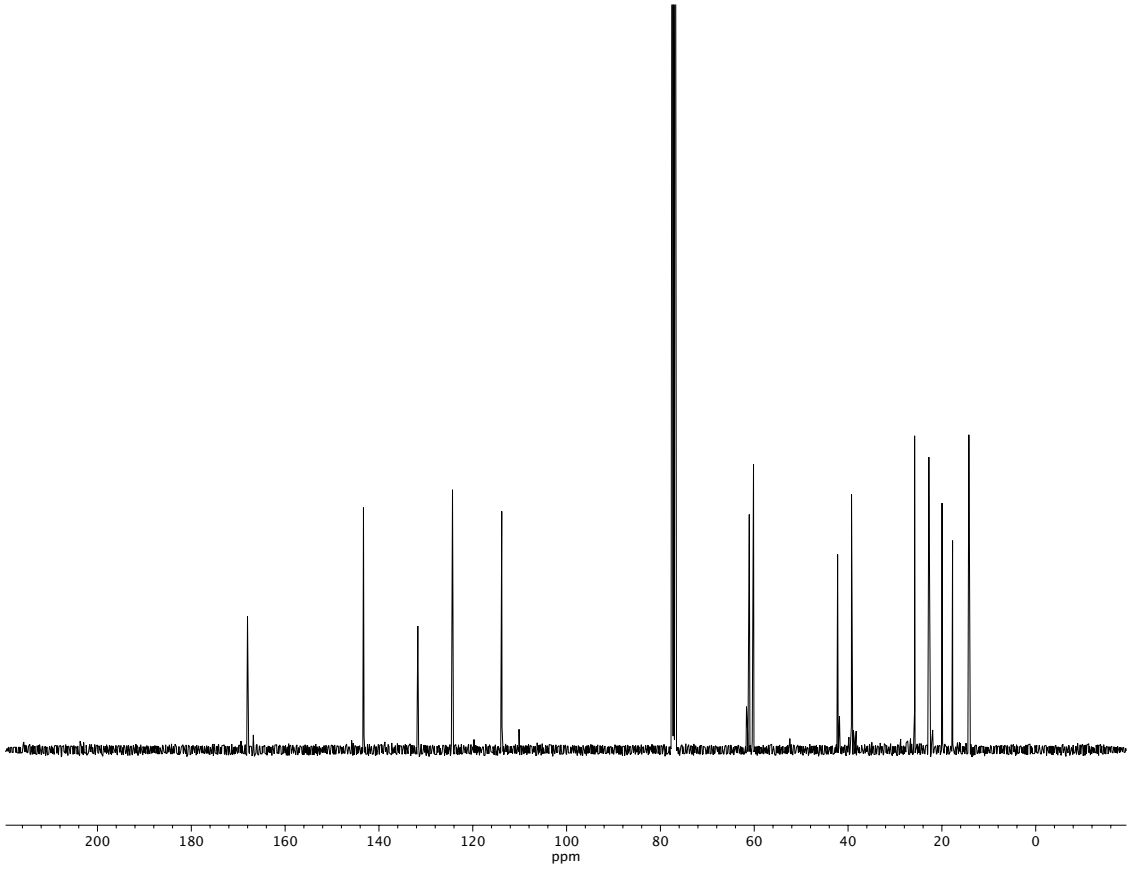


Figure A1.68 *^{13}C NMR (100 MHz, $CDCl_3$) of compound* ***32u***.

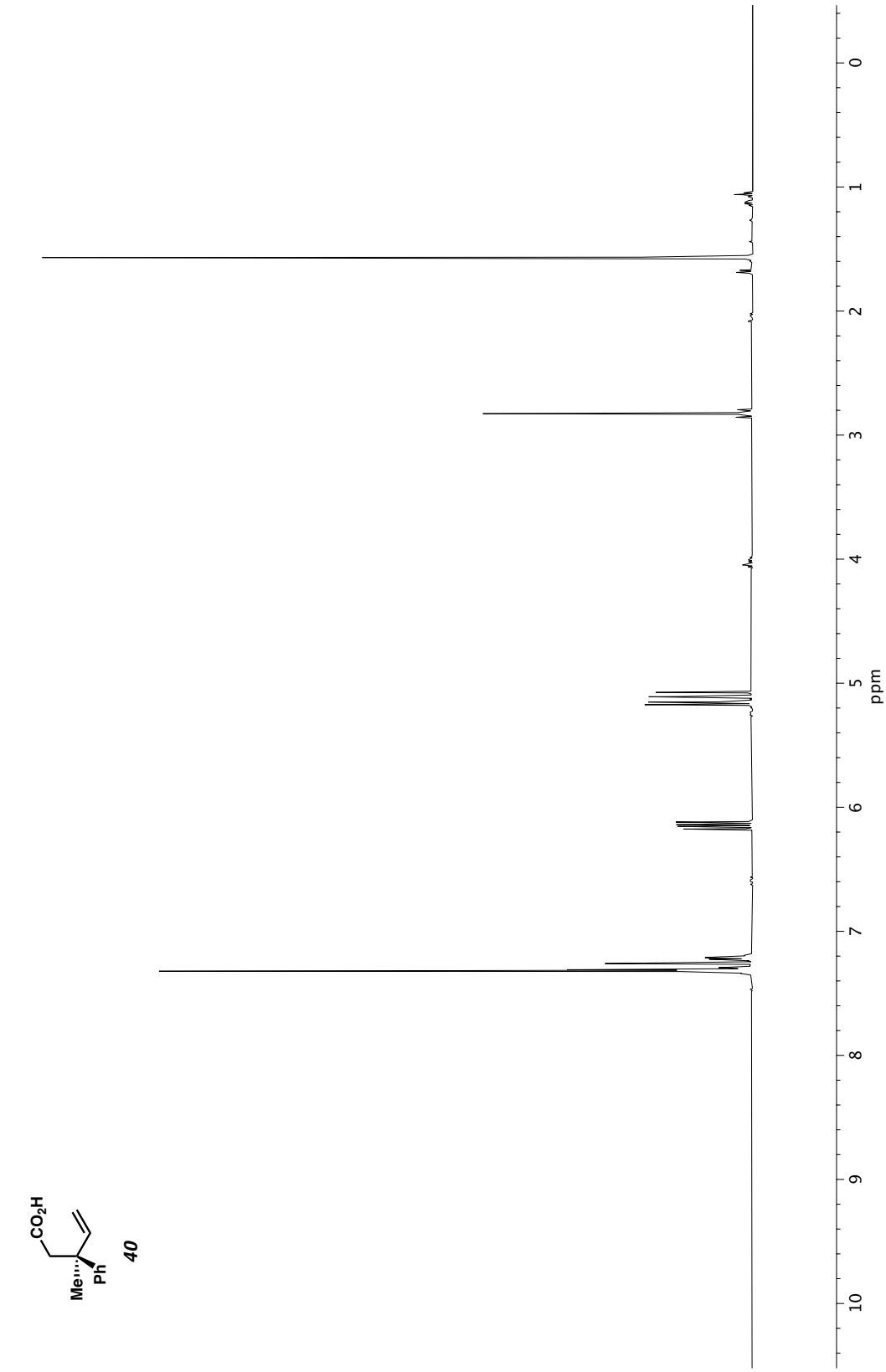


Figure A1.69 *^{1}H NMR (500 MHz, $CDCl_3$) of compound **40**.*

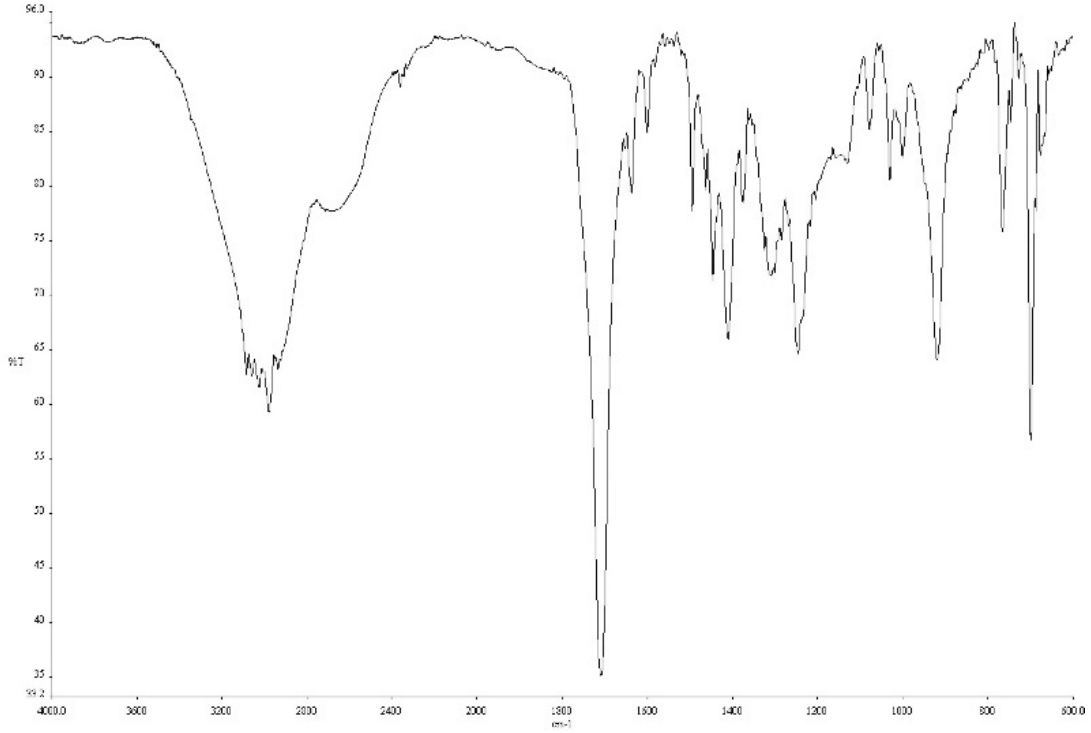


Figure A1.70 *Infrared spectrum (Thin Film, NaCl) of compound* ***40***.

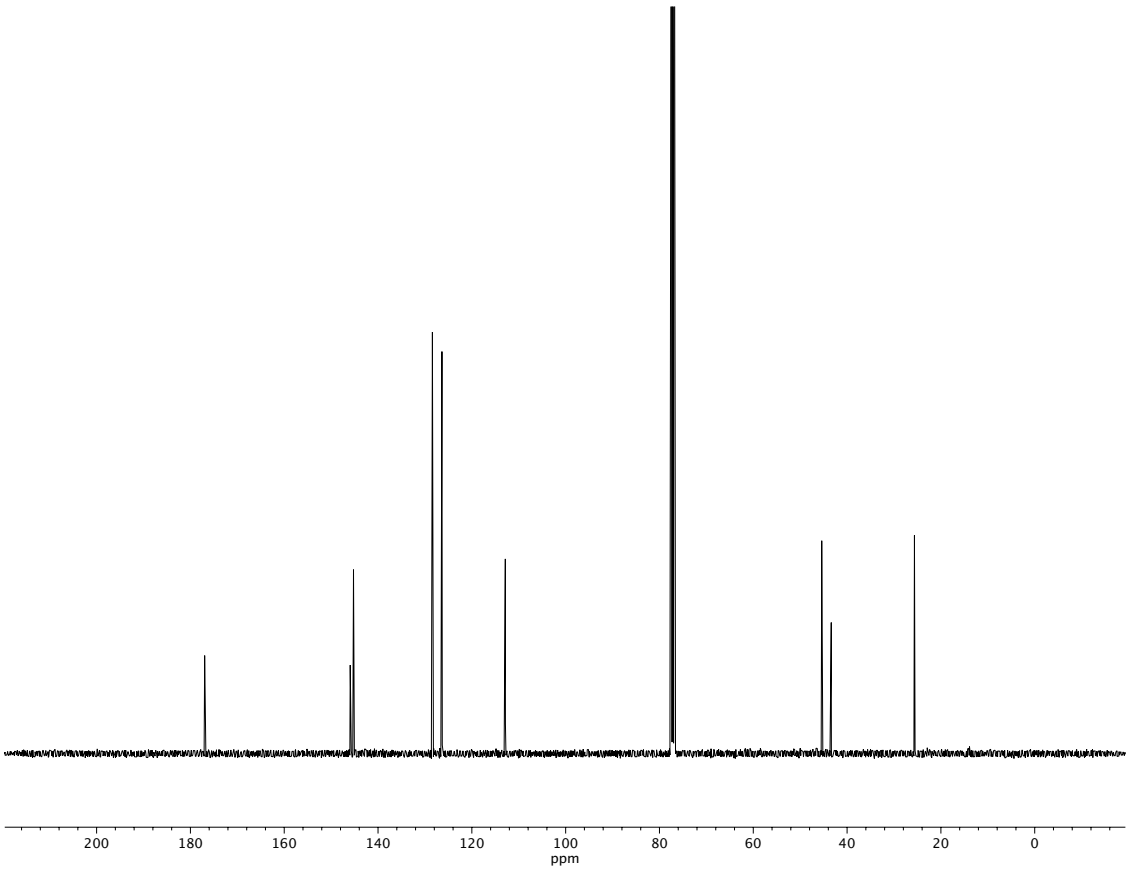


Figure A1.71 *^{13}C NMR (100 MHz, $CDCl_3$) of compound* ***40***.

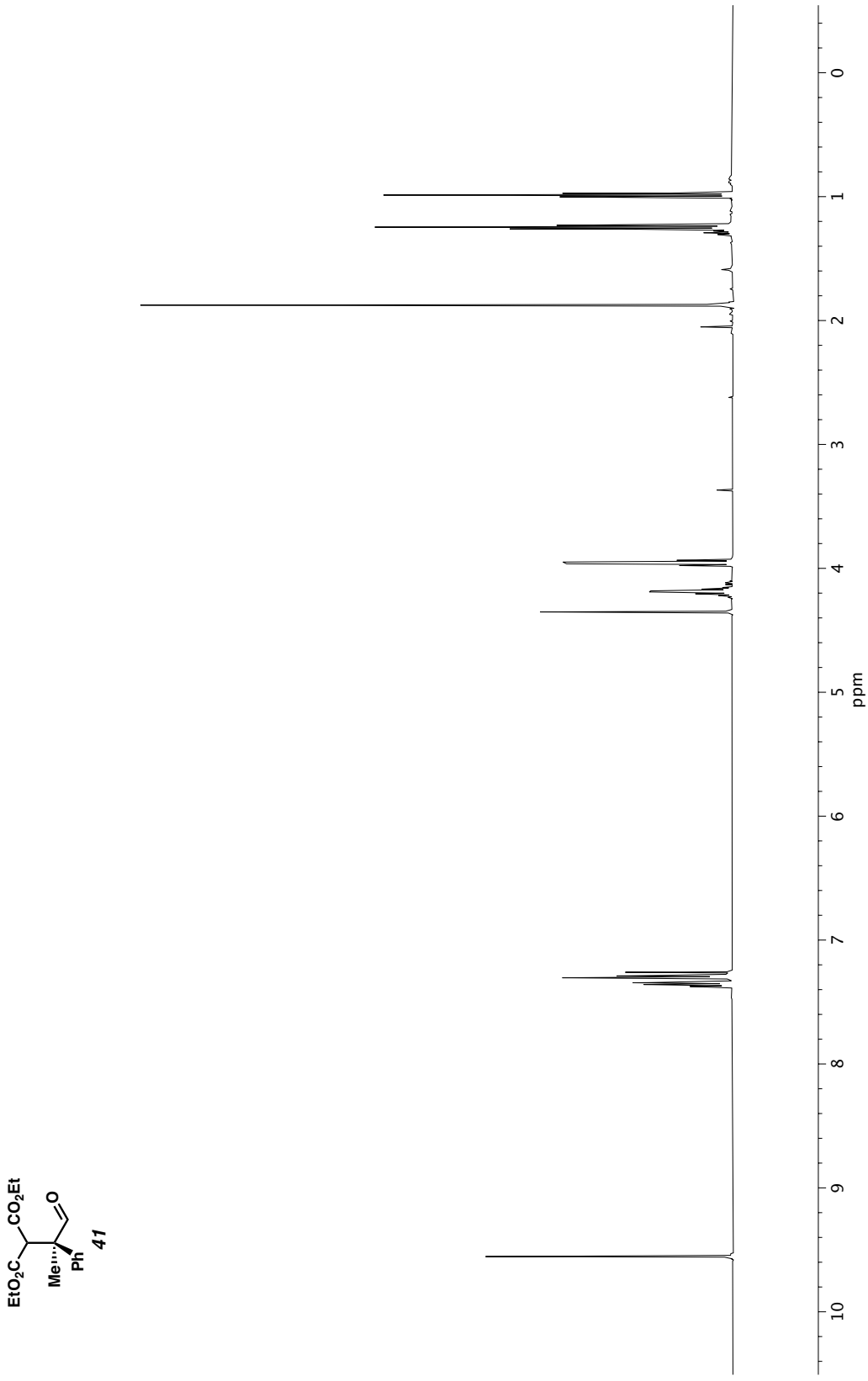


Figure A1.72 *^{1}H NMR (500 MHz, $CDCl_3$) of compound **41**.*

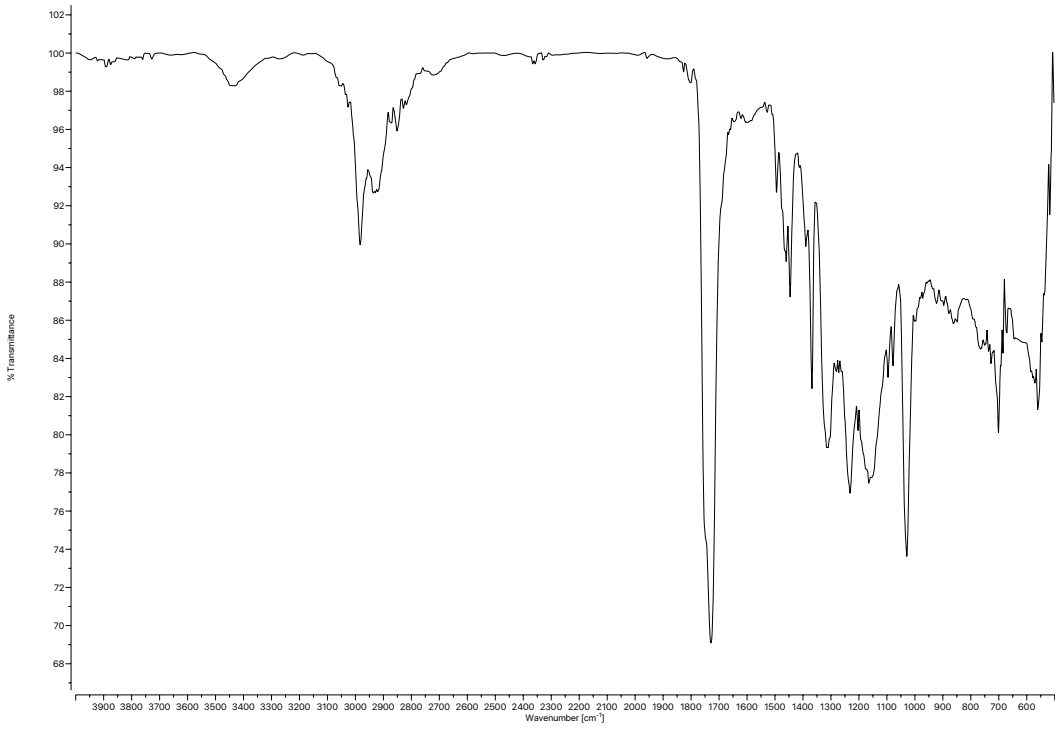


Figure A1.73 *Infrared spectrum (Thin Film, NaCl) of compound* ***41***.

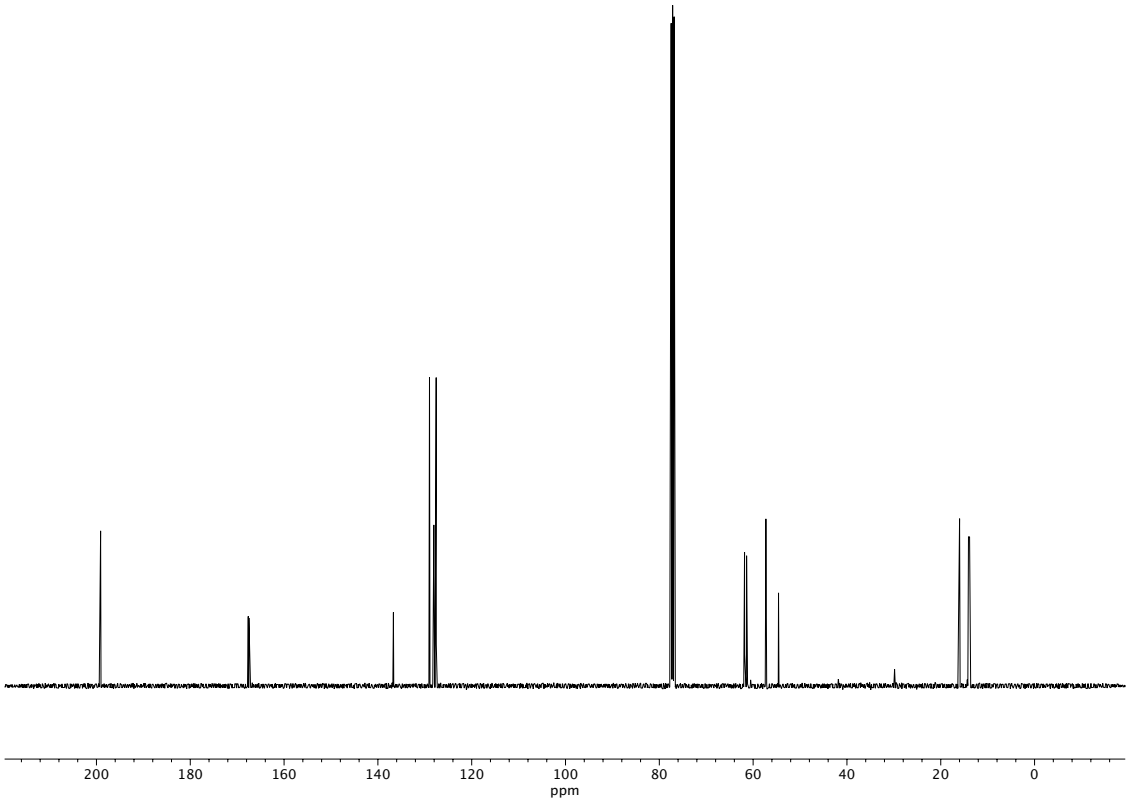


Figure A1.74 *^{13}C NMR (100 MHz, $CDCl_3$) of compound* ***41***.

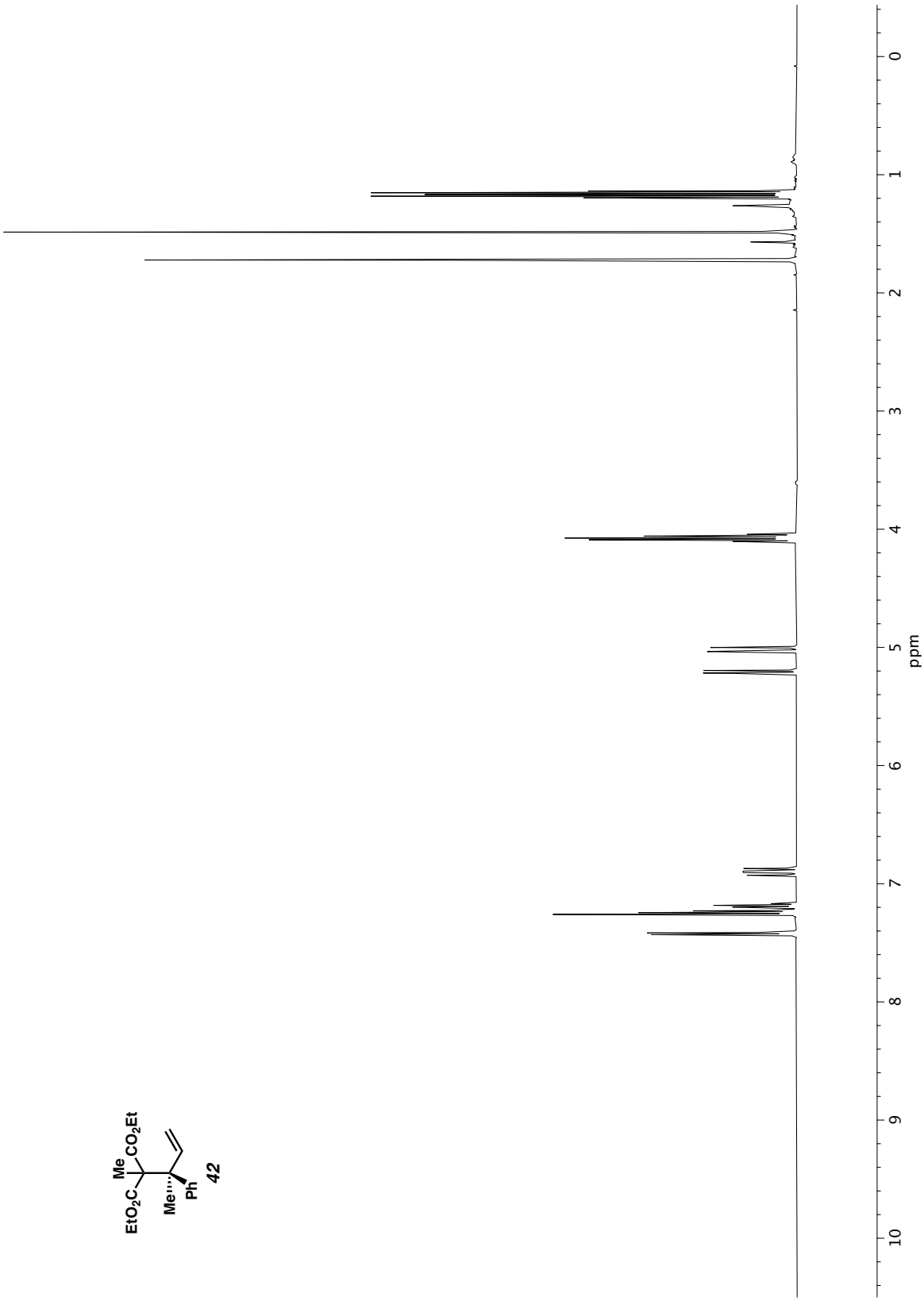


Figure A1.75 *^{1}H NMR (500 MHz, $CDCl_3$) of compound* ***42***.

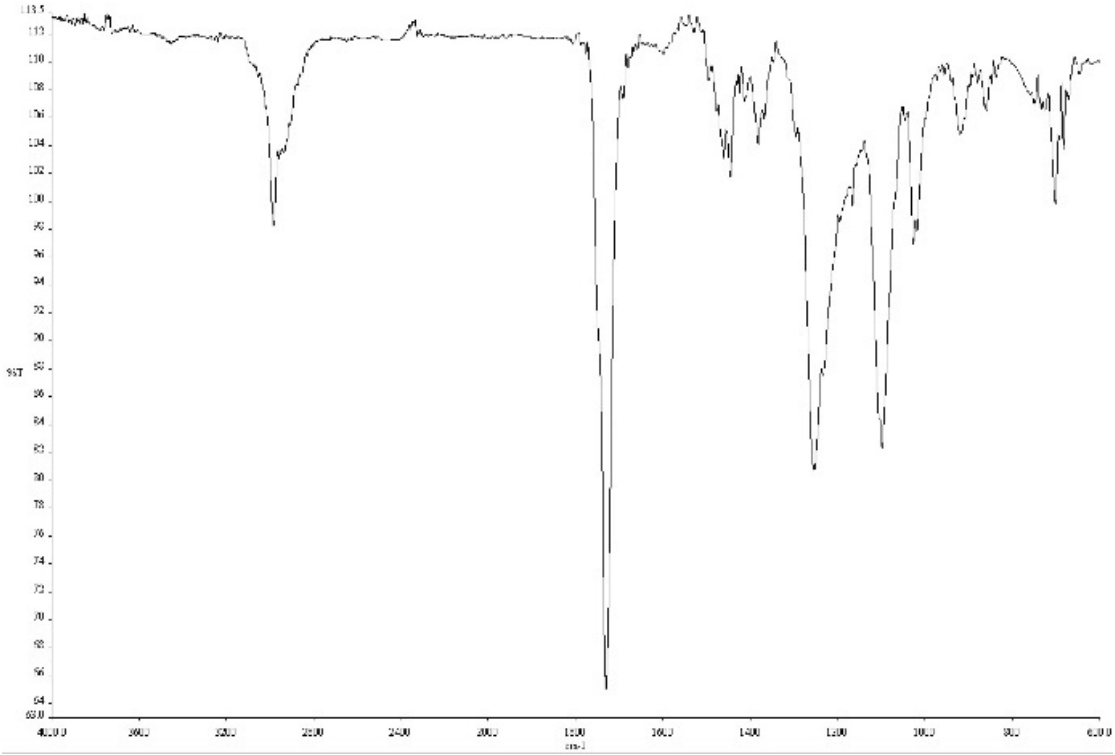


Figure A1.76 *Infrared spectrum (Thin Film, NaCl) of compound* ***42***.

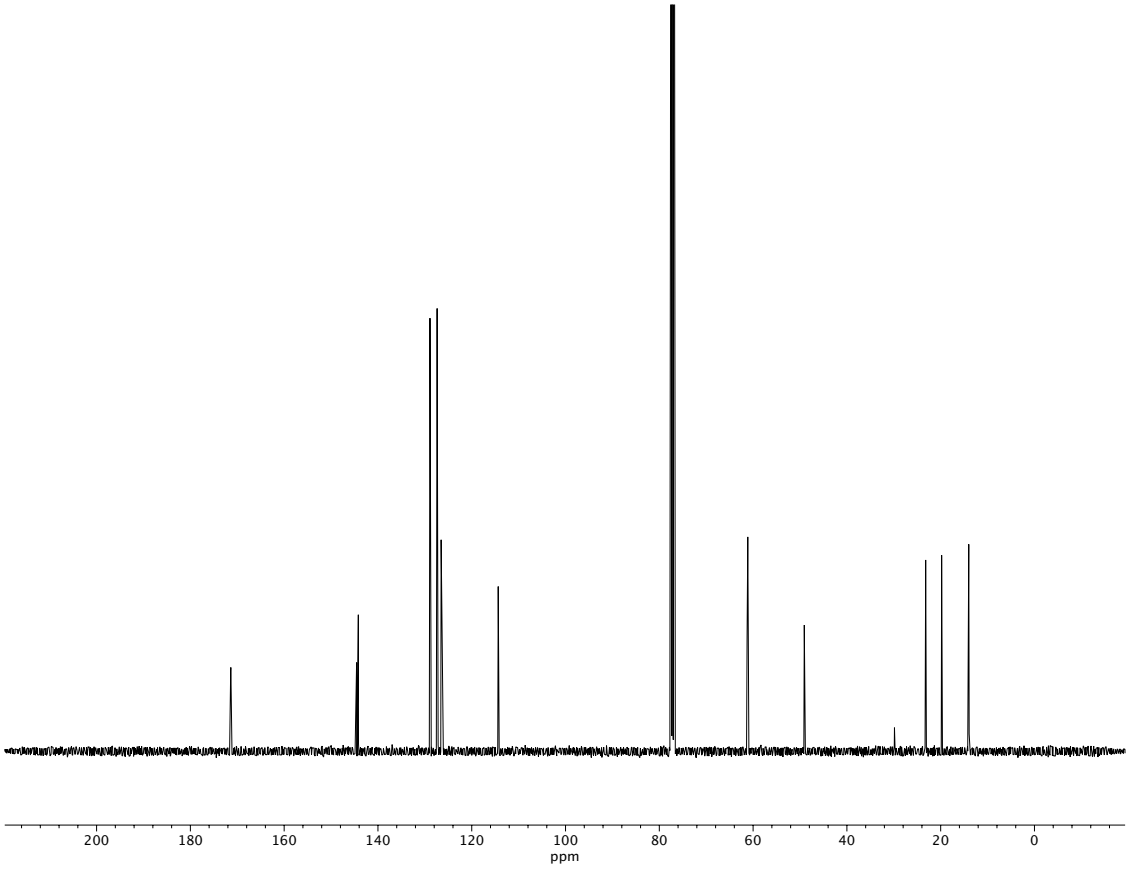


Figure A1.77 *^{13}C NMR (100 MHz, $CDCl_3$) of compound* ***42***.

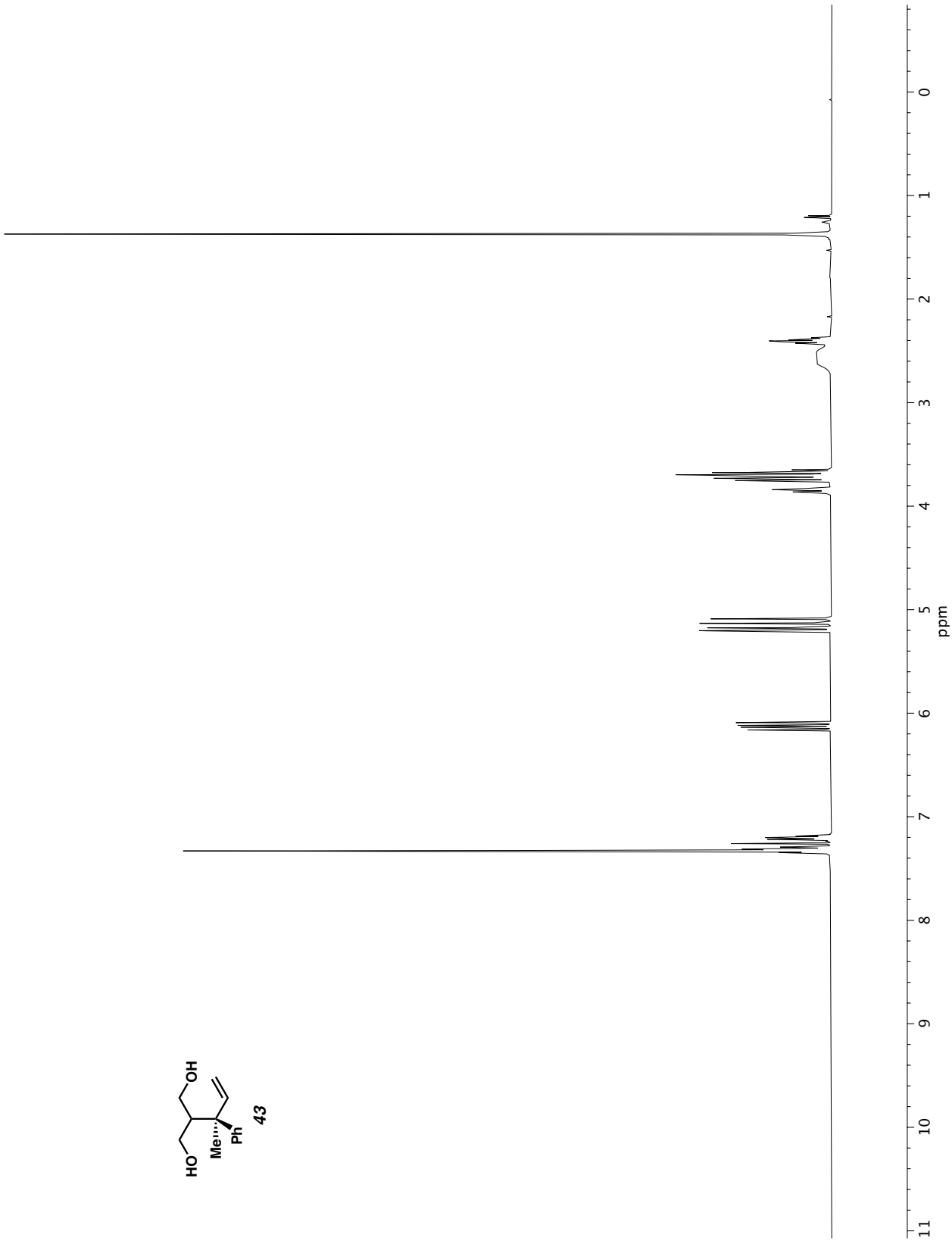


Figure A1.78 *^{1}H NMR (400 MHz, $CDCl_3$) of compound* ***43***.

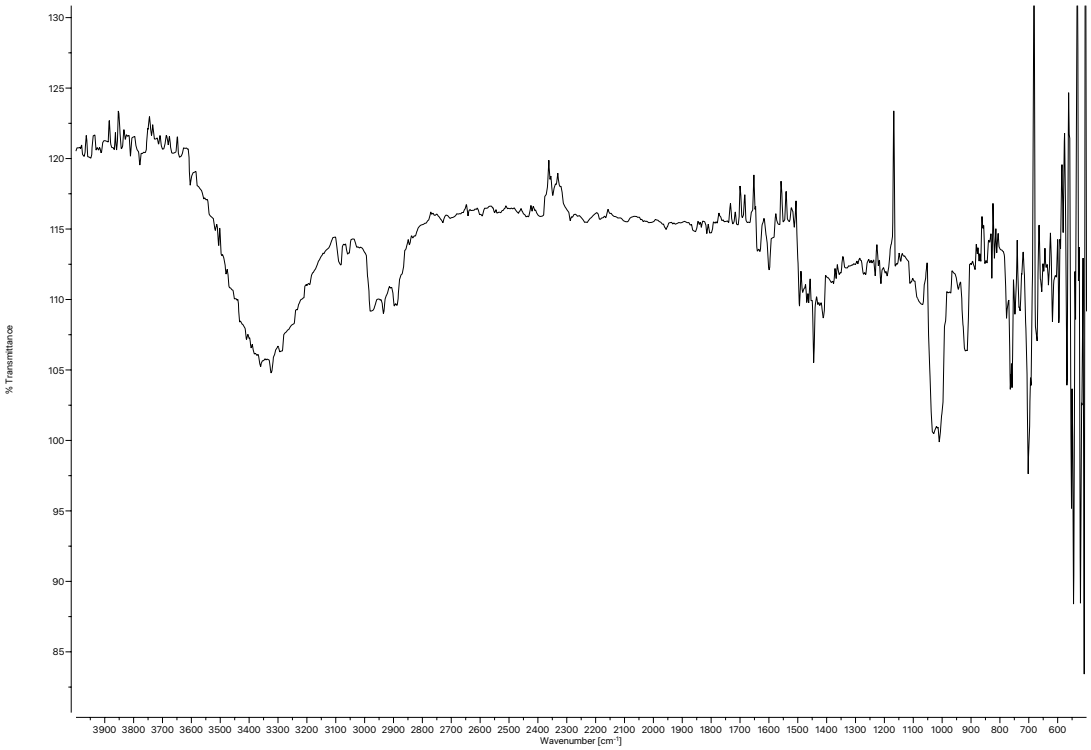


Figure A1.79 *Infrared spectrum (Thin Film, NaCl) of compound* ***43***.

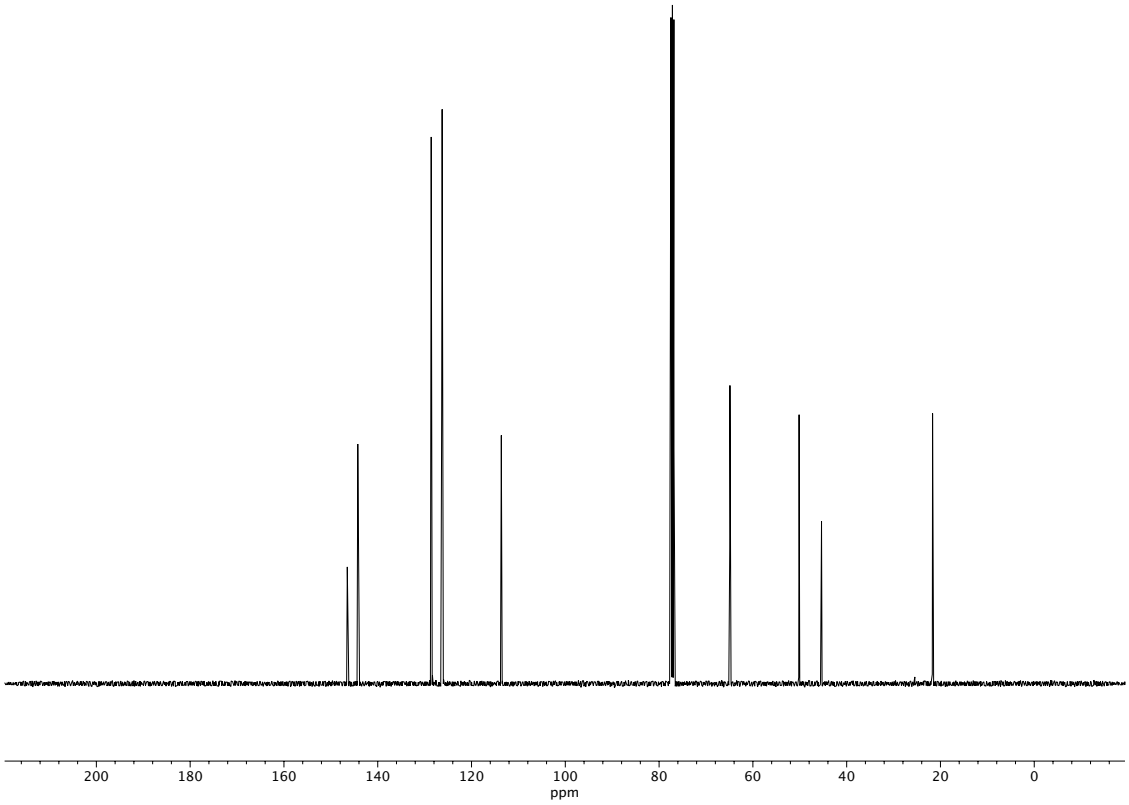


Figure A1.80 *^{13}C NMR (100 MHz, $CDCl_3$) of compound* ***43***.

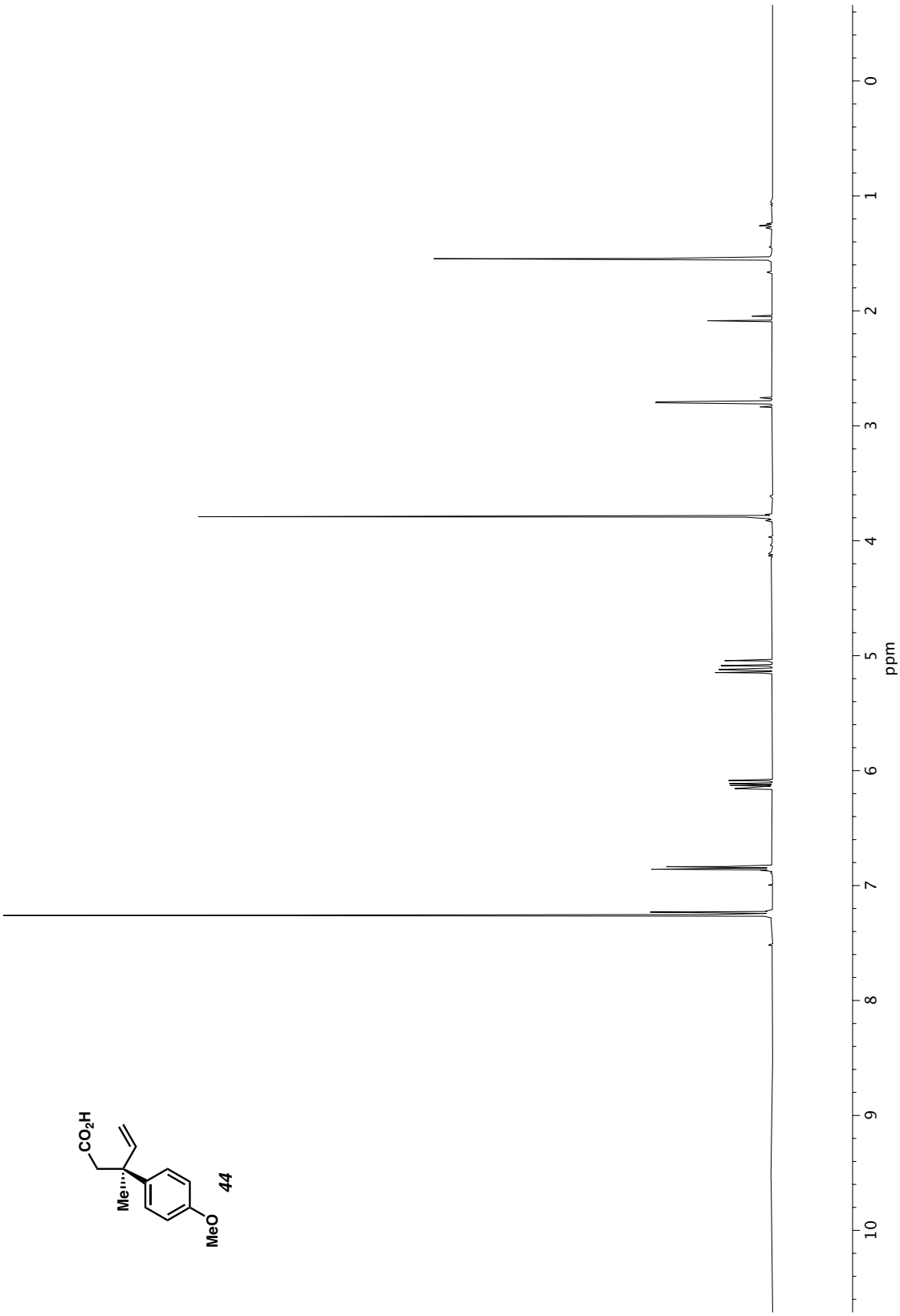


Figure A1.81 *^{1}H NMR (400 MHz, $CDCl_3$) of compound* ***44***.

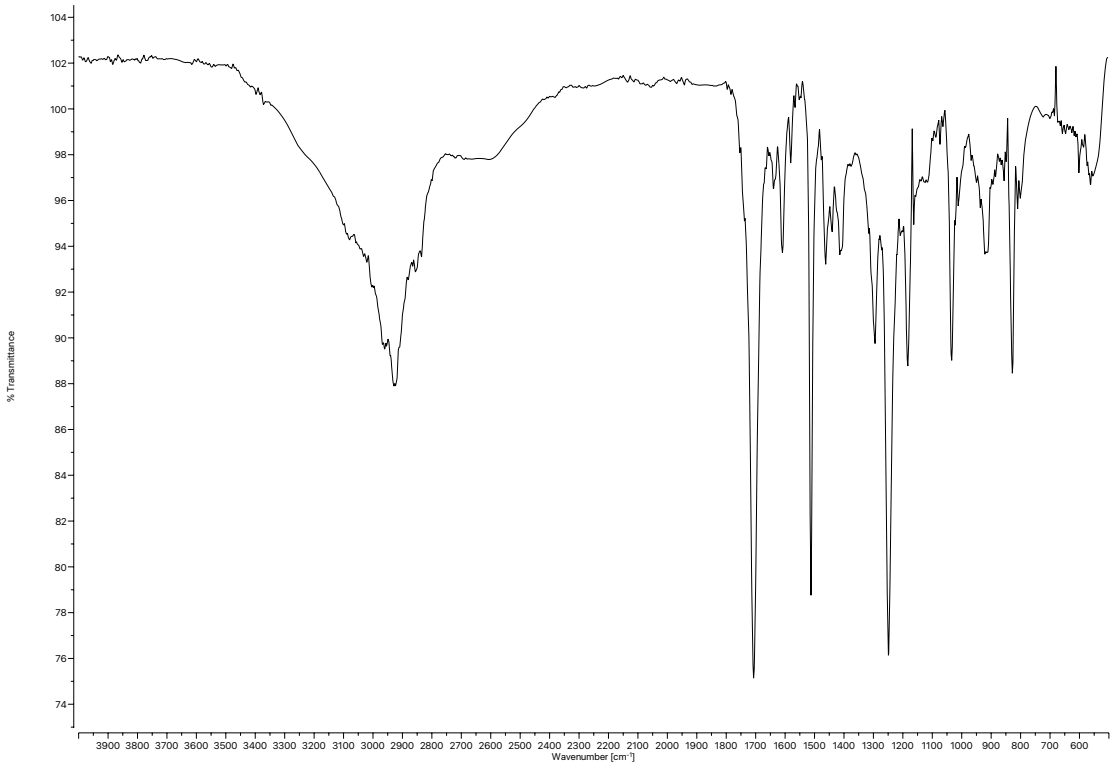


Figure A1.82 *Infrared spectrum (Thin Film, NaCl) of compound* ***44***.

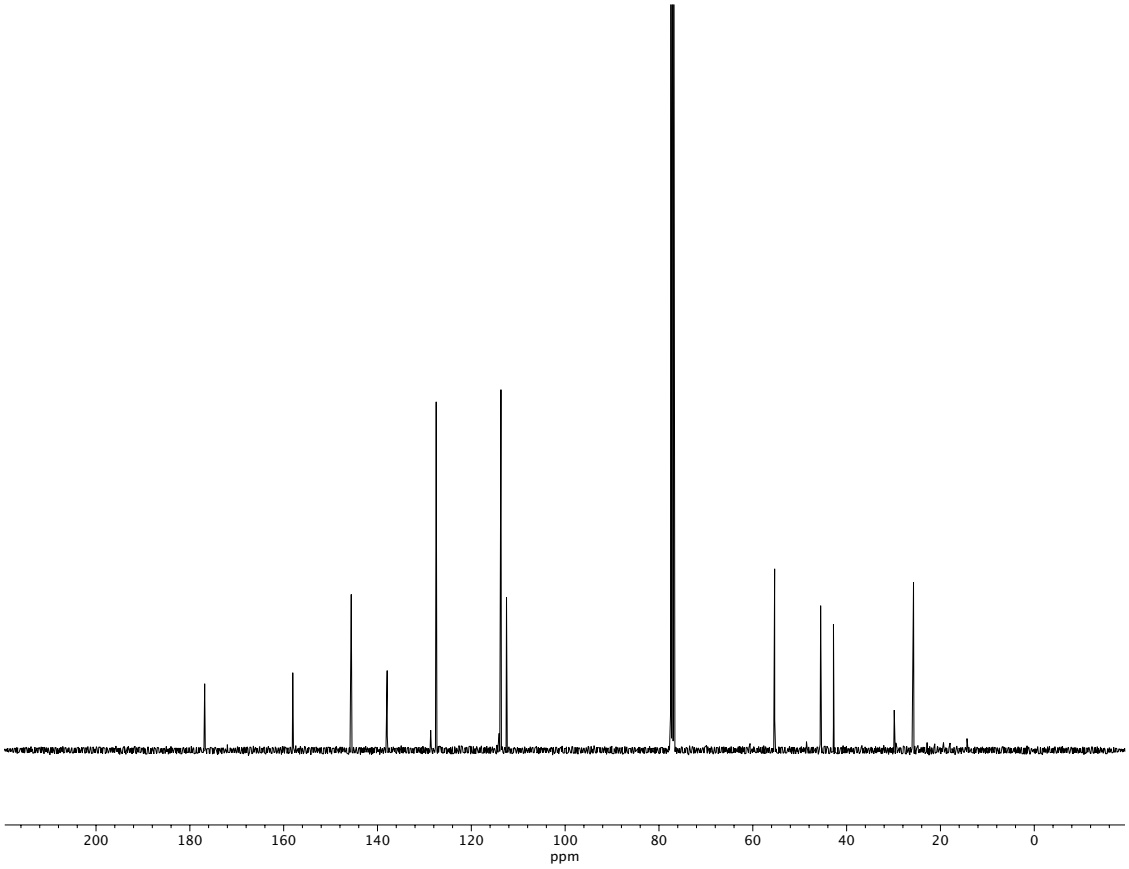


Figure A1.83 *^{13}C NMR (100 MHz, $CDCl_3$) of compound* ***44***.

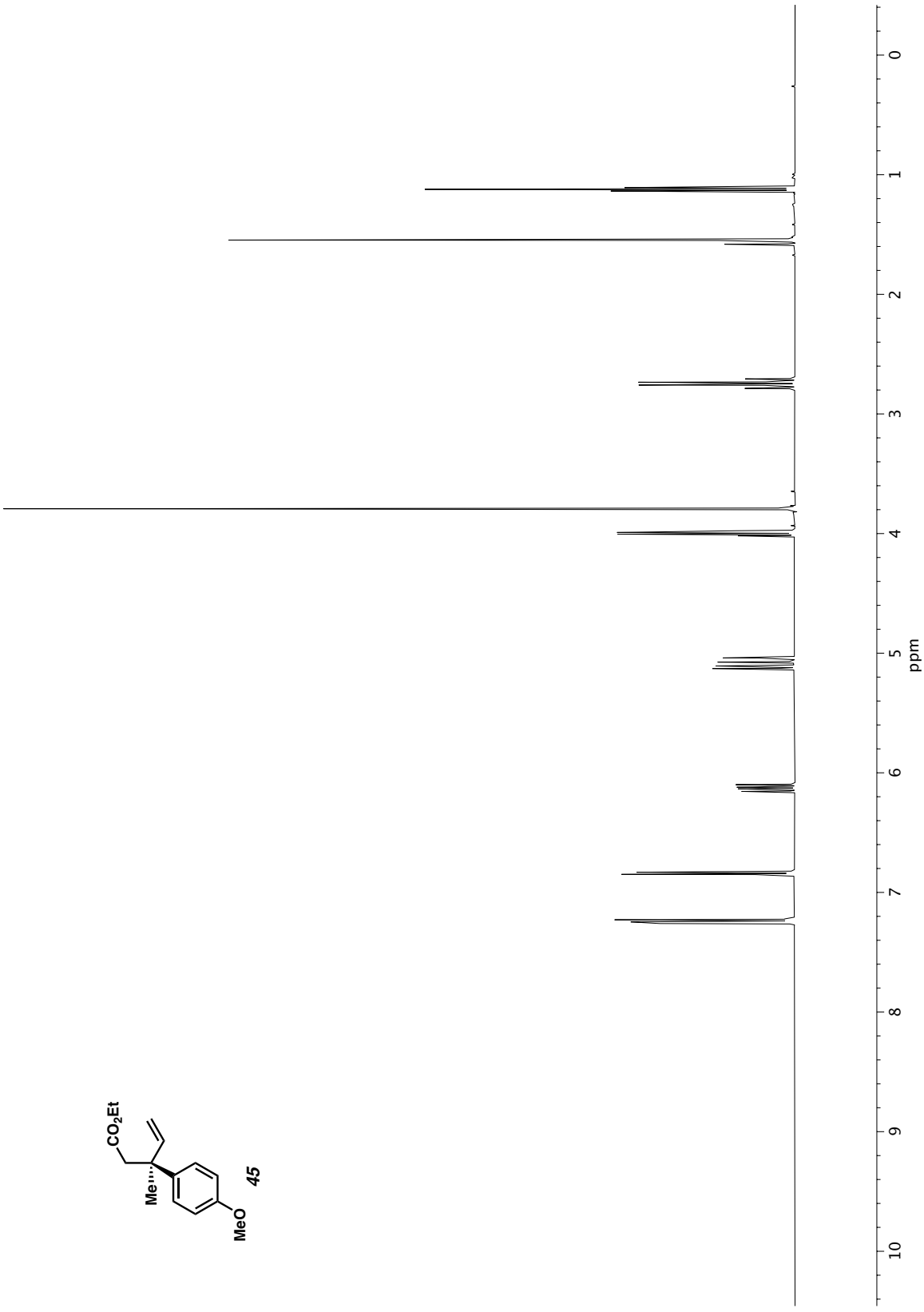


Figure A1.84 *^{1}H NMR (500 MHz, $CDCl_3$) of compound* ***45***.

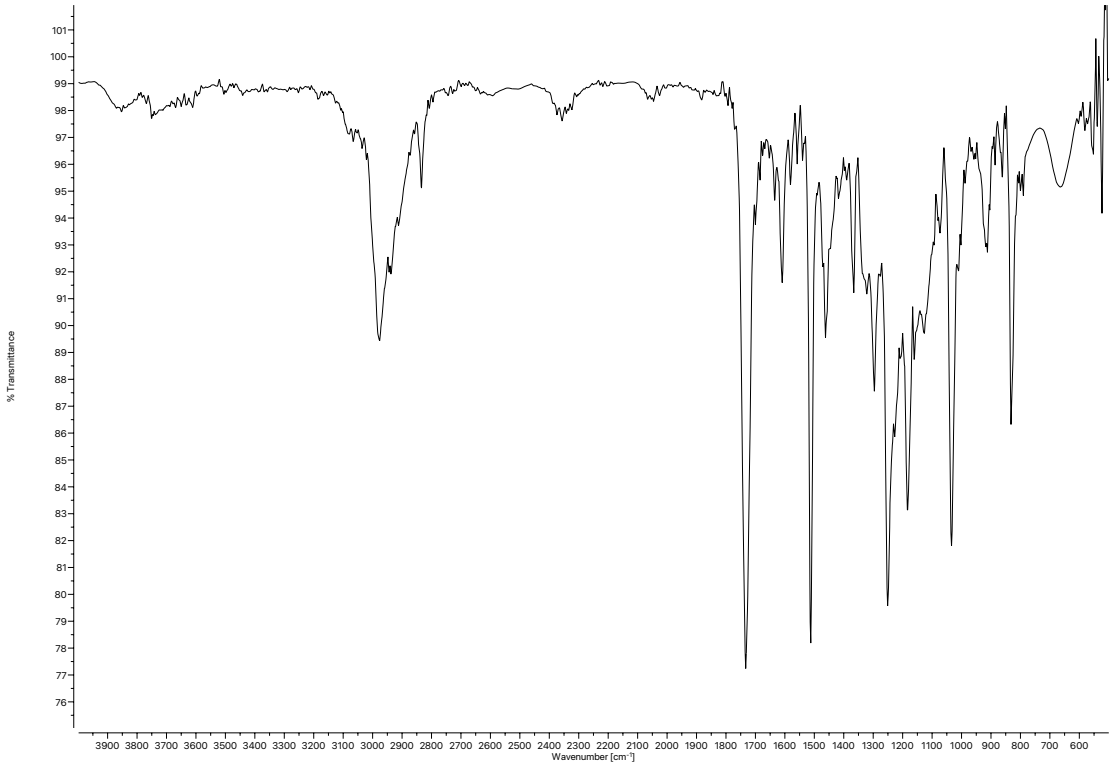


Figure A1.85 *Infrared spectrum (Thin Film, NaCl) of compound* ***45***.

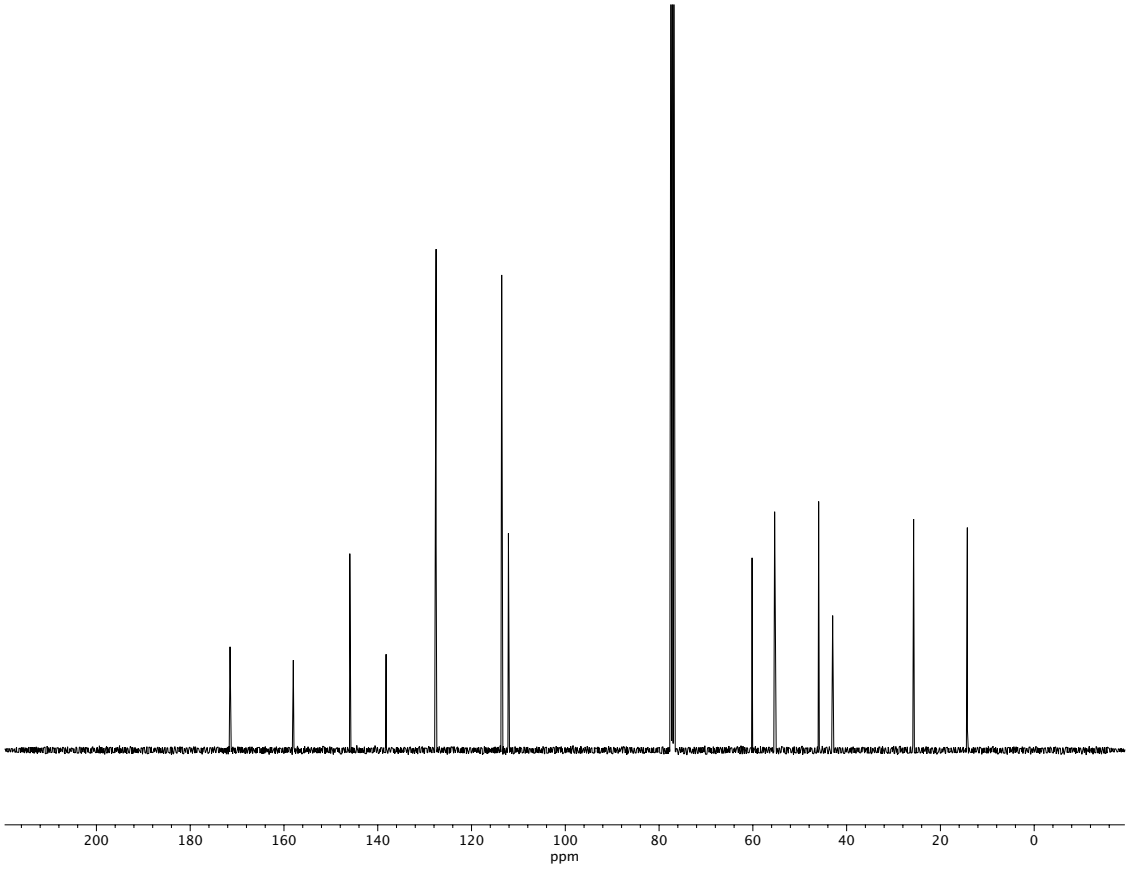


Figure A1.86 *^{13}C NMR (100 MHz, $CDCl_3$) of compound* ***45***.

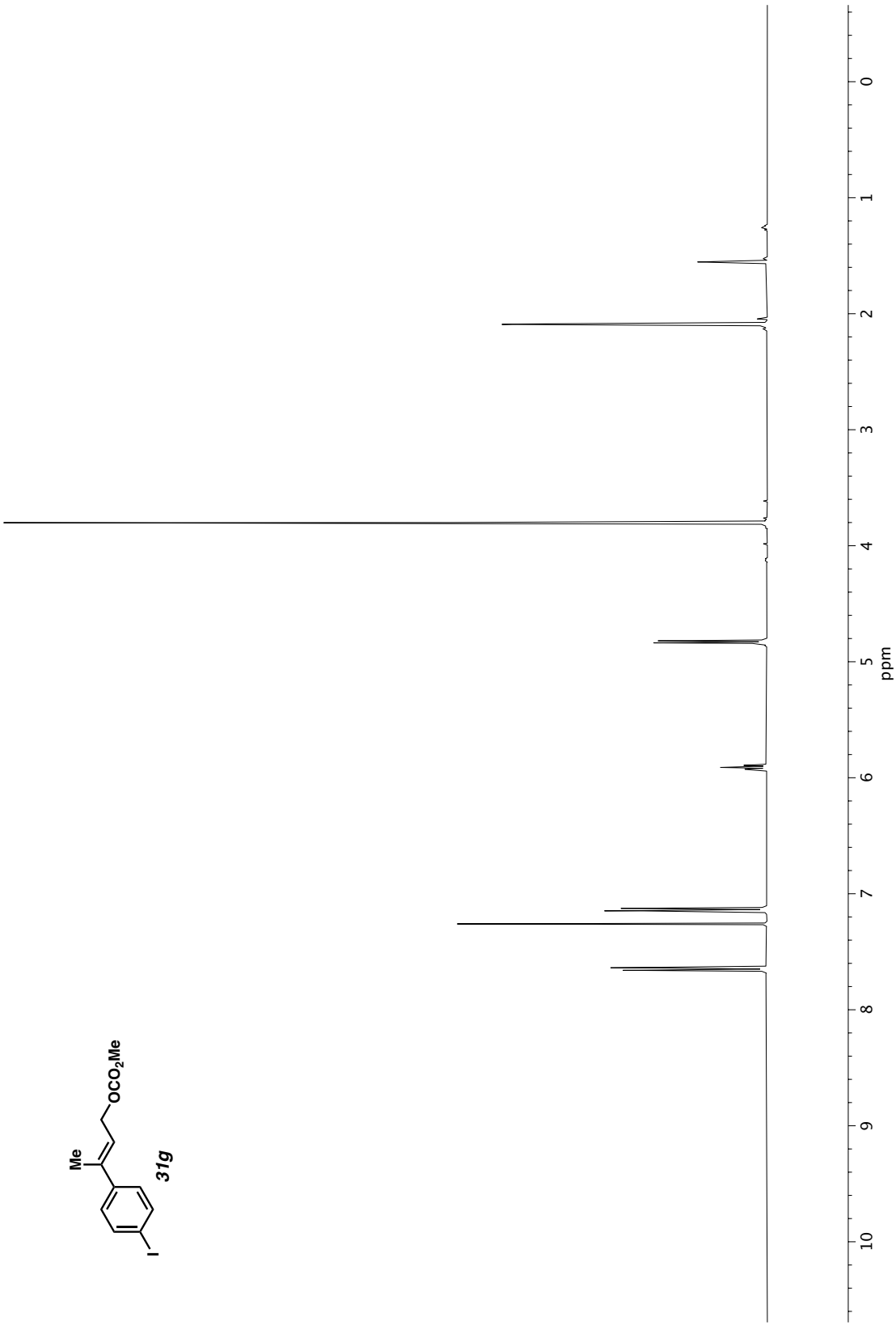


Figure A1.87 *^1H NMR (400 MHz, $CDCl_3$) of compound **31g**.*

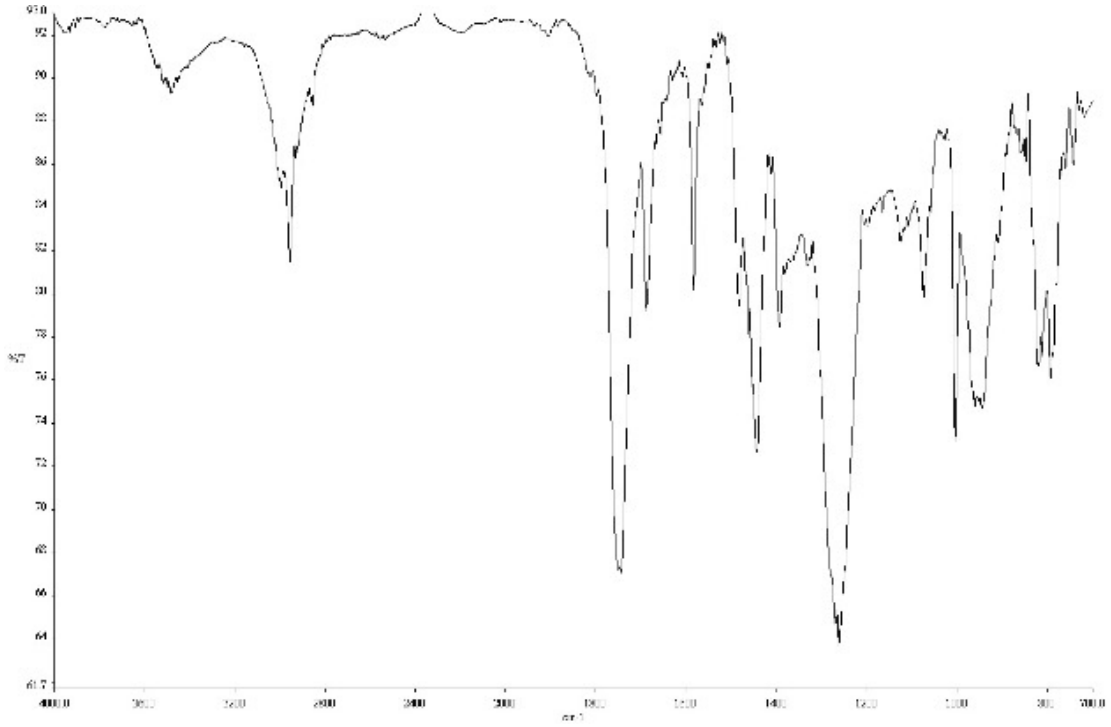


Figure A1.88 *Infrared spectrum (Thin Film, NaCl) of compound* ***31g****.*

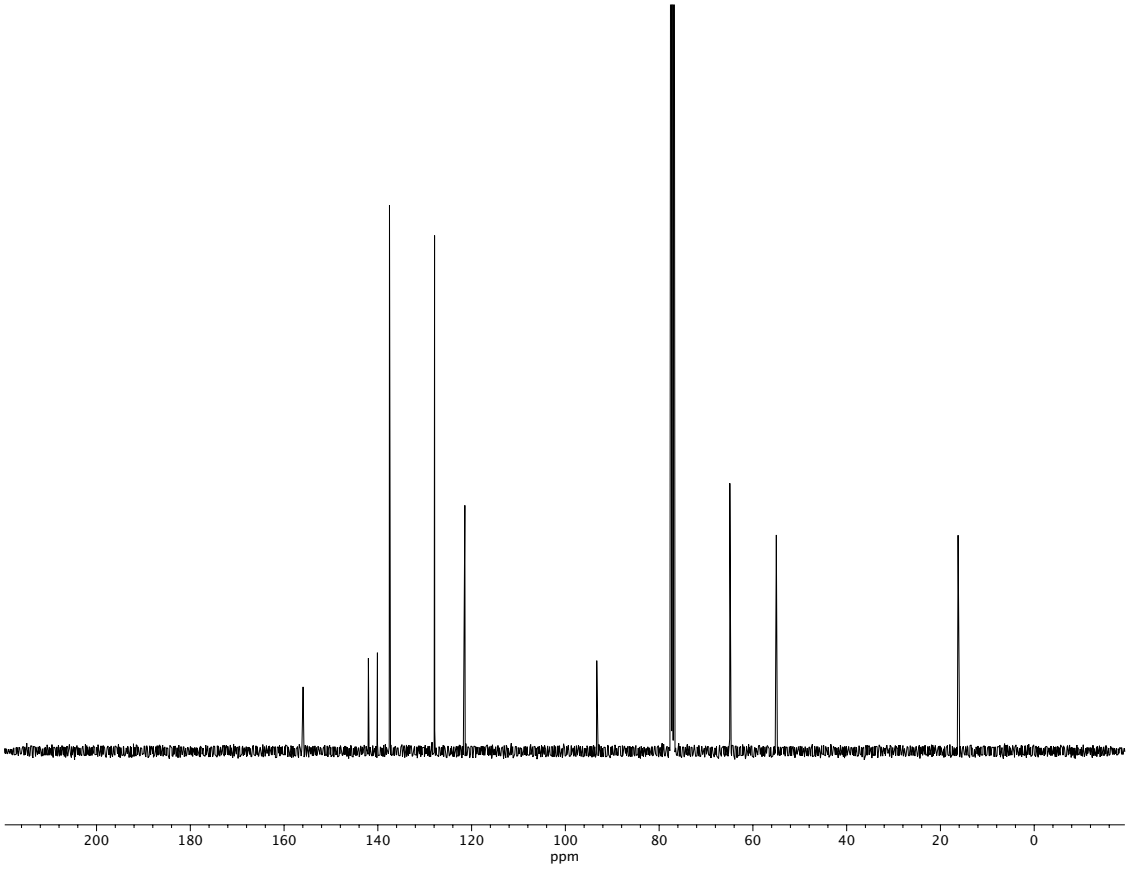


Figure A1.89 *^{13}C NMR (100 MHz, $CDCl_3$) of compound* ***31g****.*

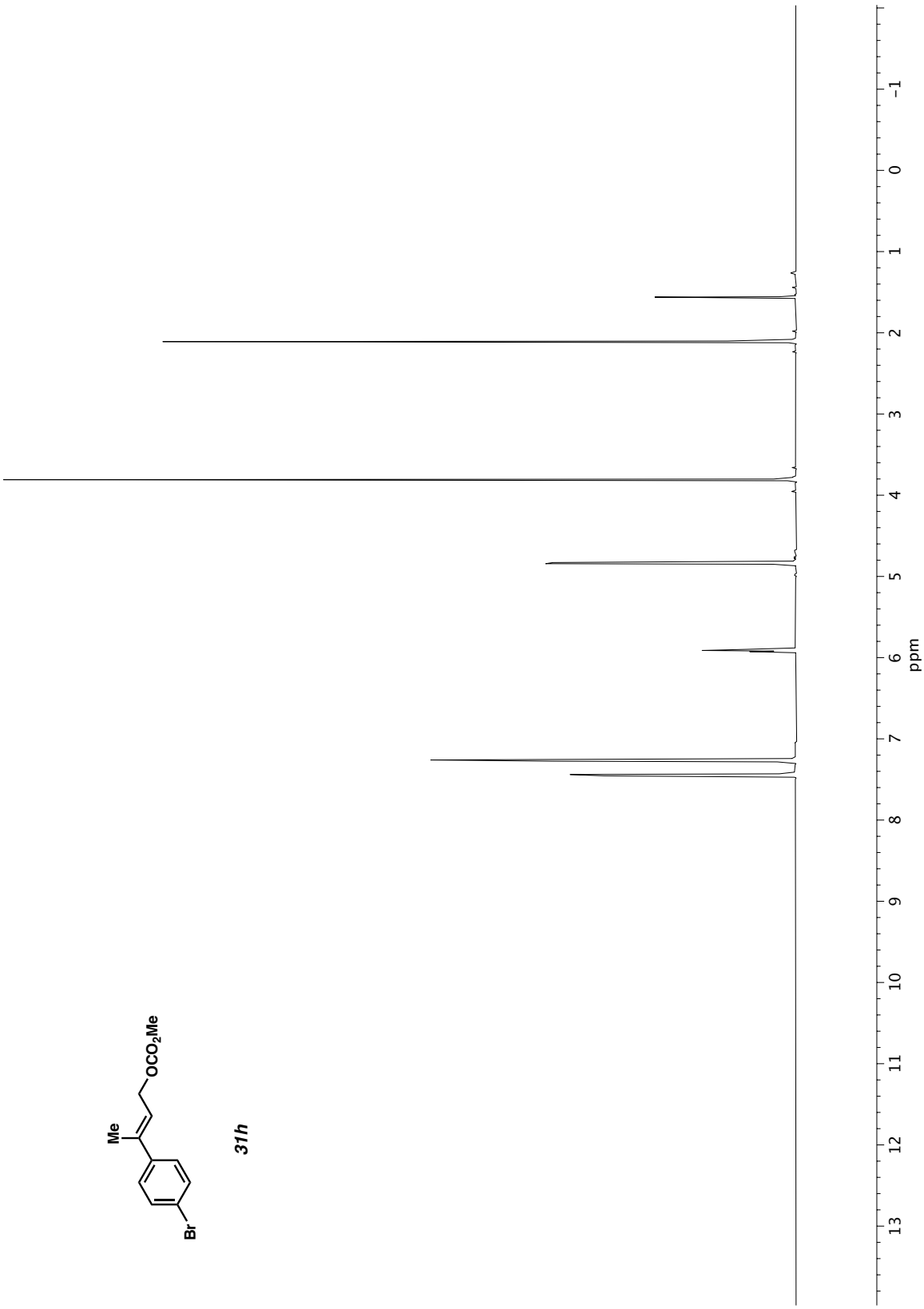


Figure A1.90 *^1H NMR (400 MHz, $CDCl_3$) of compound **31h**.*

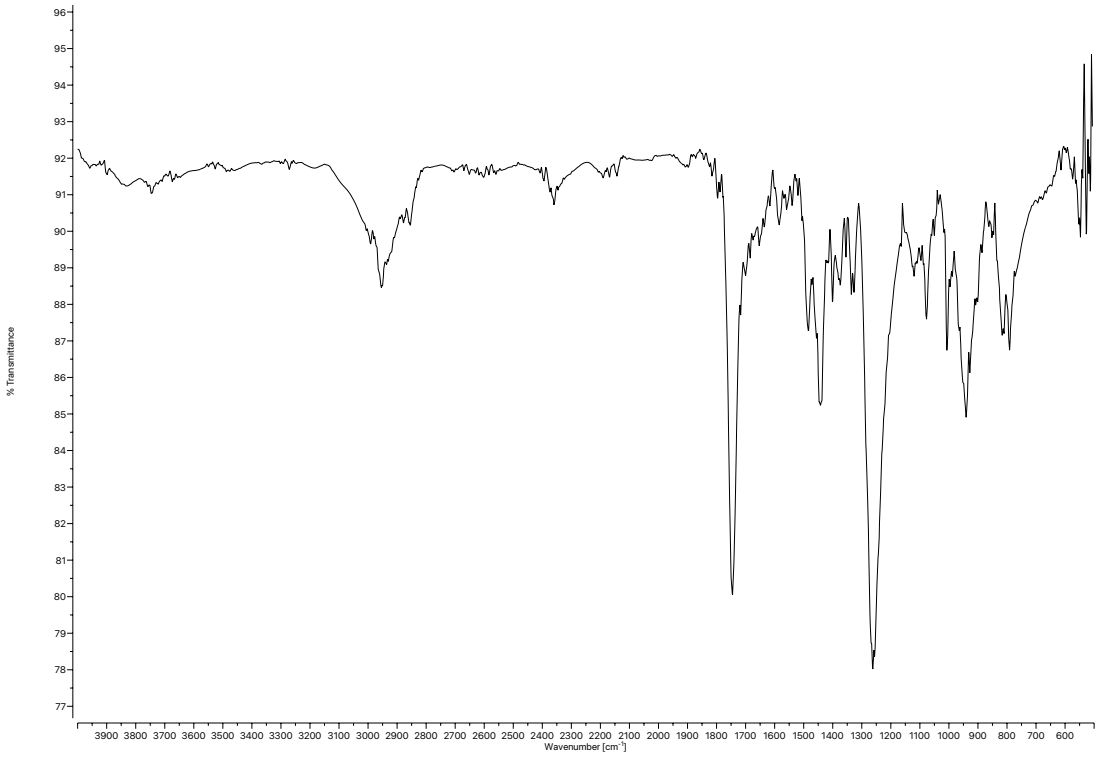


Figure A1.91 *Infrared spectrum (Thin Film, NaCl) of compound* ***31h***.

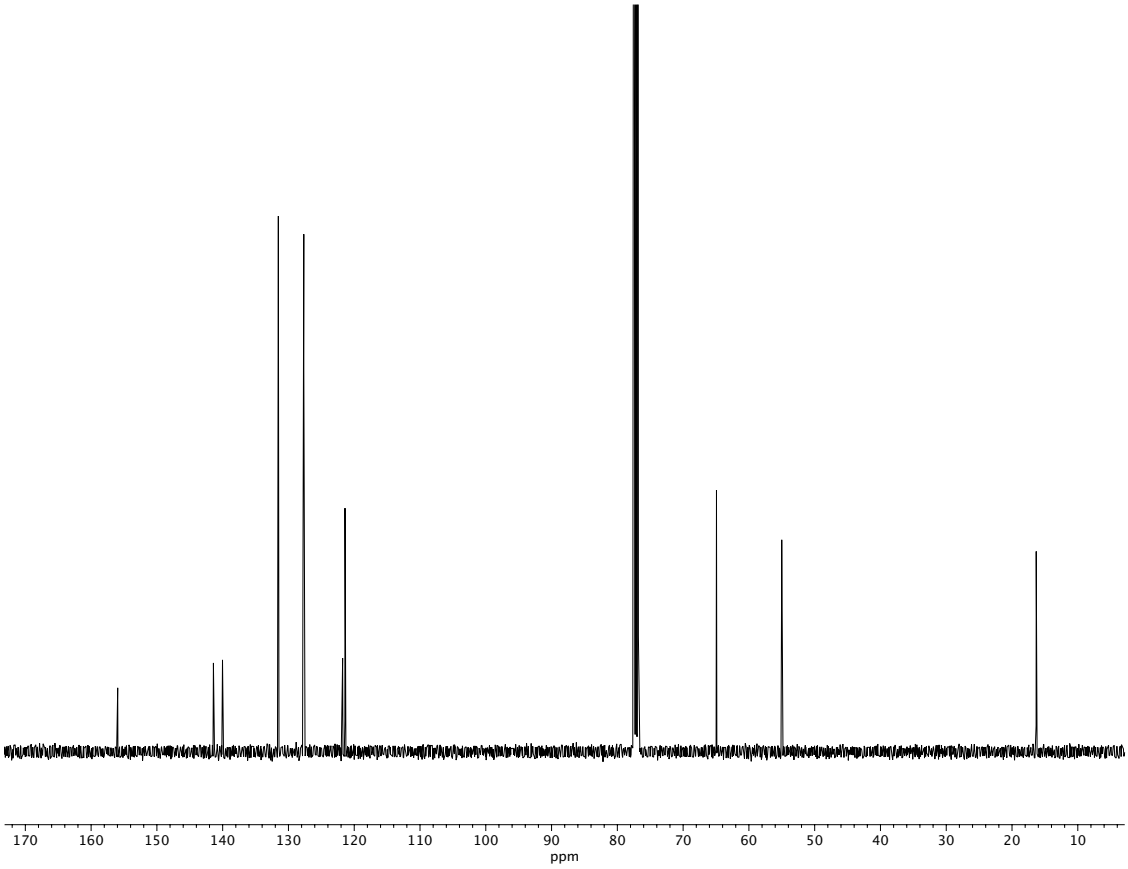


Figure A1.92 *^{13}C NMR (100 MHz, $CDCl_3$) of compound* ***31h***.

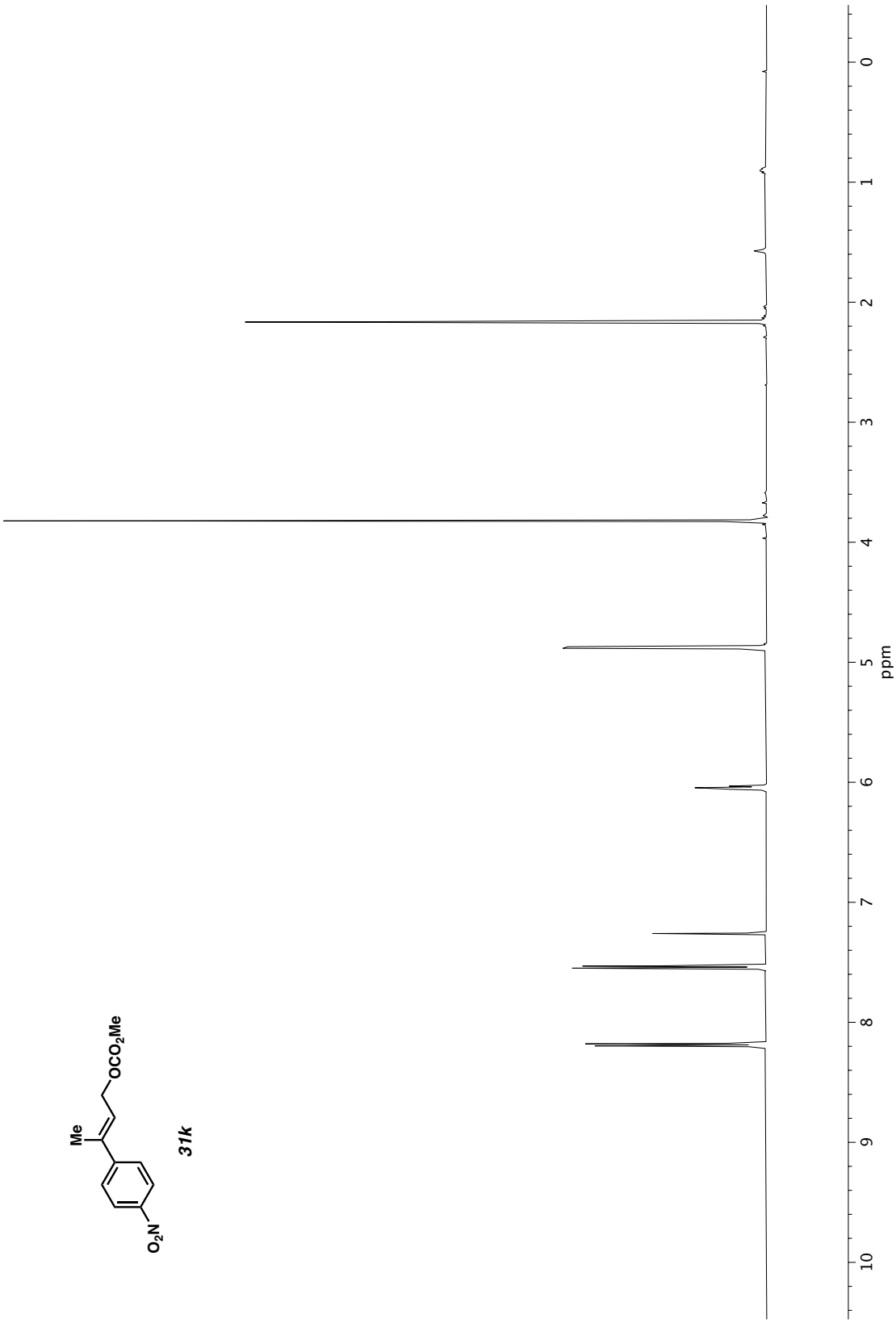


Figure A1.93 *^1H NMR (500 MHz, $CDCl_3$) of compound **31k**.*

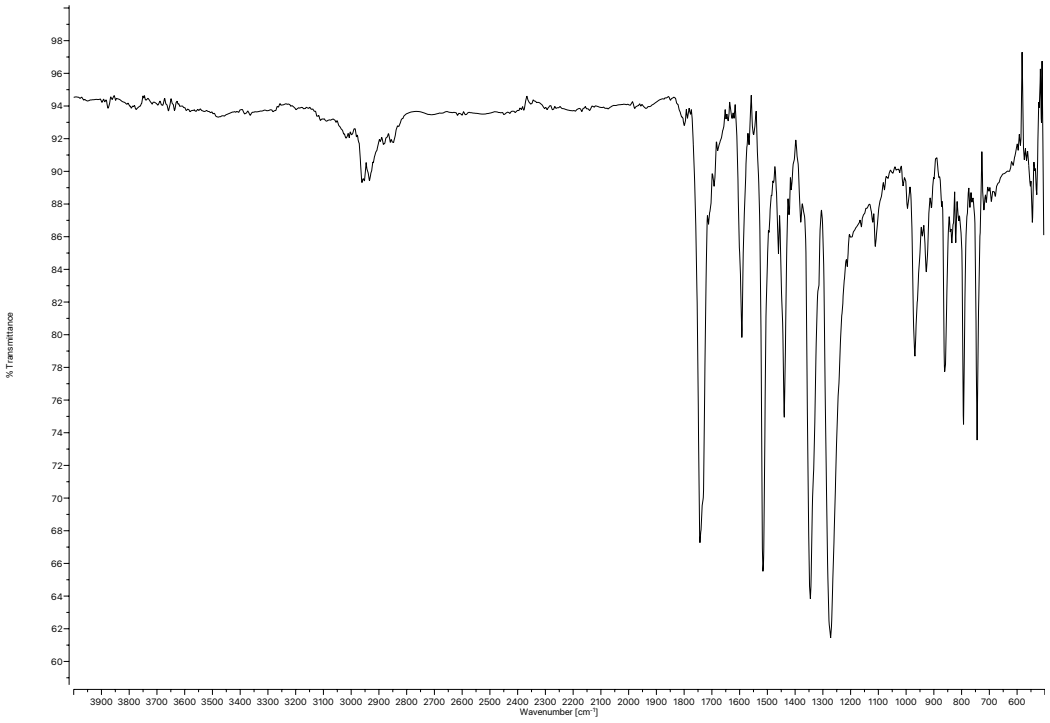


Figure A1.94 *Infrared spectrum (Thin Film, NaCl) of compound* ***31k***.

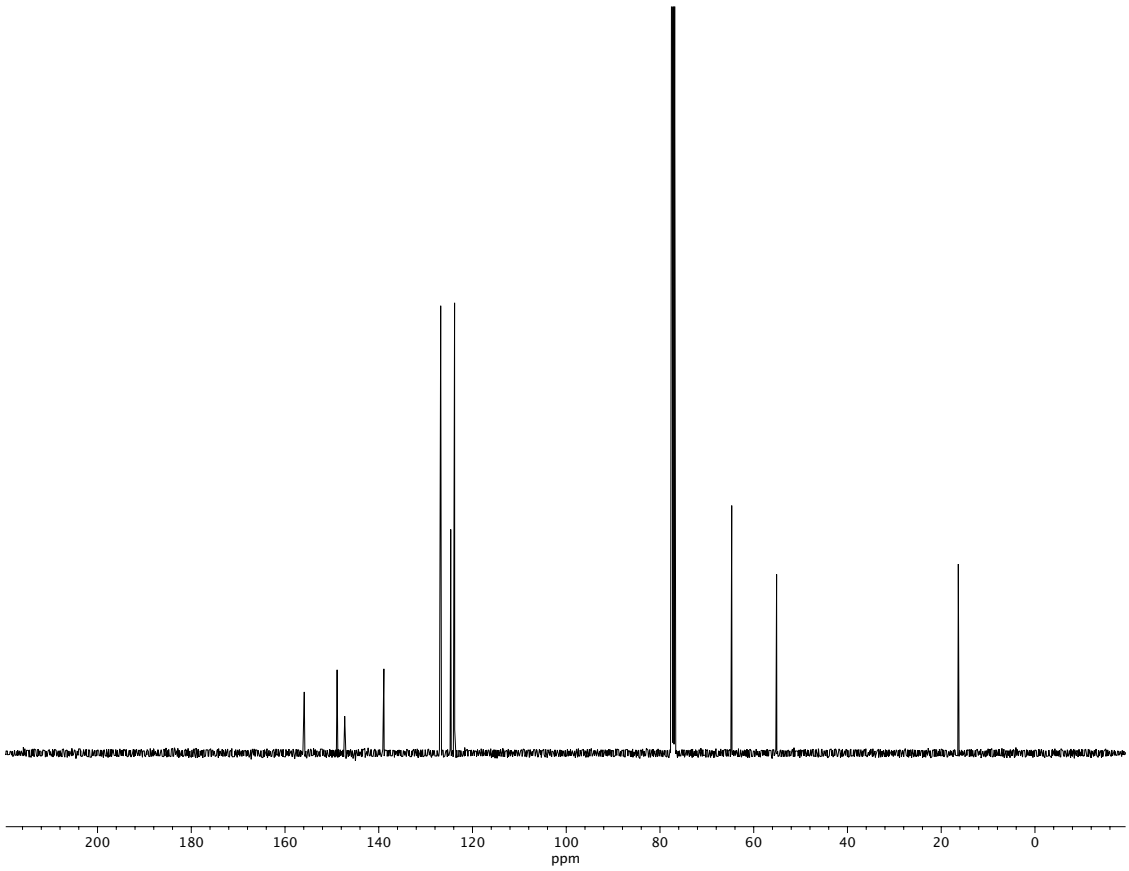


Figure A1.95 *^{13}C NMR (100 MHz, $CDCl_3$) of compound* ***31k***.

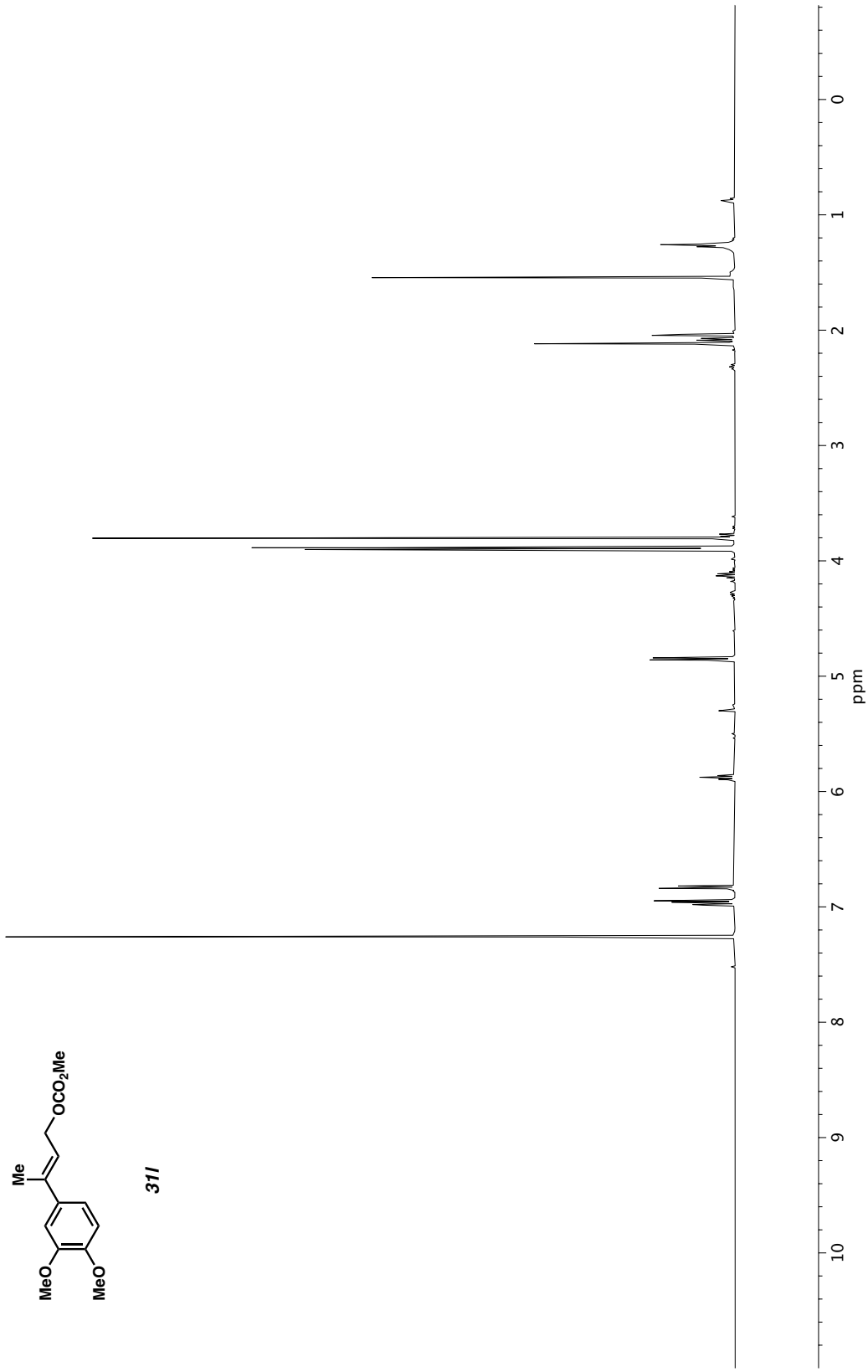


Figure A1.96 *^{1}H NMR (400 MHz, $CDCl_3$) of compound **311**.*

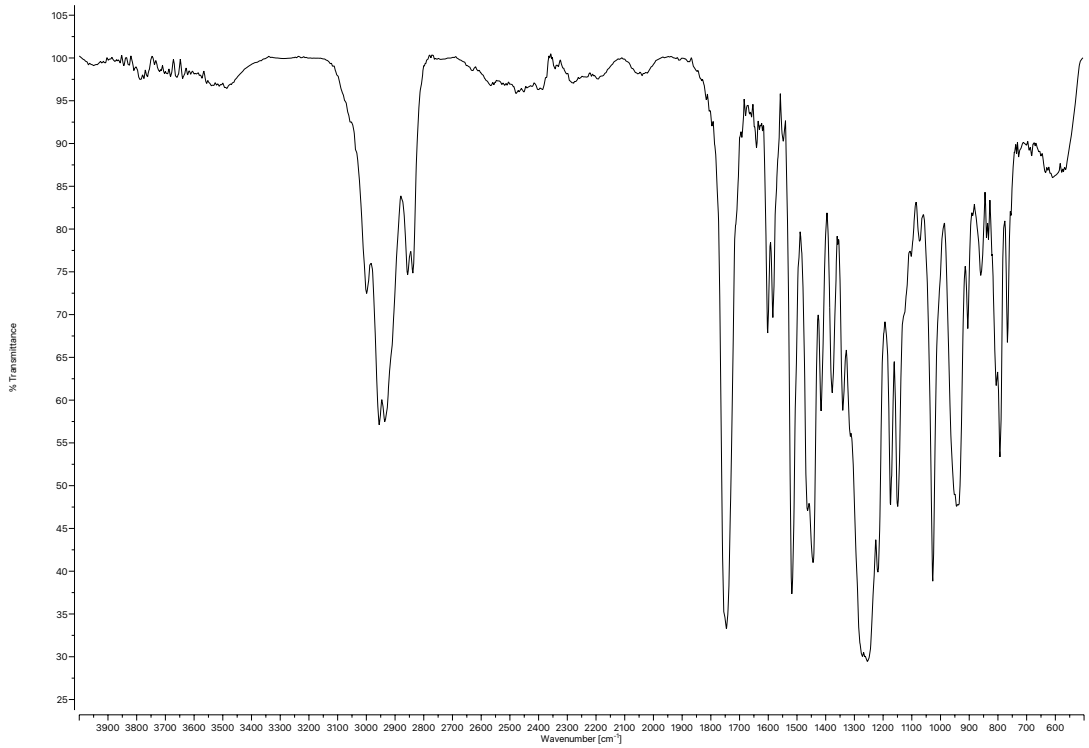


Figure A1.97 *Infrared spectrum (Thin Film, NaCl) of compound* ***31l****.*

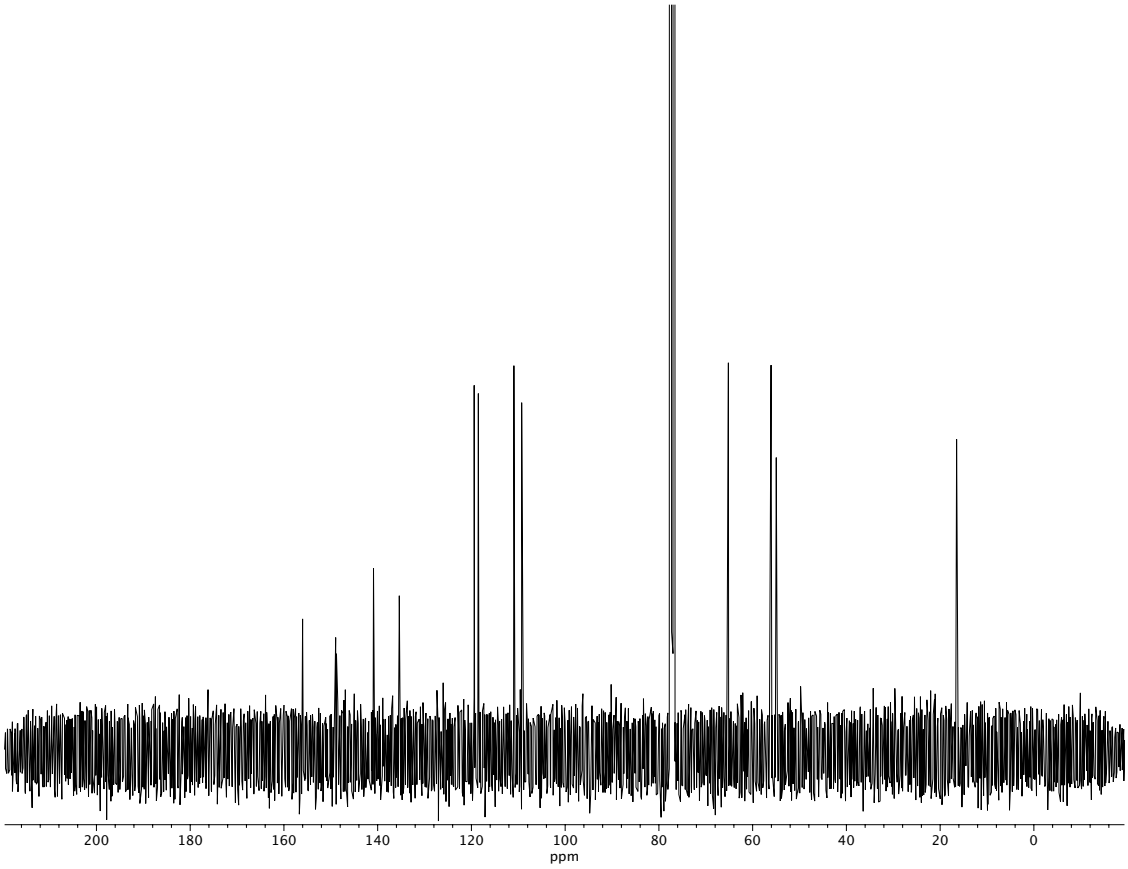


Figure A1.98 *^{13}C NMR (100 MHz, $CDCl_3$) of compound* ***31l****.*

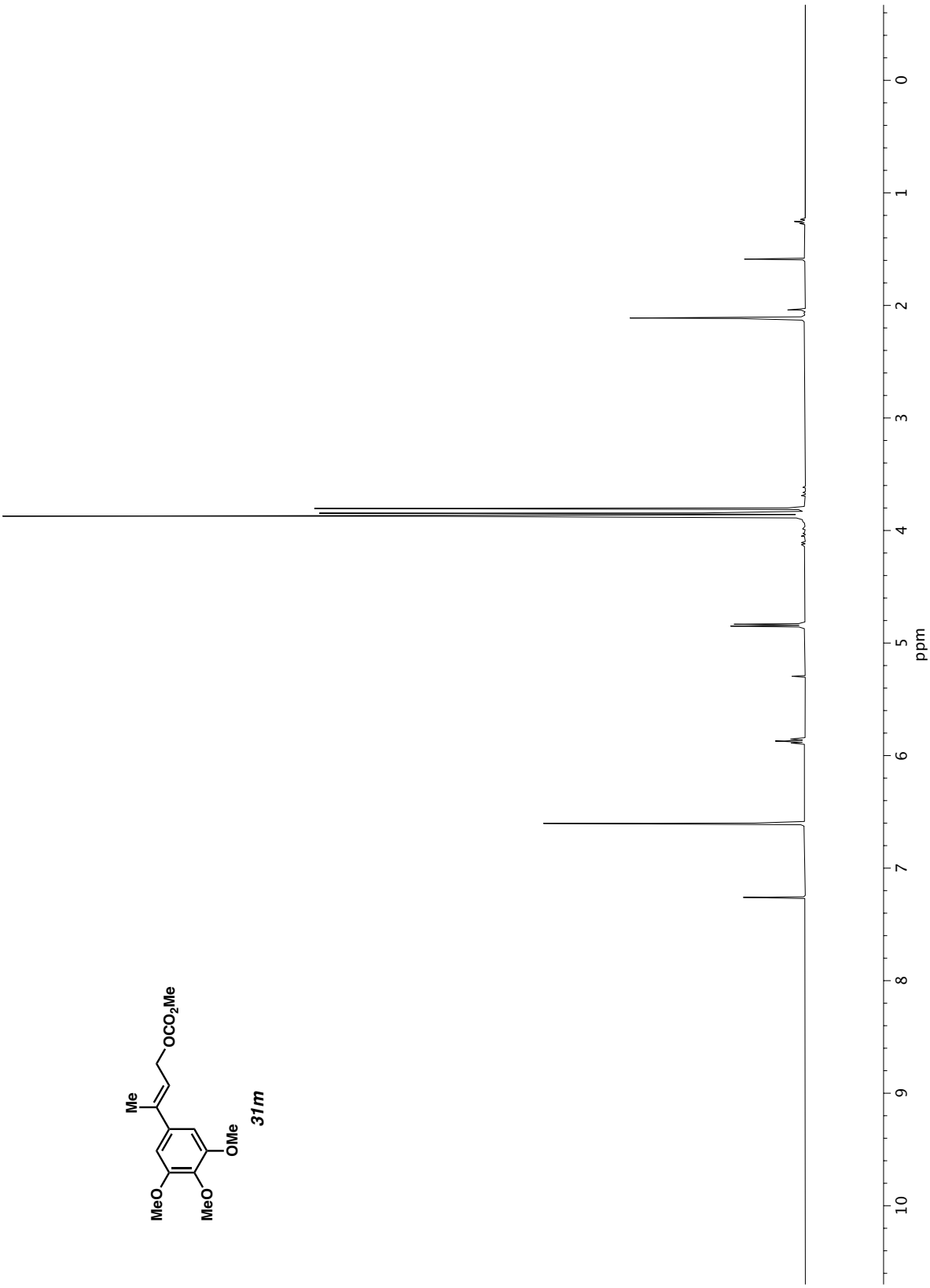


Figure A1.99 *^1H NMR (400 MHz, $CDCl_3$) of compound* ***31m****.*

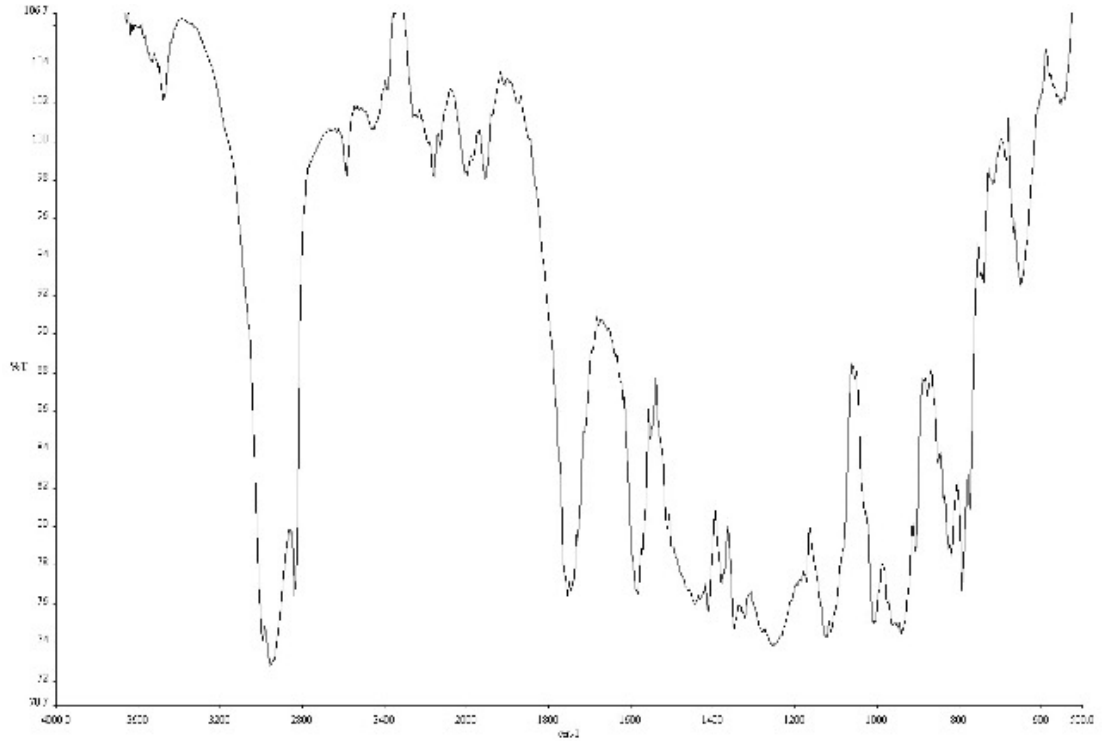


Figure A1.100 *Infrared spectrum (Thin Film, NaCl) of compound* ***31m****.*

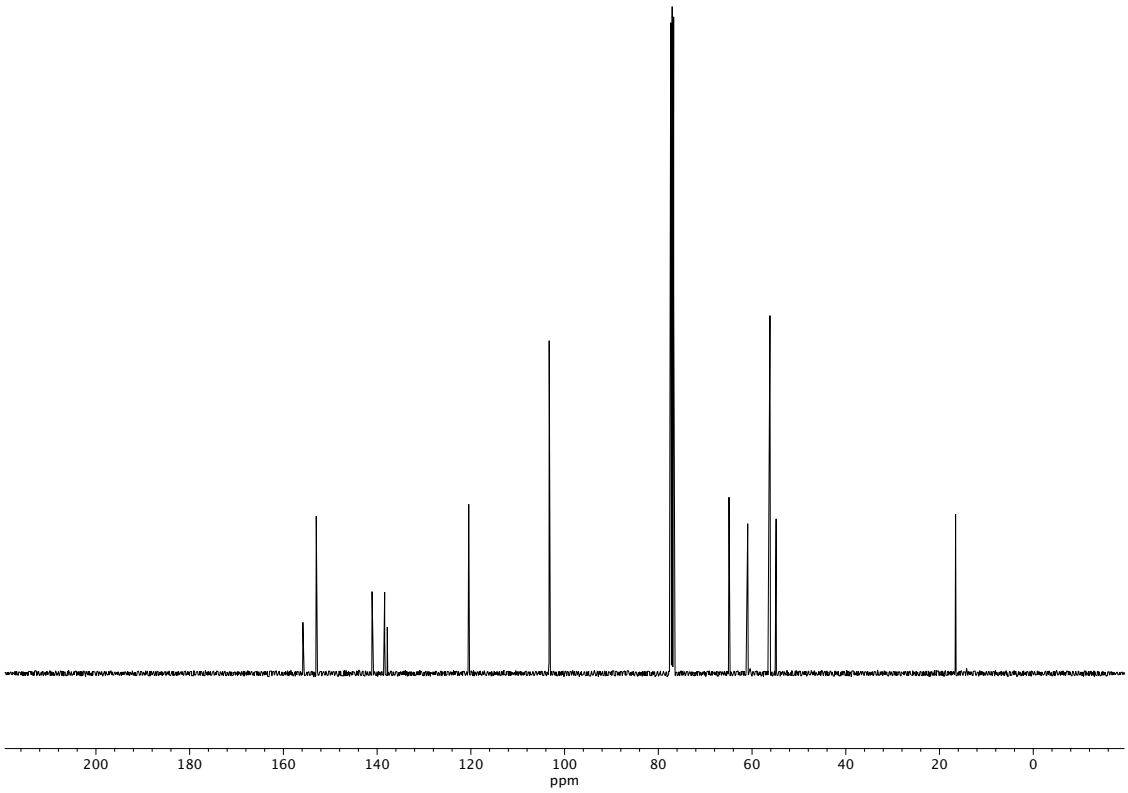


Figure A1.101 *^{13}C NMR (100 MHz, $CDCl_3$) of compound* ***31m****.*

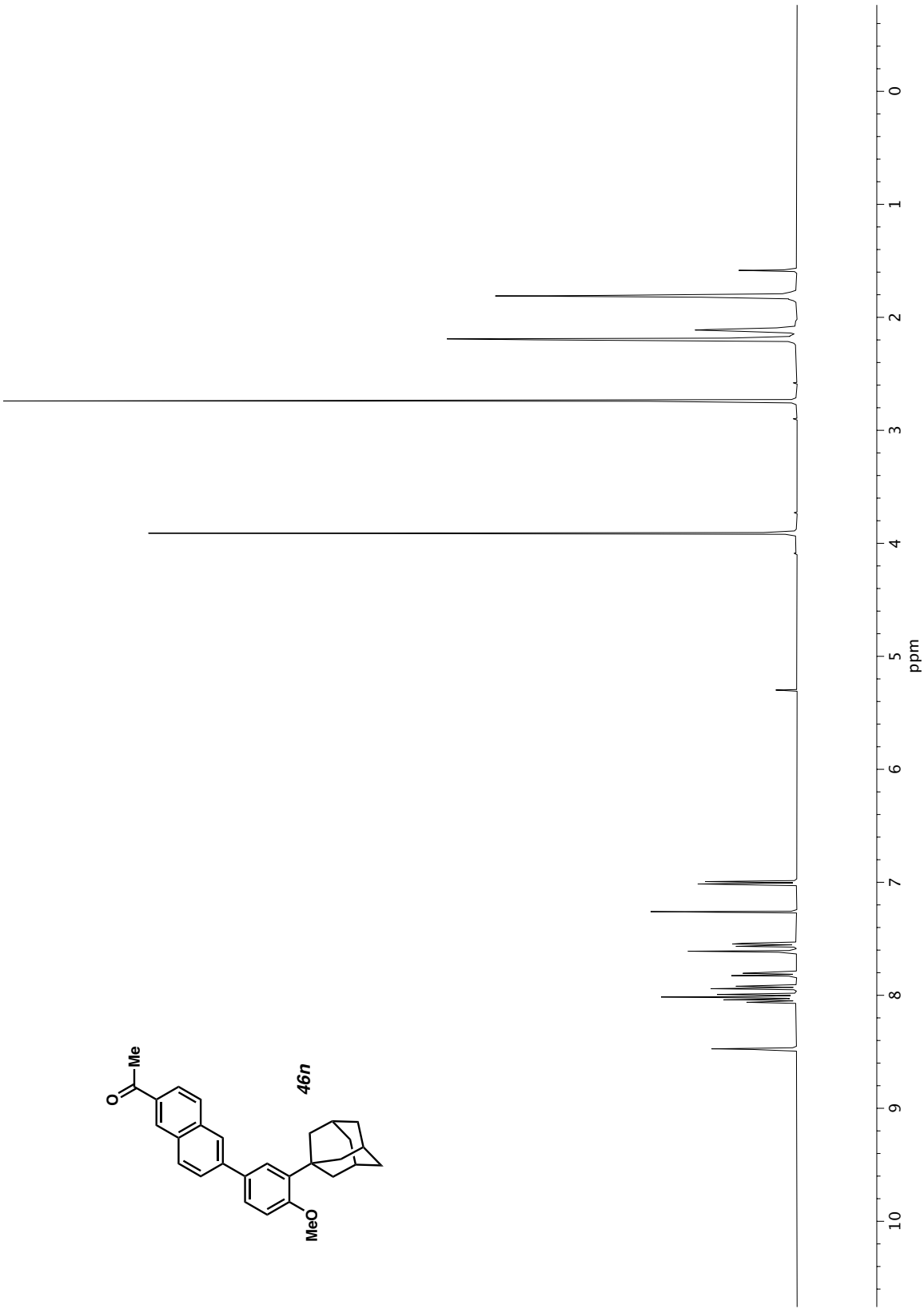


Figure A1.102 *^{1}H NMR (400 MHz, $CDCl_3$) of compound* ***46n***.

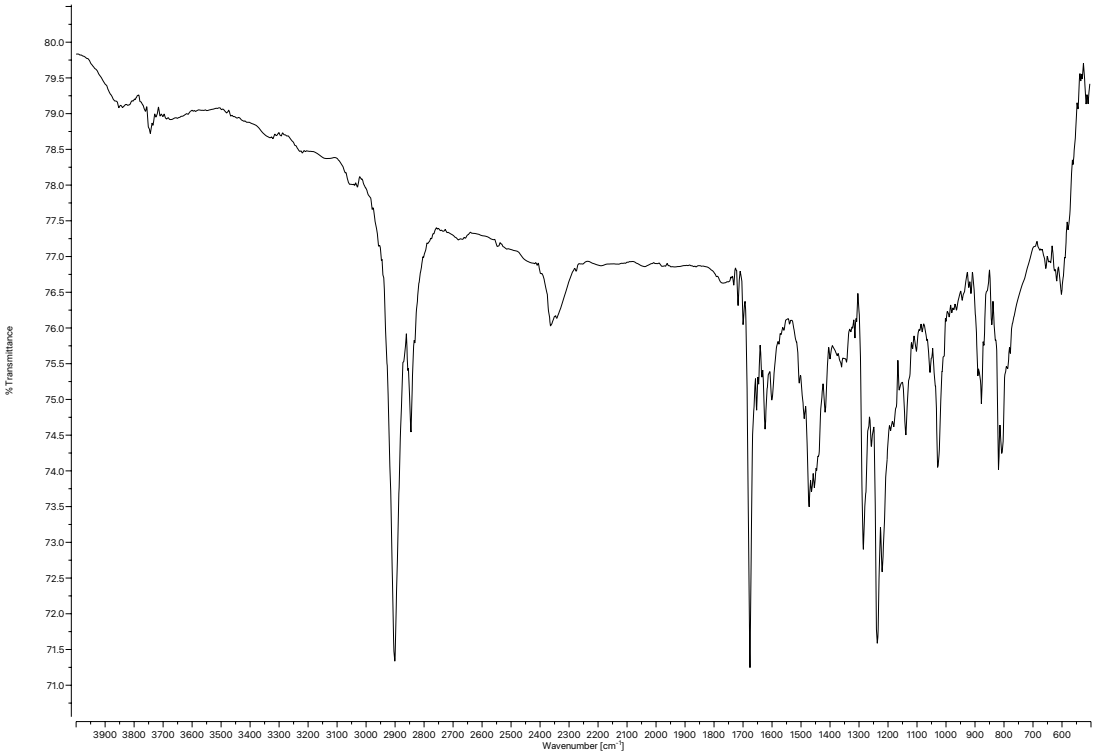


Figure A1.103 *Infrared spectrum (Thin Film, NaCl) of compound* ***46n***.

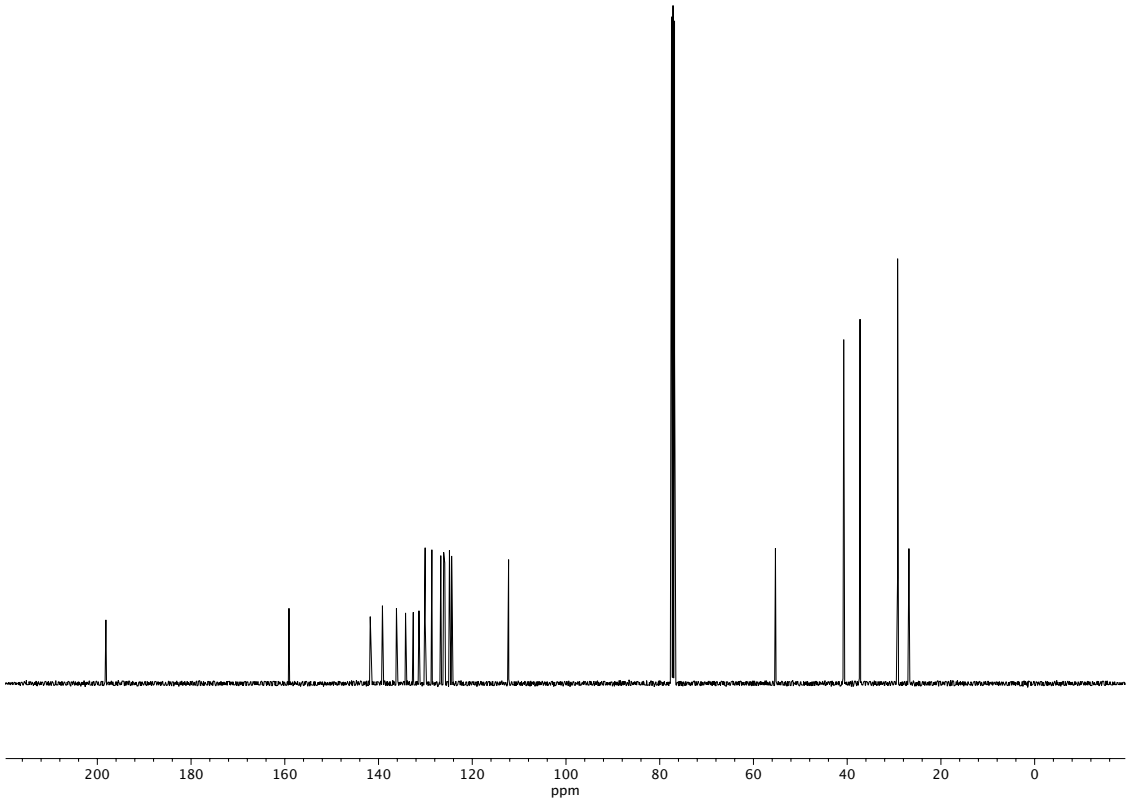


Figure A1.104 *^{13}C NMR (100 MHz, $CDCl_3$) of compound* ***46n***.

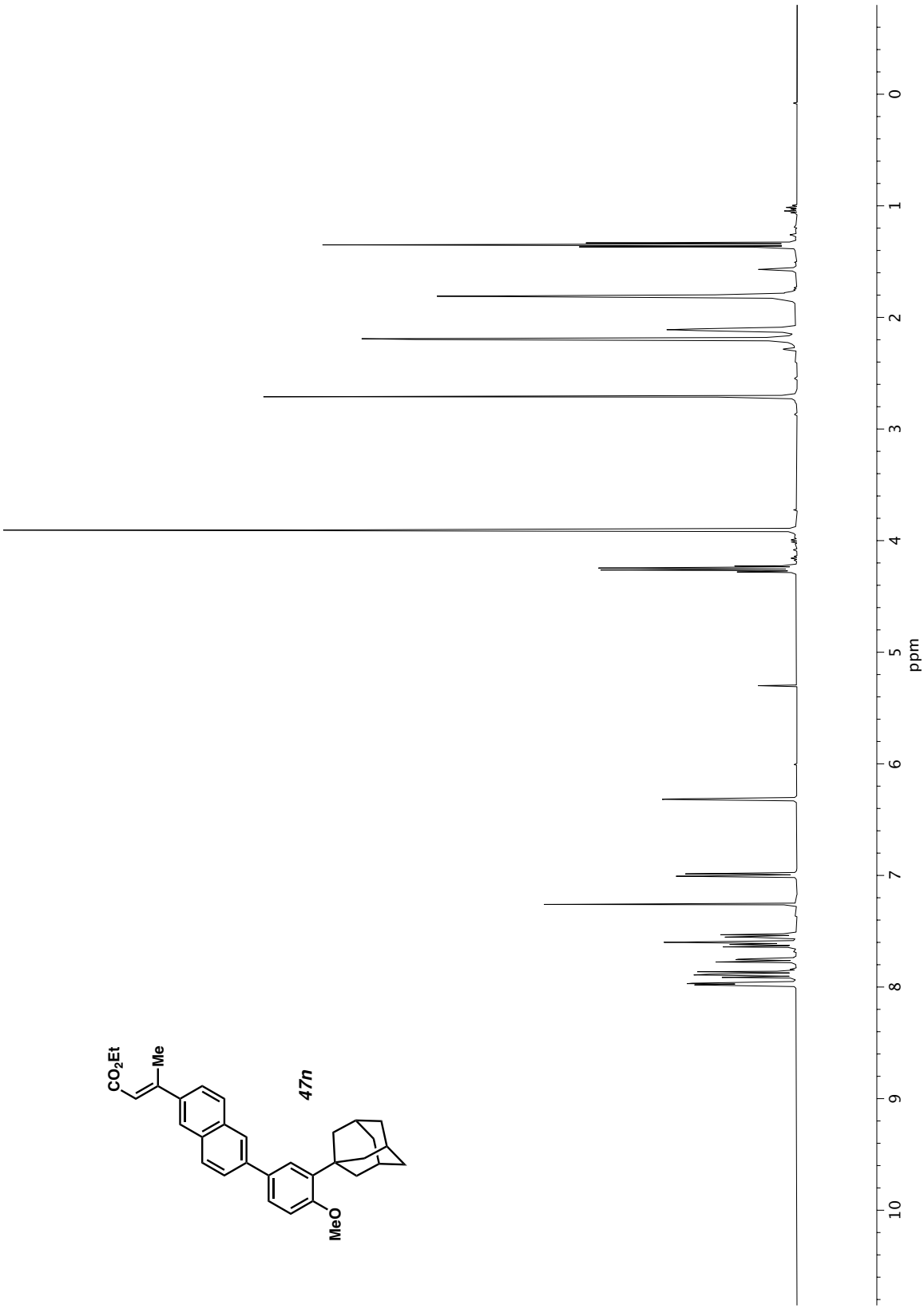


Figure A1.105 *^1H NMR (400 MHz, $CDCl_3$) of compound* ***47n***.

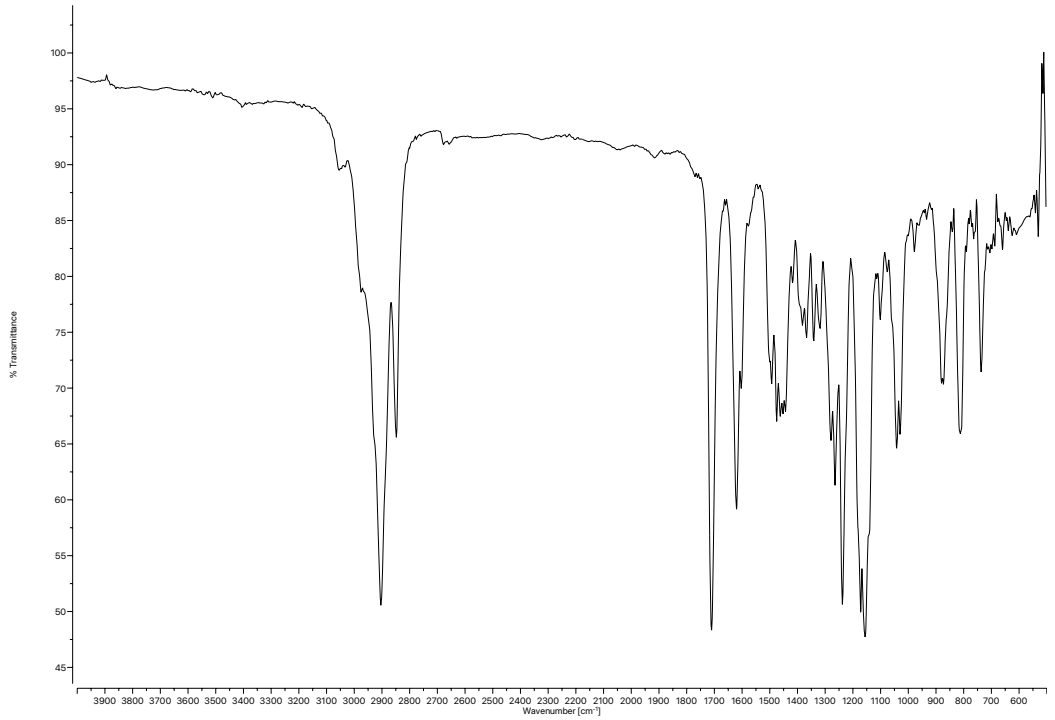


Figure A1.106 *Infrared spectrum (Thin Film, NaCl) of compound* ***47n***.

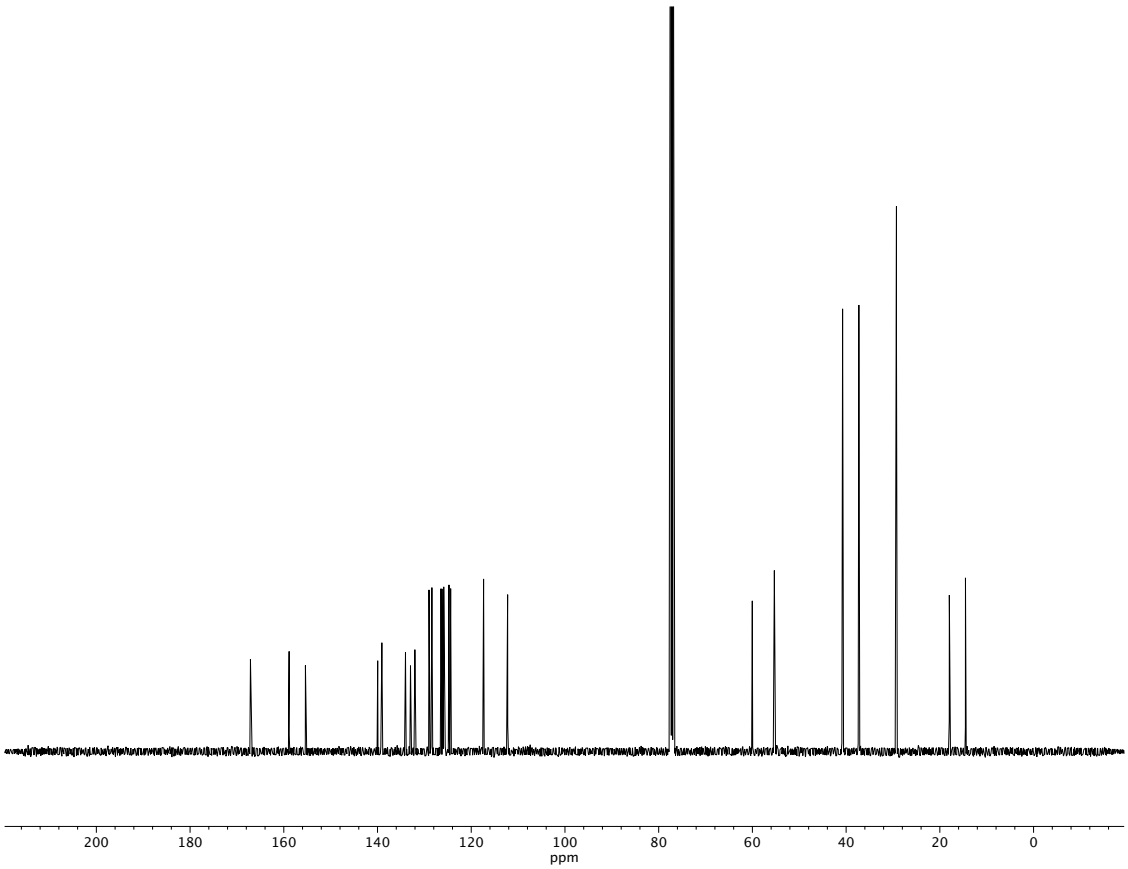


Figure A1.107 *^{13}C NMR (100 MHz, $CDCl_3$) of compound* ***47n***.

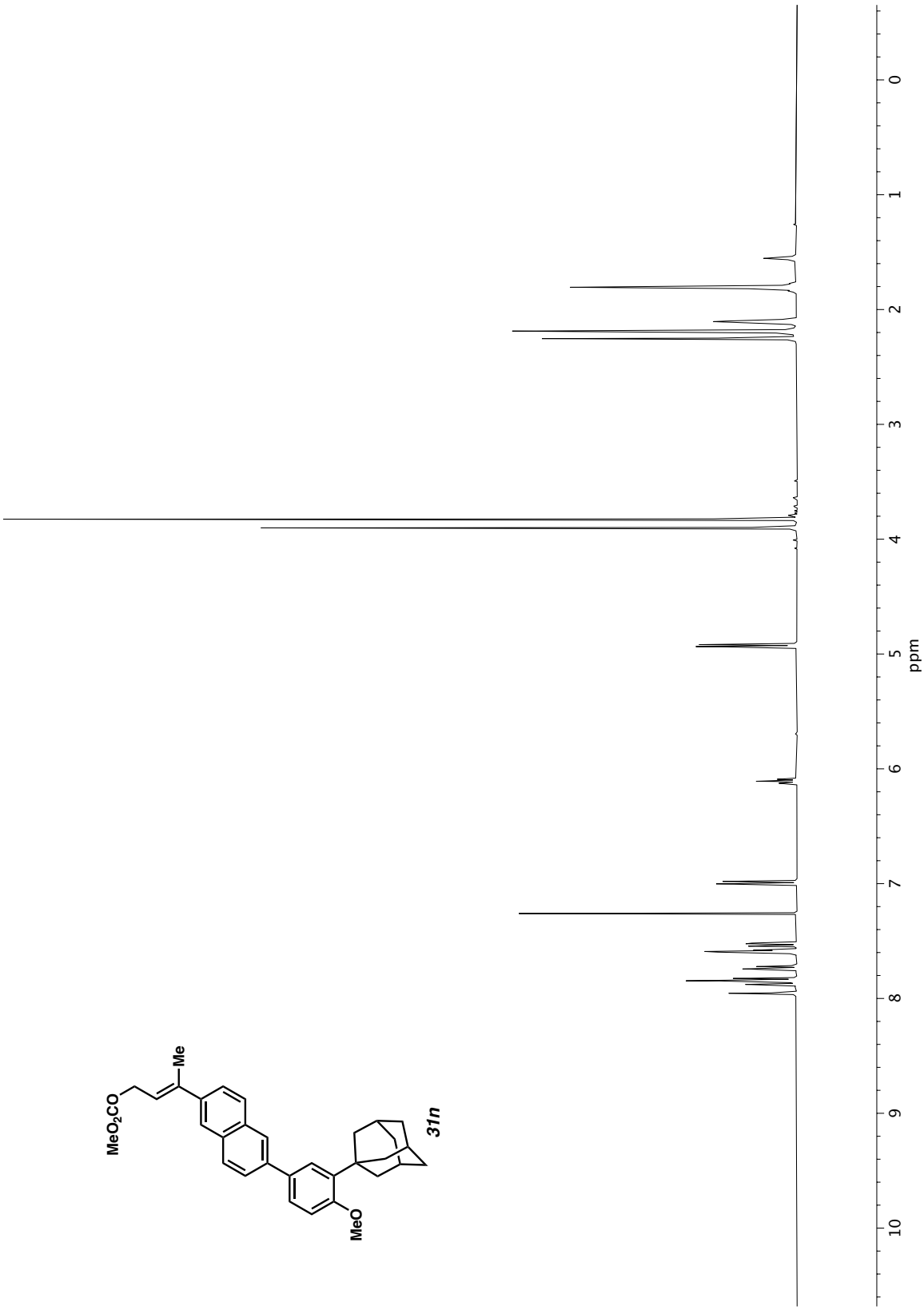


Figure A1.108 *^{1}H NMR (400 MHz, $CDCl_3$) of compound **31n**.*

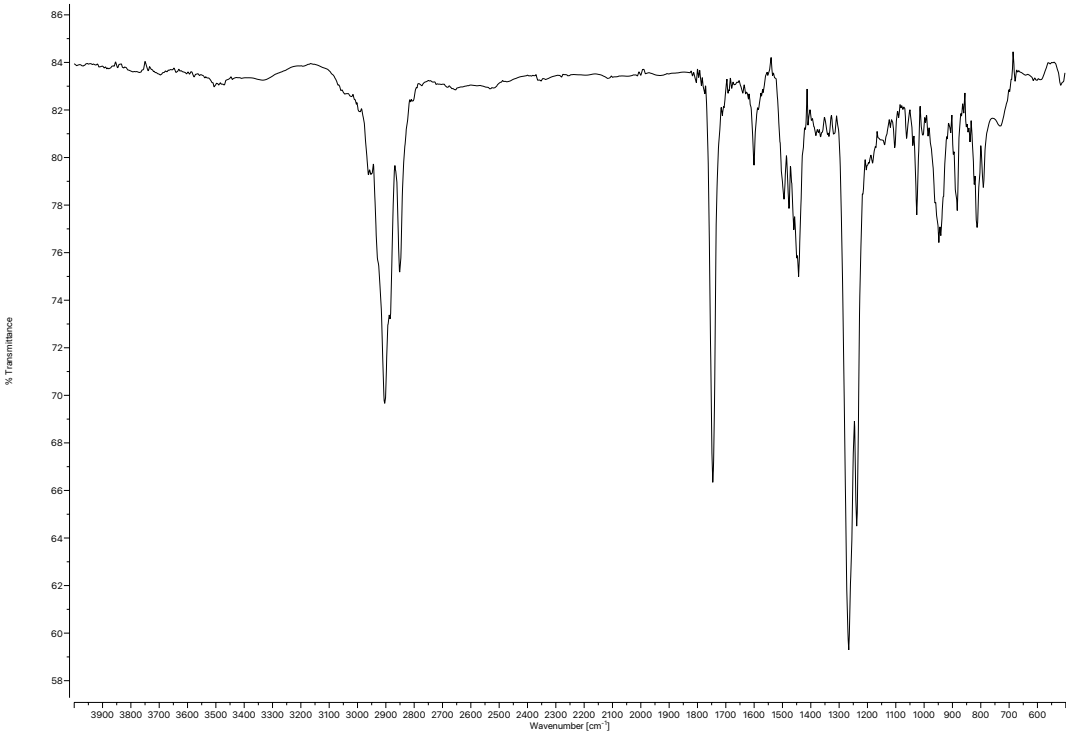


Figure A1.109 *Infrared spectrum (Thin Film, NaCl) of compound* ***31n***.

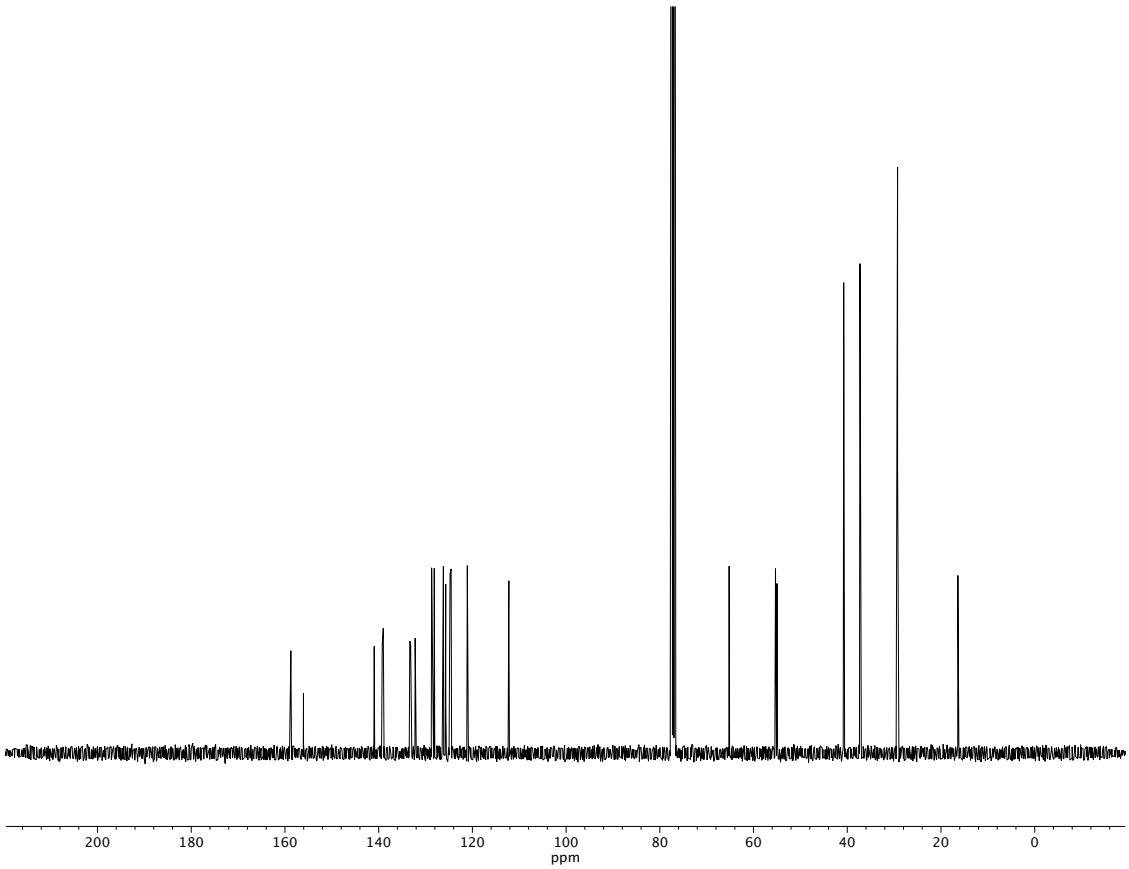


Figure A1.110 *^{13}C NMR (100 MHz, $CDCl_3$) of compound* ***31n***.

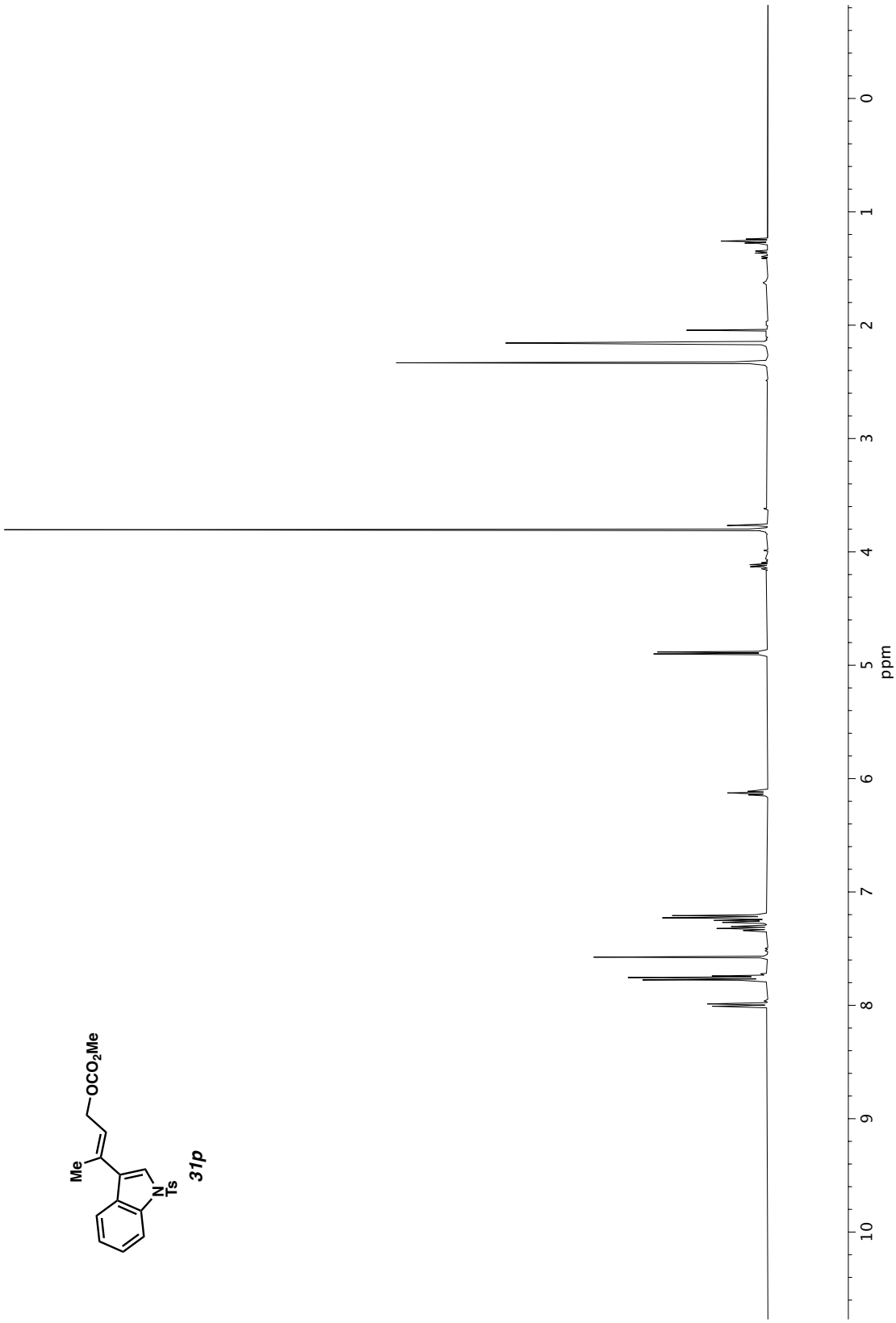


Figure A1.111 *^{1}H NMR (400 MHz, $CDCl_3$) of compound **31p**.*

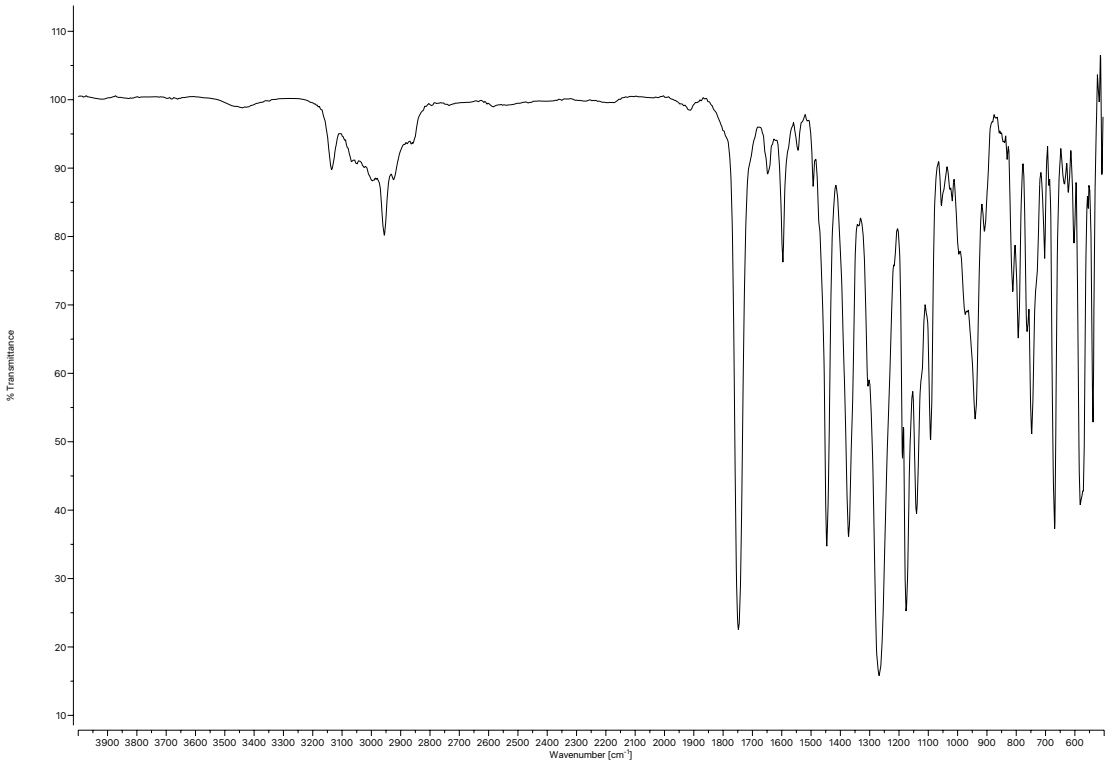


Figure A1.112 *Infrared spectrum (Thin Film, NaCl) of compound* ***31p****.*

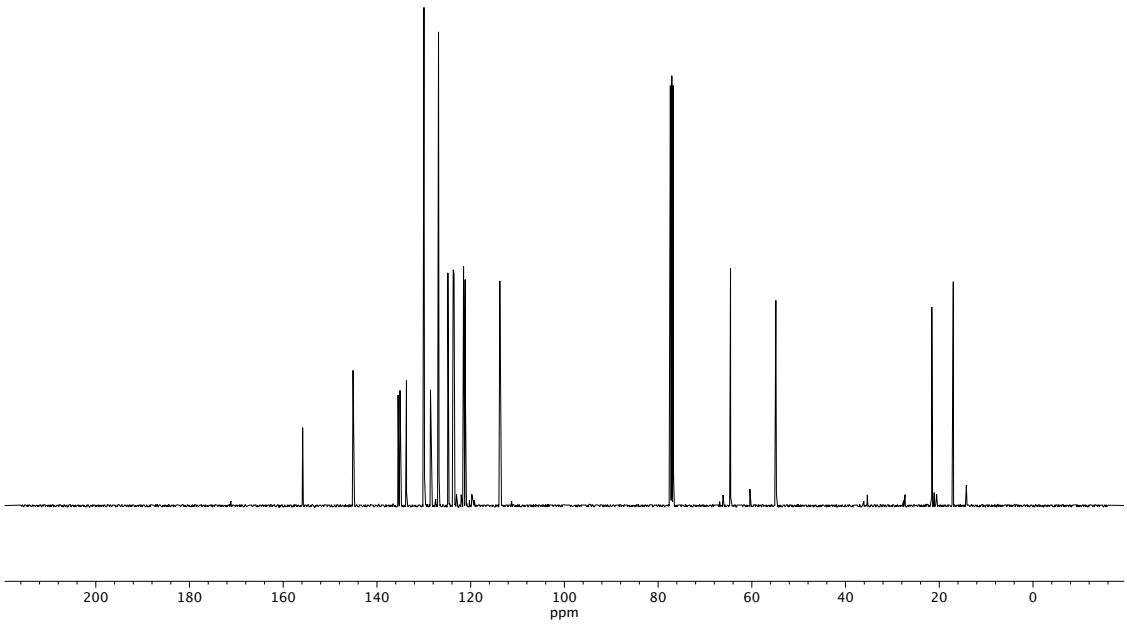


Figure A1.113 *^{13}C NMR (100 MHz, $CDCl_3$) of compound* ***31p****.*

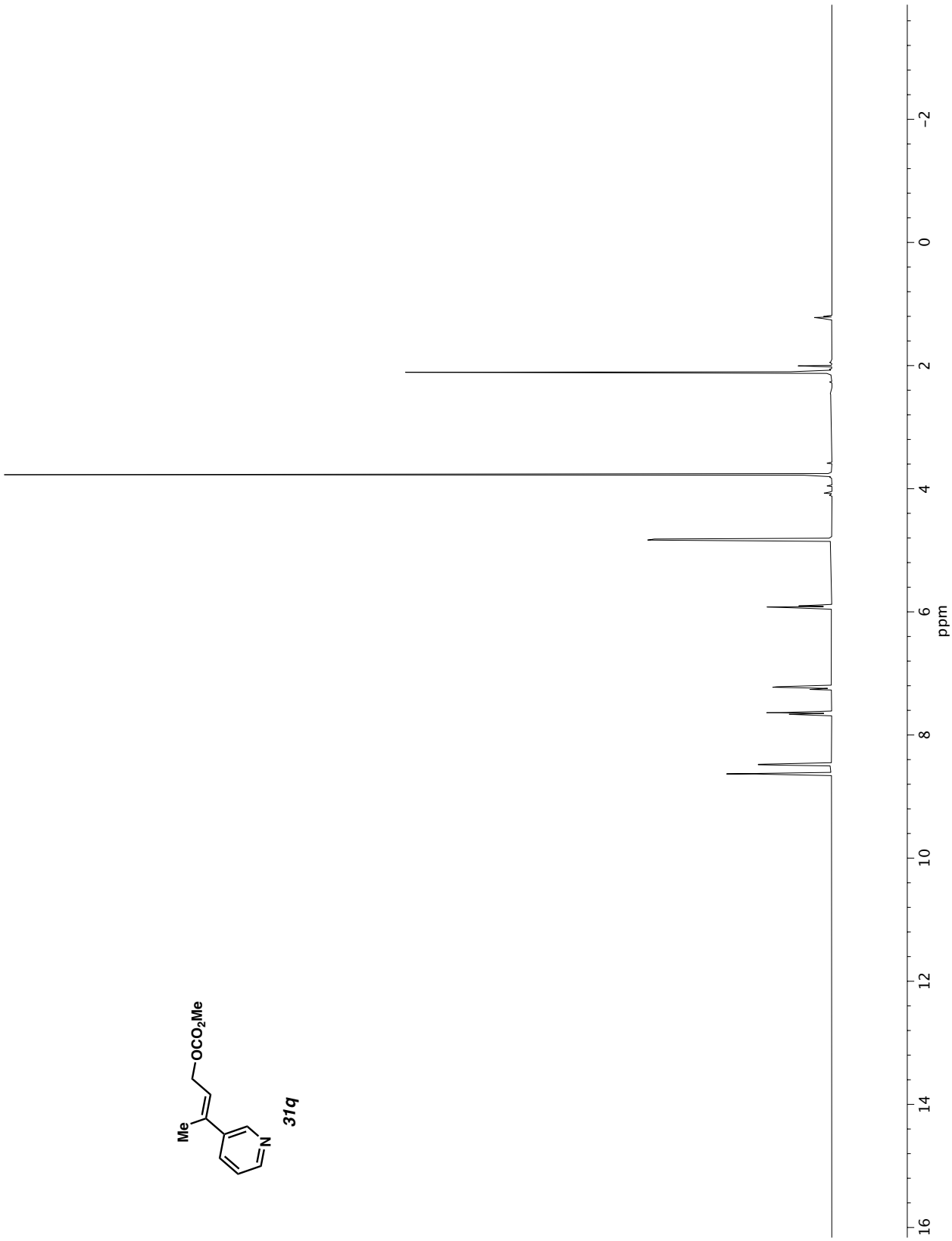


Figure A1.114 *^{1}H NMR (400 MHz, $CDCl_3$) of compound* ***31q***.

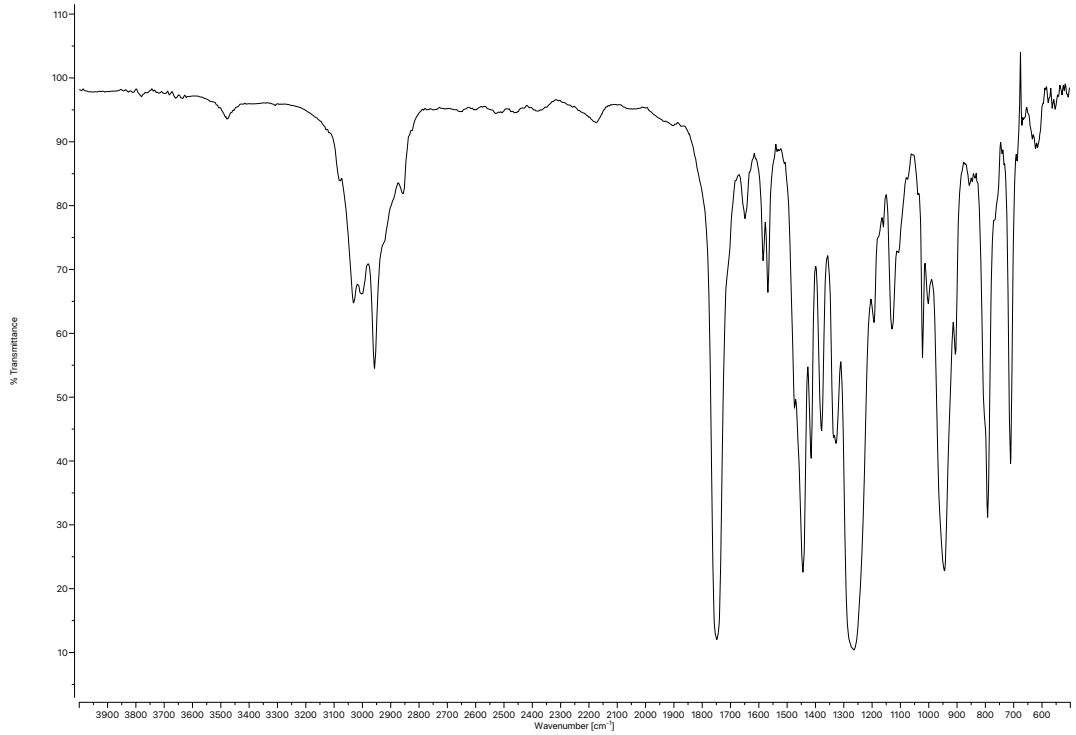


Figure A1.115 *Infrared spectrum (Thin Film, NaCl) of compound* ***31q***.

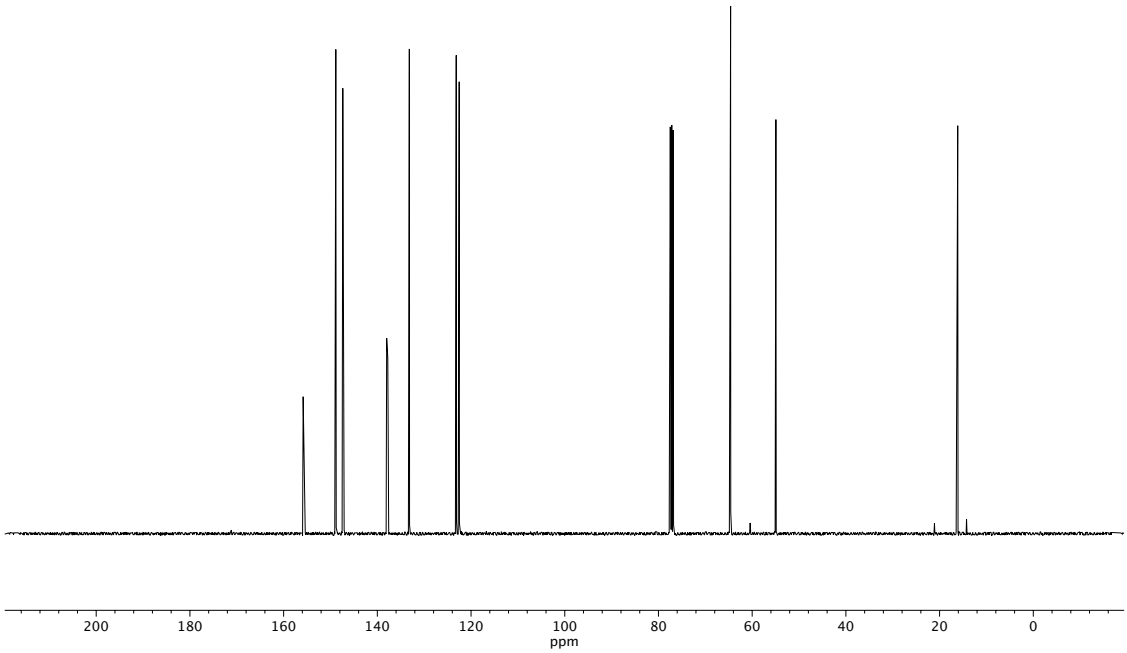


Figure A1.116 *^{13}C NMR (100 MHz, $CDCl_3$) of compound* ***31q***.

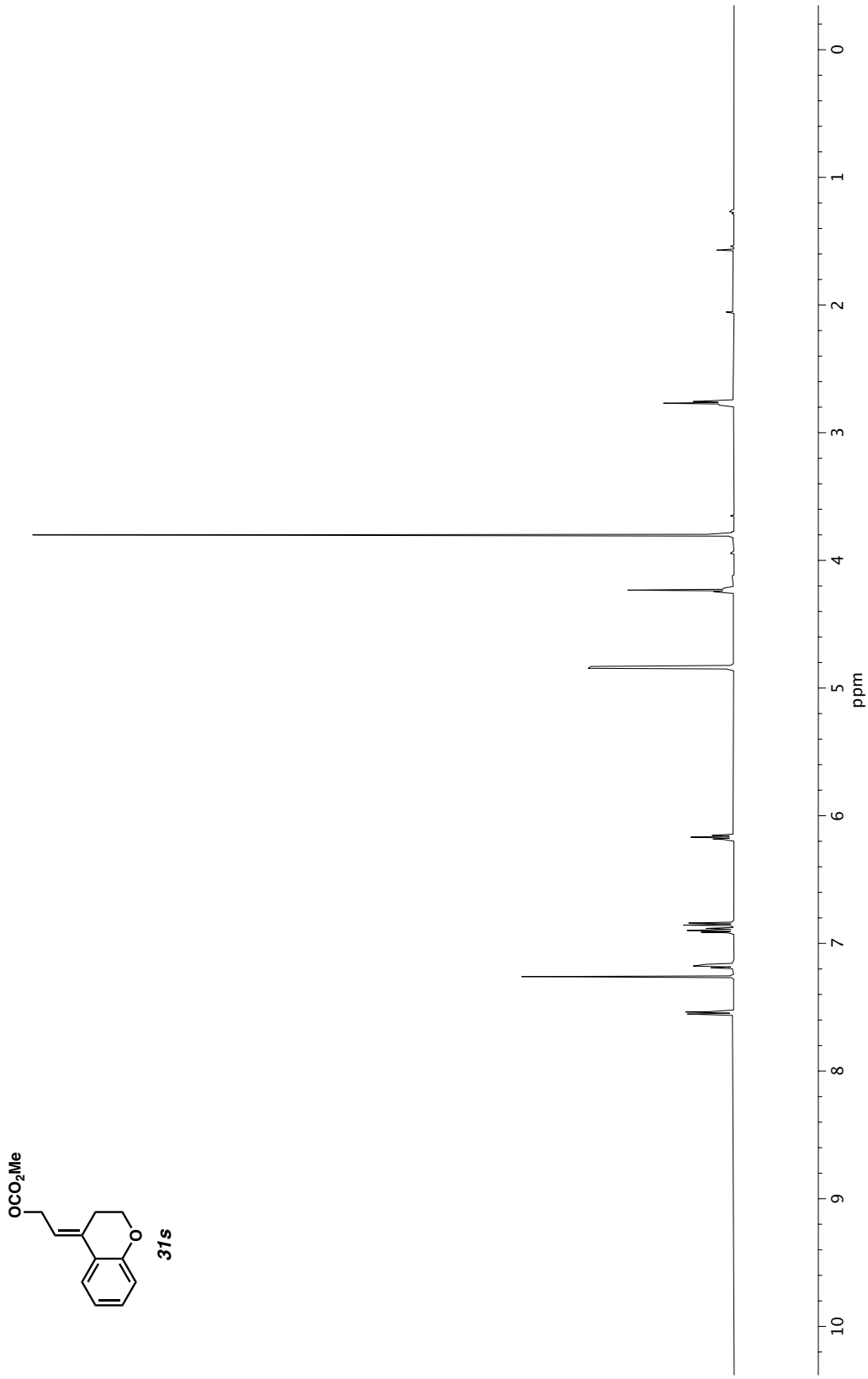


Figure A1.117 *^1H NMR (500 MHz, $CDCl_3$) of compound **31s**.*

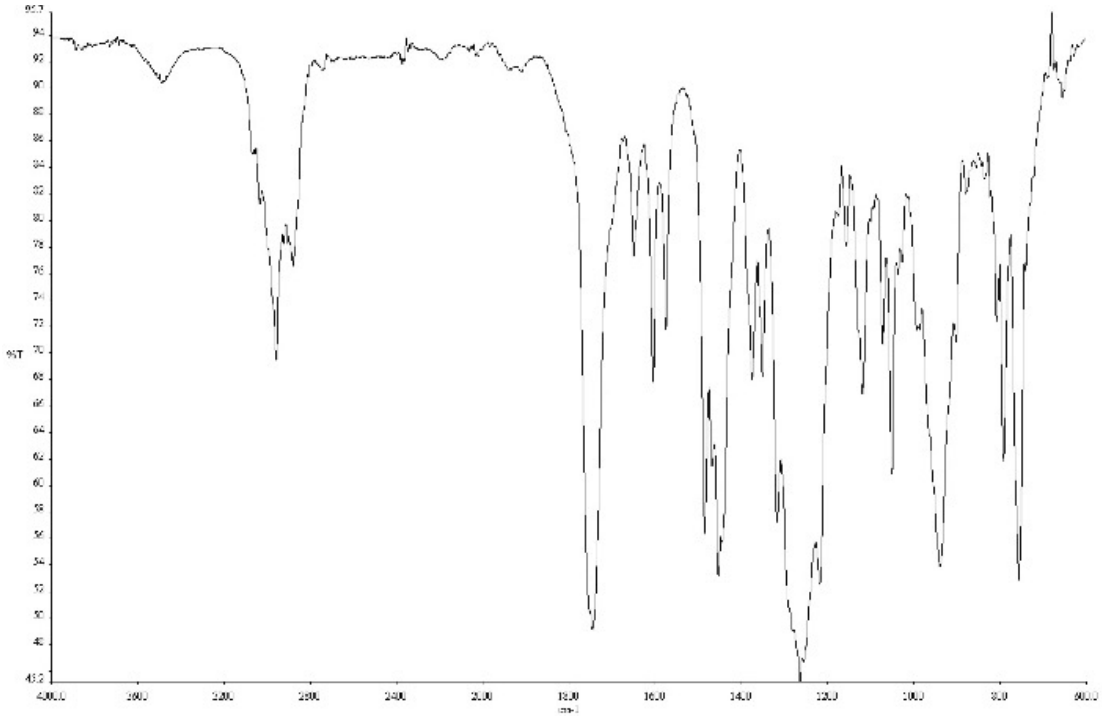


Figure A1.118 *Infrared spectrum (Thin Film, NaCl) of compound* ***31s****.*

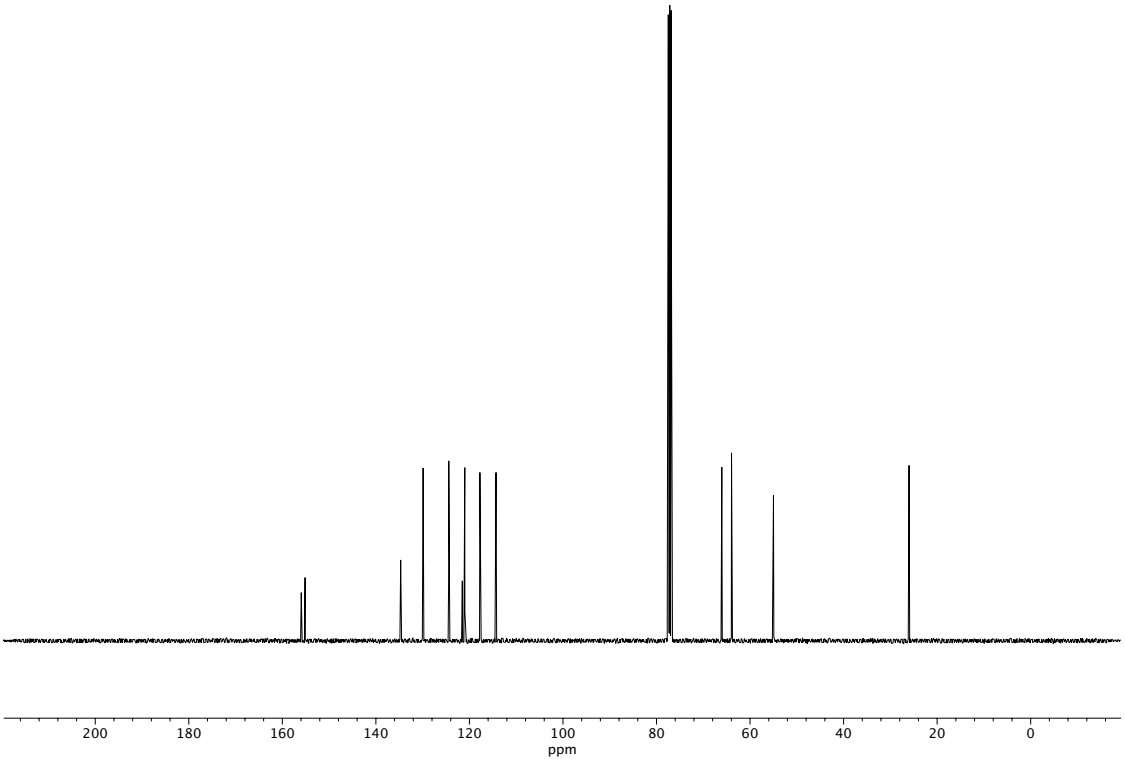


Figure A1.119 *^{13}C NMR (100 MHz, $CDCl_3$) of compound* ***31s****.*

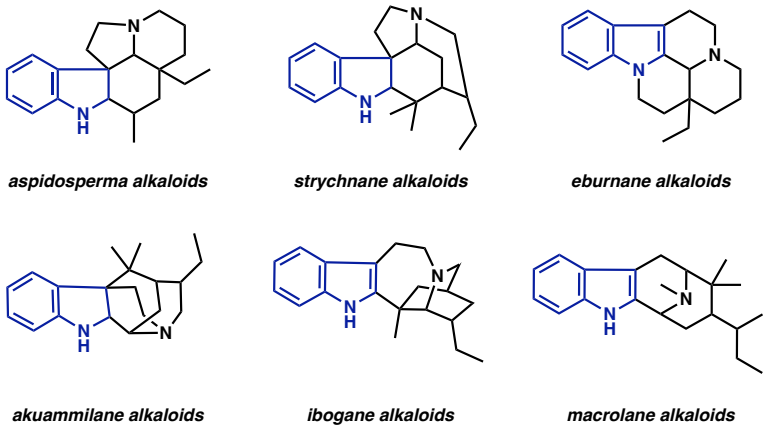
CHAPTER 2

Enantioselective Total Synthesis of Hunterine A[†]

2.1 INTRODUCTION

Monoterpene indole alkaloids (MIAs) are a structurally diverse class of natural products that have captured the attention of synthetic chemists for decades owing to their complexity and varied biological activities.[1,2] Molecules in this family are generally characterized by a conserved indole or indoline moiety bound to various rearranged terpene units. The carbon skeletons of several MIA subfamilies are shown in Figure 2.1.1.

Figure 2.1.1. *Carbon skeletons of various MIA subfamilies.*

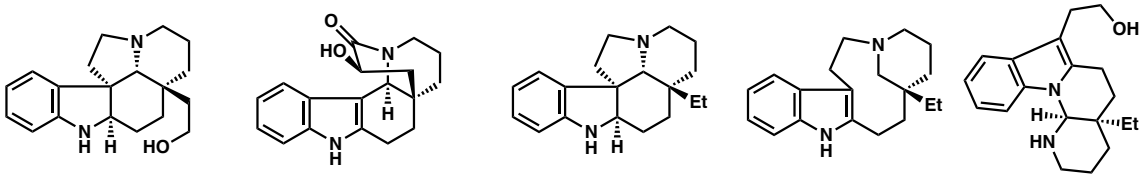


The stereochemically rich, densely functionalized molecular architectures of MIAs have made them the targets of numerous synthetic studies, and a number of elegant approaches to members of the various subfamilies have been reported.[3–8] Given our

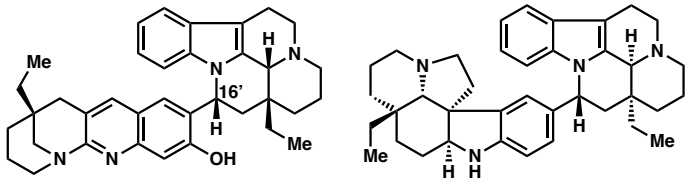
[†]This research was performed in collaboration with Kengo Inoue. Portions of this chapter have been reproduced with permission from Hicks, E. F.; Inoue, K. *J. Am. Chem. Soc.* **2024**, *146*, 4340–4345. © 2024 American Chemical Society.

laboratory's interest in the construction of structurally complex natural products, we have maintained a longstanding interest in MIAs and have completed syntheses of several members, shown in Figure 2.1.2.[9–12] These syntheses were enabled by the application of palladium-catalyzed asymmetric allylic alkylation technology developed in our laboratory.[13]

Figure 2.1.2 *MIAs and monoterpene bisindole alkaloids synthesized by the Stoltz laboratory.*



Angew. Chem. Int. Ed. **2017,** *56*, 12624. *Angew. Chem. Int. Ed.* **2016**, *55*, 13529.

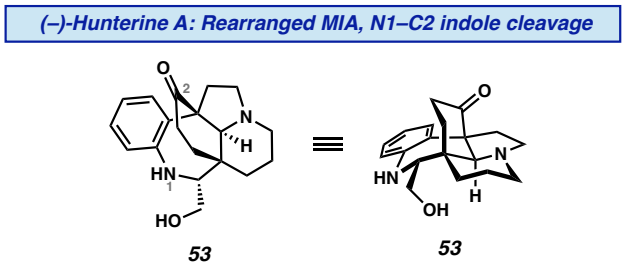


Angew. Chem. Int. Ed. **2021**, *60*, 17957. *J. Am. Chem. Soc.* **2023**, *145*, 7278.

In pursuit of synthesizing new MIA natural products, our interest was piqued by a recently reported "rearranged" monoterpene indole alkaloid, hunterine A (Figure 2.1.3, **53**), the unique structure of which is the result of an N1–C2 indole cleavage. Our efforts resulted in the first total synthesis of hunterine A (**53**) and a new synthesis of aspidospermidine (**48**), representing the first total synthesis of a rearranged MIA containing this type of structurally distinct N1–C2 indole cleavage.[14] This chapter contains an account of this research.

S

Figure 2.1.3. *Structure of Hunterine A.*

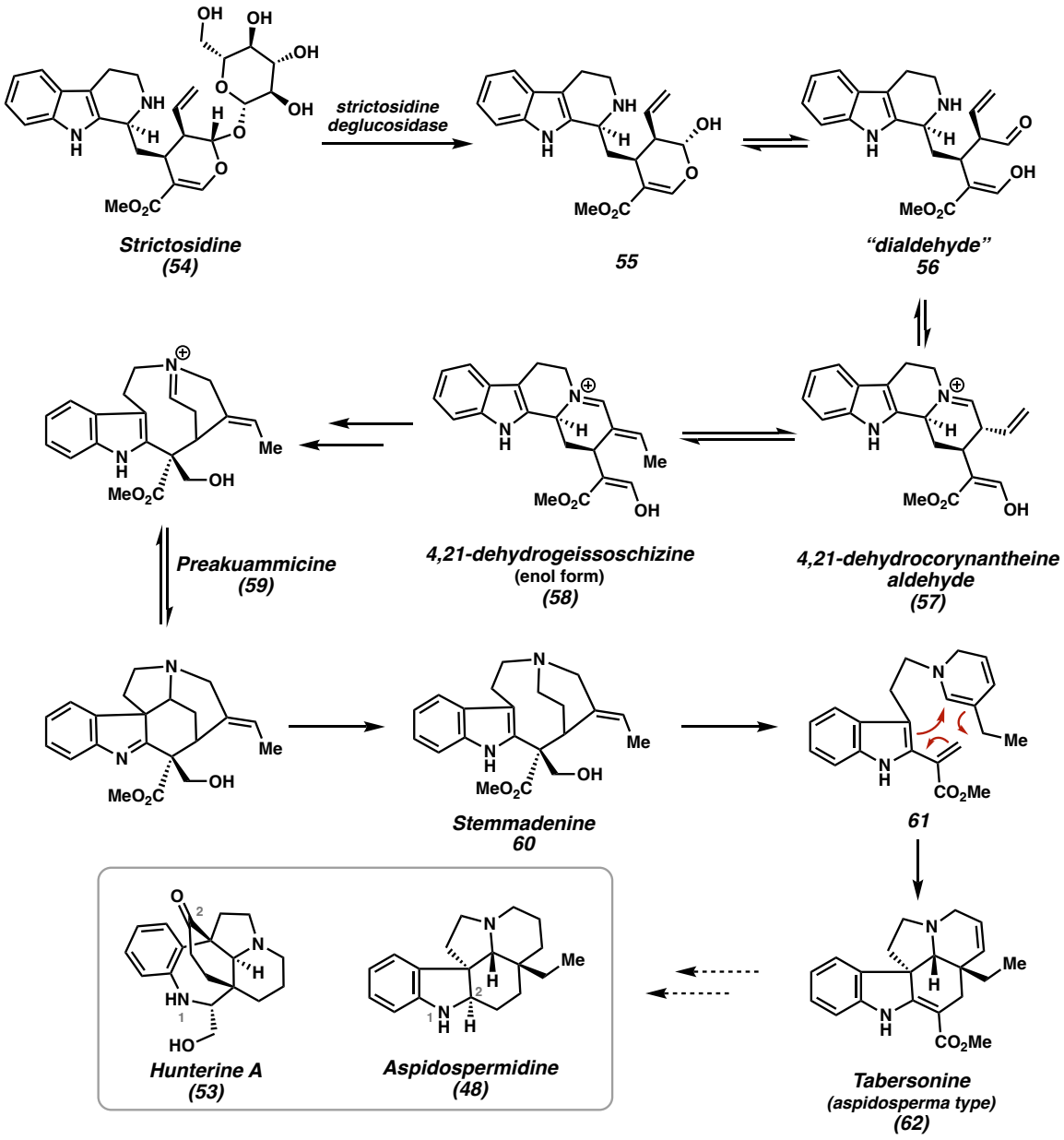


2.2 REARRANGED MONOTERPENE INDOLE ALKALOIDS

(–)-Hunterine A (**53**), isolated in 2019 by Zhang, Ye, and coworkers, belongs to the aspidosperma subfamily of MIAs (see Figure 2.1.1. for select MIA subfamilies).[15] Containing a structurally distinct N1–C2 indole bond cleavage, **53** is classified as a rearranged member of this subfamily. Biosynthetically, aspidosperma alkaloids, like all other MIAs, are believed to arise from a common precursor, strictosidine (Scheme 2.2.1,).[1,16]

The biosynthesis of aspidosperma alkaloids begins with de-glucosidation of **54**, yielding hemiacetal **55** in equilibrium with "dialdehyde" **56**. Dialdehyde **56** is also in equilibrium with its condensed form, 4,21-dehydrocorynantheine aldehyde **57**, which in turn is in equilibrium with its tautomer, 4,21-dehydrogeissoschizine (**58**), a divergent intermediate in the biosynthesis of other MIA subfamilies. In the pathway leading to aspidosperma alkaloids, **58** is converted to preakuammicine (**59**) and then reduced to stemmadenine (**60**). Stemmadenine (**60**) then undergoes isomerization, fragmentation, and tautomerization to yield enamine-diene **61**, another point of divergence that can lead to the ibogane subfamily of MIAs. Intramolecular Diels-Alder reaction of **62** yields tabersonine, the precursor to other aspidosperma MIAs. The exact pathway and intermediates involved in converting tabersonine (**62**) to other aspidosperma alkaloids (aspidospermidine (**48**), hunterine A (**53**)) has not been elucidated.

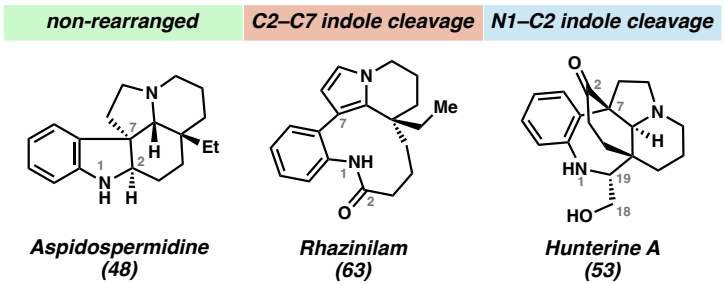
Scheme 2.2.1. *Biosynthesis of Aspidosperma MIAs.*



As has been repeatedly highlighted thus far, the N1–C2 indole ring cleavage present in hunterine A is a motif not found in any other aspidosperma MIAs to date. However, it should be noted that other "rearranged" aspidosperma MIAs have been isolated. These members, such as rhazinilam (Figure 2.2.1, **63**), contain indole ring cleavage between C2–

C7.[17,18] Side-by-side structural comparisons of these rearranged products are shown in Figure 2.2.1.

Figure 2.2.1. *Aspidospermidine (non-rearranged) and rearranged aspidosperma MIAs.*



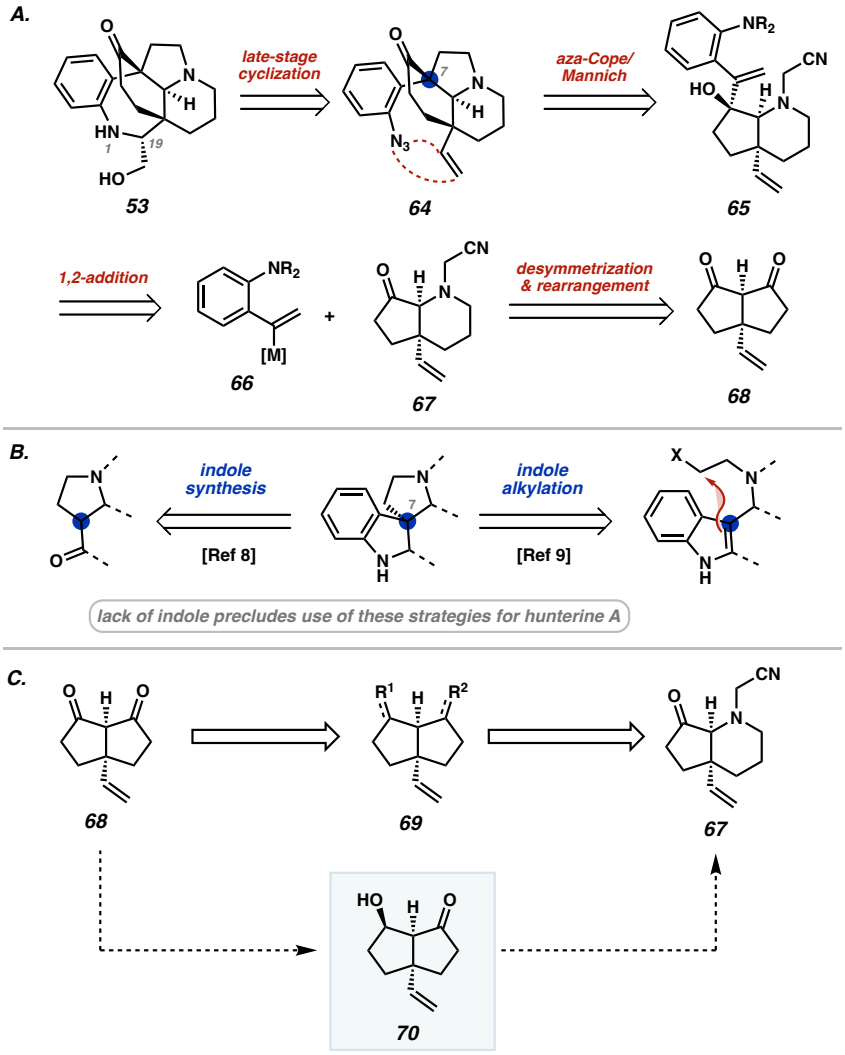
While many approaches toward the synthesis of rearranged rhazinilam-like MIAs have been disclosed,[19] there are no reported syntheses of MIAs containing and N1–C2 cleavage. Therefore, given our group's historic interest in this family of natural products coupled with the unique structure and intriguing biological activity of **53** (36 μM against HepG2 cell lines), we were motivated to pursue its total synthesis. The distinct architecture of **53** presents several new synthetic challenges such as a bridging azabicyclo[4.3.1]decane core, dissonant oxidation pattern of N1 and the C18 alcohol, and C19 stereochemistry. Consequently, this necessitated the development of a new synthetic strategy.

2.3 RETROSYNTHETIC ANALYSIS

When devising our retrosynthetic strategy, we began by focusing on the seven-membered azepane motif (Scheme 2.3.1, A). Disconnection of the C19–N1 bond within the azepane would eliminate the bridging ring system, leading to tricyclic intermediate **64**. Although at the outset of the synthesis it was unclear how this would be accomplished in the forward direction, an azide-olefin cycloaddition ultimately proved successful.[20,21] Given that **53** does not contain an indole, construction of the highlighted C7 all-carbon quaternary center could not be accomplished in the same manner as in the synthesis of related MIAs, which

commonly utilize strategies such as Fischer indole synthesis, and nucleophilic indole alkylation (Scheme 2.3.1, B).[22–31] Instead we imagined forming the C7 quaternary center via an aza-Cope/Mannich rearrangement, developed by Overman and coworkers for the synthesis of similar 3-acyl pyrrolidine motifs,[32,33] tracing back to bicyclic alcohol **65**. Alcohol **65** could be formed via a convergent, diastereoselective 1,2-addition of vinyl species **66** to ketone **67**. Finally, bicyclic ketone **67** was envisioned to arise from a desymmetrization and Beckmann rearrangement of symmetrical bicyclic diketone **68**.

Scheme 2.3.1. *A. Retrosynthetic Analysis of **53**. B. Strategies for C7 quaternary center formation. C. Possibilities for desymmetrization and use of keto-alcohol **70**.*



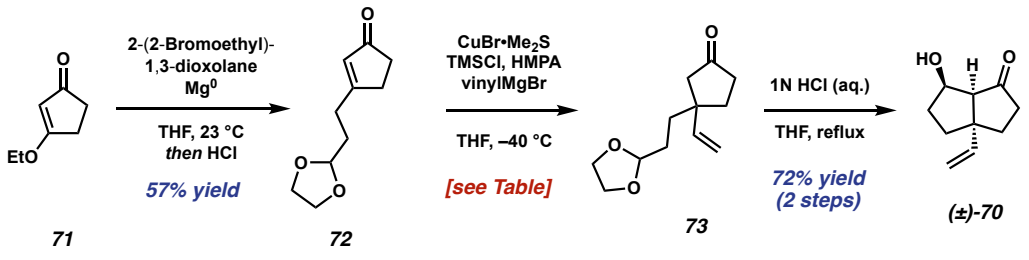
To execute the proposed desymmetrization, we imagined that **68** would need to be converted to a hypothetical intermediate **69** in which the two enantiotopic ketones would be differentiated such that the Beckmann rearrangement could be effected at the desired position (Scheme 2.3.1). While we imagined several possibilities by which this could be accomplished, the strategy we initially opted to investigate was a reductive desymmetrization to synthesize **70**, which ultimately proved successful. Thus, our initial synthetic efforts focused on construction of the bicyclic diketone **68** as well as independently synthesizing racemic keto-alcohol **70**.

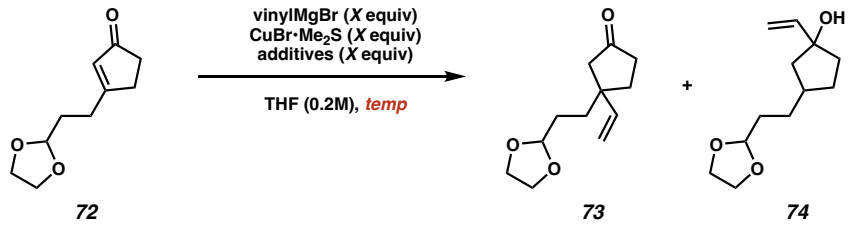
2.4 SYNTHESIS OF HUNTERINE A

Construction of racemic keto-alcohol **70** commenced from vinylogous ester **71**, inspired by the synthetic route disclosed by Piers and coworkers for the synthesis of structurally related compounds.[34] Addition of magnesiated 2-bromoethyl-1,3-dioxolane and Stork-Danheiser transposition gave enone **72**.[34] Copper-catalyzed 1,4-addition to install the necessary vinyl group required some optimization (Scheme 2.4.1). Addition of vinylmagnesium bromide at cryogenic temperature showed signs of success in the presence of TMSCl and HMPA (Entry 1) but was plagued by formation of undesired putative 1,2-addition product **74**. Raising the temperature to –40 °C improved the ratio of 1,4 and 1,2 addition products (Entry 2). In the absence of HMPA, this ratio was severely diminished (Entry 3). We found that using fewer equivalents of vinyl magnesium bromide resulted in lower yields of **73** but without formation of **74** (Entry 4), indicating that 1,2-addition may be the result of background reaction of uncomplexed excess magnesium reagent. Maintaining this relative stoichiometry of vinylMgBr, HMPA, and TMSCl, but increasing the equivalents of each reagent relative to enone **72** resulted in the best overall yield (Entry 5). This could be

further improved through the use of an "inverse addition" protocol in which vinyl magnesium bromide was added to all other reagents at low temperature.[35,36] Finally, we found that a one-pot procedure in which the crude ketone was directly treated with aqueous HCl resulted in an overall 72% yield from enone **72**, completing the synthesis of keto-alcohol **70** in racemic form. While this keto-alcohol could be oxidized to the desired diketone (**68**) for desymmetrization (not shown), we imagined constructing this motif through a more redox-efficient series of transformations through the same overall strategy.

Scheme 2.4.1. *Construction of racemic keto alcohol* ***70*** *and optimization of the 1,4-addition.*



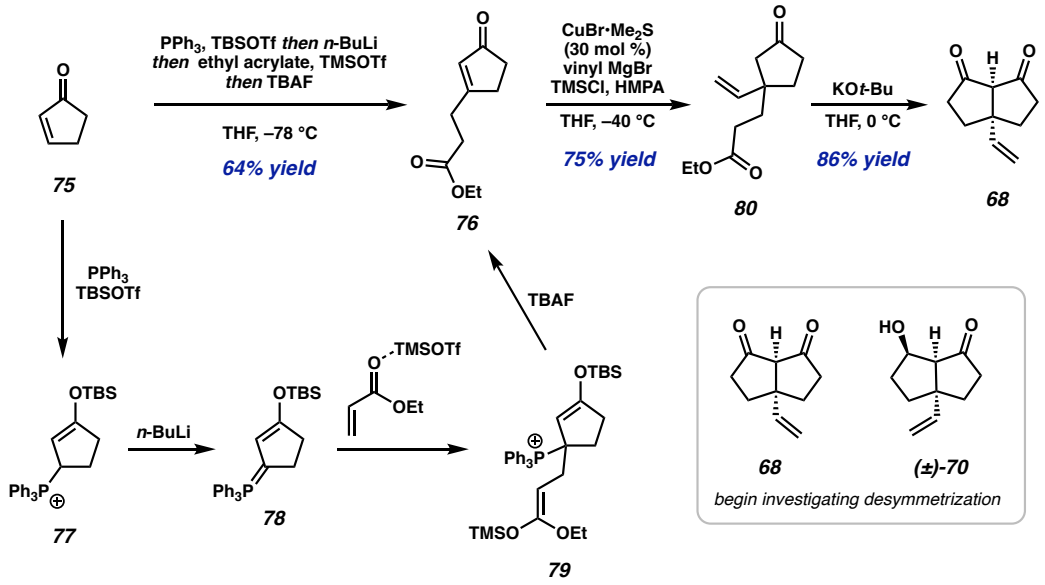


Entry	VinylMgBr	[Cu] equiv	additives	temp. (°C)	yield (1,4 pdt.)	*73* : *74*	notes
1	3.0 equiv	CuBr•Me_2S (30 mol%)	TMSCl (2 equiv) HMPA (3 equiv)	– 78	n.d.	1 : 1:.05	–
2	2.5 equiv	CuBr•Me_2S (30 mol%)	TMSCl (2 equiv) HMPA (3 equiv)	–40	56%	3.6 : 1	–
3	2.5 equiv	CuBr•Me_2S (30 mol%)	TMSCl (2 equiv)	–40	34%	1.8 : 1	–
7	1.3 equiv	CuBr•Me_2S (30 mol%)	TMSCl (2 equiv) HMPA (3 equiv)	–40	45%	1 : 0	50% conversion
10	3.0 equiv	CuBr•Me_2S (30 mol%)	TMSCl (6 equiv) HMPA (6 equiv)	–40	70%	1 : 0	vinyl MgBr added over 2 hours

Reactions conducted at 0.25 mmol scale. Yields determined by crude ^1H NMR using CH_2Br_2 as internal standard.
Reactions were conducted and quenched at the indicated temperature. Product *74* was unstable.

Construction of bicyclic diketone **68** commenced with an umpolung ylide addition of cyclopentenone to ethyl acrylate activated with TMSOTf, as disclosed by Kim and coworkers (Scheme 2.4.2).[37] In the event, cyclopentenone (**75**) is added to a mixture of PPh_3 and TBSOTf, resulting in the formation of phosphonium silyl enol ether species **77**. After cooling to cryogenic temperature, addition of *n*-BuLi leads to formation of ylide **68**. A mixture of TMSOTf and ethyl acrylate is added to the ylide, and the resulting solution is treated with TBAF to effect an E_1Cb elimination of triphenylphosphine, forming enone **76** in 64% yield in one step.

Scheme 2.4.2. *Construction of bicyclic diketone* ***68****.*



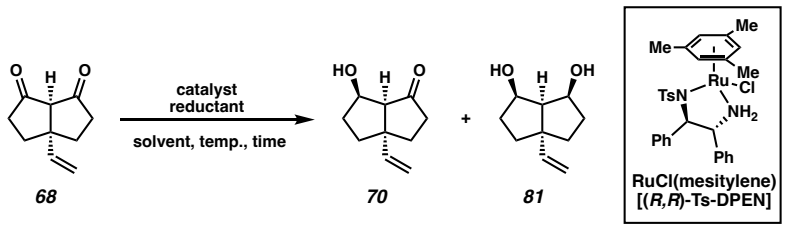
With enone **76** in hand, we next aimed to install the requisite vinyl group through Cu-catalyzed 1,4-addition. To our delight, the conditions outlined previously using the inverse addition protocol at –40 °C proved to be the key to successful 1,4-addition providing ketone **80** in 75% yield, precluding competitive 1,2-addition and addition to the ester (Scheme 2.4.2). With the vinyl group installed, an intramolecular Claisen condensation of ketone **80** cleanly afforded symmetrical diketone **68** in 86% yield.[38] With multi-gram

quantities of both symmetrical diketone **68** and racemic keto-alcohol **70** in hand, we began investigating the proposed desymmetrization.

As highlighted previously, we envisioned performing an asymmetric reduction as a means of differentiating the enantiotopic ketones. Since asymmetric reductions of simple alkyl-alkyl ketones tend to be poorly enantioselective due to difficulties in catalyst differentiation of the ketone *re*- and *si*-faces,[39] a variety of both chemical and enzymatic ketone reduction strategies were explored; representative entries are shown in the table in Scheme 2.4.3. Enantioselective reduction using Baker's yeast[40] proceeded with high levels of enantioselectivity, however in the incorrect enantiomeric series. Additionally, the long reaction time, excessive dilution required, and low conversion were all undesirable (entry 1). Reduction with CBS catalyst and catecholborane[41] was unsuccessful (entry 2). Ruthenium-catalyzed transfer hydrogenation in the presence of catalytic KOH and *i*-PrOH proceeded with low conversion and poor enantioselectivity (entries 3 and 4).[42] Ultimately, a scalable enantioselective reduction was realized through a modified version of Noyori's transfer hydrogenation conditions employing RuCl(mesitylene)(*R*,*R*-TsDPEN) and a (5:2) formic acid/triethylamine mixture[43,44] in 1,4-dioxane, which gave a separable mixture of keto-alcohol **70** (57% yield, 91% ee) and diol **81** (entry 7). Over-reduction to the *meso*-diol (**81**) was necessary as it resulted in an appreciable degree of chiral resolution, improving the enantiomeric purity of alcohol **70** (entries 8 and 9). Diol **81** was recycled to diketone **68** via oxidation with TEMPO and (diacetoxyiodo)benzene in 68% yield. To our knowledge, this is the first report of a non-enzymatic enantioselective reduction of a symmetrical [3.3.0] diketone,[45] making both enantiomers of the alcohol readily accessible. The absolute configuration of the alcohol was determined through derivatization as the 2,4-

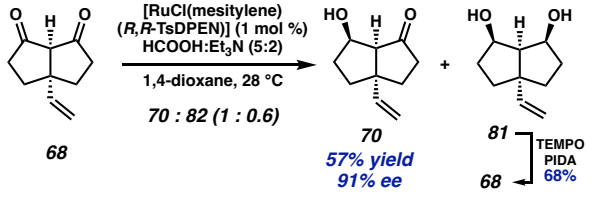
dinitrophenylhydrazone (Scheme 2.4.3), the *Z*-isomer of which proved to be crystalline (the *E* and *Z* isomers were formed in approximately equal amounts).

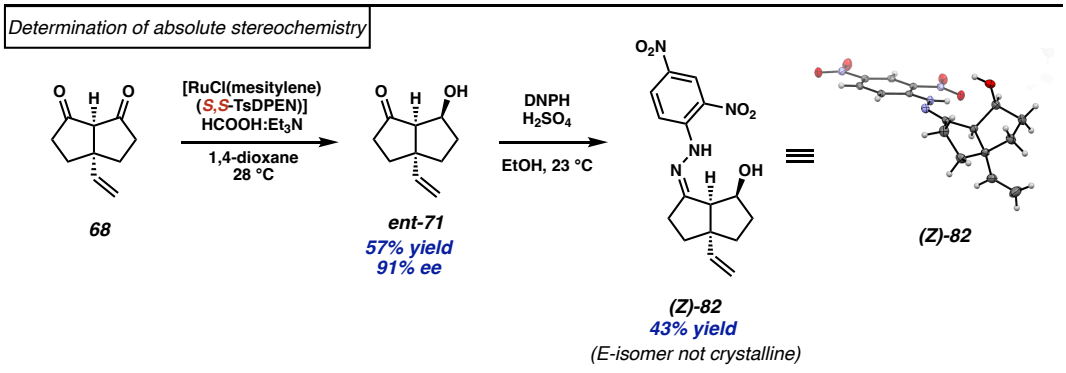
Scheme 2.4.3. *Optimization of the reductive desymmetrization and determination of absolute stereochemistry.*



Entry	Catalyst[a]	Reductant	Solv./Temp./Time	Conversion[c]	70:81	ee
1	Baker's yeast, yeast extract	—	H_2O:DMSO (70:1) 25 °C, 48 h	30%	1 : 0	–95%
2	*(S)-n*-Bu-CBS	catecholborane	toluene –78 °C, 3 h	40%	—	—
3	RuCl(*p*-cymene) [(*R,R*)-Ts-DPEN][b]	*i*-PrOH	*i*-PrOH, 28 °C 24 h	<5%	n.d.	n.d.
4	RuCl(mesitylene) [(*R,R*)-Ts-DPEN][b]	*i*-PrOH	*i*-PrOH, 28 °C 24 h	20%	1 : 0	15%
5	RuCl(mesitylene) [(*R,R*)-Ts-DPEN]	HCOOH:Et_3N (5:2) (2 equiv)	CH_2Cl_2 28 °C, 14 h	88%	1 : 1.2	79%
6	RuCl(mesitylene) [(*R,R*)-Ts-DPEN]	HCOOH:Et_3N (5:2) (2 equiv)	THF 28 °C, 14 h	99%	1 : 1	82%
7	RuCl(mesitylene) [(*R,R*)-Ts-DPEN]	HCOOH:Et_3N (5:2) (2 equiv)	1,4-dioxane 28 °C, 14 h	99%	1 : 0.6	91%
8	RuCl(mesitylene) [(*R,R*)-Ts-DPEN]	HCOOH:Et_3N (5:2) (1.5 equiv)	1,4-dioxane 28 °C, 14 h	95%	1 : 0.3	85%
9	RuCl(mesitylene) [(*R,R*)-Ts-DPEN]	HCOOH:Et_3N (5:2) (1 equiv)	1,4-dioxane 28 °C, 14 h	90%	1 : 0.12	81%

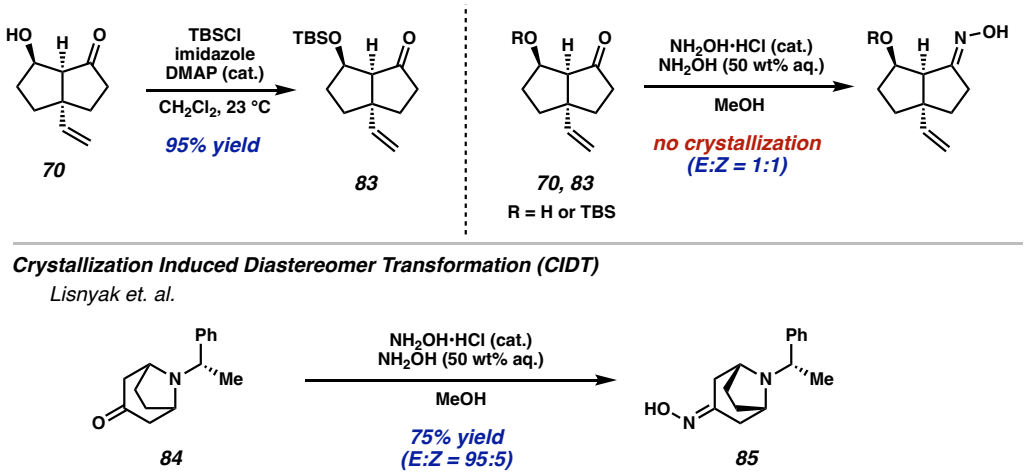
[a] Reactions were conducted with 1 mol % [Ru] catalyst [b] 5 mol % KOH added [c] Conversion determined by ^{1}H NMR ratio of remaining diketone XX relative to CH_2Br_2 internal standard





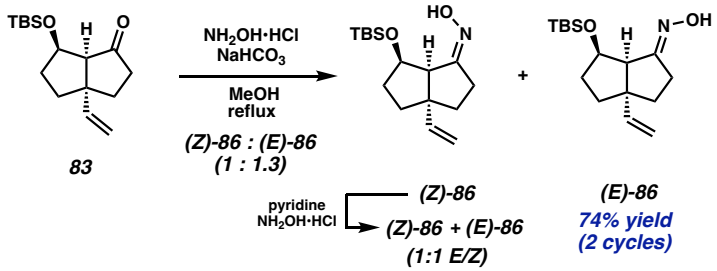
With the enantioselective desymmetrization complete, the originally envisioned Beckmann rearrangement and subsequent reduction could be performed to construct the necessary piperidine ring. To this end, enantioenriched alcohol **70** was first protected with TBSCl to give silyl ether **83** nearly quantitatively (Scheme 2.4.4). While attempts to condense hydroxylamine were successful, these condensations led to roughly equal mixtures of *E* and *Z* products. A recent report by Lisnyak and coworkers (Scheme 2.4.4) demonstrated an elegant solution to a similar *E/Z* selectivity issue during oxime formation. Implementing a crystallization-induced diastereomer transformation (CIDT), the authors were able to form the desired oxime diastereomer in 75% yield with 95:5 *E/Z* selectivity.[46] The principle of CIDT relies on crystallinity and differences in solubility of two equilibrating diastereomers such that the desired diastereomer selectivity crystallizes and the undesired remains in solution, allowing for selective formation of the desired diastereomer. Unfortunately, translation of these reaction conditions did not improve the selectivity due to a lack of product crystallinity; no precipitation was observed leading to an approximately 1:1 mixture.

Scheme 2.4.4. *CIDT reported by Lisnyak and failed CIDT of bicyclic ketones* ***70*** *and* ***83***.



Experiencing no success selectively generating one oxime isomer, alternative means to isolate the desired compound were undertaken. Condensation conditions employing hydroxylamine hydrochloride and $NaHCO_3$ slightly favored formation of the desired diastereomer, and the mixture of diastereomers was separated chromatographically (Scheme 2.4.5). After separation, the undesired diastereomer was resubjected to similar oxime formation conditions to give a 1:1 mixture that could again be separated. In two cycles, desired oxime (**(E)-86**) was isolated in 74% yield on multi-gram scale.

Scheme 2.4.5. *Oxime formation, separation, and recycling.*

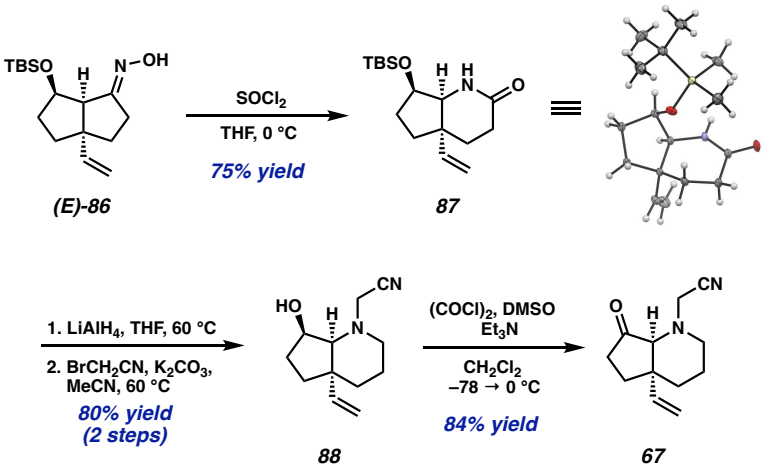


Exposure of the desired oxime to an excess of thionyl chloride resulted in smooth Beckmann rearrangement and produced lactam **87** in 75% yield (Scheme 2.4.6). The absolute and relative stereochemistry were confirmed by X-ray crystallography. It should be noted that while some reports have demonstrated that mixtures of oxime isomers can be isomerized in situ to give single Beckmann rearrangement products,[47–49] this could not be accomplished in our hands. Thus, the described protocol for separating and recycling of the oxime isomers proved crucial given that the undesired oxime isomer also undergoes a stereospecific Beckmann rearrangement to give an isomeric, undesired lactam.

Lactam **87** could be advanced through exhaustive reduction with $LiAlH_4$, which simultaneously and unexpectedly removed the silyl protecting group. This proved to be of little consequence as the crude amino alcohol was selectively alkylated with K_2CO_3 and

bromoacetonitrile to give aminonitrile **88** in 80% yield over two steps. Finally, Swern oxidation of the alcohol afforded bicyclic ketone **67** in 84% yield.

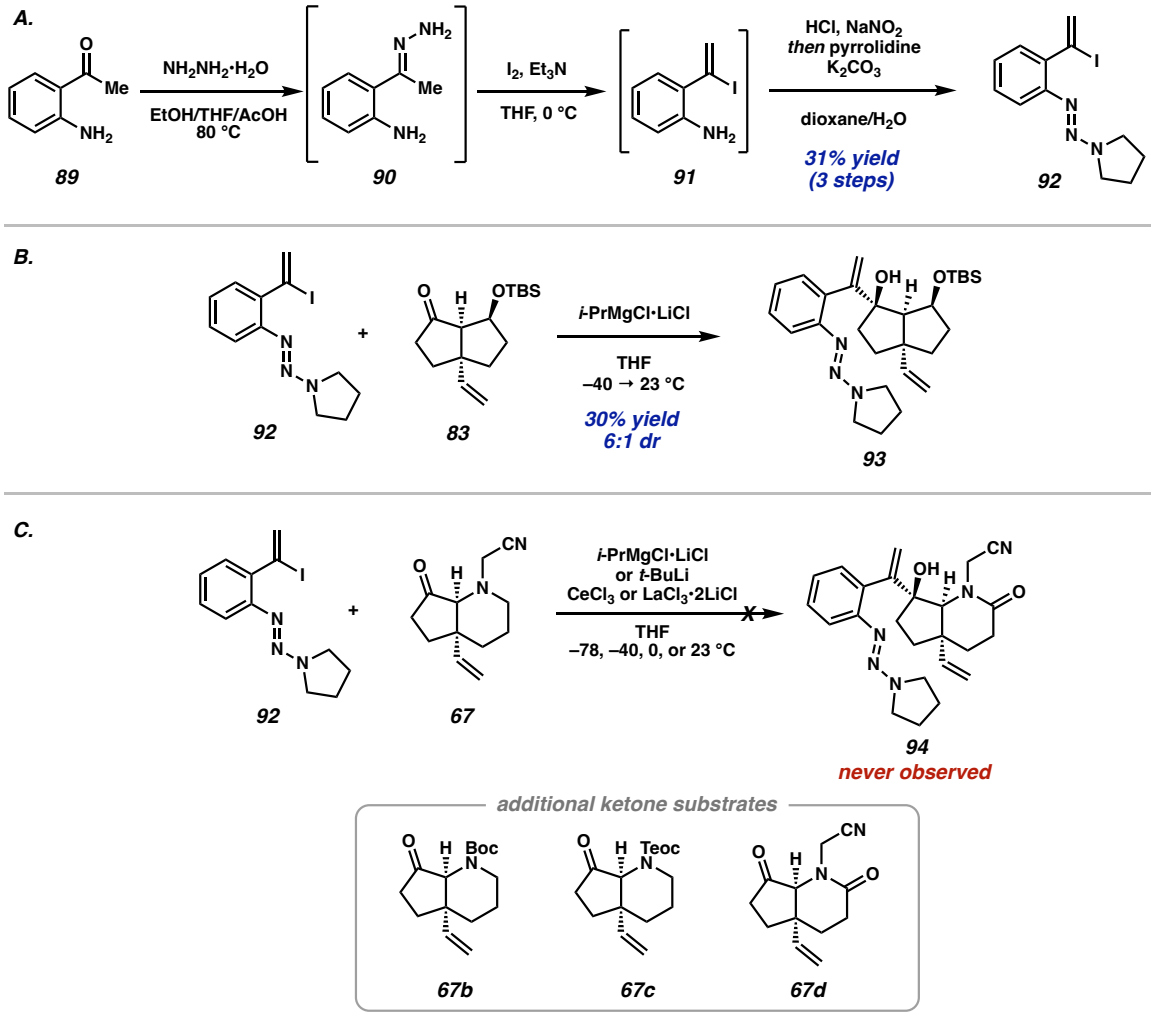
Scheme 2.4.6. *Beckmann rearrangement and synthesis of aminoketone* ***67****.*



With bicyclic aminoketone **67** in hand, a variety of 1,2-addition protocols were evaluated using different vinyl iodides as precursors to vinyl lithium or magnesium species. The incorporation of the necessary aniline nitrogen within this vinyl nucleophile was central to the success of our strategy. As such, a key consideration was how best to protect this functional group during the addition. To this end, we opted to begin our investigation of this transformation using triazene **92** (shown in Scheme 2.4.7), as triazenes have proven to be particularly robust in the context of anionic 1,2-addition reactions and can be readily converted to the parent aniline compounds or derivatized to the corresponding azide.[50–58]

Synthesis of triazene **92** began with condensation of hydrazine onto 2'-aminoacetophenone (Scheme 2.4.7). The corresponding crude hydrazone was then subjected to Barton hydrazone iodination[59] with I_2 and triethylamine resulting in the formation of **91**. Aniline **91** was converted to the triazene (**92**) by diazotization with aqueous HCl and $NaNO_2$, and subsequent trapping of the aryl diazonium with pyrrolidine.

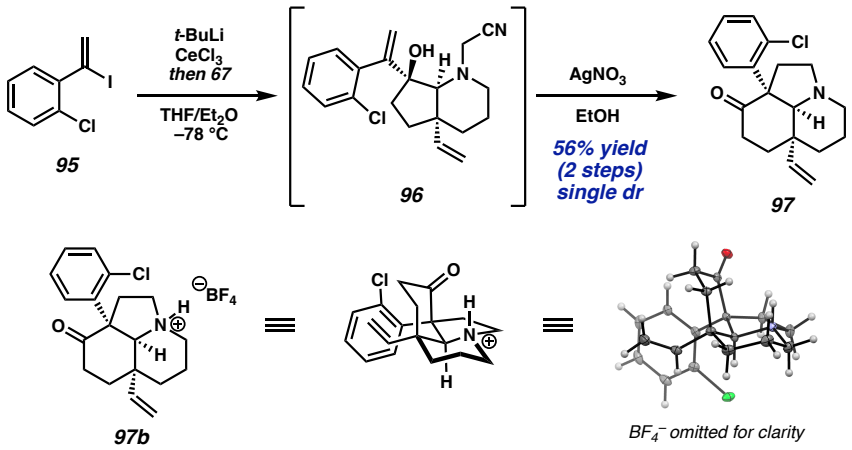
Scheme 2.4.7. *A) Synthesis of vinyl iodide nucleophile containing aryl triazene. B) Successful addition to ketone* ***83****. C) Failed addition to aminoketones* ***67b–d****.*



Early attempts to use the triazene nucleophile were promising. Treatment of **92** with *i*-PrMgCl•LiCl followed by addition of ketone **ent-83** gave **93** in 30% yield and approximately 5:1 dr. Unfortunately, this initial success never translated to successful addition to **67**. Using *i*-PrMgCl•LiCl or *t*-BuLi to generate organometallic vinyl species, neither of these vinyl nucleophiles on their own or in conjunction with Lewis acidic additives such as $CeCl_3$ and $LaCl_3$•2LiCl successfully added to the desired ketone or any derivatives thereof (Scheme 2.4.7, C).

To better understand the source of failure, we opted to perform the 1,2-addition using a simpler vinyl nucleophile. Treatment of iodovinyl aryl chloride **95** with *t*-BuLi followed by addition of the vinyllithium species to $CeCl_3$ and subsequent addition of ketone **67** gave allylic alcohol **96** (Scheme 2.4.8). Excitingly, the crude allylic alcohol could be directly treated with $AgNO_3$ to affect the desired aza-Cope/Mannich reaction,[60] giving **97**. The relative stereochemical configuration was confirmed through X-ray crystallographic analysis of its HBF_4 salt (**97b**).

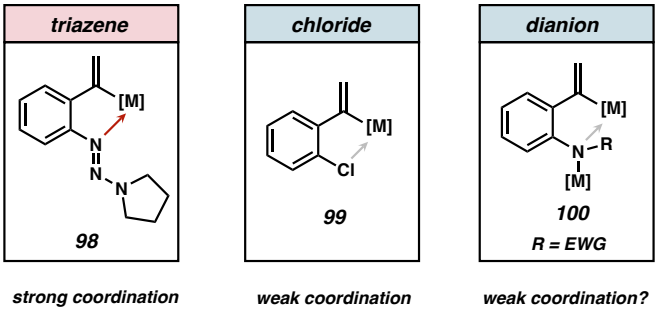
Scheme 2.4.8. *Successful 1,2-addition using chloride nucleophile and subsequent aza-Cope/Mannich reaction.*



Given these stark differences in reactivity and the knowledge that 1,2-addition to ketone **67** was indeed possible, we hypothesized that with the correct nitrogen-containing nucleophile 1,2-addition would be feasible. In an attempt to reconcile the different outcomes using the two nucleophiles, we noted that the lone pair of the aryl triazene is perfectly situated to coordinate to the metal center, making a five-membered chelate (Figure 2.4.1). It seemed possible that this might diminish the reactivity of the vinyl magnesium reagent either due to the species being stabilized or due to steric bulk as a consequence of the conformational rigidity. In contrast, the chloride likely coordinates only weakly (or perhaps not at all) to the

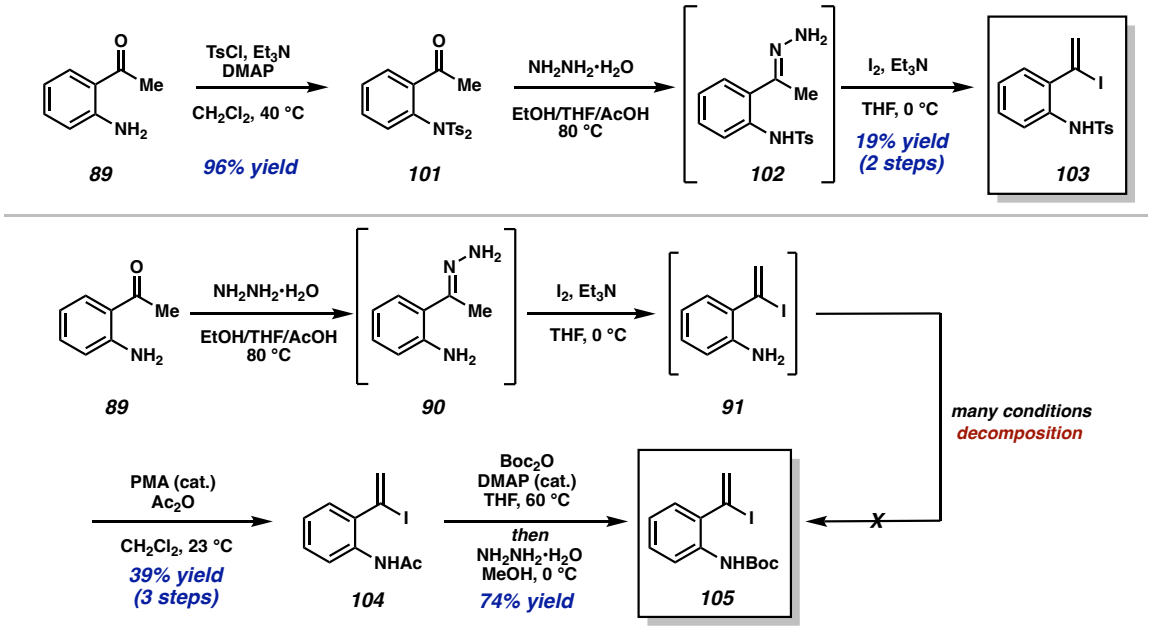
metal center. Empirically this resulted in successful 1,2-addition. If coordination were the issue with reactivity, we imagined that a dianion nucleophile with an appropriately chosen electron-withdrawing protecting group would potentially avoid this type of coordination and lead to successful in the 1,2-addition.

Figure 2.4.1. *Hypothesized differences in coordination and reactivity of different nucleophile classes.*



Synthesis of the relevant nucleophile precursors (vinyl iodides) was accomplished in a similar manner through hydrazone iodination (Scheme 2.4.9). To synthesize the N-Ts derivative, 2'amino-acetophenone was first treated with excess TsCl, Et_3N, and catalytic DMAP to give bis-tosyl derivative **101**. Condensation of hydrazine, which concomitantly removed one of the tosyl groups (**102**), was followed by hydrazone iodination to give vinyl iodide **103**. The N-Boc derivative was synthesized via an alternative order of events. After synthesizing of crude vinyl iodide **91** (as performed previously), attempts to directly protect the aniline nitrogen of **91** as the N-Boc derivative failed. Instead a two-step procedure was employed wherein the aniline was first acetylated with Ac_2O and catalytic phosphomolybdic acid to give **104**.[61] Then a one-pot procedure developed by Burk and coworkers was adapted to convert the acetylated aniline to the N-Boc compound through treatment with Boc_2O and DMAP at elevated temperature followed by treatment with hydrazine to remove the acetyl group, yielding **105**.[62]

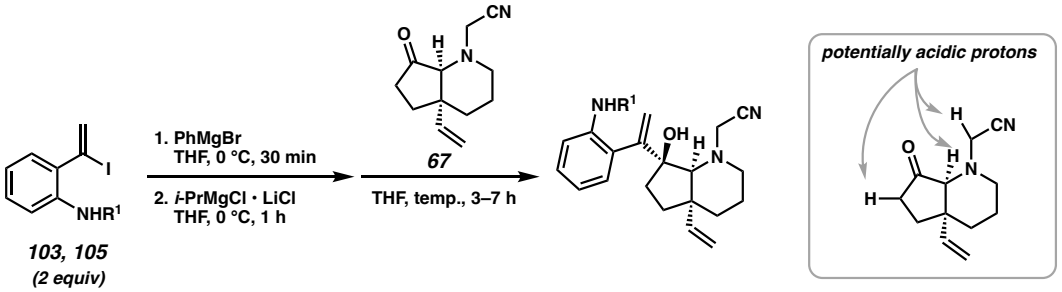
Scheme 2.4.9. *Synthesis of dianion nucleophile precursors* ***103*** *and* ***105****.*



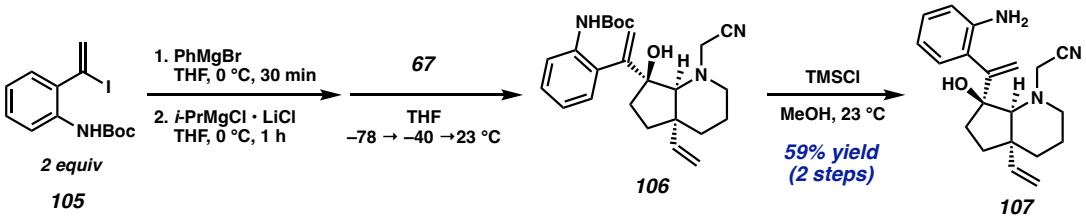
With both nucleophiles in hand, we began investigating the dianion 1,2-addition. Deprotonation of **103** with PhMgBr followed by Mg-halogen exchange with *i*-PrMgCl•LiCl and treatment with ketone **67** resulted, encouragingly, in trace formation of the desired 1,2-addition product by crude ^{1}H NMR (Scheme 2.4.10, entry 1). However, the overall reaction profile indicated formation of many unidentified side-products, perhaps due to the presence of several acidic protons. In an attempt to attenuate potential deleterious side reactions caused by deprotonation, a variety of additives were evaluated. $CeCl_3$, $ZnCl_2$, and $TMSCH_2MgCl$ (to generate the magnesium-ate complex) failed to improve the reaction in any way (entries 2–5). In striking contrast, $LaCl_3$•2LiCl[63,64] proved to be uniquely effective in promoting the desired addition, and the remaining mass was simply unreacted ketone. Encouraged by these results, we noted greater success with the N-Boc derivative **105** such that the product could be isolated in 68% yield. We speculate that the difference in reactivity has to do with improved solubility of the dianion formed when employing **105**; the N-Ts dianion suffers

from insolubility in THF even at non-cryogenic temperatures. Having developed a successful 1,2-addition protocol, it was possible to advance further by using the allylic alcohol without further purification, deprotecting the aniline with TMSCl in MeOH to give the corresponding aniline (**107**) in 59% yield over two steps (Scheme 2.4.9).

Scheme 2.4.10. *Optimization of the dianion 1,2-addition.*



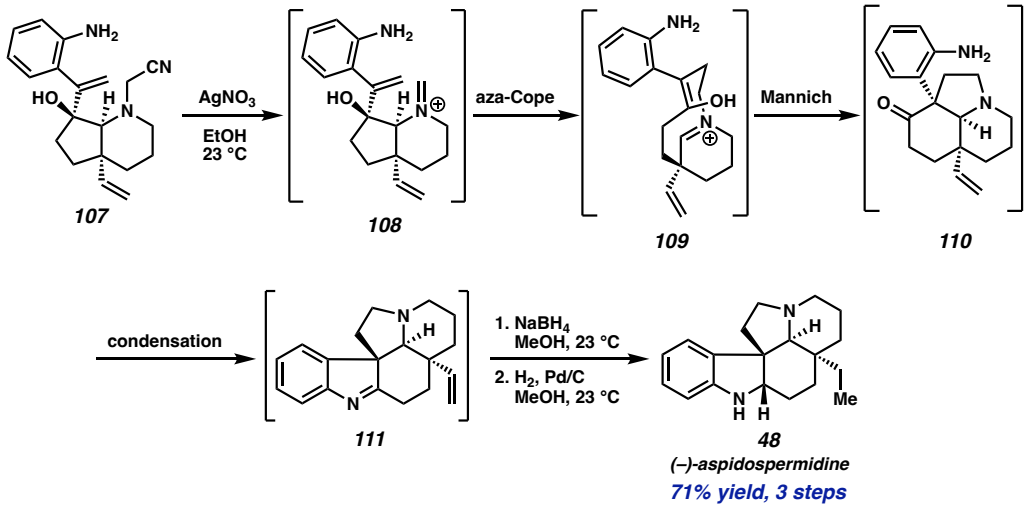
Entry	R^1 =	Additive	temp.	% yield *(NMR)*
1	Ts	–	0 °C	(<10%)
2	Ts	$ZnCl_2$	0 °C	(0%)
3	Ts	$CeCl_3$	0 °C	(<5%)
4	Ts	$CeCl_3$	–78 °C	(0%)
5	Ts	$TMSCH_2MgCl$	0 °C	(<5%)
6	Ts	$LaCl_3$·2LiCl	–78 → 23 °C	(30%)
7	Boc	$LaCl_3$·2LiCl	–78 → –40 →23 °C	68%



At this stage, we were set up to begin investigating the aza-Cope/Mannich reaction. Our results with the aryl chloride had already suggested that this transformation was feasible and proceeded to give the correct diastereomer (Scheme 2.4.8, **97**). However, given that the aniline nitrogen was now present, we were wary of performing the aza-Cope/Mannich reaction in its presence. Overman and coworkers have reported similar transformations in which an aniline nitrogen can condense onto a ketone following aza-Cope/Mannich reaction

to form an indolimine (in the case of an unprotected aniline nitrogen), albeit under rather forcing conditions.[65] Nevertheless, we decided to attempt the reaction in hopes of preventing condensation using milder reaction conditions. Treatment of **107** with $AgNO_3$ in EtOH[60] did effect the desired aza-Cope/Mannich reaction, but not unexpectedly the aforementioned condensation occurred concomitantly even under the mild reaction conditions to give **111** (Scheme 2.4.11). This transformation proceeds through initial cyanide abstraction by Ag^+ to form iminium **108** which undergoes cationic aza-Cope rearrangement to yield iminium **109** that is then trapped via an intramolecular Mannich cyclization to give tricycle **110**.[33] Unfortunately the reaction did not stop at this stage as desired. Instead, the free aniline nitrogen is then poised for a final condensation, forming **111**. Although unproductive for the synthesis of hunterine A (**53**), the crude 3,3-disubstituted indolenine (**111**) could be treated with $NaBH_4$ in MeOH and hydrogenated to give aspidospermidine (**(–)-48**) in 71% yield over 3 steps. It should be noted that reduction of indolenine **111** prior to hydrogenation is necessary, as the tertiary amine likely directs the hydride reduction to occur from the concave face of the molecule. Attempts to form aspidospermidine via direct hydrogenation of **111** resulted in the formation of *epi*-aspidospermidine (not shown), indicating that the reduction with $NaBH_4$ is likely directed.

Scheme 2.4.11. *Undesired condensation following aza-Cope/Mannich reaction and synthesis of (–)-aspidospermidine.*

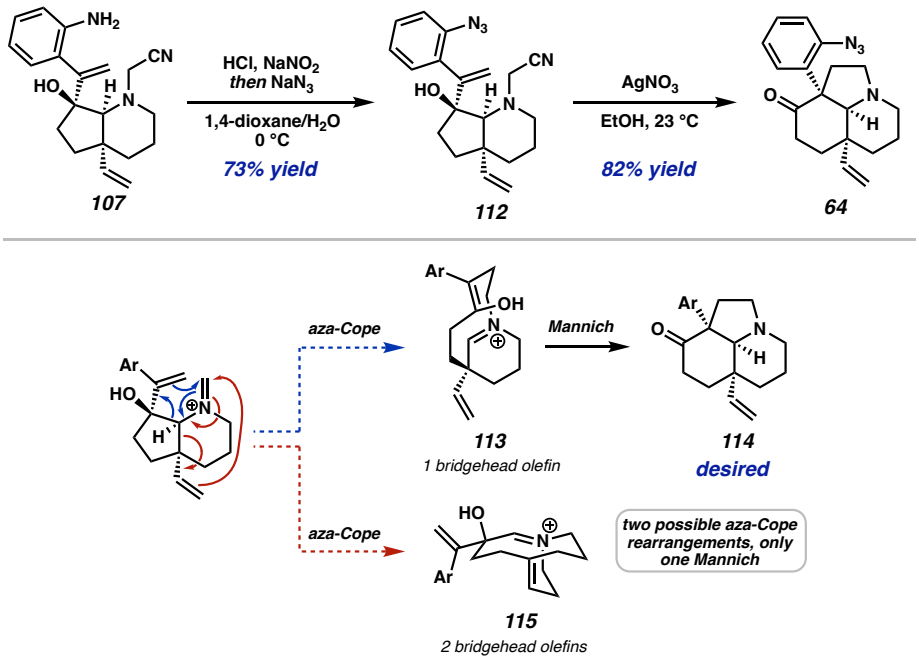


Armed with the knowledge that aza-Cope/Mannich reaction of the free aniline (**107**) was unproductive, we needed to use an alternative order of events. Ultimately, following the aza-Cope/Mannich reaction, the aniline would be converted to the corresponding azide for use in a dipolar cycloaddition. While formation of the azide prior to the aza-Cope/Mannich reaction would avoid the problematic intermediate **110**, aza-Cope/Mannich reactions in the presence of azide functional groups have not been reported. Despite the lack of precedent, we decided to proceed forward by synthesizing the necessary azide.

Conversion of aniline **107** to the corresponding aryl azide could be accomplished under standard azidation conditions using HCl and $NaNO_2$ followed by treatment with aqueous NaN_3 (Scheme 2.4.11). Gratifyingly, treatment of this intermediate with $AgNO_3$ in EtOH effected the desired aza-Cope/Mannich reaction without any noticeable interference of the azide functionality, and tricycle **64** was isolated in 82% yield. Additionally, it is worth noting that each aza-Cope/Mannich reaction presented herein, including the conversion of **96** to **97** in Scheme 2.4.7, was not affected by the presence of the terminal olefin. This is

significant as the presence of this group allows for an additional aza-Cope rearrangement possibility via the formation of **115** (Scheme 2.4.12). Although this structure would be considerably strained due to the presence of an additional bridgehead olefin, its formation could facilitate other decomposition pathways that have the potential to undermine the efficiency of the desired aza-Cope/Mannich reaction. Overall, these potential pitfalls were likely circumvented by the mild conditions used to effect this transformation by employing an *N*-cyanomethyl group as the iminium precursor for the aza-Cope rearrangement.

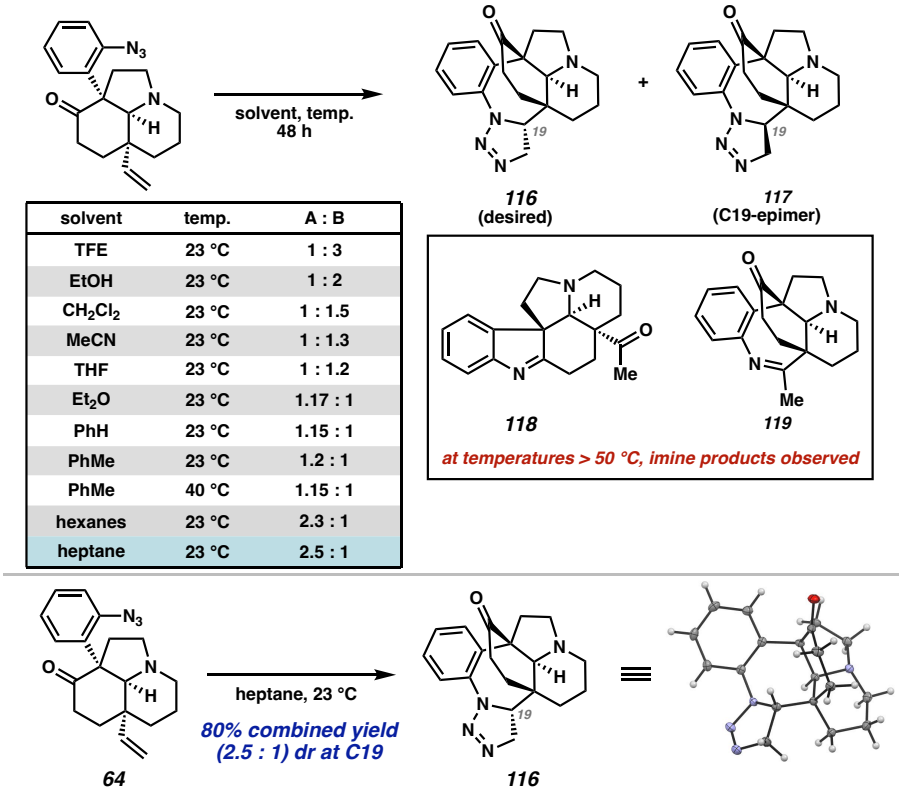
Scheme 2.4.12. *Formation of aryl azide prior to aza-Cope/Mannich and avoidance of a potential undesired aza-Cope rearrangement.*



With the tricycle complete, the remaining objectives were closure of the seven-membered azepane ring and installation of the primary alcohol. The subsequent dipolar cycloaddition proved to be spontaneous and occurred by simply dissolving azide **64** in a variety of different solvents. However, the diastereoselectivity of the cycloaddition displayed a marked solvent effect; the results are summarized in Scheme 2.4.13. It appeared that polar,

and particularly polar-protic solvents tended to favor formation of the undesired diastereomer, while nonpolar, alkane solvents favored formation of the desired diastereomer. Additionally, heating the reactions to temperatures near 50 °C resulted in the detection of imine by-products (**118** and **119**), well-characterized thermal decomposition products of aryl triazenes. Cooling the reactions reduced the rate of the cycloaddition to an impractical degree. Under the optimized conditions, dissolving the azide in heptane at ambient temperature resulted in an 80% combined yield of chromatographically separable C19 diastereomers. Additionally, the absolute and relative configurations of both diastereomers were unambiguously determined through X-ray crystallography.

Scheme 2.4.13. *Optimization of the [3+2] cycloaddition.*



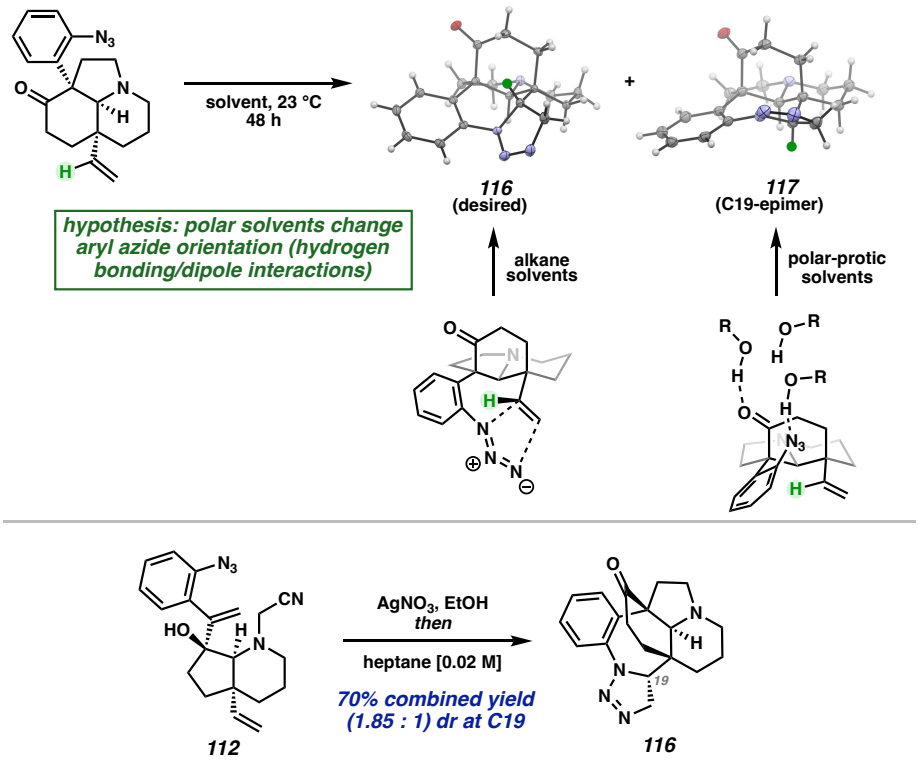
solvent	temp.	A : B
TFE	23 °C	1 : 3
EtOH	23 °C	1 : 2
CH_2Cl_2	23 °C	1 : 1.5
MeCN	23 °C	1 : 1.3
THF	23 °C	1 : 1.2
Et_2O	23 °C	1.17 : 1
PhH	23 °C	1.15 : 1
PhMe	23 °C	1.2 : 1
PhMe	40 °C	1.15 : 1
hexanes	23 °C	2.3 : 1
heptane	23 °C	2.5 : 1

We rationalize that this effect may have to do with hydrogen bonding interactions with the solvent. Looking more closely at the crystal structures of both diastereomers, the

two carbons belonging to the terminal olefin are in nearly identical positions in both **116** and **117** (Scheme 2.4.14). This indicates that the change in diastereoselectivity may have to do with changes in the orientation of the aryl azide in different solvents, prior to the cycloaddition. It seems reasonable that in the case of nonpolar, alkane solvents the preferred conformation of the aryl azide would be away from other functionality and in a conformation such that the C=O and aryl C–N dipoles are minimized (Scheme 2.4.14). In this conformation, the azide is poised to undergo cycloaddition with the olefin to preferentially give the desired diastereomer. In the case of polar protic solvents, hydrogen bonding interactions between the ketone, solvent, and azide may bring the azide and ketone in closer proximity to one another. In this conformation, the azide is poised to undergo cycloaddition with the olefin from the opposite face, leading to the formation of the undesired diastereomer.

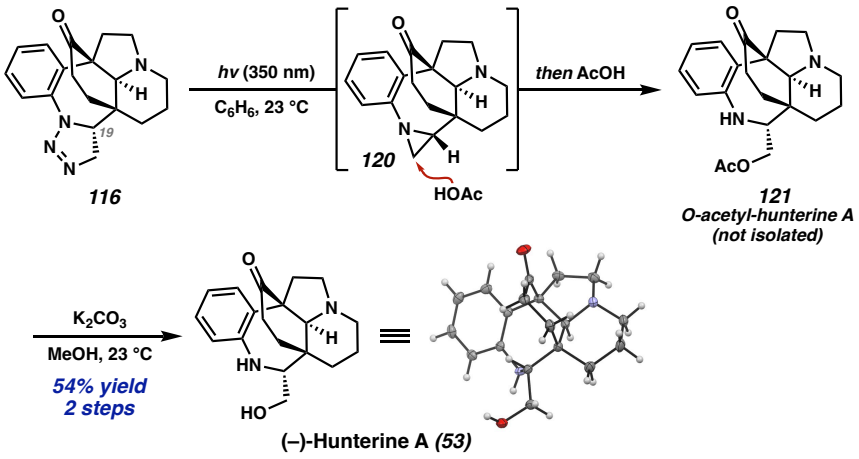
With the knowledge that polar protic solvents favor formation of the undesired diastereomer, we were able to develop a one-pot procedure for the synthesis of **116** (and **117**) beginning from allylic alcohol **112**. Treatment of this compound with $AgNO_3$ in EtOH effected the aza-Cope/Mannich reaction, and upon its completion the reaction was diluted with heptane, which gave an 70% yield of a 1.85:1 mixture of diastereomers in one step (Scheme 2.4.13). The lower diastereoselectivity is likely a feature of the presence of ethanol necessary for the aza-Cope/Mannich step. Alternative procedures involving concentration to remove the ethanol were not able to reproducibly improve the diastereoselectivity.

Scheme 2.4.14. *Rationalization of diastereoselectivity and one-pot aza-Cope/Mannich, [3+2] cycloaddition.*



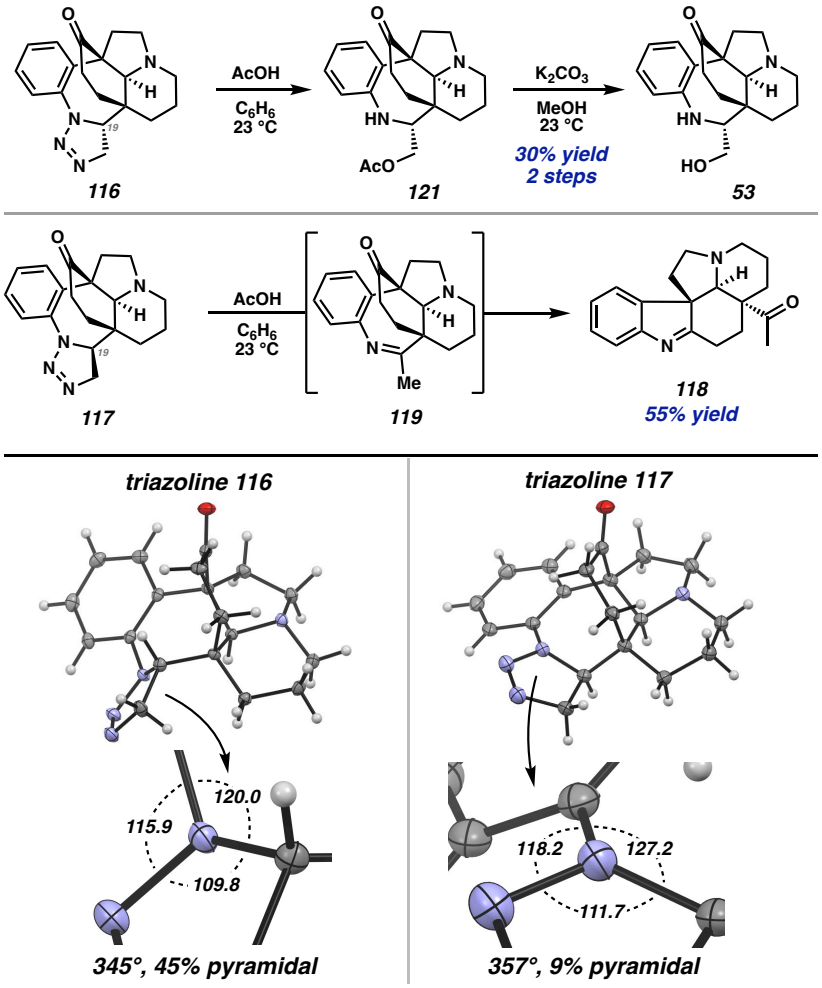
With the pentacyclic ring system complete, all that remained was functionalization of the triazoline to install the necessary alcohol. Gratifyingly, we were able to develop a two-step, one pot sequence to install the necessary oxygen atom. First, the desired diastereomer was irradiated with long wave UV light (350 nm) to form the putative aziridine **120** (Scheme 2.4.15.[66–69] Acetic acid was then added to the reaction mixture, which led to regioselective ring-opening[70,71] to form *O*-acetyl-hunterine A (**121**). With the necessary acetylated oxygen atom installed, simple treatment of *O*-acetyl-hunterine A (**121**) with K_2CO_3 in MeOH gave hunterine A (**53**) in 54% yield over the final two steps, completing the total synthesis.

Scheme 2.4.15. *Completion of the synthesis of hunterine A.*



Attempts to streamline the endgame sequence by excluding the triazoline photolysis, resulted in unexpected differences in reactivity. Treatment of triazoline **116** with acetic acid in benzene successfully generated *O*-acetyl-hunterine A, although with a poor reaction profile which resulted in a lower overall yield of (–)-hunterine A from **116** (Scheme 2.4.16). By contrast, treatment of undesired **117** with acetic acid in benzene formed imine **118** in 55% yield, likely via intermediate **119**[72,73] followed by intramolecular imine transfer to the more stable indolimine. No amount of the C19-epimer of *O*-acetyl-hunterine A was detected.

Scheme 2.4.16. *Nitrogen pyramidality and differences in reactivity of triazoline diastereomers.*



We speculate that this difference in reactivity relates to different degrees of pyramidality[74] of the respective nitrogen atoms. Summation of the relevant bond angles in the crystal structure of **116** suggests that the nitrogen atom is 45% pyramidal, while in **117** the nitrogen atom is only 9% pyramidal. Thus, the formation of imine **118** (presumably via intermediate imine **119**) from **117** may be a reflection of this diastereomer's propensity to retain a planar geometry.

2.5 CONCLUSION

In conclusion, we have developed an enantioselective total synthesis of hunterine A, a novel member of the historic monoterpene indole alkaloid (MIA) class of natural products. Key features of this synthesis are the development of a catalytic, enantioselective desymmetrization of a symmetrical bicyclo[3.3.0]diketone, a dianion 1,2-addition using $LaCl_3$•2LiCl, an aza-Cope Mannich reaction with spontaneous azide-olefin cycloaddition, and a regioselective aziridine ring opening. Additionally, we have uncovered a potential connection between the structure and divergent reactivity of late stage triazoline diastereomers. Finally, we have also demonstrated that intermediate aniline **107** provides a point of divergence to access other members of the MIA family of natural products.

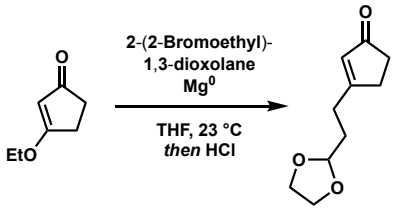
2.6 EXPERIMENTAL SECTION

2.6.1 MATERIALS AND METHODS

Unless otherwise stated, reactions were performed in flame-dried glassware under an argon or nitrogen atmosphere using dry, deoxygenated solvents. Solvents were dried by passage through an activated alumina column under argon.[75] Reaction progress was monitored by thin-layer chromatography (TLC) or Agilent 1290 UHPLC-MS. TLC was performed using E. Merck silica gel 60 F254 precoated glass plates (0.25 mm) and visualized by UV fluorescence quenching, *p*-anisaldehyde, or $KMnO_4$ staining. Silicycle Silia*Flash*® P60 Academic Silica gel (particle size 40–63 μm) was used for flash chromatography. ^1H NMR spectra were recorded on Varian Inova 500 or 600 MHz and Bruker 400 MHz spectrometers and are reported relative to residual $CHCl_3$ (δ 7.26 ppm), C_6D_5H (δ 7.16 ppm), and CD_2HOD (δ 3.31). ^{13}C NMR spectra were recorded on a Varian Inova 500 MHz spectrometer (125 MHz) and Bruker 400 MHz spectrometers (100 MHz) and are reported

relative to $CDCl_3$ (δ 77.16 ppm), C_6D_6 (δ 128.06 ppm), or CD_3OD (δ 49.00 ppm). Data for ^1H NMR are reported as follows: chemical shift (δ ppm) (multiplicity, coupling constant (Hz), integration). Multiplicities are reported as follows: s = singlet, d = doublet, t = triplet, q = quartet, p = pentet, sept = septuplet, m = multiplet, br s = broad singlet, br d = broad doublet. Data for ^{13}C NMR are reported in terms of chemical shifts (δ ppm). IR spectra were obtained by use of a Perkin Elmer Spectrum BXII spectrometer using thin films deposited on NaCl plates and reported in frequency of absorption (cm^{-1}). Optical rotations were measured with a Jasco P-2000 polarimeter operating on the sodium D-line (589 nm), using a 100 mm path-length cell. Analytical SFC was performed with an Agilent 1260 Infinity II SFC supercritical CO_2 analytical chromatography system using a Chiralpak AD-H column (4.6 mm x 250 mm, 3 micron) obtained from Daicel Chemical Industries, Ltd. High resolution mass spectra (HRMS) were obtained from the Caltech Mass Spectral Facility using a JEOL JMS-T2000GC AccuTOF^{TM} GC-Alpha High Resolution Mass Spectrometer in field ionization (FI+) or field desorption (FD+) mode, or an Agilent 6230 Series TOF with an Agilent Jet Stream ion source in electrospray ionization (ESI+) mode. Reagents were purchased from commercial sources and used as received unless otherwise stated.

2.6.2 EXPERIMENTAL PROCEDURES



71 *72*

Enone 72: Magnesium metal (15.55 g, 640 mmol, 6.4 equiv) was crushed with a mortar and pestle, then added to a 2 L, 3-necked round-bottom flask equipped with a stir bar, glass stopper, and two addition funnels. The flask was flame-dried under vacuum then allowed to cool under a stream of N_2. 2-(2-bromoethyl)-1,3-dioxolane (purchased from Combi Blocks Inc.) (37.6 mL, 320 mmol, 3.2 equiv) was added to one addition funnel with THF (330 mL). 3-Ethoxycyclopent-2-en-1-one[76] (**71**) (12.62 g, 100 mmol, 1.0 equiv) was added to the remaining addition funnel with THF (200 mL). Approximately 20 mL of the bromide solution was added to the magnesium and a small crystal of iodine (~20 mg) was added to initiate formation of the Grignard. The remaining bromide solution was then added dropwise such that a gentle reflux is maintained (added over ~30 min). The mixture was then stirred for an additional hour at ambient temperature. During this time, the mixture became cloudy. After 1 h, the solution of vinylogous ester was then added fast dropwise (~10 min) to the cloudy solution.

After 4 h, an aliquot of the reaction mixture was added to 1 N aq. HCl and extracted with ether. NMR analysis showed complete consumption of the vinylogous ester. The reaction mixture was cooled to 0 °C, and 1 N aq. HCl (600 mL) was carefully added. The cooling bath was removed, and the reaction mixture was stirred for 1 h, then the aqueous layer was extracted 3x with EtOAc (100 mL). The combined organic layers were washed with brine

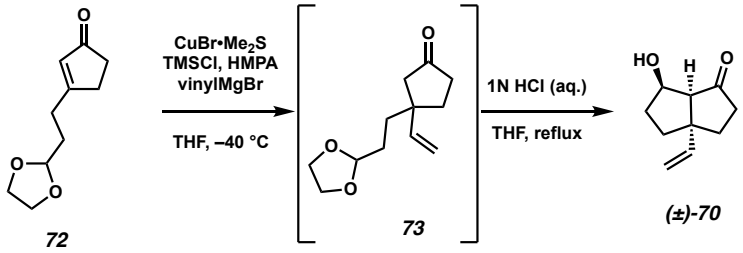
(100 mL), dried over $MgSO_4$, and concentrated under reduced pressure to give a brown oil which was purified silica gel flash column to give the title compound as a yellow/orange oil (10.50 g, 57% yield).

^{1}H NMR: (500 MHz, $CDCl_3$) δ 5.80 – 5.76 (m, 1H), 4.76 (t, *J* = 4.4 Hz, 1H), 3.86 – 3.76 (m, 2H), 3.76 – 3.65 (m, 2H), 2.45 (dt, *J* = 7.0, 1.9 Hz, 2H), 2.39 (t, *J* = 7.9 Hz, 2H), 2.26 – 2.20 (m, 2H), 1.79 (td, *J* = 8.1, 4.3 Hz, 2H)

^{13}C NMR: (125 MHz, $CDCl_3$) δ 209.5, 181.9, 129.0, 103.0, 64.8, 35.0, 31.3, 30.8, 27.3

IR: (Neat Film, NaCl) 2889, 1697, 1613, 1436, 1409, 1335, 1286, 1233, 1187, 1138, 1033, 945, 903, 843 cm^{-1}

HRMS: (ESI+) *m/z* calc'd for $C_{10}H_{15}O_3$ $[M+H]^+$: 183.1016, found 183.1015



Keto-alcohol (±)-70: To a 500 mL round-bottom flask equipped with stir bar and rubber septum was added CuBr•Me_2S (812 mg, 3.95 mmol, 30 mol %) and the vessel was purged and backfilled with N_2 three times. THF (34.7 mL) was added, followed by HMPA (14.16 g, 13.7 mL, 79.02 mmol, 6.0 equiv). The pale green mixture was then cooled to –40 °C (external temperature, dry ice/acetonitrile bath) and TMSCl (8.58 g, 10.0 mL, 79.02 mmol) was added neat, dropwise, during which time the solution became brown. Then enone **72** (2.40 g, 13.17 mmol, 1.0 equiv) in THF (20 mL) was added fast dropwise. Finally, vinylmagnesium bromide (0.7 M in THF) (56.5 mL, 39.52 mmol, 3.0 equiv) was added dropwise via syringe pump over 2 hours. After the Grignard was added, the reaction was stirred for an additional hour, then quenched with 6.34 g NH_4Cl in H_2O (20 mL). *At this stage, extraction with EtOAc and purification can be performed to give ketone **73**.*

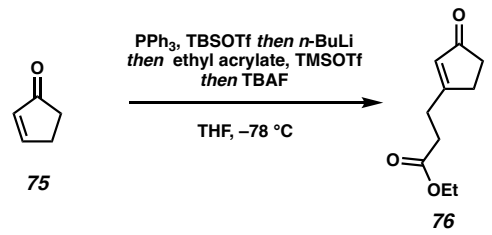
^{1}H NMR: (500 MHz, $CDCl_3$) δ 5.74 (dd, *J* = 17.5, 10.7 Hz, 1H), 5.11 (dd, *J* = 10.7, 0.7 Hz, 1H), 4.95 (dd, *J* = 17.5, 0.7 Hz, 1H), 4.87 – 4.79 (m, 1H), 3.99 – 3.90 (m, 2H), 3.88 – 3.80 (m, 2H), 2.38 (dd, *J* = 17.8, 1.9 Hz, 1H), 2.26 – 2.19 (m, 2H), 2.08 (d, *J* = 17.8 Hz, 1H), 2.04 – 1.96 (m, 1H), 1.83 (dt, *J* = 12.9, 9.1 Hz, 1H), 1.70 – 1.55 (m, 4H)

^{13}C NMR: (125 MHz, $CDCl_3$) δ 218.5, 143.0, 114.2, 104.4, 65.0, 48.7, 45.9, 36.4, 34.4, 33.6, 29.7

IR: (Neat Film, NaCl) 2954, 2883, 1741, 1403, 1165, 1141, 1034, 943, 920, 870 cm^{-1}

HRMS: (FD+) *m/z* calc'd for $C_{12}H_{18}O_3$ $[M]^+$: 210.1259, found 210.1240.

In a one-pot procedure to synthesize the keto alcohol **(±)-70**, the mixture was warmed to ambient temperature, then 1 N aq. HCl (13 mL) was added, and the reaction mixture was heated to 70 °C for 12 h. After 12 h, the mixture was cooled to ambient temperature and transferred to a separatory funnel. The aqueous layer was extracted 3x with EtOAc (50 mL). The combined organic layers were washed with satd. aqueous $NaHCO_3$ and brine, dried over $MgSO_4$ and concentrated under reduced pressure. The crude residue was purified by column chromatography (35% EtOAc in hexanes) to give the title compound as a yellow/orange oil (1.586 g, 72% yield). *The characterization data are shown in the section detailing the preparation of this alcohol in enantioenriched form.*



75 *76*

Enone 76:[37] To a 1 L round-bottom flask equipped with stir bar was added PPh_3 (27.5 g, 105 mmol, 1.05 equiv) and THF (300 mL). TBSOTf (27.76 g, 24 mL, 105 mmol, 1.05 equiv) was added followed by cyclopentenone (8.204 g, 8.27 mL, 100 mmol, 1.0 equiv). The solution was stirred for 2 h, after which time TLC indicated consumption of cyclopentenone. The solution was cooled to –78 °C and maintained for 20 min before *n*-BuLi (2.5 M in hexanes, 48 mL, 120 mmol, 1.2 equiv) was added causing the solution to turn red and then nearly black. The solution was maintained at –78 °C for 45 min. To a separate round-bottom flask equipped with stir bar was added THF (184 mL) and ethyl acrylate (purchased from Sigma Aldrich, contains 10–20 ppm MEHQ as inhibitor) (11.01 g, 11.71 mL, 110 mmol, 1.1 equiv). This solution was cooled to –78 °C and TMSOTf (25.12 g, 20.5 mL, 113 mmol, 1.13 equiv) was added in one portion. The solution was then immediately transferred rapidly by cannula to the stirring solution of ylide at –78 °C and maintained at the same temperature for 45 minutes (in instances where the solution of TMSOTf and ethyl acrylate became cloudy, another 50 mL of THF were added to complete the transfer). After this time, TBAF (1.0 M in THF, 270 mL, 270 mmol) was added. The cooling bath was removed, water (200 mL) was added, and the reaction mixture was allowed to warm to ambient temperature over 30 minutes. The reaction mixture was transferred to a separatory funnel and additional water (500 mL) was added. The aqueous layer was extracted 4x with EtOAc (200 mL). The combined organic layers were washed with brine, dried over $MgSO_4$, and concentrated under

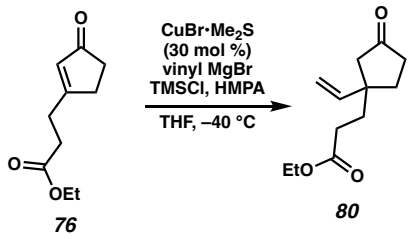
reduced pressure. The crude residue was purified by column chromatography (10 → 30% EtOAc in hexanes) to give the title compound as a yellow/orange oil (11.67 g, 64% yield)

^{1}H NMR: (400 MHz, $CDCl_3$) δ 5.93 (d, *J* = 1.5 Hz, 1H), 4.14 (qd, *J* = 7.2, 1.0 Hz, 2H), 2.72 (t, *J* = 7.4 Hz, 2H), 2.63 – 2.58 (m, 4H), 2.42 – 2.39 (m, 2H), 1.27 – 1.23 (m, 3H)

^{13}C NMR: (100 MHz, $CDCl_3$) δ 209.8, 180.6, 172.3, 129.6, 61.0, 35.4, 31.8, 31.7, 28.6, 14.3

IR: (Neat Film, NaCl) 2981, 1713, 1616, 1436, 1371, 1336, 1167, 1042, 859 cm^{-1}

HRMS: (ESI+) *m/z* calc'd for $C_{10}H_{14}O_3$ $[M+H]^+$: 183.1016, found 183.1020.



Ketone 80: To a 500 mL round-bottom flask equipped with stir bar and rubber septum was added CuBr•Me_2S (937 mg, 4.56 mmol, 30 mol %) and the vessel was purged and backfilled with N_2 three times. THF (35 mL) was added followed by HMPA (16.45 g, 15.7 mL, 91.8 mmol, 6.0 equiv). The pale green mixture was then cooled to –40 °C (dry ice/acetonitrile bath, external temperature) and TMSCl (9.973 g, 11.65 mL, 91.8 mmol) was added neat, dropwise, during which time the solution became brown. Then enone **76** (2.79 g, 15.3 mmol, 1.0 equiv) in THF (27.4 mL) was added fast dropwise. Finally, vinylmagnesium bromide (0.7 M in THF) (50 mL, 35.2 mmol, 2.3 equiv) was added dropwise via syringe pump over 2 hours. After the Grignard was added, the reaction was stirred for an additional hour then quenched AcOH (3.67 g, 3.6 mL, 61.2 mmol, 4.0 equiv). The mixture was warmed to ambient temperature, then water was added and the mixture was transferred to a separatory funnel. The aqueous layer was extracted 3x with EtOAc (40 mL). The combined organic layers were washed with satd. aqueous $NaHCO_3$ (100 mL) and brine (100 mL), dried over Na_2SO_4, and concentrated under reduced pressure. The crude residue was purified by column chromatography (10 → 30% EtOAc in hexanes) to give the title compound as a yellow oil (2.45 g, 76% yield).

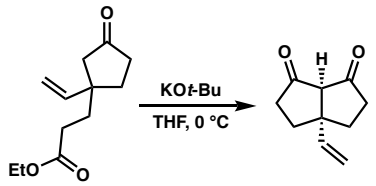
^{1}H NMR: (500 MHz, $CDCl_3$) δ 5.72 (dd, *J* = 17.5, 10.7 Hz, 1H), 5.15 (dd, *J* = 10.8, 0.6 Hz, 1H), 4.98 (d, *J* = 17.4 Hz, 1H), 4.12 (q, *J* = 7.1 Hz, 2H), 2.40 (dd, *J* = 17.7, 2.0 Hz, 1H), 2.34

– 2.18 (m, 4H), 2.09 (d, J = 17.7 Hz, 1H), 2.03 (dtd, J = 12.5, 6.1, 1.9 Hz, 1H), 1.95 – 1.81 (m, 3H), 1.26 (t, J = 7.1 Hz, 3H)

^{13}C NMR: (125 MHz, $CDCl_3$) δ 217.9, 173.5, 142.3, 114.8, 60.6, 48.3, 45.8, 36.2, 35.2, 33.5, 30.4, 14.3

IR: (Neat Film, NaCl) 3080, 2948, 2880, 1766, 1719, 1639, 1458, 1407, 1206, 1151, 1112, 1080, 998, 919 cm^{-1}

HRMS: (FI+) *m/z* calc'd for $C_{12}H_{18}O_3$ $[M]^+$: 210.1256, found 210.1265.



80 ***68***

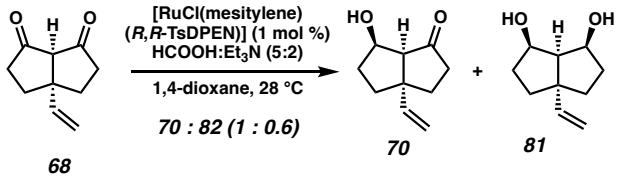
Symmetrical diketone 68: Ketone **80** (2.40 g, 11.4 mmol, 1.0 equiv) was added to a 250 mL round-bottom flask with stir bar, and THF (60 mL) was added. The solution was cooled to 0 °C. Anhydrous KO*t*-Bu (1.92 g, 17.1 mmol, 1.5 equiv) was added as a solid in one portion to the cooled solution. The mixture was stirred for 20 minutes after which time TLC indicated complete consumption of starting material. Satd. aqueous NH_4Cl was added (50 mL), and the mixture was warmed to ambient temperature. The aqueous layer was extracted 5x with EtOAc (30 mL). The combined organic layers were washed with brine (50 mL), dried over Na_2SO_4, and concentrated under reduced pressure. The crude residue was purified by silica gel flash column (20 → 30% EtOAc in hexanes). The pure product was collected and then concentrated from hexanes under reduced pressure to give the title compound as an amorphous white powder (1.61 g, 86% yield).

^{1}H NMR: (500 MHz, $CDCl_3$) δ 6.04 (dd, *J* = 17.4, 10.7 Hz, 1H), 5.15 (d, *J* = 10.7 Hz, 1H), 5.07 (d, *J* = 17.4 Hz, 1H), 3.01 (s, 1H), 2.55 – 2.37 (m, 4H), 2.13 (dddd, *J* = 13.5, 8.8, 6.5, 1.3 Hz, 2H), 2.02 (dt, *J* = 13.4, 7.9 Hz, 2H)

^{13}C NMR: (125 MHz, $CDCl_3$) δ 208.1, 141.8, 113.1, 68.2, 52.3, 37.6, 31.2

IR (Neat Film, NaCl): 3081, 2974, 1739, 1400, 1376, 1291, 1174, 1167, 1097, 1040, 925, 889, 876, 855 cm^{-1};

HRMS: (ESI+) *m/z* calc'd for $C_{10}H_{12}O_2Na$ $[M+Na]^+$: 187.0730, found 187.0732.



Keto-alcohol 10 and *meso*-diol 11: To a 250 mL round-bottom flask with stir bar was charged diketone **68** (2.668 g, 16.25 mmol, 1.0 equiv) and RuCl(mesitylene)[(*R*,*R*)-TsDPEN] (101 mg, 0.162 mmol, 1 mol %). The flask was evacuated and backfilled 3x with N_2. 1,4-Dioxane (65 mL) was added and the solution was stirred to give a homogeneous gold-colored solution. HCOOH:Et_3N (5:2) (2.86 mL, 32.5 mmol, 2.0 equiv) was degassed by bubbling Ar through the solution for 5 minutes then dissolved in 16 mL of 1,4-dioxane. The solution was then added to the solution of ketone and catalyst and maintained at 28 °C for 15 h. After 15 h, TLC indicated complete consumption of the diketone. Half-saturated aqueous $NaHCO_3$ (60 mL) was added, and the aqueous layer was extracted 4x with EtOAc (70 mL). The combined organic layers were washed with brine, dried over Na_2SO_4, and concentrated under reduced pressure. The crude residue was purified by silica gel chromatography (10 → 20 → 30% EtOAc in CH_2Cl_2) to give the desired keto-alcohol (**70**) as an orange oil (1.550 g, 57% yield) as well as *meso*-diol **81** as an orange oil (1.024 g, 37% yield).

Characterization data for keto-alcohol **70**:

Note: the ^1H NMR spectra exhibited slight variation based on sample concentration

^1H NMR: (500 MHz, $CDCl_3$) δ 5.94 (dd, *J* = 17.3, 10.6 Hz, 1H), 5.04 – 4.89 (m, 2H), 4.51 (dt, *J* = 7.7, 5.1 Hz, 1H), 2.92 (br s, 1H), 2.57 (dd, *J* = 7.8, 1.5 Hz, 1H), 2.44 – 2.29 (m, 2H), 2.04 – 1.96 (m, 3H), 1.91 (dt, *J* = 12.8, 7.3 Hz, 1H), 1.84 – 1.78 (m, 1H), 1.75 (ddt, *J* = 10.4, 6.6, 4.9 Hz, 1H)

^{13}C NMR: (125 MHz, $CDCl_3$) δ 221.1, 144.6, 110.9, 74.8, 61.6, 54.0, 39.7, 35.7, 35.2, 32.6

IR: (Neat Film, NaCl) 3445, 3081, 2953, 2873, 2249, 1738, 1639, 1455, 1413, 1268, 1167, 1104, 998, 913, 734, 695 cm^{-1}

HRMS: (FD+) *m/z* calc'd for $C_{10}H_{14}O_2N$ $[M]^+$: 166.0994, found 166.0991.

$[\alpha]_D^{23}$**:** –101 (*c* = 0.76, $CHCl_3$)

Characterization data for meso-diol **81**:

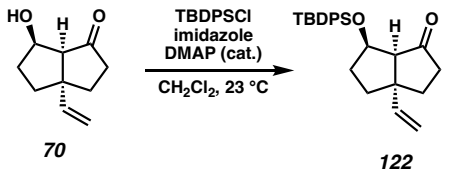
^{1}H NMR: (400 MHz, $CDCl_3$) δ 5.87 (dd, *J* = 17.4, 10.6 Hz, 1H), 4.89 (dd, *J* = 17.4, 1.0 Hz, 1H), 4.82 (dd, *J* = 10.6, 1.0 Hz, 1H), 4.44 (dt, *J* = 7.5, 5.5 Hz, 2H), 3.66 (s, 2H), 2.30 (t, *J* = 7.4 Hz, 1H), 1.87 – 1.72 (m, 6H), 1.68 – 1.58 (m, 2H)

^{13}C NMR: (100 MHz, $CDCl_3$) δ 147.3, 108.7, 76.8, 55.2, 54.7, 35.5, 35.4

IR: (Neat Film, NaCl) 3320, 2950, 2869, 1634, 1439, 1347, 1180, 1104, 1062, 1008, 938, 906, 872, 780, 680 cm^{-1}

HRMS: (FD+) *m/z* calc'd for $C_{10}H_{16}O_2$ $[M]^+$: 168.1150, found 168.1152.

Determination of enantiomeric excess: For each asymmetric reaction, a small amount (ca. 5 mg) of alcohol **70** was converted to the tert-butyldiphenylsilyl ether for SFC analysis. Synthesis of the TBDPS ether was performed using the procedure outlined for the synthesis of the TBS ether, substituting TBDPSCl for TBSCl.



70 *122*

*Characterization data for TBDPS ether **122**:*

^{1}H NMR: (500 MHz, $CDCl_3$) δ 7.71 (ddt, *J* = 16.8, 6.8, 1.6 Hz, 4H), 7.47 – 7.36 (m, 6H), 5.91 (dd, *J* = 17.3, 10.7 Hz, 1H), 4.98 – 4.87 (m, 2H), 4.64 (ddd, *J* = 7.4, 4.7, 3.0 Hz, 1H), 2.61 – 2.50 (m, 2H), 2.35 (dddd, *J* = 17.8, 8.9, 7.5, 1.6 Hz, 1H), 2.19 (ddd, *J* = 12.9, 9.1, 7.4 Hz, 1H), 2.12 – 1.99 (m, 2H), 1.75 (ddd, *J* = 12.8, 7.8, 4.9 Hz, 1H), 1.61 – 1.47 (m, 2H), 1.07 (s, 9H).

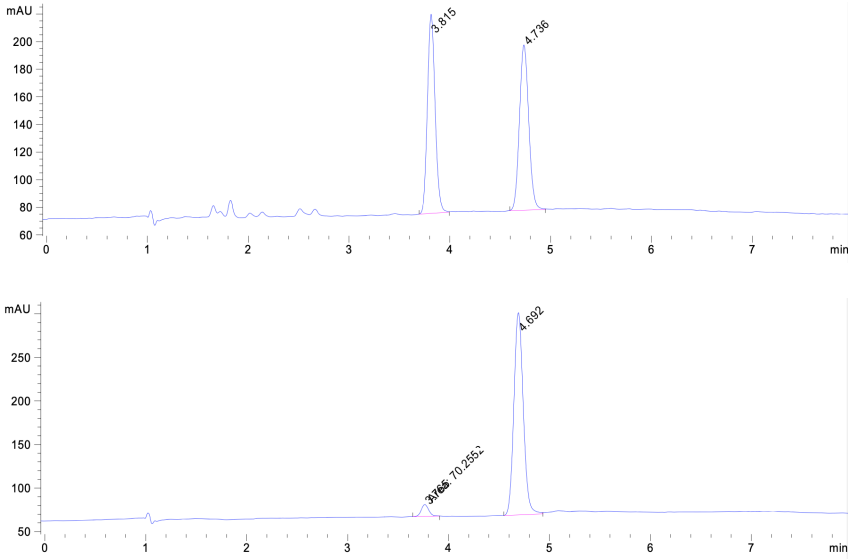
^{13}C NMR: (125 MHz, $CDCl_3$) δ 217.2, 145.0, 136.3, 136.0, 134.6, 132.9, 129.8, 129.8, 127.7, 127.7, 110.5, 77.2, 63.0, 54.1, 40.1, 37.0, 36.2, 33.2, 27.0, 19.1.

IR: (Neat Film, NaCl) 3071, 2932, 2857, 1741, 1637, 1471, 1427, 1362, 1254, 1111, 1036, 998, 911, 822, 741, 703 cm^{-1}

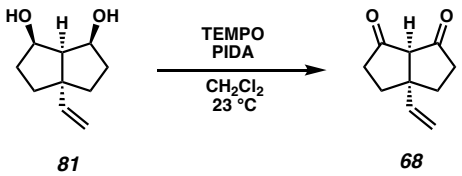
HRMS: (FD+) *m/z* calc'd for $C_{26}H_{32}O_2Si$ $[M]^+$: 404.2172, found 404.2183.

$[\alpha]_D^{23}$: –16.8 (*c* = 0.57, $CHCl_3$)

Chiral SFC: 91% ee, Daicel ADH column, 210 nm, 10% IPA/CO_2, t_r (minor) 3.77 min, t_r (major) 4.69 min

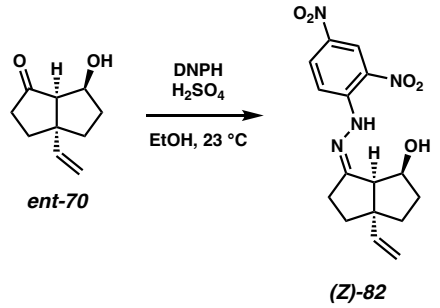


Peak #	RetTime [min]	Type	Width [min]	Area [mAU*s]	Height [mAU]	Area %
1	3.765	MM	0.0860	70.25524	13.61059	4.4659
2	4.692	BB	0.1015	1502.88928	232.32498	95.5341



81 ***68***

Oxidation of *meso*-diol 81 to diketone 68: *Meso*-diol **81** (932 mg, 5.49 mmol, 1.0 equiv) was dissolved in CH_2Cl_2 (22 mL). TEMPO (257 mg, 1.65 mmol, 0.3 equiv) was added followed by PIDA (4.44 g, 13.7 mmol, 2.5 equiv). The reaction mixture was stirred for 7 h, after which time TLC indicated complete consumption of starting material and exclusive oxidation to the symmetrical diketone. Water (50 mL) was added and the aqueous layer was extracted 3x with CH_2Cl_2 (20 mL). The combined organic extracts were washed with brine (50 mL), dried over Na_2SO_4, and concentrated under reduced pressure. The crude residue was purified by column chromatography (30% EtOAc in hexanes) to give diketone **68** as a white amorphous powder (612 mg, 68% yield).



ent-70 *(Z)-82*

Hydrazone (*Z*)-82: A stock solution of DNP stain was freshly prepared by mixing EtOH (10 mL), H_2SO_4 (3 mL), H_2O (4 mL), and 2,4-dinitrophenylhydrazine (0.6 g). To a solution of ketone **ent-70** (10 mg, 0.06 mmol) in EtOH (0.4 mL) was added 0.5 mL of the DNP stain solution. After 1 hour, the solution was diluted with water (2 mL) and extracted with CH_2Cl_2 (3x1 mL). The combined organic layers were washed with brine (1 mL), dried over $MgSO_4$ and concentrated under reduced pressure. The (*E*) and (*Z*) isomers were separated by silica gel flash column chromatography (0 → 40% Et_2O in hexanes) to give **(*Z*)-82** as an orange solid (8.9 mg, 43% yield).

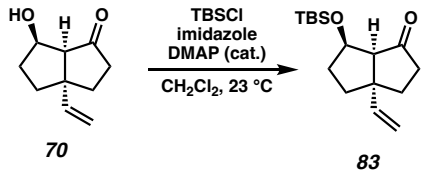
^{1}H NMR: (400 MHz, $CDCl_3$) δ 11.46 (br s, 1H), 9.11 (d, *J* = 2.6 Hz, 1H), 8.27 (ddd, *J* = 9.6, 2.6, 0.7 Hz, 1H), 7.90 (d, *J* = 9.6 Hz, 1H), 5.95 (dd, *J* = 17.4, 10.6 Hz, 1H), 5.03 (dd, *J* = 5.8, 0.7 Hz, 1H), 4.99 (d, *J* = 1.0 Hz, 1H), 4.86 (q, *J* = 6.2 Hz, 1H), 3.12 (d, *J* = 7.5 Hz, 1H), 2.81 – 2.71 (m, 2H), 2.16 – 2.06 (m, 1H), 2.00 – 1.78 (m, 5H).

^{13}C NMR: (100 MHz, $CDCl_3$) δ 167.9, 145.6, 144.7, 137.7, 129.9, 129.2, 123.7, 116.6, 111.2, 74.8, 56.3, 55.8, 36.7, 35.0, 34.8, 34.7.

IR: (Neat Film, NaCl) 3540, 2952, 2924, 1616, 1588, 1518, 1502, 1424, 1334, 1310, 1138, 1074, 918 cm^{-1}

HRMS: (ESI+) *m/z* calc'd for $C_{16}H_{19}O_5N_4$ $[M+H]^+$: 347.1350, found 347.1346.

$[\alpha]_D^{23}$: +78.8 (*c* = 0.54, $CHCl_3$)



70 ***83***

TBS ether 83: To a solution of imidazole (3.56 g, 53.6 mmol, 4.0 equiv) and *N,N*-dimethylaminopyridine (165 mg, 1.34 mmol, 0.1 equiv) in CH_2Cl_2 (67 mL) was added keto-alcohol **70** (2.23 g, 13.4 mmol, 1.0 equiv). TBSCl (6.059 g, 40.2 mmol, 3.0 equiv) was then added as a solid in one portion. The reaction mixture was stirred for 3 h, then water (100 mL) is added. The aqueous layer was extracted 3x with CH_2Cl_2 (50 mL). The combined organic layers were washed with brine (150 mL), dried over Na_2SO_4, and concentrated under reduced pressure. The crude residue was purified via silica gel flash column chromatography (5% EtOAc in hexanes) to give the title compound as a colorless oil (3.584 g, 95% yield).

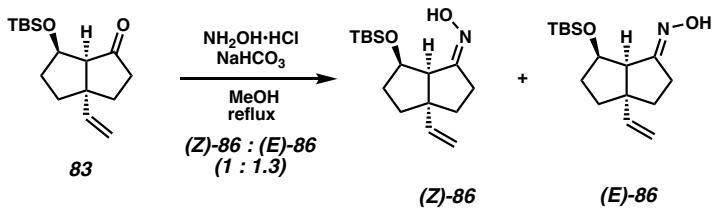
^{1}H NMR: (500 MHz, $CDCl_3$) δ 5.94 (dd, *J* = 17.3, 10.6 Hz, 1H), 4.98 – 4.89 (m, 2H), 4.54 (ddd, *J* = 6.3, 3.8, 2.3 Hz, 1H), 2.54 (d, *J* = 6.3 Hz, 1H), 2.35 (ddd, *J* = 17.7, 8.8, 6.1 Hz, 1H), 2.23 (dddd, *J* = 17.8, 8.6, 7.8, 1.5 Hz, 1H), 2.12 – 1.98 (m, 3H), 1.92 – 1.86 (m, 1H), 1.85 – 1.80 (m, 2H), 0.86 (s, 9H), 0.05 (s, 3H), 0.04 (s, 3H).

^{13}C NMR: (125 MHz, $CDCl_3$) δ 217.7, 145.3, 110.3, 76.3, 63.5, 54.1, 40.2, 37.5, 37.1, 33.6, 25.8, 18.0, –4.8, –5.2.

IR (Neat Film, NaCl): 3081, 2952, 2929, 2896, 2856, 1743, 1636, 1464, 1438, 1412, 1361, 1328, 1254, 1175, 1107, 1038, 1004, 968, 951, 910, 836, 826, 806, 777, 740, 684 cm^{-1};

HRMS: (FD+) *m/z* calc'd for $C_{16}H_{28}O_2Si$ $[M]^+$: 280.1859, found 280.1863.

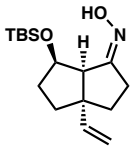
$[\boldsymbol{\alpha}]_{\boldsymbol{D}}^{\mathbf{23}}$**:** –72.9 (*c* = 0.67, $CHCl_3$)



Oximes (*Z*)-86 and (*E*)-86: TBS ether **83** (3.5836 g, 12.78 mmol, 1.0 equiv) was dissolved in MeOH (22.4 mL) and H_2O (3.2 mL). $NaHCO_3$ (3.330 g, 39.62 mmol, 3.1 equiv) and hydroxylamine hydrochloride (2.664 g , 38.34 mmol, 3.0 equiv) were sequentially added. The heterogenous reaction mixture was then heated to reflux for 4 h after which time TLC indicates complete consumption of starting material. The mixture was cooled to ambient temperature and water (100 mL) was added. The mixture was extracted 4x with CH_2Cl_2 (30 mL). The combined organic layers were then washed with brine, dried over Na_2SO_4, and concentrated under reduced pressure. The reaction mixture was then purified by silica gel flash column chromatography (2 → 5 → 10% Et_2O in hexanes) to afford undesired oxime **(*Z*)-86** with a small amount of oxime **(*E*)-86** as a viscous, pale yellow oil (1.55 g) and desired (*E*)-oxime **(*E*)-86** as an off-white/yellow, wet semi-solid (2.008 g, 56% yield (single pass)). *Note: The oxime isomers are challenging to separate. On the scale reported in this procedure, the following purification procedure was employed: Silica gel column: 26.7 cm height, 7.62 cm diameter. The column was pre-equilibrated with 100% hexanes. The crude oil was dissolved in 10% Et_2O in hexanes and loaded onto the column. The column was then eluted with 2% Et_2O in hexanes (1.5 L), then 5% Et_2O in hexanes (1.5 L), then 10% Et_2O in hexanes until the desired oximes are detected by TLC. Adequate separation was achieved with relatively few mixed fractions.*

Recycling of undesired (Z)-oxime and mixed fractions.

Undesired (Z)-oxime **13** (1.55 g, 5.25 mmol, 1.0 equiv) was dissolved in MeOH (12 mL). Pyridine (9.4 mL) was added followed by hydroxylamine hydrochloride (3.64 g, 52 mmol, 10.0 equiv). The solution was heated to reflux for 24 h. After 24 h, the solution was cooled to ambient temperature, 1N aq. HCl (50 mL) was added followed by CH_2Cl_2 (50 mL). The layers were separated, and the organic layer was extracted 3x with CH_2Cl_2 (50 mL), washed with brine (50 mL), dried over Na_2SO_4, and concentrated under reduced pressure. The crude residue was purified by silica gel flash column chromatography as described above to give (*E*)-oxime **14** (705 mg, 74% combined yield from 2 cycles).



(Z)-86

*Characterization data for undesired oxime **(Z)-86**:*

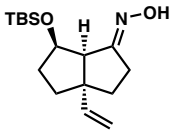
^{1}H NMR: (400 MHz, $CDCl_3$) δ 7.30 (s, 1H), 5.90 (dd, *J* = 17.4, 10.6 Hz, 1H), 4.95 – 4.87 (m, 2H), 4.64 – 4.60 (m, 1H), 3.22 (d, *J* = 5.6 Hz, 1H), 2.55 – 2.37 (m, 2H), 1.97 – 1.87 (m, 2H), 1.84 – 1.72 (m, 4H), 0.86 (s, 9H), 0.04 (s, 6H)

^{13}C NMR: (100 MHz, $CDCl_3$) δ 166.1, 145.9, 109.8, 75.1, 56.0, 55.5, 37.1, 35.9, 35.8, 31.6, 25.9, 18.0, –4.6, –5.0

IR (Neat Film, NaCl): 3231, 3144, 2931, 2894, 2856, 1639, 1467, 1380, 1255, 1055, 946, 840, 775 cm^{-1}

HRMS: (ESI+) *m/z* calc'd for $C_{16}H_{30}NO_2Si$ $[M+H]^+$: 296.2040, found 296.2045.

$[\alpha]_D^{23}$: –101 (*c* = 0.28, $CHCl_3$)



(E)-86

Characterization data for desired oxime ***(E)-86***:

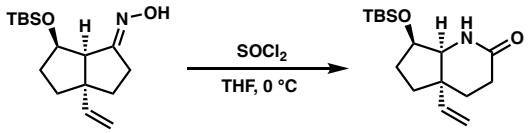
^{1}H NMR: (400 MHz, $CDCl_3$) δ 7.86 (d, *J* = 2.6 Hz, 1H), 5.86 (ddd, *J* = 17.4, 10.7, 1.4 Hz, 1H), 4.93 – 4.82 (m, 2H), 4.39 – 4.34 (m, 1H), 2.76 (d, *J* = 5.7 Hz, 1H), 2.49 (ddt, *J* = 8.7, 7.3, 1.5 Hz, 2H), 2.00 – 1.72 (m, 6H), 0.82 (d, *J* = 1.5 Hz, 9H), 0.00 (d, *J* = 1.4 Hz, 3H), –0.01 (d, *J* = 1.4 Hz, 3H).

^{13}C NMR: (100 MHz, $CDCl_3$) δ 166.8, 145.6, 110.0, 77.1 (obscured by $CHCl_3$), 59.1, 55.7, 37.0, 36.8, 36.2, 28.5, 25.9, 18.0, –4.8, –4.9.

IR (Neat Film, NaCl): 3222, 3128, 2951, 2931, 2856, 1639, 1471, 1252, 1168, 1107, 1055, 982, 962, 910, 830, 807, 775, 751 cm^{-1}

HRMS: (ESI+) *m/z* calc'd for $C_{16}H_{30}NO_2Si$ $[M+H]^+$: 296.2040, found 296.2045.

$[\alpha]_D^{23}$**:** –62.2 (*c* = 0.67, $CHCl_3$)



(E)-86 *87*

Lactam 87: In a round-bottom flask, Oxime **(*E*)-86** (2.000 g, 6.77 mmol, 1.0 equiv) was dissolved in THF (50 mL) and cooled to 0°C. In a separate flask, $SOCl_2$ (7.25g (4.42 mL), 60.93 mmol, 9.0 equiv) was dissolved in THF (15 mL). The solution of thionyl chloride was then added dropwise to the oxime solution. After 3 hours, while still at 0 °C, water (50 mL) was carefully added followed by NH_4OH (10 mL). The biphasic mixture was stirred for 10 minutes, warmed to ambient temperature, then the layers were partitioned and the aqueous layer was extracted 4x with EtOAc (50 mL). The combined organic extracts were washed with brine (100 mL), dried over Na_2SO_4, and concentrated under reduced pressure. The crude reaction mixture was purified by silica gel column chromatography (50 → 70% EtOAc in hexanes) to give the title compound as an off-white solid (1.504 g, 75% yield).

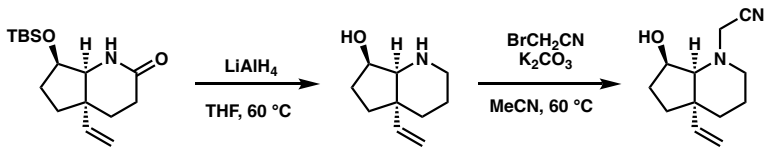
^{1}H NMR: (400 MHz, $CDCl_3$) δ 5.93 (s, 1H), 5.83 (dd, *J* = 17.6, 10.6 Hz, 1H), 5.14 – 5.02 (m, 2H), 4.22 – 4.12 (m, 1H), 3.39 (dd, *J* = 4.9, 1.6 Hz, 1H), 2.33 (dd, *J* = 7.4, 6.3 Hz, 2H), 1.98 – 1.76 (m, 4H), 1.75 – 1.60 (m, 2H), 0.87 (s, 9H), 0.04 (s, 3H), 0.04 (s, 3H).

^{13}C NMR: (100 MHz, $CDCl_3$) δ 172.5, 144.7, 112.6, 74.2, 62.5, 43.8, 31.3, 31.3, 30.3, 28.3, 25.9, 18.1, -4.6, -4.9.

IR (Neat Film, NaCl): 3294, 3085, 2951, 2901, 2854, 1647, 1470, 1461, 1407, 1358, 108, 1250, 1222, 1184, 1163, 1122, 1088, 1066, 1023, 1005, 992, 943, 917, 836, 779 cm^{-1};

HRMS: (ESI+) *m/z* calc'd for $C_{16}H_{30}NO_2Si$ $[M+H]^+$: 296.2040, found 296.2044.

$[\alpha]_D^{23}$: –2.7 (*c* = 1.0, $CHCl_3$)



87 ***123*** ***88***

Aminonitrile 88: To a round-bottom flask with stir bar was added lithium aluminum hydride (powder, 916 mg, 24.15 mmol, 5.7 equiv). The flask was cooled to 0 °C and THF (16 mL) was added. Lactam **87** (1.236 g, 4.83 mmol, 1.0 equiv) was dissolved in THF (16 mL) and the solution was added to the stirred suspension of lithium aluminum hydride at 0 °C. After stirring for 5 minutes, the cooling bath was exchanged for a heating bath, and the mixture was heated to 62 °C. After 2 h, TLC indicated complete consumption of starting lactam, and LC/MS revealed loss of the silyl protecting group. *Note: the product in which the amide has been reduced but the alcohol retains the silyl protecting group has never been observed.* The reaction mixture was then cooled to 0 °C and diluted with Et_2O (50 mL). Then Rochelle's salt (200 mL) was carefully added at 0 °C (CAUTION: EXOTHERMIC). The biphasic mixture was stirred vigorously until two clear layers were observed. The layers were partitioned, and the aqueous layer was extracted 4x with Et_2O, then 2x with EtOAc. The combined organic layers were concentrated under reduced pressure to a volume of approximately 100mL. Then the organic layers were extracted 5x with 1 N aq. HCl (aq.). To the combined aqueous layers was added solid NaOH (CAUTION: EXOTHERMIC) until the pH was >13. Then the aqueous layer was extracted 4x with EtOAc (50 mL). The combined organic layers were then washed with brine (100 mL), dried over Na_2SO_4 and concentrated under reduced pressure to give the crude amino alcohol **123** as a pale yellow solid (**123**) (620 mg) that was used directly in the next step.

To a round bottom flask with stir bar was added crude **123** (620 mg, 3.67 mmol, 1.0 equiv) and K_2CO_3 (1.546 g, 11.19 mmol, 3.05 equiv). MeCN (14.7 mL) was added and the mixture was stirred vigorously. Bromoacetonitrile (1.276 g, 0.74 mL, 10.64 mmol, 2.9 equiv) was added fast dropwise. The mixture was then heated to 60 °C. After 2 h, TLC and LC/MS indicated consumption of the starting material. Water (40 mL) was added, the layers were partitioned, and the aqueous layer was extracted 4x with Et_2O. The combined organic extracts were washed with brine, dried over Na_2SO_4, and concentrated under reduced pressure. The crude reside waws purified by silica gel flash column chromatography (30% EtOAc, 1% Et_3N in hexanes) to give a pale yellow oil (690 mg, 80% yield over 2 steps).

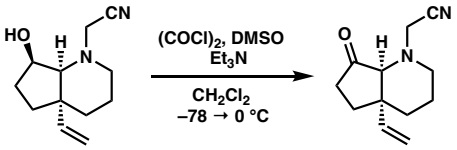
^{1}H NMR: (400 MHz, $CDCl_3$) δ 5.84 (ddd, *J* = 17.6, 10.8, 0.9 Hz, 1H), 5.14 – 4.99 (m, 2H), 4.35 – 4.29 (m, 1H), 3.91 (d, *J* = 17.1 Hz, 1H), 3.58 (d, *J* = 17.2 Hz, 1H), 2.83 – 2.75 (m, 2H), 2.73 (d, *J* = 2.6 Hz, 1H), 2.69 – 2.62 (m, 1H), 1.94 – 1.85 (m, 1H), 1.84 – 1.73 (m, 2H), 1.73 – 1.59 (m, 5H).

^{13}C NMR: (100 MHz, $CDCl_3$) δ 146.6, 115.8, 111.8, 73.6, 68.6, 48.6, 45.6, 44.6, 36.3, 31.2, 30.4, 20.0.

IR: (Neat Film, NaCl) 3457, 3078, 2938, 2860, 2750, 2232, 1650, 1634, 1467, 1439, 1336, 1236, 1132, 1104, 1064, 1039, 1000, 912, 883, 754 cm^{-1}

HRMS: (ESI+) *m/z* calc'd for $C_{12}H_{19}N_2O$ $[M+H]^+$: 207.1492, found 207.1496.

$[\alpha]_D^{23}$: –19.9 (*c* = 0.8, $CHCl_3$)



88 ***67***

Ketone 67: To a round-bottom flask with stir bar was added CH_2Cl_2 (18.6 mL) and oxalyl chloride (550 mg, 0.372 mL, 4.34 mmol, 1.4 equiv) and the solution was cooled to –78 °C. DMSO (533 mg, 0.485 mL, 6.82 mmol, 2.2 equiv) was added dropwise. The solution was allowed to stir for 30 minutes, then aminonitrile **88** (640 mg, 3.10 mmol, 1.0 equiv) was added dropwise as a solution in CH_2Cl_2 (12.4 mL). The solution was stirred an additional 30 minutes at the same temperature, then Et_3N (1.568 g, 2.16 mL, 15.5 mmol, 5 equiv) was added dropwise at –78 °C. The solution was stirred at –78 °C for 1 hour, then allowed to warm to ambient temperature and stir for an additional hour, during which time TLC indicated complete consumption of the starting material. The reaction mixture was quenched with satd. aqueous $NaHCO_3$ (50 mL). The layers were partitioned, and the aqueous layer was extracted 3x with CH_2Cl_2 (30 mL). The combined organic layers were washed with brine (50 mL), dried over Na_2SO_4, and concentrated under reduced pressure. The crude residue was purified via silica gel flash column chromatography (20% EtOAc, 1% Et_3N in hexanes) to give the title compound as a pale yellow oil (530 mg, 84% yield).

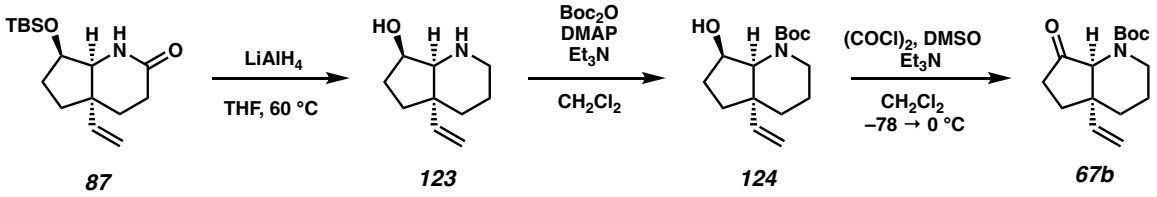
^{1}H NMR: (400 MHz, $CDCl_3$) δ 5.90 – 5.77 (m, 1H), 5.18 – 5.08 (m, 2H), 3.94 (d, J = 17.0 Hz, 1H), 3.68 (dd, J = 16.9, 1.0 Hz, 1H), 2.91 (s, 1H), 2.71 – 2.57 (m, 2H), 2.29 (ddd, J = 8.5, 7.0, 1.4 Hz, 2H), 2.11 (ddd, J = 13.2, 8.8, 6.8 Hz, 1H), 1.83 – 1.75 (m, 1H), 1.71 (p, J = 5.9 Hz, 2H), 1.61 – 1.53 (m, 1H), 1.50 – 1.42 (m, 1H)

^{13}C NMR: (100 MHz, $CDCl_3$) δ 217.0, 143.0, 116.1, 114.2, 70.1, 49.8, 44.3, 43.0, 34.1, 30.1, 28.9, 21.3

IR: (Neat Film, NaCl) 3082, 2943, 2855, 2246, 1742, 1639, 1440, 1130, 997, 921, 884, 754 cm^{-1}

HRMS: (ESI+) *m/z* calc'd for $C_{12}H_{17}N_2O$ $[M+H]^+$: 205.1335, found 205.1336.

$[\alpha]_D^{23}$: –5.0 (*c* = 0.82, $CHCl_3$)



87 ***123*** ***124*** ***67b***

*Note: The sequence was performed using racemic **87**.*

Ketone 67b: To a round-bottom flask with stir bar was added lithium aluminum hydride (powder, 916 mg, 24.15 mmol, 5.7 equiv). The flask was cooled to 0 °C and THF (16 mL) was added. Lactam **87** (1.236 g, 4.83 mmol, 1.0 equiv) was dissolved in THF (16 mL) and the solution was added to the stirred suspension of lithium aluminum hydride at 0 °C. After stirring for 5 minutes, the cooling bath was exchanged for a heating bath, and the mixture was heated to 62 °C. After 2 h, TLC indicated complete consumption of starting lactam, and LC/MS revealed loss of the silyl protecting group. *Note: the product in which the amide has been reduced but the alcohol retains the silyl protecting group has never been observed.* The reaction mixture was then cooled to 0 °C and diluted with Et_2O (50 mL). Then Rochelle's salt (200 mL) was carefully added at 0 °C (CAUTION: EXOTHERMIC). The biphasic mixture was stirred vigorously until two clear layers were observed. The layers were partitioned, and the aqueous layer was extracted 4x with Et_2O, then 2x with EtOAc. The combined organic layers were concentrated under reduced pressure to a volume of approximately 100mL. Then the organic layers were extracted 5x with 1 N aq. HCl (aq.). To the combined aqueous layers was added solid NaOH (CAUTION: EXOTHERMIC) until the pH was >13. Then the aqueous layer was extracted 4x with EtOAc (50 mL). The combined organic layers were then washed with brine (100 mL), dried over Na_2SO_4 and concentrated under reduced pressure to give the crude amino alcohol **123** as a pale yellow solid (**123**) (620 mg) a portion of which was used directly in the next step.

The crude amino alcohol (60 mg, 0.35 mmol, 1 equiv) was dissolved in CH_2Cl_2 (3.5 mL). Et_3N (75 μL, 0.53 mmol, 1.5 equiv) and DMAP (4.0 mg, 0.035 mmol, 10 mol%) were sequentially added followed by Boc_2O (94 mg, 0.43 mmol, 1.2 equiv). The reaction mixture was allowed to stir for 24 hours. After this time, the mixture was concentrated under reduced pressure and filtered through a plug of silica gel (eluting with 20% EtOAc in hexanes) and concentrated again under reduced pressure to give the N-Boc compound **124** as a crude oil (54 mg) that was used without further purification.

To a flame-dried test tube with stir bar was added CH_2Cl_2 (1.2 mL) followed by oxalyl chloride (24 μL, 0.28 mmol, 1.4 equiv) and the solution was cooled to –78 °C. DMSO (34 μL, 0.44 mmol, 2.2 equiv) was added dropwise and the solution was allowed to stir for 30 minutes. After this time, the crude alcohol (54 mg, 0.2 mmol, 1.0 equiv) in CH_2Cl_2 (0.8 mL) was added dropwise. The solution was allowed to stir for an additional 30 mintues before Et_3N (159 μL, 1 mmol, 5.0 equiv) was added dropwise. The solution was maintained at –78 °C for an additional hour before being allowed to warm to 0 °C. The reaction was quenched with satd. aq. $NaHCO_3$ (2 mL). The layers were partitioned and separated, the aqueous layer was extracted with CH_2Cl_2 (3x1 mL). The combined organic layers were washed with brine (2 mL), dried over Na_2SO_4, and concentrated under reduced pressure. The crude residue was purified by silica gel flash column chromatography (10 → 50% EtOAc in hexanes) to give the title compound as a colorless amorphous solid (36 mg, 40% yield over 3 steps).

Restricted rotation of the carbamate resulted in doubling of peaks by both ^1H and ^{13}C NMR

^{1}H NMR: (600 MHz, $CDCl_3$) δ 5.86 (ddd, *J* = 17.3, 10.8, 6.2 Hz, 1H), 5.14 (td, *J* = 13.6, 3.6 Hz, 2H), 4.63 (d, *J* = 158.0 Hz, 1H), 4.05 – 3.81 (m, 1H), 2.48 (dtd, *J* = 70.4, 13.2, 3.0 Hz,

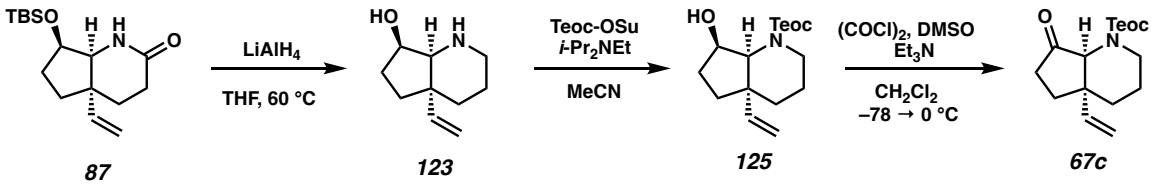
1H), 2.39 – 2.32 (m, 1H), 2.23 (ddt, J = 19.9, 13.0, 10.0 Hz, 1H), 1.95 – 1.80 (m, 2H), 1.63 (d, J = 13.9 Hz, 1H), 1.58 – 1.47 (m, 1H), 1.47 – 1.42 (m, 9H), 1.42 – 1.35 (m, 1H), 1.29 (td, J = 13.0, 3.7 Hz, 1H).

Peak doubling by ^{13}C NMR due to the carbamate complicated analysis such that all peaks observed are reported; the number of peaks is significantly more than the number of carbon atoms in the molecule.

^{13}C NMR: (150 MHz, $CDCl_3$) δ 214.0, 213.9, 155.8, 155.5, 142.7, 142.3, 114.3, 114.1, 80.2, 66.5, 65.4, 42.8, 41.3, 40.3, 32.3, 31.0, 30.2, 30.1, 28.5, 21.2, 20.9.

IR: (Neat film, NaCl) 2974, 2932, 2860, 1754, 1694, 1418, 1364, 1304, 1280, 1250, 1172, 1152, 1096, 898, 764, 680 cm^{-1}

HRMS: (FI+) *m/z* calc'd for $C_{15}H_{23}NO_3$ $[M]^+$: 265.16725, found 265.16828



87 ***123*** ***125*** ***67c***

*Note: The sequence was performed using racemic **87**.*

Ketone 67c: To a round-bottom flask with stir bar was added lithium aluminum hydride (powder, 916 mg, 24.15 mmol, 5.7 equiv). The flask was cooled to 0 °C and THF (16 mL) was added. Lactam **87** (1.236 g, 4.83 mmol, 1.0 equiv) was dissolved in THF (16 mL) and the solution was added to the stirred suspension of lithium aluminum hydride at 0 °C. After stirring for 5 minutes, the cooling bath was exchanged for a heating bath, and the mixture was heated to 62 °C. After 2 h, TLC indicated complete consumption of starting lactam, and LC/MS revealed loss of the silyl protecting group. *Note: the product in which the amide has been reduced but the alcohol retains the silyl protecting group has never been observed.* The reaction mixture was then cooled to 0 °C and diluted with Et_2O (50 mL). Then Rochelle's salt (200 mL) was carefully added at 0 °C (CAUTION: EXOTHERMIC). The biphasic mixture was stirred vigorously until two clear layers are observed. The layers were partitioned, and the aqueous layer was extracted 4x with Et_2O, then 2x with EtOAc. The combined organic layers were concentrated under reduced pressure to a volume of approximately 100mL. Then the organic layers were extracted 5x with 1 N aq. HCl (aq.). To the combined aqueous layers was added solid NaOH (CAUTION: EXOTHERMIC) until the pH was >13. Then the aqueous layer was extracted 4x with EtOAc (50 mL). The combined organic layers are then washed with brine (100 mL), dried over Na_2SO_4 and concentrated under reduced pressure to give the crude amino alcohol **123** as a pale yellow solid (**123**) (620 mg) a portion of which was used directly in the next step.

The crude amino alcohol (60 mg, 0.35 mmol, 1 equiv) was dissolved in MeCN (1.4 mL). *i*-Pr_2NEt (0.125 mL, 0.72 mmol, 2.0 equiv) and Teoc-OSu {1-[2-(Trimethylsilyl)ethoxycarbonyloxy]pyrrolidin-2,5-dione} (112 mg, 0.43 mmol, 1.2 equiv) were sequentially added. The reaction mixture was allowed to stir for 16 hours. After this time, the mixture was concentrated under reduced pressure, dissolved in CH_2Cl_2 (5 mL) and washed with satd. aq. $NaHCO_3$ (2 mL), brine (1 mL), and dried over Na_2SO_4, and concentrated under reduced pressure to give the N-Teoc compound **125** as a crude oil (108 mg) that was used without further purification.

To a round-bottom flask was added CH_2Cl_2 (2.0 mL) followed by oxalyl chloride (41 µL, 0.48 mmol, 1.4 equiv) and the solution was cooled to –78 °C. DMSO (54 µL, 0.75 mmol, 2.2 equiv) was added dropwise and the solution was allowed to stir for 30 minutes. After this time, the crude alcohol (108 mg, 0.34 mmol, 1.0 equiv) in CH_2Cl_2 (1.4 mL) was added dropwise. The solution was allowed to stir for an additional 30 mintues before Et_3N (0.24 mL, 1.7 mmol, 5.0 equiv) was added dropwise. The solution was maintained at –78 °C for an additional hour before being allowed to warm to 0 °C. The reaction was quenched with satd. aq. $NaHCO_3$ (2 mL). The layers were partitioned and separated, and the aqueous layer was extracted with CH_2Cl_2 (3x1 mL). The combined organic layers were washed with brine (2 mL), dried over Na_2SO_4, and concentrated under reduced pressure. The crude residue was purified by silica gel flash column chromatography (10 → 50% EtOAc in hexanes) to give the title compound as a white amorphous solid (64 mg, 59% yield over 3 steps).

Restricted rotation of the carbamate resulted in doubling of peaks by both ^1H and ^{13}C NMR

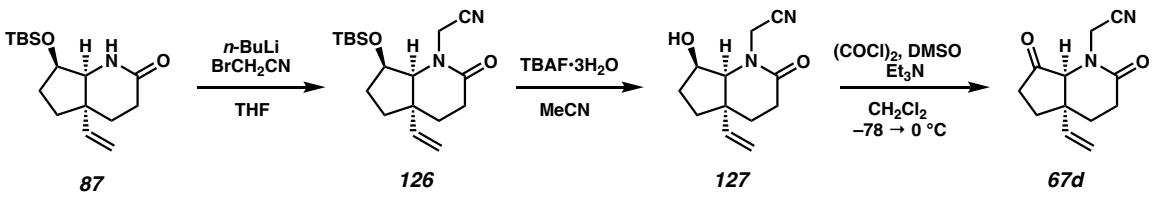
^{1}H NMR: (600 MHz, $CDCl_3$) δ 5.84 (dt, *J* = 17.4, 10.3 Hz, 1H), 5.16 – 5.07 (m, 2H), 4.65 (d, *J* = 127.7 Hz, 1H), 4.22 – 4.08 (m, 2H), 3.95 (ddt, *J* = 67.6, 13.6, 2.9 Hz, 1H), 2.50 (dtd, *J* = 50.2, 13.2, 3.0 Hz, 1H), 2.39 – 2.29 (m, 1H), 2.22 (dtd, *J* = 19.8, 10.0, 6.9 Hz, 1H), 1.94 – 1.79 (m, 2H), 1.66 – 1.60 (m, 1H), 1.51 (tdd, *J* = 13.3, 9.8, 3.8 Hz, 1H), 1.40 (ddq, *J* = 23.8, 13.5, 3.0 Hz, 1H), 1.27 (tdd, *J* = 13.6, 6.2, 3.6 Hz, 1H), 0.96 (dtq, *J* = 16.3, 6.3, 3.7 Hz, 2H), 0.00 (d, *J* = 11.3 Hz, 9H).

Peak doubling in the ^{13}C NMR spectrum due to restricted rotation of the carbamate complicated analysis such that all peaks observed are reported; the number of peaks is significantly more than the number of carbon atoms in the molecule.

^{13}C NMR: (150 MHz, $CDCl_3$) δ 213.8, 213.6, 156.7, 156.4, 142.4, 142.1, 114.4, 114.2, 66.1, 65.6, 64.0, 63.9, 42.7, 42.6, 40.9, 40.6, 32.2, 32.2, 31.0, 30.9, 30.0, 29.9, 21.0, 20.7, 17.9, 17.6, -1.4, -1.5.

IR: (Neat film, NaCl) 3082, 2950, 2860, 1756, 1694, 1432, 1346, 1302, 1248, 1184, 1154, 1094, 1046, 948, 860, 838, 766, 696, 666 cm^{-1}

HRMS: *m/z* calc'd for $C_{16}H_{27}NO_3SiNa$ $[M+Na]^+$: 332.1652, found 332.1652.



*Note: the sequence was performed with racemic **87***

Ketone 67d: To a round-bottom flask was added lactam **87** (400 mg, 1.69 mmol, 1.0 equiv) followed by THF (17 mL), and the solution was cooled to –78 °C. *n*-BuLi (2.65 M, 0.83 mL, 2.2 mmol, 1.3 equiv) was added and the solution was stirred for 30 minutes. After this time bromoacetonitrile (0.23 mL, 3.38 mmol, 2 equiv) was added, and the reaction mixture was stirred for an additional hour then warmed to 0 °C. The reaction was quenched by the addition of satd. aq. NH_4Cl (20 mL). The layers were separated, and the aqueous layer was extracted with EtOAc (3x10 mL). The combined organic layers were washed with brine (10 mL), dried over Na_2SO_4, and concentrated under reduced pressure. The crude residue was purified by passing through a plug of silica gel eluting with 10% EtOAc to remove residual starting N–H lactam to give the crude alkylated lactam **126** as a colorless oil (200 mg) that was used without further purification.

To a solution of lactam **126** (200 mg, 0.60 mmol, 1 equiv) in MeCN (8 mL) was added solid TBAF•$3H_2O$ (1.89 g, 5.98 mmol, 10 equiv). The mixture was stirred for 3 hours, then water (20 mL) was added. The aqueous layer was extracted with EtOAc (3x10 mL). The combined organic layers were washed with brine (10 mL) and Na_2SO_4 and concentrated under reduced pressure to give alcohol **127** as a colorless oil (85.2 mg) that was used without further purification.

To a round-bottom flask was added CH_2Cl_2 (2.3 mL) followed by oxalyl chloride (47 µL, 0.55 mmol, 1.4 equiv) and the solution was cooled to –78 °C. DMSO (61 µL, 0.86 mmol,

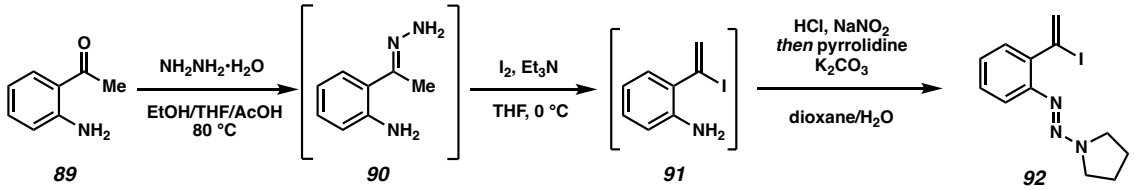
2.2 equiv) was added dropwise and the solution was allowed to stir for 30 minutes. After this time, the crude alcohol (85 mg, 0..39 mmol, 1.0 equiv) in CH_2Cl_2 (1.6 mL) was added dropwise. The solution was allowed to stir for an additional 30 mintues before Et_3N (0.27 mL, 1.95 mmol, 5.0 equiv) was added dropwise. The solution was maintained at –78 °C for an additional hour before being allowed to warm to 0 °C. The reaction was quenched with satd. aq. $NaHCO_3$ (5 mL). The layers were partitioned and separated, and the aqueous layer was extracted with CH_2Cl_2 (3x1 mL). The combined organic layers were washed with brine (2 mL), dried over Na_2SO_4, and concentrated under reduced pressure. The crude residue was purified by silica gel flash column chromatography (10 → 50% EtOAc in hexanes) to give the title compound as a white amorphous solid (73 mg, 33% yield over 3 steps).

^{1}H NMR: (600 MHz, $CDCl_3$) δ 5.91 (dd, *J* = 17.5, 10.8 Hz, 1H), 5.36 – 5.23 (m, 3H), 4.22 (d, *J* = 17.5 Hz, 1H), 4.02 (t, *J* = 1.8 Hz, 1H), 2.53 (dddd, *J* = 20.1, 8.9, 4.1, 1.4 Hz, 1H), 2.47 – 2.40 (m, 3H), 2.10 – 1.99 (m, 2H), 1.77 (ddd, *J* = 13.9, 11.3, 7.0 Hz, 1H), 1.73 – 1.68 (m, 1H).

^{13}C NMR: (150 MHz, $CDCl_3$) δ 213.3, 168.2, 139.6, 115.6, 67.4, 43.5, 33.6, 32.5, 30.5, 28.7, 27.2.

IR: (Neat film, NaCl) 2940, 1752, 1658, 1456, 1416, 1182, 1144, 1094, 928, 758, 720, 702, 670 cm^{-1}

HRMS: (FI+) *m/z* calc'd for $C_{12}H_{14}N_2O_2$ $[M]^+$: 218.10498, found 218.10447



Aryl triazene 92:

Note: The rigorous exclusion of air and moisture is not necessary for hydrazone formation. 2'-Aminoacetophenone (**89**) (purchased from Combi Blocks inc.) (1.351 g, 10 mmol, 1.0 equiv), was added to a 100 mL round-bottom flask with stir bar and dissolved in EtOH (20 mL) and THF (10 mL). Hydrazine hydrate (5 mL, 100 mmol, 10.0 equiv) was then added followed by AcOH (2 mL). The flask was fitted with a reflux condenser and heated to 80 °C for 14 h. After 14 h, the solution was cooled to ambient temperature, water (100 mL) was added, the layers were partitioned, and aqueous layer was extracted 3x with EtOAc (30 mL). The combined organic layers were washed with satd. aqueous $NaHCO_3$ (50 mL), brine (50 mL), then dried over Na_2SO_4, and concentrated under reduced pressure. The crude orange oil (**90**) was then azeotroped 2x with benzene (50 mL) and left under high-vacuum for >2 hours prior to use in the next step.

Note: It is critical that the hydrazone be completely dry prior to the iodination otherwise hydrolysis to the starting ketone is the major product. A large stir bar is also recommended to maintain stirring as the reaction mixture becomes heterogeneous. The crude, azeotropically dried hydrazone (680 mg, 4.56 mmol, 1.0 equiv) [Note: not all crude hydrazone from previous step was used] was dissolved in THF (10 mL) under an N_2 atmosphere and cooled to 0 °C. In a separate round-bottom flask under nitrogen, I_2 (3.20 g, 13.7 mmol, 3.0 equiv) was dissolved in THF (6 mL). Dry triethylamine (3.82 mL, 27.4 mmol, 6.0 equiv) was added to the flask containing the hydrazone. The solution of I_2 was then added

dropwise until the brown color if I_2 persisted in the heterogeneous solution (usually 2/3 of the I_2 solution volume). Once this point was reached, the mixture was stirred for an additional 30 min at 0 °C. Then satd. aqueous NH_4Cl (75 mL) and satd. aqueous $Na_2S_2O_3$ (75 mL) were sequentially added. The mixture was extracted 3x with CH_2Cl_2 (30 mL), washed with brine (50 mL), dried over Na_2SO_4 and concentrated under reduced pressure to give the crude vinyl iodide (**91**) as a brown, semi-solid residue, which is used directly in the next step.

The crude vinyl iodide was dissolved in dioxane (20 mL) and cooled to 0 °C. Aq. 1 N HCl (20 mL) was added followed by $NaNO_2$ (403 mg, 5.85 mmol, 1.3 equiv) in water (3 mL) and the resulting mixture was stirred for 1 hour. In a separate flask, pyrrolidine (2.66 mL, 32.4 mmol, 7.2 equiv), K_2CO_3 (2.49 g, 18 mmol, 4.0 equiv) and water (3 mL) were combined and added slowly to the diazonium solution. After 10 minutes, the reaction mixture was warmed to ambient temperature and stirred for an additional 20 minutes. Then Et_2O (50 mL) was added, the layers were separated, the aqueous layer was extracted with Et_2O (2x 20 mL), the combined organic layers were washed with satd. aq. $NaHCO_3$ (20 mL), satd. aq. $Na_2S_2O_3$ (20 mL), and brine (20 mL), dried over $MgSO_4$ and concentrated. The crude residue was purified by silica gel flash column chromatography (0 → 7% Et_2O in hexanes) to give a the title compound as a red/orange oil (455 mg, 31% yield).

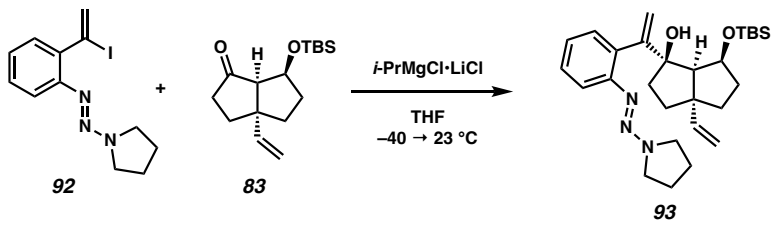
Restricted rotation of the triazene resulted in broadened and duplicated peaks in NMR spectra due to the presence of rotamers

^{1}H NMR: (400 MHz, $CDCl_3$) δ 7.37 (dd, *J* = 8.6, 1.3 Hz, 1H), 7.28 – 7.22 (m, 2H), 7.11 – 7.01 (m, 1H), 6.22 (d, *J* = 1.0 Hz, 1H), 6.10 (d, *J* = 1.0 Hz, 1H), 4.26 – 3.51 (br s, 4H), 2.08 – 1.97 (m, 4H).

^{13}C NMR: (100 MHz, $CDCl_3$) δ 147.8, 137.7, 129.5, 129.4, 129.3, 124.7, 117.2, 103.4, 51.0, 47.2, 24.0.

IR: (Neat Film, NaCl) 2970, 2870, 1614, 1408, 1338, 1316, 1272, 1220, 1158, 1100, 1058, 900, 758 cm^{-1}

HRMS: *m/z* calc'd for $C_{12}H_{15}IN_3$ $[M+H]^+$: 328.0305, found 328.0308.



*Note: The reaction was performed using racemic **70**.*

Allylic alcohol 93: To a 1 Dr vial with stir bar was added vinyl iodide **92** (19.6 mg, 0.06 mmol, 2.0 equiv) and dry THF (0.3 mL). The solution was cooled to –78 °C, then *i*-PrMgCl•LiCl (1.3 M, 51 µL, 0.066 mmol, 2.2 equiv) was added. The mixture was stirred for 20 minutes then warmed to –40 °C and stirred for an additional 2 hours. Ketone **70** (8.4 mg, 0.03 mmol, 1.0 equiv) in THF (0.3 mL) was added dropwise, then the solution was allowed to gradually warm to 0 °C over 3 hours. After this time, water (1 mL) was added. The layers were partitioned and the aqueous layer was extracted with EtOAc (3x1 mL). The combined organic layers were washed with brine, dried over Na_2SO_4 and concentrated under reduced pressure. The crude residue was purified by silica gel flash column chromatography (0 → 20% Et_2O in hexanes) to give the title compound as a yellow oil (4.3 mg, 30% yield). By NMR the compound appears to be an approximately 6:1 mixture of diastereomers.

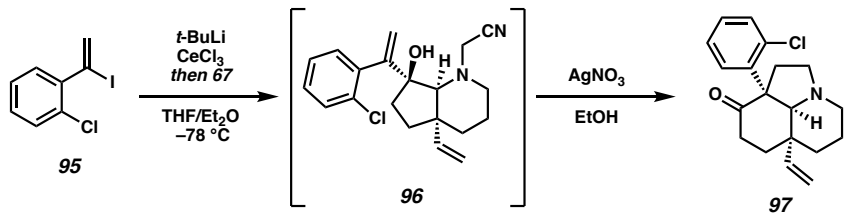
Restricted rotation of the triazene resulted in significant broadening of peaks by NMR.

^{1}H NMR: (400 MHz, $CDCl_3$) δ 7.39 – 7.32 (m, 1H), 7.24 – 7.18 (m, 2H), 7.11 – 7.05 (m, 1H), 5.70 (dd, *J* = 17.4, 10.7 Hz, 1H), 5.58 (dd, *J* = 2.2, 0.7 Hz, 1H), 5.07 (d, *J* = 2.2 Hz, 1H), 4.88 (dd, *J* = 2.2, 0.7 Hz, 1H), 4.58 (dt, *J* = 10.7, 0.9 Hz, 1H), 4.44 (d, *J* = 17.4 Hz, 1H), 4.34 (td, *J* = 9.8, 5.9 Hz, 1H), 3.73 (br s, 4H), 2.79 (d, *J* = 8.8 Hz, 1H), 2.19 – 2.02 (m, 1H), 1.96 (h, *J* = 3.7 Hz, 5H), 1.93 – 1.79 (m, 2H), 1.67 – 1.60 (m, 2H), 1.50 (dd, *J* = 12.4, 4.7 Hz, 1H), 1.34 (td, *J* = 12.5, 6.2 Hz, 1H), 0.93 (s, 9H), 0.15 (s, 3H), 0.14 (s, 3H).

^{13}C NMR: (100 MHz, $CDCl_3$) δ 153.4, 147.3, 137.1, 131.5, 127.4, 124.2, 116.6, 114.2, 108.3, 87.9, 55.6, 53.4, 39.4, 38.0, 34.8, 33.2, 29.7, 25.9, 23.8, 18.0, -4.6, -4.9. *One signal is obscured by $CDCl_3$, one signal is not observed due to restricted rotation and peak broadening, see HSQC spectrum.*

IR: 3478, 2952, 2856, 1414, 1322, 1264, 1080, 874, 854, 820, 778 cm^{-1}

HRMS: (ESI+) *m/z* calc'd for $C_{28}H_{44}O_2N_3Si$ $[M+H]^+$: 482.3197, found 482.3199.



*Note: Reaction was performed using racemic **67**.*

Tricycle 97: In a N_2 filled glovebox, to a 1 Dr vial with stir bar was added $CeCl_3$ (anhydrous, 39.4 mg, 0.16 mmol, 1.6 equiv). The vial was sealed with a rubber septum, removed from the glovebox, placed under dynamic high-vacuum and heated to 140 °C for 13 hours. After this time, the vial was cooled to ambient temperature and THF (0.5 mL) was added, and the heterogeneous mixture was stirred vigorously. In a separate 1 Dr vial, vinyl iodide **95** (37 mg, 0.14 mmol, 1.4 equiv) and Et_2O (0.23 mL) were added and cooled to –78 °C. To this solution was added *t*-BuLi (1.6 M in hexanes, 0.18 mL, 0.29 mmol) in Et_2O (0.52 mL) dropwise. The reaction was stirred for 2.5 hours at –78 °C, after which time the ketone **67** in THF (0.5 mL) was added. After 1 h, the reaction was quenched with satd. aq. NH_4Cl (1.0 mL). EtOAc was added (1.0 mL) followed by a solution of dilute aqueous AcOH (1.0 mL). The layers were partitioned and separated. The aqueous layer was extracted with EtOAc (3x1 mL), and the combined organic layers were washed with brine, dried over $MgSO_4$, and concentrated under reduced pressure to yield the crude allylic alcohol **96**.

To the crude allylic alcohol **96** in a 1 Dr vial was added EtOH (1 mL). The solution was sparged with N_2 and then $AgNO_3$ (51 mg, 0.3 mmol, 3.0 equiv) was added. The reaction was stirred for 1.5 hours then quenched by the addition of satd. aq. $NaHCO_3$ (1.0 mL). EtOAc was added (1.0 mL) followed by NH_4OH (0.2 mL). The layers were separated, the aqueous layer was extracted with EtOAc (3x1 mL), the combined organic extracts were washed with brine, dried over $MgSO_4$, and concentrated under reduced pressure. The crude residue was

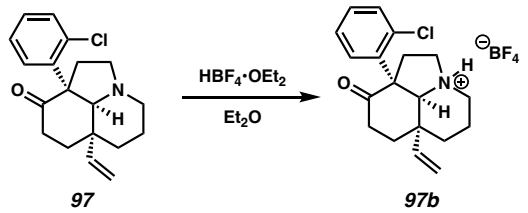
purified by silica gel flash column chromatography (0 → 10% EtOAc in hexanes) to give the title compound as an amorphous solid (17.6 mg, 56% yield over 2 steps).

^{1}H NMR: (400 MHz, $CDCl_3$) δ 7.34 (dd, *J* = 7.6, 1.8 Hz, 1H), 7.19 – 7.05 (m, 2H), 6.87 (d, *J* = 7.8 Hz, 1H), 5.56 (dd, *J* = 17.7, 10.9 Hz, 1H), 4.95 (dd, *J* = 17.7, 0.9 Hz, 1H), 4.69 (dd, *J* = 10.9, 0.9 Hz, 1H), 3.63 (s, 1H), 3.13 – 3.03 (m, 2H), 3.00 – 2.87 (m, 2H), 2.61 – 2.47 (m, 2H), 2.42 (ddd, *J* = 10.5, 8.6, 6.9 Hz, 1H), 2.05 (ddd, *J* = 12.6, 11.1, 3.3 Hz, 2H), 1.78 (qt, *J* = 12.7, 4.8 Hz, 1H), 1.65 (ddq, *J* = 12.3, 6.1, 2.0 Hz, 1H), 1.53 – 1.46 (m, 1H), 1.45 – 1.30 (m, 2H).

^{13}C NMR: (100 MHz, $CDCl_3$) δ 212.0, 143.4, 138.6, 133.4, 132.3, 130.1, 128.1, 126.8, 112.0, 73.1, 63.3, 54.0, 52.5, 39.9, 37.9, 36.1, 29.9, 28.1, 21.3.

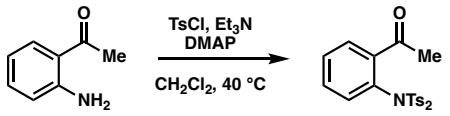
IR: 2934, 2800, 2728, 1710, 1474, 1452, 1432, 1322, 1166, 1118, 1038, 916, 752 cm^{-1}

HRMS: (ESI+) *m/z* calc'd for $C_{19}H_{23}ClNO$ $[M+H]^+$: 316.1463, found 316.1462.



97 ***97b***

HBF_4 Salt 97b: To a 1 Dr vial was added amine **97** (5.0 mg, 0.016 mmol, 1.0 equiv) and dry Et_2O (0.16 mL), and the solution was cooled to 0 °C. HBF_4•OEt_2 (2.3 µL, 0.0168 mmol, 1.05 equiv) was added and the solution was stirred for 30 mins and allowed to warm to ambient temperature. During this time, a white precipitate formed. After warming to ambient temperature, Et_2O (0.4 mL) was added, stirring was halted, and the solid was allowed to settle. The Et_2O was decanted by removal with a syringe. The solid was washed and the solvent was decanted via the same procedure with additional Et_2O (2x1 mL). The residual solid was dried under vacuum to give the title compound as a white crystalline solid (4.9 mg). Details regarding X-ray crystallographic analysis of **97b** are given in Appendix 3 (A3.4).



89 ***101***

Note: Rigorous exclusion of moisture and air is not necessary

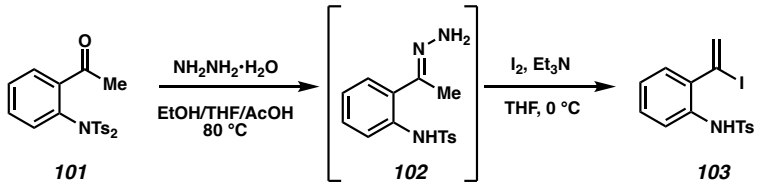
Bis-N-tosyl ketone 101: To a round-bottom flask was added ketone **89** (1.35 g, 10 mmol, 1.0 equiv) and CH_2Cl_2 (33 mL). DMAP (69 mg, 0.5 mmol, 5 mol%) and Et_3N (3.5 mL, 25 mmol, 2.5 equiv) were added followed by TsCl (4.78 g, 25 mmol, 2.5 equiv). The flask was fitted with a reflux condenser and heated to 40 °C for 21 hours. After this time, the reaction mixture was cooled to ambient temperature and water (100 mL) was added. The layers were separated and the aqueous layer was extracted with CH_2Cl_2 (2x40 mL). The combined organic layers were washed with brine (100 mL), dried over Na_2SO_4, and concentrated under reduced pressure. The crude residue was purified by silica gel flash column chromatography (10 → 50% EtOAc in hexanes) to give the title compound as a tan solid (5.11 g, 96% yield).

^{1}H NMR: (500 MHz, $CDCl_3$) δ 7.86 – 7.82 (m, 4H), 7.66 (dd, *J* = 7.7, 1.6 Hz, 1H), 7.51 (td, *J* = 7.6, 1.2 Hz, 1H), 7.39 (td, *J* = 7.7, 1.6 Hz, 1H), 7.35 – 7.28 (m, 4H), 6.96 (dd, *J* = 7.9, 1.2 Hz, 1H), 2.47 (s, 6H), 2.45 (s, 3H).

^{13}C NMR: (125 MHz, $CDCl_3$) δ 198.8, 145.3, 135.8, 133.7, 131.1, 130.2, 129.7, 129.7, 129.4, 129.1, 127.4, 29.6, 21.9.

IR: (Neat Film, NaCl) 3064, 1702, 1650, 1596, 1492, 1448, 1376, 1356, 1250, 1166, 1086, 960, 908, 862, 814, 736, 662 cm^{-1}

HRMS: *m/z* calc'd for $C_{22}H_{25}N_2O_5S_2$ $[M+NH_4]^+$: 461.1199 found 461.1204.



Note: The rigorous exclusion of moisture is not necessary for hydrazone formation.

N-Ts vinyl iodide 103: In a round bottom flask was added ketone **101** (2.2 g, 5 mmol, 1.0 equiv) followed by EtOH (10 mL), THF (5 mL), AcOH (1 mL). Hydrazine hydrate (2.45 mL, 50 mmol, 10 equiv) was added and the reaction was heated to 80 °C for 14 hours. After this time, the reaction was cooled to ambient temperature. Water (100 mL) was added and the aqueous layer was extracted with EtOAc (3x50 mL). The combined organic layers were washed with brine, dried over $MgSO_4$, and concentrated under reduced pressure to give **102**. The crude orange oil was then azeotroped 2x with benzene (50 mL) and left under high-vacuum for >2 hours prior to use in the next step.

Note: It is critical that the hydrazone be completely dry prior to the iodination otherwise hydrolysis to the starting ketone is the major product. A large stir bar is also recommended to maintain stirring as the reaction mixture becomes heterogeneous.

The crude hydrazone (**102**) was dissolved in THF (10 mL) under an N_2 atmosphere and cooled to 0 °C. In a separate round-bottom flask under nitrogen, I_2 (3.40 g, 15 mmol, 3.0 equiv) was dissolved in THF (6 mL). Dry triethylamine (4.2 mL, 30 mmol, 6.0 equiv) was added to the flask containing the hydrazone. The solution of I_2 was then added dropwise until the brown color if I_2 persisted in the heterogeneous solution (usually 2/3 of the I_2 solution volume). Once this point was reached, the mixture was stirred for an additional 30 min at 0 °C. Then satd. aqueous NH_4Cl (75 mL) and satd. aqueous $Na_2S_2O_3$ (75 mL) were sequentially added. The mixture was extracted 3x with CH_2Cl_2 (30 mL), washed with brine

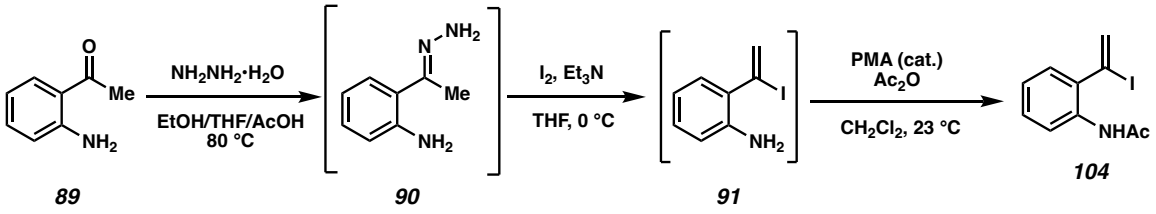
(50 mL), dried over Na_2SO_4 and concentrated under reduced pressure to give the crude vinyl iodide (**102**) as a brown, semi-solid residue. Purification by silica gel flash column chromatography (0 → 40% EtOAc in hexanes) gave the title compound as a semi-solid residue (377 mg, 19% yield over 2 steps).

^{1}H NMR: (400 MHz, $CDCl_3$) δ 7.72 – 7.65 (m, 2H), 7.60 (dt, *J* = 8.2, 1.1 Hz, 1H), 7.30 – 7.26 (m, 1H), 7.24 – 7.20 (m, 2H), 7.11 (dt, *J* = 7.7, 1.4 Hz, 1H), 7.08 – 7.02 (m, 1H), 6.79 (br s, 1H), 6.11 (t, *J* = 1.2 Hz, 1H), 5.83 (t, *J* = 1.2 Hz, 1H), 2.37 (s, 3H).

^{13}C NMR: (100 MHz, $CDCl_3$) δ 144.3, 136.2, 134.9, 133.1, 132.9, 130.0, 129.8, 129.2, 127.6, 124.6, 120.9, 98.7, 21.7.

IR: (Neat Film, NaCl) 3278, 3062, 2932, 1596, 1486, 1398, 1336, 1288, 1162, 1090, 1054, 918, 812, 758, 666 cm^{-1}

HRMS: (FD+) *m/z* calc'd for $C_{15}H_{14}NO_2SI$ $[M]^+$: 398.97844, found 398.97952.



Note: The rigorous exclusion of air and moisture is not necessary for hydrazone formation. 2'-Aminoacetophenone (**89**) (purchased from Combi Blocks inc.) (1.351 g, 10 mmol, 1.0 equiv), was added to a 100 mL round-bottom flask with stir bar and dissolved in EtOH (20 mL) and THF (10 mL). Hydrazine hydrate (5 mL, 100 mmol, 10.0 equiv) was then added followed by AcOH (2 mL). The flask was fitted with a reflux condenser and heated to 80 °C for 14 h. After 14 h, the solution was cooled to ambient temperature, water (100 mL) was added, the layers were partitioned, and aqueous layer was extracted 3x with EtOAc (30 mL). The combined organic layers were washed with satd. aqueous $NaHCO_3$ (50 mL), brine (50 mL), then dried over Na_2SO_4, and concentrated under reduced pressure. The crude orange oil (**90**) was then azeotroped 2x with benzene (50 mL) and left under high-vacuum for >2 hours prior to use in the next step.

Note: It is critical that the hydrazone be completely dry prior to the iodination otherwise hydrolysis to the starting ketone is the major product. A large stir bar is also recommended to maintain stirring as the reaction mixture becomes heterogeneous. The crude, azeotropically dried hydrazone (1.27 g) was dissolved in THF (16.5 mL) under an N_2 atmosphere and cooled to 0 °C. In a separate flame-dried flask under nitrogen, I_2 (5.94g, 25.5 mmol, 3.0 equiv) was dissolved in THF (8.5 mL). Dry triethylamine (7.1 mL, 51 mmol, 6.0 equiv) was added to the flask containing the hydrazone. The solution of I_2 was then added dropwise until the brown color if I_2 persisted in heterogeneous solution (usually 2/3 of the I_2

solution volume). Once this point was reached, the mixture was stirred for an additional 30 min at 0 °C. Then satd. aqueous NH_4Cl (75 mL) and satd. aqueous $Na_2S_2O_3$ (75 mL) were sequentially added. The mixture was extracted 3x with CH_2Cl_2 (30 mL), washed with brine (50 mL), dried over Na_2SO_4 and concentrated under reduced pressure to give the crude vinyl iodide (**91**) as a brown, semi-solid residue that was used directly in the next step.

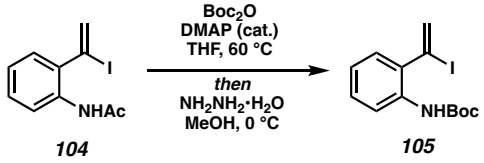
The crude vinyl iodide (**91**) was dissolved in CH_2Cl_2 (17 mL) and Ac_2O (0.964 mL, 10.2 mmol, 1.2 equiv) was added to the solution. Phosphomolybdic acid (155 mg, 0.085 mmol, 1 mol %) was added, and the reaction was maintained under an N_2 atmosphere at ambient temperature for 2 h. After TLC indicated complete consumption of the starting material, water (100 mL) was added, the layers were separated, and the aqueous layer was extracted 3x with CH_2Cl_2 (20 mL), washed with brine (50 mL), dried over Na_2SO_4, and concentrated under reduced pressure. The crude residue was purified by silica gel flash column chromatography (10 → 30% EtOAc in hexanes) to give an orange/brown solid (1.110 g, 39% yield over 3 steps).

^{1}H NMR: (400 MHz, $CDCl_3$) δ 8.14 (d, J = 8.3 Hz, 1H), 7.32 (ddd, J = 8.5, 7.5, 1.7 Hz, 1H), 7.22 (dd, J = 7.7, 1.6 Hz, 1H), 7.08 (t, J = 7.6 Hz, 1H), 6.31 (d, J = 1.3 Hz, 1H), 6.29 (d, J = 1.3 Hz, 1H), 2.23 (s, 3H)

^{13}C NMR: (100 MHz, $CDCl_3$) δ 168.2, 134.1, 133.6, 132.9, 129.9, 128.7, 124.2, 122.0, 100.2, 24.9

IR: (Neat Film, NaCl) 3265, 3097, 1670, 1577, 1517, 1444, 1368, 1297, 1269, 1036, 910, 762, 668 cm^{-1}

HRMS: (ESI+) *m/z* calc'd for $C_{10}H_{11}INO$ $[M+H]^+$: 287.9880, found 287.9878.



104 *105*

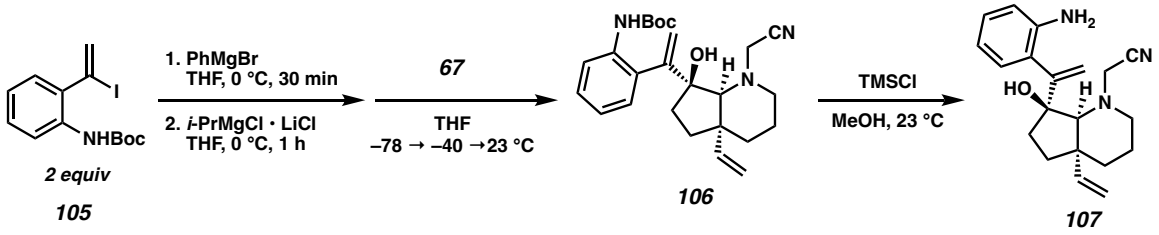
Vinyl iodide 17: In a flame-dried flask equipped with stir bar under an atmosphere of N_2, *N*-acetylated vinyl iodide **104** (1.110 g, 3.87 mmol, 1.0 equiv) was dissolved in THF (12.9 mL). Boc_2O (1.689 g, 7.74 mmol, 2.0 equiv) was added followed by DMAP (94 mg, 0.77 mmol, 0.2 equiv). The solution was then heated to 60 °C for 40 min. After this time, TLC indicated complete consumption of the starting material. The solution was cooled to 0 °C and MeOH (12.9 mL) was added followed by hydrazine hydrate (0.75 mL, 15.48 mmol, 4.0 equiv). The solution was stirred at 0 °C for 2 h. Once TLC inidicated consumption of the starting material, the reaction mixture was poured into CH_2Cl_2 (120 mL). The solution was then washed sequentially with 1 N aq. HCl (aq.) (50 mL), satd. aqueous $CuSO_4$ (50 mL), satd. aqueous $NaHCO_3$, and brine, then dried over Na_2SO_4 and concentrated under reduced pressure. The oily residue was purified by flash column chromatography (5% EtOAc in hexanes) to give the title compound as a viscous pale yellow oil (990 mg, 74% yield). *Note*: *Due to hindered rotation of the carbamate, a duplication of peaks was observed in both ^1H and ^{13}C NMR spectra. Only those peaks corresponding to the "major rotamer" were tabulated.*

^{1}H NMR: (500 MHz, $CDCl_3$) δ 8.00 (d, *J* = 8.3 Hz, 1H), 7.28 (ddd, *J* = 8.5, 7.3, 1.6 Hz, 1H), 7.19 (dd, *J* = 7.7, 1.6 Hz, 1H), 7.00 (td, *J* = 7.5, 1.2 Hz, 1H), 6.66 (s, 1H), 6.31 – 6.27 (m, 2H), 1.55 (s, 9H).

^{13}C NMR: (125 MHz, $CDCl_3$) δ 152.7, 134.6, 132.7, 129.8, 128.8, 122.8, 120.0, 100.5, 81.0, 28.5, 28.0.

IR: (Neat Film, NaCl) 3422, 2975, 1733, 1581, 1516, 1445, 1391, 1367, 1300, 1245, 1227, 1154, 1045, 1023, 912, 836, 761 cm^{-1}

HRMS: (ESI+) *m/z* calc'd for $C_9H_8INO_2$ $[M–C_4H_9+H]^+$: 289.9672, found 289.9672.



Aniline 107: Vinyl iodide **105** (690 mg , 2.0 mmol, 2.0 equiv) was azeotroped 2x with dry toluene (15 mL) and placed under high vacuum for >2 hours to remove traces of toluene. Ketone **67** (204 mg, 1.0 mmol, 1.0 equiv) was azeotroped 2x with dry toluene (10 mL) and placed under high vacuum for the same duration to remove trace amounts of toluene. Both flasks were backfilled with N_2, then vinyl iodide **105** was dissolved in THF (7.5 mL) and cooled to 0 °C (external bath temperature). PhMgBr (1.0 M in THF, 2.25 mL, 2.25 equiv) was added dropwise, and the resulting solution was allowed to stir for 30 minutes at 0 °C. The solution was then cooled to –45 °C (external temperature, dry ice/acetonitrile bath) and stirred for 10 minutes. *i*-PrMgCl•LiCl (1.3 M in THF, 1.92 mL, 2.5 equiv) was added dropwise. The resulting solution was stirred at –40 °C for 1.5 hours, then warmed to 0 °C over the course of 30 minutes. The resulting dianion solution was cooled to –78 °C (external temperature, dry ice/acetone bath). $LaCl_3$•2LiCl (0.6 M in THF, 3.5 mL, 2.1 equiv) was added dropwise. The resulting yellow/orange solution was maintained at –78 °C for 1 h. Ketone **67** was dissolved in THF (6.0 mL), the resulting solution was cooled to –78 °C for 10 minutes, and was then transferred as rapidly as possible by cannula to the stirring nucleophile (**105**) solution. *Note: The rapid cannula transfer was performed by pulling vacuum on the receiving flask while maintaining positive nitrogen flow in the transfer flask. This protocol resulted in the greatest level of reproducibility in our hands.* The solution was maintained at –78 °C for 1 h, then the solution was warmed to –40 °C for 1 h. Finally, the flask was rapidly transferred to a water bath maintained at 23 °C, and stirred for 10 minutes.

After this time, TLC and LC/MS analysis indicated complete consumption of ketone **67**. 4.5 g of silica gel were added, followed by CH_2Cl_2 (10 mL). The resulting slurry was filtered over a plug of silica gel topped with a layer of celite, and flushed with EtOAc (200 mL). The resulting solution was concentrated under reduced pressure and loaded onto a silica gel column and eluted with 5 → 30% EtOAc in hexanes to remove the protodehalogenated vinyl iodide. The semi-pure foam (295 mg) was used directly in the next step. *Characterization data of an analytically pure sample are reported, however the rotamers caused by the N-Boc group caused significant broadening and peak doubling such that the NMR data are not useful for definitive structural assignment. We are confident in this structural assignment due to interpretation of the analytical data after removal the N-Boc group.*

^{1}H NMR: (400 MHz, C_6D_6) δ 8.51 (s, 1H), 7.86 (s, 1H), 7.23 – 7.17 (m, 1H), 6.91 (tt, *J* = 7.5, 1.0 Hz, 1H), 5.56 – 5.43 (m, 2H), 4.92 – 4.74 (m, 3H), 4.24 (s, 1H), 3.11 (d, *J* = 23.8 Hz, 2H), 2.53 (d, *J* = 17.2 Hz, 1H), 2.38 (dt, *J* = 11.1, 6.7 Hz, 1H), 2.15 (dd, *J* = 10.8, 5.6 Hz, 1H), 1.89 (dt, *J* = 18.2, 6.4 Hz, 2H), 1.59 (ddd, *J* = 12.2, 10.0, 6.7 Hz, 1H), 1.45 (s, 10H), 1.39 – 1.29 (m, 1H), 1.27 – 1.07 (m, 4H), 0.59 (s, 1H).

^{13}C NMR: (100 MHz, C_6D_6) δ 153.6, 153.2, 146.7, 137.5, 130.5, 128.8, 122.9, 121.2, 117.3, 115.9, 111.8, 82.9, 79.8, 49.3, 46.6, 44.7, 38.7, 35.7, 31.2, 28.4, 19.7.

IR: (Neat Film, NaCl) 3418, 2938, 2868, 1726, 1516, 1446, 1368, 1302, 1238, 1160, 1048, 1024, 916, 745, 682 cm^{-1}

HRMS: (ESI+) *m/z* calc'd for $C_{25}H_{33}N_3O_3$ $[M+H]^+$: 424.2595, found 424.2615.

$[\alpha]_D^{23}$: –21.3 (c = 0.6, $CHCl_3$)

The semi-pure allylic alcohol (295 mg, 0.7 mmol, 1.0 equiv) was dissolved in MeOH (2.8 mL). The solution was cooled to 0 °C, then TMSCl (760 mg (0.89 mL), 7 mmol, 10.0 equiv) was added, the cooling bath removed, and the reaction was stirred for 6 h. After 6 h, LC/MS and TLC analysis indicated complete consumption of the starting material. The reaction was cooled to 0 °C, and 1 N aq. NaOH (8.2 mL) was added. The solution was then warmed to ambient temperature and extracted 5x with CH_2Cl_2 (20 mL), washed with brine (30 mL), dried over Na_2SO_4, and concentrated under reduced pressure. The crude residue was purified by flash column chromatography (10 → 30% EtOAc, 3% Et_3N in hexanes) to give the title compound as a yellow oil (190.8 mg, 59% yield over 2 steps).

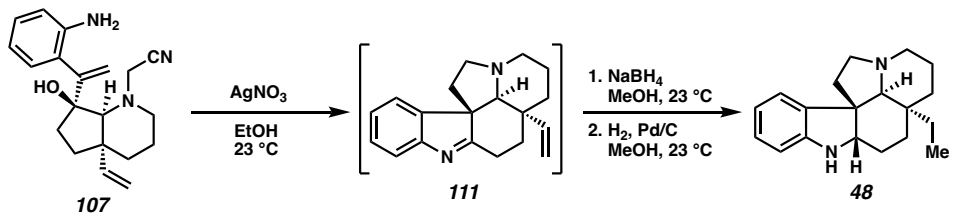
^{1}H NMR: (400 MHz, C_6D_6) δ 7.26 (dd, *J* = 7.6, 1.6 Hz, 1H), 7.00 (td, *J* = 7.7, 1.6 Hz, 1H), 6.76 (td, *J* = 7.5, 1.2 Hz, 1H), 6.37 (dd, *J* = 7.9, 1.2 Hz, 1H), 5.76 (d, *J* = 2.2 Hz, 1H), 5.55 (dd, *J* = 17.5, 10.8 Hz, 1H), 5.00 (d, *J* = 2.2 Hz, 1H), 4.85 (dd, *J* = 17.5, 0.7 Hz, 1H), 4.76 (dd, *J* = 10.9, 0.7 Hz, 1H), 4.30 (s, 1H), 3.38 (d, *J* = 17.2 Hz, 1H), 3.27 (s, 1H), 2.72 (d, *J* = 17.2 Hz, 1H), 2.56 – 2.42 (m, 1H), 2.29 (dt, *J* = 10.4, 4.7 Hz, 1H), 2.08 (ddd, *J* = 13.4, 8.8, 7.2 Hz, 1H), 1.93 (ddd, *J* = 13.4, 6.9, 5.5 Hz, 1H), 1.63 (ddd, *J* = 12.5, 8.8, 6.8 Hz, 1H), 1.54 – 1.44 (m, 1H), 1.33 – 1.20 (m, 4H).

^{13}C NMR: (100 MHz, C_6D_6) δ 154.8, 146.8, 144.9, 130.7, 128.7, 126.9, 118.1, 116.4, 115.8, 115.6, 111.6, 83.0, 70.5, 48.9, 46.6, 44.7, 38.7, 36.6, 30.4, 19.8

IR: (Neat Film, NaCl) 3447, 3375, 3077, 2940, 2862, 2242, 1616, 1493, 1449, 1300, 1137, 1078, 998, 917, 880, 750, 750, 637 cm^{-1}

HRMS: (ESI+) *m/z* calc'd for $C_{20}H_{26}N_3O$ $[M+H]^+$: 324.2070, found 324.2076.

$[\alpha]_D^{23}$: –6.8 (*c* = 1.4, $CHCl_3$)



107 *111* *48*

(–)-Aspidospermidine (48): Aniline **107** (4 mg, 0.0125 mmol, 1.0 equiv) was dissolved in EtOH (0.25 mL) and degassed by bubbling N_2 through the solution for 5 minutes. $AgNO_3$ (5 mg, 0.029 mmol, 2.3 equiv) was added in one portion. The reaction vessel was wrapped with aluminum foil to exclude light. After 6 h, all material converted to the putative imine product by TLC. Satd. aqueous $NaHCO_3$ (0.5 mL) was added followed by aqueous NH_4OH (0.1 mL). The resulting solution was extracted 4x with EtOAc (1 mL). The combined organic layers were washed with brine, dried over Na_2SO_4, and concentrated under reduced pressure.

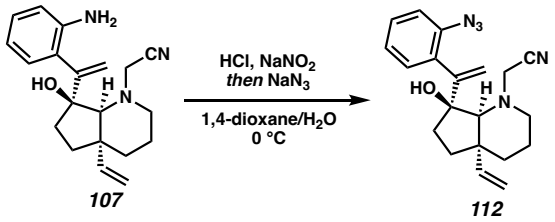
The crude residue was dissolved in MeOH (0.25 mL) and cooled to 0 °C. $NaBH_4$ (ground with a mortar and pestle, 2.9 mg, 0.067 mmol, 5.0 equiv) was added in one portion. The reaction mixture was stirred for 1 h then the cooling bath was removed and the reaction was stirred for an additional 2 h after which time TLC indicated complete consumption of starting material. Water (2 mL) was added, and the mixture was extracted 5x with CH_2Cl_2 (1 mL). The combined organic layers were washed with brine (1 mL), dried over Na_2SO_4, and concentrated under reduced pressure.

The crude residue was dissolved in MeOH (0.5 mL) under an atmosphere of N_2. 10% Pd/C (4 mg) was added. A balloon of hydrogen was used to sparge the solution for 5 minutes, and the mixture was then stirred vigorously for 1 h. After 1 h, TLC and LC/MS analysis indicated complete consumption of starting material. The reaction vessel was sparged with N_2 to expel the H_2 atmosphere. The crude reaction mixture was filtered over a pad of silica gel topped with celite and flushed with EtOAc (5 mL) and concentrated under reduced pressure. The

crude residue was purified by column chromatography 5% MeOH in CH_2Cl_2 to give (–)-aspidospermidine as a white solid (2.5 mg, 71% yield over 3 steps).

Analytical data are in agreement with those reported in the literature.[77] A ^{1}H NMR spectrum is shown for reference.

^{1}H NMR: (600 MHz, C_6D_6) δ 7.08 – 7.03 (m, 2H), 6.81 (td, *J* = 7.4, 1.0 Hz, 1H), 6.49 (dt, *J* = 7.8, 0.8 Hz, 1H), 3.43 (dd, *J* = 10.4, 6.7 Hz, 1H), 2.97 (td, *J* = 9.0, 3.4 Hz, 1H), 2.88 (ddt, *J* = 10.8, 4.0, 1.8 Hz, 1H), 2.37 (ddd, *J* = 13.1, 9.2, 7.6 Hz, 1H), 2.17 (s, 1H), 2.11 (ddd, *J* = 10.6, 8.6, 7.6 Hz, 1H), 2.03 (td, *J* = 13.1, 4.6 Hz, 1H), 1.85 (ddd, *J* = 12.4, 10.6, 2.8 Hz, 1H), 1.76 – 1.67 (m, 1H), 1.60 (dq, *J* = 15.0, 7.6 Hz, 1H), 1.52 – 1.45 (m, 3H), 1.37 – 1.30 (m, 4H), 0.94 – 0.83 (m, 3H), 0.56 (t, *J* = 7.5 Hz, 3H).



107 ***112***

Azide 112: Aniline **107** (163 mg, 0.50 mmol, 1.0 equiv) was dissolved in dioxane (3.36 mL), cooled to 0 °C, and 1N HCl (aq.) (2.5 mL) was added. An aqueous solution of $NaNO_2$ (3.0 M, 0.25 mL, 0.756 mmol, 1.5 equiv) was added slowly. The resulting solution was maintained at 0 °C for 2 h. Then, an aqueous solution of NaN_3 (3.2 M, 0.25 mL, 0.806 mmol, 1.6 equiv) was added slowly dropwise. The reaction mixture was stirred for an additional 2 hours at 0 °C. Then 2.5mL of an aqueous 2M solution of K_2CO_3 was added. The aqueous layer was extracted 3x with Et_2O (10 mL), then 3x with EtOAc (5 mL). The combined extracts were washed with brine (10 mL), dried over Na_2SO_4, and concentrated under reduced pressure. The crude residue was purified by silica gel flash column chromatography (5 → 20% EtOAc, 3% Et_3N in hexanes) to give the title compound as a yellow oil (128 mg, 73% yield).

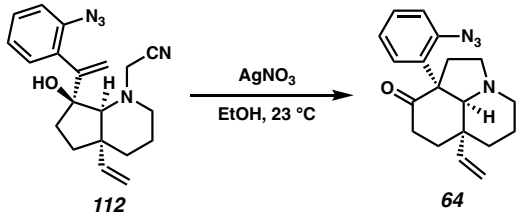
^{1}H NMR: (400 MHz, C_6D_6) δ 7.14 (dd, *J* = 7.5, 1.7 Hz, 1H), 6.89 (td, *J* = 7.6, 1.7 Hz, 1H), 6.84 – 6.76 (m, 2H), 5.88 (d, *J* = 1.9 Hz, 1H), 5.45 (dd, *J* = 17.5, 10.8 Hz, 1H), 4.96 (d, *J* = 2.0 Hz, 1H), 4.80 (dd, *J* = 17.5, 0.6 Hz, 1H), 4.70 (dd, *J* = 10.8, 0.6 Hz, 1H), 4.50 (s, 1H), 3.74 (d, *J* = 17.1 Hz, 1H), 3.28 (s, 1H), 2.61 (d, *J* = 17.1 Hz, 1H), 2.53 (td, *J* = 11.0, 4.4 Hz, 1H), 2.16 – 2.07 (m, 1H), 2.01 – 1.94 (m, 2H), 1.73 (dt, *J* = 12.4, 8.4 Hz, 1H), 1.44 (td, *J* = 10.7, 5.9 Hz, 1H), 1.38 – 1.26 (m, 1H), 1.25 – 1.14 (m, 3H).

^{13}C NMR: (100 MHz, C_6D_6) δ 153.1, 147.1, 138.6, 133.2, 132.1, 128.9, 124.2, 118.4, 116.0, 115.5, 111.4, 82.0, 69.4, 49.0, 46.9, 44.6, 38.7, 36.2, 30.9, 20.2

IR: (Neat Film, NaCl) 3255, 2940, 2123, 1634, 1570, 1462, 1290, 1137, 915, 751 cm^{-1}

HRMS: (ESI+) *m/z* calc'd for $C_{20}H_{24}N_5O$ $[M+H]^+$: 350.1975, found 350.1984.

$[\boldsymbol{\alpha}]_{\boldsymbol{D}}^{\boldsymbol{23}}$**:** –50.9 (*c* = 0.55, $CHCl_3$)



112 *64*

Tricyclic azide 2: Azide **19** (62 mg, 0.18 mmol, 1.0 equiv) was dissolved in EtOH (3.54 mL) and degassed by bubbling N_2 through the solution for 5 minutes. $AgNO_3$ (66.3 mg, 0.39 mmol, 2.2 equiv) was added in one portion, and the reaction vessel was wrapped with aluminum foil to exclude light. After 2 hours, TLC indicated complete consumption of the starting material. Satd. aqueous $NaHCO_3$ (5 mL) was added followed by aqueous NH_4OH (1 mL). The resulting solution was extracted 4x with EtOAc (5 mL). The combined organic layers were washed with brine (5 mL), dried over Na_2SO_4, and concentrated under reduced pressure. The crude residue was purified by flash column chromatography (5 → 10% EtOAc, 3% Et_3N in hexanes) to give a pale yellow oil (46.8 mg, 82% yield).

Note: Due to the fact that the subsequent cycloaddition occurred when tricyclic azide 2 was dissolved in solution, it was not possible to obtain a clean ^{13}C NMR spectrum without some amount of cycloaddition products being present.

^{1}H NMR: (600 MHz, C_6D_6) δ 6.89 (dd, *J* = 7.9, 1.5 Hz, 1H), 6.79 (ddd, *J* = 8.0, 7.3, 1.4 Hz, 1H), 6.71 (dd, *J* = 8.0, 1.3 Hz, 1H), 6.64 (td, *J* = 7.6, 1.4 Hz, 1H), 5.56 (dd, *J* = 17.6, 11.0 Hz, 1H), 4.77 (dd, *J* = 17.6, 1.0 Hz, 1H), 4.59 (dd, *J* = 11.0, 1.0 Hz, 1H), 3.46 (s, 1H), 3.24 (ddd, *J* = 12.8, 9.2, 6.6 Hz, 1H), 3.04 (td, *J* = 8.9, 3.6 Hz, 1H), 2.86 – 2.78 (m, 2H), 2.55 – 2.47 (m, 2H), 2.29 (ddd, *J* = 10.7, 8.5, 6.6 Hz, 1H), 1.85 (dddd, *J* = 16.1, 10.5, 4.9, 3.3 Hz,

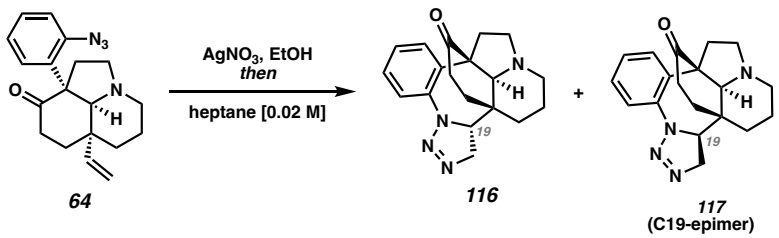
2H), 1.62 (dddd, J = 17.5, 13.2, 8.5, 4.4 Hz, 1H), 1.32 – 1.27 (m, 1H), 1.24 (td, J = 13.0, 4.2 Hz, 1H), 1.20 – 1.13 (m, 2H).

^{13}C NMR: (125 MHz, C_6D_6) δ 209.6, 144.0, 138.1, 133.4, 129.9, 128.0 (obscured by C_6H_6), 125.0, 119.9, 111.8, 74.5, 62.5, 53.8, 52.6, 40.1, 37.8, 36.1, 31.5, 28.3, 21.5.

IR: (Neat Film, NaCl) 2928, 2850, 2799, 2120, 2088, 1709, 1489, 1442, 1287, 1169, 1154, 1118, 935, 917, 748 cm^{-1}

HRMS: (ESI+) *m/z* calc'd for $C_{19}H_{23}N_4O$ $[M+H]^+$: 323.1866, found 323.1874.

$[\alpha]_D^{23}$: –117 (c = 0.31, $CHCl_3$)



Triazoline 116: Tricyclic azide **112** (36 mg, 0.11 mmol, 1.0 equiv) was added to a 2 Dr vial with stir bar. Heptane (2.5 mL) was added, and the reaction mixture was stirred for 48 h after which time TLC and LC/MS analysis indicated complete consumption of the starting material. The reaction mixture was concentrated under reduced pressure to give the title compound as a white solid (29 mg, 80% combined yield), and as a 2.5:1 mixture of C19 diastereomers pure by ^{1}H NMR. The diastereomers were separated by column chromatography (60 → 70 → 80% Et_2O in hexanes) to give undesired **117** as a white solid (6 mg), a mixture of C19 epimers (7 mg), and pure, desired diastereomer **116** as a white solid (12 mg). *Note: the diastereomers are difficult to separate and a careful gradient is required to achieve separation. By column chromatography, the diastereomeric ratio is improved to >5:1, which is sufficient for the subsequent steps. Diastereomerically pure samples were obtained by normal phase HPLC (silica gel, 70% Et_2O, 10%* i-*PrOH in hexanes, 7.0 mL/min: minor t_r = 3.8 min, major t_r = 4.5 min).*

*Characterization data for major diastereomer, triazoline **116**:*

^{1}H NMR: (400 MHz, C_6D_6) δ 7.70 (dd, *J* = 8.2, 1.4 Hz, 1H), 7.35 (dd, *J* = 7.9, 1.7 Hz, 1H), 6.96 (ddd, *J* = 8.2, 7.2, 1.6 Hz, 1H), 6.86 (td, *J* = 7.6, 1.4 Hz, 1H), 4.16 (dd, *J* = 17.6, 9.7 Hz, 1H), 3.92 (dd, *J* = 17.6, 13.4 Hz, 1H), 3.39 (dd, *J* = 13.4, 9.7 Hz, 1H), 3.30 (ddd, *J* = 12.5, 9.3, 5.7 Hz, 1H), 2.84 (td, *J* = 8.9, 4.7 Hz, 1H), 2.64 – 2.59 (m, 1H), 2.42 (d, *J* = 1.6 Hz, 1H),

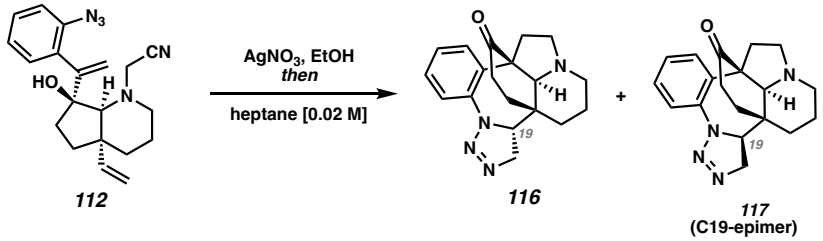
2.32 – 2.07 (m, 3H), 1.66 (ddd, J = 11.1, 8.6, 5.7 Hz, 1H), 1.46 – 1.35 (m, 3H), 1.05 (dtd, J = 9.9, 5.0, 2.6 Hz, 1H), 0.80 – 0.66 (m, 2H), 0.47 (ddt, J = 10.2, 3.7, 1.6 Hz, 1H).

^{13}C NMR: (100 MHz, C_6D_6) δ 207.1, 142.6, 130.8, 130.0, 128.0 (obscured by C_6D_6), 125.1, 120.9, 70.5, 67.8, 61.3, 61.3, 52.9, 50.9, 35.5, 34.6, 33.5, 31.7, 30.3, 21.6.

IR: (Neat Film, NaCl) 2934, 2804, 1704, 1483, 1446, 1326, 1278, 1173, 1136, 1115, 1079, 1063, 980, 928, 921 cm^{-1}

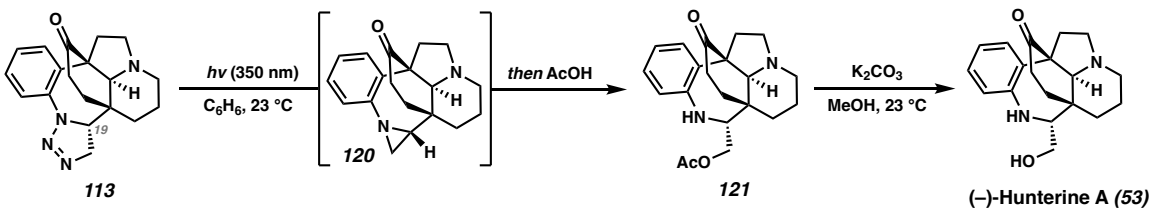
HRMS: (ESI+) *m/z* calc'd for $C_{19}H_{23}N_4O$ $[M+H]^+$: 323.1866, found 323.1874.

$[\alpha]_D^{23}$: –340 (c = 0.5, $CHCl_3$)



One pot synthesis of 116: Azide **19** (2 mg, 0.0057 mmol, 1.0 equiv) was dissolved in degassed EtOH (25 µL). $AgNO_3$ (2.4 mg, 0.013 mmol, 2.2 equiv) was added, and the reaction vessel was wrapped with aluminum foil to exclude light. After 2 hours, the mixture was concentrated under reduced pressure, diluted with heptane (0.3 mL), and stirred at ambient temperature for 48 hours. After this time, NH_4OH (10 µL) was added, the residue was concentrated, dissolved in CH_2Cl_2 and filtered through a pad of silica gel topped with celite to give a mixture of **116** and **117** . The resulting solution was extracted 4x with EtOAc (5 mL). The combined organic layers were washed with brine (5 mL), dried over Na_2SO_4, and concentrated under reduced pressure. The crude residue was purified by flash column

chromatography (5 → 10% EtOAc, 3% Et_3N in hexanes) to give a pale yellow oil (46.8 mg, 82% yield).



(–)-Hunterine A (53): Triazoline **113** (9 mg, 0.028 mmol) was dissolved in benzene (1.0 mL) and degassed by bubbling N_2 through the solution for 5 minutes. The solution was then placed in a Luzchem photobox equipped with Hitachi F8T5–BLB UVA lamps centered at 350 nm. The solution was stirred and irradiated for 4 h after which time TLC and LCMS analysis indicated complete consumption of the starting material and formation of the putative aziridine (**120**).

To this solution was added AcOH (200 µL), and the solution was maintained at 23 °C for 10 h after which time LC/MS analysis indicated complete consumption of the aziridine and formation of *O*-acetyl hunterine A (**121**). The reaction mixture was quenched with 2M aqueous K_2CO_3 (2 mL) and extracted 5x with CH_2Cl_2 (3 mL). The combined organic extracts were washed with brine (3 mL), dried over Na_2SO_4, and concentrated under reduced pressure. The crude residue was used directly in the next step.

The crude residue was dissolved in MeOH, and solid K_2CO_3 (36 mg, 0.26 mmol, 10.0 equiv) was added in one portion. After 3 h, the starting material was consumed by TLC. The mixture was concentrated under reduced pressure. Water (2 mL) was added, and the mixture was extracted 4x with EtOAc (1 mL). The combined organic extracts were washed with brine, dried over Na_2SO_4, and concentrated under reduced pressure. The crude reaction mixture was purified by column chromatography (2 → 5 → 10% MeOH in CH_2Cl_2) to give (–)-hunterine A as a white solid (4.7 mg, 54% over 2 steps).

^{1}H NMR: (600 MHz, CD_3OD) δ 7.06 (dd, *J* = 8.2, 1.6 Hz, 1H), 7.02 – 6.98 (m, 1H), 6.78 (ddd, *J* = 7.2, 6.3, 1.3 Hz, 2H), 3.87 (dd, *J* = 11.0, 3.3 Hz, 1H), 3.60 (dd, *J* = 11.0, 9.9 Hz, 1H), 3.43 (dd, *J* = 9.9, 3.3 Hz, 1H), 3.05 – 2.97 (m, 4H), 2.83 (d, *J* = 1.5 Hz, 1H), 2.54 (ddd, *J* = 13.6, 11.5, 6.6 Hz, 1H), 2.33 (ddd, *J* = 16.7, 6.5, 1.7 Hz, 1H), 2.11 – 2.05 (m, 1H), 1.97 – 1.91 (m, 1H), 1.90 – 1.80 (m, 1H), 1.76 – 1.69 (m, 1H), 1.63 – 1.54 (m, 3H), 1.42 (dd, *J* = 13.5, 5.3 Hz, 1H)

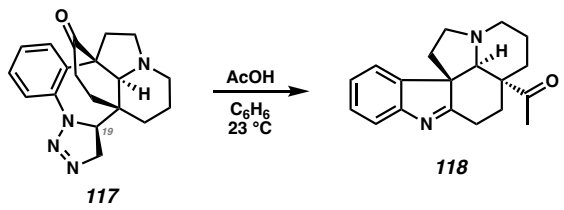
^{13}C NMR: (100 MHz, CD_3OD) δ 213.0, 150.2, 131.5, 128.9, 128.6, 121.7, 121.5, 72.3, 66.3, 61.8, 61.6, 55.1, 52.6, 37.5, 35.7, 34.9, 29.8, 29.6, 22.3

IR: (Neat Film, NaCl) 3344, 2920, 2850, 1594, 1456, 1361, 1264 cm^{-1}

HRMS: (ESI+) *m/z* calc'd for $C_{19}H_{25}N_2O_2$ $[M+H]^+$: 313.1911, found 313.1916

$[\alpha]_D^{23}$: –174 (*c* = 0.25, MeOH)

The optical rotation value is considerably greater in magnitude than that reported in the isolation of hunterine A (reported –22 (*c* = 0.23, MeOH).



117 ***118***

Imine 118: Triazoline **117** (4.0 mg, 0.028 mmol) was dissolved in benzene (1.0 mL) and AcOH (200 µL) was added. The solution was maintained at 23 °C for 10 h after which time LC/MS analysis indicated complete consumption of the starting material. The reaction mixture was quenched with 2M aqueous K_2CO_3 (1.0 mL) and extracted 5x with CH_2Cl_2 (1 mL). The combined organic extracts were washed with brine (1 mL), dried over Na_2SO_4, and concentrated under reduced pressure. The crude residue was purified by column chromatography (30% ethyl acetate, 3% triethylamine in CH_2Cl_2) to give the title compound as a colorless oil (2.2 mg, 55% yield).

Analytical data are in agreement with those reported in the literature.[78] A ^{1}H NMR spectrum is shown for reference.

^{1}H NMR: (600 MHz, C_6D_6) δ 7.67 (d, *J* = 7.6 Hz, 1H), 7.17 (m, 1 H) (obscured by C_6HD_5), 7.12 (td, *J* = 7.6, 1.3 Hz, 1H), 7.05 (t, *J* = 7.4 Hz, 1H), 2.93 (s, 1H), 2.93 – 2.88 (m, 1H), 2.80 – 2.67 (m, 3H), 2.56 – 2.49 (m, 1H), 2.38 (ddd, *J* = 11.5, 8.3, 5.1 Hz, 1H), 2.04 – 1.92 (m, 2H), 1.84 (td, *J* = 11.8, 6.6 Hz, 1H), 1.57 – 1.48 (m, 1H), 1.43 (s, 4H), 1.14 – 1.05 (m, 2H), 0.94 (td, *J* = 13.6, 5.4 Hz, 1H).

2.7 REFERENCES AND NOTES

(1) O'Connor, S. E.; Maresh, J. J. Chemistry and Biology of Monoterpene Indole Alkaloid Biosynthesis. *Nat. Prod. Rep.* **2006**, *23*, 532–547.

(2) Mauger, A.; Jarret, M.; Kouklovsky, C.; Poupon, E.; Evanno, L.; Vincent, G. The Chemistry of Mavacurane Alkaloids: A Rich Source of Bis-Indole Alkaloids. *Nat. Prod. Rep.* **2021**, *38*, 1852–1886.

(3) Ferjancic, Z.; Kukuruzar, A.; Bihelovic, F. Total Synthesis of (+)-Alstonlarsine A. *Angew. Chem. Int. Ed.* **2022**, *61*, e202210297.

(4) Yao, J.-J.; Ding, R.; Chen, X.; Zhai, H. Asymmetric Total Synthesis of (+)-Alstonlarsine A. *J. Am. Chem. Soc.* **2022**, *144*, 14396–14402.

(5) Qin, B.; Lu, Z.; Jia, Y. Divergent Total Synthesis of Four Kopsane Alkaloids: N-Carbomethoxy-10,22-Dioxokopsane, Epikopsanol-10-Lactam, 10,22-Dioxokopsane, and N-Methylkopsanone. *Angew. Chem. Int. Ed.* **2022**, *61*, e202201712.

(6) Horst, B.; Verdoorn, D. S.; Hennig, S.; van der Heijden, G.; Ruijter, E. Enantioselective Total Synthesis of (−)-Limaspermidine and (−)-Kopsinine by a Nitroaryl Transfer Cascade Strategy. *Angew. Chem. Int. Ed.* **2022**, *61*, e202210592.

(7) Zhang, Y.; Zhang, L.; Qi, X. Oxidative Coupling Approach to Sarpagine Alkaloids: Total Synthesis of (−)-Trinervine, Vellosimine, (+)-Normacusine B, and (−)-Alstomutinine C. *Angew. Chem. Int. Ed.* **2023**, *62*, e202304435.

(8) Ramakrishna, G. V.; Pop, L. P.; Latif, Z.; Suryadevara, H. K. V.; Santo, L.; Romiti, F. Streamlined Strategy for Scalable and Enantioselective Total Syntheses of the Eburnane Alkaloids. *J. Am. Chem. Soc.* **2023**, *145*, 20062–20072.

(9) Pritchett, B. P.; Kikuchi, J.; Numajiri, Y.; Stoltz, B. M. Enantioselective Pd-Catalyzed Allylic Alkylation Reactions of Dihydropyrido[1,2-a]Indolone Substrates: Efficient Syntheses of (−)-Goniomitine, (+)-Aspidospermidine, and (−)-Quebrachamine. *Angew. Chem. Int. Ed.* **2016**, *55*, 13529–13532.

(10) Pritchett, B. P.; Donckele, E. J.; Stoltz, B. M. Enantioselective Catalysis Coupled with Stereodivergent Cyclization Strategies Enables Rapid Syntheses of (+)-Limaspermidine and (+)-Kopsihainanine A. *Angew. Chem. Int. Ed.* **2017**, *56*, 12624–12627.

(11) Reimann, C. E.; Ngamnithiporn, A.; Hayashida, K.; Saito, D.; Korch, K. M.; Stoltz, B. M. The Enantioselective Synthesis of Eburnamonine, Eucophylline, and 16′-Epi-Leucophyllidine. *Angew. Chem. Int. Ed.* **2021**, *60*, 17957–17962.

(12) Rand, A. W.; Gonzalez, K. J.; Reimann, C. E.; Virgil, S. C.; Stoltz, B. M. Total Synthesis of Strempeliopidine and Non-Natural Stereoisomers through a Convergent Petasis Borono–Mannich Reaction. *J. Am. Chem. Soc.* **2023**, *145*, 7278–7287.

(13) Pritchett, B. P.; Stoltz, B. M. Enantioselective Palladium-Catalyzed Allylic Alkylation Reactions in the Synthesis of Aspidosperma and Structurally Related Monoterpene Indole Alkaloids. *Nat. Prod. Rep.* **2018**, *35*, 559–574.

(14) Zsigulics, B.; Angyal, P.; Mészáros, B. B.; Daru, J.; Varga, S.; Soós, T. Bioinspired Synthesis of (−)-Hunterine A: Deciphering the Key Step in the Biogenetic Pathway. *Chem. – Eur. J.* **2025**, *31*, e202404501.

(15) Zhang, J.; Liu, Z.-W.; Ao, Y.-L.; Hu, L.-J.; Wei, C.-J.; Zhang, Q.-H.; Yuan, M.-F.; Wang, Y.; Zhang, Q.-W.; Ye, W.-C.; Zhang, X.-Q. Hunterines A–C, Three Unusual Monoterpenoid Indole Alkaloids from Hunteria Zeylanica. *J. Org. Chem.* **2019**, *84*, 14892–14897.

(16) Hong, B.; Grzech, D.; Caputi, L.; Sonawane, P.; López, C. E. R.; Kamileen, M. O.; Hernández Lozada, N. J.; Grabe, V.; O'Connor, S. E. Biosynthesis of Strychnine. *Nature* **2022**, 1–6.

(17) Linde, H. H. A. Die Alkaloide aus Melodinus australis (F. MUELLER) PIERRE (Apocynaceae). *Helvetica Chimica Acta* **1965**, *48*, 1822–1842.

(18) Lyon, R. L.; Fong, H. H. S.; Farnsworth, N. R.; Svoboda, G. H. Biological and Phytochemical Evaluation of Plants XI: Isolation of Aspidospermine, Quebrachidine, Rhazinilam, (—)-Pyrifolidine, and Akuammidine from Aspidosperma Quebracho-Blanco (Apocynaceae). *J. Pharm. Sci.* **1973**, *62*, 218–221.

(19) Sirindil, F.; Weibel, J.-M.; Pale, P.; Blanc, A. Rhazinilam–Leuconolam Family of Natural Products: A Half Century of Total Synthesis. *Nat. Prod. Rep.* **2022**, *39*, 1574–1590.

(20) Fukuyama, T.; Yang, L. Total Synthesis of (.+-.)-Mitomycins via Isomitomycin A. *J. Am. Chem. Soc.* **1987**, *109*, 7881–7882.

(21) Ducray, R.; Ciufolini, M. A. Total Synthesis of (±)-FR66979. *Angew. Chem. Int. Ed.* **2002**, *41*, 4688–4691.

(22) Gallagher, T.; Magnus, P.; Huffman, J. Indole-2,3-Quinodimethan Route to Aspidosperma Alkaloids: Synthesis of Dl-Aspidospermidine. *J. Am. Chem. Soc.* **1982**, *104*, 1140–1141.

(23) Node, M.; Nagasawa, H.; Fuji, K. Expeditious Enantioselective Syntheses of Indole Alkaloids of Aspidosperma- and Hunteria-Type. *J. Am. Chem. Soc.* **1987**, *109*, 7901–7903.

(24) Kozmin, S. A.; Iwama, T.; Huang, Y.; Rawal, V. H. An Efficient Approach to Aspidosperma Alkaloids via [4 + 2] Cycloadditions of Aminosiloxydienes: Stereocontrolled Total Synthesis of (±)-Tabersonine. Gram-Scale Catalytic Asymmetric Syntheses of (+)-Tabersonine and (+)-16-Methoxytabersonine. Asymmetric Syntheses of (+)-Aspidospermidine and (−)-Quebrachamine. *J. Am. Chem. Soc.* **2002**, *124*, 4628–4641.

(25) Li, Z.; Zhang, S.; Wu, S.; Shen, X.; Zou, L.; Wang, F.; Li, X.; Peng, F.; Zhang, H.; Shao, Z. Enantioselective Palladium-Catalyzed Decarboxylative Allylation of Carbazolones: Total Synthesis of (−)-Aspidospermidine and (+)-Kopsihainanine A. *Angew. Chem. Int. Ed.* **2013**, *52*, 4117–4121.

(26) Mewald, M.; Medley, J. W.; Movassaghi, M. Concise and Enantioselective Total Synthesis of (−)-Mehranine, (−)-Methylenebismehranine, and Related Aspidosperma Alkaloids. *Angew. Chem. Int. Ed.* **2014**, *53*, 11634–11639.

(27) Stork, Gilbert.; Dolfini, J. E. The Total Synthesis of Dl-Aspidospermine and of Dl-Quebrachamine. *J. Am. Chem. Soc.* **1963**, *85*, 2872–2873.

(28) Iyengar, R.; Schildknegt, K.; Aubé, J. Regiocontrol in an Intramolecular Schmidt Reaction: Total Synthesis of (+)-Aspidospermidine. *Org. Lett.* **2000**, *2*, 1625–1627.

(29) Coldham, I.; Burrell, A. J. M.; White, L. E.; Adams, H.; Oram, N. Highly Efficient Synthesis of Tricyclic Amines by a Cyclization/Cycloaddition Cascade: Total Syntheses of Aspidospermine, Aspidospermidine, and Quebrachamine. *Angew. Chem. Int. Ed.* **2007**, *46*, 6159–6162.

(30) Pandey, G.; Burugu, S. K.; Singh, P. Efficient Strategy for the Construction of Both Enantiomers of the Octahydropyrroloquinolinone Ring System: Total Synthesis of (+)-Aspidospermidine. *Org. Lett.* **2016**, *18*, 1558–1561.

(31) Katahara, S.; Sugiyama, Y.; Yamane, M.; Komiya, Y.; Sato, T.; Chida, N. Five-Step Total Synthesis of (±)-Aspidospermidine by a Lactam Strategy via an Azomethine Ylide. *Org. Lett.* **2021**, *23* (8), 3058–3063. https://doi.org/10.1021/acs.orglett.1c00735.

(32) Overman, L. E.; Robertson, G. M.; Robichaud, A. J. Synthesis Applications of Cationic Aza-Cope Rearrangements. 20. Total Synthesis of (.+-.)-Meloscine and (.+-.)-Epimeloscine. *J. Org. Chem.* **1989**, *54*, 1236–1238.

(33) Overman, L. E.; Humphreys, P. G.; Welmaker, G. S. The Aza-Cope/Mannich Reaction. In *Organic Reactions*; John Wiley & Sons, Ltd, 2011; pp 747–820.

(34) Piers, E.; Renaud, J. Total Syntheses of the Triquinane Terpenoids (±)-Methyl Cantabrenonate and (±)-Methyl Epoxycantabronate. *J. Chem. Soc., Chem. Commun.* **1990**, No. 19, 1324–1326.

(35) Nielsen, E. B.; Munch-Petersen, J.; Jørgensen, P. M.; Refn, S. Conjugate Additions of Grignard Reagents to Alpha,Beta-Unsaturated Esters. V. Addition of n-Butylmagnesium Bromide to Sec-Butyl Esters of Maleic, Fumaric, Citraconic, and Mesaconic Acids. *Acta Chem. Scand.* **1959**, *13*, 1943–1954.

(36) Posner, G. H. Conjugate Addition Reactions of Organocopper Reagents. In *Organic Reactions*; John Wiley & Sons, Ltd, 2011; pp 1–114.

(37) Kim, S.; Lee, P. H. New Methods for β-Conjugate Addition and β-Hydroxyalkylation of Enones. *Tetrahedron Lett.* **1988**, *29*, 5413–5416.

(38) Guo, Y.; Guo, Z.; Lu, J.-T.; Fang, R.; Chen, S.-C.; Luo, T. Total Synthesis of (−)-Batrachotoxinin A: A Local-Desymmetrization Approach. *J. Am. Chem. Soc.* **2020**, *142*, 3675–3679.

(39) Schlatter, A.; Woggon, W.-D. Enantioselective Transfer Hydrogenation of Aliphatic Ketones Catalyzed by Ruthenium Complexes Linked to the Secondary Face of β-Cyclodextrin. *Adv. Synth. Catal.* **2008**, *350*, 995–1000.

(40) Brooks, D. W.; Mazdiyasni, H.; Grothaus, P. G. Asymmetric Microbial Reduction of Prochiral 2,2,-Disubstituted Cycloalkanediones. *J. Org. Chem.* **1987**, *52*, 3223–3232.

(41) Corey, E. J.; Helal, C. J. Reduction of Carbonyl Compounds with Chiral Oxazaborolidine Catalysts: A New Paradigm for Enantioselective Catalysis and a Powerful New Synthetic Method. *Angew. Chem. Int. Ed.* **1998**, *37*, 1986–2012.

(42) Hashiguchi, S.; Fujii, A.; Takehara, J.; Ikariya, T.; Noyori, R. Asymmetric Transfer Hydrogenation of Aromatic Ketones Catalyzed by Chiral Ruthenium(II) Complexes. *J. Am. Chem. Soc.* **1995**, *117*, 7562–7563.

(43) Fujii, A.; Hashiguchi, S.; Uematsu, N.; Ikariya, T.; Noyori, R. Ruthenium(II)-Catalyzed Asymmetric Transfer Hydrogenation of Ketones Using a Formic Acid−Triethylamine Mixture. *J. Am. Chem. Soc.* **1996**, *118*, 2521–2522.

(44) Monnereau, L.; Cartigny, D.; Scalone, M.; Ayad, T.; Ratovelomanana-Vidal, V. Efficient Synthesis of Differentiated Syn-1,2-Diol Derivatives by Asymmetric Transfer

Hydrogenation–Dynamic Kinetic Resolution of α-Alkoxy-Substituted β-Ketoesters. *Chem. – Eur. J.* **2015**, *21*, 11799–11806.

(45) Inoue, T.; Hosomi, K.; Araki, M.; Nishide, K.; Node, M. Enantioselective Reduction of σ-Symmetric Bicyclo[3.3.0]Octane-2,8-Diones with Baker's Yeast. *Tetrahedron: Asymmetry* **1995**, *6*, 31–34.

(46) Lisnyak, V. G.; Tan, Y.; Ramirez, A.; Wisniewski, S. R.; Sarjeant, A. A. Development of a Crystallization-Induced Diastereomer Transformation of Oxime Isomers for the Asymmetric Synthesis of (1S,6R)-3,9-Diazabicyclo[4.2.1]Nonane. *J. Org. Chem.* **2023**, *88*, 12493–12501.

(47) Mo, X.; Morgan, T. D. R.; Ang, H. T.; Hall, D. G. Scope and Mechanism of a True Organocatalytic Beckmann Rearrangement with a Boronic Acid/Perfluoropinacol System under Ambient Conditions. *J. Am. Chem. Soc.* **2018**, *140*, 5264–5271.

(48) Hunt, P. A.; Moody, C. J. Beckmann Rearrangements in the Bicyclo[2.2.1]Heptan-2-One Series. *Tetrahedron Lett.* **1989**, *30*, 7233–7234.

(49) De Luca, L.; Giacomelli, G.; Porcheddu, A. Beckmann Rearrangement of Oximes under Very Mild Conditions. *J. Org. Chem.* **2002**, *67*, 6272–6274.

(50) Dao, H. T.; Baran, P. S. Quinone Diazides for Olefin Functionalization. *Angew. Chem. Int. Ed.* **2014**, *53*, 14382–14386.

(51) Gross, M. L.; Blank, D. H.; Welch, W. M. The Triazene Moiety as a Protecting Group for Aromatic Amines. *J. Org. Chem.* **1993**, *58*, 2104–2109.

(52) Kimball, D. B.; Haley, M. M. Triazenes: A Versatile Tool in Organic Synthesis. *Angew. Chem. Int. Ed.* **2002**, *41*, 3338–3351.

(53) Lazny, R.; Poplawski, J.; Köbberling, J.; Enders, D.; Bräse, S. Triazenes: A Useful Protecting Strategy for Sensitive Secondary Amines. *Synlett* **1999**, *1999*, 1304–1306.

(54) Liu, C.-Y.; Knochel, P. Preparation of Polyfunctional Aryl Azides from Aryl Triazenes. A New Synthesis of Ellipticine, 9-Methoxyellipticine, Isoellipticine, and 7-Carbethoxyisoellipticine. *J. Org. Chem.* **2007**, *72*, 7106–7115.

(55) Liu, C.-Y.; Knochel, P. Preparation of Polyfunctional Arylmagnesium Reagents Bearing a Triazene Moiety. A New Carbazole Synthesis. *Org. Lett.* **2005**, *7*, 2543–2546.

(56) Suleymanov, A. A.; Severin, K. Vinyl and Alkynyl Triazenes: Synthesis, Reactivity, and Applications. *Angew. Chem. Int. Ed.* **2021**, *60*, 6879–6889.

(57) Reisman, S. E.; Ready, J. M.; Hasuoka, A.; Smith, C. J.; Wood, J. L. Total Synthesis of (±)-Welwitindolinone A Isonitrile. *J. Am. Chem. Soc.* **2006**, *128*, 1448–1449.

(58) Ready, J. M.; Reisman, S. E.; Hirata, M.; Weiss, M. M.; Tamaki, K.; Ovaska, T. V.; Wood, J. L. A Mild and Efficient Synthesis of Oxindoles: Progress Towards the Synthesis of Welwitindolinone A Isonitrile. *Angew Chem. Int. Ed.* **2004**, *43*, 1270–1272.

(59) Barton, D. H. R.; O'Brien, R. E.; Sternhell, S. 88. A New Reaction of Hydrazones. *J. Chem. Soc.* **1962**, 470–476.

(60) Dunn, T. B.; Ellis, J. M.; Kofink, C. C.; Manning, J. R.; Overman, L. E. Asymmetric Construction of Rings A−D of Daphnicyclidin-Type Alkaloids. *Org. Lett.* **2009**, *11*, 5658–5661.

(61) Kadam, S. T.; Kim, S. S. Phosphomolybdic Acid: Mild and Efficient Catalyst for Acetylation of Alcohols, Phenols, and Amines under Solvent-Free Conditions. *Synthesis* **2008**, *2008*, 267–271.

(62) Burk, M. J.; Allen, J. G. A Mild Amide to Carbamate Transformation. *J. Org. Chem.* **1997**, *62*, 7054–7057.

(63) Krasovskiy, A.; Kopp, F.; Knochel, P. Soluble Lanthanide Salts (LnCl3·2 LiCl) for the Improved Addition of Organomagnesium Reagents to Carbonyl Compounds. *Angew. Chem. Int. Ed.* **2006**, *45*, 497–500.

(64) Metzger, A.; Gavryushin, A.; Knochel, P. $LaCl_3$ ×2LiCl-CatalyzedAddition of Grignard Reagents to Ketones. *Synlett* **2009**, *2009*, 1433–1436.

(65) Angle, S. R.; Fevig, J. M.; Knight, S. D.; Marquis, R. W. Jr.; Overman, L. E. Synthesis Applications of Cationic Aza-Cope Rearrangements. 24. The Aza-Cope-Mannich Approach to Strychnos Alkaloids. Short Stereocontrolled Total Syntheses of (.+-.)-Dehydrotubifoline and (.+-.)-Akuammicine. *J. Am. Chem. Soc.* **1993**, *115*, 3966–3976.

(66) Scheiner, P. Triazoline Photodecomposition: The Preparation of Aziridines. *Tetrahedron* **1968**, *24*, 2757–2765.

(67) Scheiner, P. Photodecomposition of 1,2,3-Triazolines. A New Entry into the Aziridine Series. *J. Org. Chem.* **1965**, *30*, 7–10.

(68) Scheiner, P. Spin Inversion and Bond Rotation in 1,3-Diradicals. *J. Am. Chem. Soc.* **1966**, *88*, 4759–4760.

(69) Scheiner, P. Triazoline Photodecomposition. Stereochemistry and Mechanism. *J. Am. Chem. Soc.* **1968**, *90*, 988–992.

(70) Higashiyama, K.; Matsumura, M.; Kojima, H.; Yamauchi, T. Regio- and Stereoselective Ring-Opening Reaction of Chiral Aziridines: A Facile Synthesis of Chiral β-Amino Alcohols. *Heterocycles* **2009**, *78*, 471.

(71) Bhattacharya, D.; Ghorai, A.; Pal, U.; Maiti, N. C.; Chattopadhyay, P. Stereoselective Domino Azidation and [3 + 2] Cycloaddition: A Facile Route to Chiral Heterocyclic Scaffolds from Carbohydrate Derived Synthons. *RSC Adv.* **2013**, *4*, 4155–4162.

(72) Murthy, K. S. K.; Hassner, A. Fused β-Lactams via Intramolecular Dipolar Cycloaddition. *Tetrahedron Lett.* **1987**, *28*, 97–100.

(73) Hemming, K.; Chambers, C. S.; Jamshaid, F.; O'Gorman, P. A. Intramolecular Azide to Alkene Cycloadditions for the Construction of Pyrrolobenzodiazepines and Azetidino-Benzodiazepines. *Molecules* **2014**, *19*, 16737–16756.

(74) Brown, K. L.; Damm, L.; Dunitz, J. D.; Eschenmoser, A.; Hobi, R.; Kratky, C. Structural Studies of Crystalline Enamines. *Helv. Chim. Acta* **1978**, *61*, 3108–3135.

(75) Pangborn, A. B.; Giardello, M. A.; Grubbs, R. H.; Rosen, R. K.; Timmers, F. J. Safe and Convenient Procedure for Solvent Purification. *Organometallics* **1996**, *15*, 1518–1520.

(76) Brenninger, C.; Pöthig, A.; Bach, T. Brønsted Acid Catalysis in Visible-Light-Induced [2+2] Photocycloaddition Reactions of Enone Dithianes. *Angew. Chem. Int. Ed.* **2017**, *56*, 4337–4341.

(77) Sabot, C.; Guérard, K. C.; Canesi, S. Concise Total Synthesis of (±)-Aspidospermidinevia an Oxidative Hosomi–Sakurai Process. *Chem. Commun.* **2009**, No. 20, 2941–2943.

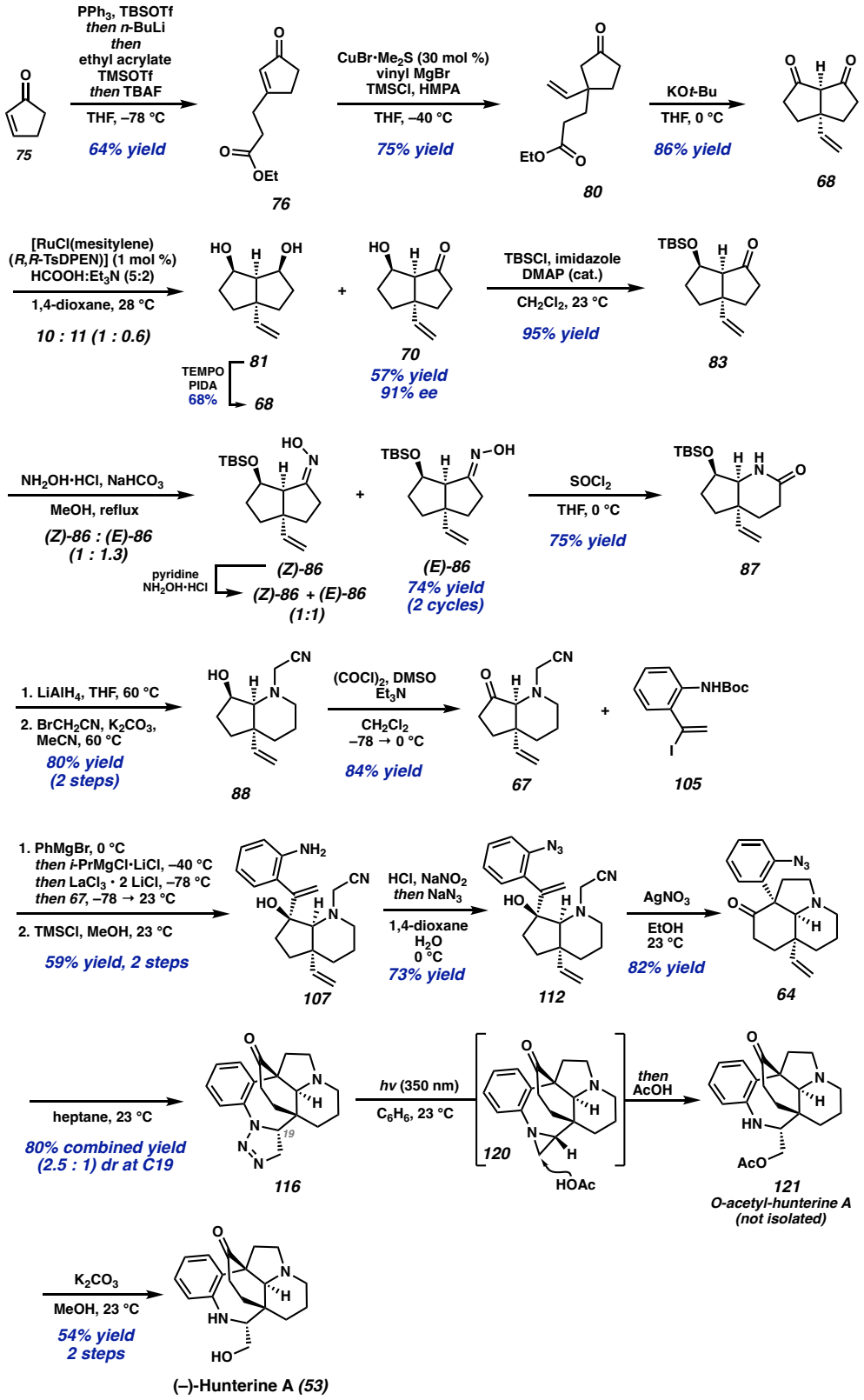
(78) Varga, S.; Angyal, P.; Martin, G.; Egyed, O.; Holczbauer, T.; Soós, T. Total Syntheses of (−)-Minovincine and (−)-Aspidofractinine through a Sequence of Cascade Reactions. *Angew. Chem. Int. Ed.* **2020**, *59*, 13547–13551.

APPENDIX 2

Synthetic Summary for Chapter 2:

Enantioselective Total Synthesis of Hunterine A

Scheme A2.1. *Synthetic Summary for Chapter 2*



APPENDIX 3

Spectra Relevant to Chapter 3:

Enantioselective Total Synthesis of Hunterine A

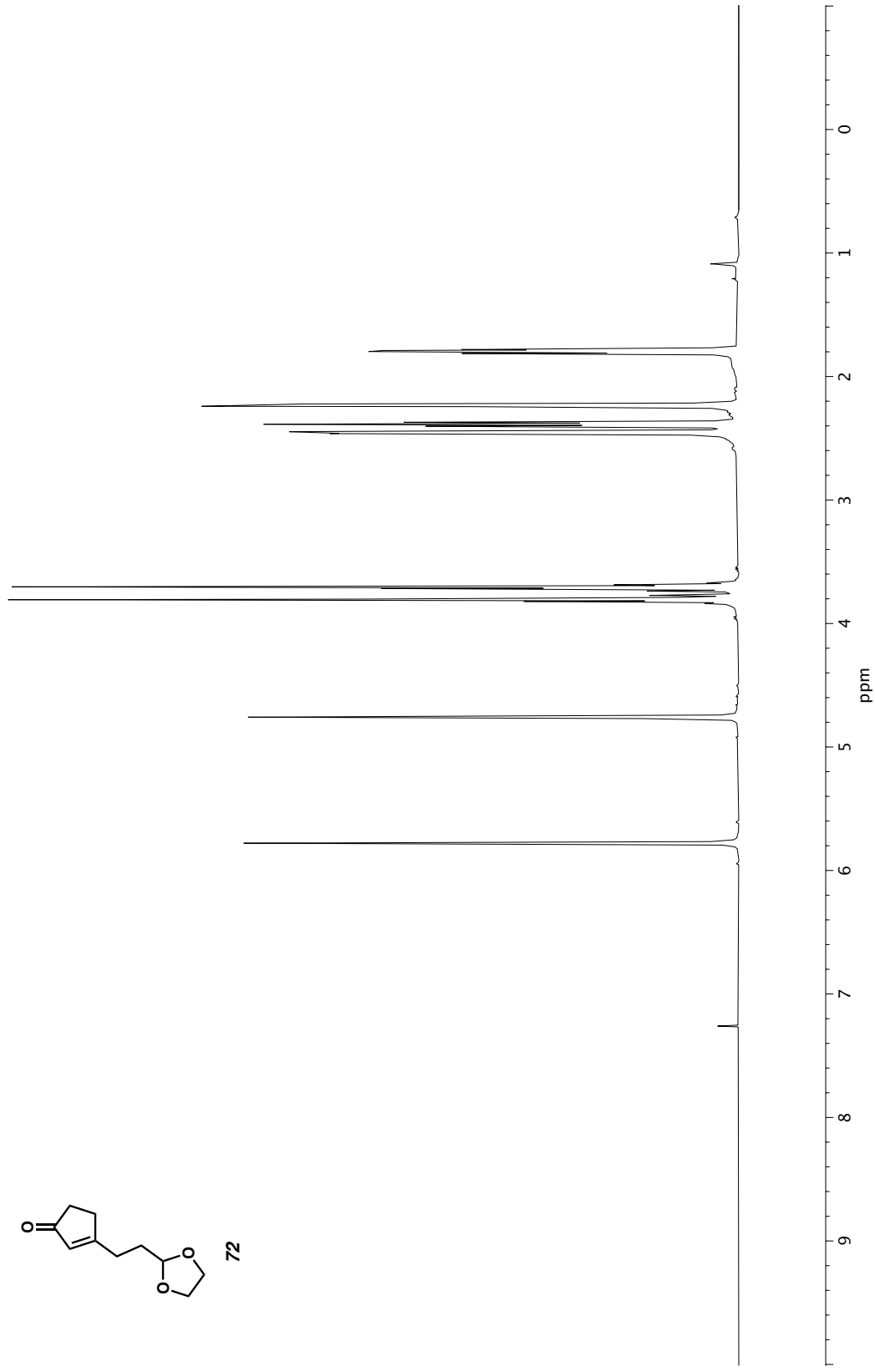


Figure A3.1 *^1H NMR (500 MHz, $CDCl_3$) of compound **72**.*

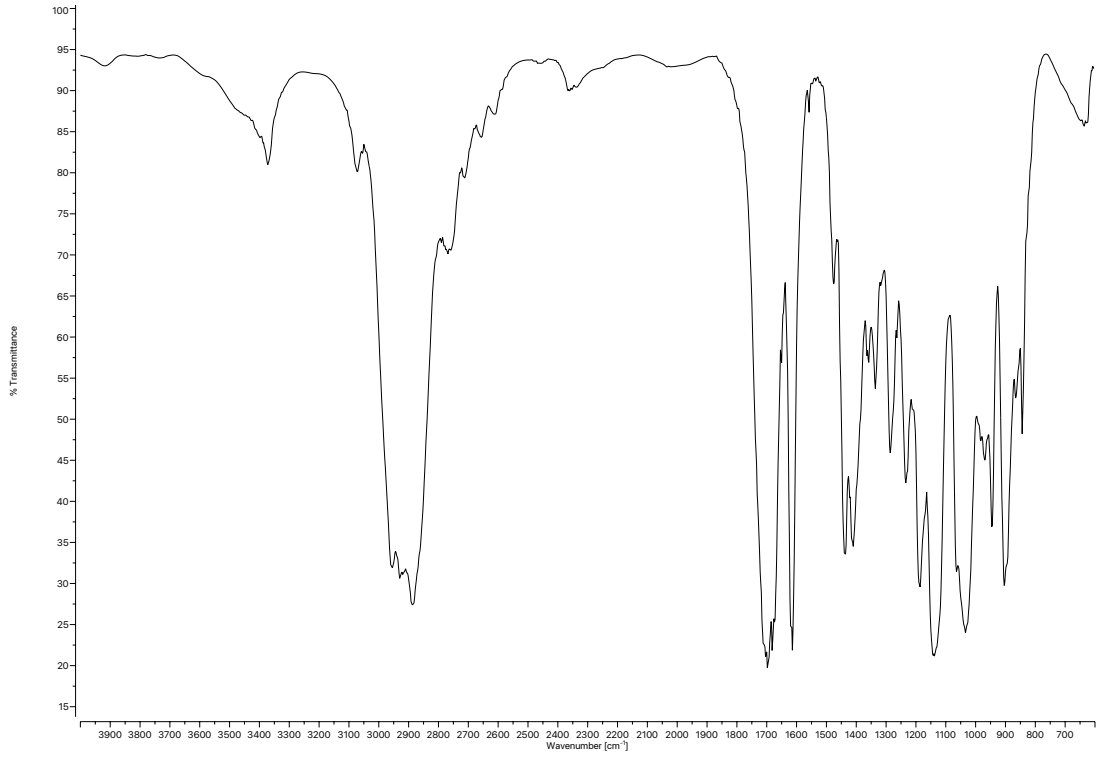


Figure A3.2 *Infrared spectrum (Thin Film, NaCl) of compound* ***72***.

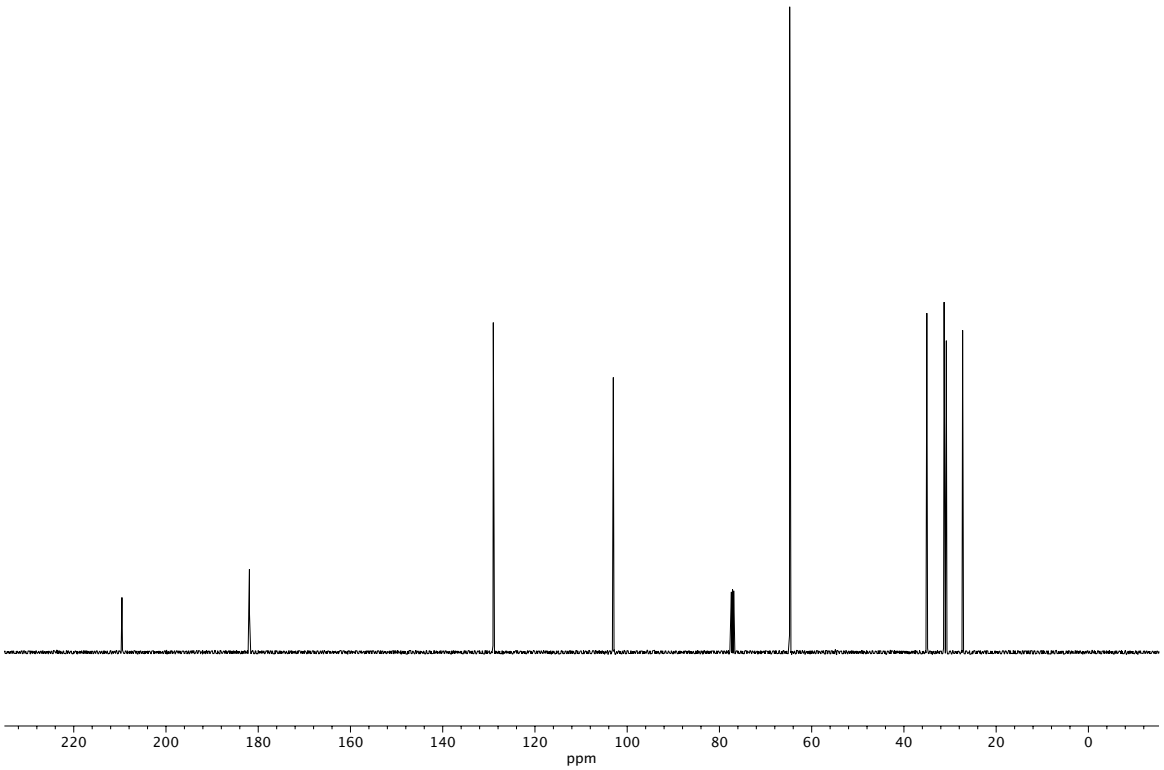


Figure A3.3 *^{13}C NMR (125 MHz, $CDCl_3$) of compound* ***72***.

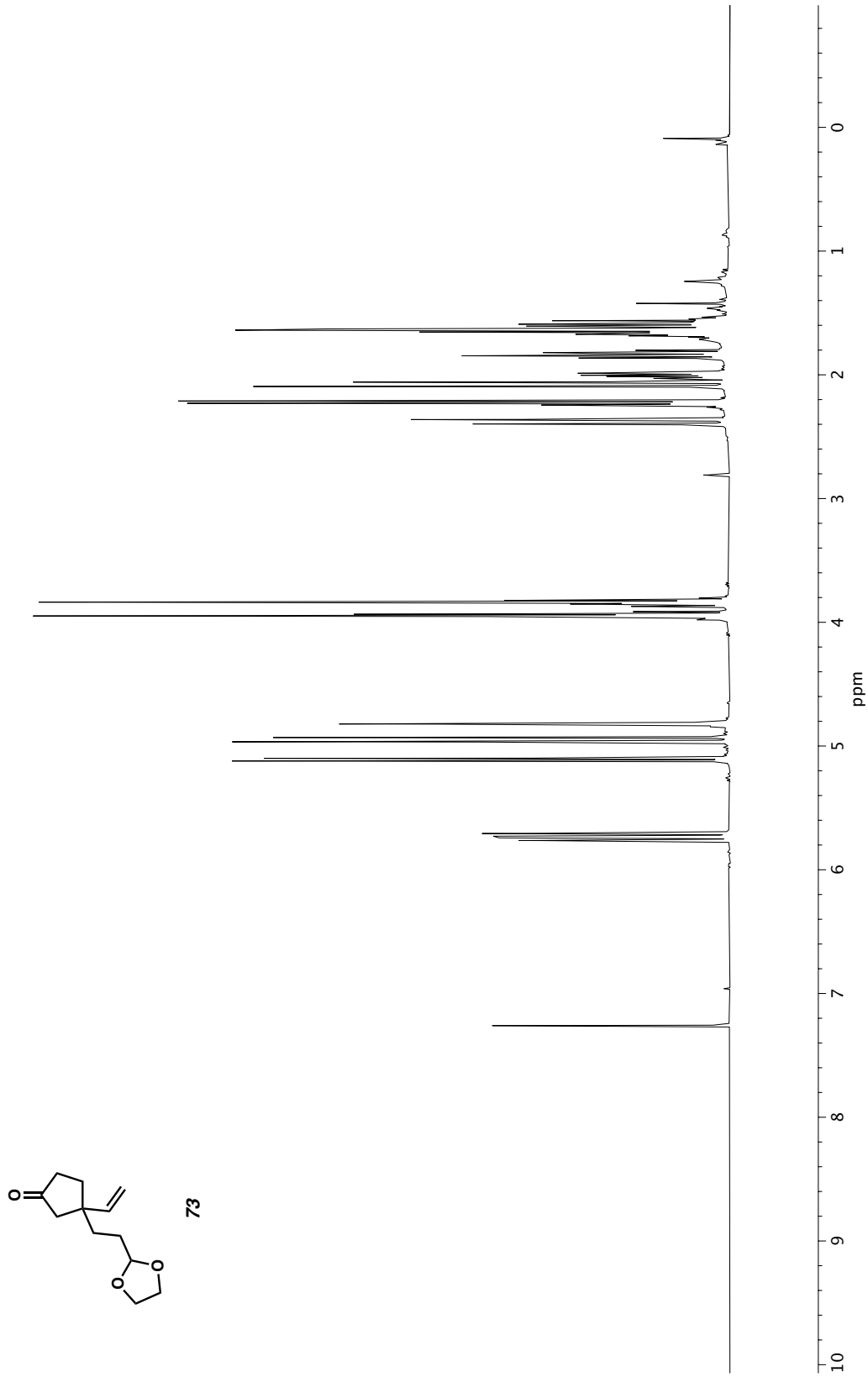


Figure A3.4 *^1H NMR (500 MHz, $CDCl_3$) of compound **73**.*

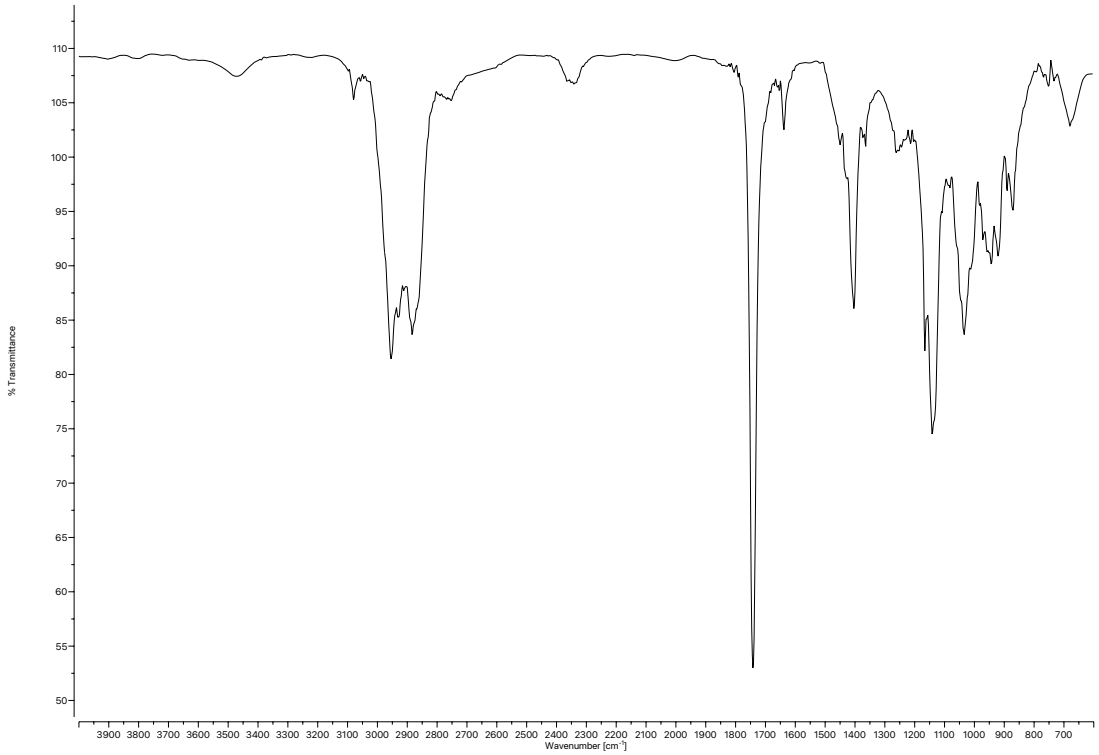


Figure A3.5 *Infrared spectrum (Thin Film, NaCl) of compound* ***73***.

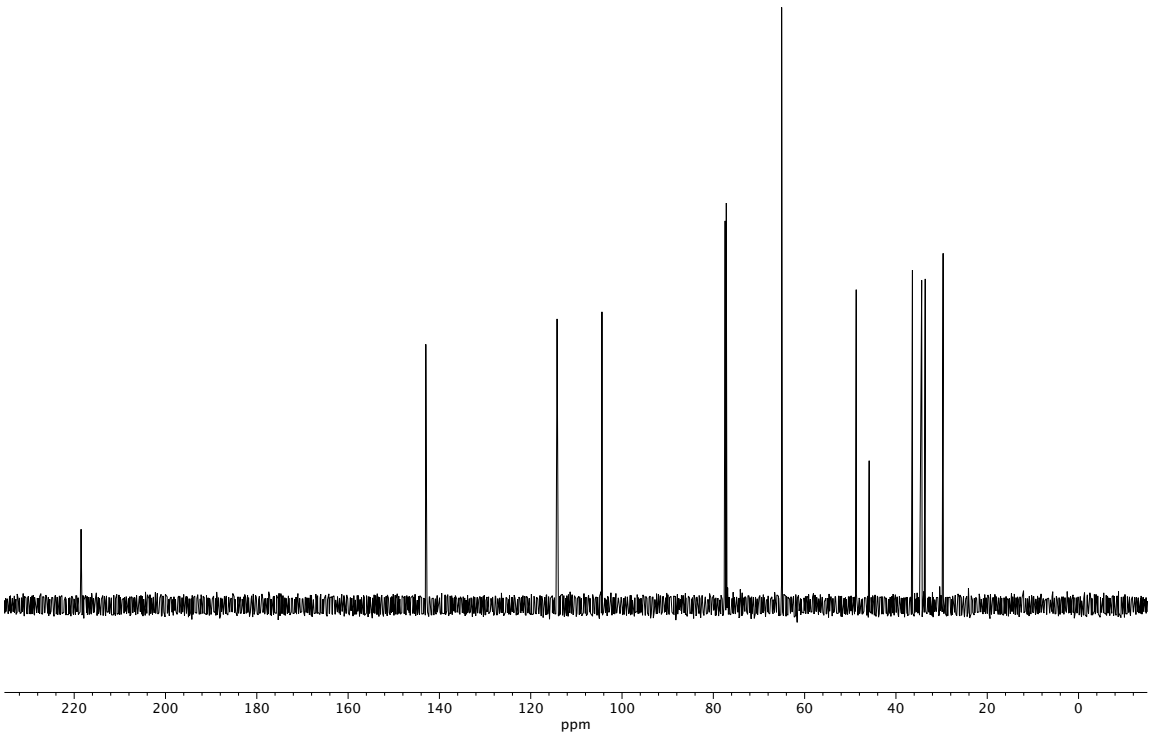


Figure A3.6 *^{13}C NMR (125 MHz, $CDCl_3$) of compound* ***73***.

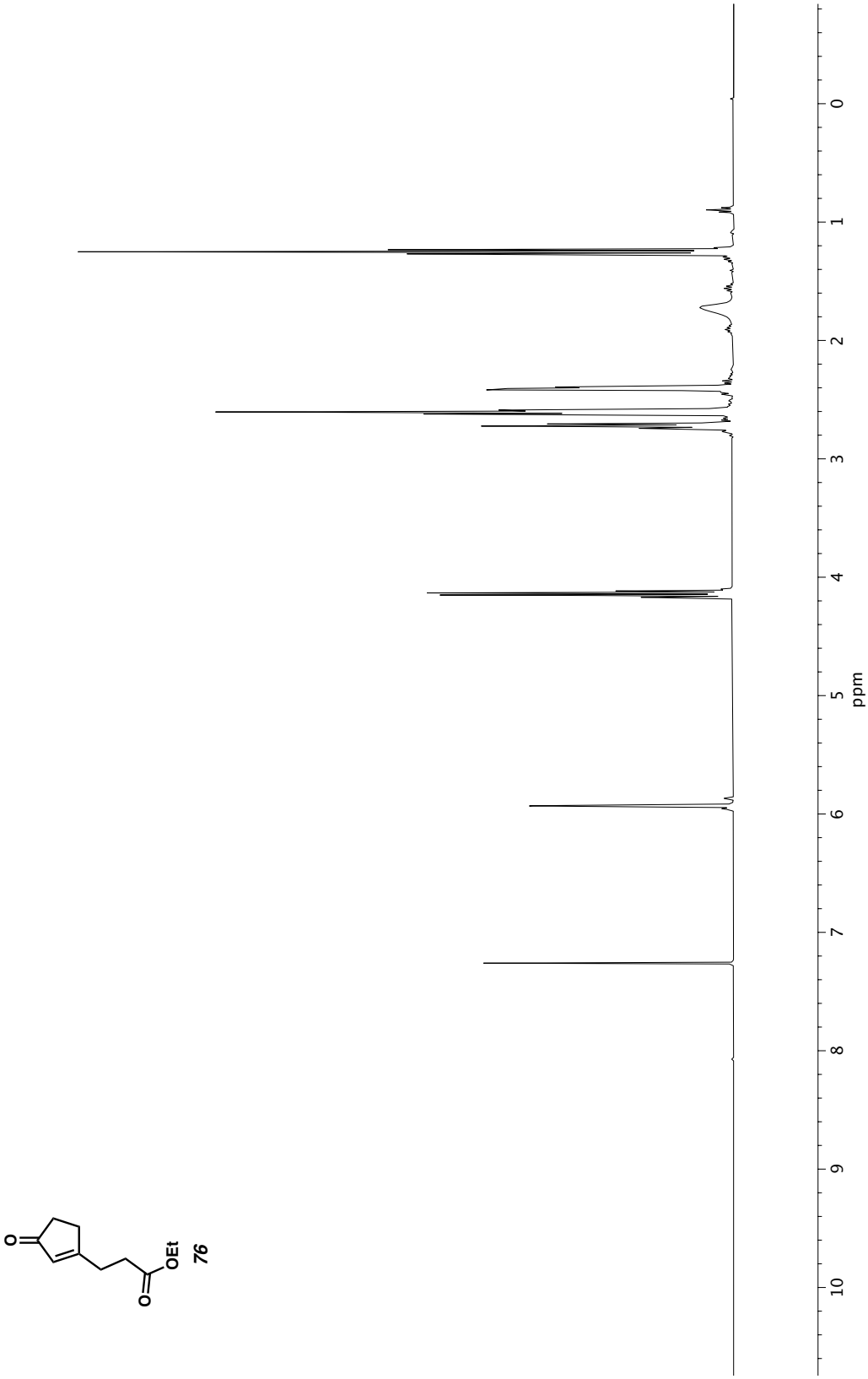


Figure A3.7 *^1H NMR (400 MHz, $CDCl_3$) of compound **76**.*

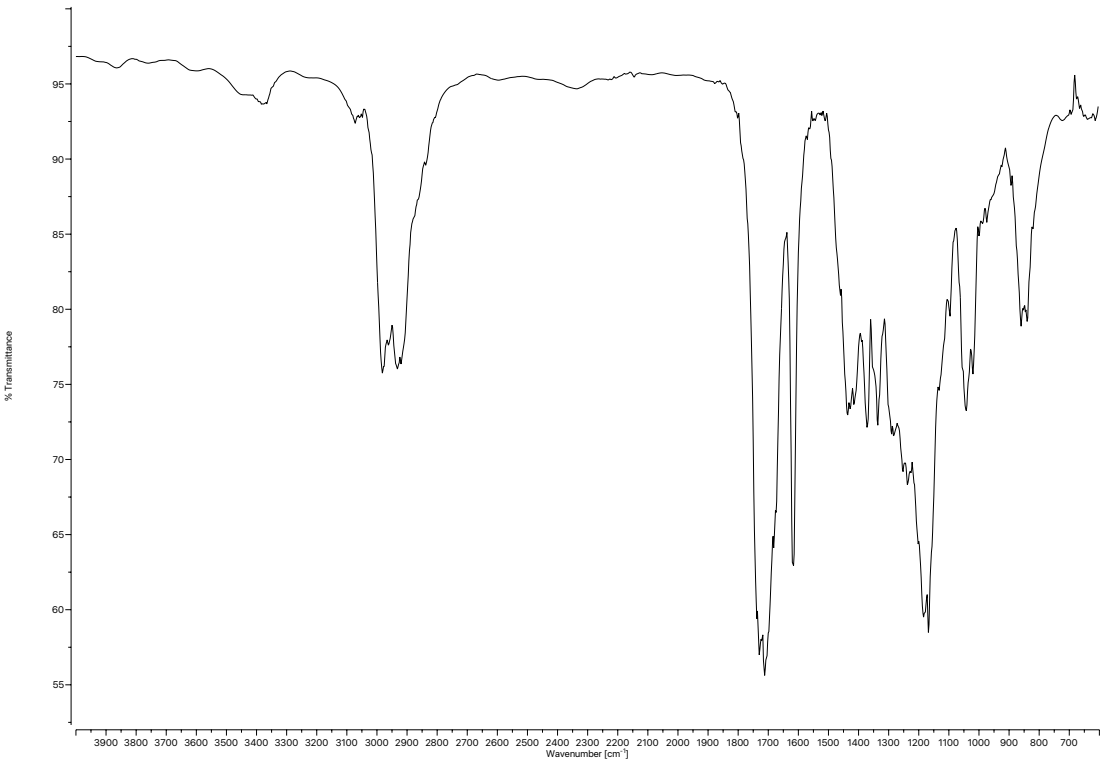


Figure A3.8 *Infrared spectrum (Thin Film, NaCl) of compound* ***76****.*

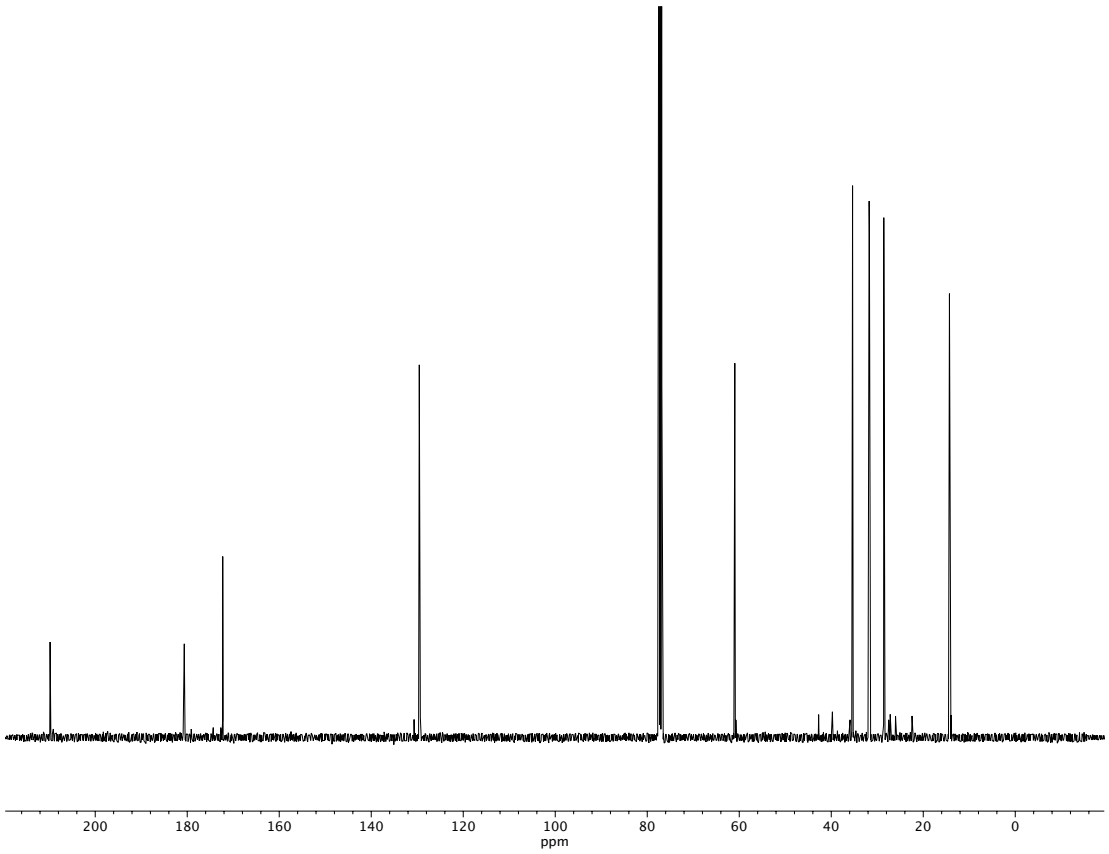


Figure A3.9 *^{13}C NMR (100 MHz, $CDCl_3$) of compound* ***76****.*

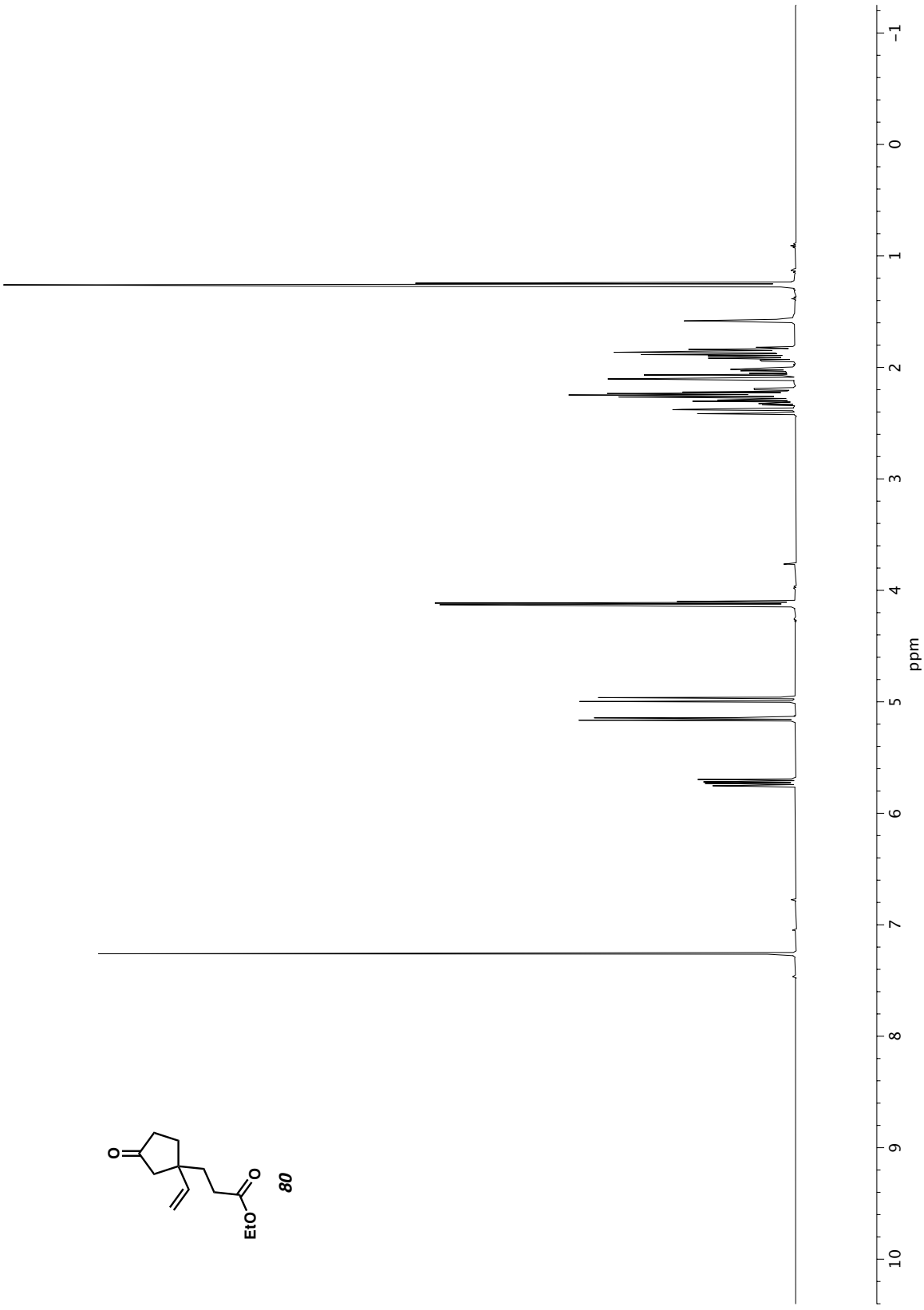


Figure A3.10 *^{1}H NMR (500 MHz, $CDCl_3$) of compound* ***80***.

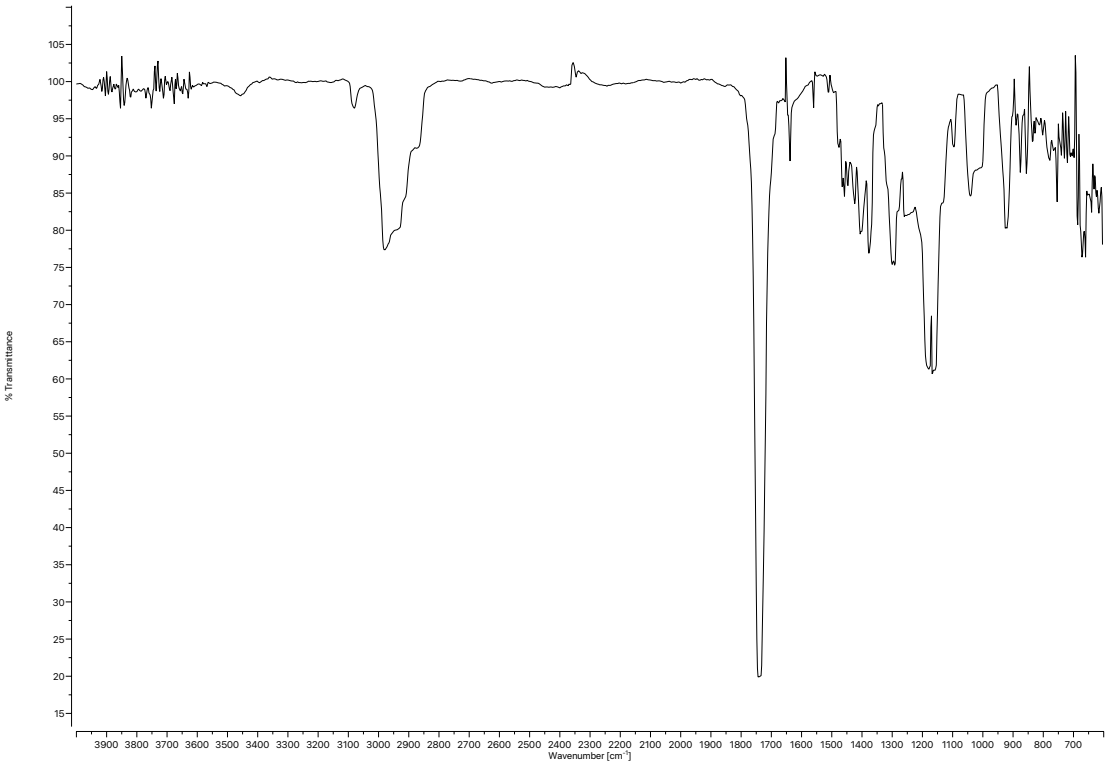


Figure A3.11 *Infrared spectrum (Thin Film, NaCl) of compound* ***80***.

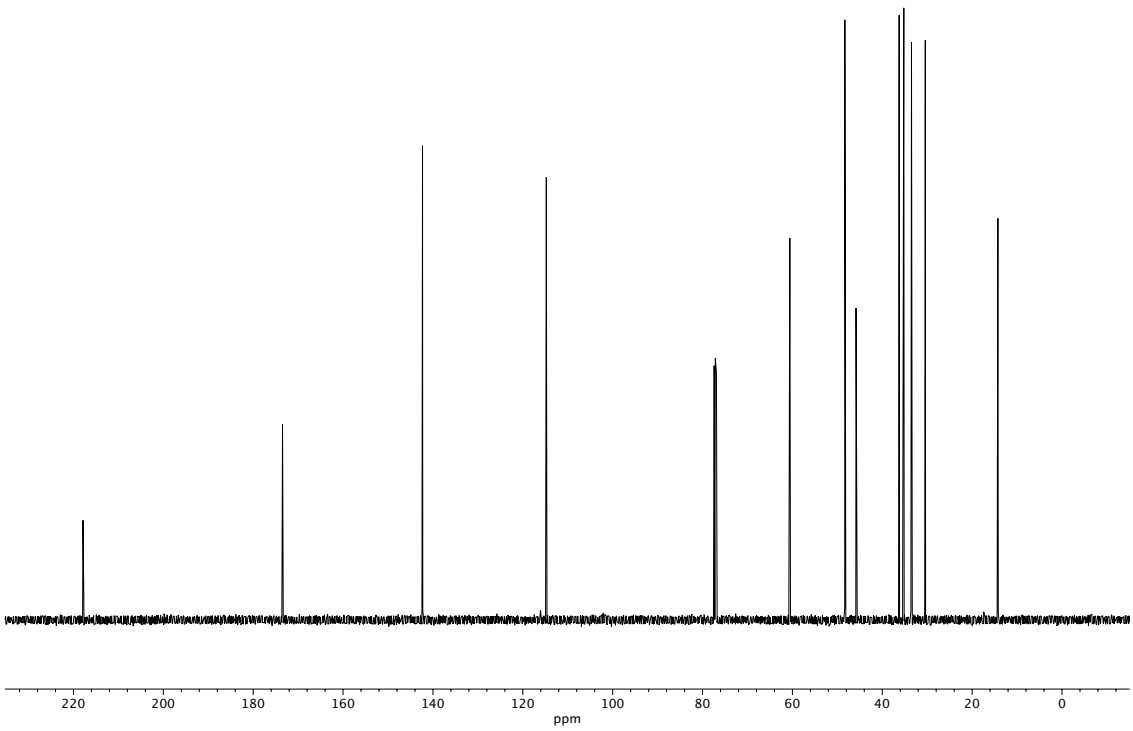


Figure A3.12 *^{13}C NMR (125 MHz, $CDCl_3$) of compound* ***80***.

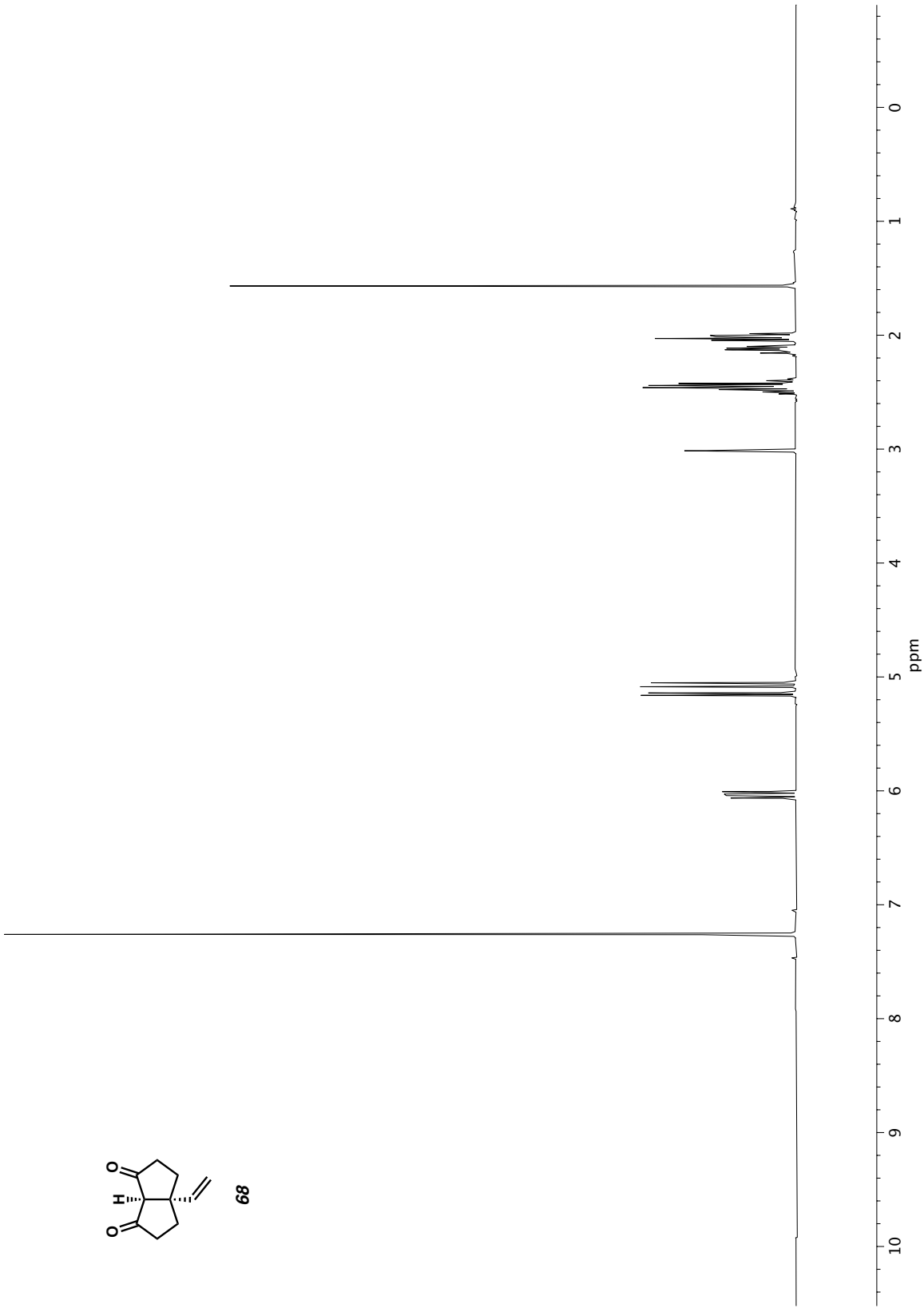


Figure A3.13 *^{1}H NMR (500 MHz, $CDCl_3$) of compound **68**.*

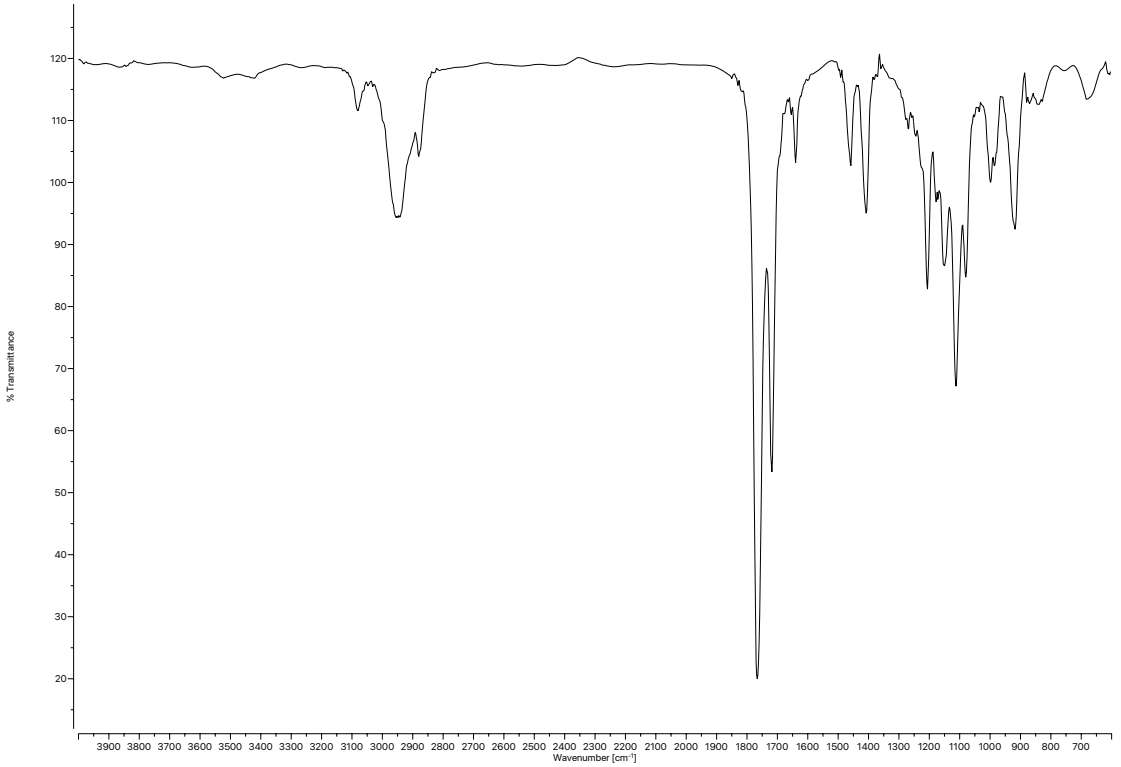


Figure A3.14 *Infrared spectrum (Thin Film, NaCl) of compound* ***68****.*

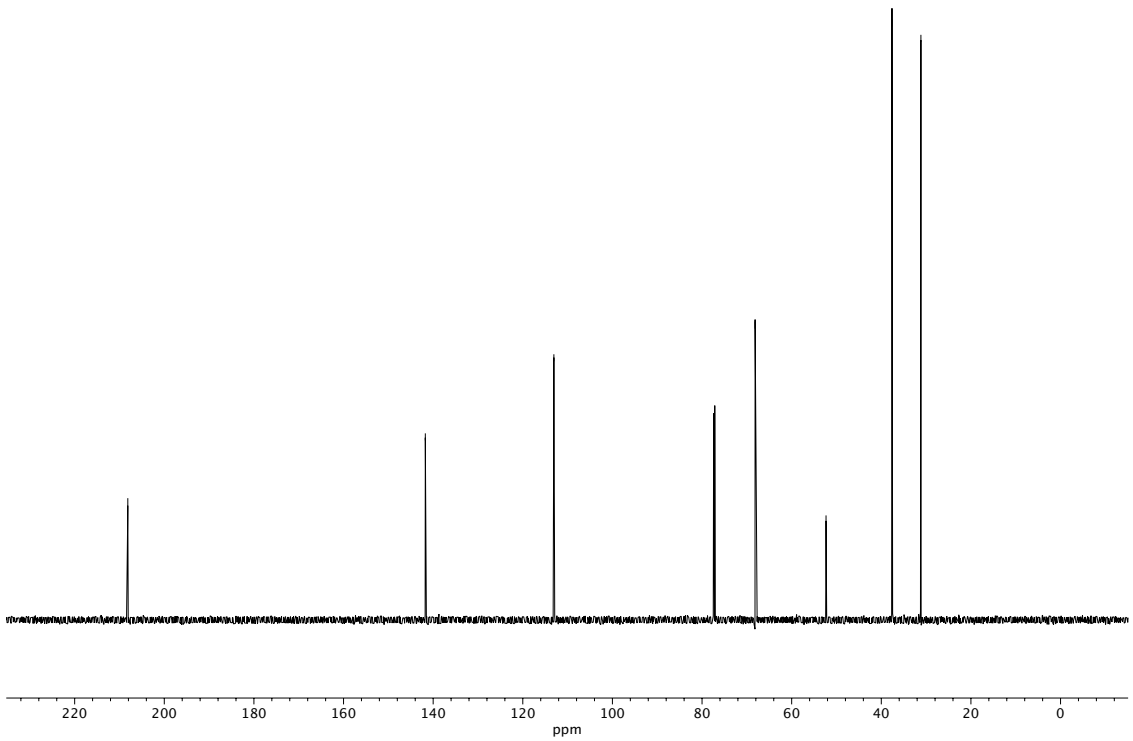
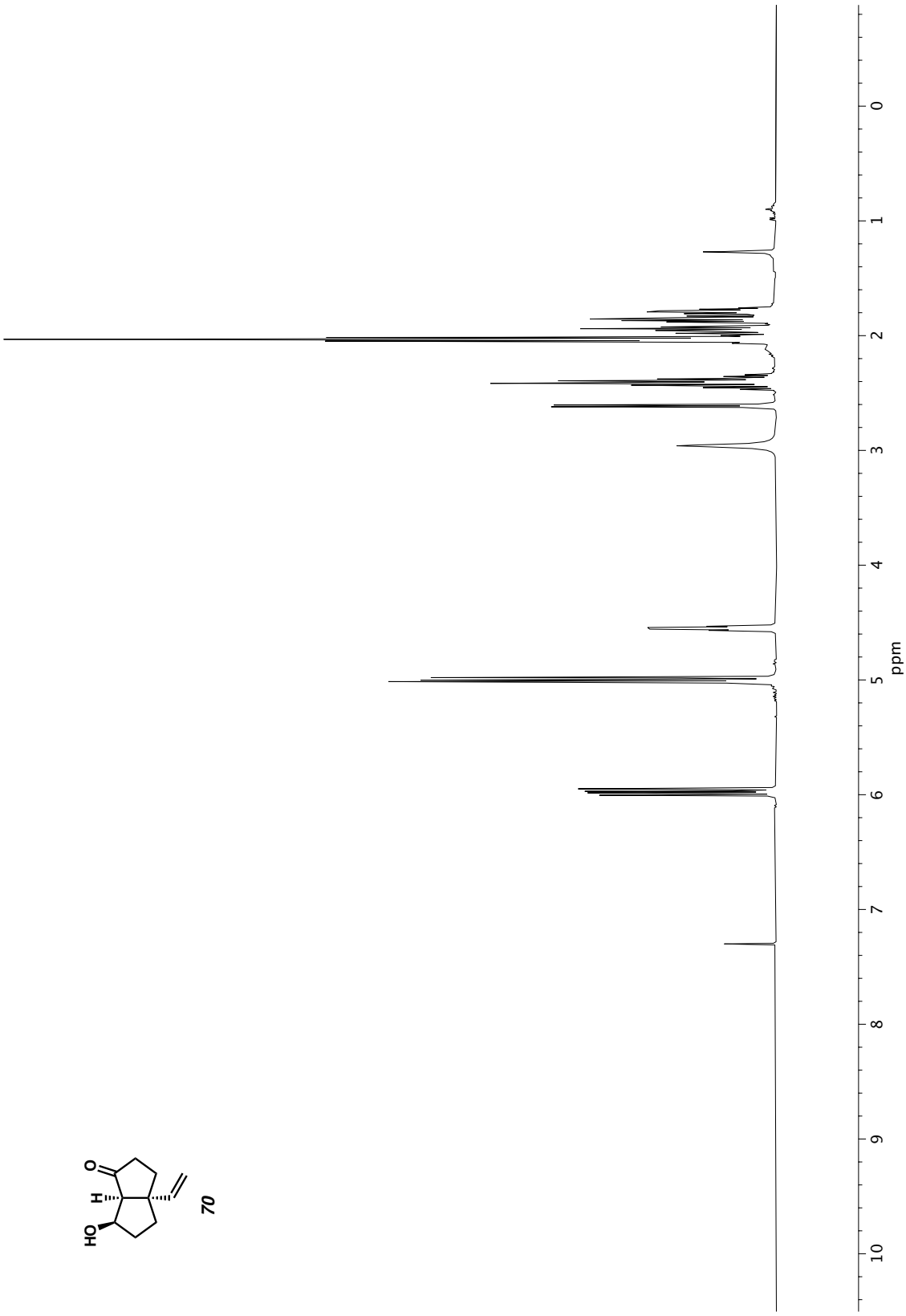


Figure A3.15 *^{13}C NMR (125 MHz, $CDCl_3$) of compound* ***68****.*



70

Figure A3.16 *^1H NMR (500 MHz, $CDCl_3$) of compound **70**.*

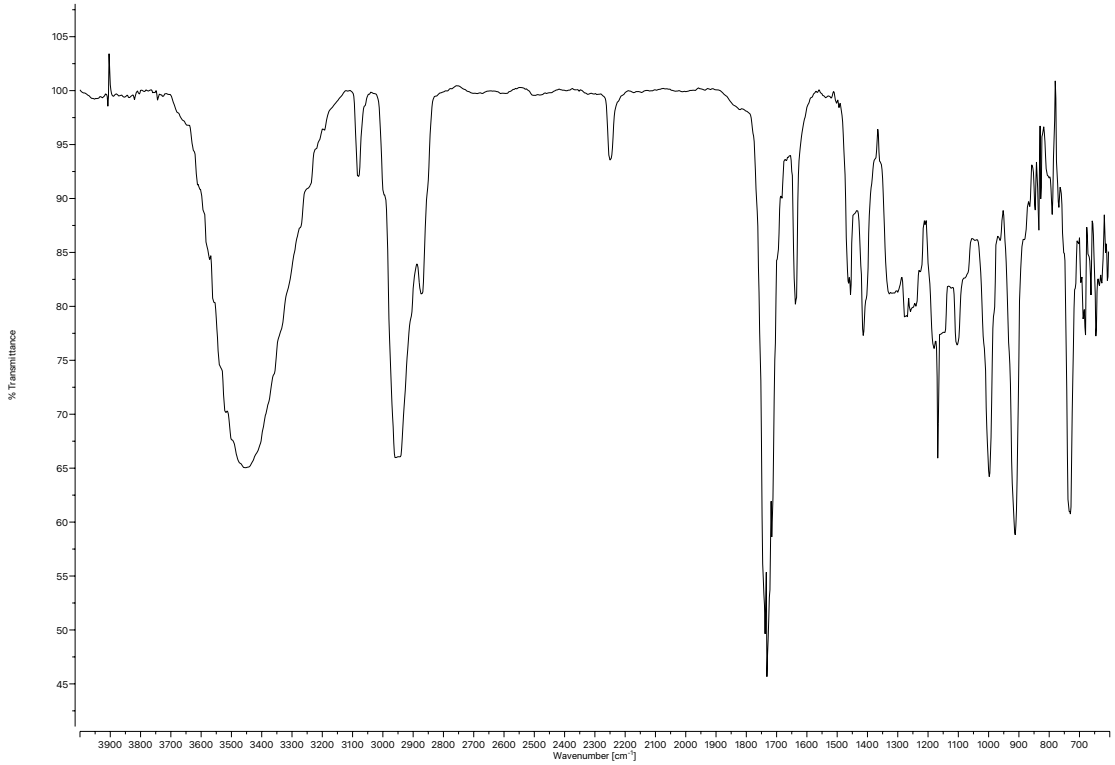


Figure A3.17 *Infrared spectrum (Thin Film, NaCl) of compound* ***70****.*

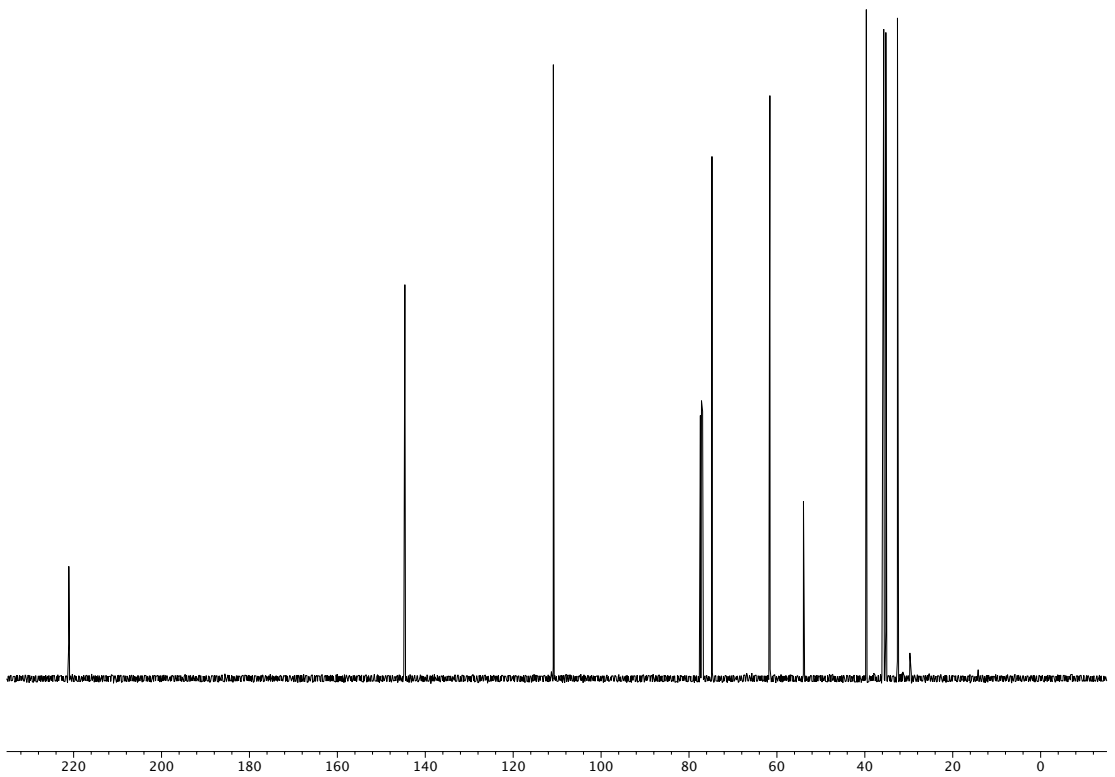


Figure A3.18 *^{13}C NMR (125 MHz, $CDCl_3$) of compound* ***70****.*

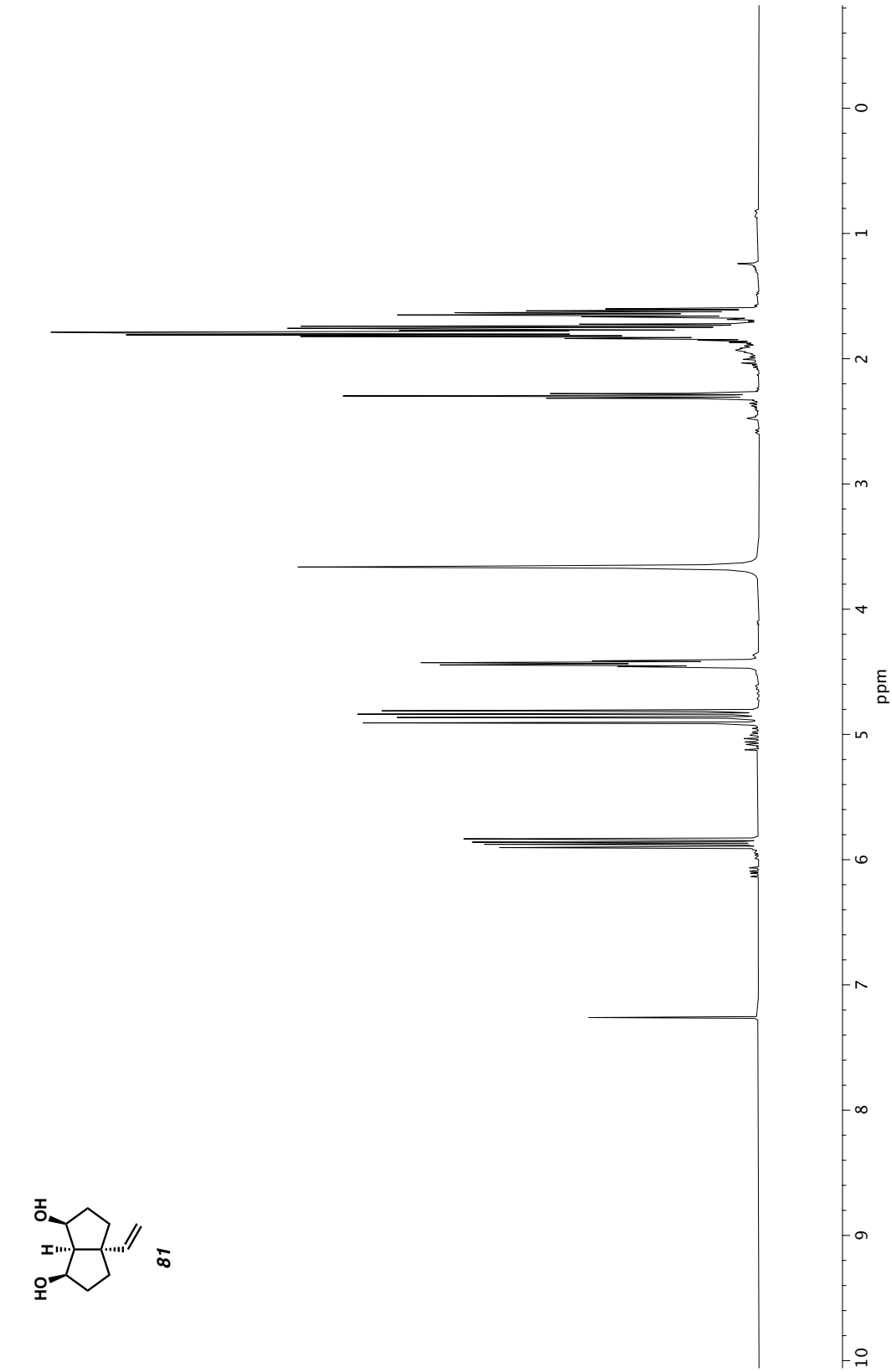


Figure A3.19 *^{1}H NMR (400 MHz, $CDCl_3$) of compound **81**.*

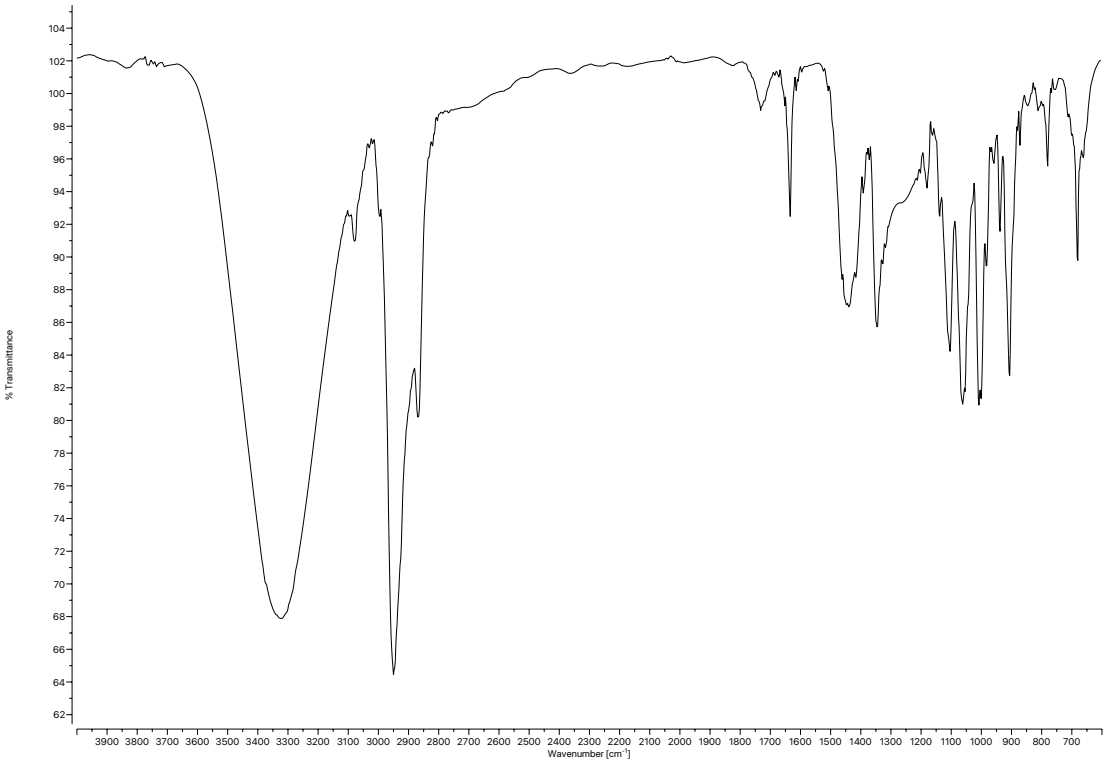


Figure A3.20 *Infrared spectrum (Thin Film, NaCl) of compound* ***81***.

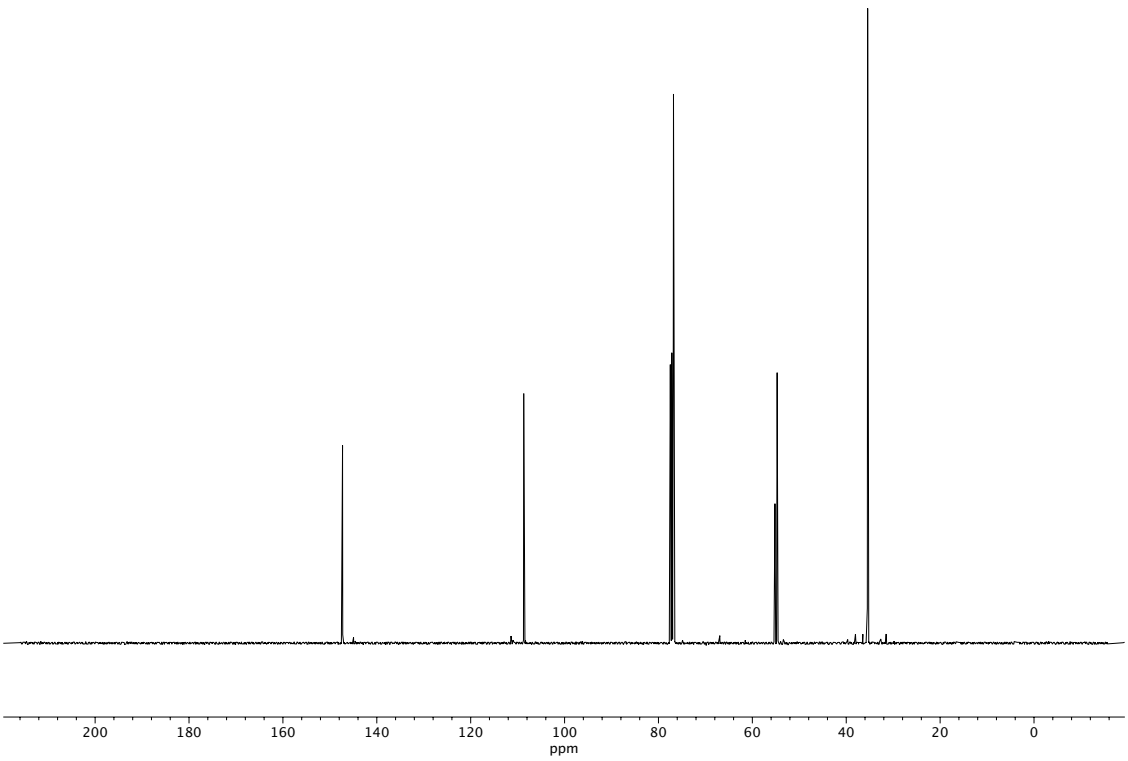


Figure A1.21 *^{13}C NMR (100 MHz, $CDCl_3$) of compound* ***81***.

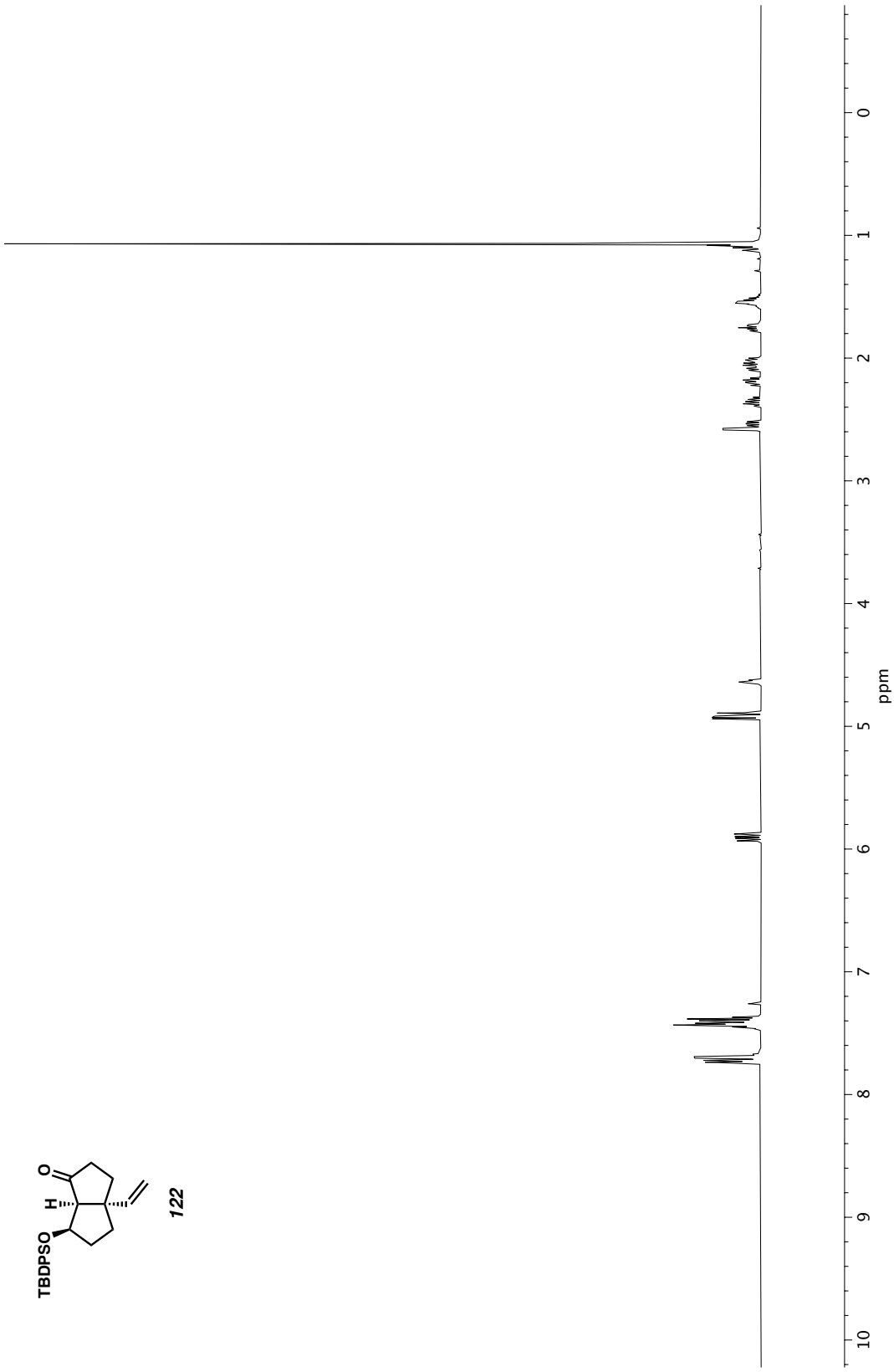


Figure A3.22 *^1H NMR (500 MHz, $CDCl_3$) of compound* ***122***.

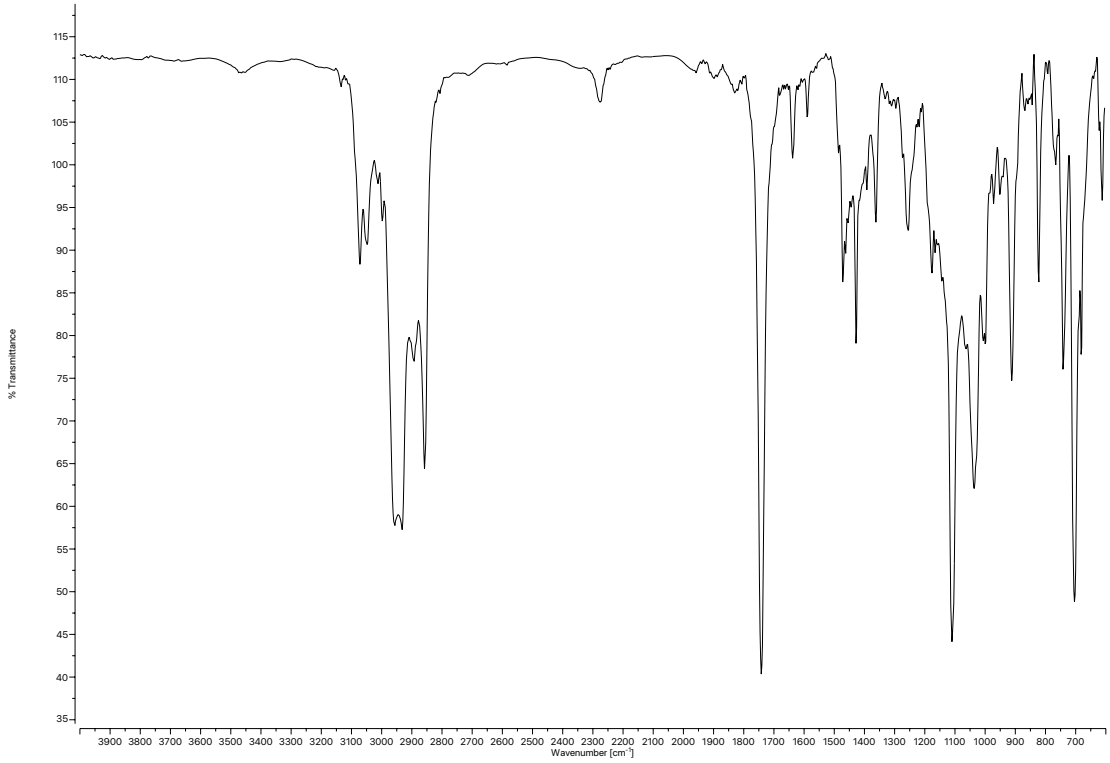


Figure A3.23 *Infrared spectrum (Thin Film, NaCl) of compound* ***122***.

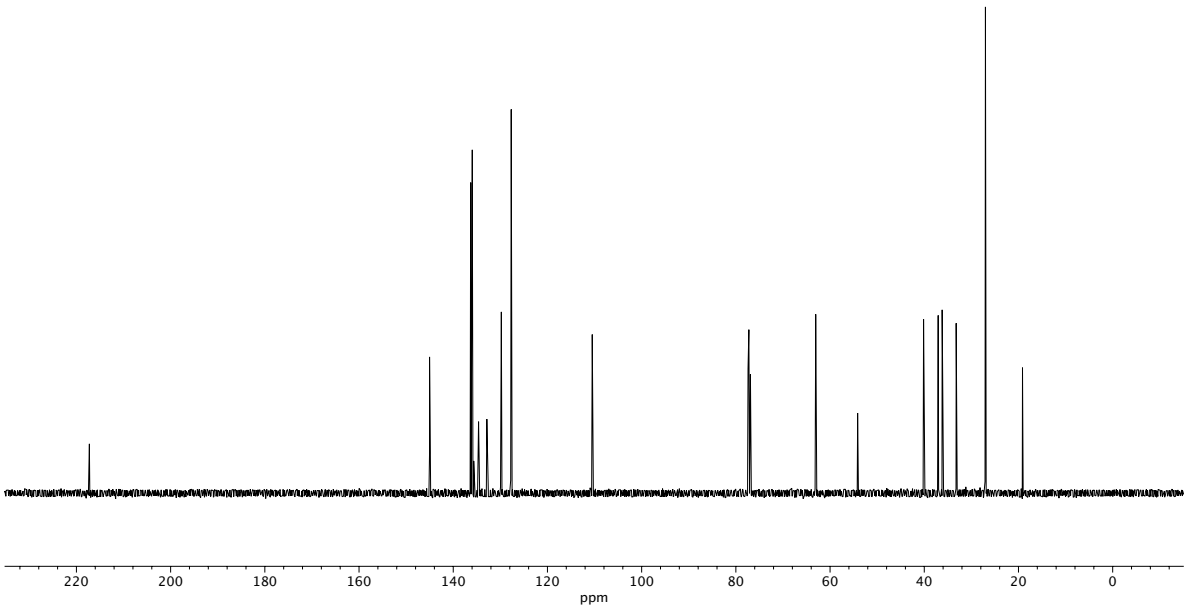


Figure A3.24 *^{13}C NMR (125 MHz, $CDCl_3$) of compound* ***122***.

Figure A3.25 *^1H NMR (400 MHz, $CDCl_3$) of compound* ***(Z)-82***.

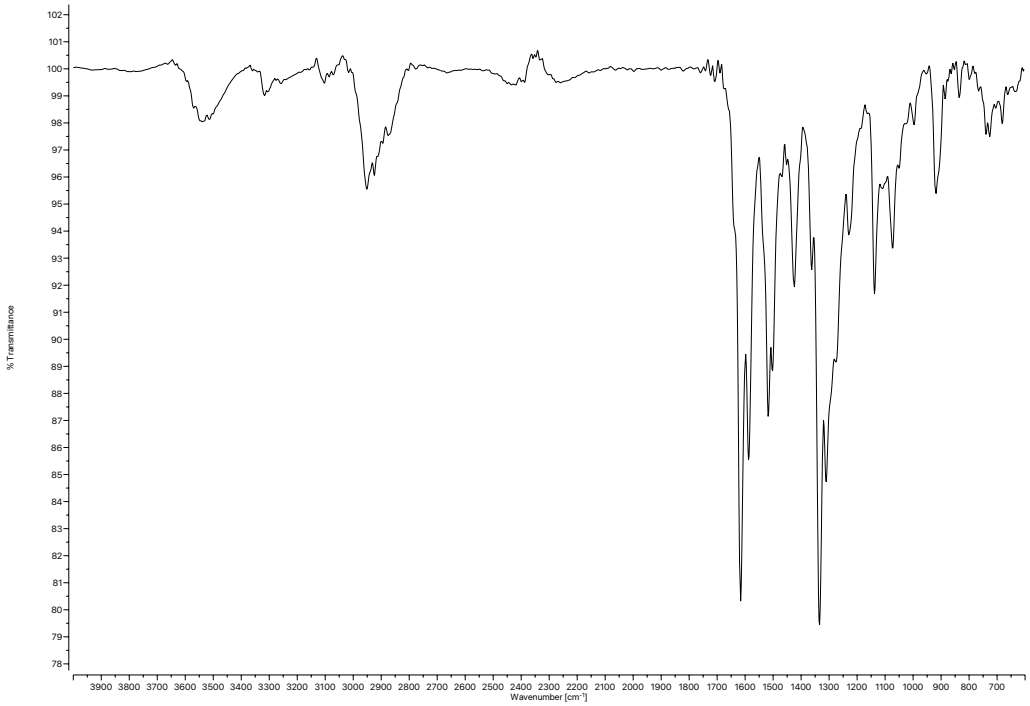


Figure A3.26 *Infrared spectrum (Thin Film, NaCl) of compound* ***82***.

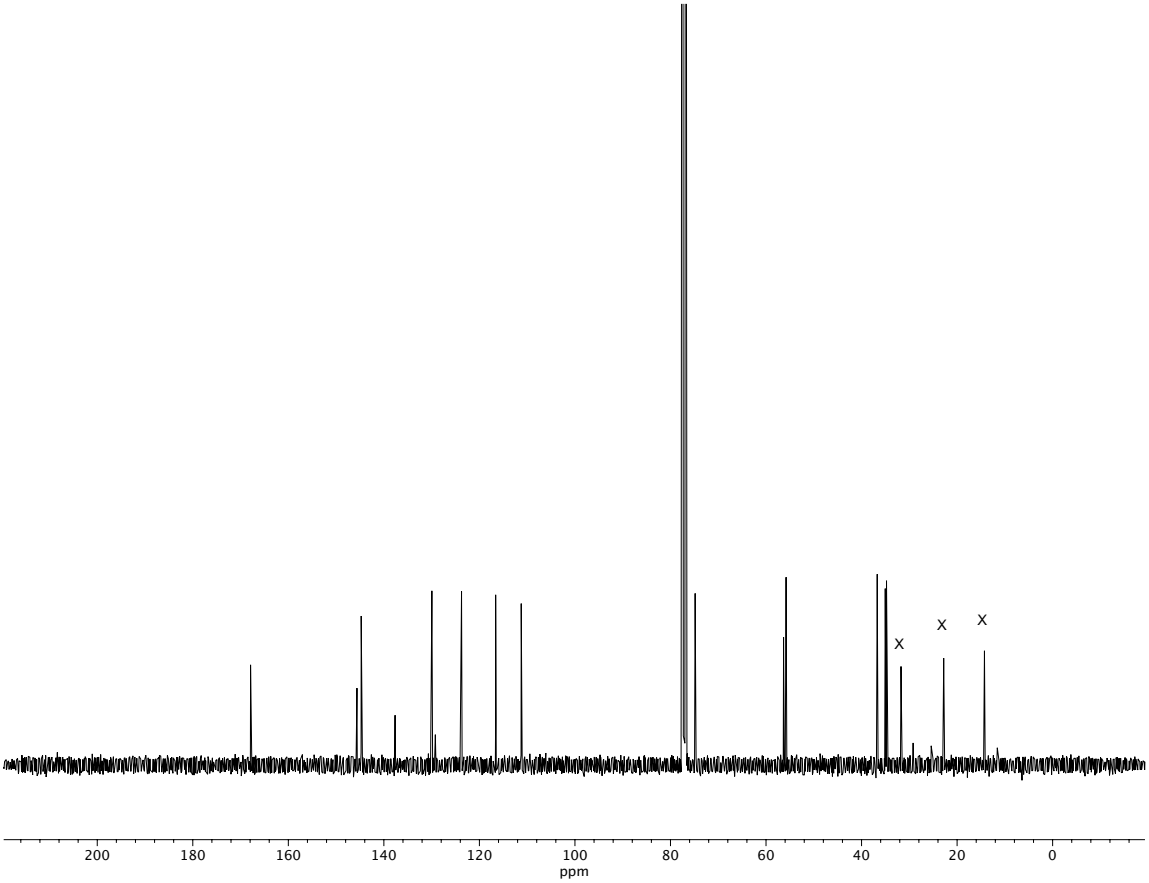
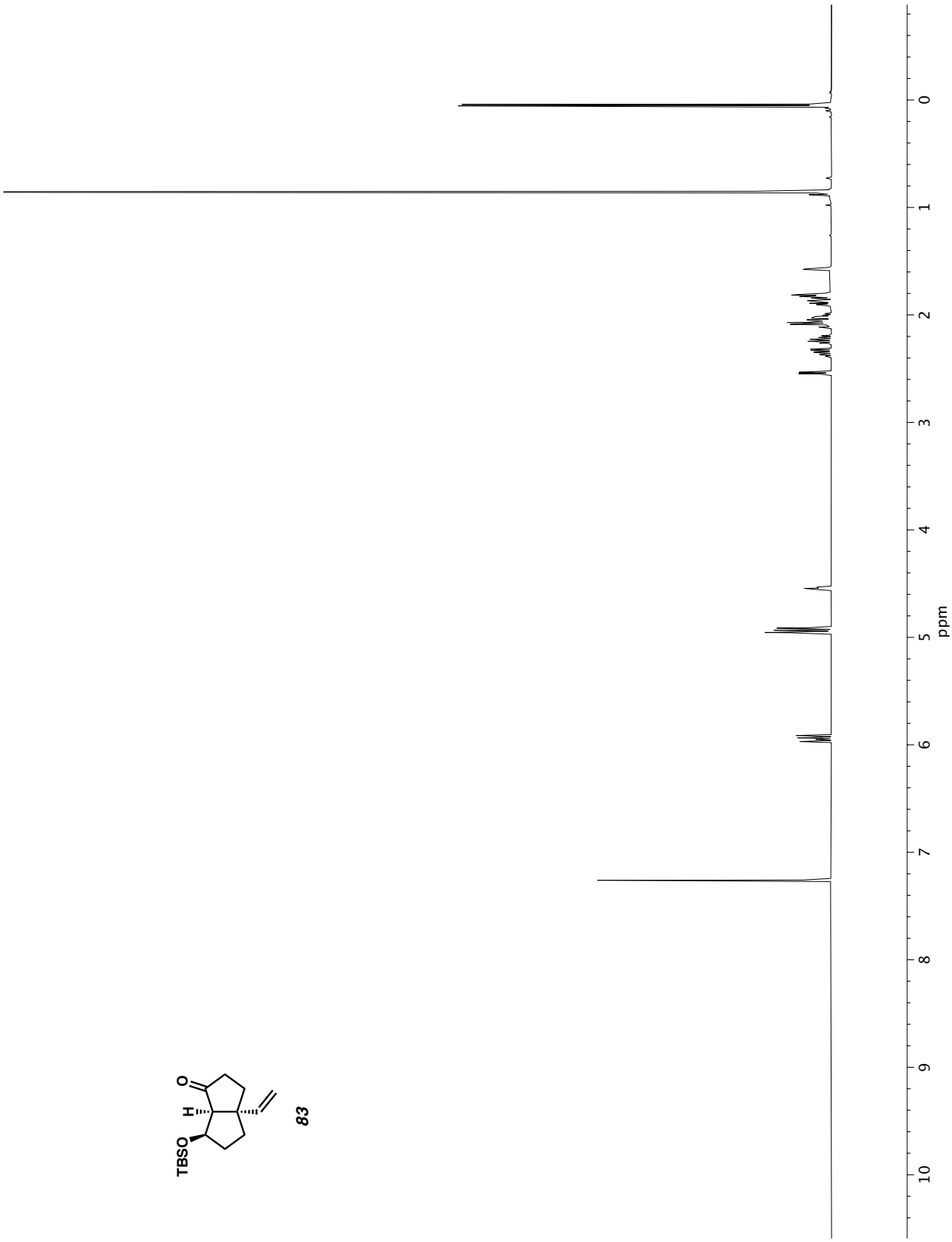


Figure A3.27 *^{13}C NMR (100 MHz, $CDCl_3$) of compound* ***82***.



83

Figure A3.28 *^{1}H NMR (500 MHz, $CDCl_3$) of compound* ***83****.*

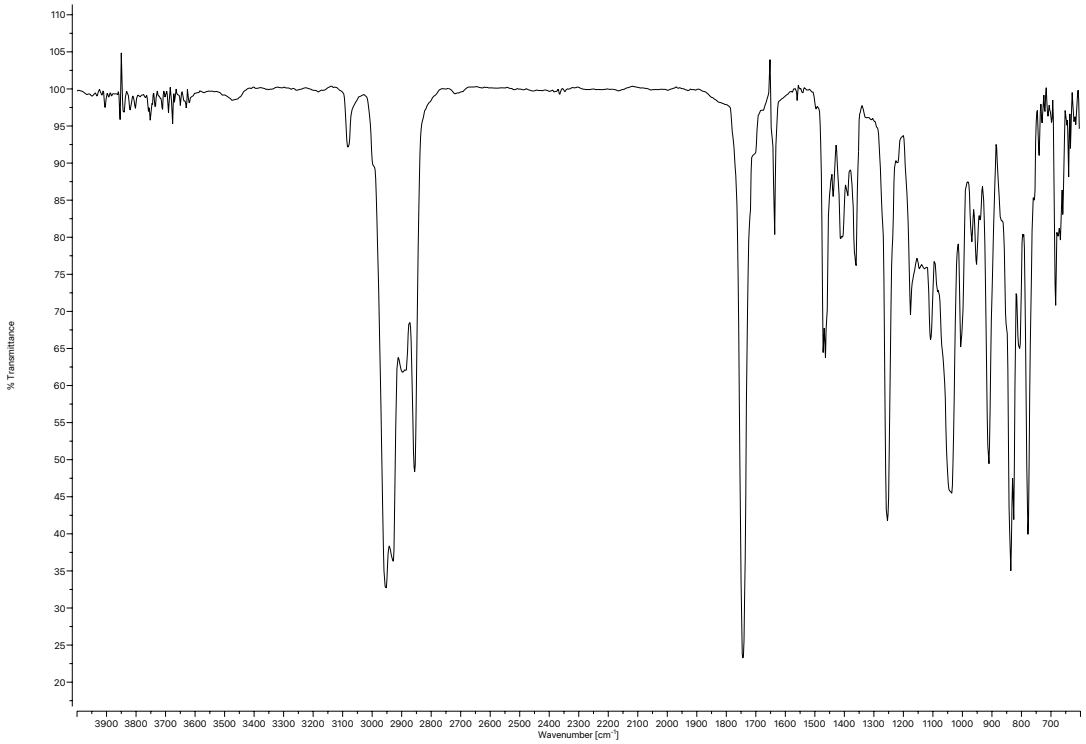


Figure A3.29 *Infrared spectrum (Thin Film, NaCl) of compound* ***83***.

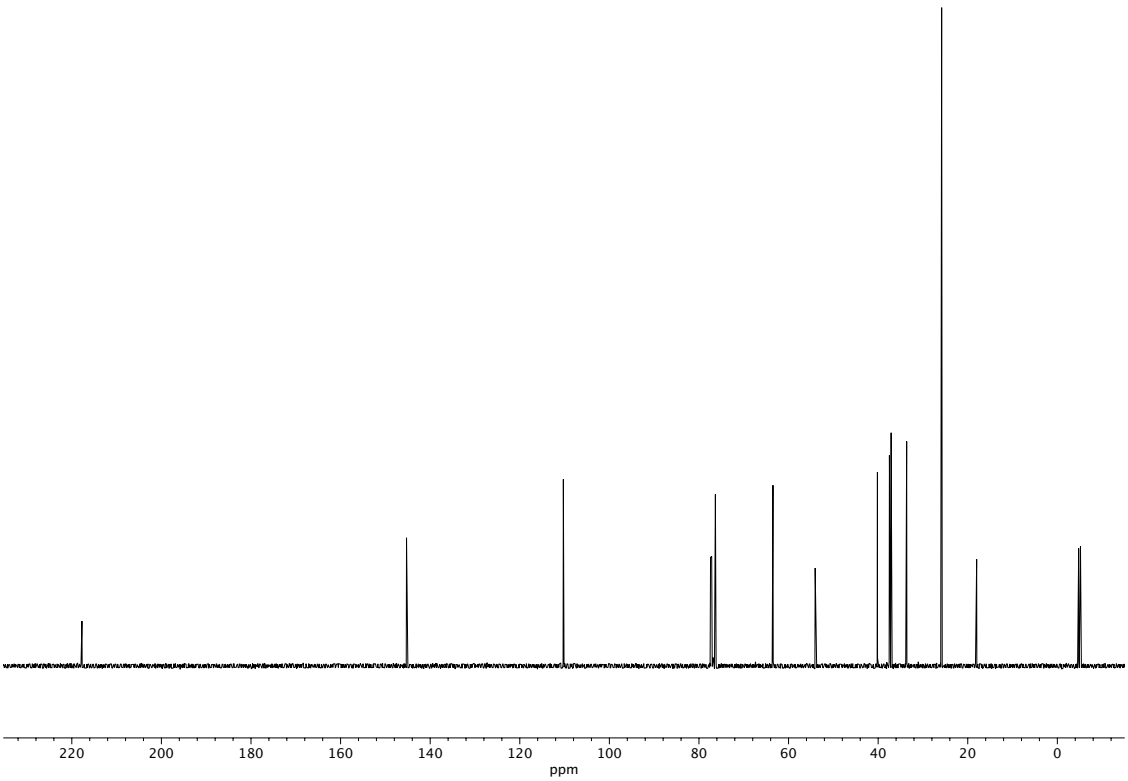
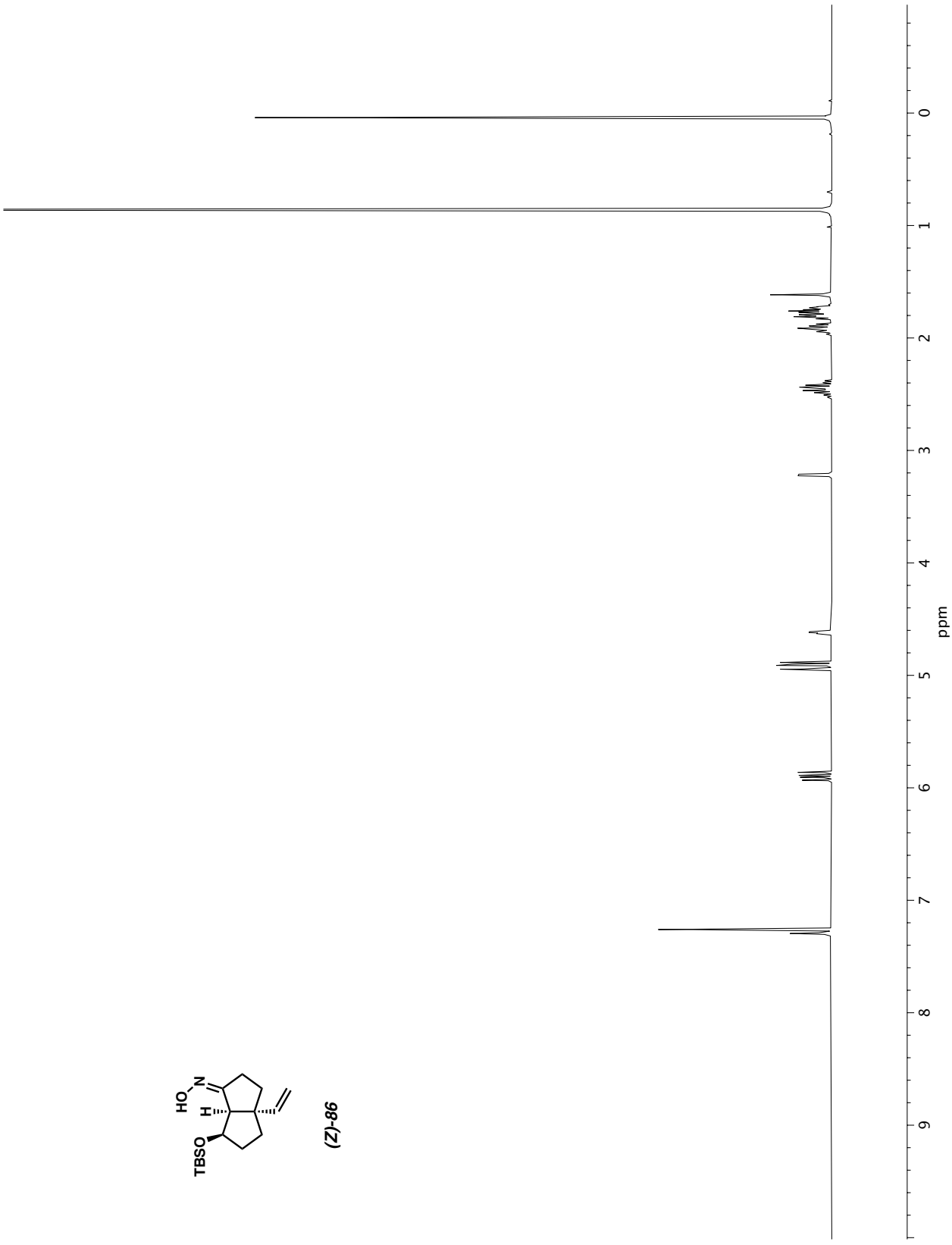


Figure A3.30 *^{13}C NMR (125 MHz, $CDCl_3$) of compound* ***83***.



(Z)-86

Figure A3.31 *^1H NMR (400 MHz, $CDCl_3$) of compound* ***(Z)-86****.*

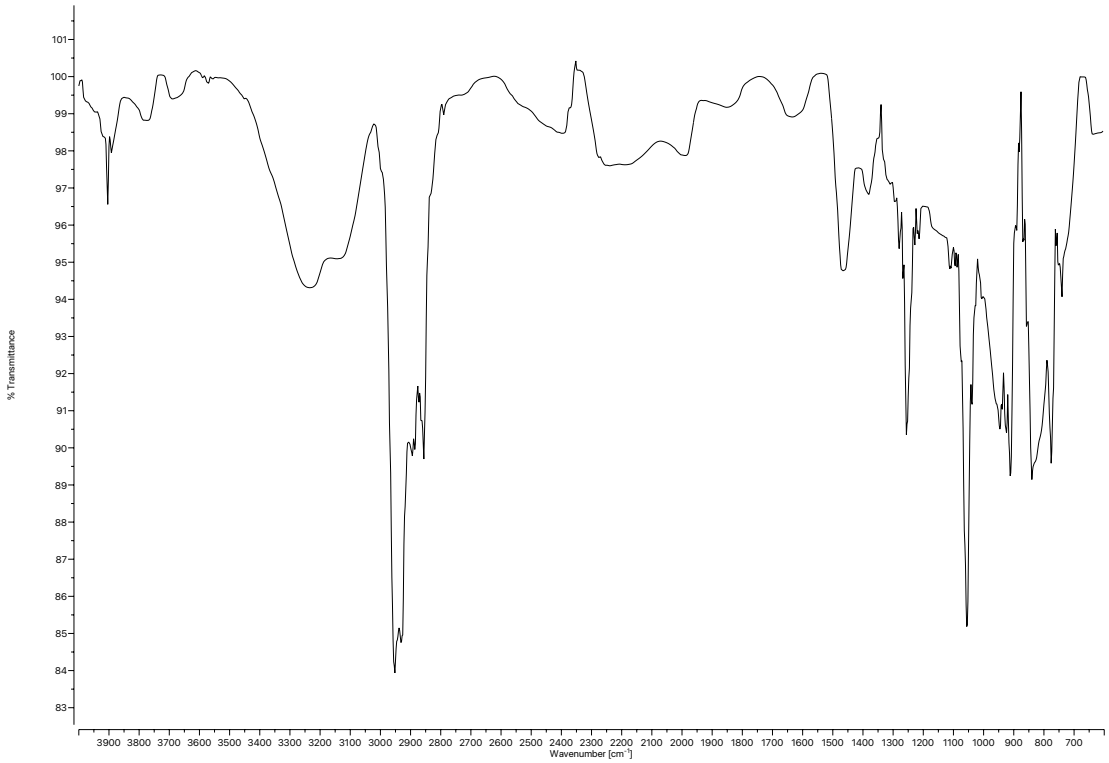


Figure A3.32 *Infrared spectrum (Thin Film, NaCl) of compound* ***(Z)-86***.

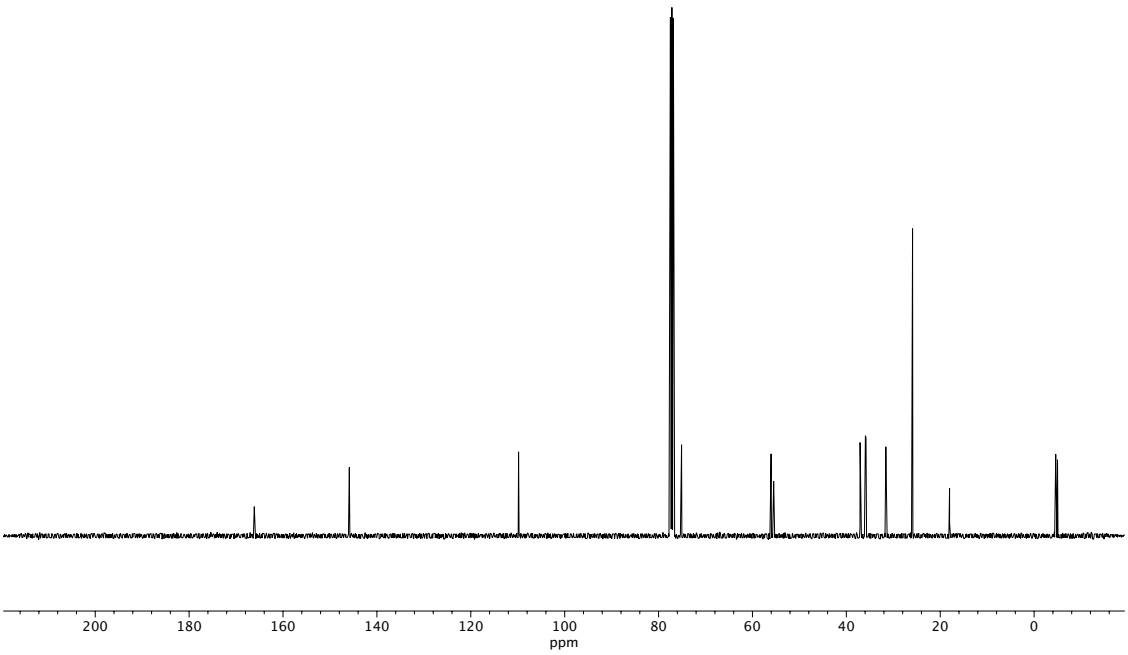


Figure A3.33 *^{13}C NMR (100 MHz, $CDCl_3$) of compound* ***(Z)-86***.

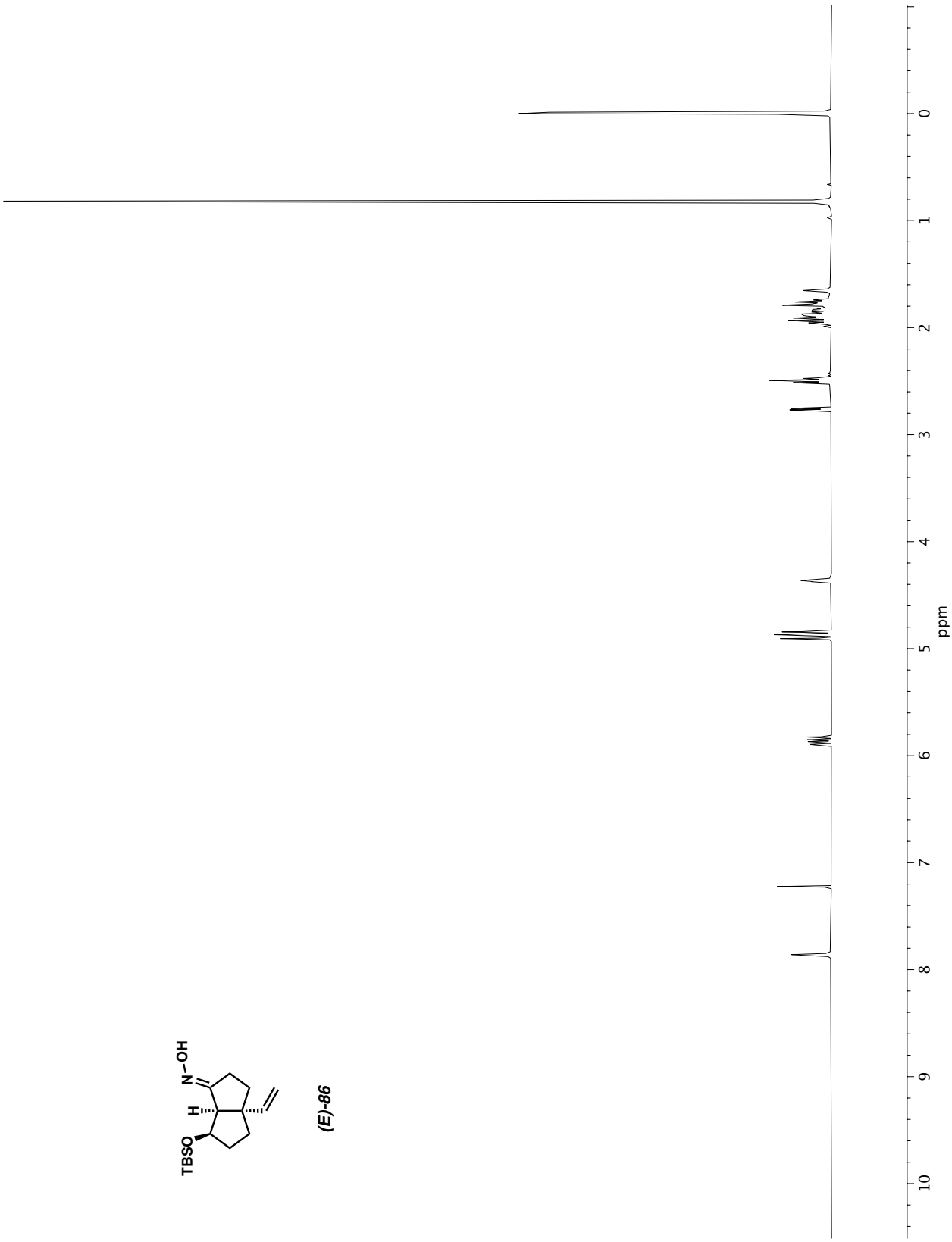


Figure A1.34 *^1H NMR (400 MHz, $CDCl_3$) of compound* ***(E)-86****.*

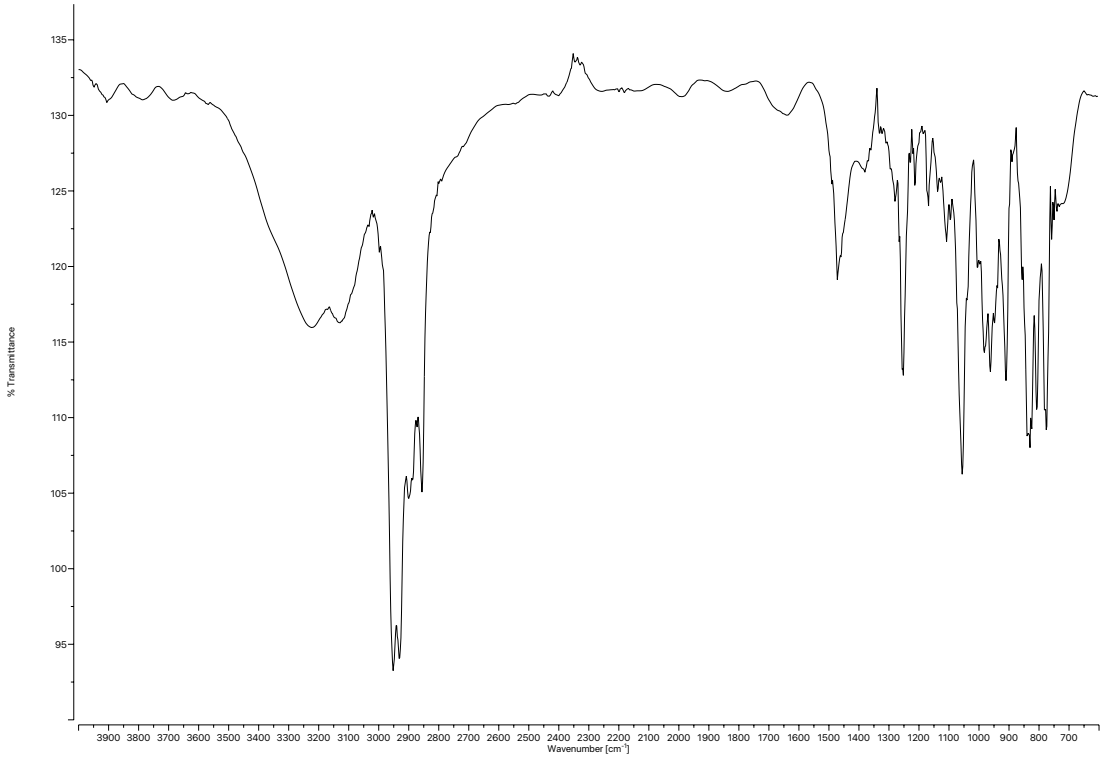


Figure A3.35 *Infrared spectrum (Thin Film, NaCl) of compound* ***(E)-86****.*

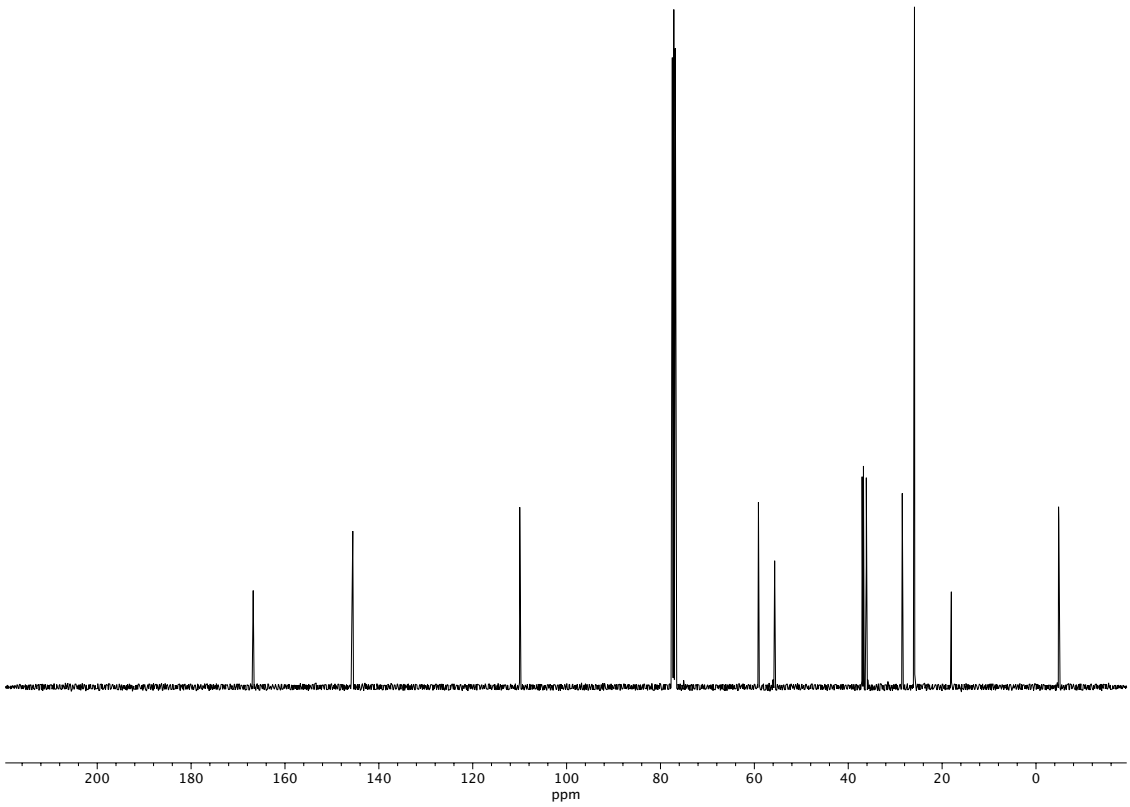


Figure A3.36 *^{13}C NMR (100 MHz, $CDCl_3$) of compound* ***(E)-86****.*

Figure A3.37 *^{1}H NMR (400 MHz, $CDCl_3$) of compound* ***87****.*

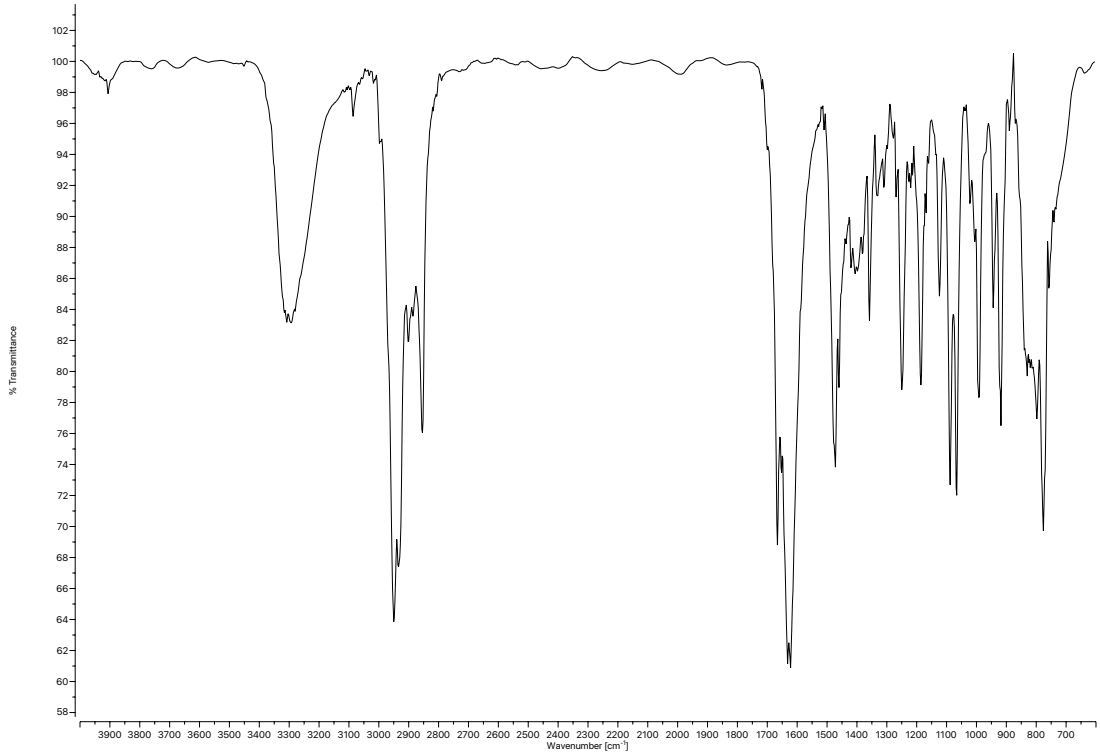


Figure A3.38 *Infrared spectrum (Thin Film, NaCl) of compound* ***87***.

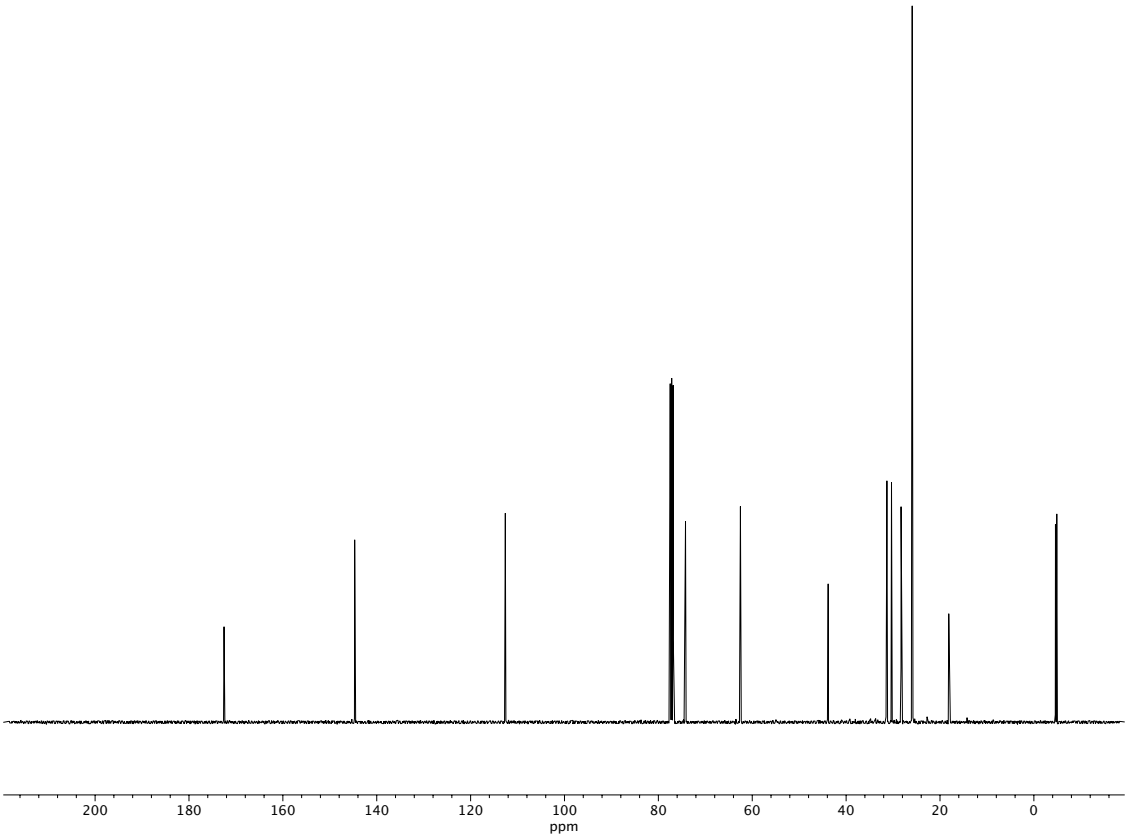
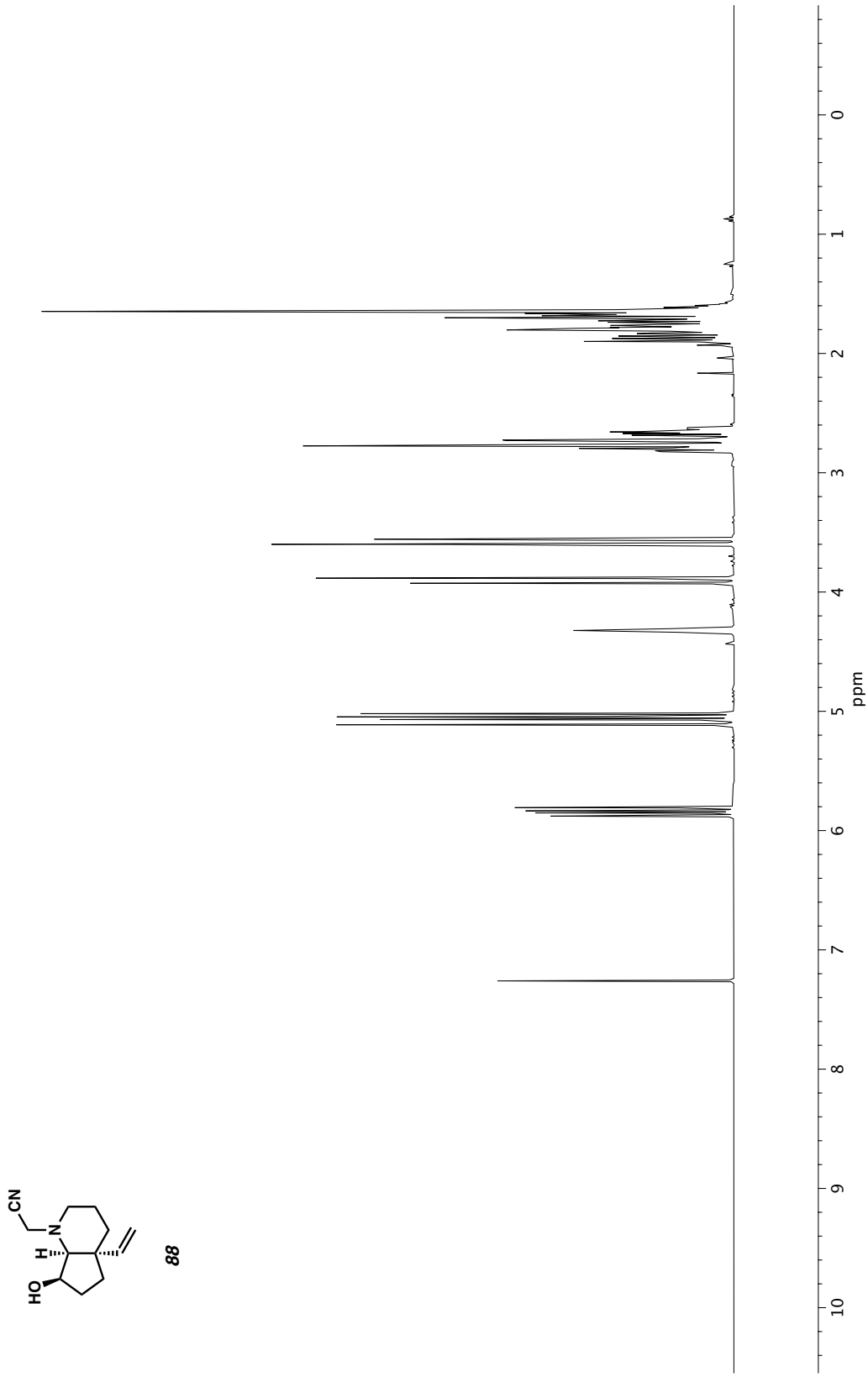


Figure A3.39 *^{13}C NMR (100 MHz, $CDCl_3$) of compound* ***87***.



88

Figure A3.40 *^{1}H NMR (400 MHz, $CDCl_3$) of compound **88**.*

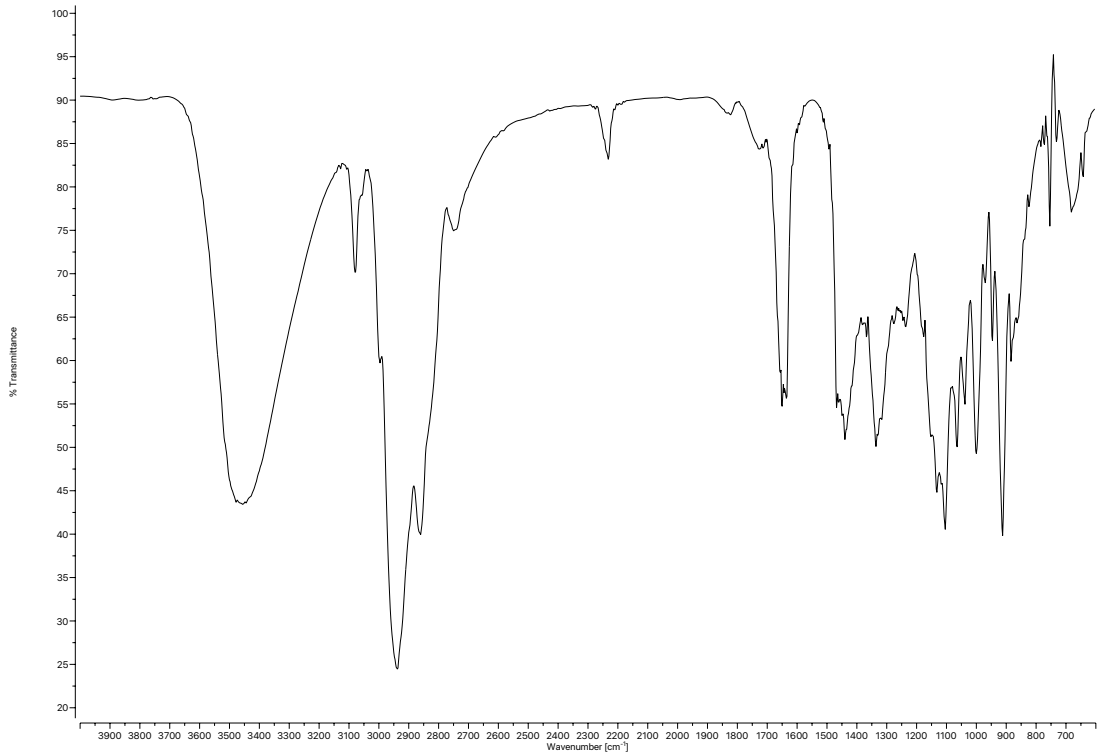


Figure A3.41 *Infrared spectrum (Thin Film, NaCl) of compound* ***88***.

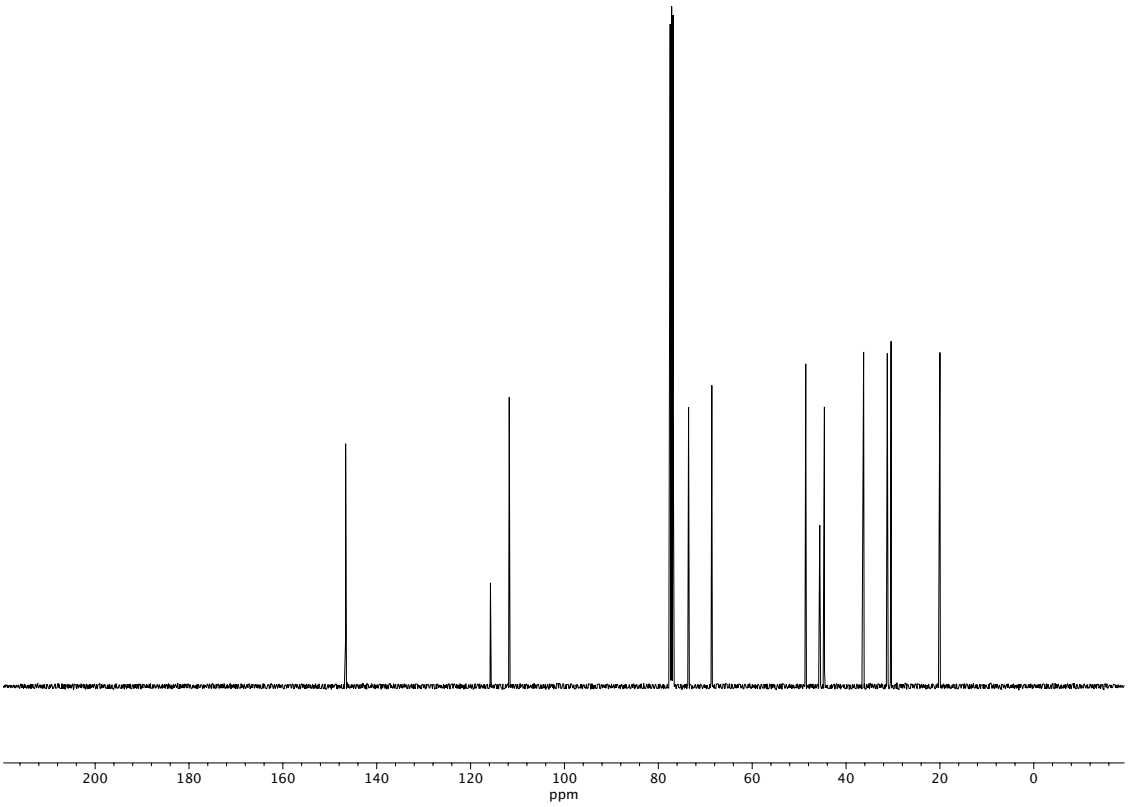


Figure A3.42 *^{13}C NMR (100 MHz, $CDCl_3$) of compound* ***88***.

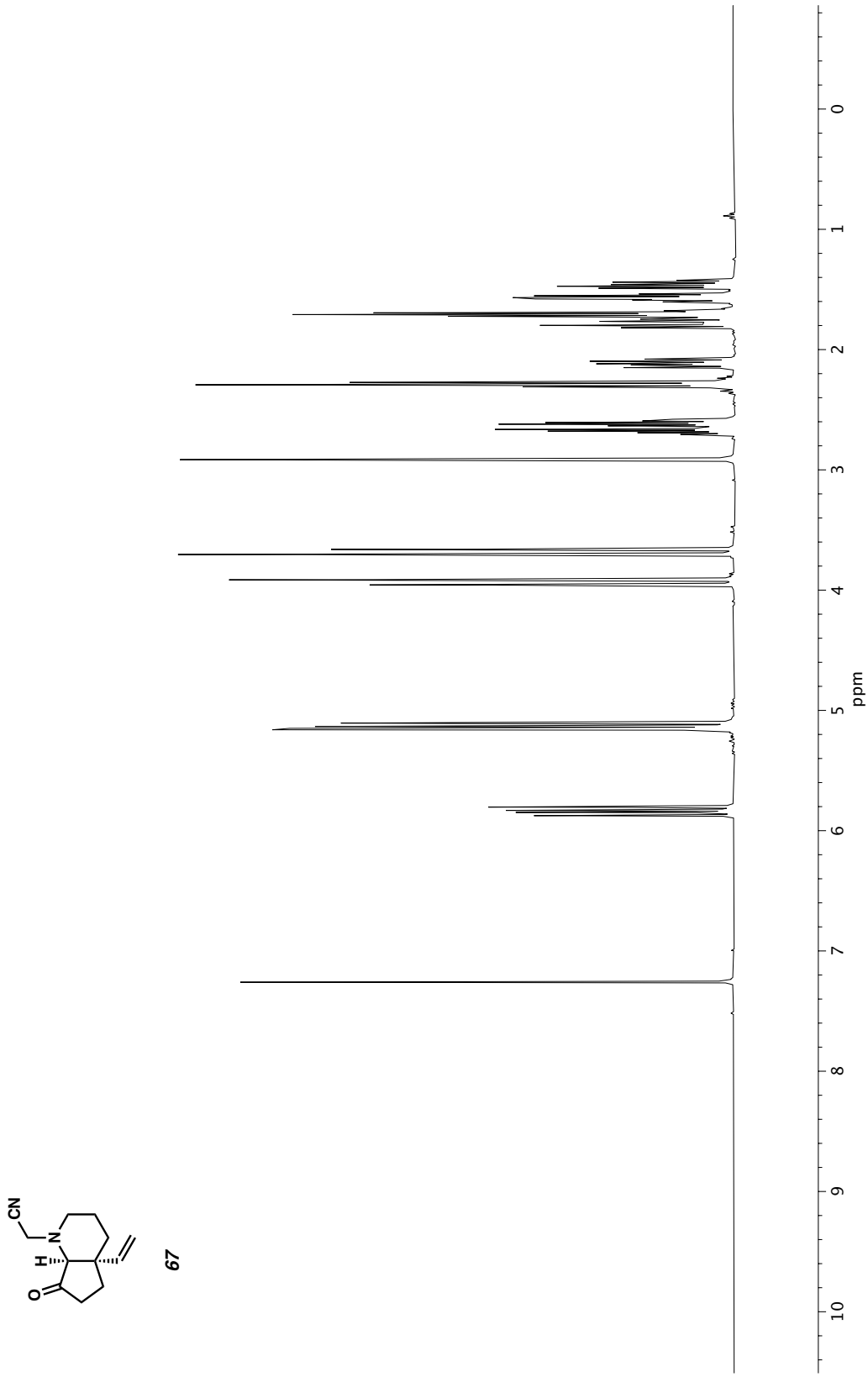


Figure A3.43 *^{1}H NMR (400 MHz, $CDCl_3$) of compound* ***67****.*

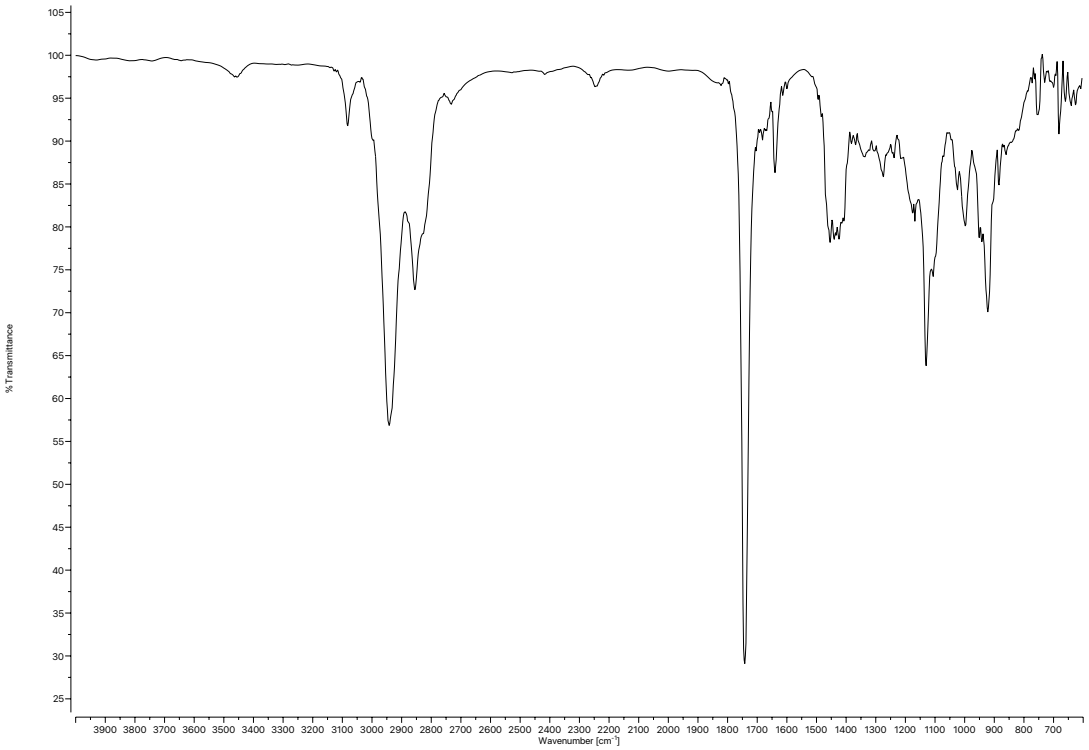


Figure A3.44 *Infrared spectrum (Thin Film, NaCl) of compound* ***67****.*

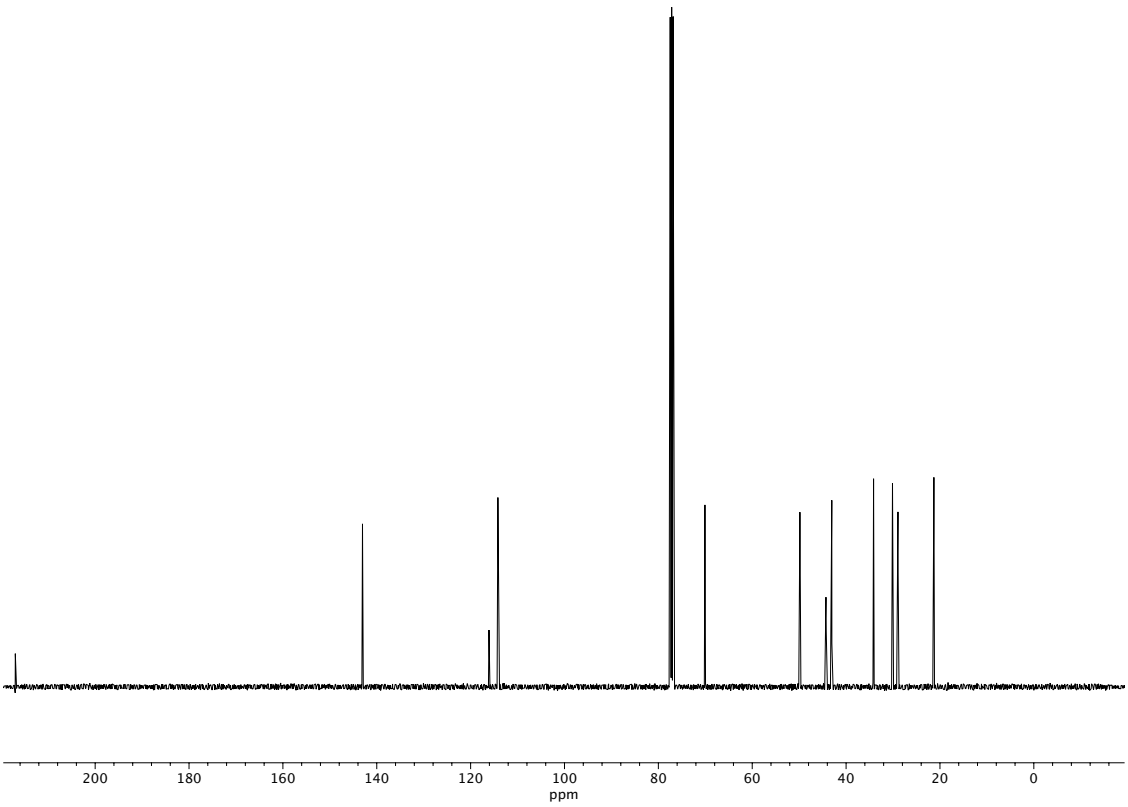


Figure A3.45 *^{13}C NMR (100 MHz, $CDCl_3$) of compound* ***67****.*

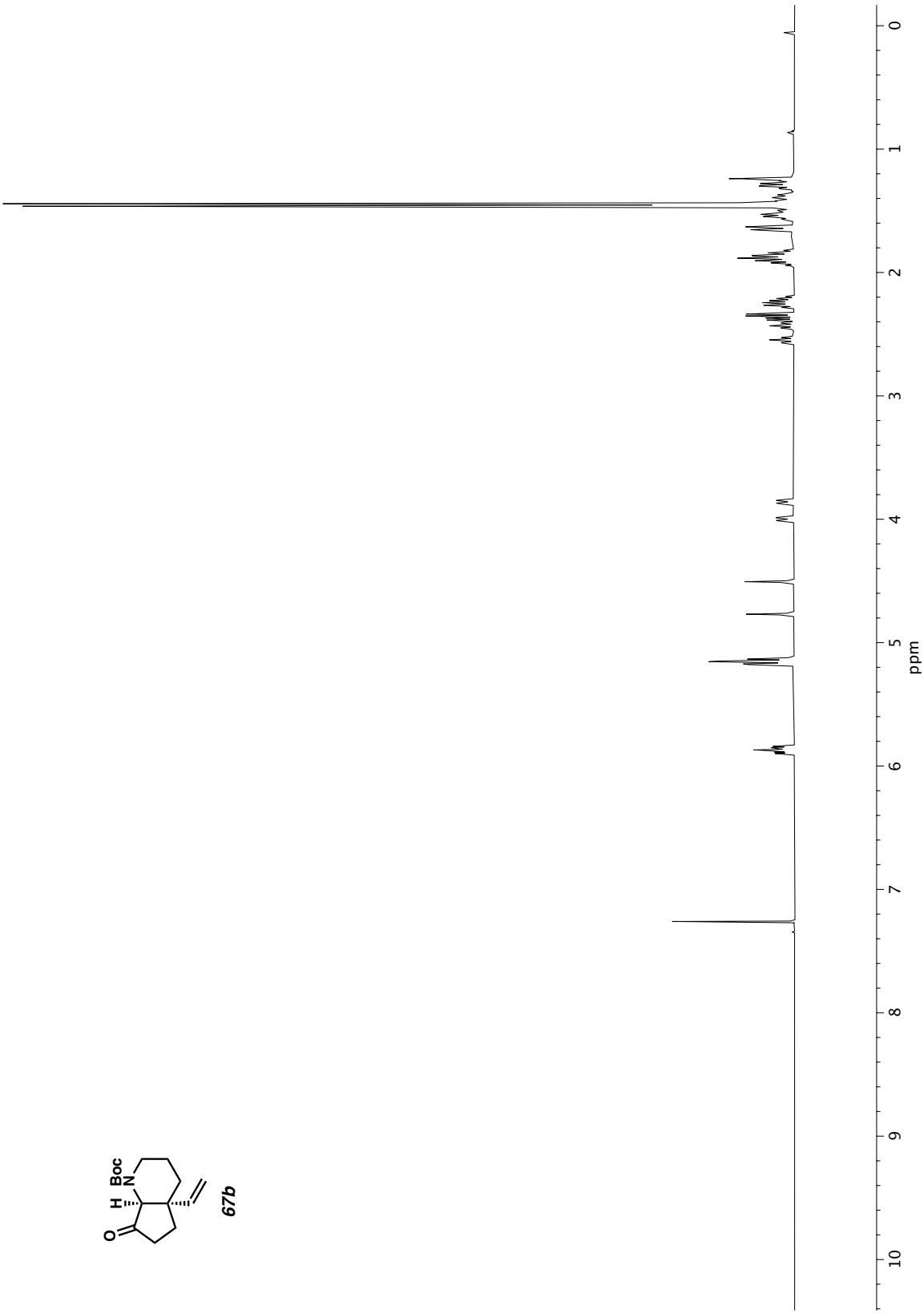


Figure A3.46 *^1H NMR (600 MHz, $CDCl_3$) of compound* ***67b****.*

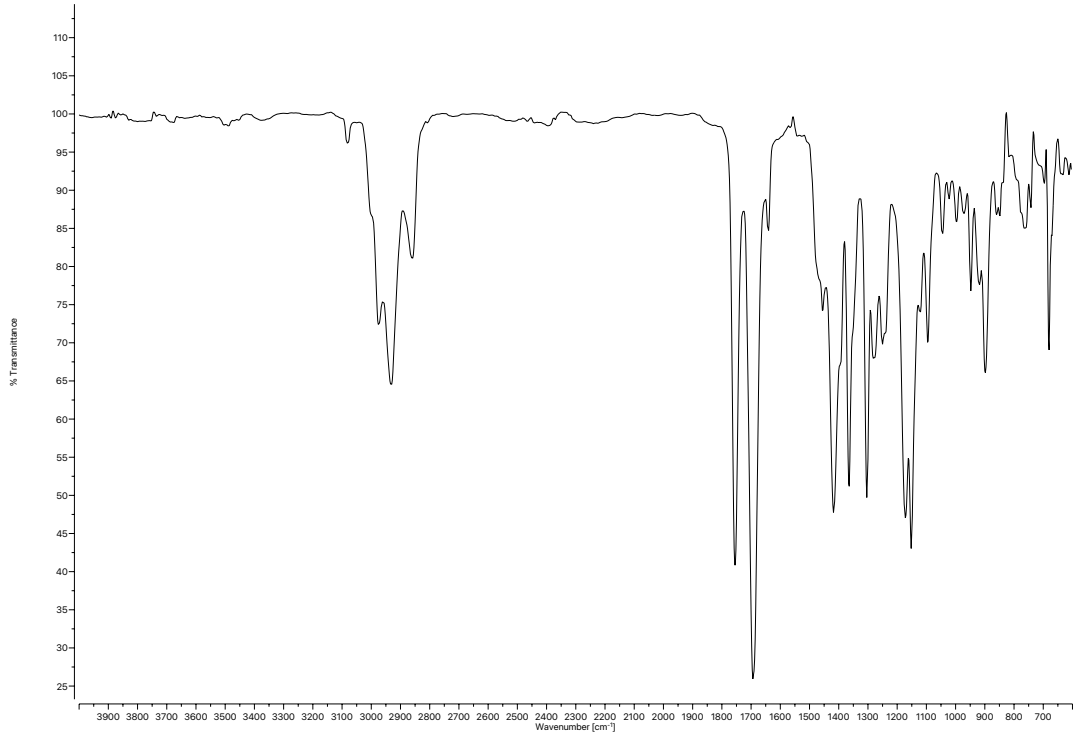


Figure A3.47 *Infrared spectrum (Thin Film, NaCl) of compound* ***67b***.

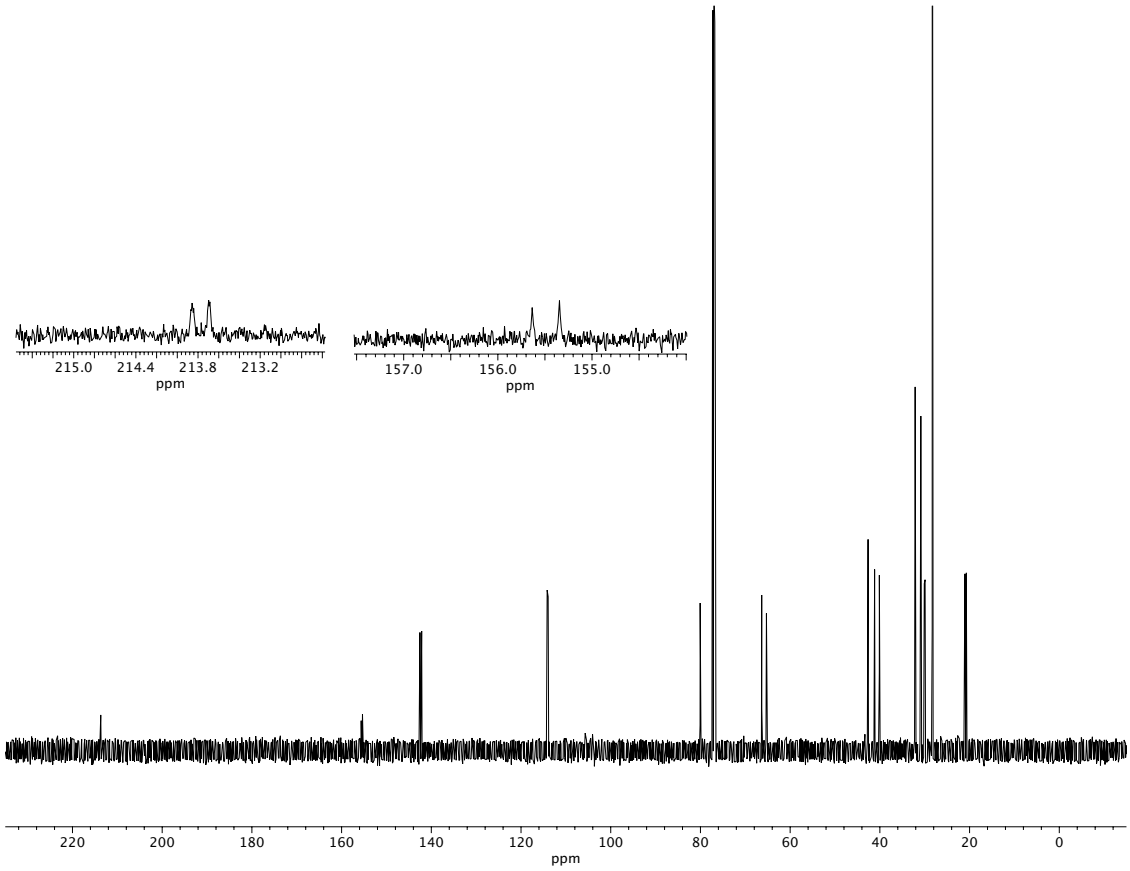
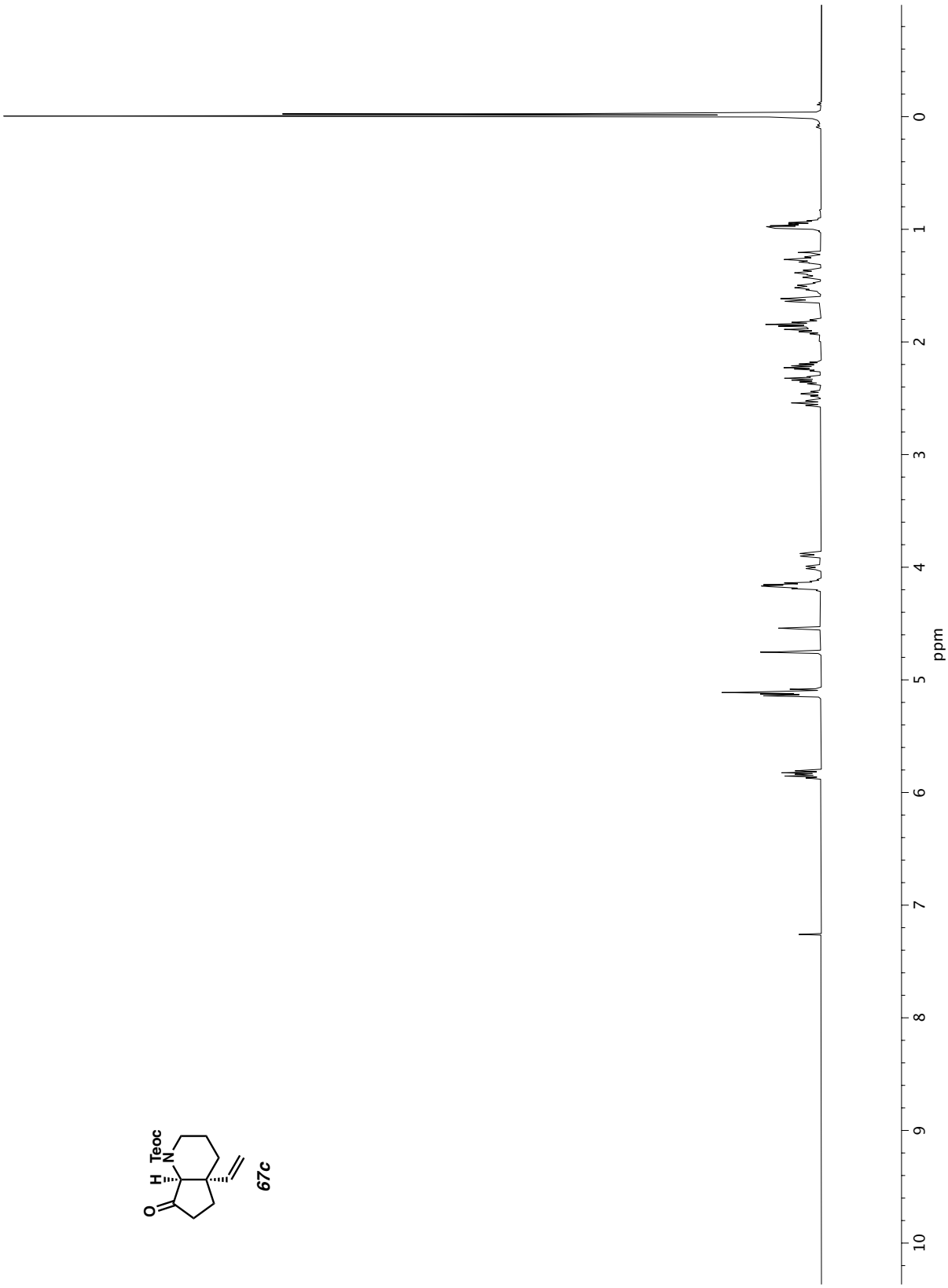


Figure A1.48 *^{13}C NMR (150 MHz, $CDCl_3$) of compound* ***67b***.



67c

Figure A3.49 *^{1}H NMR (600 MHz, $CDCl_3$) of compound* ***67c****.*

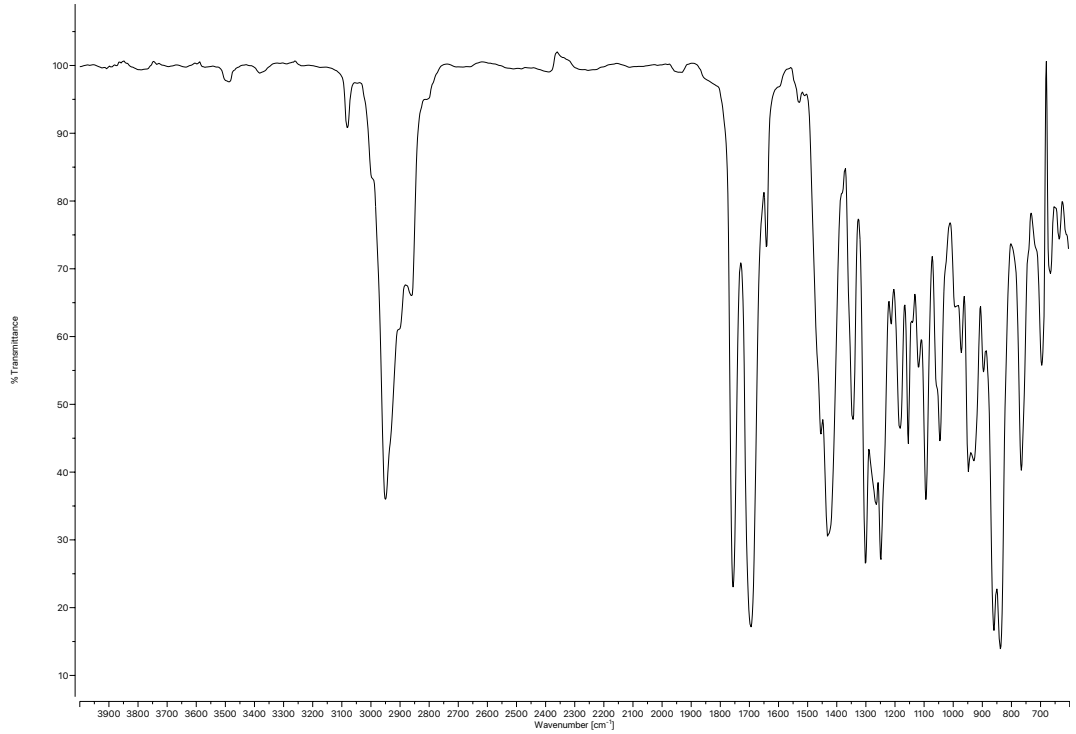


Figure A1.50 *Infrared spectrum (Thin Film, NaCl) of compound* ***67c***.

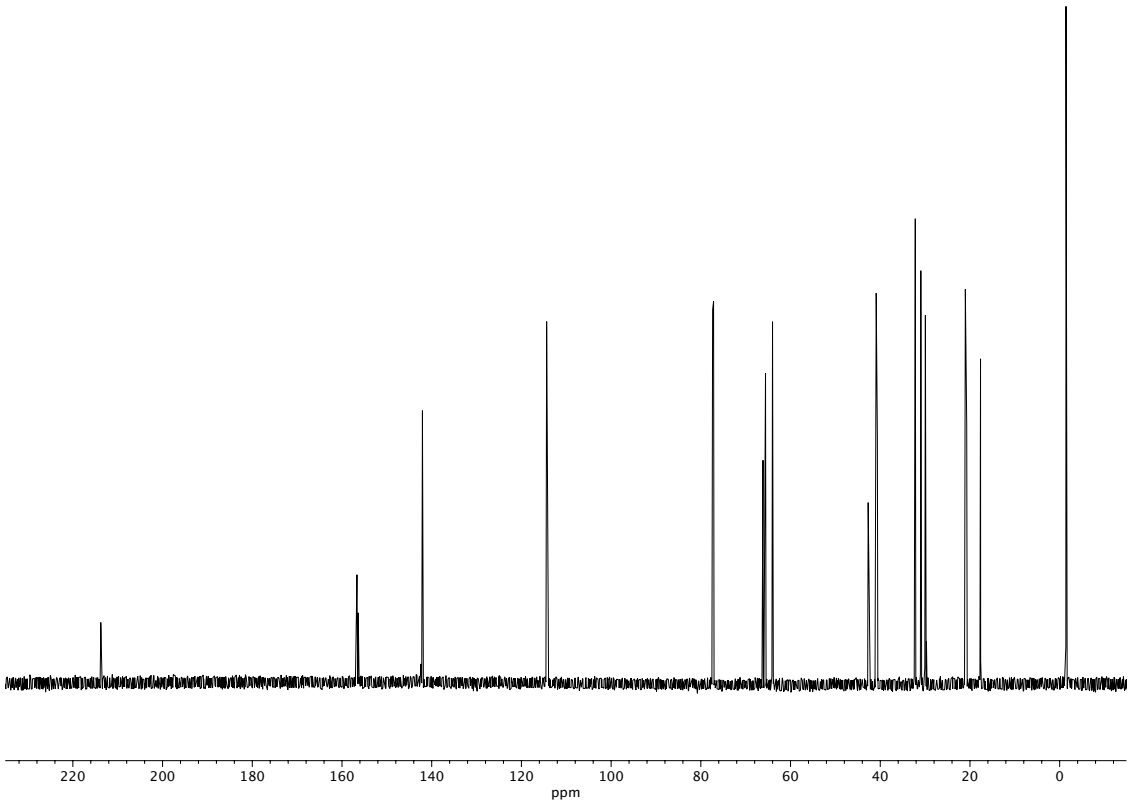


Figure A1.51 *^{13}C NMR (150 MHz, $CDCl_3$) of compound* ***67c***.

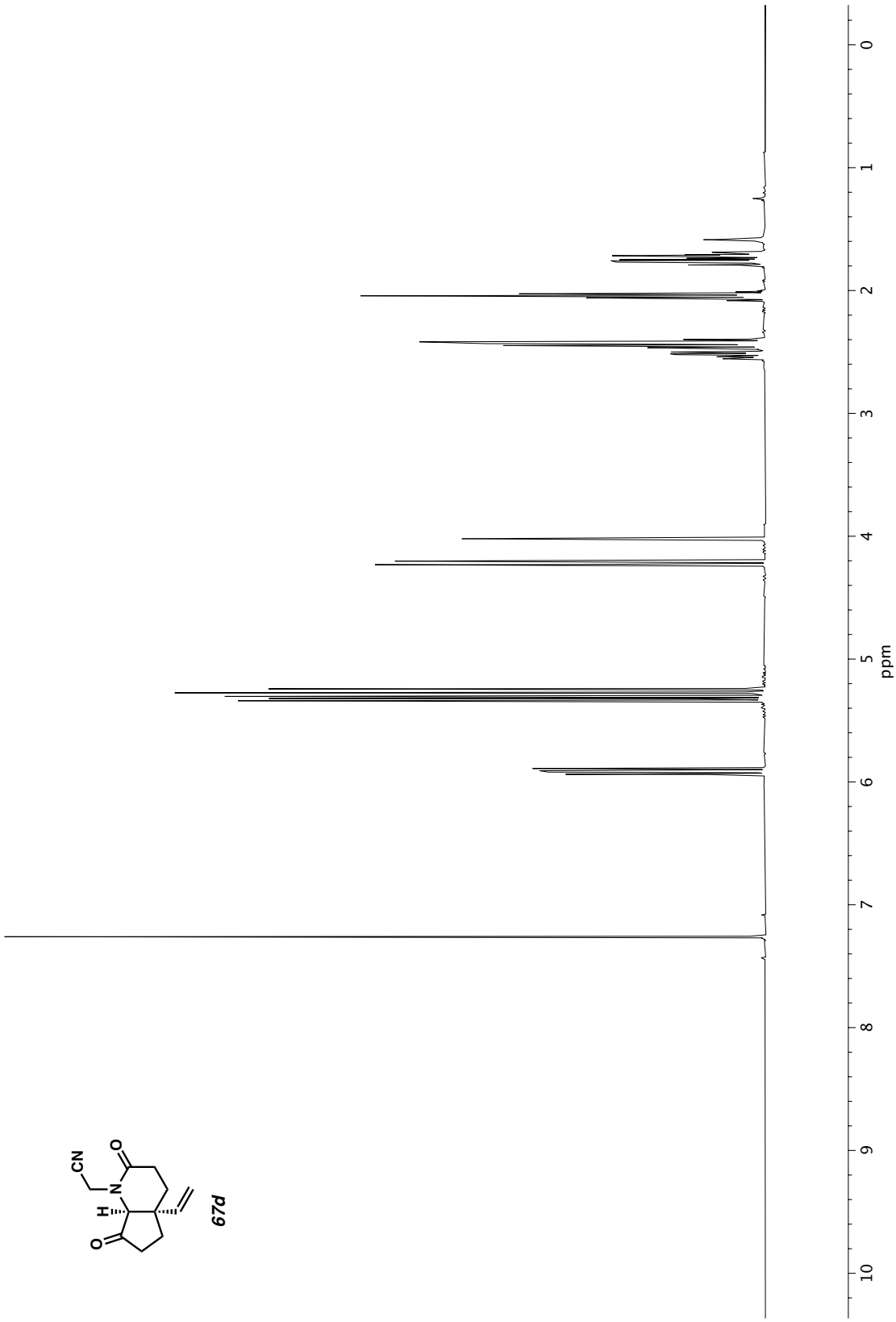


Figure A3.52 *^1H NMR (600 MHz, $CDCl_3$) of compound* ***67d****.*

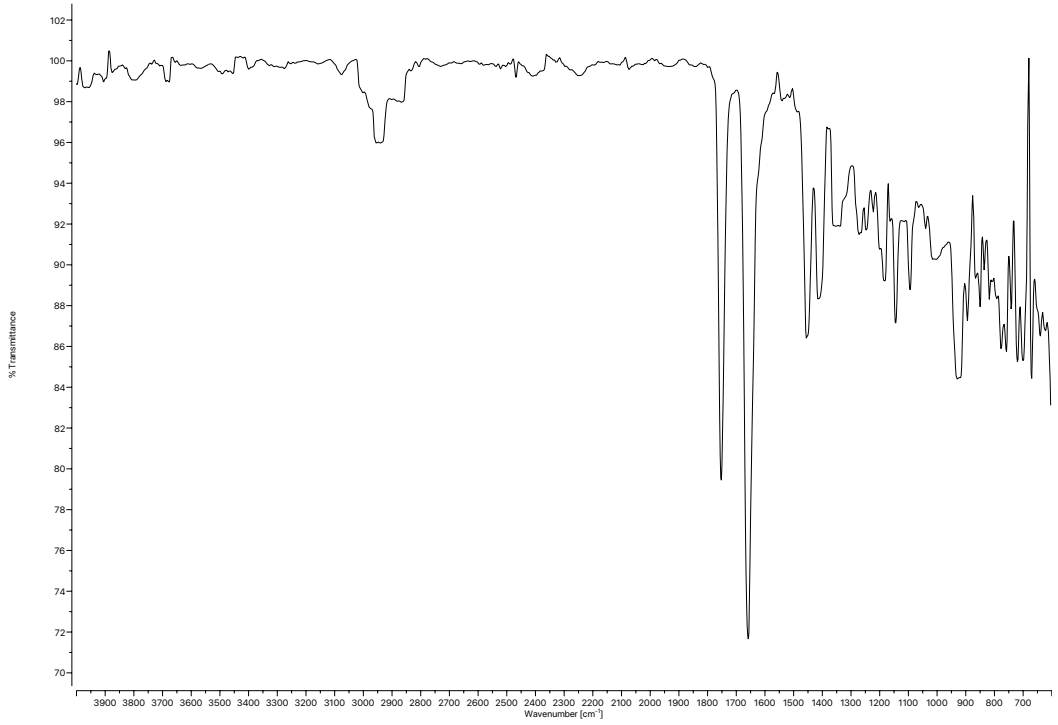


Figure A3.53 *Infrared spectrum (Thin Film, NaCl) of compound* ***67d****.*

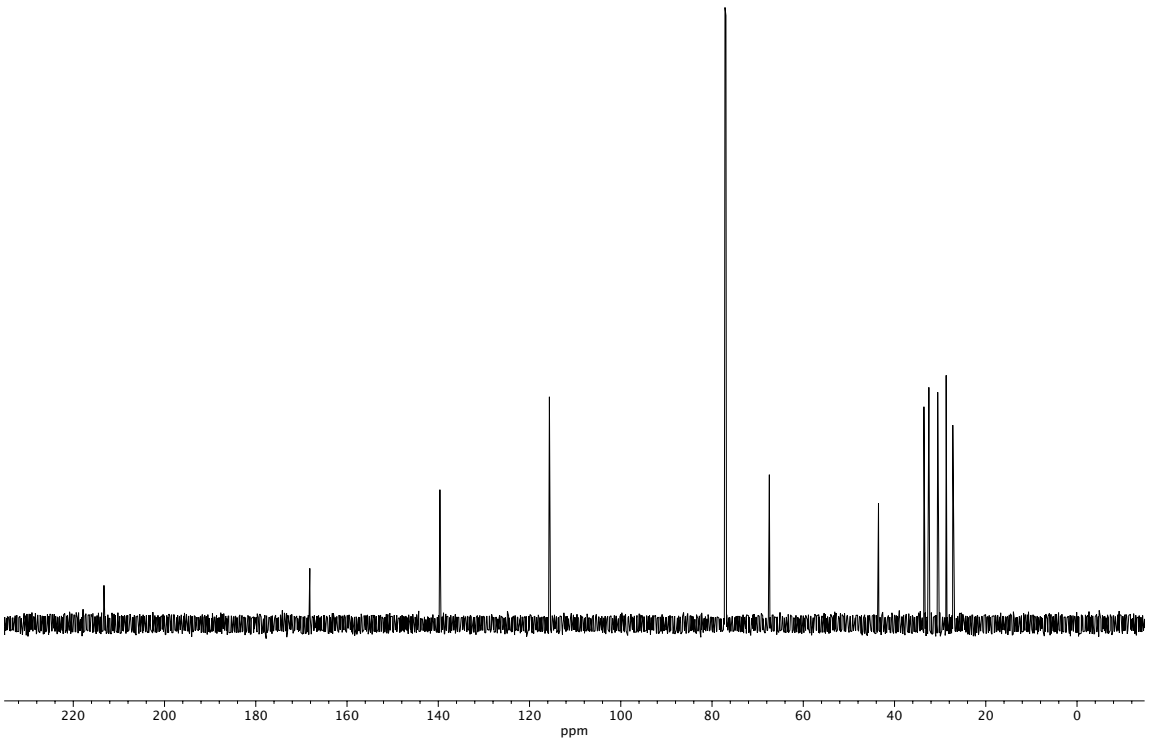


Figure A3.54 *^{13}C NMR (150 MHz, $CDCl_3$) of compound* ***67d****.*

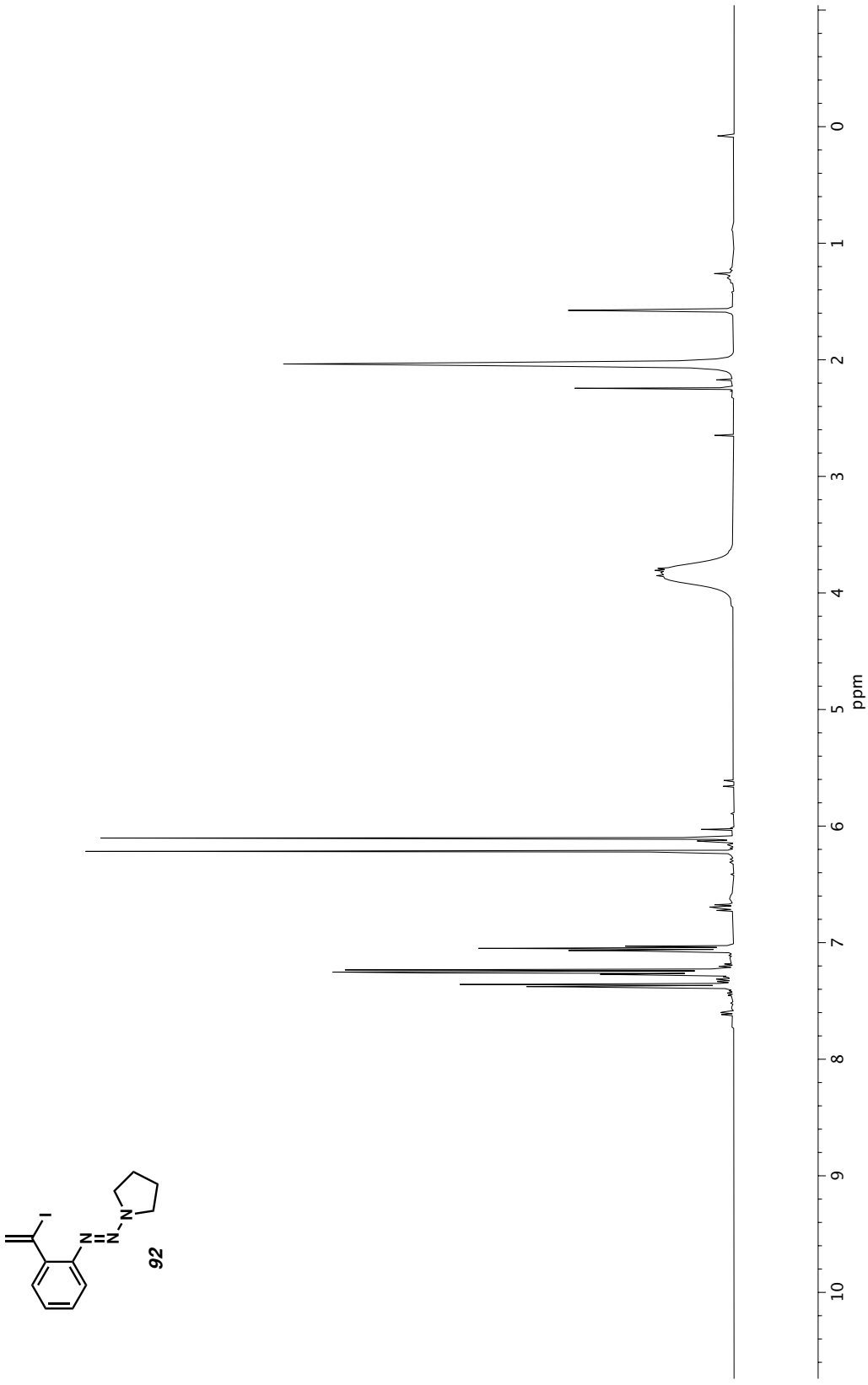


Figure A3.55 *^{1}H NMR (400 MHz, $CDCl_3$) of compound* ***92***.

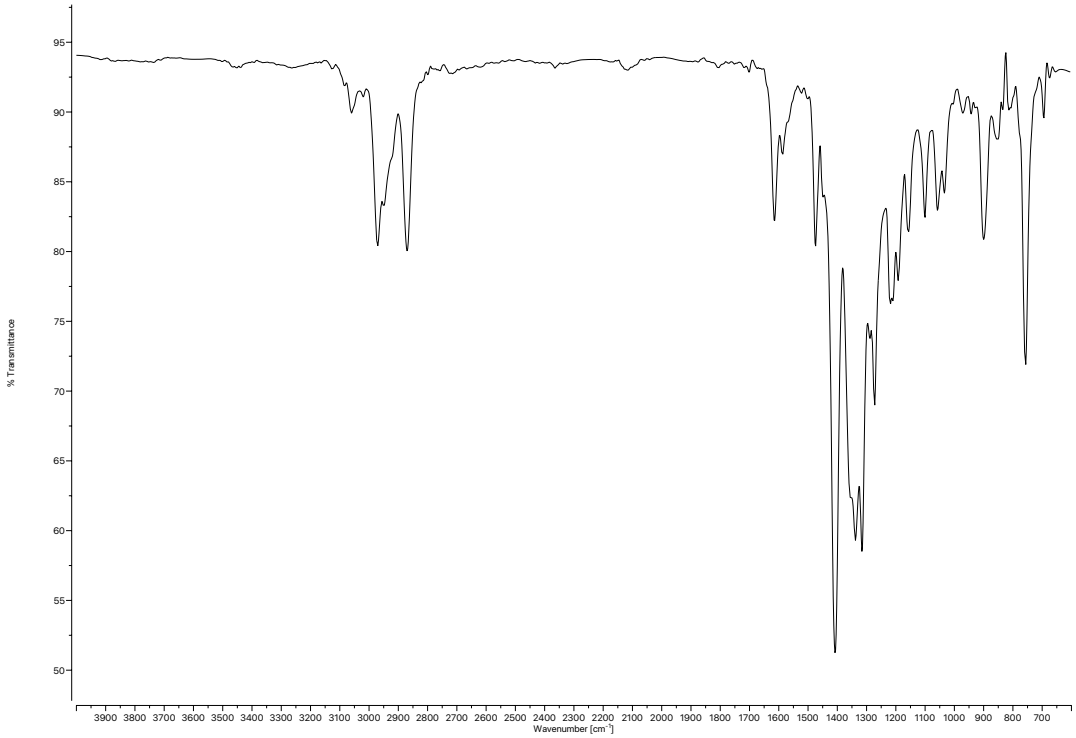


Figure A3.56 *Infrared spectrum (Thin Film, NaCl) of compound* ***92***.

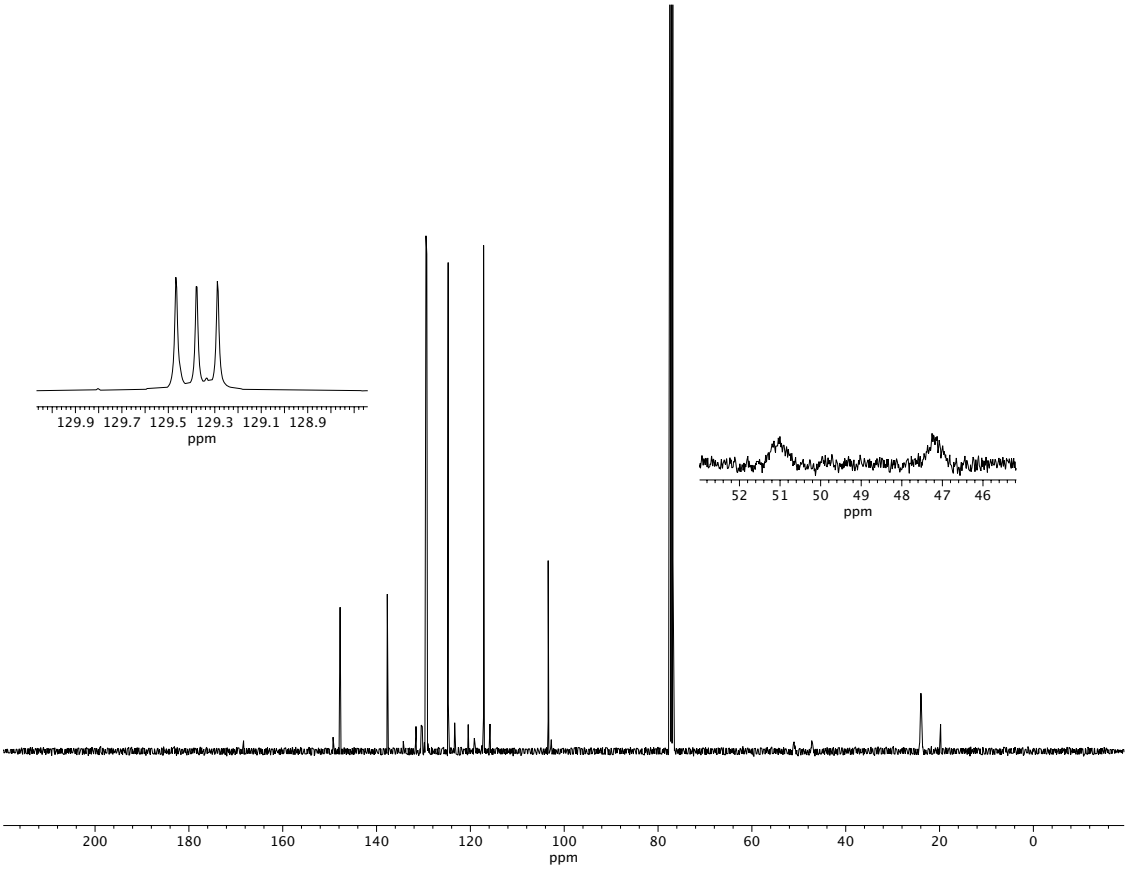


Figure A3.57 *^{13}C NMR (100 MHz, $CDCl_3$) of compound* ***92***.

Figure A3.58 *^{1}H NMR (400 MHz, $CDCl_3$) of compound **93**.*

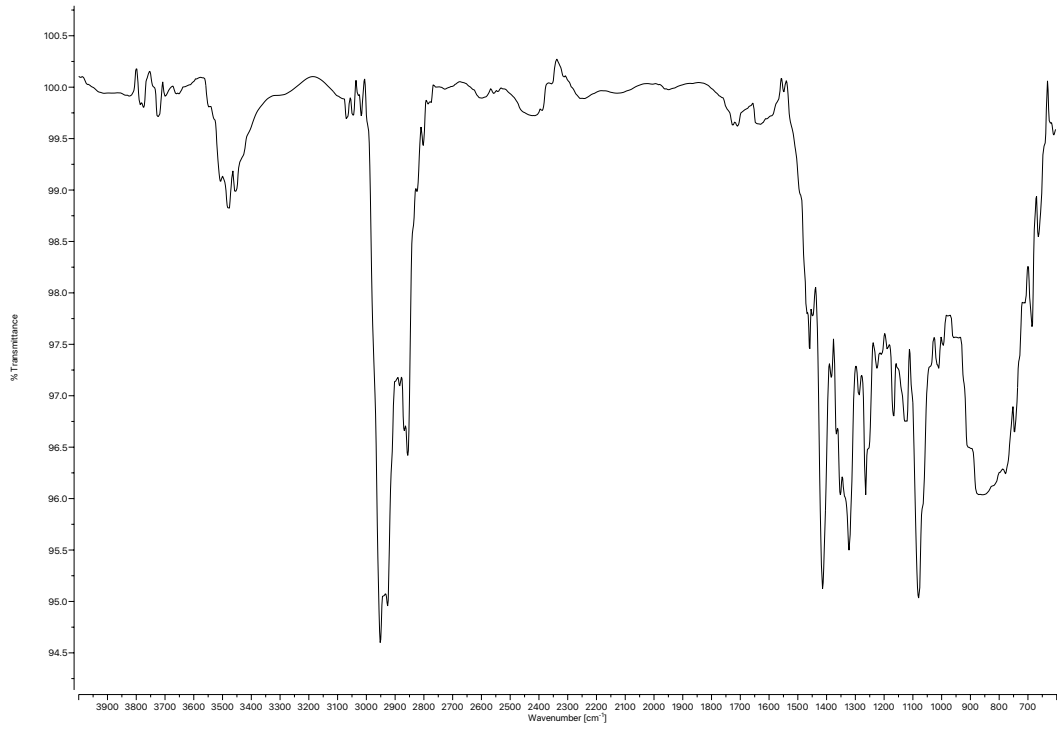


Figure A3.59 *Infrared spectrum (Thin Film, NaCl) of compound* ***93***.

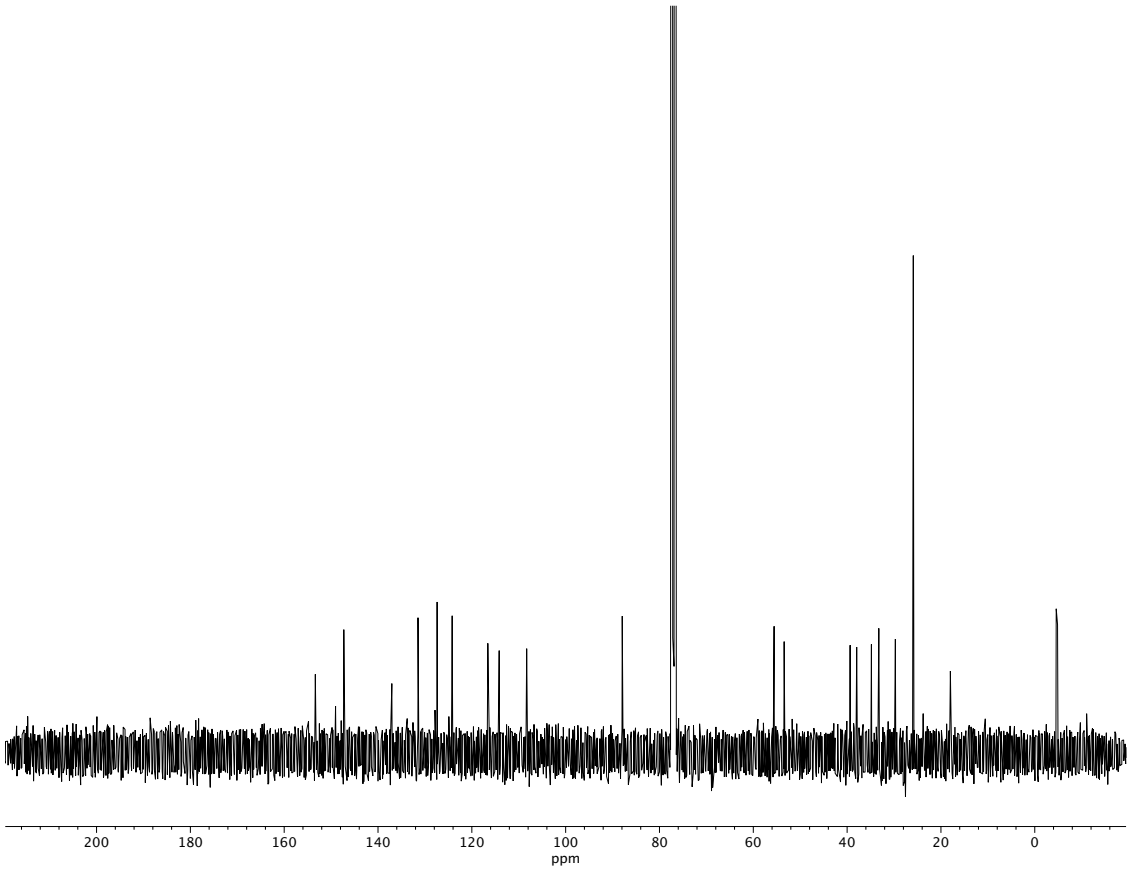


Figure A3.60 *^{13}C NMR (100 MHz, $CDCl_3$) of compound* ***93***.

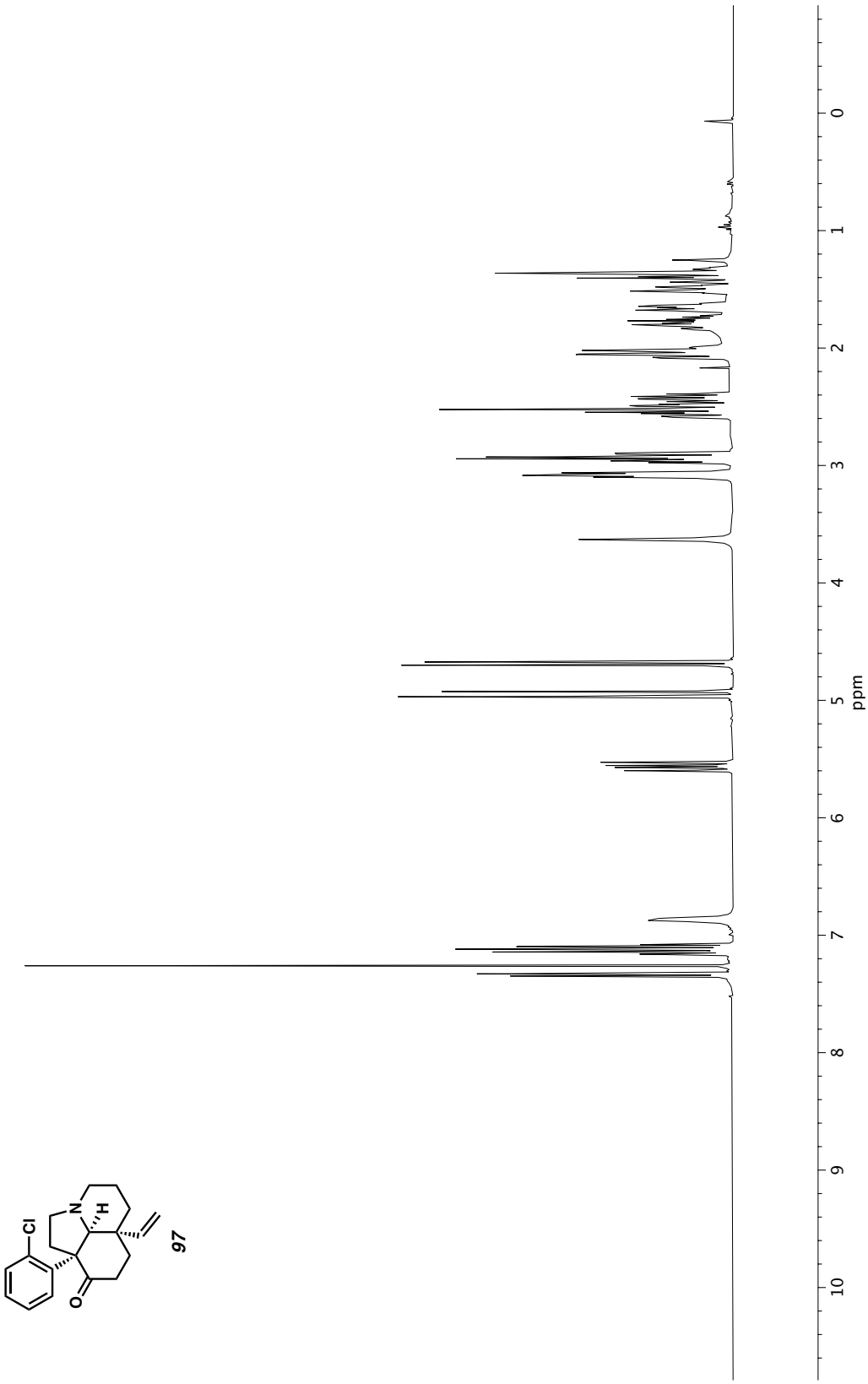


Figure A3.61 *^{1}H NMR (400 MHz, $CDCl_3$) of compound* ***97****.*

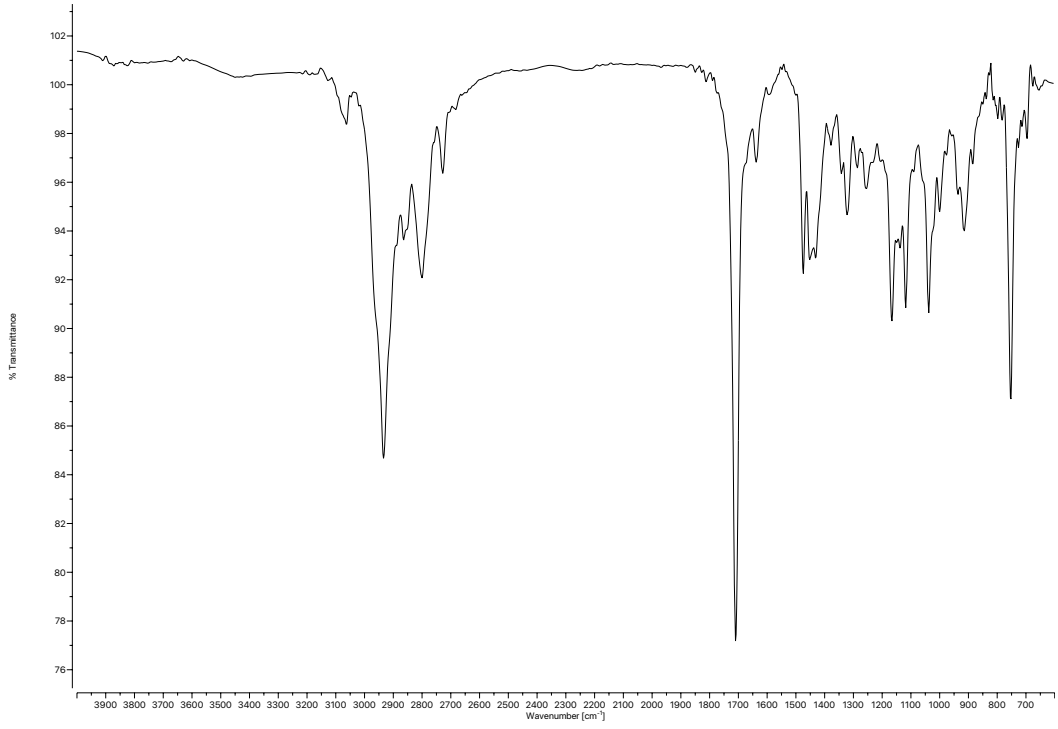


Figure A3.62 *Infrared spectrum (Thin Film, NaCl) of compound* ***97****.*

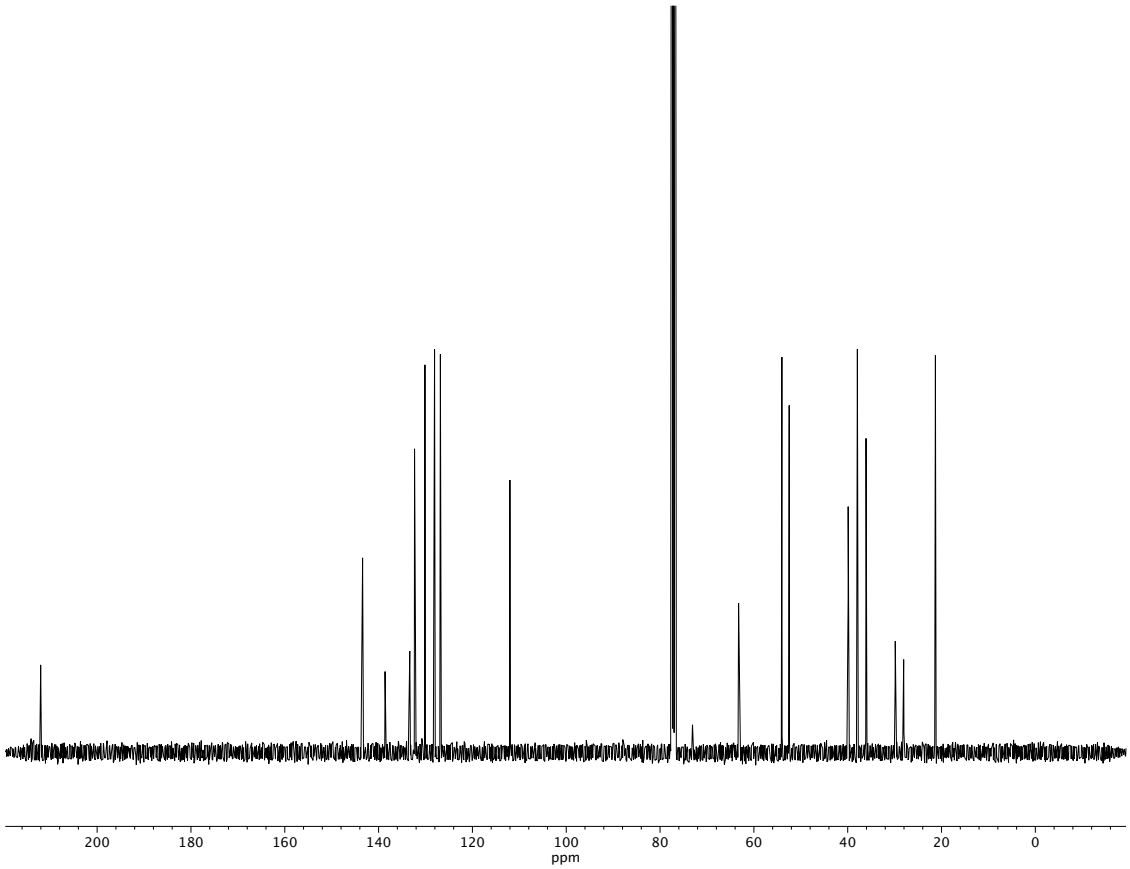


Figure A3.63 *^{13}C NMR (100 MHz, $CDCl_3$) of compound* ***97****.*

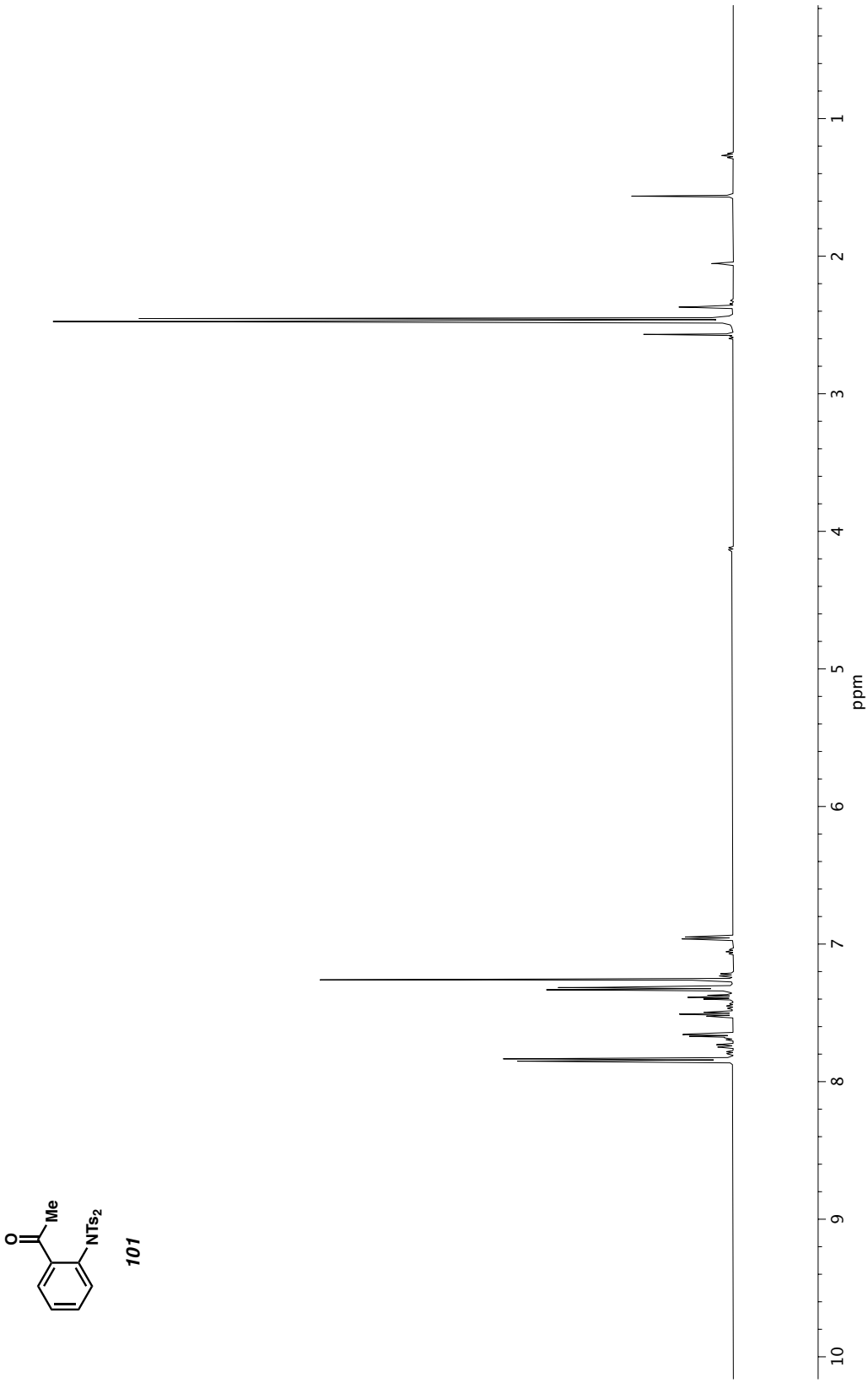


Figure A3.64 *^1H NMR (500 MHz, $CDCl_3$) of compound* ***101***.

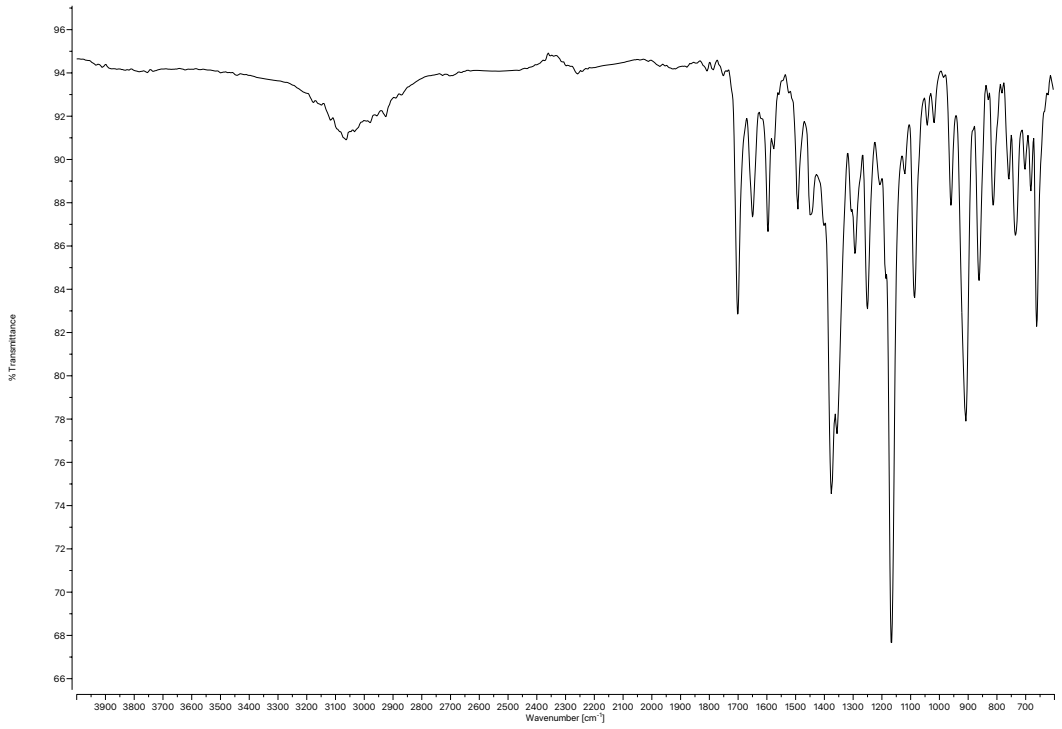


Figure A1.65 *Infrared spectrum (Thin Film, NaCl) of compound* ***101***.

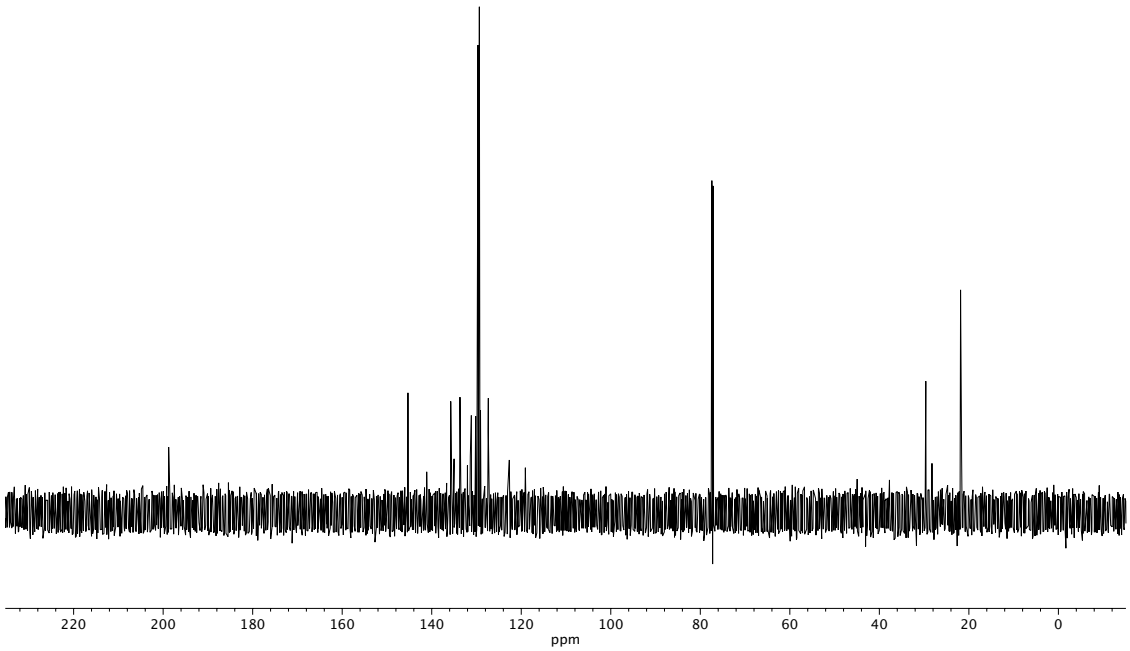


Figure A3.66 *^{13}C NMR (125 MHz, $CDCl_3$) of compound* ***101***.

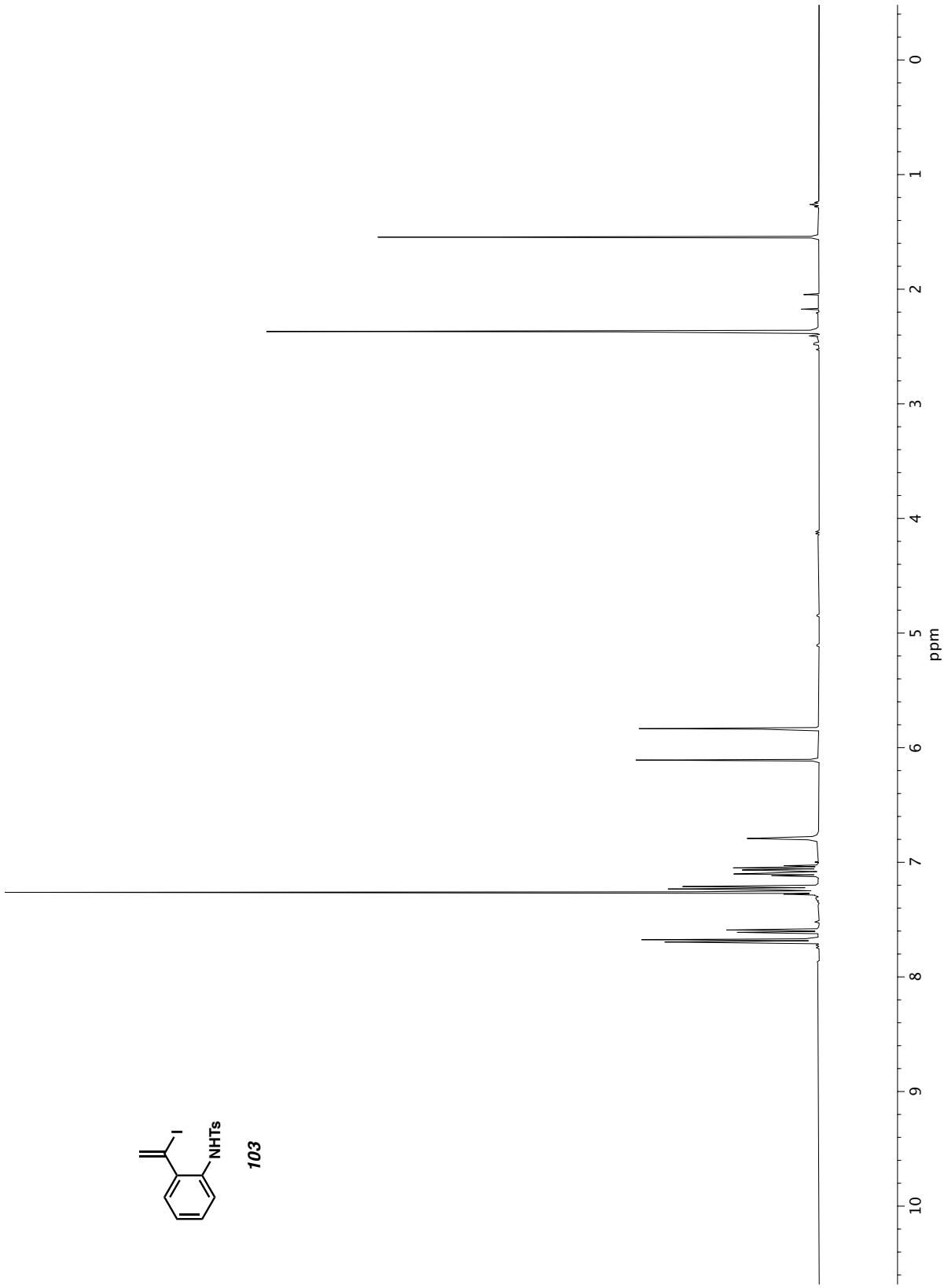


Figure A3.67 *^1H NMR (400 MHz, $CDCl_3$) of compound* ***103***.

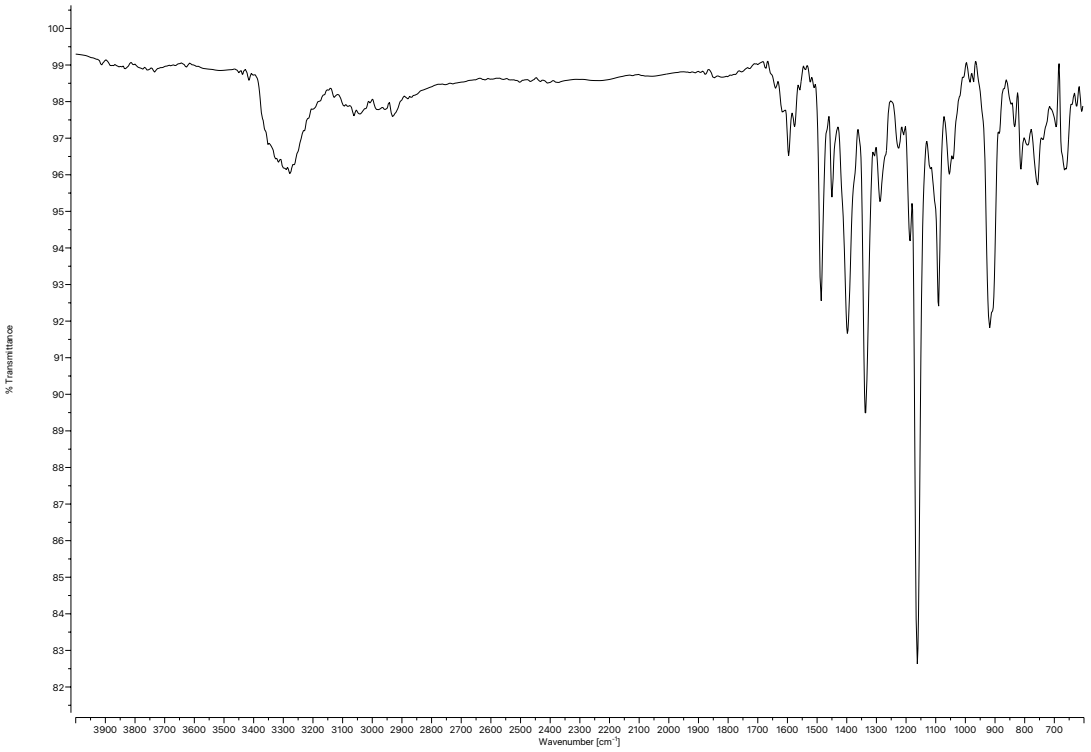


Figure A3.68 *Infrared spectrum (Thin Film, NaCl) of compound* ***103***.

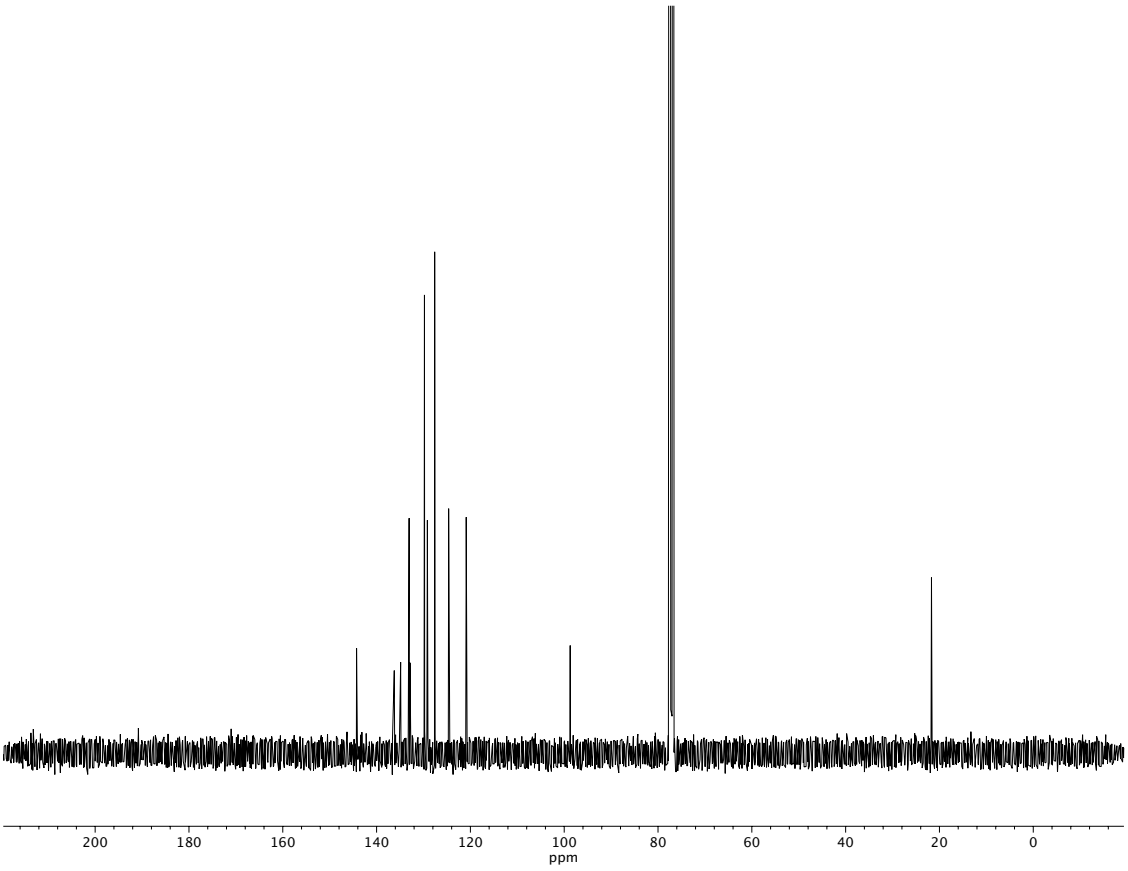


Figure A3.69 *^{13}C NMR (100 MHz, $CDCl_3$) of compound* ***103***.

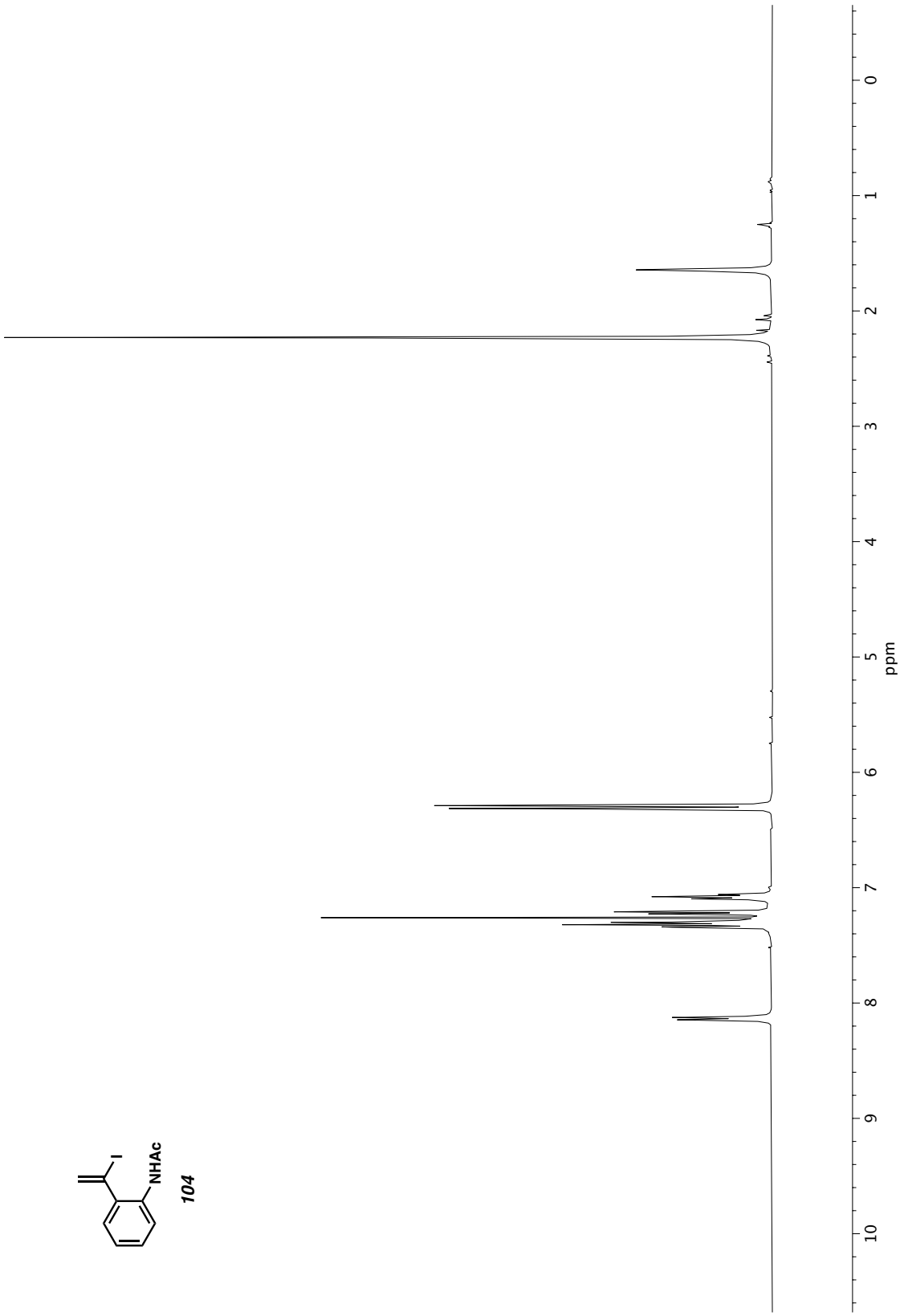


Figure A3.70 *^1H NMR (500 MHz, $CDCl_3$) of compound* ***104****.*

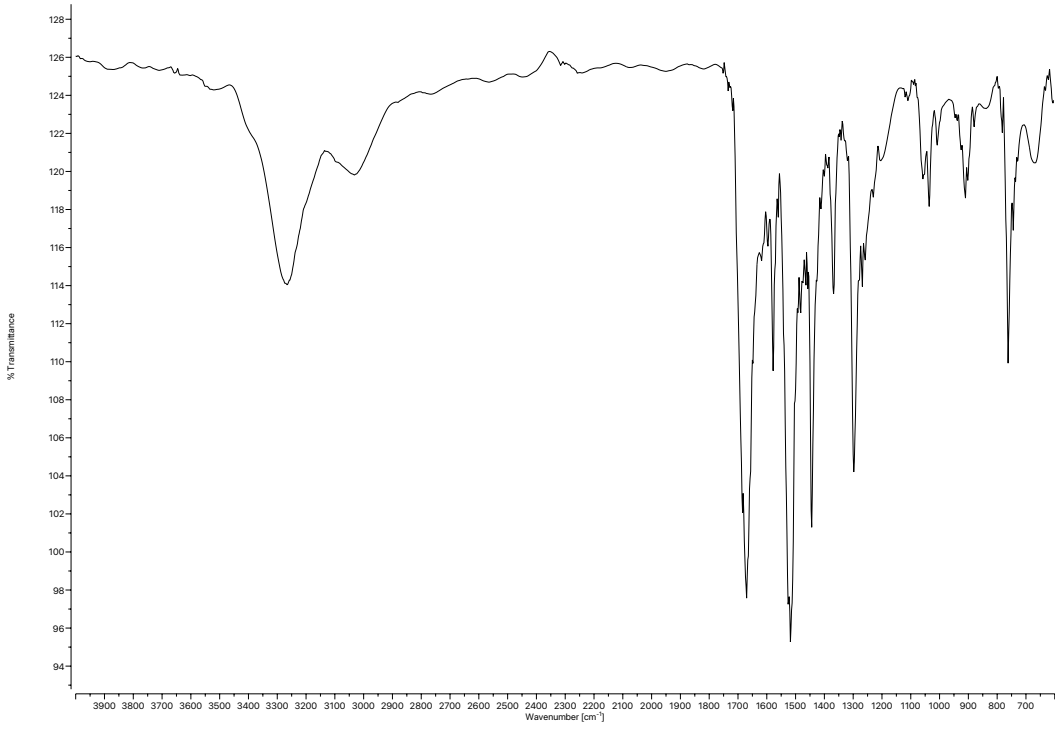


Figure A3.71 *Infrared spectrum (Thin Film, NaCl) of compound* ***104***.

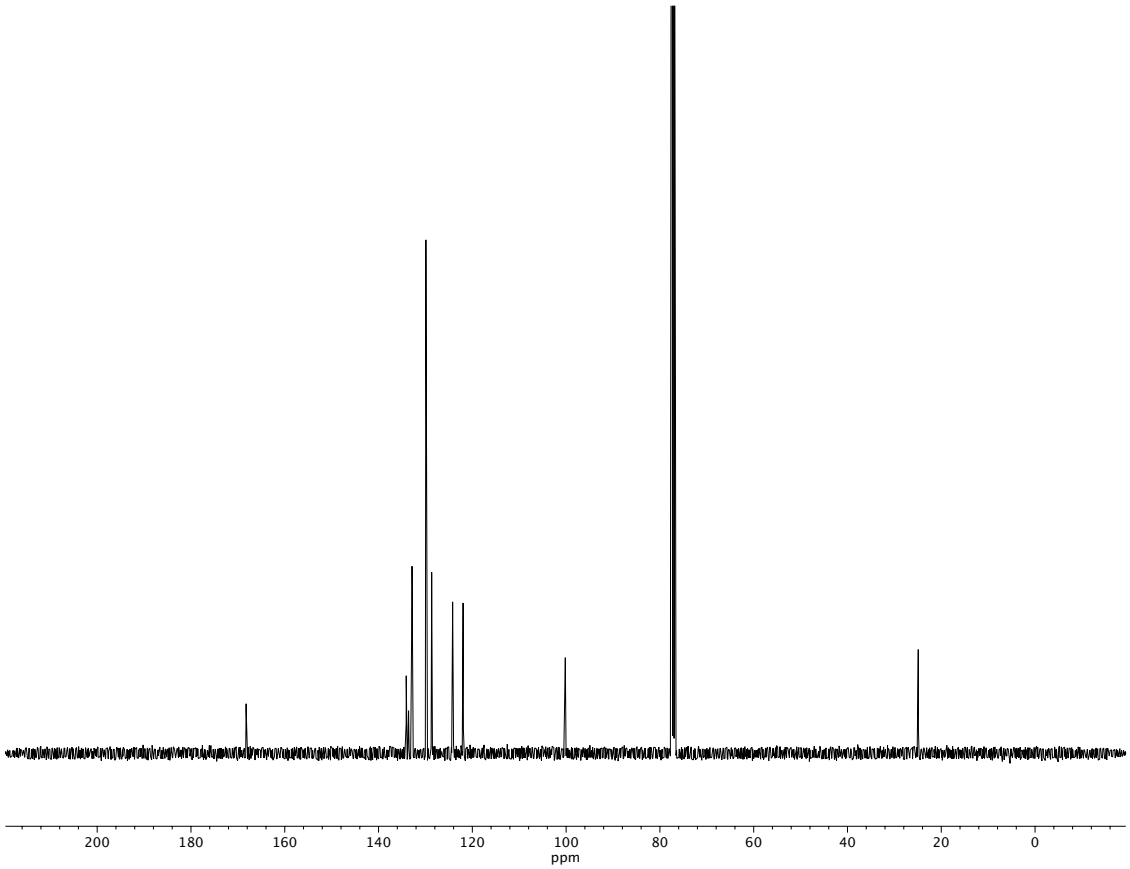


Figure A3.72 *^{13}C NMR (100 MHz, $CDCl_3$) of compound* ***104***.

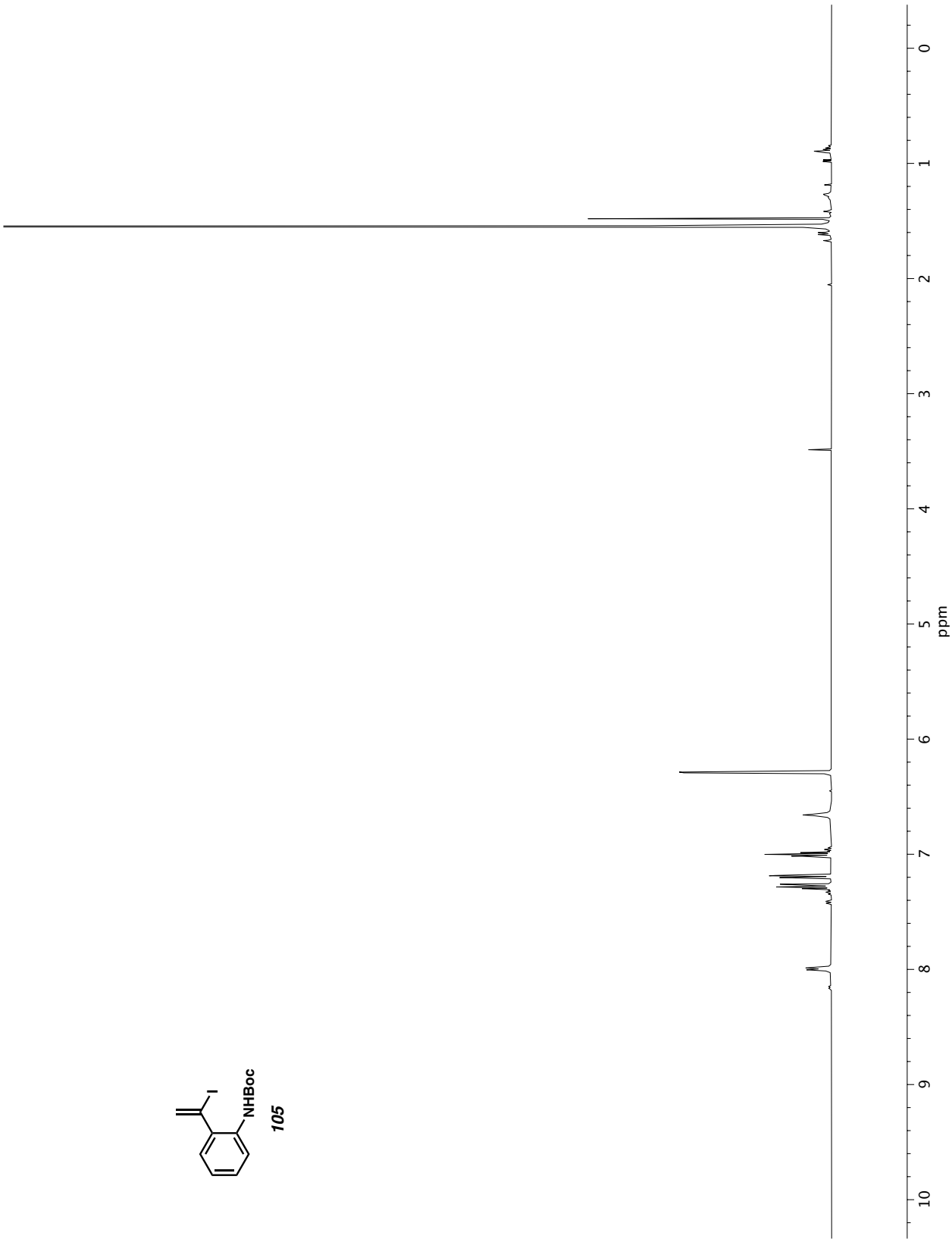


Figure A1.73 *^1H NMR (500 MHz, $CDCl_3$) of compound **105**.*

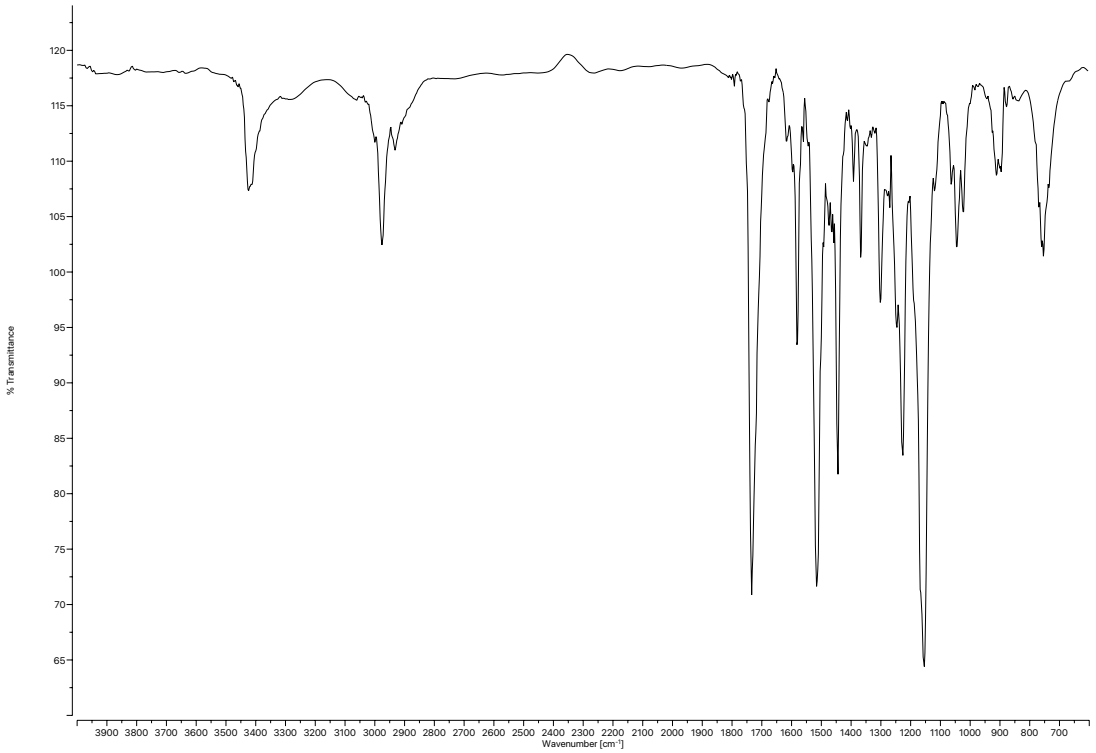


Figure A3.74 *Infrared spectrum (Thin Film, NaCl) of compound* ***105***.

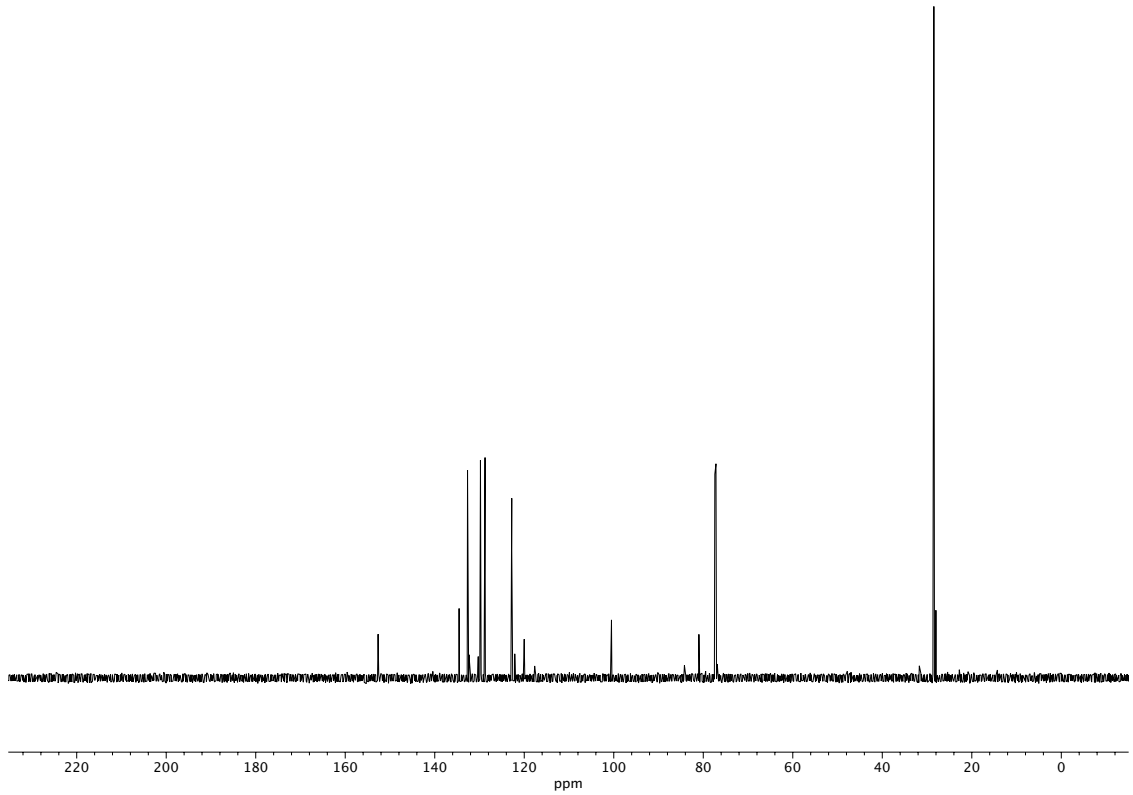


Figure A3.75 *^{13}C NMR (125 MHz, $CDCl_3$) of compound* ***105***.

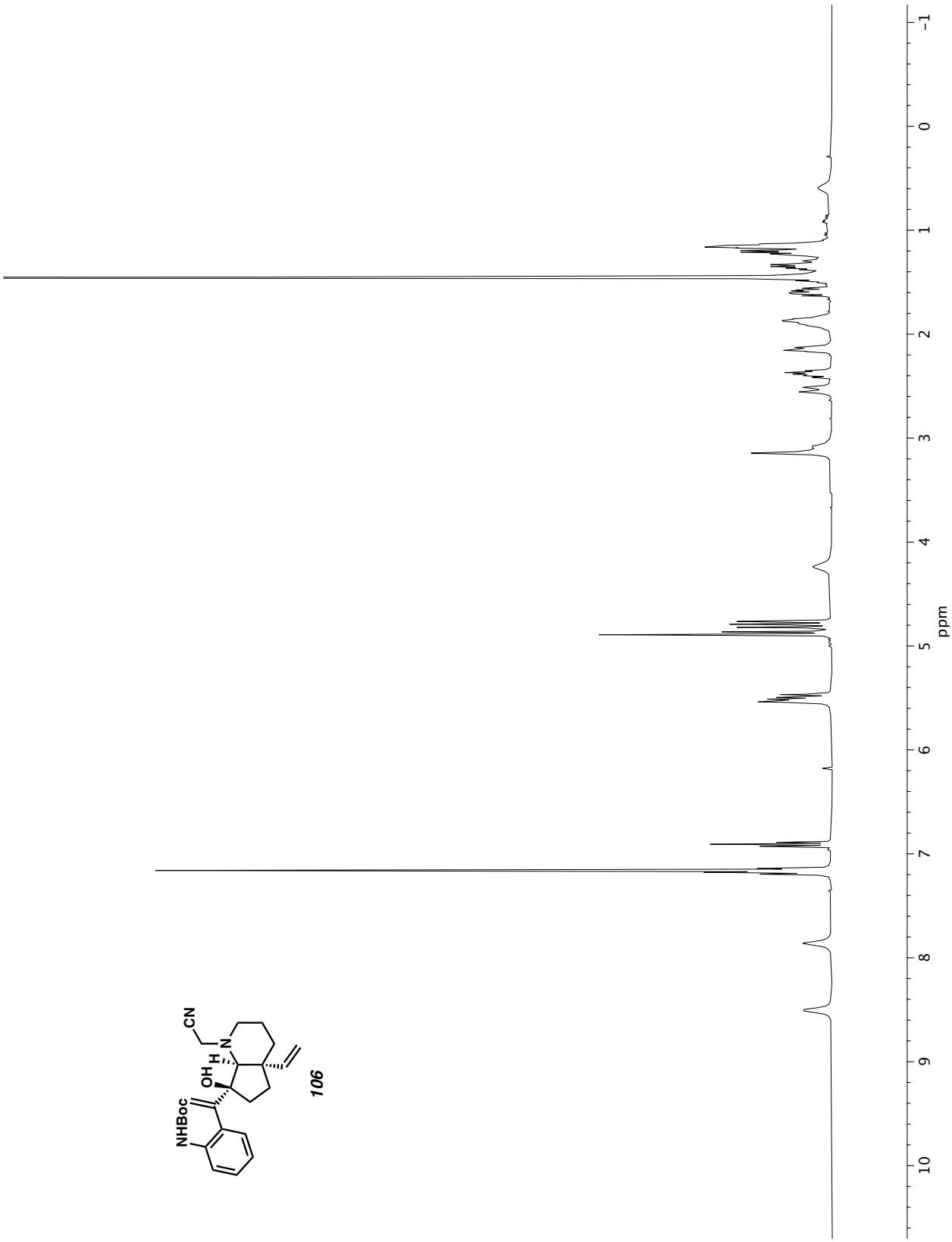


Figure A3.76 *^{1}H NMR (400 MHz, $CDCl_3$) of compound **106**.*

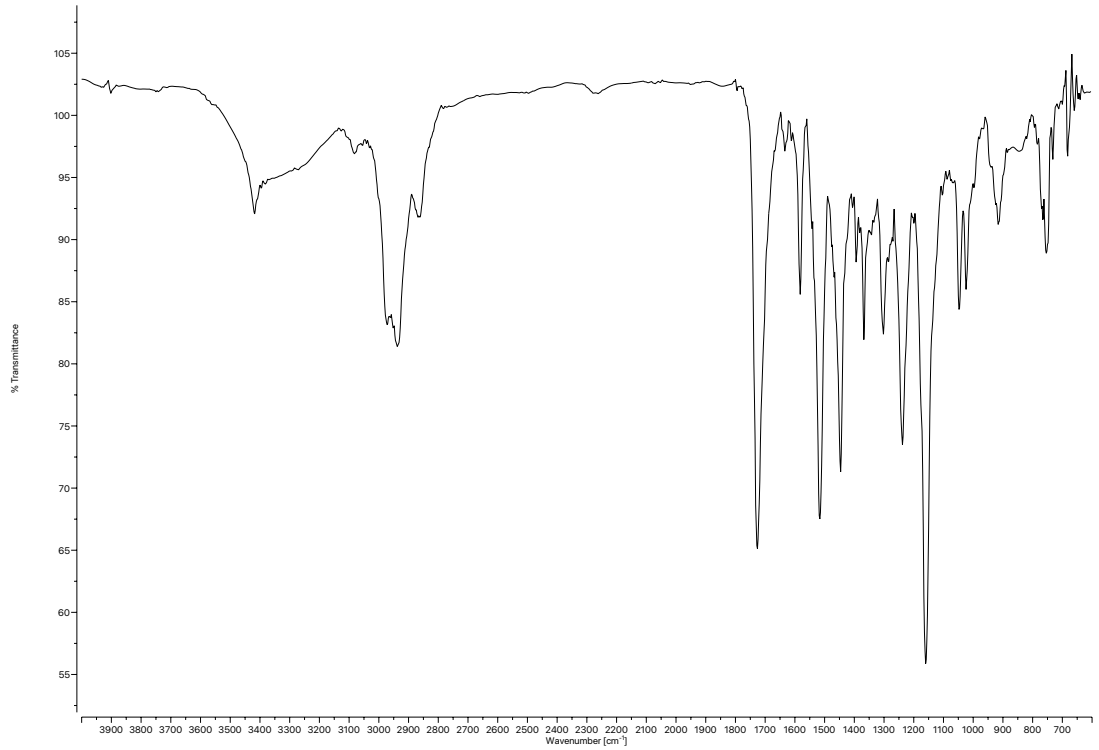


Figure A3.77 *Infrared spectrum (Thin Film, NaCl) of compound* ***106***.

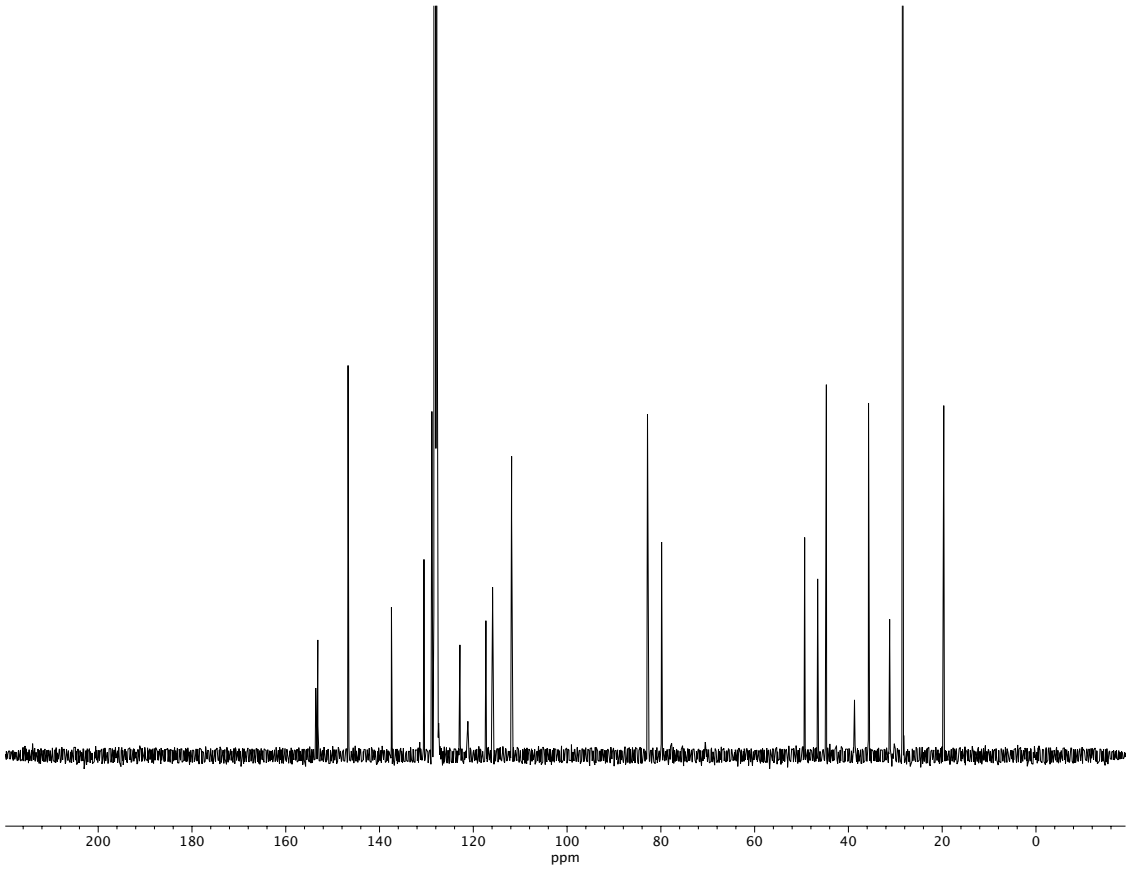


Figure A3.78 *^{13}C NMR (100 MHz, $CDCl_3$) of compound* ***106***.

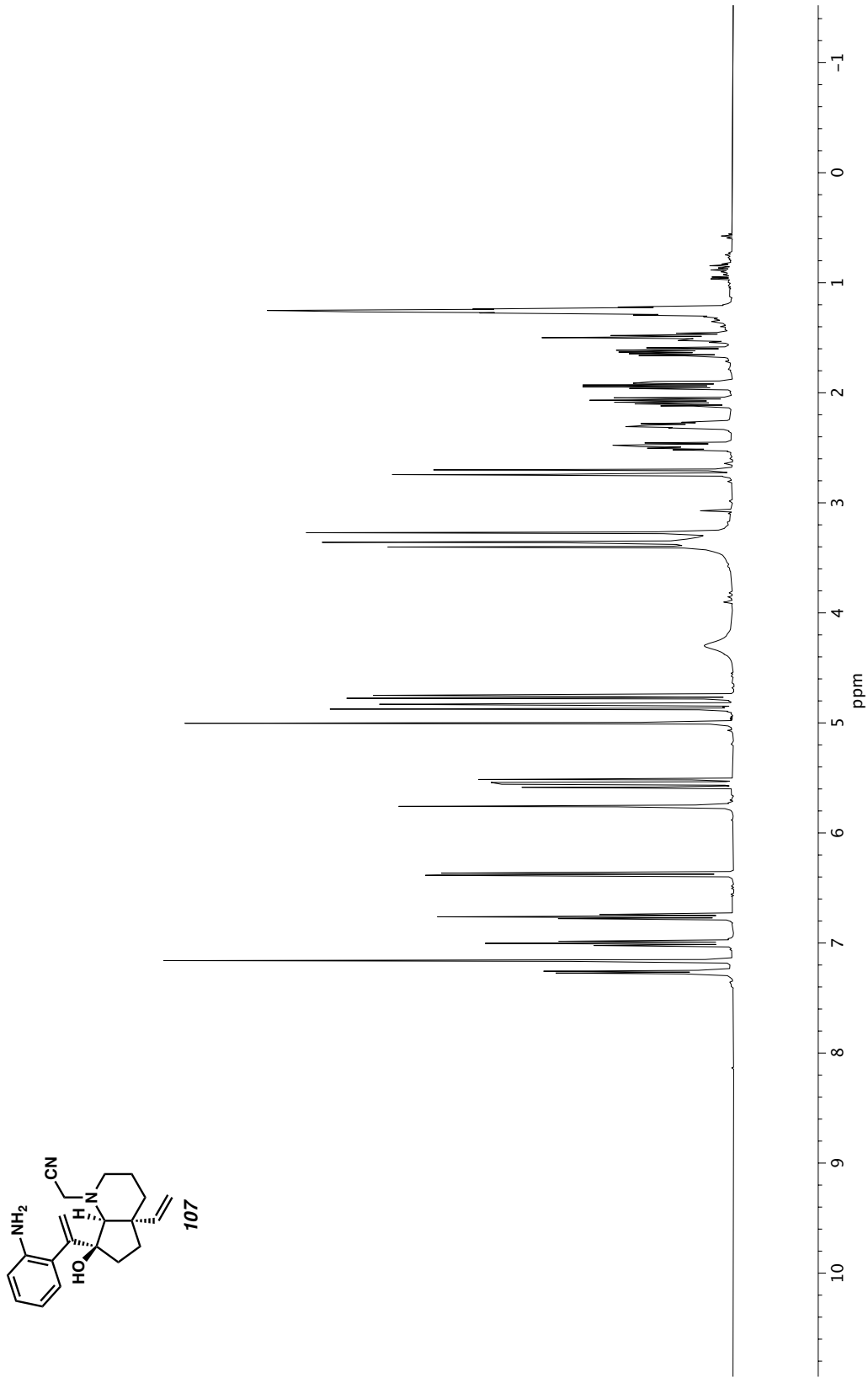


Figure A3.79 *^{1}H NMR (400 MHz, C_6D_6) of compound **107**.*

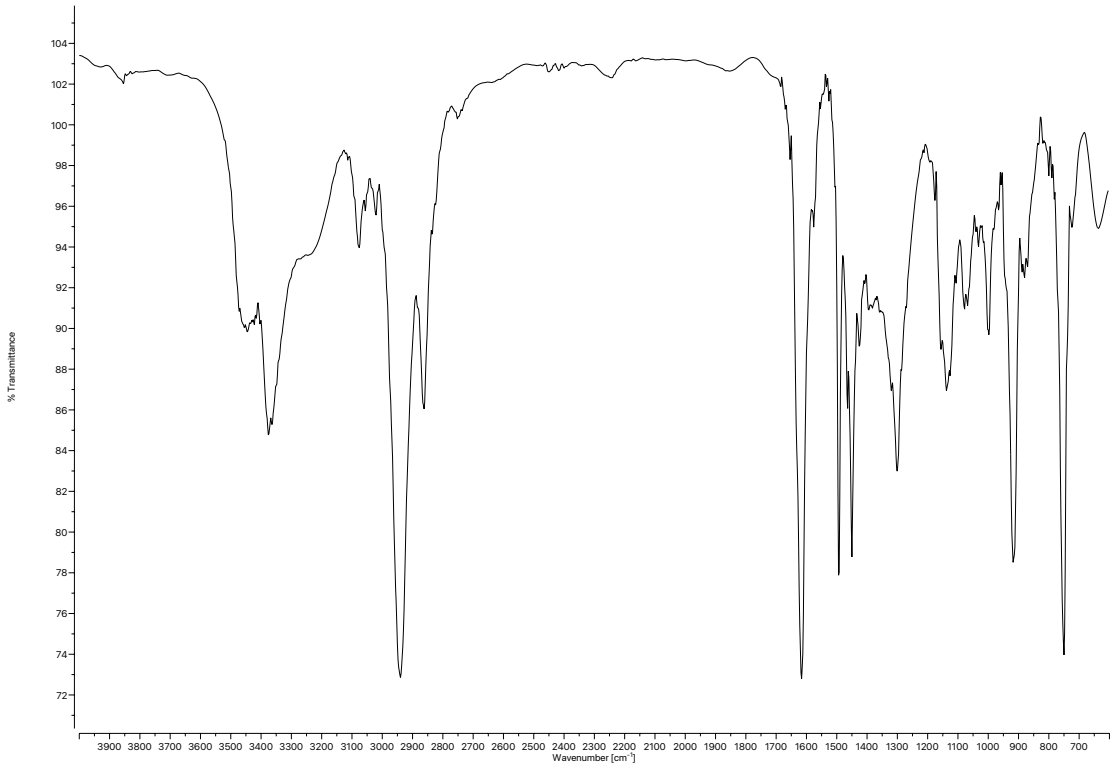


Figure A3.80 *Infrared spectrum (Thin Film, NaCl) of compound* ***107***.

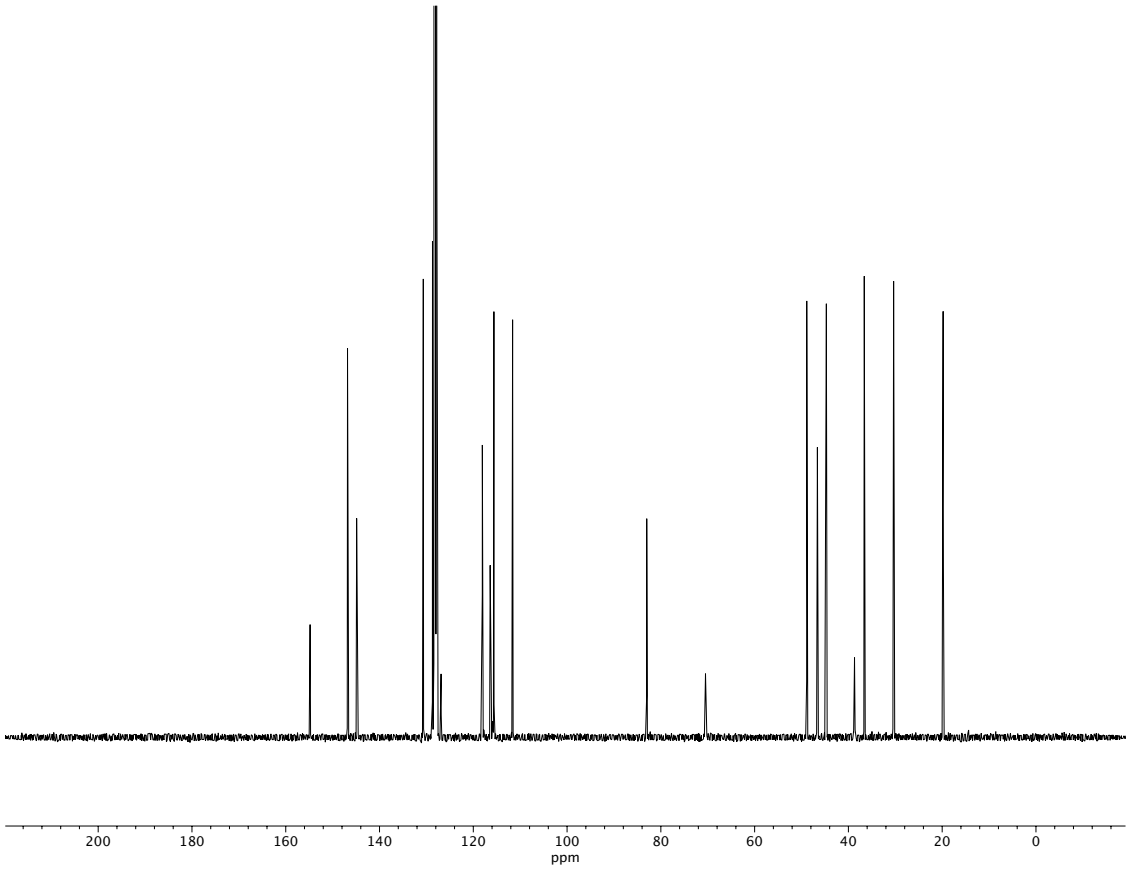


Figure A3.81 *^{13}C NMR (100 MHz, C_6D_6) of compound* ***107***.

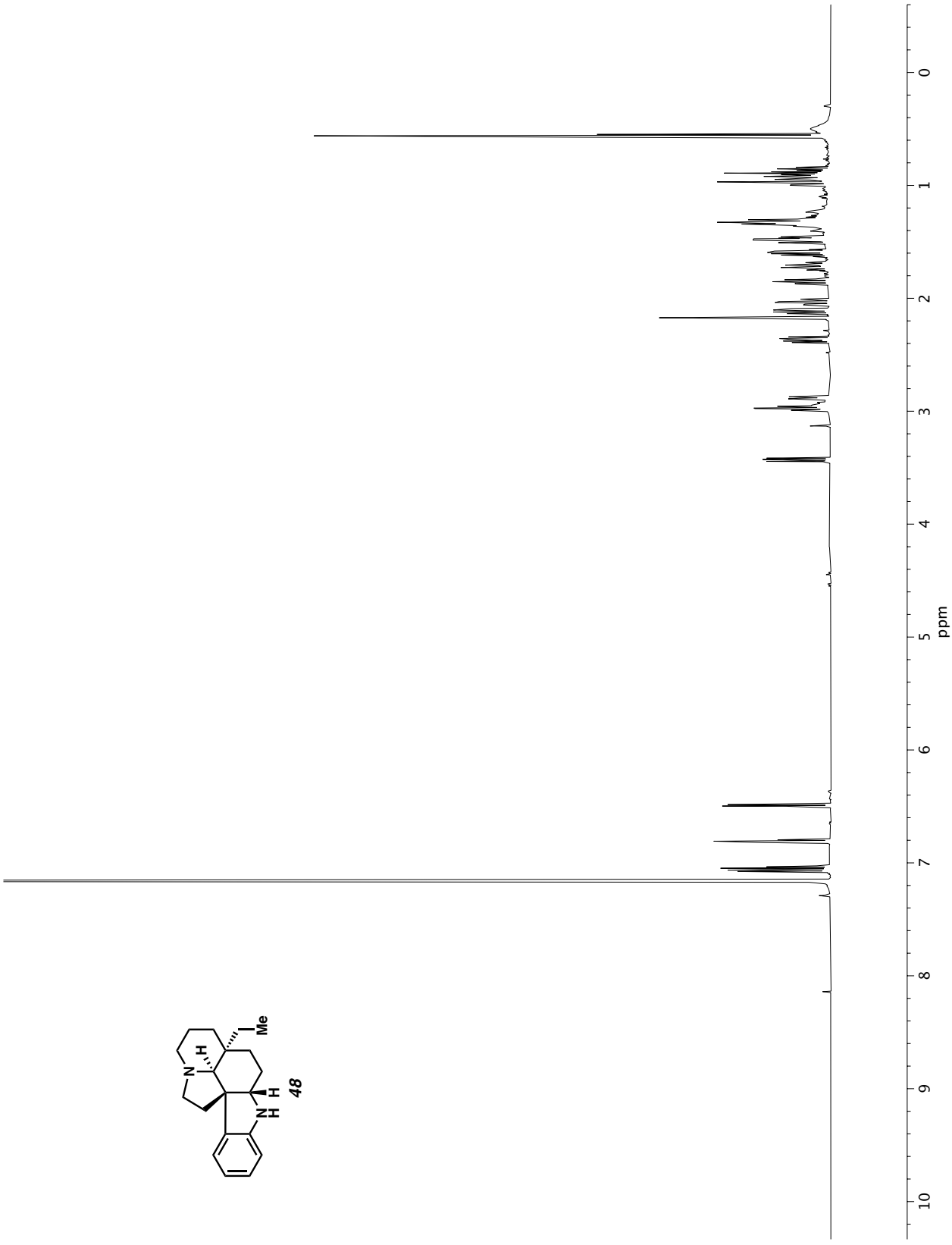


Figure A3.82 *^1H NMR (600 MHz, C_6D_6) of compound **48**.*

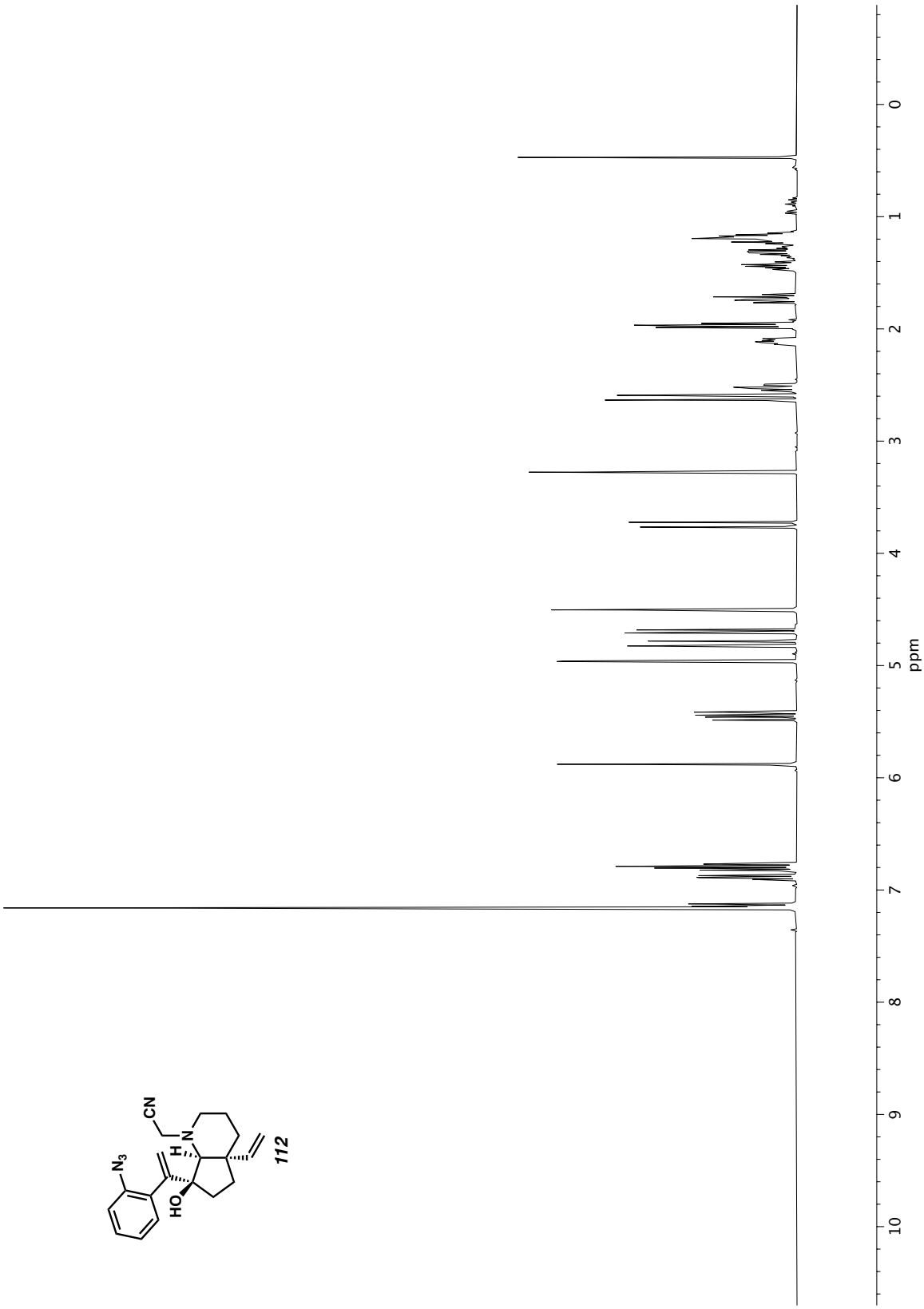


Figure A3.83 *^{1}H NMR (400 MHz, C_6D_6) of compound* ***112***.

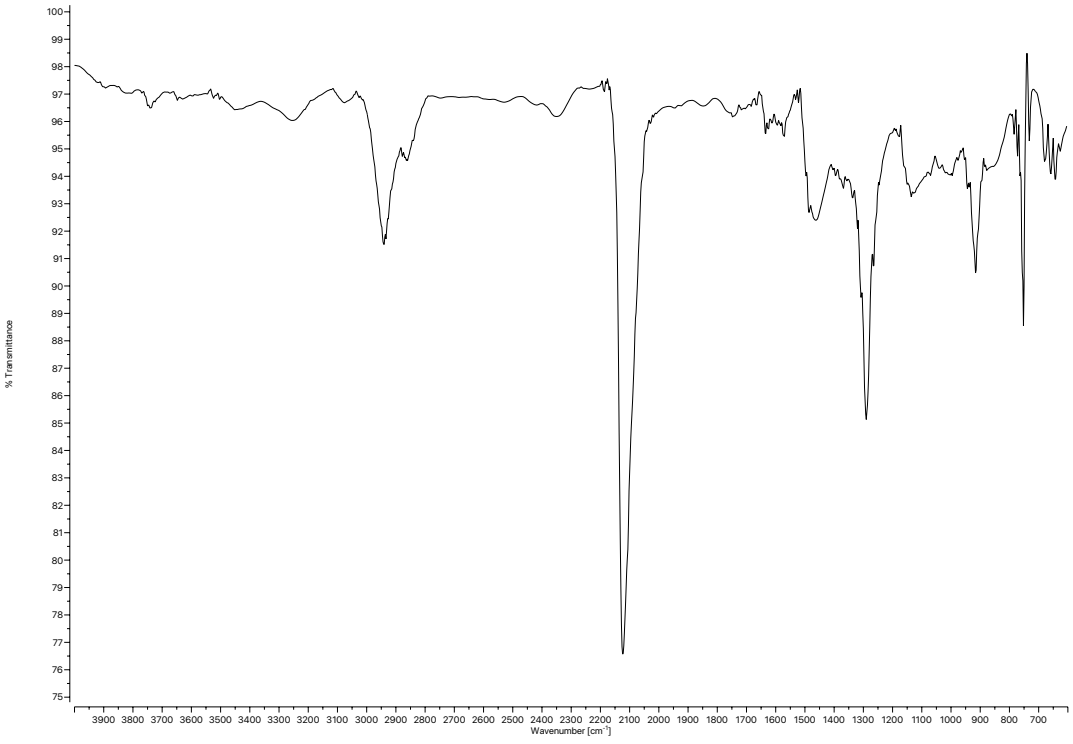


Figure A1.84 *Infrared spectrum (Thin Film, NaCl) of compound* ***112***.

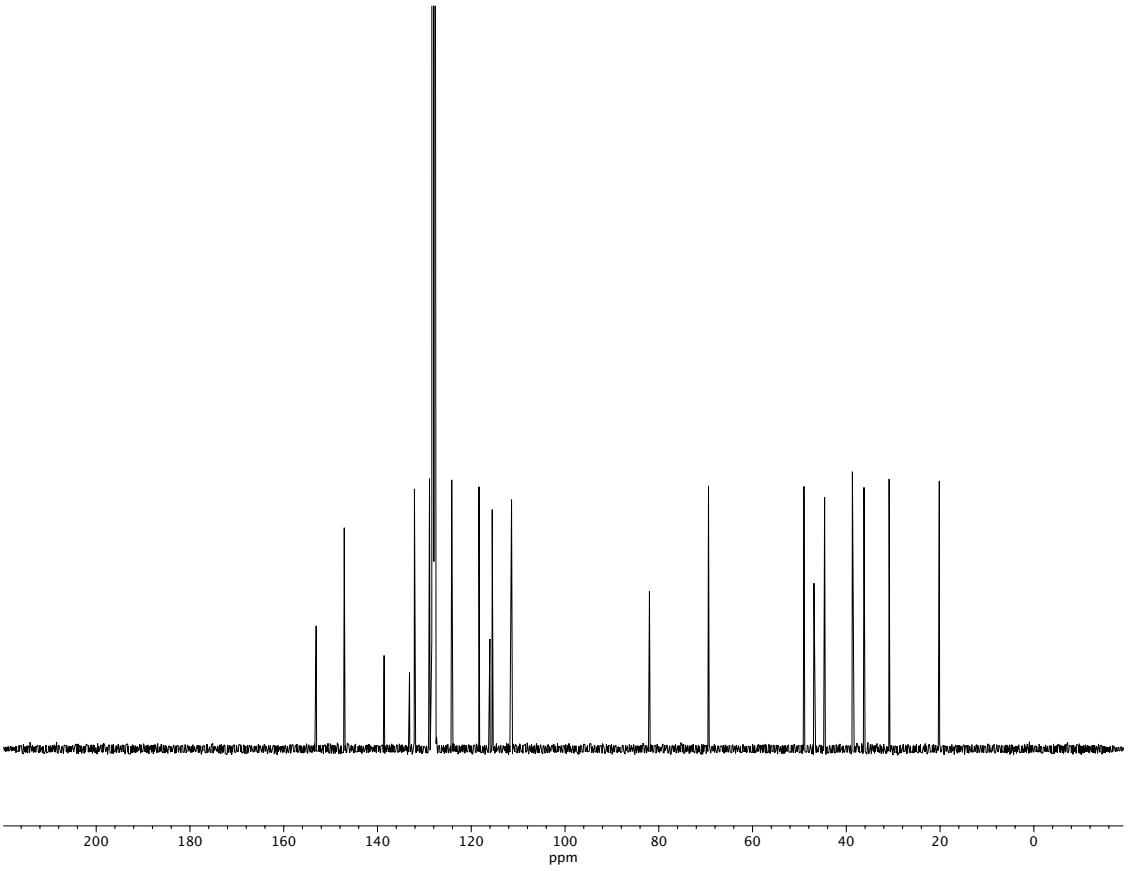


Figure A1.85 *^{13}C NMR (100 MHz, C_6D_6) of compound* ***112***.

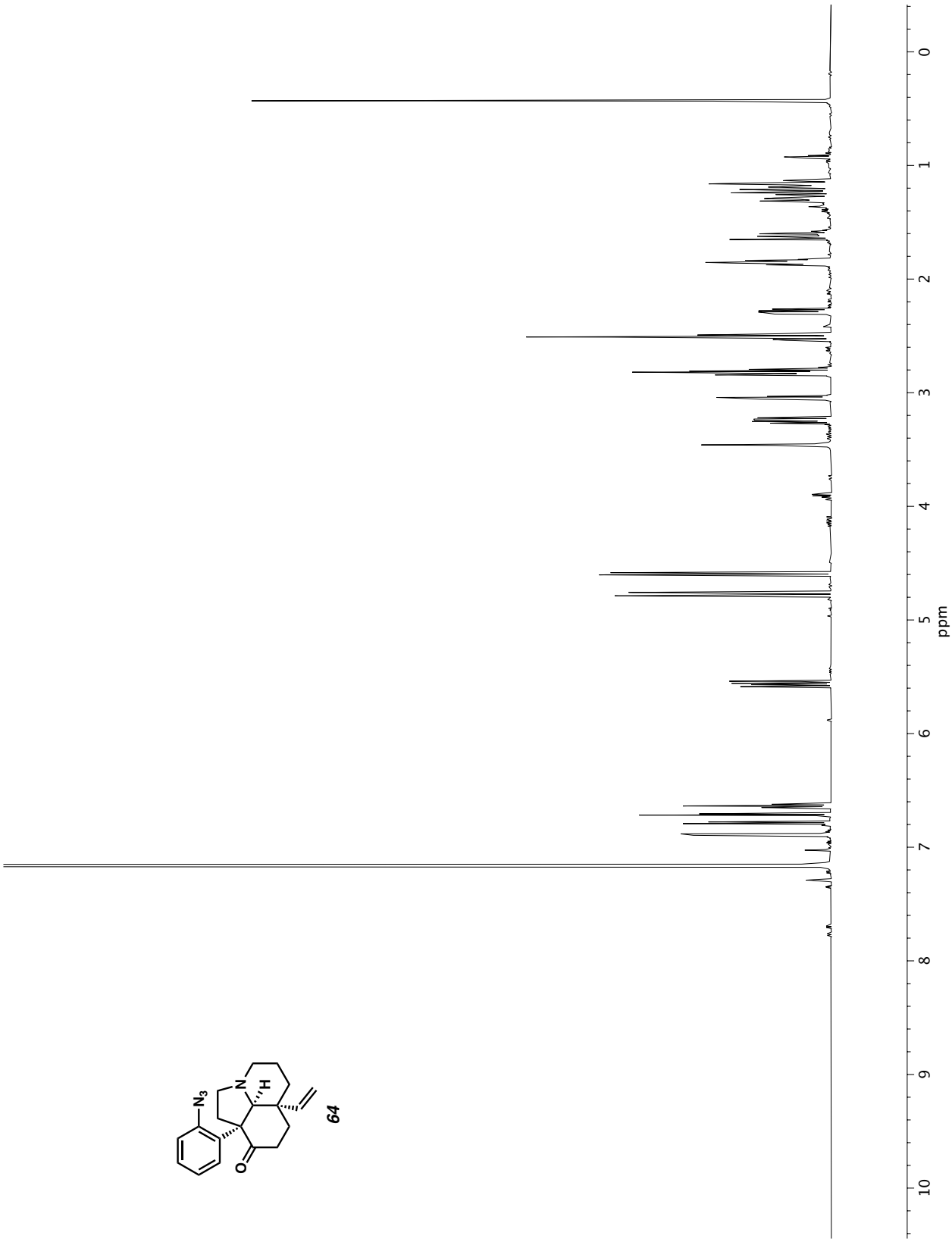


Figure A1.86 *^1H NMR (600 MHz, C_6D_6) of compound* ***64****.*

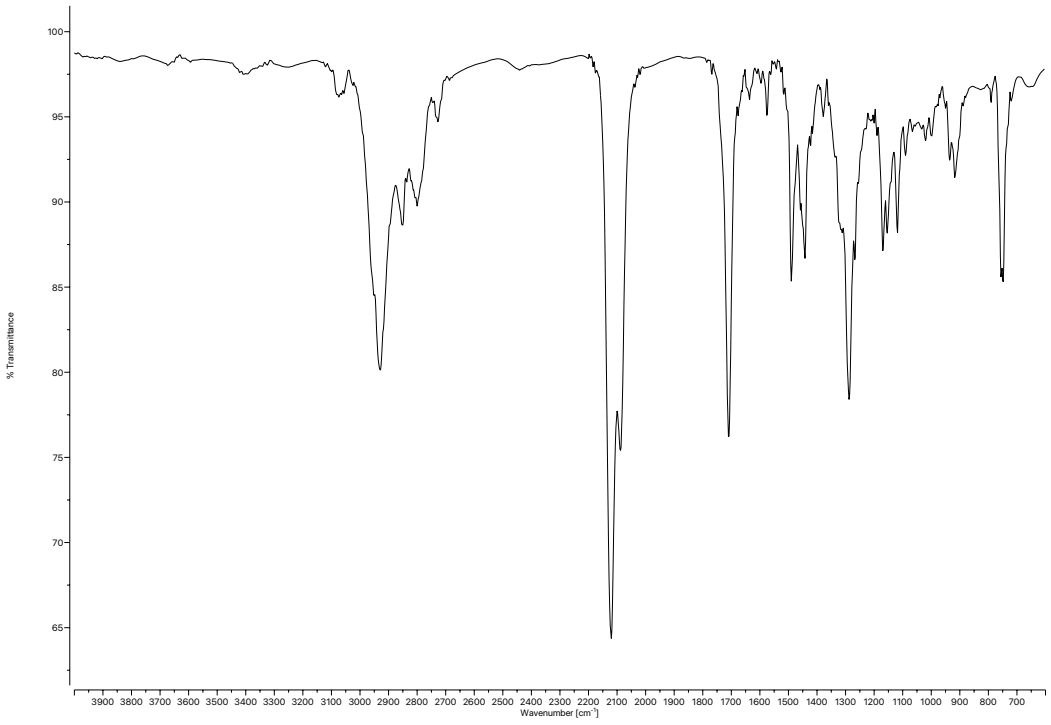


Figure A3.87 *Infrared spectrum (Thin Film, NaCl) of compound* ***64****.*

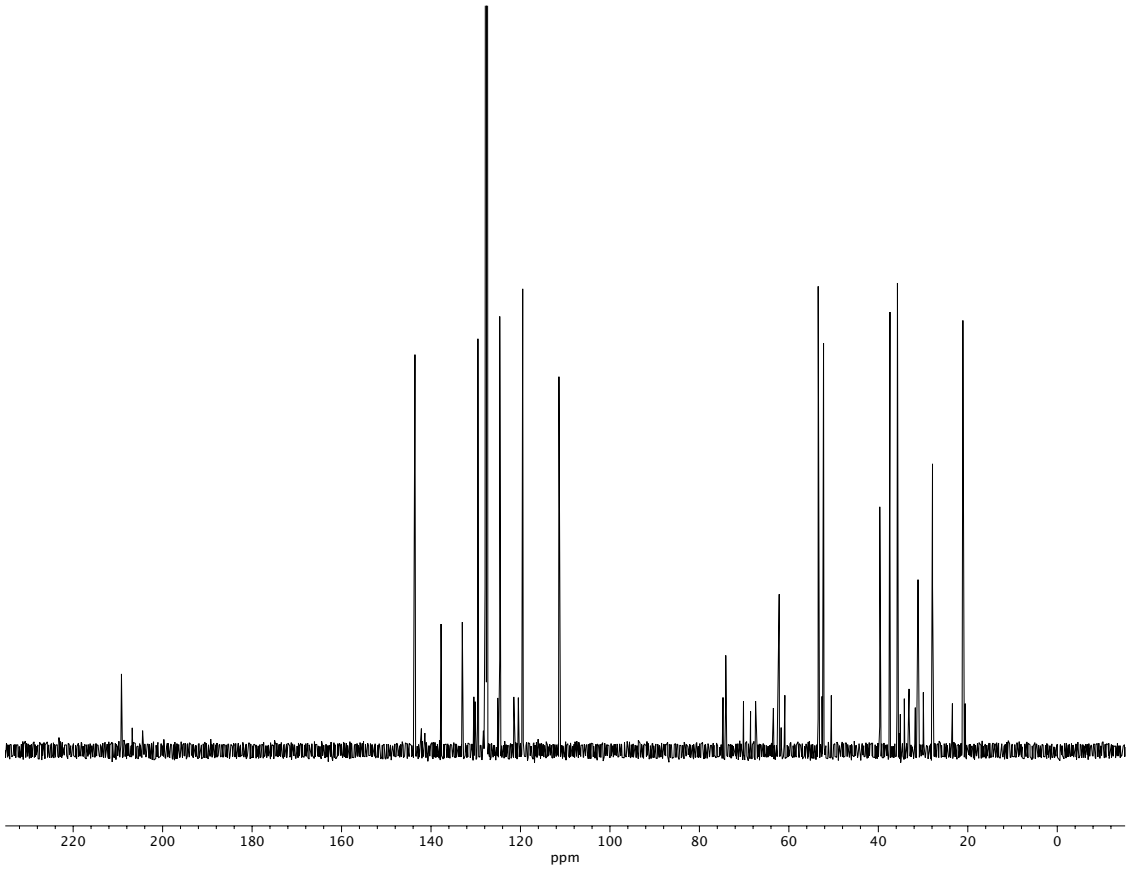


Figure A3.88 *^{13}C NMR (125 MHz, C_6D_6) of compound* ***64****.*

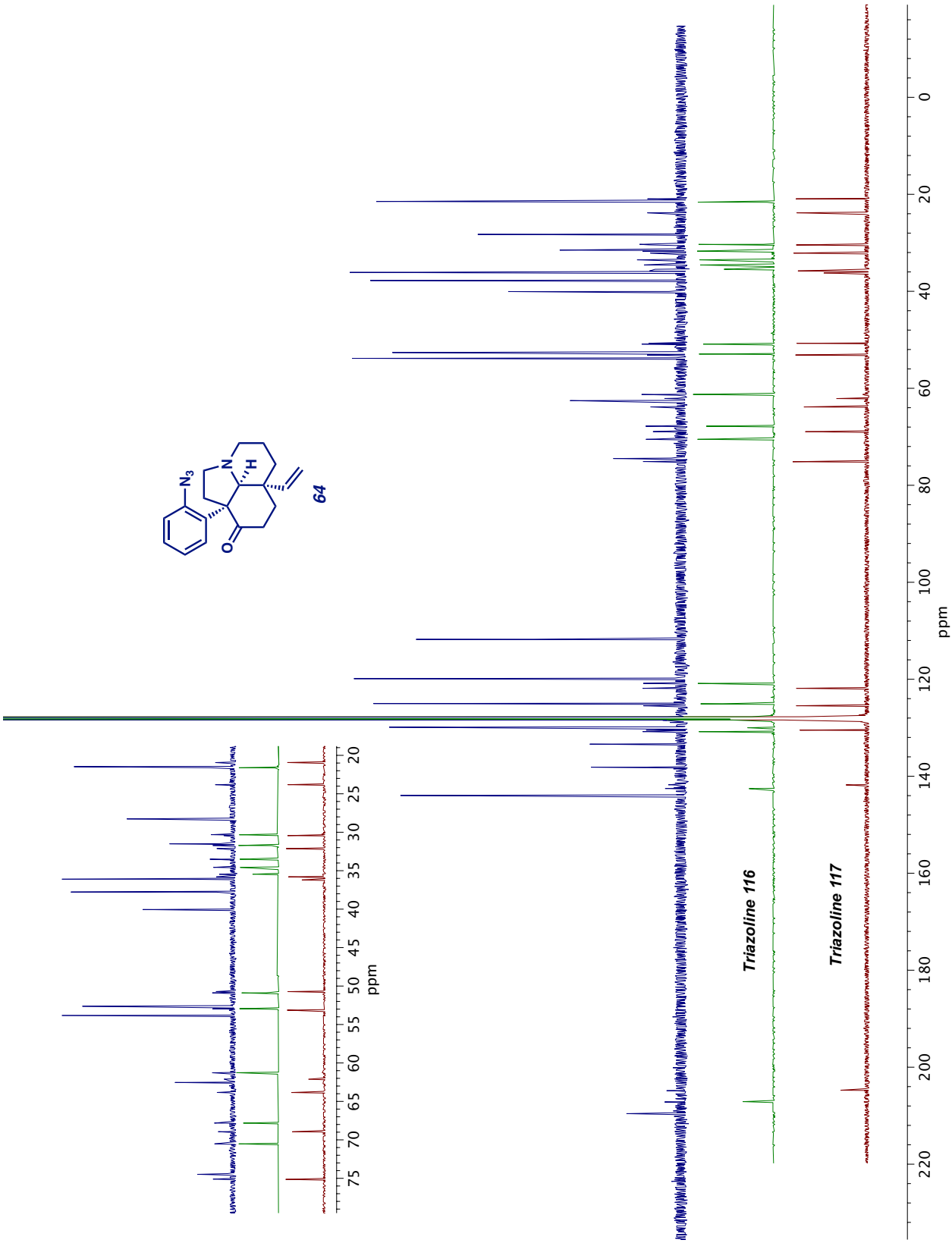


Figure A3.89 *Stacked ^{13}C NMR (C_6D_6) of compounds* ***64***, ***116***, *and* ***117***.

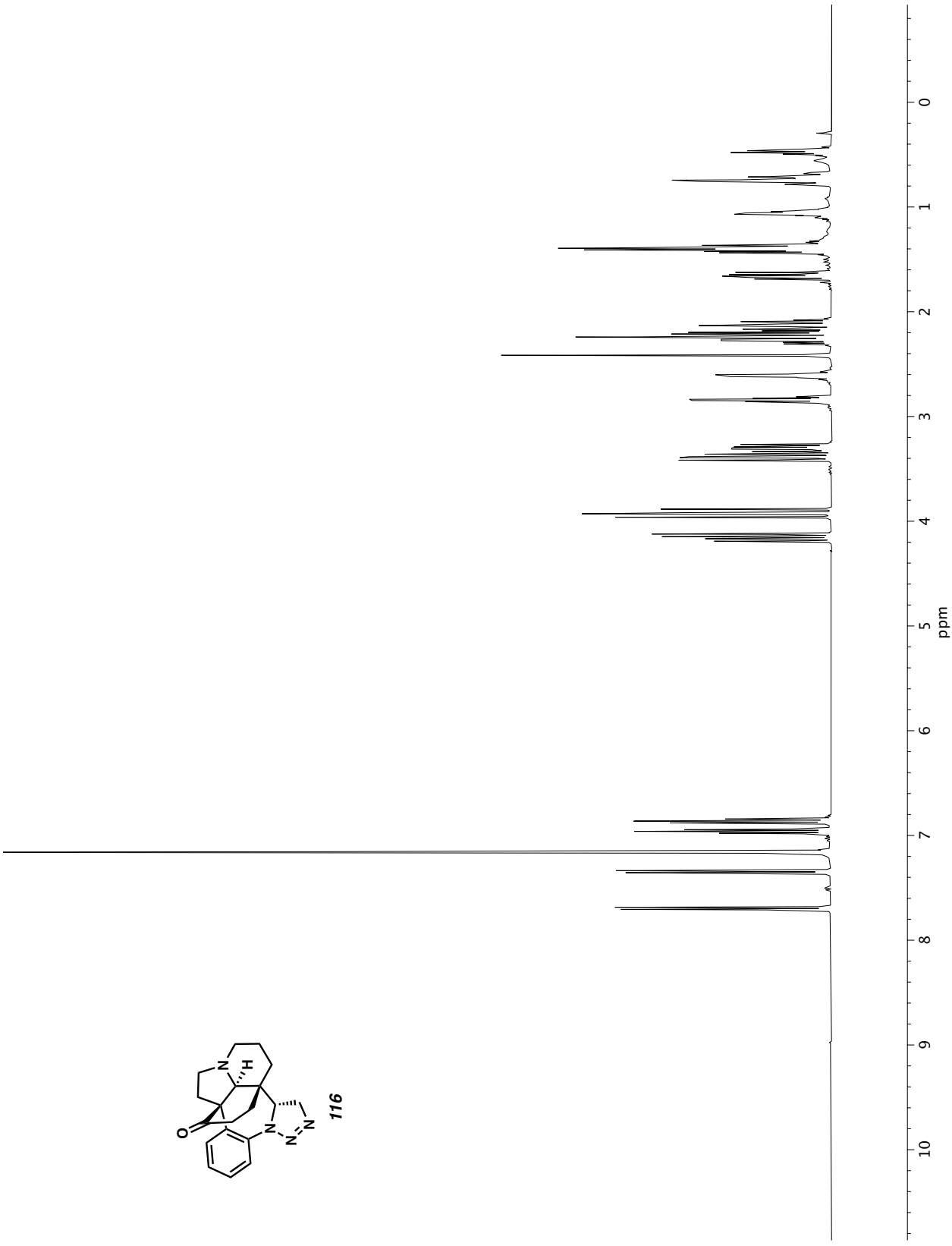


Figure A3.90 *^{1}H NMR (400 MHz, C_6D_6) of compound* ***116***.

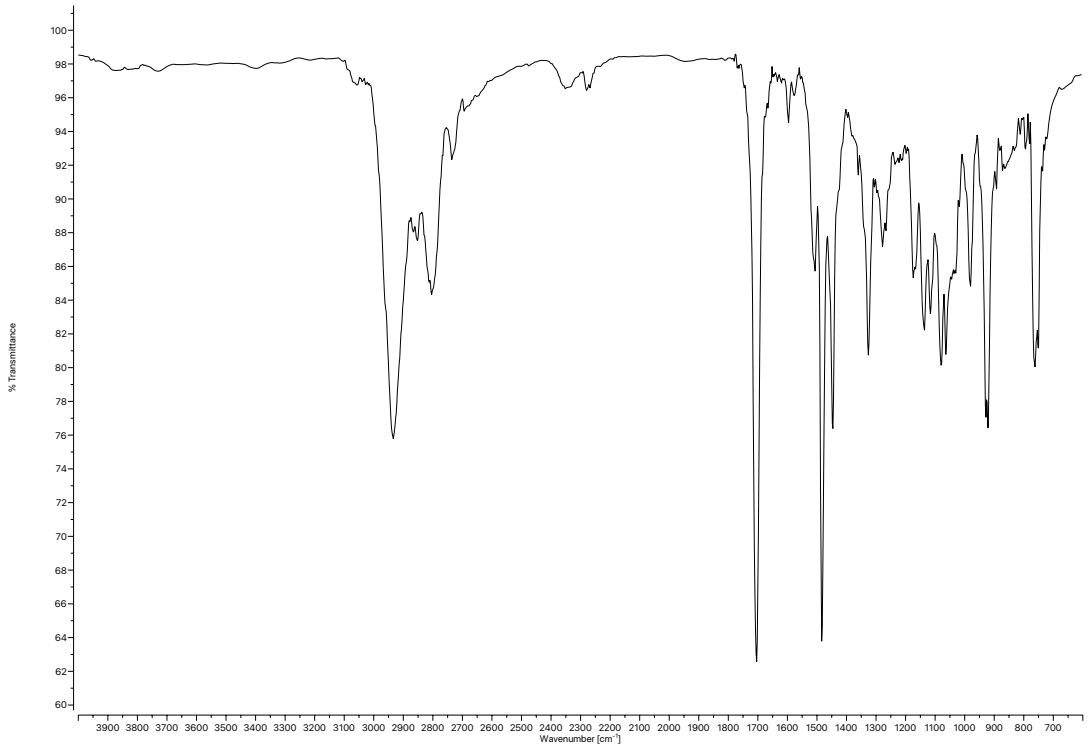


Figure A3.91 *Infrared spectrum (Thin Film, NaCl) of compound* ***116****.*

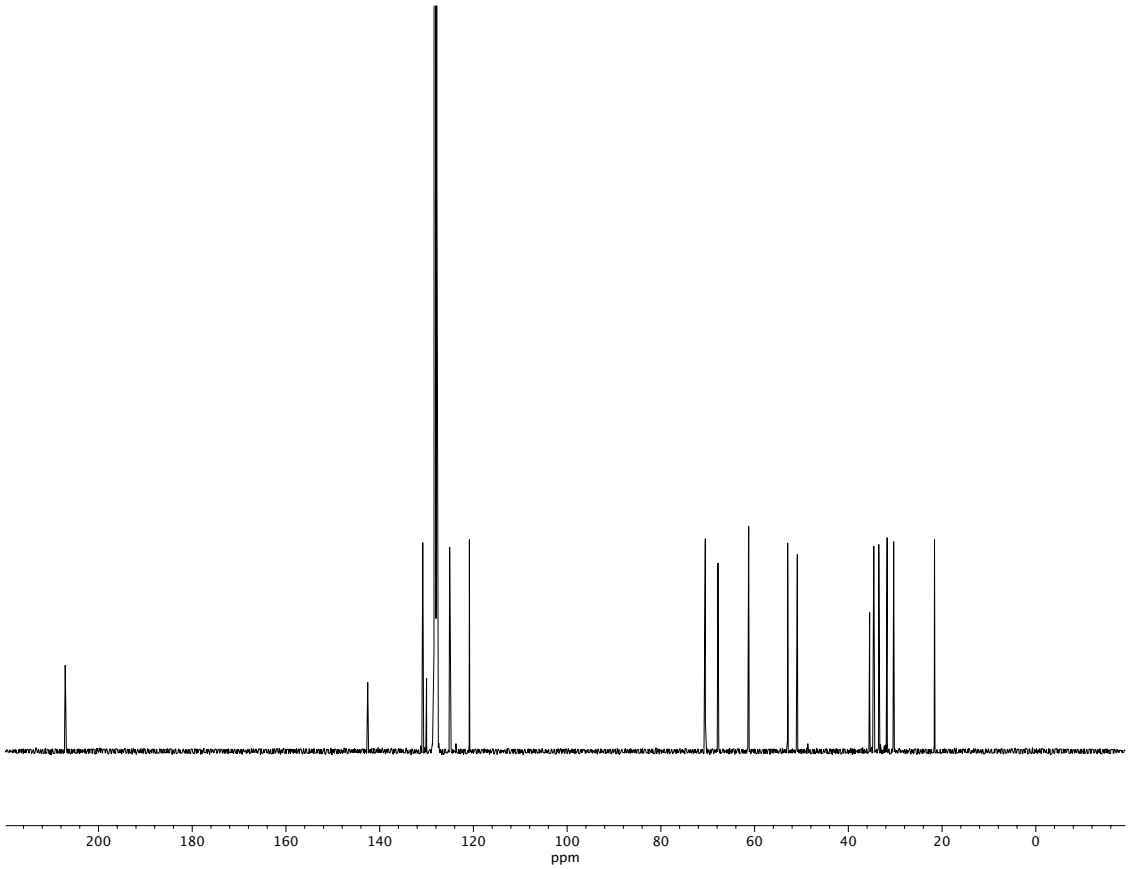


Figure A3.92 *^{13}C NMR (100 MHz, C_6D_6) of compound* ***116****.*

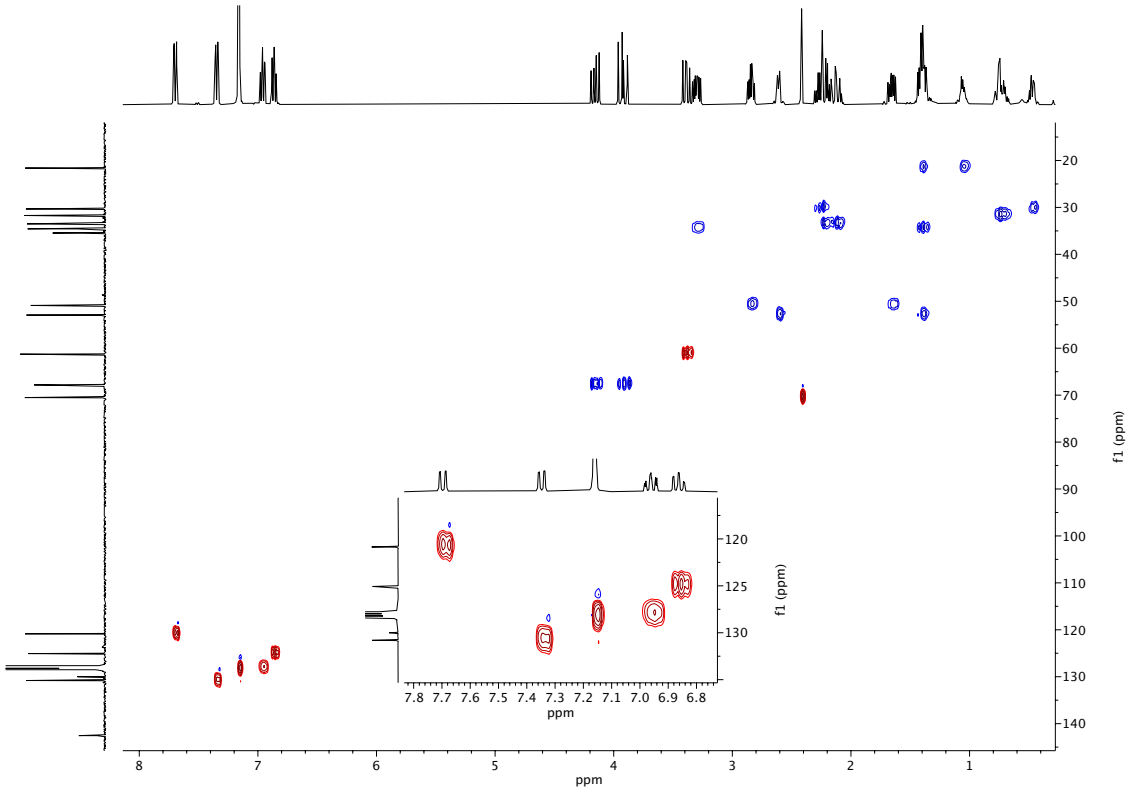


Figure A3.93 *HSQC spectrum (C_6D_6) of compound* ***116***.

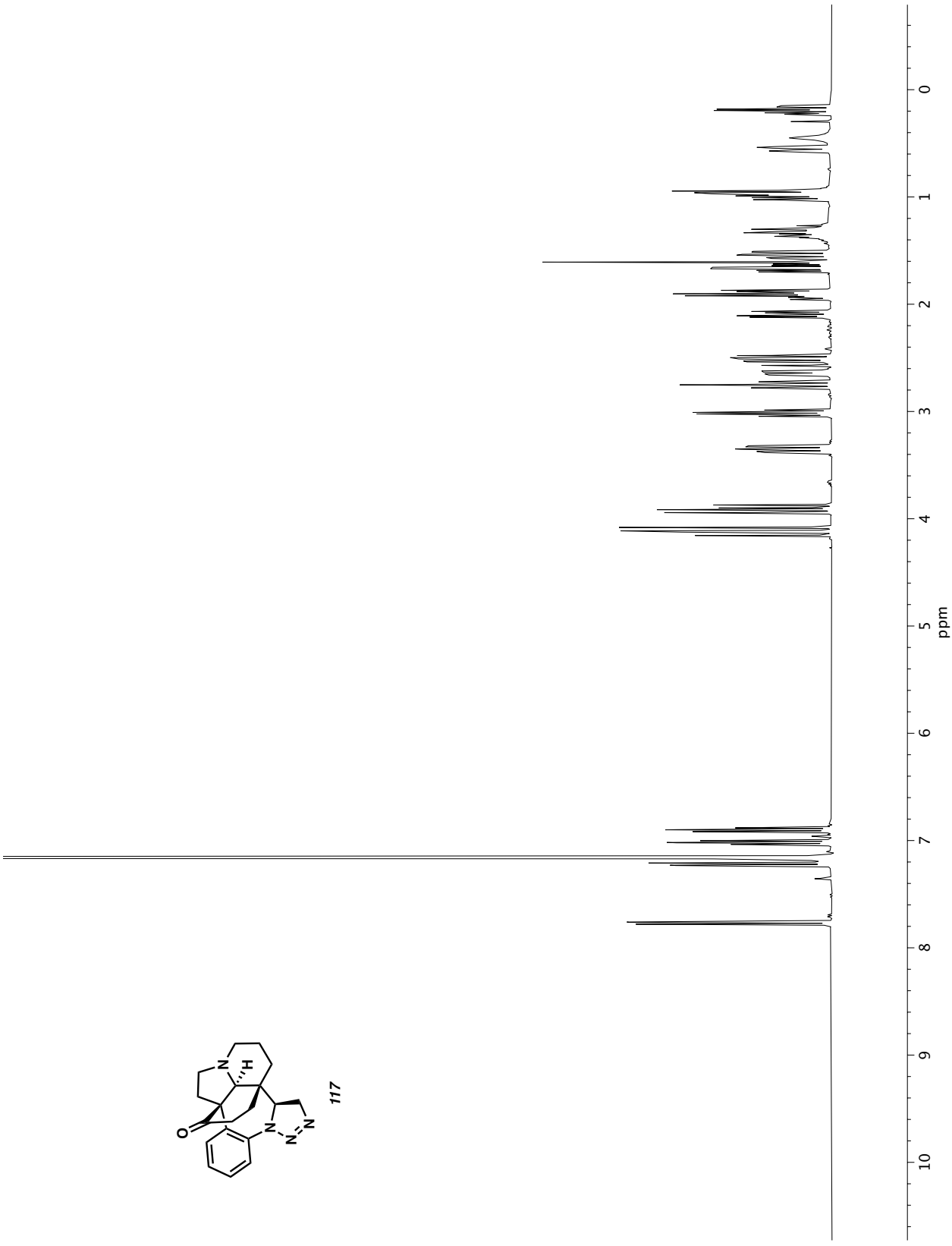


Figure A3.94 *^{1}H NMR (400 MHz, C_6D_6) of compound* ***117****.*

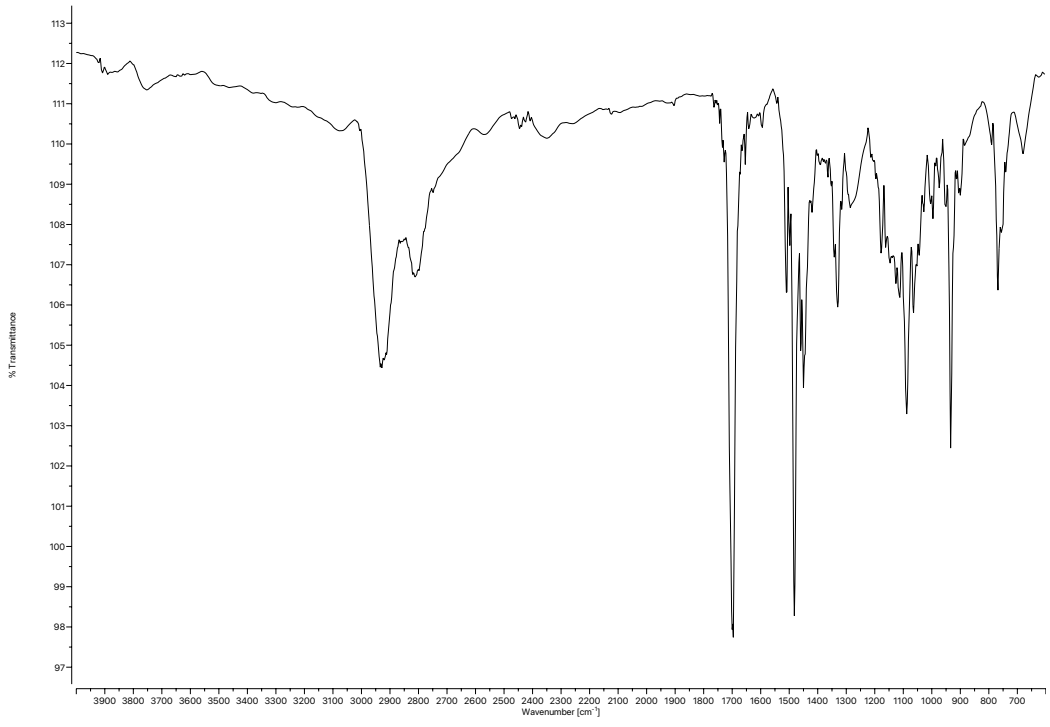


Figure A3.95 *Infrared spectrum (Thin Film, NaCl) of compound* ***117****.*

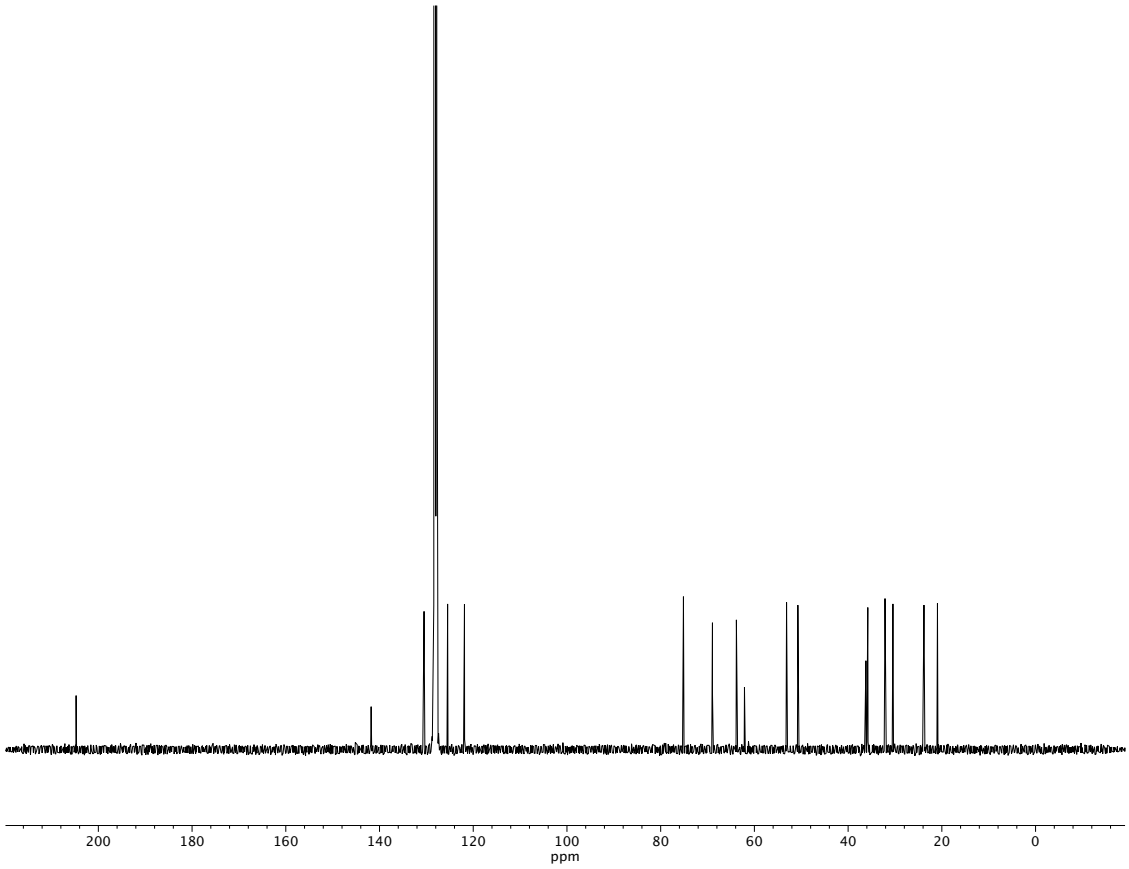


Figure A3.96 *^{13}C NMR (100 MHz, C_6D_6) of compound* ***117****.*

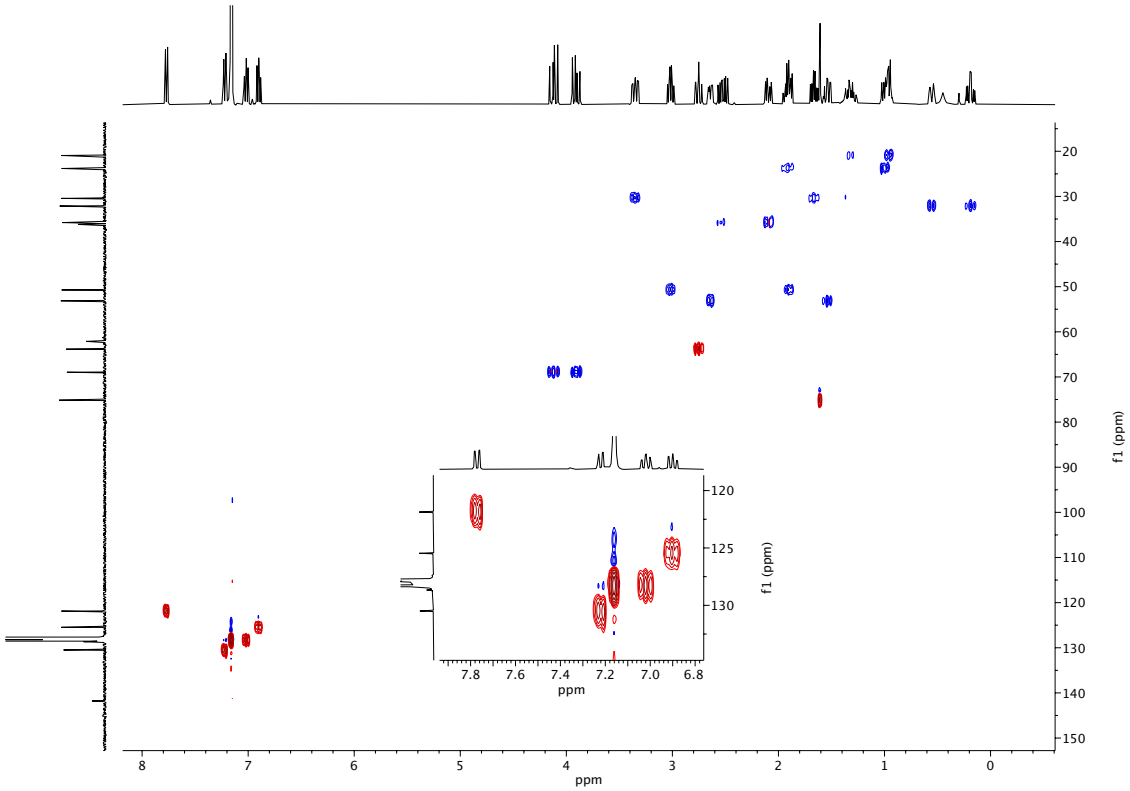
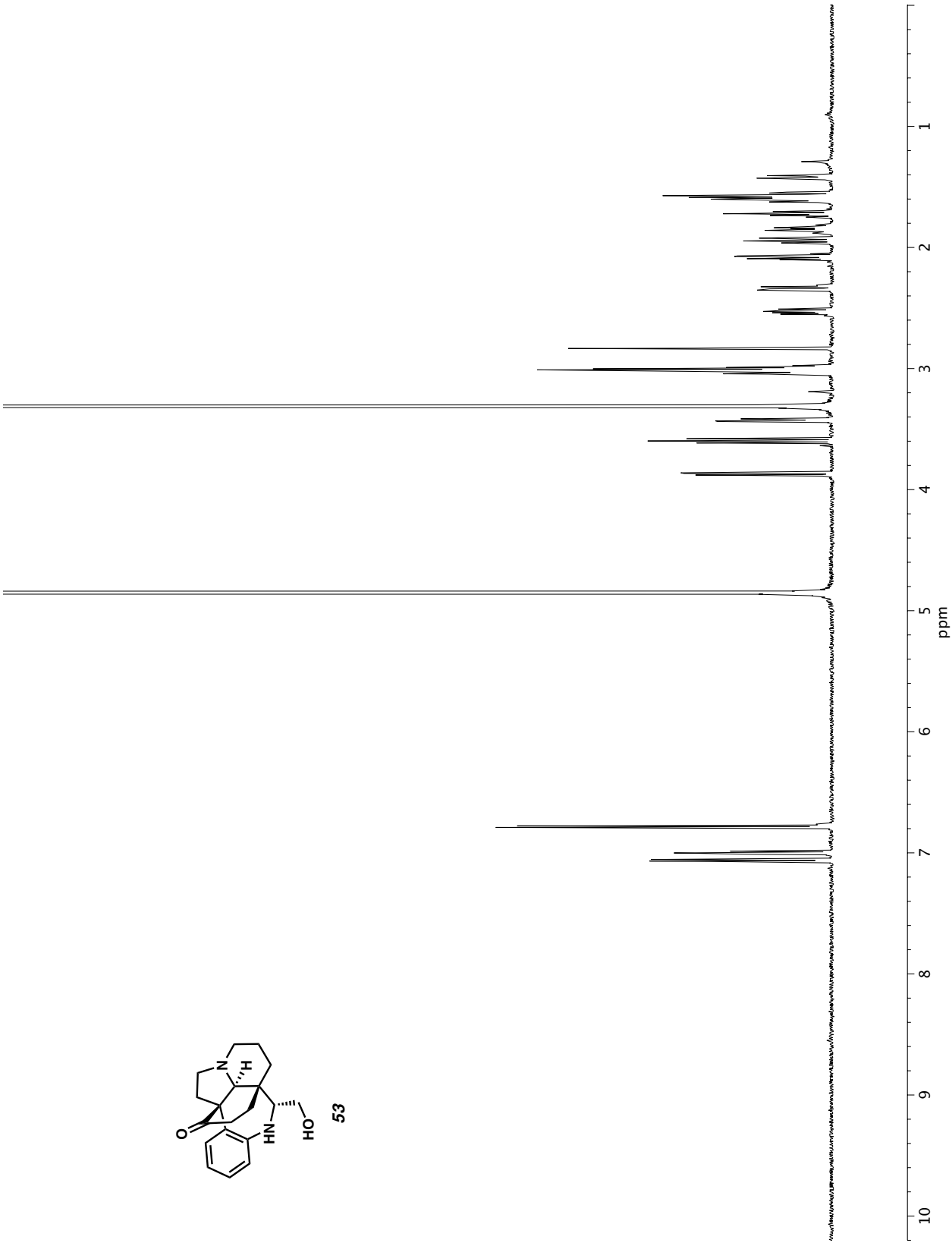


Figure A3.97 *HSQC spectrum (C_6D_6) of compound* ***117****.*



53

Figure A3.98 *^1H NMR (600 MHz, CD_3OD) of compound **53**.*

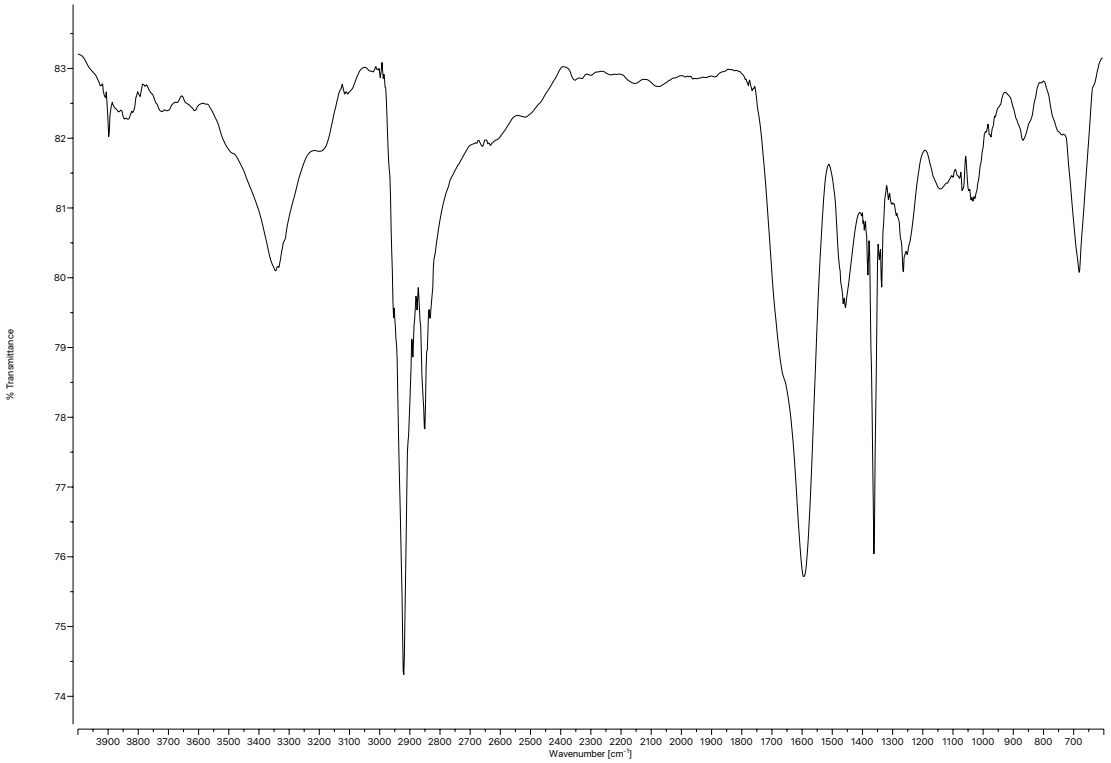


Figure A3.99 *Infrared spectrum (Thin Film, NaCl) of compound* ***53***.

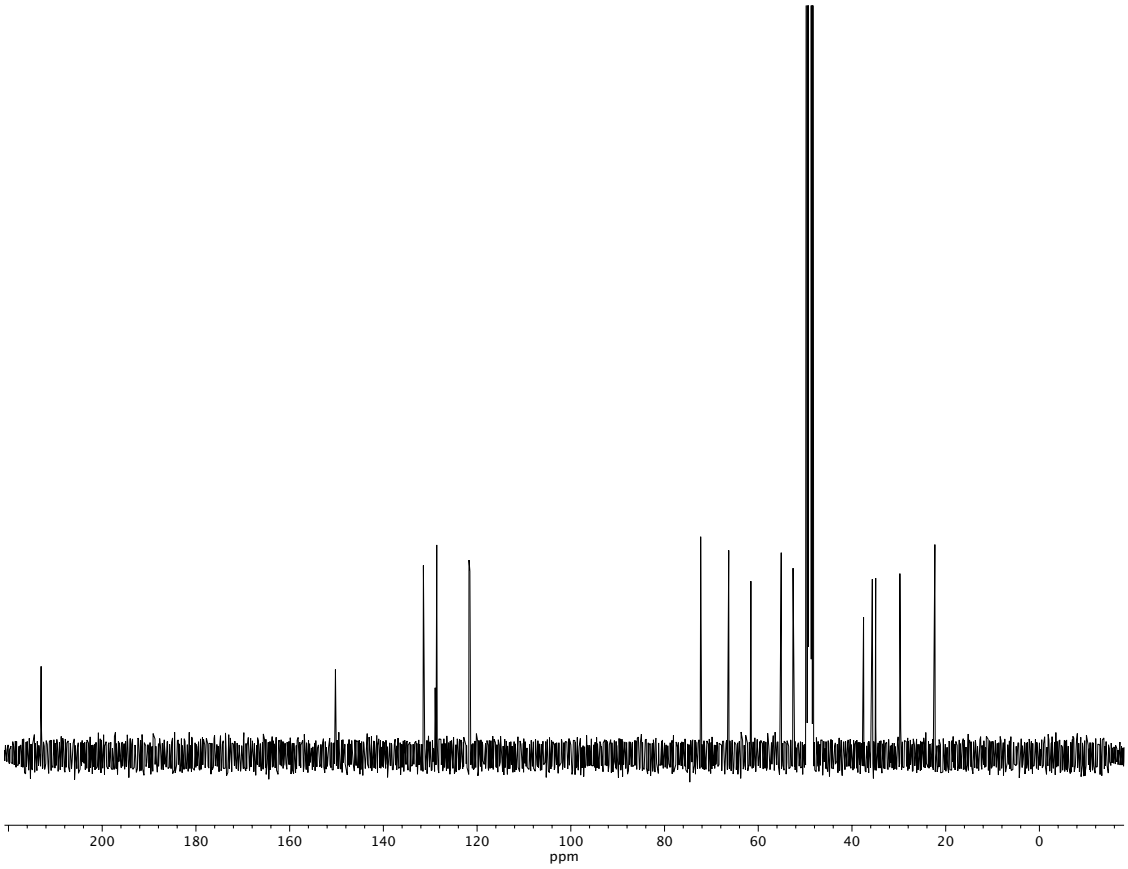


Figure A3.100 *^{13}C NMR (100 MHz, CD_3OD) of compound* ***53***.

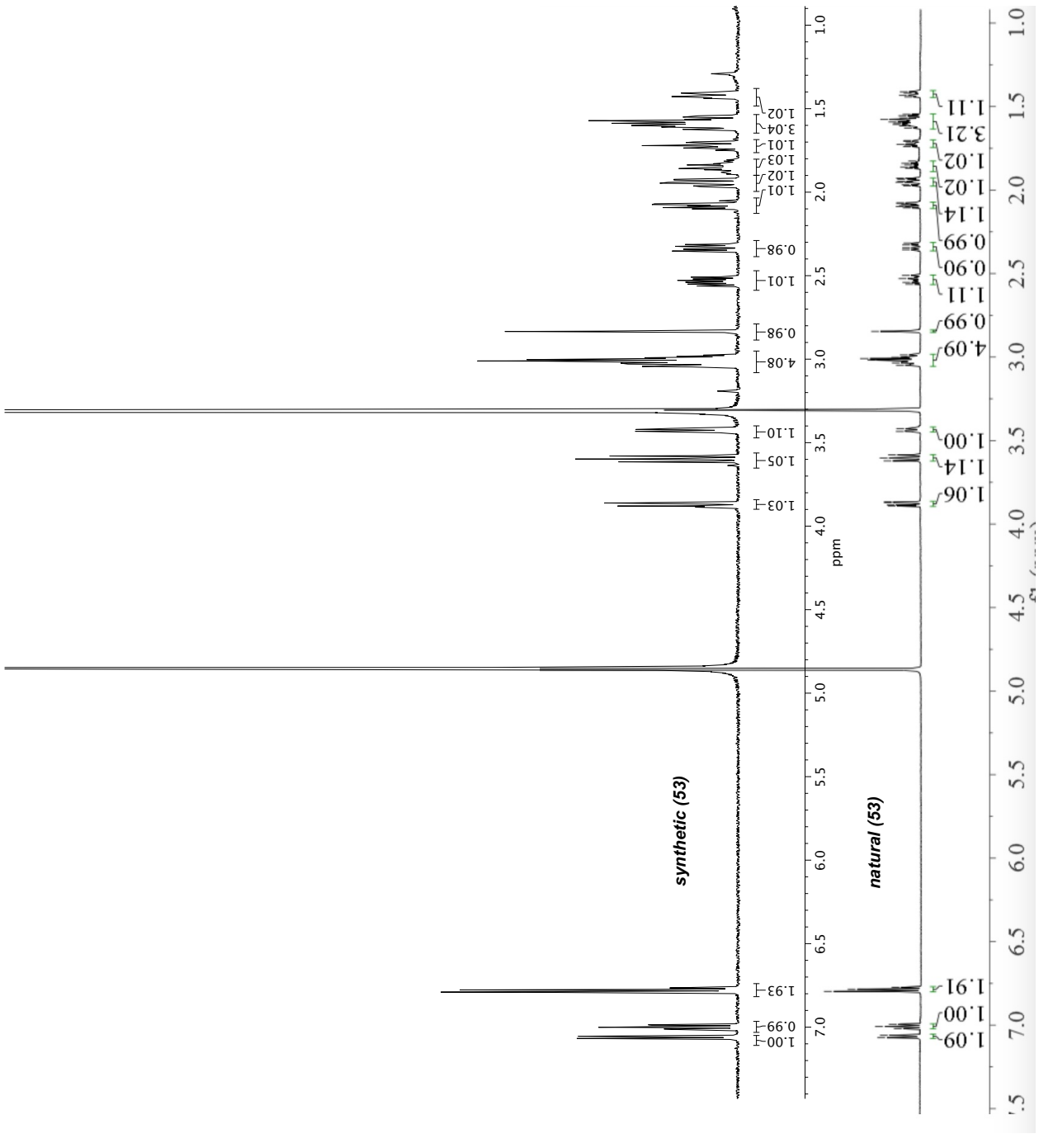


Figure A3.101 *Overlaid ^{1}H NMR (400 MHz and 600 MHz, CD_3OD) of synthetic and natural* ***53***.

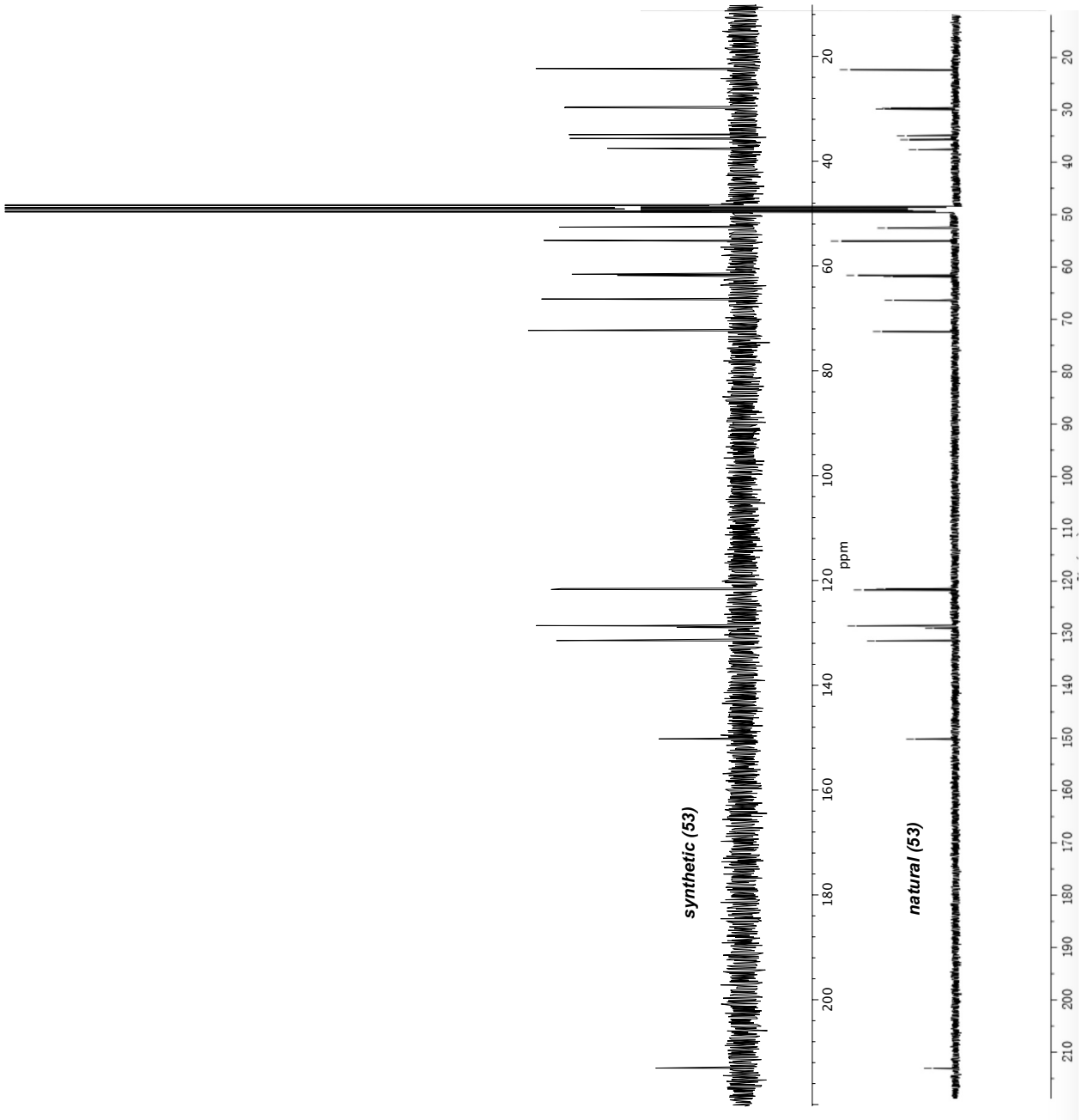


Figure A3.102 *Overlaid ^{13}C (100 MHz, CD_3OD) of synthetic and natural* ***53***.

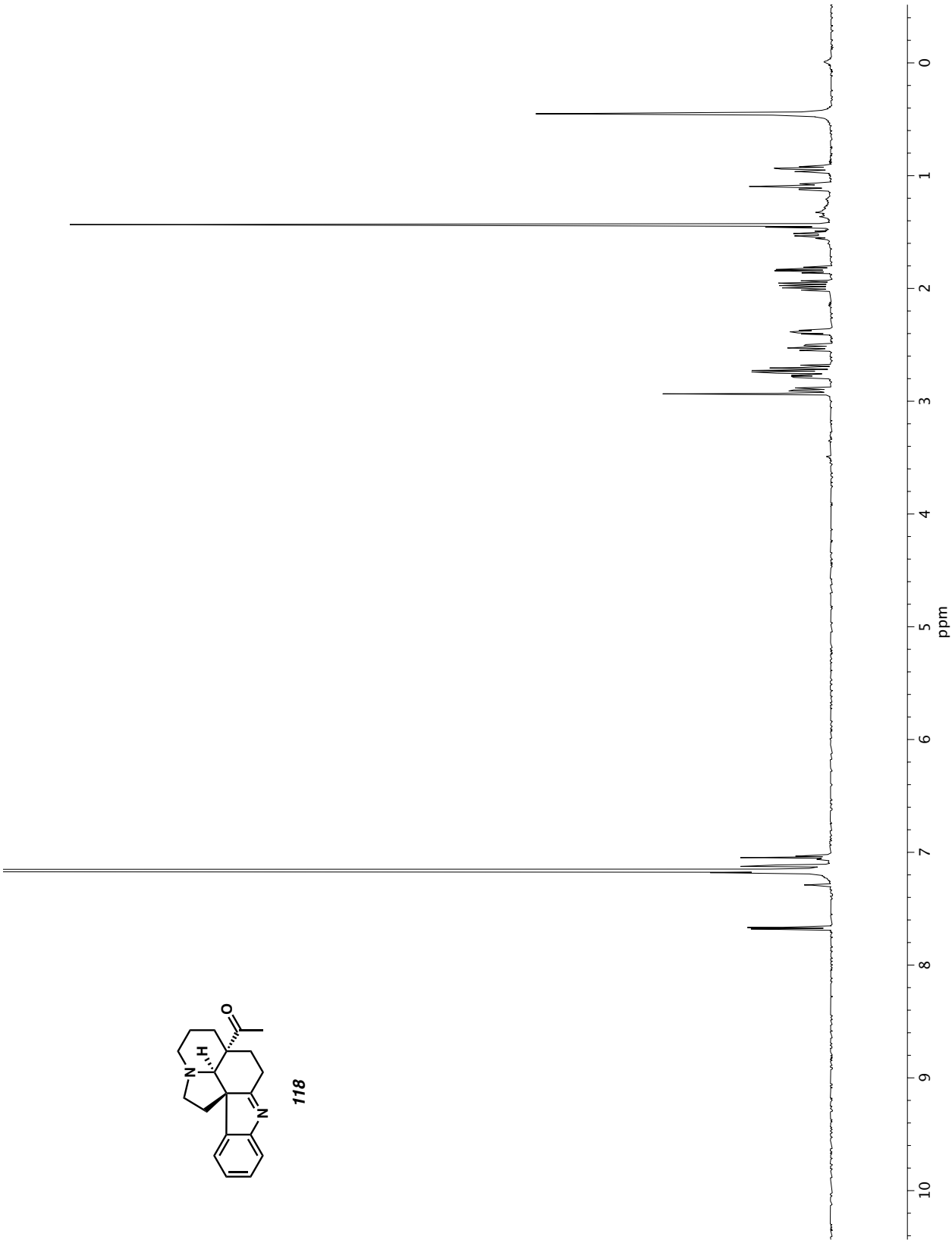


Figure A3.103 *^1H NMR (600 MHz, C_6D_6) of compound **118**.*

APPENDIX 4

X-Ray Crystallography Reports Relevant to Chapter 2:

Enantioselective Total Synthesis of Hunterine A

A4.1 GENERAL EXPERIMENTAL

X-Ray crystallographic analysis was obtained from the Caltech X-Ray Crystallography Facility using a Bruker AXS D8 VENTURE KAPPA diffractometer.

A4.2 X-RAY CRYSTAL STRUCTURE ANALYSIS OF COMPOUND (Z)–82 (V23277)

An X-Ray quality crystal of dinitrophenylhydrazone ***(Z)-82*** (compound V23277) was grown by dissolving approximately 5 mg in minimal Et_2O (approx. 30 μL) and carefully layering with pentane. Low-temperature diffraction data (ϕ-and ω-scans) were collected on a Bruker AXS D8 VENTURE KAPPA diffractometer coupled to a PHOTON II CPAD detector with Cu K_α radiation (λ = 1.54178 Å) from an IμS micro-source for the structure of compound V23277. The structure was solved by direct methods using SHELXS[1] and refined against F^2 on all data by full-matrix least squares with SHELXL-2019[2] using established refinement techniques.[3] All non-hydrogen atoms were refined anisotropically. Unless otherwise noted, all hydrogen atoms were included into the model at geometrically calculated positions and refined using a riding model. The isotropic displacement parameters of all hydrogen atoms were fixed to 1.2 times the U value of the atoms they are linked to (1.5 times for methyl groups). Compound V23277 crystallizes in the monoclinic space group $P2_1$ with one molecule in the asymmetric unit. The coordinates for the hydrogen atoms bound to N1, N101, N201, N301, O5 O105, O205, and O305 were located in the difference Fourier synthesis and refined semi-freely with the help of a restraint on the N-H or O-H distance (0.88(4) Å or 0.84(4) Å, respectively).

Figure A4.2.1 *X-Ray Coordinate of Compound* ***(Z)-82***

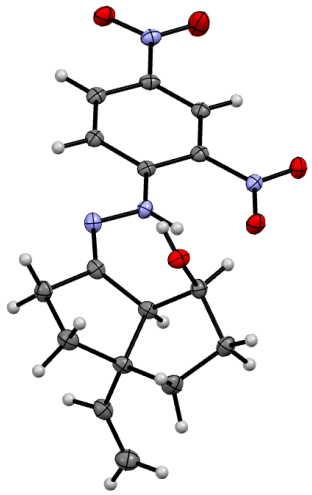


Table A4.2.1. *Crystal Data and Structure Refinement for* ***(Z)-82***

Identification code	V23277	
Empirical formula	C32 H36 N8 O10	
Formula weight	692.69	
Temperature	100(2) K	
Wavelength	1.54178 Å	
Crystal system	Monoclinic	
Space group	$P2_1$	
Unit cell dimensions	a = 17.6441(17) Å	a= 90°.
	b = 8.1909(6) Å	b= 101.734(8)°.
	c = 22.7771(14) Å	g = 90°.
Volume	3223.0(4) $Å^3$	
Z	4	
Density (calculated)	1.428 Mg/m^3	
Absorption coefficient	0.909 mm^{-1}	
F(000)	1456	
Crystal size	0.300 x 0.150 x 0.050 mm^3	
Theta range for data collection	1.981 to 74.668°.	
Index ranges	-21<=h<=22, -10<=k<=10, -28<=l<=28	
Reflections collected	64398	
Independent reflections	12967 [R(int) = 0.0677]	

Completeness to theta = 67.679°	100.0 %
Absorption correction	Semi-empirical from equivalents
Max. and min. transmission	0.7538 and 0.4744
Refinement method	Full-matrix least-squares on F^2
Data / restraints / parameters	12967 / 9 / 925
Goodness-of-fit on F^2	1.037
Final R indices [I>2sigma(I)]	R1 = 0.0493, wR2 = 0.1267
R indices (all data)	R1 = 0.0521, wR2 = 0.1298
Absolute structure parameter	-0.02(10)
Extinction coefficient	n/a
Largest diff. peak and hole	0.550 and -0.477 e.$Å^{-3}$

Table A4.2.2 *Atomic coordinates (x 10^4) and equivalent isotropic displacement parameters ($Å^2$x 10^3) for* ***(Z)-82*** *(V23277). U(eq) is defined as one third of the trace of the orthogonalized U^{ij} tensor.*

Atom	x	y	z	U(eq)
N(1)	7988(1)	2019(3)	9658(1)	16(1)
C(1)	8640(2)	1363(3)	9537(1)	15(1)
C(2)	9221(2)	2316(3)	9352(1)	15(1)
N(3)	9172(1)	4079(3)	9312(1)	17(1)
O(1)	8622(1)	4796(2)	9470(1)	20(1)
O(2)	9680(1)	4832(3)	9127(1)	22(1)
C(3)	9885(2)	1621(4)	9215(1)	16(1)
C(4)	9976(2)	-36(4)	9265(1)	17(1)
N(4)	10678(1)	-763(3)	9135(1)	18(1)
O(3)	11153(1)	138(3)	8972(1)	28(1)
O(4)	10769(1)	-2241(3)	9208(1)	24(1)
C(5)	9420(2)	-1043(3)	9448(1)	17(1)
C(6)	8770(2)	-358(3)	9586(1)	16(1)
N(2)	7444(1)	1048(3)	9854(1)	18(1)
C(7)	6950(2)	1846(3)	10087(1)	17(1)
C(8)	6918(2)	3662(3)	10205(1)	17(1)
C(9)	6489(2)	4678(4)	9662(1)	22(1)
O(5)	5971(1)	3714(3)	9235(1)	29(1)
C(10)	5977(2)	5820(4)	9938(1)	26(1)

Table A4.2.2 cont'd.

Atom	x	y	z	U(eq)
C(11)	5690(2)	4714(4)	10386(1)	25(1)
C(12)	6425(1)	3823(4)	10708(1)	18(1)
C(15)	6877(2)	4756(4)	11234(1)	26(1)
C(16)	6685(2)	6093(5)	11482(2)	44(1)
C(13)	6283(2)	2034(4)	10885(1)	24(1)
C(14)	6332(2)	994(4)	10336(1)	23(1)
N(101)	8918(1)	17070(3)	7952(1)	16(1)
C(101)	8284(1)	17723(3)	8103(1)	15(1)
C(102)	7673(2)	16759(3)	8244(1)	15(1)
N(103)	7691(1)	15003(3)	8235(1)	16(1)
O(101)	8230(1)	14291(3)	8056(1)	21(1)
O(102)	7179(1)	14229(3)	8408(1)	23(1)
C(103)	7024(2)	17457(4)	8402(1)	16(1)
C(104)	6968(1)	19123(4)	8406(1)	16(1)
N(104)	6284(1)	19867(3)	8557(1)	21(1)
O(103)	5867(1)	19028(3)	8806(1)	29(1)
O(104)	6158(1)	21311(3)	8423(1)	28(1)
C(105)	7544(2)	20135(3)	8261(1)	16(1)
C(106)	8192(2)	19445(3)	8120(1)	16(1)
N(102)	9519(1)	18065(3)	7858(1)	18(1)
C(107)	10102(2)	17285(4)	7749(1)	18(1)
C(108)	10227(2)	15456(4)	7735(1)	19(1)
C(109)	9834(2)	14664(4)	7126(1)	21(1)
O(105)	9651(1)	15942(3)	6696(1)	22(1)
C(110)	10464(2)	13556(4)	6974(2)	28(1)
C(111)	11199(2)	14566(4)	7178(1)	26(1)
C(112)	11128(2)	15241(4)	7798(1)	25(1)
C(115)	11437(2)	13942(5)	8266(2)	39(1)
C(116)	11747(3)	14133(6)	8822(2)	51(1)
C(113)	11464(2)	16973(5)	7916(2)	31(1)
C(114)	10809(2)	18139(4)	7637(2)	27(1)
N(201)	6104(1)	7470(3)	7015(1)	14(1)
C(201)	6729(1)	8151(3)	6860(1)	14(1)

Table A4.2.2 cont'd.

Atom	x	y	z	U(eq)
C(202)	7323(1)	7190(3)	6690(1)	14(1)
N(203)	7313(1)	5434(3)	6697(1)	15(1)
O(201)	6773(1)	4708(2)	6871(1)	19(1)
O(202)	7836(1)	4675(2)	6535(1)	22(1)
C(203)	7960(2)	7906(3)	6513(1)	15(1)
C(204)	8010(1)	9568(3)	6509(1)	15(1)
N(204)	8664(1)	10315(3)	6313(1)	18(1)
O(203)	9089(1)	9456(3)	6081(1)	26(1)
O(204)	8750(1)	11803(3)	6384(1)	23(1)
C(205)	7450(2)	10577(3)	6688(1)	14(1)
C(206)	6824(1)	9878(3)	6855(1)	14(1)
N(202)	5558(1)	8433(3)	7220(1)	15(1)
C(207)	4967(1)	7619(3)	7301(1)	14(1)
C(208)	4773(1)	5853(3)	7152(1)	15(1)
C(209)	5161(2)	4639(3)	7647(1)	19(1)
O(205)	5356(1)	5546(3)	8195(1)	24(1)
C(210)	4522(2)	3410(4)	7667(1)	22(1)
C(211)	3807(2)	4493(4)	7620(1)	21(1)
C(212)	3873(1)	5712(4)	7116(1)	17(1)
C(215)	3479(2)	5134(4)	6499(1)	23(1)
C(216)	3120(2)	3750(5)	6344(2)	32(1)
C(213)	3607(2)	7474(4)	7225(1)	22(1)
C(214)	4327(2)	8397(4)	7546(1)	20(1)
N(301)	7013(1)	12265(3)	5219(1)	16(1)
C(301)	6386(1)	11616(3)	5383(1)	14(1)
C(302)	5828(2)	12606(3)	5593(1)	16(1)
N(303)	5875(1)	14358(3)	5612(1)	15(1)
O(301)	6415(1)	15056(3)	5432(1)	21(1)
O(302)	5377(1)	15133(3)	5801(1)	21(1)
C(303)	5195(2)	11917(4)	5779(1)	16(1)
C(304)	5103(2)	10257(4)	5755(1)	17(1)
N(304)	4433(1)	9545(3)	5939(1)	19(1)
O(303)	4003(1)	10449(3)	6155(1)	34(1)

Table A4.2.2 cont'd.

Atom	x	y	z	U(eq)
O(304)	4327(1)	8077(3)	5868(1)	24(1)
C(305)	5629(2)	9232(3)	5543(1)	16(1)
C(306)	6254(2)	9894(4)	5359(1)	16(1)
N(302)	7550(1)	11274(3)	5021(1)	17(1)
C(307)	8038(1)	12070(4)	4780(1)	17(1)
C(308)	8069(1)	13887(3)	4675(1)	16(1)
C(309)	8385(2)	14982(3)	5222(1)	18(1)
O(305)	9040(1)	14271(3)	5613(1)	22(1)
C(310)	8673(2)	16462(4)	4932(1)	21(1)
C(311)	9091(2)	15725(4)	4462(1)	22(1)
C(312)	8661(1)	14115(4)	4255(1)	18(1)
C(315)	8222(2)	14076(4)	3611(1)	21(1)
C(316)	8077(2)	15283(4)	3226(1)	28(1)
C(313)	9181(2)	12571(4)	4386(1)	21(1)
C(314)	8653(2)	11196(4)	4526(1)	20(1)

Table A4.2.3. *Bond lengths [Å] and angles [°] for* ***(Z)-82*** *(V23277).*

Bond	Length (Å)	Bond	Length (Å)
N(1)-C(1)	1.348(3)	N(4)-O(4)	1.229(3)
N(1)-N(2)	1.389(3)	N(4)-O(3)	1.230(3)
N(1)-H(1N)	0.87(2)	C(5)-C(6)	1.368(4)
C(1)-C(2)	1.419(4)	C(5)-H(5)	0.9500
C(1)-C(6)	1.429(4)	C(6)-H(6)	0.9500
C(2)-C(3)	1.395(4)	N(2)-C(7)	1.288(4)
C(2)-N(3)	1.448(4)	C(7)-C(14)	1.500(4)
N(3)-O(2)	1.230(3)	C(7)-C(8)	1.515(4)
N(3)-O(1)	1.250(3)	C(8)-C(9)	1.555(4)
C(3)-C(4)	1.369(4)	C(8)-C(12)	1.578(4)
C(3)-H(3)	0.9500	C(8)-H(8)	1.0000
C(4)-C(5)	1.409(4)	C(9)-O(5)	1.430(4)
C(4)-N(4)	1.457(3)	C(9)-C(10)	1.523(4)

Table A4.2.3. cont'd.

Bond	Length (Å)	Bond	Length (Å)
C(9)-H(9)	1.0000	C(105)-C(106)	1.371(4)
O(5)-H(5O)	0.82(3)	C(105)-H(105)	0.9500
C(10)-C(11)	1.525(4)	C(106)-H(106)	0.9500
C(10)-H(10A)	0.9900	N(102)-C(107)	1.278(4)
C(10)-H(10B)	0.9900	C(107)-C(114)	1.496(4)
C(11)-C(12)	1.538(4)	C(107)-C(108)	1.515(4)
C(11)-H(11A)	0.9900	C(108)-C(109)	1.559(4)
C(11)-H(11B)	0.9900	C(108)-C(112)	1.576(4)
C(12)-C(15)	1.506(4)	C(108)-H(108)	1.0000
C(12)-C(13)	1.554(4)	C(109)-O(105)	1.426(4)
C(15)-C(16)	1.308(5)	C(109)-C(110)	1.529(4)
C(15)-H(15)	0.9500	C(109)-H(109)	1.0000
C(16)-H(16A)	0.9500	O(105)-H(15O)	0.85(2)
C(16)-H(16B)	0.9500	C(110)-C(111)	1.528(4)
C(13)-C(14)	1.529(4)	C(110)-H(11C)	0.9900
C(13)-H(13A)	0.9900	C(110)-H(11D)	0.9900
C(13)-H(13B)	0.9900	C(111)-C(112)	1.545(4)
C(14)-H(14A)	0.9900	C(111)-H(11E)	0.9900
C(14)-H(14B)	0.9900	C(111)-H(11F)	0.9900
N(101)-C(101)	1.346(4)	C(112)-C(115)	1.527(5)
N(101)-N(102)	1.387(3)	C(112)-C(113)	1.540(5)
N(101)-H(11N)	0.88(2)	C(115)-C(116)	1.283(6)
C(101)-C(106)	1.421(4)	C(115)-H(115)	0.9500
C(101)-C(102)	1.424(4)	C(116)-H(11G)	0.9500
C(102)-C(103)	1.391(4)	C(116)-H(11H)	0.9500
C(102)-N(103)	1.439(4)	C(113)-C(114)	1.533(5)
N(103)-O(102)	1.232(3)	C(113)-H(11I)	0.9900
N(103)-O(101)	1.253(3)	C(113)-H(11J)	0.9900
C(103)-C(104)	1.368(4)	C(114)-H(11K)	0.9900
C(103)-H(103)	0.9500	C(114)-H(11L)	0.9900
C(104)-C(105)	1.401(4)	N(201)-C(201)	1.345(3)
C(104)-N(104)	1.455(3)	N(201)-N(202)	1.397(3)
N(104)-O(103)	1.227(3)	N(201)-H(21N)	0.87(2)
N(104)-O(104)	1.231(4)	C(201)-C(206)	1.424(4)

Table A4.2.3. cont'd.

Bond	Length (Å)	Bond	Length (Å)
C(201)-C(202)	1.426(4)	C(216)-H(21E)	0.9500
C(202)-C(203)	1.399(4)	C(216)-H(21F)	0.9500
C(202)-N(203)	1.439(3)	C(213)-C(214)	1.531(4)
N(203)-O(202)	1.230(3)	C(213)-H(21G)	0.9900
N(203)-O(201)	1.253(3)	C(213)-H(21H)	0.9900
C(203)-C(204)	1.365(4)	C(214)-H(21I)	0.9900
C(203)-H(203)	0.9500	C(214)-H(21J)	0.9900
C(204)-C(205)	1.410(4)	N(301)-C(301)	1.347(3)
C(204)-N(204)	1.455(3)	N(301)-N(302)	1.390(3)
N(204)-O(203)	1.224(3)	N(301)-H(31N)	0.87(2)
N(204)-O(204)	1.234(3)	C(301)-C(306)	1.429(4)
C(205)-C(206)	1.366(4)	C(301)-C(302)	1.431(4)
C(205)-H(205)	0.9500	C(302)-C(303)	1.392(4)
C(206)-H(206)	0.9500	C(302)-N(303)	1.438(4)
N(202)-C(207)	1.281(3)	N(303)-O(302)	1.230(3)
C(207)-C(214)	1.501(4)	N(303)-O(301)	1.250(3)
C(207)-C(208)	1.509(4)	C(303)-C(304)	1.369(4)
C(208)-C(209)	1.554(4)	C(303)-H(303)	0.9500
C(208)-C(212)	1.577(3)	C(304)-C(305)	1.408(4)
C(208)-H(208)	1.0000	C(304)-N(304)	1.455(3)
C(209)-O(205)	1.434(4)	N(304)-O(304)	1.222(3)
C(209)-C(210)	1.519(4)	N(304)-O(303)	1.231(3)
C(209)-H(209)	1.0000	C(305)-C(306)	1.369(4)
O(205)-H(25O)	0.88(2)	C(305)-H(305)	0.9500
C(210)-C(211)	1.528(4)	C(306)-H(306)	0.9500
C(210)-H(21A)	0.9900	N(302)-C(307)	1.289(4)
C(210)-H(21B)	0.9900	C(307)-C(314)	1.509(4)
C(211)-C(212)	1.543(4)	C(307)-C(308)	1.510(4)
C(211)-H(21C)	0.9900	C(308)-C(309)	1.545(4)
C(211)-H(21D)	0.9900	C(308)-C(312)	1.565(4)
C(212)-C(215)	1.512(4)	C(308)-H(308)	1.0000
C(212)-C(213)	1.553(4)	C(309)-O(305)	1.431(3)
C(215)-C(216)	1.311(5)	C(309)-C(310)	1.518(4)
C(215)-H(215)	0.9500	C(309)-H(309)	1.0000

Table A4.2.3. cont'd.

Bond	Length (Å)	Atoms	Angle (°)
O(305)-H(35O)	0.84(2)	C(2)-C(3)-H(3)	120.8
C(310)-C(311)	1.541(4)	C(3)-C(4)-C(5)	121.9(3)
C(310)-H(31A)	0.9900	C(3)-C(4)-N(4)	118.5(3)
C(310)-H(31B)	0.9900	C(5)-C(4)-N(4)	119.6(3)
C(311)-C(312)	1.546(4)	O(4)-N(4)-O(3)	123.5(2)
C(311)-H(31C)	0.9900	O(4)-N(4)-C(4)	118.0(2)
C(311)-H(31D)	0.9900	O(3)-N(4)-C(4)	118.4(2)
C(312)-C(315)	1.513(4)	C(6)-C(5)-C(4)	119.7(3)
C(312)-C(313)	1.555(4)	C(6)-C(5)-H(5)	120.2
C(315)-C(316)	1.312(5)	C(4)-C(5)-H(5)	120.2
C(315)-H(315)	0.9500	C(5)-C(6)-C(1)	121.0(3)
C(316)-H(31E)	0.9500	C(5)-C(6)-H(6)	119.5
C(316)-H(31F)	0.9500	C(1)-C(6)-H(6)	119.5
C(313)-C(314)	1.535(4)	C(7)-N(2)-N(1)	114.3(2)
C(313)-H(31G)	0.9900	N(2)-C(7)-C(14)	121.6(3)
C(313)-H(31H)	0.9900	N(2)-C(7)-C(8)	128.6(2)
C(314)-H(31I)	0.9900	C(14)-C(7)-C(8)	109.5(2)
C(314)-H(31J)	0.9900	C(7)-C(8)-C(9)	114.4(2)
		C(7)-C(8)-C(12)	104.8(2)
Atoms	**Angle (°)**	C(9)-C(8)-C(12)	106.4(2)
C(1)-N(1)-N(2)	120.8(2)	C(7)-C(8)-H(8)	110.3
C(1)-N(1)-H(1N)	118(2)	C(9)-C(8)-H(8)	110.3
N(2)-N(1)-H(1N)	121(2)	C(12)-C(8)-H(8)	110.3
N(1)-C(1)-C(2)	122.6(2)	O(5)-C(9)-C(10)	105.6(2)
N(1)-C(1)-C(6)	120.5(2)	O(5)-C(9)-C(8)	112.7(2)
C(2)-C(1)-C(6)	116.8(2)	C(10)-C(9)-C(8)	103.5(2)
C(3)-C(2)-C(1)	122.2(2)	O(5)-C(9)-H(9)	111.6
C(3)-C(2)-N(3)	115.7(2)	C(10)-C(9)-H(9)	111.6
C(1)-C(2)-N(3)	122.0(2)	C(8)-C(9)-H(9)	111.6
O(2)-N(3)-O(1)	121.7(2)	C(9)-O(5)-H(5O)	114(3)
O(2)-N(3)-C(2)	118.9(2)	C(9)-C(10)-C(11)	102.6(2)
O(1)-N(3)-C(2)	119.3(2)	C(9)-C(10)-H(10A)	111.3
C(4)-C(3)-C(2)	118.4(3)	C(11)-C(10)-H(10A)	111.3
C(4)-C(3)-H(3)	120.8	C(9)-C(10)-H(10B)	111.3

Table A4.2.3. cont'd.

Atoms	Angle (°)	Atoms	Angle (°)
C(11)-C(10)-H(10B)	111.3	N(102)-N(101)-H(11N)	121(2)
H(10A)-C(10)-H(10B)	109.2	N(101)-C(101)-C(106)	120.4(2)
C(10)-C(11)-C(12)	103.8(2)	N(101)-C(101)-C(102)	122.9(3)
C(10)-C(11)-H(11A)	111.0	C(106)-C(101)-C(102)	116.6(2)
C(12)-C(11)-H(11A)	111.0	C(103)-C(102)-C(101)	122.1(3)
C(10)-C(11)-H(11B)	111.0	C(103)-C(102)-N(103)	115.8(2)
C(12)-C(11)-H(11B)	111.0	C(101)-C(102)-N(103)	122.1(2)
H(11A)-C(11)-H(11B)	109.0	O(102)-N(103)-O(101)	121.3(2)
C(15)-C(12)-C(11)	113.4(3)	O(102)-N(103)-C(102)	119.4(2)
C(15)-C(12)-C(13)	111.1(2)	O(101)-N(103)-C(102)	119.4(2)
C(11)-C(12)-C(13)	114.0(2)	C(104)-C(103)-C(102)	118.4(3)
C(15)-C(12)-C(8)	109.8(2)	C(104)-C(103)-H(103)	120.8
C(11)-C(12)-C(8)	103.3(2)	C(102)-C(103)-H(103)	120.8
C(13)-C(12)-C(8)	104.6(2)	C(103)-C(104)-C(105)	122.1(3)
C(16)-C(15)-C(12)	128.9(3)	C(103)-C(104)-N(104)	118.9(3)
C(16)-C(15)-H(15)	115.6	C(105)-C(104)-N(104)	118.9(3)
C(12)-C(15)-H(15)	115.6	O(103)-N(104)-O(104)	123.9(2)
C(15)-C(16)-H(16A)	120.0	O(103)-N(104)-C(104)	118.6(2)
C(15)-C(16)-H(16B)	120.0	O(104)-N(104)-C(104)	117.5(2)
H(16A)-C(16)-H(16B)	120.0	C(106)-C(105)-C(104)	119.3(3)
C(14)-C(13)-C(12)	105.9(2)	C(106)-C(105)-H(105)	120.3
C(14)-C(13)-H(13A)	110.5	C(104)-C(105)-H(105)	120.3
C(12)-C(13)-H(13A)	110.5	C(105)-C(106)-C(101)	121.4(3)
C(14)-C(13)-H(13B)	110.5	C(105)-C(106)-H(106)	119.3
C(12)-C(13)-H(13B)	110.5	C(101)-C(106)-H(106)	119.3
H(13A)-C(13)-H(13B)	108.7	C(107)-N(102)-N(101)	114.0(2)
C(7)-C(14)-C(13)	102.5(2)	N(102)-C(107)-C(114)	122.1(3)
C(7)-C(14)-H(14A)	111.3	N(102)-C(107)-C(108)	128.7(2)
C(13)-C(14)-H(14A)	111.3	C(114)-C(107)-C(108)	109.2(2)
C(7)-C(14)-H(14B)	111.3	C(107)-C(108)-C(109)	113.0(2)
C(13)-C(14)-H(14B)	111.3	C(107)-C(108)-C(112)	104.9(2)
H(14A)-C(14)-H(14B)	109.2	C(109)-C(108)-C(112)	107.0(2)
C(101)-N(101)-N(102)	120.4(2)	C(107)-C(108)-H(108)	110.6
C(101)-N(101)-H(11N)	118(2)	C(109)-C(108)-H(108)	110.6

Table A4.2.3. cont'd.

Atoms	Angle (°)	Atoms	Angle (°)
C(112)-C(108)-H(108)	110.6	C(112)-C(113)-H(11I)	110.6
O(105)-C(109)-C(110)	110.7(2)	C(114)-C(113)-H(11J)	110.6
O(105)-C(109)-C(108)	107.6(2)	C(112)-C(113)-H(11J)	110.6
C(110)-C(109)-C(108)	103.7(2)	H(11I)-C(113)-H(11J)	108.7
O(105)-C(109)-H(109)	111.5	C(107)-C(114)-C(113)	102.8(3)
C(110)-C(109)-H(109)	111.5	C(107)-C(114)-H(11K)	111.2
C(108)-C(109)-H(109)	111.5	C(113)-C(114)-H(11K)	111.2
C(109)-O(105)-H(15O)	98(3)	C(107)-C(114)-H(11L)	111.2
C(111)-C(110)-C(109)	102.8(2)	C(113)-C(114)-H(11L)	111.2
C(111)-C(110)-H(11C)	111.2	H(11K)-C(114)-H(11L)	109.1
C(109)-C(110)-H(11C)	111.2	C(201)-N(201)-N(202)	120.8(2)
C(111)-C(110)-H(11D)	111.2	C(201)-N(201)-H(21N)	120(2)
C(109)-C(110)-H(11D)	111.2	N(202)-N(201)-H(21N)	119(2)
H(11C)-C(110)-H(11D)	109.1	N(201)-C(201)-C(206)	121.2(2)
C(110)-C(111)-C(112)	104.5(2)	N(201)-C(201)-C(202)	121.9(2)
C(110)-C(111)-H(11E)	110.9	C(206)-C(201)-C(202)	116.9(2)
C(112)-C(111)-H(11E)	110.9	C(203)-C(202)-C(201)	121.7(2)
C(110)-C(111)-H(11F)	110.9	C(203)-C(202)-N(203)	115.7(2)
C(112)-C(111)-H(11F)	110.9	C(201)-C(202)-N(203)	122.6(2)
H(11E)-C(111)-H(11F)	108.9	O(202)-N(203)-O(201)	121.3(2)
C(115)-C(112)-C(113)	116.8(3)	O(202)-N(203)-C(202)	119.4(2)
C(115)-C(112)-C(111)	107.7(3)	O(201)-N(203)-C(202)	119.3(2)
C(113)-C(112)-C(111)	112.9(3)	C(204)-C(203)-C(202)	118.4(2)
C(115)-C(112)-C(108)	110.6(3)	C(204)-C(203)-H(203)	120.8
C(113)-C(112)-C(108)	105.0(2)	C(202)-C(203)-H(203)	120.8
C(111)-C(112)-C(108)	103.0(2)	C(203)-C(204)-C(205)	122.2(2)
C(116)-C(115)-C(112)	128.6(4)	C(203)-C(204)-N(204)	118.5(2)
C(116)-C(115)-H(115)	115.7	C(205)-C(204)-N(204)	119.3(2)
C(112)-C(115)-H(115)	115.7	O(203)-N(204)-O(204)	123.7(2)
C(115)-C(116)-H(11G)	120.0	O(203)-N(204)-C(204)	119.0(2)
C(115)-C(116)-H(11H)	120.0	O(204)-N(204)-C(204)	117.4(2)
H(11G)-C(116)-H(11H)	120.0	C(206)-C(205)-C(204)	119.3(2)
C(114)-C(113)-C(112)	105.7(2)	C(206)-C(205)-H(205)	120.4
C(114)-C(113)-H(11I)	110.6	C(204)-C(205)-H(205)	120.4

Table A4.2.3. cont'd.

Atoms	Angle (°)	Atoms	Angle (°)
C(205)-C(206)-C(201)	121.5(2)	C(211)-C(212)-C(213)	114.3(2)
C(205)-C(206)-H(206)	119.3	C(215)-C(212)-C(208)	109.8(2)
C(201)-C(206)-H(206)	119.3	C(211)-C(212)-C(208)	103.6(2)
C(207)-N(202)-N(201)	113.0(2)	C(213)-C(212)-C(208)	104.9(2)
N(202)-C(207)-C(214)	121.9(2)	C(216)-C(215)-C(212)	128.7(3)
N(202)-C(207)-C(208)	128.4(2)	C(216)-C(215)-H(215)	115.6
C(214)-C(207)-C(208)	109.7(2)	C(212)-C(215)-H(215)	115.6
C(207)-C(208)-C(209)	113.9(2)	C(215)-C(216)-H(21E)	120.0
C(207)-C(208)-C(212)	105.2(2)	C(215)-C(216)-H(21F)	120.0
C(209)-C(208)-C(212)	106.4(2)	H(21E)-C(216)-H(21F)	120.0
C(207)-C(208)-H(208)	110.4	C(214)-C(213)-C(212)	106.7(2)
C(209)-C(208)-H(208)	110.4	C(214)-C(213)-H(21G)	110.4
C(212)-C(208)-H(208)	110.4	C(212)-C(213)-H(21G)	110.4
O(205)-C(209)-C(210)	111.4(2)	C(214)-C(213)-H(21H)	110.4
O(205)-C(209)-C(208)	107.0(2)	C(212)-C(213)-H(21H)	110.4
C(210)-C(209)-C(208)	103.0(2)	H(21G)-C(213)-H(21H)	108.6
O(205)-C(209)-H(209)	111.7	C(207)-C(214)-C(213)	103.0(2)
C(210)-C(209)-H(209)	111.7	C(207)-C(214)-H(21I)	111.2
C(208)-C(209)-H(209)	111.7	C(213)-C(214)-H(21I)	111.2
C(209)-O(205)-H(25O)	105(3)	C(207)-C(214)-H(21J)	111.2
C(209)-C(210)-C(211)	102.7(2)	C(213)-C(214)-H(21J)	111.2
C(209)-C(210)-H(21A)	111.2	H(21I)-C(214)-H(21J)	109.1
C(211)-C(210)-H(21A)	111.2	C(301)-N(301)-N(302)	120.8(2)
C(209)-C(210)-H(21B)	111.2	C(301)-N(301)-H(31N)	119(2)
C(211)-C(210)-H(21B)	111.2	N(302)-N(301)-H(31N)	120(2)
H(21A)-C(210)-H(21B)	109.1	N(301)-C(301)-C(306)	121.1(2)
C(210)-C(211)-C(212)	104.0(2)	N(301)-C(301)-C(302)	121.9(2)
C(210)-C(211)-H(21C)	111.0	C(306)-C(301)-C(302)	117.0(2)
C(212)-C(211)-H(21C)	111.0	C(303)-C(302)-C(301)	121.4(3)
C(210)-C(211)-H(21D)	111.0	C(303)-C(302)-N(303)	116.1(2)
C(212)-C(211)-H(21D)	111.0	C(301)-C(302)-N(303)	122.4(2)
H(21C)-C(211)-H(21D)	109.0	O(302)-N(303)-O(301)	121.7(2)
C(215)-C(212)-C(211)	113.5(2)	O(302)-N(303)-C(302)	119.0(2)
C(215)-C(212)-C(213)	110.0(2)	O(301)-N(303)-C(302)	119.3(2)

Table A4.2.3. cont'd.

Atoms	Angle (°)	Atoms	Angle (°)
C(304)-C(303)-C(302)	119.1(3)	C(309)-O(305)-H(35O)	109(3)
C(304)-C(303)-H(303)	120.5	C(309)-C(310)-C(311)	103.9(2)
C(302)-C(303)-H(303)	120.5	C(309)-C(310)-H(31A)	111.0
C(303)-C(304)-C(305)	121.7(3)	C(311)-C(310)-H(31A)	111.0
C(303)-C(304)-N(304)	118.9(3)	C(309)-C(310)-H(31B)	111.0
C(305)-C(304)-N(304)	119.4(2)	C(311)-C(310)-H(31B)	111.0
O(304)-N(304)-O(303)	123.6(2)	H(31A)-C(310)-H(31B)	109.0
O(304)-N(304)-C(304)	117.9(2)	C(310)-C(311)-C(312)	105.8(2)
O(303)-N(304)-C(304)	118.5(2)	C(310)-C(311)-H(31C)	110.6
C(306)-C(305)-C(304)	119.8(3)	C(312)-C(311)-H(31C)	110.6
C(306)-C(305)-H(305)	120.1	C(310)-C(311)-H(31D)	110.6
C(304)-C(305)-H(305)	120.1	C(312)-C(311)-H(31D)	110.6
C(305)-C(306)-C(301)	121.0(3)	H(31C)-C(311)-H(31D)	108.7
C(305)-C(306)-H(306)	119.5	C(315)-C(312)-C(311)	115.8(2)
C(301)-C(306)-H(306)	119.5	C(315)-C(312)-C(313)	109.5(2)
C(307)-N(302)-N(301)	113.6(2)	C(311)-C(312)-C(313)	113.7(2)
N(302)-C(307)-C(314)	121.2(3)	C(315)-C(312)-C(308)	108.5(2)
N(302)-C(307)-C(308)	127.9(2)	C(311)-C(312)-C(308)	105.3(2)
C(314)-C(307)-C(308)	110.8(2)	C(313)-C(312)-C(308)	103.1(2)
C(307)-C(308)-C(309)	117.6(2)	C(316)-C(315)-C(312)	128.6(3)
C(307)-C(308)-C(312)	105.3(2)	C(316)-C(315)-H(315)	115.7
C(309)-C(308)-C(312)	104.3(2)	C(312)-C(315)-H(315)	115.7
C(307)-C(308)-H(308)	109.7	C(315)-C(316)-H(31E)	120.0
C(309)-C(308)-H(308)	109.7	C(315)-C(316)-H(31F)	120.0
C(312)-C(308)-H(308)	109.7	H(31E)-C(316)-H(31F)	120.0
O(305)-C(309)-C(310)	107.2(2)	C(314)-C(313)-C(312)	106.1(2)
O(305)-C(309)-C(308)	112.3(2)	C(314)-C(313)-H(31G)	110.5
C(310)-C(309)-C(308)	102.1(2)	C(312)-C(313)-H(31G)	110.5
O(305)-C(309)-H(309)	111.6	C(314)-C(313)-H(31H)	110.5
C(310)-C(309)-H(309)	111.6	C(312)-C(313)-H(31H)	110.5
C(308)-C(309)-H(309)	111.6	H(31G)-C(313)-H(31H)	108.7

Table A4.2.3. cont'd.

Atoms	Angle (°)	Atoms	Angle (°)
C(307)-C(314)-C(313)	104.2(2)	C(307)-C(314)-H(XXX)	110.9
C(307)-C(314)-H(31I)	110.9	C(313)-C(314)-H(31J)	110.9
C(313)-C(314)-H(31I)	110.9	H(31I)-C(314)-H(31J)	108.9

Symmetry transformations used to generate equivalent atoms:

Table A4.2.4 *Anisotropic displacement parameters ($Å^2 x\ 10^3$) for* ***(Z)-82*** *(V23277). The anisotropic displacement factor exponent takes the form: $-2p^2[\ h^2 a^{*2} U^{11} + ... + 2\ h\ k\ a^*\ b^*\ U^{12}]$*

Atom	U^{11}	U^{22}	U^{33}	U^{23}	U^{13}	U^{12}
N(1)	16(1)	13(1)	20(1)	0(1)	3(1)	0(1)
C(1)	16(1)	16(1)	11(1)	-1(1)	-2(1)	1(1)
C(2)	16(1)	14(1)	13(1)	-1(1)	-1(1)	1(1)
N(3)	18(1)	14(1)	16(1)	0(1)	-1(1)	0(1)
O(1)	19(1)	16(1)	25(1)	-1(1)	4(1)	4(1)
O(2)	19(1)	18(1)	29(1)	3(1)	6(1)	-2(1)
C(3)	16(1)	19(1)	13(1)	-1(1)	0(1)	0(1)
C(4)	15(1)	22(1)	14(1)	-2(1)	1(1)	5(1)
N(4)	18(1)	21(1)	16(1)	-3(1)	1(1)	4(1)
O(3)	22(1)	26(1)	40(1)	-1(1)	14(1)	2(1)
O(4)	26(1)	22(1)	24(1)	2(1)	5(1)	10(1)
C(5)	18(1)	14(1)	15(1)	-1(1)	-3(1)	3(1)
C(6)	16(1)	15(1)	14(1)	-1(1)	-1(1)	0(1)
N(2)	15(1)	16(1)	21(1)	0(1)	2(1)	-1(1)
C(7)	14(1)	18(1)	17(1)	2(1)	0(1)	0(1)
C(8)	16(1)	18(1)	17(1)	0(1)	5(1)	1(1)
C(9)	26(1)	20(1)	19(1)	2(1)	4(1)	1(1)
O(5)	36(1)	30(1)	18(1)	-1(1)	-3(1)	5(1)
C(10)	28(1)	25(2)	26(1)	4(1)	4(1)	10(1)
C(11)	17(1)	35(2)	25(1)	4(1)	4(1)	7(1)

Table A4.2.4 cont'd.

Atom	U^{11}	U^{22}	U^{33}	U^{23}	U^{13}	U^{12}
C(12)	16(1)	24(1)	17(1)	0(1)	6(1)	2(1)
C(15)	24(1)	32(2)	20(1)	-1(1)	4(1)	1(1)
C(16)	46(2)	50(2)	34(2)	-17(2)	5(2)	10(2)
C(13)	22(1)	26(2)	24(1)	5(1)	7(1)	-2(1)
C(14)	19(1)	21(1)	30(2)	2(1)	7(1)	-4(1)
N(101)	14(1)	16(1)	19(1)	0(1)	2(1)	-3(1)
C(101)	14(1)	18(1)	11(1)	0(1)	-2(1)	-1(1)
C(102)	16(1)	14(1)	14(1)	0(1)	-2(1)	-1(1)
N(103)	14(1)	15(1)	18(1)	0(1)	1(1)	0(1)
O(101)	17(1)	17(1)	29(1)	-2(1)	5(1)	3(1)
O(102)	20(1)	17(1)	35(1)	2(1)	10(1)	-4(1)
C(103)	14(1)	19(1)	14(1)	0(1)	0(1)	-2(1)
C(104)	14(1)	19(1)	15(1)	-3(1)	-1(1)	1(1)
N(104)	17(1)	22(1)	22(1)	-6(1)	2(1)	1(1)
O(103)	24(1)	29(1)	38(1)	-4(1)	15(1)	0(1)
O(104)	25(1)	19(1)	39(1)	-2(1)	4(1)	7(1)
C(105)	19(1)	13(1)	15(1)	-1(1)	-3(1)	0(1)
C(106)	17(1)	15(1)	14(1)	0(1)	-1(1)	-2(1)
N(102)	16(1)	21(1)	17(1)	-2(1)	4(1)	-6(1)
C(107)	16(1)	22(1)	15(1)	-3(1)	1(1)	-7(1)
C(108)	13(1)	26(2)	19(1)	2(1)	3(1)	1(1)
C(109)	17(1)	19(1)	24(1)	-3(1)	2(1)	1(1)
O(105)	22(1)	23(1)	19(1)	-3(1)	-2(1)	2(1)
C(110)	20(1)	28(2)	35(2)	-6(1)	4(1)	4(1)
C(111)	17(1)	33(2)	28(2)	-5(1)	5(1)	4(1)
C(112)	13(1)	40(2)	21(1)	-3(1)	2(1)	2(1)
C(115)	31(2)	49(2)	36(2)	2(2)	3(1)	12(2)
C(116)	62(2)	47(2)	36(2)	2(2)	-10(2)	-3(2)
C(113)	15(1)	49(2)	29(2)	-16(2)	7(1)	-10(1)
C(114)	21(1)	31(2)	31(2)	-10(1)	12(1)	-13(1)
N(201)	12(1)	11(1)	17(1)	-1(1)	2(1)	1(1)
C(201)	13(1)	15(1)	11(1)	0(1)	-1(1)	0(1)

Table A4.2.4 cont'd.

Atom	U^{11}	U^{22}	U^{33}	U^{23}	U^{13}	U^{12}
C(202)	13(1)	11(1)	16(1)	2(1)	-1(1)	0(1)
N(203)	15(1)	12(1)	16(1)	2(1)	1(1)	0(1)
O(201)	16(1)	14(1)	27(1)	2(1)	6(1)	-3(1)
O(202)	21(1)	14(1)	33(1)	-1(1)	11(1)	3(1)
C(203)	13(1)	17(1)	14(1)	-1(1)	2(1)	1(1)
C(204)	13(1)	16(1)	15(1)	2(1)	2(1)	-3(1)
N(204)	16(1)	15(1)	21(1)	1(1)	3(1)	0(1)
O(203)	24(1)	21(1)	39(1)	-1(1)	18(1)	-1(1)
O(204)	23(1)	15(1)	32(1)	-1(1)	9(1)	-6(1)
C(205)	16(1)	11(1)	13(1)	0(1)	-2(1)	1(1)
C(206)	12(1)	14(1)	13(1)	0(1)	-2(1)	1(1)
N(202)	13(1)	15(1)	16(1)	-1(1)	2(1)	2(1)
C(207)	13(1)	16(1)	14(1)	1(1)	1(1)	2(1)
C(208)	12(1)	15(1)	19(1)	-1(1)	2(1)	-1(1)
C(209)	14(1)	18(1)	25(1)	3(1)	2(1)	2(1)
O(205)	22(1)	26(1)	20(1)	4(1)	-4(1)	-2(1)
C(210)	21(1)	20(1)	26(1)	7(1)	2(1)	-2(1)
C(211)	17(1)	22(1)	24(1)	7(1)	4(1)	-3(1)
C(212)	10(1)	20(1)	20(1)	3(1)	1(1)	0(1)
C(215)	18(1)	27(2)	22(1)	4(1)	0(1)	-4(1)
C(216)	27(1)	34(2)	32(2)	-2(2)	-1(1)	-8(1)
C(213)	12(1)	22(1)	32(2)	5(1)	5(1)	2(1)
C(214)	17(1)	19(1)	25(1)	0(1)	7(1)	2(1)
N(301)	16(1)	14(1)	18(1)	-1(1)	2(1)	-1(1)
C(301)	13(1)	16(1)	12(1)	1(1)	-2(1)	-2(1)
C(302)	17(1)	17(1)	13(1)	1(1)	-1(1)	-2(1)
N(303)	15(1)	14(1)	14(1)	-1(1)	-1(1)	-2(1)
O(301)	18(1)	18(1)	26(1)	-1(1)	5(1)	-5(1)
O(302)	20(1)	19(1)	25(1)	-3(1)	6(1)	2(1)
C(303)	16(1)	19(1)	13(1)	1(1)	1(1)	1(1)
C(304)	15(1)	21(1)	14(1)	2(1)	1(1)	-3(1)
N(304)	18(1)	19(1)	19(1)	2(1)	3(1)	-2(1)

Table A4.2.4 cont'd.

Atom	U^{11}	U^{22}	U^{33}	U^{23}	U^{13}	U^{12}
O(303)	29(1)	25(1)	53(2)	1(1)	24(1)	1(1)
O(304)	25(1)	21(1)	26(1)	0(1)	6(1)	-9(1)
C(305)	16(1)	17(1)	14(1)	1(1)	-4(1)	-2(1)
C(306)	15(1)	17(1)	14(1)	0(1)	-1(1)	0(1)
N(302)	13(1)	17(1)	19(1)	-3(1)	2(1)	0(1)
C(307)	14(1)	20(1)	16(1)	-4(1)	0(1)	-2(1)
C(308)	13(1)	20(1)	16(1)	-1(1)	3(1)	-2(1)
C(309)	18(1)	17(1)	18(1)	-3(1)	3(1)	-1(1)
O(305)	23(1)	21(1)	18(1)	2(1)	-3(1)	-6(1)
C(310)	20(1)	17(1)	25(1)	1(1)	4(1)	-3(1)
C(311)	21(1)	21(1)	25(1)	-1(1)	6(1)	-9(1)
C(312)	15(1)	22(1)	17(1)	-1(1)	4(1)	-3(1)
C(315)	19(1)	25(1)	20(1)	-3(1)	3(1)	-2(1)
C(316)	27(1)	32(2)	23(1)	2(1)	3(1)	-1(1)
C(313)	14(1)	26(2)	22(1)	0(1)	4(1)	0(1)
C(314)	18(1)	19(1)	25(1)	-2(1)	6(1)	0(1)

Table A4.2.5. *Hydrogen coordinates (x 10^4) and isotropic displacement parameters ($Å^2$x 10^3) for* ***(Z)-82*** *(V23277).*

Atom	x	y	z	U(eq)
H(1N)	7930(20)	3070(30)	9640(16)	20
H(3)	10266	2281	9089	20
H(5)	9495	-2191	9476	20
H(6)	8400	-1038	9716	19
H(8)	7452	4102	10352	20
H(9)	6861	5298	9468	26
H(5O)	6180(30)	2930(40)	9110(20)	44
H(10A)	5541	6239	9631	32

Table A4.2.5 cont'd.

Atom	x	y	z	U(eq)
H(10B)	6277	6752	10142	32
H(11A)	5299	3930	10178	31
H(11B)	5461	5363	10673	31
H(15)	7368	4314	11409	31
H(16A)	6202	6602	11329	53
H(16B)	7030	6556	11816	53
H(13A)	6682	1691	11235	28
H(13B)	5767	1925	10988	28
H(14A)	6483	-144	10453	27
H(14B)	5833	987	10044	27
H(11N)	8960(20)	15990(30)	7962(16)	20
H(103)	6628	16793	8503	19
H(105)	7485	21288	8261	20
H(106)	8588	20132	8033	19
H(108)	10048	14914	8076	23
H(109)	9363	14028	7165	25
H(15O)	9480(20)	15360(50)	6389(14)	33
H(11C)	10493	12510	7195	33
H(11D)	10373	13328	6539	33
H(11E)	11226	15467	6893	31
H(11F)	11666	13876	7211	31
H(115)	11394	12845	8127	47
H(11G)	11808	15198	8990	61
H(11H)	11916	13210	9066	61
H(11I)	11626	17176	8352	37
H(11J)	11917	17119	7726	37
H(11K)	10872	19220	7835	32
H(11L)	10786	18283	7202	32
H(21N)	6040(20)	6410(30)	7004(16)	17
H(203)	8350	7250	6399	18
H(205)	7508	11730	6693	17
H(206)	6444	10558	6971	17

Table A4.2.5 cont'd.

Atom	x	y	z	U(eq)
H(208)	4903	5558	6758	18
H(209)	5627	4107	7543	23
H(25O)	5520(20)	4820(40)	8474(16)	36
H(21A)	4625	2789	8048	27
H(21B)	4463	2636	7327	27
H(21C)	3811	5069	8002	25
H(21D)	3327	3840	7513	25
H(215)	3493	5873	6180	27
H(21E)	3084	2955	6641	38
H(21F)	2896	3542	5936	38
H(21G)	3384	8009	6839	27
H(21H)	3210	7453	7476	27
H(21I)	4286	9577	7452	24
H(21J)	4409	8252	7986	24
H(31N)	7070(20)	13320(30)	5221(16)	19
H(303)	4832	12589	5921	19
H(305)	5550	8085	5527	20
H(306)	6605	9198	5213	19
H(308)	7547	14286	4468	20
H(309)	7970	15282	5444	21
H(35O)	8890(20)	13430(40)	5767(18)	33
H(31A)	9034	17117	5231	25
H(31B)	8236	17164	4739	25
H(31C)	9641	15507	4641	27
H(31D)	9065	16479	4119	27
H(315)	8027	13039	3466	25
H(31E)	8256	16352	3342	34
H(31F)	7792	15088	2831	34
H(31G)	9402	12285	4034	25
H(31H)	9611	12763	4733	25
H(31I)	8421	10588	4158	24
H(31J)	8945	10424	4823	24

Table A4.2.6. *Torsion angles [°] for* ***(Z)-82*** *(V23277).*

Atoms (A-B-C-D)	Angle (°)	Atoms (A-B-C-D)	Angle (°)
N(2)-N(1)-C(1)-C(2)	-178.2(2)	C(12)-C(8)-C(9)-C(10)	19.8(3)
N(2)-N(1)-C(1)-C(6)	2.6(4)	O(5)-C(9)-C(10)-C(11)	78.6(3)
N(1)-C(1)-C(2)-C(3)	-178.5(2)	C(8)-C(9)-C(10)-C(11)	-40.0(3)
C(6)-C(1)-C(2)-C(3)	0.8(4)	C(9)-C(10)-C(11)-C(12)	45.9(3)
N(1)-C(1)-C(2)-N(3)	3.6(4)	C(10)-C(11)-C(12)-C(15)	86.3(3)
C(6)-C(1)-C(2)-N(3)	-177.2(2)	C(10)-C(11)-C(12)-C(13)	-145.3(3)
C(3)-C(2)-N(3)-O(2)	4.5(3)	C(10)-C(11)-C(12)-C(8)	-32.5(3)
C(1)-C(2)-N(3)-O(2)	-177.4(2)	C(7)-C(8)-C(12)-C(15)	124.9(2)
C(3)-C(2)-N(3)-O(1)	-174.8(2)	C(9)-C(8)-C(12)-C(15)	-113.5(3)
C(1)-C(2)-N(3)-O(1)	3.3(4)	C(7)-C(8)-C(12)-C(11)	-113.8(2)
C(1)-C(2)-C(3)-C(4)	-0.3(4)	C(9)-C(8)-C(12)-C(11)	7.7(3)
N(3)-C(2)-C(3)-C(4)	177.8(2)	C(7)-C(8)-C(12)-C(13)	5.7(3)
C(2)-C(3)-C(4)-C(5)	0.2(4)	C(9)-C(8)-C(12)-C(13)	127.3(2)
C(2)-C(3)-C(4)-N(4)	-178.7(2)	C(11)-C(12)-C(15)-C(16)	8.2(5)
C(3)-C(4)-N(4)-O(4)	176.8(2)	C(13)-C(12)-C(15)-C(16)	-121.7(4)
C(5)-C(4)-N(4)-O(4)	-2.1(4)	C(8)-C(12)-C(15)-C(16)	123.1(4)
C(3)-C(4)-N(4)-O(3)	-1.6(4)	C(15)-C(12)-C(13)-C(14)	-144.0(2)
C(5)-C(4)-N(4)-O(3)	179.5(2)	C(11)-C(12)-C(13)-C(14)	86.4(3)
C(3)-C(4)-C(5)-C(6)	-0.6(4)	C(8)-C(12)-C(13)-C(14)	-25.6(3)
N(4)-C(4)-C(5)-C(6)	178.3(2)	N(2)-C(7)-C(14)-C(13)	142.8(3)
C(4)-C(5)-C(6)-C(1)	1.1(4)	C(8)-C(7)-C(14)-C(13)	-32.7(3)
N(1)-C(1)-C(6)-C(5)	178.1(2)	C(12)-C(13)-C(14)-C(7)	35.5(3)
C(2)-C(1)-C(6)-C(5)	-1.1(4)	N(102)-N(101)-C(101)-C(106)	5.1(4)
C(1)-N(1)-N(2)-C(7)	164.2(2)	N(102)-N(101)-C(101)-C(102)	-175.6(2)
N(1)-N(2)-C(7)-C(14)	-178.5(2)	N(101)-C(101)-C(102)-C(103)	179.7(2)
N(1)-N(2)-C(7)-C(8)	-4.0(4)	C(106)-C(101)-C(102)-C(103)	-1.0(4)
N(2)-C(7)-C(8)-C(9)	85.7(3)	N(101)-C(101)-C(102)-N(103)	-0.1(4)
C(14)-C(7)-C(8)-C(9)	-99.3(3)	C(106)-C(101)-C(102)-N(103)	179.1(2)
N(2)-C(7)-C(8)-C(12)	-158.2(3)	C(103)-C(102)-N(103)-O(102)	-5.7(4)
C(14)-C(7)-C(8)-C(12)	16.8(3)	C(101)-C(102)-N(103)-O(102)	174.1(2)
C(7)-C(8)-C(9)-O(5)	21.5(3)	C(103)-C(102)-N(103)-O(101)	174.8(2)
C(12)-C(8)-C(9)-O(5)	-93.8(3)	C(101)-C(102)-N(103)-O(101)	-5.3(4)
C(7)-C(8)-C(9)-C(10)	135.0(3)	C(101)-C(102)-C(103)-C(104)	1.4(4)

Table A4.2.6 cont'd.

Atoms (A-B-C-D)	Angle (°)	Atoms (A-B-C-D)	Angle (°)
N(103)-C(102)-C(103)-C(104)	-178.7(2)	C(109)-C(108)-C(112)-C(111)	8.1(3)
C(102)-C(103)-C(104)-C(105)	-0.3(4)	C(113)-C(112)-C(115)-C(116)	23.9(6)
C(102)-C(103)-C(104)-N(104)	178.6(2)	C(111)-C(112)-C(115)-C(116)	152.1(4)
C(103)-C(104)-N(104)-O(103)	16.7(4)	C(108)-C(112)-C(115)-C(116)	-96.0(5)
C(105)-C(104)-N(104)-O(103)	-164.4(2)	C(115)-C(112)-C(113)-C(114)	-148.6(3)
C(103)-C(104)-N(104)-O(104)	-163.2(3)	C(111)-C(112)-C(113)-C(114)	85.7(3)
C(105)-C(104)-N(104)-O(104)	15.8(4)	C(108)-C(112)-C(113)-C(114)	-25.7(3)
C(103)-C(104)-C(105)-C(106)	-1.2(4)	N(102)-C(107)-C(114)-C(113)	145.6(3)
N(104)-C(104)-C(105)-C(106)	179.8(2)	C(108)-C(107)-C(114)-C(113)	-32.1(3)
C(104)-C(105)-C(106)-C(101)	1.7(4)	C(112)-C(113)-C(114)-C(107)	35.4(3)
N(101)-C(101)-C(106)-C(105)	178.7(2)	N(202)-N(201)-C(201)-C(206)	-4.8(4)
C(102)-C(101)-C(106)-C(105)	-0.6(4)	N(202)-N(201)-C(201)-C(202)	175.5(2)
C(101)-N(101)-N(102)-C(107)	176.5(2)	N(201)-C(201)-C(202)-C(203)	178.2(2)
N(101)-N(102)-C(107)-C(114)	-179.9(2)	C(206)-C(201)-C(202)-C(203)	-1.5(4)
N(101)-N(102)-C(107)-C(108)	-2.7(4)	N(201)-C(201)-C(202)-N(203)	-2.6(4)
N(102)-C(107)-C(108)-C(109)	82.6(4)	C(206)-C(201)-C(202)-N(203)	177.6(2)
C(114)-C(107)-C(108)-C(109)	-99.9(3)	C(203)-C(202)-N(203)-O(202)	-2.1(3)
N(102)-C(107)-C(108)-C(112)	-161.2(3)	C(201)-C(202)-N(203)-O(202)	178.7(2)
C(114)-C(107)-C(108)-C(112)	16.3(3)	C(203)-C(202)-N(203)-O(201)	177.5(2)
C(107)-C(108)-C(109)-O(105)	16.1(3)	C(201)-C(202)-N(203)-O(201)	-1.7(4)
C(112)-C(108)-C(109)-O(105)	-98.8(3)	C(201)-C(202)-C(203)-C(204)	0.5(4)
C(107)-C(108)-C(109)-C(110)	133.4(2)	N(203)-C(202)-C(203)-C(204)	-178.8(2)
C(112)-C(108)-C(109)-C(110)	18.5(3)	C(202)-C(203)-C(204)-C(205)	1.4(4)
O(105)-C(109)-C(110)-C(111)	76.9(3)	C(202)-C(203)-C(204)-N(204)	-178.7(2)
C(108)-C(109)-C(110)-C(111)	-38.3(3)	C(203)-C(204)-N(204)-O(203)	10.0(4)
C(109)-C(110)-C(111)-C(112)	44.5(3)	C(205)-C(204)-N(204)-O(203)	-170.1(2)
C(110)-C(111)-C(112)-C(115)	85.0(3)	C(203)-C(204)-N(204)-O(204)	-171.1(2)
C(110)-C(111)-C(112)-C(113)	-144.6(3)	C(205)-C(204)-N(204)-O(204)	8.9(4)
C(110)-C(111)-C(112)-C(108)	-32.0(3)	C(203)-C(204)-C(205)-C(206)	-2.0(4)
C(107)-C(108)-C(112)-C(115)	133.0(3)	N(204)-C(204)-C(205)-C(206)	178.1(2)
C(109)-C(108)-C(112)-C(115)	-106.8(3)	C(204)-C(205)-C(206)-C(201)	0.8(4)
C(107)-C(108)-C(112)-C(113)	6.2(3)	N(201)-C(201)-C(206)-C(205)	-178.9(2)
C(109)-C(108)-C(112)-C(113)	126.4(3)	C(202)-C(201)-C(206)-C(205)	0.9(4)
C(107)-C(108)-C(112)-C(111)	-112.1(3)	C(201)-N(201)-N(202)-C(207)	174.4(2)

Table A4.2.6 cont'd.

Atoms (A-B-C-D)	Angle (°)	Atoms (A-B-C-D)	Angle (°)
N(201)-N(202)-C(207)-C(214)	177.1(2)	C(301)-C(302)-C(303)	1.6(4)
N(201)-N(202)-C(207)-C(208)	-5.9(4)	N(301)-C(301)-C(302)-N(303)	3.3(4)
N(202)-C(207)-C(208)-C(209)	84.7(3)	C(306)-C(301)-C(302)-N(303)	-177.1(2)
C(214)-C(207)-C(208)-C(209)	-98.0(2)	C(303)-C(302)-N(303)-O(302)	1.6(4)
N(202)-C(207)-C(208)-C(212)	-159.2(3)	C(301)-C(302)-N(303)-O(302)	-179.6(2)
C(214)-C(207)-C(208)-C(212)	18.1(3)	C(303)-C(302)-N(303)-O(301)	-177.6(2)
C(207)-C(208)-C(209)-O(205)	21.5(3)	C(301)-C(302)-N(303)-O(301)	1.2(4)
C(212)-C(208)-C(209)-O(205)	-93.9(2)	C(301)-C(302)-C(303)-C(304)	-0.7(4)
C(207)-C(208)-C(209)-C(210)	139.1(2)	N(303)-C(302)-C(303)-C(304)	178.1(2)
C(212)-C(208)-C(209)-C(210)	23.7(3)	C(302)-C(303)-C(304)-C(305)	-0.5(4)
O(205)-C(209)-C(210)-C(211)	72.6(3)	C(302)-C(303)-C(304)-N(304)	-178.8(2)
C(208)-C(209)-C(210)-C(211)	-41.8(3)	C(303)-C(304)-N(304)-O(304)	174.1(2)
C(209)-C(210)-C(211)-C(212)	44.6(3)	C(305)-C(304)-N(304)-O(304)	-4.3(4)
C(210)-C(211)-C(212)-C(215)	90.3(3)	C(303)-C(304)-N(304)-O(303)	-5.6(4)
C(210)-C(211)-C(212)-C(213)	-142.4(2)	C(305)-C(304)-N(304)-O(303)	176.1(2)
C(210)-C(211)-C(212)-C(208)	-28.8(3)	C(303)-C(304)-C(305)-C(306)	0.6(4)
C(207)-C(208)-C(212)-C(215)	120.4(2)	N(304)-C(304)-C(305)-C(306)	178.9(2)
C(209)-C(208)-C(212)-C(215)	-118.4(3)	C(304)-C(305)-C(306)-C(301)	0.5(4)
C(207)-C(208)-C(212)-C(211)	-118.0(2)	N(301)-C(301)-C(306)-C(305)	178.0(2)
C(209)-C(208)-C(212)-C(211)	3.1(3)	C(302)-C(301)-C(306)-C(305)	-1.5(4)
C(207)-C(208)-C(212)-C(213)	2.2(3)	C(301)-N(301)-N(302)-C(307)	168.2(2)
C(209)-C(208)-C(212)-C(213)	123.3(2)	N(301)-N(302)-C(307)-C(314)	-178.6(2)
C(211)-C(212)-C(215)-C(216)	-2.1(4)	N(301)-N(302)-C(307)-C(308)	-2.2(4)
C(213)-C(212)-C(215)-C(216)	-131.6(3)	N(302)-C(307)-C(308)-C(309)	75.8(3)
C(208)-C(212)-C(215)-C(216)	113.4(3)	C(314)-C(307)-C(308)-C(309)	-107.5(3)
C(215)-C(212)-C(213)-C(214)	-139.2(2)	N(302)-C(307)-C(308)-C(312)	-168.6(3)
C(211)-C(212)-C(213)-C(214)	91.7(3)	C(314)-C(307)-C(308)-C(312)	8.1(3)
C(208)-C(212)-C(213)-C(214)	-21.1(3)	C(307)-C(308)-C(309)-O(305)	40.4(3)
N(202)-C(207)-C(214)-C(213)	146.4(2)	C(312)-C(308)-C(309)-O(305)	-75.8(3)
C(208)-C(207)-C(214)-C(213)	-31.1(3)	C(307)-C(308)-C(309)-C(310)	154.9(2)
C(212)-C(213)-C(214)-C(207)	31.7(3)	C(312)-C(308)-C(309)-C(310)	38.8(3)
N(302)-N(301)-C(301)-C(306)	0.0(4)	O(305)-C(309)-C(310)-C(311)	75.1(3)
N(302)-N(301)-C(301)-C(302)	179.5(2)	C(308)-C(309)-C(310)-C(311)	-43.1(3)
N(301)-C(301)-C(302)-C(303)	-177.9(2)	C(309)-C(310)-C(311)-C(312)	31.0(3)

Table A4.2.6 cont'd.

Atoms (A-B-C-D)	Angle (°)	Atoms (A-B-C-D)	Angle (°)
C(310)-C(311)-C(312)-C(315)	113.2(3)	C(311)-C(312)-C(315)-C(316)	-9.4(4)
C(310)-C(311)-C(312)-C(313)	-118.7(3)	C(313)-C(312)-C(315)-C(316)	-139.6(3)
C(310)-C(311)-C(312)-C(308)	-6.6(3)	C(308)-C(312)-C(315)-C(316)	108.6(3)
C(307)-C(308)-C(312)-C(315)	91.3(3)	C(315)-C(312)-C(313)-C(314)	-82.4(3)
C(309)-C(308)-C(312)-C(315)	-144.2(2)	C(311)-C(312)-C(313)-C(314)	146.3(2)
C(307)-C(308)-C(312)-C(311)	-144.1(2)	C(308)-C(312)-C(313)-C(314)	32.9(3)
C(309)-C(308)-C(312)-C(311)	-19.7(3)	N(302)-C(307)-C(314)-C(313)	-170.8(2)
C(307)-C(308)-C(312)-C(313)	-24.8(3)	C(308)-C(307)-C(314)-C(313)	12.3(3)
C(309)-C(308)-C(312)-C(313)	99.7(2)	C(312)-C(313)-C(314)-C(307)	-28.1(3)

Symmetry transformations used to generate equivalent atoms:

Table A4.2.7. *Hydrogen bonds for* ***(Z)-82*** *(V23277) [Å and °].*

D-H...A	d(D-H)	d(H...A)	d(D...A)	<(DHA)
N(1)-H(1N)...O(1)	0.87(2)	1.95(3)	2.608(3)	132(3)
C(5)-H(5)...O(2)#1	0.95	2.61	3.507(4)	158.5
O(5)-H(5O)...O(104)#2	0.82(3)	2.04(3)	2.766(3)	147(5)
N(101)-H(11N)...O(101)	0.88(2)	1.94(3)	2.613(3)	131(3)
C(103)-H(103)...O(205)#3	0.95	2.44	3.282(3)	148.2
C(105)-H(105)...O(102)#3	0.95	2.51	3.443(4)	169.0
C(108)-H(108)...O(2)#3	1.00	2.61	3.535(4)	154.4
C(109)-H(109)...O(204)	1.00	2.62	3.270(3)	122.6
O(105)-H(15O)...O(305)	0.85(2)	1.99(3)	2.835(3)	172(4)
C(114)-H(11K)...O(3)#4	0.99	2.65	3.399(4)	133.0
N(201)-H(21N)...O(201)	0.87(2)	1.96(3)	2.603(3)	129(3)
C(203)-H(203)...O(105)#1	0.95	2.50	3.340(3)	147.6
C(205)-H(205)...O(202)#3	0.95	2.52	3.457(3)	167.5
C(208)-H(208)...O(302)#1	1.00	2.51	3.506(3)	171.8
O(205)-H(25O)...O(5)	0.88(2)	1.97(3)	2.827(3)	165(4)

Table A4.2.7. cont'd.

D-H...A	d(D-H)	d(H...A)	d(D...A)	<(DHA)
N(301)-H(31N)...O(301)	0.87(2)	1.95(3)	2.605(3)	131(3)
C(305)-H(305)...O(302)#1	0.95	2.53	3.453(4)	163.8
C(309)-H(309)...O(202)#3	1.00	2.59	3.334(3)	130.9
O(305)-H(35O)...O(204)	0.84(2)	1.99(3)	2.792(3)	160(4)

Symmetry transformations used to generate equivalent atoms:

#1 x,y-1,z #2 x,y-2,z #3 x,y+1,z #4 x,y+2,z

A4.3 X-RAY CRYSTAL STRUCTURE ANALYSIS OF LACTAM 87 (V23031)

An X-Ray quality crystal of lactam **87** (compound V23031) was grown by slow evaporation of a solution in Et_2O (approx. 5 mg/200µL). Low-temperature diffraction data (ϕ-and ω-scans) were collected on a Bruker AXS D8 VENTURE KAPPA diffractometer coupled to a PHOTON II CPAD detector with Mo K_α radiation ($\lambda = 0.71073$ Å) from an IμS micro-source for the structure of compound V23031. The structure was solved by direct methods using SHELXS[1] and refined against F^2 on all data by full-matrix least squares with SHELXL-2019[2] using established refinement techniques.[3] All non-hydrogen atoms were refined anisotropically. Unless otherwise noted, all hydrogen atoms were included into the model at geometrically calculated positions and refined using a riding model. The isotropic displacement parameters of all hydrogen atoms were fixed to 1.2 times the U value of the atoms they are linked to (1.5 times for methyl groups).

Compound V23031 crystallizes in the monoclinic space group $P2_1/c$ with one molecule in the asymmetric unit. The coordinates for the hydrogen atoms bound to N1 were located in the difference Fourier synthesis and refined semi-freely with the help of a restraint on the N-H distance (0.88(4) Å).

Figure A4.3.1. *X-Ray Coordinate of Lactam* ***87*** *(V23031)*

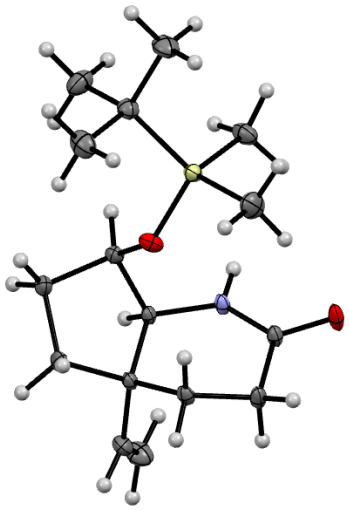


Table A4.3.1. *Crystal Data and Structure Refinement of* ***87*** *(V23031)*

Identification code	V23031	
Empirical formula	C16 H29 N O2 Si	
Formula weight	295.49	
Temperature	100(2) K	
Wavelength	0.71073 Å	
Crystal system	Monoclinic	
Space group	$P2_1/c$	
Unit cell dimensions	a = 11.480(3) Å	a= 90°.
	b = 12.741(3) Å	b= 107.367(8)°.
	c = 12.516(3) Å	g = 90°.
Volume	1747.2(8) $Å^3$	
Z	4	
Density (calculated)	1.123 Mg/m^3	
Absorption coefficient	0.137 mm^{-1}	
F(000)	648	
Crystal size	0.400 x 0.300 x 0.200 mm^3	
Theta range for data collection	2.337 to 36.332°.	
Index ranges	-19<=h<=18, -21<=k<=21, -20<=l<=20	
Reflections collected	49735	
Independent reflections	8467 [R(int) = 0.0581]	
Completeness to theta = 25.242°	100.0 %	

Absorption correction	Semi-empirical from equivalents
Max. and min. transmission	0.7471 and 0.6889
Refinement method	Full-matrix least-squares on F^2
Data / restraints / parameters	8467 / 1 / 189
Goodness-of-fit on F^2	1.050
Final R indices [I>2sigma(I)]	R1 = 0.0314, wR2 = 0.0880
R indices (all data)	R1 = 0.0456, wR2 = 0.0921
Extinction coefficient	n/a
Largest diff. peak and hole	0.518 and -0.268 e.$Å^{-3}$

Table A4.3.2. *Atomic coordinates (x 10^4) and equivalent isotropic displacement parameters ($Å^2$x 10^3) for* ***87*** *(V23031). U(eq) is defined as one third of the trace of the orthogonalized U^{ij} tensor.*

Atom	x	y	z	U(eq)
O(1)	7631(1)	7056(1)	6583(1)	17(1)
C(1)	6941(1)	7536(1)	5567(1)	14(1)
C(2)	5573(1)	7425(1)	5432(1)	12(1)
N(1)	5195(1)	6348(1)	5499(1)	14(1)
C(3)	4912(1)	5901(1)	6357(1)	14(1)
O(2)	4731(1)	4940(1)	6380(1)	20(1)
C(4)	4758(1)	6611(1)	7270(1)	17(1)
C(5)	5518(1)	7611(1)	7427(1)	14(1)
C(6)	5335(1)	8184(1)	6304(1)	12(1)
C(9)	4071(1)	8654(1)	5964(1)	17(1)
C(10)	3126(1)	8389(1)	5102(1)	26(1)
C(7)	6325(1)	9054(1)	6420(1)	17(1)
C(8)	7097(1)	8722(1)	5660(1)	17(1)
Si(1)	8591(1)	6060(1)	6793(1)	14(1)
C(11)	8691(1)	5589(1)	8227(1)	28(1)
C(12)	7991(1)	4992(1)	5760(1)	23(1)
C(13)	10118(1)	6554(1)	6726(1)	18(1)
C(14)	11074(1)	5675(1)	7045(1)	27(1)
C(15)	10012(1)	6938(1)	5537(1)	28(1)

Table A4.3.2. cont'd.

Atom	x	y	z	U(eq)
C(16)	10545(1)	7478(1)	7540(1)	28(1)

Table A4.3.3. *Bond lengths [Å] and angles [°] for* ***87*** *(V23031).*

Bond	Length (Å)	Bond	Length (Å)
O(1)-C(1)	1.4197(8)	C(7)-H(7A)	0.9900
O(1)-Si(1)	1.6488(6)	C(7)-H(7B)	0.9900
C(1)-C(8)	1.5224(10)	C(8)-H(8A)	0.9900
C(1)-C(2)	1.5357(10)	C(8)-H(8B)	0.9900
C(1)-H(1)	1.0000	Si(1)-C(12)	1.8613(8)
C(2)-N(1)	1.4493(8)	Si(1)-C(11)	1.8638(8)
C(2)-C(6)	1.5424(8)	Si(1)-C(13)	1.8874(8)
C(2)-H(2)	1.0000	C(11)-H(11A)	0.9800
N(1)-C(3)	1.3387(8)	C(11)-H(11B)	0.9800
N(1)-H(1N)	0.889(9)	C(11)-H(11C)	0.9800
C(3)-O(2)	1.2427(8)	C(12)-H(12A)	0.9800
C(3)-C(4)	1.5087(8)	C(12)-H(12B)	0.9800
C(4)-C(5)	1.5240(9)	C(12)-H(12C)	0.9800
C(4)-H(4A)	0.9900	C(13)-C(14)	1.5357(10)
C(4)-H(4B)	0.9900	C(13)-C(15)	1.5362(10)
C(5)-C(6)	1.5414(8)	C(13)-C(16)	1.5385(11)
C(5)-H(5A)	0.9900	C(14)-H(14A)	0.9800
C(5)-H(5B)	0.9900	C(14)-H(14B)	0.9800
C(6)-C(9)	1.5093(9)	C(14)-H(14C)	0.9800
C(6)-C(7)	1.5624(9)	C(15)-H(15A)	0.9800
C(9)-C(10)	1.3250(10)	C(15)-H(15B)	0.9800
C(9)-H(9)	0.9500	C(15)-H(15C)	0.9800
C(10)-H(10A)	0.9500	C(16)-H(16A)	0.9800
C(10)-H(10B)	0.9500	C(16)-H(16B)	0.9800
C(7)-C(8)	1.5404(9)	C(16)-H(16C)	0.9800

Table A4.3.3. cont'd.

Atoms	Angle (°)	Atoms	Angle (°)
C(1)-O(1)-Si(1)	129.90(4)	C(9)-C(6)-C(7)	110.89(5)
O(1)-C(1)-C(8)	109.73(5)	C(5)-C(6)-C(7)	110.73(5)
O(1)-C(1)-C(2)	109.79(5)	C(2)-C(6)-C(7)	103.47(5)
C(8)-C(1)-C(2)	101.06(5)	C(10)-C(9)-C(6)	127.79(6)
O(1)-C(1)-H(1)	111.9	C(10)-C(9)-H(9)	116.1
C(8)-C(1)-H(1)	111.9	C(6)-C(9)-H(9)	116.1
C(2)-C(1)-H(1)	111.9	C(9)-C(10)-H(10A)	120.0
N(1)-C(2)-C(1)	113.20(5)	C(9)-C(10)-H(10B)	120.0
N(1)-C(2)-C(6)	115.70(5)	H(10A)-C(10)-H(10B)	120.0
C(1)-C(2)-C(6)	104.83(4)	C(8)-C(7)-C(6)	106.52(5)
N(1)-C(2)-H(2)	107.6	C(8)-C(7)-H(7A)	110.4
C(1)-C(2)-H(2)	107.6	C(6)-C(7)-H(7A)	110.4
C(6)-C(2)-H(2)	107.6	C(8)-C(7)-H(7B)	110.4
C(3)-N(1)-C(2)	126.74(5)	C(6)-C(7)-H(7B)	110.4
C(3)-N(1)-H(1N)	116.1(7)	H(7A)-C(7)-H(7B)	108.6
C(2)-N(1)-H(1N)	116.6(7)	C(1)-C(8)-C(7)	104.12(5)
O(2)-C(3)-N(1)	121.36(5)	C(1)-C(8)-H(8A)	110.9
O(2)-C(3)-C(4)	120.95(5)	C(7)-C(8)-H(8A)	110.9
N(1)-C(3)-C(4)	117.62(5)	C(1)-C(8)-H(8B)	110.9
C(3)-C(4)-C(5)	114.04(5)	C(7)-C(8)-H(8B)	110.9
C(3)-C(4)-H(4A)	108.7	H(8A)-C(8)-H(8B)	109.0
C(5)-C(4)-H(4A)	108.7	O(1)-Si(1)-C(12)	111.16(3)
C(3)-C(4)-H(4B)	108.7	O(1)-Si(1)-C(11)	104.37(3)
C(5)-C(4)-H(4B)	108.7	C(12)-Si(1)-C(11)	109.69(4)
H(4A)-C(4)-H(4B)	107.6	O(1)-Si(1)-C(13)	108.76(3)
C(4)-C(5)-C(6)	111.21(5)	C(12)-Si(1)-C(13)	111.62(3)
C(4)-C(5)-H(5A)	109.4	C(11)-Si(1)-C(13)	111.02(4)
C(6)-C(5)-H(5A)	109.4	Si(1)-C(11)-H(11A)	109.5
C(4)-C(5)-H(5B)	109.4	Si(1)-C(11)-H(11B)	109.5
C(6)-C(5)-H(5B)	109.4	H(11A)-C(11)-H(11B)	109.5
H(5A)-C(5)-H(5B)	108.0	Si(1)-C(11)-H(11C)	109.5
C(9)-C(6)-C(5)	107.62(5)	H(11A)-C(11)-H(11C)	109.5
C(9)-C(6)-C(2)	114.05(5)	H(11B)-C(11)-H(11C)	109.5
C(5)-C(6)-C(2)	110.08(5)	Si(1)-C(12)-H(12A)	109.5

Table A4.3.3. cont'd.

Atoms	Angle (°)	Atoms	Angle (°)
Si(1)-C(12)-H(12B)	109.5	C(13)-C(14)-H(14C)	109.5
H(12A)-C(12)-H(12B)	109.5	H(14A)-C(14)-H(14C)	109.5
Si(1)-C(12)-H(12C)	109.5	H(14B)-C(14)-H(14C)	109.5
H(12A)-C(12)-H(12C)	109.5	C(13)-C(15)-H(15A)	109.5
H(12B)-C(12)-H(12C)	109.5	C(13)-C(15)-H(15B)	109.5
C(14)-C(13)-C(15)	109.08(6)	H(15A)-C(15)-H(15B)	109.5
C(14)-C(13)-C(16)	108.94(6)	C(13)-C(15)-H(15C)	109.5
C(15)-C(13)-C(16)	108.35(7)	H(15A)-C(15)-H(15C)	109.5
C(14)-C(13)-Si(1)	110.31(5)	H(15B)-C(15)-H(15C)	109.5
C(15)-C(13)-Si(1)	110.09(5)	C(13)-C(16)-H(16A)	109.5
C(16)-C(13)-Si(1)	110.03(5)	C(13)-C(16)-H(16B)	109.5
C(13)-C(14)-H(14A)	109.5	H(16A)-C(16)-H(16B)	109.5
C(13)-C(14)-H(14B)	109.5	C(13)-C(16)-H(16C)	109.5
H(14A)-C(14)-H(14B)	109.5	H(16A)-C(16)-H(16C)	109.5
		H(16B)-C(16)-H(16C)	109.5

Symmetry transformations used to generate equivalent atoms:

Table A4.3.4. *Anisotropic displacement parameters ($Å^2 x\ 10^3$) for* ***87*** *(V23031). The anisotropic displacement factor exponent takes the form: $-2p^2[\ h^2\ a^{*2}U^{11} + ... + 2\ h\ k\ a^*\ b^*\ U^{12}\ ]$*

Atom	U^{11}	U^{22}	U^{33}	U^{23}	U^{13}	U^{12}
O(1)	18(1)	17(1)	16(1)	-2(1)	4(1)	5(1)
C(1)	17(1)	12(1)	15(1)	-1(1)	7(1)	0(1)
C(2)	16(1)	9(1)	11(1)	-1(1)	4(1)	-1(1)
N(1)	21(1)	9(1)	11(1)	-2(1)	6(1)	-3(1)
C(3)	21(1)	10(1)	12(1)	-1(1)	5(1)	-2(1)
O(2)	37(1)	9(1)	17(1)	-1(1)	10(1)	-5(1)
C(4)	29(1)	11(1)	15(1)	-2(1)	12(1)	-3(1)
C(5)	21(1)	10(1)	11(1)	-1(1)	6(1)	0(1)
C(6)	15(1)	8(1)	12(1)	-1(1)	5(1)	0(1)

Table A4.3.4. cont'd.

Atom	U^{11}	U^{22}	U^{33}	U^{23}	U^{13}	U^{12}
C(9)	18(1)	14(1)	20(1)	1(1)	6(1)	3(1)
C(10)	19(1)	26(1)	28(1)	0(1)	1(1)	4(1)
C(7)	22(1)	11(1)	20(1)	-4(1)	10(1)	-4(1)
C(8)	20(1)	13(1)	22(1)	-2(1)	10(1)	-3(1)
Si(1)	16(1)	13(1)	15(1)	0(1)	5(1)	2(1)
C(11)	38(1)	27(1)	22(1)	6(1)	14(1)	4(1)
C(12)	22(1)	18(1)	29(1)	-7(1)	6(1)	1(1)
C(13)	16(1)	18(1)	20(1)	1(1)	4(1)	2(1)
C(14)	18(1)	25(1)	36(1)	2(1)	6(1)	6(1)
C(15)	24(1)	36(1)	26(1)	7(1)	12(1)	0(1)
C(16)	23(1)	23(1)	33(1)	-6(1)	2(1)	-2(1)

Table A4.3.5. *Hydrogen coordinates (x 10^4) and isotropic displacement parameters ($Å^2$x 10^3) for* ***87*** *(V23031).*

Atom	x	y	z	U(eq)
H(1)	7157	7249	4907	17
H(2)	5116	7697	4673	14
H(1N)	5257(10)	5917(8)	4960(8)	16
H(4A)	4985	6217	7984	21
H(4B)	3886	6805	7095	21
H(5A)	6392	7433	7755	17
H(5B)	5281	8082	7956	17
H(9)	3935	9206	6424	21
H(10A)	3206	7842	4612	31
H(10B)	2370	8745	4974	31
H(7A)	5934	9742	6180	20
H(7B)	6843	9111	7207	20
H(8A)	6794	9058	4915	21
H(8B)	7965	8913	6001	21
H(11A)	8973	6162	8764	42

Table A4.3.5. cont'd.

Atom	x	y	z	U(eq)
H(11B)	9270	5003	8427	42
H(11C)	7885	5353	8245	42
H(12A)	7244	4705	5871	35
H(12B)	8604	4436	5866	35
H(12C)	7810	5275	5000	35
H(14A)	10803	5078	6536	40
H(14B)	11174	5450	7815	40
H(14C)	11855	5935	6985	40
H(15A)	9419	7512	5337	41
H(15B)	9740	6358	5007	41
H(15C)	10810	7187	5510	41
H(16A)	11330	7738	7489	42
H(16B)	10638	7243	8306	42
H(16C)	9938	8043	7342	42

Table A4.3.6. *Torsion angles [°] for* ***87*** *(V23031).*

Atoms (A-B-C-D)	Angle (°)	Atoms (A-B-C-D)	Angle (°)
Si(1)-O(1)-C(1)-C(8)	-131.43(5)	C(4)-C(5)-C(6)-C(9)	71.63(6)
Si(1)-O(1)-C(1)-C(2)	118.35(5)	C(4)-C(5)-C(6)-C(2)	-53.21(7)
O(1)-C(1)-C(2)-N(1)	-54.99(6)	C(4)-C(5)-C(6)-C(7)	-167.02(5)
C(8)-C(1)-C(2)-N(1)	-170.84(4)	N(1)-C(2)-C(6)-C(9)	-85.53(6)
O(1)-C(1)-C(2)-C(6)	71.99(6)	C(1)-C(2)-C(6)-C(9)	149.04(5)
C(8)-C(1)-C(2)-C(6)	-43.85(5)	N(1)-C(2)-C(6)-C(5)	35.54(7)
C(1)-C(2)-N(1)-C(3)	105.81(7)	C(1)-C(2)-C(6)-C(5)	-89.89(5)
C(6)-C(2)-N(1)-C(3)	-15.21(9)	N(1)-C(2)-C(6)-C(7)	153.91(5)
C(2)-N(1)-C(3)-O(2)	-171.85(6)	C(1)-C(2)-C(6)-C(7)	28.48(5)
C(2)-N(1)-C(3)-C(4)	11.08(9)	C(5)-C(6)-C(9)-C(10)	-112.82(8)
O(2)-C(3)-C(4)-C(5)	154.04(6)	C(2)-C(6)-C(9)-C(10)	9.61(9)
N(1)-C(3)-C(4)-C(5)	-28.87(8)	C(7)-C(6)-C(9)-C(10)	125.93(8)
C(3)-C(4)-C(5)-C(6)	50.73(7)	C(9)-C(6)-C(7)-C(8)	-125.18(6)

Table A4.3.6. cont'd.

Atoms (A-B-C-D)	Angle (°)	Atoms (A-B-C-D)	Angle (°)
C(5)-C(6)-C(7)-C(8)	115.42(6)	C(12)-Si(1)-C(13)-C(14)	-63.18(6)
C(2)-C(6)-C(7)-C(8)	-2.49(6)	C(11)-Si(1)-C(13)-C(14)	59.54(6)
O(1)-C(1)-C(8)-C(7)	-74.32(6)	O(1)-Si(1)-C(13)-C(15)	-65.75(6)
C(2)-C(1)-C(8)-C(7)	41.56(6)	C(12)-Si(1)-C(13)-C(15)	57.25(6)
C(6)-C(7)-C(8)-C(1)	-24.49(7)	C(11)-Si(1)-C(13)-C(15)	179.97(5)
C(1)-O(1)-Si(1)-C(12)	-42.14(7)	O(1)-Si(1)-C(13)-C(16)	53.59(5)
C(1)-O(1)-Si(1)-C(11)	-160.31(6)	C(12)-Si(1)-C(13)-C(16)	176.59(5)
C(1)-O(1)-Si(1)-C(13)	81.14(6)O(1)-	C(11)-Si(1)-C(13)-C(16)	-60.69(6)
Si(1)-C(13)-C(14)	173.82(5)		

Symmetry transformations used to generate equivalent atoms:

Table A4.3.7. *Hydrogen bonds for* ***87*** *(V23031) [Å and °].*

D-H...A	d(D-H)	d(H...A)	d(D...A)	<(DHA)
N(1)-H(1N)...O(2)#1	0.889(9)	2.005(9)	2.8900(8)	173.5(10)

Symmetry transformations used to generate equivalent atoms:
#1 -x+1,-y+1,-z+1

A4.4 X-RAY CRYSTAL STRUCTURE ANALYSIS OF HBF_4 SALT 97b (V23134)

An X-ray quality crystal of compound **97b** (V23134) was grown by dissolving **97b** (4 mg) in MeCN (approx. 0.1 mL) and placing the small tube in a 1 Dr vial filled with Et_2O (approx. 1 mL). The vial-in-vial setup was placed in a –10 °C freezer to allow for slow vapor diffusion of Et_2O into the MeCN solution *(Note: compound **97b** is racemic)*. Low-temperature diffraction data (ϕ-and ω-scans) were collected on a Bruker AXS D8 VENTURE KAPPA diffractometer coupled to a PHOTON II CPAD detector with Cu K_α radiation (λ = 1.54178 Å) from an IμS micro-source for the structure of compound V23134. The structure was solved by direct methods using SHELXS[1] and refined against F^2 on all data by full-matrix least squares with SHELXL-2019[2] using established refinement techniques.[3] All non-hydrogen atoms were refined anisotropically. Unless otherwise noted, all hydrogen atoms were included into the model at geometrically calculated positions and refined using a riding model. The isotropic displacement parameters of all hydrogen atoms were fixed to 1.2 times the U value of the atoms they are linked to (1.5 times for methyl groups).

Compound V23134 crystallizes in the monoclinic space group $P2_1/c$ with one molecule in the asymmetric unit. The coordinates for the hydrogen atoms bound to N1 were located in the difference Fourier synthesis and refined semi-freely with the help of a restraint on the N-H distance (0.91(4) Å).

Figure A4.4.1. *X-Ray Coordinate for* ***97b*** *(V23134)*

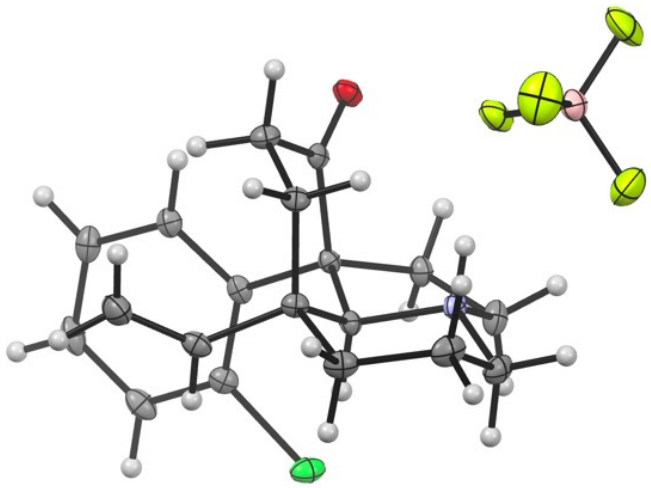


Table A4.4.1. *Crystal data and structure refinement for* ***97b*** *(V23134).*

Identification code	V23134	
Empirical formula	C19 H23 B Cl F4 N O	
Formula weight	403.64	
Temperature	100(2) K	
Wavelength	1.54178 Å	
Crystal system	Monoclinic	
Space group	$P2_1/c$	
Unit cell dimensions	a = 11.8613(9) Å	a= 90°.
	b = 11.9757(7) Å	b= 98.397(9)°.
	c = 13.0930(12) Å	g = 90°.
Volume	1839.9(2) $Å^3$	
Z	4	
Density (calculated)	1.457 Mg/m^3	
Absorption coefficient	2.277 mm^{-1}	
F(000)	840	
Crystal size	0.300 x 0.250 x 0.200 mm^3	
Theta range for data collection	3.767 to 74.599°.	
Index ranges	-14<=h<=14, -14<=k<=14, -16<=l<=16	
Reflections collected	50321	
Independent reflections	3752 [R(int) = 0.0362]	
Completeness to theta = 67.679°	99.9 %	

Absorption correction	Semi-empirical from equivalents
Max. and min. transmission	0.7538 and 0.6473
Refinement method	Full-matrix least-squares on F^2
Data / restraints / parameters	3752 / 1 / 247
Goodness-of-fit on F^2	1.054
Final R indices [I>2sigma(I)]	R1 = 0.0288, wR2 = 0.0733
R indices (all data)	R1 = 0.0297, wR2 = 0.0739
Extinction coefficient	n/a
Largest diff. peak and hole	0.335 and -0.240 e.$Å^{-3}$

Table A4.4.2. *Atomic coordinates (x 10^4) and equivalent isotropic displacement parameters ($Å^2$x 10^3) for V23134. U(eq) is defined as one third of the trace of the orthogonalized Uij tensor.*

Atom	x	y	z	U(eq)
N(1)	1586(1)	2708(1)	7914(1)	14(1)
C(1)	2676(1)	3358(1)	8206(1)	12(1)
C(2)	2449(1)	4594(1)	8406(1)	13(1)
C(12)	3568(1)	5097(1)	8916(1)	16(1)
C(13)	3942(1)	6115(1)	8793(1)	23(1)
C(3)	1955(1)	5185(1)	7398(1)	15(1)
C(4)	2674(1)	4990(1)	6531(1)	16(1)
C(5)	2923(1)	3779(1)	6353(1)	13(1)
O(1)	2843(1)	3383(1)	5494(1)	17(1)
C(6)	3352(1)	3044(1)	7315(1)	11(1)
C(14)	4651(1)	3203(1)	7568(1)	12(1)
C(15)	5331(1)	2691(1)	8406(1)	14(1)
Cl(1)	4762(1)	1768(1)	9229(1)	19(1)
C(16)	6502(1)	2863(1)	8627(1)	19(1)
C(17)	7047(1)	3511(1)	7974(1)	20(1)
C(18)	6419(1)	3984(1)	7108(1)	18(1)
C(19)	5242(1)	3843(1)	6925(1)	14(1)

Table A4.4.2. cont'd.

Atom	x	y	z	U(eq)
C(7)	3005(1)	1803(1)	7076(1)	15(1)
C(8)	1986(1)	1570(1)	7649(1)	18(1)
C(9)	829(1)	2732(1)	8735(1)	19(1)
C(10)	534(1)	3943(1)	8927(1)	21(1)
C(11)	1604(1)	4658(1)	9207(1)	18(1)
B(1)	-717(1)	3244(1)	5944(1)	18(1)
F(1)	481(1)	3308(1)	5972(1)	24(1)
F(2)	-907(1)	2443(1)	6668(1)	39(1)
F(3)	-1110(1)	4262(1)	6225(1)	40(1)
F(4)	-1207(1)	2935(1)	4970(1)	34(1)

Table A4.4.3. *Bond lengths [Å] and angles [°] for* ***97b*** *(V23134).*

Bond	Length (Å)	Bond	Length (Å)
N(1)-C(9)	1.4987(15)	C(3)-H(3B)	0.9900
N(1)-C(8)	1.4996(15)	C(4)-C(5)	1.5050(16)
N(1)-C(1)	1.5096(14)	C(4)-H(4A)	0.9900
N(1)-H(1N)	0.900(13)	C(4)-H(4B)	0.9900
C(1)-C(2)	1.5339(15)	C(5)-O(1)	1.2114(14)
C(1)-C(6)	1.5554(15)	C(5)-C(6)	1.5601(15)
C(1)-H(1)	1.0000	C(6)-C(14)	1.5403(15)
C(2)-C(12)	1.5194(16)	C(6)-C(7)	1.5617(15)
C(2)-C(3)	1.5362(15)	C(14)-C(19)	1.3998(16)
C(2)-C(11)	1.5542(15)	C(14)-C(15)	1.4039(16)
C(12)-C(13)	1.3156(18)	C(15)-C(16)	1.3919(16)
C(12)-H(12)	0.9500	C(15)-Cl(1)	1.7465(12)
C(13)-H(13A)	0.9500	C(16)-C(17)	1.3833(19)
C(13)-H(13B)	0.9500	C(16)-H(16)	0.9500
C(3)-C(4)	1.5330(16)	C(17)-C(18)	1.3837(18)
C(3)-H(3A)	0.9900	C(17)-H(17)	0.9500

Table A4.4.3. cont'd.

Bond	Length (Å)	Bond	Angle (°)
C(18)-C(19)	1.3911(16)	C(12)-C(2)-C(1)	107.05(9)
C(18)-H(18)	0.9500	C(12)-C(2)-C(3)	113.19(9)
C(19)-H(19)	0.9500	C(1)-C(2)-C(3)	110.62(9)
C(7)-C(8)	1.5388(16)	C(12)-C(2)-C(11)	106.95(9)
C(7)-H(7A)	0.9900	C(1)-C(2)-C(11)	108.01(9)
C(7)-H(7B)	0.9900	C(3)-C(2)-C(11)	110.77(9)
C(8)-H(8A)	0.9900	C(13)-C(12)-C(2)	127.00(11)
C(8)-H(8B)	0.9900	C(13)-C(12)-H(12)	116.5
C(9)-C(10)	1.5209(18)	C(2)-C(12)-H(12)	116.5
C(9)-H(9A)	0.9900	C(12)-C(13)-H(13A)	120.0
C(9)-H(9B)	0.9900	C(12)-C(13)-H(13B)	120.0
C(10)-C(11)	1.5319(18)	H(13A)-C(13)-H(13B)	120.0
C(10)-H(10A)	0.9900	C(4)-C(3)-C(2)	112.49(9)
C(10)-H(10B)	0.9900	C(4)-C(3)-H(3A)	109.1
C(11)-H(11A)	0.9900	C(2)-C(3)-H(3A)	109.1
C(11)-H(11B)	0.9900	C(4)-C(3)-H(3B)	109.1
B(1)-F(4)	1.3733(16)	C(2)-C(3)-H(3B)	109.1
B(1)-F(3)	1.3747(16)	H(3A)-C(3)-H(3B)	107.8
B(1)-F(2)	1.3907(16)	C(5)-C(4)-C(3)	113.83(9)
B(1)-F(1)	1.4173(15)	C(5)-C(4)-H(4A)	108.8
		C(3)-C(4)-H(4A)	108.8
Bond	**Angle (°)**	C(5)-C(4)-H(4B)	108.8
C(9)-N(1)-C(8)	115.21(9)	C(3)-C(4)-H(4B)	108.8
C(9)-N(1)-C(1)	112.88(9)	H(4A)-C(4)-H(4B)	107.7
C(8)-N(1)-C(1)	103.89(8)	O(1)-C(5)-C(4)	122.07(10)
C(9)-N(1)-H(1N)	108.7(10)	O(1)-C(5)-C(6)	119.99(10)
C(8)-N(1)-H(1N)	106.8(10)	C(4)-C(5)-C(6)	117.87(9)
C(1)-N(1)-H(1N)	109.1(10)	C(14)-C(6)-C(1)	114.71(9)
N(1)-C(1)-C(2)	112.10(9)	C(14)-C(6)-C(5)	107.57(9)
N(1)-C(1)-C(6)	101.58(8)	C(1)-C(6)-C(5)	108.99(9)
C(2)-C(1)-C(6)	118.98(9)	C(14)-C(6)-C(7)	112.77(9)
N(1)-C(1)-H(1)	107.9	C(1)-C(6)-C(7)	103.39(9)
C(2)-C(1)-H(1)	107.9	C(5)-C(6)-C(7)	109.28(9)
C(6)-C(1)-H(1)	107.9	C(19)-C(14)-C(15)	115.34(10)

Table A4.4.3. cont'd.

Bond	Angle (°)	Bond	Angle (°)
C(19)-C(14)-C(6)	120.78(10)	N(1)-C(8)-H(8B)	110.9
C(15)-C(14)-C(6)	123.80(10)	C(7)-C(8)-H(8B)	110.9
C(16)-C(15)-C(14)	122.66(11)	H(8A)-C(8)-H(8B)	108.9
C(16)-C(15)-Cl(1)	115.38(9)	N(1)-C(9)-C(10)	108.27(9)
C(14)-C(15)-Cl(1)	121.94(9)	N(1)-C(9)-H(9A)	110.0
C(17)-C(16)-C(15)	119.76(11)	C(10)-C(9)-H(9A)	110.0
C(17)-C(16)-H(16)	120.1	N(1)-C(9)-H(9B)	110.0
C(15)-C(16)-H(16)	120.1	C(10)-C(9)-H(9B)	110.0
C(16)-C(17)-C(18)	119.48(11)	H(9A)-C(9)-H(9B)	108.4
C(16)-C(17)-H(17)	120.3	C(9)-C(10)-C(11)	111.72(10)
C(18)-C(17)-H(17)	120.3	C(9)-C(10)-H(10A)	109.3
C(17)-C(18)-C(19)	119.84(11)	C(11)-C(10)-H(10A)	109.3
C(17)-C(18)-H(18)	120.1	C(9)-C(10)-H(10B)	109.3
C(19)-C(18)-H(18)	120.1	C(11)-C(10)-H(10B)	109.3
C(18)-C(19)-C(14)	122.76(11)	H(10A)-C(10)-H(10B)	107.9
C(18)-C(19)-H(19)	118.6	C(10)-C(11)-C(2)	113.85(10)
C(14)-C(19)-H(19)	118.6	C(10)-C(11)-H(11A)	108.8
C(8)-C(7)-C(6)	106.09(9)	C(2)-C(11)-H(11A)	108.8
C(8)-C(7)-H(7A)	110.5	C(10)-C(11)-H(11B)	108.8
C(6)-C(7)-H(7A)	110.5	C(2)-C(11)-H(11B)	108.8
C(8)-C(7)-H(7B)	110.5	H(11A)-C(11)-H(11B)	107.7
C(6)-C(7)-H(7B)	110.5	F(4)-B(1)-F(3)	111.90(11)
H(7A)-C(7)-H(7B)	108.7	F(4)-B(1)-F(2)	111.01(11)
N(1)-C(8)-C(7)	104.20(9)	F(3)-B(1)-F(2)	109.54(11)
N(1)-C(8)-H(8A)	110.9	F(4)-B(1)-F(1)	108.99(11)
C(7)-C(8)-H(8A)	110.9	F(3)-B(1)-F(1)	108.85(11)
		F(2)-B(1)-F(1)	106.37(10)

Symmetry transformations used to generate equivalent atoms:

Table A4.4.4. *Anisotropic displacement parameters ($Å^2 x\ 10^3$) for* ***97b*** *(V23134). The anisotropic displacement factor exponent takes the form: $-2p^2[\ h^2\ a^{*2}U^{11} + \ldots + 2\ h\ k\ a^*\ b^*\ U^{12}\ ]$*

Atom	U^{11}	U^{22}	U^{33}	U^{23}	U^{13}	U^{12}
N(1)	10(1)	15(1)	16(1)	2(1)	2(1)	0(1)
C(1)	9(1)	14(1)	12(1)	0(1)	1(1)	0(1)
C(2)	14(1)	14(1)	12(1)	0(1)	3(1)	2(1)
C(12)	17(1)	17(1)	13(1)	-3(1)	0(1)	3(1)
C(13)	26(1)	22(1)	20(1)	-2(1)	-3(1)	-4(1)
C(3)	15(1)	15(1)	14(1)	1(1)	1(1)	3(1)
C(4)	18(1)	16(1)	14(1)	3(1)	2(1)	2(1)
C(5)	7(1)	18(1)	13(1)	1(1)	2(1)	-1(1)
O(1)	14(1)	24(1)	12(1)	-3(1)	2(1)	-1(1)
C(6)	10(1)	12(1)	12(1)	-1(1)	1(1)	0(1)
C(14)	11(1)	12(1)	14(1)	-4(1)	2(1)	1(1)
C(15)	15(1)	16(1)	14(1)	-2(1)	3(1)	3(1)
Cl(1)	17(1)	23(1)	17(1)	6(1)	4(1)	6(1)
C(16)	14(1)	22(1)	19(1)	-5(1)	-2(1)	5(1)
C(17)	11(1)	21(1)	29(1)	-8(1)	2(1)	-1(1)
C(18)	15(1)	15(1)	26(1)	-4(1)	7(1)	-2(1)
C(19)	14(1)	13(1)	16(1)	-3(1)	2(1)	1(1)
C(7)	16(1)	13(1)	18(1)	-3(1)	2(1)	-2(1)
C(8)	16(1)	14(1)	27(1)	-1(1)	4(1)	-2(1)
C(9)	14(1)	23(1)	20(1)	5(1)	7(1)	1(1)
C(10)	15(1)	26(1)	22(1)	3(1)	9(1)	5(1)
C(11)	19(1)	21(1)	16(1)	0(1)	6(1)	5(1)
B(1)	13(1)	21(1)	21(1)	0(1)	2(1)	0(1)
F(1)	12(1)	41(1)	18(1)	-1(1)	1(1)	-1(1)
F(2)	37(1)	39(1)	40(1)	15(1)	7(1)	-11(1)
F(3)	36(1)	29(1)	58(1)	-6(1)	16(1)	9(1)
F(4)	18(1)	54(1)	28(1)	-8(1)	-6(1)	-4(1)

Table A4.4.5. *Hydrogen coordinates (x 104) and isotropic displacement parameters ($Å^2$x 10^3) for* ***97b*** *(V23134).*

Atom	x	y	z	U(eq)
H(1N)	1202(12)	2996(12)	7329(10)	16
H(1)	3087	3032	8859	14
H(12)	4048	4625	9372	19
H(13A)	3495	6622	8345	28
H(13B)	4659	6343	9152	28
H(3A)	1172	4910	7172	18
H(3B)	1910	5997	7529	18
H(4A)	2268	5311	5883	19
H(4B)	3405	5396	6701	19
H(16)	6925	2536	9224	22
H(17)	7846	3630	8118	24
H(18)	6790	4405	6640	22
H(19)	4823	4195	6339	17
H(7A)	2786	1692	6324	18
H(7B)	3646	1296	7323	18
H(8A)	1377	1163	7201	22
H(8B)	2223	1125	8281	22
H(9A)	1225	2393	9379	22
H(9B)	125	2300	8509	22
H(10A)	69	3976	9496	25
H(10B)	72	4250	8299	25
H(11A)	2004	4415	9888	22
H(11B)	1372	5446	9274	22

Table A4.4.6. *Torsion angles [°] for* ***97b*** *(V23134).*

Atoms (A-B-C-D)	Angle (°)	Atoms (A-B-C-D)	Angle (°)
C(9)-N(1)-C(1)-C(2)	-60.07(12)	C(4)-C(5)-C(6)-C(7)	152.76(10)
C(8)-N(1)-C(1)-C(2)	174.44(9)	C(1)-C(6)-C(14)-C(19)	-126.35(11)
C(9)-N(1)-C(1)-C(6)	171.84(9)	C(5)-C(6)-C(14)-C(19)	-4.93(13)
C(8)-N(1)-C(1)-C(6)	46.35(10)	C(7)-C(6)-C(14)-C(19)	115.64(11)
N(1)-C(1)-C(2)-C(12)	167.72(9)	C(1)-C(6)-C(14)-C(15)	56.80(14)
C(6)-C(1)-C(2)-C(12)	-74.09(12)	C(5)-C(6)-C(14)-C(15)	178.23(10)
N(1)-C(1)-C(2)-C(3)	-68.53(11)	C(7)-C(6)-C(14)-C(15)	-61.21(14)
C(6)-C(1)-C(2)-C(3)	49.66(13)	C(19)-C(14)-C(15)-C(16)	4.01(16)
N(1)-C(1)-C(2)-C(11)	52.86(11)	C(6)-C(14)-C(15)-C(16)	-178.98(10)
C(6)-C(1)-C(2)-C(11)	171.05(9)	C(19)-C(14)-C(15)-Cl(1)	-174.52(8)
C(1)-C(2)-C(12)-C(13)	145.11(12)	C(6)-C(14)-C(15)-Cl(1)	2.48(15)
C(3)-C(2)-C(12)-C(13)	22.96(17)	C(14)-C(15)-C(16)-C(17)	-3.64(18)
C(11)-C(2)-C(12)-C(13)	-99.31(14)	Cl(1)-C(15)-C(16)-C(17)	174.98(9)
C(12)-C(2)-C(3)-C(4)	68.62(12)	C(15)-C(16)-C(17)-C(18)	0.19(18)
C(1)-C(2)-C(3)-C(4)	-51.51(12)	C(16)-C(17)-C(18)-C(19)	2.57(18)
C(11)-C(2)-C(3)-C(4)	-171.26(10)	C(17)-C(18)-C(19)-C(14)	-2.09(18)
C(2)-C(3)-C(4)-C(5)	51.69(13)	C(15)-C(14)-C(19)-C(18)	-1.15(16)
C(3)-C(4)-C(5)-O(1)	135.80(11)	C(6)-C(14)-C(19)-C(18)	-178.25(10)
C(3)-C(4)-C(5)-C(6)	-47.22(13)	C(14)-C(6)-C(7)-C(8)	136.54(10)
N(1)-C(1)-C(6)-C(14)	-158.34(9)	C(1)-C(6)-C(7)-C(8)	12.07(11)
C(2)-C(1)-C(6)-C(14)	78.13(12)	C(5)-C(6)-C(7)-C(8)	-103.88(10)
N(1)-C(1)-C(6)-C(5)	81.01(10)	C(9)-N(1)-C(8)-C(7)	-162.84(9)
C(2)-C(1)-C(6)-C(5)	-42.52(12)	C(1)-N(1)-C(8)-C(7)	-38.84(11)
N(1)-C(1)-C(6)-C(7)	-35.15(10)	C(6)-C(7)-C(8)-N(1)	15.80(12)
C(2)-C(1)-C(6)-C(7)	-158.68(9)	C(8)-N(1)-C(9)-C(10)	178.45(10)
O(1)-C(5)-C(6)-C(14)	92.54(12)	C(1)-N(1)-C(9)-C(10)	59.32(12)
C(4)-C(5)-C(6)-C(14)	-84.49(11)	N(1)-C(9)-C(10)-C(11)	-55.77(13)
O(1)-C(5)-C(6)-C(1)	-142.52(10)	C(9)-C(10)-C(11)-C(2)	54.40(13)
C(4)-C(5)-C(6)-C(1)	40.44(12)	C(12)-C(2)-C(11)-C(10)	-166.06(10)
O(1)-C(5)-C(6)-C(7)	-30.20(14)	C(1)-C(2)-C(11)-C(10)	-51.13(12)
		C(3)-C(2)-C(11)-C(10)	70.17(13)

Symmetry transformations used to generate equivalent atoms:

Table A4.4.7. *Hydrogen bonds for* ***97b*** *(V23134) [Å and °].*

D-H...A	d(D-H)	d(H...A)	d(D...A)	<(DHA)
N(1)-H(1N)...F(1)	0.900(13)	1.894(13)	2.7798(13)	167.6(14)
C(1)-H(1)...Cl(1)	1.00	2.49	3.2523(11)	132.8
C(4)-H(4A)...F(4)#1	0.99	2.61	3.4729(15)	145.2
C(16)-H(16)...F(4)#2	0.95	2.36	3.1614(14)	142.4
C(7)-H(7B)...Cl(1)	0.99	2.71	3.2523(12)	115.0
C(9)-H(9A)...O(1)#3	0.99	2.42	3.3453(15)	155.1
C(9)-H(9A)...F(1)#3	0.99	2.53	3.2640(14)	131.3
C(9)-H(9B)...F(2)	0.99	2.54	3.1712(16)	121.1

Symmetry transformations used to generate equivalent atoms:
#1 -x,-y+1,-z+1 #2 x+1,-y+1/2,z+1/2 #3 x,-y+1/2,z+1/2

A4.5 X-RAY CRYSTAL STRUCTURE ANALYSIS OF TRIAZOLINE 116 (V23324)

An X-ray quality crystal of **116** was grown by dissolving 116 in minimal CH_2Cl_2 (approx. 10 mg/0.5 mL) and layering with heptane. Low-temperature diffraction data (ϕ-and ω-scans) were collected on a Bruker AXS D8 VENTURE KAPPA diffractometer coupled to a PHOTON II CPAD detector with Cu K_α radiation (λ = 1.54178 Å) from an IμS micro-source for the structure of compound V23324. The structure was solved by direct methods using SHELXS[1] and refined against F^2 on all data by full-matrix least squares with SHELXL-2019[2] using established refinement techniques.[3] All non-hydrogen atoms were refined anisotropically. All hydrogen atoms were included into the model at geometrically calculated positions and refined using a riding model. The isotropic displacement parameters of all hydrogen atoms were fixed to 1.2 times the U value of the atoms they are linked to (1.5 times for methyl groups). Compound V23324 crystallizes in the monoclinic space group $P2_1$ with one molecule in the asymmetric unit.

Figure A4.5.1. *X-Ray Coordinate for* ***116*** *(V23324)*

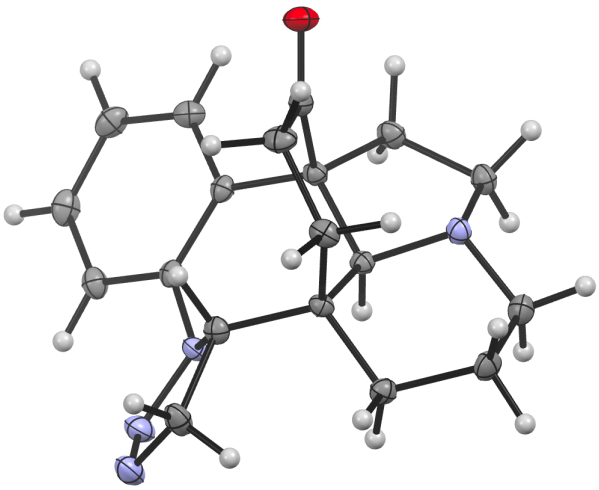


Table A4.5.1. *Crystal data and structure refinement for* ***116*** *(V23324).*

Identification code	V23324	
Empirical formula	C19 H22 N4 O	
Formula weight	322.40	
Temperature	100(2) K	
Wavelength	1.54178 Å	
Crystal system	Monoclinic	
Space group	$P2_1$	
Unit cell dimensions	a = 8.8173(12) Å	a= 90°.
	b = 8.3934(6) Å	b= 111.249(7)°.
	c = 11.3020(11) Å	g = 90°.
Volume	779.56(15) $Å^3$	
Z	2	
Density (calculated)	1.374 Mg/m^3	
Absorption coefficient	0.697 mm^{-1}	
F(000)	344	
Crystal size	0.150 x 0.150 x 0.050 mm^3	
Theta range for data collection	4.197 to 74.555°.	
Index ranges	-10<=h<=9, -10<=k<=10, -14<=l<=14	
Reflections collected	16511	
Independent reflections	3170 [R(int) = 0.0396]	
Completeness to theta = 67.679°	100.0 %	

Absorption correction	Semi-empirical from equivalents
Max. and min. transmission	0.7538 and 0.6681
Refinement method	Full-matrix least-squares on F^2
Data / restraints / parameters	3170 / 1 / 217
Goodness-of-fit on F^2	1.069
Final R indices [I>2sigma(I)]	R1 = 0.0290, wR2 = 0.0690
R indices (all data)	R1 = 0.0309, wR2 = 0.0705
Absolute structure parameter	-0.05(11)
Extinction coefficient	n/a
Largest diff. peak and hole	0.205 and -0.161 e.$Å^{-3}$

Table A4.5.2. *Atomic coordinates (x 10^4) and equivalent isotropic displacement parameters ($Å^2$x 10^3) for V23324. U(eq) is defined as one third of the trace of the orthogonalized Uij tensor.*

Atom	x	y	z	U(eq)
O(1)	10804(2)	2163(2)	8321(1)	22(1)
C(1)	9510(2)	2684(2)	8292(2)	16(1)
C(2)	9006(2)	2479(3)	9428(2)	20(1)
C(3)	7171(2)	2403(2)	9161(2)	16(1)
C(4)	6195(2)	3616(2)	8157(2)	12(1)
C(5)	6699(2)	5309(2)	8721(2)	15(1)
C(6)	5599(3)	6141(2)	9314(2)	20(1)
N(1)	5315(2)	7758(2)	8745(2)	22(1)
N(2)	5961(2)	7906(2)	7939(2)	21(1)
N(3)	6715(2)	6515(2)	7766(2)	14(1)
C(7)	8136(2)	6723(2)	7463(2)	14(1)
C(8)	8694(2)	8267(2)	7377(2)	18(1)
C(9)	10148(2)	8497(2)	7187(2)	20(1)
C(10)	11068(2)	7200(3)	7085(2)	21(1)
C(11)	10483(2)	5679(2)	7124(2)	18(1)
C(12)	9005(2)	5396(2)	7279(2)	14(1)

Table A4.5.2. cont'd.

Atom	x	y	z	U(eq)
C(13)	8414(2)	3665(2)	7148(2)	13(1)
C(14)	8462(2)	2913(2)	5899(2)	17(1)
C(15)	6986(2)	1785(2)	5442(2)	18(1)
N(4)	6298(2)	1838(2)	6450(2)	15(1)
C(16)	4561(2)	1479(2)	5988(2)	19(1)
C(17)	3881(2)	1681(2)	7042(2)	19(1)
C(18)	4355(2)	3295(2)	7718(2)	15(1)
C(19)	6627(2)	3451(2)	6966(2)	12(1)

Table A4.5.3. *Bond lengths [Å] and angles [°] for* ***97b*** *(V23324).*

Bond	Length (Å)	Bond	Length (Å)
O(1)-C(1)	1.211(2)	N(3)-C(7)	1.424(2)
C(1)-C(2)	1.513(3)	C(7)-C(8)	1.401(3)
C(1)-C(13)	1.542(3)	C(7)-C(12)	1.409(3)
C(2)-C(3)	1.535(2)	C(8)-C(9)	1.389(3)
C(2)-H(2A)	0.9900	C(8)-H(8)	0.9500
C(2)-H(2B)	0.9900	C(9)-C(10)	1.387(3)
C(3)-C(4)	1.535(3)	C(9)-H(9)	0.9500
C(3)-H(3A)	0.9900	C(10)-C(11)	1.383(3)
C(3)-H(3B)	0.9900	C(10)-H(10)	0.9500
C(4)-C(19)	1.532(2)	C(11)-C(12)	1.397(3)
C(4)-C(18)	1.539(2)	C(11)-H(11)	0.9500
C(4)-C(5)	1.555(3)	C(12)-C(13)	1.533(2)
C(5)-N(3)	1.484(2)	C(13)-C(19)	1.524(2)
C(5)-C(6)	1.533(2)	C(13)-C(14)	1.561(2)
C(5)-H(5)	1.0000	C(14)-C(15)	1.539(3)
C(6)-N(1)	1.484(3)	C(14)-H(14A)	0.9900
C(6)-H(6A)	0.9900	C(14)-H(14B)	0.9900
C(6)-H(6B)	0.9900	C(15)-N(4)	1.472(2)
N(1)-N(2)	1.245(2)	C(15)-H(15A)	0.9900
N(2)-N(3)	1.392(2)	C(15)-H(15B)	0.9900

Table A4.5.3. cont'd.

Bond	**Length (Å)**	**Atoms**	**Angle (°)**
N(4)-C(16)	1.459(2)	N(3)-C(5)-C(6)	100.51(14)
N(4)-C(19)	1.461(2)	N(3)-C(5)-C(4)	113.67(15)
C(16)-C(17)	1.525(3)	C(6)-C(5)-C(4)	117.59(15)
C(16)-H(16A)	0.9900	N(3)-C(5)-H(5)	108.2
C(16)-H(16B)	0.9900	C(6)-C(5)-H(5)	108.2
C(17)-C(18)	1.536(3)	C(4)-C(5)-H(5)	108.2
C(17)-H(17A)	0.9900	N(1)-C(6)-C(5)	105.14(15)
C(17)-H(17B)	0.9900	N(1)-C(6)-H(6A)	110.7
C(18)-H(18A)	0.9900	C(5)-C(6)-H(6A)	110.7
C(18)-H(18B)	0.9900	N(1)-C(6)-H(6B)	110.7
C(19)-H(19)	1.0000	C(5)-C(6)-H(6B)	110.7
		H(6A)-C(6)-H(6B)	108.8
Atoms	**Angle (°)**	N(2)-N(1)-C(6)	111.01(16)
O(1)-C(1)-C(2)	119.99(17)	N(1)-N(2)-N(3)	112.82(17)
O(1)-C(1)-C(13)	120.84(17)	N(2)-N(3)-C(7)	115.92(15)
C(2)-C(1)-C(13)	119.02(15)	N(2)-N(3)-C(5)	109.81(14)
C(1)-C(2)-C(3)	116.74(16)	C(7)-N(3)-C(5)	119.98(14)
C(1)-C(2)-H(2A)	108.1	C(8)-C(7)-C(12)	119.82(16)
C(3)-C(2)-H(2A)	108.1	C(8)-C(7)-N(3)	119.41(16)
C(1)-C(2)-H(2B)	108.1	C(12)-C(7)-N(3)	120.75(16)
C(3)-C(2)-H(2B)	108.1	C(9)-C(8)-C(7)	120.40(17)
H(2A)-C(2)-H(2B)	107.3	C(9)-C(8)-H(8)	119.8
C(4)-C(3)-C(2)	112.74(15)	C(7)-C(8)-H(8)	119.8
C(4)-C(3)-H(3A)	109.0	C(10)-C(9)-C(8)	120.29(18)
C(2)-C(3)-H(3A)	109.0	C(10)-C(9)-H(9)	119.9
C(4)-C(3)-H(3B)	109.0	C(8)-C(9)-H(9)	119.9
C(2)-C(3)-H(3B)	109.0	C(11)-C(10)-C(9)	119.06(17)
H(3A)-C(3)-H(3B)	107.8	C(11)-C(10)-H(10)	120.5
C(19)-C(4)-C(3)	109.74(14)	C(9)-C(10)-H(10)	120.5
C(19)-C(4)-C(18)	105.64(14)	C(10)-C(11)-C(12)	122.41(17)
C(3)-C(4)-C(18)	111.44(15)	C(10)-C(11)-H(11)	118.8
C(19)-C(4)-C(5)	108.52(14)	C(12)-C(11)-H(11)	118.8
C(3)-C(4)-C(5)	107.63(15)	C(11)-C(12)-C(7)	117.79(17)
C(18)-C(4)-C(5)	113.80(14)	C(11)-C(12)-C(13)	116.67(16)

Table A4.5.3. cont'd.

Atoms	Angle (°)	Atoms	Angle (°)
C(7)-C(12)-C(13)	125.41(16)	N(4)-C(16)-H(16A)	109.5
C(19)-C(13)-C(12)	115.04(15)	C(17)-C(16)-H(16A)	109.5
C(19)-C(13)-C(1)	110.69(15)	N(4)-C(16)-H(16B)	109.5
C(12)-C(13)-C(1)	109.71(15)	C(17)-C(16)-H(16B)	109.5
C(19)-C(13)-C(14)	101.29(14)	H(16A)-C(16)-H(16B)	108.0
C(12)-C(13)-C(14)	110.56(15)	C(16)-C(17)-C(18)	111.92(15)
C(1)-C(13)-C(14)	109.19(15)	C(16)-C(17)-H(17A)	109.2
C(15)-C(14)-C(13)	104.80(14)	C(18)-C(17)-H(17A)	109.2
C(15)-C(14)-H(14A)	110.8	C(16)-C(17)-H(17B)	109.2
C(13)-C(14)-H(14A)	110.8	C(18)-C(17)-H(17B)	109.2
C(15)-C(14)-H(14B)	110.8	H(17A)-C(17)-H(17B)	107.9
C(13)-C(14)-H(14B)	110.8	C(17)-C(18)-C(4)	112.30(15)
H(14A)-C(14)-H(14B)	108.9	C(17)-C(18)-H(18A)	109.1
N(4)-C(15)-C(14)	104.91(14)	C(4)-C(18)-H(18A)	109.1
N(4)-C(15)-H(15A)	110.8	C(17)-C(18)-H(18B)	109.1
C(14)-C(15)-H(15A)	110.8	C(4)-C(18)-H(18B)	109.1
N(4)-C(15)-H(15B)	110.8	H(18A)-C(18)-H(18B)	107.9
C(14)-C(15)-H(15B)	110.8	N(4)-C(19)-C(13)	102.06(14)
H(15A)-C(15)-H(15B)	108.8	N(4)-C(19)-C(4)	110.98(15)
C(16)-N(4)-C(19)	111.39(14)	C(13)-C(19)-C(4)	116.41(15)
C(16)-N(4)-C(15)	112.99(15)	N(4)-C(19)-H(19)	109.0
C(19)-N(4)-C(15)	105.02(14)	C(13)-C(19)-H(19)	109.0
N(4)-C(16)-C(17)	110.90(15)	C(4)-C(19)-H(19)	109.0

Symmetry transformations used to generate equivalent atoms:

Table A4.5.4. *Anisotropic displacement parameters ($Å^2 x\ 10^3$) for* ***116*** *V23324. The anisotropic displacement factor exponent takes the form: $-2p^2[\ h^2\ a^{*2}U^{11} + \ldots + 2\ h\ k\ a^*\ b^*\ U^{12}\ ]$*

Atom	U^{11}	U^{22}	U^{33}	U^{23}	U^{13}	U^{12}
O(1)	15(1)	24(1)	28(1)	3(1)	8(1)	6(1)
C(1)	14(1)	13(1)	18(1)	-2(1)	4(1)	-1(1)
C(2)	18(1)	23(1)	16(1)	4(1)	4(1)	5(1)
C(3)	19(1)	16(1)	14(1)	3(1)	8(1)	2(1)
C(4)	13(1)	12(1)	13(1)	1(1)	6(1)	1(1)
C(5)	16(1)	16(1)	13(1)	-1(1)	6(1)	-1(1)
C(6)	25(1)	17(1)	23(1)	-4(1)	15(1)	-1(1)
N(1)	23(1)	16(1)	33(1)	-4(1)	16(1)	0(1)
N(2)	20(1)	15(1)	30(1)	-1(1)	11(1)	3(1)
N(3)	16(1)	11(1)	17(1)	0(1)	8(1)	2(1)
C(7)	14(1)	15(1)	11(1)	0(1)	3(1)	-1(1)
C(8)	22(1)	13(1)	17(1)	0(1)	7(1)	-1(1)
C(9)	24(1)	17(1)	19(1)	3(1)	8(1)	-6(1)
C(10)	18(1)	26(1)	21(1)	2(1)	9(1)	-4(1)
C(11)	16(1)	19(1)	19(1)	2(1)	7(1)	2(1)
C(12)	14(1)	15(1)	11(1)	1(1)	3(1)	-1(1)
C(13)	13(1)	14(1)	12(1)	-1(1)	5(1)	1(1)
C(14)	18(1)	20(1)	16(1)	-2(1)	9(1)	1(1)
C(15)	21(1)	17(1)	16(1)	-4(1)	8(1)	0(1)
N(4)	16(1)	16(1)	14(1)	-3(1)	6(1)	-1(1)
C(16)	18(1)	18(1)	20(1)	-4(1)	6(1)	-3(1)
C(17)	16(1)	19(1)	23(1)	-3(1)	8(1)	-5(1)
C(18)	15(1)	15(1)	17(1)	1(1)	7(1)	-1(1)
C(19)	13(1)	12(1)	12(1)	1(1)	4(1)	1(1)

Table A4.5.5. *Hydrogen coordinates (x 10^4) and isotropic displacement parameters (Å^{2}x 10^3) for* ***116*** *(V23324).*

Atom	x	y	z	U(eq)
H(2A)	9468	3374	10020	23
H(2B)	9508	1487	9872	23
H(3A)	6771	1317	8867	19
H(3B)	6983	2604	9960	19
H(5)	7820	5242	9379	18
H(6A)	4559	5559	9111	24
H(6B)	6141	6203	10249	24
H(8)	8073	9161	7450	21
H(9)	10515	9547	7126	24
H(10)	12085	7354	6990	25
H(11)	11110	4794	7041	21
H(14A)	8371	3747	5258	21
H(14B)	9487	2315	6066	21
H(15A)	6179	2155	4624	21
H(15B)	7328	689	5332	21
H(16A)	4381	371	5668	23
H(16B)	3978	2200	5275	23
H(17A)	4297	813	7670	23
H(17B)	2680	1595	6676	23
H(18A)	4019	3316	8464	18
H(18B)	3761	4154	7133	18
H(19)	5959	4223	6310	15

Table A4.5.6. *Torsion angles [°] for* ***116*** *(V23324).*

Atoms (A-B-C-D)	Angle (°)	Atoms (A-B-C-D)	Angle (°)
O(1)-C(1)-C(2)-C(3)	-151.58(18)	N(3)-C(7)-C(12)-C(11)	-173.10(17)
C(13)-C(1)-C(2)-C(3)	32.8(3)	C(8)-C(7)-C(12)-C(13)	-170.36(17)
C(1)-C(2)-C(3)-C(4)	-41.4(2)	N(3)-C(7)-C(12)-C(13)	11.2(3)
C(2)-C(3)-C(4)-C(19)	52.1(2)	C(11)-C(12)-C(13)-C(19)	-164.20(17)
C(2)-C(3)-C(4)-C(18)	168.75(16)	C(7)-C(12)-C(13)-C(19)	11.6(3)
C(2)-C(3)-C(4)-C(5)	-65.82(19)	C(11)-C(12)-C(13)-C(1)	70.2(2)
C(19)-C(4)-C(5)-N(3)	26.6(2)	C(7)-C(12)-C(13)-C(1)	-113.97(19)
C(3)-C(4)-C(5)-N(3)	145.34(15)	C(11)-C(12)-C(13)-C(14)	-50.2(2)
C(18)-C(4)-C(5)-N(3)	-90.66(18)	C(7)-C(12)-C(13)-C(14)	125.54(19)
C(19)-C(4)-C(5)-C(6)	143.62(16)	O(1)-C(1)-C(13)-C(19)	150.33(18)
C(3)-C(4)-C(5)-C(6)	-97.68(19)	C(2)-C(1)-C(13)-C(19)	-34.1(2)
C(18)-C(4)-C(5)-C(6)	26.3(2)	O(1)-C(1)-C(13)-C(12)	-81.7(2)
N(3)-C(5)-C(6)-N(1)	-6.91(19)	C(2)-C(1)-C(13)-C(12)	93.9(2)
C(4)-C(5)-C(6)-N(1)	-130.80(17)	O(1)-C(1)-C(13)-C(14)	39.7(2)
C(5)-C(6)-N(1)-N(2)	3.5(2)	C(2)-C(1)-C(13)-C(14)	-144.76(17)
C(6)-N(1)-N(2)-N(3)	2.0(2)	C(19)-C(13)-C(14)-C(15)	-22.66(18)
N(1)-N(2)-N(3)-C(7)	-147.00(17)	C(12)-C(13)-C(14)-C(15)	-145.07(15)
N(1)-N(2)-N(3)-C(5)	-7.0(2)	C(1)-C(13)-C(14)-C(15)	94.13(17)
C(6)-C(5)-N(3)-N(2)	8.33(19)	C(13)-C(14)-C(15)-N(4)	-4.62(19)
C(4)-C(5)-N(3)-N(2)	134.88(16)	C(14)-C(15)-N(4)-C(16)	153.57(15)
C(6)-C(5)-N(3)-C(7)	146.43(16)	C(14)-C(15)-N(4)-C(19)	31.97(18)
C(4)-C(5)-N(3)-C(7)	-87.02(19)	C(19)-N(4)-C(16)-C(17)	-57.5(2)
N(2)-N(3)-C(7)-C(8)	0.9(2)	C(15)-N(4)-C(16)-C(17)	-175.40(16)
C(5)-N(3)-C(7)-C(8)	-134.77(18)	N(4)-C(16)-C(17)-C(18)	50.3(2)
N(2)-N(3)-C(7)-C(12)	179.40(17)	C(16)-C(17)-C(18)-C(4)	-51.2(2)
C(5)-N(3)-C(7)-C(12)	43.7(2)	C(19)-C(4)-C(18)-C(17)	55.13(19)
C(12)-C(7)-C(8)-C(9)	-3.8(3)	C(3)-C(4)-C(18)-C(17)	-64.0(2)
N(3)-C(7)-C(8)-C(9)	174.68(17)	C(5)-C(4)-C(18)-C(17)	174.08(15)
C(7)-C(8)-C(9)-C(10)	-0.3(3)	C(16)-N(4)-C(19)-C(13)	-169.83(14)
C(8)-C(9)-C(10)-C(11)	2.6(3)	C(15)-N(4)-C(19)-C(13)	-47.19(17)
C(9)-C(10)-C(11)-C(12)	-0.9(3)	C(16)-N(4)-C(19)-C(4)	65.48(18)
C(10)-C(11)-C(12)-C(7)	-3.1(3)	C(15)-N(4)-C(19)-C(4)	-171.87(14)
C(10)-C(11)-C(12)-C(13)	173.04(18)	C(12)-C(13)-C(19)-N(4)	161.45(14)
C(8)-C(7)-C(12)-C(11)	5.4(3)	C(1)-C(13)-C(19)-N(4)	-73.49(17)

Table A4.5.6. cont'd.

Atoms (A-B-C-D)	Angle (°)	Atoms (A-B-C-D)	Angle (°)
C(14)-C(13)-C(19)-N(4)	42.20(16)	C(18)-C(4)-C(19)-N(4)	-62.06(18)
C(12)-C(13)-C(19)-C(4)	-77.6(2)	C(5)-C(4)-C(19)-N(4)	175.54(14)
C(1)-C(13)-C(19)-C(4)	47.5(2)	C(3)-C(4)-C(19)-C(13)	-57.9(2)
C(14)-C(13)-C(19)-C(4)	163.20(16)	C(18)-C(4)-C(19)-C(13)	-178.19(15)
C(3)-C(4)-C(19)-N(4)	58.18(19)	C(5)-C(4)-C(19)-C(13)	59.4(2)

Symmetry transformations used to generate equivalent atoms:

A4.6 X-RAY CRYSTAL STRUCTURE ANALYSIS OF TRIAZOLINE 117 (V23195)

An X-ray quality crystal of **117** was grown by dissolving **117** in minimal EtOAc (approx. 5 mg/300μL), layering with hexanes, and allowing the solution to slowly evaporate. *(Note: the crystal of **117** was grown using a racemic sample).* Low-temperature diffraction data (ϕ-and ω-scans) were collected on a Bruker AXS D8 VENTURE KAPPA diffractometer coupled to a PHOTON II CPAD detector with Cu K_α radiation (λ = 1.54178 Å) from an IμS micro-source for the structure of compound V23195. The structure was solved by direct methods using SHELXS[1] and refined against F^2 on all data by full-matrix least squares with SHELXL-2019[2] using established refinement techniques.[3] All non-hydrogen atoms were refined anisotropically. All hydrogen atoms were included into the model at geometrically calculated positions and refined using a riding model. The isotropic displacement parameters of all hydrogen atoms were fixed to 1.2 times the U value of the atoms they are linked to (1.5 times for methyl groups). Compound V23195 crystallizes in the monoclinic space group $P2_1/c$ with one molecule in the asymmetric unit.

Figure A4.6.1. *X-Ray Coordinate of* ***117*** *(V23195)*

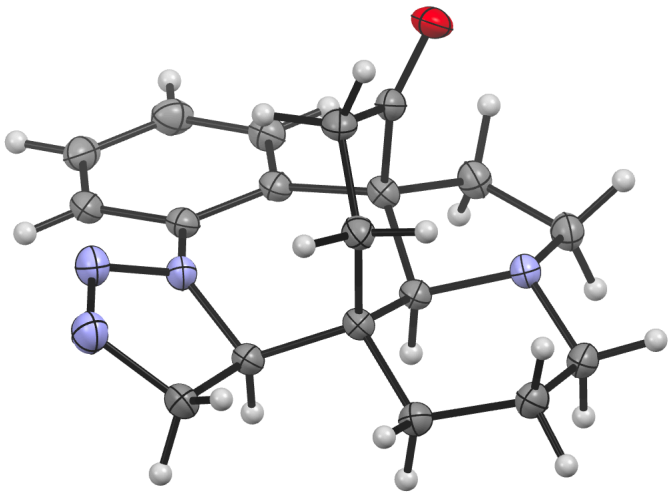


Table A4.6.1. *Crystal data and structure refinement for* ***117*** *(V23195).*

Identification code	V23195	
Empirical formula	C19 H22 N4 O	
Formula weight	322.40	
Temperature	100(2) K	
Wavelength	1.54178 Å	
Crystal system	Monoclinic	
Space group	$P2_1/c$	
Unit cell dimensions	a = 14.4626(13) Å	a= 90°.
	b = 7.9984(10) Å	b= 103.749(12)°.
	c = 13.6506(15) Å	g = 90°.
Volume	1533.8(3) $Å^3$	
Z	4	
Density (calculated)	1.396 Mg/m^3	
Absorption coefficient	0.709 mm^{-1}	
F(000)	688	
Crystal size	0.300 x 0.200 x 0.050 mm^3	
Theta range for data collection	3.146 to 74.492°.	
Index ranges	-18<=h<=18, -9<=k<=9, -17<=l<=15	
Reflections collected	23274	

Independent reflections	3123 [R(int) = 0.0603]
Completeness to theta = 67.679°	100.0 %
Absorption correction	Semi-empirical from equivalents
Max. and min. transmission	0.7538 and 0.6193
Refinement method	Full-matrix least-squares on F^2
Data / restraints / parameters	3123 / 0 / 217
Goodness-of-fit on F^2	1.060
Final R indices [I>2sigma(I)]	R1 = 0.0397, wR2 = 0.0955
R indices (all data)	R1 = 0.0476, wR2 = 0.1019
Extinction coefficient	n/a
Largest diff. peak and hole	0.290 and -0.204 e.$Å^{-3}$

Table A4.6.2. *Atomic coordinates (x 10^4) and equivalent isotropic displacement parameters ($Å^2$x 10^3) for* ***117*** *(V23195). U(eq) is defined as one third of the trace of the orthogonalized U^{ij} tensor.*

Atom	x	y	z	U(eq)
O(1)	2671(1)	4860(1)	7478(1)	28(1)
C(1)	2426(1)	4435(2)	6601(1)	21(1)
C(2)	1424(1)	4688(2)	5988(1)	23(1)
C(3)	1002(1)	3230(2)	5288(1)	22(1)
C(4)	1695(1)	2353(2)	4752(1)	19(1)
C(5)	1820(1)	3326(2)	3821(1)	21(1)
C(6)	917(1)	3535(2)	2971(1)	26(1)
N(1)	761(1)	5355(2)	2843(1)	30(1)
N(2)	1417(1)	6142(2)	3425(1)	27(1)
N(3)	2063(1)	5094(2)	4035(1)	22(1)
C(7)	2959(1)	5757(2)	4530(1)	21(1)
C(8)	3295(1)	7134(2)	4078(1)	24(1)
C(9)	4142(1)	7901(2)	4545(1)	27(1)
C(10)	4672(1)	7286(2)	5455(1)	27(1)
C(11)	4343(1)	5917(2)	5894(1)	25(1)
C(12)	3485(1)	5112(2)	5454(1)	21(1)

Table A4.6.2. cont'd.

Atom	x	y	z	U(eq)
C(13)	3151(1)	3697(2)	6047(1)	20(1)
C(14)	3965(1)	2862(2)	6835(1)	24(1)
C(15)	3571(1)	1125(2)	7002(1)	24(1)
N(4)	2621(1)	1059(1)	6319(1)	21(1)
C(16)	2311(1)	-643(2)	6012(1)	24(1)
C(17)	1339(1)	-609(2)	5270(1)	25(1)
C(18)	1332(1)	588(2)	4394(1)	23(1)
C(19)	2674(1)	2141(2)	5466(1)	19(1)

Table A4.6.3. *Bond lengths [Å] and angles [°] for* ***117*** *(V23195).*

Bond	Length (Å)	Bond	Length (Å)
O(1)-C(1)	1.2132(17)	N(2)-N(3)	1.3777(17)
C(1)-C(2)	1.505(2)	N(3)-C(7)	1.4150(18)
C(1)-C(13)	1.5478(19)	C(7)-C(8)	1.403(2)
C(2)-C(3)	1.539(2)	C(7)-C(12)	1.4077(19)
C(2)-H(2A)	0.9900	C(8)-C(9)	1.383(2)
C(2)-H(2B)	0.9900	C(8)-H(8)	0.9500
C(3)-C(4)	1.5434(18)	C(9)-C(10)	1.386(2)
C(3)-H(3A)	0.9900	C(9)-H(9)	0.9500
C(3)-H(3B)	0.9900	C(10)-C(11)	1.386(2)
C(4)-C(19)	1.5260(19)	C(10)-H(10)	0.9500
C(4)-C(5)	1.5369(18)	C(11)-C(12)	1.400(2)
C(4)-C(18)	1.5443(19)	C(11)-H(11)	0.9500
C(5)-N(3)	1.4689(18)	C(12)-C(13)	1.5342(19)
C(5)-C(6)	1.5365(19)	C(13)-C(14)	1.5448(19)
C(5)-H(5)	1.0000	C(13)-C(19)	1.5475(19)
C(6)-N(1)	1.477(2)	C(14)-C(15)	1.539(2)
C(6)-H(6A)	0.9900	C(14)-H(14A)	0.9900
C(6)-H(6B)	0.9900	C(14)-H(14B)	0.9900
N(1)-N(2)	1.2525(19)	C(15)-N(4)	1.4671(18)

Table A4.6.3. cont'd.

Bond	Length (Å)	Atoms	Angle (°)
C(15)-H(15A)	0.9900	C(5)-C(4)-C(18)	107.44(11)
C(15)-H(15B)	0.9900	C(3)-C(4)-C(18)	110.82(11)
N(4)-C(16)	1.4627(18)	N(3)-C(5)-C(6)	99.55(11)
N(4)-C(19)	1.4683(17)	N(3)-C(5)-C(4)	113.13(11)
C(16)-C(17)	1.525(2)	C(6)-C(5)-C(4)	115.67(12)
C(16)-H(16A)	0.9900	N(3)-C(5)-H(5)	109.4
C(16)-H(16B)	0.9900	C(6)-C(5)-H(5)	109.4
C(17)-C(18)	1.5295(19)	C(4)-C(5)-H(5)	109.4
C(17)-H(17A)	0.9900	N(1)-C(6)-C(5)	105.92(12)
C(17)-H(17B)	0.9900	N(1)-C(6)-H(6A)	110.6
C(18)-H(18A)	0.9900	C(5)-C(6)-H(6A)	110.6
C(18)-H(18B)	0.9900	N(1)-C(6)-H(6B)	110.6
C(19)-H(19)	1.0000	C(5)-C(6)-H(6B)	110.6
		H(6A)-C(6)-H(6B)	108.7
Atoms	**Angle (°)**	N(2)-N(1)-C(6)	110.43(12)
O(1)-C(1)-C(2)	121.81(13)	N(1)-N(2)-N(3)	112.34(12)
O(1)-C(1)-C(13)	121.07(13)	N(2)-N(3)-C(7)	118.21(12)
C(2)-C(1)-C(13)	117.03(11)	N(2)-N(3)-C(5)	111.70(11)
C(1)-C(2)-C(3)	115.52(12)	C(7)-N(3)-C(5)	127.18(12)
C(1)-C(2)-H(2A)	108.4	C(8)-C(7)-C(12)	120.79(13)
C(3)-C(2)-H(2A)	108.4	C(8)-C(7)-N(3)	117.25(12)
C(1)-C(2)-H(2B)	108.4	C(12)-C(7)-N(3)	121.93(12)
C(3)-C(2)-H(2B)	108.4	C(9)-C(8)-C(7)	120.46(13)
H(2A)-C(2)-H(2B)	107.5	C(9)-C(8)-H(8)	119.8
C(2)-C(3)-C(4)	115.60(12)	C(7)-C(8)-H(8)	119.8
C(2)-C(3)-H(3A)	108.4	C(8)-C(9)-C(10)	119.74(14)
C(4)-C(3)-H(3A)	108.4	C(8)-C(9)-H(9)	120.1
C(2)-C(3)-H(3B)	108.4	C(10)-C(9)-H(9)	120.1
C(4)-C(3)-H(3B)	108.4	C(11)-C(10)-C(9)	119.63(14)
H(3A)-C(3)-H(3B)	107.4	C(11)-C(10)-H(10)	120.2
C(19)-C(4)-C(5)	108.08(11)	C(9)-C(10)-H(10)	120.2
C(19)-C(4)-C(3)	110.89(11)	C(10)-C(11)-C(12)	122.57(14)
C(5)-C(4)-C(3)	112.32(11)	C(10)-C(11)-H(11)	118.7
C(19)-C(4)-C(18)	107.07(11)	C(12)-C(11)-H(11)	118.7

Table A4.6.3. cont'd.

Atoms	Angle (°)	Atoms	Angle (°)
C(11)-C(12)-C(7)	116.79(13)	N(4)-C(16)-C(17)	110.18(11)
C(11)-C(12)-C(13)	118.09(12)	N(4)-C(16)-H(16A)	109.6
C(7)-C(12)-C(13)	124.93(13)	C(17)-C(16)-H(16A)	109.6
C(12)-C(13)-C(14)	113.76(12)	N(4)-C(16)-H(16B)	109.6
C(12)-C(13)-C(19)	118.75(11)	C(17)-C(16)-H(16B)	109.6
C(14)-C(13)-C(19)	100.48(11)	H(16A)-C(16)-H(16B)	108.1
C(12)-C(13)-C(1)	108.11(11)	C(16)-C(17)-C(18)	111.33(12)
C(14)-C(13)-C(1)	108.49(11)	C(16)-C(17)-H(17A)	109.4
C(19)-C(13)-C(1)	106.63(11)	C(18)-C(17)-H(17A)	109.4
C(15)-C(14)-C(13)	104.26(11)	C(16)-C(17)-H(17B)	109.4
C(15)-C(14)-H(14A)	110.9	C(18)-C(17)-H(17B)	109.4
C(13)-C(14)-H(14A)	110.9	H(17A)-C(17)-H(17B)	108.0
C(15)-C(14)-H(14B)	110.9	C(17)-C(18)-C(4)	112.76(11)
C(13)-C(14)-H(14B)	110.9	C(17)-C(18)-H(18A)	109.0
H(14A)-C(14)-H(14B)	108.9	C(4)-C(18)-H(18A)	109.0
N(4)-C(15)-C(14)	105.19(11)	C(17)-C(18)-H(18B)	109.0
N(4)-C(15)-H(15A)	110.7	C(4)-C(18)-H(18B)	109.0
C(14)-C(15)-H(15A)	110.7	H(18A)-C(18)-H(18B)	107.8
N(4)-C(15)-H(15B)	110.7	N(4)-C(19)-C(4)	110.89(11)
C(14)-C(15)-H(15B)	110.7	N(4)-C(19)-C(13)	99.70(10)
H(15A)-C(15)-H(15B)	108.8	C(4)-C(19)-C(13)	118.08(11)
C(16)-N(4)-C(15)	113.13(11)	N(4)-C(19)-H(19)	109.2
C(16)-N(4)-C(19)	113.03(11)	C(4)-C(19)-H(19)	109.2
C(15)-N(4)-C(19)	105.37(11)	C(13)-C(19)-H(19)	109.2

Symmetry transformations used to generate equivalent atoms:

Table A4.6.4. *Anisotropic displacement parameters ($Å^2 x\ 10^3$) for* ***117*** *(V23195). The anisotropic displacement factor exponent takes the form: $-2p^2[h^2\ a^{*2}U^{11} + ... + 2\ h\ k\ a^*\ b^*\ U^{12}]$*

Atom	U^{11}	U^{22}	U^{33}	U^{23}	U^{13}	U^{12}
O(1)	38(1)	30(1)	19(1)	-6(1)	10(1)	-3(1)
C(1)	30(1)	16(1)	18(1)	0(1)	9(1)	-2(1)
C(2)	29(1)	21(1)	21(1)	-1(1)	10(1)	4(1)
C(3)	25(1)	22(1)	19(1)	2(1)	7(1)	3(1)
C(4)	24(1)	19(1)	16(1)	0(1)	6(1)	1(1)
C(5)	28(1)	19(1)	16(1)	-1(1)	7(1)	-1(1)
C(6)	35(1)	24(1)	17(1)	1(1)	4(1)	0(1)
N(1)	34(1)	27(1)	26(1)	4(1)	2(1)	1(1)
N(2)	32(1)	25(1)	23(1)	4(1)	5(1)	3(1)
N(3)	30(1)	18(1)	18(1)	2(1)	3(1)	0(1)
C(7)	27(1)	19(1)	18(1)	-2(1)	8(1)	-1(1)
C(8)	36(1)	21(1)	18(1)	0(1)	11(1)	1(1)
C(9)	37(1)	20(1)	28(1)	-2(1)	18(1)	-4(1)
C(10)	29(1)	27(1)	28(1)	-5(1)	10(1)	-7(1)
C(11)	28(1)	25(1)	21(1)	-2(1)	7(1)	-1(1)
C(12)	27(1)	19(1)	18(1)	-1(1)	9(1)	0(1)
C(13)	24(1)	21(1)	16(1)	0(1)	6(1)	0(1)
C(14)	26(1)	27(1)	20(1)	3(1)	4(1)	0(1)
C(15)	27(1)	24(1)	21(1)	4(1)	6(1)	4(1)
N(4)	26(1)	19(1)	17(1)	2(1)	6(1)	1(1)
C(16)	34(1)	17(1)	23(1)	2(1)	9(1)	1(1)
C(17)	32(1)	19(1)	24(1)	0(1)	9(1)	-3(1)
C(18)	29(1)	20(1)	20(1)	-1(1)	6(1)	-2(1)
C(19)	24(1)	18(1)	17(1)	0(1)	7(1)	1(1)

Table A4.6.5. *Hydrogen coordinates (x 10^4) and isotropic displacement parameters (Å^{2}x 10^3) for* ***117*** *(V23195).*

Atom	x	y	z	U(eq)
H(2A)	1410	5706	5572	28
H(2B)	1009	4896	6457	28
H(3A)	454	3658	4768	26
H(3B)	753	2386	5691	26
H(5)	2327	2782	3546	25
H(6A)	1005	3025	2339	31
H(6B)	366	2994	3156	31
H(8)	2937	7541	3448	29
H(9)	4360	8846	4243	32
H(10)	5258	7800	5776	33
H(11)	4713	5510	6519	30
H(14A)	4546	2763	6575	29
H(14B)	4117	3512	7470	29
H(15A)	3983	232	6838	29
H(15B)	3530	991	7712	29
H(16A)	2273	-1308	6613	29
H(16B)	2781	-1181	5692	29
H(17A)	850	-253	5626	30
H(17B)	1174	-1749	5002	30
H(18A)	675	675	3972	27
H(18B)	1738	121	3970	27
H(19)	3118	1631	5089	23

Table A4.6.6. *Torsion angles [°] for* ***177*** *(V23195).*

Atoms (A-B-C-D)	Angle (°)	Atoms (A-B-C-D)	Angle (°)
O(1)-C(1)-C(2)-C(3)	-138.86(14)	N(3)-C(7)-C(12)-C(11)	-177.26(12)
C(13)-C(1)-C(2)-C(3)	44.55(17)	C(8)-C(7)-C(12)-C(13)	175.46(13)
C(1)-C(2)-C(3)-C(4)	-39.06(16)	N(3)-C(7)-C(12)-C(13)	-2.3(2)
C(2)-C(3)-C(4)-C(19)	40.85(16)	C(11)-C(12)-C(13)-C(14)	-23.55(17)
C(2)-C(3)-C(4)-C(5)	-80.20(15)	C(7)-C(12)-C(13)-C(14)	161.56(13)
C(2)-C(3)-C(4)-C(18)	159.62(11)	C(11)-C(12)-C(13)-C(19)	-141.47(13)
C(19)-C(4)-C(5)-N(3)	-71.09(14)	C(7)-C(12)-C(13)-C(19)	43.64(19)
C(3)-C(4)-C(5)-N(3)	51.56(16)	C(11)-C(12)-C(13)-C(1)	97.01(14)
C(18)-C(4)-C(5)-N(3)	173.68(11)	C(7)-C(12)-C(13)-C(1)	-77.88(16)
C(19)-C(4)-C(5)-C(6)	175.00(11)	O(1)-C(1)-C(13)-C(12)	-96.91(15)
C(3)-C(4)-C(5)-C(6)	-62.36(15)	C(2)-C(1)-C(13)-C(12)	79.70(14)
C(18)-C(4)-C(5)-C(6)	59.77(15)	O(1)-C(1)-C(13)-C(14)	26.89(18)
N(3)-C(5)-C(6)-N(1)	-1.54(14)	C(2)-C(1)-C(13)-C(14)	-156.50(12)
C(4)-C(5)-C(6)-N(1)	119.97(13)	O(1)-C(1)-C(13)-C(19)	134.35(13)
C(5)-C(6)-N(1)-N(2)	2.56(16)	C(2)-C(1)-C(13)-C(19)	-49.03(15)
C(6)-N(1)-N(2)-N(3)	-2.48(17)	C(12)-C(13)-C(14)-C(15)	-157.41(11)
N(1)-N(2)-N(3)-C(7)	163.52(13)	C(19)-C(13)-C(14)-C(15)	-29.40(13)
N(1)-N(2)-N(3)-C(5)	1.40(17)	C(1)-C(13)-C(14)-C(15)	82.23(13)
C(6)-C(5)-N(3)-N(2)	0.26(14)	C(13)-C(14)-C(15)-N(4)	1.42(14)
C(4)-C(5)-N(3)-N(2)	-123.07(12)	C(14)-C(15)-N(4)-C(16)	153.34(11)
C(6)-C(5)-N(3)-C(7)	-159.88(13)	C(14)-C(15)-N(4)-C(19)	29.39(14)
C(4)-C(5)-N(3)-C(7)	76.79(17)	C(15)-N(4)-C(16)-C(17)	-177.59(11)
N(2)-N(3)-C(7)-C(8)	-26.08(18)	C(19)-N(4)-C(16)-C(17)	-57.94(15)
C(5)-N(3)-C(7)-C(8)	132.93(14)	N(4)-C(16)-C(17)-C(18)	51.93(15)
N(2)-N(3)-C(7)-C(12)	151.76(13)	C(16)-C(17)-C(18)-C(4)	-52.40(16)
C(5)-N(3)-C(7)-C(12)	-49.2(2)	C(19)-C(4)-C(18)-C(17)	54.27(15)
C(12)-C(7)-C(8)-C(9)	-1.2(2)	C(5)-C(4)-C(18)-C(17)	170.17(12)
N(3)-C(7)-C(8)-C(9)	176.71(13)	C(3)-C(4)-C(18)-C(17)	-66.78(15)
C(7)-C(8)-C(9)-C(10)	1.2(2)	C(16)-N(4)-C(19)-C(4)	62.76(14)
C(8)-C(9)-C(10)-C(11)	-0.7(2)	C(15)-N(4)-C(19)-C(4)	-173.21(11)
C(9)-C(10)-C(11)-C(12)	0.0(2)	C(16)-N(4)-C(19)-C(13)	-172.04(11)
C(10)-C(11)-C(12)-C(7)	0.1(2)	C(15)-N(4)-C(19)-C(13)	-48.02(12)
C(10)-C(11)-C(12)-C(13)	-175.25(13)	C(5)-C(4)-C(19)-N(4)	-173.65(10)
C(8)-C(7)-C(12)-C(11)	0.5(2)	C(3)-C(4)-C(19)-N(4)	62.83(14)

Table A4.6.6. cont'd.

Atoms (A-B-C-D)	**Angle (°)**	**Atoms (A-B-C-D)**	**Angle (°)**
C(18)-C(4)-C(19)-N(4)	-58.18(13)	C(14)-C(13)-C(19)-N(4)	46.84(12)
C(5)-C(4)-C(19)-C(13)	72.27(14)	C(1)-C(13)-C(19)-N(4)	-66.23(12)
C(3)-C(4)-C(19)-C(13)	-51.24(15)	C(12)-C(13)-C(19)-C(4)	-68.42(16)
C(18)-C(4)-C(19)-C(13)	-172.26(11)	C(14)-C(13)-C(19)-C(4)	166.92(11)
C(12)-C(13)-C(19)-N(4)	171.50(11)	C(1)-C(13)-C(19)-C(4)	53.85(14)

Symmetry transformations used to generate equivalent atoms:

A4.7 X-RAY CRYSTAL STRUCTURE ANALYSIS OF HUNTERINE A (53) (V23353)

An X-ray quality crystal of **53** was grown by dissolving in minimal CH_2Cl_2 with 1% added MeOH (approx. 4 mg/0.1 mL) and layering with pentane. Low-temperature diffraction data (ϕ-and ω-scans) were collected on a Bruker AXS D8 VENTURE KAPPA diffractometer coupled to a PHOTON II CPAD detector with Cu K_α radiation (λ = 1.54178 Å) from an IμS micro-source for the structure of compound V23353. The structure was solved by direct methods using SHELXS[1] and refined against F^2 on all data by full-matrix least squares with SHELXL-2019[2] using established refinement techniques.[3] All non-hydrogen atoms were refined anisotropically. Unless otherwise noted, all hydrogen atoms were included into the model at geometrically calculated positions and refined using a riding model. The isotropic displacement parameters of all hydrogen atoms were fixed to 1.2 times the U value of the atoms they are linked to (1.5 times for methyl groups). Compound V23353 crystallizes in the orthorhombic space group $P2_12_12_1$ with one molecule in the asymmetric unit. The coordinates for the hydrogen atoms bound to N1 and O2 were located in the difference Fourier synthesis and refined semi-freely with the help of a restraint on the O-H or N-H distance (0.84(4) Å or 0.91(4) Å, respectively).

Figure A4.7.1. *X-Ray Coordinate of* ***53***

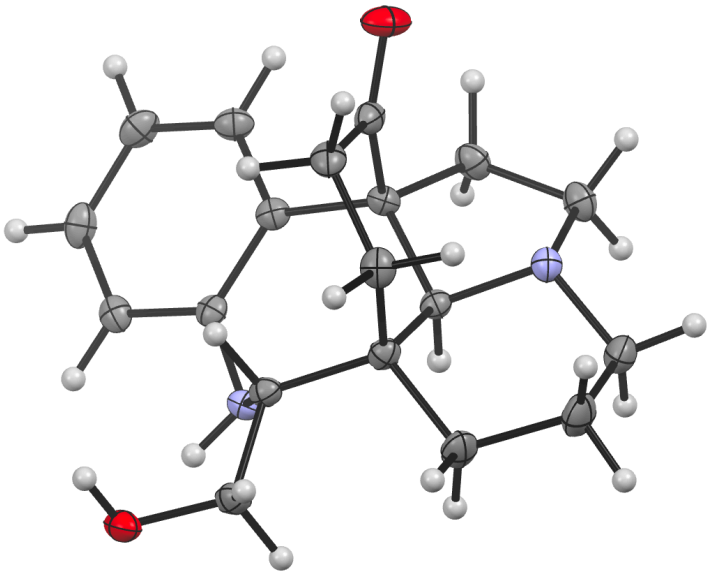


Table A4.7.1. *Crystal data and structure refinement for* ***53*** *(V23353).*

Identification code	V23353	
Empirical formula	C19 H24 N2 O2	
Formula weight	312.40	
Temperature	100(2) K	
Wavelength	1.54178 Å	
Crystal system	Orthorhombic	
Space group	$P2_12_12_1$	
Unit cell dimensions	a = 9.6582(10) Å	a= 90°.
	b = 11.3016(9) Å	b= 90°.
	c = 14.7369(12) Å	g = 90°.
Volume	1608.6(2) $Å^3$	
Z	4	
Density (calculated)	1.290 Mg/m^3	
Absorption coefficient	0.666 mm^{-1}	
F(000)	672	
Crystal size	0.200 x 0.200 x 0.100 mm^3	
Theta range for data collection	4.931 to 74.486°.	
Index ranges	-12<=h<=12, -13<=k<=14, -18<=l<=18	
Reflections collected	25356	
Independent reflections	3278 [R(int) = 0.0414]	

Completeness to theta = 67.679°	100.0 %
Absorption correction	Semi-empirical from equivalents
Max. and min. transmission	0.7538 and 0.6724
Refinement method	Full-matrix least-squares on F^2
Data / restraints / parameters	3278 / 2 / 216
Goodness-of-fit on F^2	1.050
Final R indices [I>2sigma(I)]	R1 = 0.0276, wR2 = 0.0696
R indices (all data)	R1 = 0.0286, wR2 = 0.0700
Absolute structure parameter	-0.04(6)
Extinction coefficient	n/a
Largest diff. peak and hole	0.174 and -0.165 e.$Å^{-3}$

Table A4.7.2. *Atomic coordinates (x 10^4) and equivalent isotropic displacement parameters ($Å^2$x 10^3) for* ***53*** *(V23353). U(eq) is defined as one third of the trace of the orthogonalized U^{ij} tensor.*

Atom	x	y	z	U(eq)
O(1)	2989(1)	3912(1)	3930(1)	28(1)
C(1)	3400(2)	3654(1)	4686(1)	18(1)
C(2)	3835(2)	2414(2)	4922(1)	20(1)
C(3)	3424(2)	2006(1)	5880(1)	20(1)
C(4)	3716(2)	2940(1)	6616(1)	16(1)
C(5)	5321(2)	3042(1)	6735(1)	16(1)
C(19)	5890(2)	2327(2)	7534(1)	20(1)
O(2)	7360(1)	2397(1)	7577(1)	21(1)
C(6)	6080(2)	4911(1)	6030(1)	15(1)
N(1)	5816(1)	4274(1)	6836(1)	16(1)
C(7)	7380(2)	5445(1)	5914(1)	18(1)
C(8)	7696(2)	6107(1)	5150(1)	22(1)
C(9)	6725(2)	6224(2)	4461(1)	22(1)
C(10)	5442(2)	5697(1)	4566(1)	20(1)
C(11)	5082(2)	5058(1)	5346(1)	15(1)
C(12)	3590(2)	4617(1)	5407(1)	15(1)
C(13)	2523(2)	5620(1)	5263(1)	21(1)

Table A4.7.2. cont'd.

Atom	x	y	z	U(eq)
C(14)	1214(2)	5183(2)	5754(1)	21(1)
N(2)	1621(1)	4060(1)	6185(1)	17(1)
C(15)	887(2)	3819(2)	7030(1)	22(1)
C(16)	1383(2)	2646(2)	7425(1)	26(1)
C(17)	2969(2)	2614(2)	7509(1)	24(1)
C(18)	3125(2)	4136(1)	6326(1)	15(1)

Table A4.7.3. *Bond lengths [Å] and angles [°] for* ***53*** *(V23353).*

Bond	Length (Å)	Bond	Length (Å)
O(1)-C(1)	1.218(2)	N(1)-H(1N)	0.886(18)
C(1)-C(2)	1.504(2)	C(7)-C(8)	1.385(2)
C(1)-C(12)	1.531(2)	C(7)-H(7)	0.9500
C(2)-C(3)	1.537(2)	C(8)-C(9)	1.389(2)
C(2)-H(2A)	0.9900	C(8)-H(8)	0.9500
C(2)-H(2B)	0.9900	C(9)-C(10)	1.383(2)
C(3)-C(4)	1.540(2)	C(9)-H(9)	0.9500
C(3)-H(3A)	0.9900	C(10)-C(11)	1.401(2)
C(3)-H(3B)	0.9900	C(10)-H(10)	0.9500
C(4)-C(18)	1.527(2)	C(11)-C(12)	1.528(2)
C(4)-C(17)	1.545(2)	C(12)-C(18)	1.528(2)
C(4)-C(5)	1.564(2)	C(12)-C(13)	1.546(2)
C(5)-N(1)	1.480(2)	C(13)-C(14)	1.538(2)
C(5)-C(19)	1.530(2)	C(13)-H(13A)	0.9900
C(5)-H(5)	1.0000	C(13)-H(13B)	0.9900
C(19)-O(2)	1.423(2)	C(14)-N(2)	1.473(2)
C(19)-H(19A)	0.9900	C(14)-H(14A)	0.9900
C(19)-H(19B)	0.9900	C(14)-H(14B)	0.9900
O(2)-H(2O)	0.85(2)	N(2)-C(15)	1.459(2)
C(6)-C(7)	1.403(2)	N(2)-C(18)	1.4701(19)
C(6)-C(11)	1.405(2)	C(15)-C(16)	1.525(2)
C(6)-N(1)	1.413(2)	C(15)-H(15A)	0.9900

Table A4.7.3. cont'd.

Bond	Length (Å)	Atoms	Angle (°)
C(15)-H(15B)	0.9900	C(19)-C(5)-H(5)	107.1
C(16)-C(17)	1.538(2)	C(4)-C(5)-H(5)	107.1
C(16)-H(16A)	0.9900	O(2)-C(19)-C(5)	111.32(13)
C(16)-H(16B)	0.9900	O(2)-C(19)-H(19A)	109.4
C(17)-H(17A)	0.9900	C(5)-C(19)-H(19A)	109.4
C(17)-H(17B)	0.9900	O(2)-C(19)-H(19B)	109.4
C(18)-H(18)	1.0000	C(5)-C(19)-H(19B)	109.4
		H(19A)-C(19)-H(19B)	108.0
Atoms	**Angle (°)**	C(19)-O(2)-H(2O)	106.3(18)
O(1)-C(1)-C(2)	121.72(14)	C(7)-C(6)-C(11)	118.42(14)
O(1)-C(1)-C(12)	120.22(15)	C(7)-C(6)-N(1)	118.91(14)
C(2)-C(1)-C(12)	117.90(13)	C(11)-C(6)-N(1)	122.65(14)
C(1)-C(2)-C(3)	114.84(14)	C(6)-N(1)-C(5)	116.97(12)
C(1)-C(2)-H(2A)	108.6	C(6)-N(1)-H(1N)	108.0(14)
C(3)-C(2)-H(2A)	108.6	C(5)-N(1)-H(1N)	108.9(14)
C(1)-C(2)-H(2B)	108.6	C(8)-C(7)-C(6)	121.88(15)
C(3)-C(2)-H(2B)	108.6	C(8)-C(7)-H(7)	119.1
H(2A)-C(2)-H(2B)	107.5	C(6)-C(7)-H(7)	119.1
C(2)-C(3)-C(4)	113.19(13)	C(7)-C(8)-C(9)	119.78(15)
C(2)-C(3)-H(3A)	108.9	C(7)-C(8)-H(8)	120.1
C(4)-C(3)-H(3A)	108.9	C(9)-C(8)-H(8)	120.1
C(2)-C(3)-H(3B)	108.9	C(10)-C(9)-C(8)	118.82(15)
C(4)-C(3)-H(3B)	108.9	C(10)-C(9)-H(9)	120.6
H(3A)-C(3)-H(3B)	107.8	C(8)-C(9)-H(9)	120.6
C(18)-C(4)-C(3)	109.93(12)	C(9)-C(10)-C(11)	122.40(15)
C(18)-C(4)-C(17)	105.97(12)	C(9)-C(10)-H(10)	118.8
C(3)-C(4)-C(17)	110.52(13)	C(11)-C(10)-H(10)	118.8
C(18)-C(4)-C(5)	109.69(12)	C(10)-C(11)-C(6)	118.63(14)
C(3)-C(4)-C(5)	108.07(13)	C(10)-C(11)-C(12)	116.77(14)
C(17)-C(4)-C(5)	112.65(13)	C(6)-C(11)-C(12)	124.53(13)
N(1)-C(5)-C(19)	107.66(12)	C(11)-C(12)-C(18)	116.45(13)
N(1)-C(5)-C(4)	113.57(12)	C(11)-C(12)-C(1)	107.71(12)
C(19)-C(5)-C(4)	113.80(13)	C(18)-C(12)-C(1)	109.11(12)
N(1)-C(5)-H(5)	107.1	C(11)-C(12)-C(13)	112.39(13)

Table A4.7.3. cont'd.

Atoms	**Angle (°)**	**Atoms**	**Angle (°)**
C(18)-C(12)-C(13)	100.74(12)	C(16)-C(15)-H(15B)	109.8
C(1)-C(12)-C(13)	110.27(13)	H(15A)-C(15)-H(15B)	108.2
C(14)-C(13)-C(12)	104.35(13)	C(15)-C(16)-C(17)	111.38(14)
C(14)-C(13)-H(13A)	110.9	C(15)-C(16)-H(16A)	109.4
C(12)-C(13)-H(13A)	110.9	C(17)-C(16)-H(16A)	109.4
C(14)-C(13)-H(13B)	110.9	C(15)-C(16)-H(16B)	109.4
C(12)-C(13)-H(13B)	110.9	C(17)-C(16)-H(16B)	109.4
H(13A)-C(13)-H(13B)	108.9	H(16A)-C(16)-H(16B)	108.0
N(2)-C(14)-C(13)	105.09(13)	C(16)-C(17)-C(4)	112.99(14)
N(2)-C(14)-H(14A)	110.7	C(16)-C(17)-H(17A)	109.0
C(13)-C(14)-H(14A)	110.7	C(4)-C(17)-H(17A)	109.0
N(2)-C(14)-H(14B)	110.7	C(16)-C(17)-H(17B)	109.0
C(13)-C(14)-H(14B)	110.7	C(4)-C(17)-H(17B)	109.0
H(14A)-C(14)-H(14B)	108.8	H(17A)-C(17)-H(17B)	107.8
C(15)-N(2)-C(18)	111.70(12)	N(2)-C(18)-C(4)	110.94(12)
C(15)-N(2)-C(14)	113.53(13)	N(2)-C(18)-C(12)	100.66(12)
C(18)-N(2)-C(14)	105.93(12)	C(4)-C(18)-C(12)	116.95(12)
N(2)-C(15)-C(16)	109.56(13)	N(2)-C(18)-H(18)	109.3
N(2)-C(15)-H(15A)	109.8	C(4)-C(18)-H(18)	109.3
C(16)-C(15)-H(15A)	109.8	C(12)-C(18)-H(18)	109.3
N(2)-C(15)-H(15B)	109.8		

Symmetry transformations used to generate equivalent atoms:

Table A4.7.4. *Anisotropic displacement parameters ($Å^2$x 10^3) for* ***53*** *(V23353). The anisotropic displacement factor exponent takes the form: $-2p^2[h^2 a^{*2}U^{11} + ... + 2 h k a^* b^* U^{12}]$*

Atom	U^{11}	U^{22}	U^{33}	U^{23}	U^{13}	U^{12}
O(1)	37(1)	30(1)	16(1)	0(1)	-6(1)	-9(1)
C(1)	15(1)	23(1)	16(1)	-3(1)	1(1)	-5(1)
C(2)	20(1)	20(1)	20(1)	-8(1)	-1(1)	-1(1)
C(3)	20(1)	13(1)	26(1)	-1(1)	1(1)	-1(1)
C(4)	18(1)	15(1)	16(1)	2(1)	2(1)	1(1)
C(5)	18(1)	15(1)	14(1)	0(1)	1(1)	2(1)
C(19)	22(1)	21(1)	16(1)	2(1)	-1(1)	5(1)
O(2)	23(1)	24(1)	17(1)	-3(1)	-4(1)	6(1)
C(6)	17(1)	12(1)	15(1)	-4(1)	1(1)	1(1)
N(1)	17(1)	16(1)	15(1)	0(1)	-3(1)	0(1)
C(7)	17(1)	15(1)	22(1)	-3(1)	-1(1)	1(1)
C(8)	18(1)	16(1)	31(1)	-1(1)	5(1)	-2(1)
C(9)	27(1)	18(1)	22(1)	4(1)	5(1)	-2(1)
C(10)	25(1)	17(1)	17(1)	2(1)	-1(1)	-1(1)
C(11)	18(1)	12(1)	16(1)	-1(1)	0(1)	0(1)
C(12)	16(1)	14(1)	14(1)	0(1)	-2(1)	-1(1)
C(13)	21(1)	19(1)	22(1)	3(1)	-3(1)	3(1)
C(14)	18(1)	18(1)	26(1)	0(1)	-2(1)	3(1)
N(2)	15(1)	18(1)	19(1)	-1(1)	1(1)	1(1)
C(15)	18(1)	27(1)	22(1)	-1(1)	5(1)	1(1)
C(16)	22(1)	29(1)	28(1)	7(1)	9(1)	-1(1)
C(17)	22(1)	27(1)	22(1)	9(1)	5(1)	2(1)
C(18)	16(1)	14(1)	14(1)	-1(1)	0(1)	0(1)

Table A4.7.5. *Hydrogen coordinates (x 10^4) and isotropic displacement parameters (Å^{2}x 10^3) for* ***53*** *(V23353).*

Atom	U^{11}	U^{22}	U^{33}	U^{23}	U^{13}	U^{12}
H(2A)		4854	2357	4863		24
H(2B)		3422	1864	4475		24
H(3A)		3940	1274	6029		23
H(3B)		2424	1813	5885		23
H(5)		5754	2716	6171		19
H(19A)		5490	2632	8106		24
H(19B)		5609	1489	7468		24
H(2O)		7660(30)	2020(20)	7117(15)		40(7)
H(1N)		6583(19)	4273(19)	7165(14)		24(5)
H(7)		8062	5350	6372		22
H(8)		8574	6480	5098		26
H(9)		6938	6658	3927		27
H(10)		4781	5771	4092		24
H(13A)		2858	6371	5531		25
H(13B)		2340	5745	4609		25
H(14A)		910	5763	6215		25
H(14B)		450	5055	5317		25
H(15A)		-122	3782	6914		27
H(15B)		1062	4465	7469		27
H(16A)		1073	1990	7028		31
H(16B)		964	2529	8031		31
H(17A)		3258	1810	7697		28
H(17B)		3260	3172	7990		28
H(18)		3324	4736	6807		18

Table A7.7.6. *Torsion angles [°] for* ***53*** *(V23353).*

Atoms (A-B-C-D)	Angle (°)	Atoms (A-B-C-D)	Angle (°)
O(1)-C(1)-C(2)-C(3)	-141.77(16)	C(6)-C(11)-C(12)-C(13)	123.98(15)
C(12)-C(1)-C(2)-C(3)	42.7(2)	O(1)-C(1)-C(12)-C(11)	-91.59(18)
C(1)-C(2)-C(3)-C(4)	-44.98(19)	C(2)-C(1)-C(12)-C(11)	83.99(16)
C(2)-C(3)-C(4)-C(18)	49.60(17)	O(1)-C(1)-C(12)-C(18)	141.16(15)
C(2)-C(3)-C(4)-C(17)	166.23(13)	C(2)-C(1)-C(12)-C(18)	-43.27(18)
C(2)-C(3)-C(4)-C(5)	-70.09(17)	O(1)-C(1)-C(12)-C(13)	31.4(2)
C(18)-C(4)-C(5)-N(1)	18.53(17)	C(2)-C(1)-C(12)-C(13)	-153.04(14)
C(3)-C(4)-C(5)-N(1)	138.37(13)	C(11)-C(12)-C(13)-C(14)	-155.29(13)
C(17)-C(4)-C(5)-N(1)	-99.24(15)	C(18)-C(12)-C(13)-C(14)	-30.64(15)
C(18)-C(4)-C(5)-C(19)	142.19(13)	C(1)-C(12)-C(13)-C(14)	84.52(15)
C(3)-C(4)-C(5)-C(19)	-97.98(15)	C(12)-C(13)-C(14)-N(2)	4.05(16)
C(17)-C(4)-C(5)-C(19)	24.42(19)	C(13)-C(14)-N(2)-C(15)	148.74(13)
N(1)-C(5)-C(19)-O(2)	-56.56(16)	C(13)-C(14)-N(2)-C(18)	25.80(16)
C(4)-C(5)-C(19)-O(2)	176.64(13)	C(18)-N(2)-C(15)-C(16)	-60.01(17)
C(7)-C(6)-N(1)-C(5)	-126.30(14)	C(14)-N(2)-C(15)-C(16)	-179.71(14)
C(11)-C(6)-N(1)-C(5)	55.29(19)	N(2)-C(15)-C(16)-C(17)	52.62(19)
C(19)-C(5)-N(1)-C(6)	147.18(13)	C(15)-C(16)-C(17)-C(4)	-52.0(2)
C(4)-C(5)-N(1)-C(6)	-85.89(16)	C(18)-C(4)-C(17)-C(16)	53.74(18)
C(11)-C(6)-C(7)-C(8)	0.1(2)	C(3)-C(4)-C(17)-C(16)	-65.31(18)
N(1)-C(6)-C(7)-C(8)	-178.38(14)	C(5)-C(4)-C(17)-C(16)	173.68(14)
C(6)-C(7)-C(8)-C(9)	-2.0(2)	C(15)-N(2)-C(18)-C(4)	65.91(16)
C(7)-C(8)-C(9)-C(10)	1.7(2)	C(14)-N(2)-C(18)-C(4)	-170.01(12)
C(8)-C(9)-C(10)-C(11)	0.6(2)	C(15)-N(2)-C(18)-C(12)	-169.64(12)
C(9)-C(10)-C(11)-C(6)	-2.4(2)	C(14)-N(2)-C(18)-C(12)	-45.55(14)
C(9)-C(10)-C(11)-C(12)	174.76(15)	C(3)-C(4)-C(18)-N(2)	59.71(15)
C(7)-C(6)-C(11)-C(10)	2.1(2)	C(17)-C(4)-C(18)-N(2)	-59.74(15)
N(1)-C(6)-C(11)-C(10)	-179.52(14)	C(5)-C(4)-C(18)-N(2)	178.41(12)
C(7)-C(6)-C(11)-C(12)	-174.92(13)	C(3)-C(4)-C(18)-C(12)	-54.91(17)
N(1)-C(6)-C(11)-C(12)	3.5(2)	C(17)-C(4)-C(18)-C(12)	-174.36(13)
C(10)-C(11)-C(12)-C(18)	-168.52(13)	C(5)-C(4)-C(18)-C(12)	63.79(16)
C(6)-C(11)-C(12)-C(18)	8.5(2)	C(11)-C(12)-C(18)-N(2)	167.95(12)
C(10)-C(11)-C(12)-C(1)	68.62(17)	C(1)-C(12)-C(18)-N(2)	-69.92(14)
C(6)-C(11)-C(12)-C(1)	-114.35(16)	C(13)-C(12)-C(18)-N(2)	46.12(14)
C(10)-C(11)-C(12)-C(13)	-53.04(18)	C(11)-C(12)-C(18)-C(4)	-71.81(17)

Table A7.7.6. cont'd.

Atoms (A-B-C-D)	Angle (°)	Atoms (A-B-C-D)	Angle (°)
C(1)-C(12)-C(18)-C(4)	50.32(17)	C(13)-C(12)-C(18)-C(4)	166.36(13)

Symmetry transformations used to generate equivalent atoms:

Table A4.7.7. *Hydrogen bonds for* ***53*** *[Å and °].*

D-H...A	d(D-H)	d(H...A)	d(D...A)	<(DHA)
O(2)-H(2O)...O(1)#1	0.85(2)	1.90(2)	2.7372(17)	169(3)
N(1)-H(1N)...O(2)	0.886(18)	2.33(2)	2.8136(18)	114.5(16)

Symmetry transformations used to generate equivalent atoms:
#1 x+1/2,-y+1/2,-z+1

A4.8 REFERENCES AND NOTES

(1) Sheldrick, G. M. Phase Annealing in SHELX-90: Direct Methods for Larger Structures. *Acta. Crystallogr. A Found. Crystallogr.* **1990**, *46*, 467–473.

(2) Sheldrick, G. M. Crystal Structure Refinement with *SHELXL*. *Acta. Crystallogr. C Struct. Chem.* **2015**, *71*, 3–8.

(3) Müller, P. Practical Suggestions for Better Crystal Structures. *Crystallogr. Rev.* **2009**, *15*, 57–83.

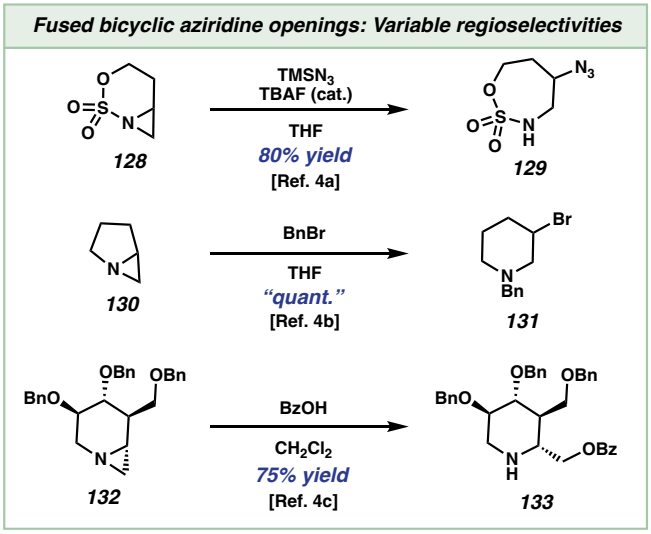
CHAPTER 3

PREPARATION AND REGIOSELECTIVE RING OPENING REACTIONS OF FUSED BICYCLIC AZIRIDINES†

3.1 INTRODUCTION

Aziridines are three-membered heterocycles that frequently serve as key intermediates in synthetic organic chemistry.[1] The strained nature of aziridines enables myriad ring opening reactions that make them useful building blocks for the preparation of nitrogen-containing molecules.[2] As such, central to their synthetic utility is the ability to control or predict the site at which these ring opening reactions occur. While the regioselectivities of these transformations vary according to the structure of the aziridine and reaction conditions, these systems have been well-studied and general trends have been established for the well-studied class of "*standard*" aziridines, defined herein as aziridines in which the nitrogen substituent is not connected to either of the aziridine carbon atoms.[2b,3]

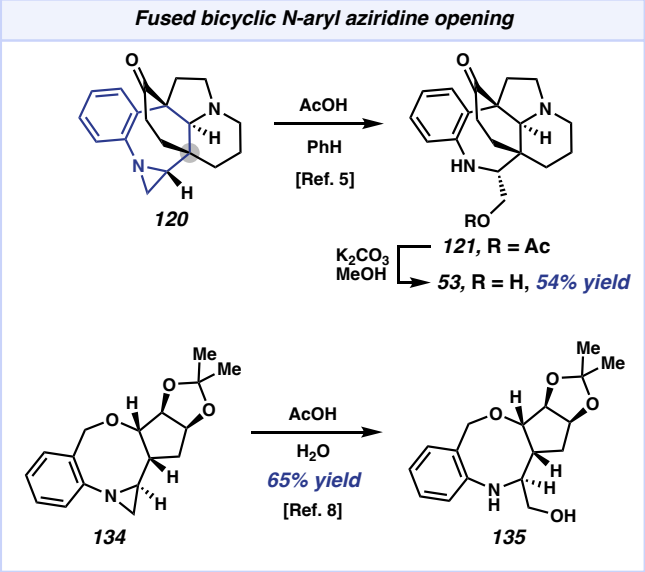
Scheme 3.1.1 *Ring opening reactions of fused bicyclic aziridines*



†This research was performed in collaboration with Leanne Fuentes Ruiz, Bryce E. Gaskins, and Michael K. Takase. A manuscript has been submitted for publication.

In contrast, ring opening reactions of "*fused bicyclic*" aziridines, those in which the nitrogen substituent is connected to one of the aziridine carbon atoms, have been the subject of fewer studies[4] and general reactivity trends have not been elucidated nor systematically evaluated. Therefore, the reaction site can be considerably more challenging to predict. Scheme 3.1.1 highlights select examples that showcase the disparate nature of fused bicyclic aziridine ring opening regioselectivity.

Scheme 3.1.2 *Ring opening reactions of fused bicyclic N-aryl aziridines*

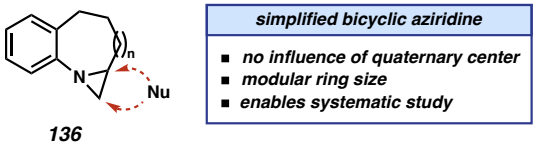


In our recent synthesis of hunterine A (**53**), a late-stage, regioselective ring opening of N-aryl aziridine **120** was crucial for the installation of the necessary hydroxymethyl moiety found in the natural product (Scheme 3.1.2).[5] We reasoned that the steric bias of the neighboring quaternary center would significantly influence the regiochemical outcome of the reaction. However, since few bicyclic N-aryl aziridines have been reported and studied in the context of ring opening[6,7] this strategy carried some degree of risk. We were gratified to observe that ring opening yielded the desired product **121** that could be deacetylated to give the natural product (**53**). In a related eight-membered system, Chattopadhyay and

coworkers observed a similar outcome when treating **134** with AcOH in H_2O.[8] The additional neighboring substitution may also play a role in the regiochemical outcome of this transformation.

The success of our synthetic strategy coupled with a paucity of studies concerned with bicyclic N-aryl aziridine ring opening prompted us to further investigate the reactivity of these systems. Based on the results in Scheme 2, it appeared that achieving exclusive regioselectivity was possible and that through a more systematic evaluation of related compounds we might be able to elucidate general trends in reactivity, as have been established for "*standard*" aziridines. To do so, we aimed to synthesize a series of simplified bicyclic N-aryl aziridines (**136**, Scheme 3.1.3) that would allow for modulation of the ring size and that would not be affected by the same steric influence and conformational restrictions of **7**. Additionally, the variety of outcomes observed in the ring openings of other bicyclic aziridines shown in Scheme 1 suggested that the site of reaction could vary according to reaction conditions and size of the fused ring.

Scheme 3.1.3 *Proposed simplified bicyclic N-aryl aziridine for systematic study of ring opening*

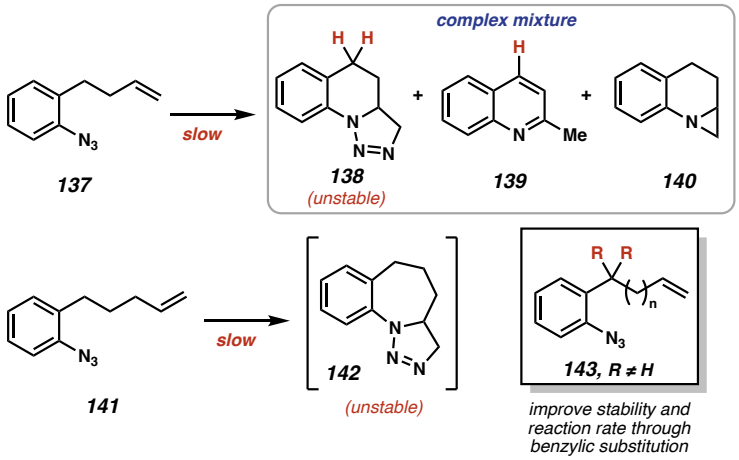


3.2 ATTEMPTED SYNTHESIS OF SIMPLIFIED AZIRIDINES

Preparation of the simplified bicyclic N-aryl aziridines proved to be more challenging than initially envisioned. We attempted to employ an azide/alkene intramolecular dipolar cycloaddition and triazoline photolysis to synthesize these aziridines. However, our initial attempts to execute this set of transformations were met with failure (Scheme 3.2.1). In our

hands, azide **137** was slow to undergo dipolar cycloaddition, and the cycloadduct appeared to decompose, as evidenced by observation of quinoline **139** as one of the major products by crude ^{1}H NMR, along with a small amount of what we tentatively assigned as putative aziridine **140**. Unfortunately, attempts to purify the mixture and verify the formation of this aziridine only led to further decomposition. Azide **141** was even slower to react and the putative cycloadduct was not stable to any attempted forms of purification. We hypothesized that incorporating substituents at the benzylic position (**143**) would accelerate the rate of intramolecular cycloaddition[9] as well as prevent any potentially deleterious reactions resulting from elimination/oxidation at the benzylic position and provide a more robust route to the desired compounds. We expected that the benzylic substituents would have little steric influence on the aziridine opening due to their distal location relative to the possible sites of reaction. This strategy ultimately proved successful.

Scheme 3.2.1 *Initial attempts to synthesize simplified bicyclic N-aryl aziridines*

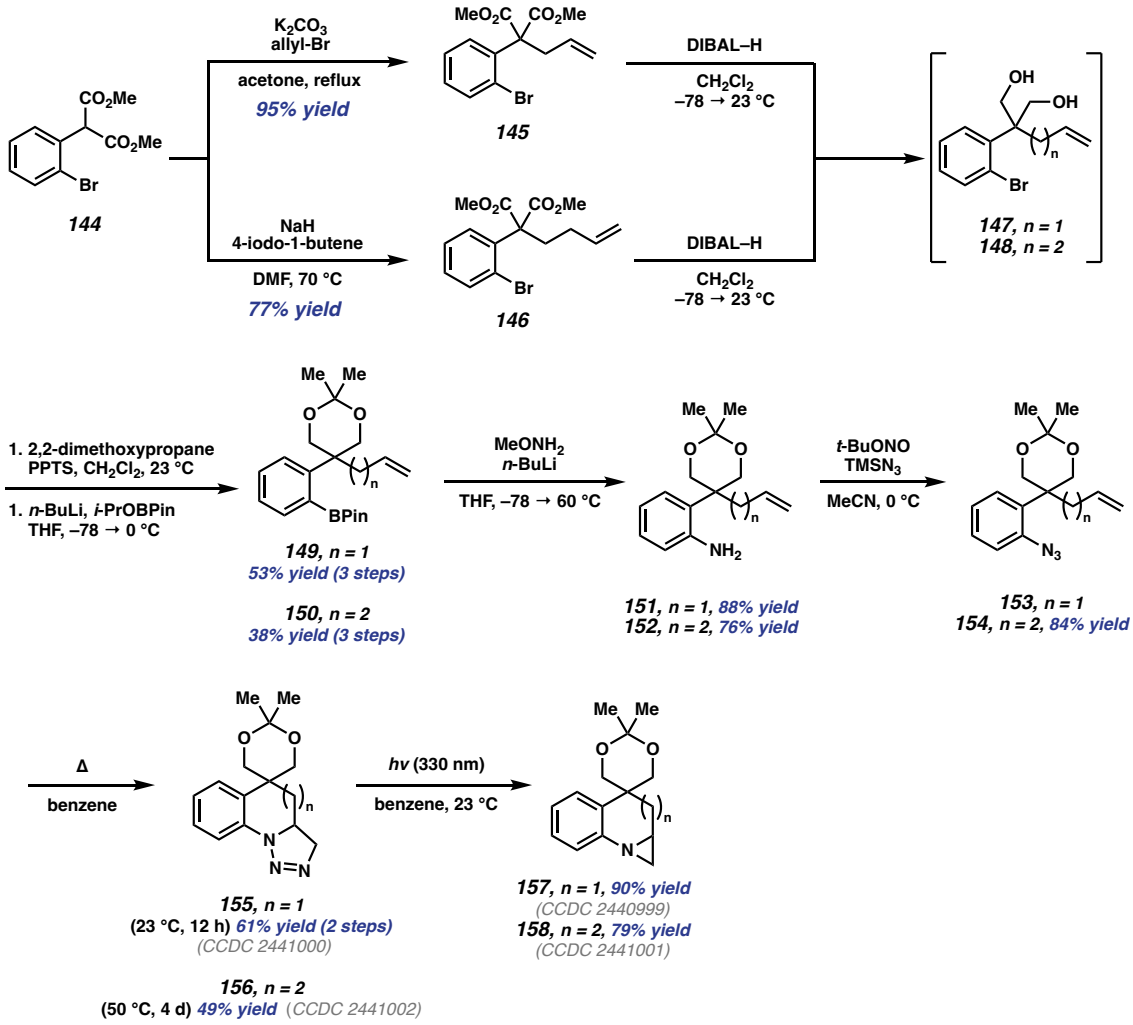


3.3 SUCCESSFUL SYNTHESIS AND RING OPENING OF SIMPLIFIED AZIRIDINES

Malonate **144** was alkylated in a divergent manner to access the products containing pendant olefins with different methylene spacer lengths (Scheme 3.3.1). Treatment of **144**

with K_2CO_3 and allyl bromide in acetone afforded **145** in 95% yield. Alternatively, treatment with NaH and 4-iodo-1-butene in DMF afforded **146** in 77% yield. With both intermediates of different tether lengths in hand, identical synthetic sequences could be performed to arrive at the desired aziridines. Treatment of the alkylated compounds with DIBAL–H, followed by protection of the diol as the acetonide, and finally a lithiation/borylation sequence gave aryl BPin compounds **149** and **150** in respective 53% and 38% yields over three steps. While attempts to perform Chan-Evans-Lam couplings or Buchwald-Hartwig aminations from the aryl BPin or bromide compounds were unsuccessful, installation of the necessary nitrogen atom was accomplished through a protocol developed by Morken and coworkers.[10] The aryl BPin compounds were treated with a mixture of $MeONH_2$ and *n*-BuLi at cryogenic temperature, followed by heating to 60 °C, allowing for isolation of the anilines **151** and **152** in 88% and 76% yields. Conversion of the anilines to the corresponding aryl azides was accomplished with *t*-BuONO and $TMSN_3$.[11] It should be noted attempts to directly convert the aryl bromides or BPin compounds to the corresponding azides (**153**, **154**) were also unsuccessful. Allowing azide **153** to stand in benzene at ambient temperature for twelve hours led to formation of triazoline **155** in 61% yield over two steps. Formation of **156** required heating to 50 °C for 4 days. Both compounds were crystalline solids, the structures of which could be unambiguously determined by X-ray crystallography (CCDC 2441000 and 2441002). Overall, these results highlight the improved stability and reaction rates imparted by benzylic substitution. Finally, irradiation of each compound with long-wave UV light (centered at 330 nm)[12] gave the desired aziridines **157** and **158**. We did not attempt to synthesize the aziridine fused to a five-membered ring (n = 0) because the benzylic substituents would be likely to disfavor reaction at the neighboring site.

Scheme 3.3.1 *Successful synthesis of fused bicyclic N-aryl aziridines*

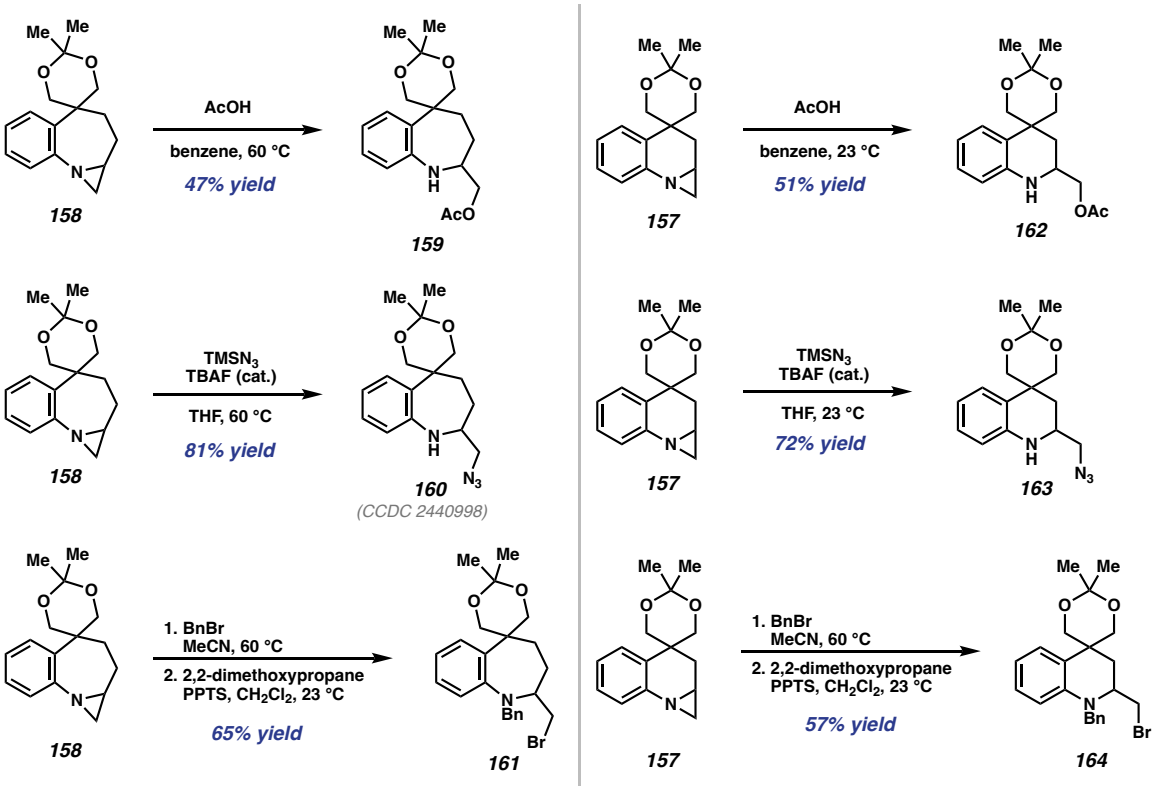


Our investigation of the aziridine ring opening reactions began with the seven-membered aziridine **158** that was most similar to our previous synthetic intermediate **120**. Gratifyingly, ring-opening with acetic acid proceeded smoothly to deliver **159** in 47% yield (Scheme 3.3.2). It is noteworthy that the reaction did not proceed at ambient temperature and required heating to 60 °C for conversion to the ring-opened product. We were unable to detect the formation of any other products or constitutional isomers resulting from the alternative ring opening reaction. Because our previous report had also used acetic acid and led to the same outcome, the subsequent ring openings were performed using reactants other

than oxygen-based nucleophiles and conditions that did not involve protic acids. Dauban and Dodd reported ring opening of **128** at the *more substituted* aziridine carbon (shown in Scheme 3.1.1) using $TMSN_3$ and catalytic TBAF.[4a] When treating **158** with the same reagents at 60 °C, we again observed exclusive ring opening at the least-substituted position, forming **160** in 81% yield, the structure of which was unambiguously determined by X-ray crystallography (CCDC 2440998). As a final test, we opted to perform a ring opening analogous to that reported by Hayashi in which treatment of the non-activated bicyclic aziridine **130** (shown in Scheme 1) with BnBr resulted in ring opening at the more substituted position.[4b] Treatment of **158** with BnBr in MeCN at 60 °C did allow for ring opening to occur, although with partial removal of the acetonide protecting group. Thus, a two-step procedure of ring opening and reprotection was employed. This enabled clean isolation of **161** in 65% yield with no indication of products resulting from alternative ring opening reactions. The results of these experiments led us to hypothesize that the regioselectivity of these transformations is influenced primarily by the nature of the aziridine.

With these results in hand, we turned our attention to evaluating the same ring opening reactions using six-membered substrate **157** and were surprised to observe the same exclusively regioselective outcomes. Opening with acetic acid proceeded in a similar 51% yield to give **162**, the reaction with $TMSN_3$ afforded **157** in 72% yield, and opening with BnBr followed by reprotection gave **164** in 57% yield. The transformations involving $TMSN_3$ and AcOH proceeded at milder temperatures than in the seven-membered case. We assumed that this reflected increased strain in the azabicyclo[4.1.0]heptane motif of **157** relative to the azabicyclo[5.1.0]octane motif found in **158**, discussed later in Figure 3.3.1. In all cases, no constitutional isomers resulting from the alternative ring opening were observed.

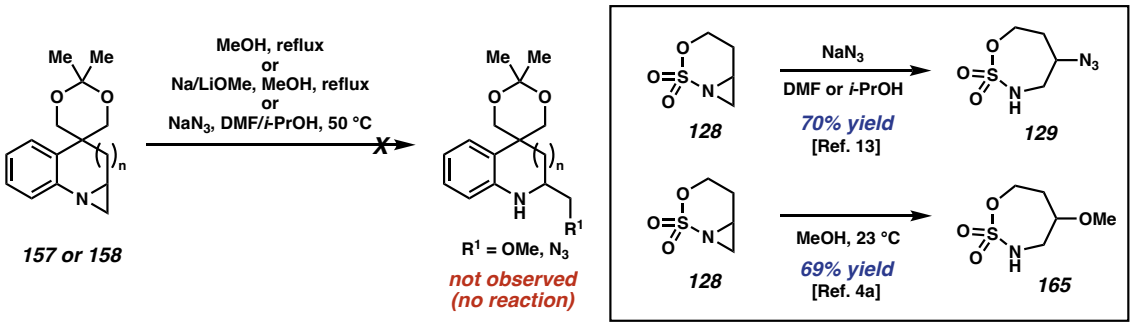
Scheme 3.3.2 *Ring opening of fused bicyclic N-aryl aziridines*



While these transformations are not an exhaustive evaluation of all ring opening conditions reported for aziridines, they are representative of diverse conditions in which different sites of reaction have been observed. In a mechanistic sense, each transformation likely proceeds in a similar manner via initial activation (protonation, silylation, alkylation) of the aziridine nitrogen, followed by nucleophilic attack. Therefore, as a final test we thought it pertinent to evaluate whether this type of activation was necessary for the ring opening to proceed. Du Bois[13] as well as Dauban and Dodd[4a] have reported that bicyclic aziridines derived from sulfamates can undergo ring-opening reactions in the absence of strong activation; **128** will undergo ring opening in the presence of methanol, amines, and in the presence of NaN_3 in DMF with an exclusive preference for opening at the more substituted position (**129** and **165**, Scheme 3.3.3). Treatment of **157** and **158** with MeOH

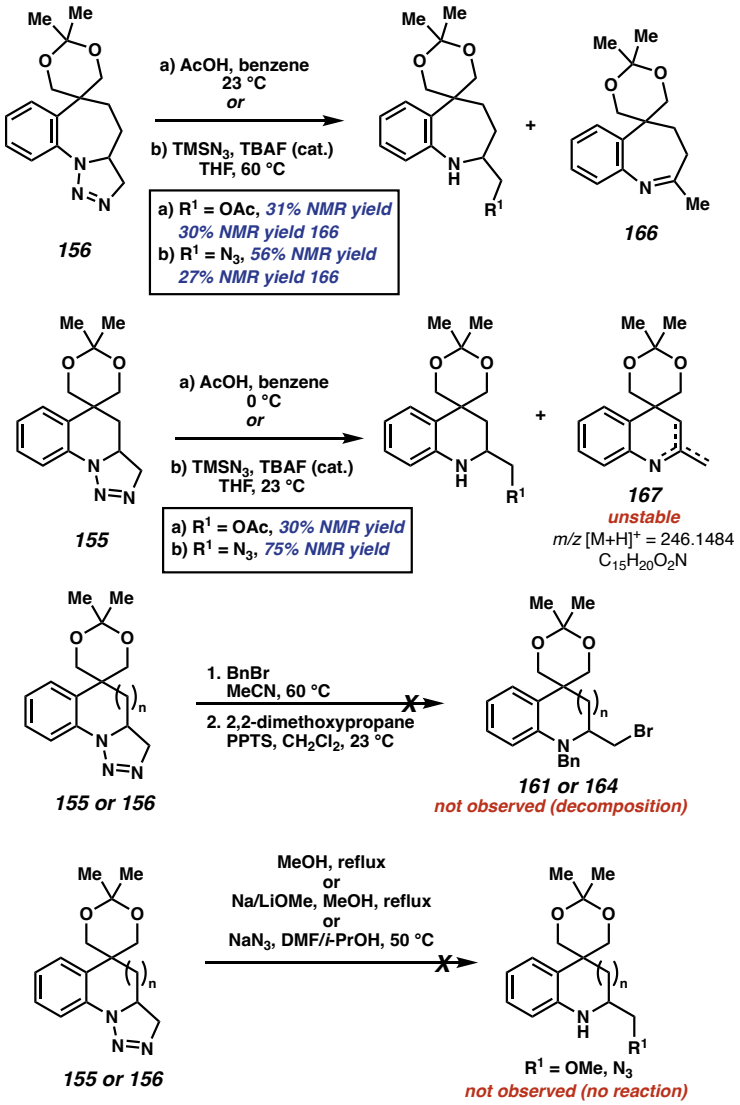
resulted in no reaction even at elevated temperature. Likewise, both aziridines failed to react in the presence of NaOMe or the more Lewis acidic LiOMe in refluxing MeOH. Furthermore, there were no signs of ring opening in the presence of NaN_3 (Scheme 3.3.3). Thus, stronger activation of these aziridines appears to be necessary for ring opening to occur.

Scheme 3.3.3 *Failed ring opening without strong activation*



Having evaluated ring opening reactions of the N-aryl bicyclic aziridines, we considered the possibility of performing similar reactions using the triazoline precursors, as such transformations have been documented.[14] Treating triazoline **156** with acetic acid at ambient temperature resulted in ring opening to give the same acetylated product **159** in 31% NMR yield (Scheme 7). This was accompanied by formation of the imine product **166**, a frequently encountered decomposition product of this type of triazoline.[12c,15] A similar outcome was observed when treating **156** with $TMSN_3$ and TBAF at 60 °C with azide **160** being observed in 56% NMR yield, accompanied by 27% of the imine. Treatment with benzyl bromide resulted only in non-specific decomposition.

Scheme 3.3.4 *Ring opening of triazolines and formation of imine/enamine byproducts*



**NMR yields reported with respect to a 2,4,6-trimethoxybenzene internal standard*

As in the case of the opening of aziridines, the six-membered substrates reacted at lower temperatures. Treatment of **155** with acetic acid resulted in formation of **162** in 30% yield by NMR. This was accompanied by formation of a putative imine/enamine product (**167**), assigned by analogy to the seven-membered product. Unlike the seven-membered analog, this product proved to be highly unstable and recalcitrant to purification. We were able to obtain high-resolution mass spectrometry data that suggested the molecule had a

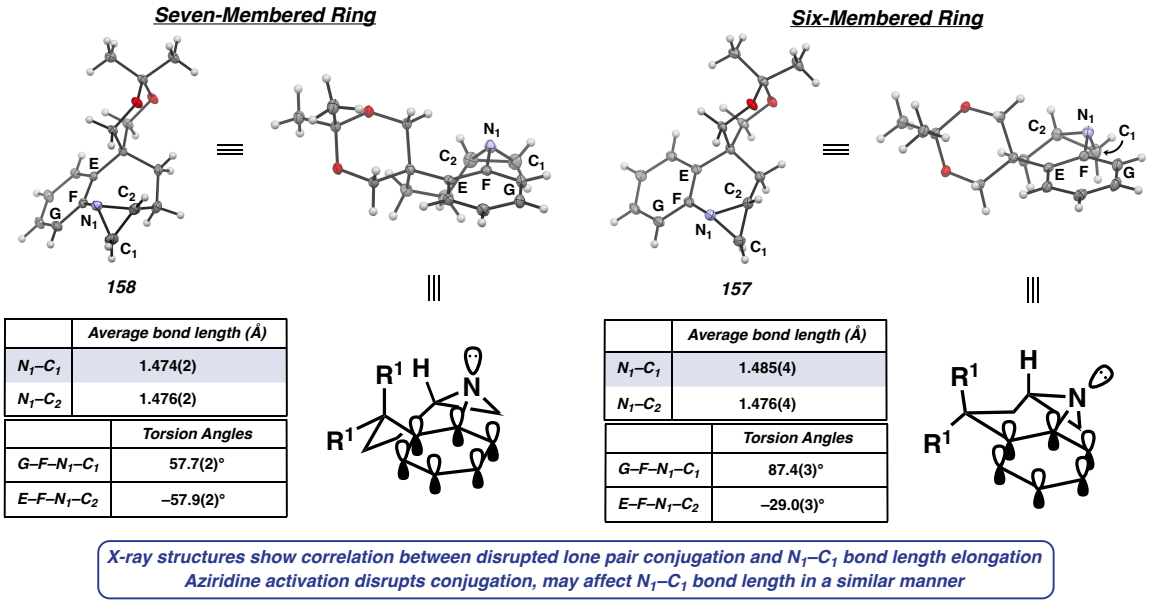
formula consistent with this imine/enamine. Ring opening with $TMSN_3$ performed similarly to give **163** in 75% NMR yield, and treatment with BnBr again resulted only in a complex profile. Additionally, both triazolines also failed to react in the presence of methanol, NaOMe or LiOMe at elevated temperature, or NaN_3. Taken together, these results indicate that triazolines behave similarly to the analogous N-aryl aziridines with respect to the regioselectivity of ring opening but are more prone to decomposition in these transformations.

Since the origin of regioselectivity for the ring opening of bicyclic aziridines is substrate dependent (as seen in Scheme 1), we sought to better understand the exclusive regioselectivities observed through analysis of the crystal structures of **157** and **158** (Figure 3.3.1, CCDC 2441001 and 2440999). Of course, the solid state aziridine structures may not reflect the solution phase conformations of these molecules, and activation of the aziridine under the reaction conditions likely distorts both ground state structures. Unfortunately, it was not possible to obtain a crystal structure of a protonated or otherwise activated aziridine intermediate. However, analysis of these ground state structures still provides valuable information that may help understand the reactivity of these systems, discussed below. It should be noted that both aziridines crystallized with two molecules in the asymmetric unit, thus bond lengths and torsion angles are shown as averages and the uncertainties shown in parentheses have been propagated.

In the seven-membered substrate **158**, the molecule is oriented such that the aziridine lone pair is nearly perfectly aligned with the aromatic π-system, made clear by the nearly identical torsion angles (Figure 1, left). In contrast, **157** adopts a conformation in which the aziridine lone pair does not overlap as effectively with the aromatic π-system and

results in a considerable difference in the same torsion angles (Figure 1, right). When comparing the relevant bond lengths of the seven-membered and six-membered substrates, it appears that this loss of conjugation does not significantly affect the length of the N1–C2 bond (1.476(2) for **158** and 1.476(4) for **157**), while the N1–C1 bond length increases with loss of conjugation (1.474(2) for **158** and 1.485(4) for **157**). This difference may be due to improved orbital overlap between the aromatic π-system and the N1–C1 σ* orbital in this conformation of **157**, supported by the G–F–N_1–C_1 torsion angle being nearly 90°. Experimentally these differences in conjugation are supported by the observation that reactions of the seven-membered aziridine require elevated temperatures relative to the six-membered aziridine. These differences in ground state structure do not on their own explain why both aziridines undergo ring opening at the same position (C1) but instead call attention to the correlation between loss of lone pair conjugation and N1–C1 bond elongation.

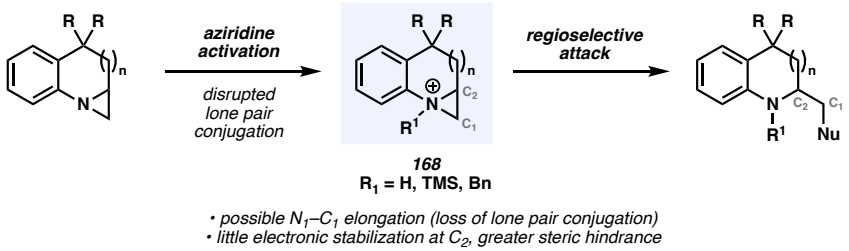
Figure 3.3.1 *Conformational analysis of aziridines and identification of a relationship between lone pair conjugation and N1–C1 bond length*



While we do not wish to speculate too heavily, we believe that the correlation between loss of conjugation and bond elongation could be an important factor in explaining the observed regioselectivity. Each ring opening likely proceeds through activation (protonation, silylation, alkylation) to form an aziridinium where lone pair conjugation would be disrupted (Scheme Figure 1, intermediate **168**). In turn, this could engender a conformational change that causes N1–C1 bond elongation in an analogous fashion to that observed when comparing **158** and **157**. The greater reactivity of **157** could be due to a predisposed elongation in the ground state. Although not perfectly analogous, bond elongation due to stabilization of cationic species by hyperconjugation has been observed.[16] Overall, we believe elongation of the N1–C1 bond relative to the N1–C2 bond may be a factor that contributes to preferential opening at C1.

While N1–C1 bond elongation could contribute to regioselective opening at C1, steric and electronic factors likely contribute as well. Electronic stabilization that would favor attack at C2 is likely to be weak, a phenomenon that has been observed in certain ring opening reactions of similarly substituted epoxides.[17] Steric factors may also contribute to preferential attack at the less hindered C1 position. Taken together, these considerations suggest that in a general sense, ring openings of bicyclic N-aryl aziridines bearing similar substitution patterns to the substrates described herein are likely to occur preferentially at the C1 position.

Scheme 3.3.5 *Possible factors influencing regioselective attack*



3.4 CONCLUSION

In conclusion, we have disclosed a reliable synthetic route for the preparation of fused bicyclic N-aryl aziridines and have performed a systematic evaluation of the ring opening reactions of these molecules with a variety of heteroatom nucleophiles, inspired by our recent total synthesis efforts. Notably, each ring opening proceeds with exclusive regioselectivity. Mechanistically, the reactions are believed to proceed via initial activation of the aziridine followed by nucleophilic attack. Additionally, we found that the triazoline precursors to these aziridines were also competent substrates for ring opening reactions, albeit with concomitant formation of imine/enamine byproducts. Through X-ray crystallographic analysis of the aziridines, we were able to glean information about aziridine lone pair conjugation and its correlation with N–C bond lengths that may contribute to the exclusive regioselectivities observed. We hope these insights will help inform future studies involving fused bicyclic N-aryl aziridines as well as those concerned with elucidating the origins of aziridine ring opening regioselectivity.

3.5 EXPERIMENTAL SECTION

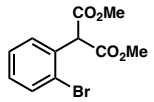
3.5.1 GENERAL INFORMATION

Unless otherwise stated, reactions were performed in flame-dried glassware under an argon or nitrogen atmosphere using dry, deoxygenated solvents. Solvents were dried by passage through an activated alumina column under argon.[18] Reaction progress was monitored by thin-layer chromatography (TLC) or Agilent 1290 UHPLC-MS. TLC was performed using E. Merck silica gel 60 F254 precoated glass plates (0.25 mm) and visualized by UV fluorescence quenching, *p*-anisaldehyde, or $KMnO_4$ staining. Silicycle Silia*Flash*® P60 Academic Silica gel (particle size 40–63 μm) was used for flash chromatography. ^1H NMR spectra were recorded on Varian Inova 500 MHz and Bruker 400 MHz spectrometers and are reported relative to residual $CHCl_3$ (δ 7.26 ppm) or C_6D_5H (δ 7.16 ppm). ^{13}C NMR spectra were recorded on a Varian Inova 500 MHz spectrometer (125 MHz) and Bruker 400 MHz spectrometers (100 MHz) and are reported relative to $CDCl_3$ (δ 77.16 ppm) or C_6D_6 (δ 128.06) . Data for ^1H NMR are reported as follows: chemical shift (δ ppm) (multiplicity, coupling constant (Hz), integration). Multiplicities are reported as follows: s = singlet, d = doublet, t = triplet, q = quartet, p = pentet, sept = septuplet, m = multiplet, br s = broad singlet, br d = broad doublet. Data for ^{13}C NMR are reported in terms of chemical shifts (δ ppm). IR spectra were obtained by use of a Perkin Elmer Spectrum BXII spectrometer using thin films deposited on NaCl plates and reported in frequency of absorption (cm^{-1}). High resolution mass spectra (HRMS) were obtained from an Agilent 6230 Series TOF with an Agilent Jet Stream ion source in electrospray ionization (ESI+) mode. Reagents were purchased from commercial sources and used as received unless otherwise stated.

3.5.2 SAFETY

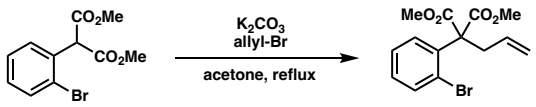
Azides and triazolines are reactive, potentially explosive and toxic molecules. Although these compounds displayed relative thermal stability and no incidents occurred during the preparation of any compounds described herein, they should be handled with care. Additionally, $TMSN_3$ can rapidly hydrolyze in the presence of water to hydrazoic acid (HN_3) which is volatile, toxic, and explosive.

3.5.3 EXPERIMENTAL PROCEDURES



Dimethyl 2-(2-bromophenyl)malonate (**144**): Prepared according to a modified procedure from Cai and coworkers.[19] To a flame-dried flask with stir bar was added methyl 2-(2-bromophenyl)acetate (prepared according to Coe and coworkers[20]) (9.76 g, 40.3 mmol, 1.0 equiv). Dimethyl carbonate (129 mL) was added and the solution was cooled to 0 °C. NaH (60% wt, 5.11 g, 121 mmol, 3.0 equiv) was added portionwise. The cooling bath was removed, and the mixture was heated to 50 °C for 14 hours. After cooling to ambient temperature, water (500 mL) was added, the layers were separated, the aqueous layer was extracted with EtOAc (3x75 mL). The combined organic layers were washed with brine (100 mL), dried over Na_2SO_4, and concentrated under reduced pressure. The crude reside was purified by flash column chromatography (30% EtOAc in hexanes) to give the title compound as a white solid (9.17 g, 75% yield). Characterization data were in accord with those reported in the literature;[21] a ^{1}H NMR spectrum is provided for reference.

^{1}H NMR: (600 MHz, $CDCl_3$) δ 7.60 (dd, *J* = 8.0, 1.3 Hz, 1H), 7.48 (dd, *J* = 7.8, 1.7 Hz, 1H), 7.34 (td, *J* = 7.6, 1.3 Hz, 1H), 7.20 (ddd, *J* = 8.0, 7.4, 1.2 Hz, 1H), 5.28 (s, 1H), 3.79 (s, 6H)



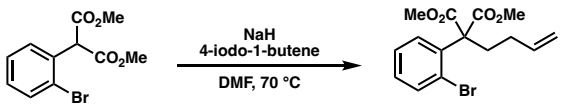
Dimethyl 2-allyl-2-(2-bromophenyl)malonate (**145**): Malonate **144** (3.85 g, 13.4 mmol, 1.0 equiv) was charged to round bottom flask equipped with a magnetic stir bar. Acetone (45 mL, 0.3 M) was added followed by K_2CO_3 (7.42 g, 53.7 mmol, 4 equiv) and allyl bromide (4.87 g, 3.48 mL, 40.2 mmol, 3 equiv). A reflux condenser was added to the flask and the system was flushed with nitrogen before refluxing for 14 hours. After this time, the mixture was cooled to ambient temperature. Water (200 mL) was added and the mixture was extracted with Et_2O (3x100 mL). The combined organic layers were washed with brine, dried over Na_2SO_4 and concentrated under reduced pressure to give a colorless oil (4.39 g, 95% yield) that was sufficiently pure for use without further purification.

^{1}H NMR: (400 MHz, $CDCl_3$) δ 7.58 (dd, *J* = 7.8, 1.4 Hz, 1H), 7.29 (ddd, *J* = 8.0, 7.2, 1.4 Hz, 1H), 7.21 – 7.10 (m, 2H), 5.77 (ddt, *J* = 17.2, 10.2, 7.1 Hz, 1H), 5.02 (ddt, *J* = 17.1, 2.0, 1.4 Hz, 1H), 4.93 (ddt, *J* = 10.1, 2.1, 1.1 Hz, 1H), 3.79 (s, 6H), 3.23 (dt, *J* = 7.2, 1.3 Hz, 2H).

^{13}C NMR: (100 MHz, $CDCl_3$) δ 170.30, 137.19, 134.78, 133.59, 130.13, 129.14, 127.38, 123.93, 118.52, 64.91, 53.21, 38.92.

IR: (neat film, NaCl) 2950, 1746, 1470, 1432, 1256, 1212, 1136, 1026, 918, 744 cm^{-1}

HRMS: (ESI^+) *m/z* calc'd for $C_{14}H_{15}BrO_4Na$ $[M+Na]^+$: 349.0046 found 349.0044



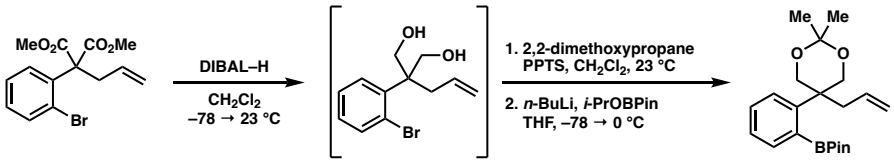
Dimethyl 2-(2-bromophenyl)-2-(but-3-en-1-yl)malonate (**146**): To a flame-dried flask with stir bar was added a mineral oil dispersion of NaH (60 wt%, 1.92g, 47.91 mmol, 1.5 equiv). The flask was purged and backfilled three times and cooled to 0 °C. DMF was added to the flask (15 mL), followed by malonate **144** (9.17 g, 31.94 mmol, 1.0 equiv) as a solution in DMF (15 mL) and stirred for 10 minutes at 0 °C then 20 minutes at ambient temperature. 4-iodo-1-butene[22] (11.63 g, 63.9 mmol, 2.0 equiv) was added as a solution in DMF (15 mL) to the reaction mixture. The flask was heated in a heating block at 70 °C for 15 h. After this time, the reaction mixture was cooled to ambient temperature. Water (250 mL) was added and the mixture was extracted with EtOAc (3x75 mL). The combined organic layers were washed with 10% aq. LiCl (100 mL), brine (100 mL), dried over Na_2SO_4, and concentrated under reduced pressure. The crude oil was purified by flash column chromatography (20 → 30% Et_2O in hexanes) to give the title compound as a colorless oil (8.35 g, 77% yield).

^{1}H NMR: (500 MHz, $CDCl_3$) δ 7.59 (dd, *J* = 7.9, 1.5 Hz, 1H), 7.32 – 7.28 (m, 1H), 7.19 – 7.14 (m, 2H), 5.78 (ddt, *J* = 16.8, 10.1, 6.5 Hz, 1H), 4.99 (dd, *J* = 17.1, 1.7 Hz, 1H), 4.93 (dd, *J* = 10.2, 1.6 Hz, 1H), 3.79 (s, 6H), 2.58 – 2.53 (m, 2H), 1.99 – 1.90 (m, 2H)

^{13}C NMR: (125 MHz, $CDCl_3$) δ 170.6, 137.9, 137.2, 134.8, 130.1, 129.1, 127.5, 124.0, 115.0, 64.5, 53.2, 33.6, 29.9

IR: (neat film, NaCl) 2950, 1738, 1432, 1256, 1205, 1022, 912, 748, 674 cm^{-1}

HRMS: (ESI^+) *m/z* calc'd for $C_{15}H_{17}BrO_4Na$ $[M+Na]^+$: 363.0205 found 363.0209



2-(2-(5-Allyl-2,2-dimethyl-1,3-dioxan-5-yl)phenyl)-4,4,5,5-tetramethyl-1,3,2-dioxaborolane (**149**): To a flame-dried flask equipped with stir bar was added compound **145** (4.20 g, 12.8 mmol, 1.0 equiv). The flask was purged and backfilled with nitrogen three times. CH_2Cl_2 (32 mL) was added and the stirred solution was cooled to –78 °C. DIBAL–H (neat, 16.0 mL, 89.6 mmol, 7 equiv) was added dropwise and the solution was allowed to warm to ambient temperature over the course of three hours and stirred for an additional twelve hours at the same temperature. After this time, the solution was cooled to 0 °C. EtOAc (10 mL) was added carefully. Then Et_2O (250 mL) was added followed by aqueous Rochelle's salt solution (250 mL) and stirred vigorously until two relatively clear layers formed. The layers were separated and the aqueous layer was extracted with EtOAc (3x75 mL). The combined organic layers were washed with brine, dried over Na_2SO_4 and concentrated under reduced pressure to give a colorless oil (2.40 g) that was used without further purification.

The crude oil (2.40 g) was added to a flame-dried flask with stir bar. CH_2Cl_2 (44 mL) was added followed by 2,2,-dimethoxypropane (6.5 mL, 53.1 mmol, 6 equiv), and the resulting solution was cooled to 0 °C. Pyridinium *p*-toluenesulfonate (0.222 g, 0.885 mmol, 10 mol %) was added. The reaction was warmed to ambient temperature and stirred for two hours, after which time TLC indicated consumption of the diol. The solution was cooled to 0 °C and satd. Aq. $NaHCO_3$ (50 mL) was added. The layers were separated, and the aqueous layer was extracted with CH_2Cl_2 (3x20 mL). The combined organic layers were washed with

brine, dried over Na_2SO_4 and concentrated under reduced pressure to give a colorless oil (2.2 g).

The crude oil (2.2 g) was azeotroped with benzene then dried under high vacuum for >2 hours. After this time an oven-dried stir bar was added followed by THF (44 mL) and the solution was cooled to –78 °C. *n*-BuLi (2.5 M in hexanes, 5.32 mL, 13.3 mmol, 1.5 equiv) was added dropwise at –78 °C and stirred for one hour. Isopropylpinacolylborate (3.25 mL, 15.93 mmol, 1.8 equiv) was added dropwise at –78 °C. The solution was then warmed to 0 °C and stirred for two hours. The reaction was quenched with water 50 mL. The layers were separated and the aqueous layer was extracted with EtOAc (3x15 mL). The combined organic layers were washed with brine, dried over Na_2SO_4, and concentrated under reduced pressure. The crude residue was purified by flash column chromatography (0 → 30% Et_2O in hexanes) to afford compound **149** as a colorless oil (1.592 g, 53% yield over 3 steps).

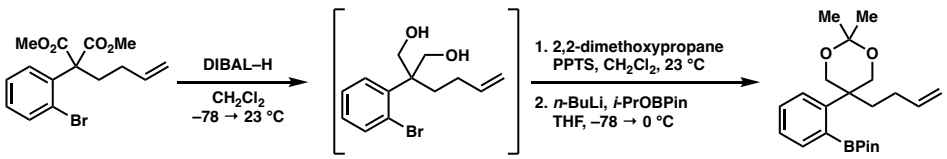
^{1}H NMR: (400 MHz, $CDCl_3$) δ 7.63 (dd, *J* = 7.4, 1.7 Hz, 1H), 7.35 (td, *J* = 7.5, 1.6 Hz, 1H), 7.25 – 7.18 (m, 2H), 5.39 (ddt, *J* = 17.4, 10.1, 7.3 Hz, 1H), 5.02 (ddt, *J* = 17.0, 2.4, 1.3 Hz, 1H), 4.92 (ddd, *J* = 10.1, 2.3, 1.1 Hz, 1H), 4.15 (s, 4H), 2.84 (dt, *J* = 7.4, 1.2 Hz, 2H), 1.48 (s, 3H), 1.38 (overlapping singlets, 15H).

^{13}C NMR: (100 MHz, $CDCl_3$) δ 146.6, 135.6, 134.4, 129.9, 126.7, 125.8, 117.7, 98.0, 84.2, 67.6, 41.2, 39.3, 26.3, 24.9, 21.7 *One aromatic signal is not observed due to boron quadrupolar relaxation.*

^{11}B NMR: (128 MHz, $CDCl_3$) δ 32.5. Externally referenced to BF_3•OEt_2 (δ 0.0)

IR: (neat film, NaCl) 3070, 2980, 2938, 2870, 1488, 1436, 1372, 1340, 1304, 1200, 1144, 1090, 916, 860, 838, 760, 748, 670 cm^{-1}

HRMS: (ESI^+) *m/z* calc'd for $C_{21}H_{32}BO_4$ $[M+H]^+$: 359.2388 found 359.2390



2-(2-(5-(But-3-en-1-yl)-2,2-dimethyl-1,3-dioxan-5-yl)phenyl)-4,4,5,5-tetramethyl-1,3,2-dioxaborolane (**150**): To a flame-dried flask equipped with stir bar was added compound **146** (4.78 g, 14.00 mmol, 1.0 equiv). The flask was purged and backfilled with nitrogen three times. CH_2Cl_2 (46 mL) was added and the stirred solution was cooled to –78 °C. DIBAL–H (neat, 17.47 mL, 98.0 mmol, 7 equiv) was added dropwise and the solution was allowed to warm to ambient temperature over the course of 3 hours, and stirred for an additional 12 hours at this temperature. After this time, the solution was cooled to 0 °C. EtOAc (10 mL) was added carefully. Then Et_2O (250 mL) was added followed by aqueous Rochelle's salt solution (250 mL) and stirred vigorously until two relatively clear layers formed. The layers were separated and the aqueous layer was extracted with EtOAc (3x75 mL). The combined organic layers were washed with brine (100 mL), dried over Na_2SO_4 and concentrated under reduced pressure to give a crude oil (2.8 g) that was used without further purification.

The crude oil (2.8 g) was added to a flame dried flask with stir bar. CH_2Cl_2 (43 mL) was added followed by 2,2,-dimethoxypropane (6.32 mL, 51.6 mmol, 6 equiv), and the resulting solution was cooled to 0 °C. Pyridinium *p*-toluenesulfonate (0.216 g, 0.859 mmol, 10 mol %) was added. The reaction was warmed to ambient temperature and stirred for 2 hours, after which time TLC indicated consumption of the diol. The solution was cooled to 0 °C and satd. aq. $NaHCO_3$ (50 mL) was added. The layers were separated, and the aqueous layer was extracted with CH_2Cl_2 (3x20 mL). The combined organic layers were washed with brine (100 mL), dried over Na_2SO_4 and concentrated under reduced pressure to give a colorless oil (2.3 g).

The crude oil (2.3 g) was azeotroped with benzene then dried under high vacuum for >2 hours. After this time an oven-dried stir bar was added followed by THF (35 mL) and the solution was cooled to –78 °C. *n*-BuLi (2.5 M in hexanes, 4.25 mL, 10.6 mmol, 1.5 equiv) was added dropwise at –78 °C and stirred for 1 hour. Isopropylpinacolylborate (2.60 mL, 12.74 mmol, 1.8 equiv) was added dropwise at –78 °C. The solution was then warmed to 0 °C and stirred for 2 hours. The reaction was quenched with water (50 mL). The layers were separated and the aqueous layer was extracted with EtOAc (3x15 mL). The combined organic layers were washed with brine (100 mL), dried over Na_2SO_4, and concentrated under reduced pressure. The crude residue was purified by flash column chromatography (0 → 30% Et_2O in hexanes) to afford compound **150** as a colorless oil (1.975 g, 38% yield over 3 steps).

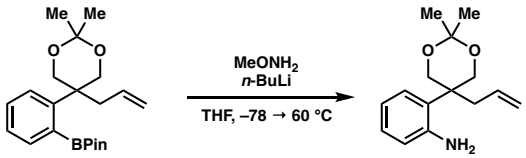
^{1}H NMR: (400 MHz, $CDCl_3$) δ 7.60 (dd, *J* = 7.4, 1.6 Hz, 1H), 7.36 (ddd, *J* = 8.0, 7.1, 1.6 Hz, 1H), 7.30 (dd, *J* = 8.0, 1.3 Hz, 1H), 7.22 (td, *J* = 7.3, 1.3 Hz, 1H), 5.73 (ddt, *J* = 16.8, 10.2, 6.5 Hz, 1H), 4.92 (dq, *J* = 17.1, 1.7 Hz, 1H), 4.86 (ddt, *J* = 10.2, 2.2, 1.2 Hz, 1H), 4.21 (d, *J* = 11.6 Hz, 2H), 4.12 (d, *J* = 11.6 Hz, 2H), 2.13 – 2.04 (m, 2H), 1.70 (dddd, *J* = 9.1, 6.4, 3.9, 1.4 Hz, 2H), 1.47 (s, 3H), 1.39 – 1.35 (overlapping singlets, 15H)

^{13}C NMR: (100 MHz, $CDCl_3$) δ 146.7, 139.0, 135.4, 129.8, 127.0, 125.7, 114.3, 98.1, 84.2, 68.2, 41.7, 34.3, 28.3, 25.6, 25.0, 22.4. *One aromatic signal is not observed due to boron quadrupolar relaxation.*

^{11}B NMR: (128 MHz, $CDCl_3$) δ 32.9. Externally referenced to BF_3•OEt_2 (δ 0.0)

IR: (neat film, NaCl) 3066, 2978, 2936, 2862, 1436, 1372, 1340, 1302, 1258, 1144, 1090, 1050, 858, 838, 752, 670 cm^{-1}

HRMS: (ESI$^+$) *m/z* calc'd for $C_{22}H_{34}BO_4$ $[M+H]^+$: 373.2545 found 373.2542



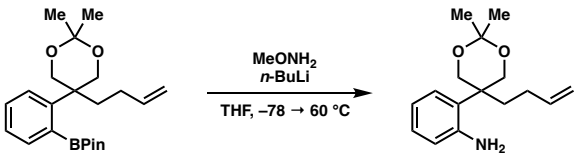
2-(5-Allyl-2,2-dimethyl-1,3-dioxan-5-yl)aniline (**151**): To a flame dried flask with stir bar was added a THF solution of $MeONH_2$ (1.6 M, 12.9 mL, 20.65 mmol, 4.6 equiv) followed by an addition 60 mL of THF. The solution was cooled to –78 °C and stirred for 10 minutes. *n*-BuLi (2.5 M, 8.3 mL, 20.65 mmol, 4.6 equiv) was added dropwise. The resulting solution was stirred at –78 °C for 30 minutes. BPin **149** (1.592 g, 4.44 mmol, 1.0 equiv) was added dropwise as a solution in THF (10 mL). The resulting solution was stirred 5 minutes at –78 °C, then the cooling bath was removed and the solution was allowed to warm to ambient temperature (~30 mins). After warming to ambient temperature, the reaction mixture was heated to 60 °C for an additional 15 hours. After this time, the reaction was cooled to 0 °C and quenched by the addition of water (150 mL). EtOAc (50 mL) was added, the layers were separated, and the aqueous layer was extracted with EtOAc (3x50 mL). The combined organic extracts were washed with brine, dried over Na_2SO_4 and concentrated under reduced pressure. The crude residue was purified by flash column chromatography (30 → 50% Et_2O in hexanes) to afford aniline **151** as a pale yellow oil (972 mg, 88% yield).

^{1}H NMR: (500 MHz, $CDCl_3$) δ 7.10 – 7.01 (m, 2H), 6.75 – 6.70 (m, 1H), 6.67 (dd, *J* = 7.8, 1.4 Hz, 1H), 5.64 (ddt, *J* = 17.1, 10.1, 6.9 Hz, 1H), 5.15 (dd, *J* = 17.0, 1.8 Hz, 1H), 5.08 – 5.01 (m, 1H), 4.41 (s, 2H), 4.08 (d, *J* = 11.9 Hz, 2H), 3.87 (d, *J* = 11.9 Hz, 2H), 2.86 (dt, *J* = 7.0, 1.4 Hz, 2H), 1.48 (s, 3H), 1.44 (s, 3H)

^{13}C NMR: (125 MHz, $CDCl_3$) δ 145.9, 134.2, 128.3, 127.8, 125.5, 118.1, 118.1, 118.1, 99.5, 66.3, 42.3, 39.1, 25.0, 23.2.

IR: (neat film, NaCl) 3460, 3362, 2988, 2876, 1640, 1498, 1450, 1372, 1258, 1226, 1200, 1162, 1088, 920, 834, 746 cm^{-1}.

HRMS: (ESI^+) *m/z* calc'd for $C_{15}H_{21}NO_2$ $[M+H]^+$: 248.1645 found 248.1647



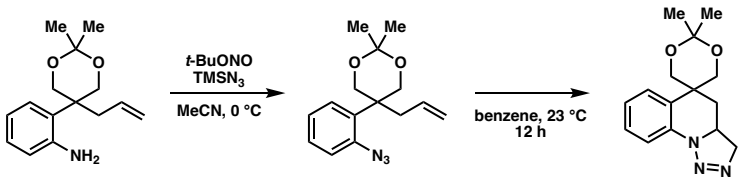
2-(5-(But-3-en-1-yl)-2,2-dimethyl-1,3-dioxan-5-yl)aniline (**152**): To a flame dried flask with stir bar was added a THF solution of $MeONH_2$ (1.8 M, 8.85 mL, 15.93 mmol, 3.0 equiv) followed by an additional 48 mL of THF. The solution was cooled to –78 °C and stirred for 10 minutes. *n*-BuLi (2.5 M, 6.37 mL, 15.93 mmol, 3.0 equiv) was added dropwise. The resulting solution was stirred at –78 °C for 30 minutes. BPin **150** (1.975 g, 5.31 mmol, 1.0 equiv) was added dropwise as a solution in THF (14 mL). The resulting solution was stirred 5 minutes at –78 °C, then the cooling bath was removed, and the solution was allowed to warm to ambient temperature (~30 mins). After warming to ambient temperature, the reaction mixture was heated to 60 °C for an additional 15 hours. After this time, the reaction was cooled to 0 °C and quenched by the addition of water (150 mL). Ethyl acetate (50 mL) was added, the layers were separated, and the aqueous layer was extracted with EtOAc (3x50 mL). The combined organic extracts were washed with brine (50 mL), dried over Na_2SO_4 and concentrated under reduced pressure. The crude residue was purified by flash column chromatography (30 → 50% Et_2O in hexanes) to afford aniline **152** as a colorless oil (1.049 g, 76% yield).

^{1}H NMR: (500 MHz, $CDCl_3$) δ 7.09 – 7.00 (m, 2H), 6.77 – 6.70 (m, 1H), 6.66 (dd, *J* = 7.9, 1.4 Hz, 1H), 5.83 (ddt, *J* = 16.7, 10.1, 6.4 Hz, 1H), 5.01 (dt, *J* = 17.1, 1.8 Hz, 1H), 4.95 (dd, *J* = 10.2, 1.8 Hz, 1H), 4.33 (br s, 2H), 4.13 (d, *J* = 11.8 Hz, 2H), 3.90 (d, *J* = 11.9 Hz, 2H), 2.16 – 2.09 (m, 2H), 1.94 – 1.86 (m, 2H), 1.49 (s, 3H), 1.43 (s, 3H)

^{13}C NMR: (125 MHz, $CDCl_3$) δ 146.0, 138.7, 128.3, 127.8, 125.3, 118.3, 118.2, 114.6, 99.3, 66.9, 42.4, 33.6, 28.4, 24.9, 23.2.

IR: (neat film, NaCl) 1456, 3366, 3076, 2990, 2940, 2876, 1640, 1500, 1450, 1374, 1258, 1226, 1200, 1166, 1090, 912, 834, 750 cm^{-1}

HRMS: (ESI^+) *m/z* calc'd for $C_{16}H_{24}NO_2$ $[M+H]^+$: 262.1802 found 262.1803



2',2'-Dimethyl-3a,4-dihydro-3H-spiro[[1,2,3]triazolo[1,5-a]quinoline-5,5'-[1,3]dioxane] (**155**): To a flame-dried test tube with stir bar was added aniline **151** (100 mg, 0.40 mmol, 1.0 equiv). The vessel was evacuated and backfilled with nitrogen three times. Acetonitrile (2.0 mL) was added and the solution was cooled to 0 °C. *Tert*-butyl nitrite (167 mg, 0.192 mL, 1.6 mmol, 4.0 equiv) was added and the solution was stirred for five minutes. Then $TMSN_3$ (140 mg, 0.16 mL, 1.2 mmol, 3.0 equiv) was added dropwise. After fifteen minutes bubbling ceased, and TLC analysis indicated complete consumption of the aniline. The reaction was warmed to ambient temperature, concentrated under reduced pressure and purified by flash column chromatography (1 → 5 → 10% Et_2O in hexanes) to give azide **153** as a colorless oil (100 mg, 91% yield). *Note: Azide **153** rapidly undergoes intramolecular cycloaddition (half life ~3 h in solution). Concentration of the crude reaction mixture should be performed with bath temperatures ≤ 25 °C, and flash column purification should be performed with haste. As such, it was not possible to obtain sufficiently pure samples of azide **153** without contamination of triazoline **155**, therefore, characterization data are only reported for the triazoline product **155** following cycloaddition.*

To the obtained azide **153** (100 mg, 0.365 mmol, 1.0 equiv) in a 20 mL vial was added benzene (5 mL). The vial was flushed with nitrogen and the solution was allowed to stir at ambient temperature for 12 hours, protected from light. After this time, the reaction mixture was concentrated under reduced pressure. Hexanes (5 mL) were added causing precipitation of a white solid. The mixture was concentrated under reduced pressure, hexanes (5 mL) were again added, the mixture was filtered, and triazoline **155** was collected as a

white crystalline solid (67 mg, 61% yield over 2 steps, 67% yield from azide **153**). *This triazoline proved more sensitive than the seven-membered analog. Therefore, it was not stored for periods >1 week and was protected from light, as prolonged exposure to light (>24 hours at ambient temperature) resulted in discoloration of the solid.* Crystals for X-ray analysis were grown by layer diffusion of heptane into a solution of **155** dissolved in minimal Et_2O at –20 °C (protected from light).

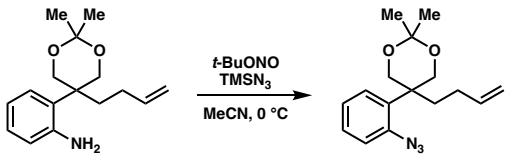
^{1}H NMR: (400 MHz, C_6D_6) δ 7.90 (dd, *J* = 8.1, 1.3 Hz, 1H), 7.20 (dd, *J* = 7.9, 1.4 Hz, 1H), 7.08 (ddd, *J* = 8.1, 7.3, 1.4 Hz, 1H), 6.87 (ddd, *J* = 7.9, 7.3, 1.3 Hz, 1H), 4.01 (d, *J* = 11.6 Hz, 1H), 3.84 (dd, *J* = 16.6, 11.3 Hz, 1H), 3.68 (dd, *J* = 12.0, 1.6 Hz, 1H), 3.60 (dd, *J* = 16.7, 7.1 Hz, 1H), 3.37 (dd, *J* = 12.0, 2.2 Hz, 1H), 3.07 – 2.94 (m, 2H), 2.22 – 2.13 (m, 1H), 1.42 (s, 3H), 1.34 (s, 3H), 0.70 – 0.58 (m, 1H).

^{13}C NMR: (100 MHz, C_6D_6) δ 138.8, 127.0, 125.2, 122.9, 119.1, 98.3, 72.4, 69.6, 67.2, 46.8, 36.5, 32.3, 28.0, 19.9. *One aromatic signal is obscured by C_6D_6.*

IR: (neat film, NaCl) 3040, 2990, 2942, 2874, 1604, 1484, 1454, 1372, 1258, 1200, 1158, 1092, 1010, 906, 830, 756 cm^{-1}.

HRMS: (ESI^+) *m/z* calc'd for $C_{15}H_{19}NO_2$ $[M–N_2]^+$: 246.1489 found 246.1483.

MP: 92 °C (dec.).



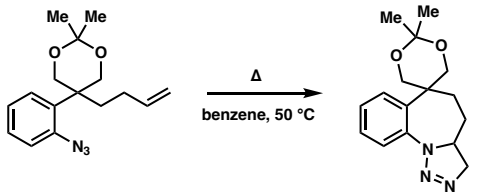
5-(2-Azidophenyl)-5-(but-3-en-1-yl)-2,2-dimethyl-1,3-dioxane (**154**): To a flame dried flask with stir bar was added aniline **152** (0.999 g, 3.82 mmol, 1.0 equiv). The flask was evacuated and backfilled with nitrogen three times. Acetonitrile (19 mL) was added and the solution was cooled to 0 °C. *Tert*-butyl nitrite (1.82 mL, 15.28 mmol, 4.0 equiv) was added and the resulting solution was stirred for 5 minutes. Then $TMSN_3$ (1.51 mL, 11.46 mmol, 3.0 equiv) was added dropwise. The solution was maintained at 0 °C for 10 minutes then warmed to ambient temperature. After maintaining at ambient temperature for an additional 15 minutes, TLC analysis indicated complete consumption of the starting material. The reaction mixture was concentrated under reduced pressure and purified by flash column chromatography (0 → 20% Et_2O in hexanes) to afford azide **154** as a colorless oil (0.921 g, 84% yield).

^{1}H NMR: (400 MHz, C_6D_6) δ 7.27 – 7.21 (m, 1H), 6.89 – 6.83 (m, 2H), 6.71 – 6.67 (m, 1H), 5.66 (ddt, *J* = 16.8, 10.2, 6.5 Hz, 1H), 4.94 – 4.84 (m, 2H), 4.21 – 4.16 (m, 2H), 3.96 (d, *J* = 11.8 Hz, 2H), 2.14 – 2.07 (m, 2H), 1.68 – 1.53 (m, 2H), 1.42 (s, 3H), 1.30 (s, 3H).

^{13}C NMR: (100 MHz, C_6D_6) δ 139.0, 138.2, 133.3, 130.3, 128.2, 124.8, 119.6, 114.5, 98.2, 67.2, 41.2, 32.1, 28.8, 24.3, 23.9.

IR: (neat film, NaCl) 3080, 2990, 2938, 2870, 2126, 1484, 1444, 1370, 1288, 1258, 1200, 1092, 910, 844, 834, 750 cm^{-1}.

HRMS: (ESI^+) *m/z* calc'd for $C_{16}H_{22}N_3O_2$ $[M+H]^+$: 288.1707 found 288.1710.



2',2'-Dimethyl-3,3a,4,5-tetrahydrospiro[benzo[f][1,2,3]triazolo[1,5-a]azepine-6,5'-[1,3]dioxane] (**156**): Azide **154** (0.920 g, 3.20 mmol, 1.0 equiv) was charged to a flask followed by benzene (64 mL). The flask was flushed with nitrogen then heated to 50 °C in a heating block for 96 h under a nitrogen atmosphere. After this time, an NMR aliquot indicated complete consumption of the starting azide. The solution was cooled to ambient temperature and concentrated under reduced pressure. 50 mL of hexanes were added to the flask, causing precipitation of a white solid. This mixture was again concentrated under reduced pressure. Hexanes (50 mL) were again added, and the mixture was filtered. The solid residue was washed with hexanes (10 mL) and dried under vacuum to give triazoline **156** as a white crystalline solid (0.454 g, 49% yield). ***156*** *is stable at ambient temperature for several months without showing signs of decomposition, however, as a precaution it was protected from light during prolonged storage.* Crystals suitable for X-ray analysis were grown by layer diffusion of pentane into a solution of **156** in minimal CH_2Cl_2.

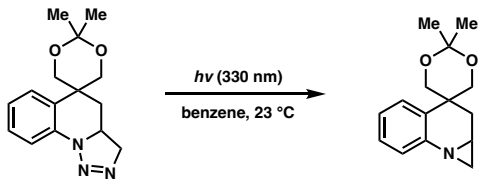
^{1}H NMR: (400 MHz, C_6D_6) δ 7.61 (dt, *J* = 7.9, 1.0 Hz, 1H), 7.03 – 6.97 (m, 1H), 6.95 – 6.92 (m, 2H), 4.35 (dd, *J* = 12.1, 2.7 Hz, 1H), 4.21 (d, *J* = 11.1 Hz, 1H), 4.15 (dd, *J* = 16.6, 11.0 Hz, 1H), 3.65 – 3.54 (m, 2H), 3.31 (dd, *J* = 16.6, 13.3 Hz, 1H), 2.59 – 2.44 (m, 2H), 1.66 – 1.53 (m, 1H), 1.46 (s, 3H), 1.39 (ddt, *J* = 14.3, 4.4, 3.2 Hz, 1H), 1.23 (s, 3H), 0.95 (td, *J* = 13.7, 3.2 Hz, 1H).

^{13}C NMR: (101 MHz, C_6D_6) δ 144.4, 134.9, 128.0, 126.3, 125.7, 122.5, 98.2, 74.3, 68.7, 63.7, 59.0, 39.7, 29.13, 29.11, 27.8, 20.3.

IR: (neat film, NaCl) 2990, 2940, 2858, 1508, 1486, 1450, 1386, 1370, 1202, 1170, 1094, 1058, 978, 832, 756, 684, 676, 648 cm^{-1}.

HRMS: (ESI^+) *m/z* calc'd for $C_{16}H_{22}N_3O_2$ $[M+H]^+$: 288.1707 found 288.1715.

MP: 127 °C (dec.)



2',2'-Dimethyl-1a,2-dihydro-1H-spiro[azirino[1,2-a]quinoline-3,5'-[1,3]dioxane] (**157**): Triazoline **155** (62 mg, 0.2268 mmol) was charged to a flask with stir bar and 4.5 mL of benzene were added. Argon gas was bubbled through the solution for 5 minutes with stirring to remove oxygen then sealed. The flask was placed in a Lutzchem photobox equipped with Hitachi F8T5-BLB UVA lamps centered at 350 nm and irradiated for 4 hours. After this time the solution was concentrated under reduced pressure. The crude aziridine was purified by flash column chromatography (10 → 50% EtOAc in hexanes) to afford aziridine **157** as a crystalline solid (50 mg, 90% yield). Crystals suitable for X-ray diffraction were grown by adding dissolving **157** in minimal Et_2O and carefully layering with pentane.

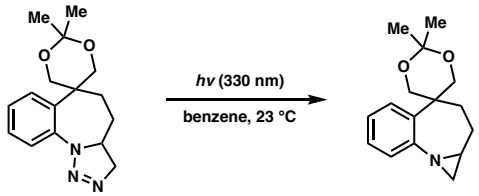
^{1}H NMR: (400 MHz, C_6D_6) δ 7.28 (ddd, *J* = 7.7, 2.5, 1.4 Hz, 2H), 7.08 (ddd, *J* = 7.9, 7.3, 1.5 Hz, 1H), 6.89 (td, *J* = 7.5, 1.3 Hz, 1H), 4.20 (d, *J* = 11.5 Hz, 1H), 4.01 (dd, *J* = 11.7, 1.9 Hz, 1H), 3.78 (dd, *J* = 11.8, 1.2 Hz, 1H), 3.38 (dd, *J* = 11.5, 1.8 Hz, 1H), 2.67 (dd, *J* = 13.4, 7.2 Hz, 1H), 2.35 (dddd, *J* = 8.2, 7.2, 4.7, 3.5 Hz, 1H), 2.18 (dd, *J* = 4.7, 1.2 Hz, 1H), 1.48 (s, 3H), 1.38 (s, 3H), 1.20 (dd, *J* = 3.5, 1.2 Hz, 1H), 0.60 (ddd, *J* = 13.4, 8.3, 1.2 Hz, 1H).

^{13}C NMR: (100 MHz, C_6D_6) δ 150.0, 132.5, 128.6, 125.2, 124.3, 122.5, 98.3, 67.5, 67.2, 42.1, 36.0, 30.2, 29.7, 26.2, 21.8.

IR: (neat film, NaCl) 2990, 2862, 1484, 1450, 1370, 1312, 1196, 1088, 984, 834, 750 cm^{-1}.

HRMS: (ESI^+) *m/z* calc'd for $C_{15}H_{20}NO_2$ $[M+H]^+$: 246.1489 found 246.1487.

MP: 86–90 °C



2',2'-Dimethyl-1,1a,2,3-tetrahydrospiro[azirino[1,2-a]benzo[f]azepine-4,5'-[1,3]dioxane] (**158**): Triazoline **156** (0.365 g, 1.27 mmol) was charged to a flask with stir bar and 25 mL of benzene were added. Argon gas was bubbled through the solution for 5 minutes with stirring to remove oxygen and sealed. The flask was placed in a Lutzchem photobox equipped with Hitachi F8T5-BLB UVA lamps centered at 350 nm and irradiated for 8 hours. After this time the solution was concentrated under reduced pressure. The crude aziridine was purified by flash column chromatography (10 → 50% EtOAc in hexanes) to afford aziridine **158** as a crystalline solid (0.260 g, 79% yield). Crystals suitable for X-ray diffraction were grown by adding one drop of EtOAc to 3 mg of aziridine **158**, heating the sealed vial to 80 °C, and allowing the solution to slowly cool to ambient temperature.

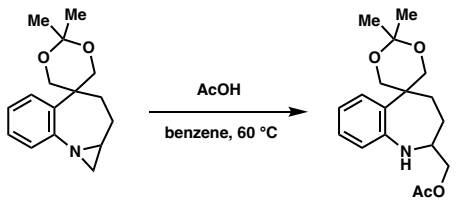
^{1}H NMR: (400 MHz, C_6D_6) δ 7.11 – 7.00 (m, 2H), 6.92 – 6.87 (m, 1H), 6.86 (dd, *J* = 7.8, 1.4 Hz, 1H), 4.64 (dd, *J* = 11.7, 1.9 Hz, 1H), 4.46 – 4.38 (m, 1H), 4.15 (d, *J* = 11.3 Hz, 1H), 3.70 (d, *J* = 1.9 Hz, 1H), 2.22 (ddd, *J* = 14.4, 13.1, 5.4 Hz, 1H), 2.13 (d, *J* = 4.7 Hz, 1H), 1.98 (dtd, *J* = 11.1, 4.3, 2.8 Hz, 1H), 1.66 (ddt, *J* = 14.3, 5.1, 2.3 Hz, 1H), 1.51 (s, 3H), 1.38 (d, *J* = 3.5 Hz, 1H), 1.30 (s, 3H), 1.15 – 1.03 (m, 1H), 0.72 (dddd, *J* = 14.3, 13.1, 11.4, 5.5 Hz, 1H).

^{13}C NMR: (100 MHz, C_6D_6) δ 151.5, 130.1, 126.7, 122.7, 122.2, 98.1, 69.9, 67.7, 39.4, 38.3, 35.4, 28.8, 26.7, 25.8, 22.5. *One carbon signal is obscured by C_6D_6.*

IR: (neat film, NaCl) 3054, 2986, 2924, 2860, 1482, 1446, 1370, 1312, 1260, 1196, 1166, 1090, 838, 762, 748 cm^{-1}.

HRMS: (ESI^+) *m/z* calc'd for $C_{16}H_{22}NO_2$ $[M+H]^+$: 260.1645 found 260.1651.

MP: 96–99 °C



(2',2'-Dimethyl-1,2,3,4-tetrahydrospiro[benzo[b]azepine-5,5'-[1,3]dioxan]-2-yl)methyl acetate (**159**): To a 1 Dr vial with stir bar was added aziridine **158** (20 mg, 0.077 mmol, 1.0 equiv). Benzene (0.77 mL) was added followed by AcOH (22 μL, 0.385 mmol, 5.0 equiv). The vial was flushed with argon, sealed, and heated to 60 °C for 24 hours. After this time the vial was cooled to ambient temperature and concentrated under reduced pressure. The residue was re-dissolved in EtOAc (1 mL) and cautiously quenched with satd. aq. $NaHCO_3$ (1 mL). The layers were separated and the aqueous layer was extracted with EtOAc (2x1 mL). The combined organic layers were washed with brine, dried over Na_2SO_4 and concentrated under reduced pressure. The crude residue was purified by flash column chromatography (20 → 60 % Et_2O in hexanes) to give acetyl compound **159** as a white amorphous solid (11.6 mg, 47% yield). Synthesis of **159** beginning with triazoline **156** was performed in an analogous fashion at ambient temperature instead of 60 °C. Flash column chromatography afforded imine **166** in sufficient purity for structural assignment.

^{1}H NMR: (400 MHz, C_6D_6) δ 7.12 (dd, *J* = 7.8, 1.6 Hz, 1H), 6.97 (td, *J* = 7.5, 1.6 Hz, 1H), 6.89 (td, *J* = 7.5, 1.4 Hz, 1H), 6.54 (dd, *J* = 7.7, 1.4 Hz, 1H), 4.44 (dd, *J* = 11.7, 2.2 Hz, 1H), 4.23 (d, *J* = 11.3 Hz, 1H), 4.03 (d, *J* = 11.6 Hz, 1H), 3.96 – 3.84 (m, 2H), 3.66 (dd, *J* = 11.2, 9.0 Hz, 1H), 3.49 (s, 1H), 2.78 (dddd, *J* = 10.3, 9.1, 3.7, 2.8 Hz, 1H), 2.24 (ddd, *J* = 15.1, 7.0, 3.3 Hz, 1H), 1.62 (m, 4H), 1.49 (s, 3H), 1.47 – 1.33 (m, 2H), 1.31 (s, 3H)

^{13}C NMR: (100 MHz, C_6D_6) δ 169.9, 148.4, 134.8, 127.5, 127.2, 122.5, 122.4, 98.1, 68.2, 67.5, 65.1, 57.0, 39.8, 29.8, 27.7, 26.9, 21.4, 20.3

IR: (neat film, NaCl) 3356, 2990, 2940, 2868, 1744, 1602, 1474, 1370, 1234, 1200, 1088, 1044, 972, 932, 836, 756 cm^{-1}

HRMS: (ESI$^+$) *m/z* calc'd for $C_{18}H_{25}NO_4$ $[M+H]^+$:320.1856 found 320.1858

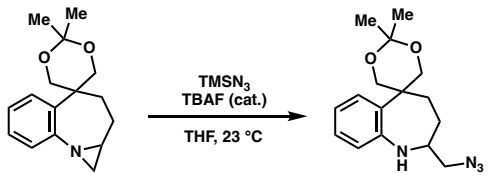
Characterization data for (**166**):

^{1}H NMR: (400 MHz, C_6D_6) δ 7.28 (ddd, J = 7.4, 1.5, 0.8 Hz, 1H), 7.14 (m, 2H), 6.97 (ddd, J = 8.1, 7.1, 1.5 Hz, 1H), 3.96 – 3.87 (m, 2H), 3.82 – 3.74 (m, 2H), 2.07 (t, J = 7.1 Hz, 2H), 1.91 (s, 3H), 1.75 (dd, J = 7.6, 6.7 Hz, 2H), 1.43 (s, 3H), 1.20 (s, 3H).

^{13}C NMR: (100 MHz, C_6D_6) δ 174.1, 150.3, 132.3, 126.5, 125.7, 124.7, 98.1, 68.2, 39.1, 38.6, 31.2, 27.2, 26.3, 21.7

IR: (neat film, NaCl) 2990, 2940, 2862, 1644, 1478, 1454, 1372, 1256, 1198, 1090, 1032, 838, 752, 745 cm^{-1}

HRMS: (ESI$^+$) *m/z* calc'd for $C_{16}H_{22}NO_2$ $[M+H]^+$: 260.1645 found 260.1640



2-(Azidomethyl)-2',2'-dimethyl-1,2,3,4-tetrahydrospiro[benzo[b]azepine-5,5'-[1,3]dioxane] (**160**): To a flame-dried 1 Dr vial with stir bar was added aziridine **158** (20 mg, 0.077 mmol, 1.0 equiv). The vial was purged and backfilled with nitrogen three times. THF (0.77 mL) was added, followed by $TMSN_3$ (20.3 μL, 0.154 mmol, 2.0 equiv) then TBAF (1.0 M in THF, 15 μL, 0.015 mmol, 20 mol %). The vial was then sealed and heated to 60 °C for 18 hours. After this time, the reaction mixture was passed through a plug of silica gel, eluting with EtOAc (2 mL). The filtrate was concentrated under reduced pressure. The crude reside was purified by flash column chromatography (10 → 30% Et_2O in hexanes) to give azide **160** as a colorless solid (18.9 mg, 81% yield). Crystals suitable for X-ray analysis were grown by dissolving **160** in minimal hot Et_2O, followed by addition of hexanes, and allowing to stand at –20 °C. Synthesis of **160** beginning with triazoline **156** was performed in an analogous fashion.

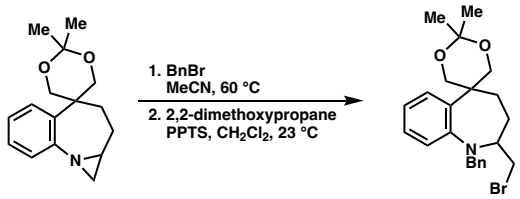
^{1}H NMR: (400 MHz, $CDCl_3$) δ 7.15 (dd, *J* = 7.8, 1.5 Hz, 1H), 7.10 (td, *J* = 7.5, 1.5 Hz, 1H), 6.97 (td, *J* = 7.6, 1.4 Hz, 1H), 6.81 (dd, *J* = 7.7, 1.4 Hz, 1H), 4.43 (dd, *J* = 11.8, 2.3 Hz, 1H), 4.32 (d, *J* = 11.4 Hz, 1H), 4.00 (d, *J* = 11.7 Hz, 1H), 3.95 (dd, *J* = 11.5, 2.3 Hz, 1H), 3.70 (s, 1H), 3.48 (dd, *J* = 12.2, 3.7 Hz, 1H), 3.26 (dd, *J* = 12.2, 10.1 Hz, 1H), 2.97 (tt, *J* = 9.7, 3.6 Hz, 1H), 2.30 (ddd, *J* = 13.9, 6.1, 3.5 Hz, 1H), 1.86 – 1.67 (m, 2H), 1.60 (ddd, *J* = 14.9, 10.7, 4.1 Hz, 1H), 1.46 (s, 3H), 1.42 (s, 3H)

^{13}C NMR: (100 MHz, $CDCl_3$) δ 147.6, 134.2, 127.7, 126.6, 122.8, 122.4, 98.2, 67.9, 64.9, 56.8, 56.2, 39.5, 29.4, 28.7, 26.9, 21.1

IR: (neat film, NaCl) 3338, 2992, 2936, 2868, 2100, 1602, 1472, 1454, 1372, 1258, 1200, 1084, 836, 756, 682 cm^{-1}

HRMS: (ESI^+) *m/z* calc'd for $C_{16}H_{23}N_4O_2$ $[M+H]^+$: 303.1816 found 303.1815

MP: 93–96 °C



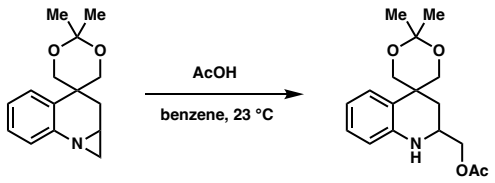
1-Benzyl-2-(bromomethyl)-2',2'-dimethyl-1,2,3,4-tetrahydrospiro[benzo[b]azepine-5,5'-[1,3]dioxane] (**161**): To a flame-dried 1 Dr vial with stir bar was added aziridine **158** (20 mg, 0.077 mmol, 1.0 equiv). The vial was evacuated and backfilled with nitrogen three times. Acetonitrile (0.26 mL) was added followed by BnBr (15.8 mg, 11 µL, 0.093 mmol, 1.2 equiv). The vial was sealed and heated to 60 °C for 18 h. After this time, the reaction mixture was concentrated under reduced pressure. Dry CH_2Cl_2 (0.25 mL) was added to the crude reaction mixture followed by 2,2-dimethoxypropane (48 mg, 56 µL, 6 equiv) and PPTS (1.9 mg, 0.0077 mmol, 10 mol%). The reaction mixture was stirred under a nitrogen atmosphere for six hours, then satd. aq. $NaHCO_3$ (1 mL) was added. The layers were separated, and the aqueous layer was extracted with CH_2Cl_2 (3x1 mL). The combined organic extracts were washed with brine, dried over Na_2SO_4 and concentrated under reduced pressure. The crude residue was purified by flash column chromatography (0 → 20% Et_2O in hexanes) to give **37** as a white foam (21.6 mg, 65% yield).

^{1}H NMR: (400 MHz, C_6D_6) δ 7.24 (dt, *J* = 8.7, 2.1 Hz, 3H), 7.14 – 7.00 (m, 4H), 6.99 – 6.94 (m, 1H), 6.91 (dd, *J* = 7.9, 1.4 Hz, 1H), 4.49 (d, *J* = 11.4 Hz, 1H), 4.20 (d, *J* = 11.3 Hz, 1H), 4.12 – 4.01 (m, 3H), 3.57 (dd, *J* = 11.4, 1.8 Hz, 1H), 3.29 (dq, *J* = 8.1, 5.3 Hz, 1H), 3.12 (dd, *J* = 10.1, 5.5 Hz, 1H), 2.63 (dd, *J* = 10.1, 8.4 Hz, 1H), 1.94 – 1.75 (m, 2H), 1.45 (s, 3H), 1.34 (m, 4H), 1.23 – 1.11 (m, 1H)

^{13}C NMR: (100 MHz, C_6D_6) δ 147.2, 138.8, 137.6, 129.7, 128.8, 127.7, 127.5, 127.4, 123.8, 123.3, 98.0, 69.1, 66.0, 57.9, 57.8, 40.2, 32.4, 27.7, 26.6, 25.6, 22.7

IR: (neat film, NaCl) 2990, 2936, 2860, 1594, 1492, 1452, 1370, 1254, 1198, 1092, 930, 834, 754, 700 cm^{-1}

HRMS: (ESI^+) *m/z* calc'd for $C_{23}H_{29}BrNO_2$ $[M+H]^+$: 430.1376 found 430.1372



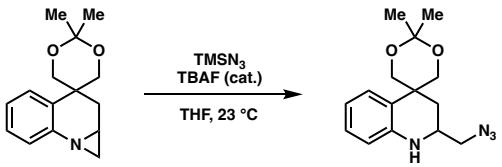
(2',2'-Dimethyl-2,3-dihydro-1H-spiro[quinoline-4,5'-[1,3]dioxan]-2-yl)methyl acetate (**162**): To a 1 Dr vial with stir bar was added aziridine **157** (10 mg, 0.0408 mmol, 1.0 equiv) followed by benzene (0.4 mL) and acetic acid (14.7 mg, 14 μL, 0.245, 6.0 equiv). The vial was flushed with nitrogen and stirred at ambient temperature for 24 hours. After this time, the reaction was concentrated under reduced pressure. The residue was dissolved in EtOAc (1 mL) and satd. aq. $NaHCO_3$ (1 mL) was carefully added. The layers were separated and the aqueous layer was extracted with EtOAc (2x1 mL). The combined organic extracts were washed with brine, dried over Na_2SO_4 and concentrated under reduced pressure. The crude residue was purified by flash column chromatography (5% Et_2O/45% CH_2Cl_2/50% hexanes) to give acetate **162** as an amorphous solid (6.3 mg, 51% yield). Synthesis of **162** from **155** was performed in an analogous fashion at 0 °C.

^{1}H NMR: (400 MHz, C_6D_6) δ 7.20 (dd, *J* = 7.8, 1.5 Hz, 1H), 6.97 (ddd, *J* = 8.1, 7.2, 1.4 Hz, 1H), 6.75 – 6.66 (m, 1H), 6.26 (dd, *J* = 8.0, 1.3 Hz, 1H), 4.19 (d, *J* = 11.5 Hz, 1H), 3.99 (dd, *J* = 11.0, 3.6 Hz, 1H), 3.82 (dd, *J* = 11.9, 1.7 Hz, 1H), 3.77 (s, 1H), 3.68 (dd, *J* = 11.0, 7.4 Hz, 1H), 3.60 (dd, *J* = 11.9, 2.2 Hz, 1H), 3.34 (dd, *J* = 11.5, 2.2 Hz, 1H), 3.20 – 3.09 (m, 1H), 2.51 (dd, *J* = 13.2, 2.6 Hz, 1H), 1.64 (s, 3H), 1.49 (s, 3H), 1.38 (s, 3H), 1.22 (ddd, *J* = 13.4, 11.9, 1.7 Hz, 1H)

^{13}C NMR: (101 MHz, C_6D_6) δ 170.0, 145.5, 127.9, 127.3, 122.7, 118.1, 115.4, 98.2, 70.2, 68.9, 68.1, 47.2, 35.7, 32.2, 28.3, 20.3, 19.9

IR: (neat film, NaCl) 3364, 2990, 2944, 2862, 1738, 1606, 1496, 1370, 1228, 10990, 1036, 828, 752 cm^{-1}

HRMS: (ESI^+) *m/z* calc'd for $C_{17}H_{24}NO_4$ $[M+H]^+$: 306.1700 found 306.1698



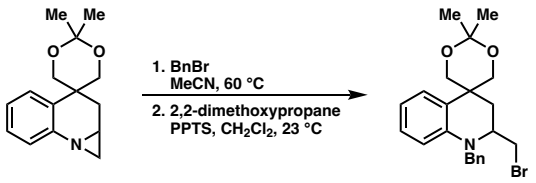
2-(Azidomethyl)-2',2'-dimethyl-2,3-dihydro-1H-spiro[quinoline-4,5'-[1,3]dioxane] (**163**): To a flame-dried 1 Dr vial with stir bar was added aziridine **157** (20 mg, 0.082 mmol, 1.0 equiv). The vial was purged and backfilled with nitrogen three times. THF (0.82 mL) was added, followed by $TMSN_3$ (18.8 mg, 21.4 µL, 0.163 mmol, 2.0 equiv) then TBAF (1.0 M in THF, 16.3 µL, 0.0163 mmol, 20 mol %). The vial was then sealed and stirred at ambient temperature for 18 hours. After this time, the reaction mixture was passed through a plug of silica gel, eluting with EtOAc (2 mL). The filtrate was concentrated under reduced pressure. The crude reside was purified by flash column chromatography (10 → 30% Et_2O in hexanes) to give azide **163** as a colorless solid (17.0 mg, 72% yield). Synthesis of azide **163** from triazoline **155** was performed in an analogous fashion.

^{1}H NMR: (400 MHz, C_6D_6) δ 7.13 (dd, *J* = 7.8, 1.5 Hz, 1H), 6.96 (ddd, *J* = 8.1, 7.2, 1.5 Hz, 1H), 6.70 (td, *J* = 7.5, 1.3 Hz, 1H), 6.22 (dd, *J* = 8.0, 1.3 Hz, 1H), 4.18 (d, *J* = 11.6 Hz, 1H), 3.78 (dd, *J* = 11.9, 1.7 Hz, 1H), 3.68 (s, 1H), 3.50 (dd, *J* = 11.9, 2.3 Hz, 1H), 3.29 (dd, *J* = 11.5, 2.3 Hz, 1H), 2.92 – 2.81 (m, 1H), 2.60 (dd, *J* = 11.8, 3.8 Hz, 1H), 2.52 (dd, *J* = 11.8, 8.7 Hz, 1H), 2.40 (dt, *J* = 13.2, 2.4 Hz, 1H), 1.50 (s, 3H), 1.36 (s, 3H), 1.04 (ddd, *J* = 13.4, 11.6, 1.7 Hz, 1H).

^{13}C NMR: (100 MHz, C_6D_6) δ 145.4, 128.0, 127.1, 122.6, 118.2, 115.6, 98.1, 70.2, 68.9, 56.5, 47.3, 35.8, 33.1, 28.7, 19.5

IR: (neat film, NaCl) 3664, 2990, 2940, 2870, 2104, 1606, 1490, 1448, 1268, 1194, 1090, 1032, 930, 830, 750 cm^{-1}

HRMS: (ESI^+) *m/z* calc'd for $C_{15}H_{21}N_4O_2$ $[M+H]^+$: 289.1659 found 289.1655



1-Benzyl-2-(bromomethyl)-2',2'-dimethyl-2,3-dihydro-1H-spiro[quinoline-4,5'-[1,3]dioxane] (**164**): To a flame-dried 1 Dr vial with stir bar was added aziridine **157** (20 mg, 0.082 mmol, 1.0 equiv). The vial was evacuated and backfilled with nitrogen three times. Acetonitrile (0.3 mL) was added followed by BnBr (16.7 mg, 11.6 µL, 0.098 mmol, 1.2 equiv). The vial was sealed and heated to 60 °C for 18 h. After this time, the reaction mixture was concentrated under reduced pressure. Dry CH_2Cl_2 (0.3 mL) was added to the crude reaction mixture followed by 2,2-dimethoxypropane (51 mg, 60 µL, 6 equiv) and PPTS (2.0 mg, 0.0082 mmol, 10 mol%). The reaction mixture was stirred under a nitrogen atmosphere for six hours, then satd. aq. $NaHCO_3$ (1 mL) was added. The layers were separated and the aqueous layer was extracted with CH_2Cl_2 (3x1 mL). The combined organic extracts were washed with brine, dried over Na_2SO_4 and concentrated under reduced pressure. The crude residue was purified by flash column chromatography (0 → 30% Et_2O in hexanes) to give bromide **164** as an orange oil (19.2 mg, 57% yield). *Note: the product is somewhat unstable and degrades over the course of several weeks.*

^{1}H NMR: (400 MHz, C_6D_6) δ 7.35 (dd, *J* = 7.7, 1.7 Hz, 1H), 7.13 – 7.06 (m, 2H), 7.06 – 7.00 (m, 3H), 6.96 (ddd, *J* = 8.5, 7.3, 1.6 Hz, 1H), 6.73 (td, *J* = 7.5, 1.2 Hz, 1H), 6.57 (dd, *J* = 8.3, 1.2 Hz, 1H), 4.23 – 4.11 (m, 2H), 3.96 (d, *J* = 16.9 Hz, 1H), 3.80 (d, *J* = 11.6 Hz, 1H), 3.66 (dd, *J* = 11.6, 1.8 Hz, 1H), 3.51 (dd, *J* = 11.6, 1.8 Hz, 1H), 3.25 (dddd, *J* = 9.5, 7.9, 4.9, 3.1 Hz, 1H), 3.07 (dd, *J* = 10.5, 3.1 Hz, 1H), 2.97 (dd, *J* = 10.5, 7.5 Hz, 1H), 2.48 (dd, *J* = 13.7, 5.0 Hz, 1H), 1.85 (dd, *J* = 13.7, 9.4 Hz, 1H), 1.47 (s, 3H), 1.41 (s, 3H)

^{13}C NMR: (100 MHz, C_6D_6) δ 146.3, 139.2, 128.8, 128.4, 127.3, 127.1, 126.5, 126.2, 118.4, 114.7, 98.4, 68.8, 68.7, 55.5, 54.8, 36.2, 34.9, 34.4, 26.6, 21.6

IR: (neat film, NaCl) 2986, 2940, 2866, 1492, 1450, 1370, 1224, 1196, 1090, 830, 754, 742, 730 cm^{-1}

HRMS: (ESI^+) *m/z* calc'd for $C_{22}H_{27}BrNO_2$ $[M+H]^+$: 416.1220 found 416.1217

3.6 REFERENCES AND NOTES

(1) Dequina, H. J.; Jones, C. L.; Schomaker, J. M. Recent Updates and Future Perspectives in Aziridine Synthesis and Reactivity. *Chem* **2023**, *9*, 1658–1701.

(2) (a) Ju, X.; Lee, M.; Leung, J. C.; Lee, J. Synthesis and Functionalization of Aziridines: A Perspective View from Pharmaceutical Industries. *Eur. J. Org. Chem.* **2025**, *28*, e202401414. For an elegant application of this concept in a recent total synthesis see: (b) Schneider, F.; Guo, Y.; Lin, Y.-C.; Eberle, K. J.; Chiodi, D.; Greene, J. A.; Lu, C.; Baran, P. S. Total Synthesis of Dynobactin A. *J. Am. Chem. Soc.* **2024**, *146* (10), 6444–6448.

(3) The number of reported ring opening reactions of "*standard"* aziridines is far too large to comprehensively cite. For examples, see the following references and the citations therein: (a) Argouarch, G.; Gibson, C. L.; Stones, G.; Sherrington, D. C. The Synthesis of Chiral Annulet 1,4,7-Triazacyclononanes. *Tetrahedron Lett.* **2002**, *43*, 3795–3798. (b) Bornholdt, J.; Felding, J.; Clausen, R. P.; Kristensen, J. L. Ring Opening of Pymisyl-Protected Aziridines with Organocuprates. *Chem. – Eur. J.* **2010**, *16*, 12474–12480. (c) Bornholdt, J.; Felding, J.; Kristensen, J. L. Synthesis of Enantiopure 3-Substituted Morpholines. *J. Org. Chem.* **2010**, *75*, 7454–7457. (d) Ottesen, L. K.; Jaroszewski, J. W.; Franzyk, H. Ring Opening of a Resin-Bound Chiral Aziridine with Phenol Nucleophiles. *J. Org. Chem.* **2010**, *75*, 4983–4991. (e) Sureshkumar, D.; Ganesh, V.; Vidyarini, R. S.; Chandrasekaran, S. Direct Synthesis of Functionalized Unsymmetrical β-Sulfonamido Disulfides by Tetrathiomolybdate Mediated Aziridine Ring-Opening Reactions. *J. Org. Chem.* **2009**, *74*, 7958–7961. (f) Liu, J.; Wang, C. Zinc-Catalyzed Hydroxyl-Directed Regioselective Ring Opening of Aziridines in S_N2 Reaction

Pathway. *ACS Catal.* **2020**, *10*, 556–561. (g) Yang, S.; Li, L.; Wang, F.; Dong, X.; Jiang, J.; Zhang, Y.-Q. Water-Mediated Radical Kinetic Resolution of Terminal Activated N-Carbamate Aziridines. *J. Am. Chem. Soc.* **2025**, *147*, 13039–13049. (h) D'hooghe, M.; Catak, S.; Stanković, S.; Waroquier, M.; Kim, Y.; Ha, H.-J.; Van Speybroeck, V.; De Kimpe, N. Systematic Study of Halide-Induced Ring Opening of 2-Substituted Aziridinium Salts and Theoretical Rationalization of the Reaction Pathways. *Eur. J. Org. Chem.* **2010**, *2010*, 4920–4931. (i) Higashiyama, K.; Matsumura, M.; Kojima, H.; Yamauchi, T. Regio- and Stereoselective Ring-Opening Reaction of Chiral Aziridines: A Facile Synthesis of Chiral β-Amino Alcohols. *Heterocycles* **2009**, *78*, 471. (j) Choi, S.-K.; Lee, J.-S.; Kim, J.-H.; Lee, W. K. Efficient Syntheses of (1R,2R)- and (1S,2S)-2-Amino-1-Alkyl(or Aryl)-1,3-Propanediols by Regioselective Ring Opening of Aziridine-2-Methanols. *J. Org. Chem.* **1997**, *62*, 743–745. (k) Yun, J. M.; Sim, T. B.; Hahm, H. S.; Lee, W. K.; Ha, H.-J. Efficient Synthesis of Enantiomerically Pure 2-Acylaziridines: Facile Syntheses of N-Boc-Safingol, N-Boc-d-Erythro-Sphinganine, and N-Boc-Spisulosine from a Common Intermediate. *J. Org. Chem.* **2003**, *68*, 7675–7680. (l) Katagiri, T.; Takahashi, M.; Fujiwara, Y.; Ihara, H.; Uneyama, K. General Syntheses of Optically Active α-Trifluoromethylated Amines via Ring-Opening Reactions of N-Benzyl-2-Trifluoromethylaziridine. *J. Org. Chem.* **1999**, *64*, 7323–7329. (m) Yook, C.-M.; Eum, H.-S.; Ha, H.-J.; Kang, K.-Y.; Lee, W.-K. Regiochemical Pathway in the Ring Opening of 2-Acylaziridines. *Bull. Korean Chem. Soc.* **2011**, *32*, 2879–2880. (n) Kim, Y.; Ha, H.-J.; Yun, S. Y.; Lee, W. K. The Preparation of Stable Aziridinium Ions and Their Ring-Openings. *Chem. Commun.* **2008**, 4363–4365. (o) Zheng, B.; Taylor, M. S. Regioselective, Lewis Acid-Catalyzed

Ring-Openings of 2,3-Aziridyl Alcohols with Azoles. *J. Org. Chem.* **2025**. ASAP. https://doi.org/10.1021/acs.joc.5c00380. (p) Stanković, S.; D'hooghe, M.; Catak, S.; Eum, H.; Waroquier, M.; Speybroeck, V. V.; Kimpe, N. D.; Ha, H.-J. Regioselectivity in the Ring Opening of Non-Activated Aziridines. *Chem. Soc. Rev.* **2012**, *41*, 643–665.

(4) For examples of fused bicyclic aziridine ring openings see: (a) Duran, F.; Leman, L.; Ghini, A.; Burton, G.; Dauban, P.; Dodd, R. H. Intramolecular PhIO Mediated Copper-Catalyzed Aziridination of Unsaturated Sulfamates: A New Direct Access to Polysubstituted Amines from Simple Homoallylic Alcohols. *Org. Lett.* **2002**, *4*, 2481–2483.. (b) Hayashi, K.; Kujime, E.; Katayama, H.; Sano, S.; Shiro, M.; Nagao, Y. Synthesis and Reaction of 1-Azabicyclo[3.1.0]Hexane. *Chem. Pharm. Bull.* **2009**, *57*, 1142–1146. (c) Goujon, J.-Y.; Gueyrard, D.; Compain, P.; Martin, O. R.; Ikeda, K.; Kato, A.; Asano, N. General Synthesis and Biological Evaluation of α-1-*C*-Substituted Derivatives of Fagomine (2-Deoxynojirimycin-α-*C*-Glycosides). *Bioorg. Med. Chem.* **2005**, *13*, 2313–2324. (d) Yadav, N. N.; Ha, H.-J. Preparation of Stable Bicyclic Aziridinium Ions and Their Ring-Opening for the Synthesis of Azaheterocycles. *J. Vis. Exp.* **2018**, 57572.

(5) Hicks, E. F.; Inoue, K.; Stoltz, B. M. Enantioselective Total Synthesis of (−)-Hunterine A Enabled by a Desymmetrization/Rearrangement Strategy. *J. Am. Chem. Soc.* **2024**, *146*, 4340–4345.

(6) For an example of a similar ring opening of an analogous seven-membered fused bicyclic aziridine see: Santer, G.; Ongania, K. H. Synthese von benzanellierten Carbacephamen, 1. Mitt. *Monatshefte Für Chem. Chem. Mon.* **1994**, *125*, 71–78.

(7) Ciufolini and coworkers have reported ring openings of related aziridines that proceed in an intramolecular fashion: (a) Ducray, R.; Cramer, N.; Ciufolini, M. A. Homo-Brook Route to Benzazocenols and Congeners via Allylsilane-Derived Aziridines. *Tetrahedron Lett.* **2001**, *42*, 9175–9178. (b) Ducray, R.; Ciufolini, M. A. Total Synthesis of (±)-FR66979. *Angew. Chem. Int. Ed.* **2002**, *41*, 4688–4691.

(8) Bhattacharya, D.; Ghorai, A.; Pal, U.; Maiti, N. C.; Chattopadhyay, P. Stereoselective Domino Azidation and [3 + 2] Cycloaddition: A Facile Route to Chiral Heterocyclic Scaffolds from Carbohydrate Derived Synthons. *RSC Adv.* **2013**, *4*, 4155–4162.

(9) (a) Jung, M. E.; Piizzi, G. Gem-Disubstituent Effect: Theoretical Basis and Synthetic Applications. *Chem. Rev.* **2005**, *105*, 1735–1766. (b) Jung, M. E. New Gem- and Vic-Disubstituent Effects on Cyclizations. *Synlett* **1999**, *1999*, 843–846.

(10) Mlynarski, S. N.; Karns, A. S.; Morken, J. P. Direct Stereospecific Amination of Alkyl and Aryl Pinacol Boronates. *J. Am. Chem. Soc.* **2012**, *134*, 16449–16451.

(11) Barral, K.; Moorhouse, A. D.; Moses, J. E. Efficient Conversion of Aromatic Amines into Azides: A One-Pot Synthesis of Triazole Linkages. *Org. Lett.* **2007**, *9*, 1809–1811.

(12) (a) Scheiner, P. Triazoline Photodecomposition: The Preparation of Aziridines. *Tetrahedron* **1968**, *24*, 2757–2765. (b) Scheiner, P. Photodecomposition of 1,2,3-Triazolines. A New Entry into the Aziridine Series. *J. Org. Chem.* **1965**, *30*, 7–10. (c) Scheiner, P. Triazoline Photodecomposition. Stereochemistry and Mechanism. *J. Am. Chem. Soc.* **1968**, *90*, 988–992.

(13) Guthikonda, K.; Wehn, P. M.; Caliando, B. J.; Du Bois, J. Rh-Catalyzed Alkene Oxidation: A Highly Efficient and Selective Process for Preparing N-Alkoxysulfonyl Aziridines. *Tetrahedron* **2006**, *62*, 11331–11342.

(14) For select examples see: (a) Saryazdi, S.; Parkin, S.; Grossman, R. B. 1,2-Diamination of Alkenes via 1,3-Dipolar Cycloaddition with Azidium Ions or Azides. *Org. Lett.* **2023**, *25*, 331–335. (b) Hong, K. B.; Donahue, M. G.; Johnston, J. N. On the Nature of Rate Acceleration in the Synthesis and Fragmentation of Triazolines by Brønsted Acid: Secondary Catalysis by Water (Hydronium Triflate). *J. Am. Chem. Soc.* **2008**, *130*, 2323–2328. (c) Moynihan, L.; Chadda, R.; McArdle, P.; Murphy, P. V. Allylic Azide Rearrangement in Tandem with Huisgen Cycloaddition for Stereoselective Annulation: Synthesis of C-Glycosyl Iminosugars. *Org. Lett.* **2015**, *17*, 6226–6229.

(15) (a) Murthy, K. S. K.; Hassner, A. Fused β-Lactams via Intramolecular Dipolar Cycloaddition. *Tetrahedron Lett.* **1987**, *28*, 97–100. (b) Hemming, K.; Chambers, C. S.; Jamshaid, F.; O'Gorman, P. A. Intramolecular Azide to Alkene Cycloadditions for the Construction of Pyrrolobenzodiazepines and Azetidino-Benzodiazepines. *Molecules* **2014**, *19*, 16737–16756.

(16) Laube, T. First Crystal Structure Analysis of an Aliphatic Carbocation—Stabilization of the 3,5,7-Trimethyl-1-Adamantyl Cation by C–C Hyperconjugation. *Angew. Chem. Int. Ed.* **1986**, *25*, 349–350.

(17) Chini, M.; Crotti, P.; Gardelli, C.; Macchia, F. Regio- and Stereoselective Synthesis of β-Halohydrins from 1,2-Epoxides with Ammonium Halides in the Presence of Metal Salts. *Tetrahedron* **1992**, *48*, 3805–3812.

(18) Pangborn, A. B.; Giardello, M. A.; Grubbs, R. H.; Rosen, R. K.; Timmers, F. J. Safe and Convenient Procedure for Solvent Purification. *Organometallics* **1996**, *15*, 1518–1520.

(19) Yang, W.; Liu, Y.; Zhang, S.; Cai, Q. Copper-Catalyzed Intramolecular Desymmetric Aryl C–O Coupling for the Enantioselective Construction of Chiral Dihydrobenzofurans and Dihydrobenzopyrans. *Angew Chem. Int. Ed.* **2015**, *54*, 8805–8808.

(20) Bashore, C. G.; Samardjiev, I. J.; Bordner, J.; Coe, J. W. Twisted Amide Reduction under Wolff−Kishner Conditions: Synthesis of a Benzo-1-Aza-Adamantane Derivative. *J. Am. Chem. Soc.* **2003**, *125*, 3268–3272.

(21) Chaumontet, M.; Piccardi, R.; Audic, N.; Hitce, J.; Peglion, J.-L.; Clot, E.; Baudoin, O. Synthesis of Benzocyclobutenes by Palladium-Catalyzed C−H Activation of Methyl Groups: Method and Mechanistic Study. *J. Am. Chem. Soc.* **2008**, *130*, 15157–15166.

(22) Fry, A. J.; Little, R. D.; Leonetti, J. A General Mechanistic Scheme for Intramolecular Electrochemical Hydrocyclizations. Mechanism of the Electroreductive Cyclization of .Omega.-Keto .Alpha.,.Beta.-Unsaturated Esters. *J. Org. Chem.* **1994**, *59*, 5017–5026.

APPENDIX 5

Spectra Relevant to Chapter 3:

Preparation and Regioselective Ring Opening Reactions of Fused Bicyclic N-Aryl Aziridines

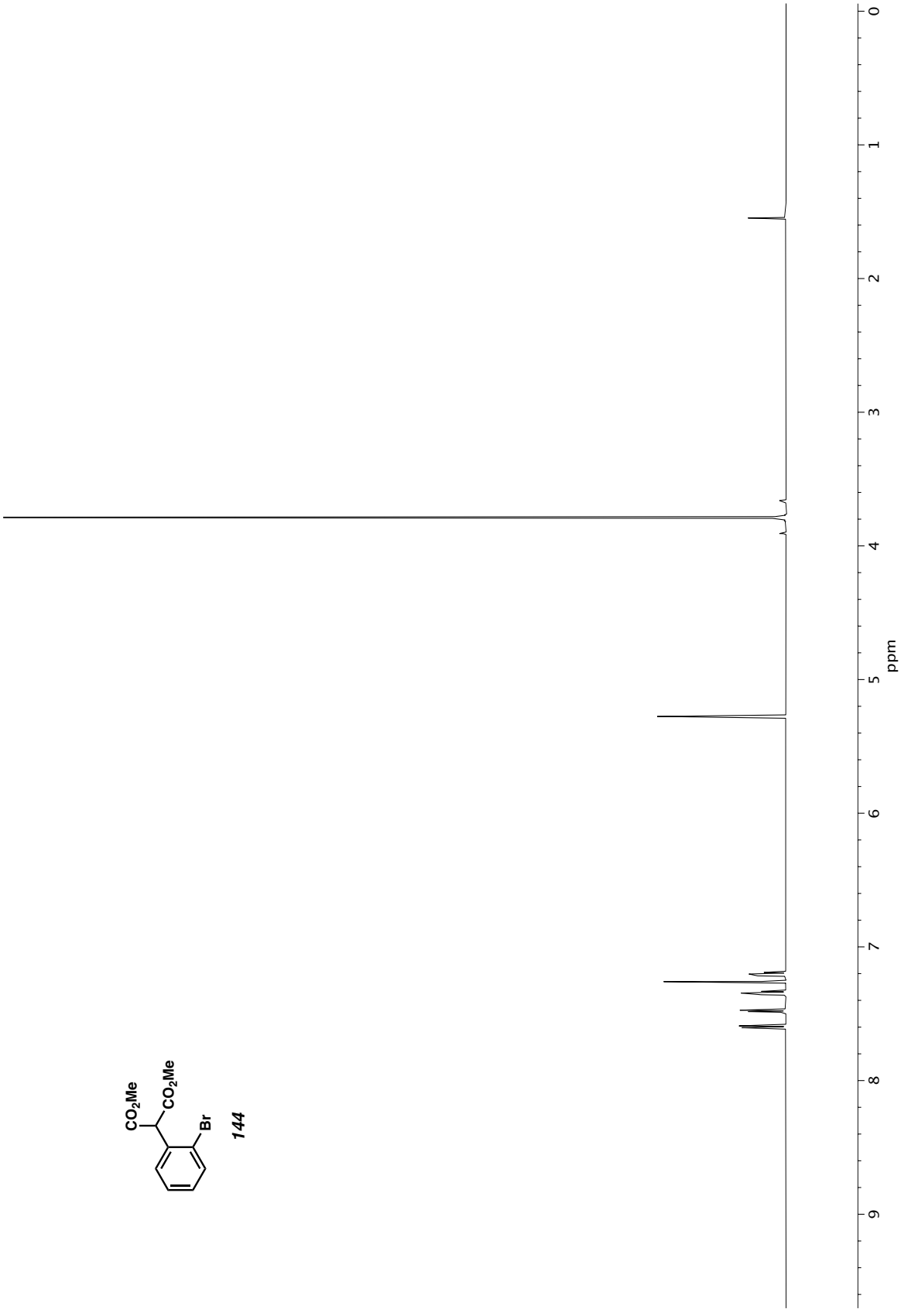


Figure A5.1 *^1H NMR (600 MHz, $CDCl_3$) of compound* ***144****.*

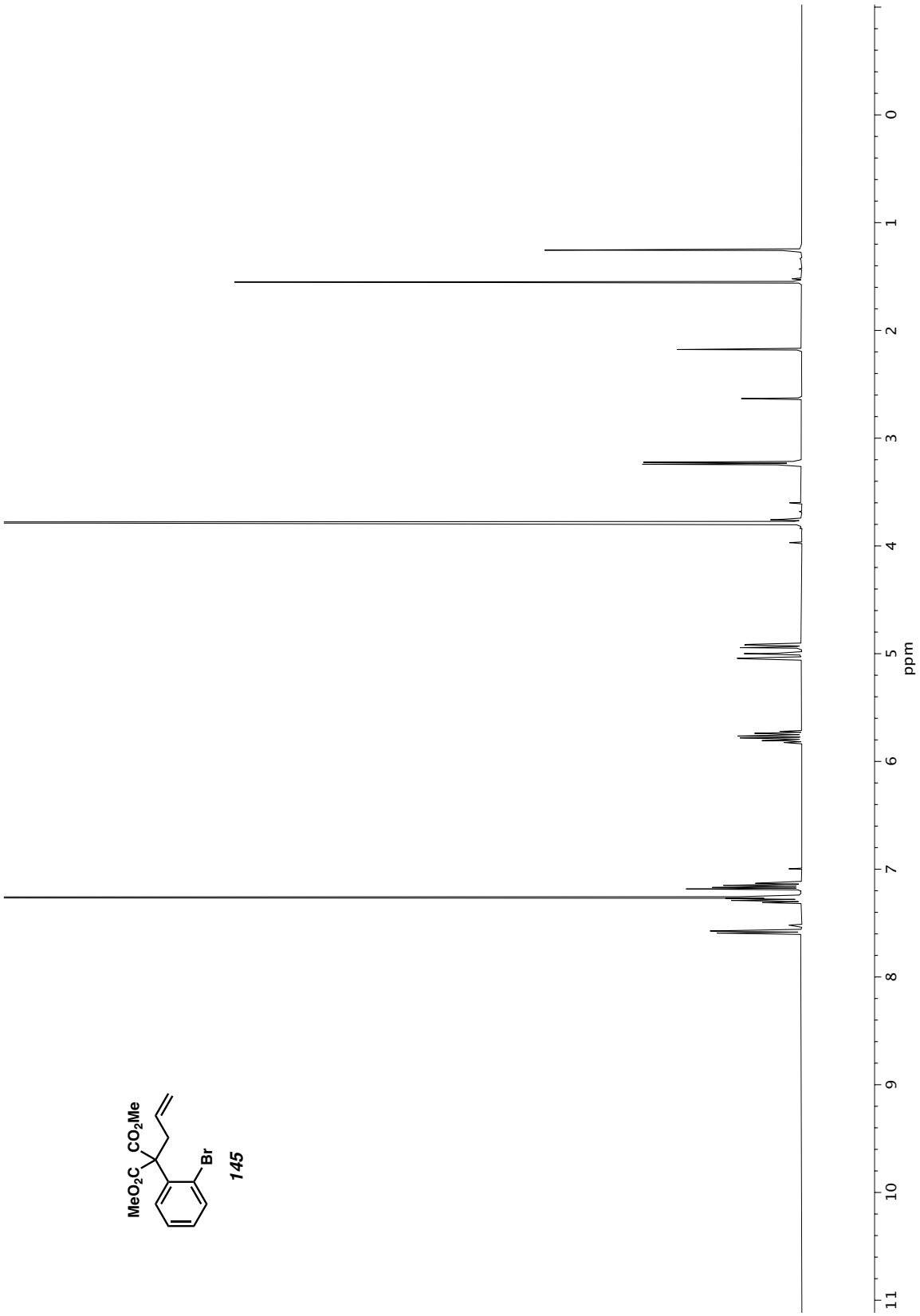


Figure A5.2 *^1H NMR (400 MHz, $CDCl_3$) of compound* ***145***.

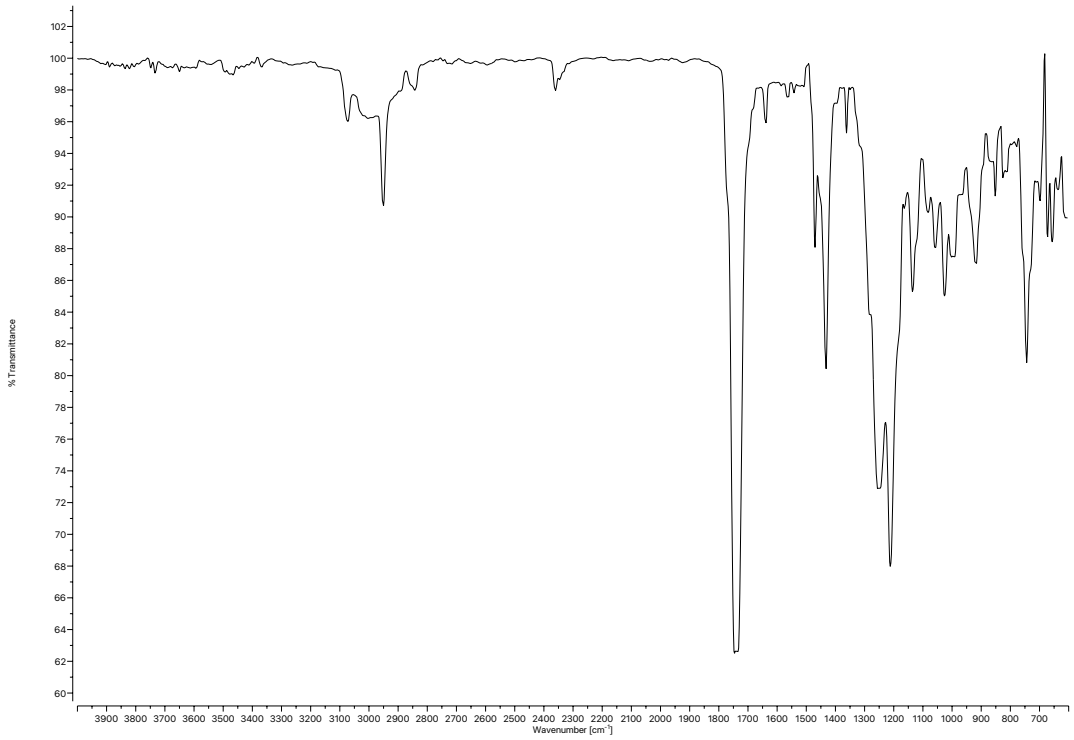


Figure A5.3 *Infrared spectrum (Thin Film, NaCl) of compound* ***145***.

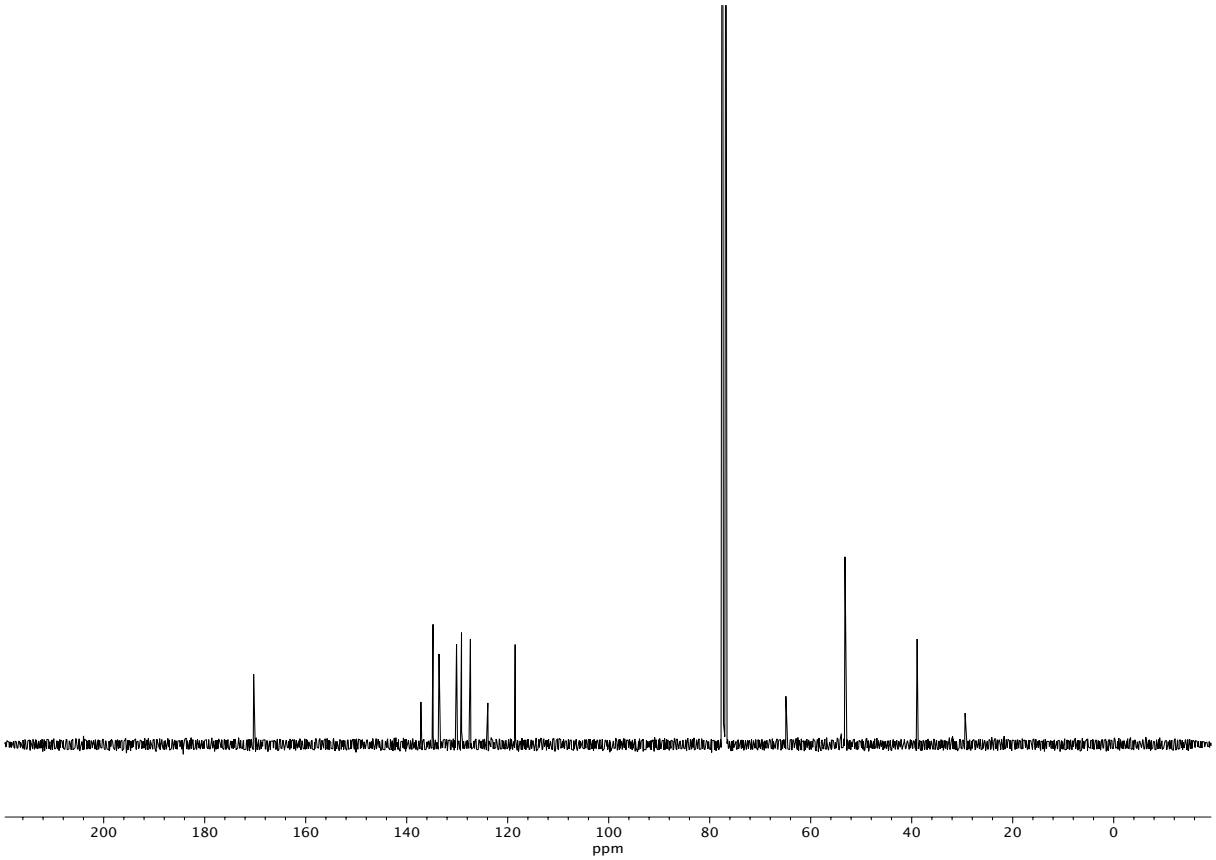


Figure A5.4 *^{13}C NMR (100 MHz, $CDCl_3$) of compound* ***145***.

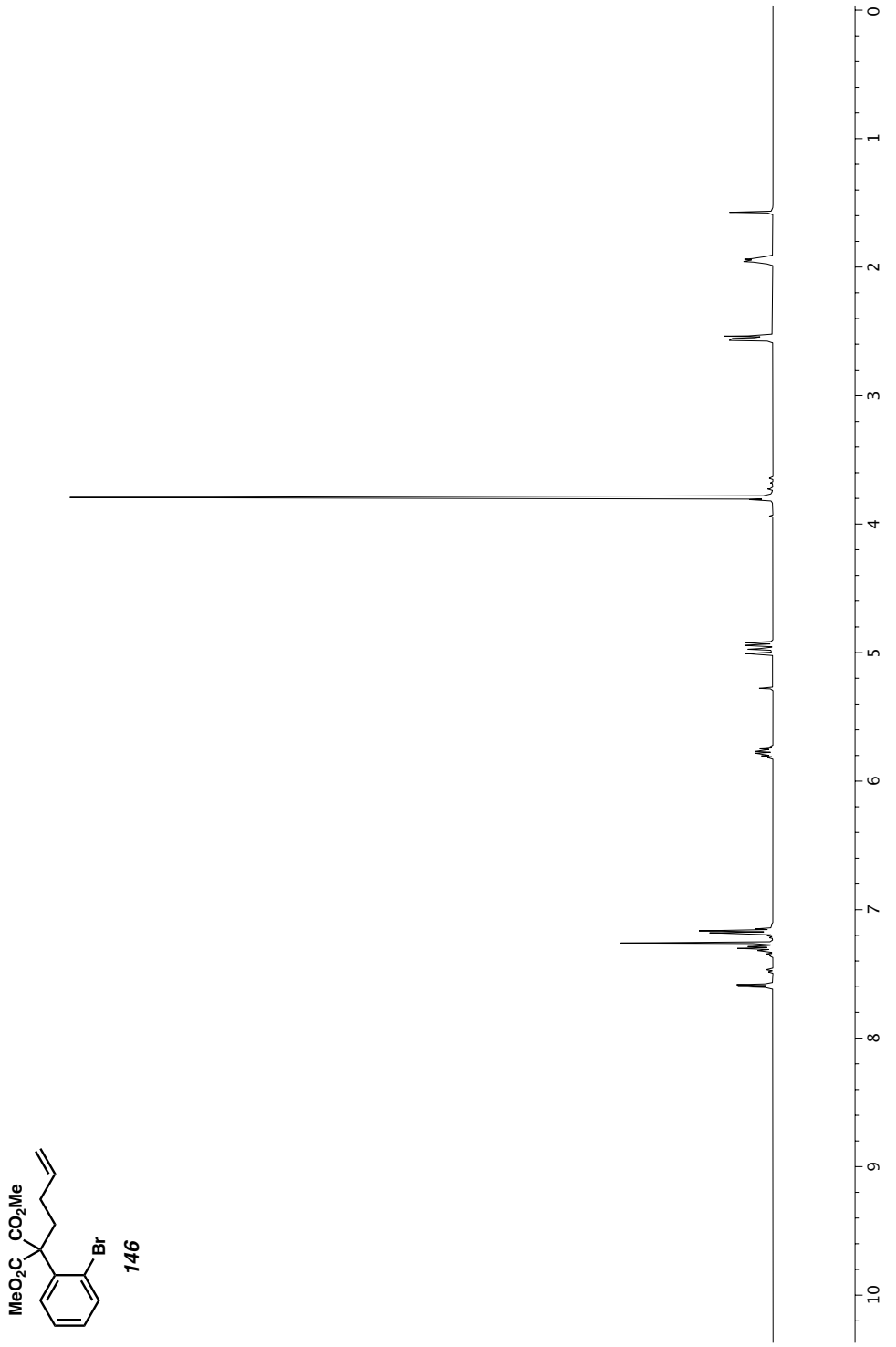


Figure A5.5 *^1H NMR (500 MHz, $CDCl_3$) of compound* ***146***.

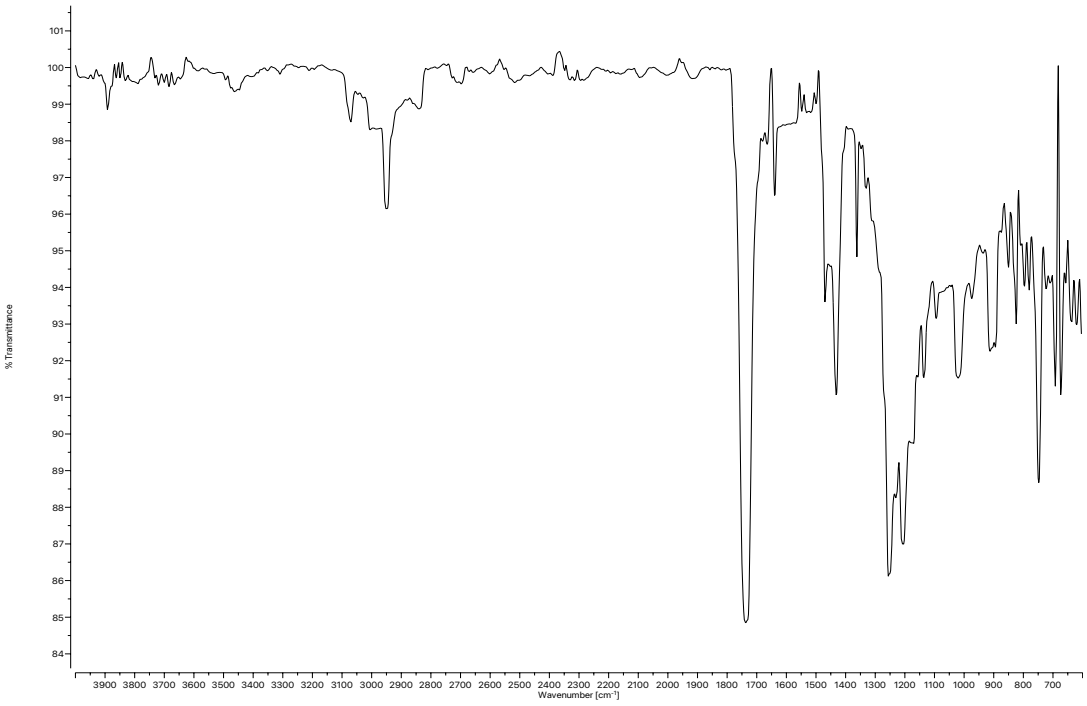


Figure A5.6 *Infrared spectrum (Thin Film, NaCl) of compound* ***146***.

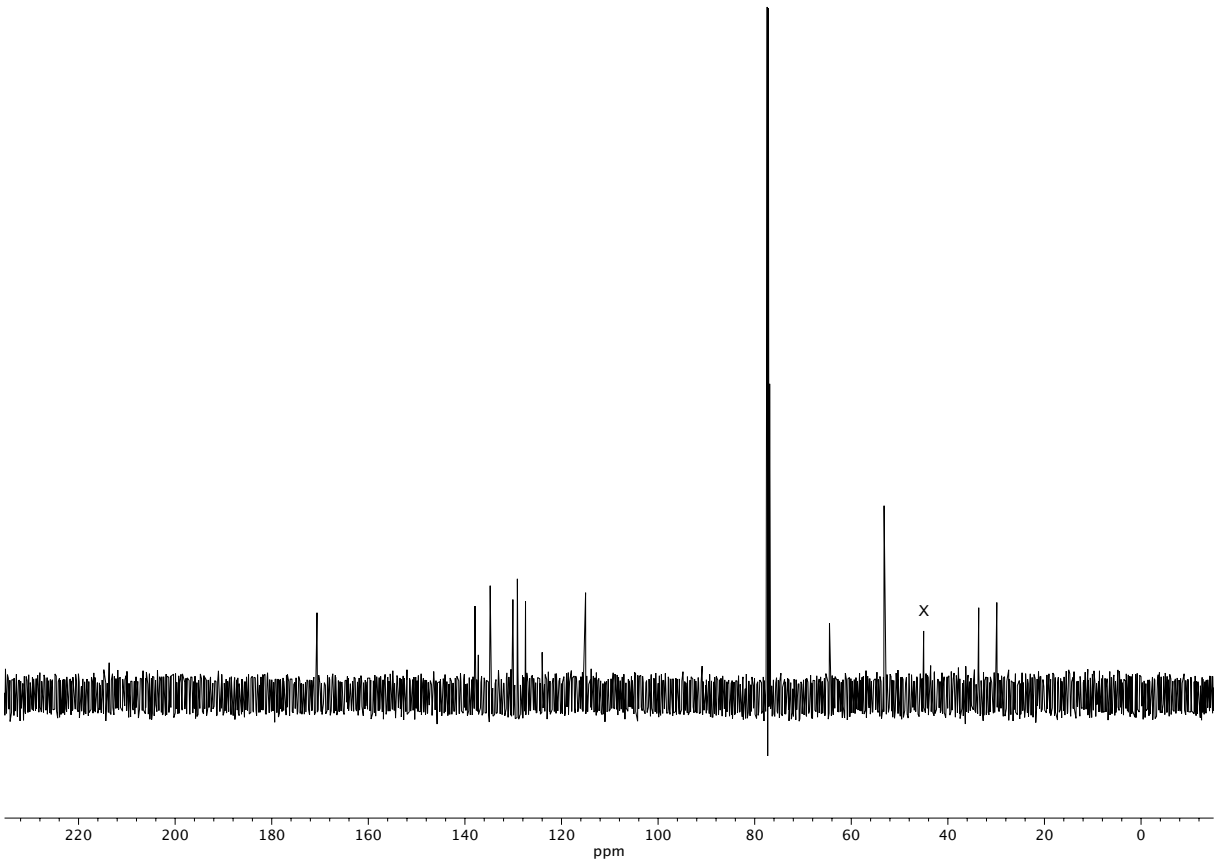


Figure A5.7 *^{13}C NMR (125 MHz, $CDCl_3$) of compound* ***146***.

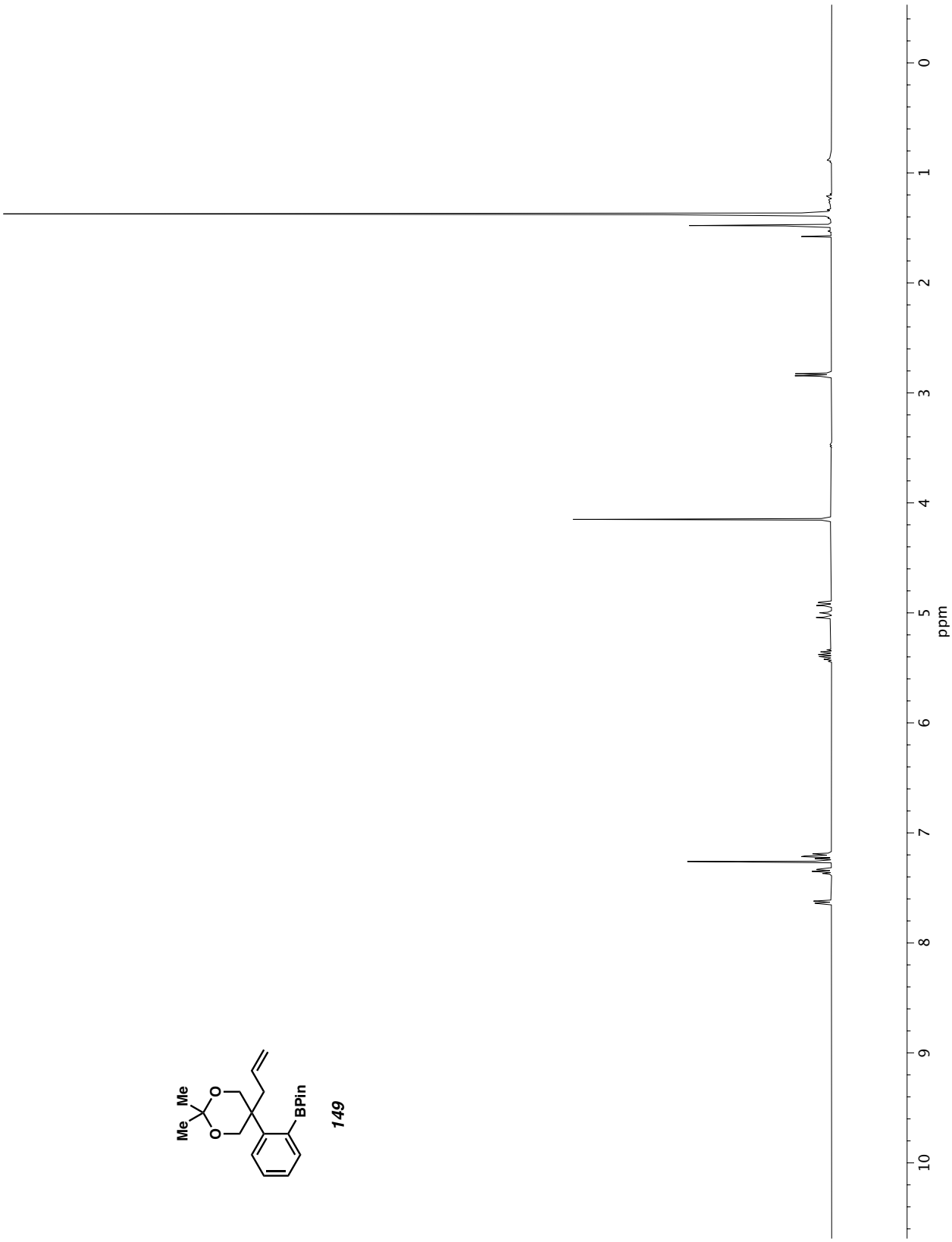


Figure A5.8 *^1H NMR (400 MHz, $CDCl_3$) of compound* ***149***.

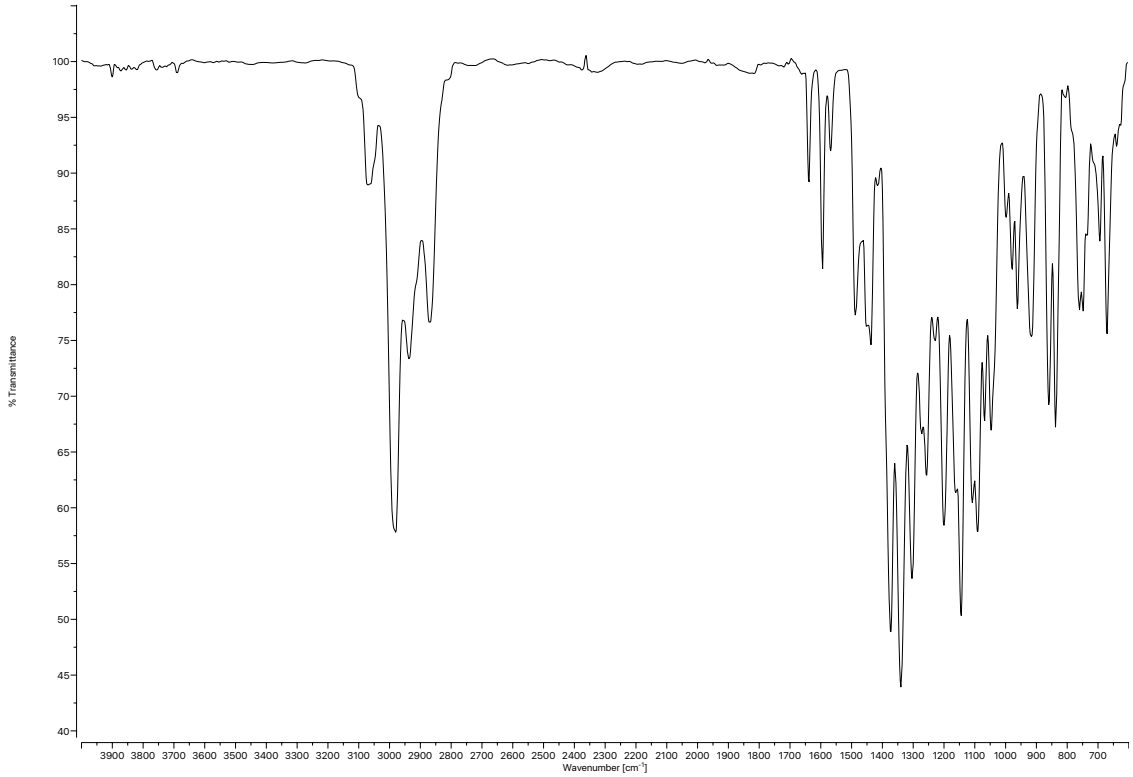


Figure A5.9 *Infrared spectrum (Thin Film, NaCl) of compound* ***149****.*

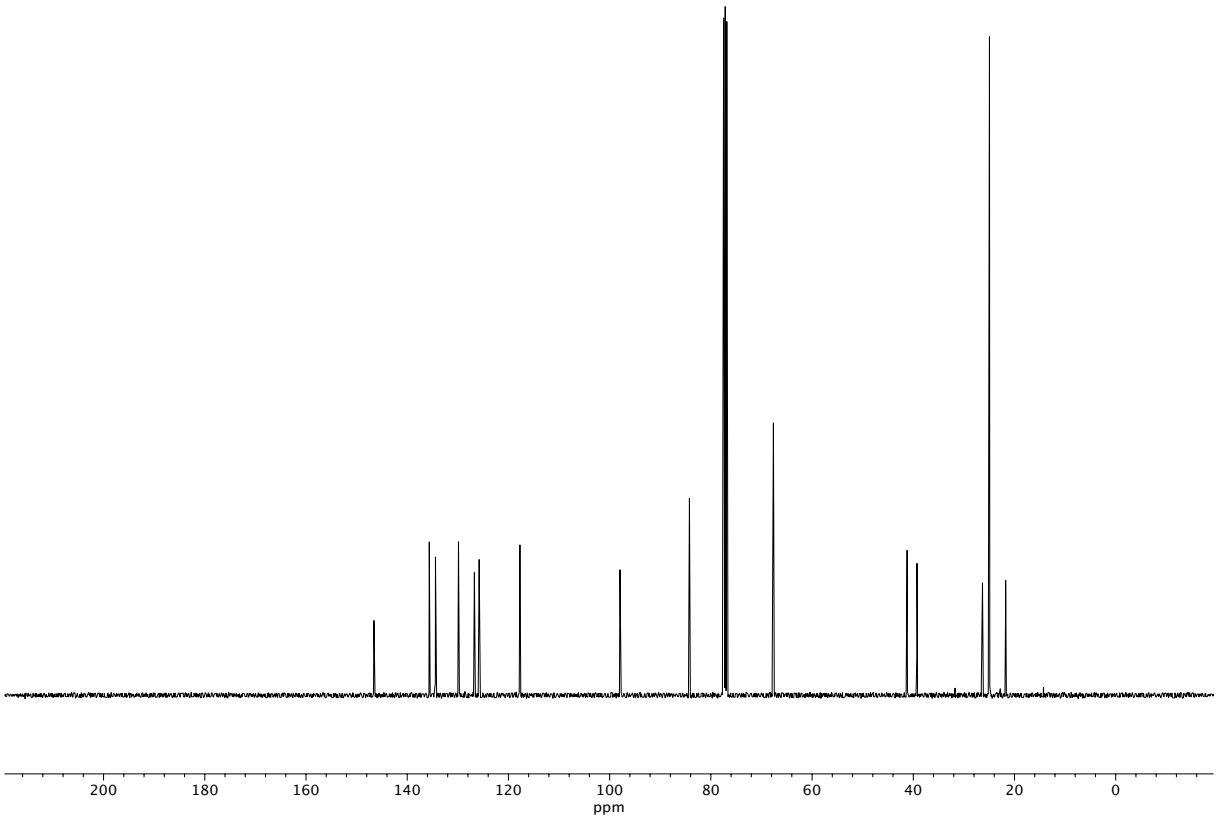


Figure A5.10 *^{13}C NMR (100 MHz, $CDCl_3$) of compound* ***149****.*

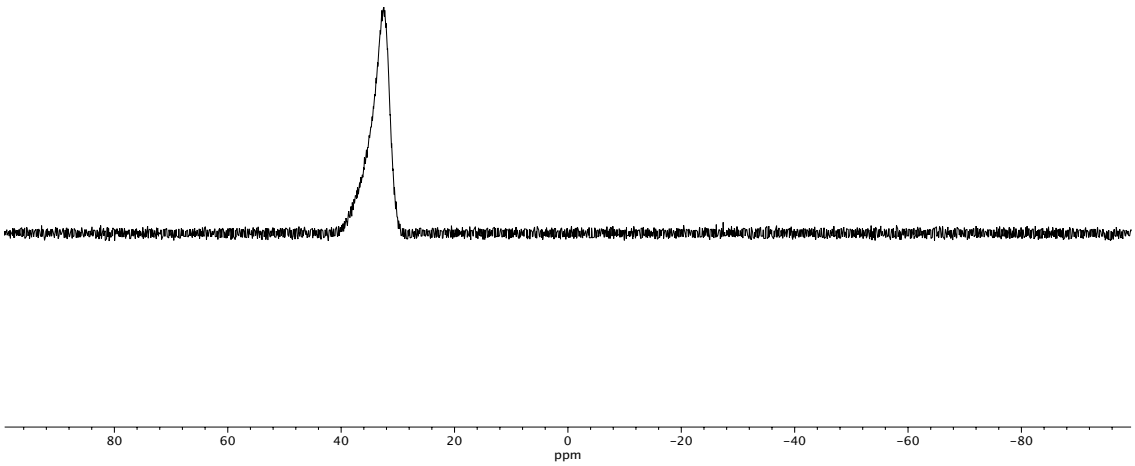


Figure A5.11 *^{11}B NMR spectrum (128 MHz, $CDCl_3$) of compound* ***149****.*

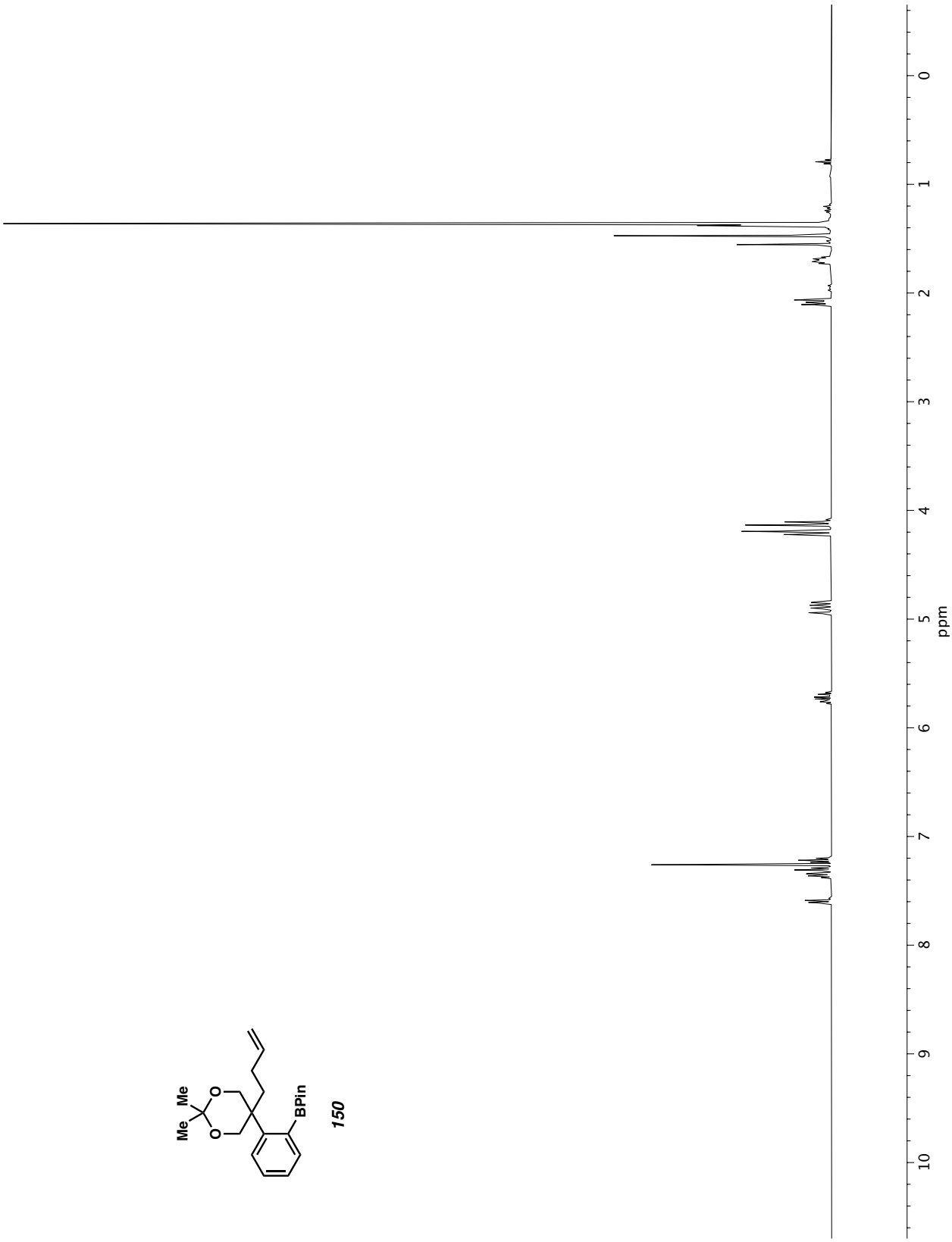


Figure A5.12 *^1H NMR (400 MHz, $CDCl_3$) of compound* ***150***.

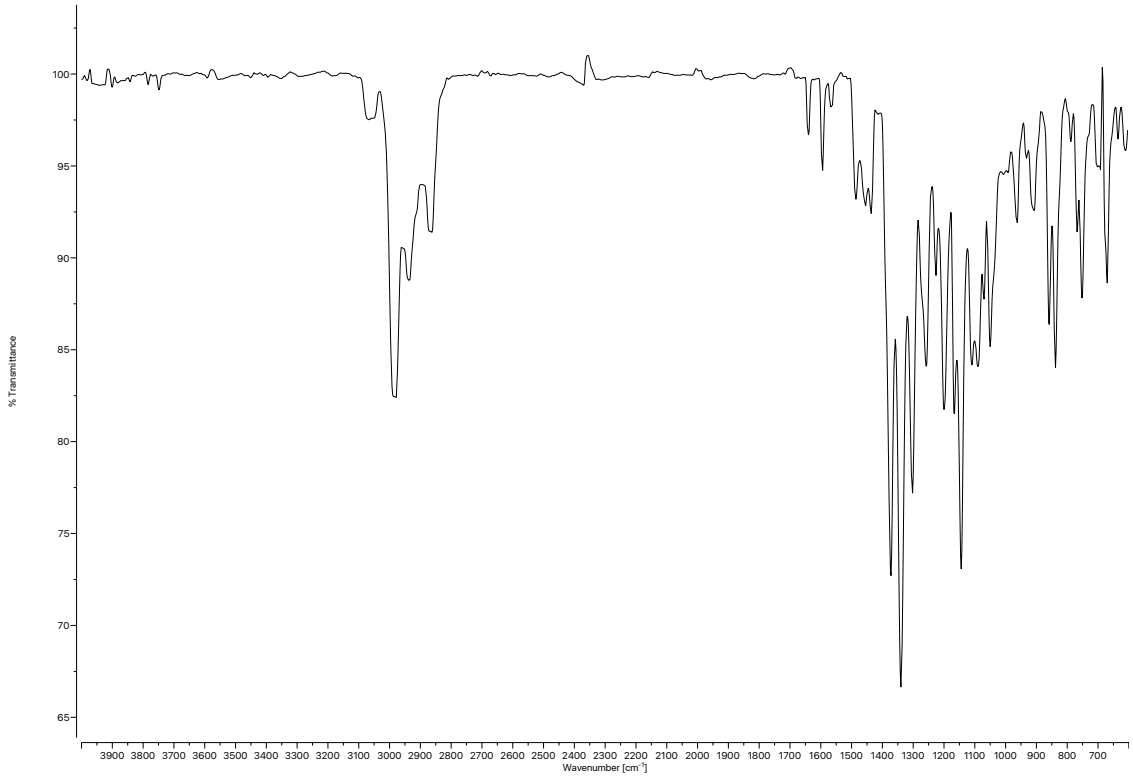


Figure A5.13 *Infrared spectrum (Thin Film, NaCl) of compound* ***150****.*

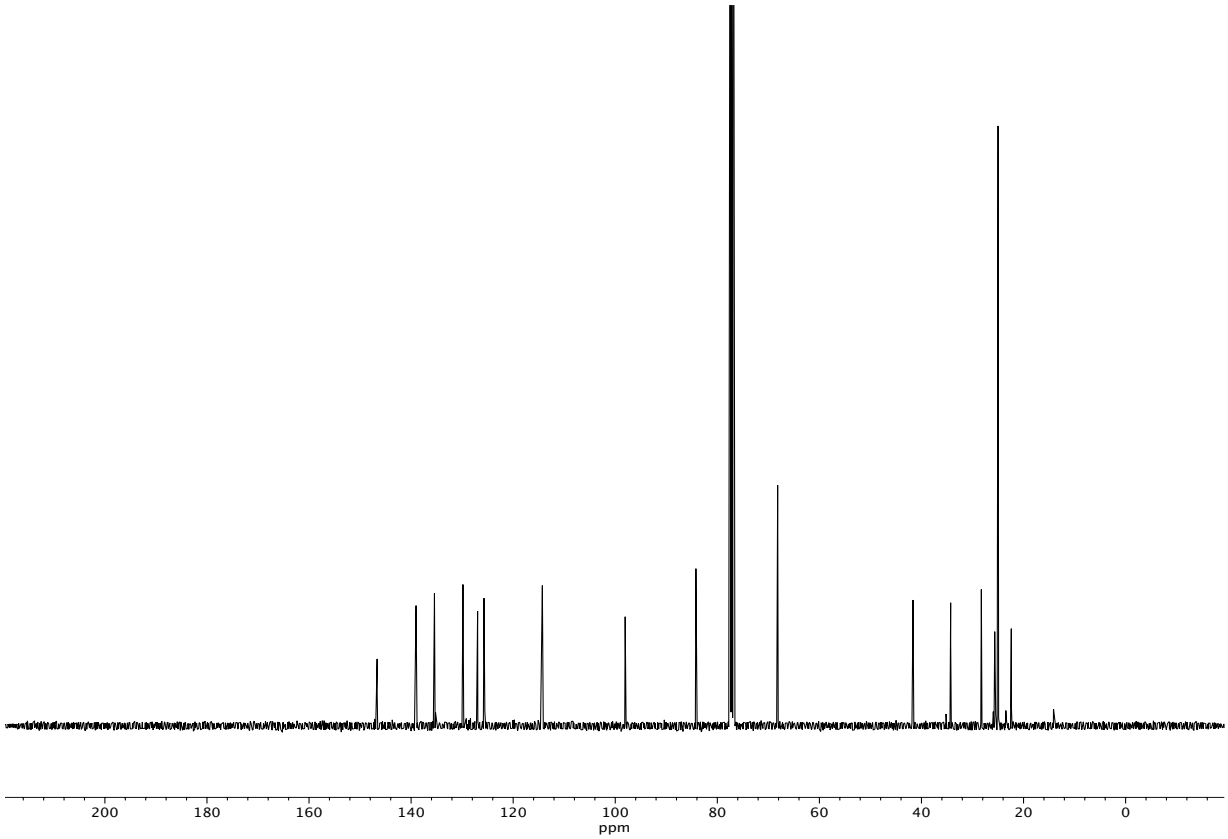


Figure A5.14 *^{13}C NMR (100 MHz, $CDCl_3$) of compound* ***150****.*

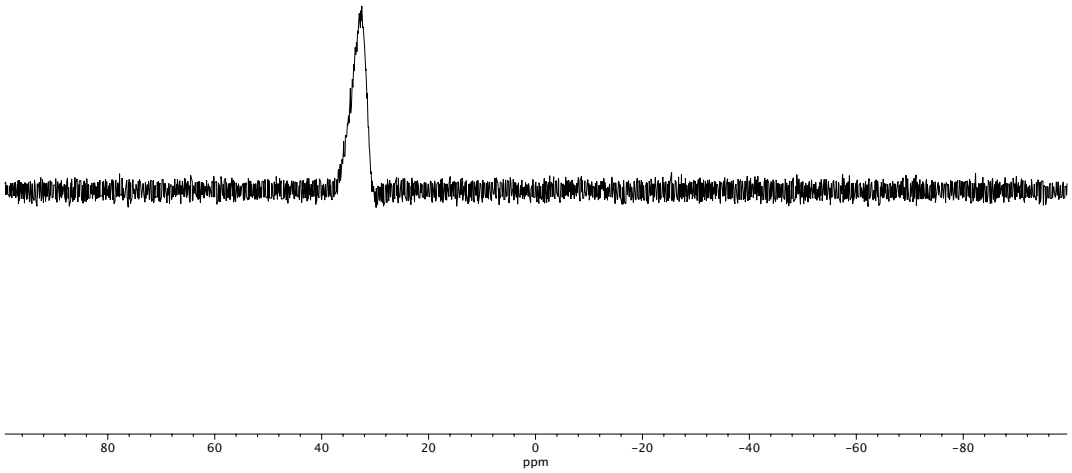


Figure A5.15 *^{11}B NMR spectrum (128 MHz, $CDCl_3$) of compound* ***150****.*

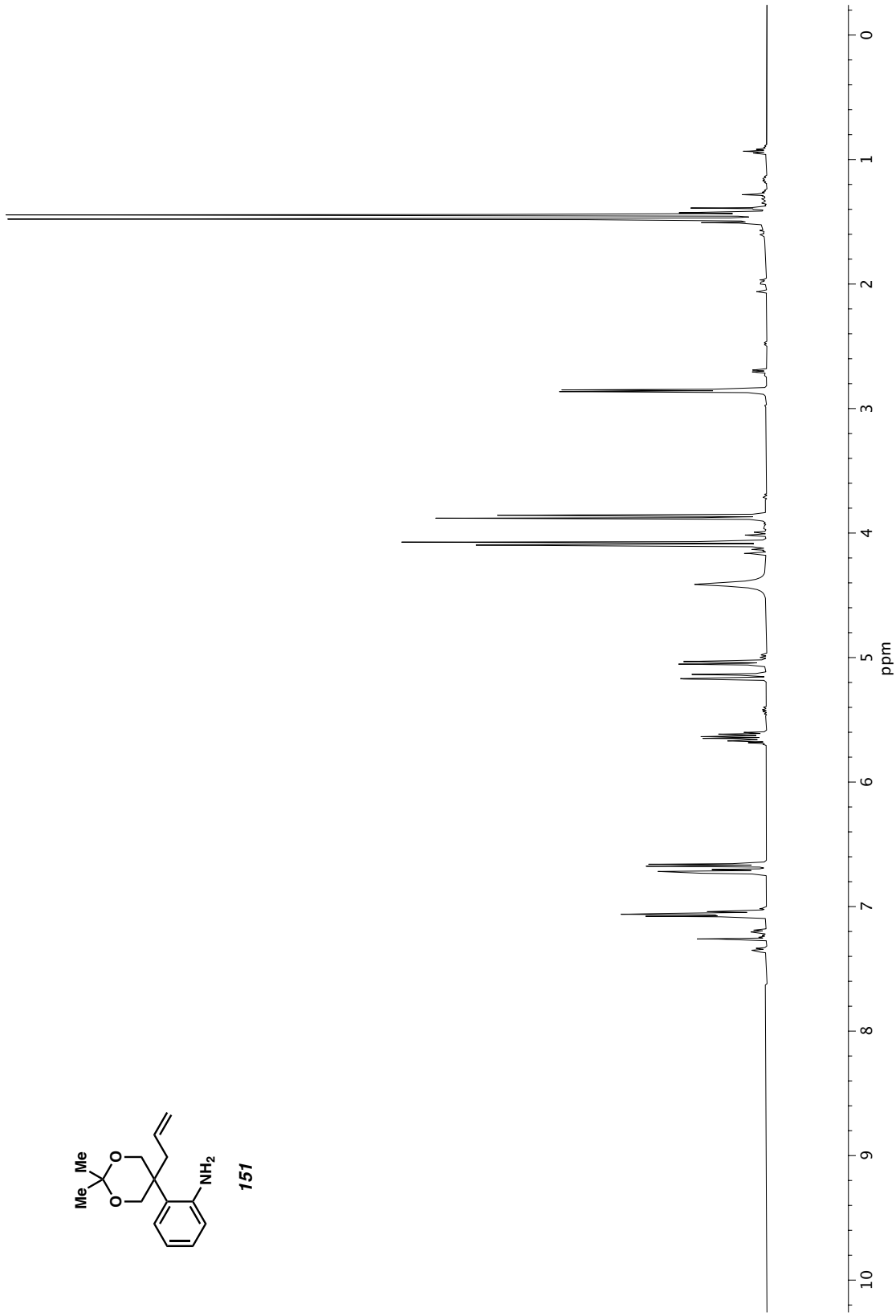


Figure A5.16 *^1H NMR (500 MHz, $CDCl_3$) of compound* ***151****.*

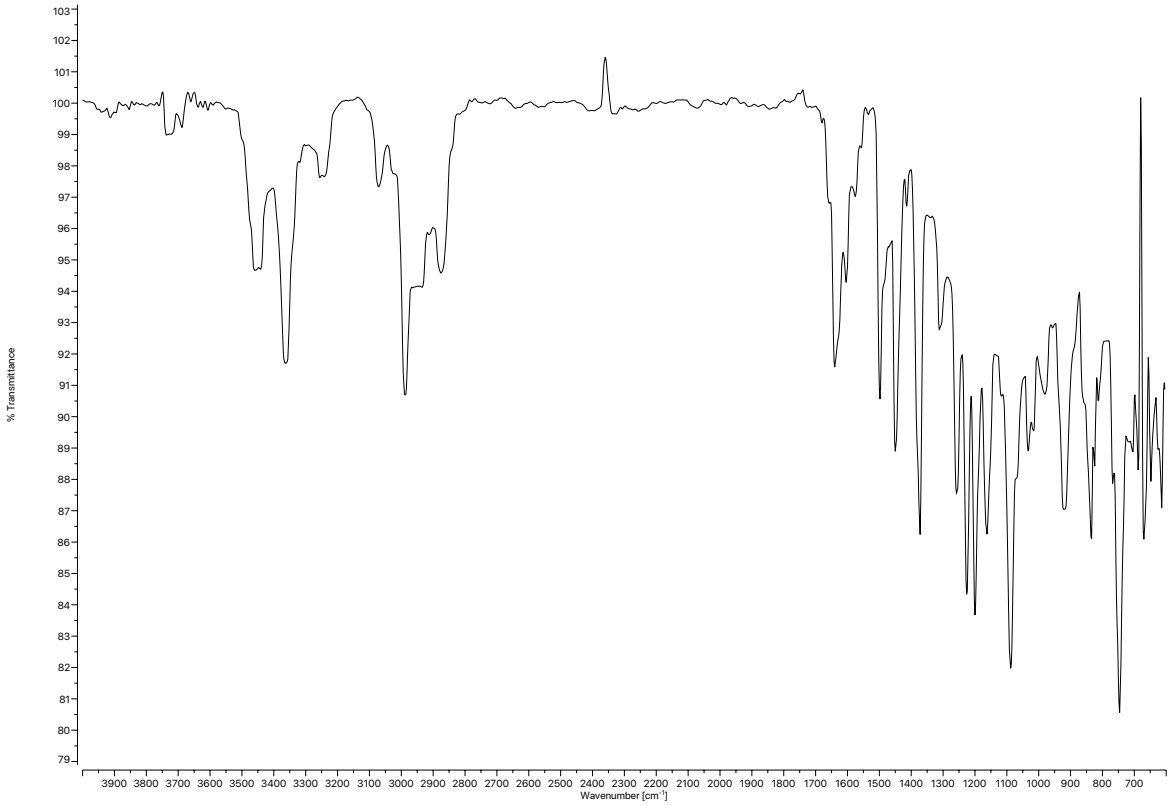


Figure A5.17 *Infrared spectrum (Thin Film, NaCl) of compound* ***151***.

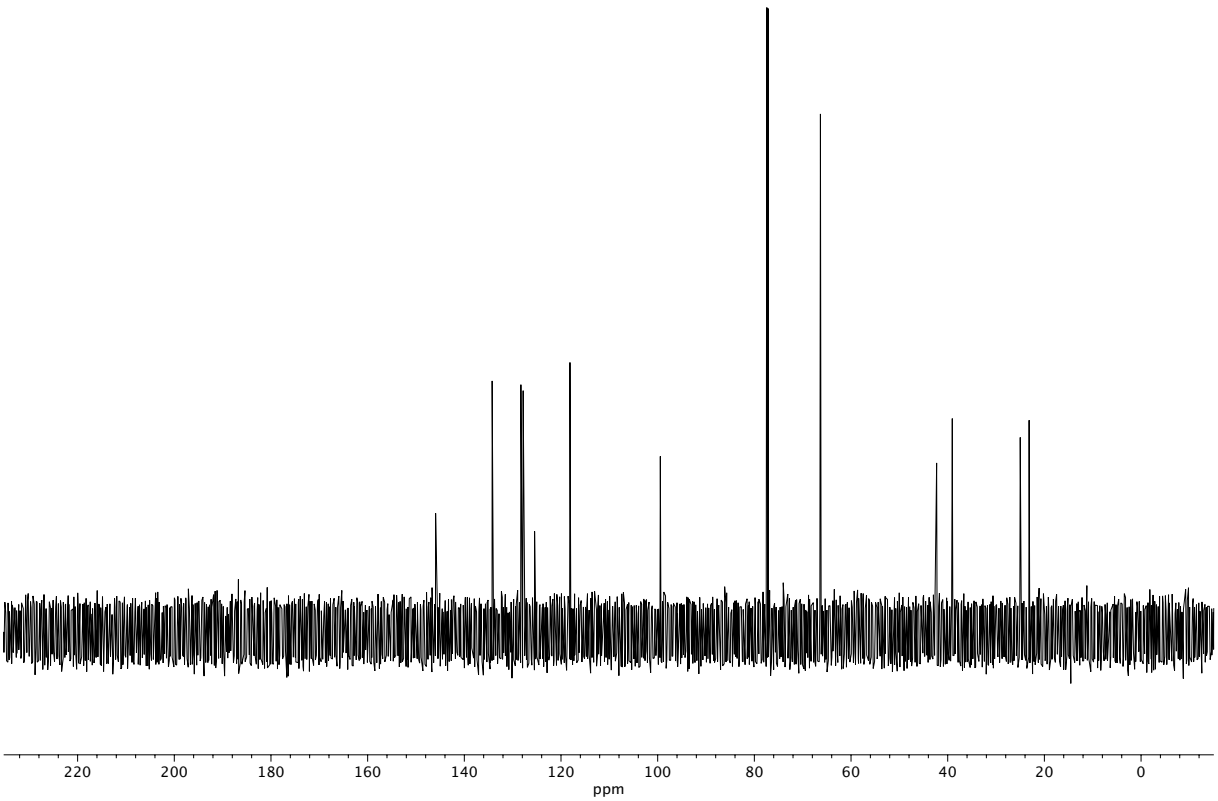


Figure A5.18 *^{13}C NMR (125 MHz, $CDCl_3$) of compound* ***151***.

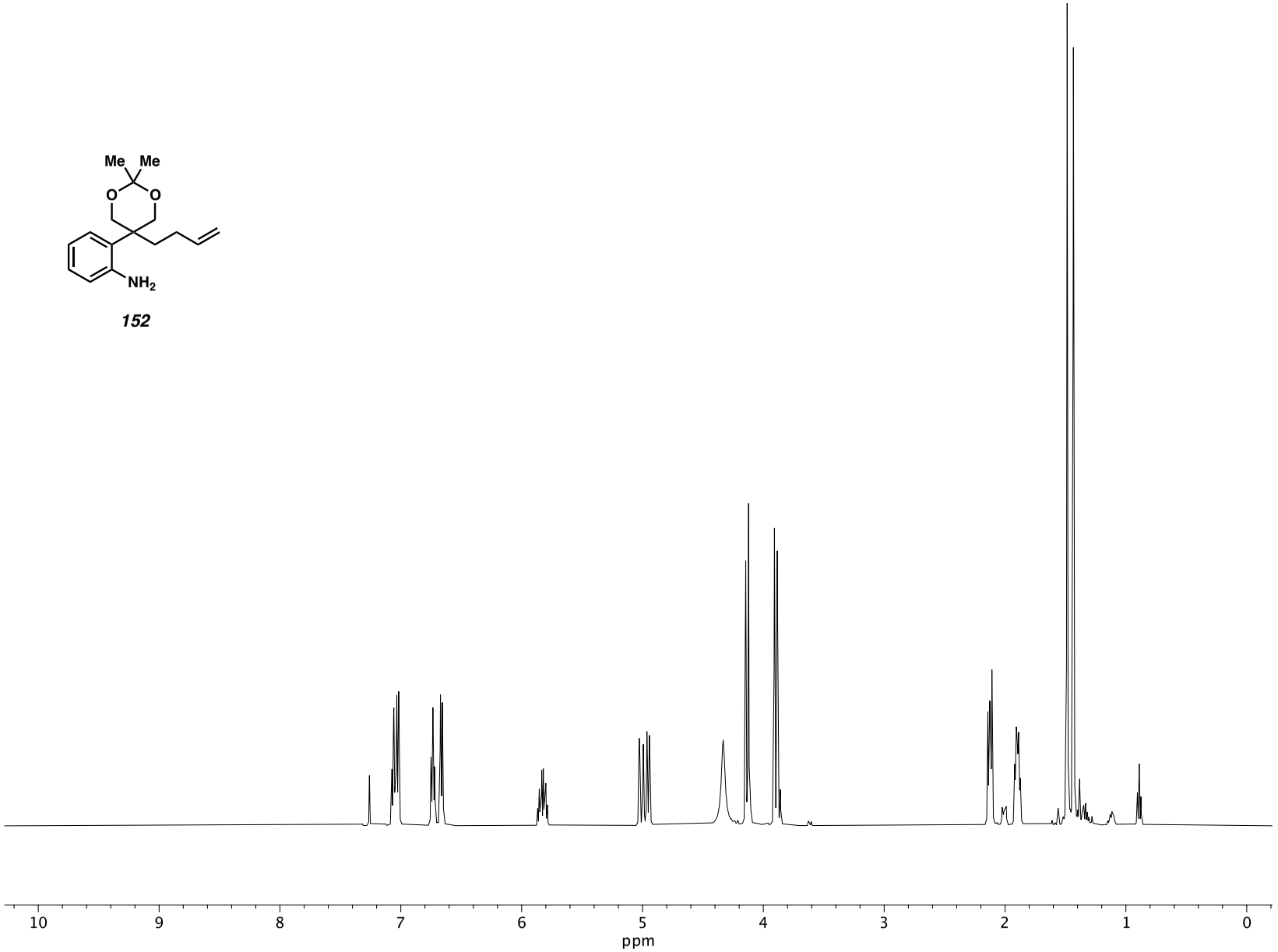


Figure A5.19 *^{1}H NMR (500 MHz, $CDCl_3$) of compound* ***152***.

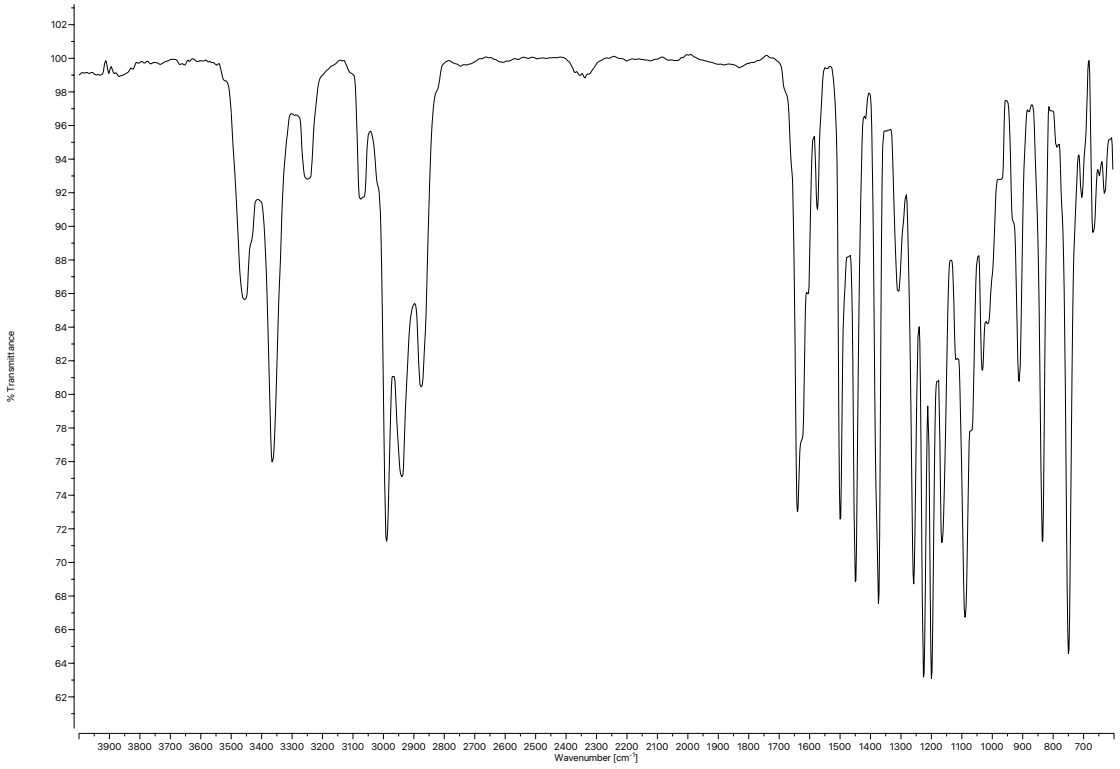


Figure A5.20 *Infrared spectrum (Thin Film, NaCl) of compound* ***152***.

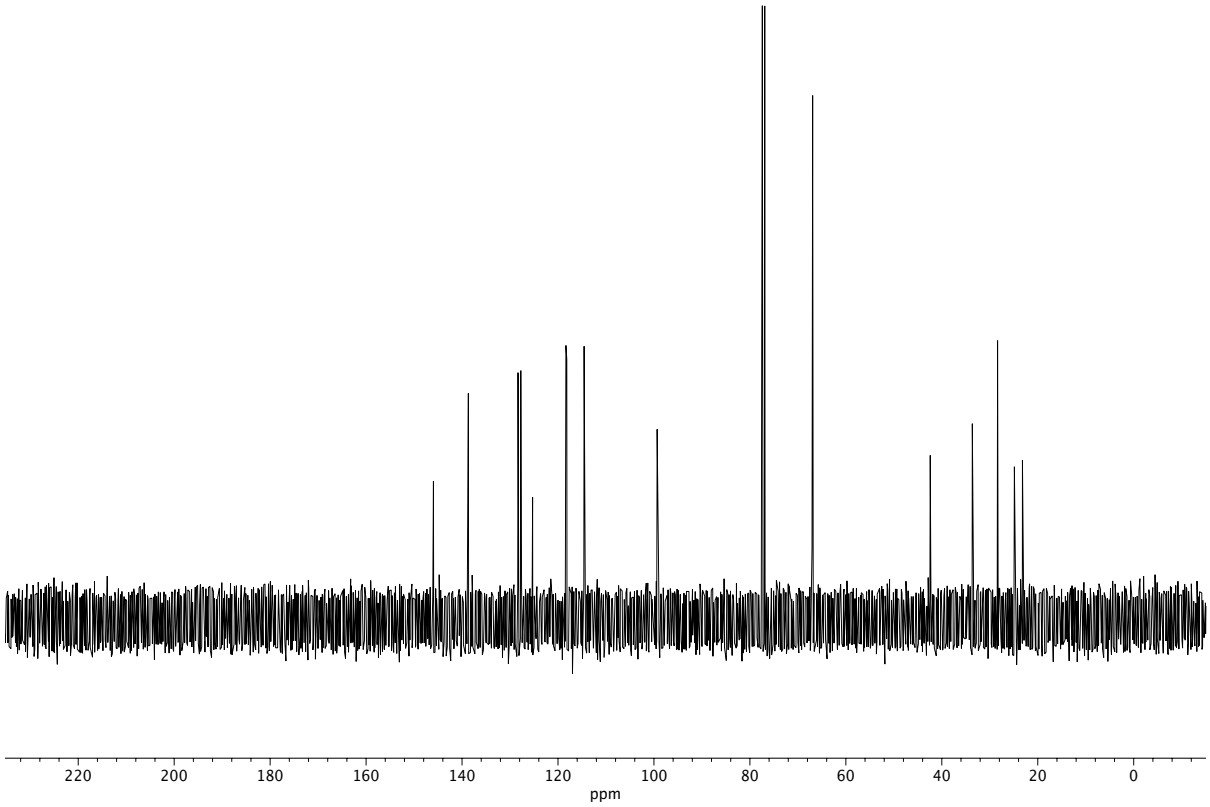


Figure A5.21 *^{13}C NMR (125 MHz, $CDCl_3$) of compound* ***152***.

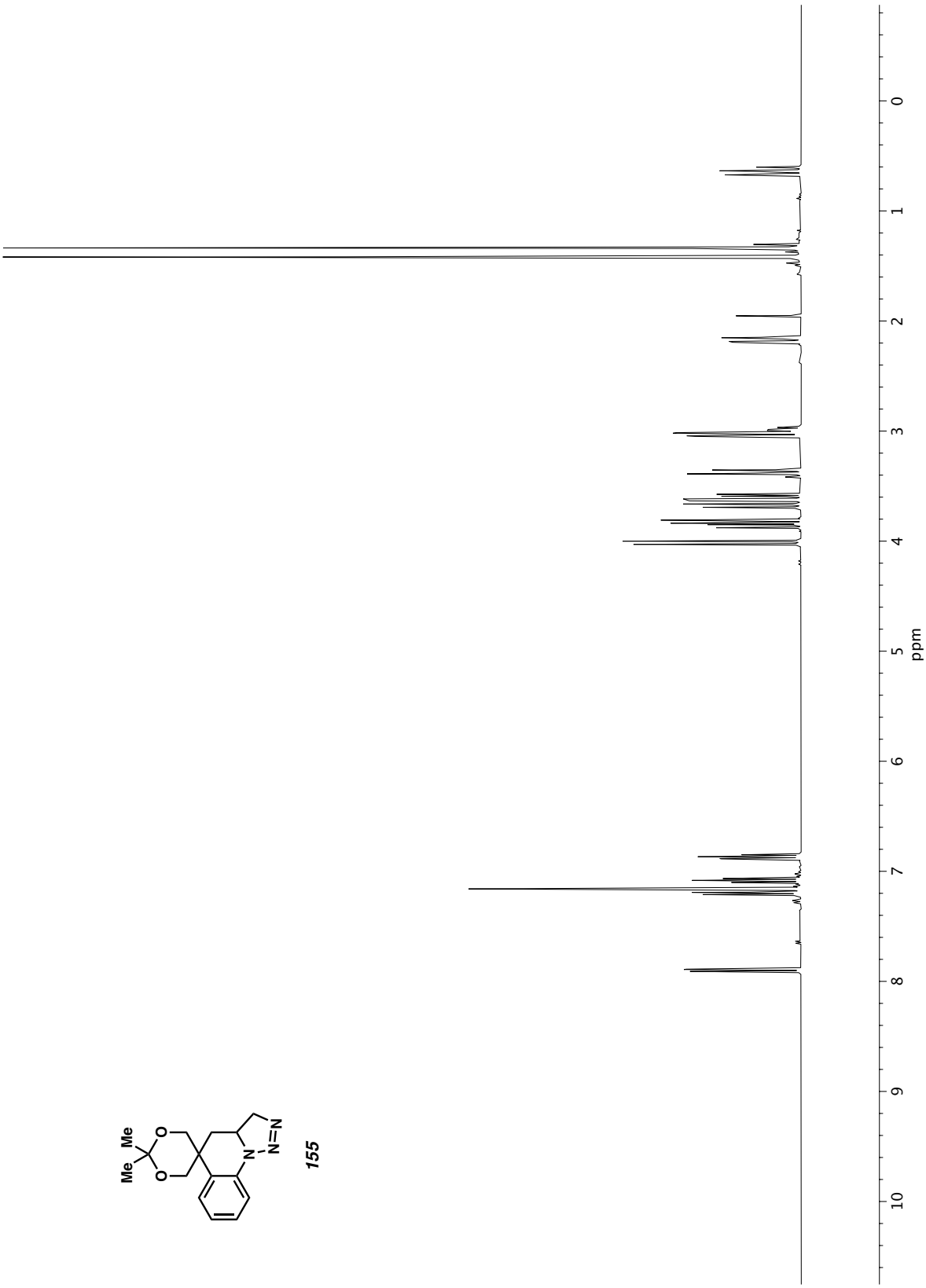


Figure A5.22 *^1H NMR (400 MHz, C_6D_6) of compound **155**.*

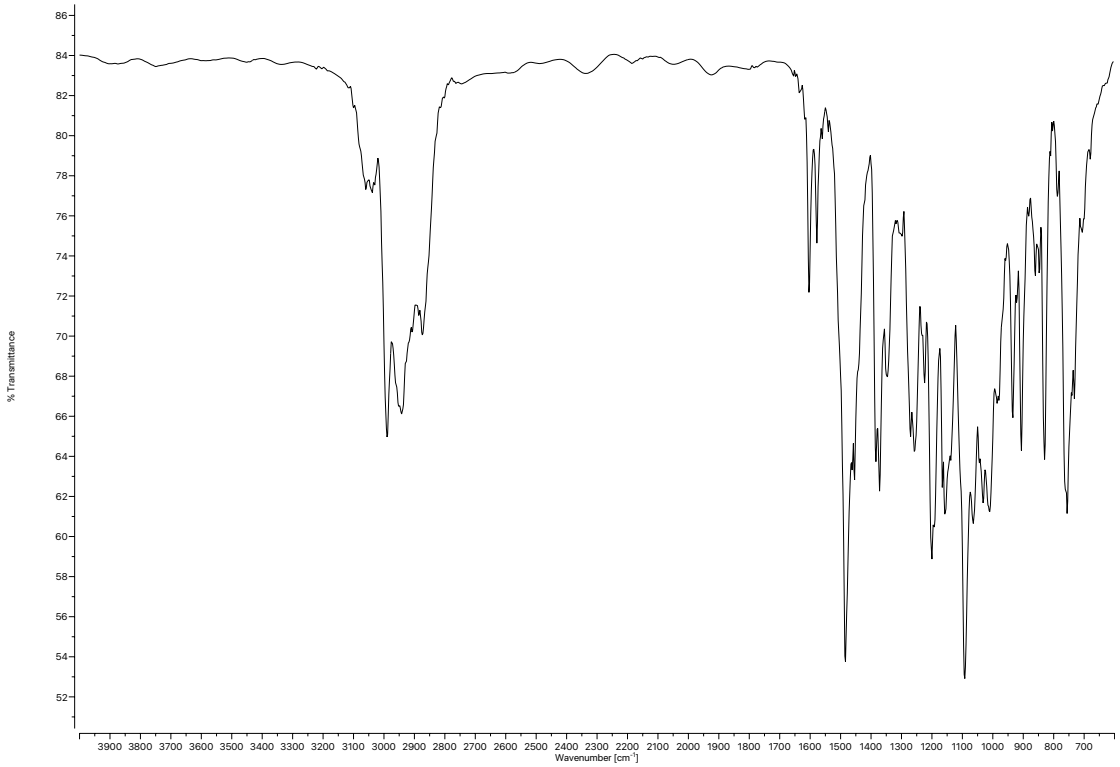


Figure A5.23 *Infrared spectrum (Thin Film, NaCl) of compound* ***155***.

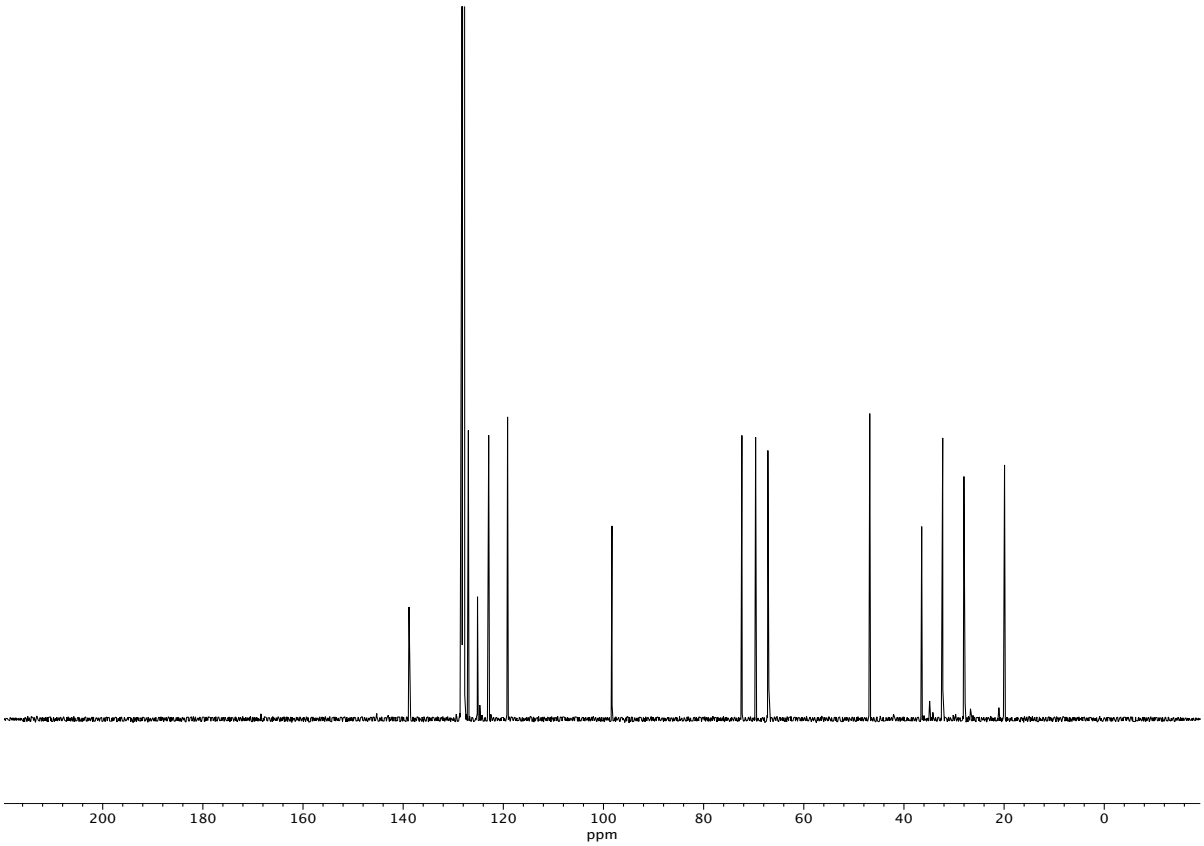


Figure A5.24 *^{13}C NMR (100 MHz, C_6D_6) of compound* ***155***.

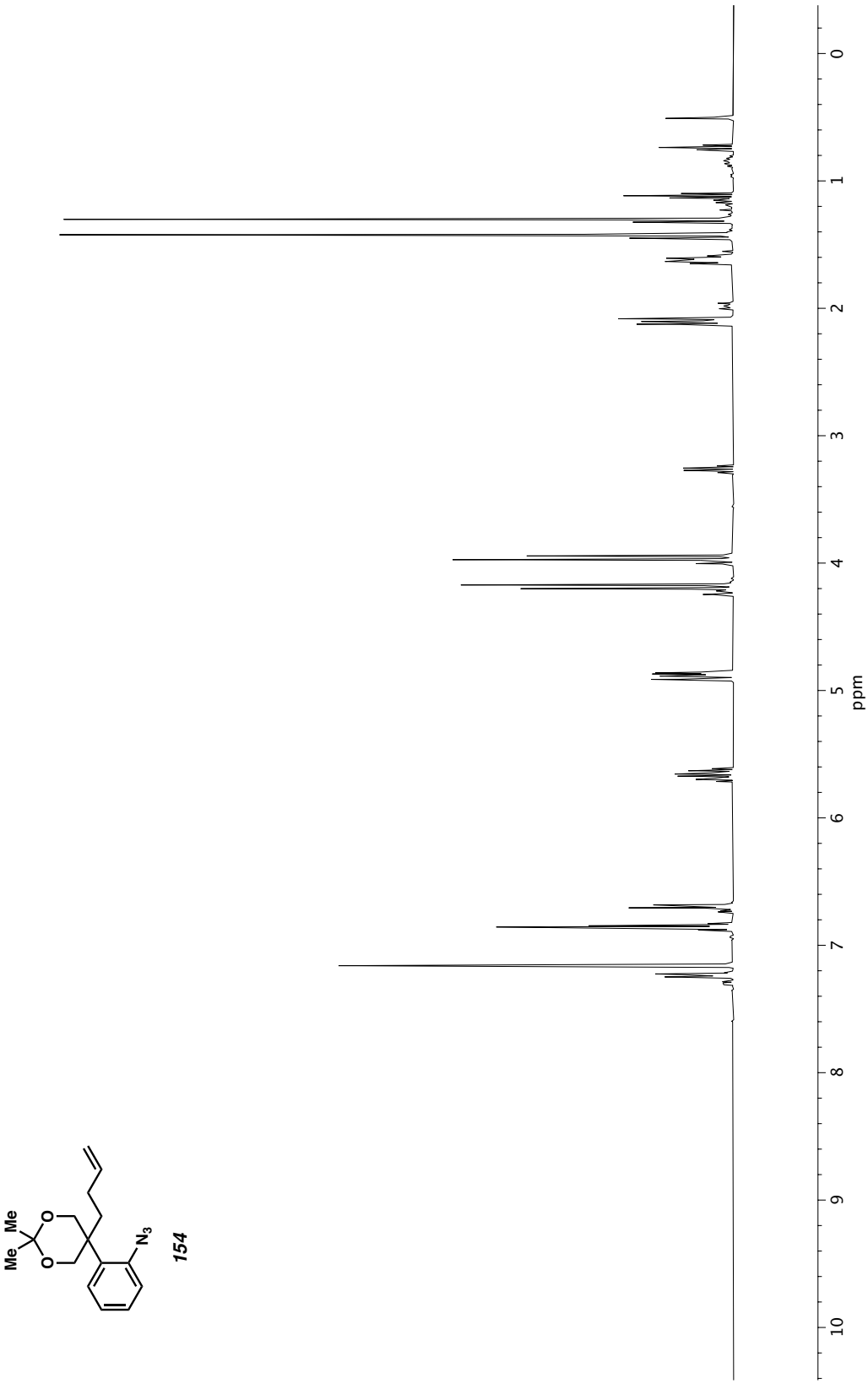


Figure A5.25 *^1H NMR (400 MHz, C_6D_6) of compound* ***154***.

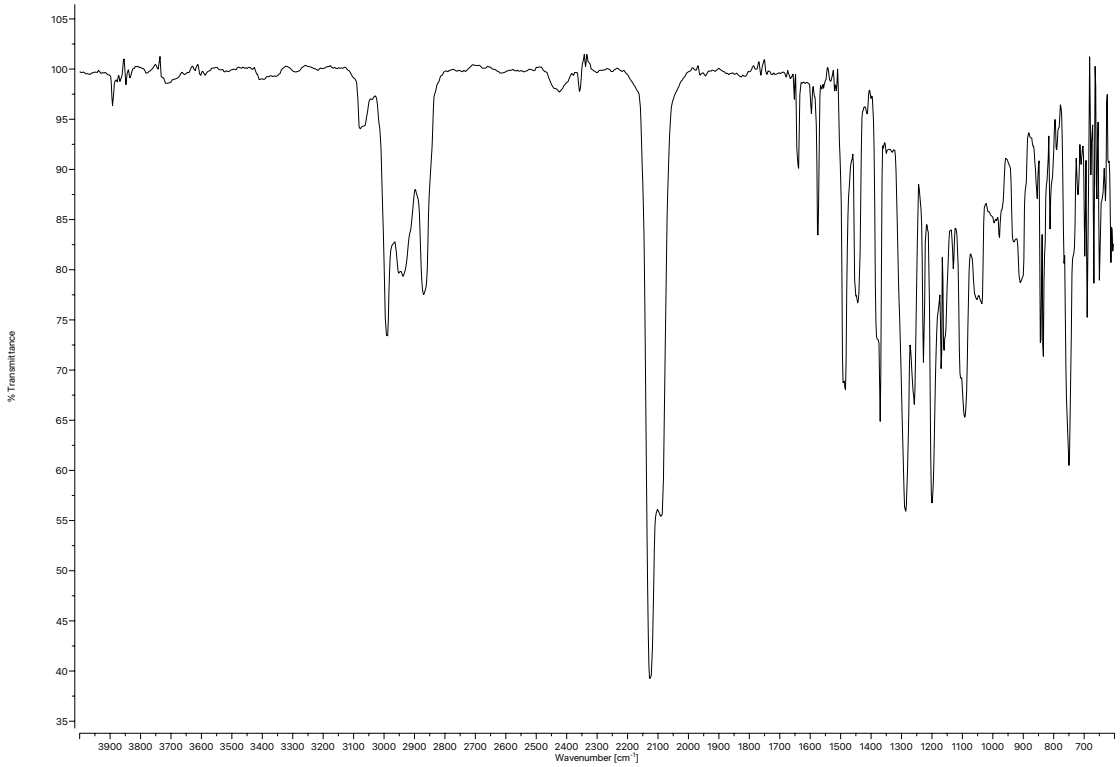


Figure A5.26 *Infrared spectrum (Thin Film, NaCl) of compound* ***154****.*

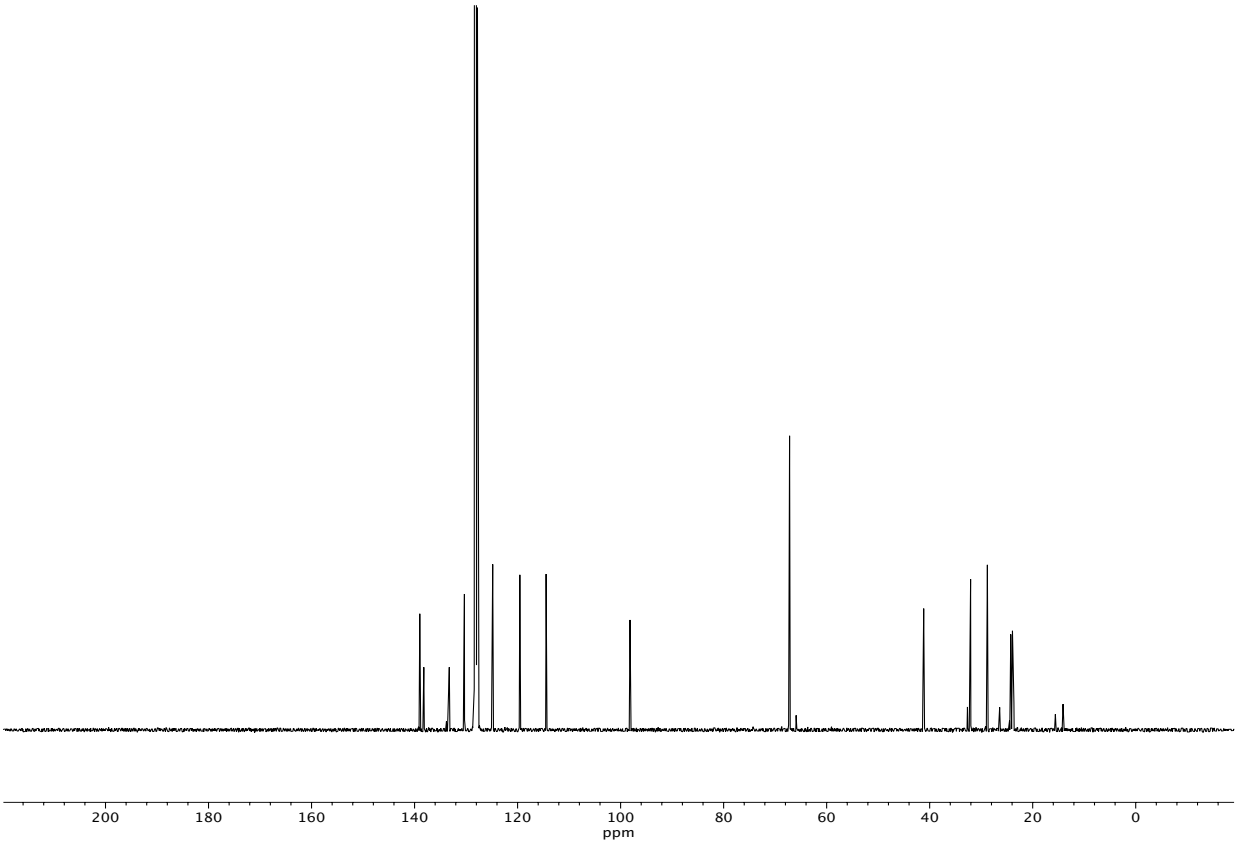


Figure A5.27 *^{13}C NMR (100 MHz, C_6D_6) of compound* ***154****.*

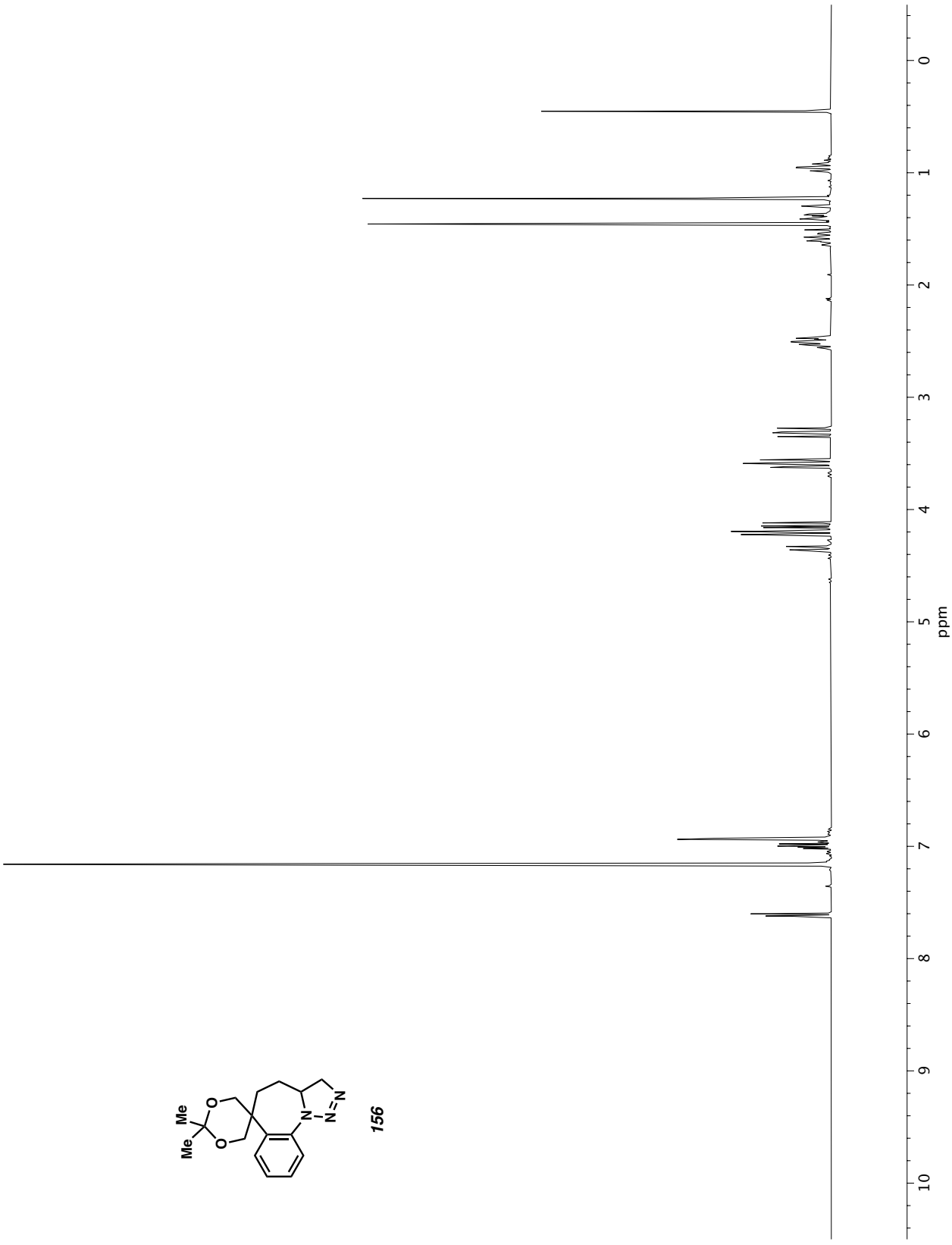


Figure A5.28 *^1H NMR (400 MHz, C_6D_6) of compound* ***156***.

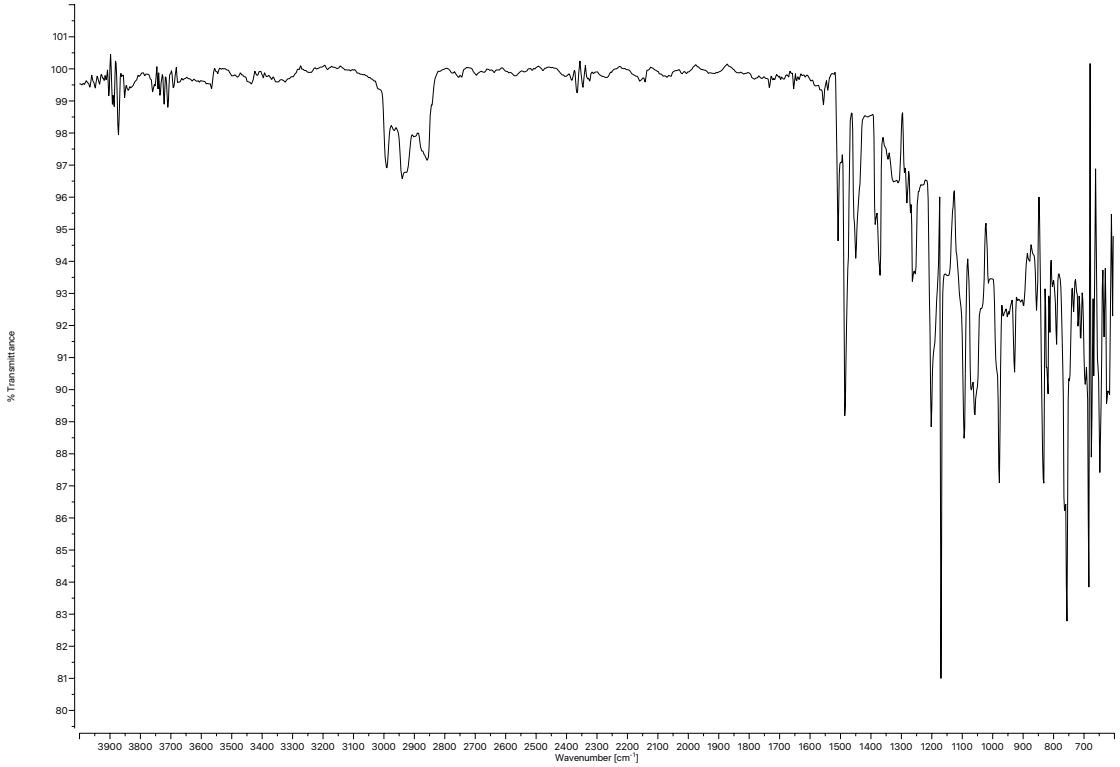


Figure A5.29 *Infrared spectrum (Thin Film, NaCl) of compound* ***156***.

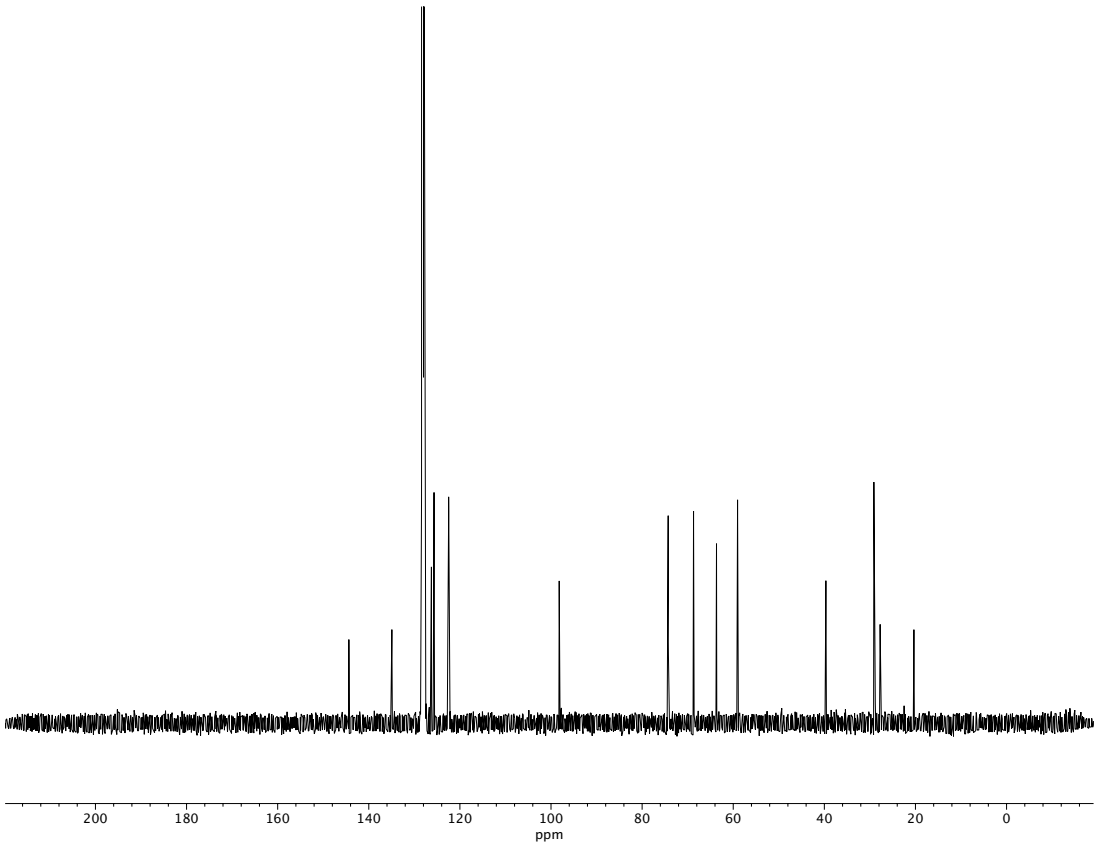


Figure A5.30 *^{13}C NMR (100 MHz, C_6D_6) of compound* ***156***.

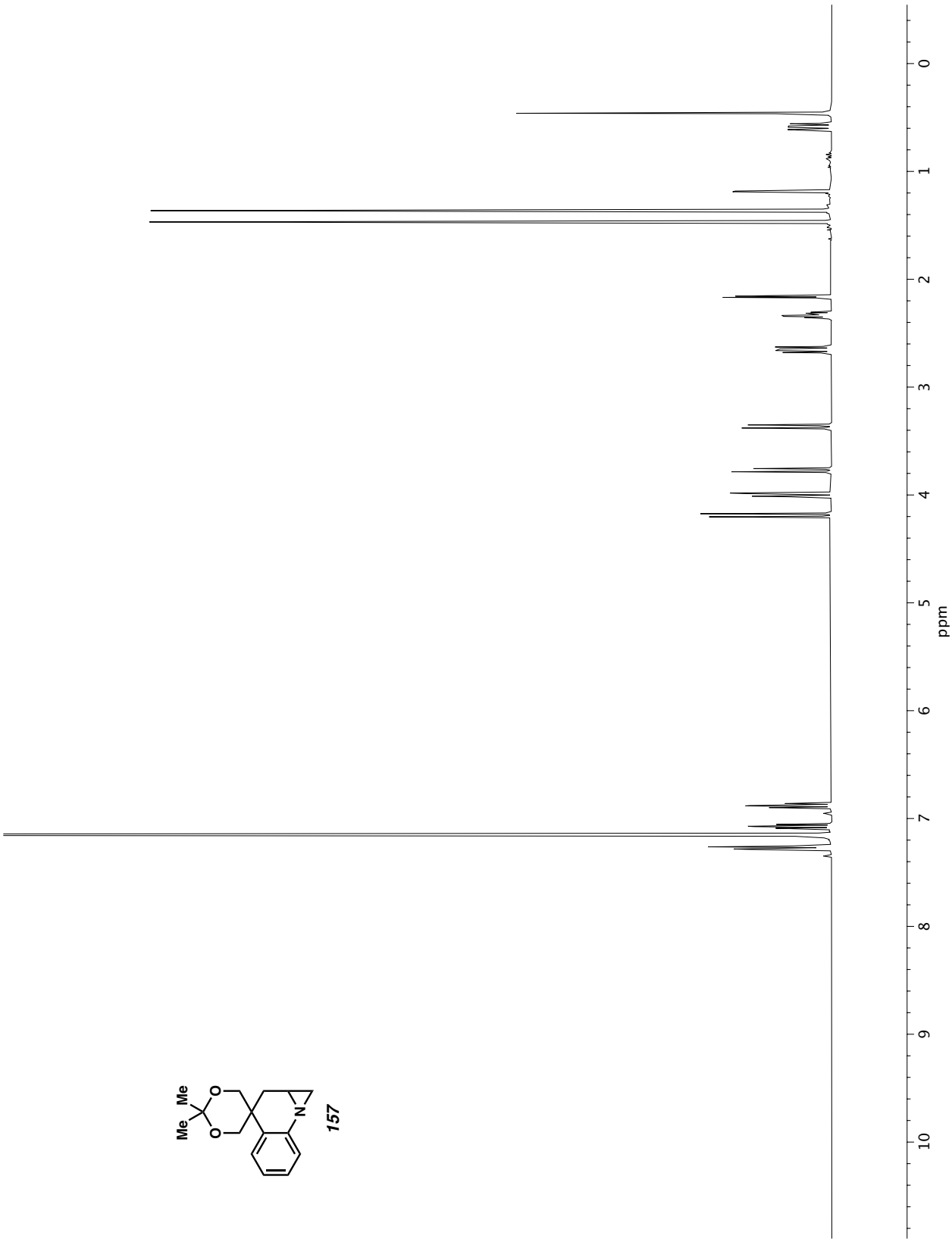


Figure A5.31 *^{1}H NMR (400 MHz, C_6D_6) of compound* ***157****.*

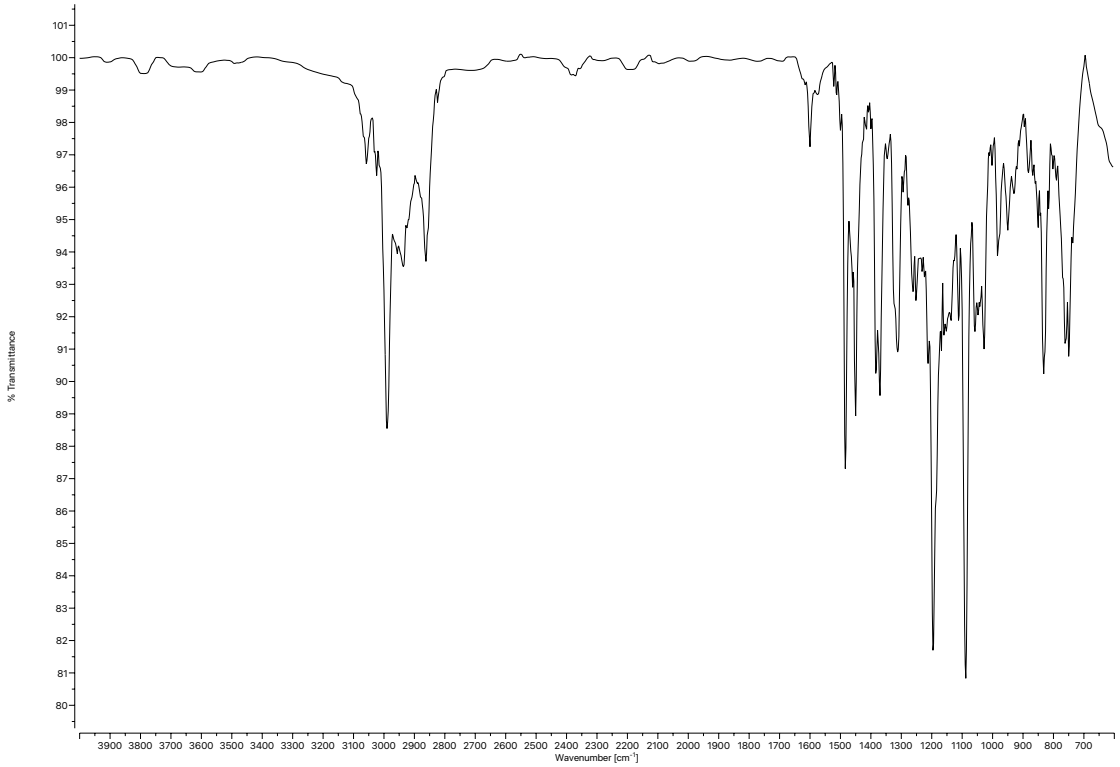


Figure A5.32 *Infrared spectrum (Thin Film, NaCl) of compound* ***157****.*

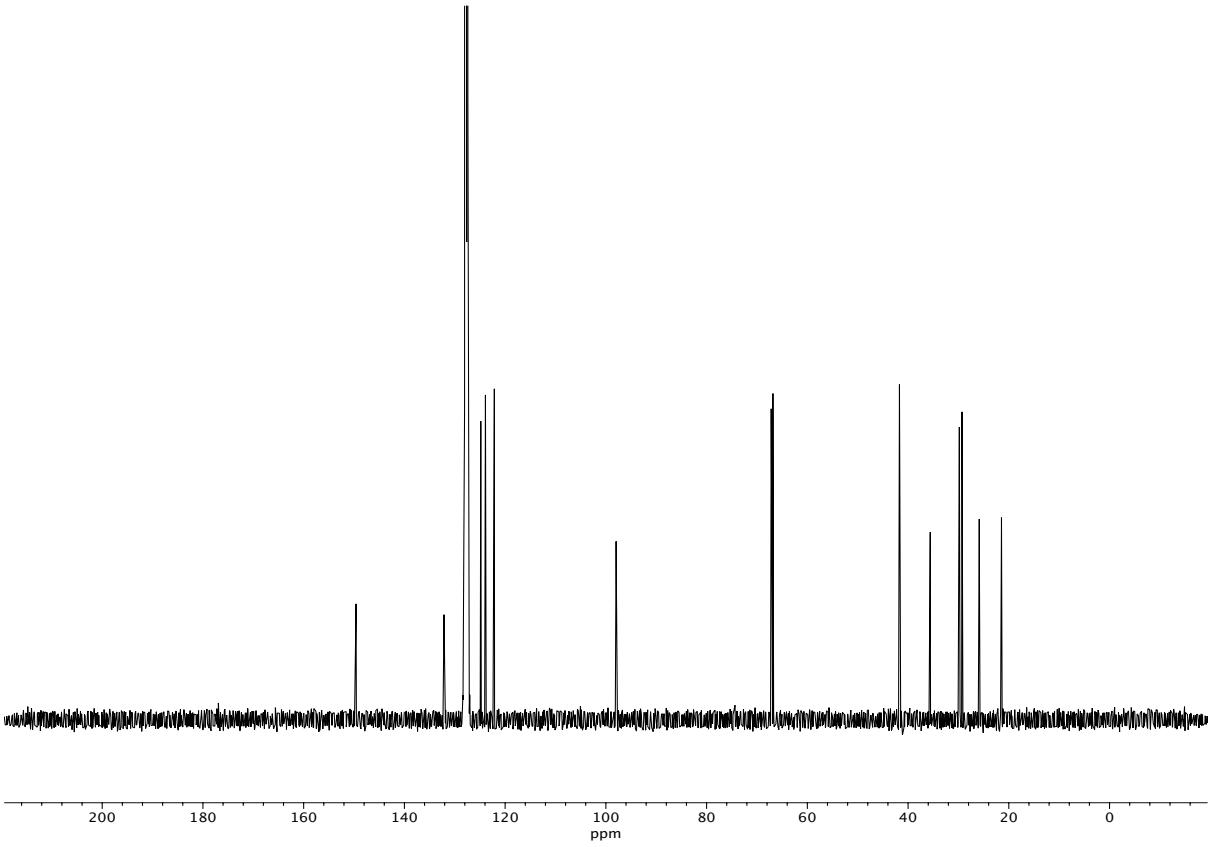


Figure A5.33 *^{13}C NMR (100 MHz, C_6D_6) of compound* ***157****.*

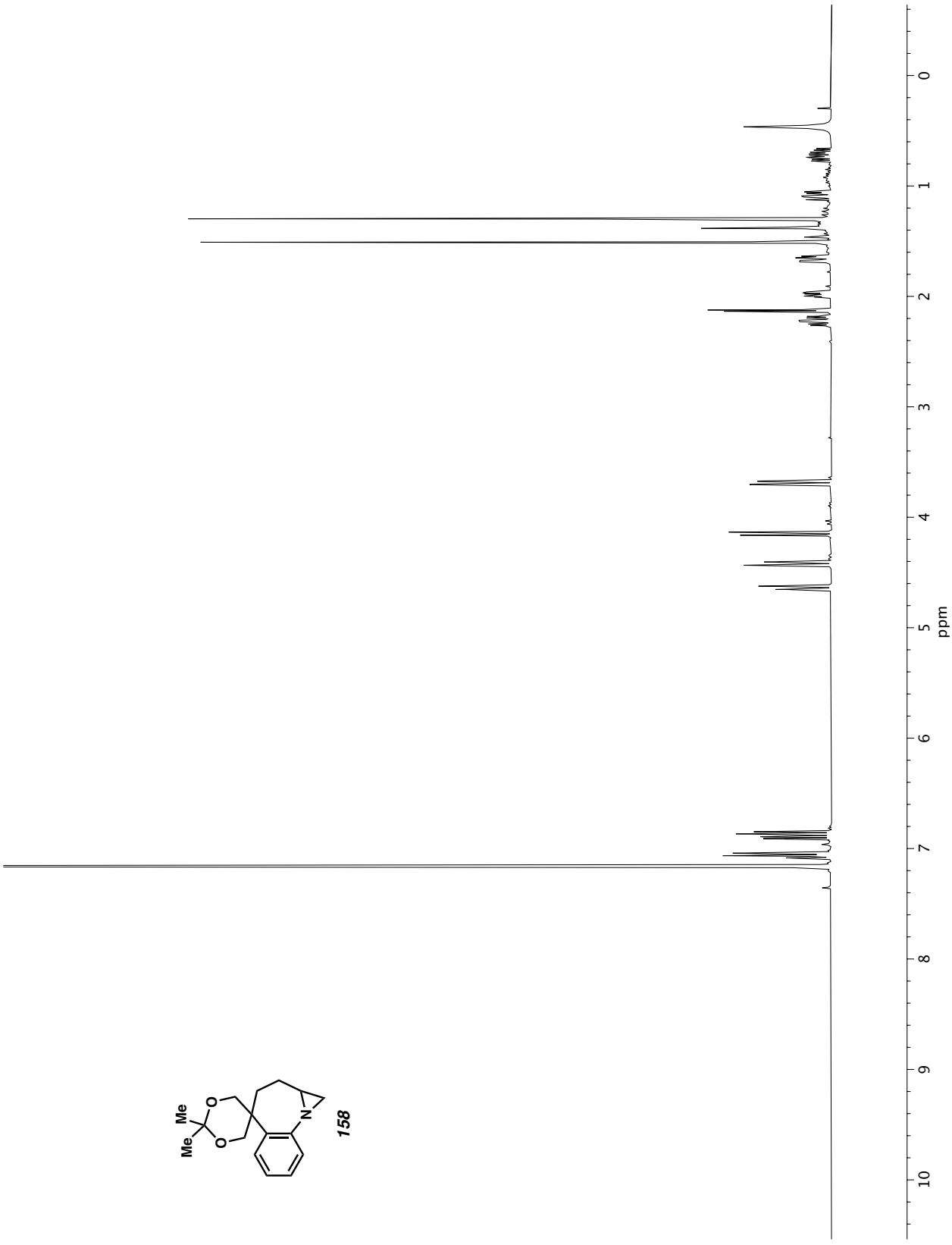


Figure A5.34 *^{1}H NMR (400 MHz, C_6D_6) of compound **158**.*

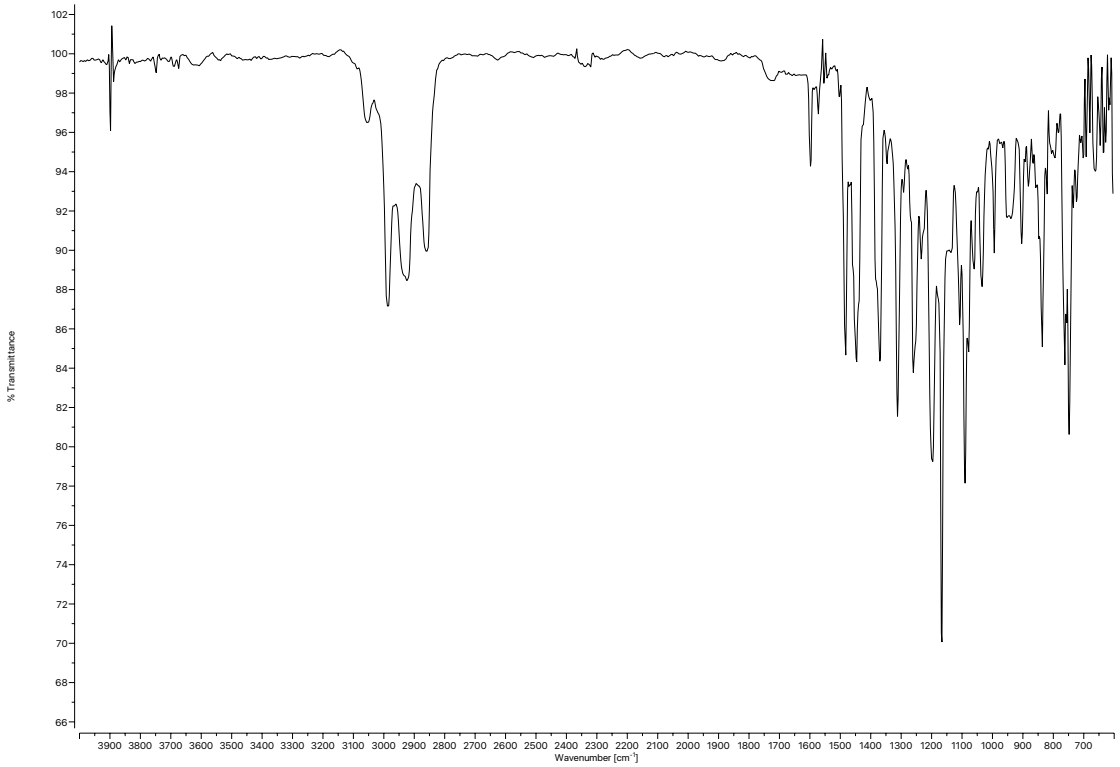


Figure A5.35 *Infrared spectrum (Thin Film, NaCl) of compound* ***158****.*

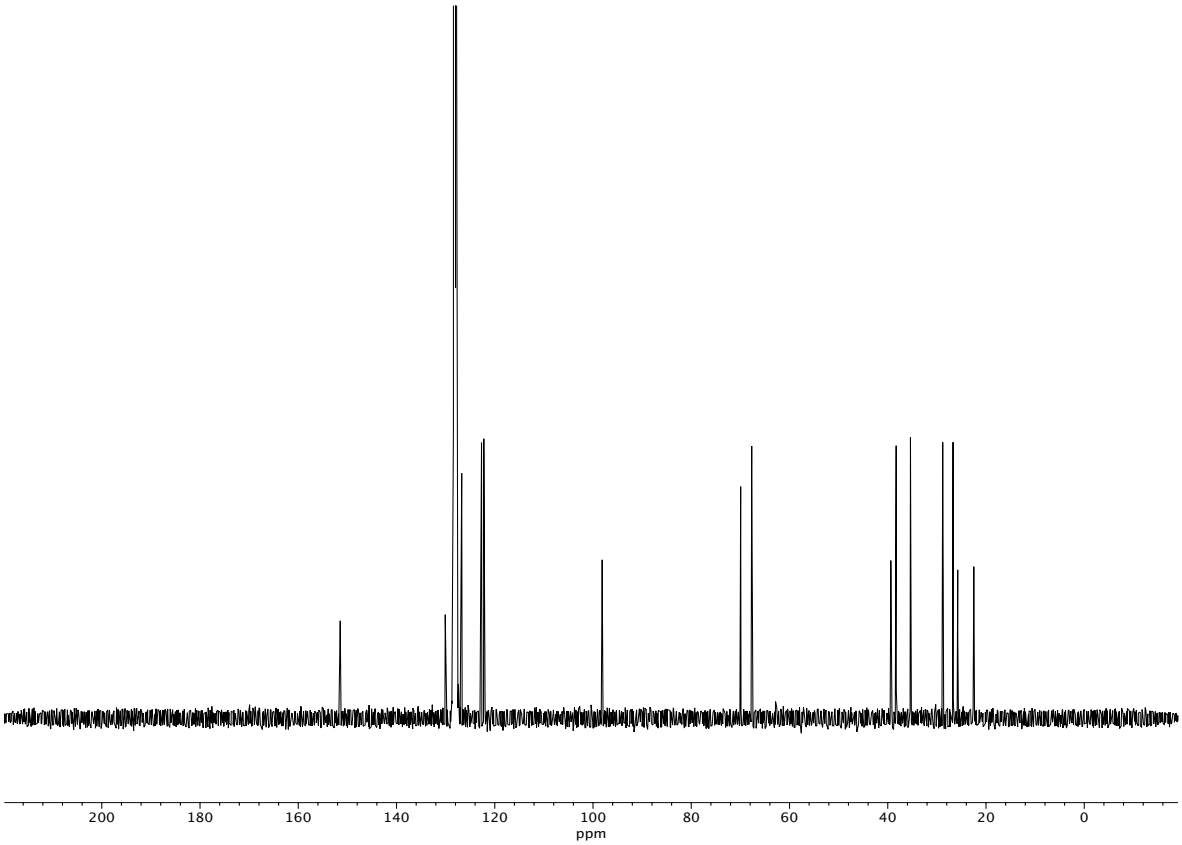
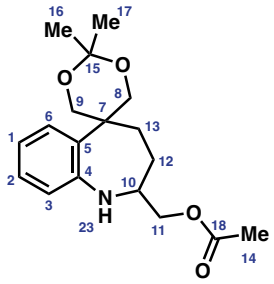


Figure A5.36 *^{13}C NMR (100 MHz, C_6D_6) of compound* ***158****.*

Table A5.1 *2D NMR Correlations for* ***159***



159

No	δ_H	δ_C	HSQC	HMBC	COSY
6	7.12	127.5	127.5(6)	39.8(7), 127.2(2),148.4(4)	6.88(1)
2	6.96	127.2	127.2(2)	127.5(6),148.4(4)	6.53(3),6.88(1)
1	6.88	122.4	122.4(1)	122.5(3),134.8(5)	6.96(2),7.12(6)
3	6.53	122.5	122.5(3)	134.8(5)	6.96(2)
8"	4.44	65.1	65.1(8)	29.8(13), 39.8(7), 68.2(9), 98.1(15),134.8(5)	4.03(8')
9'	4.23	68.2	68.2(9)	29.8(13), 39.8(7), 65.1(8), 98.1(15),134.8(5)	3.88(9")
8'	4.03	65.1	65.1(8)	29.8(13), 39.8(7), 68.2(9), 98.1(15),134.8(5)	4.44(8")
11"	3.91	67.5	67.5(11)	57.0(10),148.4(4), 169.9(18)	2.78(10), 3.67(11')
9"	3.88	68.2	68.2(9)	29.8(13), 39.8(7), 65.1(8), 98.1(15),134.8(5)	4.23(9')
11'	3.67	67.5	67.5(11)	57.0(10), 169.9(18)	2.78(10), 3.91(11")
23	3.49	-	-	-	-
10	2.78	57.0	57.0(10)	27.7(12), 29.8(13), 67.5(11),148.4(4)	1.41(12"), 1.59(12'), 3.67(11'), 3.91(11")
13"	2.25	29.8	29.8(13)	27.7(12), 39.8(7), 57.0(10), 68.2(9),134.8(5)	1.41(12"), 1.41(13'), 1.59(12')
14	1.62	20.3	20.3(14)	169.9(18)	-
12'	1.59	27.7	27.7(12)	39.8(7),57.0(10), 67.5(11)	2.25(13"),2.78(10)
16	1.49	26.9	26.9(16)	21.4(17),98.1(15)	-
12"	1.41	27.7	27.7(12)	39.8(7),57.0(10), 65.1(8), 67.5(11)	2.25(13"),2.78(10)
13'	1.41	29.8	29.8(13)	27.7(12), 39.8(7), 57.0(10), 68.2(9),134.8(5)	2.25(13")
17	1.31	21.4	21.4(17)	26.9(16),98.1(15)	-
5	-	134.8	-	1.41(13'),2.25(13"), 3.88(9"), 4.03(8'), 4.23(9'), 4.44(8"), 6.53(3), 6.88(1)	-
4	-	148.4	-	2.78(10), 3.91(11"), 6.96(2), 7.12(6)	-
7	-	39.8	-	1.41(12"), 1.41(13'), 1.59(12'), 2.25(13"), 3.88(9"), 4.03(8'), 4.23(9'), 4.44(8"), 7.12(6)	-
15	-	98.1	-	1.31(17), 1.49(16), 3.88(9"), 4.03(8'), 4.23(9'),4.44(8")	-
18	-	169.9	-	1.62(14), 3.67(11'),3.91(11")	-

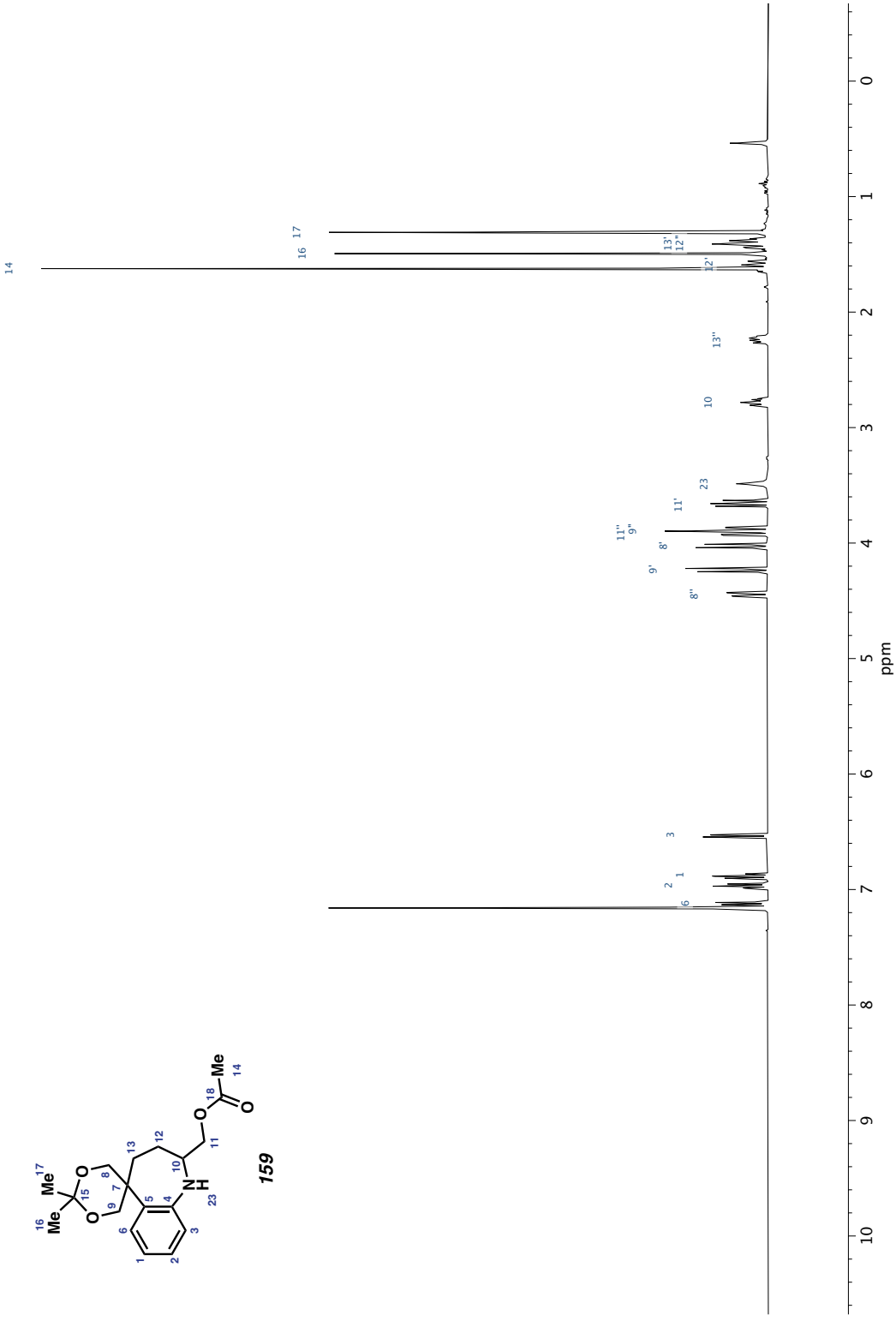


Figure A5.37 *^{1}H NMR (400 MHz, C_6D_6) of compound* ***159***.

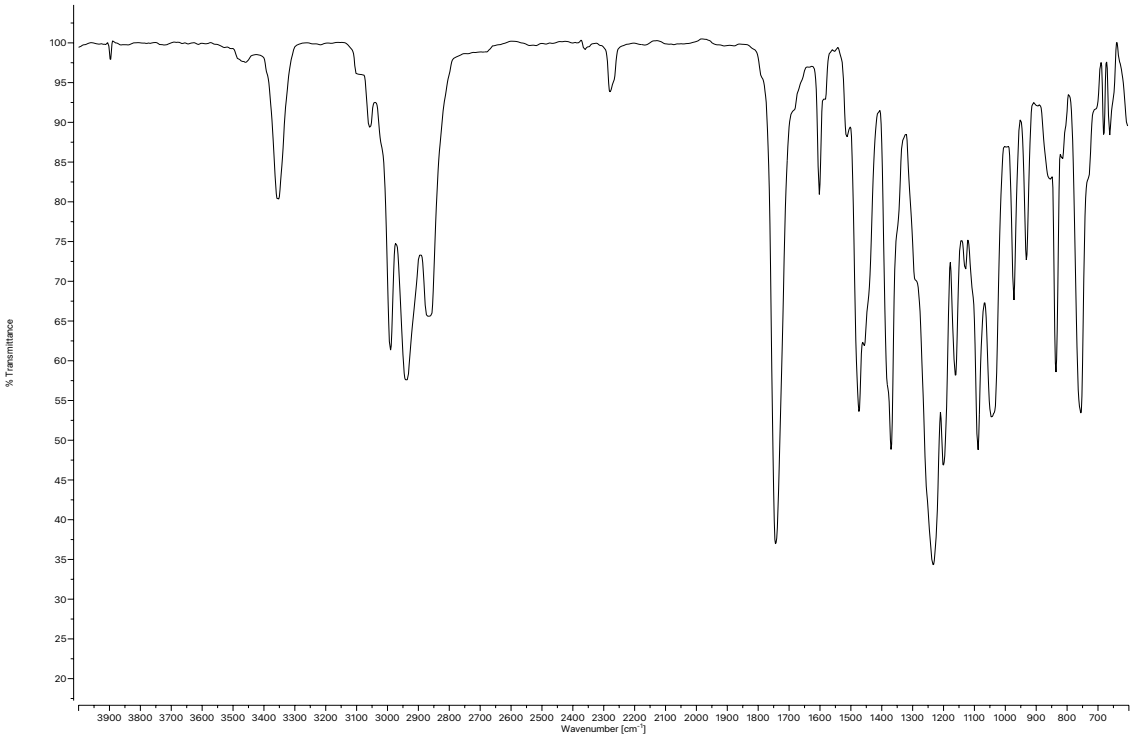


Figure A.38 *Infrared spectrum (Thin Film, NaCl) of compound* ***159****.*

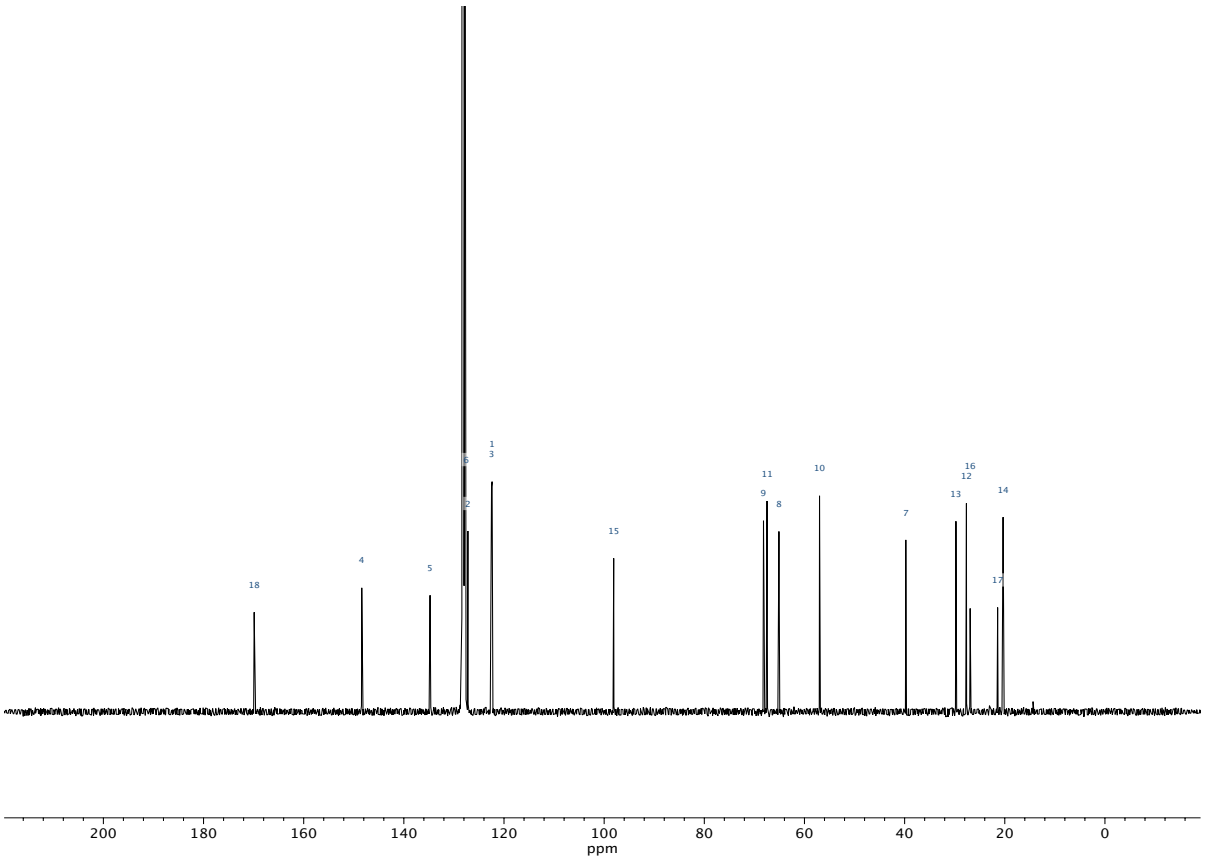


Figure A.39 *^{13}C NMR (100 MHz, C_6D_6) of compound* ***159****.*

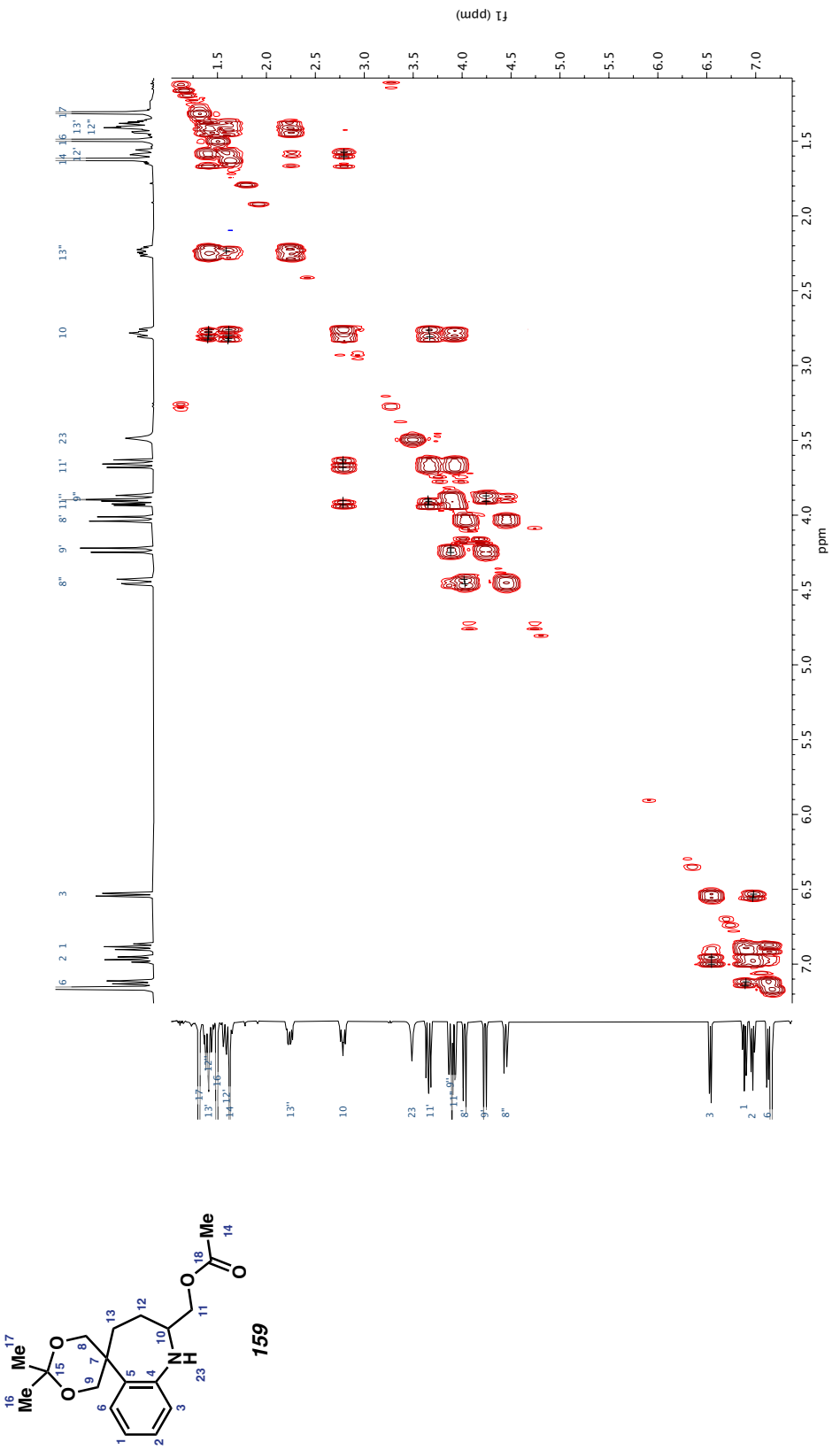


Figure A.40 *COSY spectrum (C_6D_6) of compound* ***159***.

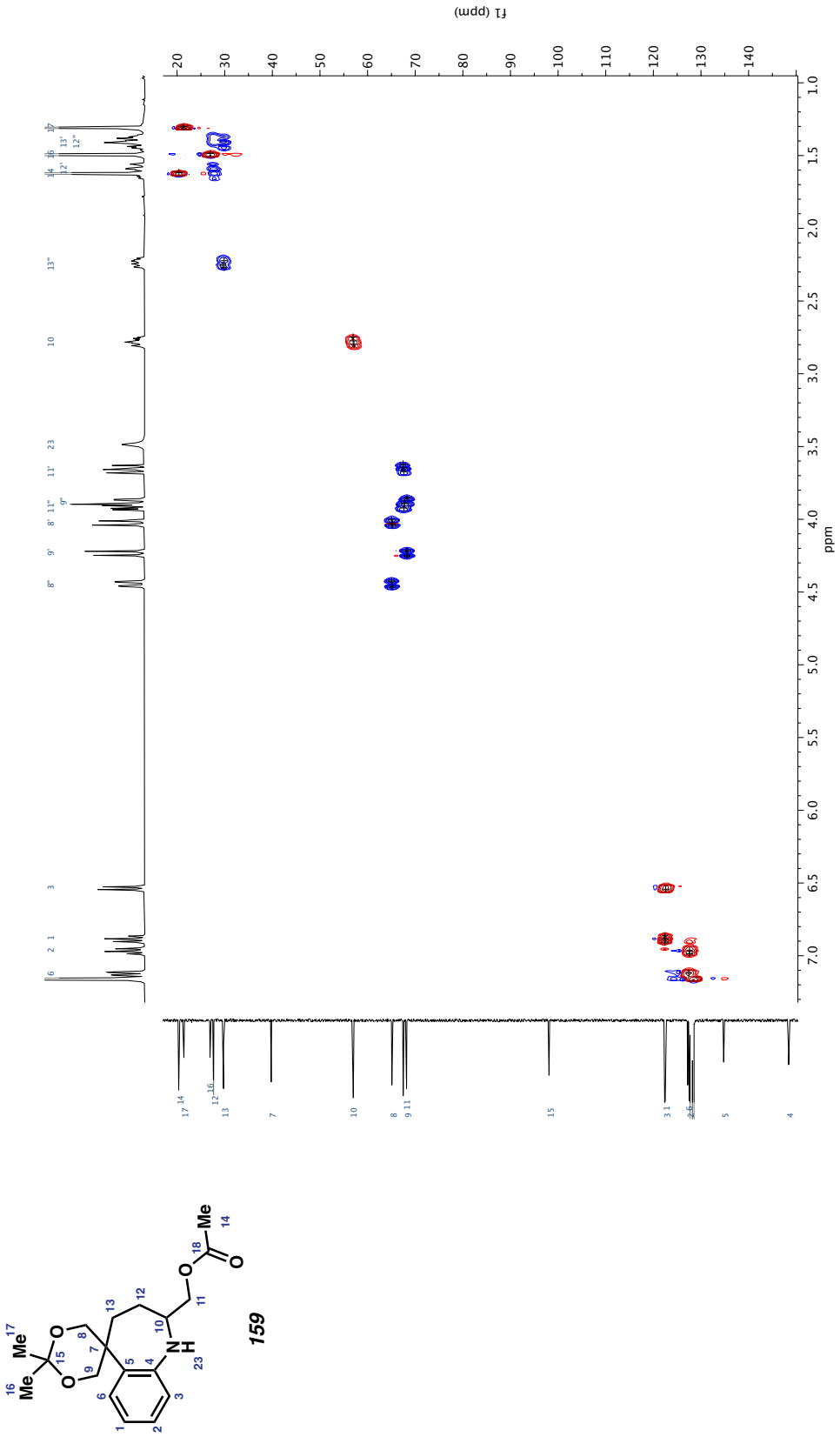


Figure A.41 *HSQC spectrum (C_6D_6) of compound* ***159***.

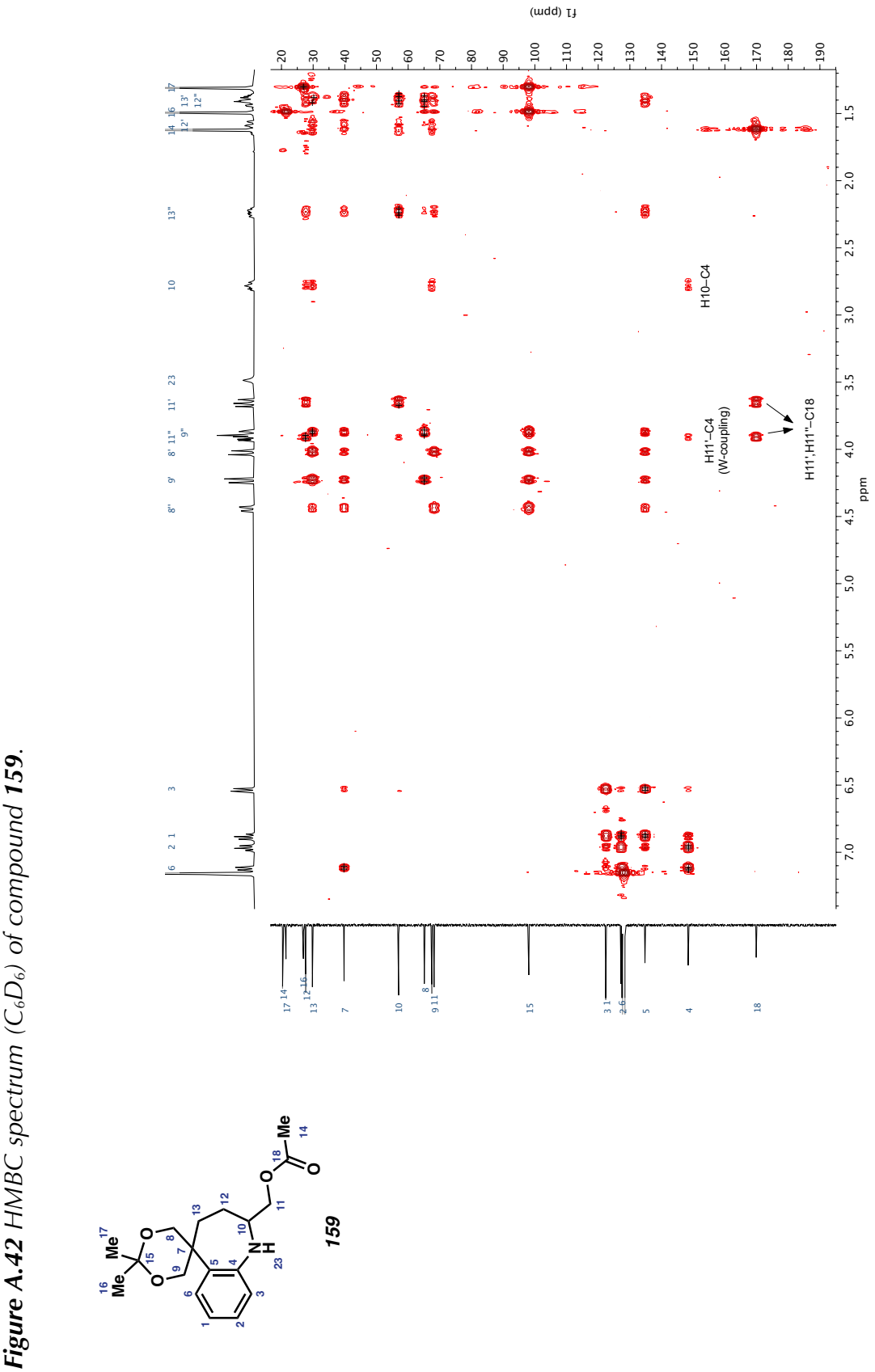


Figure A.42 *HMBC spectrum (C_6D_6) of compound* ***159***.

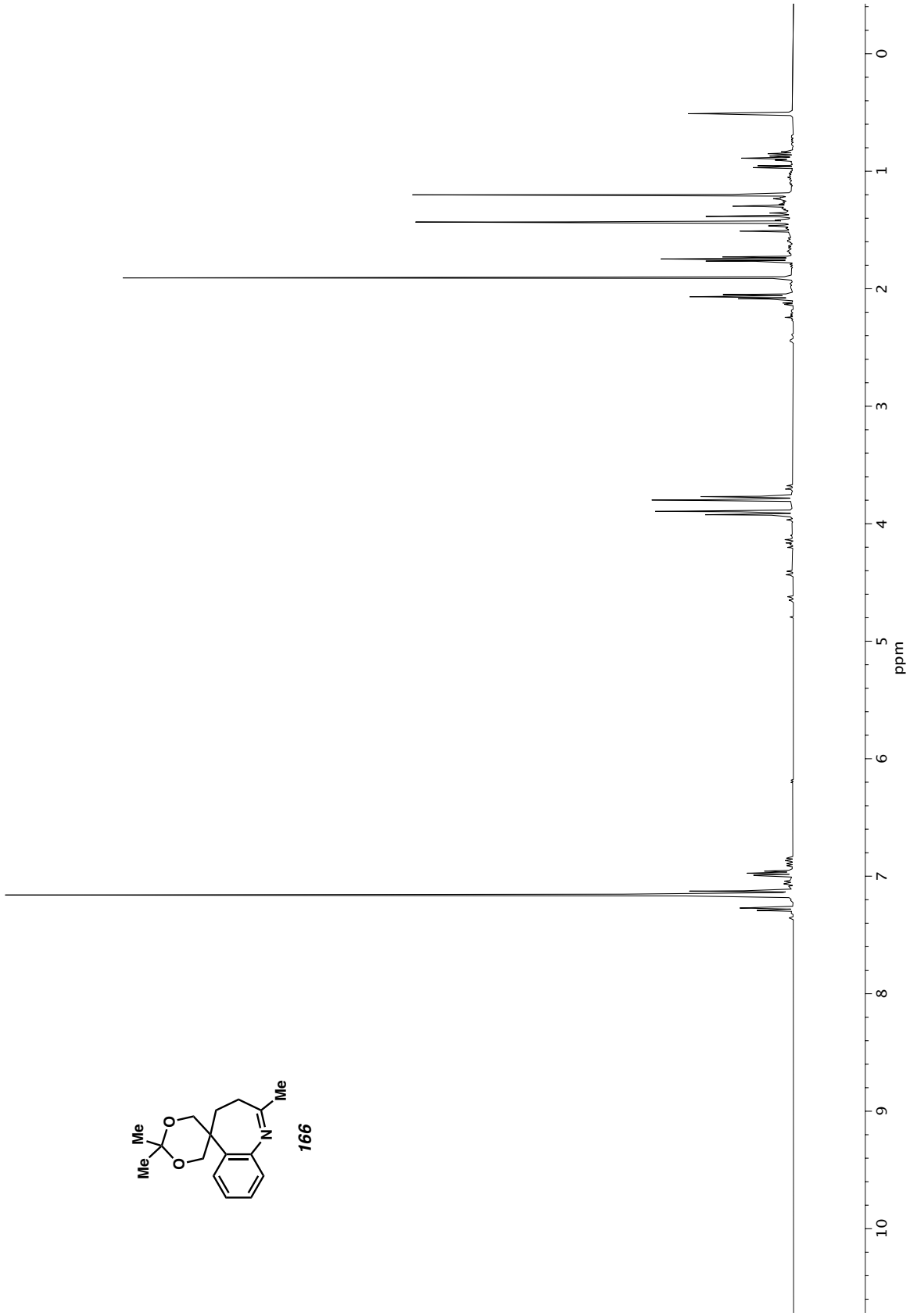


Figure A5.43 *^1H NMR (400 MHz, C_6D_6) of compound* ***166****.*

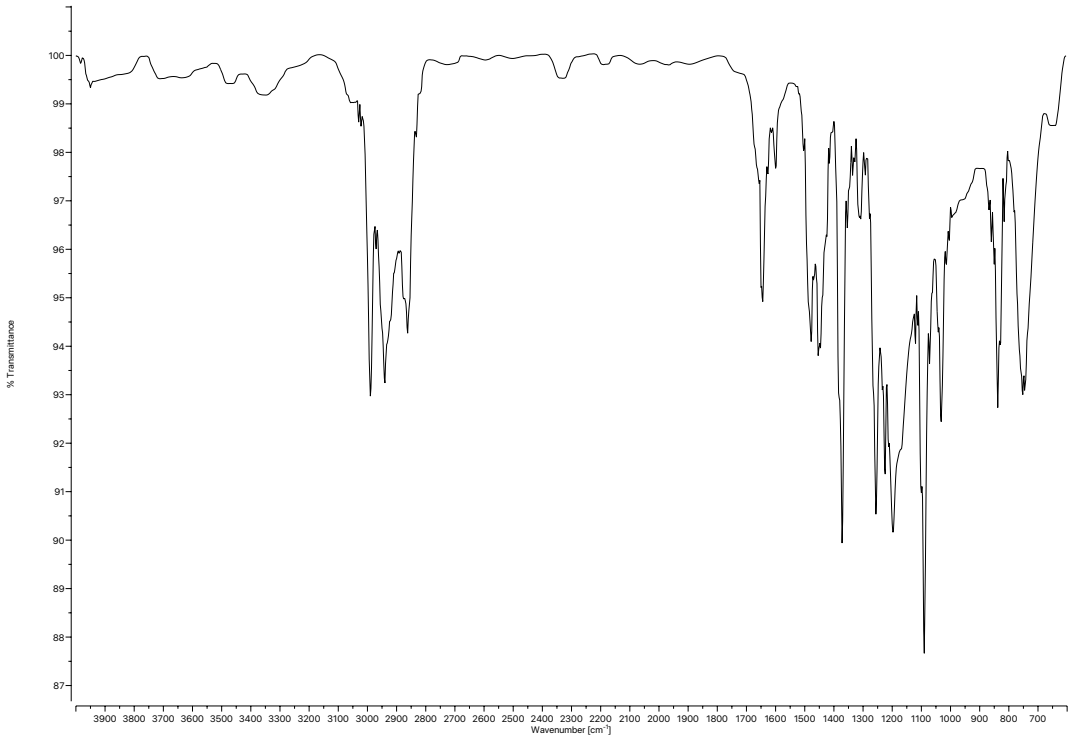


Figure A5.44 *Infrared spectrum (Thin Film, NaCl) of compound* ***166****.*

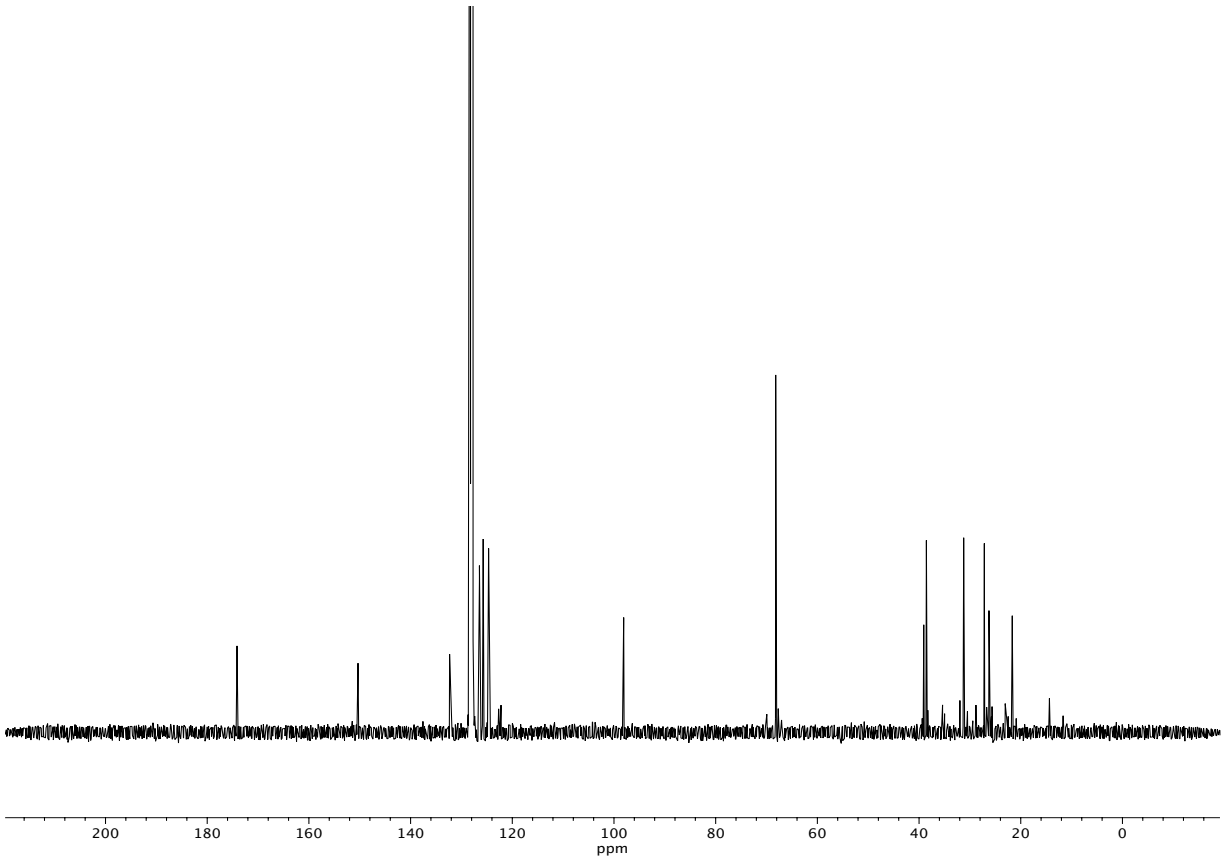
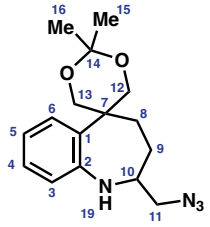


Figure A5.45 *^{13}C NMR (100 MHz, C_6D_6) of compound* ***166****.*

Table A5.2 *2D NMR Correlations for* ***160***



160

No	δ_H	δ_C	HSQC	HMBC	COSY
6	7.14	126.6	126.6(6)	39.5(7), 127.7(4),147.6(2)	6.96(5)
4	7.10	127.7	127.7(4)	147.6(2)	6.81(3),6.96(5)
5	6.96	122.4	122.4(5)	122.8(3),134.2(1)	7.10(4),7.14(6)
3	6.81	122.8	122.8(3)	122.4(5),134.2(1)	7.10(4)
13"	4.43	64.9	64.9(13)	29.4(8), 39.5(7), 67.9(12), 98.2(14),134.2(1)	4.00(13')
12"	4.32	67.9	67.9(12)	29.4(8), 39.5(7), 64.9(13), 98.2(14),134.2(1)	3.95(12')
13'	4.00	64.9	64.9(13)	29.4(8), 39.5(7), 67.9(12), 98.2(14),134.2(1)	4.43(13")
12'	3.95	67.9	67.9(12)	29.4(8), 39.5(7), 64.9(13), 98.2(14),134.2(1)	4.32(12")
19	3.70	-	-	-	-
11'	3.49	56.2	56.2(11)	28.7(9), 56.8(10),147.6(2)	2.96(10), 3.24(11")
11"	3.24	56.2	56.2(11)	28.7(9),56.8(10)	2.96(10), 3.49(11')
10	2.96	56.8	56.8(10)	29.4(8), 56.2(11),147.6(2)	1.78(9"), 3.24(11"), 3.49(11')
8'	2.29	29.4	29.4(8)	28.7(9), 39.5(7), 56.8(10), 67.9(12),134.2(1)	1.60(8"),1.78(9"), 1.78(9')
9'	1.78	28.7	28.7(9)	56.8(10)	1.60(8"), 2.29(8')
9"	1.78	28.7	28.7(9)	29.4(8), 39.5(7),56.8(10)	1.60(8"), 2.29(8'),2.96(10)
8"	1.60	29.4	29.4(8)	28.7(9), 39.5(7), 56.8(10), 64.9(13),134.2(1)	1.78(9"), 1.78(9'), 2.29(8')
16	1.46	26.9	26.9(16)	21.1(15),98.2(14)	-
15	1.42	21.1	21.1(15)	26.9(16),98.2(14)	-
1	-	134.2	-	1.60(8"), 2.29(8'), 3.95(12'), 4.00(13'), 4.32(12"), 4.43(13"), 6.81(3), 6.96(5)	-
2	-	147.6	-	2.96(10), 3.49(11'), 7.10(4), 7.14(6)	-
7	-	39.5	-	1.60(8"),1.78(9"), 2.29(8'), 3.95(12'), 4.00(13'), 4.32(12"), 4.43(13"), 7.14(6)	-
14	-	98.2	-	1.42(15), 1.46(16), 3.95(12'), 4.00(13'),4.32(12"), 4.43(13")	-

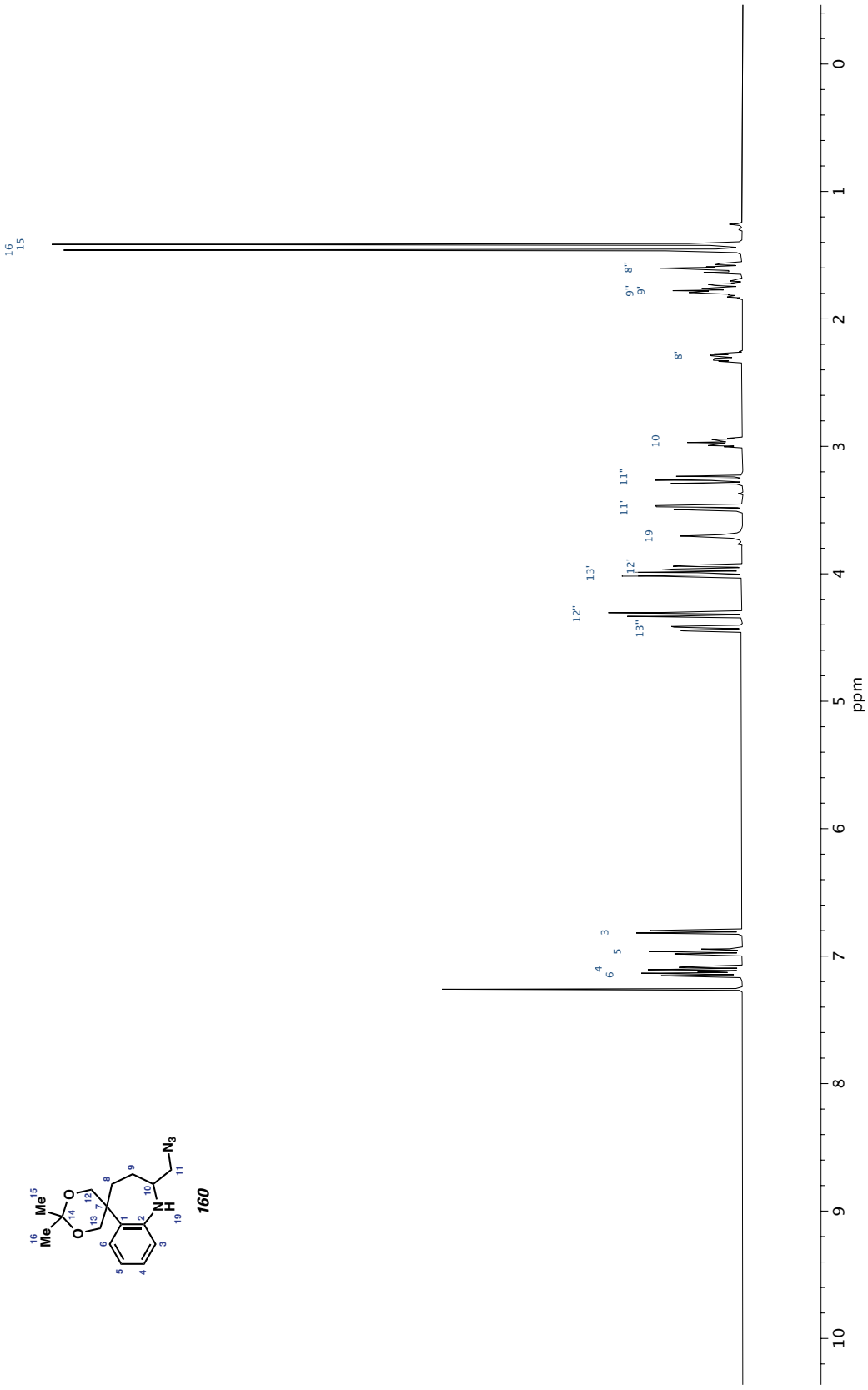


Figure A5.46 *^{1}H NMR (400 MHz, $CDCl_3$) of compound* ***160****.*

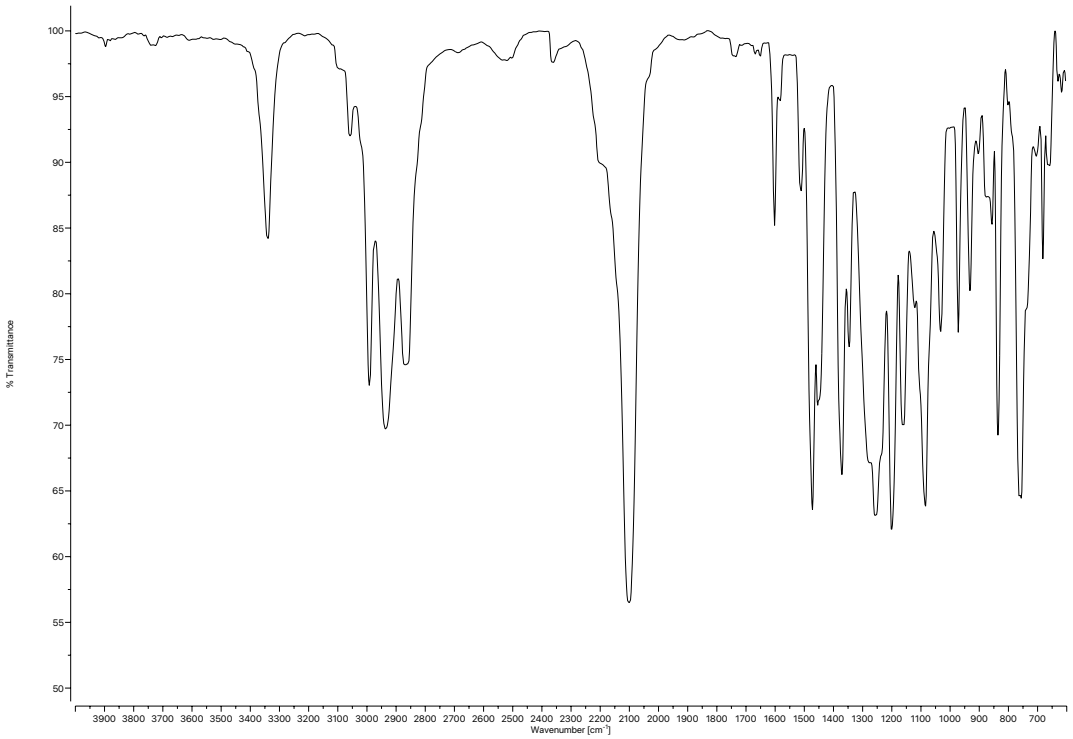


Figure A5.47 *Infrared spectrum (Thin Film, NaCl) of compound* ***160***.

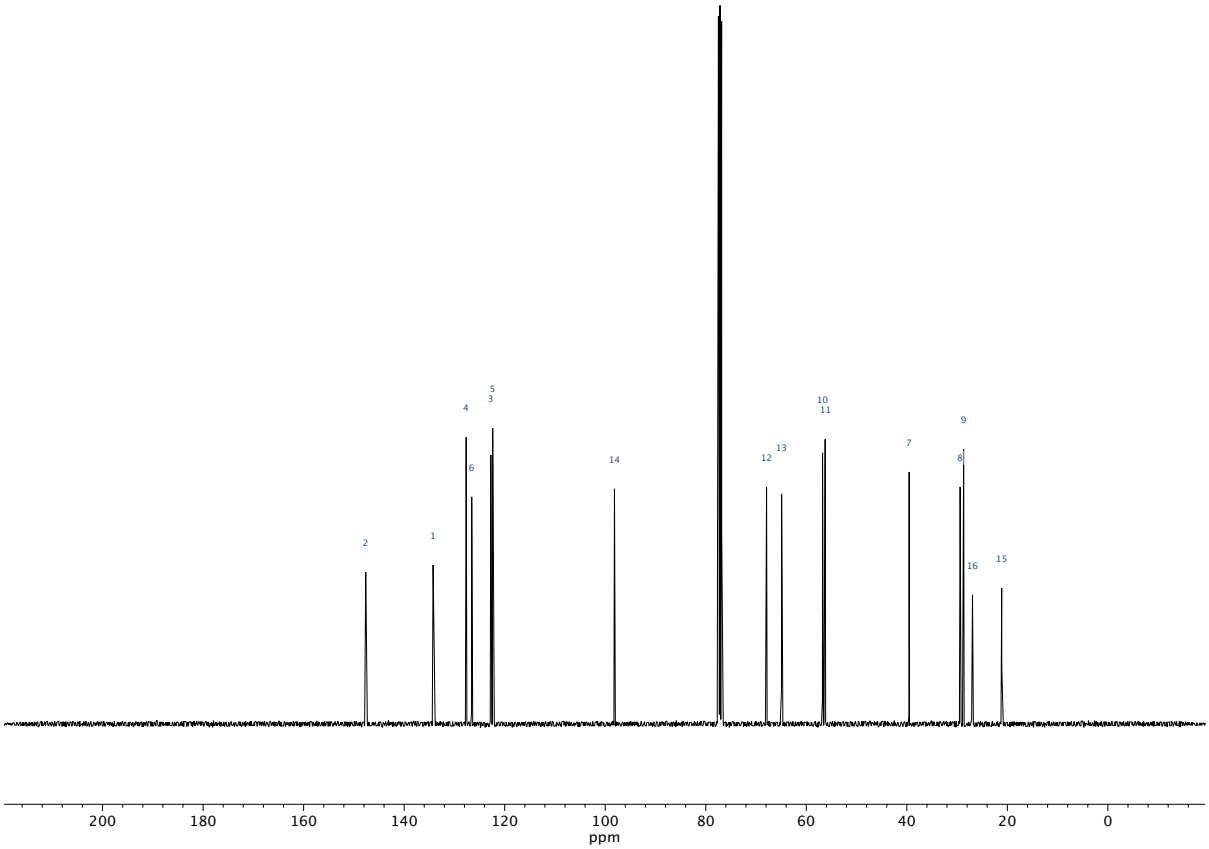


Figure A5.48 *^{13}C NMR (100 MHz, $CDCl_3$) of compound* ***160***.

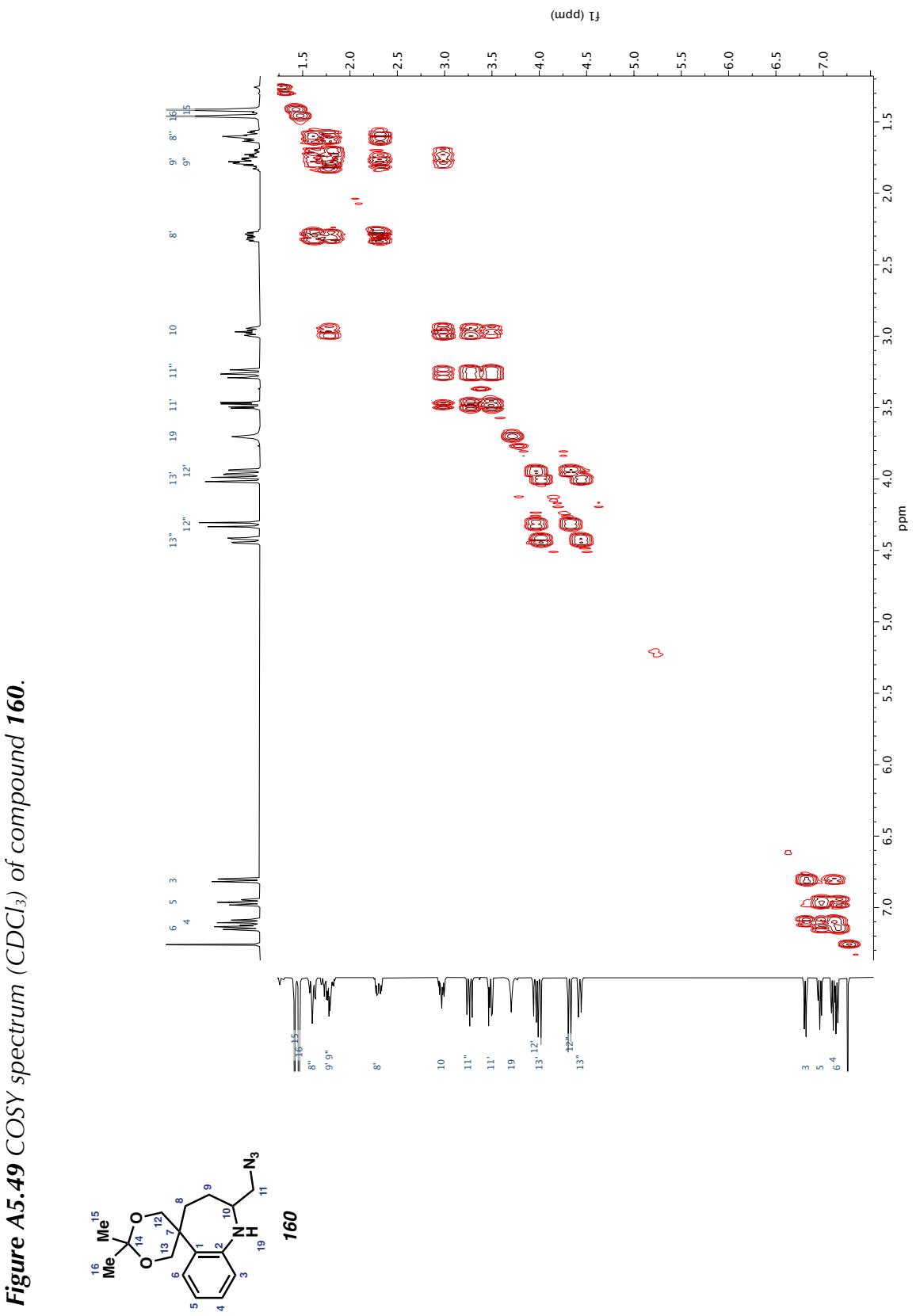


Figure A5.49 *COSY spectrum ($CDCl_3$) of compound* ***160***.

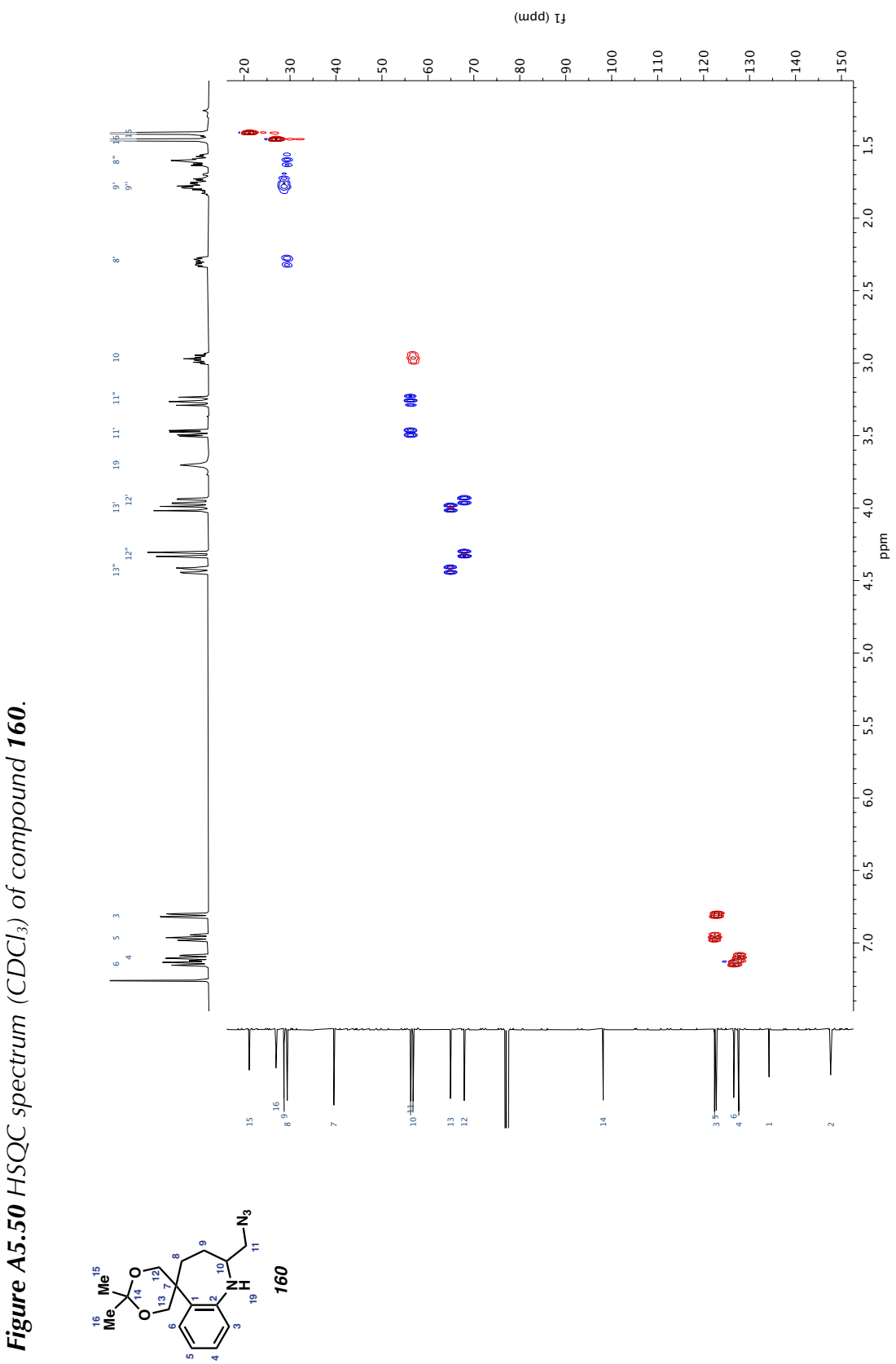


Figure A5.50 *HSQC spectrum ($CDCl_3$) of compound* ***160***.

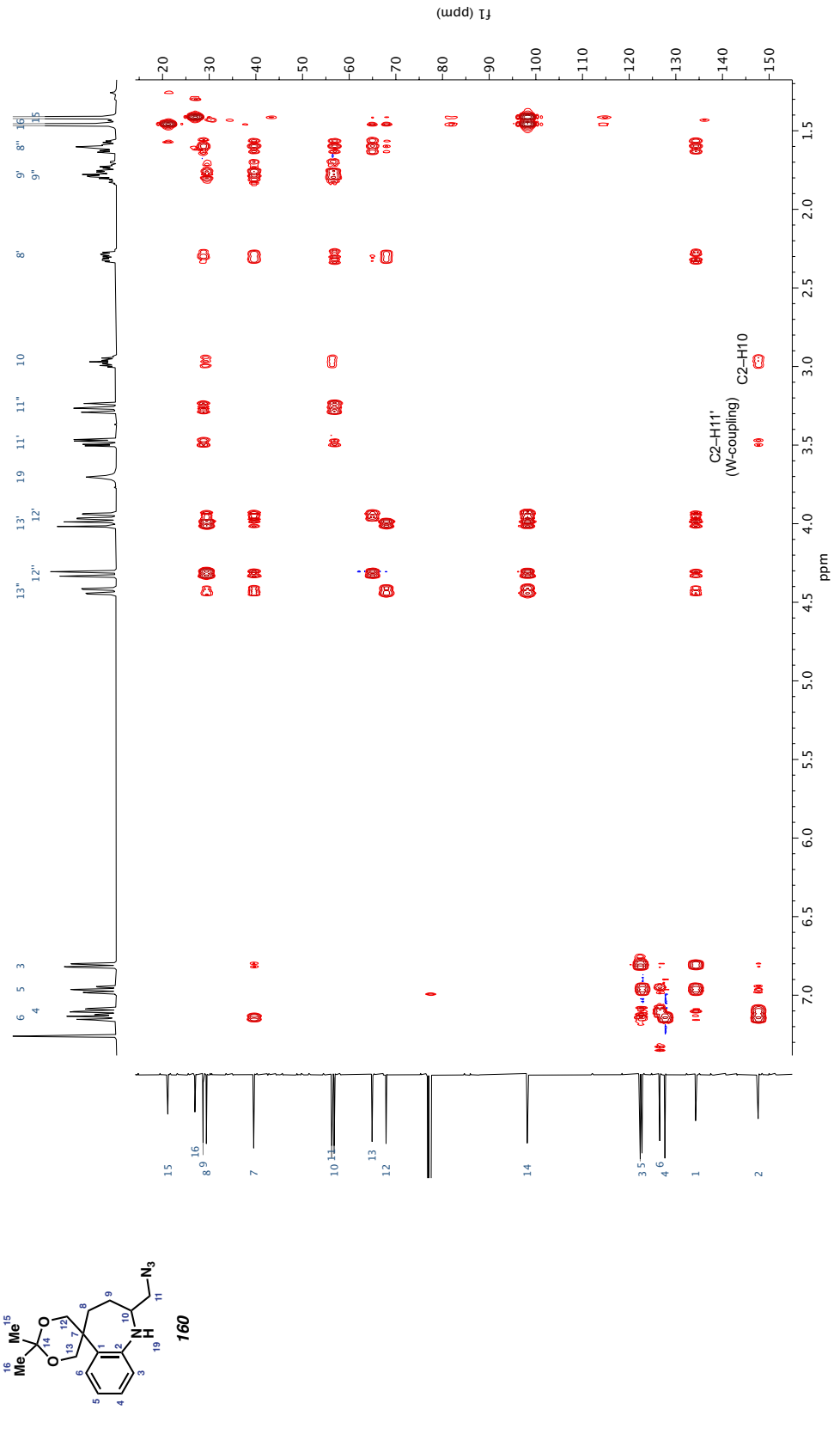
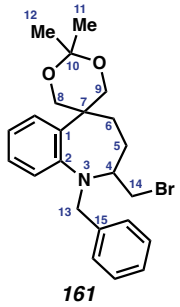


Figure A5.51 *HMBC spectrum ($CDCl_3$) of compound* ***160***.

Table A5.3 *2D NMR Correlations for* ***161***



161

Due to the presence of many overlapping peaks in the aromatic region, not all hydrogen and carbon atoms could be definitively assigned. This did not affect the structural assignment of compound ***161****. The carbon shifts of C4 and C14 are particularly diagnostic.*

No	δ_H	δ_C	HSQC	HMBC	COSY
8"	4.49	66.0	66.0(8)	26.6(6), 40.2(7), 69.1(9), 98.0(10)	4.08(8')
9'	4.20	69.1	69.1(9)	26.6(6), 40.2(7), 66.0(8), 98.0(10),137.5(1)	3.57(9")
8'	4.08	66.0	66.0(8)	26.6(6), 40.2(7), 69.1(9), 98.0(10)	4.49(8")
13'	4.07	57.8	57.8(13)	57.9(4), 138.8(15),147.3(2)	-
13"	4.07	57.8	57.8(13)	57.9(4), 138.8(15),147.3(2)	-
9"	3.57	69.1	69.1(9)	26.6(6), 40.2(7), 66.0(8), 98.0(10),137.5(1)	4.20(9')
4	3.28	57.9	57.9(4)	27.6(5), 32.4(14), 57.8(13),147.3(2)	1.32(5"), 1.82(5'), 2.63(14"), 3.12(14')
14'	3.12	32.4	32.4(14)	27.6(5),57.9(4)	2.63(14"),3.28(4)
14"	2.63	32.4	32.4(14)	27.6(5),57.9(4)	3.12(14'),3.28(4)
6"	1.89	26.6	26.6(6)	27.6(5), 40.2(7),137.5(1)	1.18(6'),1.32(5"), 1.82(5')
5'	1.82	27.6	-	32.4(14),40.2(7)	1.18(6'), 1.89(6"),3.28(4)
12	1.44	25.6	25.6(12)	98.0(10)	-
11	1.33	22.7	22.7(11)	98.0(10)	-
5"	1.32	27.6	-	40.2(7)	1.18(6'), 1.89(6"),3.28(4)
6'	1.18	26.6	26.6(6)	27.6(5), 40.2(7)	1.32(5"), 1.82(5'), 1.89(6")
1	-	137.5	-	1.89(6"), 3.57(9"), 4.20(9')	-
2	-	147.3	-	3.28(4), 4.07(13"), 4.07(13')	-
7	-	40.2	-	1.18(6'),1.32(5"), 1.82(5'), 1.89(6"), 3.57(9"), 4.08(8'), 4.20(9'), 4.49(8")	-
10	-	98.0	-	1.33(11), 1.44(12),3.57(9"), 4.08(8'), 4.20(9'), 4.49(8")	-
15	-	138.8	-	4.07(13"), 4.07(13')	-

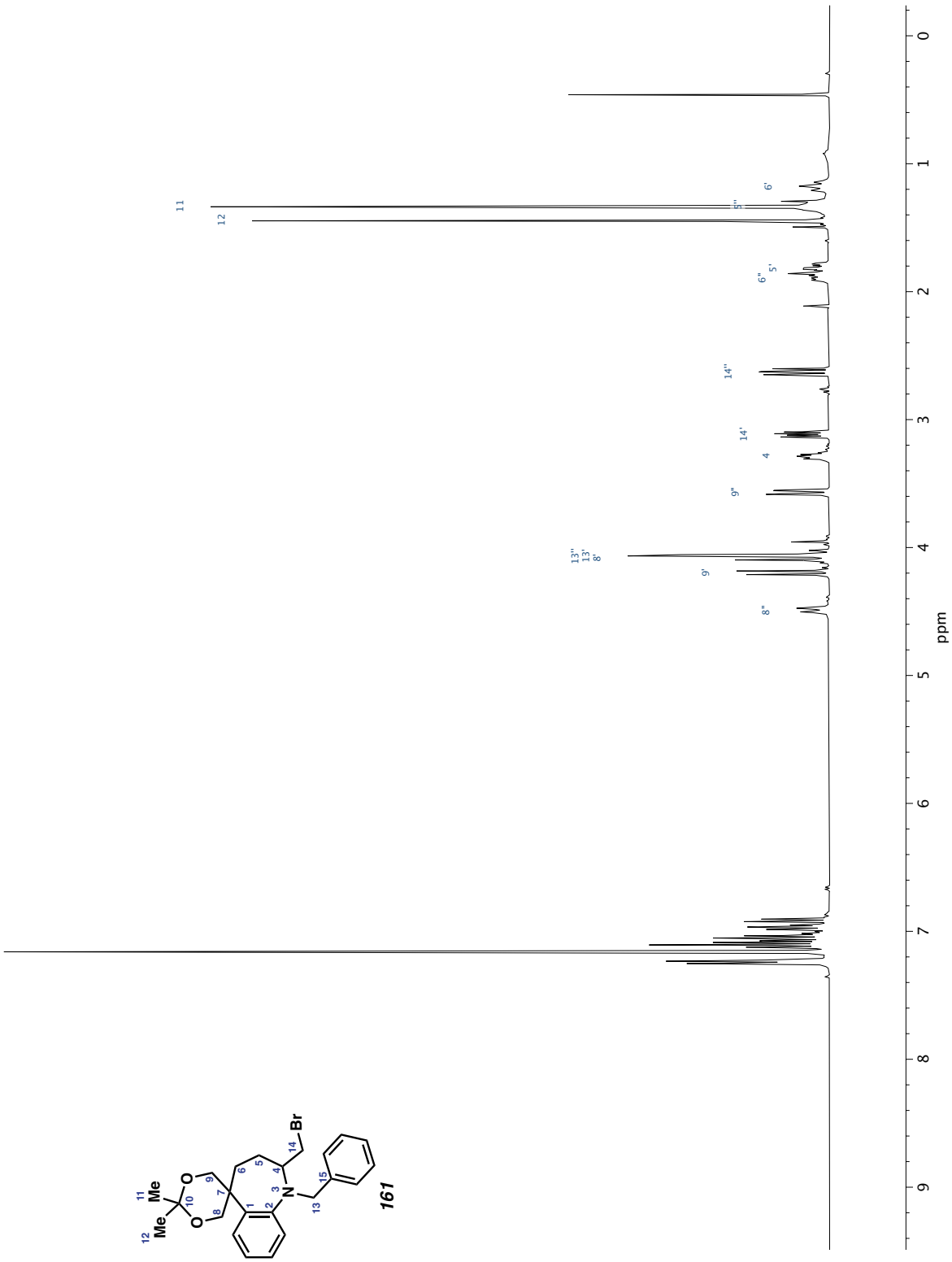


Figure A5.52 *^{1}H NMR (400 MHz, C_6D_6) of compound* ***161****.*

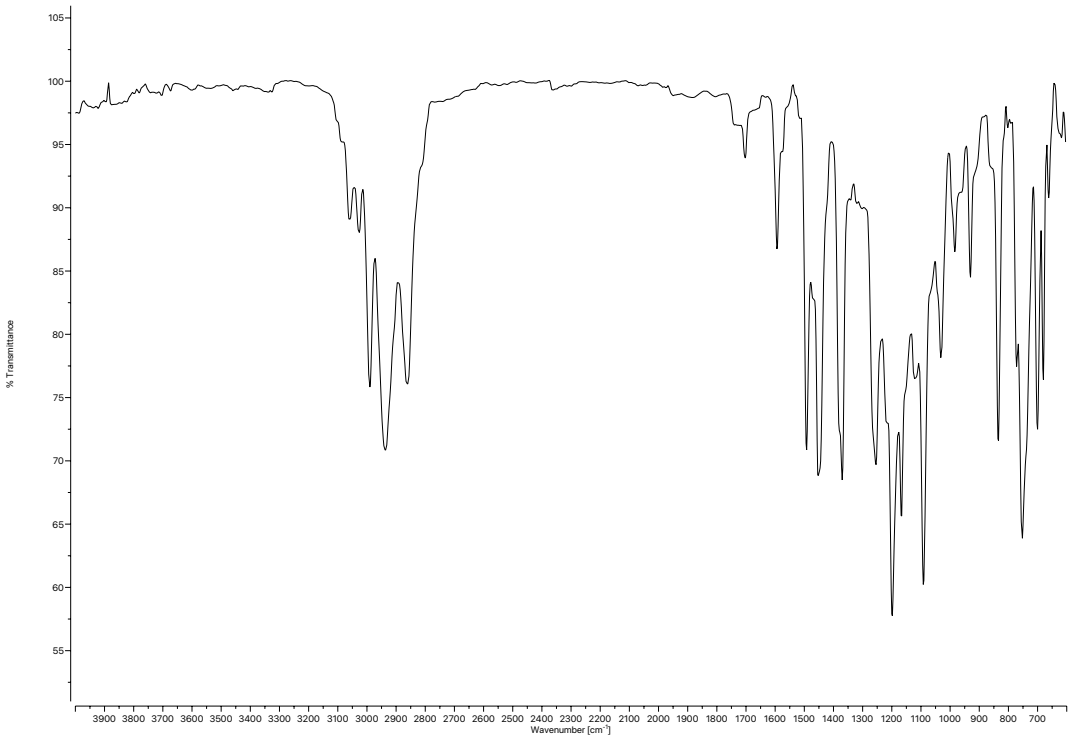


Figure A.53 *Infrared spectrum (Thin Film, NaCl) of compound* ***161***.

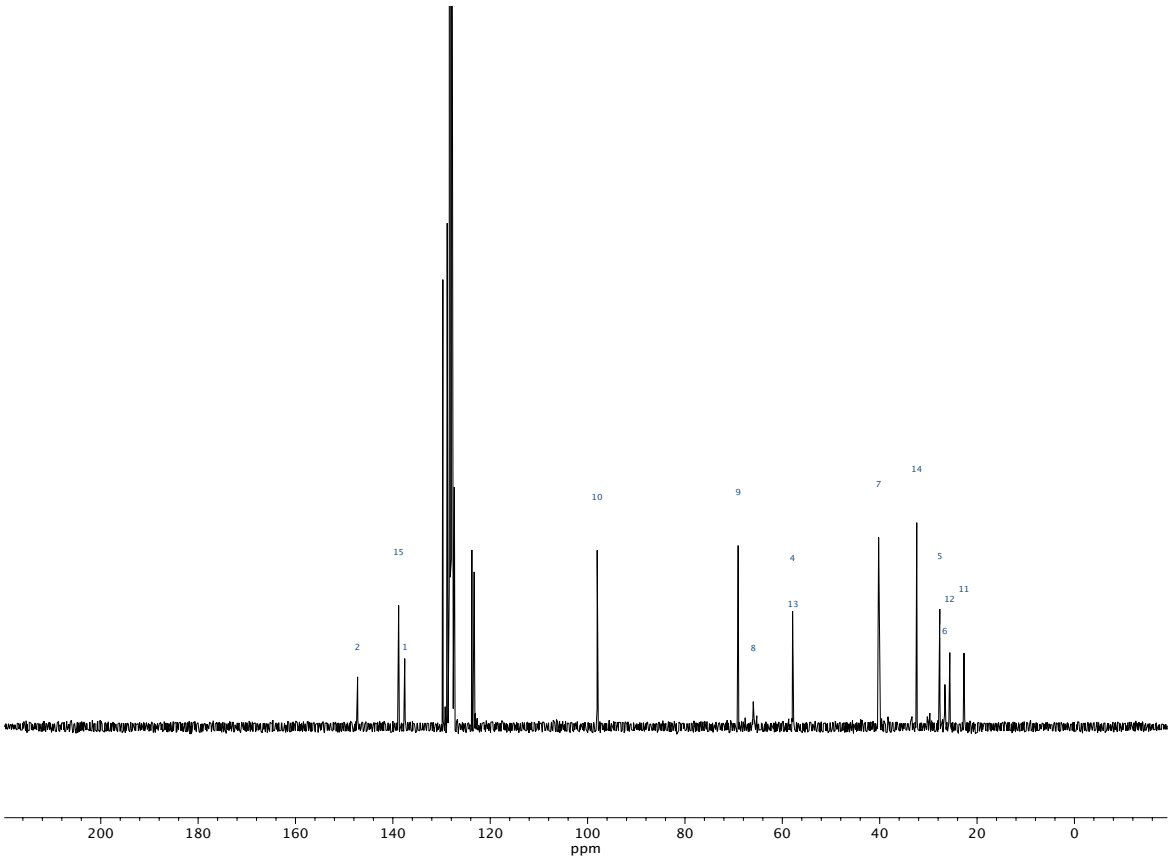


Figure A.54 *^{13}C NMR (100 MHz, C_6D_6) of compound* ***161***.

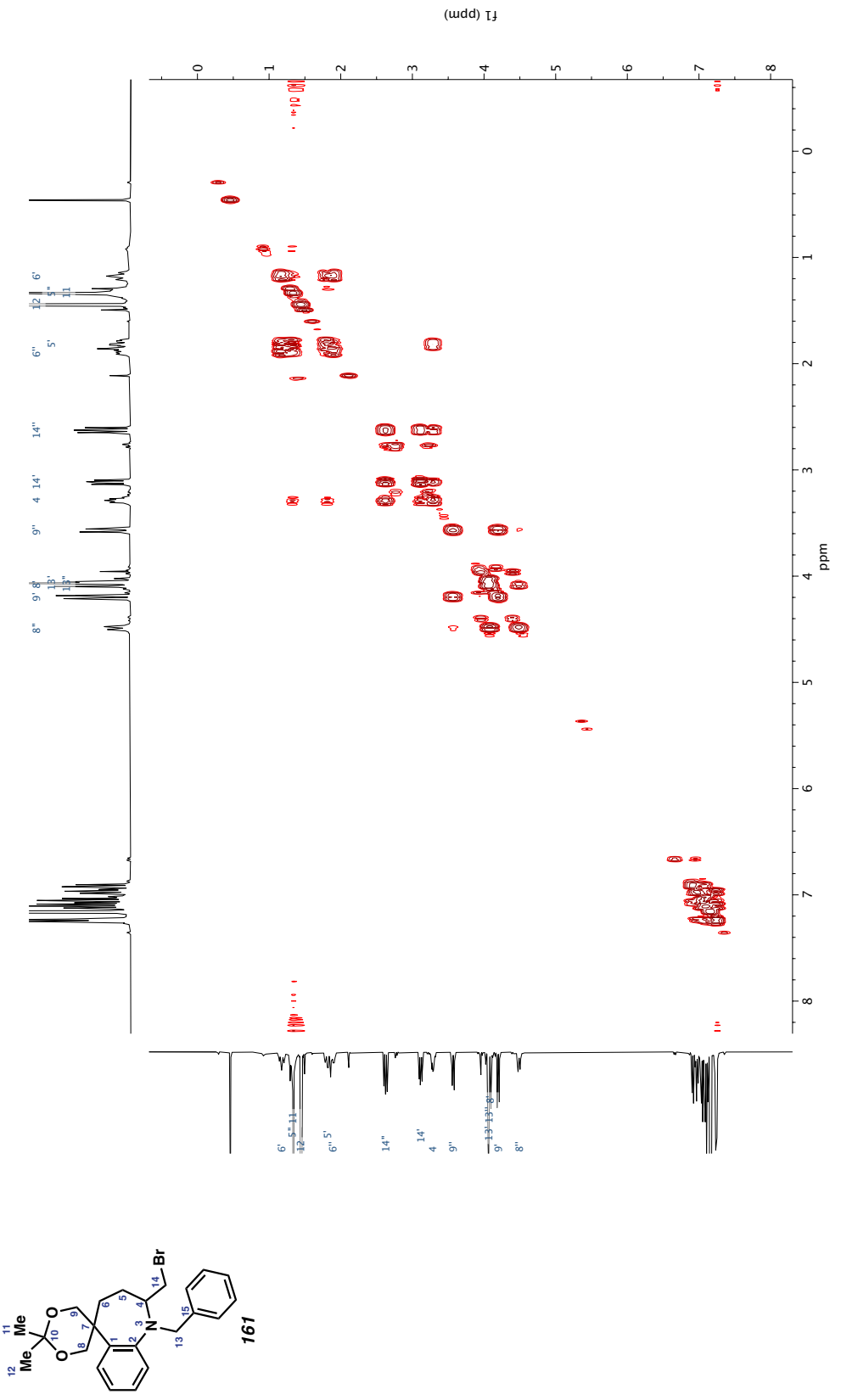


Figure A.55 *COSY spectrum* (C_6D_6) *of compound* ***161***.

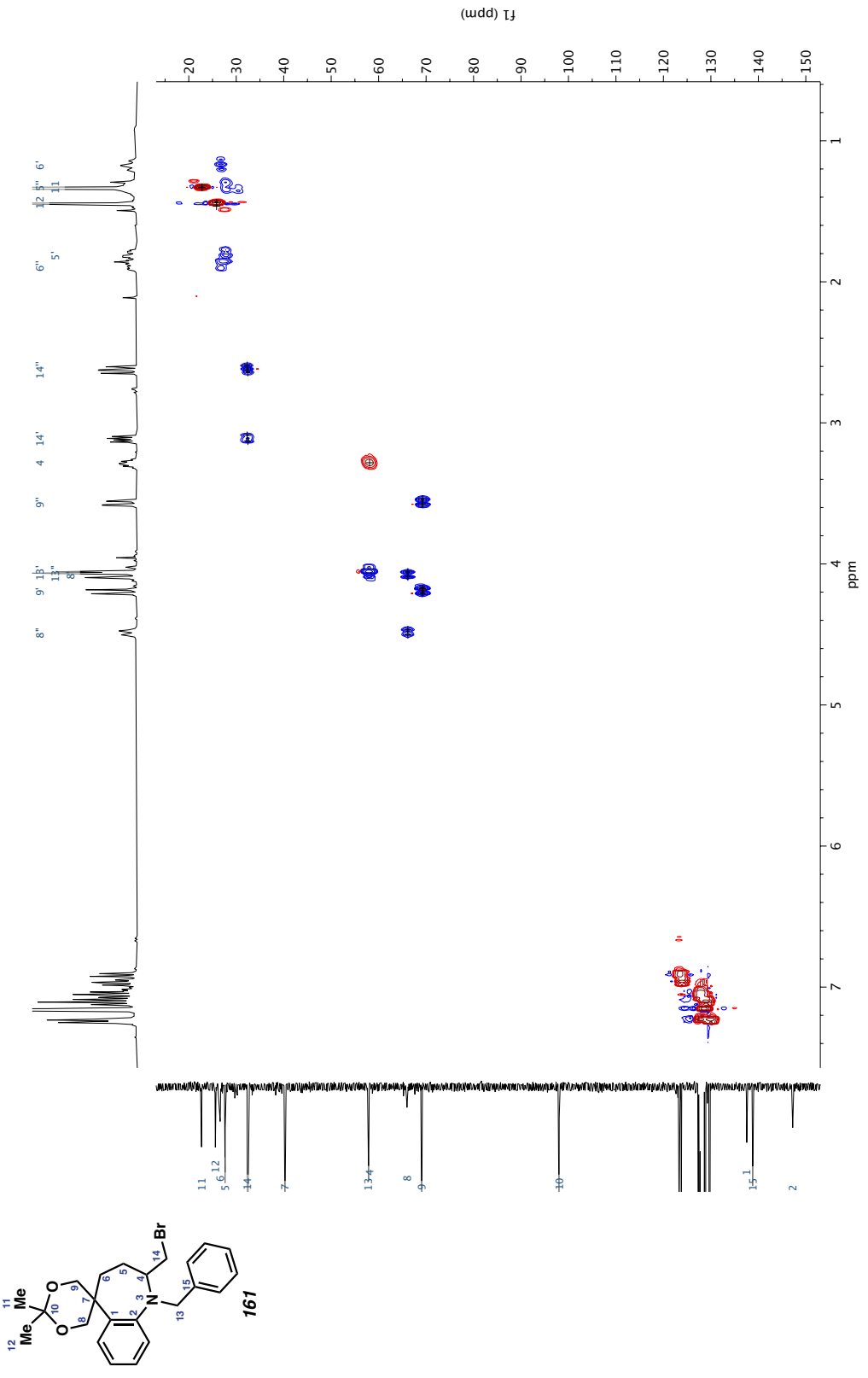


Figure A.56 *HSQC spectrum (C_6D_6) of compound* ***161***.

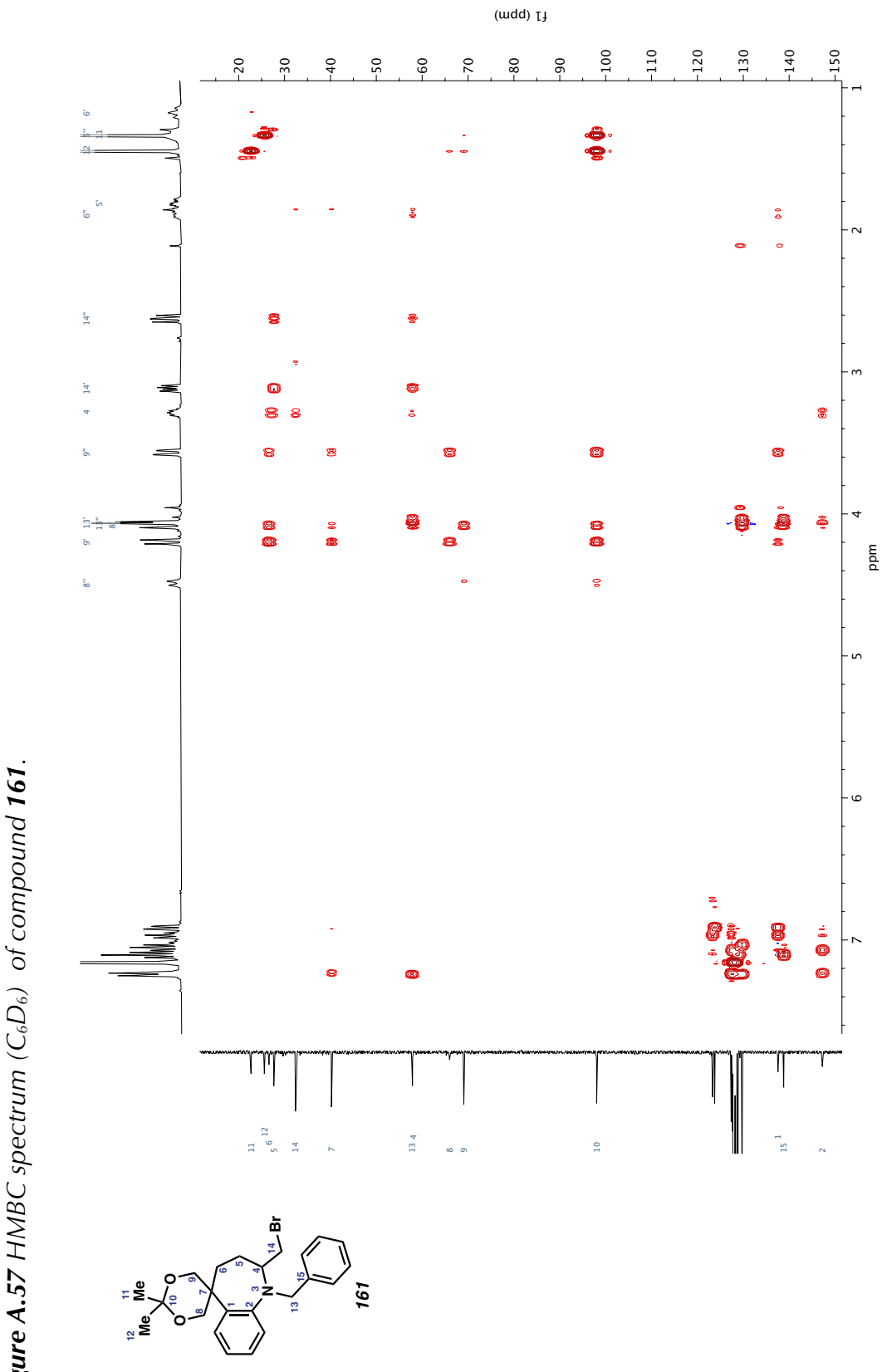
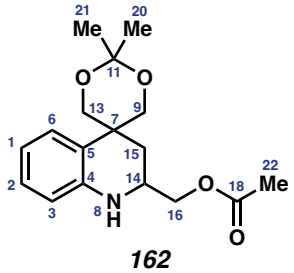


Figure A.57 *HMBC spectrum (C_6D_6) of compound* ***161***.

Table A5.4 *2D NMR Correlations for* ***162***



162

No	δ_H	δ_C	HSQC	HMBC	COSY
6	7.20	127.3	127.3(6)	35.7(7),127.9(2), 145.5(4)	6.70(1)
2	6.97	127.9	127.9(2)	127.3(6),145.5(4)	6.26(3),6.70(1)
1	6.70	118.2	118.2(1)	115.4(3), 122.7(5),127.9(2)	6.97(2), 7.20(6)
3	6.26	115.4	115.4(3)	118.2(1), 122.7(5)	6.97(2)
9"	4.19	70.3	70.3(9)	32.2(15), 47.1(14), 69.0(13), 98.2(11),122.7(5)	3.34(9')
16"	3.99	68.0	68.0(16)	32.2(15),47.1(14), 170.0(18)	3.14(14), 3.70(16')
13"	3.83	69.0	69.0(13)	32.2(15), 70.3(9), 98.2(11),122.7(5)	3.60(13')
8	3.77	-	-	32.2(15)	-
16'	3.70	68.0	68.0(16)	32.2(15),47.1(14), 170.0(18)	3.14(14), 3.99(16")
13'	3.60	69.0	69.0(13)	32.2(15),35.7(7), 70.3(9), 98.2(11)	3.34(9'), 3.83(13")
9'	3.34	70.3	70.3(9)	32.2(15), 69.0(13), 98.2(11),122.7(5)	3.60(13'),4.19(9")
14	3.14	47.1	47.1(14)	32.2(15),35.7(7), 68.0(16)	1.22(15'),2.51(15"), 3.70(16'), 3.99(16")
15"	2.51	32.2	32.2(15)	35.7(7), 47.1(14), 69.0(13),122.7(5)	1.22(15'),3.14(14)
22	1.65	20.3	20.3(22)	170.0(18)	-
21	1.50	28.4	28.4(21)	20.0(20),98.2(11)	-
20	1.38	20.0	20.0(20)	28.4(21),98.2(11)	-
15'	1.22	32.2	32.2(15)	35.7(7), 47.1(14), 69.0(13)	2.51(15"),3.14(14)
4	-	145.5	-	6.97(2), 7.20(6)	-
5	-	122.7	-	2.51(15"), 3.34(9'), 3.83(13"), 4.19(9"), 6.26(3),6.70(1)	-
7	-	35.7	-	1.22(15'), 2.51(15"), 3.14(14), 3.60(13'),7.20(6)	-
11	-	98.2	-	1.38(20), 1.50(21), 3.34(9'), 3.60(13'), 3.83(13"),4.19(9")	-
18	-	170.0	-	1.65(22), 3.70(16'),3.99(16")	-

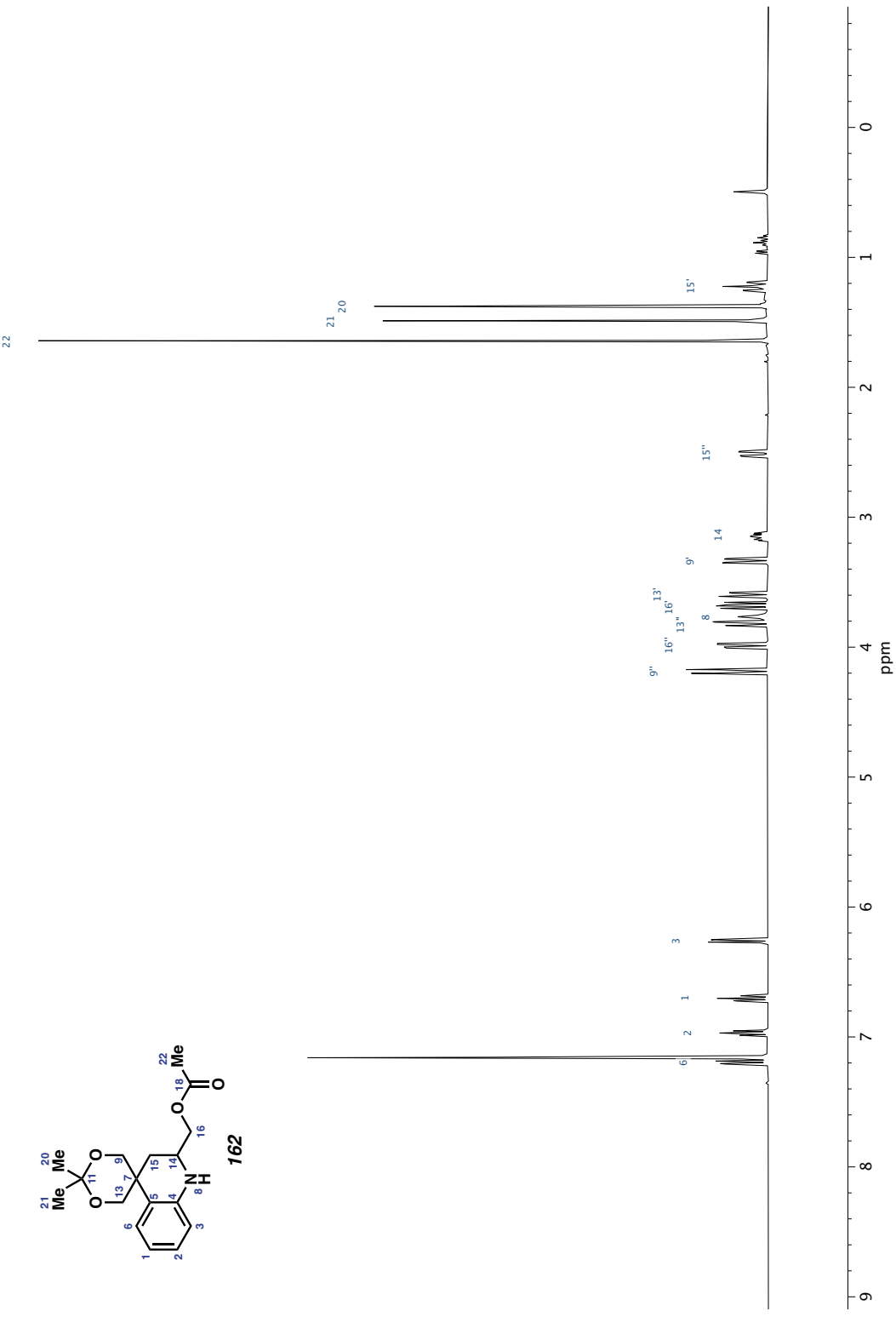


Figure A5.58 *^{1}H NMR (400 MHz, C_6D_6) of compound* ***162****.*

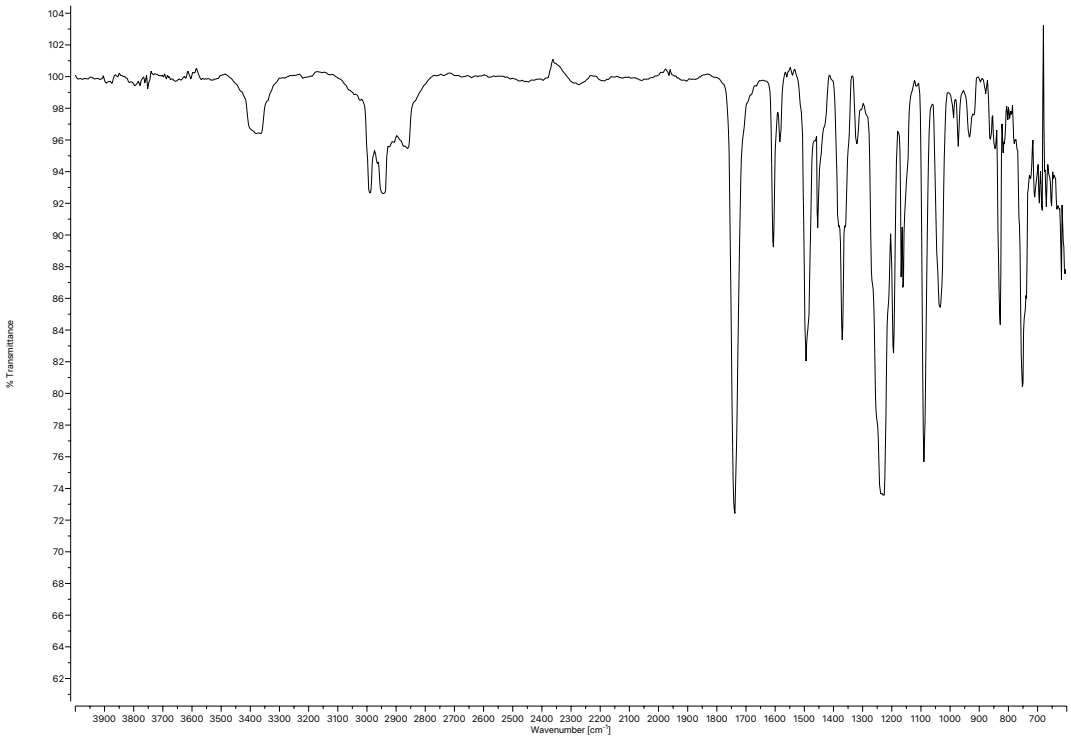


Figure A.59 *Infrared spectrum (Thin Film, NaCl) of compound* ***162****.*

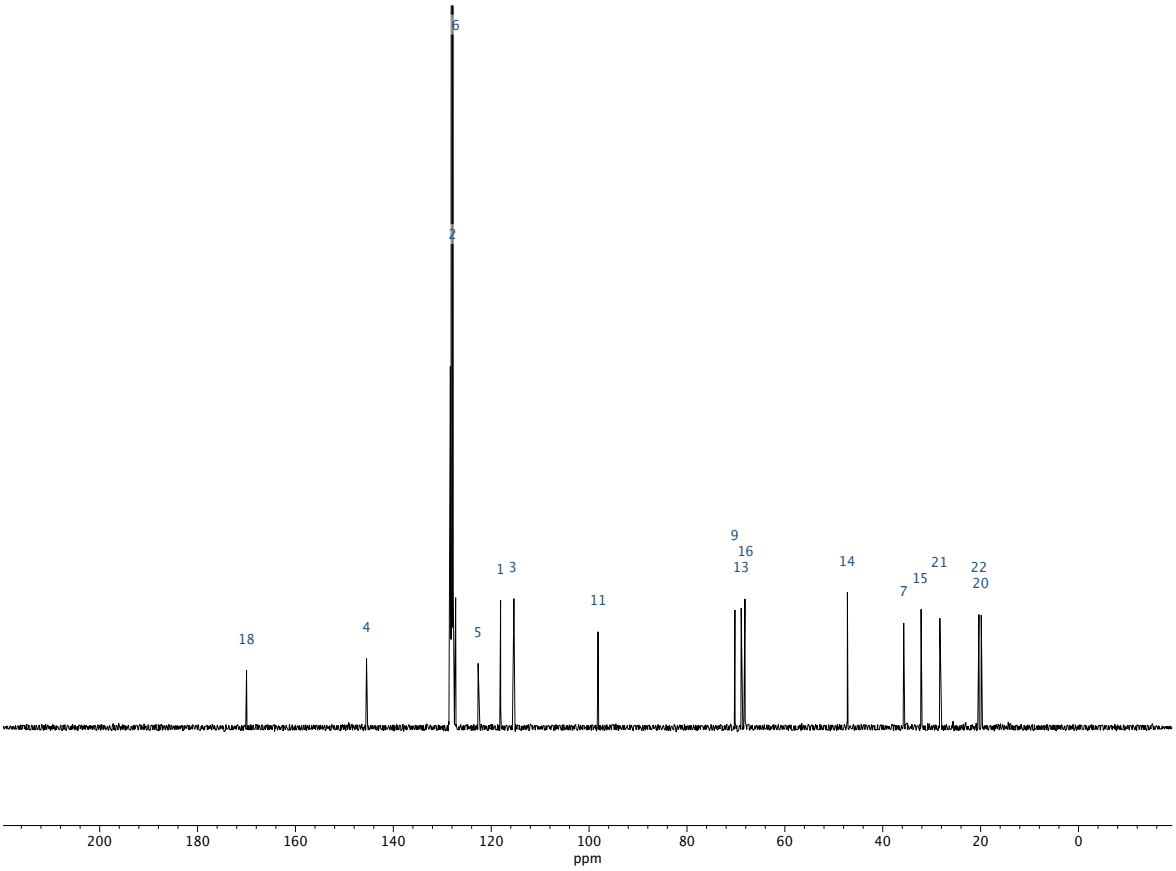


Figure A.60 *^{13}C NMR (100 MHz, C_6D_6) of compound* ***162****.*

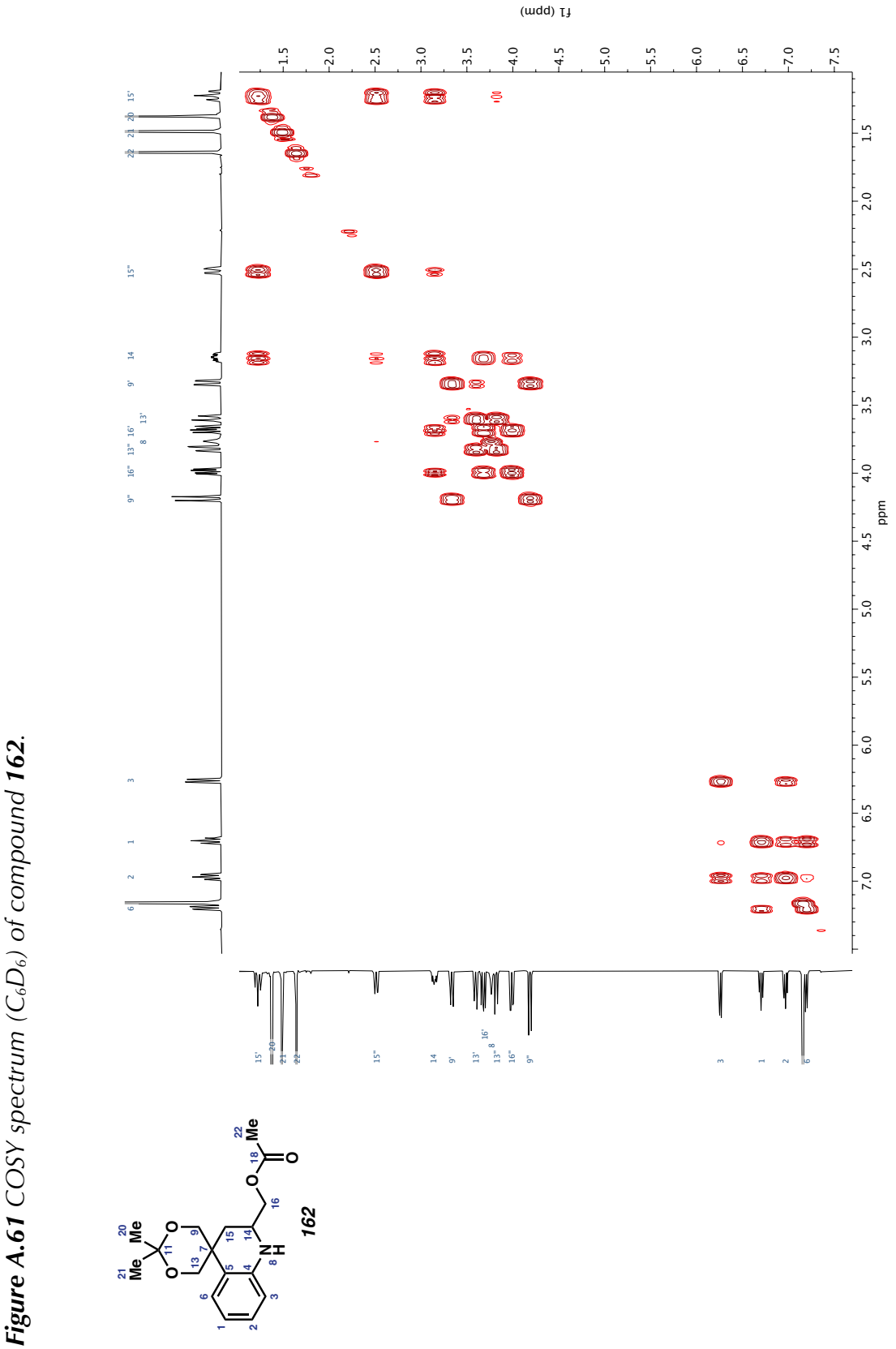


Figure A.61 *COSY spectrum (C_6D_6) of compound* ***162***.

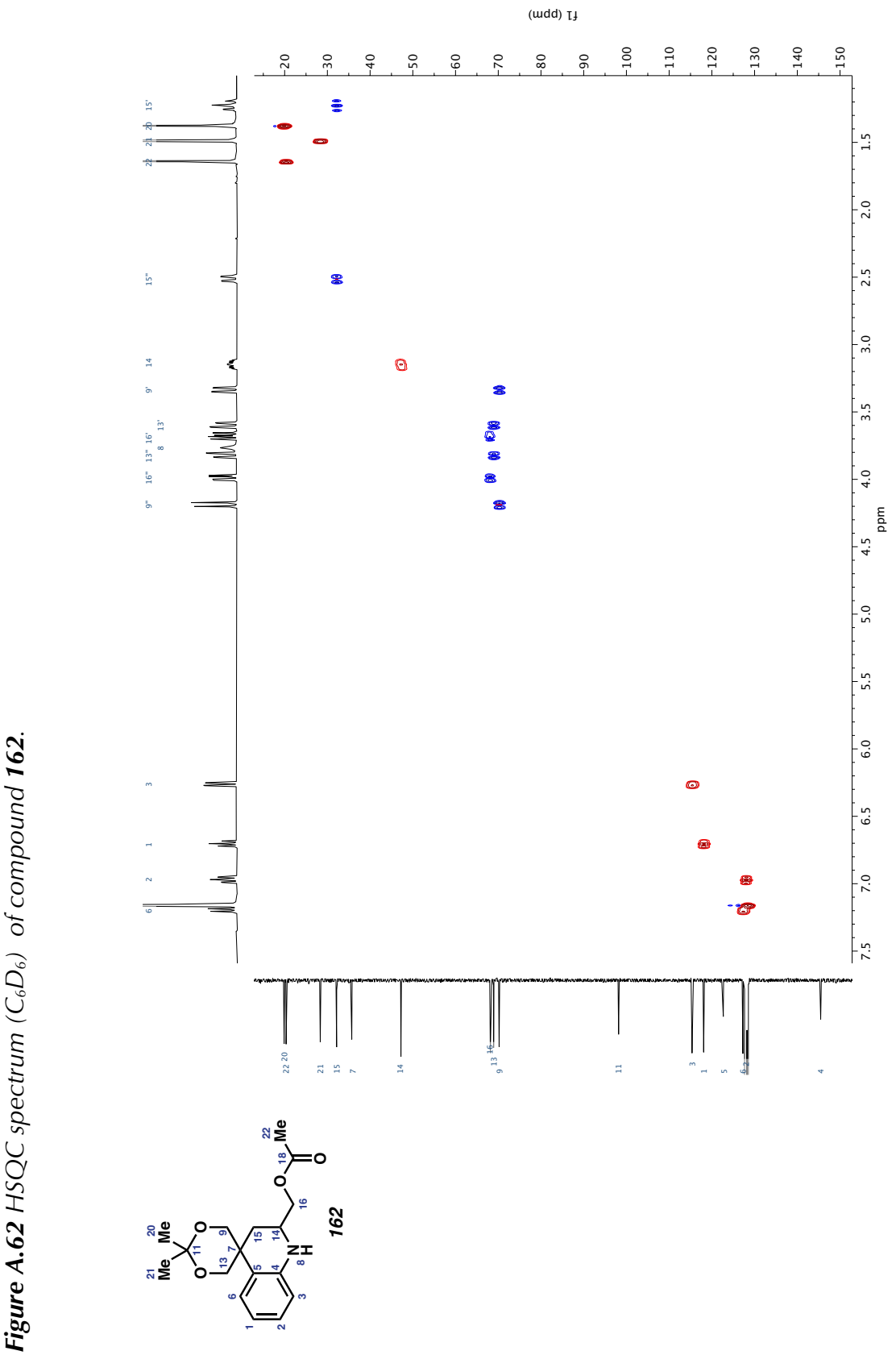


Figure A.62 *HSQC spectrum (C_6D_6) of compound* ***162****.*

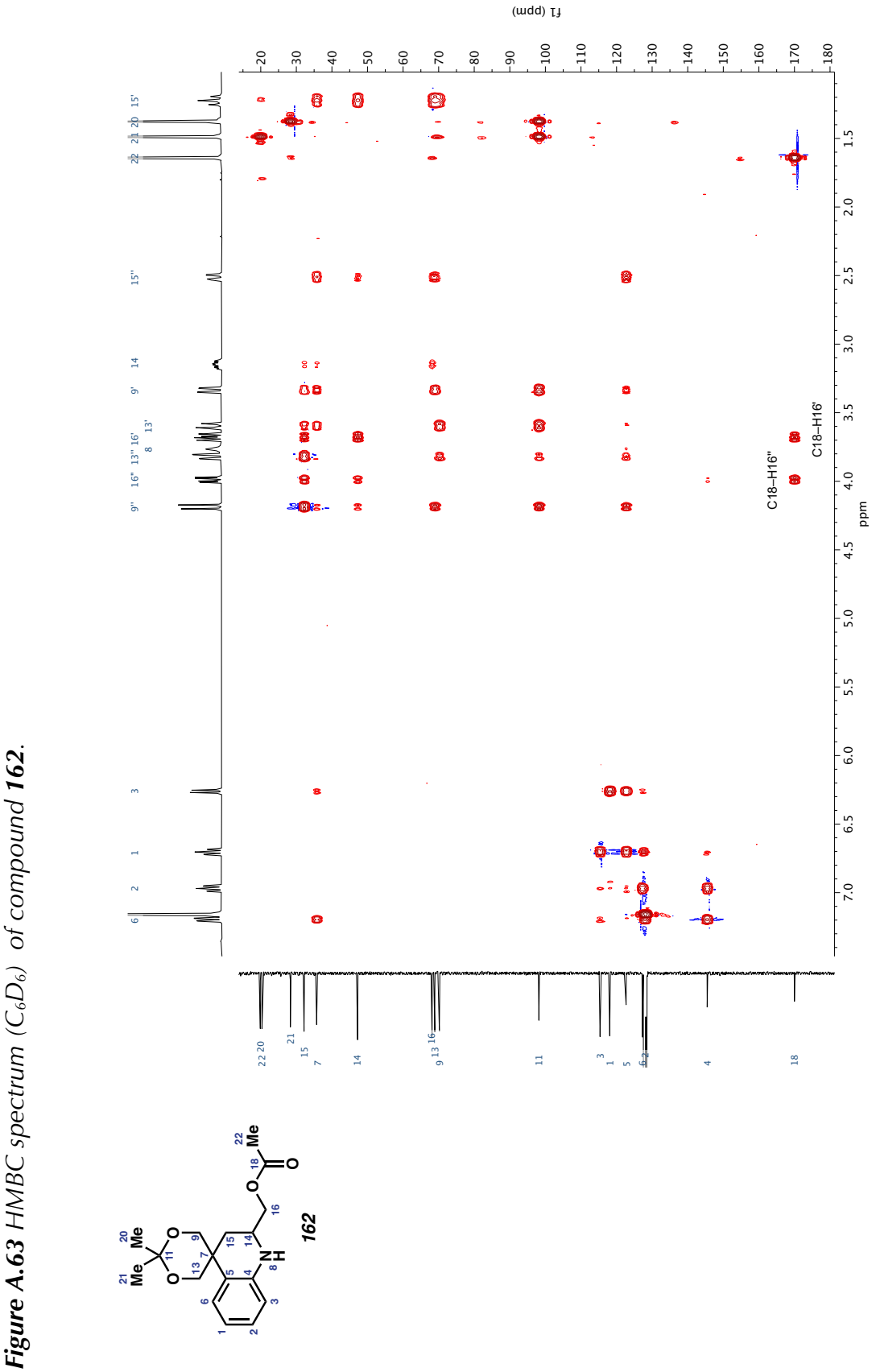
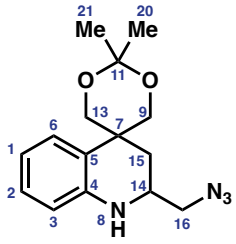


Figure A.63 *HMBC spectrum (C_6D_6) of compound* ***162***.

Table A5.5 *2D NMR Correlations for* ***163***



163

No	δ_H	δ_C	HSQC	HMBC	COSY
6	7.12	127.1	127.1(6)	35.8(7),128.0(2), 145.4(4)	6.70(1)
2	6.95	128.0	128.0(2)	145.4(4)	6.22(3),6.70(1)
1	6.70	118.2	118.2(1)	115.6(3), 122.6(5)	6.95(2), 7.12(6)
3	6.22	115.6	115.6(3)	118.2(1), 122.6(5)	6.95(2)
9"	4.17	70.2	70.2(9)	33.1(15), 47.3(14), 68.9(13), 98.1(11),122.6(5)	3.28(9')
13"	3.77	68.9	68.9(13)	33.1(15), 70.2(9), 98.1(11),122.6(5)	3.49(13')
8	3.68	-	-	-	-
13'	3.49	68.9	68.9(13)	33.1(15), 35.8(7), 70.2(9), 98.1(11),122.6(5)	3.77(13")
9'	3.28	70.2	70.2(9)	33.1(15), 35.8(7), 68.9(13), 98.1(11),122.6(5)	4.17(9")
14	2.85	47.3	47.3(14)	56.5(16)	1.03(15"), 2.52(16"), 2.58(16')
16'	2.58	56.5	56.5(16)	33.1(15), 47.3(14),145.4(4)	2.52(16"),2.85(14)
16"	2.52	56.5	56.5(16)	33.1(15),47.3(14)	2.58(16'),2.85(14)
15'	2.39	33.1	33.1(15)	35.8(7), 56.5(16), 68.9(13),122.6(5)	1.03(15")
17	1.50	28.7	28.7(17)	19.5(18),98.1(11)	-
18	1.36	19.5	19.5(18)	28.7(17),98.1(11)	-
15"	1.03	33.1	33.1(15)	35.8(7), 47.3(14), 56.5(16), 68.9(13), 70.2(9)	2.39(15'),2.85(14)
4	-	145.4	-	2.58(16'),6.95(2), 7.12(6)	-
5	-	122.6	-	2.39(15'), 3.28(9'), 3.49(13'), 3.77(13"), 4.17(9"), 6.22(3),6.70(1)	-
7	-	35.8	-	1.03(15"), 2.39(15'), 3.28(9'), 3.49(13'),7.12(6)	-
11	-	98.1	-	1.36(18), 1.50(17), 3.28(9'), 3.49(13'), 3.77(13"),4.17(9")	-

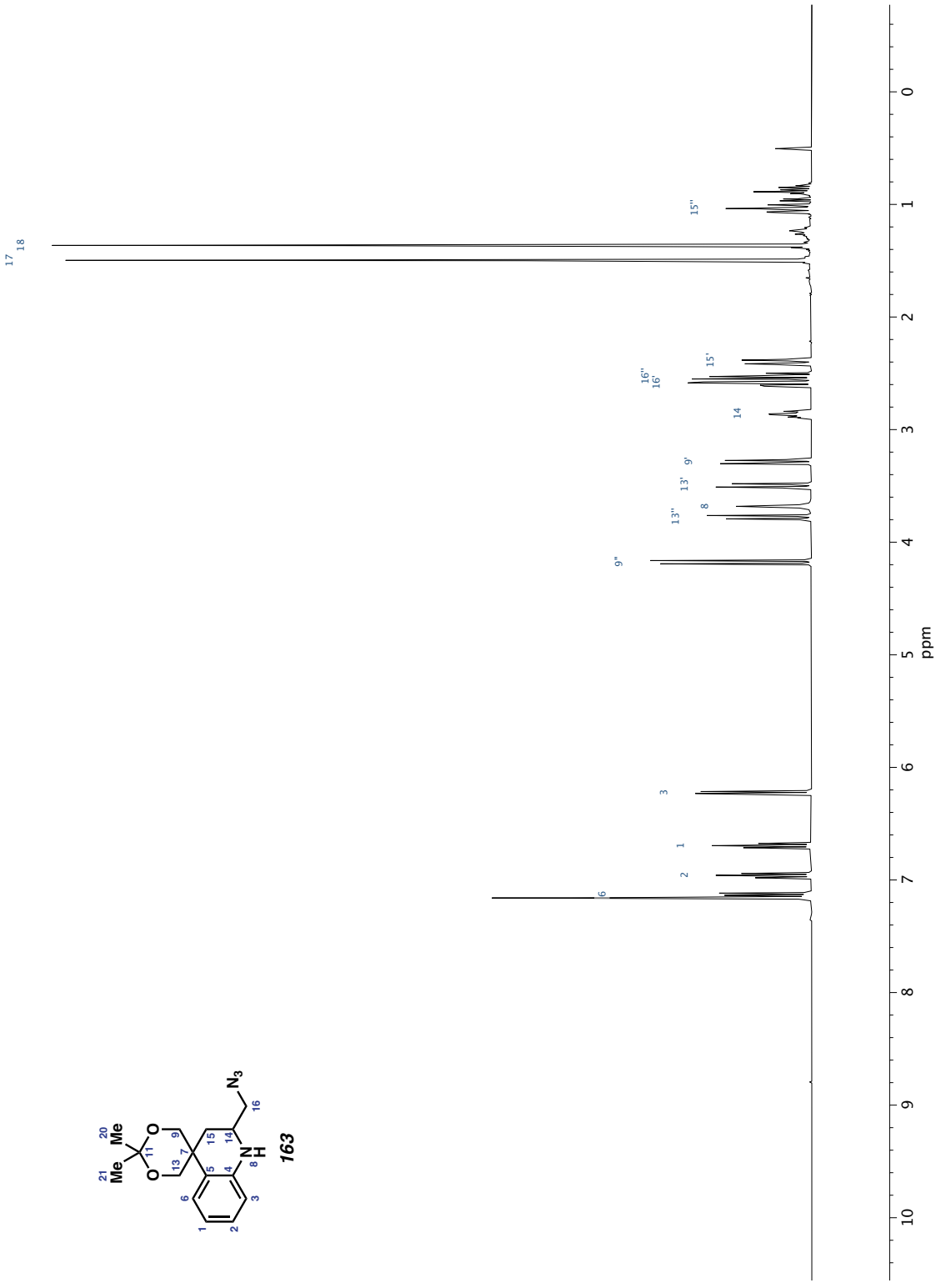


Figure A5.64 *^{1}H NMR (400 MHz, C_6D_6) of compound* ***163****.*

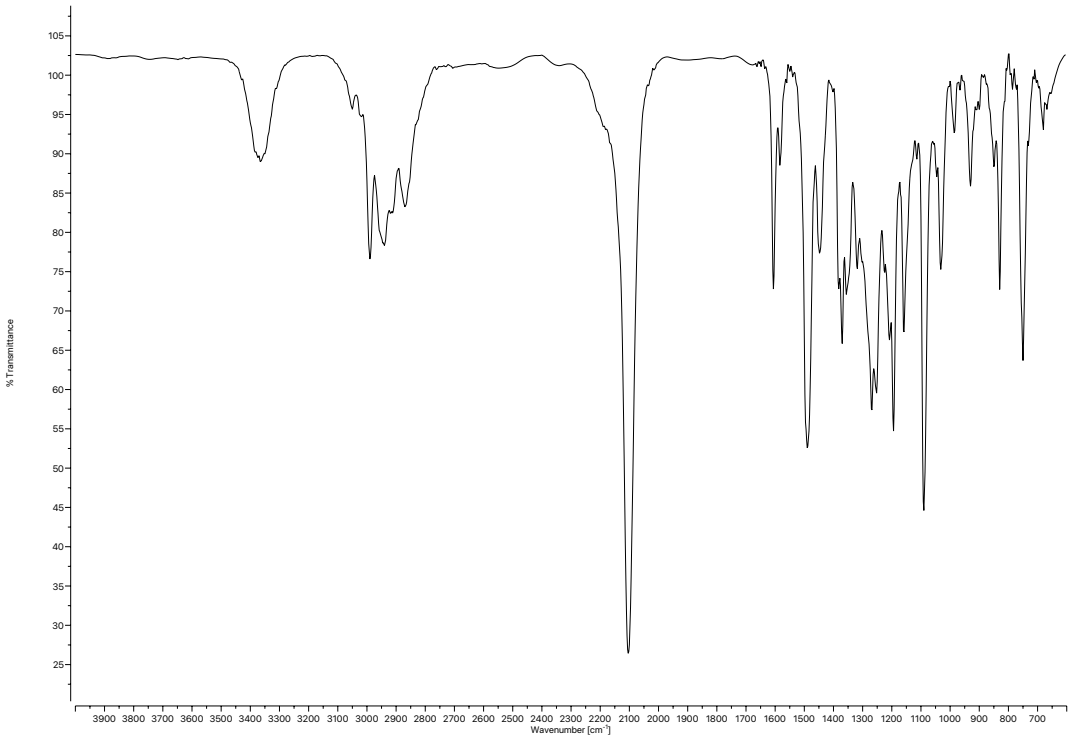


Figure A.65 *Infrared spectrum (Thin Film, NaCl) of compound* ***163***.

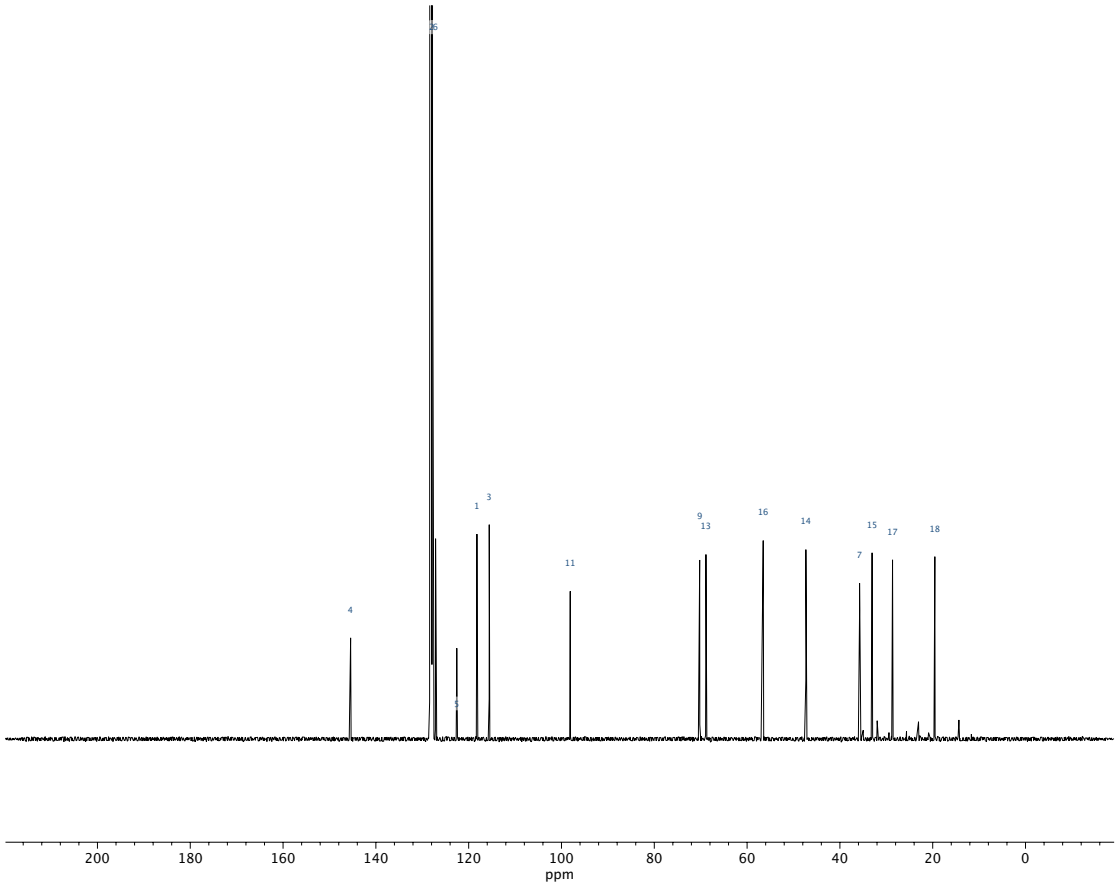


Figure A.66 *^{13}C NMR (100 MHz, C_6D_6) of compound* ***163***.

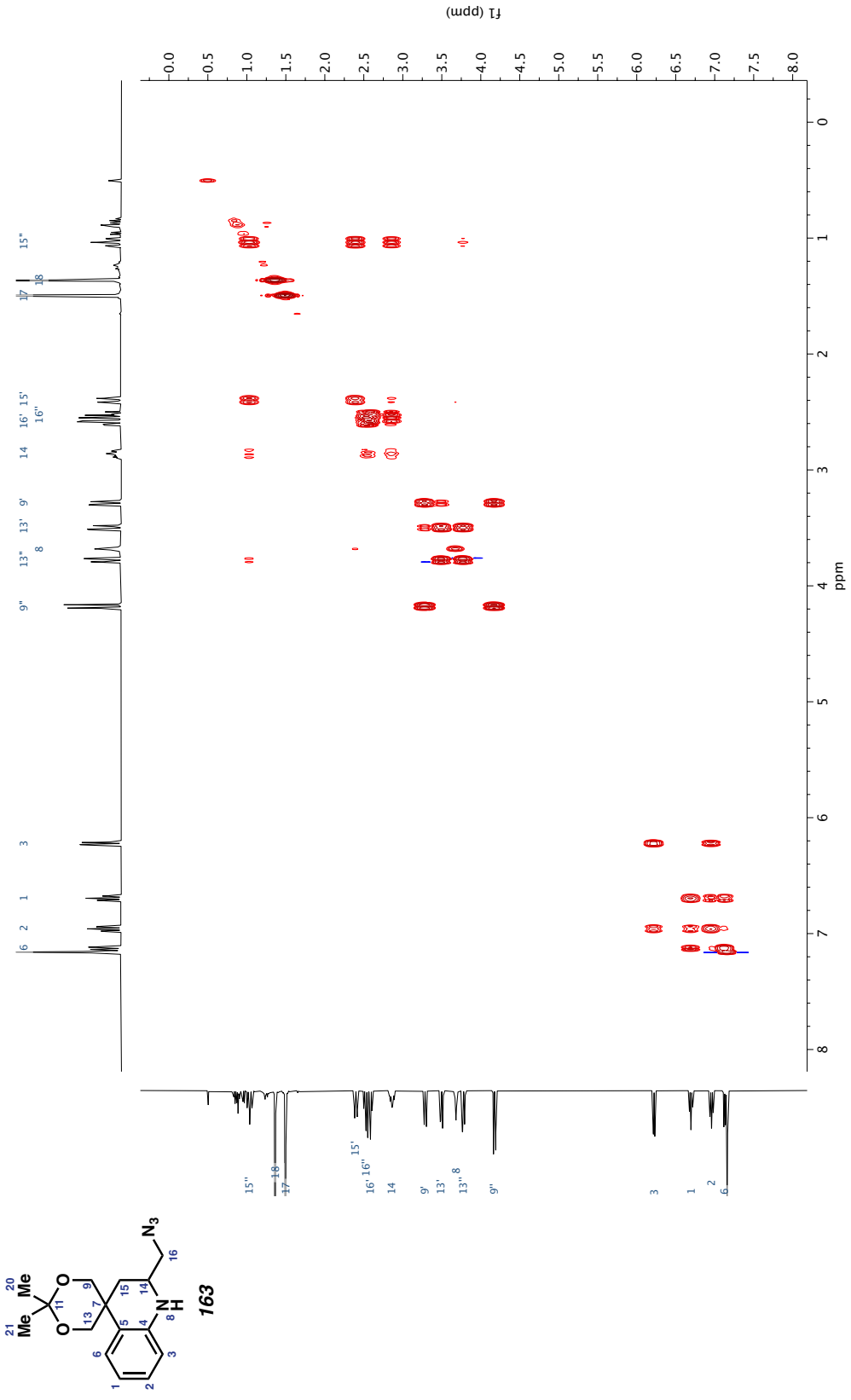


Figure A.67 *COSY spectrum (C_6D_6) of compound* ***163***.

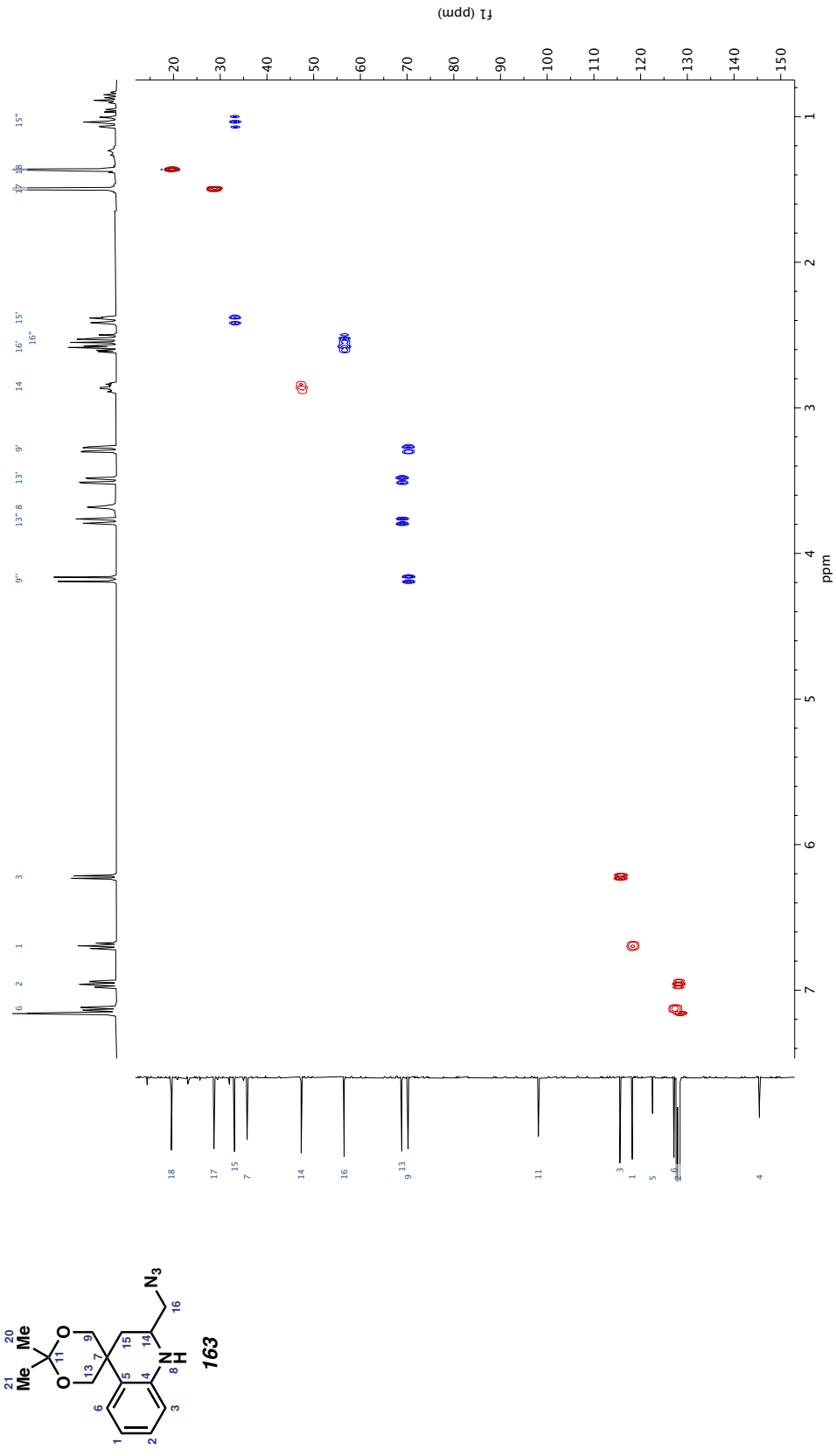


Figure A.68 *HSQC spectrum (C_6D_6) of compound* ***163***.

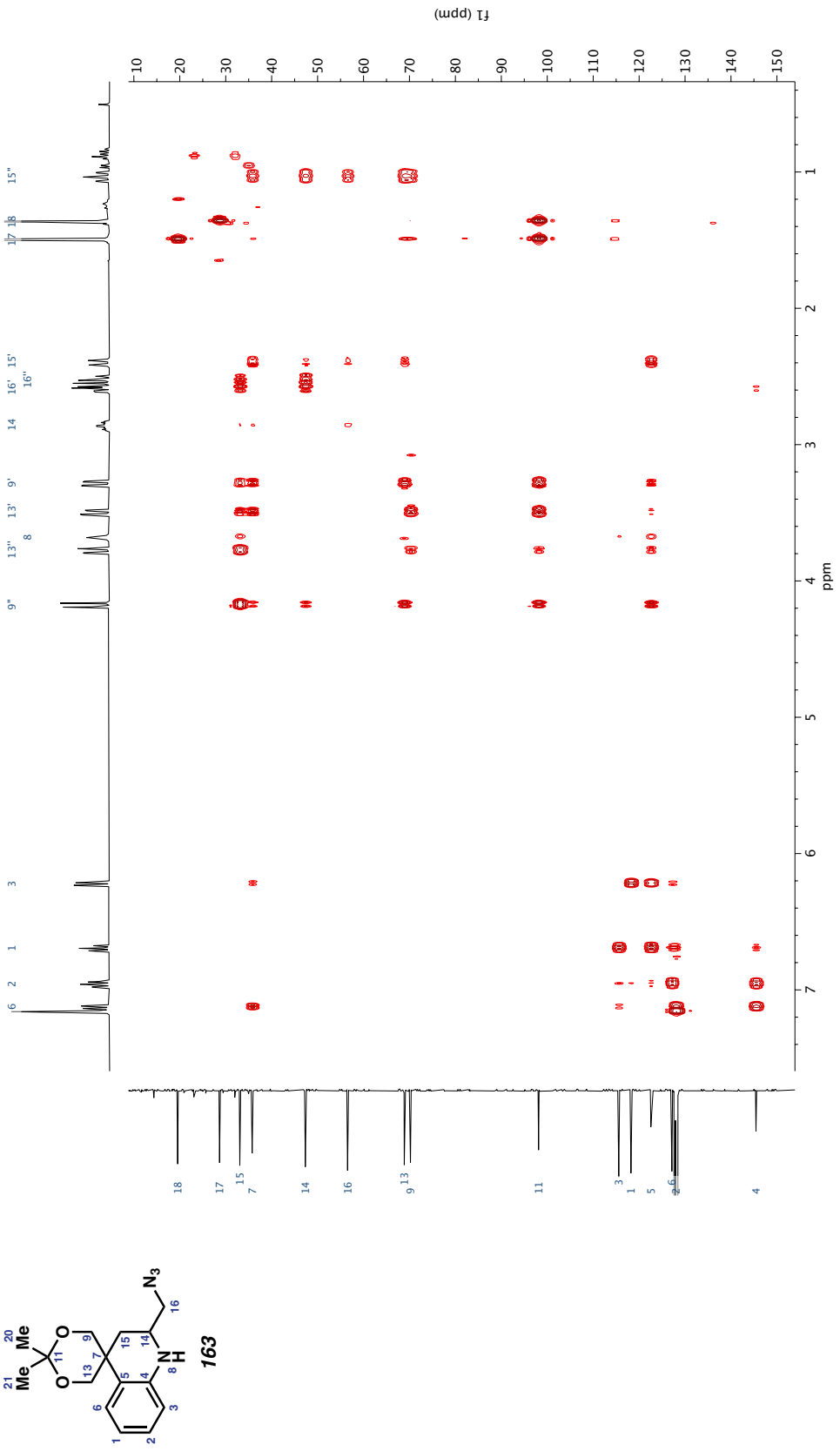
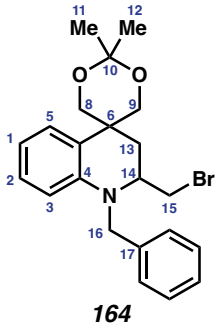


Figure A.69 *HMBC spectrum (C_6D_6) of compound* ***163***.

Table A5.6 *2D NMR Correlations for* ***164***



164

Due to the presence of several overlapping aromatic hydrogen and carbon signals, not all atoms were assigned. This did not affect the overall structural assignment of ***164****. The* ^{1}H *and* ^{13}C *shifts of 14 and 15 are particularly diagnostic in assigning the structure of* ***164****.*

No	δ_H	δ_C	HSQC	HMBC	COSY
5	7.35	126.2	126.2(5)	34.9(6),114.8(3), 146.3(4)	6.73(1)
2	6.96	128.4	128.4(2)	146.3(4)	6.57(3),6.73(1)
1	6.73	118.4	118.4(1)	114.8(3)	6.96(2), 7.35(5)
3	6.57	114.8	114.8(3)	118.4(1)	6.96(2)
8"	4.18	68.7	68.7(8)	34.4(13),34.9(6), 68.8(9), 98.4(10)	3.51(8')
16"	4.15	54.8	54.8(16)	55.5(14), 139.2(17)	3.96(16')
16'	3.96	54.8	54.8(16)	55.5(14), 139.2(17)	4.15(16")
9"	3.80	68.8	68.8(9)	34.4(13),34.9(6), 68.7(8), 98.4(10)	3.66(9')
9'	3.66	68.8	68.8(9)	34.4(13),34.9(6), 68.7(8), 98.4(10)	3.80(9")
8'	3.51	68.7	68.7(8)	34.4(13),34.9(6), 68.8(9), 98.4(10)	4.18(8")
14	3.25	55.5	55.5(14)	-	1.85(13"), 2.48(13'), 2.99(15"), 3.07(15')
15'	3.07	36.2	36.2(15)	34.4(13),55.5(14)	2.99(15"),3.25(14)
15"	2.99	36.2	36.2(15)	34.4(13),55.5(14)	3.07(15'),3.25(14)
13'	2.48	34.4	34.4(13)	55.5(14),68.7(8), 68.8(9)	1.85(13"),3.25(14)
13"	1.85	34.4	34.4(13)	55.5(14),68.7(8), 68.8(9)	2.48(13'),3.25(14)
11	1.47	26.6	26.6(11)	98.4(10)	-
12	1.41	21.6	21.6(12)	98.4(10)	-
4	-	146.3	-	6.96(2), 7.35(5)	-
6	-	34.9	-	3.51(8'), 3.66(9'), 3.80(9"), 4.18(8"),7.35(5)	-
10	-	98.4	-	1.41(12), 1.47(11), 3.51(8'), 3.66(9'), 3.80(9"),4.18(8")	-
17	-	139.2	-	3.96(16'),4.15(16")	-

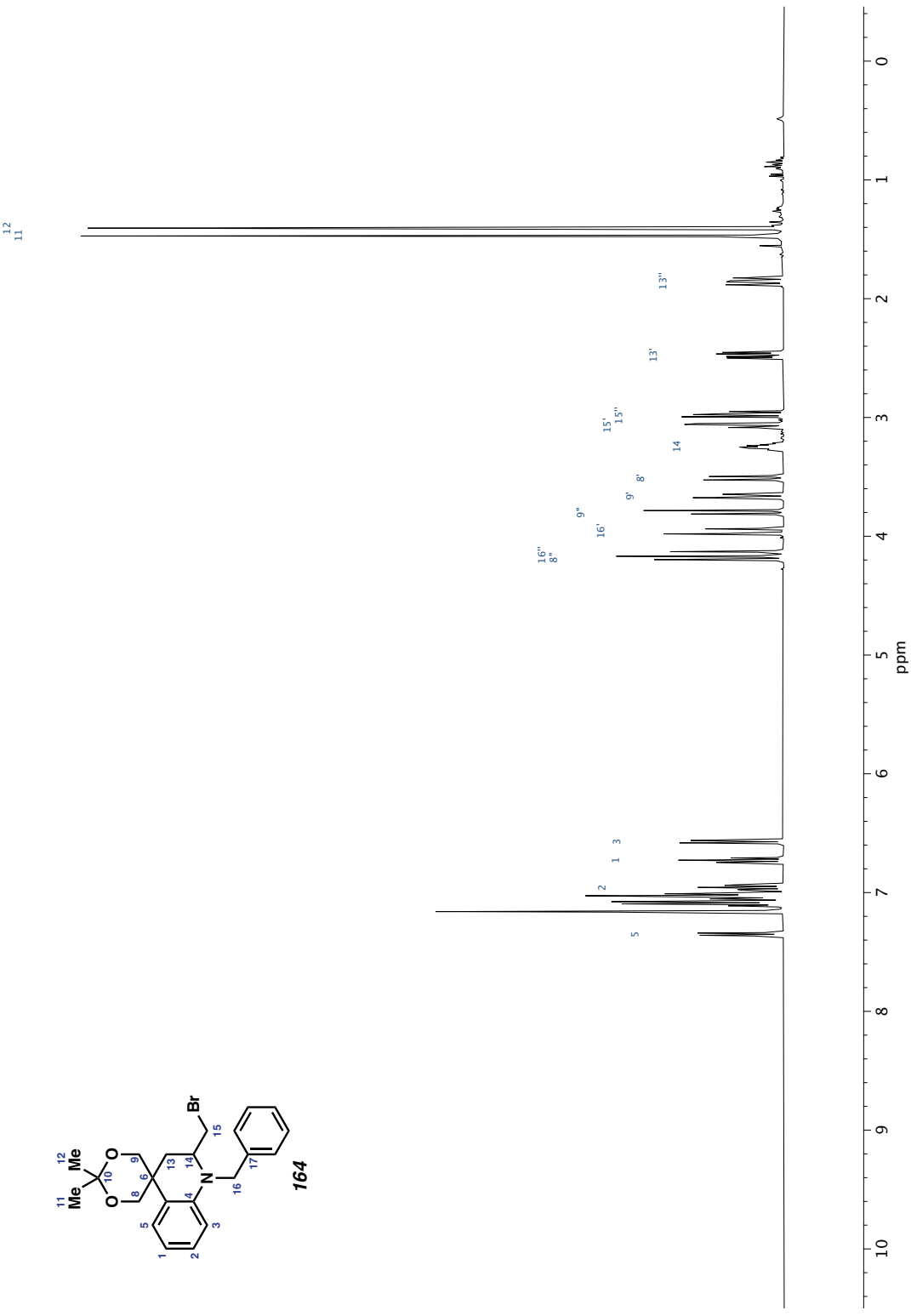


Figure A5.70 *^{1}H NMR (400 MHz, C_6D_6) of compound* ***164****.*

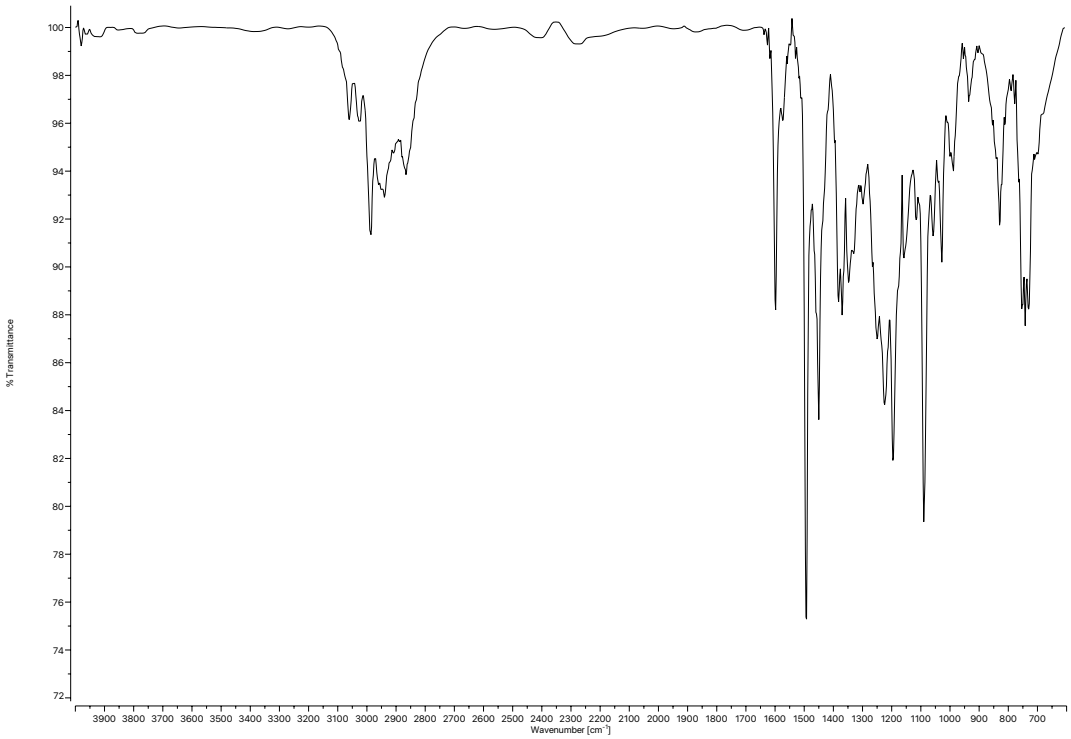


Figure A.71 *Infrared spectrum (Thin Film, NaCl) of compound* ***164****.*

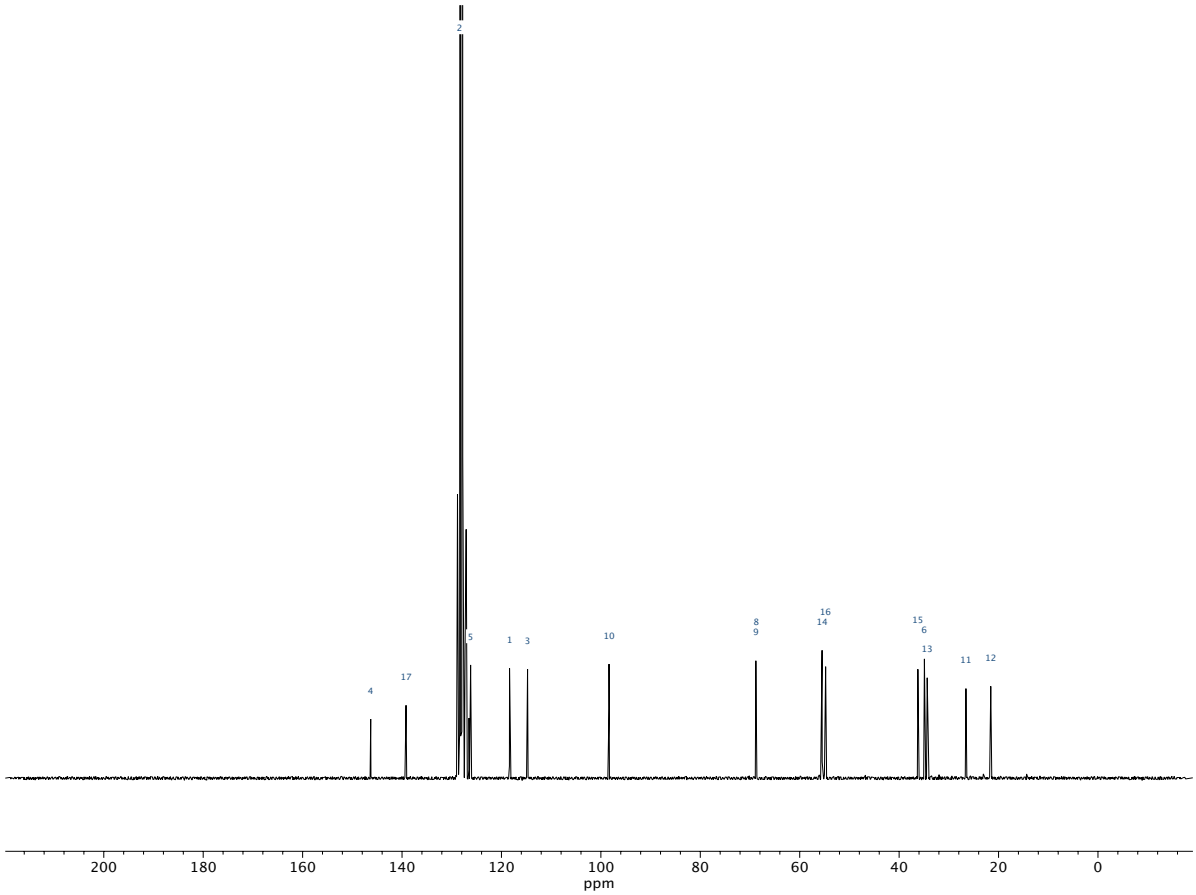


Figure A.72 *^{13}C NMR (100 MHz, C_6D_6) of compound* ***164****.*

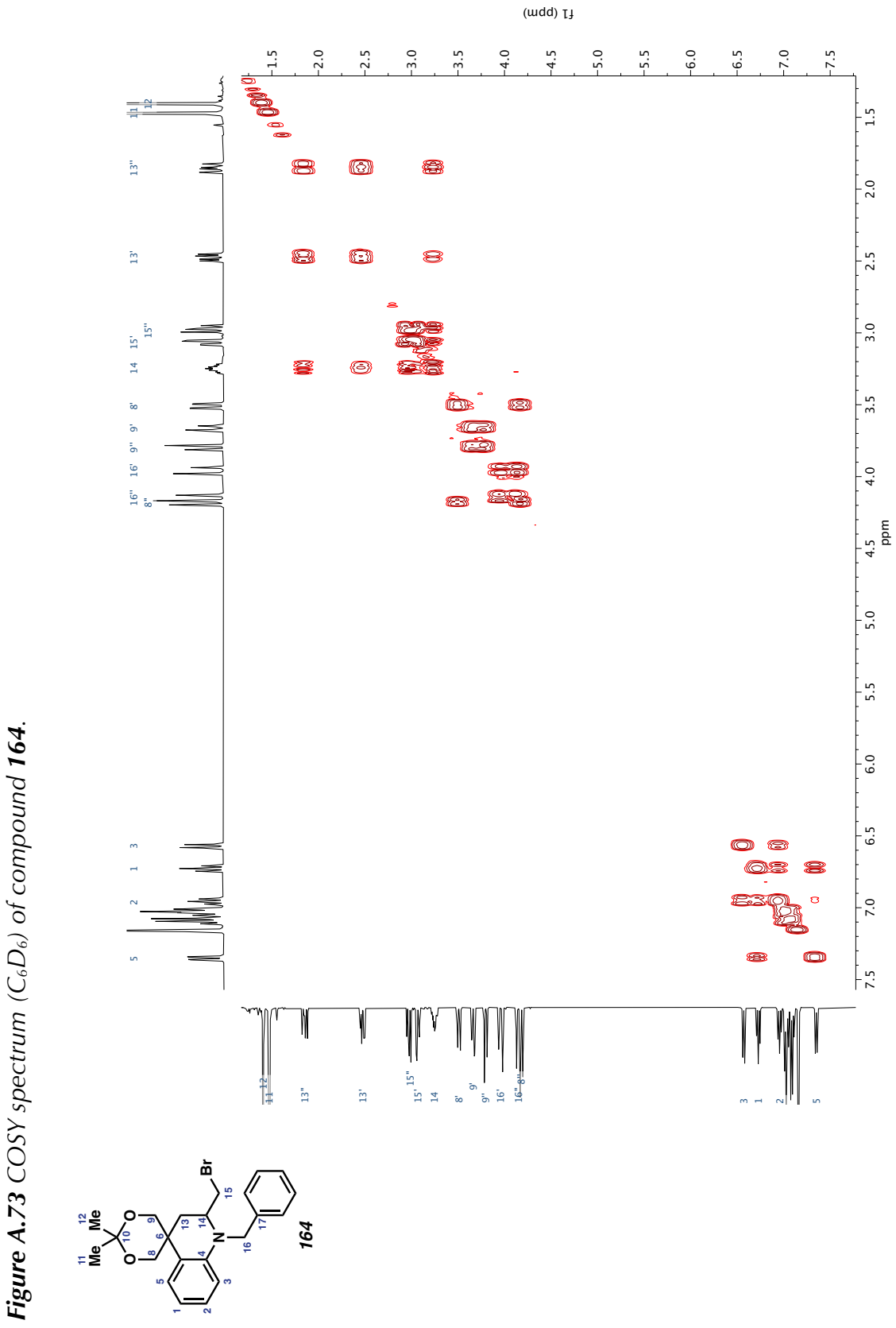


Figure A.73 *COSY spectrum (C_6D_6) of compound* ***164***.

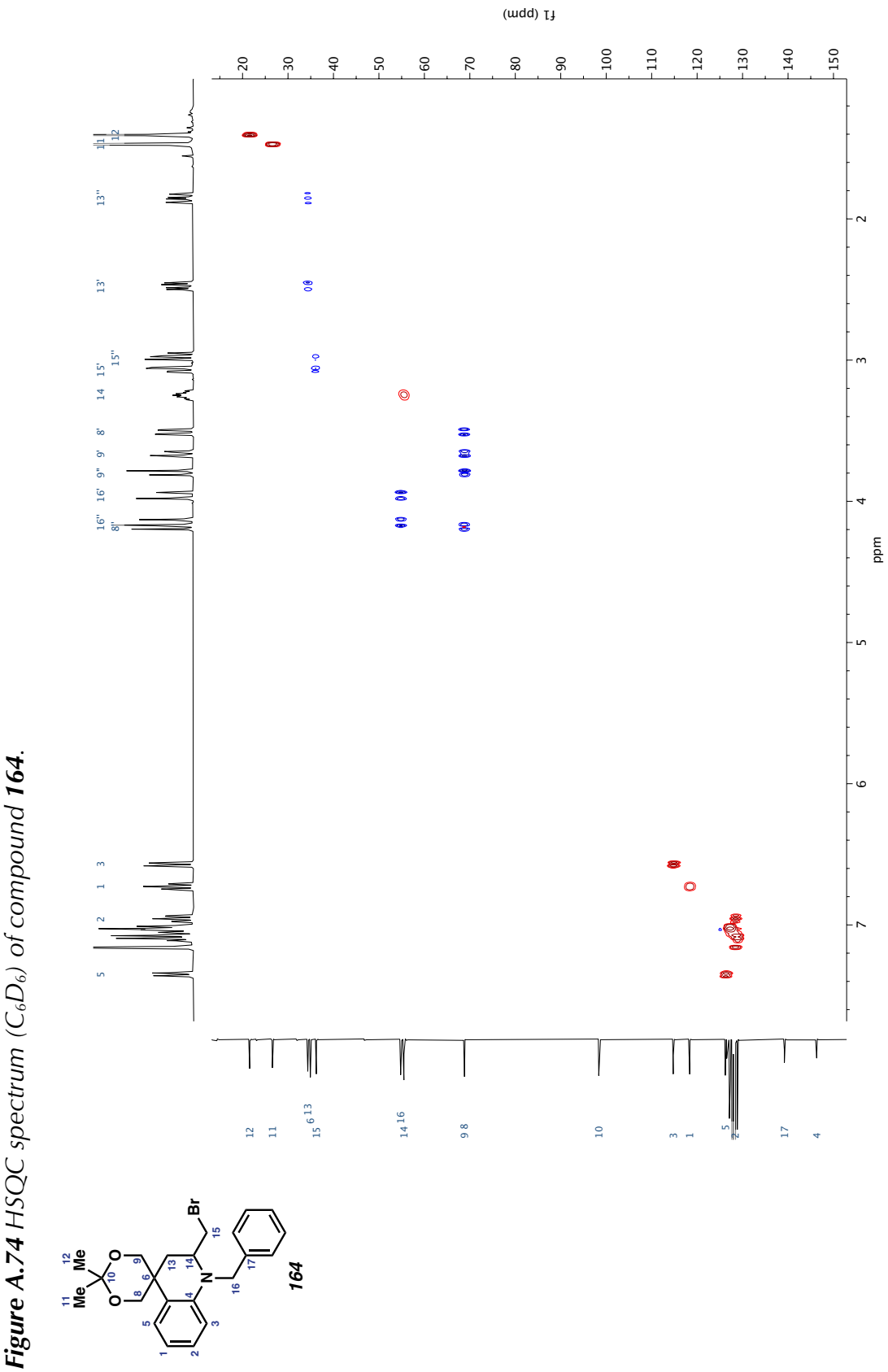


Figure A.74 *HSQC spectrum (C_6D_6) of compound* ***164****.*

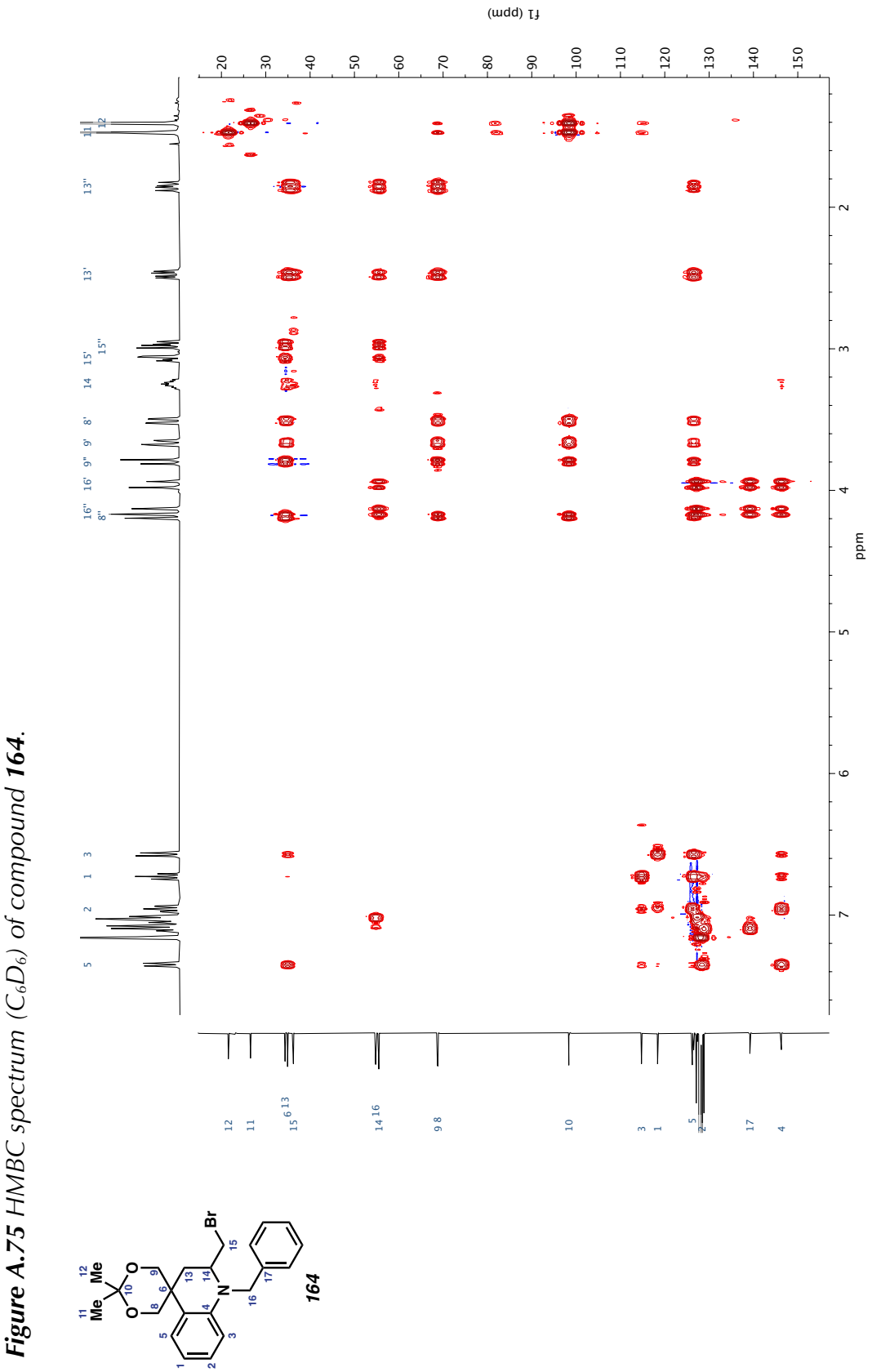


Figure A.75 *HMBC spectrum (C_6D_6) of compound* ***164****.*

APPENDIX 6

X-Ray Crystallography Reports Relevant to Chapter 3:

Preparation and Regioselective Ring Opening Reactions of Fused Bicyclic N-Aryl Aziridines

A6.1 GENERAL EXPERIMENTAL

X-Ray crystallographic analysis was obtained from the Caltech X-Ray Crystallography Facility using a Bruker AXS D8 VENTURE KAPPA diffractometer.

A6.2 X-RAY CRYSTAL STRUCTURE ANALYSIS OF COMPOUND 155 (V24324)

Crystals suitable for X-ray diffraction were grown by dissolving **155** in minimal Et_2O and carefully layering with pentane. Low-temperature diffraction data (ϕ-and ω-scans) were collected on a Bruker AXS D8 VENTURE KAPPA diffractometer coupled to a PHOTON II CPAD detector with Cu K_α radiation (λ = 1.54178 Å) from an IμS micro-source for the structure of compound V24324. The structure was solved by direct methods using SHELXS[1] and refined against F^2 on all data by full-matrix least squares with SHELXL-2019[2] using established refinement techniques.[3] All non-hydrogen atoms were refined anisotropically. All hydrogen atoms were included into the model at geometrically calculated positions and refined using a riding model. The isotropic displacement parameters of all hydrogen atoms were fixed to 1.2 times the U value of the atoms they are linked to (1.5 times for methyl groups). Compound V24324 crystallizes in the monoclinic space group $P2_1/c$ with one molecule in the asymmetric unit.

Figure A6.2.1 *X-Ray Coordinate of Compound* ***155***

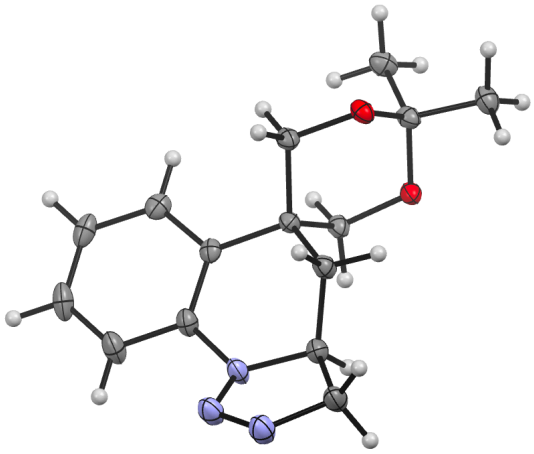


Table A6.2.1 *Crystal data and structure refinement for* ***155***.

Identification code	V24324	
Empirical formula	C15 H19 N3 O2	
Formula weight	273.33	
Temperature	100(2) K	
Wavelength	1.54178 Å	
Crystal system	Monoclinic	
Space group	$P2_1/c$	
Unit cell dimensions	a = 5.7352(6) Å	a= 90°.
	b = 22.0610(14) Å	b= 91.493(6)°.
	c = 10.8363(7) Å	g = 90°.
Volume	1370.59(19) $Å^3$	
Z	4	
Density (calculated)	1.325 Mg/m^3	
Absorption coefficient	0.726 mm^{-1}	
F(000)	584	
Crystal size	0.150 x 0.150 x 0.150 mm^3	
Theta range for data collection	4.008 to 74.500°.	
Index ranges	-6<=h<=7, -27<=k<=27, -13<=l<=13	
Reflections collected	32931	
Independent reflections	2802 [R(int) = 0.0560]	
Completeness to theta = 67.679°	100.0 %	
Absorption correction	Semi-empirical from equivalents	

Max. and min. transmission	0.7538 and 0.6508
Refinement method	Full-matrix least-squares on F^2
Data / restraints / parameters	2802 / 0 / 183
Goodness-of-fit on F^2	1.044
Final R indices [I>2sigma(I)]	R1 = 0.0411, wR2 = 0.0969
R indices (all data)	R1 = 0.0481, wR2 = 0.1030
Extinction coefficient	n/a
Largest diff. peak and hole	0.383 and -0.241 e.$Å^{-3}$

Table A6.2.2 *Atomic coordinates (x 10^4) and equivalent isotropic displacement parameters ($Å^2$x 10^3) for* ***155****. U(eq) is defined as one third of the trace of the orthogonalized U^{ij} tensor.*

Atom	x	y	z	U(eq)
C(1)	2829(2)	4080(1)	6882(1)	19(1)
C(2)	3819(2)	4528(1)	7813(1)	20(1)
C(3)	2033(3)	4812(1)	8670(1)	25(1)
N(1)	2524(2)	4538(1)	9903(1)	29(1)
N(2)	4280(2)	4206(1)	9877(1)	27(1)
N(3)	5314(2)	4211(1)	8728(1)	24(1)
C(4)	6630(2)	3699(1)	8416(1)	21(1)
C(5)	8161(3)	3448(1)	9309(1)	29(1)
C(6)	9494(3)	2950(1)	9027(2)	29(1)
C(7)	9368(2)	2702(1)	7849(2)	25(1)
C(8)	7889(2)	2960(1)	6960(1)	22(1)
C(9)	6466(2)	3455(1)	7218(1)	17(1)
C(10)	4765(2)	3718(1)	6251(1)	16(1)
C(11)	6071(2)	4109(1)	5320(1)	18(1)
O(1)	4514(2)	4310(1)	4346(1)	19(1)
C(12)	3308(2)	3834(1)	3698(1)	19(1)
C(14)	1411(3)	4142(1)	2935(1)	24(1)
C(15)	4959(3)	3473(1)	2902(1)	24(1)
O(2)	2110(2)	3457(1)	4546(1)	19(1)
C(13)	3601(2)	3206(1)	5491(1)	18(1)

Table A6.2.3. *Bond lengths [Å] and angles [°] for* ***155***.

Bond	**Length (Å)**	**Bond**	**Length (Å)**
C(1)-C(2)	1.5128(19)	C(14)-H(14A)	0.9800
C(1)-C(10)	1.5419(19)	C(14)-H(14B)	0.9800
C(1)-H(1A)	0.9900	C(14)-H(14C)	0.9800
C(1)-H(1B)	0.9900	C(15)-H(15A)	0.9800
C(2)-N(3)	1.4715(17)	C(15)-H(15B)	0.9800
C(2)-C(3)	1.534(2)	C(15)-H(15C)	0.9800
C(2)-H(2)	1.0000	O(2)-C(13)	1.4287(16)
C(3)-N(1)	1.4869(19)	C(13)-H(13A)	0.9900
C(3)-H(3A)	0.9900	C(13)-H(13B)	0.9900
C(3)-H(3B)	0.9900		
N(1)-N(2)	1.2463(19)	**Atoms**	**Angle (Å)**
N(2)-N(3)	1.3932(18)	C(2)-C(1)-C(10)	111.87(11)
N(3)-C(4)	1.4046(19)	C(2)-C(1)-H(1A)	109.2
C(4)-C(5)	1.4037(19)	C(10)-C(1)-H(1A)	109.2
C(4)-C(9)	1.406(2)	C(2)-C(1)-H(1B)	109.2
C(5)-C(6)	1.377(2)	C(10)-C(1)-H(1B)	109.2
C(5)-H(5)	0.9500	H(1A)-C(1)-H(1B)	107.9
C(6)-C(7)	1.388(2)	N(3)-C(2)-C(1)	109.91(11)
C(6)-H(6)	0.9500	N(3)-C(2)-C(3)	99.95(11)
C(7)-C(8)	1.388(2)	C(1)-C(2)-C(3)	115.24(12)
C(7)-H(7)	0.9500	N(3)-C(2)-H(2)	110.4
C(8)-C(9)	1.3956(19)	C(1)-C(2)-H(2)	110.4
C(8)-H(8)	0.9500	C(3)-C(2)-H(2)	110.4
C(9)-C(10)	1.5275(17)	N(1)-C(3)-C(2)	105.31(11)
C(10)-C(11)	1.5364(18)	N(1)-C(3)-H(3A)	110.7
C(10)-C(13)	1.5396(17)	C(2)-C(3)-H(3A)	110.7
C(11)-O(1)	1.4352(15)	N(1)-C(3)-H(3B)	110.7
C(11)-H(11A)	0.9900	C(2)-C(3)-H(3B)	110.7
C(11)-H(11B)	0.9900	H(3A)-C(3)-H(3B)	108.8
O(1)-C(12)	1.4319(16)	N(2)-N(1)-C(3)	110.68(12)
C(12)-O(2)	1.4288(16)	N(1)-N(2)-N(3)	112.26(12)
C(12)-C(14)	1.5111(19)	N(2)-N(3)-C(4)	116.94(12)
C(12)-C(15)	1.522(2)	N(2)-N(3)-C(2)	110.60(11)

Table A6.2.3. cont'd.

Atoms	Angle (Å)	Atoms	Angle (Å)
C(4)-N(3)-C(2)	121.84(11)	C(10)-C(11)-H(11B)	109.5
C(5)-C(4)-N(3)	118.82(13)	H(11A)-C(11)-H(11B)	108.1
C(5)-C(4)-C(9)	120.71(13)	C(12)-O(1)-C(11)	114.61(10)
N(3)-C(4)-C(9)	120.44(12)	O(2)-C(12)-O(1)	110.28(10)
C(6)-C(5)-C(4)	120.20(15)	O(2)-C(12)-C(14)	105.24(11)
C(6)-C(5)-H(5)	119.9	O(1)-C(12)-C(14)	105.65(11)
C(4)-C(5)-H(5)	119.9	O(2)-C(12)-C(15)	112.08(11)
C(5)-C(6)-C(7)	120.13(13)	O(1)-C(12)-C(15)	111.21(11)
C(5)-C(6)-H(6)	119.9	C(14)-C(12)-C(15)	112.04(12)
C(7)-C(6)-H(6)	119.9	C(12)-C(14)-H(14A)	109.5
C(6)-C(7)-C(8)	119.52(14)	C(12)-C(14)-H(14B)	109.5
C(6)-C(7)-H(7)	120.2	H(14A)-C(14)-H(14B)	109.5
C(8)-C(7)-H(7)	120.2	C(12)-C(14)-H(14C)	109.5
C(7)-C(8)-C(9)	122.11(14)	H(14A)-C(14)-H(14C)	109.5
C(7)-C(8)-H(8)	118.9	H(14B)-C(14)-H(14C)	109.5
C(9)-C(8)-H(8)	118.9	C(12)-C(15)-H(15A)	109.5
C(8)-C(9)-C(4)	117.30(12)	C(12)-C(15)-H(15B)	109.5
C(8)-C(9)-C(10)	121.74(12)	H(15A)-C(15)-H(15B)	109.5
C(4)-C(9)-C(10)	120.95(12)	C(12)-C(15)-H(15C)	109.5
C(9)-C(10)-C(11)	110.50(10)	H(15A)-C(15)-H(15C)	109.5
C(9)-C(10)-C(13)	110.40(11)	H(15B)-C(15)-H(15C)	109.5
C(11)-C(10)-C(13)	105.80(10)	C(13)-O(2)-C(12)	113.41(10)
C(9)-C(10)-C(1)	110.29(11)	O(2)-C(13)-C(10)	110.04(10)
C(11)-C(10)-C(1)	111.68(11)	O(2)-C(13)-H(13A)	109.7
C(13)-C(10)-C(1)	108.06(11)	C(10)-C(13)-H(13A)	109.7
O(1)-C(11)-C(10)	110.63(10)	O(2)-C(13)-H(13B)	109.7
O(1)-C(11)-H(11A)	109.5	C(10)-C(13)-H(13B)	109.7
C(10)-C(11)-H(11A)	109.5	H(13A)-C(13)-H(13B)	108.2
O(1)-C(11)-H(11B)	109.5		

Symmetry transformations used to generate equivalent atoms:

Table A6.2.4 *Anisotropic displacement parameters ($Å^2 x\ 10^3$) for **155**. The anisotropic displacement factor exponent takes the form: $-2p^2[\ h^2\ a^{*2}U^{11} + ... + 2\ h\ k\ a^*\ b^*\ U^{12}\ ]$*

Atom	U^{11}	U^{22}	U^{33}	U^{23}	U^{13}	U^{12}
C(1)	17(1)	23(1)	18(1)	-1(1)	-2(1)	2(1)
C(2)	21(1)	20(1)	20(1)	0(1)	-3(1)	2(1)
C(3)	28(1)	28(1)	20(1)	-3(1)	-3(1)	9(1)
N(1)	32(1)	33(1)	21(1)	-1(1)	0(1)	9(1)
N(2)	30(1)	34(1)	16(1)	-1(1)	-1(1)	7(1)
N(3)	26(1)	30(1)	15(1)	-1(1)	-4(1)	10(1)
C(4)	19(1)	24(1)	20(1)	4(1)	-1(1)	4(1)
C(5)	27(1)	39(1)	20(1)	6(1)	-3(1)	8(1)
C(6)	22(1)	35(1)	30(1)	16(1)	-1(1)	6(1)
C(7)	18(1)	19(1)	39(1)	9(1)	3(1)	3(1)
C(8)	17(1)	20(1)	28(1)	0(1)	1(1)	-1(1)
C(9)	14(1)	16(1)	20(1)	3(1)	0(1)	-2(1)
C(10)	15(1)	17(1)	17(1)	0(1)	-2(1)	0(1)
C(11)	17(1)	18(1)	18(1)	2(1)	-3(1)	-2(1)
O(1)	21(1)	17(1)	18(1)	2(1)	-5(1)	-2(1)
C(12)	19(1)	21(1)	17(1)	0(1)	-1(1)	-4(1)
C(14)	21(1)	28(1)	22(1)	4(1)	-5(1)	-1(1)
C(15)	23(1)	28(1)	20(1)	-3(1)	1(1)	0(1)
O(2)	17(1)	23(1)	17(1)	1(1)	-2(1)	-4(1)
C(13)	19(1)	18(1)	18(1)	1(1)	-2(1)	-4(1)

Table A6.2.5 *Hydrogen coordinates ($x\ 10^4$) and isotropic displacement parameters ($Å^2 x\ 10^3$) for **155**.*

Atom	x	y	z	U(eq)
H(1A)	1894	4301	6246	23
H(1B)	1779	3795	7303	23
H(2)	4722	4851	7389	24
H(3A)	2223	5258	8703	30

Table A6.2.5 cont'd.

Atom	x	y	z	U(eq)
H(3B)	423	4718	8380	30
H(5)	8279	3622	10110	34
H(6)	10501	2775	9639	35
H(7)	10286	2359	7653	30
H(8)	7846	2795	6151	26
H(11A)	6766	4464	5748	21
H(11B)	7352	3869	4966	21
H(14A)	445	3835	2514	36
H(14B)	2120	4406	2320	36
H(14C)	438	4386	3475	36
H(15A)	6239	3311	3421	36
H(15B)	5592	3738	2267	36
H(15C)	4108	3137	2507	36
H(13A)	4815	2952	5113	22
H(13B)	2680	2945	6039	22

Table A6.2.6. *Torsion angles [°] for* ***155***.

Atoms (A-B-C-D)	Angle (°)	Atoms (A-B-C-D)	Angle (°)
C(10)-C(1)-C(2)-N(3)	-55.97(15)	N(2)-N(3)-C(4)-C(5)	-43.77(19)
C(10)-C(1)-C(2)-C(3)	-167.93(11)	C(2)-N(3)-C(4)-C(5)	174.95(13)
N(3)-C(2)-C(3)-N(1)	-8.98(14)	N(2)-N(3)-C(4)-C(9)	138.19(14)
C(1)-C(2)-C(3)-N(1)	108.72(13)	C(2)-N(3)-C(4)-C(9)	-3.1(2)
C(2)-C(3)-N(1)-N(2)	4.52(17)	N(3)-C(4)-C(5)-C(6)	-179.30(14)
C(3)-N(1)-N(2)-N(3)	2.65(18)	C(9)-C(4)-C(5)-C(6)	-1.3(2)
N(1)-N(2)-N(3)-C(4)	-154.72(13)	C(4)-C(5)-C(6)-C(7)	1.5(2)
N(1)-N(2)-N(3)-C(2)	-9.30(18)	C(5)-C(6)-C(7)-C(8)	0.0(2)
C(1)-C(2)-N(3)-N(2)	-110.66(13)	C(6)-C(7)-C(8)-C(9)	-1.7(2)
C(3)-C(2)-N(3)-N(2)	10.93(15)	C(7)-C(8)-C(9)-C(4)	1.9(2)
C(1)-C(2)-N(3)-C(4)	32.78(18)	C(7)-C(8)-C(9)-C(10)	-177.20(12)
C(3)-C(2)-N(3)-C(4)	154.37(13)	C(5)-C(4)-C(9)-C(8)	-0.4(2)

Table A6.2.6. cont'd.

Atoms (A-B-C-D)	Angle (°)	Atoms (A-B-C-D)	Angle (°)
N(3)-C(4)-C(9)-C(8)	177.62(13)	C(13)-C(10)-C(11)-O(1)	55.16(13)
C(5)-C(4)-C(9)-C(10)	178.69(13)	C(1)-C(10)-C(11)-O(1)	-62.17(14)
N(3)-C(4)-C(9)-C(10)	-3.3(2)	C(10)-C(11)-O(1)-C(12)	-56.14(14)
C(8)-C(9)-C(10)-C(11)	-77.34(15)	C(11)-O(1)-C(12)-O(2)	54.32(14)
C(4)-C(9)-C(10)-C(11)	103.62(14)	C(11)-O(1)-C(12)-C(14)	167.55(11)
C(8)-C(9)-C(10)-C(13)	39.35(17)	C(11)-O(1)-C(12)-C(15)	-70.66(14)
C(4)-C(9)-C(10)-C(13)	-139.69(13)	O(1)-C(12)-O(2)-C(13)	-56.28(14)
C(8)-C(9)-C(10)-C(1)	158.70(12)	C(14)-C(12)-O(2)-C(13)	-169.78(11)
C(4)-C(9)-C(10)-C(1)	-20.34(17)	C(15)-C(12)-O(2)-C(13)	68.21(14)
C(2)-C(1)-C(10)-C(9)	49.93(15)	C(12)-O(2)-C(13)-C(10)	60.18(14)
C(2)-C(1)-C(10)-C(11)	-73.35(14)	C(9)-C(10)-C(13)-O(2)	-176.89(10)
C(2)-C(1)-C(10)-C(13)	170.69(11)	C(11)-C(10)-C(13)-O(2)	-57.32(13)
C(9)-C(10)-C(11)-O(1)	174.66(10)	C(1)-C(10)-C(13)-O(2)	62.42(13)

Symmetry transformations used to generate equivalent atoms:

A6.3 X-RAY CRYSTAL STRUCTURE ANALYSIS OF COMPOUND 156 (V24183)

Crystals suitable for X-ray analysis were grown by layer diffusion of pentane into a solution of **156** in minimal CH_2Cl_2. Low-temperature diffraction data (ϕ-and ω-scans) were collected on a Bruker AXS D8 VENTURE KAPPA diffractometer coupled to a PHOTON II CPAD detector with or Cu K_α radiation (λ = 1.54178 Å) from an IμS micro-source for the structure of compound V24183. The structure was solved by direct methods using SHELXS[1] and refined against F^2 on all data by full-matrix least squares with SHELXL-2019[2] using established refinement techniques.[3] All non-hydrogen atoms were refined anisotropically. All hydrogen atoms were included into the model at geometrically calculated positions and refined using a riding model. The isotropic displacement parameters of all hydrogen atoms were fixed to 1.2 times the U value of the atoms they are linked to (1.5 times for methyl groups). Compound **156** crystallizes in the monoclinic space group $P2_1/n$ with one molecule in the asymmetric unit.

Figure A6.3.1 *X-Ray Coordinate of Compound* ***156***

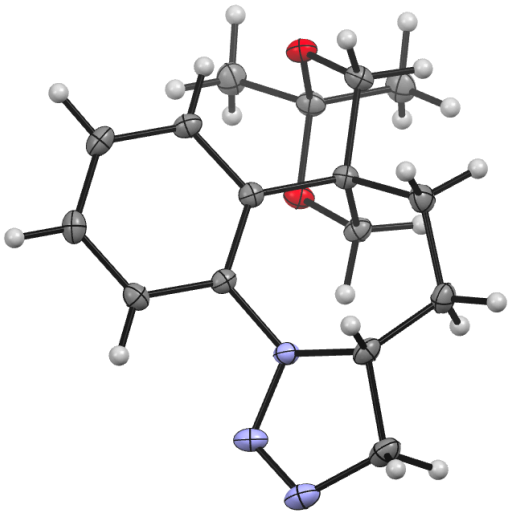


Table A6.3.1 *Crystal data and structure refinement for* ***156***.

Identification code	V24183	
Empirical formula	C16 H21 N3 O2	
Formula weight	287.36	
Temperature	100(2) K	
Wavelength	1.54178 Å	
Crystal system	Monoclinic	
Space group	$P2_1/n$	
Unit cell dimensions	a = 12.3987(13) Å	a= 90°.
	b = 6.4964(5) Å	b= 104.422(5)°.
	c = 19.0596(18) Å	g = 90°.
Volume	1486.8(2) $Å^3$	
Z	4	
Density (calculated)	1.284 Mg/m^3	
Absorption coefficient	0.694 mm^{-1}	
F(000)	616	
Crystal size	0.500 x 0.400 x 0.300 mm^3	
Theta range for data collection	4.791 to 74.394°.	
Index ranges	-15<=h<=15, -8<=k<=8, -23<=l<=23	
Reflections collected	37072	
Independent reflections	3036 [R(int) = 0.0327]	
Completeness to theta = 67.679°	100.0 %	

Absorption correction	Semi-empirical from equivalents
Max. and min. transmission	0.7538 and 0.6557
Refinement method	Full-matrix least-squares on F^2
Data / restraints / parameters	3036 / 0 / 192
Goodness-of-fit on F^2	1.049
Final R indices [I>2sigma(I)]	R1 = 0.0343, wR2 = 0.0843
R indices (all data)	R1 = 0.0345, wR2 = 0.0844
Extinction coefficient	n/a
Largest diff. peak and hole	0.255 and -0.290 e.$Å^{-3}$

Table A6.3.2 *Atomic coordinates (x 10^4) and equivalent isotropic displacement parameters ($Å^2$x 10^3) for* ***156****. U(eq) is defined as one third of the trace of the orthogonalized U^{ij} tensor.*

Atom	x	y	z	U(eq)
C(1)	6910(1)	5290(2)	3507(1)	16(1)
O(1)	7144(1)	6896(1)	4038(1)	17(1)
C(2)	7180(1)	6245(2)	4758(1)	17(1)
C(15)	7204(1)	8200(2)	5193(1)	23(1)
C(16)	8187(1)	4876(2)	5069(1)	21(1)
O(2)	6162(1)	5249(1)	4775(1)	17(1)
C(3)	5864(1)	3598(2)	4270(1)	17(1)
C(4)	5783(1)	4269(2)	3484(1)	14(1)
C(5)	4835(1)	5813(2)	3207(1)	13(1)
C(6)	4164(1)	6498(2)	3651(1)	16(1)
C(7)	3333(1)	7964(2)	3422(1)	18(1)
C(8)	3142(1)	8795(2)	2732(1)	18(1)
C(9)	3778(1)	8126(2)	2273(1)	16(1)
C(10)	4612(1)	6653(2)	2504(1)	13(1)
N(1)	5225(1)	5949(1)	2009(1)	15(1)
N(2)	5258(1)	7252(1)	1438(1)	19(1)
N(3)	5389(1)	6298(2)	896(1)	23(1)
C(11)	5437(1)	4051(2)	1036(1)	22(1)
C(12)	5125(1)	3788(2)	1758(1)	17(1)

Table A6.3.2 cont'd.

Atom	x	y	z	U(eq)
C(13)	5889(1)	2367(2)	2290(1)	19(1)
C(14)	5637(1)	2258(2)	3035(1)	18(1)

Table A6.3.3 *Bond lengths [Å] and angles [°] for* ***156****.*

Bond	Length (Å)	Bond	Length (Å)
C(1)-O(1)	1.4313(12)	C(7)-H(7)	0.9500
C(1)-C(4)	1.5376(13)	C(8)-C(9)	1.3863(14)
C(1)-H(1A)	0.9900	C(8)-H(8)	0.9500
C(1)-H(1B)	0.9900	C(9)-C(10)	1.3976(14)
O(1)-C(2)	1.4257(12)	C(9)-H(9)	0.9500
C(2)-O(2)	1.4251(12)	C(10)-N(1)	1.4252(12)
C(2)-C(15)	1.5134(14)	N(1)-N(2)	1.3870(12)
C(2)-C(16)	1.5277(14)	N(1)-C(12)	1.4786(13)
C(15)-H(15A)	0.9800	N(2)-N(3)	1.2512(13)
C(15)-H(15B)	0.9800	N(3)-C(11)	1.4829(15)
C(15)-H(15C)	0.9800	C(11)-C(12)	1.5304(14)
C(16)-H(16A)	0.9800	C(11)-H(11A)	0.9900
C(16)-H(16B)	0.9800	C(11)-H(11B)	0.9900
C(16)-H(16C)	0.9800	C(12)-C(13)	1.5164(14)
O(2)-C(3)	1.4273(12)	C(12)-H(12)	1.0000
C(3)-C(4)	1.5382(13)	C(13)-C(14)	1.5281(14)
C(3)-H(3A)	0.9900	C(13)-H(13A)	0.9900
C(3)-H(3B)	0.9900	C(13)-H(13B)	0.9900
C(4)-C(5)	1.5356(13)	C(14)-H(14A)	0.9900
C(4)-C(14)	1.5480(13)	C(14)-H(14B)	0.9900
C(5)-C(6)	1.3997(13)		
C(5)-C(10)	1.4090(13)	**Atoms**	**Angle (°)**
C(6)-C(7)	1.3911(14)	O(1)-C(1)-C(4)	110.99(8)
C(6)-H(6)	0.9500	O(1)-C(1)-H(1A)	109.4
C(7)-C(8)	1.3854(15)	C(4)-C(1)-H(1A)	109.4

Table A6.3.3 cont'd.

Atoms	Angle (°)	Atoms	Angle (°)
O(1)-C(1)-H(1B)	109.4	C(3)-C(4)-C(14)	105.67(8)
C(4)-C(1)-H(1B)	109.4	C(6)-C(5)-C(10)	116.60(9)
H(1A)-C(1)-H(1B)	108.0	C(6)-C(5)-C(4)	121.20(8)
C(2)-O(1)-C(1)	114.57(8)	C(10)-C(5)-C(4)	122.18(8)
O(2)-C(2)-O(1)	109.97(7)	C(7)-C(6)-C(5)	122.14(9)
O(2)-C(2)-C(15)	105.37(8)	C(7)-C(6)-H(6)	118.9
O(1)-C(2)-C(15)	105.69(8)	C(5)-C(6)-H(6)	118.9
O(2)-C(2)-C(16)	111.65(9)	C(8)-C(7)-C(6)	120.26(9)
O(1)-C(2)-C(16)	111.90(8)	C(8)-C(7)-H(7)	119.9
C(15)-C(2)-C(16)	111.90(8)	C(6)-C(7)-H(7)	119.9
C(2)-C(15)-H(15A)	109.5	C(7)-C(8)-C(9)	119.14(9)
C(2)-C(15)-H(15B)	109.5	C(7)-C(8)-H(8)	120.4
H(15A)-C(15)-H(15B)	109.5	C(9)-C(8)-H(8)	120.4
C(2)-C(15)-H(15C)	109.5	C(8)-C(9)-C(10)	120.58(9)
H(15A)-C(15)-H(15C)	109.5	C(8)-C(9)-H(9)	119.7
H(15B)-C(15)-H(15C)	109.5	C(10)-C(9)-H(9)	119.7
C(2)-C(16)-H(16A)	109.5	C(9)-C(10)-C(5)	121.26(9)
C(2)-C(16)-H(16B)	109.5	C(9)-C(10)-N(1)	119.12(8)
H(16A)-C(16)-H(16B)	109.5	C(5)-C(10)-N(1)	119.59(9)
C(2)-C(16)-H(16C)	109.5	N(2)-N(1)-C(10)	116.54(8)
H(16A)-C(16)-H(16C)	109.5	N(2)-N(1)-C(12)	110.03(8)
H(16B)-C(16)-H(16C)	109.5	C(10)-N(1)-C(12)	120.18(8)
C(2)-O(2)-C(3)	114.08(7)	N(3)-N(2)-N(1)	112.42(9)
O(2)-C(3)-C(4)	112.77(8)	N(2)-N(3)-C(11)	110.28(9)
O(2)-C(3)-H(3A)	109.0	N(3)-C(11)-C(12)	105.31(8)
C(4)-C(3)-H(3A)	109.0	N(3)-C(11)-H(11A)	110.7
O(2)-C(3)-H(3B)	109.0	C(12)-C(11)-H(11A)	110.7
C(4)-C(3)-H(3B)	109.0	N(3)-C(11)-H(11B)	110.7
H(3A)-C(3)-H(3B)	107.8	C(12)-C(11)-H(11B)	110.7
C(5)-C(4)-C(1)	109.88(8)	H(11A)-C(11)-H(11B)	108.8
C(5)-C(4)-C(3)	112.29(8)	N(1)-C(12)-C(13)	111.90(8)
C(1)-C(4)-C(3)	104.81(8)	N(1)-C(12)-C(11)	99.51(8)
C(5)-C(4)-C(14)	112.76(8)	C(13)-C(12)-C(11)	114.44(8)
C(1)-C(4)-C(14)	111.10(8)	N(1)-C(12)-H(12)	110.2

C(13)-C(12)-H(12)	110.2	H(13A)-C(13)-H(13B)	107.6
C(11)-C(12)-H(12)	110.2	C(13)-C(14)-C(4)	116.86(8)
C(12)-C(13)-C(14)	114.28(8)	C(13)-C(14)-H(14A)	108.1
C(12)-C(13)-H(13A)	108.7	C(4)-C(14)-H(14A)	108.1
C(14)-C(13)-H(13A)	108.7	C(13)-C(14)-H(14B)	108.1
C(12)-C(13)-H(13B)	108.7	C(4)-C(14)-H(14B)	108.1
C(14)-C(13)-H(13B)	108.7	H(14A)-C(14)-H(14B)	107.3

Symmetry transformations used to generate equivalent atoms:

Table A6.3.4 *Anisotropic displacement parameters ($Å^2 x\ 10^3$) for* ***156****. The anisotropic displacement factor exponent takes the form: $-2p^2[\ h^2\ a^{*2}U^{11} + \ldots + 2\ h\ k\ a^*\ b^*\ U^{12}\ ]$*

Atom	U^{11}	U^{22}	U^{33}	U^{23}	U^{13}	U^{12}
C(1)	14(1)	19(1)	14(1)	-1(1)	3(1)	0(1)
O(1)	18(1)	18(1)	13(1)	0(1)	2(1)	-3(1)
C(2)	17(1)	19(1)	13(1)	1(1)	2(1)	-1(1)
C(15)	27(1)	21(1)	19(1)	-3(1)	2(1)	2(1)
C(16)	20(1)	24(1)	17(1)	-1(1)	-1(1)	3(1)
O(2)	18(1)	21(1)	13(1)	0(1)	4(1)	-1(1)
C(3)	19(1)	17(1)	15(1)	2(1)	4(1)	-1(1)
C(4)	14(1)	14(1)	13(1)	1(1)	4(1)	0(1)
C(5)	12(1)	13(1)	13(1)	-2(1)	2(1)	-2(1)
C(6)	15(1)	20(1)	13(1)	-1(1)	4(1)	-2(1)
C(7)	16(1)	20(1)	19(1)	-6(1)	6(1)	0(1)
C(8)	15(1)	14(1)	23(1)	-2(1)	3(1)	1(1)
C(9)	16(1)	14(1)	16(1)	0(1)	2(1)	-2(1)
C(10)	13(1)	13(1)	13(1)	-3(1)	4(1)	-3(1)
N(1)	17(1)	15(1)	12(1)	0(1)	5(1)	-1(1)
N(2)	21(1)	24(1)	14(1)	2(1)	6(1)	-3(1)
N(3)	25(1)	30(1)	15(1)	-1(1)	8(1)	-1(1)
C(11)	22(1)	28(1)	15(1)	-4(1)	6(1)	2(1)
C(12)	17(1)	18(1)	16(1)	-5(1)	5(1)	-2(1)

Table A6.3.4 cont'd.

Atom	U^{11}	U^{22}	U^{33}	U^{23}	U^{13}	U^{12}
C(13)	22(1)	16(1)	20(1)	-4(1)	6(1)	2(1)
C(14)	23(1)	14(1)	19(1)	0(1)	5(1)	0(1)

Table A6.3.5 *Hydrogen coordinates (x 10^4) and isotropic displacement parameters ($Å^2$x 10^3) for* ***156****.*

Atom	x	y	z	U(eq)
H(1A)	7507	4242	3625	19
H(1B)	6897	5870	3025	19
H(15A)	6538	9019	4984	34
H(15B)	7870	8998	5182	34
H(15C)	7219	7848	5696	34
H(16A)	8166	4418	5556	32
H(16B)	8872	5656	5097	32
H(16C)	8168	3674	4755	32
H(3A)	5137	3029	4302	20
H(3B)	6426	2490	4402	20
H(6)	4281	5945	4126	19
H(7)	2896	8397	3739	22
H(8)	2582	9810	2576	21
H(9)	3645	8674	1796	19
H(11A)	6196	3514	1068	26
H(11B)	4904	3310	644	26
H(12)	4335	3314	1673	20
H(13A)	6667	2838	2353	23
H(13B)	5832	965	2081	23
H(14A)	6125	1195	3323	22
H(14B)	4859	1784	2966	22

Table A6.3.6 *Torsion angles [°] for* ***156****.*

Atoms	Angle (°)	Atoms	Angle (°)
C(4)-C(1)-O(1)-C(2)	58.84(10)	C(8)-C(9)-C(10)-C(5)	-0.21(15)
C(1)-O(1)-C(2)-O(2)	-55.69(10)	C(8)-C(9)-C(10)-N(1)	177.91(9)
C(1)-O(1)-C(2)-C(15)	-168.95(8)	C(6)-C(5)-C(10)-C(9)	1.23(14)
C(1)-O(1)-C(2)-C(16)	69.01(10)	C(4)-C(5)-C(10)-C(9)	-177.09(9)
O(1)-C(2)-O(2)-C(3)	53.84(10)	C(6)-C(5)-C(10)-N(1)	-176.89(8)
C(15)-C(2)-O(2)-C(3)	167.31(8)	C(4)-C(5)-C(10)-N(1)	4.79(14)
C(16)-C(2)-O(2)-C(3)	-71.00(10)	C(9)-C(10)-N(1)-N(2)	23.15(12)
C(2)-O(2)-C(3)-C(4)	-56.45(10)	C(5)-C(10)-N(1)-N(2)	-158.69(8)
O(1)-C(1)-C(4)-C(5)	66.45(10)	C(9)-C(10)-N(1)-C(12)	-114.01(10)
O(1)-C(1)-C(4)-C(3)	-54.41(10)	C(5)-C(10)-N(1)-C(12)	64.14(12)
O(1)-C(1)-C(4)-C(14)	-168.07(8)	C(10)-N(1)-N(2)-N(3)	-152.90(9)
O(2)-C(3)-C(4)-C(5)	-65.24(10)	C(12)-N(1)-N(2)-N(3)	-11.62(11)
O(2)-C(3)-C(4)-C(1)	54.00(10)	N(1)-N(2)-N(3)-C(11)	1.59(12)
O(2)-C(3)-C(4)-C(14)	171.45(8)	N(2)-N(3)-C(11)-C(12)	8.45(12)
C(1)-C(4)-C(5)-C(6)	-115.12(10)	N(2)-N(1)-C(12)-C(13)	136.58(8)
C(3)-C(4)-C(5)-C(6)	1.11(13)	C(10)-N(1)-C(12)-C(13)	-83.77(11)
C(14)-C(4)-C(5)-C(6)	120.35(10)	N(2)-N(1)-C(12)-C(11)	15.28(10)
C(1)-C(4)-C(5)-C(10)	63.13(11)	C(10)-N(1)-C(12)-C(11)	154.93(8)
C(3)-C(4)-C(5)-C(10)	179.36(8)	N(3)-C(11)-C(12)-N(1)	-13.71(10)
C(14)-C(4)-C(5)-C(10)	-61.40(12)	N(3)-C(11)-C(12)-C(13)	-133.16(9)
C(10)-C(5)-C(6)-C(7)	-1.23(14)	N(1)-C(12)-C(13)-C(14)	62.60(11)
C(4)-C(5)-C(6)-C(7)	177.11(9)	C(11)-C(12)-C(13)-C(14)	174.84(9)
C(5)-C(6)-C(7)-C(8)	0.21(15)	C(12)-C(13)-C(14)-C(4)	-63.58(12)
C(6)-C(7)-C(8)-C(9)	0.87(15)	C(5)-C(4)-C(14)-C(13)	75.25(11)
C(7)-C(8)-C(9)-C(10)	-0.86(15)	C(1)-C(4)-C(14)-C(13)	-48.61(11)
		C(3)-C(4)-C(14)-C(13)	-161.74(8)

Symmetry transformations used to generate equivalent atoms:

A6.4 X-RAY CRYSTAL STRUCTURE ANALYSIS OF COMPOUND 157 (V24328)

Low-temperature diffraction data (ϕ-and ω-scans) were collected on a Bruker AXS D8 VENTURE KAPPA diffractometer coupled to a PHOTON II CPAD detector with Cu K_α radiation (λ = 1.54178 Å) from an IμS micro-source for the structure of compound **157**. The structure was solved by direct methods using SHELXS[1] and refined against F^2 on all data by full-matrix least squares with SHELXL-2019[2] using established refinement techniques.[3] All non-hydrogen atoms were refined anisotropically. All hydrogen atoms were included into the model at geometrically calculated positions and refined using a riding model. The isotropic displacement parameters of all hydrogen atoms were fixed to 1.2 times the U value of the atoms they are linked to (1.5 times for methyl groups). Compound **157** crystallizes in the monoclinic space group *Pn* with two molecules in the asymmetric unit.

Figure A6.4.1 *X-Ray Coordinate of Compound* ***157***

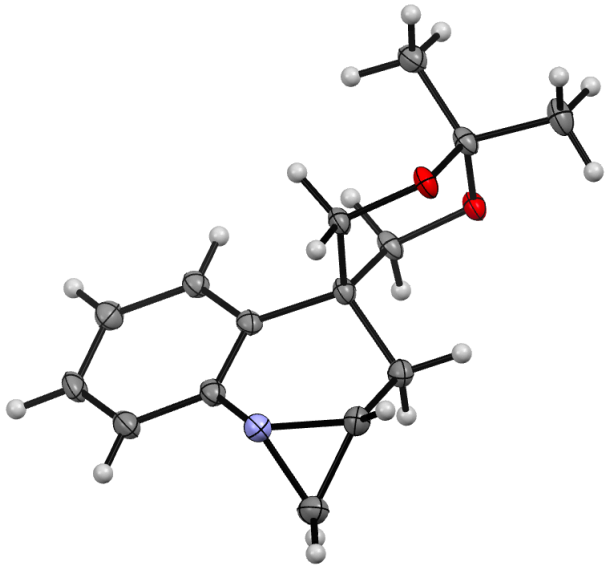


Table A6.4.1 *Crystal data and structure refinement for* ***157***.

Identification code	V24328	
Empirical formula	C15 H19 N O2	
Formula weight	245.31	
Temperature	100(2) K	
Wavelength	1.54178 Å	
Crystal system	Monoclinic	
Space group	Pn	
Unit cell dimensions	a = 14.6342(14) Å	a= 90°.
	b = 5.5370(4) Å	b= 91.015(11)°.
	c = 15.6925(13) Å	g = 90°.
Volume	1271.36(19) $Å^3$	
Z	4	
Density (calculated)	1.282 Mg/m^3	
Absorption coefficient	0.674 mm^{-1}	
F(000)	528	
Crystal size	0.200 x 0.100 x 0.100 mm^3	
Theta range for data collection	4.094 to 69.712°.	
Index ranges	-17<=h<=17, -6<=k<=6, -19<=l<=19	
Reflections collected	32042	
Independent reflections	4767 [R(int) = 0.0603]	

Completeness to theta = 67.679°	100.0 %
Absorption correction	Semi-empirical from equivalents
Max. and min. transmission	0.7532 and 0.5963
Refinement method	Full-matrix least-squares on F^2
Data / restraints / parameters	4767 / 2 / 329
Goodness-of-fit on F^2	1.037
Final R indices [I>2sigma(I)]	R1 = 0.0290, wR2 = 0.0723
R indices (all data)	R1 = 0.0296, wR2 = 0.0729
Absolute structure parameter	0.21(7)
Extinction coefficient	n/a
Largest diff. peak and hole	0.130 and -0.218 e.Å^{-3}

Table A6.4.2 *Atomic coordinates (x 10^4) and equivalent isotropic displacement parameters (Å^{2}x 10^3) for* ***157****. U(eq) is defined as one third of the trace of the orthogonalized U^{ij} tensor.*

Atom	x	y	z	U(eq)
N(1)	4869(1)	7691(3)	8717(1)	20(1)
C(1)	5191(2)	5396(4)	9105(1)	25(1)
C(2)	4322(2)	5480(3)	8599(1)	21(1)
C(3)	4262(2)	4440(4)	7710(1)	19(1)
C(4)	4176(1)	6457(3)	7033(1)	15(1)
C(11)	3261(1)	7790(3)	7128(1)	16(1)
O(1)	3059(1)	9262(2)	6398(1)	16(1)
C(12)	3021(1)	7949(3)	5616(1)	18(1)
C(14)	2223(1)	6169(4)	5580(2)	24(1)
C(15)	2942(2)	9844(4)	4921(1)	22(1)
O(2)	3871(1)	6760(2)	5480(1)	17(1)
C(13)	4159(1)	5203(3)	6165(1)	16(1)
C(5)	4979(1)	8168(3)	7159(1)	15(1)
C(6)	5412(1)	9336(3)	6485(1)	17(1)
C(7)	6180(1)	10773(4)	6622(1)	21(1)
C(8)	6544(1)	11040(4)	7444(2)	24(1)
C(9)	6117(1)	9942(4)	8118(1)	23(1)
C(10)	5332(1)	8545(3)	7987(1)	17(1)

Table A6.4.2

Atom	x	y	z	U(eq)
N(101)	5114(1)	7021(3)	1274(1)	19(1)
C(101)	4975(2)	9468(4)	901(1)	23(1)
C(102)	5713(1)	9037(3)	1549(1)	19(1)
C(103)	5618(1)	9933(3)	2454(1)	18(1)
C(104)	5457(1)	7808(3)	3070(1)	15(1)
C(111)	5352(1)	8798(4)	3976(1)	17(1)
O(101)	6198(1)	9815(2)	4285(1)	18(1)
C(112)	6939(1)	8137(3)	4294(1)	17(1)
C(114)	7781(2)	9595(4)	4520(1)	24(1)
C(115)	6793(2)	6075(4)	4922(1)	21(1)
O(102)	7079(1)	7242(2)	3449(1)	18(1)
C(113)	6282(1)	6095(3)	3090(1)	16(1)
C(105)	4625(1)	6403(3)	2757(1)	16(1)
C(106)	4011(1)	5267(3)	3302(1)	18(1)
C(107)	3261(1)	3998(4)	2983(1)	22(1)
C(108)	3101(1)	3865(4)	2107(1)	23(1)
C(109)	3704(2)	4957(4)	1560(1)	22(1)
C(110)	4470(1)	6187(3)	1874(1)	17(1)

Table A6.4.3 *Bond lengths [Å] and angles [°] for* ***157****.*

Bond	Length (Å)	Bond	Length (Å)
N(1)-C(10)	1.423(3)	C(3)-H(3A)	0.9900
N(1)-C(2)	1.473(3)	C(3)-H(3B)	0.9900
N(1)-C(1)	1.482(3)	C(4)-C(5)	1.520(3)
C(1)-C(2)	1.488(3)	C(4)-C(13)	1.529(3)
C(1)-H(1A)	0.9900	C(4)-C(11)	1.538(3)
C(1)-H(1B)	0.9900	C(11)-O(1)	1.432(2)
C(2)-C(3)	1.511(3)	C(11)-H(11A)	0.9900
C(2)-H(2)	1.0000	C(11)-H(11B)	0.9900
C(3)-C(4)	1.544(3)	O(1)-C(12)	1.427(2)

Table A6.4.3 cont'd.

Bond	Length (Å)	Bond	Length (Å)
C(12)-O(2)	1.427(2)	C(104)-C(111)	1.534(3)
C(12)-C(15)	1.516(3)	C(104)-C(113)	1.536(3)
C(12)-C(14)	1.528(3)	C(111)-O(101)	1.436(2)
C(14)-H(14A)	0.9800	C(111)-H(11C)	0.9900
C(14)-H(14B)	0.9800	C(111)-H(11D)	0.9900
C(14)-H(14C)	0.9800	O(101)-C(112)	1.428(2)
C(15)-H(15A)	0.9800	C(112)-O(102)	1.434(2)
C(15)-H(15B)	0.9800	C(112)-C(114)	1.510(3)
C(15)-H(15C)	0.9800	C(112)-C(115)	1.526(3)
O(2)-C(13)	1.436(2)	C(114)-H(11E)	0.9800
C(13)-H(13A)	0.9900	C(114)-H(11F)	0.9800
C(13)-H(13B)	0.9900	C(114)-H(11G)	0.9800
C(5)-C(6)	1.400(3)	C(115)-H(11H)	0.9800
C(5)-C(10)	1.405(3)	C(115)-H(11I)	0.9800
C(6)-C(7)	1.391(3)	C(115)-H(11J)	0.9800
C(6)-H(6)	0.9500	O(102)-C(113)	1.434(2)
C(7)-C(8)	1.394(3)	C(113)-H(11K)	0.9900
C(7)-H(7)	0.9500	C(113)-H(11L)	0.9900
C(8)-C(9)	1.380(3)	C(105)-C(106)	1.400(3)
C(8)-H(8)	0.9500	C(105)-C(110)	1.406(3)
C(9)-C(10)	1.397(3)	C(106)-C(107)	1.390(3)
C(9)-H(9)	0.9500	C(106)-H(106)	0.9500
N(101)-C(110)	1.421(3)	C(107)-C(108)	1.392(3)
N(101)-C(102)	1.479(3)	C(107)-H(107)	0.9500
N(101)-C(101)	1.488(3)	C(108)-C(109)	1.382(3)
C(101)-C(102)	1.489(3)	C(108)-H(108)	0.9500
C(101)-H(10A)	0.9900	C(109)-C(110)	1.394(3)
C(101)-H(10B)	0.9900	C(109)-H(109)	0.9500
C(102)-C(103)	1.513(3)		
C(102)-H(102)	1.0000	**Atoms**	**Angle (°)**
C(103)-C(104)	1.544(3)	C(10)-N(1)-C(2)	116.14(16)
C(103)-H(10C)	0.9900	C(10)-N(1)-C(1)	117.56(16)
C(103)-H(10D)	0.9900	C(2)-N(1)-C(1)	60.47(13)
C(104)-C(105)	1.519(3)	N(1)-C(1)-C(2)	59.45(13)

Table A6.4.3 cont'd.

Atoms	Angle (°)	Atoms	Angle (°)
N(1)-C(1)-H(1A)	117.8	O(1)-C(12)-C(14)	112.32(16)
C(2)-C(1)-H(1A)	117.8	C(15)-C(12)-C(14)	111.76(17)
N(1)-C(1)-H(1B)	117.8	C(12)-C(14)-H(14A)	109.5
C(2)-C(1)-H(1B)	117.8	C(12)-C(14)-H(14B)	109.5
H(1A)-C(1)-H(1B)	115.0	H(14A)-C(14)-H(14B)	109.5
N(1)-C(2)-C(1)	60.08(13)	C(12)-C(14)-H(14C)	109.5
N(1)-C(2)-C(3)	117.10(16)	H(14A)-C(14)-H(14C)	109.5
C(1)-C(2)-C(3)	121.06(18)	H(14B)-C(14)-H(14C)	109.5
N(1)-C(2)-H(2)	115.7	C(12)-C(15)-H(15A)	109.5
C(1)-C(2)-H(2)	115.7	C(12)-C(15)-H(15B)	109.5
C(3)-C(2)-H(2)	115.7	H(15A)-C(15)-H(15B)	109.5
C(2)-C(3)-C(4)	111.24(16)	C(12)-C(15)-H(15C)	109.5
C(2)-C(3)-H(3A)	109.4	H(15A)-C(15)-H(15C)	109.5
C(4)-C(3)-H(3A)	109.4	H(15B)-C(15)-H(15C)	109.5
C(2)-C(3)-H(3B)	109.4	C(12)-O(2)-C(13)	114.19(14)
C(4)-C(3)-H(3B)	109.4	O(2)-C(13)-C(4)	113.25(15)
H(3A)-C(3)-H(3B)	108.0	O(2)-C(13)-H(13A)	108.9
C(5)-C(4)-C(13)	113.49(15)	C(4)-C(13)-H(13A)	108.9
C(5)-C(4)-C(11)	111.14(15)	O(2)-C(13)-H(13B)	108.9
C(13)-C(4)-C(11)	107.67(15)	C(4)-C(13)-H(13B)	108.9
C(5)-C(4)-C(3)	107.93(15)	H(13A)-C(13)-H(13B)	107.7
C(13)-C(4)-C(3)	106.51(15)	C(6)-C(5)-C(10)	117.77(18)
C(11)-C(4)-C(3)	109.97(15)	C(6)-C(5)-C(4)	123.30(17)
O(1)-C(11)-C(4)	111.34(15)	C(10)-C(5)-C(4)	118.89(17)
O(1)-C(11)-H(11A)	109.4	C(7)-C(6)-C(5)	121.55(18)
C(4)-C(11)-H(11A)	109.4	C(7)-C(6)-H(6)	119.2
O(1)-C(11)-H(11B)	109.4	C(5)-C(6)-H(6)	119.2
C(4)-C(11)-H(11B)	109.4	C(6)-C(7)-C(8)	119.80(19)
H(11A)-C(11)-H(11B)	108.0	C(6)-C(7)-H(7)	120.1
C(12)-O(1)-C(11)	113.70(14)	C(8)-C(7)-H(7)	120.1
O(2)-C(12)-O(1)	110.08(15)	C(9)-C(8)-C(7)	119.53(19)
O(2)-C(12)-C(15)	105.47(16)	C(9)-C(8)-H(8)	120.2
O(1)-C(12)-C(15)	105.50(16)	C(7)-C(8)-H(8)	120.2
O(2)-C(12)-C(14)	111.35(16)	C(8)-C(9)-C(10)	120.85(19)

Table A6.4.3 cont'd.

Atoms	Angle (°)	Atoms	Angle (°)
C(8)-C(9)-H(9)	119.6	C(104)-C(111)-H(11C)	109.5
C(10)-C(9)-H(9)	119.6	O(101)-C(111)-H(11D)	109.5
C(9)-C(10)-C(5)	120.41(18)	C(104)-C(111)-H(11D)	109.5
C(9)-C(10)-N(1)	117.88(17)	H(11C)-C(111)-H(11D)	108.1
C(5)-C(10)-N(1)	121.52(17)	C(112)-O(101)-C(111)	113.48(14)
C(110)-N(101)-C(102)	116.68(16)	O(101)-C(112)-O(102)	109.61(14)
C(110)-N(101)-C(101)	117.92(17)	O(101)-C(112)-C(114)	105.74(15)
C(102)-N(101)-C(101)	60.26(13)	O(102)-C(112)-C(114)	105.79(15)
N(101)-C(101)-C(102)	59.55(13)	O(101)-C(112)-C(115)	112.25(16)
N(101)-C(101)-H(10A)	117.8	O(102)-C(112)-C(115)	111.27(16)
C(102)-C(101)-H(10A)	117.8	C(114)-C(112)-C(115)	111.83(17)
N(101)-C(101)-H(10B)	117.8	C(112)-C(114)-H(11E)	109.5
C(102)-C(101)-H(10B)	117.8	C(112)-C(114)-H(11F)	109.5
H(10A)-C(101)-H(10B)	115.0	H(11E)-C(114)-H(11F)	109.5
N(101)-C(102)-C(101)	60.19(13)	C(112)-C(114)-H(11G)	109.5
N(101)-C(102)-C(103)	117.18(17)	H(11E)-C(114)-H(11G)	109.5
C(101)-C(102)-C(103)	120.66(18)	H(11F)-C(114)-H(11G)	109.5
N(101)-C(102)-H(102)	115.8	C(112)-C(115)-H(11H)	109.5
C(101)-C(102)-H(102)	115.8	C(112)-C(115)-H(11I)	109.5
C(103)-C(102)-H(102)	115.8	H(11H)-C(115)-H(11I)	109.5
C(102)-C(103)-C(104)	110.85(15)	C(112)-C(115)-H(11J)	109.5
C(102)-C(103)-H(10C)	109.5	H(11H)-C(115)-H(11J)	109.5
C(104)-C(103)-H(10C)	109.5	H(11I)-C(115)-H(11J)	109.5
C(102)-C(103)-H(10D)	109.5	C(112)-O(102)-C(113)	112.81(14)
C(104)-C(103)-H(10D)	109.5	O(102)-C(113)-C(104)	111.61(15)
H(10C)-C(103)-H(10D)	108.1	O(102)-C(113)-H(11K)	109.3
C(105)-C(104)-C(111)	112.97(16)	C(104)-C(113)-H(11K)	109.3
C(105)-C(104)-C(113)	108.40(14)	O(102)-C(113)-H(11L)	109.3
C(111)-C(104)-C(113)	107.07(15)	C(104)-C(113)-H(11L)	109.3
C(105)-C(104)-C(103)	108.54(16)	H(11K)-C(113)-H(11L)	108.0
C(111)-C(104)-C(103)	109.09(15)	C(106)-C(105)-C(110)	118.08(17)
C(113)-C(104)-C(103)	110.78(16)	C(106)-C(105)-C(104)	123.44(17)
O(101)-C(111)-C(104)	110.66(15)	C(110)-C(105)-C(104)	118.46(17)
O(101)-C(111)-H(11C)	109.5	C(107)-C(106)-C(105)	121.18(19)

Table A6.4.3 cont'd.

Atoms	Angle (°)	Atoms	Angle (°)
C(107)-C(106)-H(106)	119.4	C(109)-C(108)-H(108)	120.2
C(107)-C(108)-H(108)	120.2	C(108)-C(109)-C(110)	120.82(19)
C(105)-C(106)-H(106)	119.4	C(108)-C(109)-H(109)	119.6
C(106)-C(107)-C(108)	120.04(19)	C(110)-C(109)-H(109)	119.6
C(106)-C(107)-H(107)	120.0	C(109)-C(110)-C(105)	120.29(18)
C(108)-C(107)-H(107)	120.0	C(109)-C(110)-N(101)	117.61(18)
C(109)-C(108)-C(107)	119.53(18)	C(105)-C(110)-N(101)	121.90(17)

Symmetry transformations used to generate equivalent atoms:

Table A6.4.4 *Anisotropic displacement parameters ($Å^2 x\ 10^3$) for **157**. The anisotropic displacement factor exponent takes the form: $-2p^2[\ h^2\ a^{*2}U^{11} + \ldots + 2\ h\ k\ a^*\ b^*\ U^{12}\ ]$*

Atom	U^{11}	U^{22}	U^{33}	U^{23}	U^{13}	U^{12}
N(1)	22(1)	19(1)	18(1)	0(1)	-4(1)	4(1)
C(1)	34(1)	22(1)	18(1)	0(1)	-6(1)	8(1)
C(2)	25(1)	17(1)	20(1)	2(1)	1(1)	2(1)
C(3)	21(1)	16(1)	20(1)	2(1)	-2(1)	0(1)
C(4)	13(1)	15(1)	17(1)	0(1)	-2(1)	0(1)
C(11)	14(1)	18(1)	17(1)	1(1)	-1(1)	0(1)
O(1)	14(1)	17(1)	18(1)	-2(1)	-4(1)	1(1)
C(12)	13(1)	20(1)	19(1)	-4(1)	-4(1)	3(1)
C(14)	14(1)	24(1)	33(1)	-8(1)	-6(1)	-2(1)
C(15)	22(1)	23(1)	21(1)	-2(1)	-6(1)	6(1)
O(2)	14(1)	21(1)	16(1)	-1(1)	-3(1)	4(1)
C(13)	16(1)	16(1)	18(1)	-1(1)	-4(1)	1(1)
C(5)	12(1)	14(1)	20(1)	-1(1)	-2(1)	3(1)
C(6)	14(1)	17(1)	21(1)	0(1)	-1(1)	3(1)
C(7)	15(1)	19(1)	30(1)	1(1)	2(1)	0(1)
C(8)	12(1)	20(1)	39(1)	-6(1)	-4(1)	0(1)
C(9)	18(1)	21(1)	29(1)	-6(1)	-9(1)	4(1)

Table A6.4.4 cont'd.

Atom	U^{11}	U^{22}	U^{33}	U^{23}	U^{13}	U^{12}
C(10)	14(1)	15(1)	21(1)	-1(1)	-2(1)	6(1)
N(101)	19(1)	19(1)	19(1)	0(1)	-2(1)	-1(1)
C(101)	28(1)	21(1)	20(1)	1(1)	-3(1)	1(1)
C(102)	19(1)	17(1)	20(1)	0(1)	0(1)	-2(1)
C(103)	20(1)	16(1)	20(1)	-2(1)	-3(1)	-1(1)
C(104)	12(1)	16(1)	18(1)	-2(1)	-2(1)	-1(1)
C(111)	11(1)	21(1)	19(1)	-4(1)	-3(1)	2(1)
O(101)	14(1)	18(1)	21(1)	-4(1)	-4(1)	-1(1)
C(112)	12(1)	20(1)	19(1)	-4(1)	-4(1)	1(1)
C(114)	16(1)	27(1)	29(1)	-7(1)	-2(1)	-3(1)
C(115)	20(1)	23(1)	22(1)	-1(1)	-5(1)	1(1)
O(102)	11(1)	23(1)	20(1)	-5(1)	-2(1)	-2(1)
C(113)	12(1)	17(1)	19(1)	-3(1)	-4(1)	-1(1)
C(105)	12(1)	14(1)	20(1)	-1(1)	-3(1)	2(1)
C(106)	15(1)	19(1)	20(1)	-1(1)	-3(1)	0(1)
C(107)	15(1)	22(1)	28(1)	2(1)	-2(1)	0(1)
C(108)	15(1)	22(1)	31(1)	-2(1)	-9(1)	-3(1)
C(109)	20(1)	21(1)	23(1)	-2(1)	-7(1)	0(1)
C(110)	14(1)	16(1)	21(1)	-2(1)	-3(1)	1(1)

Table A6.4.5 *Hydrogen coordinates (x 10^4) and isotropic displacement parameters ($Å^2$x 10^3) for* ***157***.

Atom	x	y	z	U(eq)
H(1A)	5150	5221	9731	30
H(1B)	5722	4587	8848	30
H(2)	3749	5391	8936	25
H(3A)	3725	3357	7663	23
H(3B)	4816	3468	7601	23
H(11A)	2766	6596	7201	20
H(11B)	3289	8818	7644	20

Table A6.4.5 cont'd.

Atom	x	y	z	U(eq)
H(14A)	2327	4886	6001	36
H(14B)	2177	5459	5008	36
H(14C)	1655	7020	5706	36
H(15A)	2365	10724	4978	33
H(15B)	2955	9057	4362	33
H(15C)	3454	10977	4974	33
H(13A)	4779	4585	6046	20
H(13B)	3741	3800	6188	20
H(6)	5176	9142	5922	21
H(7)	6457	11571	6156	26
H(8)	7081	11970	7538	28
H(9)	6360	10139	8679	27
H(10A)	4432	10396	1079	27
H(10B)	5156	9725	303	27
H(102)	6350	9002	1327	23
H(10C)	5098	11073	2481	22
H(10D)	6179	10810	2631	22
H(11C)	4870	10054	3976	21
H(11D)	5162	7479	4360	21
H(11E)	7834	10951	4123	36
H(11F)	8324	8565	4481	36
H(11G)	7733	10213	5103	36
H(11H)	6701	6738	5493	32
H(11I)	7331	5020	4931	32
H(11J)	6253	5142	4746	32
H(11K)	6134	4648	3431	19
H(11L)	6412	5558	2503	19
H(106)	4110	5367	3901	22
H(107)	2857	3220	3362	26
H(108)	2581	3031	1887	28
H(109)	3596	4867	962	26

Table A6.4.6 *Torsion angles [°] for* ***157****.*

Atoms (A-B-C-D)	Angle (°)	Atoms (A-B-C-D)	Angle (°)
C(10)-N(1)-C(1)-C(2)	-105.99(19)	C(6)-C(7)-C(8)-C(9)	-2.3(3)
C(10)-N(1)-C(2)-C(1)	108.33(19)	C(7)-C(8)-C(9)-C(10)	0.8(3)
C(10)-N(1)-C(2)-C(3)	-3.6(3)	C(8)-C(9)-C(10)-C(5)	2.0(3)
C(1)-N(1)-C(2)-C(3)	-112.0(2)	C(8)-C(9)-C(10)-N(1)	-173.07(18)
N(1)-C(1)-C(2)-C(3)	105.5(2)	C(6)-C(5)-C(10)-C(9)	-3.2(3)
N(1)-C(2)-C(3)-C(4)	-39.3(2)	C(4)-C(5)-C(10)-C(9)	174.58(16)
C(1)-C(2)-C(3)-C(4)	-109.1(2)	C(6)-C(5)-C(10)-N(1)	171.74(16)
C(2)-C(3)-C(4)-C(5)	55.6(2)	C(4)-C(5)-C(10)-N(1)	-10.5(3)
C(2)-C(3)-C(4)-C(13)	177.82(17)	C(2)-N(1)-C(10)-C(9)	-154.57(17)
C(2)-C(3)-C(4)-C(11)	-65.8(2)	C(1)-N(1)-C(10)-C(9)	-85.9(2)
C(5)-C(4)-C(11)-O(1)	74.36(19)	C(2)-N(1)-C(10)-C(5)	30.4(2)
C(13)-C(4)-C(11)-O(1)	-50.52(19)	C(1)-N(1)-C(10)-C(5)	99.1(2)
C(3)-C(4)-C(11)-O(1)	-166.18(15)	C(110)-N(101)-C(101)-C(102)	106.4(3)
C(4)-C(11)-O(1)-C(12)	57.95(19)	C(110)-N(101)-C(102)-C(101)	-108.5(2)
C(11)-O(1)-C(12)-O(2)	-58.6(2)	C(110)-N(101)-C(102)-C(103)	3.0(3)
C(11)-O(1)-C(12)-C(15)	-171.90(15)	C(101)-N(101)-C(102)-C(103)	111.5(2)
C(11)-O(1)-C(12)-C(14)	66.1(2)	N(101)-C(101)-C(102)-C(103)	-105.8(2)
O(1)-C(12)-O(2)-C(13)	55.5(2)	N(101)-C(102)-C(103)-C(104)	38.4(2)
C(15)-C(12)-O(2)-C(13)	168.83(15)	C(101)-C(102)-C(103)-C(104)	108.2(2)
C(14)-C(12)-O(2)-C(13)	-69.8(2)	C(102)-C(103)-C(104)-C(105)	-55.8(2)
C(12)-O(2)-C(13)-C(4)	-52.9(2)	C(102)-C(103)-C(104)-C(111)	-179.3(2)
C(5)-C(4)-C(13)-O(2)	-75.00(19)	C(102)-C(103)-C(104)-C(113)	63.1(2)
C(11)-C(4)-C(13)-O(2)	48.5(2)	C(105)-C(104)-C(111)-O(101)	172.0(2)
C(3)-C(4)-C(13)-O(2)	166.38(15)	C(113)-C(104)-C(111)-O(101)	52.8(2)
C(13)-C(4)-C(5)-C(6)	27.2(2)	C(103)-C(104)-C(111)-O(101)	-67.2(2)
C(11)-C(4)-C(5)-C(6)	-94.4(2)	C(104)-C(111)-O(101)-C(112)	-58.3(2)
C(3)-C(4)-C(5)-C(6)	144.98(17)	C(111)-O(101)-C(112)-O(102)	59.0(2)
C(13)-C(4)-C(5)-C(10)	-150.45(16)	C(111)-O(101)-C(112)-C(114)	172.6(2)
C(11)-C(4)-C(5)-C(10)	88.0(2)	C(111)-O(101)-C(112)-C(115)	-65.2(2)
C(3)-C(4)-C(5)-C(10)	-32.6(2)	O(101)-C(112)-O(102)-C(113)	-58.1(2)
C(10)-C(5)-C(6)-C(7)	1.6(3)	C(114)-C(112)-O(102)-C(113)	-171.7(2)
C(4)-C(5)-C(6)-C(7)	-176.02(17)	C(115)-C(112)-O(102)-C(113)	66.6(2)
C(5)-C(6)-C(7)-C(8)	1.1(3)	C(112)-O(102)-C(113)-C(104)	57.3(2)

Table A6.4.6 cont'd.

Atoms (A-B-C-D)	Angle (°)	Atoms (A-B-C-D)	Angle (°)
C(105)-C(104)-C(113)-O(102)	-175.1(2)	C(106)-C(107)-C(108)-C(109)	1.5(3)
C(111)-C(104)-C(113)-O(102)	-52.9(2)	C(107)-C(108)-C(109)-C(110)	0.0(3)
C(103)-C(104)-C(113)-O(102)	66.0(2)	C(108)-C(109)-C(110)-C(105)	-2.0(3)
C(111)-C(104)-C(105)-C(106)	-24.9(2)	C(108)-C(109)-C(110)-N(101)	172.9(2)
C(113)-C(104)-C(105)-C(106)	93.6(2)	C(106)-C(105)-C(110)-C(109)	2.6(3)
C(103)-C(104)-C(105)-C(106)	-146.1(2)	C(104)-C(105)-C(110)-C(109)	-178.6(2)
C(111)-C(104)-C(105)-C(110)	156.3(2)	C(106)-C(105)-C(110)-N(101)	-172.1(2)
C(113)-C(104)-C(105)-C(110)	-85.2(2)	C(104)-C(105)-C(110)-N(101)	6.7(3)
C(103)-C(104)-C(105)-C(110)	35.2(2)	C(102)-N(101)-C(110)-C(109)	157.7(2)
C(110)-C(105)-C(106)-C(107)	-1.1(3)	C(101)-N(101)-C(110)-C(109)	88.9(2)
C(104)-C(105)-C(106)-C(107)	-179.9(2)	C(102)-N(101)-C(110)-C(105)	-27.5(3)
C(105)-C(106)-C(107)-C(108)	-0.9(3)	C(101)-N(101)-C(110)-C(105)	-96.3(2)

Symmetry transformations used to generate equivalent atoms:

A6.5 X-RAY CRYSTAL STRUCTURE ANALYSIS OF COMPOUND 158 (V24321)

Crystals suitable for X-ray diffraction were grown by adding one drop of EtOAc to 3 mg of aziridine **158**, heating the sealed vial to 80 °C, and allowing the solution to slowly cool to ambient temperature. Low-temperature diffraction data (ϕ-and ω-scans) were collected on a Bruker AXS D8 VENTURE KAPPA diffractometer coupled to a PHOTON II CPAD detector with Cu K_α radiation (λ = 1.54178 Å) from an IμS micro-source for the structure of compound V24321. The structure was solved by direct methods using SHELXS[i] and refined against F^2 on all data by full-matrix least squares with SHELXL-2019[ii] using established refinement techniques.[iii] All non-hydrogen atoms were refined anisotropically. All hydrogen atoms were included into the model at geometrically calculated positions and refined using a riding model. The isotropic displacement parameters of all hydrogen atoms were fixed to 1.2 times the U value of the atoms they are linked to (1.5 times for methyl groups). Compound **158** crystallizes in the triclinic space group P-1 with two molecules in the asymmetric unit.

Figure A6.5.1 *X-Ray Coordinate of Compound* ***158***

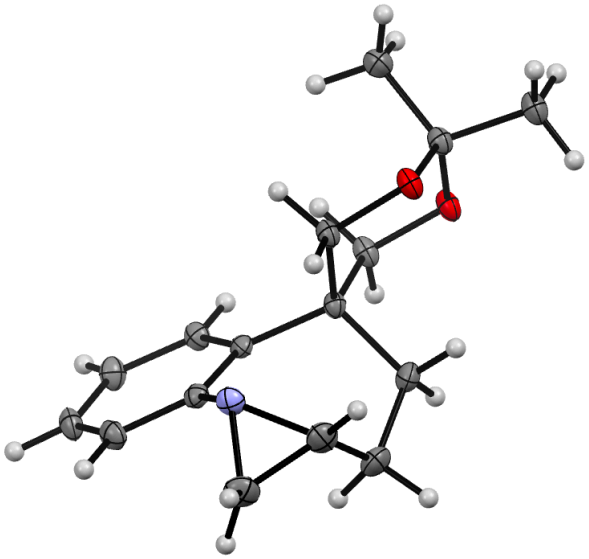


Table A6.5.1 *Crystal data and structure refinement for* ***158***.

Identification code	V24321	
Empirical formula	C16 H21 N O2	
Formula weight	259.34	
Temperature	100(2) K	
Wavelength	1.54178 Å	
Crystal system	Triclinic	
Space group	P-1	
Unit cell dimensions	a = 10.6789(11) Å	a= 108.035(7)°.
	b = 10.7870(6) Å	b= 91.204(8)°.
	c = 13.9886(9) Å	g = 116.063(5)°.
Volume	1352.9(2) $Å^3$	
Z	4	
Density (calculated)	1.273 Mg/m^3	
Absorption coefficient	0.660 mm^{-1}	
F(000)	560	
Crystal size	0.400 x 0.300 x 0.200 mm^3	
Theta range for data collection	3.380 to 74.431°.	
Index ranges	-13<=h<=13, -13<=k<=13, -17<=l<=17	
Reflections collected	35179	
Independent reflections	5526 [R(int) = 0.0351]	

Completeness to theta = 67.679°	99.9 %
Absorption correction	Semi-empirical from equivalents
Max. and min. transmission	0.7538 and 0.6350
Refinement method	Full-matrix least-squares on F^2
Data / restraints / parameters	5526 / 0 / 347
Goodness-of-fit on F^2	1.032
Final R indices [I>2sigma(I)]	R1 = 0.0388, wR2 = 0.0979
R indices (all data)	R1 = 0.0404, wR2 = 0.0986
Extinction coefficient	n/a
Largest diff. peak and hole	0.271 and -0.284 e.$Å^{-3}$

Table A6.5.2 *Atomic coordinates (x 10^4) and equivalent isotropic displacement parameters ($Å^2$x 10^3) for* ***158****. U(eq) is defined as one third of the trace of the orthogonalized U^{ij} tensor.*

Atom	x	y	z	U(eq)
C(1)	8302(1)	6335(1)	3227(1)	14(1)
C(2)	8076(1)	6694(1)	2384(1)	16(1)
C(3)	9104(1)	7893(1)	2187(1)	20(1)
C(4)	10392(1)	8788(1)	2853(1)	21(1)
C(5)	10657(1)	8455(1)	3691(1)	19(1)
C(6)	9640(1)	7233(1)	3879(1)	15(1)
N(1)	10039(1)	6863(1)	4684(1)	18(1)
C(7)	10569(1)	7997(1)	5718(1)	24(1)
C(8)	9142(1)	6685(1)	5469(1)	23(1)
C(9)	7810(1)	6814(1)	5330(1)	24(1)
C(10)	6667(1)	5468(1)	4463(1)	20(1)
C(11)	7143(1)	5013(1)	3424(1)	14(1)
C(12)	5821(1)	4198(1)	2573(1)	17(1)
O(1)	4800(1)	2881(1)	2702(1)	18(1)
C(13)	5320(1)	1855(1)	2636(1)	16(1)
O(2)	6567(1)	2518(1)	3390(1)	17(1)
C(15)	5587(1)	1248(1)	1563(1)	24(1)
C(16)	4203(1)	643(1)	2931(1)	21(1)

Table A6.5.2 cont'd.

Atom	x	y	z	U(eq)
C(14)	7669(1)	3868(1)	3349(1)	15(1)
C(21)	3192(1)	6256(1)	2477(1)	14(1)
C(22)	2950(1)	6783(1)	3467(1)	16(1)
C(23)	4047(1)	7853(1)	4278(1)	19(1)
C(24)	5423(1)	8452(1)	4107(1)	20(1)
C(25)	5700(1)	7976(1)	3132(1)	18(1)
C(26)	4606(1)	6877(1)	2322(1)	14(1)
N(2)	4987(1)	6332(1)	1368(1)	15(1)
C(27)	5799(1)	7419(1)	895(1)	18(1)
C(28)	4294(1)	6317(1)	437(1)	16(1)
C(29)	3123(1)	6739(1)	536(1)	17(1)
C(30)	1787(1)	5541(1)	703(1)	16(1)
C(31)	1971(1)	5042(1)	1606(1)	13(1)
C(32)	2201(1)	3661(1)	1253(1)	14(1)
O(3)	1028(1)	2432(1)	498(1)	15(1)
O(4)	-547(1)	3301(1)	1170(1)	16(1)
C(33)	-318(1)	2041(1)	810(1)	16(1)
C(35)	-1424(1)	1004(1)	-150(1)	22(1)
C(36)	-459(1)	1310(1)	1607(1)	22(1)
C(34)	551(1)	4516(1)	1979(1)	16(1)

Table A6.5.3 *Bond lengths [Å] and angles [°] for* ***158****.*

Bond	Length (Å)	Bond	Length (Å)
C(1)-C(2)	1.3978(15)	C(4)-C(5)	1.3858(16)
C(1)-C(6)	1.4121(15)	C(4)-H(4)	0.9500
C(1)-C(11)	1.5318(14)	C(5)-C(6)	1.3979(15)
C(2)-C(3)	1.3922(15)	C(5)-H(5)	0.9500
C(2)-H(2)	0.9500	C(6)-N(1)	1.4201(14)
C(3)-C(4)	1.3830(16)	N(1)-C(7)	1.4737(15)
C(3)-H(3)	0.9500	N(1)-C(8)	1.4743(15)

Table A6.5.3 cont'd.

Bond	Length (Å)	Bond	Length (Å)
C(7)-C(8)	1.4914(17)	C(23)-C(24)	1.3827(17)
C(7)-H(7A)	0.9900	C(23)-H(23)	0.9500
C(7)-H(7B)	0.9900	C(24)-C(25)	1.3879(16)
C(8)-C(9)	1.5032(18)	C(24)-H(24)	0.9500
C(8)-H(8)	1.0000	C(25)-C(26)	1.3968(15)
C(9)-C(10)	1.5364(16)	C(25)-H(25)	0.9500
C(9)-H(9A)	0.9900	C(26)-N(2)	1.4286(13)
C(9)-H(9B)	0.9900	N(2)-C(27)	1.4746(14)
C(10)-C(11)	1.5564(15)	N(2)-C(28)	1.4768(13)
C(10)-H(10A)	0.9900	C(27)-C(28)	1.4879(15)
C(10)-H(10B)	0.9900	C(27)-H(27A)	0.9900
C(11)-C(12)	1.5403(14)	C(27)-H(27B)	0.9900
C(11)-C(14)	1.5452(14)	C(28)-C(29)	1.5019(15)
C(12)-O(1)	1.4298(12)	C(28)-H(28)	1.0000
C(12)-H(12A)	0.9900	C(29)-C(30)	1.5308(15)
C(12)-H(12B)	0.9900	C(29)-H(29A)	0.9900
O(1)-C(13)	1.4212(13)	C(29)-H(29B)	0.9900
C(13)-O(2)	1.4262(13)	C(30)-C(31)	1.5577(14)
C(13)-C(16)	1.5122(14)	C(30)-H(30A)	0.9900
C(13)-C(15)	1.5290(16)	C(30)-H(30B)	0.9900
O(2)-C(14)	1.4338(12)	C(31)-C(34)	1.5341(14)
C(15)-H(15A)	0.9800	C(31)-C(32)	1.5473(14)
C(15)-H(15B)	0.9800	C(32)-O(3)	1.4346(12)
C(15)-H(15C)	0.9800	C(32)-H(32A)	0.9900
C(16)-H(16A)	0.9800	C(32)-H(32B)	0.9900
C(16)-H(16B)	0.9800	O(3)-C(33)	1.4290(13)
C(16)-H(16C)	0.9800	O(4)-C(33)	1.4262(13)
C(14)-H(14A)	0.9900	O(4)-C(34)	1.4321(12)
C(14)-H(14B)	0.9900	C(33)-C(35)	1.5139(15)
C(21)-C(22)	1.4010(15)	C(33)-C(36)	1.5277(15)
C(21)-C(26)	1.4110(15)	C(35)-H(35A)	0.9800
C(21)-C(31)	1.5308(14)	C(35)-H(35B)	0.9800
C(22)-C(23)	1.3914(15)	C(35)-H(35C)	0.9800
C(22)-H(22)	0.9500	C(36)-H(36A)	0.9800

Table A6.5.3 cont'd.

Bond	Length (Å)	Bond	Angle (°)
C(36)-H(36B)	0.9800	N(1)-C(8)-C(9)	117.73(10)
C(36)-H(36C)	0.9800	C(7)-C(8)-C(9)	121.15(11)
C(34)-H(34A)	0.9900	N(1)-C(8)-H(8)	115.6
C(34)-H(34B)	0.9900	C(7)-C(8)-H(8)	115.6
		C(9)-C(8)-H(8)	115.6
Bond	**Angle (°)**	C(8)-C(9)-C(10)	111.90(10)
C(2)-C(1)-C(6)	117.15(9)	C(8)-C(9)-H(9A)	109.2
C(2)-C(1)-C(11)	120.99(9)	C(10)-C(9)-H(9A)	109.2
C(6)-C(1)-C(11)	121.86(9)	C(8)-C(9)-H(9B)	109.2
C(3)-C(2)-C(1)	122.41(10)	C(10)-C(9)-H(9B)	109.2
C(3)-C(2)-H(2)	118.8	H(9A)-C(9)-H(9B)	107.9
C(1)-C(2)-H(2)	118.8	C(9)-C(10)-C(11)	116.16(9)
C(4)-C(3)-C(2)	119.56(10)	C(9)-C(10)-H(10A)	108.2
C(4)-C(3)-H(3)	120.2	C(11)-C(10)-H(10A)	108.2
C(2)-C(3)-H(3)	120.2	C(9)-C(10)-H(10B)	108.2
C(3)-C(4)-C(5)	119.55(10)	C(11)-C(10)-H(10B)	108.2
C(3)-C(4)-H(4)	120.2	H(10A)-C(10)-H(10B)	107.4
C(5)-C(4)-H(4)	120.2	C(1)-C(11)-C(12)	110.81(8)
C(4)-C(5)-C(6)	121.08(10)	C(1)-C(11)-C(14)	109.00(8)
C(4)-C(5)-H(5)	119.5	C(12)-C(11)-C(14)	104.72(8)
C(6)-C(5)-H(5)	119.5	C(1)-C(11)-C(10)	112.68(9)
C(5)-C(6)-C(1)	120.19(10)	C(12)-C(11)-C(10)	107.73(9)
C(5)-C(6)-N(1)	117.97(9)	C(14)-C(11)-C(10)	111.62(9)
C(1)-C(6)-N(1)	121.63(9)	O(1)-C(12)-C(11)	110.60(8)
C(6)-N(1)-C(7)	117.86(9)	O(1)-C(12)-H(12A)	109.5
C(6)-N(1)-C(8)	118.17(9)	C(11)-C(12)-H(12A)	109.5
C(7)-N(1)-C(8)	60.78(8)	O(1)-C(12)-H(12B)	109.5
N(1)-C(7)-C(8)	59.63(7)	C(11)-C(12)-H(12B)	109.5
N(1)-C(7)-H(7A)	117.8	H(12A)-C(12)-H(12B)	108.1
C(8)-C(7)-H(7A)	117.8	C(13)-O(1)-C(12)	112.70(8)
N(1)-C(7)-H(7B)	117.8	O(1)-C(13)-O(2)	110.09(8)
C(8)-C(7)-H(7B)	117.8	O(1)-C(13)-C(16)	105.76(9)
H(7A)-C(7)-H(7B)	114.9	O(2)-C(13)-C(16)	106.11(9)
N(1)-C(8)-C(7)	59.59(7)	O(1)-C(13)-C(15)	111.72(9)

Table A6.5.3 cont'd.

Bond	Angle (°)	Bond	Angle (°)
O(2)-C(13)-C(15)	111.38(9)	C(24)-C(25)-H(25)	119.6
C(16)-C(13)-C(15)	111.49(9)	C(26)-C(25)-H(25)	119.6
C(13)-O(2)-C(14)	114.27(8)	C(25)-C(26)-C(21)	120.38(10)
C(13)-C(15)-H(15A)	109.5	C(25)-C(26)-N(2)	117.60(9)
C(13)-C(15)-H(15B)	109.5	C(21)-C(26)-N(2)	121.82(9)
H(15A)-C(15)-H(15B)	109.5	C(26)-N(2)-C(27)	116.96(9)
C(13)-C(15)-H(15C)	109.5	C(26)-N(2)-C(28)	118.43(8)
H(15A)-C(15)-H(15C)	109.5	C(27)-N(2)-C(28)	60.55(7)
H(15B)-C(15)-H(15C)	109.5	N(2)-C(27)-C(28)	59.80(7)
C(13)-C(16)-H(16A)	109.5	N(2)-C(27)-H(27A)	117.8
C(13)-C(16)-H(16B)	109.5	C(28)-C(27)-H(27A)	117.8
H(16A)-C(16)-H(16B)	109.5	N(2)-C(27)-H(27B)	117.8
C(13)-C(16)-H(16C)	109.5	C(28)-C(27)-H(27B)	117.8
H(16A)-C(16)-H(16C)	109.5	H(27A)-C(27)-H(27B)	114.9
H(16B)-C(16)-H(16C)	109.5	N(2)-C(28)-C(27)	59.65(7)
O(2)-C(14)-C(11)	111.83(8)	N(2)-C(28)-C(29)	117.64(9)
O(2)-C(14)-H(14A)	109.3	C(27)-C(28)-C(29)	121.78(9)
C(11)-C(14)-H(14A)	109.3	N(2)-C(28)-H(28)	115.4
O(2)-C(14)-H(14B)	109.3	C(27)-C(28)-H(28)	115.4
C(11)-C(14)-H(14B)	109.3	C(29)-C(28)-H(28)	115.4
H(14A)-C(14)-H(14B)	107.9	C(28)-C(29)-C(30)	111.35(9)
C(22)-C(21)-C(26)	117.23(10)	C(28)-C(29)-H(29A)	109.4
C(22)-C(21)-C(31)	121.19(9)	C(30)-C(29)-H(29A)	109.4
C(26)-C(21)-C(31)	121.57(9)	C(28)-C(29)-H(29B)	109.4
C(23)-C(22)-C(21)	122.25(10)	C(30)-C(29)-H(29B)	109.4
C(23)-C(22)-H(22)	118.9	H(29A)-C(29)-H(29B)	108.0
C(21)-C(22)-H(22)	118.9	C(29)-C(30)-C(31)	116.55(8)
C(24)-C(23)-C(22)	119.50(10)	C(29)-C(30)-H(30A)	108.2
C(24)-C(23)-H(23)	120.2	C(31)-C(30)-H(30A)	108.2
C(22)-C(23)-H(23)	120.2	C(29)-C(30)-H(30B)	108.2
C(23)-C(24)-C(25)	119.86(10)	C(31)-C(30)-H(30B)	108.2
C(23)-C(24)-H(24)	120.1	H(30A)-C(30)-H(30B)	107.3
C(25)-C(24)-H(24)	120.1	C(21)-C(31)-C(34)	111.45(8)
C(24)-C(25)-C(26)	120.74(10)	C(21)-C(31)-C(32)	108.48(8)

Table A6.5.3 cont'd.

Bond	Angle (°)	Bond	Angle (°)
C(34)-C(31)-C(32)	104.13(8)	C(33)-C(35)-H(35A)	109.5
C(21)-C(31)-C(30)	113.17(8)	C(33)-C(35)-H(35B)	109.5
C(34)-C(31)-C(30)	107.11(8)	H(35A)-C(35)-H(35B)	109.5
C(32)-C(31)-C(30)	112.15(8)	C(33)-C(35)-H(35C)	109.5
O(3)-C(32)-C(31)	111.55(8)	H(35A)-C(35)-H(35C)	109.5
O(3)-C(32)-H(32A)	109.3	H(35B)-C(35)-H(35C)	109.5
C(31)-C(32)-H(32A)	109.3	C(33)-C(36)-H(36A)	109.5
O(3)-C(32)-H(32B)	109.3	C(33)-C(36)-H(36B)	109.5
C(31)-C(32)-H(32B)	109.3	H(36A)-C(36)-H(36B)	109.5
H(32A)-C(32)-H(32B)	108.0	C(33)-C(36)-H(36C)	109.5
C(33)-O(3)-C(32)	114.49(8)	H(36A)-C(36)-H(36C)	109.5
C(33)-O(4)-C(34)	113.58(8)	H(36B)-C(36)-H(36C)	109.5
O(4)-C(33)-O(3)	110.39(8)	O(4)-C(34)-C(31)	110.11(8)
O(4)-C(33)-C(35)	105.46(9)	O(4)-C(34)-H(34A)	109.6
O(3)-C(33)-C(35)	106.25(9)	C(31)-C(34)-H(34A)	109.6
O(4)-C(33)-C(36)	111.74(9)	O(4)-C(34)-H(34B)	109.6
O(3)-C(33)-C(36)	111.44(9)	C(31)-C(34)-H(34B)	109.6
C(35)-C(33)-C(36)	111.26(9)	H(34A)-C(34)-H(34B)	108.2

Symmetry transformations used to generate equivalent atoms:

Table A6.5.4 *Anisotropic displacement parameters ($Å^2 x\ 10^3$) for* ***158****. The anisotropic displacement factor exponent takes the form: $-2p^2[\ h^2\ a^{*2}U^{11} + \ldots + 2\ h\ k\ a^*\ b^*\ U^{12}\ ]$*

Atom	U^{11}	U^{22}	U^{33}	U^{23}	U^{13}	U^{12}
C(1)	12(1)	14(1)	16(1)	5(1)	5(1)	7(1)
C(2)	13(1)	17(1)	18(1)	6(1)	2(1)	7(1)
C(3)	19(1)	23(1)	22(1)	13(1)	5(1)	10(1)
C(4)	15(1)	19(1)	28(1)	12(1)	7(1)	6(1)
C(5)	12(1)	18(1)	23(1)	6(1)	1(1)	5(1)
C(6)	14(1)	16(1)	15(1)	5(1)	4(1)	9(1)
N(1)	16(1)	19(1)	16(1)	5(1)	-1(1)	7(1)

Table A6.5.4 cont'd.

Atom	U^{11}	U^{22}	U^{33}	U^{23}	U^{13}	U^{12}
C(7)	26(1)	25(1)	16(1)	4(1)	-3(1)	10(1)
C(8)	27(1)	25(1)	14(1)	7(1)	2(1)	10(1)
C(9)	26(1)	26(1)	17(1)	6(1)	9(1)	12(1)
C(10)	18(1)	21(1)	21(1)	9(1)	9(1)	9(1)
C(11)	11(1)	15(1)	16(1)	6(1)	3(1)	6(1)
C(12)	13(1)	16(1)	22(1)	10(1)	2(1)	5(1)
O(1)	11(1)	17(1)	27(1)	10(1)	3(1)	5(1)
C(13)	13(1)	16(1)	20(1)	7(1)	2(1)	6(1)
O(2)	13(1)	16(1)	22(1)	10(1)	1(1)	4(1)
C(15)	21(1)	19(1)	23(1)	4(1)	5(1)	5(1)
C(16)	16(1)	19(1)	26(1)	11(1)	4(1)	5(1)
C(14)	11(1)	14(1)	20(1)	7(1)	3(1)	5(1)
C(21)	15(1)	14(1)	13(1)	5(1)	1(1)	7(1)
C(22)	17(1)	17(1)	16(1)	6(1)	4(1)	9(1)
C(23)	24(1)	20(1)	13(1)	3(1)	2(1)	11(1)
C(24)	19(1)	18(1)	16(1)	0(1)	-3(1)	7(1)
C(25)	14(1)	18(1)	20(1)	5(1)	1(1)	8(1)
C(26)	16(1)	14(1)	14(1)	5(1)	2(1)	9(1)
N(2)	12(1)	16(1)	14(1)	5(1)	2(1)	6(1)
C(27)	17(1)	19(1)	20(1)	8(1)	6(1)	8(1)
C(28)	18(1)	18(1)	14(1)	7(1)	4(1)	9(1)
C(29)	18(1)	19(1)	16(1)	8(1)	3(1)	10(1)
C(30)	15(1)	18(1)	15(1)	6(1)	0(1)	8(1)
C(31)	12(1)	14(1)	13(1)	4(1)	2(1)	6(1)
C(32)	12(1)	14(1)	15(1)	4(1)	2(1)	6(1)
O(3)	13(1)	14(1)	15(1)	2(1)	2(1)	5(1)
O(4)	12(1)	15(1)	18(1)	2(1)	1(1)	5(1)
C(33)	14(1)	15(1)	18(1)	5(1)	4(1)	6(1)
C(35)	16(1)	19(1)	22(1)	1(1)	1(1)	6(1)
C(36)	22(1)	20(1)	25(1)	11(1)	7(1)	7(1)
C(34)	14(1)	15(1)	14(1)	2(1)	2(1)	6(1)

Table A6.5.5 *Hydrogen coordinates (x 10^4) and isotropic displacement parameters (Å^{2}x 10^3)for* ***158****.*

Atom	x	y	z	U(eq)
H(2)	7190	6099	1928	20
H(3)	8922	8095	1599	24
H(4)	11089	9625	2736	25
H(5)	11544	9066	4145	23
H(7A)	10611	8962	5808	29
H(7B)	11336	8044	6162	29
H(8)	9070	5921	5758	27
H(9A)	8037	7717	5176	28
H(9B)	7437	6912	5976	28
H(10A)	5871	5673	4345	24
H(10B)	6298	4615	4696	24
H(12A)	5394	4853	2592	20
H(12B)	6101	3943	1898	20
H(15A)	4757	927	1056	35
H(15B)	5754	406	1505	35
H(15C)	6420	2021	1440	35
H(16A)	3975	1080	3585	31
H(16B)	4564	-24	2999	31
H(16C)	3346	89	2402	31
H(14A)	8022	3657	2700	18
H(14B)	8470	4286	3920	18
H(22)	2005	6397	3588	20
H(23)	3851	8169	4944	23
H(24)	6178	9186	4655	24
H(25)	6645	8404	3015	21
H(27A)	6541	7287	530	22
H(27B)	6016	8459	1252	22
H(28)	4144	5493	-207	19
H(29A)	2898	6898	-93	20
H(29B)	3446	7678	1119	20
H(30A)	1390	4663	66	19

Table A6.5.5 cont'd.

Atom	x	y	z	U(eq)
H(30B)	1077	5904	816	19
H(32A)	3080	3894	964	17
H(32B)	2321	3391	1851	17
H(35A)	-1284	1486	-657	32
H(35B)	-2372	755	16	32
H(35C)	-1333	101	-429	32
H(36A)	-448	368	1299	33
H(36B)	-1355	1136	1850	33
H(36C)	334	1959	2185	33
H(34A)	631	4209	2565	19
H(34B)	311	5337	2213	19

Table A6.5.6 *Torsion angles [°] for* ***158****.*

Atoms	Angle (°)	Atoms	Angle (°)
C(6)-C(1)-C(2)-C(3)	-0.88(16)	C(6)-N(1)-C(8)-C(7)	-107.93(11)
C(11)-C(1)-C(2)-C(3)	179.59(10)	C(6)-N(1)-C(8)-C(9)	3.73(15)
C(1)-C(2)-C(3)-C(4)	-1.20(17)	C(7)-N(1)-C(8)-C(9)	111.66(12)
C(2)-C(3)-C(4)-C(5)	1.85(17)	N(1)-C(7)-C(8)-C(9)	-106.00(12)
C(3)-C(4)-C(5)-C(6)	-0.43(17)	N(1)-C(8)-C(9)-C(10)	72.31(13)
C(4)-C(5)-C(6)-C(1)	-1.70(16)	C(7)-C(8)-C(9)-C(10)	141.79(11)
C(4)-C(5)-C(6)-N(1)	173.12(10)	C(8)-C(9)-C(10)-C(11)	-50.49(13)
C(2)-C(1)-C(6)-C(5)	2.30(15)	C(2)-C(1)-C(11)-C(12)	1.78(13)
C(11)-C(1)-C(6)-C(5)	-178.18(9)	C(6)-C(1)-C(11)-C(12)	-177.72(9)
C(2)-C(1)-C(6)-N(1)	-172.33(9)	C(2)-C(1)-C(11)-C(14)	116.51(10)
C(11)-C(1)-C(6)-N(1)	7.20(15)	C(6)-C(1)-C(11)-C(14)	-62.99(12)
C(5)-C(6)-N(1)-C(7)	57.43(14)	C(2)-C(1)-C(11)-C(10)	-119.00(11)
C(1)-C(6)-N(1)-C(7)	-127.83(11)	C(6)-C(1)-C(11)-C(10)	61.49(13)
C(5)-C(6)-N(1)-C(8)	127.36(11)	C(9)-C(10)-C(11)-C(1)	-31.75(13)
C(1)-C(6)-N(1)-C(8)	-57.91(14)	C(9)-C(10)-C(11)-C(12)	-154.27(10)
C(6)-N(1)-C(7)-C(8)	108.43(11)	C(9)-C(10)-C(11)-C(14)	91.29(11)

TableA6.5.6 cont'd.

Atoms	Angle (°)	Atoms	Angle (°)
C(1)-C(11)-C(12)-O(1)	174.06(8)	C(26)-N(2)-C(28)-C(27)	106.64(10)
C(14)-C(11)-C(12)-O(1)	56.68(11)	C(26)-N(2)-C(28)-C(29)	-5.84(14)
C(10)-C(11)-C(12)-O(1)	-62.26(11)	C(27)-N(2)-C(28)-C(29)	-112.48(11)
C(11)-C(12)-O(1)-C(13)	-61.88(11)	N(2)-C(27)-C(28)-C(29)	105.64(11)
C(12)-O(1)-C(13)-O(2)	58.19(11)	N(2)-C(28)-C(29)-C(30)	-71.41(12)
C(12)-O(1)-C(13)-C(16)	172.40(9)	C(27)-C(28)-C(29)-C(30)	-141.14(10)
C(12)-O(1)-C(13)-C(15)	-66.12(11)	C(28)-C(29)-C(30)-C(31)	53.71(12)
O(1)-C(13)-O(2)-C(14)	-55.08(11)	C(22)-C(21)-C(31)-C(34)	-1.30(13)
C(16)-C(13)-O(2)-C(14)	-169.07(8)	C(26)-C(21)-C(31)-C(34)	178.00(9)
C(15)-C(13)-O(2)-C(14)	69.42(11)	C(22)-C(21)-C(31)-C(32)	-115.37(10)
C(13)-O(2)-C(14)-C(11)	55.50(11)	C(26)-C(21)-C(31)-C(32)	63.92(12)
C(1)-C(11)-C(14)-O(2)	-172.21(8)	C(22)-C(21)-C(31)-C(30)	119.50(10)
C(12)-C(11)-C(14)-O(2)	-53.60(11)	C(26)-C(21)-C(31)-C(30)	-61.21(12)
C(10)-C(11)-C(14)-O(2)	62.68(11)	C(29)-C(30)-C(31)-C(21)	28.45(12)
C(26)-C(21)-C(22)-C(23)	-1.32(16)	C(29)-C(30)-C(31)-C(34)	151.68(9)
C(31)-C(21)-C(22)-C(23)	178.01(10)	C(29)-C(30)-C(31)-C(32)	-94.67(11)
C(21)-C(22)-C(23)-C(24)	1.64(17)	C(21)-C(31)-C(32)-O(3)	174.79(8)
C(22)-C(23)-C(24)-C(25)	-0.36(17)	C(34)-C(31)-C(32)-O(3)	55.99(10)
C(23)-C(24)-C(25)-C(26)	-1.20(17)	C(30)-C(31)-C(32)-O(3)	-59.48(11)
C(24)-C(25)-C(26)-C(21)	1.51(16)	C(31)-C(32)-O(3)-C(33)	-55.82(11)
C(24)-C(25)-C(26)-N(2)	-173.41(10)	C(34)-O(4)-C(33)-O(3)	-55.68(11)
C(22)-C(21)-C(26)-C(25)	-0.26(15)	C(34)-O(4)-C(33)-C(35)	-170.05(8)
C(31)-C(21)-C(26)-C(25)	-179.58(9)	C(34)-O(4)-C(33)-C(36)	68.94(11)
C(22)-C(21)-C(26)-N(2)	174.44(9)	C(32)-O(3)-C(33)-O(4)	52.70(11)
C(31)-C(21)-C(26)-N(2)	-4.88(15)	C(32)-O(3)-C(33)-C(35)	166.56(8)
C(25)-C(26)-N(2)-C(27)	-58.12(13)	C(32)-O(3)-C(33)-C(36)	-72.09(11)
C(21)-C(26)-N(2)-C(27)	127.05(10)	C(33)-O(4)-C(34)-C(31)	61.61(11)
C(25)-C(26)-N(2)-C(28)	-127.51(10)	C(21)-C(31)-C(34)-O(4)	-175.21(8)
C(21)-C(26)-N(2)-C(28)	57.65(13)	C(32)-C(31)-C(34)-O(4)	-58.46(10)
C(26)-N(2)-C(27)-C(28)	-109.04(10)	C(30)-C(31)-C(34)-O(4)	60.51(10)

Symmetry transformations used to generate equivalent atoms:

A6.6 X-RAY CRYSTAL STRUCTURE ANALYSIS OF COMPOUND 160 (V25163)

Crystals suitable for X-ray analysis were grown by dissolving **160** in minimal hot Et_2O, followed by addition of hexanes, and allowing to stand at –20 °C. Low-temperature diffraction data (ϕ-and ω-scans) were collected on a Bruker AXS D8 VENTURE KAPPA diffractometer coupled to a PHOTON II CPAD detector with Cu K_α radiation (λ = 1.54178 Å) from an IμS micro-source for the structure of compound **160**. The structure was solved by direct methods using SHELXS[iv] and refined against F^2 on all data by full-matrix least squares with SHELXL-2019[v] using established refinement techniques.[vi] All non-hydrogen atoms were refined anisotropically. Unless otherwise noted, all hydrogen atoms were included into the model at geometrically calculated positions and refined using a riding model. The isotropic displacement parameters of all hydrogen atoms were fixed to 1.2 times the *U* value of the atoms they are linked to (1.5 times for methyl groups). Compound **160** crystallizes in the orthorhombic space group $Pna2_1$ with one molecule in the asymmetric unit. The coordinates for the hydrogen atoms bound to N1were located in the difference Fourier synthesis and refined semi-freely with the help of a restraint on the N-H distance (0.91(4) Å).

Figure A6.6.1 *X-Ray Coordinate of Compound* ***160***

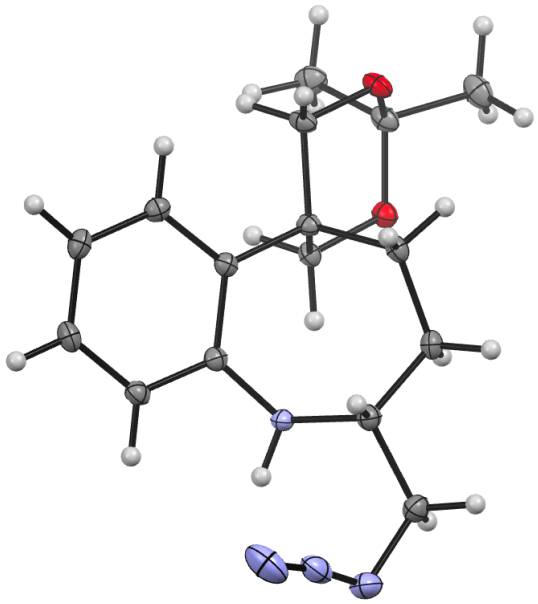


Table A6.6.1 *Crystal data and structure refinement for* ***160***.

Identification code	V25163	
Empirical formula	C16 H22 N4 O2	
Formula weight	302.37	
Temperature	100(2) K	
Wavelength	1.54178 Å	
Crystal system	Orthorhombic	
Space group	$Pna2_1$	
Unit cell dimensions	a = 27.317(4) Å	a= 90°.
	b = 8.2030(11) Å	b= 90°.
	c = 6.9111(10) Å	g = 90°.
Volume	1548.6(4) $Å^3$	
Z	4	
Density (calculated)	1.297 Mg/m^3	
Absorption coefficient	0.711 mm^{-1}	
F(000)	648	
Crystal size	0.400 x 0.200 x 0.150 mm^3	
Theta range for data collection	3.236 to 74.479°.	
Index ranges	-33<=h<=34, -10<=k<=10, -8<=l<=8	
Reflections collected	23964	

Independent reflections	3107 [R(int) = 0.0478]
Completeness to theta = 67.679°	100.0 %
Absorption correction	Semi-empirical from equivalents
Max. and min. transmission	0.7538 and 0.5911
Refinement method	Full-matrix least-squares on F^2
Data / restraints / parameters	3107 / 2 / 204
Goodness-of-fit on F^2	1.061
Final R indices [I>2sigma(I)]	R1 = 0.0288, wR2 = 0.0728
R indices (all data)	R1 = 0.0291, wR2 = 0.0731
Absolute structure parameter	0.04(6)
Extinction coefficient	n/a
Largest diff. peak and hole	0.186 and -0.232 e.$Å^{-3}$

Table A6.6.2 *Atomic coordinates (x 10^4) and equivalent isotropic displacement parameters ($Å^2$x 10^3) for* ***160****. U(eq) is defined as one third of the trace of the orthogonalized U^{ij} tensor.*

Atom	x	y	z	U(eq)
N(1)	6267(1)	6687(2)	4601(2)	14(1)
C(1)	6169(1)	6146(2)	2603(2)	15(1)
C(11)	6386(1)	7364(2)	1177(3)	19(1)
N(2)	6182(1)	9037(2)	1284(2)	25(1)
N(3)	5754(1)	9168(2)	1809(2)	25(1)
N(4)	5367(1)	9474(2)	2313(3)	39(1)
C(2)	6390(1)	4464(2)	2210(2)	16(1)
C(3)	6171(1)	3087(2)	3409(2)	15(1)
C(4)	6238(1)	3192(2)	5620(2)	12(1)
C(12)	6772(1)	3559(2)	6204(2)	13(1)
O(1)	7095(1)	2348(1)	5433(2)	16(1)
C(13)	6989(1)	732(2)	6065(3)	16(1)
O(2)	6486(1)	331(1)	5699(2)	17(1)
C(15)	7284(1)	-372(2)	4749(3)	23(1)
C(16)	7120(1)	488(2)	8190(3)	21(1)
C(14)	6140(1)	1482(2)	6453(3)	15(1)

Table A6.6.2 cont'd.

Atom	x	y	z	U(eq)
C(5)	5900(1)	4463(2)	6536(2)	12(1)
C(6)	5552(1)	4023(2)	7926(2)	14(1)
C(7)	5252(1)	5161(2)	8833(2)	16(1)
C(8)	5293(1)	6795(2)	8349(3)	16(1)
C(9)	5627(1)	7263(2)	6939(2)	15(1)
C(10)	5932(1)	6131(2)	6025(2)	13(1)

Table A6.6.3 *Bond lengths [Å] and angles [°] for* ***160****.*

Bond	Length (Å)	Bond	Length (Å)
N(1)-C(10)	1.419(2)	C(12)-H(12A)	0.9900
N(1)-C(1)	1.475(2)	C(12)-H(12B)	0.9900
N(1)-H(1N)	0.895(18)	O(1)-C(13)	1.4247(19)
C(1)-C(11)	1.524(2)	C(13)-O(2)	1.4356(18)
C(1)-C(2)	1.530(2)	C(13)-C(15)	1.515(2)
C(1)-H(1)	1.0000	C(13)-C(16)	1.525(2)
C(11)-N(2)	1.484(2)	O(2)-C(14)	1.4335(18)
C(11)-H(11A)	0.9900	C(15)-H(15A)	0.9800
C(11)-H(11B)	0.9900	C(15)-H(15B)	0.9800
N(2)-N(3)	1.231(2)	C(15)-H(15C)	0.9800
N(3)-N(4)	1.141(3)	C(16)-H(16A)	0.9800
C(2)-C(3)	1.523(2)	C(16)-H(16B)	0.9800
C(2)-H(2A)	0.9900	C(16)-H(16C)	0.9800
C(2)-H(2B)	0.9900	C(14)-H(14A)	0.9900
C(3)-C(4)	1.541(2)	C(14)-H(14B)	0.9900
C(3)-H(3A)	0.9900	C(5)-C(6)	1.400(2)
C(3)-H(3B)	0.9900	C(5)-C(10)	1.416(2)
C(4)-C(5)	1.528(2)	C(6)-C(7)	1.391(2)
C(4)-C(14)	1.540(2)	C(6)-H(6)	0.9500
C(4)-C(12)	1.5432(19)	C(7)-C(8)	1.386(2)
C(12)-O(1)	1.4312(18)	C(7)-H(7)	0.9500

Table A6.6.3 cont'd.

Bond	Length (Å)	Atoms	Angle (°)
C(8)-C(9)	1.390(2)	H(3A)-C(3)-H(3B)	107.3
C(8)-H(8)	0.9500	C(5)-C(4)-C(14)	111.23(13)
C(9)-C(10)	1.397(2)	C(5)-C(4)-C(3)	112.17(12)
C(9)-H(9)	0.9500	C(14)-C(4)-C(3)	107.38(13)
		C(5)-C(4)-C(12)	109.22(12)
Atoms	**Angle (°)**	C(14)-C(4)-C(12)	104.08(12)
C(10)-N(1)-C(1)	115.81(12)	C(3)-C(4)-C(12)	112.46(13)
C(10)-N(1)-H(1N)	110.6(14)	O(1)-C(12)-C(4)	110.47(12)
C(1)-N(1)-H(1N)	109.4(15)	O(1)-C(12)-H(12A)	109.6
N(1)-C(1)-C(11)	109.72(12)	C(4)-C(12)-H(12A)	109.6
N(1)-C(1)-C(2)	111.52(13)	O(1)-C(12)-H(12B)	109.6
C(11)-C(1)-C(2)	108.82(14)	C(4)-C(12)-H(12B)	109.6
N(1)-C(1)-H(1)	108.9	H(12A)-C(12)-H(12B)	108.1
C(11)-C(1)-H(1)	108.9	C(13)-O(1)-C(12)	114.03(12)
C(2)-C(1)-H(1)	108.9	O(1)-C(13)-O(2)	110.64(12)
N(2)-C(11)-C(1)	115.35(14)	O(1)-C(13)-C(15)	105.36(13)
N(2)-C(11)-H(11A)	108.4	O(2)-C(13)-C(15)	105.38(13)
C(1)-C(11)-H(11A)	108.4	O(1)-C(13)-C(16)	111.71(13)
N(2)-C(11)-H(11B)	108.4	O(2)-C(13)-C(16)	111.37(13)
C(1)-C(11)-H(11B)	108.4	C(15)-C(13)-C(16)	112.04(14)
H(11A)-C(11)-H(11B)	107.5	C(14)-O(2)-C(13)	114.59(11)
N(3)-N(2)-C(11)	116.95(14)	C(13)-C(15)-H(15A)	109.5
N(4)-N(3)-N(2)	172.23(17)	C(13)-C(15)-H(15B)	109.5
C(3)-C(2)-C(1)	114.68(13)	H(15A)-C(15)-H(15B)	109.5
C(3)-C(2)-H(2A)	108.6	C(13)-C(15)-H(15C)	109.5
C(1)-C(2)-H(2A)	108.6	H(15A)-C(15)-H(15C)	109.5
C(3)-C(2)-H(2B)	108.6	H(15B)-C(15)-H(15C)	109.5
C(1)-C(2)-H(2B)	108.6	C(13)-C(16)-H(16A)	109.5
H(2A)-C(2)-H(2B)	107.6	C(13)-C(16)-H(16B)	109.5
C(2)-C(3)-C(4)	116.84(13)	H(16A)-C(16)-H(16B)	109.5
C(2)-C(3)-H(3A)	108.1	C(13)-C(16)-H(16C)	109.5
C(4)-C(3)-H(3A)	108.1	H(16A)-C(16)-H(16C)	109.5
C(2)-C(3)-H(3B)	108.1	H(16B)-C(16)-H(16C)	109.5
C(4)-C(3)-H(3B)	108.1	O(2)-C(14)-C(4)	110.50(13)

Table A6.6.3 cont'd.

Atoms	Angle (°)	Atoms	Angle (°)
O(2)-C(14)-H(14A)	109.6	C(8)-C(7)-H(7)	120.3
C(4)-C(14)-H(14A)	109.6	C(6)-C(7)-H(7)	120.3
O(2)-C(14)-H(14B)	109.6	C(7)-C(8)-C(9)	119.30(14)
C(4)-C(14)-H(14B)	109.6	C(7)-C(8)-H(8)	120.3
H(14A)-C(14)-H(14B)	108.1	C(9)-C(8)-H(8)	120.3
C(6)-C(5)-C(10)	117.44(14)	C(8)-C(9)-C(10)	121.63(14)
C(6)-C(5)-C(4)	121.27(13)	C(8)-C(9)-H(9)	119.2
C(10)-C(5)-C(4)	121.30(13)	C(10)-C(9)-H(9)	119.2
C(7)-C(6)-C(5)	122.49(14)	C(9)-C(10)-C(5)	119.61(14)
C(7)-C(6)-H(6)	118.8	C(9)-C(10)-N(1)	118.89(13)
C(5)-C(6)-H(6)	118.8	C(5)-C(10)-N(1)	121.50(14)
C(8)-C(7)-C(6)	119.49(14)		

Symmetry transformations used to generate equivalent atoms:

Table A6.6.4 *Anisotropic displacement parameters ($Å^2 x\ 10^3$) for* ***160****. The anisotropic displacement factor exponent takes the form: $-2p^2[\ h^2\ a^{*2}U^{11} + \ldots + 2\ h\ k\ a^*\ b^*\ U^{12}\ ]$*

Atom	U^{11}	U^{22}	U^{33}	U^{23}	U^{13}	U^{12}
N(1)	18(1)	11(1)	12(1)	0(1)	0(1)	-3(1)
C(1)	17(1)	15(1)	13(1)	0(1)	-1(1)	-1(1)
C(11)	24(1)	18(1)	15(1)	2(1)	0(1)	-2(1)
N(2)	36(1)	18(1)	23(1)	4(1)	2(1)	-4(1)
N(3)	38(1)	15(1)	22(1)	-2(1)	-6(1)	1(1)
N(4)	40(1)	24(1)	52(1)	-9(1)	-2(1)	7(1)
C(2)	17(1)	18(1)	12(1)	-3(1)	1(1)	1(1)
C(3)	15(1)	15(1)	16(1)	-4(1)	-1(1)	0(1)
C(4)	11(1)	11(1)	15(1)	0(1)	1(1)	-1(1)
C(12)	13(1)	13(1)	13(1)	-2(1)	-1(1)	0(1)
O(1)	13(1)	15(1)	19(1)	-1(1)	2(1)	1(1)
C(13)	14(1)	14(1)	22(1)	-2(1)	-1(1)	1(1)

Table A6.6.4 cont'd.

Atom	U^{11}	U^{22}	U^{33}	U^{23}	U^{13}	U^{12}
O(2)	13(1)	12(1)	25(1)	-3(1)	0(1)	1(1)
C(15)	18(1)	22(1)	28(1)	-6(1)	1(1)	4(1)
C(16)	20(1)	19(1)	24(1)	3(1)	-1(1)	3(1)
C(14)	13(1)	11(1)	22(1)	-1(1)	2(1)	1(1)
C(5)	12(1)	12(1)	12(1)	0(1)	-2(1)	0(1)
C(6)	14(1)	15(1)	14(1)	1(1)	-1(1)	0(1)
C(7)	14(1)	22(1)	13(1)	0(1)	1(1)	-1(1)
C(8)	15(1)	17(1)	16(1)	-5(1)	0(1)	2(1)
C(9)	18(1)	13(1)	15(1)	-2(1)	-2(1)	-1(1)
C(10)	14(1)	14(1)	12(1)	-1(1)	-2(1)	-2(1)

Table A6.6.5 *Hydrogen coordinates (x 10^4) and isotropic displacement parameters ($Å^2$x 10^3) for* ***160****.*

Atom	x	y	z	U(eq)
H(1N)	6290(8)	7780(20)	4630(30)	17
H(1)	5807	6090	2400	18
H(11A)	6744	7424	1401	23
H(11B)	6336	6943	-151	23
H(2A)	6345	4203	822	19
H(2B)	6746	4514	2464	19
H(3A)	6317	2048	2962	18
H(3B)	5816	3035	3132	18
H(12A)	6868	4646	5711	16
H(12B)	6799	3576	7633	16
H(15A)	7188	-180	3401	34
H(15B)	7220	-1512	5088	34
H(15C)	7633	-138	4906	34
H(16A)	7458	848	8414	32

Table A6.6.5 cont'd

Atom	x	y	z	U(eq)
H(16B)	7090	-669	8523	32
H(16C)	6897	1129	8999	32
H(14A)	6166	1516	7881	18
H(14B)	5804	1133	6112	18
H(6)	5518	2906	8262	17
H(7)	5021	4821	9777	20
H(8)	5094	7587	8974	20
H(9)	5650	8380	6588	18

Table A6.6.6 *Torsion angles [°] for* ***160****.*

Atoms (A-B-C-D)	Angle (°)	Atoms (A-B-C-D)	Angle (°)
C(10)-N(1)-C(1)-C(11)	154.30(13)	C(15)-C(13)-O(2)-C(14)	-166.20(14)
C(10)-N(1)-C(1)-C(2)	-85.06(16)	C(16)-C(13)-O(2)-C(14)	72.09(16)
N(1)-C(1)-C(11)-N(2)	-61.81(18)	C(13)-O(2)-C(14)-C(4)	57.77(18)
C(2)-C(1)-C(11)-N(2)	175.92(14)	C(5)-C(4)-C(14)-O(2)	-175.23(12)
C(1)-C(11)-N(2)-N(3)	-29.9(2)	C(3)-C(4)-C(14)-O(2)	61.68(16)
N(1)-C(1)-C(2)-C(3)	64.16(17)	C(12)-C(4)-C(14)-O(2)	-57.74(16)
C(11)-C(1)-C(2)-C(3)	-174.67(13)	C(14)-C(4)-C(5)-C(6)	-0.8(2)
C(1)-C(2)-C(3)-C(4)	-62.93(18)	C(3)-C(4)-C(5)-C(6)	119.46(15)
C(2)-C(3)-C(4)-C(5)	74.96(17)	C(12)-C(4)-C(5)-C(6)	-115.16(16)
C(2)-C(3)-C(4)-C(14)	-162.53(12)	C(14)-C(4)-C(5)-C(10)	178.55(14)
C(2)-C(3)-C(4)-C(12)	-48.62(18)	C(3)-C(4)-C(5)-C(10)	-61.15(18)
C(5)-C(4)-C(12)-O(1)	177.58(12)	C(12)-C(4)-C(5)-C(10)	64.23(18)
C(14)-C(4)-C(12)-O(1)	58.71(16)	C(10)-C(5)-C(6)-C(7)	-1.8(2)
C(3)-C(4)-C(12)-O(1)	-57.20(16)	C(4)-C(5)-C(6)-C(7)	177.64(14)
C(4)-C(12)-O(1)-C(13)	-59.50(17)	C(5)-C(6)-C(7)-C(8)	0.5(2)
C(12)-O(1)-C(13)-O(2)	53.49(17)	C(6)-C(7)-C(8)-C(9)	1.1(2)
C(12)-O(1)-C(13)-C(15)	166.91(13)	C(7)-C(8)-C(9)-C(10)	-1.4(2)
C(12)-O(1)-C(13)-C(16)	-71.20(16)	C(8)-C(9)-C(10)-C(5)	0.1(2)
O(1)-C(13)-O(2)-C(14)	-52.79(18)	C(8)-C(9)-C(10)-N(1)	-179.79(14)

Table A6.6.6 cont'd.

Atoms (A-B-C-D)	Angle (°)	Atoms (A-B-C-D)	Angle (°)
C(6)-C(5)-C(10)-C(9)	1.5(2)	C(4)-C(5)-C(10)-N(1)	1.9(2)
C(4)-C(5)-C(10)-C(9)	-177.94(14)	C(1)-N(1)-C(10)-C(9)	-112.83(15)
C(6)-C(5)-C(10)-N(1)	-178.67(14)	C(1)-N(1)-C(10)-C(5)	67.32(18)

Symmetry transformations used to generate equivalent atoms:

Table A6.6.7 *Hydrogen bonds for* ***160*** *[Å and °].*

D-H...A	d(D-H)	d(H...A)	d(D...A)	<(DHA)
N(1)-H(1N)...N(2)	0.895(18)	2.55(2)	3.004(2)	112.3(17)
N(1)-H(1N)...N(3)	0.895(18)	2.69(2)	3.135(2)	111.8(16)
N(1)-H(1N)...O(2)#1	0.895(18)	2.288(19)	3.1417(17)	160(2)
C(12)-H(12A)...N(1)	0.99	2.47	3.117(2)	122.9

Symmetry transformations used to generate equivalent atoms:
#1 x,y+1,z

A6.7 REFERENCES AND NOTES

(1) Sheldrick, G. M. Phase Annealing in SHELX-90: Direct Methods for Larger Structures. *Acta. Crystallogr. A Found. Crystallogr.* **1990**, *46*, 467–473.

(2) Sheldrick, G. M. Crystal Structure Refinement with *SHELXL*. *Acta. Crystallogr. C Struct. Chem.* **2015**, *71*, 3–8.

(3) Müller, P. Practical Suggestions for Better Crystal Structures. *Crystallogr. Rev.* **2009**, *15*, 57–83.

CHAPTER 4

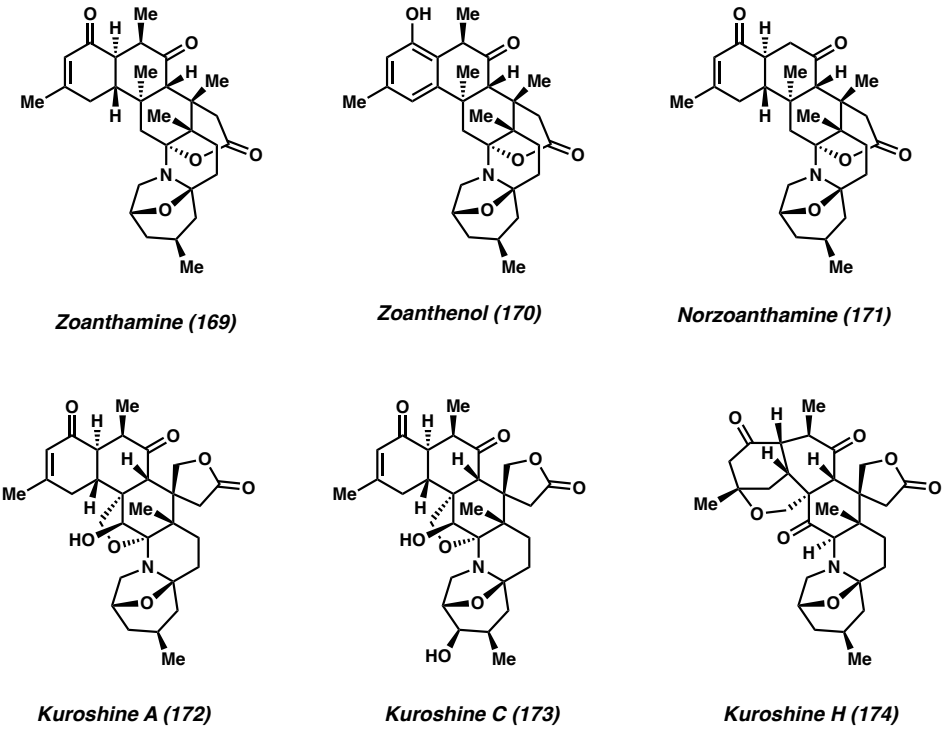
PROGRESS TOWARD THE SYNTHESIS OF KUROSHINE A

4.1 INTRODUCTION

The zoanthamine alkaloids represent a structurally diverse class of molecules isolated from species in the order Zoantharia.[1] These alkaloids possess a variety of attractive biological and pharmacological properties that have made them the targets of extensive study in the areas of medicinal chemistry, pharmacology, and synthetic organic chemistry.[2,3] For example, members of this family display anti-osteoporotic, anti-inflammatory, antibacterial, anticancer, and neuroprotective activities as well as the ability to inhibit human platelet aggregation.[2,4]

Since the initial discovery of the zoanthamine alkaloids, dating back to the isolation of zoanthamine (**169**) in 1984,[5] many new molecules belonging to this family have been isolated and characterized. Recent endeavors have uncovered new, highly oxidized natural products that belong to this same class (Figure 4.1.1). These molecules have been collectively referred to as "kuroshines," named after zoanthid *Zoanthus kuroshio*, from which the first member of this family, kuroshine A (**172**), was isolated.[6] Since this initial report, other members containing higher degrees of oxidation have been uncovered including kuroshine C (**173**) and kuroshine H (**174**).[7,8]

Figure 4.1.1 *Zoanthamine alkaloids and highly oxidized subfamily of "kuroshines"*



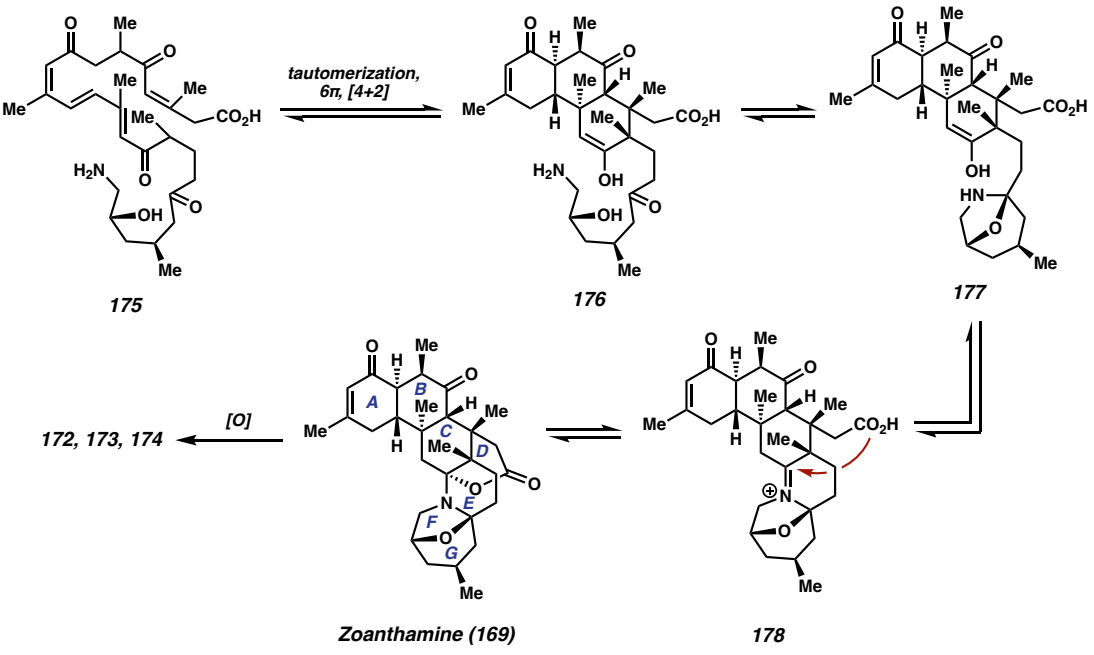
The potential therapeutic properties and intricate structures of zoanthamine alkaloids have made these molecules the focus of numerous synthetic studies, with almost all efforts concentrating on those members with lower overall oxidation levels (**169**, **170**, **171**), discussed further in Section 4.3. However, given our laboratory's longstanding interest in and progress toward the synthesis of zoanthamine alkaloids, we were interested in developing a new strategy for the construction of the highly oxidized members of this family that have yet to succumb to total synthesis. In these initial efforts, we chose to focus on kuroshine A (**172**), although we believe our approach to be applicable to many similar highly oxygenated scaffolds. This chapter contains an account of our synthetic progress.

4.2 SYNTHESIS OF ZOANTHAMINE ALKALOIDS

The intricate structures of zoanthamine alkaloids are believed to arise, biosynthetically, from sequential cyclizations and condensations beginning with linear

precursor **175** (Scheme 4.2.1). Tautomerization and electrocyclization form the A ring (not shown), followed by Diels-Alder reaction of the conformationally restricted intermediate gives rise to **176**, marking completion of the B and C rings, and complete construction of the carbocyclic framework of the molecule. Additional condensation forms **177**, and tautomerization of the enol allows for condensation of the amine to form iminium **178** that can be subsequently trapped by the pendant carboxylic acid to give zoanthamine (**169**). Through this condensation cascade, the entire southern bridged bicyclic DEFG ring system is constructed from an acyclic linear chain. Subsequent oxidations give rise to additional members of the zoanthamine alkaloid family, including those of the "kuroshine" subclass.

Scheme 4.2.1 *Proposed biosynthesis of* ***169*** *and oxidation leading to* ***172***, ***173***, *and* ***174***

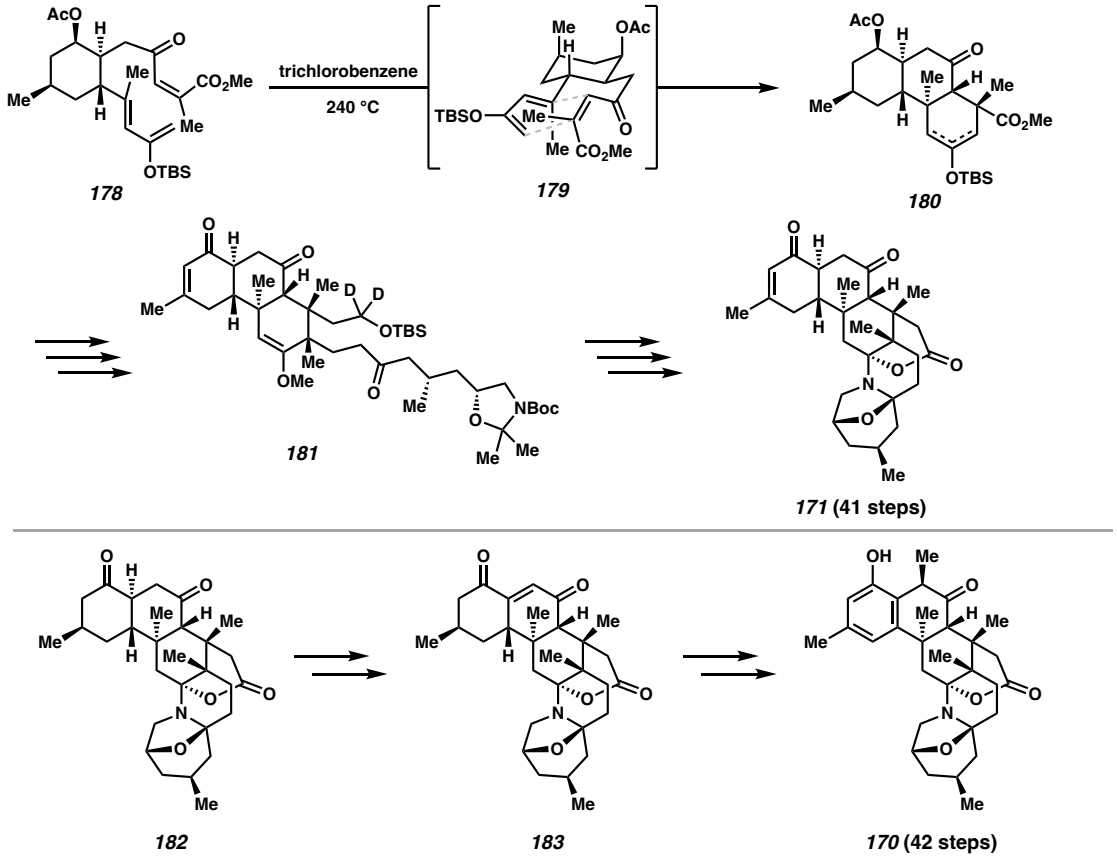


The high degree of structural and stereochemical complexity coupled with potentially valuable therapeutic properties of the zoanthamine alkaloids have attracted the attention of synthetic chemists for the past several decades. While many approaches to the synthesis of

these molecules, or portions of their ring systems have been disclosed,[2] few completed syntheses of these molecules have been reported.

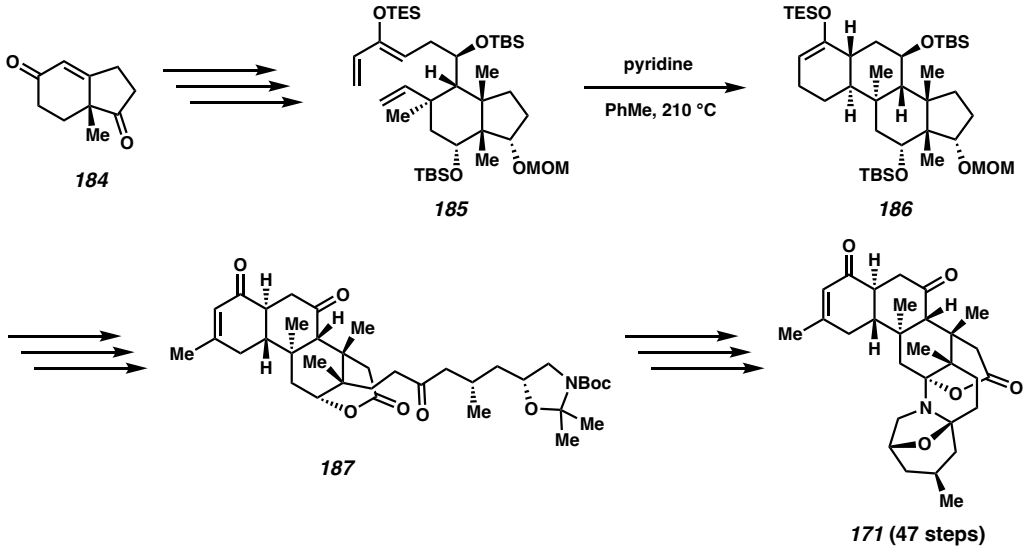
In 2004, Miyashita and coworkers reported the first completed total synthesis of **170**,[3] which represented the first completed total synthesis of any member of the zoanthamine family (Scheme 4.2.2). Their approach relied on an intramolecular Diels-Alder reaction to construct the carbocyclic ABC ring system (intermediate **180**). Installation of a linear side chain (**181**), reminiscent of that seen in the proposed biosynthesis of **171**, could be installed, and through a series of condensations enabled the completion of **171**. Five years later, the group reported a procedure for A ring oxidation of an advanced intermediate to access **170**.[9]

Scheme 4.2.2. *Total syntheses of **171** and **170** by Miyashita and coworkers*



In 2009, Kobayashi and coworkers reported a total synthesis of **171** via an alternative approach.[10,11] Their synthesis began with Hajos-Parrish ketone (**184**), the cyclohexanone portion of which served as the central C ring building block. Construction of the A and B rings was achieved through intramolecular Diels-Alder reaction of siloxy diene **185**. Further functionalization and installation of a linear chain followed by a series of condensations analogous to those discussed previously gave rise to **171**.

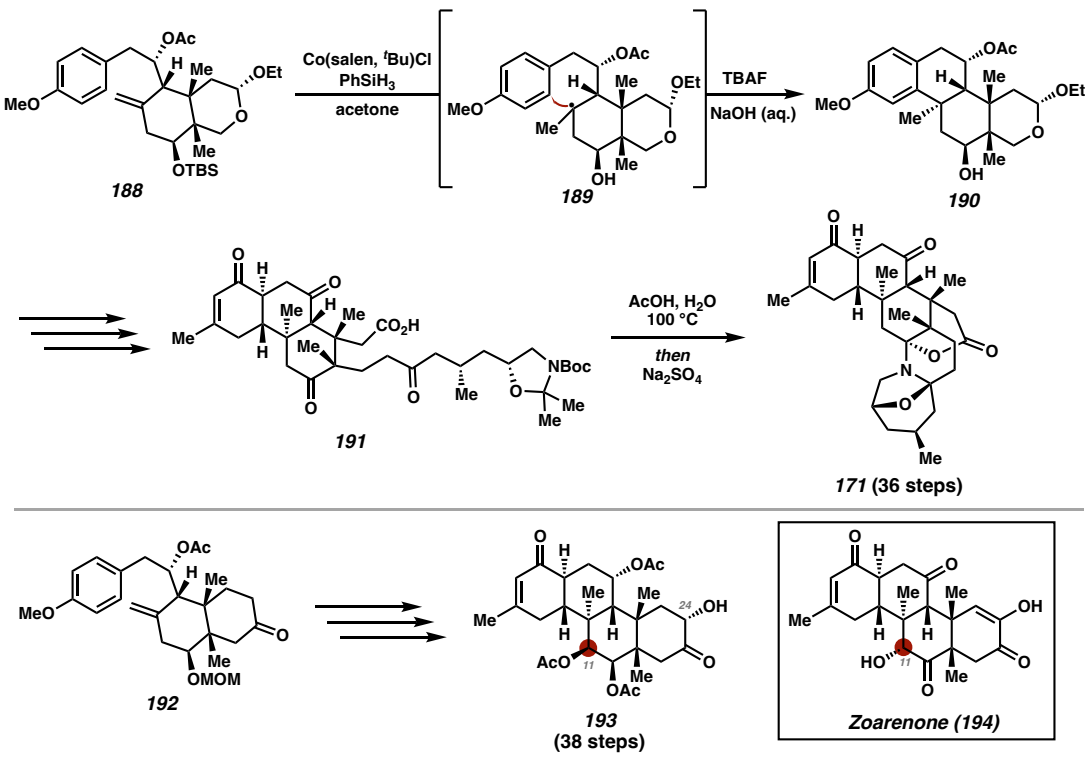
Scheme 4.2.3 *Total synthesis of **171** by Kobayashi and coworkers*



In 2022, Gao and coworkers completed a total synthesis of **171** that made extensive use of radical chemistry, including recently developed methods for radical functionalization and hydrogenation through metal hydrogen atom transfer (MHAT) reactions.[12] Key to their strategy was the use of a cobalt-catalyzed MHAT cyclization of **188** (via **189**) to form the B ring. Further elaboration allowed access to tetracycle **190** to which the necessary linear chain could be appended that allowed for subsequent condensations to access **171**. The group later reported a similar strategy toward the synthesis of zoarenone (**194**). MHAT radical cyclization of **192** again closed the B ring that was advanced to intermediate **193** that contains

oxidation at C11 (**193**).[13] Unfortunately, attempts to oxidize the C24 position failed, possibly due to the alcohol being unfavorably positioned on the concave face of the molecule, and ultimately thwarted further advancement and completion of **194**. To our knowledge this is the only reported attempt to synthesize any zoanthamine-like skeleton with oxidation at C11, a feature present in the "kuroshine" subfamily. The large number of steps required to access the intermediate with oxidation at this uncommon position underscores the challenge associated with synthesizing highly oxidized members of this family.

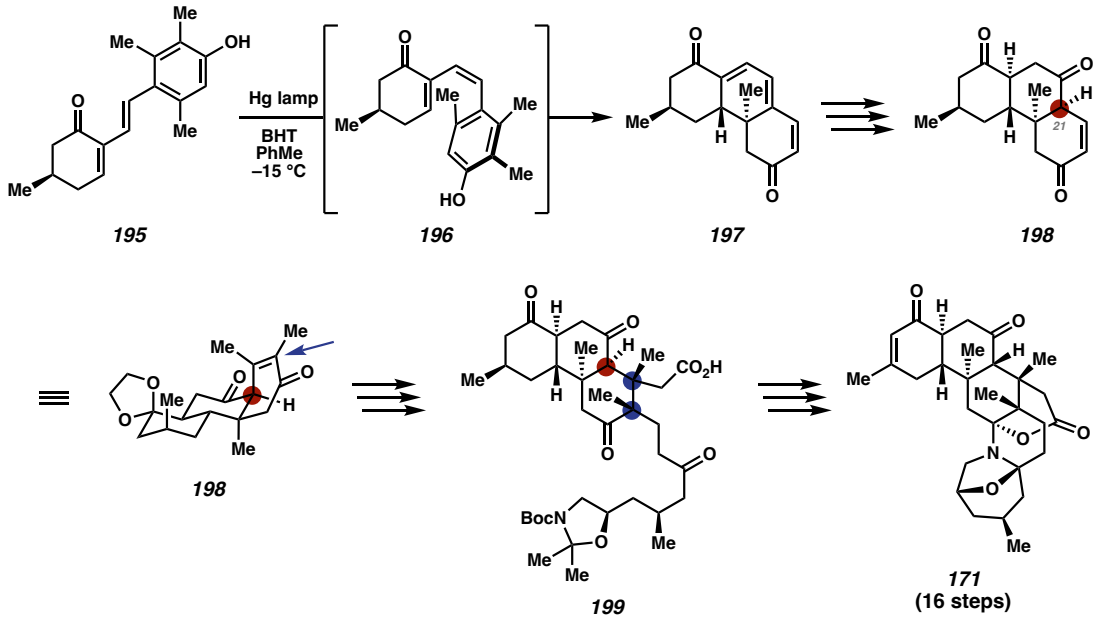
Scheme 4.2.4. *Total synthesis of* ***171*** *and attempted synthesis of* ***194*** *by Gao and coworkers*



Finally, in 2024 Sun and coworkers disclosed an expedient synthesis of **171** that made use of several modern photocatalytic methods.[14] Construction of the ABC ring system was achieved through a dearomative electrocyclization of **195** to give **197**. A key advance made by Sun and coworkers was the recognition that improper stereochemistry at C21

renders the molecule severely stereochemically biased such that transformations occur with exquisite preference for reaction on the convex (α) face of the molecule. Making use of this spatial arrangement, intermediate **198** could be advanced through a series of diastereoselective photochemical transformations to **199**. The final condensation cascade rectified the incorrect C21 stereochemistry, yielding the all-*trans* ring system of **171**. This strategy allowed for completion of **171** in a longest linear sequence of 16 steps, highlighting the power of strategic application of recently developed methods to the synthesis of the zoanthamine alkaloids.

Scheme 4.2.5 *Efficient total synthesis of* ***171*** *by Sun and coworkers*



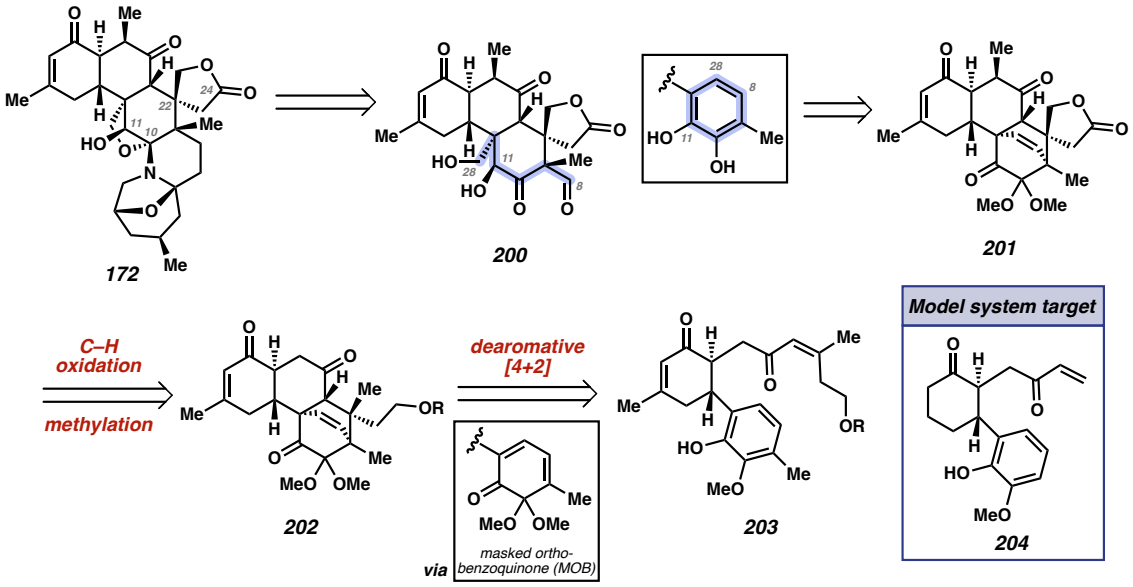
From the perspective of synthetic strategy, these approaches provide several pedagogical features that can aid in designing synthetic approaches to zoanthamine alkaloids. First, they demonstrate that formation of the southern DEFG ring system can be strategically and efficiently performed by a series of condensations from an acyclic precursor. Second, pericyclic reactions to construct various portions of the carbocyclic ABC ring system are highly enabling. Finally, strategic application of recently developed technologies can greatly

facilitate syntheses of these complex alkaloids. These insights were instructive in our retrosynthetic analysis of kuroshine A (**172**).

4.3 RETROSYNTHETIC ANALYSIS OF KUROSHINE A (172)

With these principles in mind, we devised our retrosynthesis of **172** (Figure 4.3.1). We envisioned the same series of late-stage condensations to form the southern DEFG ring system from an acyclic precursor. This moiety is commonly installed through addition of a derivative of the linear chain to a carbonyl compound. Thus, we imagined tracing the entire DEFG ring system back to hypothetical β-keto-aldehyde **200**. From this intermediate, we were faced with the challenge of installing the six highlighted carbons. Two of the six are all-carbon quaternary and the remaining four possess some degree of oxidation. Therefore, it was challenging to imagine sequentially installing the necessary oxygen atoms from a less-oxidized precursor. Instead, we imagined simultaneous installation of these six atoms in the form of an aromatic ring where the necessary oxidation would already be embedded.

Figure 4.3.1. *Retrosynthetic analysis of* ***172***



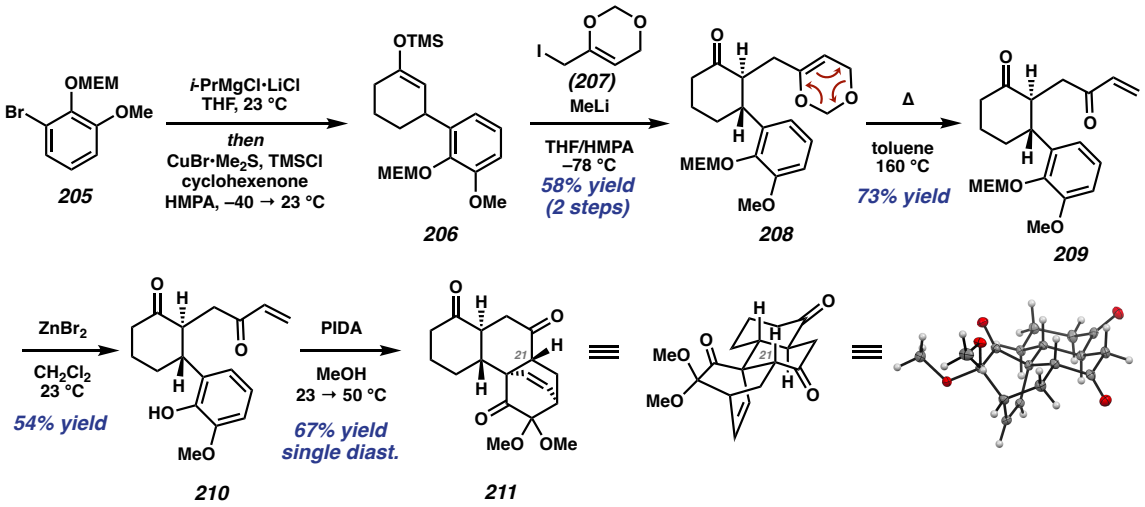
To arrive at this type of aromatic precursor, we noted that the primary alcohol (C28) and aldehyde (C8) constitute a 1,6-dioxygenation pattern that can be retrosynthetically connected, leading back to bridged bicycle **201**. The molecule can be additionally simplified by disconnecting the lactone through C–H oxidation and the methyl group through alkylation, leading to **202**.[15–19] The [2.2.2] bicycle bearing a high degree of oxidation could then be formed through a dearomative [4+2] cycloaddition via an intermediate masked *ortho*-benzoquinone (MOB) species. Dearomative cycloaddition strategies of this type have found a growing number of applications in recent total synthetic efforts.[20–23] As drawn, the proposed dearomative cycloaddition would form two all carbon quaternary centers and set four contiguous stereocenters in a single step. To our knowledge, reactions of MOBs to form products with such extensive substitution patterns have not been studied in either inter- or intramolecular settings. Additionally, we were unsure of the general feasibility of this approach to the ABC ring system of **172**. Therefore, we initiated our study by constructing a simplified, less-substituted model system to understand if this general type of reaction could be applied to the synthesis of the kuroshine ABC ring system.

4.4 MODEL SYSTEM EVALUATION OF THE DEAROMATIVE [4+2] REACTION

Beginning with cyclohexenone, copper catalyzed conjugate addition of aryl magnesium bromide generated from **205** and trapping of the resulting enolate as the TMS silyl enol ether followed by treatment with methyllithium and allylic iodide **207**, a derivative of that prepared by Funk and coworkers,[24] afforded difunctionalized product **208**. Heating **208** in toluene facilitated retro-[4+2] cycloaddition to reveal the terminally unsubstituted enone **209**. Removal of the MEM protecting group with $ZnBr_2$ generated the corresponding

free phenol, setting the stage for the dearomative cycloaddition. Treatment of phenol with bisacetoxyiodobenzene in MeOH led to in situ formation of the corresponding masked *ortho*-benzoquinone species that smoothly undergoes [4+2] cycloaddition with the pendant enone to give bridged bicycle **211** in 67% yield as a single diastereomer with the correct stereochemistry at C21. Although this model system lacks the extensive substitution required for elaboration to **172**, it clearly establishes the viability of this strategy for the construction of the ABC ring system.

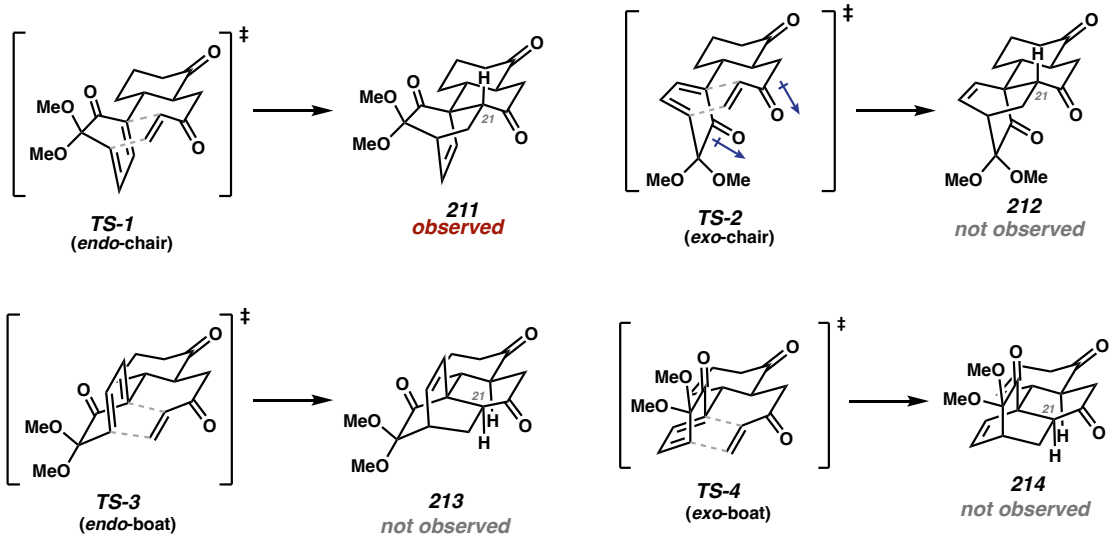
Scheme 4.4.1 *Successful synthesis of the ABC ring system using a model system*



We believe the origins of diastereoselectivity in the MOB cycloaddition to be twofold (shown in Figure 4.4.1). The first, intuitive factor is preference for an *endo*-transition state commonly observed in this type of cycloaddition when the dieneophile bears an electron-withdrawing group, in accord with frontier-molecular orbital theory.[25–28]. The second factor that likely influences the diastereoselectivity of the cycloaddition is a preference for the forming B ring to adopt a chair-like conformation. Of the four possible transition states, only **TS-1** accommodates the *endo* and chair-like preferences. The *exo*-chair **TS-2** may experience additional repulsive dipole interactions between the two carbonyls that disfavor

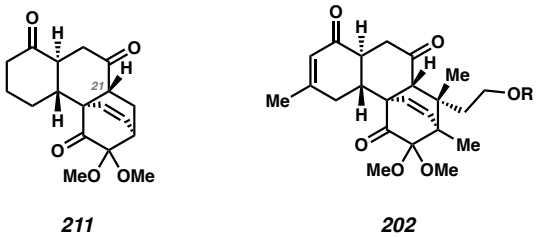
this pathway. The two "boat" transition structures **TS-3** and **TS-4** likely experience eclipsing and steric interactions that render them unfavorable. As a result, only product **211** with the desired C21 stereochemistry is observed.

Figure 4.4.1 *Rationalization of the MOB cycloaddition stereochemical outcome through transition state analysis*



Having established a viable framework from which the ABC carbocyclic skeleton could be constructed, we were poised to begin investigating the fully elaborated system that could be advanced to **172**. These changes would involve additional methyl substitution on the aromatic ring, increased substitution at the terminus of the enone, and an A ring methyl-substituted enone, or some derivative thereof (Scheme XX).

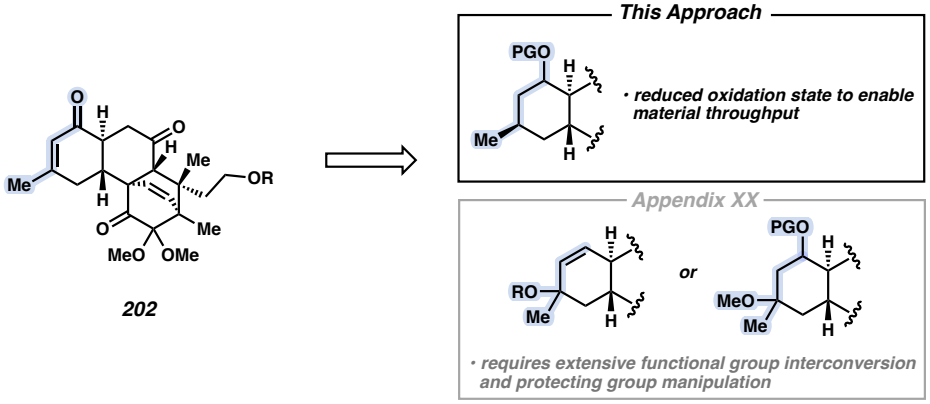
Scheme XX. *Comparison of the model and fully functionalized systems*



4.5 SYNTHETIC PROGRESS TOWARD A FULLY FUNCTIONALIZED ABC RING SYSTEM

A central issue in our initial quest to incorporate the necessary additional substituents was how best to incorporate the A ring methyl-substituted enone (Figure 4.5.1). We explored a number of possible strategies, that involved masking the A ring enone while maintaining a relatively high oxidation level, discussed in Appendix 9. These approaches necessitated a considerable number of steps due to extensive functional group interconversions that prohibited advancement of large quantities of material to be able to test the key dearomative cycloaddition step. Based on these difficulties, we opted to decrease the oxidation level of this ring and concede that installing the necessary oxidation would be achieved through a late stage desaturation, a tactic previously employed in the synthesis of norzoanthamine (**171**).[3,14]

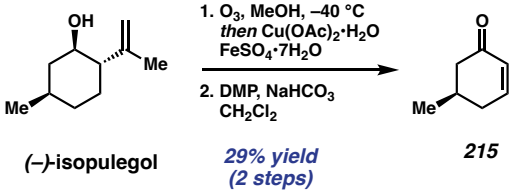
Figure 4.5.1 *Strategies to mask the A ring methyl enone*



In this approach, we chose to follow a synthetic pathway analogous to the conjugate addition/alkylation tactics used to construct the model system. Thus, our synthesis began with construction of a chiral methylated cyclohexenone derivative. Synthesis of this compound from (–)-isopulegone was performed using the oxidative fragmentation procedure

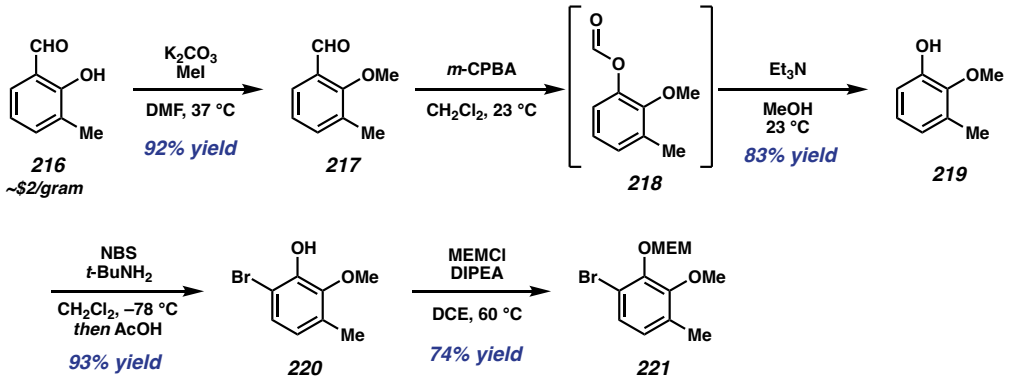
outlined by Newhouse and coworkers[29] followed by the oxidation protocol of Pronin and coworkers[30] to give chiral cyclohexenone **215** (Scheme 4.5.1).

Scheme 4.5.1 *Synthesis of chiral cyclohexenone derivative through known procedures*



Synthesis of the aryl bromide coupling partner was accomplished through a four-step sequence beginning with readily available 2-hydroxy-3-methylbenzaldehyde (**216)** (Scheme 4.5.2). Alkylation of **216** with MeI proceeded nearly quantitatively and was followed by Dakin-type oxidation of the benzaldehyde derivative, cleaving the intermediate formate ester with MeOH and Et_3N to give **218** in 83% yield. Bromination was effected by addition of a mixture of NBS and *t*-$BuNH_2$ to a cooled solution of phenol **219** to form bromoarene **220**, contaminated with <5% of the dibrominated product. Finally, protection of the phenol as the MEM ether completed the synthesis of the necessary bromoarene coupling partner **221**.

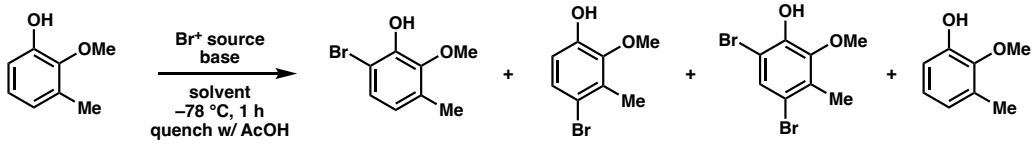
Scheme 4.5.2 *Synthesis of aryl bromide coupling partner*



It should be noted that selective *ortho*-bromination of phenol **219** required optimization to achieve full conversion and suppress formation of the unwanted bromination constitutional isomer **222** as well as doubly brominated product **223.** The results of this

optimization are shown in Table 4.5.1. Key to this transformation was the combination of the amine base and brominating reagent prior to addition to the phenol. The combination of Br_2 and *t*-$BuNH_2$ gave reasonable selectivity, however the heterogeneous nature of the reaction led to poor conversion (Entry 1). The combination of NBS with various amine bases provided varied levels of success. Higher levels of conversion were achieved by addition of a pre-stirred mixture of amine and NBS to the phenol (Entries 3–6). Ultimately, combination of NBS and *t*-$BuNH_2$ proved to be ideal (Entry 6).

Table 4.5.1 *Optimization of the ortho-phenol bromination*



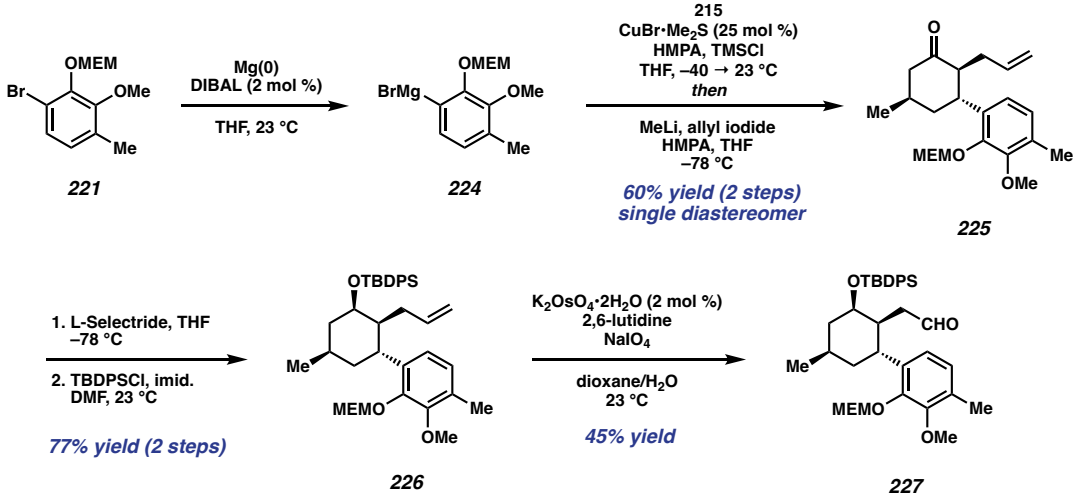
219 ***220*** ***222*** ***223*** ***219***

Entry	*Br⁺ source (1 equiv)*	*base (2 equiv)*	*solvent*	*220:222:223:219 (crude ^{1}H NMR NMR ratio)*	*notes*
1	Br_2	*t*-$BuNH_2$	PhMe/CH_2Cl_2	1.0 : 0.13 : 0.1 : 0.5	pre-stir Br_2 + *t*-$BuNH_2$ add phenol
2	NBS	*i*-Pr_2NH	CH_2Cl_2, 0 °C	1.0 : 0.39 : 0.56 : 1.5	add NBS in CH_2Cl_2 slowly
3	NBS	TMG	CH_2Cl_2	1.0 : 0.28 : 0.17 : 0.18	pre-stir NBS+TMG, *add to phenol*
4	NBS	TMG	CH_2Cl_2/PhMe	1.0 : 0.31 : 0.11 : 0.05	pre-stir NBS+TMG, *add to phenol*
5	NBS	DBU	CH_2Cl_2	1.0 : 0.82 : 0.36 : 0.87	pre-stir NBS+DBU, *add to phenol*
6	NBS	*t*-$BuNH_2$	CH_2Cl_2	1.0 : 0.02 : 0.04 : 0.08	pre-stir NBS+*t*-$BuNH_2$, *add to phenol*

With both coupling partners in hand, we began investigating the conjugate addition/alkylation. We found that formation of the necessary Grignard reagent could be accessed in a scalable fashion by treatment of bromide **221** with activated magnesium metal.[31] Slow addition of the Grignard reagent to a cooled mixture of CuBr•Me_2S, TMSCl, HMPA, and cyclohexeneone **215** followed by basic workup allowed for isolation of the corresponding silyl enol ether that was used without further purification. Treatment of the

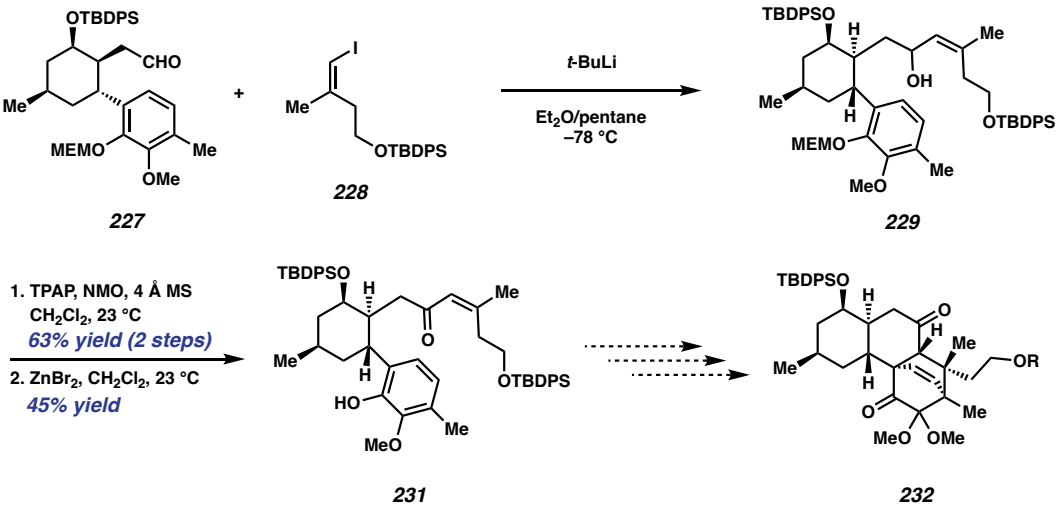
crude silyl enol ether with methyllithium in the presence of HMPA, followed by addition of allyl iodide at cryogenic temperatures led to formation of ketone **225** in an overall 60% yield. Reduction of the ketone with L-selectride and protection of the secondary alcohol proceeded smoothly. Lemieux–Johnson oxidation of the terminal olefin yielded aldehyde **227**.

Scheme 4.5.3 *Conjugate addition/alkylation and further manipulation*



With aldehyde **227** in hand, we envisioned installing the dieneophile through addition of various vinyl nucleophiles followed by oxidation of the allylic alcohol. To this end, treatment of vinyl iodide **228** with *t*-BuLi followed by addition of aldehyde **227** smoothly produced a diastereomeric (inconsequential) mixture of allylic alcohols that gave the corresponding enone (**230**, not shown) upon oxidation under Ley-Griffith conditions (TPAP, NMO) in 63% yield from aldehyde **227**. Deprotection of the phenol using $ZnBr_2$ proceeded in an unoptimized 45% yield to give **231**. Efforts are underway to advance this compound to bridged bicycle **232**. We envision that 1,2-additions to aldehyde **227** will provide a modular platform through which a variety of dieneophiles with differing substitution patterns and electronic character may be installed.

Scheme 4.5.4 *Installation of the dieneophile*



4.6 CONCLUSION

This chapter presents a new approach to access oxidized members of the zoanthamine alkaloid family. A key feature of our synthetic route is a masked *ortho*-benzoquinone (MOB) cycloaddition to construct the ABC ring system of the molecule. We have demonstrated the feasibility of this strategy through construction of a model system, in which we observed exquisite diastereoselectivity to access a simplified ABC ring system with the correct C21 stereochemistry. Construction of the fully elaborated system is underway. By utilizing an A ring in a lower oxidation state have been able to advance the material smoothly without experiencing complications due to many reactive functional groups. Future efforts are directed toward construction of the highly substituted bridged bicycle **232**.

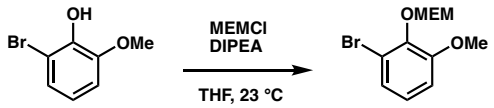
4.7 EXPERIMENTAL SECTION

4.7.1 MATERIALS AND METHODS

Unless otherwise stated, reactions were performed in flame-dried glassware under an argon or nitrogen atmosphere using dry, deoxygenated solvents. Solvents were dried by passage through an activated alumina column under argon.[32] Reaction progress was

monitored by thin-layer chromatography (TLC) or Agilent 1290 UHPLC-MS. TLC was performed using E. Merck silica gel 60 F254 precoated glass plates (0.25 mm) and visualized by UV fluorescence quenching, *p*-anisaldehyde, or $KMnO_4$ staining. Silicycle Silia*Flash*® P60 Academic Silica gel (particle size 40–63 μm) was used for flash chromatography. ^1H NMR spectra were recorded on Varian Inova 500 or 600 MHz and Bruker 400 MHz spectrometers and are reported relative to residual $CHCl_3$ (δ 7.26 ppm), C_6D_5H (δ 7.16 ppm), and CD_2HOD (δ 3.31). ^{13}C NMR spectra were recorded on a Varian Inova 500 MHz spectrometer (125 MHz) and Bruker 400 MHz spectrometers (100 MHz) and are reported relative to $CDCl_3$ (δ 77.16 ppm) or C_6D_6 (δ 128.06 ppm). Data for ^1H NMR are reported as follows: chemical shift (δ ppm) (multiplicity, coupling constant (Hz), integration). Multiplicities are reported as follows: s = singlet, d = doublet, t = triplet, q = quartet, p = pentet, sept = septuplet, m = multiplet, br s = broad singlet, br d = broad doublet. Data for ^{13}C NMR are reported in terms of chemical shifts (δ ppm). IR spectra were obtained by use of a Perkin Elmer Spectrum BXII spectrometer using thin films deposited on NaCl plates and reported in frequency of absorption (cm^{-1}). Optical rotations were measured with a Jasco P-2000 polarimeter operating on the sodium D-line (589 nm), using a 100 mm path-length cell. High resolution mass spectra (HRMS) were obtained from the Caltech Mass Spectral Facility using a JEOL JMS-T2000GC AccuTOF^{TM} GC-Alpha High Resolution Mass Spectrometer in field ionization (FI+) or field desorption (FD+) mode, or an Agilent 6230 Series TOF with an Agilent Jet Stream ion source in electrospray ionization (ESI+) mode. Reagents were purchased from commercial sources and used as received unless otherwise stated.

4.7.2 EXPERIMENTAL PROCEDURES



205

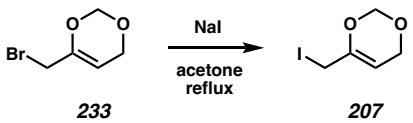
Bromide 205: To a round bottom flask was added 2-bromo-6-methoxyphenol[33] (1.00 g, 4.93 mmol, 1.0 equiv) followed by THF (10 mL). DIPEA (2.58 mL, 14.79 mmol, 3.0 equiv) was added and the solution was stirred at ambient temperature. MEMCl (1.69 mL, 14.79 mmol, 3.0 equiv) was added slowly and the solution was allowed to stir for 12 hours. After this time, the reaction mixture was quenched with 1N NaOH (15 mL) and stirred for 30 minutes. The layers were partitioned and separated. The aqueous layer was extracted with CH_2Cl_2 (3x20 mL). The combined organic layers were washed with brine, dried over Na_2SO_4, and concentrated under reduced pressure. The crude reside was purified by silica gel flash column chromatography (40% Et_2O in hexanes) to give a colorless oil that solidified upon standing at low temperature to give the title compound as an oily colorless solid (1.29 g, 90% yield).

^{1}H NMR: (400 MHz, $CDCl_3$) δ 7.13 (dt, *J* = 8.0, 1.6 Hz, 1H), 6.93 (td, *J* = 8.2, 1.7 Hz, 1H), 6.85 (dt, *J* = 8.2, 1.6 Hz, 1H), 5.25 (d, *J* = 1.7 Hz, 2H), 4.09 – 3.99 (m, 2H), 3.83 (d, *J* = 1.6 Hz, 3H), 3.63 – 3.55 (m, 2H), 3.38 (d, *J* = 1.7 Hz, 3H)

^{13}C NMR: (100 MHz, $CDCl_3$) δ 153.7, 143.4, 125.3, 125.2, 118.1, 111.7, 97.5, 71.9, 69.4, 59.2, 56.1

IR: (neat film, NaCl) 2932, 2886, 2808, 1582, 1464, 1256, 1170, 1106, 1034, 938, 824, 766, 696, 618 cm^{-1}

HRMS: *m/z* calc'd for $C_{11}H_{15}O_4BrNa$ $[M+Na]^+$: 314.0043, found 314.0046



233 ***207***

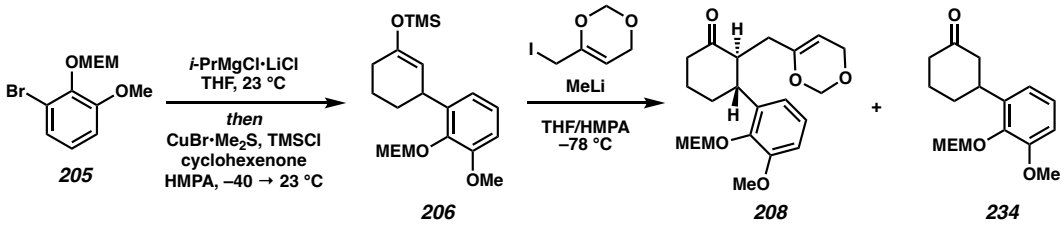
Allylic iodide 207: To a round-bottom flask was charged bromide **233**[24] (2.00 g, 11.17 mmol, 2.0 equiv). Acetone (37.3 mL) was added followed by NaI (3.35 g, 22.4 mmol, 2.0 equiv). The flask was purged with a stream of nitrogen, then fitted with a reflux condenser equipped with a nitrogen inlet and heated to reflux for 2 hours. After this time, the solution was cooled to ambient temperature. The mixture was concentrated under reduced pressure. The residue was reconstituted with Et_2O (50 mL) and washed with water (50 mL). The aqeuous washing was extracted with Et_2O (3x10 mL). The combined organic extracts were washed with brine (20 mL), dried over Na_2SO_4, and concentrated under reduced pressure. The crude residue was purified by silica gel flash column chromatography (0 → 20% Et_2O in hexanes) to give the title compound as an off-white solid (1.757 g, 69% yield).

^{1}H NMR: (400 MHz, $CDCl_3$) δ 4.70 (s, 2H), 4.32 (t, *J* = 2.8 Hz, 1H), 3.58 (dt, *J* = 2.6, 1.1 Hz, 2H), 3.29 – 3.24 (m, 2H)

^{13}C NMR: (100 MHz, $CDCl_3$) δ 149.0, 97.7, 89.1, 61.7, 0.0

IR: (neat film, NaCl) 3004, 2944, 2872, 1666, 1414, 1368, 1306, 1152, 1086, 1012, 978, 926, 842, 658 cm^{-1}

HRMS: (FI+) *m/z* calc'd for $C_5H_7O_2I$ $[M]^+$: 225.94852, found 225.94928.



Ketone 208: To a round-bottom flask with stir bar was added aryl bromide **205** (200 mg, 0.69 mmol, 1.0 equiv). The bromide was azeotroped from toluene (2x3 mL), then placed under high-vacuum for >3 hours. After this time, THF (0.69 mL) was added and the solution was cooled to 0 °C. *i*-PrMgCl•LiCl (1.3 M, 0.74 mL, 0.96 mmol, 1.4 equiv) was added and the solution was warmed to ambient temperature and stirred for 6 hours. After this time, to a separate flask was added CuBr•Me_2S (14.2 mg, 0.069 mmol, 10 mol%). HMPA (0.36 mL) was added and the solution was cooled to 0 °C. TMSCl (131 µL, 1.04 mmol, 1.5 equiv) and cyclohexenone (66.3 mg, 0.69 mmol, 1 equiv) were sequentially added. The stirring Grignard solution was cooled to –40 °C. Then the copper/enone solution was added to the cooled Grignard solution and the solution was allowed to warm to ambient temperature over 10 hours. After this time, the solution was cooled to –78 °C. Et_3N (289 µL, 2.07 mmol, 3.0 equiv) was added and stirred for 20 minutes. Then satd. aq. $NaHCO_3$ (2.0 mL) was added followed by aq. NH_4OH (0.2 mL) and EtOAc (2.0 mL). The solution was allowed to reach ambient temperature then the layers were separated and the aqueous layer was extracted with EtOAc (3x2 mL). The combined organic layers were washed with brine (5 mL), dried over Na_2SO_4 and concentrated under reduced pressure. The crude oil was azeotroped with benzene (3 mL) and placed under high vacuum for direct use in the next step without further purification.

To the crude, azeotroped silyl enol ether (190 mg, 0.5 mmol, 1.0 equiv) was added THF (0.44 mL) and HMPA (0.44 mL), and the solution was cooled to 0 °C. MeLi (1.7 M in

Et_2O, 0.63mL, 1.0 mmol, 2.0 equiv) was added dropwise. After stirring for 30 minutes, the solution was cooled to –78 °C. To a separate flask was charged allylic iodide **XX** (396 mg, 1.75 mmol, 3.5 equiv). HMPA (0.34 mL) and THF (0.67 mL) were sequentially added and stirred the mixture was stirred until it became homogeneous. The solution of allylic iodide was added dropwise to the –78 enolate solution. After addition, the reaction mixture was allowed to stir for 6 hours at –78 °C then quenched by addition of satd. aq. NH_4Cl (2 mL). After the mixture reached ambient temperature it was extracted with EtOAc (3x5 mL). The combined organic layers were washed with brine, dried over Na_2SO_4, and concentrated under reduced pressure. The crude reside was purified by silica gel flash column chromatography (0 → 50% EtOAc in hexanes) to give the title compound as a colorless oil contaminated with a small amount of unalkylated ketone **234** (162 mg, 58% yield over 2 steps).

^{1}H NMR: (400 MHz, $CDCl_3$) δ 7.06 (q, *J* = 7.6 Hz, 1H), 6.90 (dd, *J* = 7.9, 1.5 Hz, 1H), 6.77 (dd, *J* = 8.1, 1.4 Hz, 1H), 5.15 – 5.10 (m, 2H), 4.88 (d, *J* = 5.3 Hz, 1H), 4.82 (d, *J* = 5.3 Hz, 1H), 4.44 (dq, *J* = 2.6, 1.3 Hz, 1H), 4.08 (ddt, *J* = 14.8, 2.9, 1.6 Hz, 1H), 3.98 (dq, *J* = 14.7, 1.9 Hz, 1H), 3.94 – 3.84 (m, 2H), 3.82 (d, *J* = 1.9 Hz, 3H), 3.62 – 3.49 (m, 2H), 3.37 (s, 3H), 3.31 (td, *J* = 11.8, 3.8 Hz, 1H), 2.94 (ddd, *J* = 12.1, 8.3, 3.6 Hz, 1H), 2.59 – 2.52 (m, 1H), 2.51 – 2.45 (m, 2H), 2.16 – 2.08 (m, 1H), 2.01 – 1.93 (m, 1H), 1.88 (td, *J* = 12.0, 3.4 Hz, 1H), 1.83 – 1.70 (m, 2H).

^{13}C NMR: (100 MHz, $CDCl_3$) δ 211.3, 152.7, 152.3, 144.1, 137.3, 124.7, 119.0, 110.3, 98.2, 97.6, 90.5, 71.8, 69.2, 64.1, 59.2, 55.8, 51.9, 43.8, 42.5, 34.4, 31.0, 27.1.

IR: (neat film, NaCl) 2934, 1710, 1584, 1476, 1368, 1292, 1264, 1200, 1168, 1070, 1024, 966, 844, 782, 750, 680 cm^{-1}

HRMS: (ESI+) *m/z* calc'd for $C_{22}H_{31}O_7$ $[M+H]^+$: 407.2064, found 207.2065

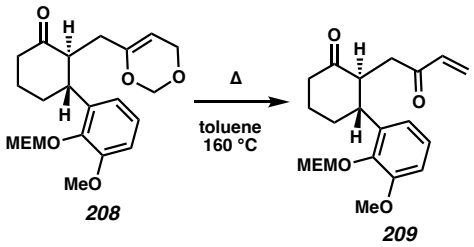
Ketone **234**

^{1}H NMR: (400 MHz, $CDCl_3$) δ 7.06 (t, *J* = 8.0 Hz, 1H), 6.84 (dd, *J* = 7.9, 1.4 Hz, 1H), 6.80 (dd, *J* = 8.2, 1.4 Hz, 1H), 5.16 (s, 2H), 3.94 – 3.84 (m, 2H), 3.83 (s, 3H), 3.62 – 3.51 (m, 3H), 2.57 (ddt, *J* = 13.9, 4.1, 1.9 Hz, 1H), 2.52 – 2.30 (m, 3H), 2.14 (dqt, *J* = 13.4, 6.9, 3.4 Hz, 1H), 2.03 (dtt, *J* = 9.3, 3.5, 2.1 Hz, 1H), 1.88 – 1.71 (m, 2H).

^{13}C NMR: (100 MHz, $CDCl_3$) δ 211.4, 152.2, 143.7, 138.5, 124.6, 118.4, 110.5, 98.3, 71.8, 69.3, 59.2, 55.9, 48.3, 41.5, 37.7, 32.2, 25.8.

IR: (neat film, NaCl) 2926, 1710, 1584, 1466, 1262, 1172, 1066, 962, 784, 754, 706, 682, 628, 606 cm^{-1}

HRMS: (ESI+) *m/z* calc'd for $C_{17}H_{24}O_5Na$ $[M+Na]^+$: 331.1516, found 331.1517



208 ***209***

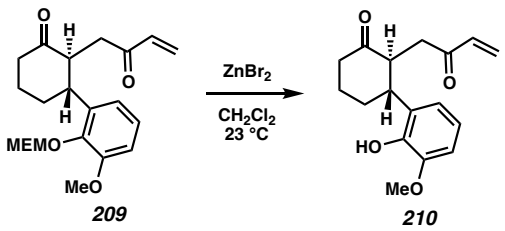
Enone 209: To a flame-dried microwave vial was added ketone **208** (20 mg, 0.0492 mmol, 1.0 equiv) and toluene (0.5 mL). The reaction vessel was placed in a preheated oil bath at 180 °C. After 1 hour, the solution was cooled to ambient temperature. The solution was concentrated under reduced pressure. The crude residue was purified by silica gel flash column chromatography (0 → 25% acetone in hexanes) to give the title compound as a colorless oil (13.6 mg, 73% yield).

^{1}H NMR: (400 MHz, $CDCl_3$) δ 7.06 (t, *J* = 8.0 Hz, 1H), 6.94 – 6.86 (m, 1H), 6.77 (dd, *J* = 8.1, 1.4 Hz, 1H), 6.25 (ddd, *J* = 17.6, 10.4, 0.8 Hz, 1H), 6.12 (dt, *J* = 17.6, 1.1 Hz, 1H), 5.71 (dt, *J* = 10.5, 1.1 Hz, 1H), 5.20 – 5.09 (m, 2H), 3.94 – 3.86 (m, 2H), 3.83 (d, *J* = 0.7 Hz, 3H), 3.62 – 3.53 (m, 2H), 3.37 (d, *J* = 0.8 Hz, 5H), 3.05 (dd, *J* = 17.5, 9.1 Hz, 1H), 2.62 – 2.44 (m, 2H), 2.16 (dh, *J* = 12.3, 3.0 Hz, 1H), 2.06 – 1.84 (m, 3H), 1.75 (qt, *J* = 13.2, 4.5 Hz, 1H)

^{13}C NMR: (100 MHz, $CDCl_3$) δ 210.5, 199.5, 152.1, 144.0, 137.0, 136.5, 127.8, 125.0, 118.4, 110.2, 98.3, 71.7, 69.2, 59.1, 55.7, 51.5, 42.4, 41.7, 36.9, 33.9, 26.7. *One signal is not observed due to peak broadening.*

IR: (neat film, NaCl) 2934, 1710, 1476, 1290, 1262, 1168, 1070, 968, 812, 740, 680 cm^{-1}

HRMS: (ESI+) *m/z* calc'd for $C_{21}H_{28}O_6Na$ $[M+Na]^+$: 399.1778, found 399.1787



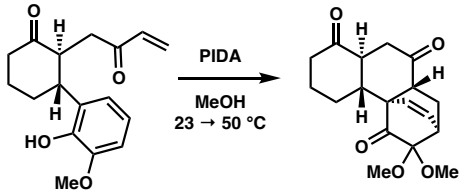
Phenol 210: In an nitrogen-filled glovebox, $ZnBr_2$ (finely powdered, 138.5 mg, 0.615 mmol, 5.0 equiv) was charged to a round bottom flask. The flask was sealed with a rubber septum, removed from the glovebox, and connected to a nitrogen inlet line. Enone **209** (46.3 mg, 0.123 mmol, 1.0 equiv) was added as a solution in CH_2Cl_2 (2.1 mL), and the solution was stirred for 5 hours. After this time, satd. aq. $NaHCO_3$ was added and the layers were separated. The aqueous layer was extracted with CH_2Cl_2 (3x1 mL). The combined organic layers were washed with brine, dried over Na_2SO_4, and concentrated under reduced pressure. The crude reside was purified by silica gel flash column chromatography (0 → 40% EtOAc in hexanes) to give the title compound as a white foam (19.0 mg, 54% yield).

^{1}H NMR: (400 MHz, $CDCl_3$) δ 6.86 – 6.78 (m, 2H), 6.78 – 6.70 (m, 1H), 6.26 (dd, *J* = 17.6, 10.5 Hz, 1H), 6.12 (dd, *J* = 17.6, 1.3 Hz, 1H), 5.77 (s, 1H), 5.71 (dd, *J* = 10.5, 1.3 Hz, 1H), 3.89 (s, 3H), 3.50 (t, *J* = 11.0 Hz, 1H), 3.19 (t, *J* = 12.1 Hz, 1H), 3.01 (dd, *J* = 17.4, 9.2 Hz, 1H), 2.64 – 2.42 (m, 2H), 2.21 – 1.94 (m, 4H), 1.79 (tt, *J* = 13.1, 4.5 Hz, 1H)

^{13}C NMR: (100 MHz, $CDCl_3$) δ 210.9, 199.7, 146.6, 143.4, 136.7, 128.6, 127.7, 120.1, 108.9, 56.1, 51.1, 41.8, 37.2, 32.6, 26.7

IR: (neat film, NaCl) 3400, 2934, 1708, 1614, 1478, 1442, 1368, 1264, 1170, 1074, 834, 824, 752, 734, 696 cm^{-1}

HRMS: (ESI+) *m/z* calc'd for $C_{17}H_{20}O_4Na$ $[M+Na]^+$: 311.1254, found 311.1253



210 ***211***

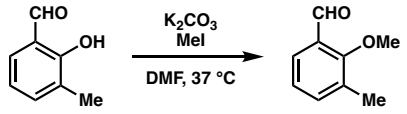
Cycloadduct 211: Phenol **210** (19.0 mg, 0.066 mmol, 1.0 equiv) was charged to a round-bottom flask and MeOH (degassed with Ar, 1.32 mL) was added under nitrogen. Iodobenzene diacetate (25.5 mg, 0.079 mmol, 1.2 equiv) was added and the solution was stirred vigorously for 20 minutes. After this time addition MeOH (degassed with Ar, 5.3 mL) was added and the solution was heated to 50 °C for 10 hours. After this time, the reaction mixture was concentrated under reduced pressure. The crude product was purified by silica gel flash column chromatography (30% EtOAc in hexanes) to give the title compound as a colorless crystalline solid (14 mg, 67% yield).

^{1}H NMR: (400 MHz, $CDCl_3$) δ 6.59 – 6.51 (m, 1H), 5.93 (dd, *J* = 8.5, 1.4 Hz, 1H), 3.35 (s, 3H), 3.27 (s, 3H), 3.17 (dtd, *J* = 4.5, 2.9, 1.4 Hz, 1H), 2.65 – 2.42 (m, 6H), 2.41 – 2.28 (m, 1H), 2.26 – 2.10 (m, 3H), 1.93 – 1.74 (m, 2H), 1.57 – 1.41 (m, 1H)

^{13}C NMR: (100 MHz, $CDCl_3$) δ 208.9, 206.1, 201.2, 136.8, 122.9, 94.5, 59.0, 50.8, 50.7, 49.6, 42.5, 41.5, 40.3, 38.1, 26.8, 25.9, 19.7

IR: (neat film, NaCl) 2946, 1714, 1450, 1312, 1248, 1144, 1084, 1058, 1018, 992, 916, 730 cm^{-1}

HRMS: (FD+): The compound did not ionize to give an expected mass. It appears to ionize with loss of CO to give an *m/z* of $C_{17}H_{22}O_4$ $[M]^+$: 290.1513, found 290.1503. All other data are consistent with the structure of **211**, which has been confirmed by X-ray crystallography.

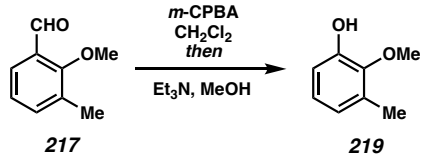


216 ***217***

Aldehyde 216: To a round-bottom flask was charged 2-hydroxy-3-methyl benzaldehyde (24.90 g, 183 mmol, 1.0 equiv). DMF (100 mL) was added followed by K_2CO_3 (30.3 g, 219 mmol, 1.2 equiv). MeI (17.1 mL, 274.5 mmol, 1.5 equiv) was added in one portion and the reaction mixture was heated to 37 °C for 14 hours. After this time, the mixture was cooled to ambient temperature. The reaction mixture was poured into water (250 mL) then 3 N HCl (approx. 25 mL) was added to adjust the pH of the solution to ~7–8. The mixture was then extracted with EtOAc (4x70 mL). The combined organic layers were washed with brine, dried over Na_2SO_4, and concentrated under reduced pressure. The crude oil was allowed to stand at –10 °C during which time it solidified to give the title compound as a gold solid (25.3 g, 92% yield).

The physical data were in accord with those reported in the literature.[34]

^{1}H NMR: (500 MHz, $CDCl_3$) δ 10.38 (d, *J* = 0.8 Hz, 1H), 7.69 (dd, *J* = 7.8, 1.8 Hz, 1H), 7.48 – 7.42 (m, 1H), 7.14 (t, *J* = 7.6 Hz, 1H), 3.89 (s, 3H), 2.36 (s, 3H).

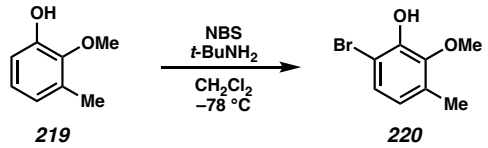


217 ***219***

Phenol 219: To a round-bottom flask was charged aldehyde **217** (19.00 g, 126.5 mmol, 1.0 equiv). The aldehyde was dissolved in CH_2Cl_2 (320 mL, not rigorously anhydrous or purified by passage through activated alumnia) and cooled to 0 °C *m*-CPBA (46.8 g (>70% purity), 189.8 mmol, 1.5 equiv) was added in three portions to the cooled solution. The reaction mixture was allowed to gradually warm to ambient temperature over the course of 12 hours and the reaction color became pale yellow with formation of a white precipitate. After this time, the solution was cooled to 0 °C. Satd. aq. $NaHCO_3$ (500 mL) and satd. aq. $Na_2S_2O_3$ (500 mL) and stirred until peroxide test paper indicated that no peroxides were present. The layers were then partitioned and separated. The aqeuous layer was extracted with CH_2Cl_2 (3x100 mL). The combined organic layers were washed with brine, dried over Na_2SO_4, and concentrated under reduced pressure. The crude residue was dissolved in MeOH (100 mL), Et_3N (6 mL) was added, and the mixture was stirred for 30 minutes. Then the reaction was concentrated under reduced pressure to give a brown oil that was purified by silica gel flash column chromatography (0 → 20% EtOAc in hexanes) to give the title compound as a yellow/gold oil (14.6 g, 83% yield).

The physical data were in accord with those reported in the literature.[35]

^{1}H NMR: (500 MHz, $CDCl_3$) δ 6.91 (t, *J* = 7.8 Hz, 1H), 6.81 (dd, *J* = 8.1, 1.6 Hz, 1H), 6.73 – 6.67 (m, 1H), 5.63 (d, *J* = 1.6 Hz, 1H), 3.81 (s, 3H), 2.31 (s, 3H).

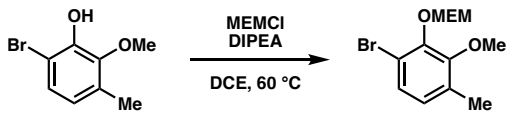


219 ***220***

Bromophenol 220: To a round-bottom flask was added phenol **219** (2.26 g, 16.36 mmol, 1.0 equiv). The phenol was dissolved in CH_2Cl_2 (160 mL, not purified by passage through alumina) and cooled to –78 °C. In a separate round-bottom flask, NBS (recrystallized, 2.853 g, 16.03 mmol, 0.99 equiv) was added followed by CH_2Cl_2 (48 mL, not purified by passage through alumina). *t*-$BuNH_2$ (3.44 mL, 32.7 mmol, 2.0 equiv) was added slowly and the solution turned pale yellow. The mixture was stirred until it became homogeneous (approx. 5 minutes). Then the amine solution was transferred by cannula to the cooled phenol solution. The solution was maintained at –78 °C for 2 hours, then AcOH (1.87 mL, 13.7 mmol, 2.0 equiv) was added, and the solution was allowed to warm to ambient temperature. The mixture was passed through a pad of silica gel, eluting with CH_2Cl_2 (300 mL). The filtrate was concentrated to give the title compound as a white/off-white amorphous solid (3.3 g, 93% yield).

The physical data were in agreement with those reported in the literature.[36]

^{1}H NMR: (500 MHz, $CDCl_3$) δ 7.12 (d, J = 8.3 Hz, 1H), 6.62 (dd, J = 8.3, 0.8 Hz, 1H), 5.79 (s, 1H), 3.83 (s, 3H), 2.26 (s, 3H).



220 ***221***

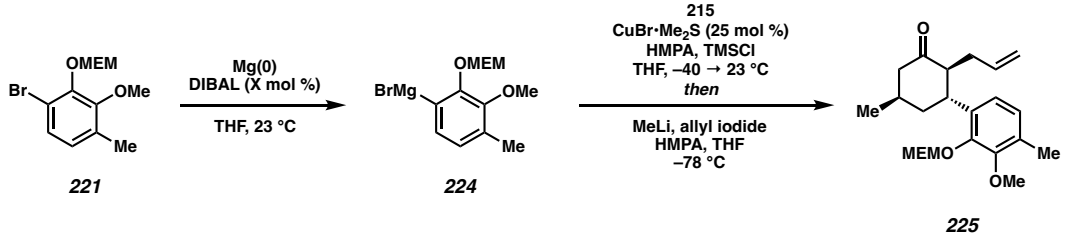
MEM ether 221: Bromophenol **220** (4.8 g, 22.1 mmol, 1.0 equiv) was charged to a round-bottom flask. 1,2-dichloroethane (73 mL) was added followed by DIPEA (11.84 mL, 66.3 mmol, 3.0 equiv). MEMCl (7.57 mL, 66.3 mmol, 3.0 equiv) was added slowly and the solution turned yellow. The reaction was then heated to 60 °C and maintained at this temperature for 12 hours. The solution was cooled to ambient temperature and 1 N NaOH (100 mL) was added. The layers were separated and the aqueous layer was extracted with CH_2Cl_2 (3x50 mL). The combined organic extracts were washed with brine, dried over Na_2SO_4, and concentrated under reduced pressure. The crude residue was purified by silica gel flash column chromatography (0 → 40% Et_2O in hexanes) to give the title compound as a colorless oil (4.97 g, 74% yield).

^{1}H NMR: (400 MHz, $CDCl_3$) δ 7.18 (d, *J* = 8.2 Hz, 1H), 6.80 (dq, *J* = 8.3, 0.7 Hz, 1H), 5.26 (s, 2H), 4.07 – 3.98 (m, 2H), 3.79 (s, 3H), 3.64 – 3.56 (m, 2H), 3.39 (s, 3H), 2.21 (d, *J* = 0.8 Hz, 3H)

^{13}C NMR: (100 MHz, $CDCl_3$) δ 152.5, 147.5, 132.4, 127.9, 127.2, 114.9, 97.9, 71.9, 69.5, 60.4, 59.2, 15.9

IR: (neat film, NaCl) 2938, 1468, 1454, 1392, 1270, 1168, 1114, 1008, 964, 910, 844, 796, 738, 718, 646, 616 cm^{-1}

HRMS: (ESI+) *m/z* calc'd for $C_{12}H_{17}BrO_4Na$ $[M+Na]^+$: 327.0202, found 327.0203



Ketone 225: To a round-bottom flask was added magnesium metal (crushed with mortar and pestle, 119 mg, 4.9 mmol, 3 equiv). The flask containing magnesium was flame dried under vacuum and allowed to cool then backfilled with nitrogen. In a separate flask, bromide **221** (748 mg, 2.45 mmol, 1.5 equiv) was prepared as a solution in THF (2.7 mL). A freshly prepared solution of DIBAL (1.0 M in toluene, 0.05 mL, 0.05 mmol, 3 mol% relative to Mg) was added to the magnesium. 0.4 mL of the bromide/THF solution were added to the magnesium metal and stirred. Initiation occurred within 10 minutes and could be observed by color change of the solution from colorless to a dark yellow/green. If initiation did not occur, the solution was gently heated with a heat gun until a slight color change was observed. The remaining bromide/THF solution was added dropwise such that the solution did not reach temperatures that caused the solvent to boil. After complete addition of the bromide solution, the mixture was allowed to stir for an additional 20 minutes. At this time all bromide was consumed. *Note: to check for consumption of the bromide, an aliquot of the solution (<50 μL) was removed and quenched with water. Addition of Et_2O and TLC (25% Et_2O in hexanes) analysis of the organic layer against bromide 221 revealed complete consumption.*

To a separate round-bottom flask was added CuBr•Me_2S (84 mg, 0.41 mmol, 25 mol %), followed by THF (2.0 mL) and HMPA (1.71 mL, 9.8 mmol, 6 equiv). The solution was cooled to –40 °C (dry ice/acetonitrile), then TMSCl (0.31 mL, 2.45 mmol, 1.5 equiv) was added, and finally enone **215**[29,30] (180 mg, 1.63 mool, 1 equiv). The Grignard solution

was added dropwise to the cooled solution over the course of 30 minutes. The solution was maintained at –40 °C, and allowed to stir for an additional 2 hours before being gradually warmed to ambient temperature. After warming, the solution was cooled to –78 °C and Et_3N was added. The solution was stirred for 10 minutes. Satd. aq. $NaHCO_3$ (5 mL) was added and the frozen solution was allowed to gradually warm to ambient temperature. NH_4OH (0.2 mL) was added followed by EtOAc (5 mL) and water (10 mL). The layers were separated and the aqueous layer was extracted with EtOAc (3x15 mL). The combined organic layers were washed with water (2x15 mL), brine (10 mL), dried over Na_2SO_4 and concentrated. The crude residue was azeotroped with benzene (15 mL) and placed under high-vacuum for >2 h. The material was used without further purification.

To the dried silyl enol ether was added THF (2.0 mL) and HMPA (0.853 mL, 4.90 mmol, 3 equiv), and the solution was cooled to –10 °C (NaCl/ice bath). MeLi (1.32 mL, 1.716 mmol, 1.05 equiv) was added dropwise to the stirring solution, resulting in a pale deep red solution. The solution was stirred for 20 minutes, then cooled to –78 °C. Allyl iodide (0.448 mL, 4.9 mmol, 3 equiv) and HMPA (0.853 mL) were added dropwise as a solution in THF. The mixture was maintained at –78 °C for 5.5 hours then quenched by addition of NH_4Cl (5 mL) and $Na_2S_2O_3$ (1 mL), then warmed to ambient temperature. EtOAc (5 mL) was added followed by water (10 mL) and the layers were separated. The aqueous layer was extracted with EtOAc (3x15 mL), washed with water (10 mL), brine (10 mL), dried over Na_2SO_4, and concentrated. The crude residue was purified by silica gel flash column (0 → 30 % Et_2O in hexanes) to give the title compound as a pale yellow oil (371 mg, 60% yield over 2 steps)

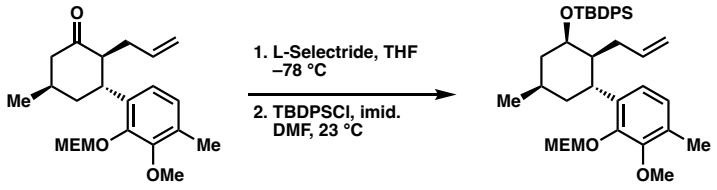
^{1}H NMR: (400 MHz, $CDCl_3$) δ 6.93 – 6.88 (m, 1H), 6.86 (d, *J* = 8.0 Hz, 1H), 5.72 (ddt, *J* = 17.0, 10.3, 6.9 Hz, 1H), 5.18 (d, *J* = 5.6 Hz, 1H), 5.15 (d, *J* = 5.5 Hz, 1H), 4.90 – 4.81 (m, 2H), 3.94 – 3.84 (m, 2H), 3.75 (s, 3H), 3.62 – 3.48 (m, 3H), 3.38 (s, 4H), 2.72 – 2.58 (m, 2H), 2.40 – 2.29 (m, 2H), 2.28 – 2.20 (m, 4H), 2.08 – 1.92 (m, 2H), 1.77 (dtd, *J* = 13.7, 4.4, 1.6 Hz, 1H), 1.02 (d, *J* = 7.1 Hz, 3H).

^{13}C NMR: (100 MHz, $CDCl_3$) δ 212.3, 151.2, 148.1, 136.8, 135.7, 130.5, 126.3, 122.2, 115.9, 98.4, 71.8, 69.3, 60.0, 59.2, 54.8, 48.4, 39.2, 38.1, 32.2, 30.6, 19.6, 15.8.

IR: (neat film, NaCl) 2922, 1710, 1448, 1420, 1272, 1170, 1110, 1056, 1016, 974, 916, 850, 826, 756, 684, 622 cm^{-1}

HRMS: (ESI+) *m/z* calc'd for $C_{24}H_{31}O_5$ $[M+H]^+$: 399.2166 found 399.2141

$[\alpha]_D^{23}$: 20.0 (*c* = 1, $CHCl_3$)



225 ***226***

Silyl ether 226: In a round-bottom flask, a solution of ketone **225** (450 mg, 1.195 mmol, 1 equiv) in THF (6.0 mL) was cooled to –78 °C. L-selectride (1.0 M in THF, 1.375 mL, 1.375 mmol, 1.15 equiv) was added dropwise. The solution was stirred at –78 °C for two hours before being warmed to ambient temperature and stirred for an additional eight hours. The solution was cooled to 0 °C and NaOH (2.0 M, 0.7 mL) was added followed by H_2O_2 (27% w/w, 0.7 mL) and the solution was stirred at 0 °C for two hours. Water (10 mL) and $Na_2S_2O_3$ (5 mL) were added. The layers were separated, and the aqueous layer was extracted with Et_2O (3x10 mL). The combined organic layers were washed with brine (10 mL), dried over Na_2SO_4, and concentrated. The crude oil was passed through a plug of silica gel, eluting with 30% EtOAc in hexanes, concentrated, and used without further purification. A portion of the crude oil was used in the next step.

To the crude alcohol (200 mg, assumed 100% purity, 0.528 mmol, 1 equiv) was added DMF (1.76 mL) and imidazole (144 mg, 2.1 mmol, 4 equiv). TBDPSCl (0.28 μL, 1.06 mmol, 2 equiv) was added dropwise and the mixture was stirred for 12 hours. Water (20 mL) was added followed by Et_2O (10 mL). The layers were separated, and the aqueous layer was extracted with Et_2O (3x7 mL). The combined organic layers were washed with brine (10 mL), dried over Na_2SO_4, and concentrated. The crude residue was purified by silica gel flash column (10 % Et_2O in hexanes) to give the title compound as a colorless oil (290 mg, 77% yield over 2 steps).

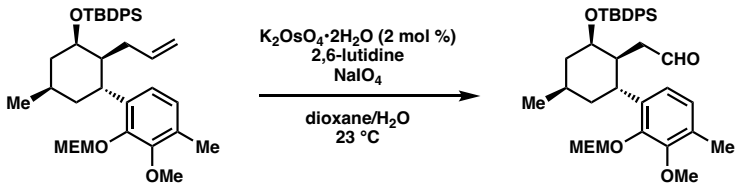
^{1}H NMR: (400 MHz, $CDCl_3$) δ 7.76 – 7.64 (m, 4H), 7.47 – 7.30 (m, 6H), 6.62 – 6.55 (m, 1H), 6.40 (d, *J* = 8.0 Hz, 1H), 5.64 (dddd, *J* = 16.8, 9.9, 8.3, 5.4 Hz, 1H), 5.19 (d, *J* = 5.2 Hz, 1H), 5.04 (d, *J* = 5.3 Hz, 1H), 4.97 – 4.86 (m, 2H), 4.16 (dt, *J* = 8.6, 4.2 Hz, 1H), 3.96 – 3.82 (m, 2H), 3.72 (s, 3H), 3.57 (t, *J* = 4.7 Hz, 2H), 3.39 (s, 4H), 2.75 – 2.64 (m, 1H), 2.20 (s, 3H), 2.01 (dt, *J* = 14.2, 8.9 Hz, 1H), 1.88 (dq, *J* = 8.2, 3.9 Hz, 1H), 1.76 – 1.67 (m, 1H), 1.64 – 1.56 (m, 1H), 1.56 – 1.35 (m, 3H), 1.08 (s, 9H), 0.92 (d, *J* = 5.8 Hz, 3H).

^{13}C NMR: (100 MHz, $CDCl_3$) δ 151.2, 148.0, 139.2, 138.2, 136.2, 136.1, 134.9, 134.7, 134.3, 129.68, 129.65, 129.61, 127.7, 127.6, 125.3, 122.7, 115.3, 98.0, 71.9, 71.0, 69.3, 60.0, 59.2, 44.2, 38.8, 35.2, 34.4, 31.6, 27.7, 27.3, 22.6, 19.5, 15.8.

IR: (neat film, NaCl)

HRMS: (ESI+) *m/z* calc'd for $C_{38}H_{52}O_5SiNa$ $[M+Na]^+$: 639.3476, found 639.3478

$[\alpha]_D^{23}$: –5.7 (*c* = 1, $CHCl_3$)



226 ***227***

Rigorous exclusion of air and moisture is not necessary

Aldehyde 227: To a round bottom flask was added **226** (245 mg, 0.397 mmol, 1 equiv). Dioxane (1.5 mL) and water (0.5 mL) were added followed by 2,6-lutidine (92 µL, 0.794 mmol, 2 equiv). The mixture was vigorously stirred. $K_2OsO_4•2H_2O$ (3 mg, 0.0079 mmol, 2 mol %) was added followed by $NaIO_4$ (340 mg, 1.59 mmol, 4 equiv). The mixture was stirred vigorously for 3 hours, after which time TLC indicated complete consumption of the olefin. Water was added followed by EtOAc. The layers were separated, and the aqueous layer was extracted with EtOAc (3x2 mL). The combined organic layers were washed with brine, dried over Na_2SO_4, and concentrated. The crude residue was purified by silica gel flash column to give the title compound as a brown oil (94 mg, 45% yield).

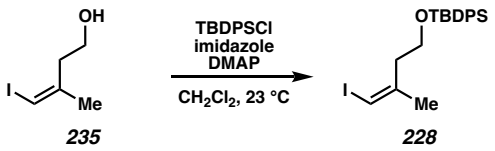
^{1}H NMR: (500 MHz, C_6D_6) δ 9.08 (s, 1H), 7.81 (dt, *J* = 5.8, 1.7 Hz, 2H), 7.78 – 7.73 (m, 2H), 7.29 – 7.16 (m, 6H), 6.70 (d, *J* = 8.0 Hz, 1H), 6.66 (d, *J* = 8.0 Hz, 1H), 5.33 (d, *J* = 5.4 Hz, 1H), 5.30 (d, *J* = 5.5 Hz, 1H), 4.35 (dt, *J* = 6.6, 3.7 Hz, 1H), 3.97 – 3.84 (m, 2H), 3.77 (td, *J* = 7.4, 4.4 Hz, 1H), 3.56 (s, 3H), 3.41 (ddd, *J* = 5.7, 4.4, 1.4 Hz, 2H), 3.12 (s, 3H), 2.63 (dd, *J* = 17.2, 6.7 Hz, 1H), 2.53 (qd, *J* = 6.7, 3.3 Hz, 1H), 2.17 (s, 4H), 1.86 – 1.53 (m, 4H), 1.21 (s, 9H), 1.17 (d, *J* = 6.7 Hz, 3H).

^{13}C NMR: (125 MHz, C_6D_6) δ 200.4, 151.7, 148.9, 137.6, 136.6, 134.5, 134.3, 130.2, 130.1, 130.0, 128.6, 126.1, 122.6, 98.7, 72.3, 71.7, 69.9, 59.7, 58.7, 44.2, 40.9, 38.5, 37.9, 33.3, 28.2, 27.5, 22.5, 19.7, 15.8.

IR: (neat film, NaCl) 3070, 2930, 2722, 1722, 1454, 1428, 1404, 1274, 1110, 1056, 1018, 972, 928, 858, 822, 740 704 cm^{-1}

HRMS: (ESI+) *m/z* calc'd for $C_{37}H_{50}O_6SiNa$ $[M+Na]^+$: 641.3269, found 641.3270

$[\boldsymbol{\alpha}]_{\boldsymbol{D}}^{\boldsymbol{23}}$**:** 14.3 (*c* = 1, $CHCl_3$)



235 ***228***

Vinyl iodide 228: To a round-bottom flask was added alcohol **235** (674 mg, 3.179 mmol, 1 equiv) (prepared according to May[37]) and CH_2Cl_2 (15 mL). Imidazole (303 mg, 4.45 mmol, 1.4 equiv) and DMAP (39 mg, 0.317 mmol, 10 mol%) were sequentially added. The solution was then cooled to 0 °C and TBDPSCl (0.91 mL, 3.497 mmol, 1.1 equiv) was added. The solution was warmed to ambient temperature and maintained for 1 hour. Water (50 mL) was added, the layers were separated, and the aqueous layer was extracted with CH_2Cl_2 (3x15 mL). The combined organic layers were washed with brine (10 mL), dried over Na_2SO_4, and concentrated. The crude oil was purified by silica gel flash column (0→5% EtOAc in hexanes) to give the title compound as a colorless oil that solidified upon cooling to –20 °C (1.31 g, 92% yield).

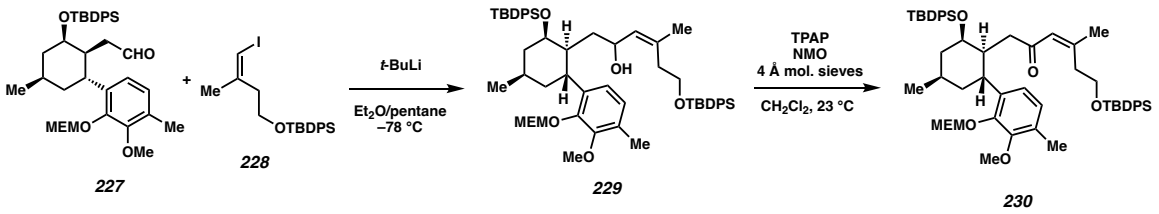
EFH-XII-295

^{1}H NMR: (500 MHz, $CDCl_3$) δ 7.71 – 7.64 (m, 4H), 7.46 – 7.35 (m, 6H), 5.92 (q, *J* = 1.5 Hz, 1H), 3.76 (t, *J* = 6.8 Hz, 2H), 2.50 (t, *J* = 6.8 Hz, 2H), 1.89 (d, *J* = 1.5 Hz, 3H), 1.06 (s, 9H).

^{13}C NMR: (125 MHz, $CDCl_3$) δ 145.3, 135.8, 133.8, 129.8, 127.8, 75.7, 61.6, 41.7, 27.0, 24.4, 19.3.

IR: (neat film, NaCl) 3070, 2930, 2856, 1472, 1428, 1264, 1110, 910, 824, 740, 702, 610 cm^{-1}

HRMS: (FD+) *m/z* calc'd for $C_{21}H_{27}OSiI$ $[M]^+$: 450.08704, found 450.08543



Enone 230: To a flame-dried test tube with stir bar was charged aldehyde **227** (40 mg, 0.0646 mmol, 1 equiv). The aldehyde was azeotroped from benzene (1 mL) and placed under high vacuum for > 2 hours prior to use. In a separate flame-dried test tube, vinyl iodide **228** (58.2 mg, 0.129 mmol, 2 equiv) was added, azeotroped from benzene (1 mL) and placed under high vacuum for >2 hours prior to use. To the test tube containing vinyl iodide **228** was added Et_2O (0.35 mL), and the solution was cooled to –78 °C. *tert*-Butyllithium (1.7 M in pentane, 0.14 mL, 0.236 mmol, 3.65 equiv) was added dropwise and stirred for 40 minutes. The solution became pale yellow in color. The solution was then warmed to 0 °C and stirred for 20 minutes. During this time the solution became colorless. Then the solution was again cooled to –78 °C. Aldehyde **227** was dissolved in Et_2O (0.65 mL) and added dropwise to the stirring vinyllithium species. And additional 0.35 mL of Et_2O were used to wash the test tube and complete the transfer. The solution was stirred at –78 °C for 2 hours and then quenched by addition of aq. pH = 6 phosphate buffer (1 mL) and $Na_2S_2O_3$ (0.2 mL). The layers were separated, and the aqueous layer was extracted with Et_2O (3x1 mL). The combined organic layers were washed with brine (1 mL), dried over Na_2SO_4, and concentrated. The crude residue was passed through a pad of silica gel, eluting first with 2% acetone in hexanes (15 mL) to remove protodehalogenated vinyl species. Then with 30% acetone in hexanes (30 mL) to collect all remaining material. The crude mixture of diastereomeric allylic alcohols was concentrated and used without further purification (48 mg).

To a flame dried test tube was added 4Å molecular sieves (powder, freshly microwave activated, 185 mg). The diastereomeric mixture of alcohols (48 mg) was added as a solution in CH_2Cl_2 (1.0 mL). N-Methyl morpholine N-oxide (17.9 mg,, 0.153 mmol, 3 equiv) was added and the solution was allowed to stir for 5 minutes. TPAP (0.35 mg, 0.001 mmol, 2 mol %) was added, and the mixture was stirred for 12 hours. After this time, the contents of the reaction were filtered through a pad of celite, eluting with CH_2Cl_2 and the filtrate was concentrated. The crude residue was purified by silica gel flash column (20% EtOAc in hexanes) to give the title compound as a colorless oil (38.1 mg, 63% yield over 2 steps).

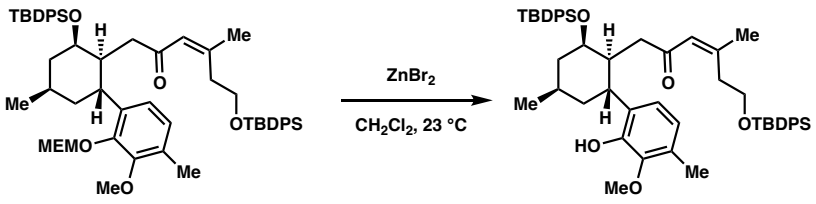
^{1}H NMR: (500 MHz, $CDCl_3$) δ 7.75 – 7.60 (m, 8H), 7.44 – 7.29 (m, 12H), 6.65 (d, *J* = 7.9 Hz, 1H), 6.55 (d, *J* = 8.0 Hz, 1H), 5.62 (s, 1H), 5.22 (d, *J* = 5.4 Hz, 1H), 5.13 (d, *J* = 5.4 Hz, 1H), 4.25 (dt, *J* = 6.8, 3.5 Hz, 1H), 3.98 – 3.90 (m, 2H), 3.76 (s, 3H), 3.72 (t, *J* = 6.5 Hz, 2H), 3.60 – 3.47 (m, 3H), 3.37 (s, 3H), 2.73 (dt, *J* = 12.6, 6.4 Hz, 1H), 2.68 – 2.56 (m, 2H), 2.38 (dtd, *J* = 9.1, 6.0, 3.1 Hz, 1H), 2.23 – 2.08 (m, 4H), 1.82 – 1.72 (m, 4H), 1.72 – 1.54 (m, 2H), 1.12 (d, *J* = 6.9 Hz, 3H), 1.09 (s, 9H), 1.04 (s, 9H).

^{13}C NMR: (125 MHz, $CDCl_3$) δ 199.5, 155.7, 151.1, 148.0, 137.5, 136.3, 136.3, 135.7, 134.4, 134.2, 133.9, 129.7, 129.6 127.72, 127.70, 127.63, 127.59, 126.0, 124.9, 122.8, 98.1, 71.9, 71.8, 69.3, 63.4, 60.0, 59.1, 43.8, 41.2, 38.3, 37.1, 27.6, 27.4, 27.0, 26.9, 22.4, 19.7, 19.3, 15.8.

IR: (neat film, NaCl) 3070, 2930, 2856, 1684, 1616, 1458, 1428, 1274, 1110, 1056, 976, 912, 822, 736, 704, 686, 613 cm^{-1}

HRMS: (ESI+) *m/z* calc'd for $C_{58}H_{76}O_7Si_2Na$ $[M+Na]^+$: 963.5022, found 963.5022

$[\alpha]_D^{23}$: 32.6 (c = 1, $CHCl_3$)



230 ***231***

Phenol 231: In a nitrogen filled glovebox, $ZnBr_2$ (finely crushed to a powder, 64 mg, 0.282 mmol, 7 equiv) was added to a test tube, sealed with a septum, and removed from the glovebox. Enone **230** (38 mg, 0.0404 mmol, 1 equiv) was transferred to the reaction vessel as a solution in CH_2Cl_2 (0.5 mL). The resulting heterogeneous mixture was vigorously stirred for 6 hours, after which time TLC analysis indicated complete consumption of the starting material. The reaction was quenched by addition of satd. aq. $NaHCO_3$ (1 mL). The layers were separated and the aqueous layer was extracted with CH_2Cl_2 (5x0.5 mL). The combined organic layers were washed with brine, dried over Na_2SO_4, and concentrated. The crude residue was purified by silica gel flash column (0 → 20% Et_2O in hexanes) to give the title compound as a white foam (15 mg, 45% yield).

^{1}H NMR: (400 MHz, $CDCl_3$) δ 8.17 (s, 1H), 7.73 – 7.62 (m, 4H), 7.60 – 7.52 (m, 2H), 7.47 – 7.42 (m, 2H), 7.38 (dtd, *J* = 12.7, 5.1, 2.4 Hz, 7H), 7.29 (ddt, *J* = 8.1, 6.6, 1.1 Hz, 3H), 7.17 (ddd, *J* = 8.0, 6.7, 1.2 Hz, 2H), 6.59 (d, *J* = 8.0 Hz, 1H), 6.45 – 6.38 (m, 1H), 6.13 (d, *J* = 1.6 Hz, 1H), 3.85 (t, *J* = 6.3 Hz, 3H), 3.81 (s, 3H), 3.14 – 3.05 (m, 2H), 2.99 (dt, *J* = 12.6, 6.3 Hz, 1H), 2.82 (dt, *J* = 12.4, 6.2 Hz, 1H), 2.56 (dd, *J* = 18.7, 10.5 Hz, 1H), 2.43 – 2.34 (m, 1H), 2.25 (s, 3H), 1.97 (d, *J* = 1.3 Hz, 3H), 1.92 – 1.84 (m, 1H), 1.80 – 1.71 (m, 1H), 1.62 (dt, *J* = 12.5, 3.8 Hz, 1H), 1.42 – 1.32 (m, 1H), 1.31 – 1.20 (m, 2H), 1.05 (s, 10H), 0.97 (s, 9H), 0.94 (d, *J* = 6.5 Hz, 3H).

^{13}C NMR: (100 MHz, $CDCl_3$) δ 202.1, 148.0, 146.4, 135.8, 135.7, 135.6, 134.6, 133.9, 133.6, 129.7, 129.6, 129.5, 129.04, 128.97, 127.8, 127.6, 127.5, 124.7, 122.2, 120.4, 69.9, 63.3, 60.1, 41.4, 39.5, 38.4, 37.1, 35.5, 34.8, 32.5, 31.7, 28.5, 27.2, 27.1, 27.0, 22.9, 19.3, 19.3, 15.8, 14.3.

IR: (neat film, NaCl) 3324, 3072, 2928, 2858, 1614, 1460, 1428, 1388, 1250, 1220, 1108, 1062, 908, 822, 736, 702, 612 cm^{-1}

HRMS: (ESI+) *m/z* calc'd for $C_{54}H_{69}O_5Si_2$ $[M+H]^+$: 853.4605, found 853.4679.

$[\alpha]_D^{23}$: –2.6 (*c* = 1, $CHCl_3$)

4.8 REFERENCES AND NOTES

(1) Guillen, P. O.; Jaramillo, K. B.; Genta-Jouve, G.; Thomas, O. P. Marine Natural Products from Zoantharians: Bioactivity, Biosynthesis, Systematics, and Ecological Roles. *Nat. Prod. Rep.* **2020**, *37*, 515–540.

(2) Behenna, D. C.; Stockdill, J. L.; Stoltz, B. M. The Biology and Chemistry of the Zoanthamine Alkaloids. *Angew. Chem. Int. Ed.* **2008**, *47*, 2365–2386.

(3) Miyashita, M.; Sasaki, M.; Hattori, I.; Sakai, M.; Tanino, K. Total Synthesis of Norzoanthamine. *Science* **2004**, *305*, 495–499.

(4) Guillen, P. O.; Gegunde, S.; Jaramillo, K. B.; Alfonso, A.; Calabro, K.; Alonso, E.; Rodriguez, j.; Botana, L. M.; Thomas, O. P. Zoanthamine Alkaloids form the Zoantharian *Zoanthus* cf. *pulchellus* and Their Effects in Neuroinflammation. *Mar. Drugs* **2018**, *16*, 242.

(5) Rao, C. B.; Anjaneyula, A. S. R.; Sarma, N. S.; Venkatateswarlu, Y.; Rosser, R. M.; Faulkner, D. J.; Chen, M. H. M.; Clardy, J. Zoanthamine; a Novel Alkaloid from a Marine Zoanthid. *J. Am. Chem. Soc.* **1984**, *106*, 7983–7984.

(6) Cheng, Y.-B.; Lan, C.-C.; Liu, W.-C.; Lai, W.-C.; Tsai, Y.-C.; Chiang, M. Y.; Wu, Y.-C.; Chang, F.-R. Kuroshines A and B, New Alkaloids from Zoanthus Kuroshio. *Tetrahedron Lett.* **2014**, *55*, 5369–5372.

(7) Chen, S.-R.; Wang, S.-W.; Chang, F.-R.; Cheng, Y.-B. Anti-Lymphangiogenic Alkaloids from the Zoanthid Zoanthus Vietnamensis Collected in Taiwan. *J. Nat. Prod.* **2019**, *82*, 2790–2799.

(8) Cheng, Y.-B.; Lo, I.-W.; Shyur, L.-F.; Yang, C.-C.; Hsu, Y.-M.; Su, J.-H.; Lu, M.-C.; Chiou, S.-F.; Lan, C.-C.; Wu, Y.-C.; Chang, F.-R. New Alkaloids from Formosan Zoanthid *Zoanthus Kuroshio*. *Tetrahedron* **2015**, *71*, 8601–8606.

(9) Takahashi, Y.; Yoshimura, F.; Tanino, K.; Miyashita, M. Total Synthesis of Zoanthenol. *Angew. Chem. Int. Ed.* **2009**, *48*, 8905–8908.

(10) Murata, Y.; Yamashita, D.; Kitahara, K.; Minasako, Y.; Nakazaki, A.; Kobayashi, S. Synthetic Study of (−)-Norzoanthamine: Construction of the ABC Ring Moiety. *Angew. Chem. Int. Ed.* **2009**, *48*, 1400–1403.

(11) Yamashita, D.; Murata, Y.; Hikage, N.; Takao, K.; Nakazaki, A.; Kobayashi, S. Total Synthesis of (−)-Norzoanthamine. *Angew. Chem. Int. Ed.* **2009**, *48*, 1404–1406.

(12) Xin, Z.; Wang, H.; He, H.; Zhao, X.; Gao, S. Asymmetric Total Synthesis of Norzoanthamine. *Angew. Chem. Int. Ed.* **2021**, *60*, 12807–12812.

(13) Wen, G.; Gu, S.; Chen, J.; He, H.; Gao, S. Synthetic Studies of Zoaramine: Construction of the Tetracyclic Skeleton in High Oxidation State. *Org. Lett.* **2025**, *27*, 2310–2316.

(14) Sun, Y.; Zhang, X.; Jiang, F.; Zhang, M.; Wu, W.; Sun, Y. Concise Synthesis of Norzoanthamine Enabled by a Set of Photochemical Transformations. *J. Am. Chem. Soc.* **2024**, *146*, 32305–32310.

(15) Zhuang, Z.; Sheng, T.; Qiao, J. X.; Yeung, K.-S.; Yu, J.-Q. Versatile Copper-Catalyzed γ-C(Sp3)–H Lactonization of Aliphatic Acids. *J. Am. Chem. Soc.* **2024,** *146*, 17311–17317.

(16) Call, A.; Cianfanelli, M.; Besalú-Sala, P.; Olivo, G.; Palone, A.; Vicens, L.; Ribas, X.; Luis, J. M.; Bietti, M.; Costas, M. Carboxylic Acid Directed γ-Lactonization of Unactivated Primary C–H Bonds Catalyzed by Mn Complexes: Application to

Stereoselective Natural Product Diversification. *J. Am. Chem. Soc.* **2022**, *144*, 19542–19558.

(17) Call, A.; Capocasa, G.; Palone, A.; Vicens, L.; Aparicio, E.; Choukairi Afailal, N.; Siakavaras, N.; López Saló, M. E.; Bietti, M.; Costas, M. Highly Enantioselective Catalytic Lactonization at Nonactivated Primary and Secondary γ-C–H Bonds. *J. Am. Chem. Soc.* **2023**, *145*, 18094–18103.

(18) Richers, J.; Heilmann, M.; Drees, M.; Tiefenbacher, K. Synthesis of Lactones via C–H Functionalization of Nonactivated C(Sp3)–H Bonds. *Org. Lett.* **2016**, *18*, 6472–6475.

(19) Xu, T.; Mal, S.; van Gemmeren, M. The Direct Pd-Catalyzed γ-Lactonization of Aliphatic Carboxylic Acids. *ACS Catal.* **2025**, 2735–2741.

(20) Chen, C.-M.; Hsieh, H.-P. Recent Advances in Total Synthesis of Natural Products by Masked Ortho-Benzoquinones. *J. Chin. Chem. Soc.* **2022**, *69*, 1210–1222.

(21) Liao, C.-C. Masked O-Benzoquinone Strategy in Organic Synthesis: Short and Efficient Construction of Cis-Decalins and Linear Triquinanes from 2-Methoxyphenols. *Pure Appl. Chem.* **2005**, *77*, 1221–1234.

(22) Liao, C.-C.; Peddinti, R. K. Masked O-Benzoquinones in Organic Synthesis. *Acc. Chem. Res.* **2002**, *35*, 856–866. h

(23) Harry, N. A.; Saranya, S.; Krishnan, K. K.; Anilkumar, G. Recent Advances in the Chemistry of Masked *Ortho* -Benzoquinones and Their Applications in Organic Synthesis. *Asian J. Org. Chem.* **2017**, *6*, 945–966.

(24) Greshock, T. J.; Funk, R. L. 6-Bromomethyl-4H-1,3-Dioxin: A Versatile Bromomethyl Vinyl Ketone Equivalent for Heterocycle and Carbocycle Construction. *J. Am. Chem. Soc.* **2002**, *124*, 754–755.

(25) Lai, C.-H.; Shen, Y.-L.; Wang, M.-N.; Kameswara Rao, N. S.; Liao, C.-C. Intermolecular Diels−Alder Reactions of Brominated Masked O-Benzoquinones with Electron-Deficient Dienophiles. A Detour Method to Synthesize Bicyclo[2.2.2]Octenones from 2-Methoxyphenols. *J. Org. Chem.* **2002**, *67*, 6493–6502.

(26) Surasani, S. R.; Rajora, V. S.; Bodipati, N.; Peddinti, R. K. Diels–Alder Reactions of Halogenated Masked *o*-Benzoquinones: Synthesis of Halogen-Substituted Bicyclo[2.2.2]Octenones. *Tetrahedron Lett.* **2009**, *50*, 773–775.

(27) Georgopanou, E.; Martini, K.-I.; Pantazis, P.; Pelagias, P.; Voulgari, P.; Hadjiarapoglou, L. P. Diels–Alder Cycloadditions of Masked o-Benzoquinones with Alkenes. *J. Org. Chem.* **2015**, *80*, 9682–9690.

(28) Chittimalla, S. K.; Liao, C.-C. Diels–Alder Reactions of Masked *o*-Benzoquinones with Acrylonitrile. *Tetrahedron* **2003**, *59*, 4039–4046.

(29) Huang, D.; Schuppe, A. W.; Liang, M. Z.; Newhouse, T. R. Scalable Procedure for the Fragmentation of Hydroperoxides Mediated by Copper and Iron Tetrafluoroborate Salts. *Org. Biomol. Chem.* **2016**, *14*, 6197–6200.

(30) Thomas, W. P.; Pronin, S. V. A Concise Enantioselective Approach to Quassinoids. *J. Am. Chem. Soc.* **2022**, *144*, 118–122.

(31) Tilstam, U.; Weinmann, H. Activation of Mg Metal for Safe Formation of Grignard Reagents on Plant Scale. *Org. Process Res. Dev.* **2002**, *6*, 906–910.

(32) Pangborn, A. B.; Giardello, M. A.; Grubbs, R. H.; Rosen, R. K.; Timmers, F. J. Safe and Convenient Procedure for Solvent Purification. *Organometallics* **1996**, *15*, 1518–1520.

(33) Sisa, M.; Dvorakova, M.; Temml, V.; Jarosova, V.; Vanek, T.; Landa, P. Synthesis, Inhibitory Activity and *in Silico* Docking of Dual COX/5-LOX Inhibitors with Quinone and Resorcinol Core. *Eur. J. Med. Chem.* **2020**, *204*, 112620.

(34) Prins, L. J.; Blázquez, M. M.; Kolarović, A.; Licini, G. Effective Synthesis of *Ortho*-Substituted Triphenol Amines via Reductive Amination. *Tetrahedron Lett.* **2006**, *47*, 2735–2738.

(35) Bertrand, F.; Basketter, D. A.; Roberts, D. W.; Lepoittevin, J.-P. Skin Sensitization to Eugenol and Isoeugenol in Mice: Possible Metabolic Pathways Involving Ortho-Quinone and Quinone Methide Intermediates. *Chem. Res. Toxicol.* **1997**, *10*, 335–343.

(36) Sun, D.; Chen, R.; Tang, D.; Xia, Q.; Zhao, Y.; Liu, C.-H.; Ding, H. Total Synthesis of (−)-Retigeranic Acid A: A Reductive Skeletal Rearrangement Strategy. *J. Am. Chem. Soc.* **2023**, *145*, 11927–11932.

(37) Luo, J.; May, J. A. Enantioselective Total Synthesis of Cannabinoids via a Tandem Conjugate Addition/Enolate Alkylation Annulation with Ambiphilic Organoboronates. *Org. Lett.* **2023**, *25*, 708–713.

APPENDIX 7

Spectra Relevant to Chapter 4:

Progress Toward the Total Synthesis of Kuroshine A

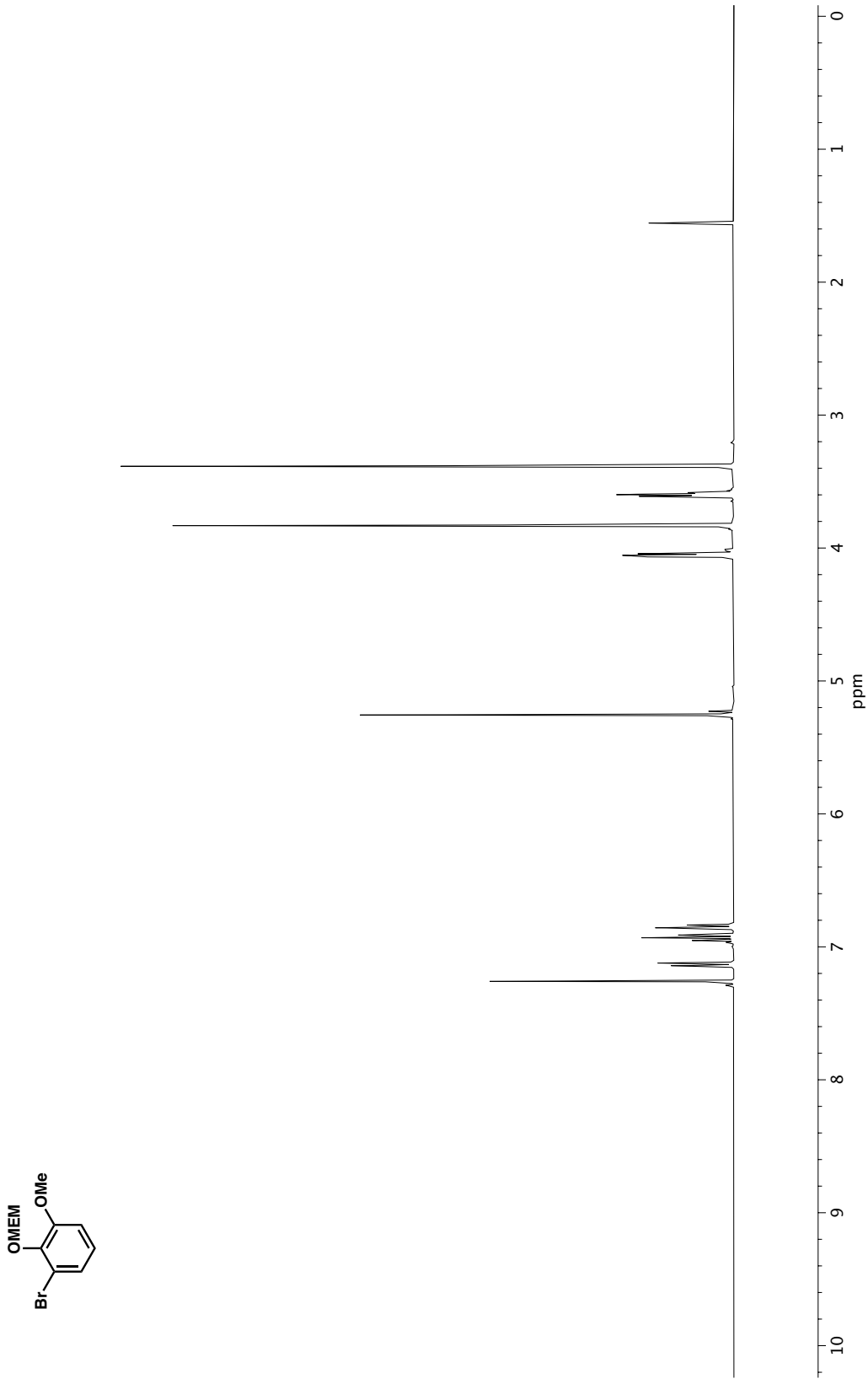


Figure A7.1 *^1H NMR (400 MHz, $CDCl_3$) of compound* ***205***.

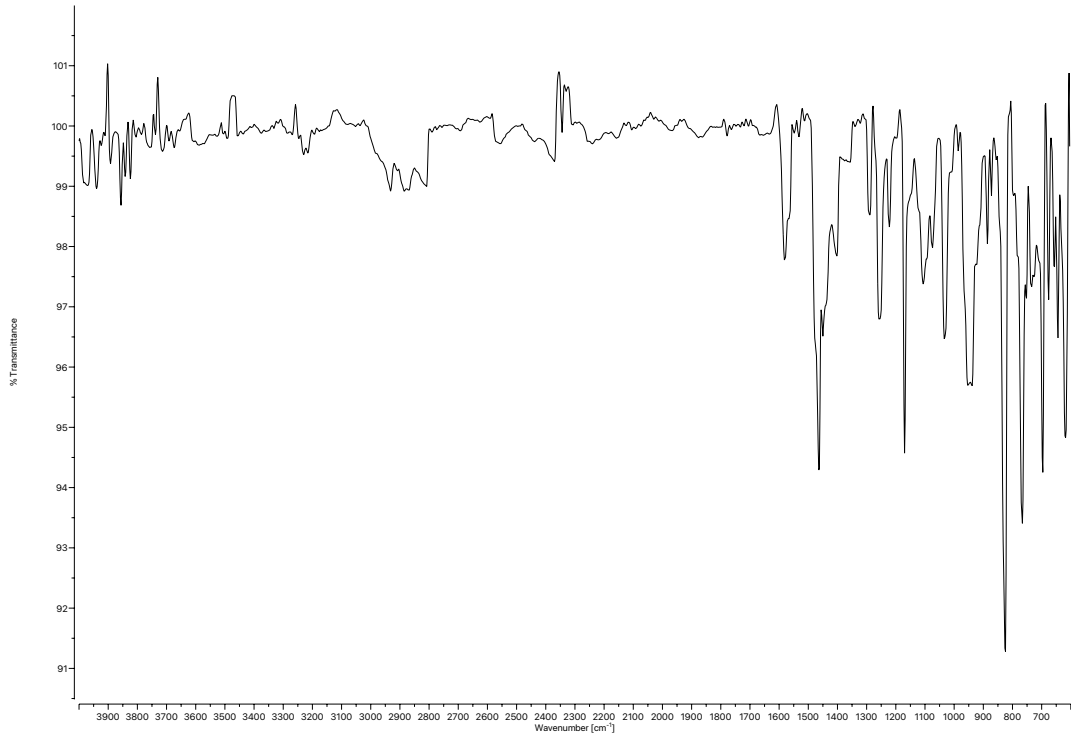


Figure A7.2 *Infrared spectrum (Thin Film, NaCl) of compound* ***205***.

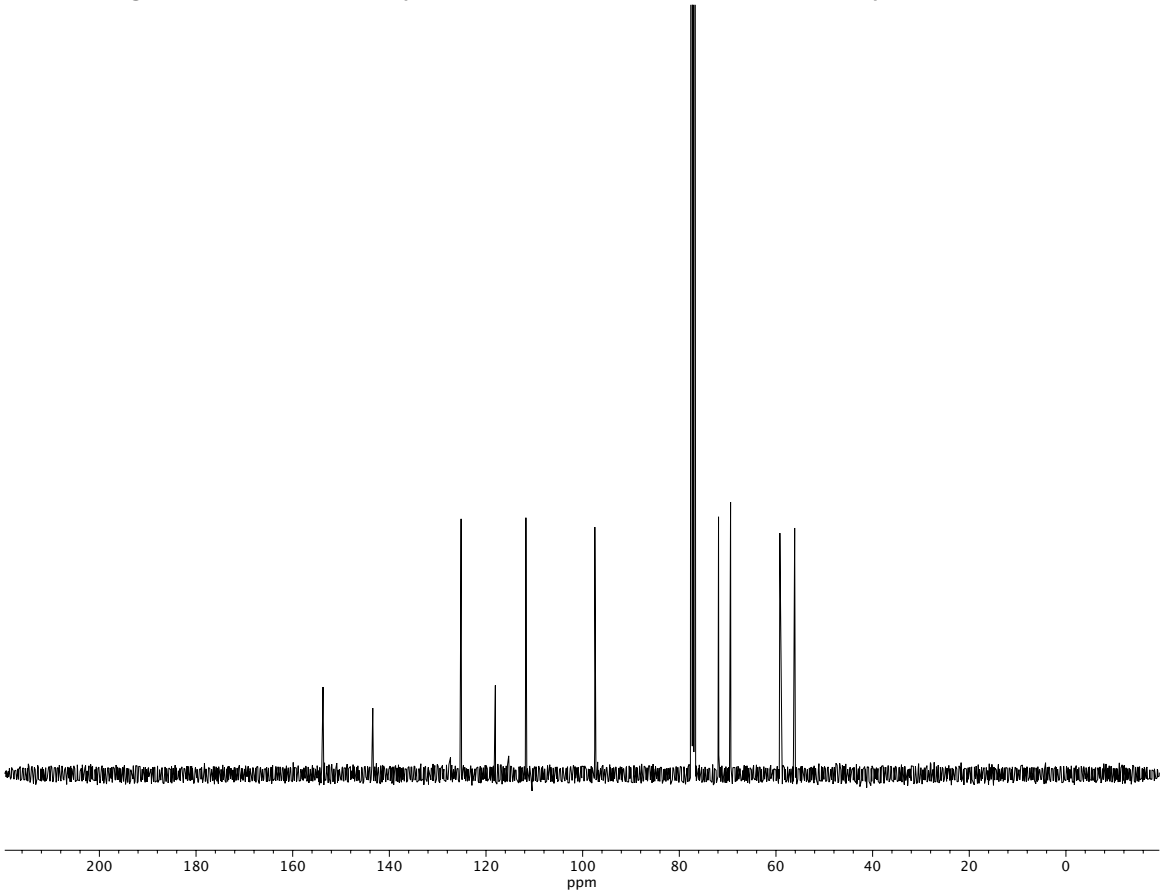


Figure A7.3 *^{13}C NMR (100 MHz, $CDCl_3$) of compound* ***205***.

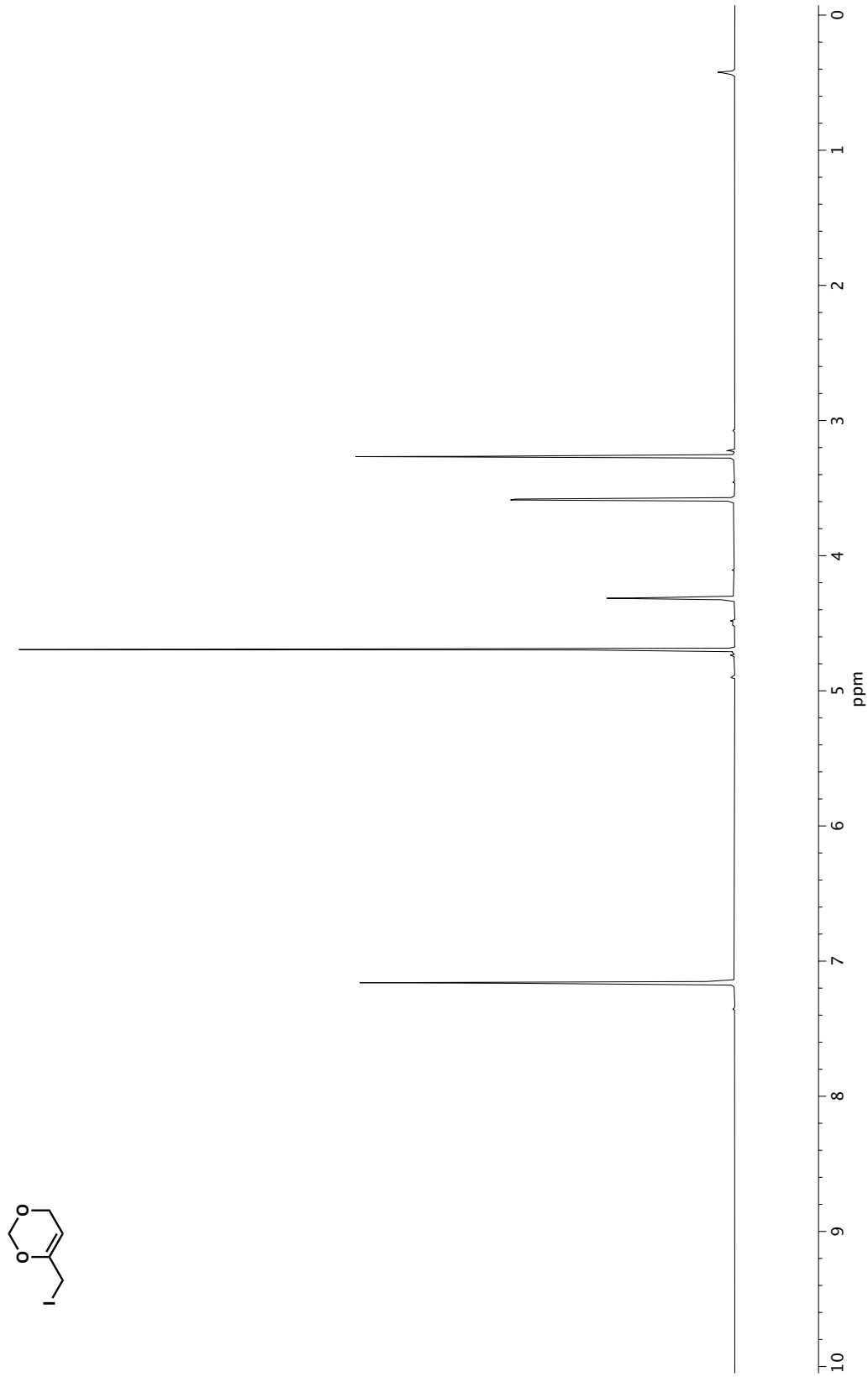


Figure A7.4 *^{1}H NMR (400 MHz, $CDCl_3$) of compound* ***207****.*

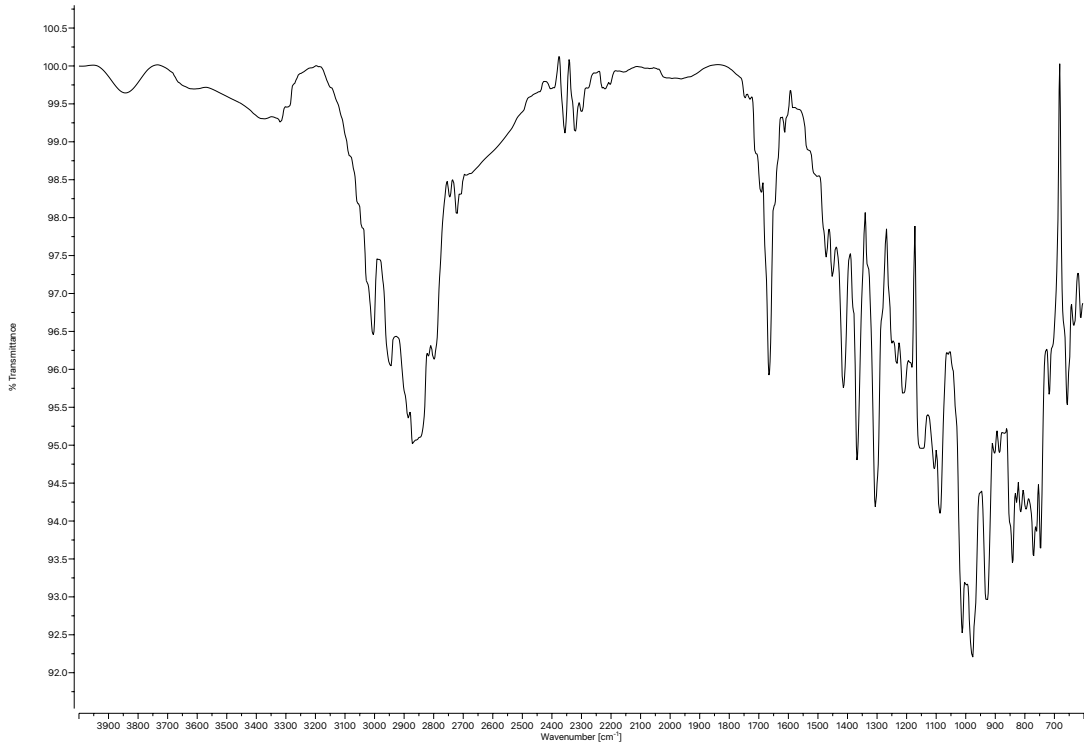


Figure A7.5 *Infrared spectrum (Thin Film, NaCl) of compound* ***207***.

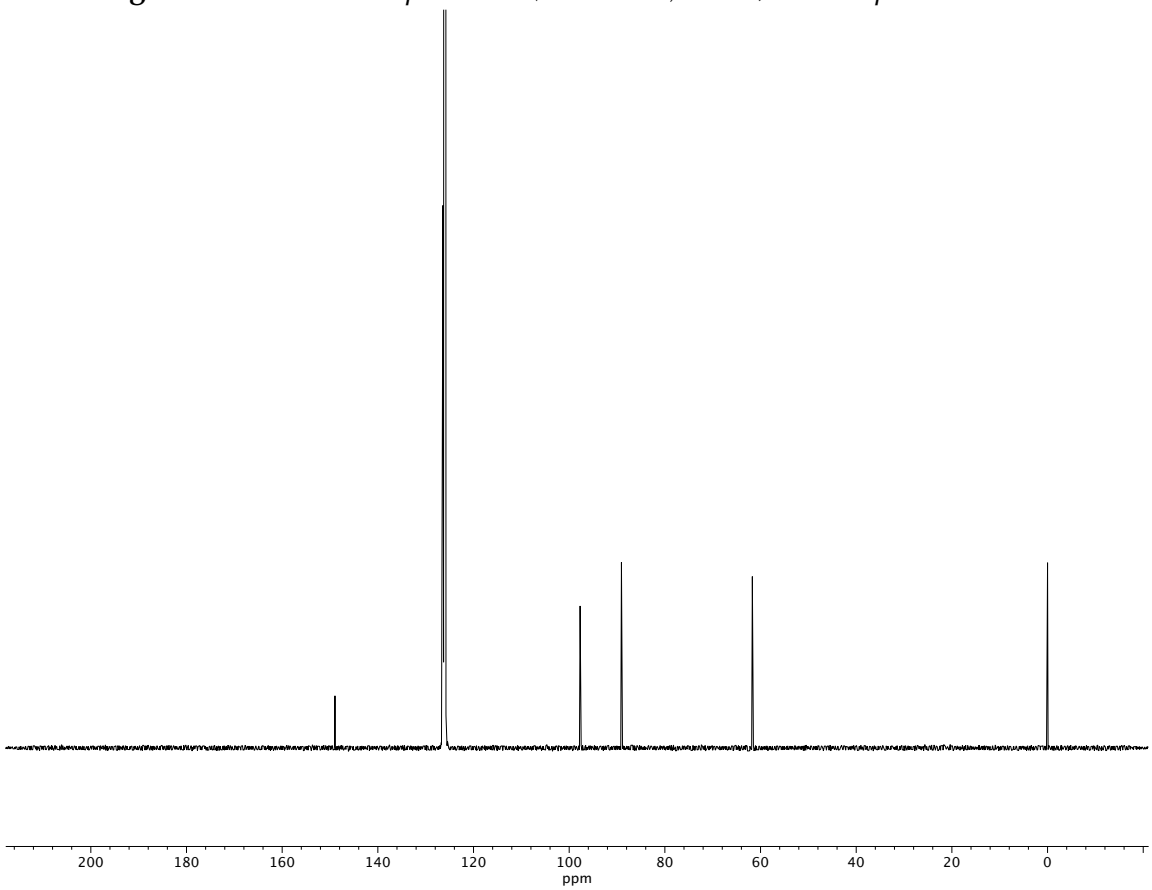


Figure A7.6 *^{13}C NMR (100 MHz, $CDCl_3$) of compound* ***207***.

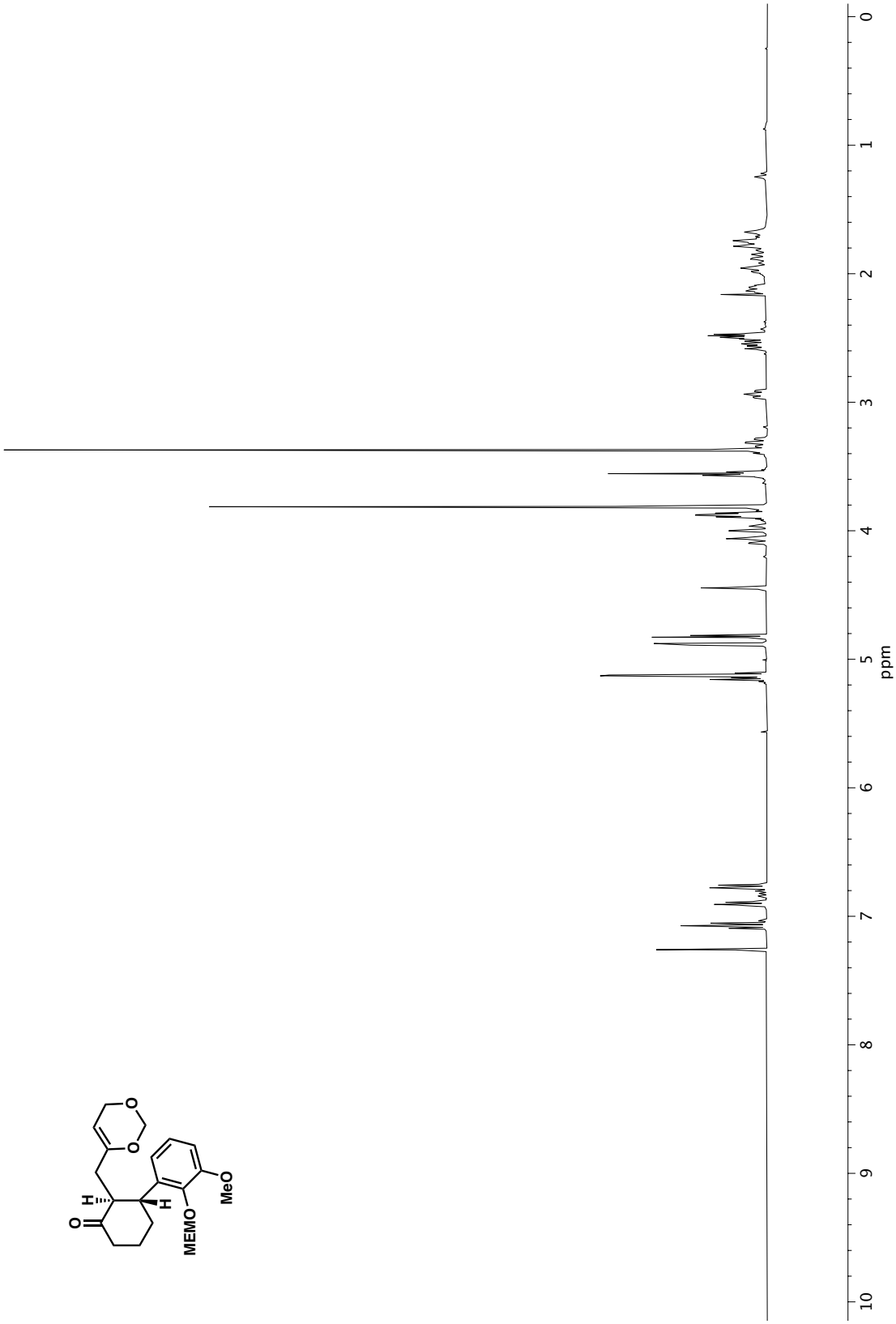


Figure A7.7 *^1H NMR (400 MHz, $CDCl_3$) of compound* ***208***.

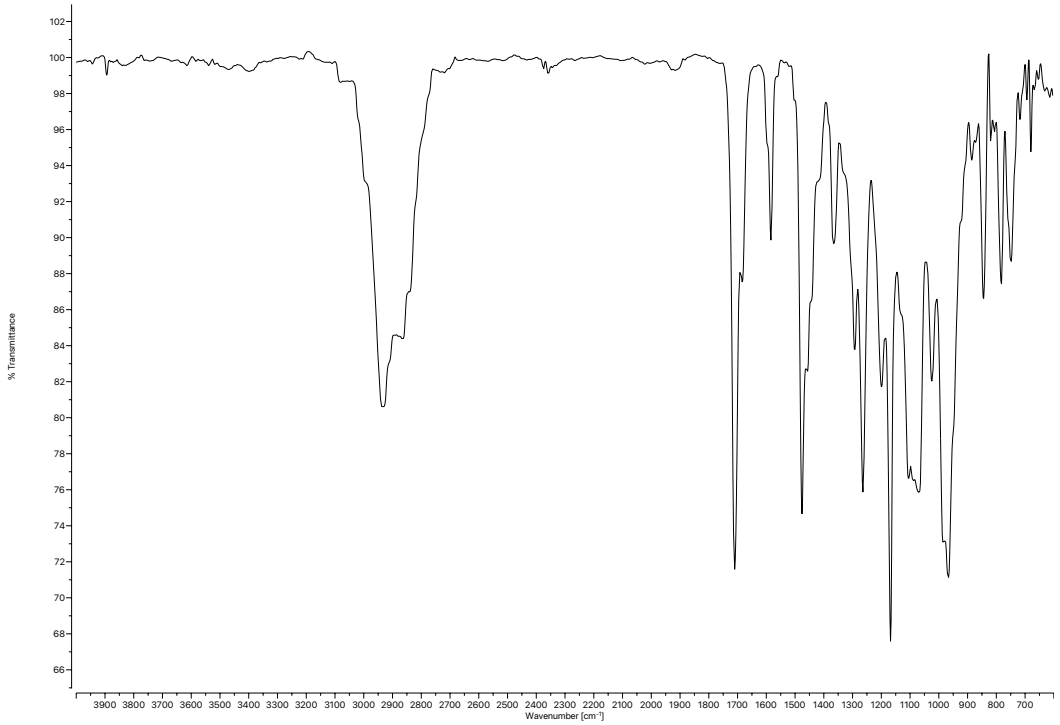


Figure A7.8 *Infrared spectrum (Thin Film, NaCl) of compound* ***208***.

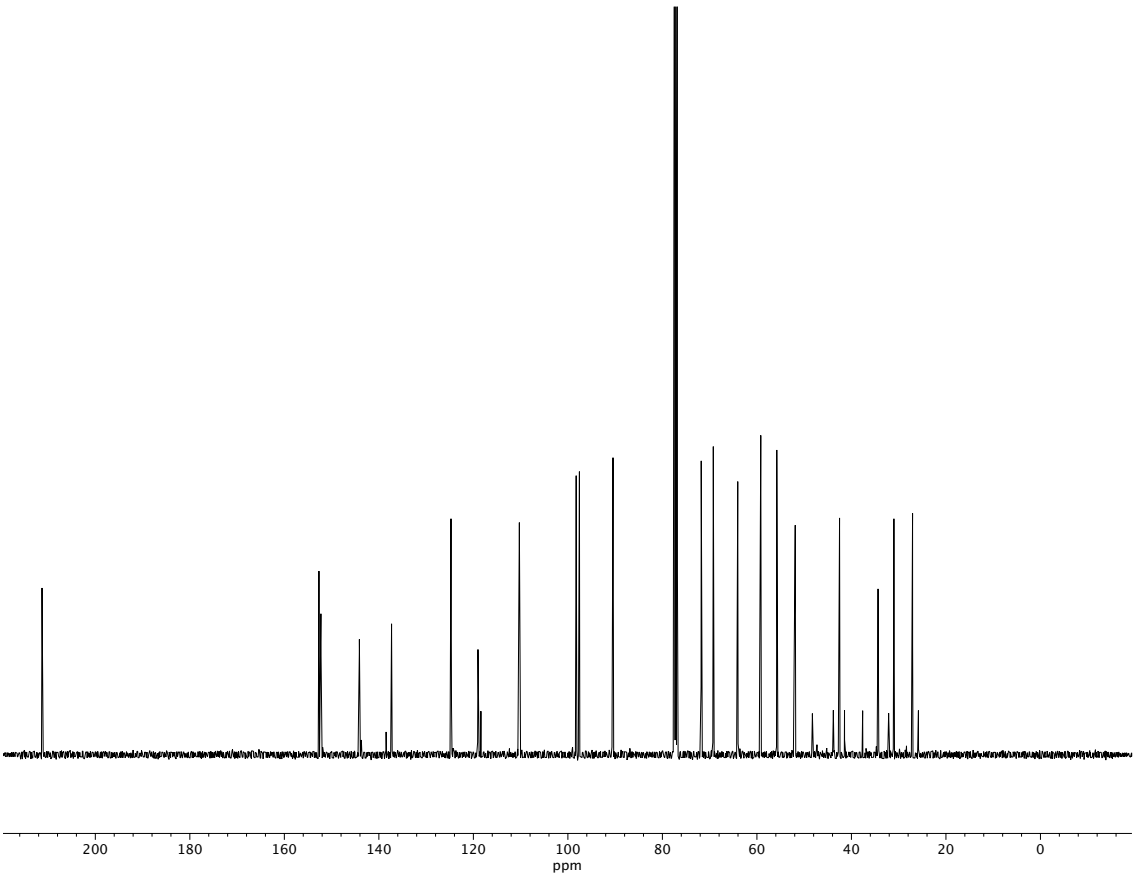


Figure A7.9 *^{13}C NMR (100 MHz, $CDCl_3$) of compound* ***208***.

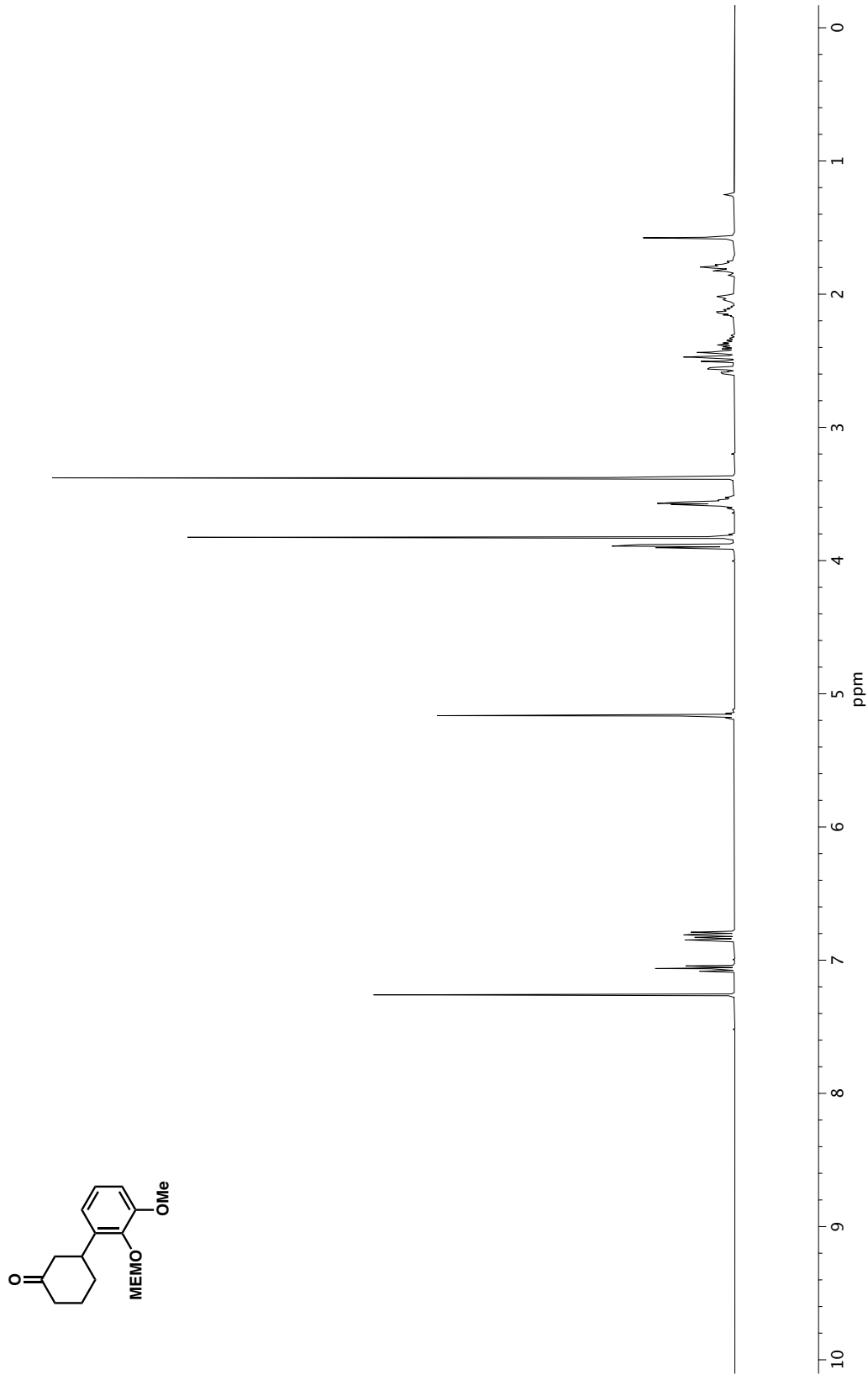


Figure A7.10 *^1H NMR (400 MHz, $CDCl_3$) of compound* ***233***.

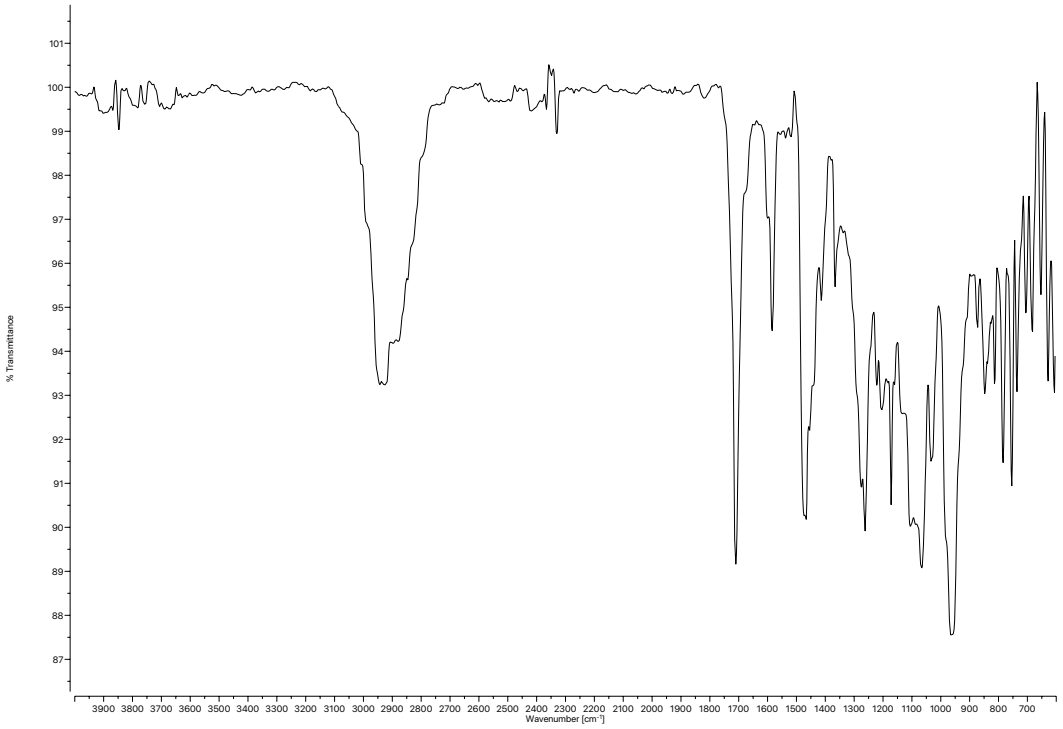


Figure A7.11 *Infrared spectrum (Thin Film, NaCl) of compound* ***233***.

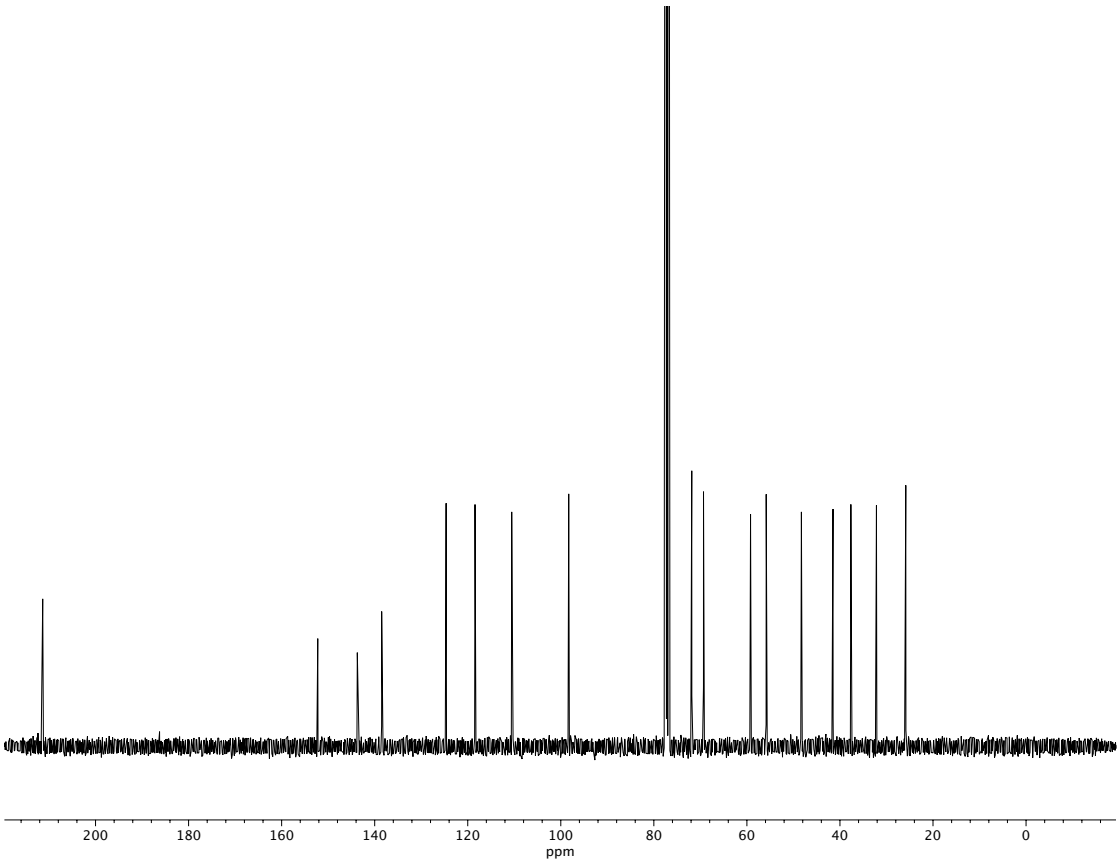


Figure A7.12 *^{13}C NMR (100 MHz, $CDCl_3$) of compound* ***234***.

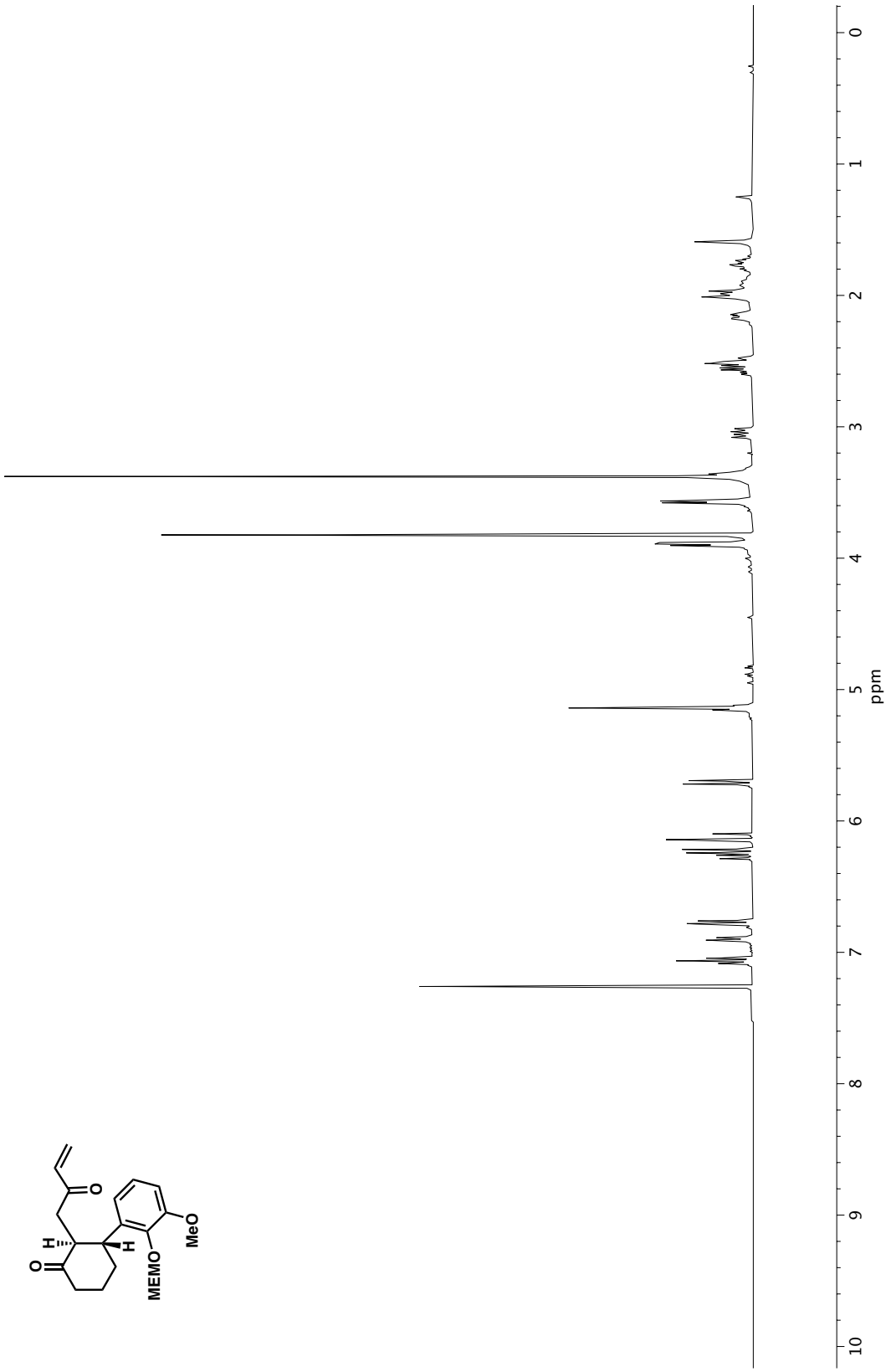


Figure A7.13 *^1H NMR (400 MHz, $CDCl_3$) of compound **209**.*

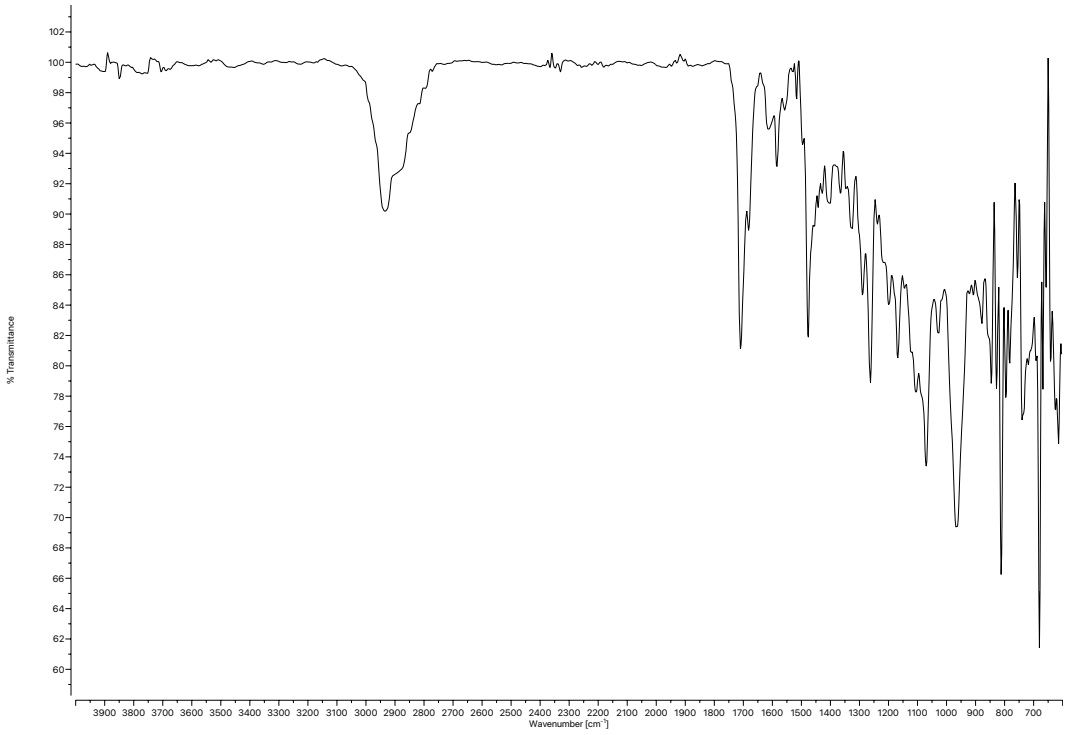


Figure A7.14 *Infrared spectrum (Thin Film, NaCl) of compound* ***209***.

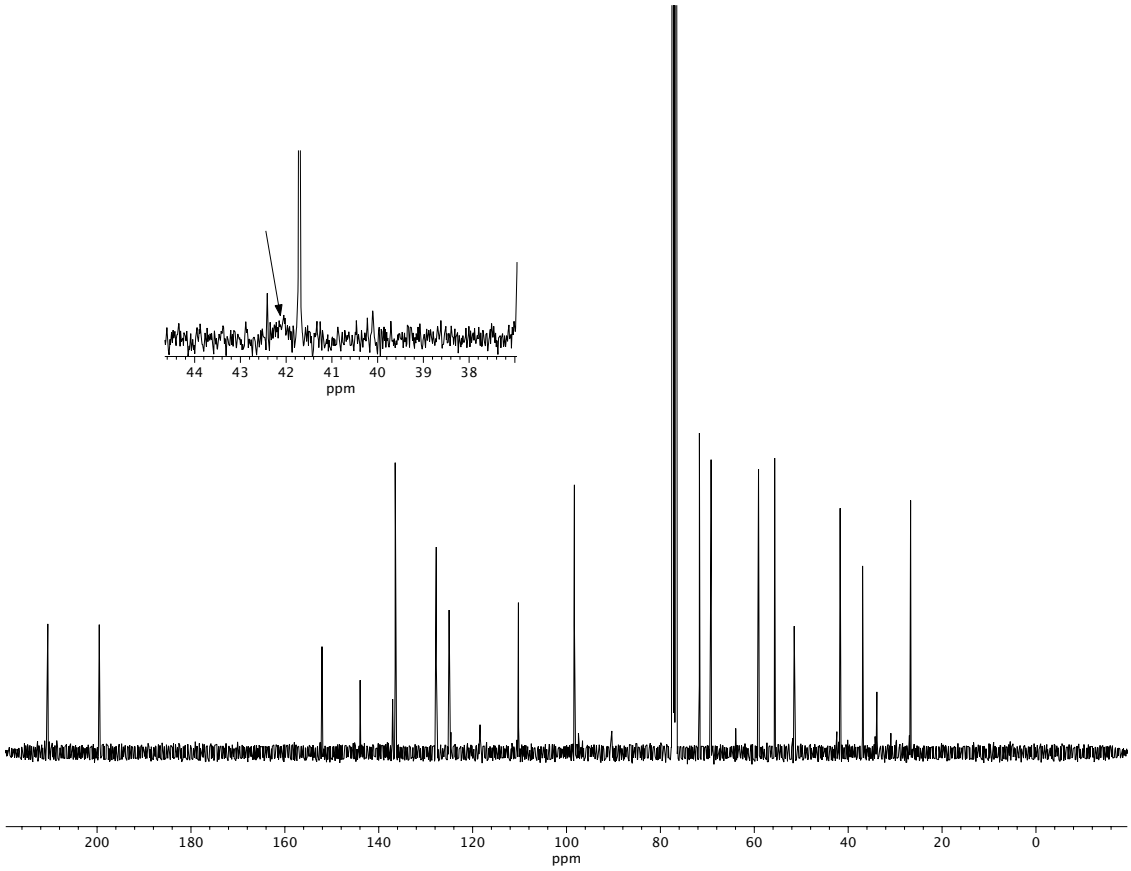


Figure A7.15 *^{13}C NMR (100 MHz, $CDCl_3$) of compound* ***209***.

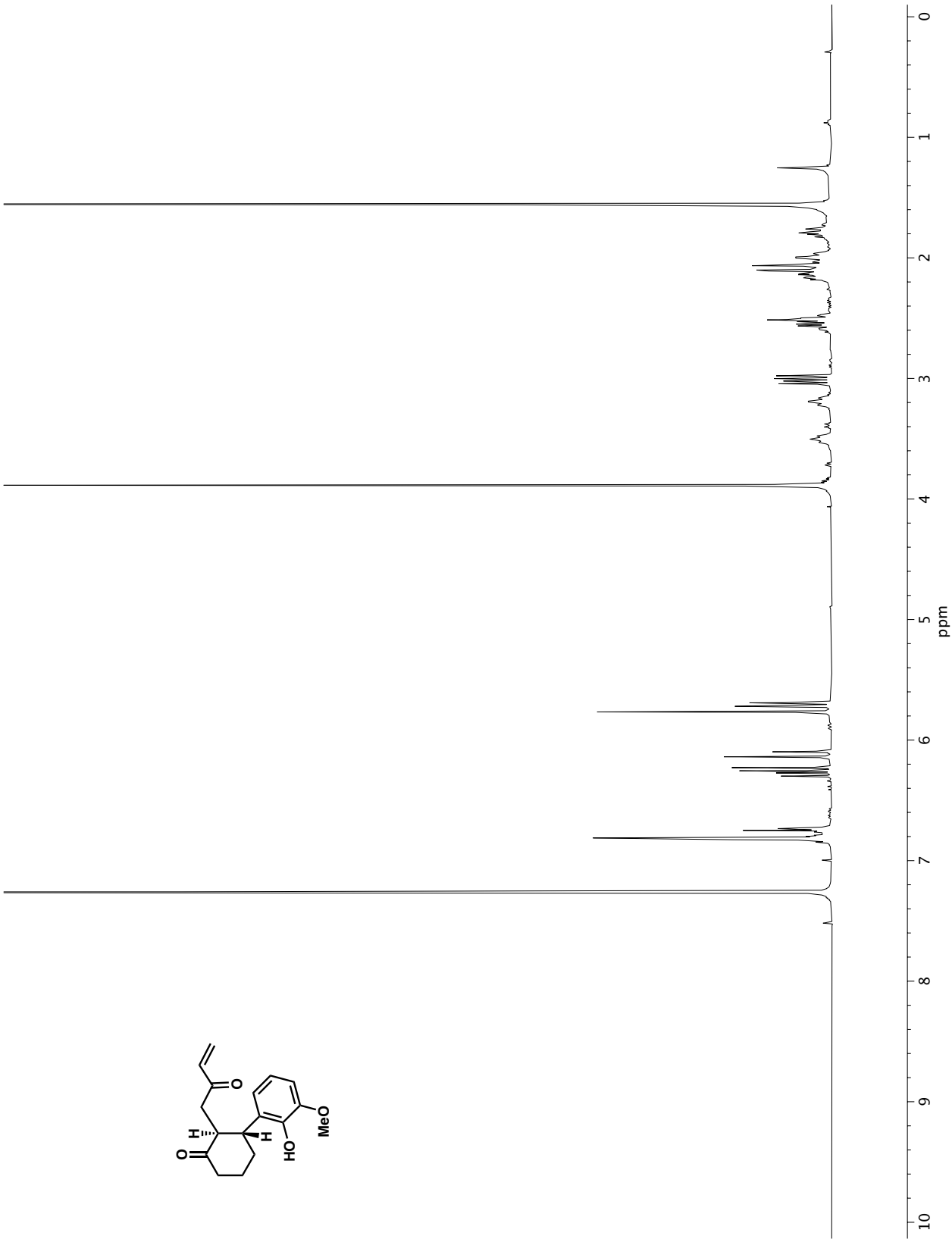


Figure A7.16 *^{1}H NMR (400 MHz, $CDCl_3$) of compound **210**.*

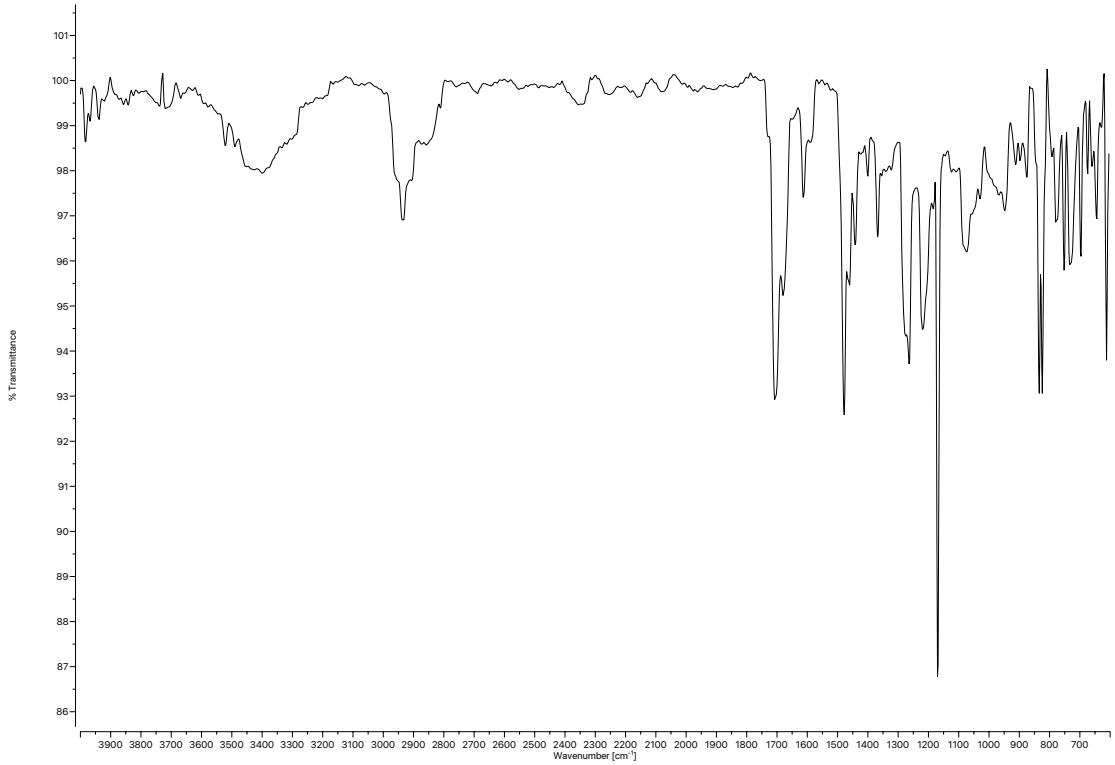


Figure A7.17 *Infrared spectrum (Thin Film, NaCl) of compound* ***210***.

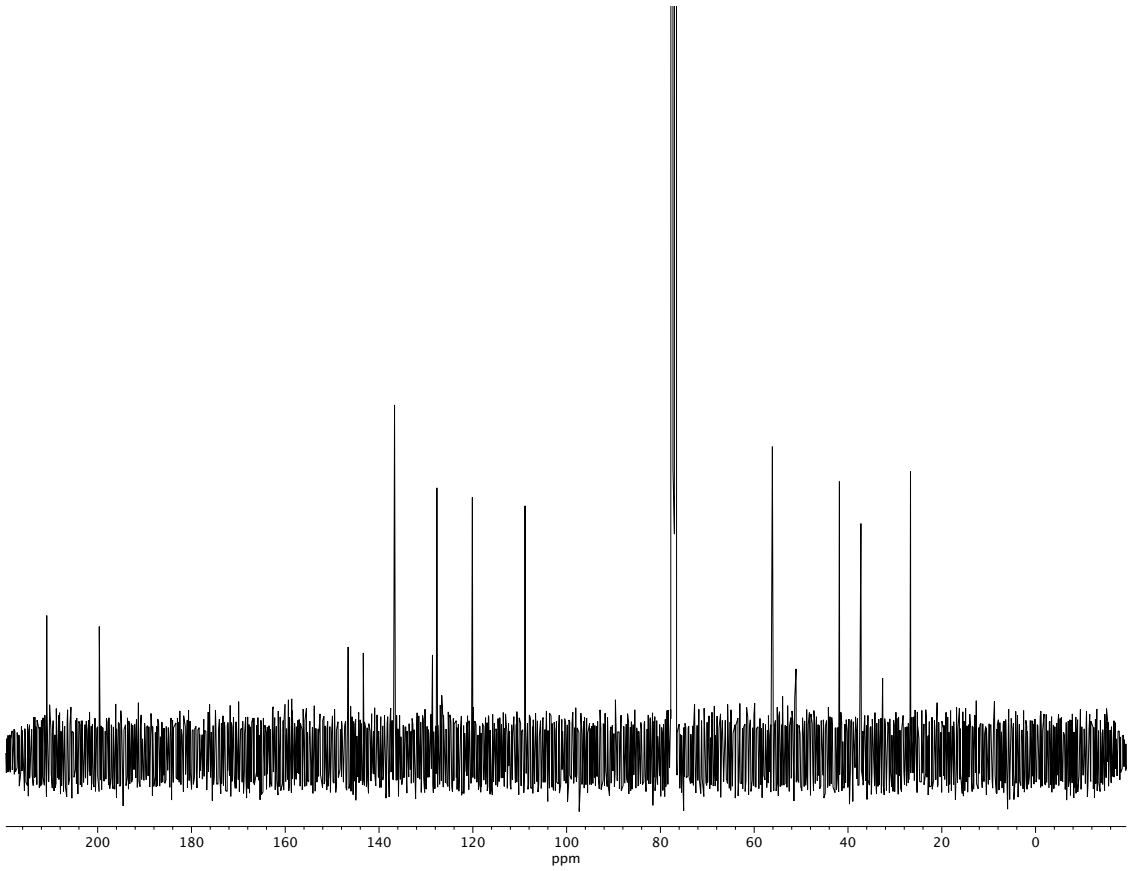


Figure A7.18 *^{13}C NMR (100 MHz, $CDCl_3$) of compound* ***210***.

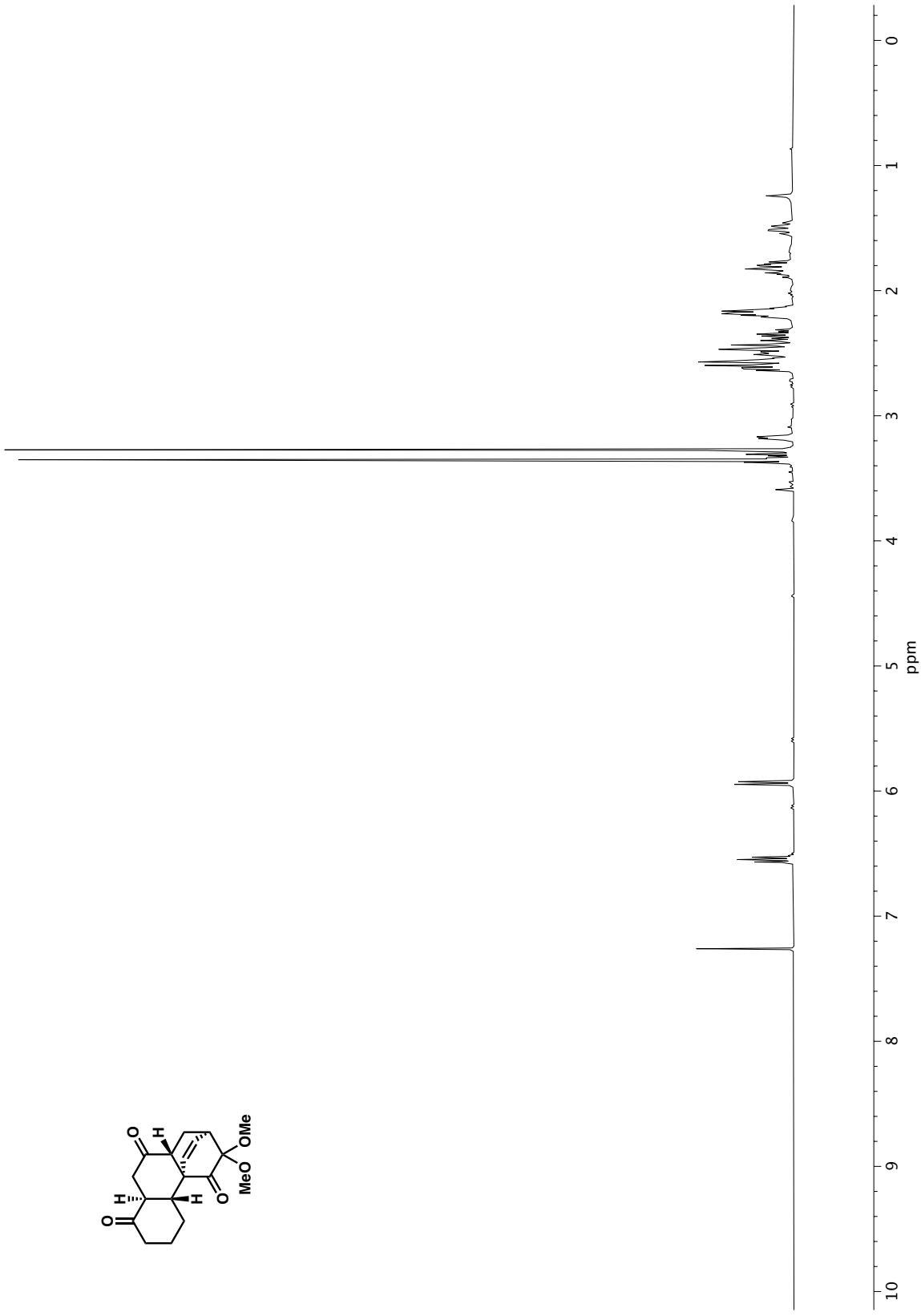


Figure A7.19 *^{1}H NMR (400 MHz, $CDCl_3$) of compound **211**.*

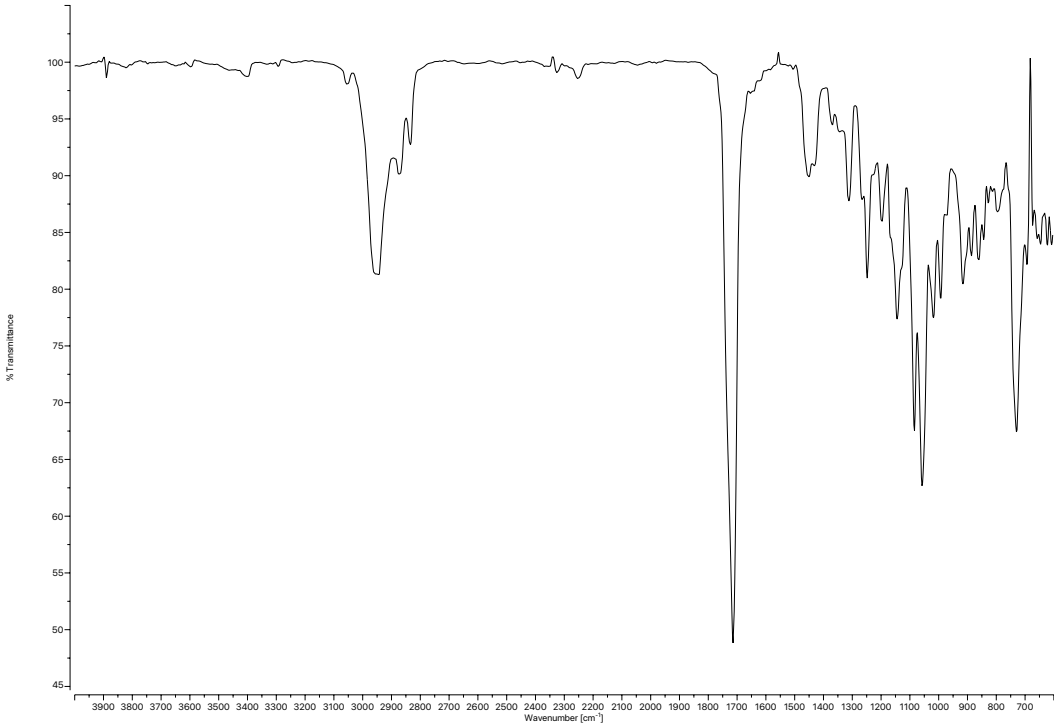


Figure A7.20 *Infrared spectrum (Thin Film, NaCl) of compound* ***211****.*

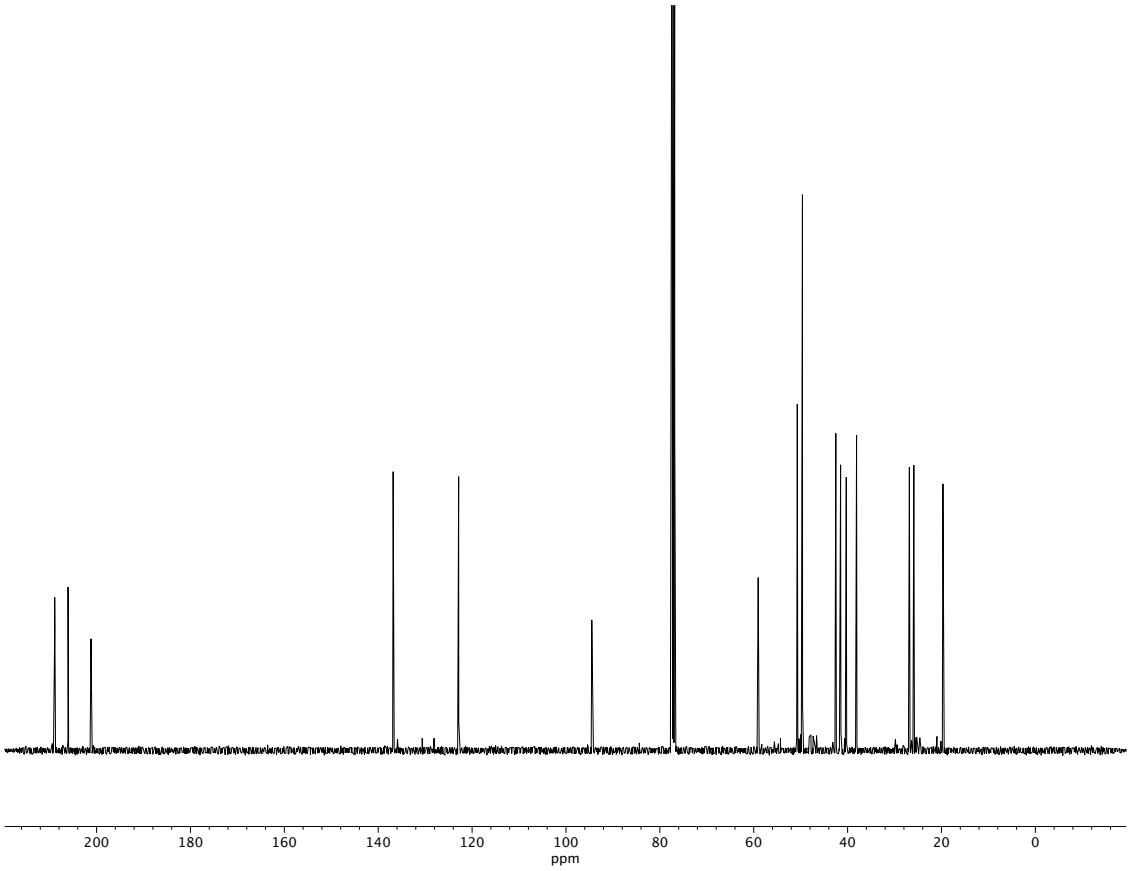


Figure A7.21 *^{13}C NMR (100 MHz, $CDCl_3$) of compound* ***211****.*

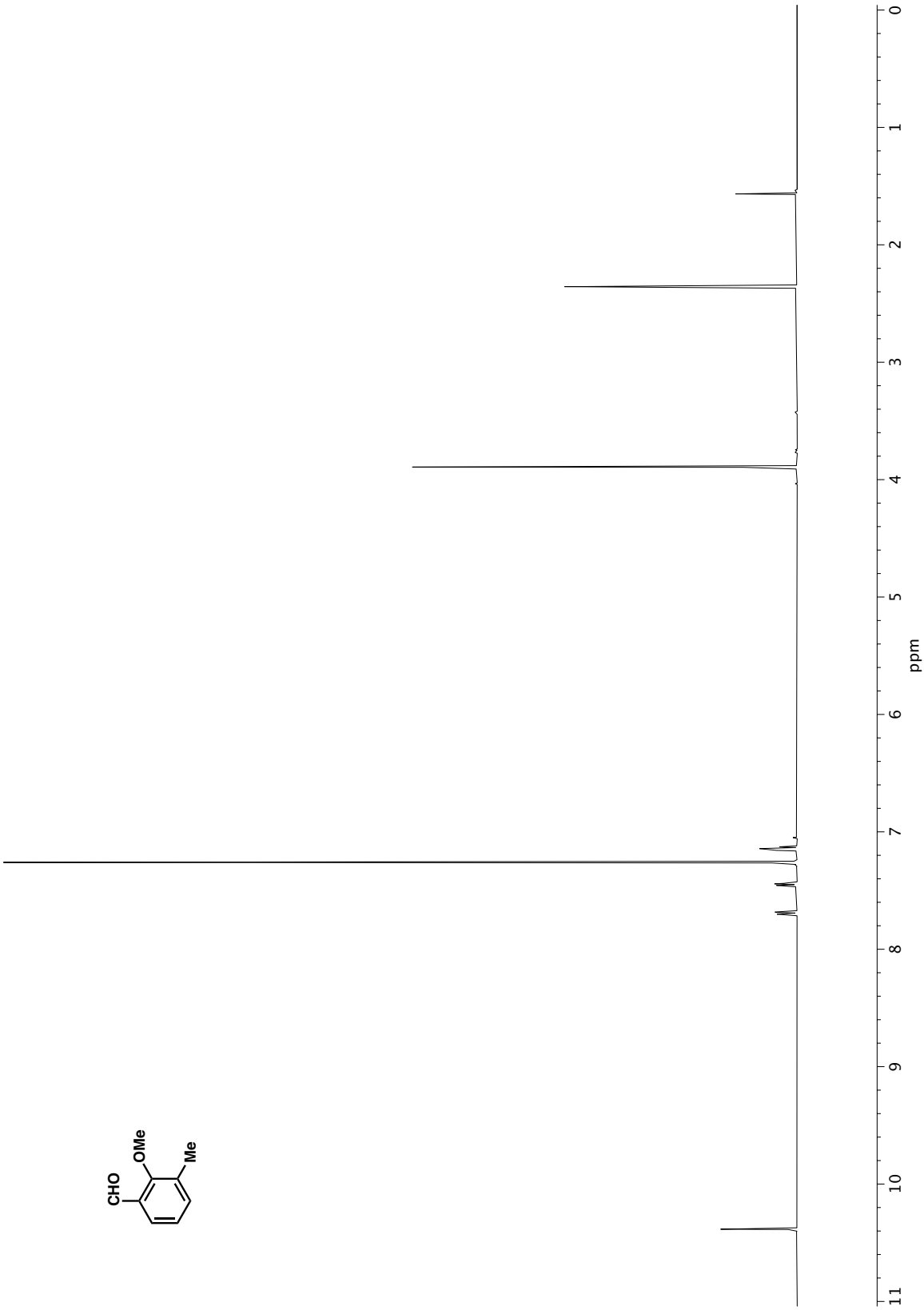


Figure A7.22 *^1H NMR (500 MHz, $CDCl_3$) of compound* ***217****.*

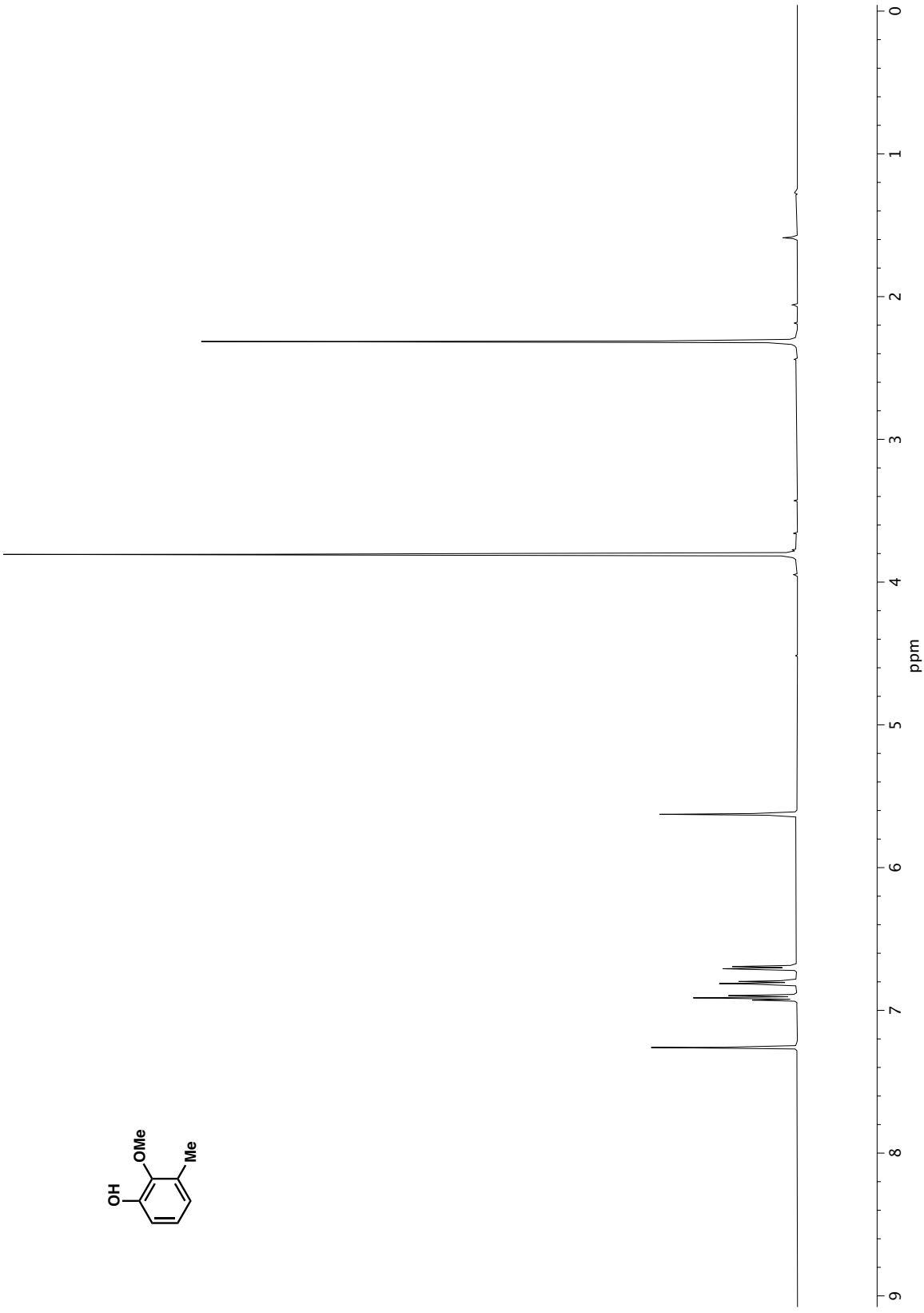


Figure A7.23 *^{1}H NMR (500 MHz, $CDCl_3$) of compound* ***219***.

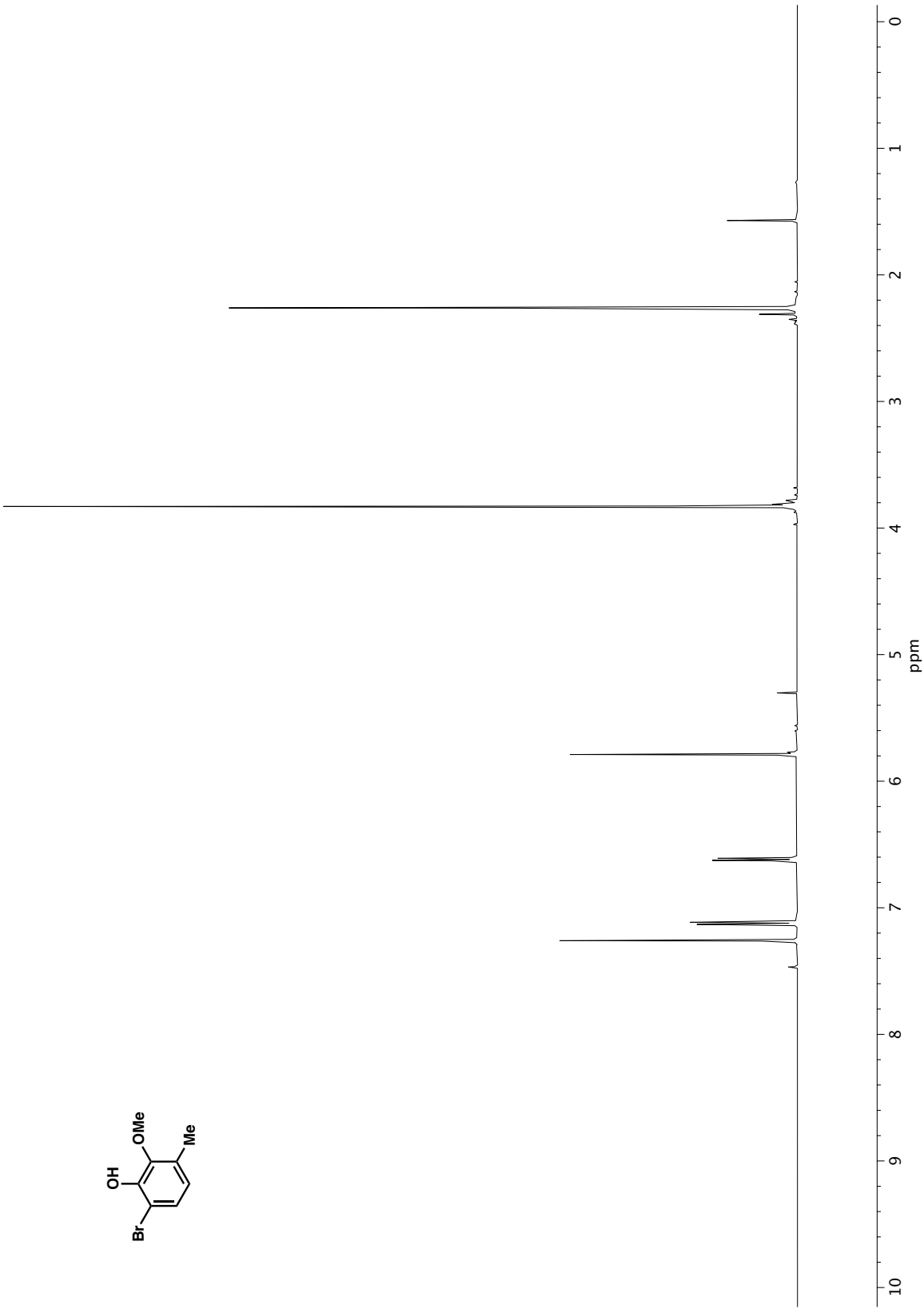


Figure A7.24 *^1H NMR (500 MHz, $CDCl_3$) of compound* ***220****.*

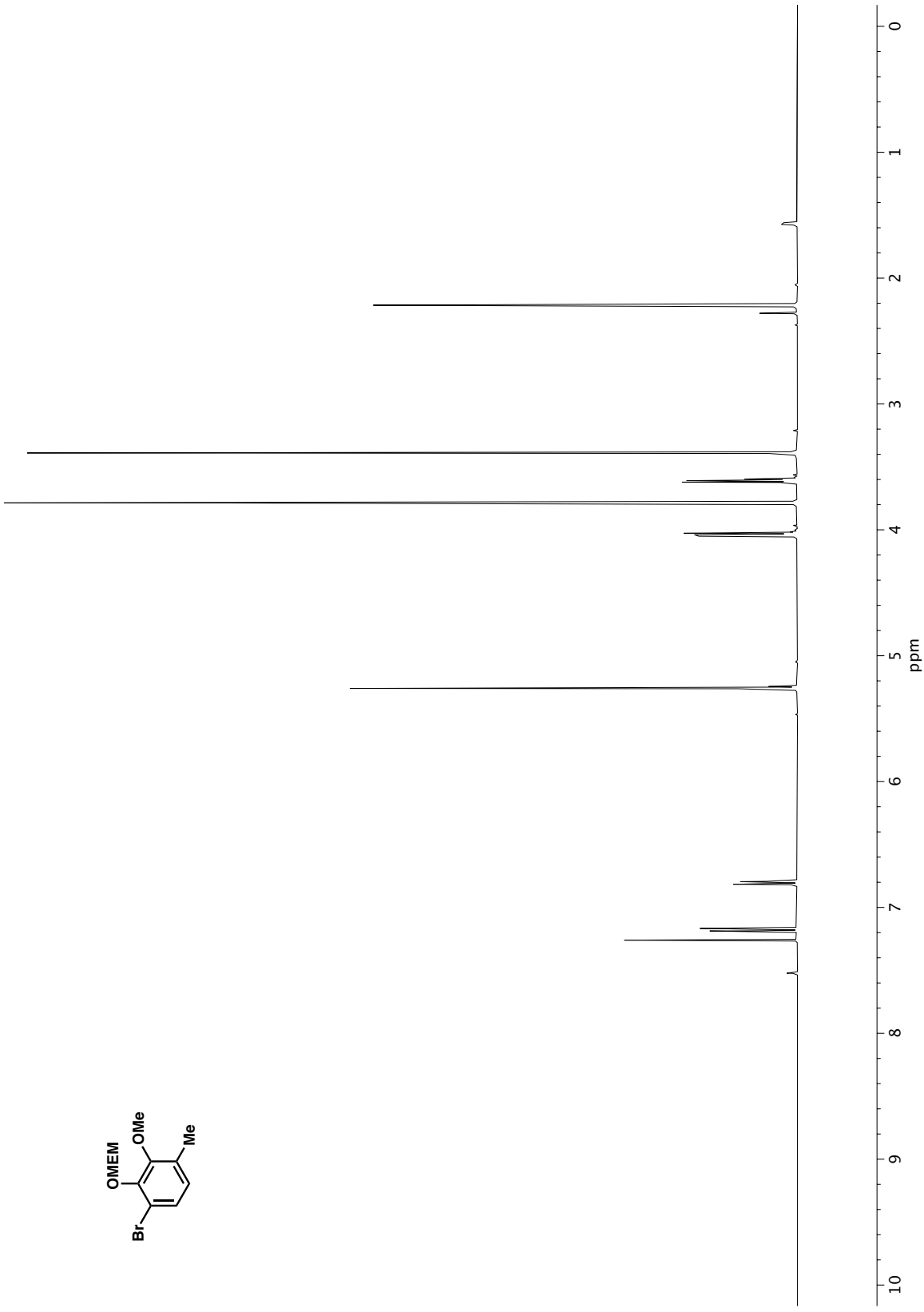


Figure A7.25 *^1H NMR (400 MHz, $CDCl_3$) of compound* ***221****.*

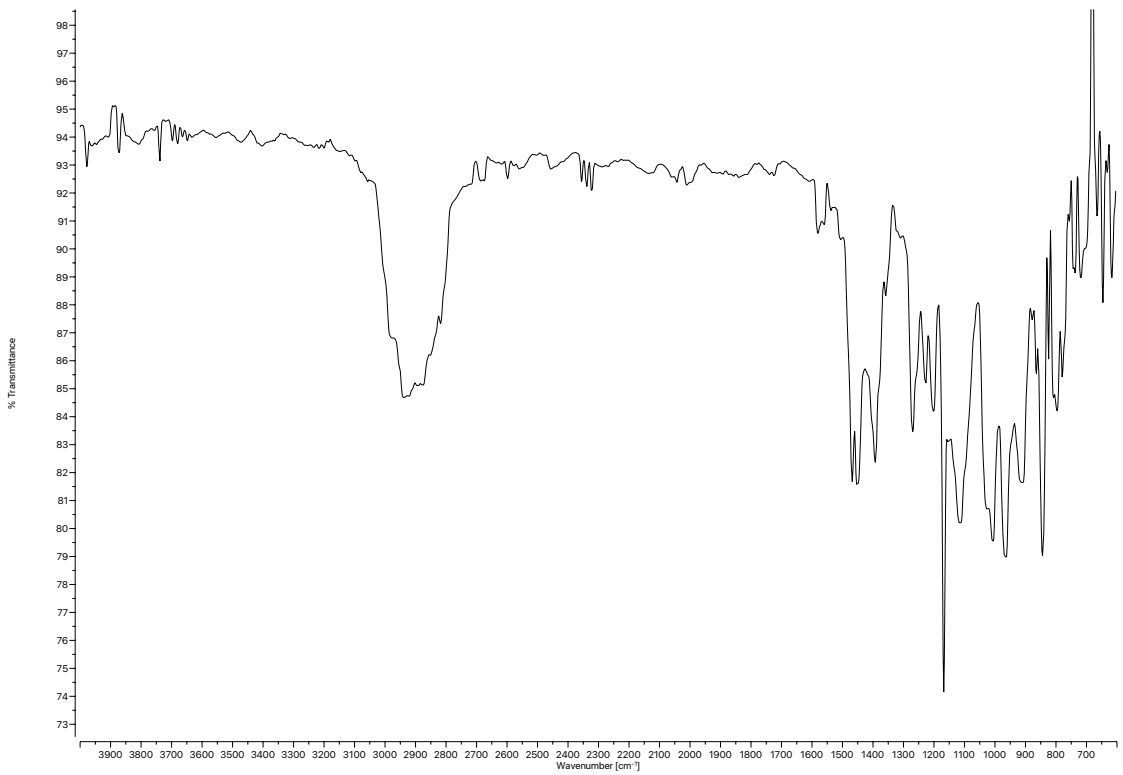


Figure A7.26 *Infrared spectrum (Thin Film, NaCl) of compound* ***221***.

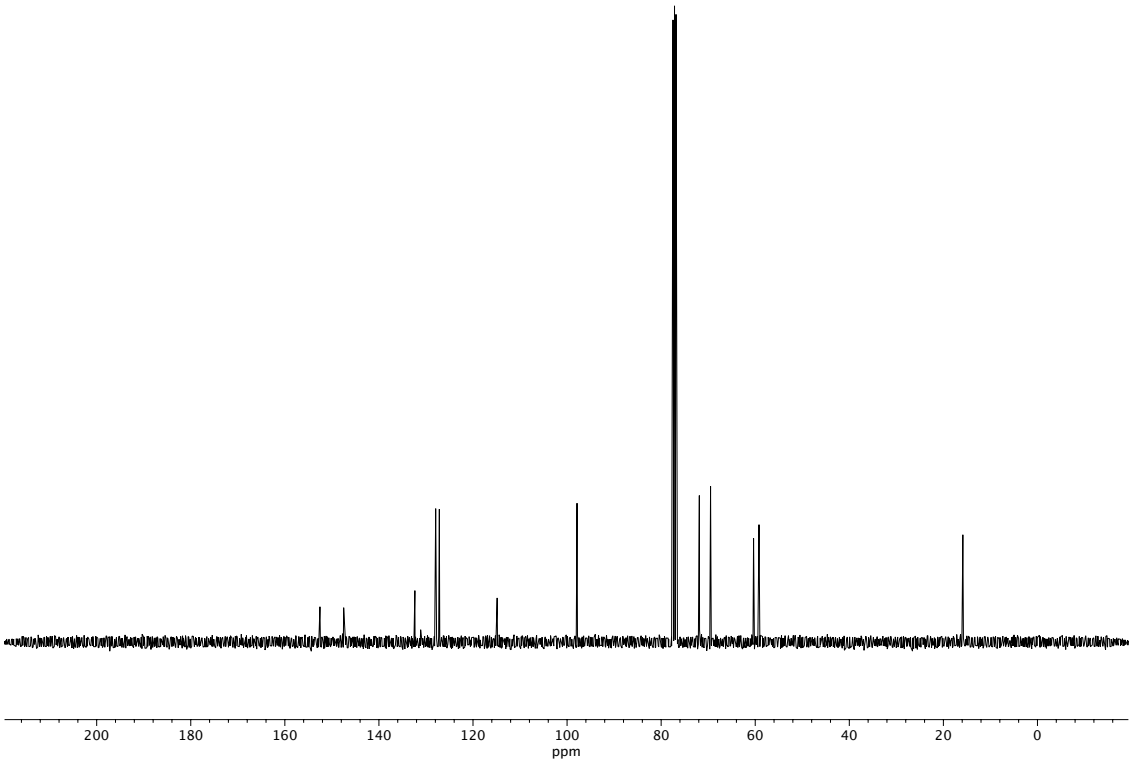


Figure A7.27 *^{13}C NMR (100 MHz, $CDCl_3$) of compound* ***221***.

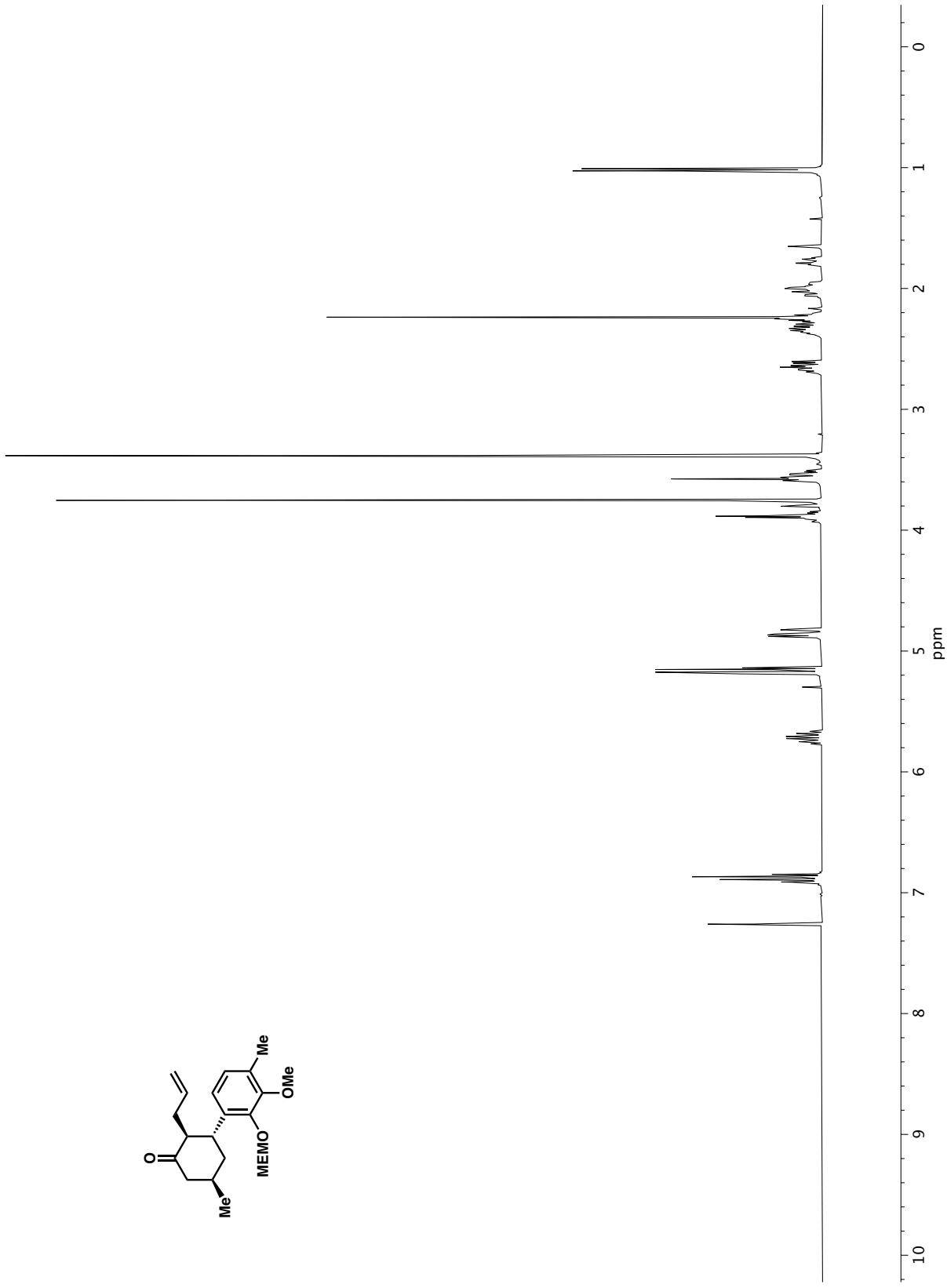


Figure A7.28 *^{1}H NMR (400 MHz, $CDCl_3$) of compound* ***225****.*

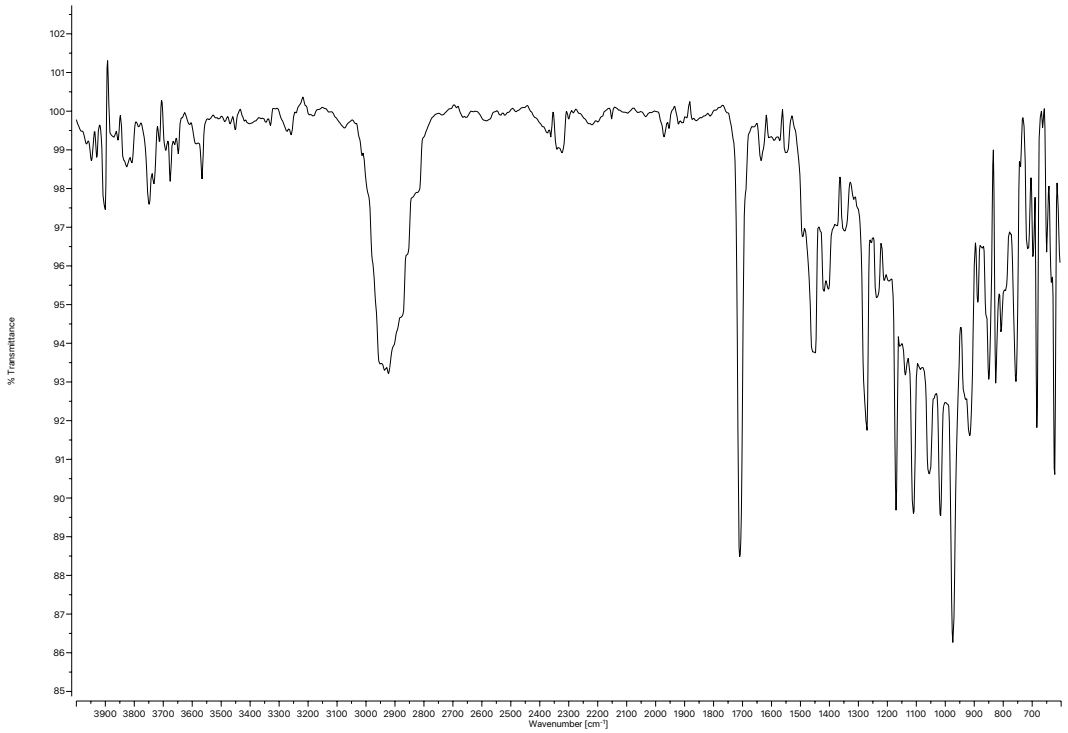


Figure A7.29 *Infrared spectrum (Thin Film, NaCl) of compound* ***225****.*

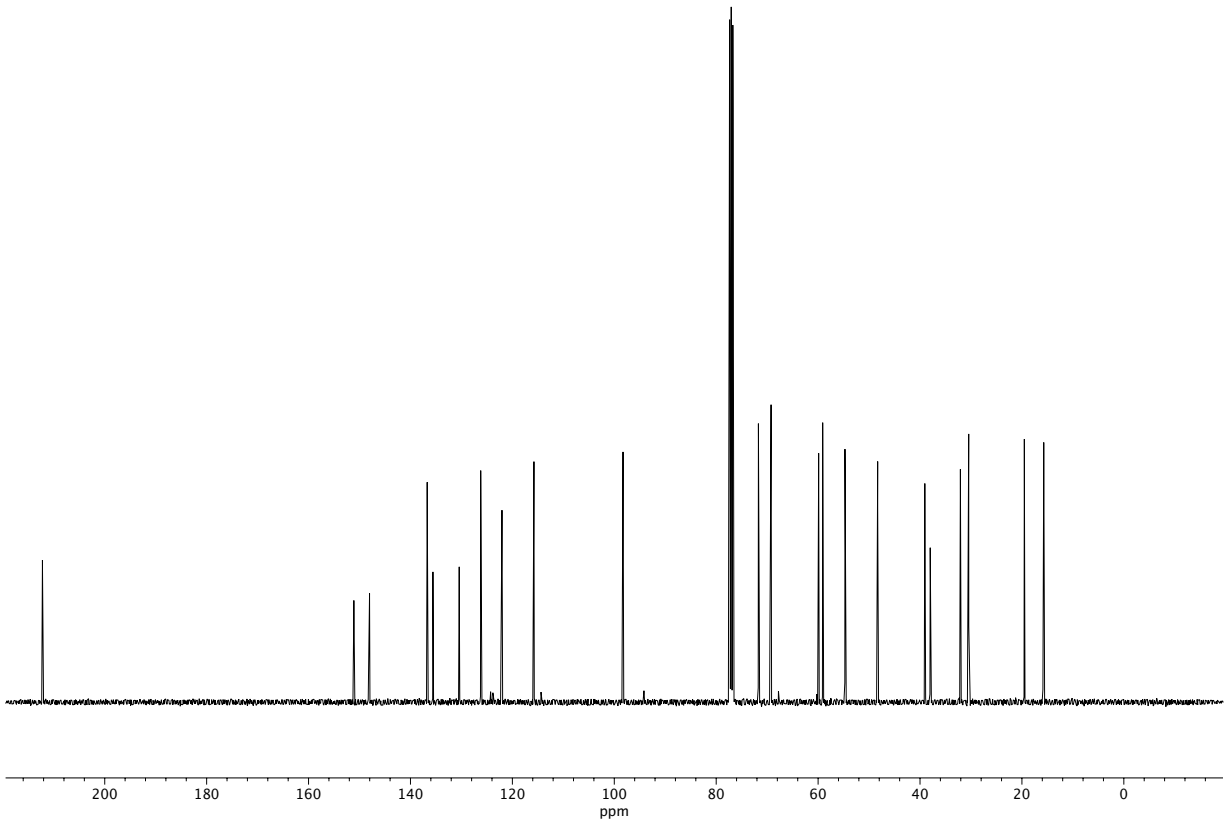


Figure A7.30 *^{13}C NMR (100 MHz, $CDCl_3$) of compound* ***225****.*

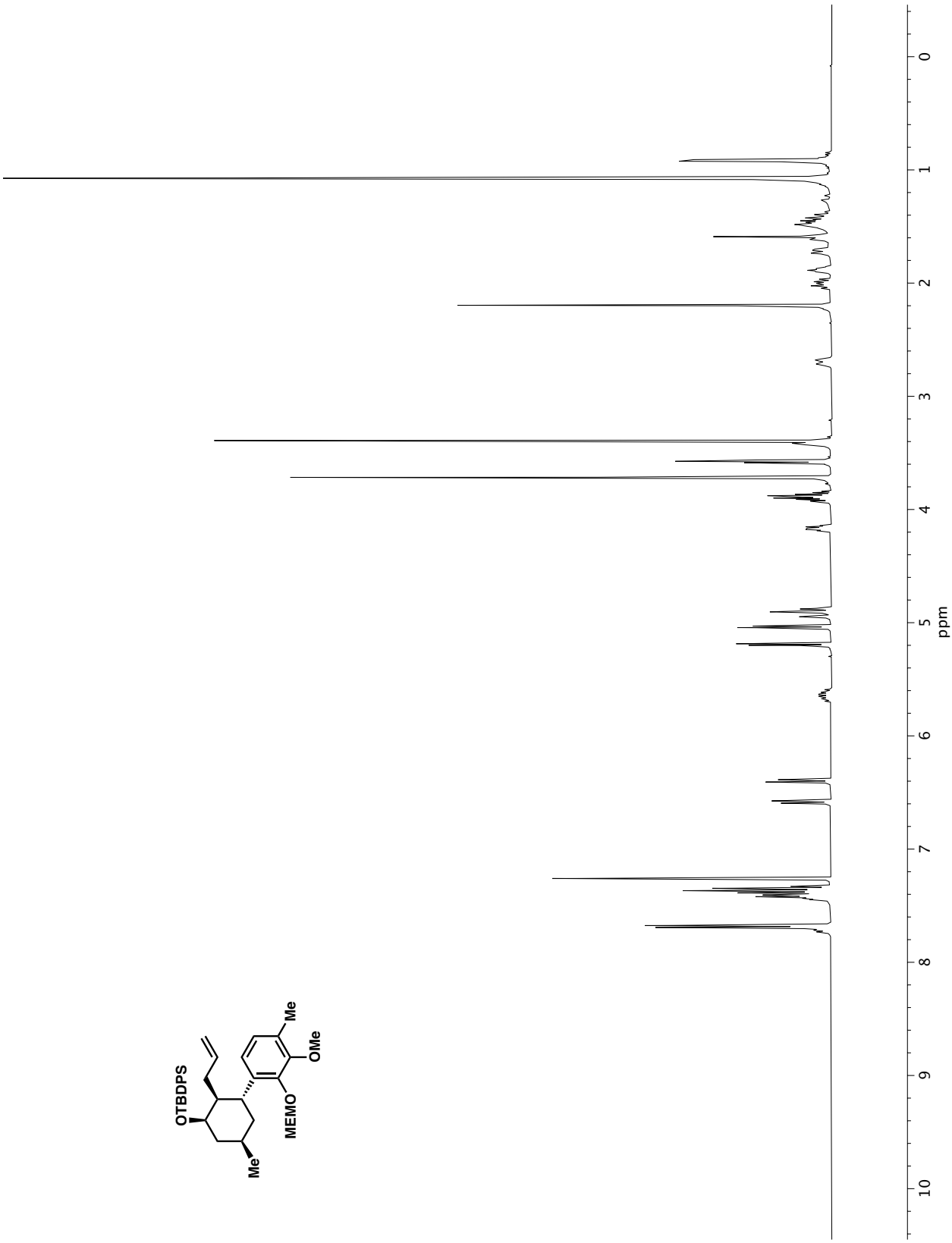


Figure A7.31 *^1H NMR (400 MHz, $CDCl_3$) of compound* ***226****.*

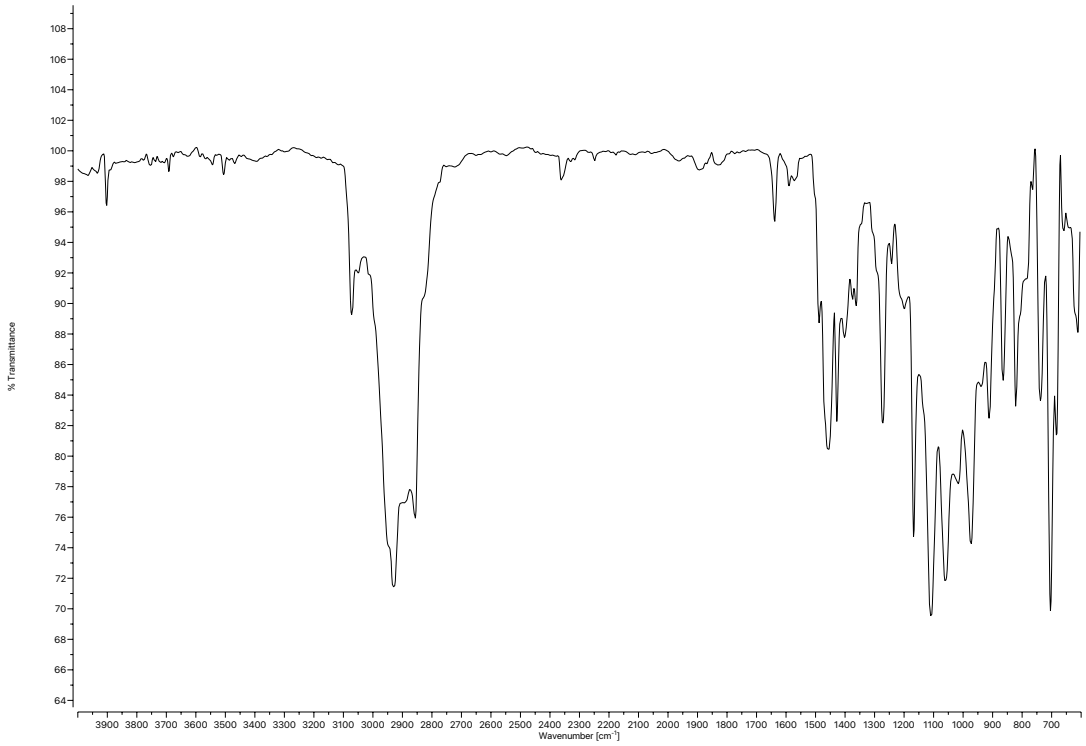


Figure A7.32 *Infrared spectrum (Thin Film, NaCl) of compound* ***226***.

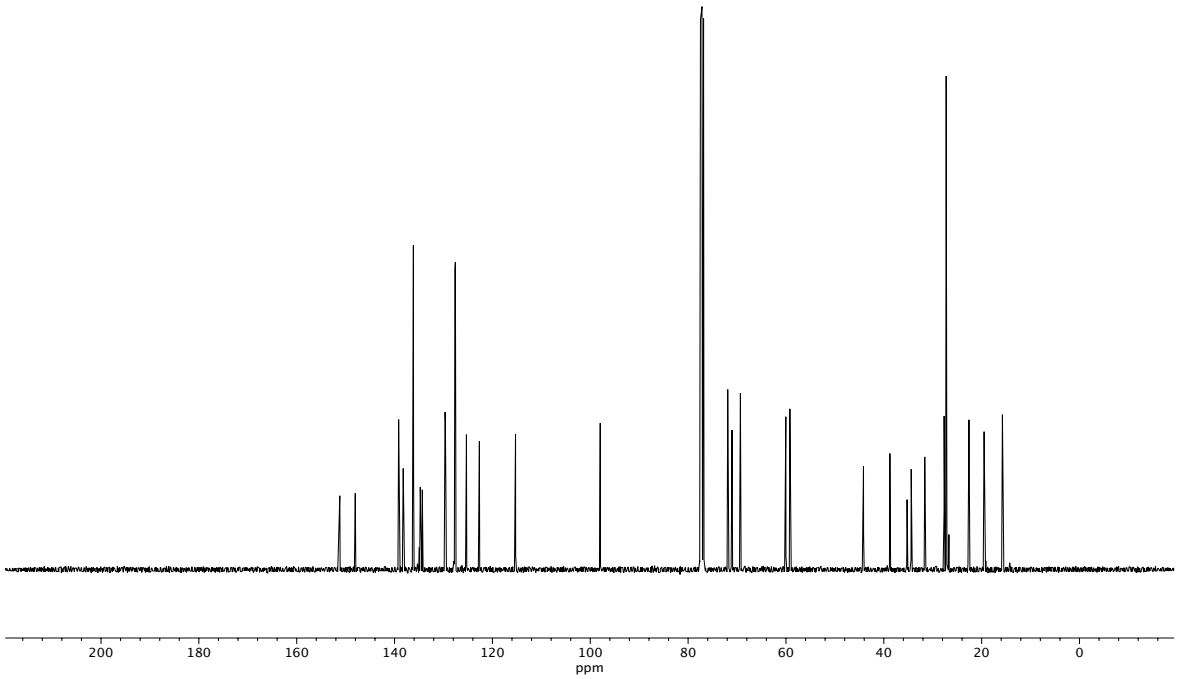


Figure A7.33 *^{13}C NMR (100 MHz, $CDCl_3$) of compound* ***226***.

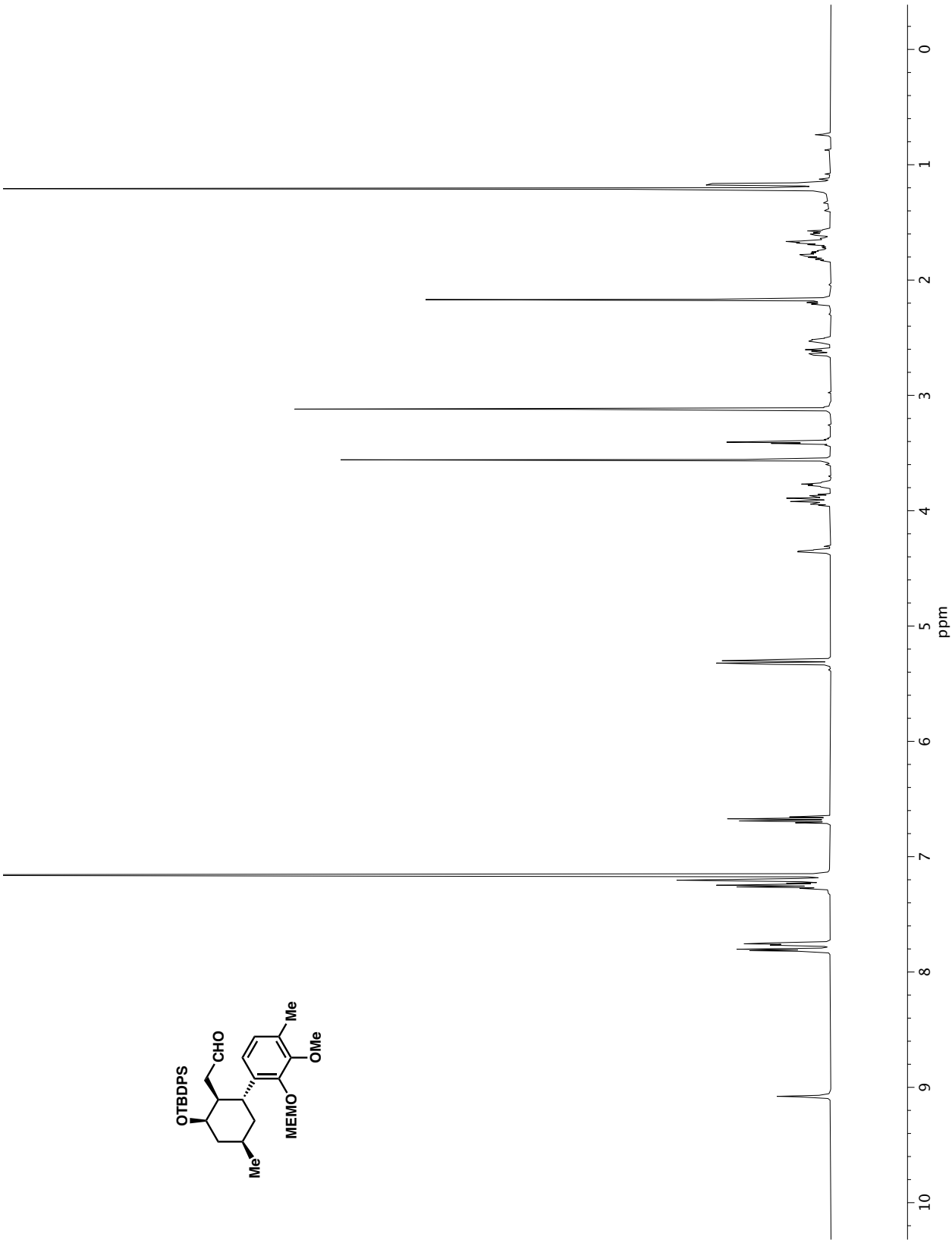


Figure A7.34 *^{1}H NMR (500 MHz, C_6D_6) of compound* ***227****.*

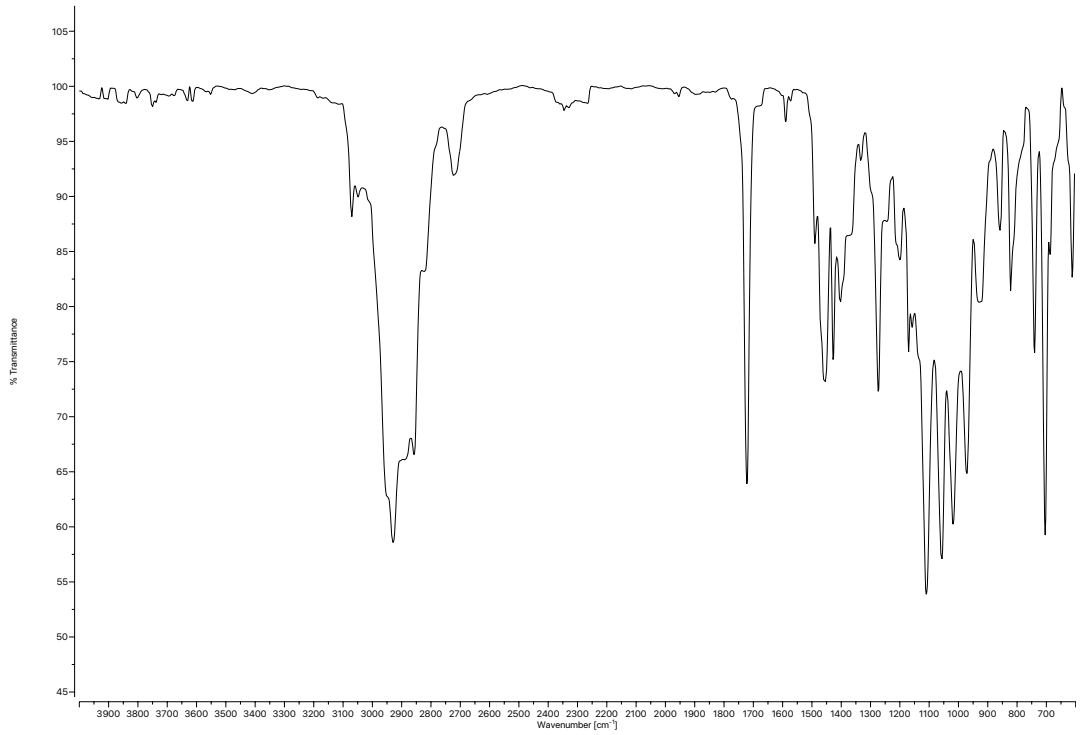


Figure A7.35 *Infrared spectrum (Thin Film, NaCl) of compound* ***227****.*

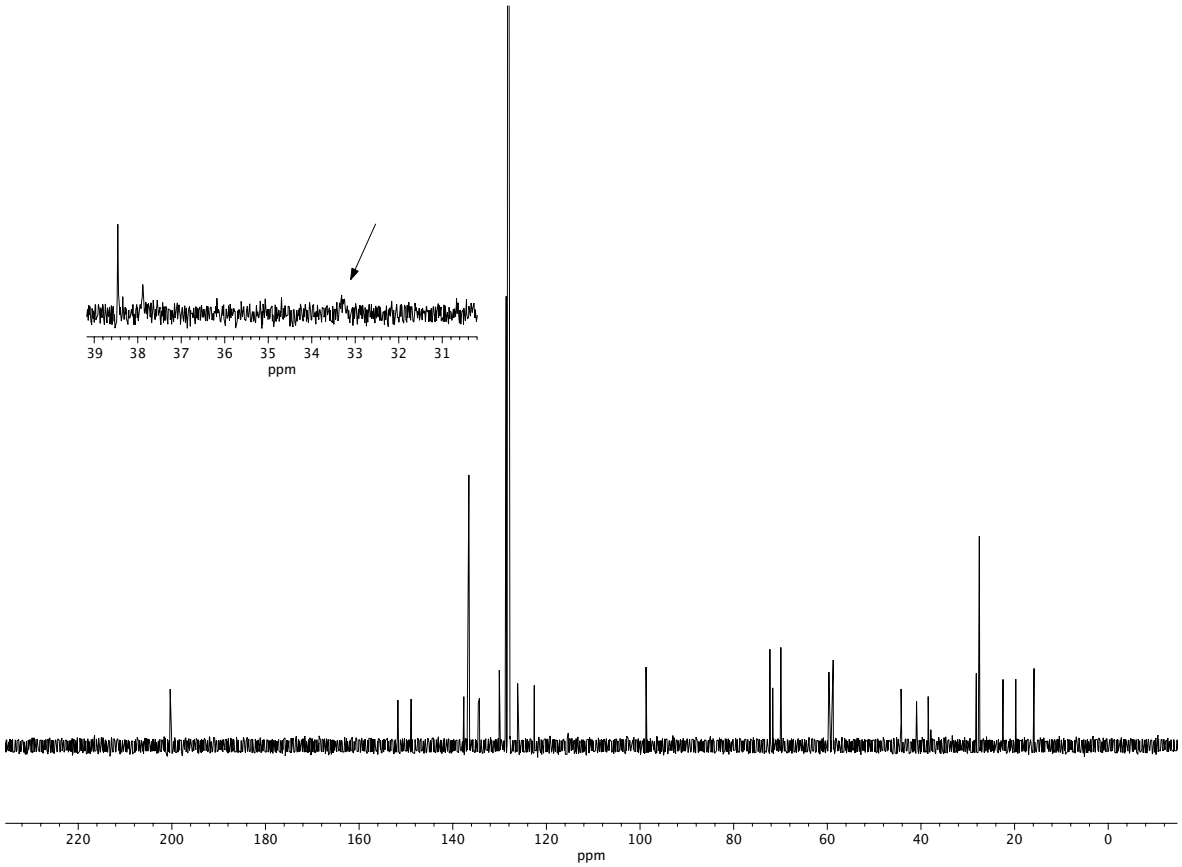


Figure A7.36 *^{13}C NMR (125 MHz, $CDCl_3$) of compound* ***227****.*

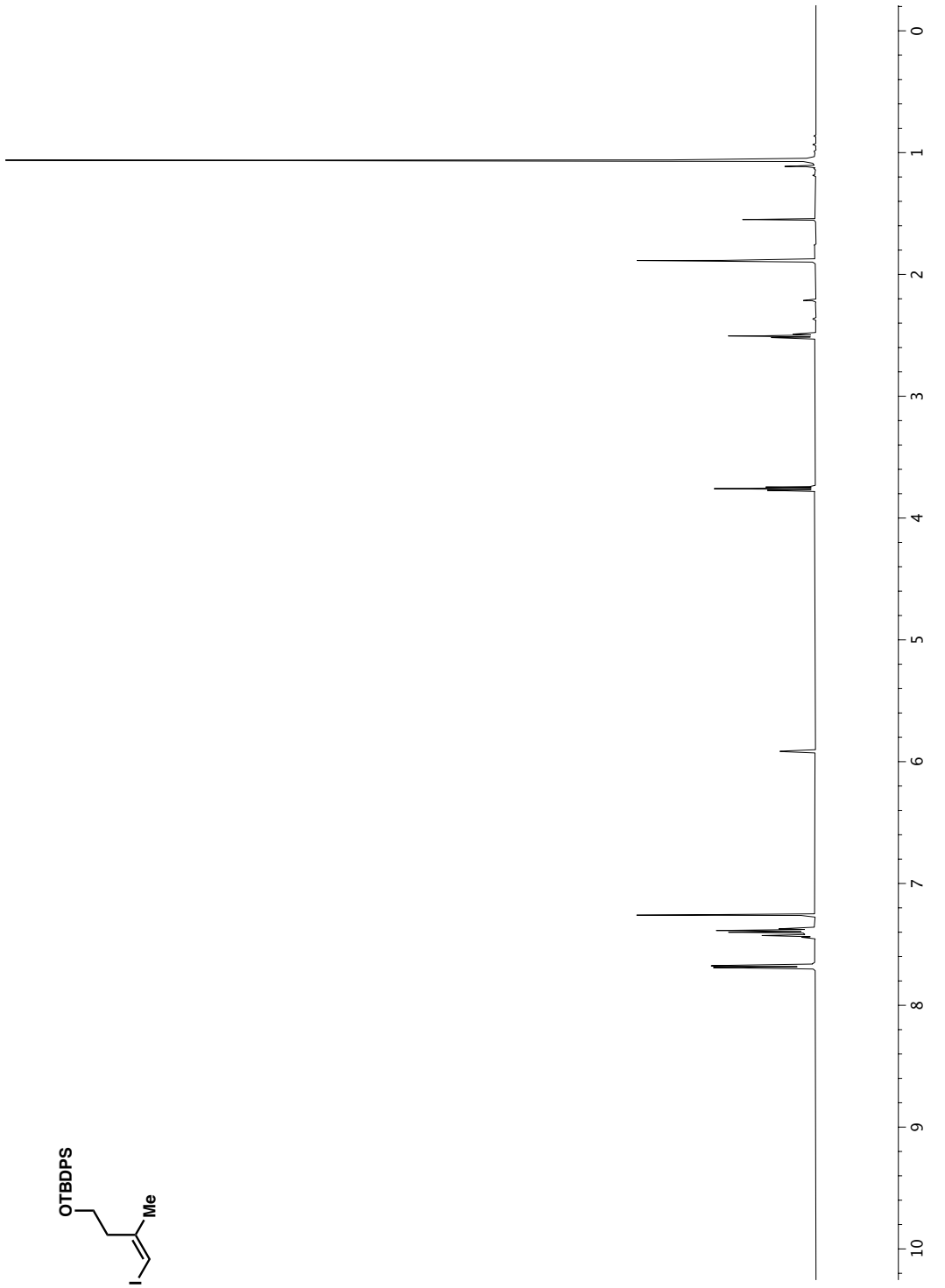


Figure A7.37 *^1H NMR (500 MHz, $CDCl_3$) of compound* ***228****.*

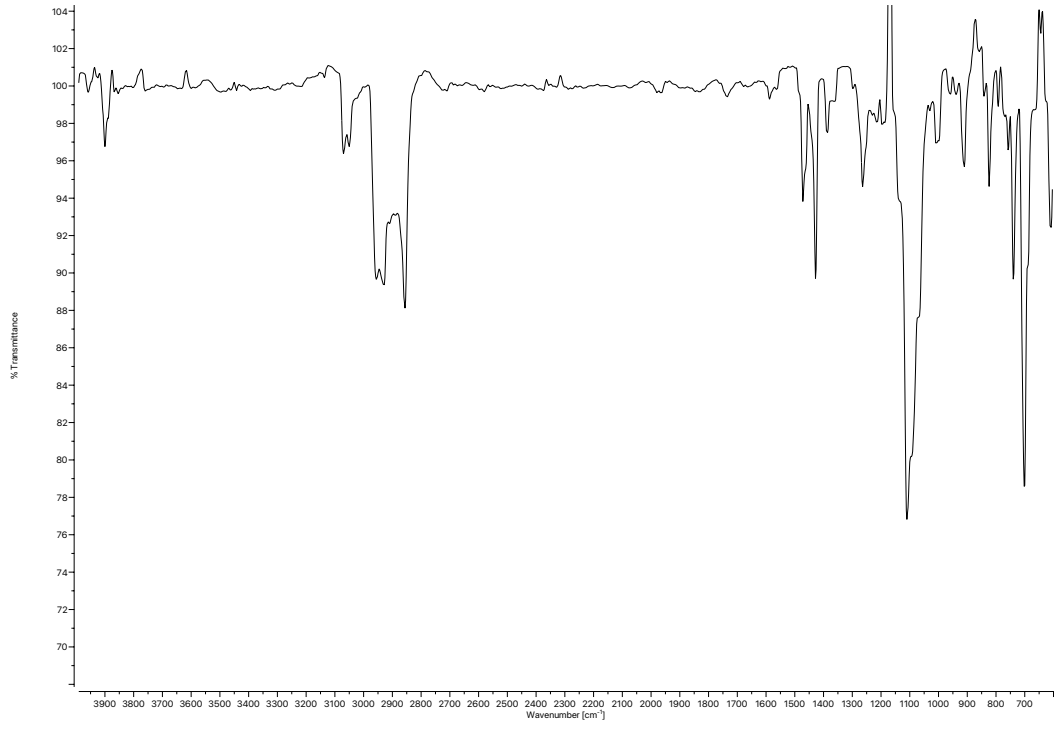


Figure A7.38 *Infrared spectrum (Thin Film, NaCl) of compound* ***228****.*

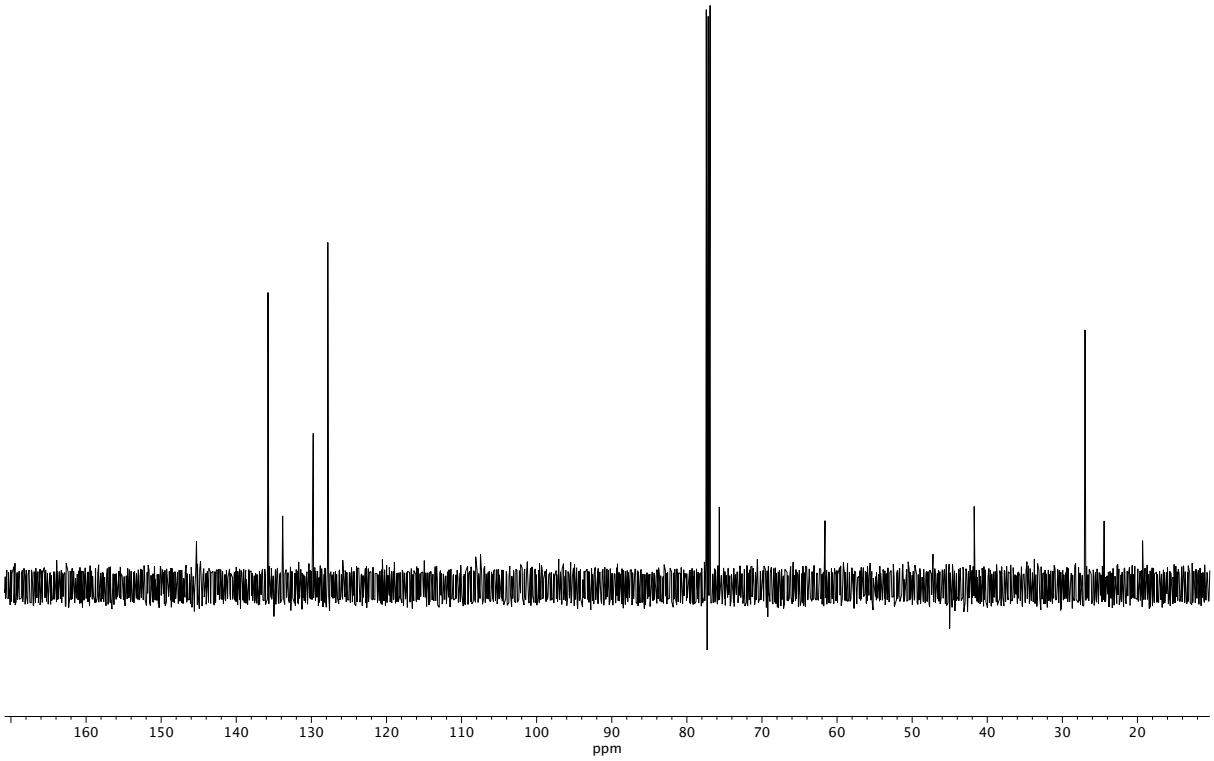


Figure A7.39 *^{13}C NMR (100 MHz, $CDCl_3$) of compound* ***228****.*

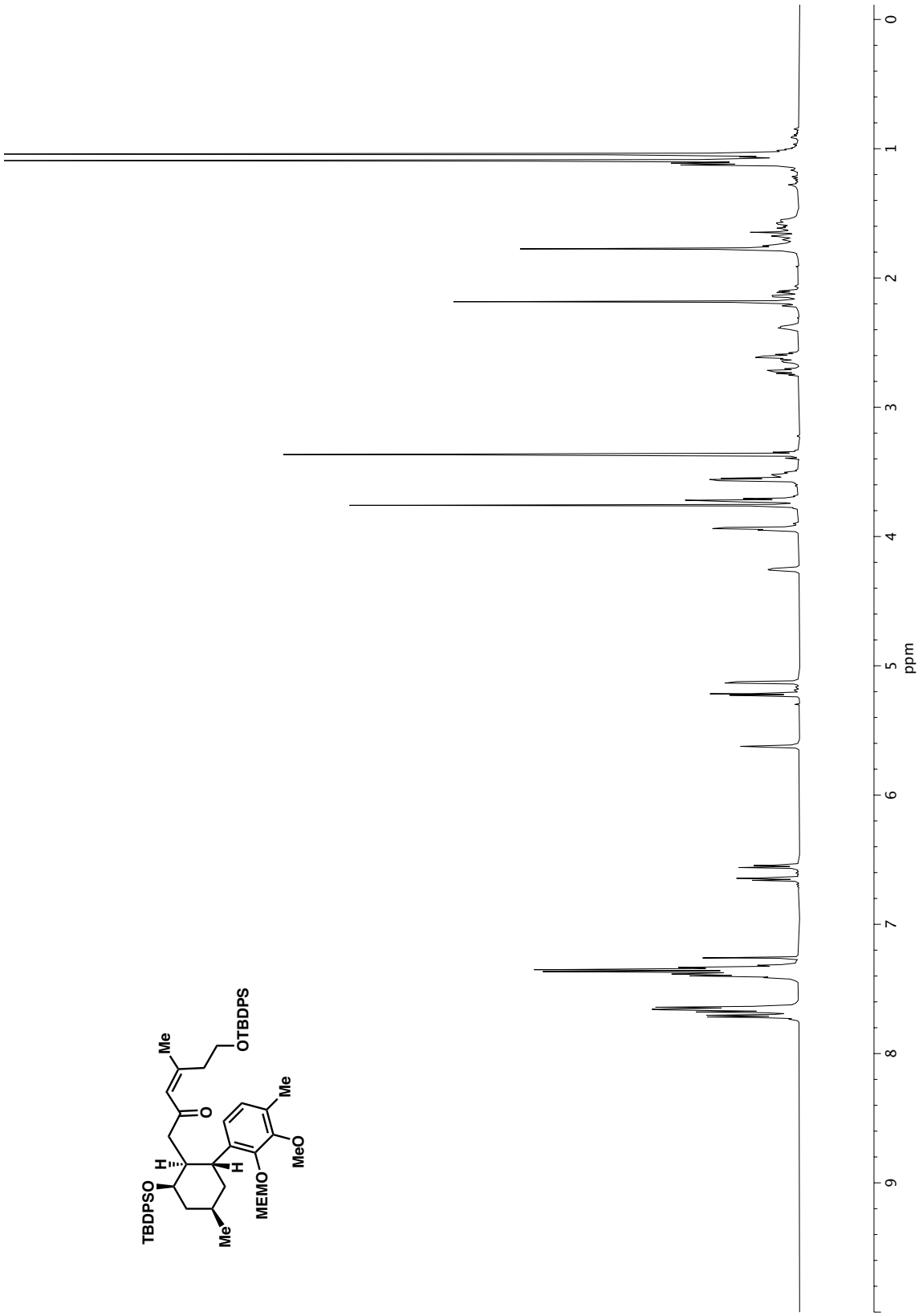


Figure A7.40 *^1H NMR (500 MHz, $CDCl_3$) of compound* ***230***.

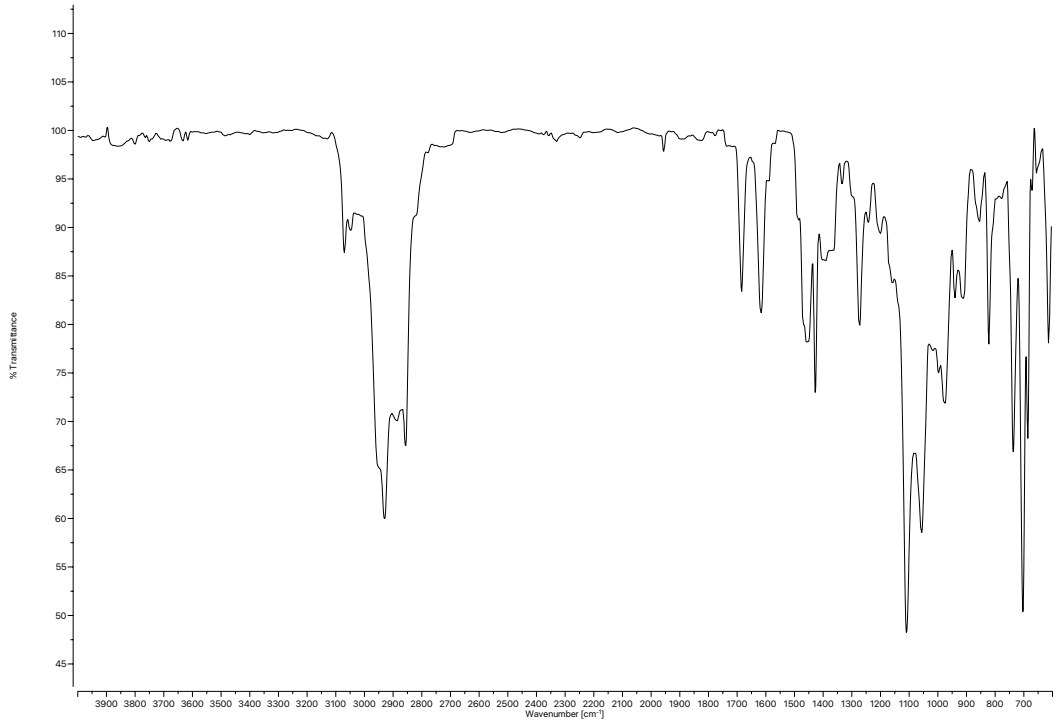


Figure A7.41 *Infrared spectrum (Thin Film, NaCl) of compound* ***230****.*

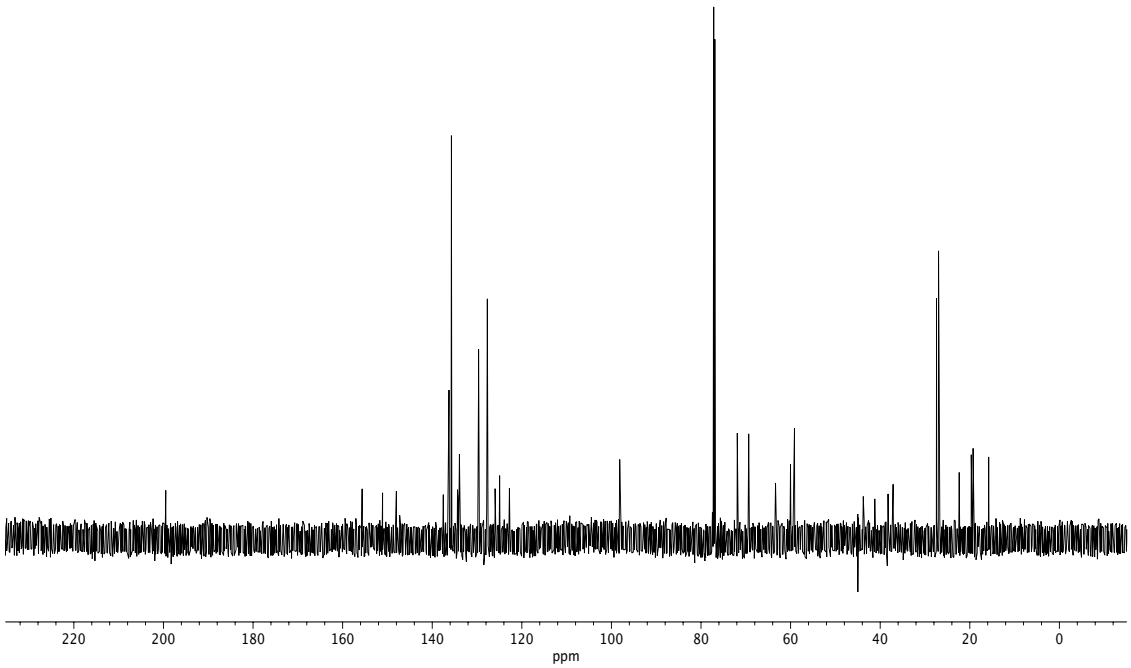


Figure A7.42 *^{13}C NMR (100 MHz, $CDCl_3$) of compound* ***230****.*

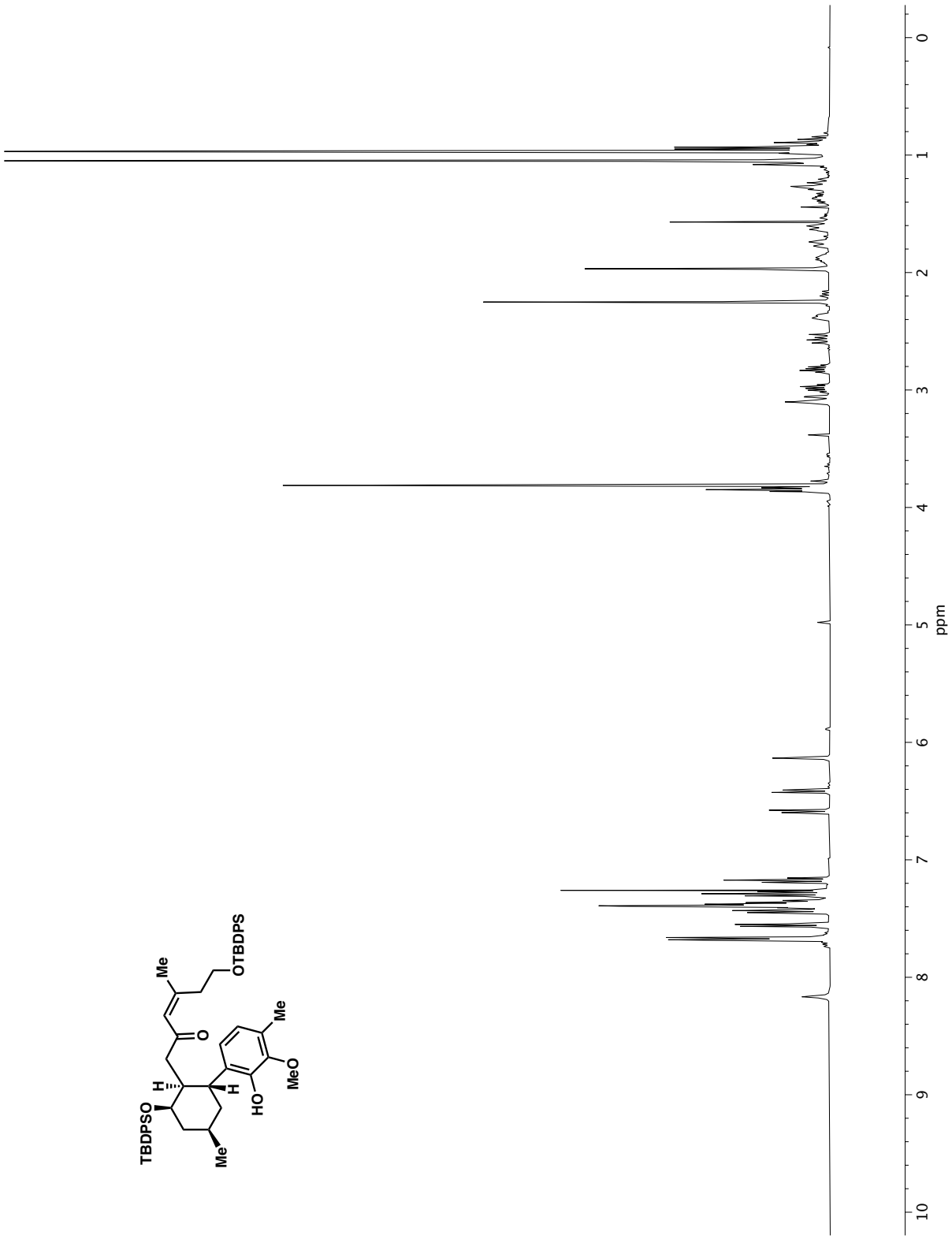


Figure A7.40 *^1H NMR (500 MHz, $CDCl_3$) of compound* ***231****.*

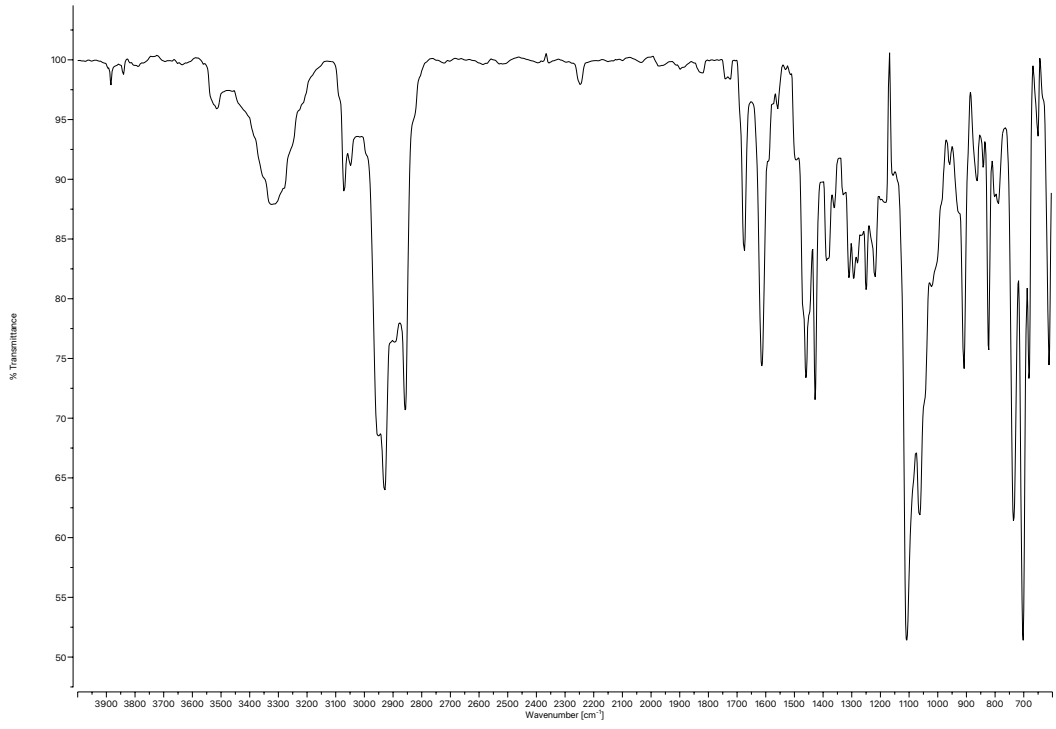


Figure A7.41 *Infrared spectrum (Thin Film, NaCl) of compound* ***231****.*

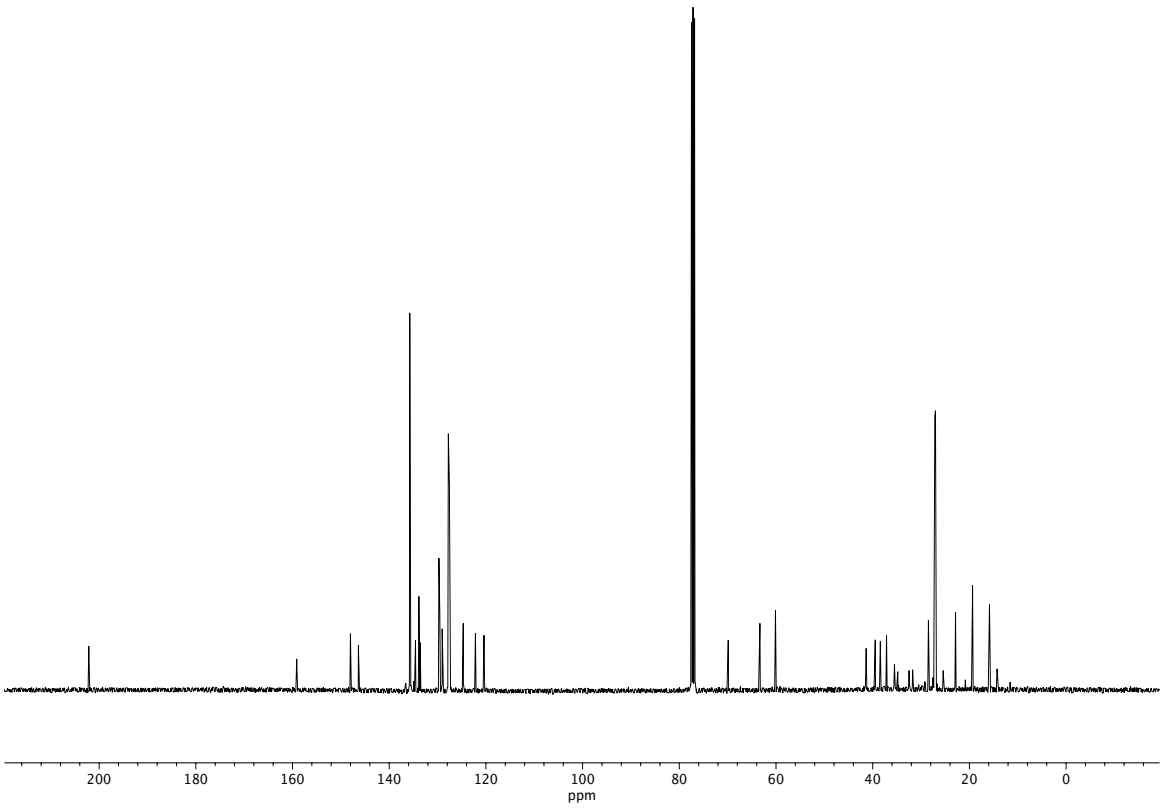


Figure A7.42 *^{13}C NMR (100 MHz, $CDCl_3$) of compound* ***231****.*

APPENDIX 8

X-Ray Crystallography Reports Relevant to Chapter 4:

Progress Toward the Synthesis of Kuroshine A

A8.1 GENERAL EXPERIMENTAL

X-Ray crystallographic analysis was obtained from the Caltech X-Ray Crystallography Facility using a Bruker A8S D8 VENTURE KAPPA diffractometer.

A8.2 X-RAY CRYSTAL STRUCTURE ANALYSIS OF COMPOUND 211 (V24053)

Crystals suitable for X-ray diffraction were grown by dissolving **211** in minimal CH_2Cl_2 and carefully layering with pentane. Low-temperature diffraction data (ϕ-and ω-scans) were collected on a Bruker A8S D8 VENTURE KAPPA diffractometer coupled to a PHOTON II CPAD detector with Cu K_α radiation ($\lambda = 1.54178$ Å) from an IμS micro-source for the structure of compound V24053. The structure was solved by direct methods using SHELXS[1] and refined against F^2 on all data by full-matrix least squares with SHELXL-2019[2] using established refinement techniques.[3] All non-hydrogen atoms were refined anisotropically. All hydrogen atoms were included into the model at geometrically calculated positions and refined using a riding model. The isotropic displacement parameters of all hydrogen atoms were fixed to 1.2 times the U value of the atoms they are linked to (1.5 times for methyl groups). Compound V24053 crystallizes in the monoclinic space group $P2_1/n$ with one molecule in the asymmetric unit.

Figure A8.2.1 *X-Ray coordinate of compound* ***211***

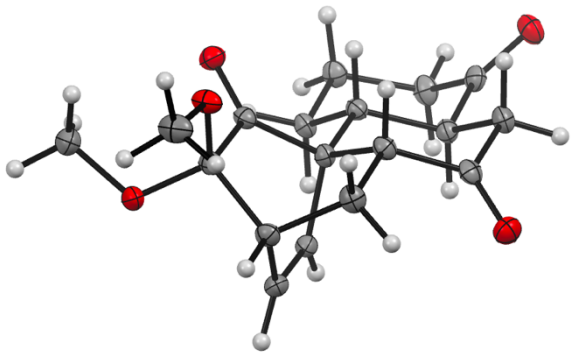


Table A8.2.1 *Crystal data and structure refinement for* ***211***.

Identification code	V24053	
Empirical formula	C18 H22 O5	
Formula weight	318.35	
Temperature	100(2) K	
Wavelength	1.54178 Å	
Crystal system	Monoclinic	
Space group	$P2_1/n$	
Unit cell dimensions	a = 6.9480(7) Å	a= 90°.
	b = 11.0134(14) Å	b= 96.189(5)°.
	c = 19.757(2) Å	g = 90°.
Volume	1503.0(3) $Å^3$	
Z	4	
Density (calculated)	1.407 Mg/m^3	
Absorption coefficient	0.839 mm^{-1}	
F(000)	680	
Crystal size	0.250 x 0.050 x 0.050 mm^3	
Theta range for data collection	4.502 to 74.580°.	
Index ranges	-8<=h<=8, -13<=k<=13, -24<=l<=24	
Reflections collected	23603	
Independent reflections	3075 [R(int) = 0.0578]	
Completeness to theta = 67.679°	100.0 %	
Absorption correction	Semi-empirical from equivalents	
MA8. and min. transmission	0.7538 and 0.5851	
Refinement method	Full-matrix least-squares on F^2	

Data / restraints / parameters	3075 / 0 / 210
Goodness-of-fit on F^2	1.049
Final R indices [I>2sigma(I)]	R1 = 0.0413, wR2 = 0.1071
R indices (all data)	R1 = 0.0491, wR2 = 0.1165
Extinction coefficient	n/a
Largest diff. peak and hole	0.396 and -0.298 e.Å^{-3}

Table A8.2.2 *Atomic coordinates (x 10^4) and equivalent isotropic displacement parameters (Å^{2}x 10^3) for V24053. U(eq) is defined as one third of the trace of the orthogonalized U^{ij} tensor.*

Atom	x	y	z	U(eq)
C(1)	3346(2)	3732(1)	5584(1)	15(1)
O(1)	2884(2)	4610(1)	5237(1)	19(1)
C(2)	3056(2)	3676(1)	6353(1)	16(1)
O(2)	1078(1)	3709(1)	6461(1)	18(1)
C(17)	62(2)	4805(1)	6255(1)	22(1)
O(3)	4087(2)	4691(1)	6634(1)	19(1)
C(18)	4026(2)	4845(1)	7353(1)	25(1)
C(3)	3827(2)	2447(1)	6634(1)	17(1)
C(4)	6008(2)	2392(1)	6547(1)	19(1)
C(5)	6321(2)	2550(1)	5793(1)	16(1)
C(6)	7552(2)	1556(1)	5521(1)	17(1)
O(4)	8093(2)	664(1)	5846(1)	23(1)
C(7)	7943(2)	1747(1)	4794(1)	18(1)
C(8)	5991(2)	1721(1)	4350(1)	16(1)
C(9)	6246(2)	1931(1)	3602(1)	18(1)
O(5)	7801(2)	2193(1)	3414(1)	23(1)
C(10)	4397(2)	1846(1)	3128(1)	21(1)
C(11)	2904(2)	2748(1)	3360(1)	18(1)
C(12)	2624(2)	2558(1)	4110(1)	16(1)
C(13)	4552(2)	2685(1)	4565(1)	14(1)
C(14)	4309(2)	2591(1)	5329(1)	14(1)
C(15)	3094(2)	1533(1)	5531(1)	15(1)
C(16)	2828(2)	1474(1)	6189(1)	17(1)

Table A8.2.3 *Bond lengths [Å] and angles [°] for* ***211***.

Bond	**Length (Å)**	**Bond**	**Length (Å)**
C(1)-O(1)	1.2068(17)	C(10)-C(11)	1.541(2)
C(1)-C(14)	1.5339(18)	C(10)-H(10A)	0.9900
C(1)-C(2)	1.5569(18)	C(10)-H(10B)	0.9900
C(2)-O(3)	1.4087(17)	C(11)-C(12)	1.5300(18)
C(2)-O(2)	1.4136(17)	C(11)-H(11A)	0.9900
C(2)-C(3)	1.5369(19)	C(11)-H(11B)	0.9900
O(2)-C(17)	1.4347(18)	C(12)-C(13)	1.5370(18)
C(17)-H(17A)	0.9800	C(12)-H(12A)	0.9900
C(17)-H(17B)	0.9800	C(12)-H(12B)	0.9900
C(17)-H(17C)	0.9800	C(13)-C(14)	1.5393(18)
O(3)-C(18)	1.4359(17)	C(13)-H(13)	1.0000
C(18)-H(18A)	0.9800	C(14)-C(15)	1.5180(18)
C(18)-H(18B)	0.9800	C(15)-C(16)	1.334(2)
C(18)-H(18C)	0.9800	C(15)-H(15)	0.9500
C(3)-C(16)	1.5077(19)	C(16)-H(16)	0.9500
C(3)-C(4)	1.5441(19)		
C(3)-H(3)	1.0000	**Atoms**	**Angle (°)**
C(4)-C(5)	1.5391(18)	O(1)-C(1)-C(14)	124.66(12)
C(4)-H(4A)	0.9900	O(1)-C(1)-C(2)	122.07(12)
C(4)-H(4B)	0.9900	C(14)-C(1)-C(2)	113.25(11)
C(5)-C(6)	1.5227(19)	O(3)-C(2)-O(2)	112.41(11)
C(5)-C(14)	1.5877(18)	O(3)-C(2)-C(3)	114.44(11)
C(5)-H(5)	1.0000	O(2)-C(2)-C(3)	105.97(11)
C(6)-O(4)	1.2119(18)	O(3)-C(2)-C(1)	103.81(10)
C(6)-C(7)	1.5051(19)	O(2)-C(2)-C(1)	112.14(11)
C(7)-C(8)	1.5339(19)	C(3)-C(2)-C(1)	108.14(11)
C(7)-H(7A)	0.9900	C(2)-O(2)-C(17)	115.84(11)
C(7)-H(7B)	0.9900	O(2)-C(17)-H(17A)	109.5
C(8)-C(9)	1.5243(19)	O(2)-C(17)-H(17B)	109.5
C(8)-C(13)	1.5490(19)	H(17A)-C(17)-H(17B)	109.5
C(8)-H(8)	1.0000	O(2)-C(17)-H(17C)	109.5
C(9)-O(5)	1.2144(18)	H(17A)-C(17)-H(17C)	109.5
C(9)-C(10)	1.509(2)	H(17B)-C(17)-H(17C)	109.5

Table A8.2.3 cont'd.

Atoms	Angle (°)	Atoms	Angle (°)
C(2)-O(3)-C(18)	114.52(11)	C(9)-C(8)-C(7)	111.28(11)
O(3)-C(18)-H(18A)	109.5	C(9)-C(8)-C(13)	107.93(11)
O(3)-C(18)-H(18B)	109.5	C(7)-C(8)-C(13)	112.77(11)
H(18A)-C(18)-H(18B)	109.5	C(9)-C(8)-H(8)	108.2
O(3)-C(18)-H(18C)	109.5	C(7)-C(8)-H(8)	108.2
H(18A)-C(18)-H(18C)	109.5	C(13)-C(8)-H(8)	108.2
H(18B)-C(18)-H(18C)	109.5	O(5)-C(9)-C(10)	123.45(13)
C(16)-C(3)-C(2)	107.15(11)	O(5)-C(9)-C(8)	122.17(13)
C(16)-C(3)-C(4)	107.60(11)	C(10)-C(9)-C(8)	114.31(12)
C(2)-C(3)-C(4)	107.60(11)	C(9)-C(10)-C(11)	109.31(11)
C(16)-C(3)-H(3)	111.4	C(9)-C(10)-H(10A)	109.8
C(2)-C(3)-H(3)	111.4	C(11)-C(10)-H(10A)	109.8
C(4)-C(3)-H(3)	111.4	C(9)-C(10)-H(10B)	109.8
C(5)-C(4)-C(3)	110.28(11)	C(11)-C(10)-H(10B)	109.8
C(5)-C(4)-H(4A)	109.6	H(10A)-C(10)-H(10B)	108.3
C(3)-C(4)-H(4A)	109.6	C(12)-C(11)-C(10)	111.09(11)
C(5)-C(4)-H(4B)	109.6	C(12)-C(11)-H(11A)	109.4
C(3)-C(4)-H(4B)	109.6	C(10)-C(11)-H(11A)	109.4
H(4A)-C(4)-H(4B)	108.1	C(12)-C(11)-H(11B)	109.4
C(6)-C(5)-C(4)	113.85(11)	C(10)-C(11)-H(11B)	109.4
C(6)-C(5)-C(14)	108.07(11)	H(11A)-C(11)-H(11B)	108.0
C(4)-C(5)-C(14)	110.77(11)	C(11)-C(12)-C(13)	111.08(11)
C(6)-C(5)-H(5)	108.0	C(11)-C(12)-H(12A)	109.4
C(4)-C(5)-H(5)	108.0	C(13)-C(12)-H(12A)	109.4
C(14)-C(5)-H(5)	108.0	C(11)-C(12)-H(12B)	109.4
O(4)-C(6)-C(7)	122.85(13)	C(13)-C(12)-H(12B)	109.4
O(4)-C(6)-C(5)	123.33(13)	H(12A)-C(12)-H(12B)	108.0
C(7)-C(6)-C(5)	113.73(12)	C(12)-C(13)-C(14)	112.68(11)
C(6)-C(7)-C(8)	107.65(11)	C(12)-C(13)-C(8)	108.95(11)
C(6)-C(7)-H(7A)	110.2	C(14)-C(13)-C(8)	111.45(11)
C(8)-C(7)-H(7A)	110.2	C(12)-C(13)-H(13)	107.9
C(6)-C(7)-H(7B)	110.2	C(14)-C(13)-H(13)	107.9
C(8)-C(7)-H(7B)	110.2	C(8)-C(13)-H(13)	107.9
H(7A)-C(7)-H(7B)	108.5	C(15)-C(14)-C(1)	105.54(11)

Table A8.2.3 cont'd.

Atoms	Angle (°)	Atoms	Angle (°)
C(15)-C(14)-C(13)	115.66(11)	C(16)-C(15)-H(15)	122.1
C(1)-C(14)-C(13)	111.38(11)	C(14)-C(15)-H(15)	122.1
C(15)-C(14)-C(5)	107.80(11)	C(15)-C(16)-C(3)	115.46(12)
C(1)-C(14)-C(5)	102.82(10)	C(15)-C(16)-H(16)	122.3
C(13)-C(14)-C(5)	112.63(11)	C(3)-C(16)-H(16)	122.3
C(16)-C(15)-C(14)	115.72(12)		

Symmetry transformations used to generate equivalent atoms:

Table A8.2.4 *Anisotropic displacement parameters ($Å^2 x\ 10^3$) for* ***211****. The anisotropic displacement factor exponent takes the form: $-2p^2[\ h^2\ a^{*2}U^{11} + \ldots + 2\ h\ k\ a^*\ b^*\ U^{12}\ ]$*

Atom	U^{11}	U^{22}	U^{33}	U^{23}	U^{13}	U^{12}
C(1)	15(1)	15(1)	15(1)	-1(1)	3(1)	-3(1)
O(1)	24(1)	16(1)	18(1)	1(1)	4(1)	1(1)
C(2)	17(1)	16(1)	15(1)	-2(1)	5(1)	-1(1)
O(2)	19(1)	16(1)	22(1)	1(1)	8(1)	1(1)
C(17)	22(1)	19(1)	27(1)	0(1)	6(1)	2(1)
O(3)	26(1)	18(1)	14(1)	-3(1)	5(1)	-6(1)
C(18)	35(1)	23(1)	16(1)	-5(1)	6(1)	-6(1)
C(3)	20(1)	17(1)	13(1)	1(1)	4(1)	1(1)
C(4)	18(1)	24(1)	15(1)	-1(1)	1(1)	0(1)
C(5)	15(1)	18(1)	15(1)	0(1)	1(1)	-1(1)
C(6)	12(1)	20(1)	19(1)	-1(1)	0(1)	-3(1)
O(4)	23(1)	22(1)	23(1)	3(1)	2(1)	3(1)
C(7)	14(1)	21(1)	19(1)	-1(1)	4(1)	1(1)
C(8)	14(1)	17(1)	18(1)	-1(1)	3(1)	0(1)
C(9)	20(1)	16(1)	18(1)	-2(1)	6(1)	3(1)
O(5)	21(1)	28(1)	22(1)	-2(1)	9(1)	-1(1)
C(10)	21(1)	25(1)	16(1)	-4(1)	4(1)	1(1)
C(11)	18(1)	22(1)	15(1)	0(1)	2(1)	1(1)

Table A8.2.4 cont'd.

Atom	U^{11}	U^{22}	U^{33}	U^{23}	U^{13}	U^{12}
C(12)	14(1)	18(1)	16(1)	0(1)	4(1)	0(1)
C(13)	14(1)	15(1)	15(1)	0(1)	3(1)	-1(1)
C(14)	14(1)	15(1)	14(1)	0(1)	3(1)	0(1)
C(15)	14(1)	13(1)	19(1)	0(1)	2(1)	1(1)
C(16)	17(1)	14(1)	20(1)	2(1)	4(1)	1(1)

Table A8.2.5 *Hydrogen coordinates (x 10^4) and isotropic displacement parameters ($Å^2$x 10^3) for* ***211***.

Atom	x	y	z	U(eq)
H(17A)	883	5507	6388	33
H(17B)	-1131	4854	6477	33
H(17C)	-261	4802	5760	33
H(18A)	2683	4783	7459	37
H(18B)	4546	5645	7491	37
H(18C)	4807	4212	7599	37
H(3)	3595	2340	7122	20
H(4A)	6700	3042	6820	23
H(4B)	6543	1601	6714	23
H(5)	6991	3344	5743	19
H(7A)	8799	1098	4651	22
H(7B)	8590	2539	4746	22
H(8)	5401	900	4394	19
H(10A)	3877	1009	3133	25
H(10B)	4659	2039	2657	25
H(11A)	3350	3589	3293	22
H(11B)	1650	2637	3078	22
H(12A)	2079	1739	4171	19
H(12B)	1690	3163	4250	19

Table A8.2.5 cont'd.

Atom	x	y	z	U(eq)
H(13)	5096	3505	4481	17
H(15)	2556	950	5210	19
H(16)	2062	859	6366	20

Table A8.2.6 *Torsion angles [°] for* ***211***.

Atoms (A-B-C-D)	Angle (°)	Atoms (A-B-C-D)	Angle (°)
O(1)-C(1)-C(2)-O(3)	-57.17(16)	C(14)-C(5)-C(6)-O(4)	-117.15(14)
C(14)-C(1)-C(2)-O(3)	121.33(12)	C(4)-C(5)-C(6)-C(7)	-176.98(11)
O(1)-C(1)-C(2)-O(2)	64.42(16)	C(14)-C(5)-C(6)-C(7)	59.51(14)
C(14)-C(1)-C(2)-O(2)	-117.08(12)	O(4)-C(6)-C(7)-C(8)	114.15(14)
O(1)-C(1)-C(2)-C(3)	-179.10(12)	C(5)-C(6)-C(7)-C(8)	-62.53(15)
C(14)-C(1)-C(2)-C(3)	-0.60(15)	C(6)-C(7)-C(8)-C(9)	178.98(11)
O(3)-C(2)-O(2)-C(17)	52.39(15)	C(6)-C(7)-C(8)-C(13)	57.53(15)
C(3)-C(2)-O(2)-C(17)	178.09(11)	C(7)-C(8)-C(9)-O(5)	-6.13(19)
C(1)-C(2)-O(2)-C(17)	-64.12(15)	C(13)-C(8)-C(9)-O(5)	118.10(14)
O(2)-C(2)-O(3)-C(18)	58.15(15)	C(7)-C(8)-C(9)-C(10)	176.66(12)
C(3)-C(2)-O(3)-C(18)	-62.81(15)	C(13)-C(8)-C(9)-C(10)	-59.11(15)
C(1)-C(2)-O(3)-C(18)	179.55(11)	O(5)-C(9)-C(10)-C(11)	-120.98(15)
O(3)-C(2)-C(3)-C(16)	-169.19(11)	C(8)-C(9)-C(10)-C(11)	56.19(16)
O(2)-C(2)-C(3)-C(16)	66.36(13)	C(9)-C(10)-C(11)-C(12)	-53.58(16)
C(1)-C(2)-C(3)-C(16)	-54.06(14)	C(10)-C(11)-C(12)-C(13)	57.39(15)
O(3)-C(2)-C(3)-C(4)	-53.73(14)	C(11)-C(12)-C(13)-C(14)	175.85(11)
O(2)-C(2)-C(3)-C(4)	-178.18(10)	C(11)-C(12)-C(13)-C(8)	-59.91(14)
C(1)-C(2)-C(3)-C(4)	61.40(13)	C(9)-C(8)-C(13)-C(12)	58.70(14)
C(16)-C(3)-C(4)-C(5)	57.16(15)	C(7)-C(8)-C(13)-C(12)	-177.97(11)
C(2)-C(3)-C(4)-C(5)	-58.00(14)	C(9)-C(8)-C(13)-C(14)	-176.34(11)
C(3)-C(4)-C(5)-C(6)	-127.56(12)	C(7)-C(8)-C(13)-C(14)	-53.01(15)
C(3)-C(4)-C(5)-C(14)	-5.53(16)	O(1)-C(1)-C(14)-C(15)	-128.21(14)
C(4)-C(5)-C(6)-O(4)	6.36(19)	C(2)-C(1)-C(14)-C(15)	53.34(14)

Table A8.2.6 cont'd.

Atoms (A-B-C-D)	Angle (°)	Atoms (A-B-C-D)	Angle (°)
O(1)-C(1)-C(14)-C(13)	-1.95(18)	C(4)-C(5)-C(14)-C(15)	-48.37(14)
C(2)-C(1)-C(14)-C(13)	179.60(10)	C(6)-C(5)-C(14)-C(1)	-171.80(11)
O(1)-C(1)-C(14)-C(5)	118.91(14)	C(4)-C(5)-C(14)-C(1)	62.84(13)
C(2)-C(1)-C(14)-C(5)	-59.54(13)	C(6)-C(5)-C(14)-C(13)	-51.81(14)
C(12)-C(13)-C(14)-C(15)	47.93(15)	C(4)-C(5)-C(14)-C(13)	-177.16(11)
C(8)-C(13)-C(14)-C(15)	-74.92(14)	C(1)-C(14)-C(15)-C(16)	-54.28(15)
C(12)-C(13)-C(14)-C(1)	-72.56(14)	C(13)-C(14)-C(15)-C(16)	-177.88(12)
C(8)-C(13)-C(14)-C(1)	164.59(11)	C(5)-C(14)-C(15)-C(16)	55.07(15)
C(12)-C(13)-C(14)-C(5)	172.52(11)	C(14)-C(15)-C(16)-C(3)	-1.74(17)
C(8)-C(13)-C(14)-C(5)	49.67(14)	C(2)-C(3)-C(16)-C(15)	59.13(15)
C(6)-C(5)-C(14)-C(15)	76.99(13)	C(4)-C(3)-C(16)-C(15)	-56.33(15)

Symmetry transformations used to generate equivalent atoms:

A8.7 REFERENCES AND NOTES

(1) Sheldrick, G. M. Phase Annealing in SHELX-90: Direct Methods for Larger Structures. *Acta. Crystallogr. A Found. Crystallogr.* **1990**, *46*, 467–473.

(2) Sheldrick, G. M. Crystal Structure Refinement with *SHELXL*. *Acta. Crystallogr. C Struct. Chem.* **2015**, *71*, 3–8.

(3) Müller, P. Practical Suggestions for Better Crystal Structures. *Crystallogr. Rev.* **2009**, *15*, 57–83.

APPENDIX 9

Alternative Masked "A" Ring Strategies

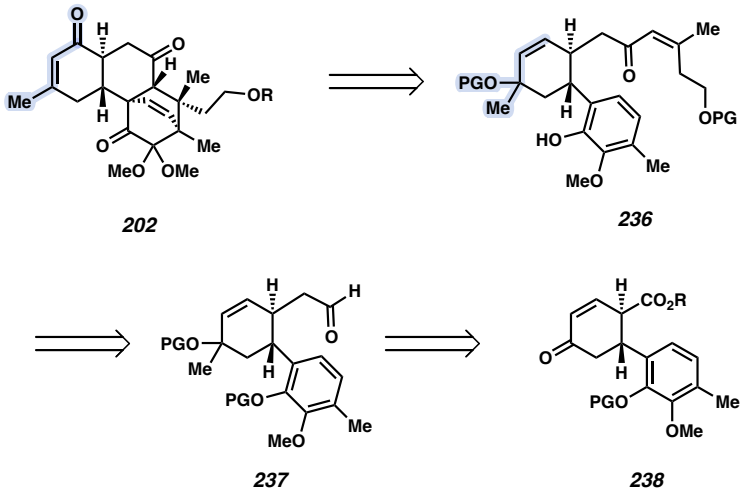
A9.1 INTRODUCTION

Our initial efforts to prepare the fully functionalized intermediate for the proposed dearomative [4+2] reaction were undermined by challenges associated with appropriately masking the A ring methyl enone via intermediates with decreased A ring oxidation states. This appendix details our efforts, progress, and potential future directions using masked intermediates in a higher oxidation level than those described in Chapter 4.

A9.2 TERTIARY ALLYLIC ALCOHOL

Our initial efforts aimed to mask the A ring enone as a tertiary allylic alcohol, a tactic utilized by Gao and coworkers in their synthesis of **171**,[1] and targeted **236** as the desired substrate for dearomative cycloaddition. In a retrosynthetic sense, we imagined synthesizing **236** from aldehyde **237** that would arise from cyclohexeneone **238**.

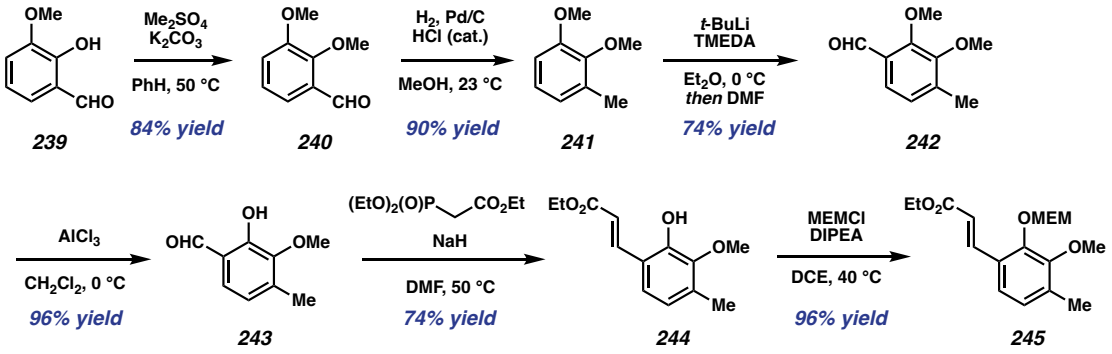
Figure A9.2.1 *Initial retrosynthesis masking the A ring enone as a tertiary allylic alcohol*



In the forward sense, beginning with *ortho*-vanillin (**239**), methylation and exhaustive reduction of the benzaldehyde derivative provided catechol derivative **241** (Scheme A9.2.1).[2] Directed *ortho*-lithiation with *t*-BuLi and TMEDA followed by trapping with DMF afforded aldehyde **242**.[3] Selective demethylation with $AlCl_3$[4] in CH_2Cl_2 provided

phenol **242** nearly quantitatively. Finally, Horner-Wadsworth-Emmons olefination followed by protection of the phenol as the MEM ether provided cinnamyl ester **245**.

Scheme A9.2.1 *Synthesis of substituted arene* ***245***

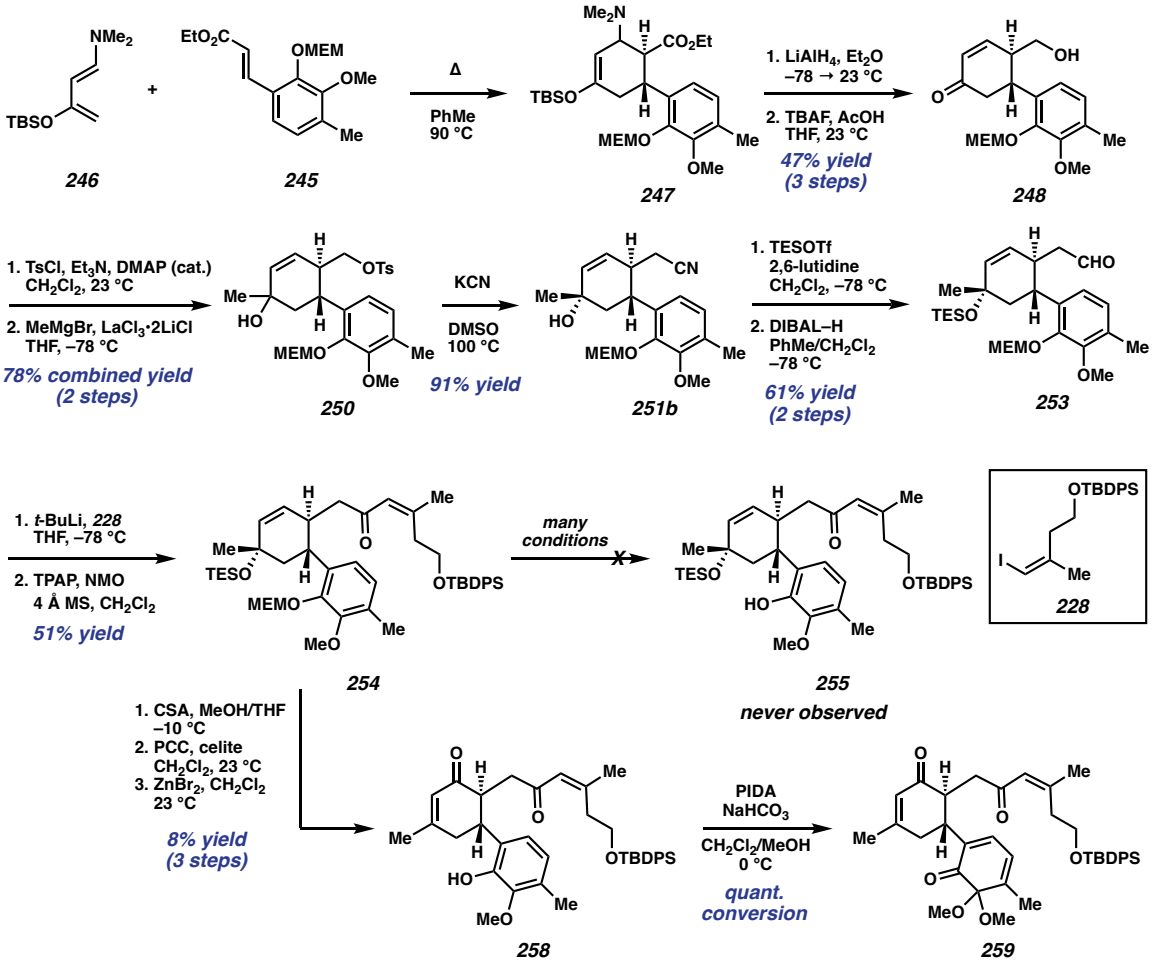


Treatment of **245** with multiple equivalents of Rawal's diene (**246**) at high temperature resulted in the formation of **247** as an inconsequential mixture of α- and β-dimethylamino diastereomers (Scheme A9.2.2). Treatment of the ester with $LiAlH_4$ in Et_2O exhaustively reduced the ester to the corresponding alcohol. Elimination of the dimethylamino substituent was performed by subjecting the silyl enol ether to a mixture of TBAF and AcOH, resulting in the formation of enone **247**. At this stage, tosylation of the primary alcohol and 1,2-addition of MeMgBr in the presence of $LaCl_3$•2LiCl gave a separable mixture of diastereomers (**250**), the major diastereomer (**250b**) of which was advanced.

With the tertiary allylic alcohol installed, we shifted our focus to constructing the dienophile. To that end, displacement of the primary tosylate with cyanide gave **251b**. TES protection of the alcohol and reduction of the nitrile to the corresponding aldehyde gave **253**. 1,2-addition of an organolithium derived from vinyl iodide **228** to the aldehyde yielded the corresponding allylic alcohol that was oxidized to the enone using Ley-Griffith conditions (i.e. TPAP; NMO). To test the dearomative cycloaddition, all that remained was removal of

the MEM protecting group. Despite many attempts to remove this group, we experienced no success in performing this selectively. The tertiary allylic alcohol proved problematic in all cases and led to degradation. Use of bulkier protecting groups did not remedy this issue.

Scheme A9.2.2 *Elaboration of arene* ***245****, failed deprotection, and formation of A ring enone*

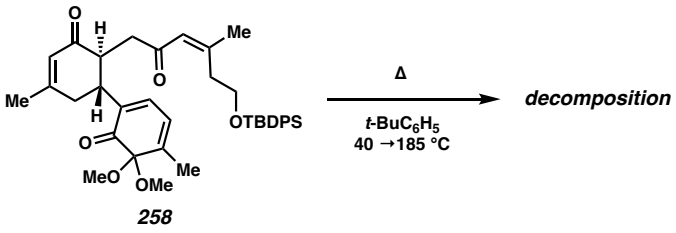


Experiencing no success with the deprotection, we decided at this stage to change our substrate to avoid deprotection in the presence of the tertiary allylic alcohol. The tertiary allylic alcohol was selectively deprotected using CSA in a mixture of methanol and THF. To obviate the complications caused by the tertiary allylic alcohol, we opted to perform oxidative transposition to form the enone. Unfortunately, the yield of the oxidation of the

tertiary allylic alcohol with PCC was exceptionally low yielding (16% yield). Oxidation with TEMPO•BF_4 was equally poor. Alternative chromium oxidants were not attempted but may hold promise for future studies. Excitingly, in the absence of the tertiary allylic alcohol, removal of the MEM protecting group was possible to give enone **258** in an overall 8% yield from **254**. Oxidation of the phenol with PIDA in the presence of MeOH led to formation of masked *ortho*-quinone **259**.

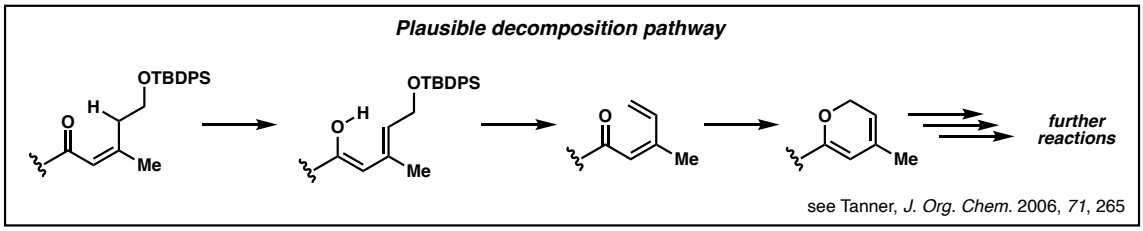
Unfortunately, unlike in the model system, the desired cycloaddition did not occur readily. Attempted gradual heating of the sample led to decomposition at high temperature, perhaps through decomposition of the dieneophile, as thermal degradation of similar species has been documented by Tanner and coworkers (Scheme A9.3.3).[5]

Scheme A9.2.3 *Failed cycloaddition of MOB* ***258*** *and potential decomposition pathway*



258

poor material throughput prevented further optimization



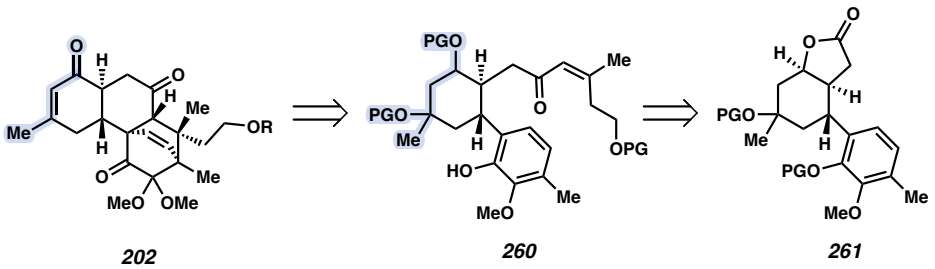
Our ability to optimize this transformation was limited at this stage due to poor material throughput. Formation of masked *ortho*-quinone **258** represents the 20th step in the longest linear sequence beginning with *ortho*-vanillin (**238**). Our attempt to circumvent the sensitivity imparted by the tertiary allylic alcohol introduced another potentially reactive

enone into our system as well as a low yielding series of steps. Furthermore, we imagined that even if the desired cycloaddition would occur, this reactive moiety would again need to be protected during subsequent elaborations that would be necessary to access kuroshine A. Therefore, avoiding premature formation of the enone seemed strategic, leading us to design a new strategy that made use of our previously accessed intermediates.

A9.3 LACTONE SYNTHESIS

We reasoned that it would be possible to maintain the same A ring oxidation level while avoiding the allylic alcohol intermediate if we could access an intermediate such as **259**. We imagined that this compound would be accessible via lactone **260**, taking inspiration from Tanner's approach to norzoanthamine (**171**).[5–7]

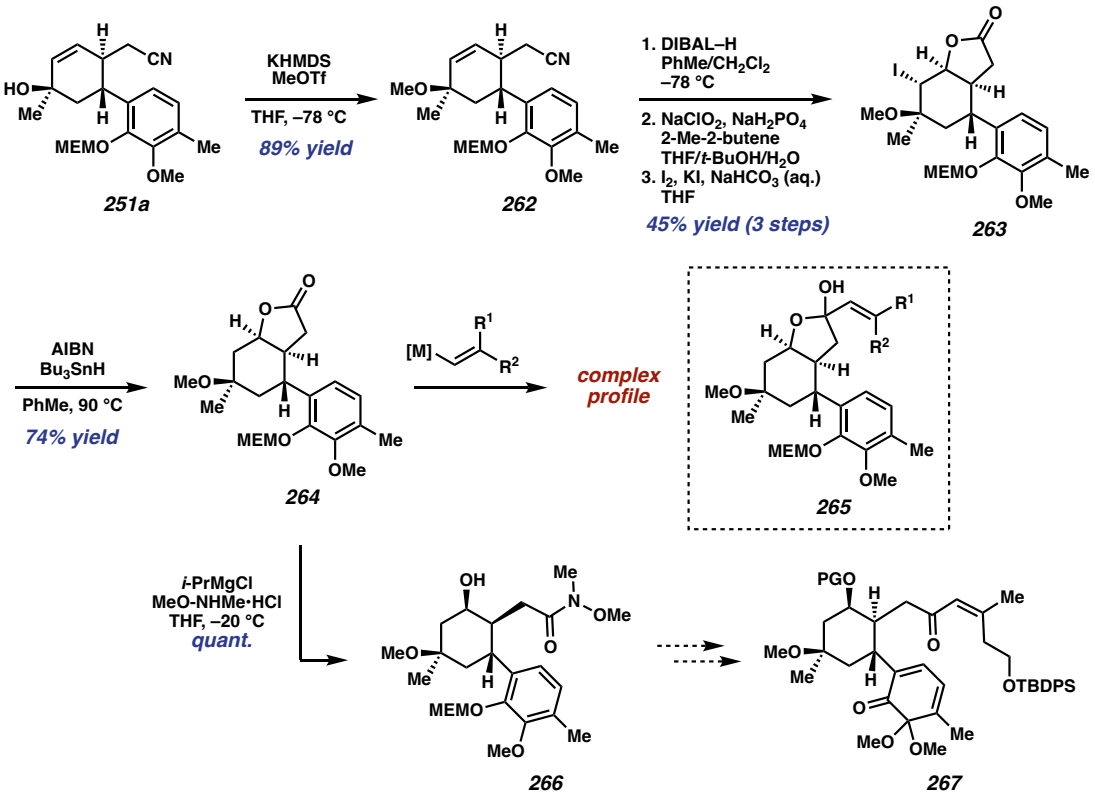
Figure A9.3.1 *Revised synthetic approach to preserve A ring oxidation level*



Beginning with intermediate **251a**, derived from the minor diastereomer of the methyl 1,2 addition (Scheme A9.2.2), methylation of the tertiary allylic alcohol with KHMDS and MeOTf effectively gave methyl ether **262** in 89% yield without undesired reaction of the nitrile. Reduction of the nitrile followed by Pinnick oxidation of the aldehyde gave the corresponding carboxylic acid which was subjected to iodolactonization to give iodide **263** in 48% yield over 3 steps. Radical deiodination afforded **264**. Initial attempts to affect 1,2-addition to the lactone led to complex reaction profiles, but this may be due to the fact that two possible lactol diastereomers can form in addition to the possible ring opened

isomer. Ring opening of the lactone to synthesize **266** proceeded smoothly, and efforts are ongoing to protect this secondary alcohol and advance to intermediate **267**. We believe that this synthetic sequence involving formation of the lactone represents an especially promising path forward.

Scheme A9.3.1. *Revised synthetic approach to avoid allylic alcohol and preserve A ring oxidation*



A9.4 CONCLUSION

While we believe there is merit to approaches toward **172** that utilize intermediates with higher A ring oxidation states, at present the lack of material throughput has dramatically affected our ability to test and optimize the key MOB cycloaddition. Assuming that this step can be evaluated through the route described in Chapter 4, we believe the approaches described herein may be worth exploring in future endeavors as they contain

additional oxidation at necessary positions that will obviate the need for late-stage desaturation. Ultimately, our decision to pursue an alternative route was motivated by a desire to expediently synthesize the substrates necessary to evaluate the key transformation.

A9.6 EXPERIMENTAL SECTION

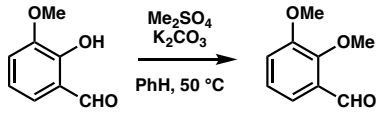
Only ^{1}H NMR characterization data are shown for all compounds in this Appendix. The spectra are included for reference, but may still contain residual solvent or other impurities.

A9.6.1 MATERIALS AND METHODS

Unless otherwise stated, reactions were performed in flame-dried glassware under an argon or nitrogen atmosphere using dry, deoxygenated solvents. Solvents were dried by passage through an activated alumina column under argon.[8] Reaction progress was monitored by thin-layer chromatography (TLC) or Agilent 1290 UHPLC-MS. TLC was performed using E. Merck silica gel 60 F254 precoated glass plates (0.25 mm) and visualized by UV fluorescence quenching, *p*-anisaldehyde, or $KMnO_4$ staining. Silicycle Silia*Flash*® P60 Academic Silica gel (particle size 40–63 μm) was used for flash chromatography. ^{1}H NMR spectra were recorded on Varian Inova 500 or 600 MHz and Bruker 400 MHz spectrometers and are reported relative to residual $CHCl_3$ (δ 7.26 ppm), C_6D_5H (δ 7.16 ppm), and CD_2HOD (δ 3.31). ^{13}C NMR spectra were recorded on a Varian Inova 500 MHz spectrometer (125 MHz) and Bruker 400 MHz spectrometers (100 MHz) and are reported relative to $CDCl_3$ (δ 77.16 ppm) or C_6D_6 (δ 128.06 ppm). Data for ^{1}H NMR are reported as follows: chemical shift (δ ppm) (multiplicity, coupling constant (Hz), integration). Multiplicities are reported as follows: s = singlet, d = doublet, t = triplet, q = quartet, p = pentet, sept = septuplet, m = multiplet, br s = broad singlet, br d = broad doublet. Data for

^{13}C NMR are reported in terms of chemical shifts (δ ppm). IR spectra were obtained by use of a Perkin Elmer Spectrum BXII spectrometer using thin films deposited on NaCl plates and reported in frequency of absorption (cm^{-1}). Optical rotations were measured with a Jasco P-2000 polarimeter operating on the sodium D-line (589 nm), using a 100 mm path-length cell. High resolution mass spectra (HRMS) were obtained from the Caltech Mass Spectral Facility using a JEOL JMS-T2000GC AccuTOF^{TM} GC-Alpha High Resolution Mass Spectrometer in field ionization (FI+) or field desorption (FD+) mode, or an Agilent 6230 Series TOF with an Agilent Jet Stream ion source in electrospray ionization (ESI+) mode. Reagents were purchased from commercial sources and used as received unless otherwise stated.

A9.6.2 EXPERIMENTAL PROCEDURES

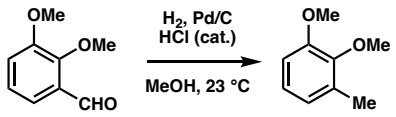


239 ***240***

Aldehyde 240: *ortho*-Vanilin (27.0 g, 178 mmol, 1 equiv) was added to a round bottom flask with stir bar. Benzene (150 mL) was added followed by K_2CO_3 (50.0 g, 362 mmol, 2 equiv) and resulting mixture was stirred vigorously. Me_2SO_4 (24 mL, 240 mmol, 1.4 equiv) was added and mixture was heated to 50 °C and stirred for 48 hours. After this time, water (300 mL) and 1N aq. NaOH (50 mL) were added and mixture was stirred for 30 mins. Then the layers were partitioned and the aqueous layers was extracted with Et_2O (3x100 mL). The combined organic layers were washed with brine (100 mL), dried over Na_2SO_4, and concentrated to give a thick oil. 1N NaOH (approx. 100 mL) was added and after slight agitation resulted in the precipitation of a solid. The solid was filtered and collected in a

Büchner funnel, washed with water (3x 20 mL), and dried under vacuum to give an off-white/tan solid (24.7 g, 84% yield).

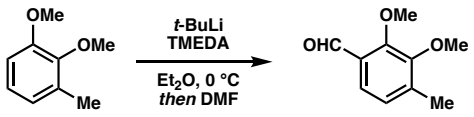
^{1}H NMR: (500 MHz, $CDCl_3$) δ 10.43 (d, *J* = 0.7 Hz, 1H), 7.42 (dd, *J* = 6.7, 2.7 Hz, 1H), 7.19 – 7.10 (m, 2H), 4.00 (s, 3H), 3.92 (s, 3H).



240 ***241***

1,2-Dimethoxy-3-methylbenzene (241): To a round-bottom flask was added aldehyde **240** (10.0 g, 60.2 mmol, 1.0 equiv) followed by palladium on carbon (10% wt, 700 mg), MeOH (240 mL), and concentrated HCl (0.8 mL). The flask was fitted with a glass 3-way stop valve. One valve was connected to a vacuum line, the other to an N_2 line. The flask was cycled between vacuum and N_2 10 times, approximately 5–10 seconds per vacuum cycle. Then the N_2 line was exchanged for a balloon of H_2. The flask was then cycled between vacuum and H_2 10 times, approximately 5–10 seconds per vacuum cycle. The three way valve was closed, the partially depleted H_2 balloon was replaced with a full H_2 balloon, the valve was re-opened to H_2 and the mixture was vigorously stirred for 12 hours. After this time, the valve was closed, the H_2 balloon was swapped for an N_2 line. The flask was cycled between vacuum and N_2 10 times, approximately 5–10 seconds per vacuum cycle. The mixture was filtered through celite, eluting with EtOAc (200 mL). *SAFETY NOTE: The celite/Pd/C should be kept wet and disposed of in a separate waste container to prevent sparking or combustion.* The filtrate was concentrated to give the title compound as a thick oil (8.20 g, 90% yield).

^{1}H NMR: (500 MHz, $CDCl_3$) δ 6.96 (t, J = 7.9 Hz, 1H), 6.80 – 6.73 (m, 2H), 3.86 (s, 3H), 3.81 (d, J = 0.8 Hz, 3H), 2.29 (s, 3H).

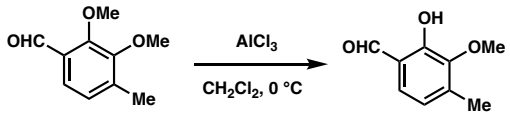


241 ***242***

Benzaldehyde 242: To a round-bottom flask with stir bar was added arene **241** (10.0 g, 65.7 mmol, 1.0 equiv). The flask was evacuated and backfilled with N_2 three times. Dry Et_2O (365 mL) was added followed by tetramethylethylenediamine (13.8 mL, 92 mmol, 1.4 equiv) and the solution was cooled to 0 °C. *tert*-Butyllithium (1.7M in pentane, 47 mL, 78.8 mmol, 1.2 equiv) was added dropwise over 1.5 hours, then the cooling bath was removed and the solution was allowed to stir for an additional 12 hours. After this time, the solution was cooled to 0 °C and DMF (10.2 mL, 131.4 mmol, 2.0 equiv) was added over 1 hour. The solution was stirred for an additional 20 minutes then quenched by the careful addition of ice water (360 mL) followed by 2N aq. HCl (12 mL). The layers were partitioned and the aqueous layer was extracted with Et_2O (3x75 mL). The combined organic layers were washed with brine (75 mL), dried over Na_2SO_4 and concentrated. The crude oil was purified by silica gel flash column (0 → 20% Et_2O in hexanes) to give the title compound as a colorless oil (8.69 g, 74% yield).

EFH-XI-199

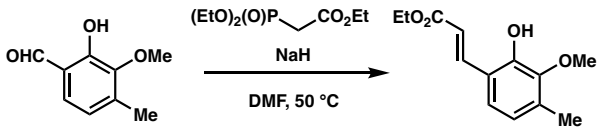
^{1}H NMR: (500 MHz, $CDCl_3$) δ 10.33 (d, J = 0.9 Hz, 1H), 7.48 (d, J = 7.9 Hz, 1H), 7.00 (dq, J = 7.9, 0.7 Hz, 1H), 4.00 (s, 3H), 3.86 (s, 3H), 2.33 (d, J = 0.8 Hz, 3H).



242 ***243***

Phenol 243: To a round-bottom flask was added benzaldehyde **242** (10.2 g, 56.6 mmol, 1.0 equiv). The flask was evacuated and backfilled with N_2 three times. CH_2Cl_2 (275 mL) was added and the solution was cool to –5 °C. $AlCl_3$ (11.32g, 84.9 mmol, 1.5 equiv) was added in two portions stirring for 5 minutes in between the two additions. The solution was warmed to ambient temperature, stirred for an additional hour until TLC indicated complete consumption of the starting material. Then the reaction mixture was poured into ice water (400 mL). The layers were separated and the aqueous layer was extracted with CH_2Cl_2 (3x75 mL). The combined organic layers were washed with satd. aq. $NaHCO_3$ (200 mL), brine (70 mL), dried over Na_2SO_4, and concentrated. The crude oil was passed through a pad of silica gel eluting with 20% EtOAc in hexanes to give the title compound an orange oil (8.72 g, 93% yield).

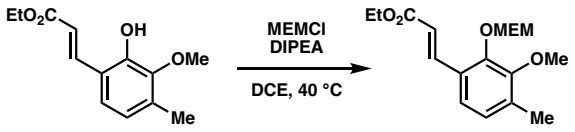
^{1}H NMR: (500 MHz, $CDCl_3$) δ 11.14 (s, 1H), 9.82 (d, J = 1.3 Hz, 1H), 7.20 (d, J = 7.9 Hz, 1H), 6.85 – 6.79 (m, 1H), 3.90 (s, 3H), 2.34 (s, 3H).



243 ***244***

Cinnamyl ester 244: To a round-bottom flask was added NaH (60% wt mineral oil dispersion, 2.71 g, 67.8 mmol, 2.5 equiv). The flask was evacuated and backfilled with nitrogen three times then cooled to 0 °C. DMF (27 mL) was added followed by triethylphosphonoacetate (15.19 g, 67.8 mmol, 2.5 equiv) added dropwise. The mixture was allowed to stir for 10 minutes then warmed to ambient temperature and stirred for an additional 30 minutes. Phenol **243** (4.50 g, 27.1 mmol, 1.0 equiv) in DMF (27 mL) was added dropwise. The mixture was heated to 50 °C for 10 hours. After this time, the reaction was cooled to 0 °C and quenched by addition of water (100 mL) and NH_4Cl (50 mL) then Et_2O (100 mL) was added. The layers were separated, and the aqueous layer was extracted with Et_2O (5x75 mL). The combined organic layers were washed with aq. LiCl (2x50 mL), brine (50 mL), dried over Na_2SO_4 and concentrated under reduced pressure. The crude oil was purified by silica gel flash column (30% Et_2O in hexanes) to give the title compound as a colorless solid (4.764 g, 74% yield).

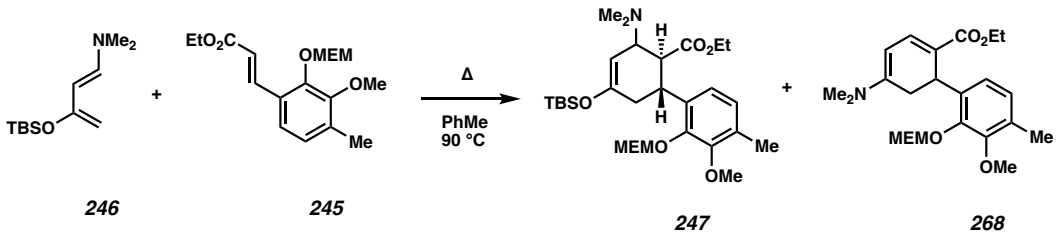
^{1}H NMR: (500 MHz, $CDCl_3$) δ 7.87 (d, *J* = 16.1 Hz, 1H), 7.13 (d, *J* = 8.1 Hz, 1H), 6.70 (d, *J* = 8.1 Hz, 1H), 6.58 (d, *J* = 16.1 Hz, 1H), 6.19 (d, *J* = 2.9 Hz, 1H), 4.26 (q, *J* = 7.1 Hz, 2H), 3.81 (s, 3H), 2.32 (s, 3H), 1.34 (t, *J* = 7.1 Hz, 3H).



244 ***245***

MEM ether 245: To a round bottom flask was added cinnamyl ester **244** (4.76 g, 20.2 mmol, 1 equiv). The flask was evacuated and backfilled with N_2 three times. CH_2Cl_2 (100 mL) was added followed by DIPEA (10.79 mL, 60.5 mmol, 3 equiv). MEMCl (6.9 mL, 60.5 mmol, 3 equiv) was added slowly. Then the solution was heated to 40 °C for 12 hours. After this time, the reaction was cooled to ambient temperature and satd. aq. $NaHCO_3$ (100 mL) was added and mixture was stirred vigorously. The layers were partitioned and separated. The aqueous layer was extracted with CH_2Cl_2 (3x50 mL). The combined organic layers were washed with brine (50 mL), dried over Na_2SO_4, and concentrated. The crude residue was purified by silica gel flash column (30% EtOAc in hexanes) to give the tile compound as a colorless oil (6.27 g, 96% yield).

^{1}H NMR: (500 MHz, $CDCl_3$) δ 8.00 (d, *J* = 16.1 Hz, 1H), 7.21 (d, *J* = 8.0 Hz, 1H), 6.92 (d, *J* = 7.9 Hz, 1H), 6.40 (d, *J* = 16.2 Hz, 1H), 5.23 (d, *J* = 1.6 Hz, 2H), 4.28 – 4.21 (m, 2H), 3.98 – 3.93 (m, 2H), 3.78 (d, *J* = 1.7 Hz, 3H), 3.59 – 3.54 (m, 2H), 3.36 (d, *J* = 1.4 Hz, 3H), 2.27 (s, 3H), 1.32 (td, *J* = 7.1, 1.7 Hz, 3H).



246 ***245*** ***247*** ***268***

Silyl Enol Ether 247: To a round-bottom flask with stir bar was added MEM ether **245** (5.06 g, 15.6 mmol, 1 equiv) and toluene (15 mL). Rawal's diene[9] (11.0 g, 48.4 mmol, 3.1 equiv) was added and the solution was evacuated and backfilled rapidly with N_2 five times. Then the solution was sparged with N_2 for five minutes. The reaction was heated to 90 °C and maintained at this temperature for 36 hours. After this time, crude mixture was purified by silica gel flash column (0 → 25% EtOAc in 95:5 hexanes/triethylamine) to give the title compound as a yellow/orange oil (6.30 g). Under these conditions, partial separation of the α- and β-NMe_2 diastereomers was achieved. Separation of these diastereomers is not necessary and is simply provided for ease of characterization. We also noted the appearance of a byproduct when the reaction was performed on larger scales, the structure of which is tentatively assigned to be **268**.

EFH-XII-169

Major Diastereomer:

^{1}H NMR: (500 MHz, C_6D_6) δ 7.00 (br s, 1H), 6.80 (br s, 1H), 5.44 – 5.30 (m, 2H), 5.13 (s, 1H), 4.21 – 4.14 (m, 1H), 4.03 (dt, *J* = 10.4, 4.9 Hz, 1H), 3.98 – 3.91 (m, 2H), 3.74 (s, 1H), 3.52 (s, 3H), 3.49 – 3.43 (m, 2H), 3.16 (s, 4H), 2.71 – 2.56 (m, 1H), 2.35 (s, 6H), 2.14 (s, 3H), 0.98 (s, 9H), 0.74 (s, 2H), 0.48 (s, 3H), 0.19 (overlapping singlets, *J* = 4.1 Hz, 6H).

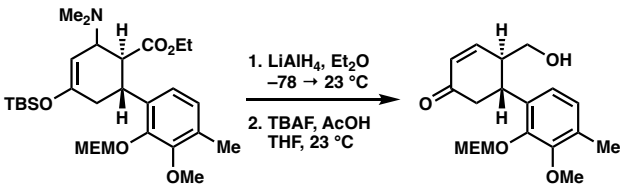
Minor Diastereomer:

^{1}H NMR: (500 MHz, C_6D_6) δ 6.74 (q, *J* = 8.0 Hz, 2H), 5.51 (d, *J* = 5.2 Hz, 1H), 5.46 (d, *J* = 5.2 Hz, 1H), 5.16 (dd, *J* = 4.8, 1.8 Hz, 1H), 4.36 (d, *J* = 17.6 Hz, 1H), 4.11 – 3.99 (m, 2H),

3.96 (ddd, *J* = 10.7, 6.0, 4.5 Hz, 1H), 3.92 – 3.84 (m, 1H), 3.55 (s, 3H), 3.51 – 3.42 (m, 2H), 3.34 – 3.24 (m, 1H), 3.15 (s, 3H), 2.71 (dd, *J* = 17.2, 5.7 Hz, 1H), 2.42 (s, 6H), 2.14 (s, 4H), 0.98 (s, 9H), 0.49 (s, 3H), 0.21 (s, 3H), 0.19 (s, 3H).

*Byproduct **268***

^{1}H NMR: (500 MHz, C_6D_6) δ 7.98 (d, *J* = 6.9 Hz, 1H), 7.29 (d, *J* = 7.9 Hz, 1H), 6.73 (dd, *J* = 7.9, 0.8 Hz, 1H), 5.59 – 5.52 (m, 2H), 5.01 (dd, *J* = 9.6, 1.8 Hz, 1H), 4.72 – 4.67 (m, 1H), 4.21 – 4.07 (m, 3H), 3.98 (ddd, *J* = 10.9, 5.7, 4.1 Hz, 1H), 3.56 (s, 3H), 3.47 (dt, *J* = 5.7, 3.9 Hz, 2H), 3.13 (s, 3H), 2.90 (dd, *J* = 16.4, 1.9 Hz, 1H), 2.73 (ddd, *J* = 16.3, 9.7, 1.6 Hz, 1H), 2.07 (overlapping singlets, *J* = 3.2 Hz, 9H), 1.05 (t, *J* = 7.1 Hz, 3H).

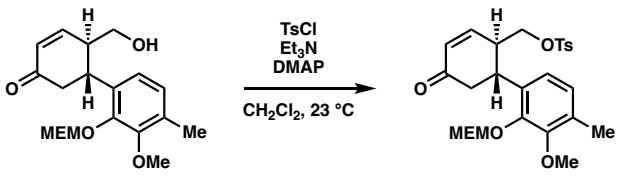


247 ***248***

Enone 248: To a round bottom flask was added solid $LiAlH_4$ (powder, 1.303 g, 34.3 mmol, 3 equiv). The flask was cooled to –78 °C. Then Et_2O (45 mL) was added and the solution was stirred for 5 minutes. Silyl enol ether **247** (mixture of diastereomers, 6.30 g, 11.42 mmol, 1 equiv) was added slowly as a solution in Et_2O (45 mL). The solution was allowed to warm to ambient temperature for 4 hours, then stirred for an additional 10 hours. After this time, the solution was cooled to 0 °C and diluted with Et_2O (90 mL). 6.7 mL of water was cautiously added and the mixture was stirred for 1 hour. Then the solution was further diluted with Et_2O (180 mL) and 45 g Na_2SO_4 were added. The mixture was vigorously stirred for 30 minutes, then filtered, the solid washed with Et_2O and the filtrate concentrated to give an oil that was used without further purification.

To the crude oil in a round-bottom flask was added THF (80 mL) and the solution was cooled to 0 °C. AcOH (1.71 mL, 30 mmol, 3 equiv) was added and the solution was stirred for 5 minutes. Then TBAF (1.0 M in THF, 20 mL, 20 mmol, 2 equiv) was added and the solution was maintained at 0 °C for 45 minutes. Water (150 mL) was added, the layers were separated, and the aqueous layer was extracted with EtOAc (3x40 mL). The combined organic layers were washed with brine (50 mL), dried over Na_2SO_4, and concentrated. The crude residue was purified by silica gel flash column (0→ 50% EtOAc in hexanes) to give the title compound as a pale gold oil (2.58g, 47% overall yield from MEM ether **245**).

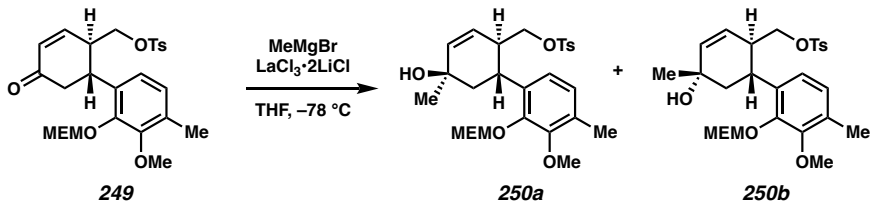
^{1}H NMR: (500 MHz, $CDCl_3$) δ 7.08 (dd, *J* = 10.2, 2.1 Hz, 1H), 6.96 (d, *J* = 8.0 Hz, 1H), 6.91 (d, *J* = 8.0 Hz, 1H), 6.18 (ddd, *J* = 10.0, 3.1, 0.9 Hz, 1H), 5.24 (d, *J* = 1.2 Hz, 2H), 3.90 – 3.79 (m, 3H), 3.77 (s, 3H), 3.66 (ddd, *J* = 11.8, 8.6, 3.3 Hz, 1H), 3.53 (dd, *J* = 5.1, 4.1 Hz, 2H), 3.49 (ddd, *J* = 11.8, 5.1, 3.8 Hz, 1H), 3.35 (s, 3H), 2.91 (dd, *J* = 8.7, 5.1 Hz, 1H), 2.76 – 2.58 (m, 3H), 2.27 (d, *J* = 0.6 Hz, 3H).



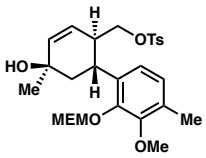
248 ***249***

Tosylate 249: To a round-bottom flask with stir bar was added enone **248** (2.58 g, 7.36 mmol, 1 equiv) and CH_2Cl_2 (9.8 mL). TsCl (3.51 g, 18.4 mmol, 2.5 equiv) was added followed by Et_3N (2.67 mL, 19.14 mmol, 2.6 equiv) and DMAP (90 mg, 0.74 mmol, 10 mol%). The reaction was stirred for 12 hours. Water (100 mL) was added and the layers were separated. The aqueous layer was extracted with CH_2Cl_2 (3x20 mL). The combined organic layers were washed with brine (30 mL), dried over Na_2SO_4, and concentrated. The crude oil was purified by silica gel flash column (0→30% EtOAc in hexanes) to give the title compound as a pale yellow oil (2.97g, 81% yield).

^{1}H NMR: (500 MHz, $CDCl_3$) δ 7.76 – 7.67 (m, 2H), 7.32 – 7.28 (m, 2H), 6.92 – 6.85 (m, 2H), 6.78 (d, *J* = 7.9 Hz, 1H), 6.15 – 6.09 (m, 1H), 5.15 (d, *J* = 1.1 Hz, 2H), 4.00 (dd, *J* = 10.0, 3.9 Hz, 1H), 3.85 (dd, *J* = 10.0, 7.6 Hz, 1H), 3.78 (td, *J* = 5.0, 4.0 Hz, 2H), 3.72 (s, 3H), 3.62 (ddd, *J* = 13.5, 10.9, 4.4 Hz, 1H), 3.54 – 3.43 (m, 2H), 3.33 (s, 3H), 3.06 (s, 0H), 2.69 (dd, *J* = 16.5, 13.4 Hz, 1H), 2.63 – 2.55 (m, 1H), 2.45 (s, 3H), 2.28 – 2.23 (m, 3H).



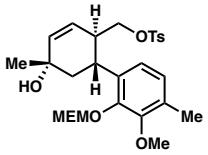
Alcohol 250: To a round-bottom flask was added MeMgBr (3.0 M in Et_2O, 5.11 mL, 15.3 mmol, 2.6 equiv) and the solution was cooled to –78 °C. During this time the solution tended to solidify. $LaCl_3$•2LiCl (0.6 M in THF, 25.6 mL, 15.33 mmol, 2.6 equiv) was added. The mixture was warmed as needed until stirring resumed and the solution became homogeneous, then cooled to –78 °C. Tosylate **249** (2.97 g, 5.90 mmol, 1 equiv) was added dropwise as a solution in THF (58 mL). The solution was maintained at –78 °C for 1 hour then warmed to 0 °C for 30 minutes. MeOH (3 mL) was added to quench the reaction then SiO_2 was added (approx. 10 g). The slurry was filtered through a plug of silica gel eluting with EtOAc. The filtrate was concentrated and the crude residue was purified by silica gel flash column (0→30% acetone in hexanes) to give first the minor diastereomer **250a** (1.13 g) then the second, major diastereomer **250b** (1.87 g) both as thick colorless oils (combined 98% yield). The relative stereochemistry of each compound was confirmed by nOE experiments of subsequent intermediates. *Note: while the diastereomers are ultimately inconsequential, they were separated at this stage for ease of analysis of subsequent transformations.*



*Minor Diastereomer **250a***

^{1}H NMR (500 MHz, $CDCl_3$) δ 7.71 – 7.65 (m, 2H), 7.26 (obscured by $CHCl_3$, 2H), 6.85 (d, J = 8.0 Hz, 1H), 6.76 (d, J = 8.0 Hz, 1H), 5.84 – 5.76 (m, 2H), 5.15 (d, J = 6.5 Hz, 1H), 5.05

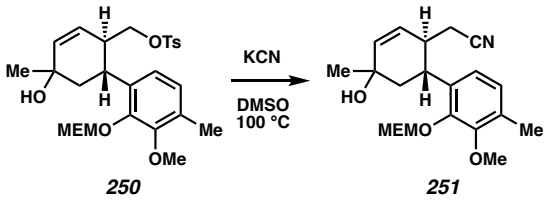
(d, *J* = 6.5 Hz, 1H), 3.98 (ddd, *J* = 11.0, 6.8, 2.5 Hz, 1H), 3.94 – 3.83 (m, 2H), 3.79 (t, *J* = 9.5 Hz, 1H), 3.73 (s, 3H), 3.57 (qdd, *J* = 10.6, 5.9, 2.4 Hz, 2H), 3.45 (t, *J* = 12.1 Hz, 1H), 3.29 (s, 3H), 2.59 (s, 1H), 2.43 (s, 3H), 2.24 (s, 3H), 1.89 (dd, *J* = 13.1, 2.9 Hz, 1H), 1.70 (t, *J* = 13.3 Hz, 1H), 1.27 (s, 1H).



Major Diastereomer ***250b***

^{1}H NMR (500 MHz, $CDCl_3$) δ 7.71 – 7.65 (m, 2H), 7.29 – 7.26 (m, 2H), 6.84 (d, *J* = 7.9 Hz, 1H), 6.75 (d, *J* = 7.9 Hz, 1H), 5.76 – 5.69 (m, 1H), 5.61 (dd, *J* = 10.1, 2.0 Hz, 1H), 5.17 (d, *J* = 5.6 Hz, 1H), 5.12 (d, *J* = 5.6 Hz, 1H), 3.95 – 3.85 (m, 2H), 3.82 (dt, *J* = 10.9, 4.4 Hz, 1H), 3.78 – 3.72 (m, 1H), 3.72 (s, 3H), 3.56 (t, *J* = 4.6 Hz, 2H), 3.37 (s, 3H), 3.15 (t, *J* = 12.0 Hz, 1H), 2.65 (s, 1H), 2.43 (s, 3H), 2.26 – 2.16 (m, 3H), 2.05 (s, 1H), 1.89 (ddd, *J* = 12.6, 3.1, 1.6 Hz, 1H), 1.73 – 1.56 (m, 1H), 1.37 (s, 3H).

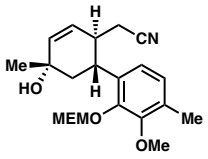
Note: all transformations shown from this point forward can be performed using either diastereomer with no significant changes in reactivity. The characterization data shown are for the diastereomer that is indicated. The nitrile compounds derived from the substitution of the tosylate diastereomers were used to investigate the two strategies described in this Appendix.



250 ***251***

Safety note: KCN is highly toxic. As a solution in DMSO, it can readily absorb into the skin. Extreme caution should be taken to avoid contact with the KCN solutions. All aqueous waste was separately treated with $NaHCO_3$ and NaOCl and appropriately stored in a separate waste container and discarded.

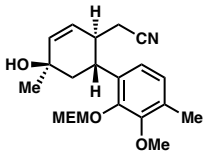
Nitrile 251: To a round-bottom flask was added added KCN (702 mg, 10.78 mmol, 3 equiv) and the flask was evacuated and backfilled with N_2 three times. Alcohol **250** (1.87 g, 3.59 mmol, 1 equiv) was added as a solution in DMSO (23 mL). The reaction was heated to 100 °C in an oil bath. After 2 hours the solution was cooled to ambient temperature. Water (120 mL) was added followed by satd. aq. $NaHCO_3$ (4 mL). The aqueous layer was extracted with EtOAc (3x15 mL). The combined organic layers were washed with brine (20 mL), dried over Na_2SO_4, and concentrated. The crude residue was purified by silica gel flash column (0⟶ 40% EtOAc in hexanes) to give the title compound as a colorless oil (1.25 g, 91% yield).



*From major diastereomer **251b***

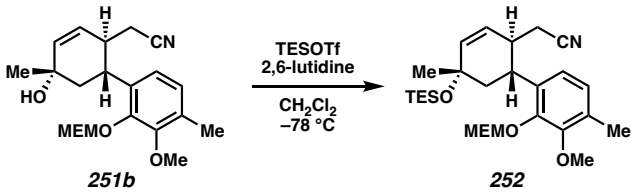
^{1}H NMR: (500 MHz, $CDCl_3$) δ 6.92 (dd, *J* = 7.9, 0.8 Hz, 1H), 6.85 (d, *J* = 7.9 Hz, 1H), 5.84 (ddd, *J* = 10.1, 2.7, 1.7 Hz, 1H), 5.71 (dd, *J* = 10.0, 2.0 Hz, 1H), 5.26 – 5.18 (m, 2H), 3.95 (ddd, *J* = 10.9, 5.4, 4.1 Hz, 1H), 3.85 (ddd, *J* = 10.9, 4.9, 3.8 Hz, 1H), 3.77 (s, 3H), 3.57 (ddd, *J* = 4.7, 3.7, 0.8 Hz, 2H), 3.37 (s, 3H), 3.20 (d, *J* = 12.4 Hz, 1H), 2.67 (s, 1H), 2.32 (dd, *J* =

16.7, 4.4 Hz, 1H), 2.26 (d, *J* = 0.7 Hz, 3H), 2.22 (dd, *J* = 16.8, 8.3 Hz, 1H), 2.11 (t, *J* = 10.8 Hz, 1H), 1.94 (ddd, *J* = 12.7, 2.9, 1.7 Hz, 1H), 1.73 (s, 1H), 1.44 (s, 3H).



*From minor diastereomer (**251a**)*

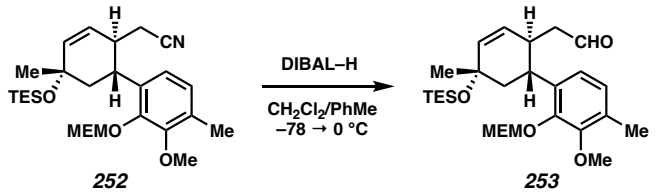
^{1}H NMR: (500 MHz, $CDCl_3$) δ 6.94 (dd, *J* = 7.9, 0.8 Hz, 1H), 6.84 (d, *J* = 8.0 Hz, 1H), 5.94 – 5.86 (m, 2H), 5.20 (d, *J* = 6.5 Hz, 1H), 5.12 (d, *J* = 6.6 Hz, 1H), 4.02 (ddd, *J* = 10.9, 6.4, 2.8 Hz, 1H), 3.91 (ddd, *J* = 10.9, 5.0, 2.7 Hz, 1H), 3.77 (s, 3H), 3.66 – 3.56 (m, 2H), 3.51 (t, *J* = 12.1 Hz, 1H), 3.38 (s, 3H), 2.57 (q, *J* = 7.4 Hz, 1H), 2.33 (dd, *J* = 16.8, 4.4 Hz, 1H), 2.27 – 2.22 (m, 4H), 1.92 (ddd, *J* = 13.6, 3.1, 1.3 Hz, 1H), 1.77 (t, *J* = 13.5 Hz, 1H), 1.32 (s, 3H).



251b ***252***

TES ether 252: To a round-bottom flask was added nitrile **251b** (200 mg, 0.533 mmol, 1 equiv) and CH_2Cl_2 (2.67 mL). The solution was cooled to –78 °C then 2,6-lutidine (0.25 mL, 2.13 mmol, 4 equiv) was added. TESOTf (0.242 mL, 1.07 mmol, 2 equiv) was added dropwise. The solution was maintained for 1 hour, then warmed to 0 °C and quenched with NH_4Cl. The aqueous layer was extracted with CH_2Cl_2 (3x5 mL). The combined organic layers were washed with brine (5 mL), dried over Na_2SO_4, and concentrated. The residue was purified by silica gel flash column (0→ 10% EtOAc in hexanes) to give the title compound as a colorless oil (200 mg, 77% yield).

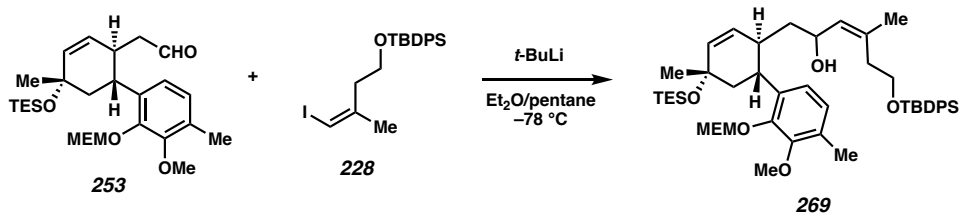
^{1}H NMR: (500 MHz, $CDCl_3$) δ 6.94 (d, *J* = 7.9 Hz, 1H), 6.86 (d, *J* = 7.9 Hz, 1H), 5.85 (dt, *J* = 10.1, 2.1 Hz, 1H), 5.64 (dd, *J* = 10.1, 1.9 Hz, 1H), 5.23 – 5.17 (m, 2H), 3.93 (dt, *J* = 10.8, 4.7 Hz, 1H), 3.87 (dt, *J* = 10.9, 4.5 Hz, 1H), 3.78 (s, 3H), 3.56 (t, *J* = 4.6 Hz, 2H), 3.37 (s, 3H), 3.26 – 3.22 (m, 1H), 2.57 (s, 1H), 2.30 (dd, *J* = 16.8, 4.4 Hz, 1H), 2.26 (d, *J* = 0.7 Hz, 3H), 2.20 (dd, *J* = 16.8, 8.5 Hz, 1H), 2.08 (t, *J* = 13.2 Hz, 1H), 1.87 (dt, *J* = 12.5, 2.5 Hz, 1H), 1.43 (s, 3H), 0.96 (t, *J* = 7.9 Hz, 9H), 0.60 (q, *J* = 7.9 Hz, 6H).



252 ***253***

Aldehyde 252: To a round-bottom flask was added TES ether **252** (200 mg, 0.408 mmol, 1 equiv) and CH_2Cl_2 (4 mL). The solution was cooled to –78 °C. A solution of DIBAL in tolune (freshly prepared, 1.0 M, 0.82 mL, 0.82 mmol, 2 equiv) was added dropwise. The solution was stirred at –78 °C for 1.5 hours, warmed to 0 °C for 10 minutes, then cooled to –78 °C and quenched by the addition of EtOAc (0.3 mL). The solution was then diluted with Et_2O (50 mL) and stirred vigorously with half-saturated Rochelle's salt solution (50 mL) until two clear layers formed. The layers were separated, and the aqueous layer was extracted with Et_2O (3x15 mL). The combined organic layers were washed with brine (10 mL), dried over Na_2SO_4, and concentrated. The crude residue was purified by silica gel flash column (20→50% Et_2O in hexanes) to give the title compound as a colorless oil (161 mg, 80% yield).

^{1}H NMR: (500 MHz, $CDCl_3$) δ 9.53 (t, *J* = 1.8 Hz, 1H), 6.91 (q, *J* = 8.0 Hz, 2H), 5.70 (dt, *J* = 10.1, 2.2 Hz, 1H), 5.48 (dd, *J* = 10.1, 1.9 Hz, 1H), 5.20 – 5.14 (m, 2H), 3.96 – 3.89 (m, 1H), 3.89 – 3.83 (m, 1H), 3.77 (s, 3H), 3.62 – 3.53 (m, 2H), 3.38 (s, 3H), 3.26 (d, *J* = 22.4 Hz, 1H), 2.81 (s, 1H), 2.37 (ddd, *J* = 17.2, 4.8, 1.7 Hz, 1H), 2.29 (td, *J* = 8.6, 2.1 Hz, 1H), 2.25 (s, 3H), 2.09 (t, *J* = 13.2 Hz, 1H), 1.87 (dt, *J* = 12.4, 2.3 Hz, 1H), 1.40 (s, 3H), 0.95 (t, *J* = 7.9 Hz, 9H), 0.59 (q, *J* = 8.0 Hz, 6H).



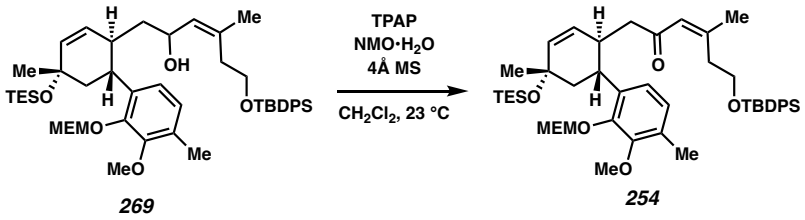
Allylic alcohol 269: In separate flame-dried test tubes were added vinyl iodide **228** (183 mg, 0.406 mmol, 2 equiv) and aldehyde **253** (100 mg, 0.203 mmol, 1 equiv). Both starting materials were azeotroped with toluene (2x1 mL) and left under high-vacuum for >2 hours to remove traces of toluene. Vinyl iodide **228** (prepared according to procedure in Chapter 4) was dissolved in Et_2O (0.8 mL) and cooled to –78 °C. *tert*-Butyllithium (1.7 M in pentane, 0.418 mL, 0.71 mmol, 3.5 equiv) was added dropwise. The solution was maintained at –78 °C for 45 minutes then warmed to 0 °C and stirred for 30 minutes, during which time the solution became almost colorless. The solution was cooled again to –78 °C. Aldehyde **253** was dissolved in Et_2O (2 mL) and added dropise to the cooled vinyllithium species. The reaction was stirred for 2 hours at –78 °C then pH = 6 aq. phosphate buffer was added to quench the reaction. The layers were separated, and the aqueous layer was extracted with EtOAc (3x1 mL). The combined organic layers were washed with brine (1 mL), dried over Na_2SO_4, and concentrated. The crude residue was purified by silica gel flash column (0→30% Et_2O in hexanes) to give the title compound as a colorless oil (135 mg, 83% combined yield). Use of this gradient separated both diastereomers for the purposes of characterization. The diastereomers are inconsequential and separation of these stereoisomers is not necessary.

Diastereomer 1 (relative configuration unassigned), isolated as a mixture with unreacted vinyl iodide. Only the peaks corresponding to the title compound are reported.

^{1}H NMR: (600 MHz, C_6D_6) δ 7.76 (dddd, *J* = 8.1, 6.9, 3.1, 2.0 Hz, 4H), 7.29 – 7.23 (m, 6H), 7.09 (s, 1H), 6.81 (d, *J* = 7.9 Hz, 1H), 5.99 (dd, *J* = 10.3, 1.9 Hz, 1H), 5.89 (d, *J* = 10.1 Hz, 1H), 5.29 (s, 2H), 5.25 – 5.21 (m, 1H), 4.56 (s, 1H), 3.90 – 3.78 (m, 2H), 3.61 (dq, *J* = 13.4, 6.6 Hz, 2H), 3.54 (s, 3H), 3.36 – 3.31 (m, 2H), 3.08 (s, 3H), 3.01 (s, 1H), 2.45 (dt, *J* = 14.0, 7.2 Hz, 1H), 2.33 (s, 1H), 2.26 – 2.19 (m, 1H), 2.15 (s, 3H), 1.88 (d, *J* = 1.3 Hz, 3H), 1.86 – 1.83 (m, 1H), 1.66 (s, 3H), 1.47 (d, *J* = 1.4 Hz, 3H), 1.17 (s, 9H), 1.09 (obscured, 9H), 0.73 (q, *J* = 8.0 Hz, 6H).

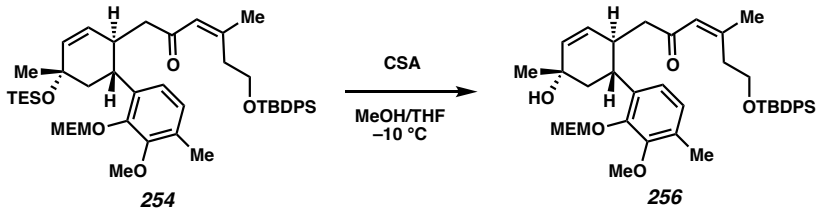
Diastereomer 2 (relative configuration unassigned)

^{1}H NMR: (600 MHz, C_6D_6) δ 7.80 – 7.73 (m, 4H), 7.29 – 7.21 (m, 6H), 6.98 (d, *J* = 8.0 Hz, 1H), 6.81 (d, *J* = 7.9 Hz, 1H), 5.92 (dd, *J* = 10.7, 1.7 Hz, 1H), 5.86 (dt, *J* = 10.4, 2.0 Hz, 1H), 5.27 (s, 2H), 5.26 – 5.22 (m, 1H), 4.42 (q, *J* = 7.5 Hz, 1H), 3.89 – 3.79 (m, 2H), 3.61 (ddd, *J* = 7.9, 5.5, 1.8 Hz, 2H), 3.52 (s, 3H), 3.38 – 3.32 (m, 2H), 3.09 (s, 3H), 2.61 (s, 1H), 2.50 (dt, *J* = 14.1, 7.4 Hz, 1H), 2.29 (s, 1H), 2.16 (s, 4H), 1.95 (dt, *J* = 13.3, 5.2 Hz, 2H), 1.78 – 1.71 (m, 2H), 1.64 (s, 3H), 1.49 (d, *J* = 1.4 Hz, 3H), 1.17 (s, 9H), 1.14 – 1.04 (m, 9H), 0.71 (q, *J* = 8.0 Hz, 6H).



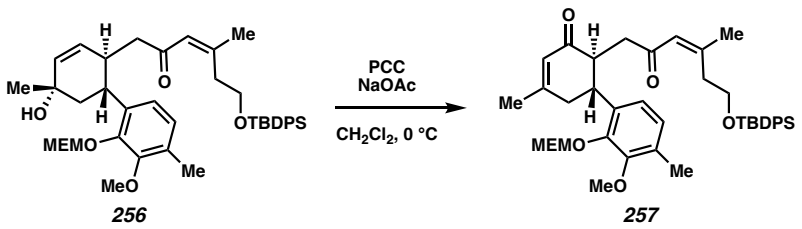
Enone 254: To a round bottom flask was charged allylic alcohol **269** (mixture of dr's, 130 mg, 0.159 mmol, 1 equiv) and NMO•H_2O (106 mg, 0.9 mmol, 5.6 equiv). CH_2Cl_2 (3.18 mL) was added followed by 4Å molecular sieves (freshly microwave activated, 1.20 g). The heterogeneous mixture was stirred vigorously for 5 minutes. Then tetrapropylammonium perruthenate (6.0 mg, 0.15 mmol, 10 mol%) was added and the mixture was stirred for 2 hours. After this time, the mixture was passed through a pad of celite and concentrated, eluting with CH_2Cl_2. The crude residue was purified by silica gel flash column (0→30% EtOAc/hexanes) to give the title compound as a colorless oil (84 mg, 64% yield).

^{1}H NMR: (500 MHz, C_6D_6) δ 7.81 – 7.73 (m, 4H), 7.24 (ddd, *J* = 4.1, 2.8, 1.4 Hz, 6H), 6.95 (d, *J* = 8.0 Hz, 1H), 6.73 (d, *J* = 8.0 Hz, 1H), 5.84 (s, 2H), 5.75 (d, *J* = 1.5 Hz, 1H), 5.31 – 5.24 (m, 2H), 3.94 – 3.86 (m, 3H), 3.79 (dt, *J* = 10.6, 4.9 Hz, 1H), 3.53 (s, 3H), 3.37 – 3.30 (m, 2H), 3.24 (d, *J* = 5.4 Hz, 1H), 3.09 (s, 3H), 2.94 (td, *J* = 6.4, 4.4 Hz, 2H), 2.56 (dd, *J* = 16.9, 3.2 Hz, 1H), 2.36 (dd, *J* = 16.8, 10.5 Hz, 2H), 2.21 – 2.15 (m, 1H), 2.14 (s, 3H), 1.64 (s, 3H), 1.58 (d, *J* = 1.3 Hz, 3H), 1.16 (s, 9H), 1.09 (t, *J* = 7.9 Hz, 9H), 0.73 (q, *J* = 7.9 Hz, 5H).



Tertiary allylic alcohol 256: To a round bottom flask was added enone **254** (68 mg, 0.0841 mmol, 1 equiv) followed by MeOH (1.40 mL). The solution was cooled to –10 °C. Camphorsulfonic acid (1.37 mg, 0.0059 mmol, 7 mol %) was added as a solution in THF (0.28 mL). The solution was maintained at the specified temperature for 1 hour, then quenched by the addition of satd. aq. $NaHCO_3$ (50 μL). The mixture was concentrated to remove MeOH, then water was added and the mixture was extracted with EtOAc (3x2 mL). The combined organic layers were washed with brine (1 mL), dried over Na_2SO_4, and concentrated. The crude residue was purified by silica gel flash column (10→50% EtOAc/hexanes) to give the title compound as a colorless oil (54 mg, 91% yield).

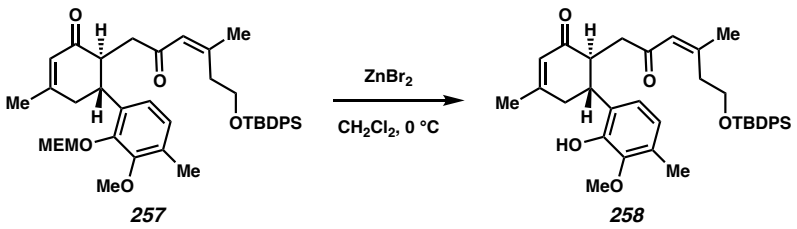
^{1}H NMR: (600 MHz, C_6D_6) δ 7.81 – 7.74 (m, 4H), 7.23 (ddt, *J* = 4.5, 3.3, 1.5 Hz, 6H), 6.86 (d, *J* = 7.9 Hz, 1H), 6.75 (d, *J* = 8.0 Hz, 1H), 5.79 (dd, *J* = 10.1, 2.0 Hz, 1H), 5.74 (d, *J* = 1.6 Hz, 1H), 5.71 – 5.63 (m, 1H), 5.25 (d, *J* = 5.5 Hz, 1H), 5.23 (d, *J* = 5.5 Hz, 1H), 3.88 – 3.84 (m, 1H), 3.72 (dt, *J* = 10.9, 4.8 Hz, 1H), 3.52 (s, 3H), 3.40 (s, 1H), 3.31 (t, *J* = 4.9 Hz, 2H), 3.20 – 3.13 (m, 1H), 3.07 (s, 3H), 2.94 (td, *J* = 6.4, 3.3 Hz, 2H), 2.52 (dd, *J* = 16.9, 3.3 Hz, 1H), 2.31 (dd, *J* = 16.9, 10.6 Hz, 1H), 2.15 (s, 3H), 2.00 (t, *J* = 14.8 Hz, 2H), 1.58 (d, *J* = 1.3 Hz, 3H), 1.48 (s, 3H), 1.15 (s, 9H).



256 ***257***

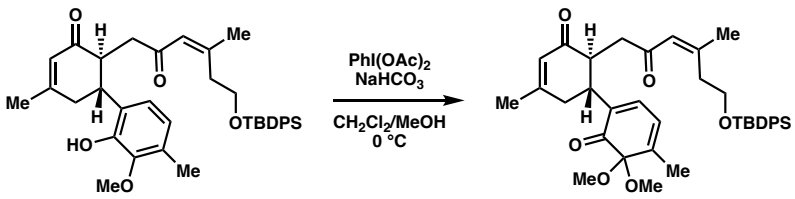
Bis-enone 257: To a flame-dried test tube was added NaOAc (12.6 mg) followed by allylic alcohol **256** (54 mg, 0.077 mmol, 1 equiv) as a solution in CH_2Cl_2 (0.4 mL). PCC (25 mg, 0.116 mmol, 1.5 equiv) was added and the mixture was stirred vigorously. Five additional portions of NaOAc (13 mg) and PCC (25 mg) were added every 30 minutes until the reaction reached complete conversion by TLC. Then pyridine (56 μL) was added and the reaction was concentrated. The crude residue was purified by silica gel flash column (0 → 50% EtOAc in hexanes) to give the title compound as a colorless oil (8.3 mg, 16% yield).

^{1}H NMR: (500 MHz, C_6D_6) δ 7.83 – 7.74 (m, 3H), 7.75 – 7.69 (m, 1H), 7.30 – 7.20 (m, 6H), 6.89 (dd, *J* = 15.8, 8.0 Hz, 1H), 6.81 – 6.74 (m, 1H), 6.00 (t, *J* = 3.5 Hz, 1H), 5.91 (d, *J* = 1.5 Hz, 1H), 5.18 (d, *J* = 6.7 Hz, 2H), 3.94 (t, *J* = 6.6 Hz, 2H), 3.71 (dt, *J* = 9.7, 4.8 Hz, 2H), 3.52 (s, 3H), 3.31 – 3.22 (m, 2H), 3.08 (d, *J* = 3.1 Hz, 3H), 3.04 – 2.94 (m, 1H), 2.88 (dt, *J* = 12.2, 6.4 Hz, 1H), 2.40 (dd, *J* = 16.9, 3.2 Hz, 1H), 2.29 – 2.19 (m, 1H), 2.14 (d, *J* = 2.6 Hz, 3H), 1.59 – 1.53 (m, 3H), 1.43 (s, 3H), 1.18 (s, 9H).



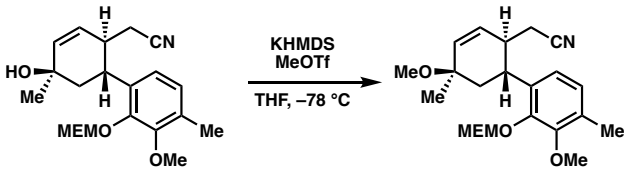
Phenol 258: In a nitrogen-filled glovebox, $ZnBr_2$ (finely powdered, 26.7 mg, 0.1187 mmol, 10 equiv) was added to a test tube with stir bar. The vessel was sealed, removed from the glovebox and connected to an N_2 line. Bis-enone **257** (8.3 mg, 0.0119 mmol, 1 equiv) was added as a solution in CH_2Cl_2 (0.4 mL). The mixture was stirred vigorously for 5 hours. Satd. aq. $NaHCO_3$ (1 mL) was added. And the mixture was extracted with CH_2Cl_2 (3x1 mL). The combined organic layers were washed with brine (0.5 mL), dried over Na_2SO_4, and concentrated. The crude residue was purified by silica gel flash column (0→60% Et_2O in hexanes) to give the title compound as a colorless oil (4.3 mg, 60% yield).

^{1}H NMR: (600 MHz, C_6D_6) δ 7.80 (ddt, *J* = 6.3, 4.5, 1.9 Hz, 4H), 7.29 – 7.20 (m, 6H), 6.75 (d, *J* = 7.9 Hz, 1H), 6.53 (d, *J* = 7.9 Hz, 1H), 5.96 (s, 1H), 5.86 (d, *J* = 1.7 Hz, 1H), 5.80 (s, 1H), 3.92 (t, *J* = 6.6 Hz, 2H), 3.73 – 3.64 (m, 1H), 3.54 (ddd, *J* = 13.4, 6.8, 3.8 Hz, 1H), 3.22 (s, 2H), 2.97 (dt, *J* = 12.9, 6.7 Hz, 1H), 2.88 (dt, *J* = 12.4, 6.5 Hz, 1H), 2.80 (dd, *J* = 16.8, 6.8 Hz, 1H), 2.47 – 2.38 (m, 2H), 2.06 (s, 3H), 2.06 – 2.01 (m, 1H), 1.56 (d, *J* = 1.2 Hz, 3H), 1.34 (s, 3H), 1.17 (s, 9H).



Masked *ortho*-benzoquinone 259: To a test tube was added phenol **258** (2.0 mg, 0.00327 mmol, 1 equiv) followed by CH_2Cl_2 (11 µL) and MeOH (22 µL) and the solution was cooled to 0 °C. $NaHCO_3$ (0.83 mg, 0.00982 mmol, 3 equiv) was added followed by $PhI(OAc)_2$ (1.2 mg, 0.0036 mmol, 1.1 equiv). The mixture was stirred for 30 minutes. No change in polarity was observed by TLC, but the reaction mixture turned yellow and a new yellow spot was visible by TLC without UV fluorescence quenching with the same Rf as the starting material. Satd. aq. $NaHCO_3$ (0.5 mL) and $Na_2S_2O_3$ (0.1 mL) were added and the mixture was extracted with Et_2O (3x0.5 mL). The combined organic layers were dried over Na_2SO_4, and concentrated. The crude residue was passed through a plug of silica gel eluting with CH_2Cl_2 and Et_2O and concentrated to give the title compound, contaminated by a small amount of iodobenzene (2.5 mg total)

^{1}H NMR: (600 MHz, C_6D_6) δ 7.79 (ddt, *J* = 7.5, 3.0, 1.8 Hz, 4H), 7.29 – 7.20 (m, 6H), 6.26 (d, *J* = 6.4 Hz, 1H), 5.95 (d, *J* = 1.5 Hz, 1H), 5.90 (dd, *J* = 2.4, 1.4 Hz, 1H), 5.56 (dq, *J* = 6.3, 1.6 Hz, 1H), 3.94 (t, *J* = 6.7 Hz, 2H), 3.38 – 3.26 (m, 3H), 3.22 (s, 3H), 3.18 (s, 3H), 3.05 – 2.92 (m, 2H), 2.79 (dd, *J* = 17.0, 5.9 Hz, 1H), 2.39 (dd, *J* = 17.0, 3.2 Hz, 1H), 2.16 – 2.09 (m, 1H), 1.85 – 1.81 (m, 1H), 1.80 (d, *J* = 1.6 Hz, 3H), 1.59 (d, *J* = 1.4 Hz, 3H), 1.30 (d, *J* = 1.3 Hz, 3H), 1.17 (s, 9H).



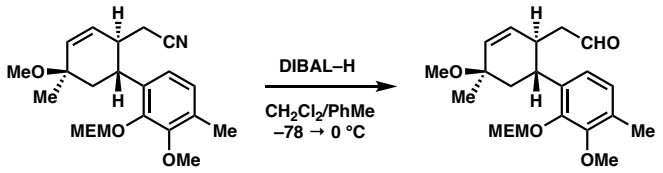
251a ***262***

Note: the transformations described in this section were performed using the minor diastereomer of nitrile ***251a***

Methyl ether 261: To a round bottom flask was charged nitrile **250a** (226 mg, 0.602 mmol, 1 equiv) and THF (3.0 mL). The solution was cooled to –78 °C. KHMDS (1.0 M in THF, 0.69 mL, 0.69 mmol, 1.15 equiv) was added dropwise and stirred for 1 hour. MeOTf (0.102 mL, 0.90 mmol, 1.5 equiv) was added dropwise to the cooled solution and the reaction was stirred for 1.5 hours. Satd. aq. NH_4Cl (10 mL) was added and the mixture was warmed to ambient temperature. The mixture was extracted with EtOAc (3x10 mL). The combined organic layers were washed with brine (5 mL), dried over Na_2SO_4, and concentrated. The crude residue was purified by silica gel flash column (20% EtOAc in hexanes) to give the title compound as a pale yellow oil (229 mg, 89% yield).

XIII-129

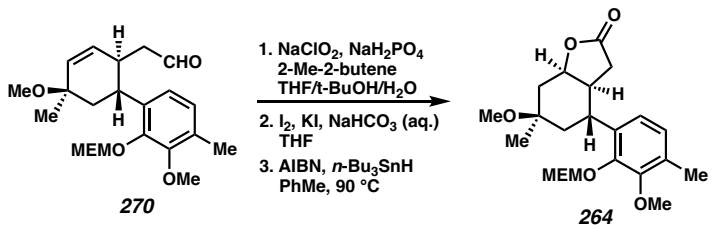
^{1}H NMR: (500 MHz, $CDCl_3$) δ 6.92 (d, *J* = 7.9 Hz, 1H), 6.82 (d, *J* = 7.9 Hz, 1H), 5.98 (dd, *J* = 10.0, 1.9 Hz, 1H), 5.90 (dt, *J* = 10.0, 2.0 Hz, 1H), 5.24 – 5.16 (m, 2H), 4.03 (dt, *J* = 10.9, 4.7 Hz, 1H), 3.90 (dt, *J* = 10.9, 4.2 Hz, 1H), 3.77 (s, 3H), 3.58 (dd, *J* = 5.2, 4.1 Hz, 2H), 3.38 (s, 4H), 3.26 (s, 3H), 2.53 (s, 1H), 2.35 (dd, *J* = 16.8, 4.3 Hz, 1H), 2.25 (s, 3H), 2.25 (s, 1H), 1.97 (dt, *J* = 13.6, 2.5 Hz, 1H), 1.70 (t, *J* = 13.4 Hz, 1H), 1.27 (s, 3H).



262 ***270***

Aldehyde 270: To a round-bottom flask was added methyl ether **262** (323 mg, 0.829 mmol, 1 equiv) and CH_2Cl_2 (8 mL). The solution was cooled to –78 °C. A solution of DIBAL in tolune (freshly prepared, 1.0 M, 1.66 mL, 1.66 mmol, 2 equiv) was added dropwise. The solution was stirred at –78 °C for 1.5 hours, warmed to 0 °C for 10 minutes, then cooled to –78 °C and quenched by the addition of EtOAc (0.3 mL). The solution was then diluted with Et_2O (50 mL) and stirred vigorously with half-saturated Rochelle's salt solution (50 mL) until two clear layers formed. The layers were separated, and the aqueous layer was extracted with Et_2O (3x15 mL). The combined organic layers were washed with brine (10 mL), dried over Na_2SO_4, and concentrated. The crude residue was purified by silica gel flash column (20→50% Et_2O in hexanes) to give the title compound as a colorless oil (240 mg, 73% yield).

^{1}H NMR: (500 MHz, $CDCl_3$) δ 9.58 (t, *J* = 1.7 Hz, 1H), 6.90 (d, *J* = 8.0 Hz, 1H), 6.85 (d, *J* = 8.0 Hz, 1H), 5.81 – 5.72 (m, 2H), 5.22 – 5.15 (m, 2H), 4.06 – 3.99 (m, 1H), 3.97 – 3.88 (m, 1H), 3.77 (s, 3H), 3.59 (dd, *J* = 5.1, 4.2 Hz, 2H), 3.39 (s, 4H), 3.24 (s, 3H), 2.78 (s, 1H), 2.43 (ddd, *J* = 17.5, 4.6, 1.6 Hz, 1H), 2.35 (ddd, *J* = 17.4, 8.7, 1.9 Hz, 1H), 2.27 – 2.22 (m, 3H), 1.98 (ddd, *J* = 13.7, 2.9, 1.5 Hz, 1H), 1.69 (t, *J* = 13.6 Hz, 1H), 1.26 (s, 3H).

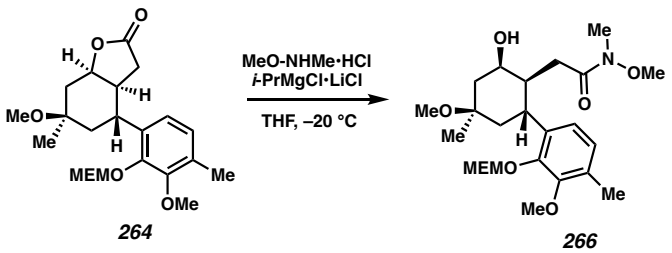


Lactone 264: To a round bottom flask was added aldehyde **270** (240 mg, 0.612 mmol, 1 equiv) followed by *tert*-butanol (3 mL) and THF (3 mL) and 2-methyl-2-butene (0.648 mL, 6.12 mmol, 10 equiv). In a separate vial was added water (1.53 mL), $NaClO_2$ (~80% pure, 207 mg, 1.83 mmol, 3 equiv), and NaH_2PO_4 (440 mg, 3.67 mmol, 6 equiv). The aqueous salt solution was added to the organic solution and stirred vigorously for 1.5 hours. Then the solution was adjusted to approx. pH = 1 using 1N aq. HCl. The mixture was extracted with EtOAc (4x5 mL). The combined organic layers were washed with brine (5 mL), dried over Na_2SO_4 and concentrated to afford the corresponding acid as a colorless oil that was used without further purification.

The acid was dissolved in THF (1.53 mL), cooled to 0 °C, and satd. aq. $NaHCO_3$ (4.86 mL) was added. The mixture was stirred vigorously for 20 minutes. In a separate vial, I_2 (466 mg, 1.83 mmol, 3 equiv) and KI (914 mg, 5.5 mmol, 9 equiv) were added to water (1.7 mL). The solution was then added to the stirring, cooled solution and maintained at the specified temperature for 1.5 hours. After this time, satd. $Na_2S_2O_3$ (20 mL) was added, and the mixture was extracted with EtOAc (3x10 mL). The combined organic layers were washed with brine (5 mL), dried over Na_2SO_4, and concentrated. The crude residue was purified by silica gel flash column (15% EtOAc in hexanes) to give the title compound as a colorless oil (200 mg) that was used without further purification.

AIBN (16 mg, 0.095 mmol, 0.3 equiv) was added to a round-bottom flask and the flask was purged and backfilled with N_2 three times. The previously formed iodolactone (**263)** (170 mg, 0.318 mmol, 1 equiv) was added as a solution in PhMe (4 mL). Tri-*n*-butyltin hydride (94 μL, 0.35 mmol, 1.1 equiv) was added and the solution was heated to 90 °C for 1.5 hours. The solution was then cooled to ambient temperature. The solution was loaded directly onto a silica gel column pre-equilibrated with 90:10 hexanes/Et_3N. The column was eluted with this solvent mixture (100 mL) until the tin byproducts were removed, then the column was eluted with 10% Et_2O in hexanes to give the title compound as a colorless oil (94 mg, 74% yield).

^{1}H NMR: (500 MHz, $CDCl_3$) δ 6.90 (d, *J* = 7.9 Hz, 1H), 6.81 (d, *J* = 7.9 Hz, 1H), 5.20 (s, 2H), 4.65 (td, *J* = 4.6, 2.0 Hz, 1H), 3.99 (ddd, *J* = 11.0, 5.3, 3.9 Hz, 1H), 3.92 (ddd, *J* = 11.0, 5.2, 4.0 Hz, 1H), 3.77 (s, 3H), 3.60 (ddd, *J* = 5.1, 3.7, 1.1 Hz, 2H), 3.51 (d, *J* = 12.7 Hz, 1H), 3.39 (s, 3H), 3.23 (s, 3H), 2.65 (d, *J* = 16.2 Hz, 1H), 2.47 (td, *J* = 17.5, 7.0 Hz, 2H), 2.33 (d, *J* = 16.5 Hz, 1H), 2.24 (d, *J* = 0.7 Hz, 3H), 1.90 (dt, *J* = 13.7, 3.0 Hz, 1H), 1.57 – 1.46 (m, 2H), 1.34 – 1.24 (m, 1H), 1.19 (s, 3H).



Weinreb amide 266: Lactone **264** (10 mg, 0.0245 mmol, 1 equiv) was charged to a test tube with N,O-diemthylhydroxylamine•HCl (9.94 mg, 0.102 mmol, 4.15 equiv). The vessel was evacuated and backfilled with N_2 three times. THF (0.35 mL) was added and the solution was cooled to –20 °C. *i*-PrMgCl•LiCl (2.0 M in Et_2O, 0.098 mL, 0.196 mmol, 8 equiv) was added dropwise. The solution was maintained at –20 °C for 30 minutes, then warmed to 0 °C. The reaction was quenched by addition of satd. aq. NH_4Cl (1 mL) and extracted with EtOAc (3x0.5 mL). The combined organic layers were dried over Na_2SO_4 and concentrated. The crude residue was purified by silica gel flash column (20→50% EtOAc in hexanes) to give the title compound as a colorless oil (11.6 mg, quantitative yield).

^{1}H NMR: (500 MHz, C_6D_6) δ 7.04 (d, *J* = 8.0 Hz, 1H), 6.83 (d, *J* = 8.0 Hz, 1H), 5.31 (d, *J* = 0.8 Hz, 2H), 4.40 (dd, *J* = 9.8, 2.8 Hz, 1H), 4.34 (d, *J* = 9.9 Hz, 1H), 4.04 (ddd, *J* = 10.7, 5.5, 4.1 Hz, 1H), 3.99 – 3.86 (m, 1H), 3.80 (td, *J* = 12.5, 3.3 Hz, 1H), 3.54 (s, 3H), 3.51 – 3.41 (m, 2H), 3.33 (s, 1H), 3.22 (s, 3H), 3.14 (s, 3H), 3.06 (s, 3H), 2.88 (s, 3H), 2.66 (ddt, *J* = 12.9, 10.7, 2.5 Hz, 1H), 2.32 (d, *J* = 16.8 Hz, 1H), 2.20 – 2.13 (m, 4H), 2.04 (dt, *J* = 14.2, 3.2 Hz, 1H), 1.34 (dd, *J* = 14.6, 3.1 Hz, 1H), 1.18 – 1.08 (m, 1H), 0.79 (s, 3H).

APPENDIX 10

Spectra Relevant to Appendix 9

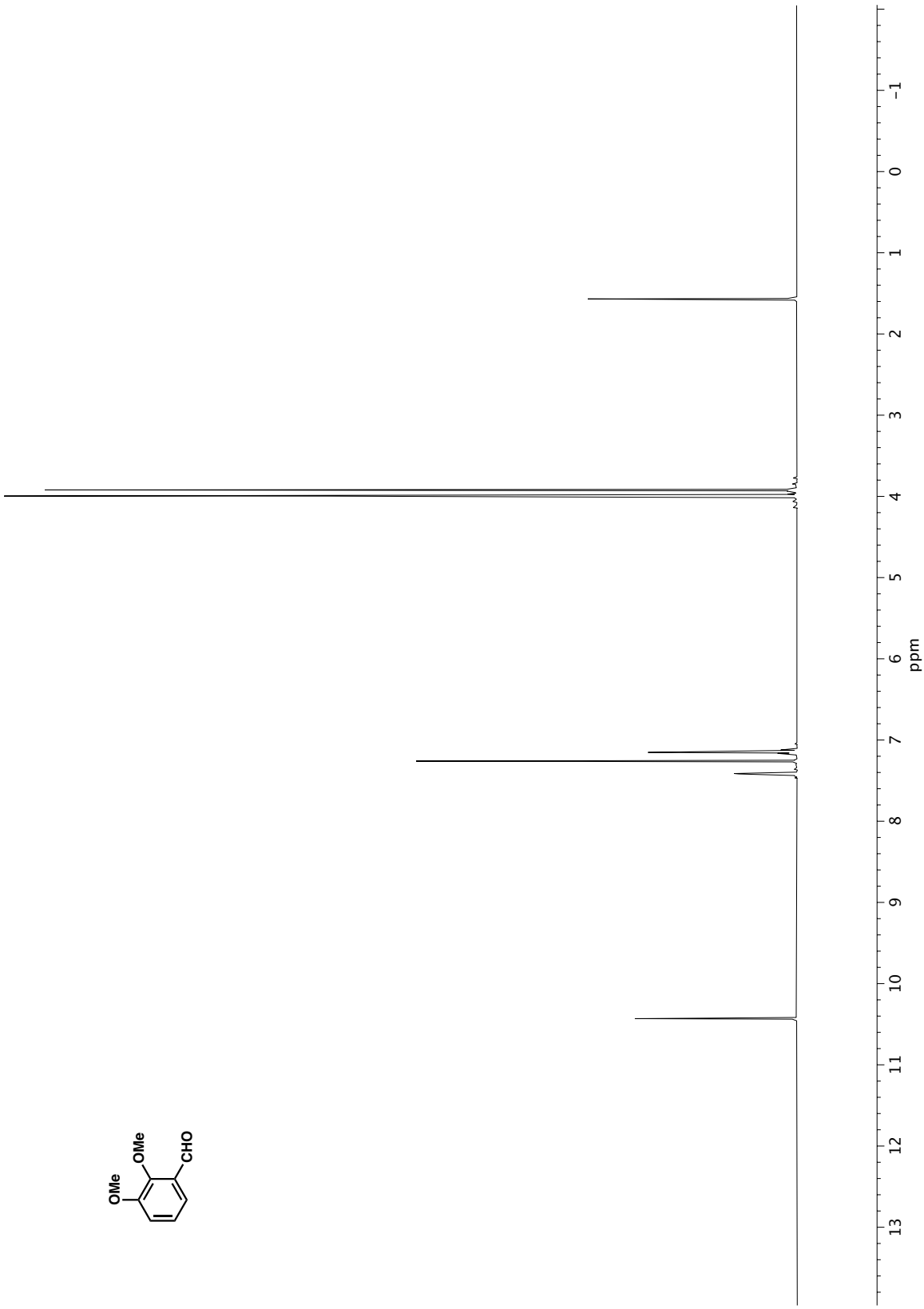


Figure A10.1 *^1H NMR (500 MHz, $CDCl_3$) of compound* ***240****.*

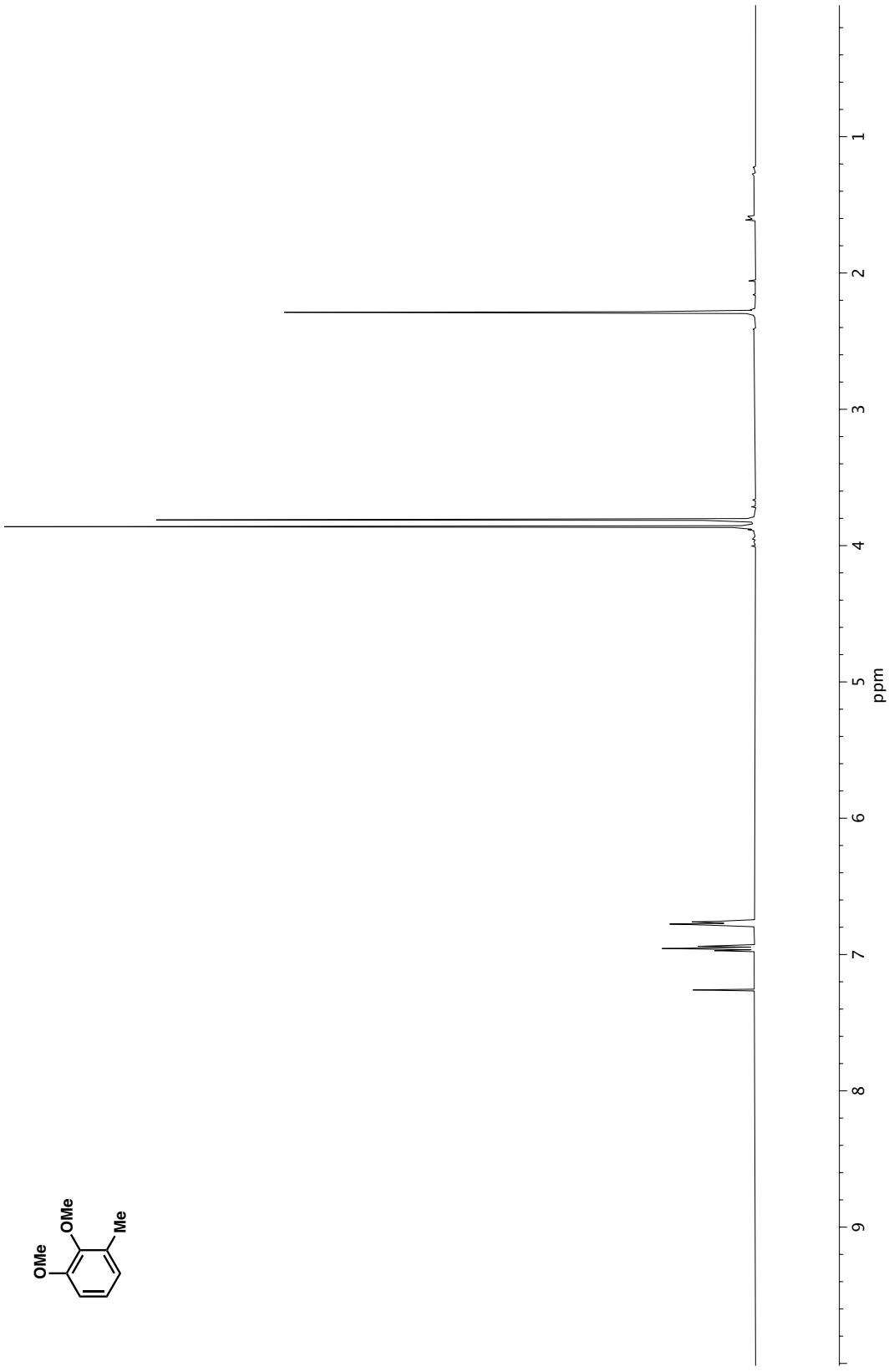


Figure A10.2 *^1H NMR (500 MHz, $CDCl_3$) of compound* ***241****.*

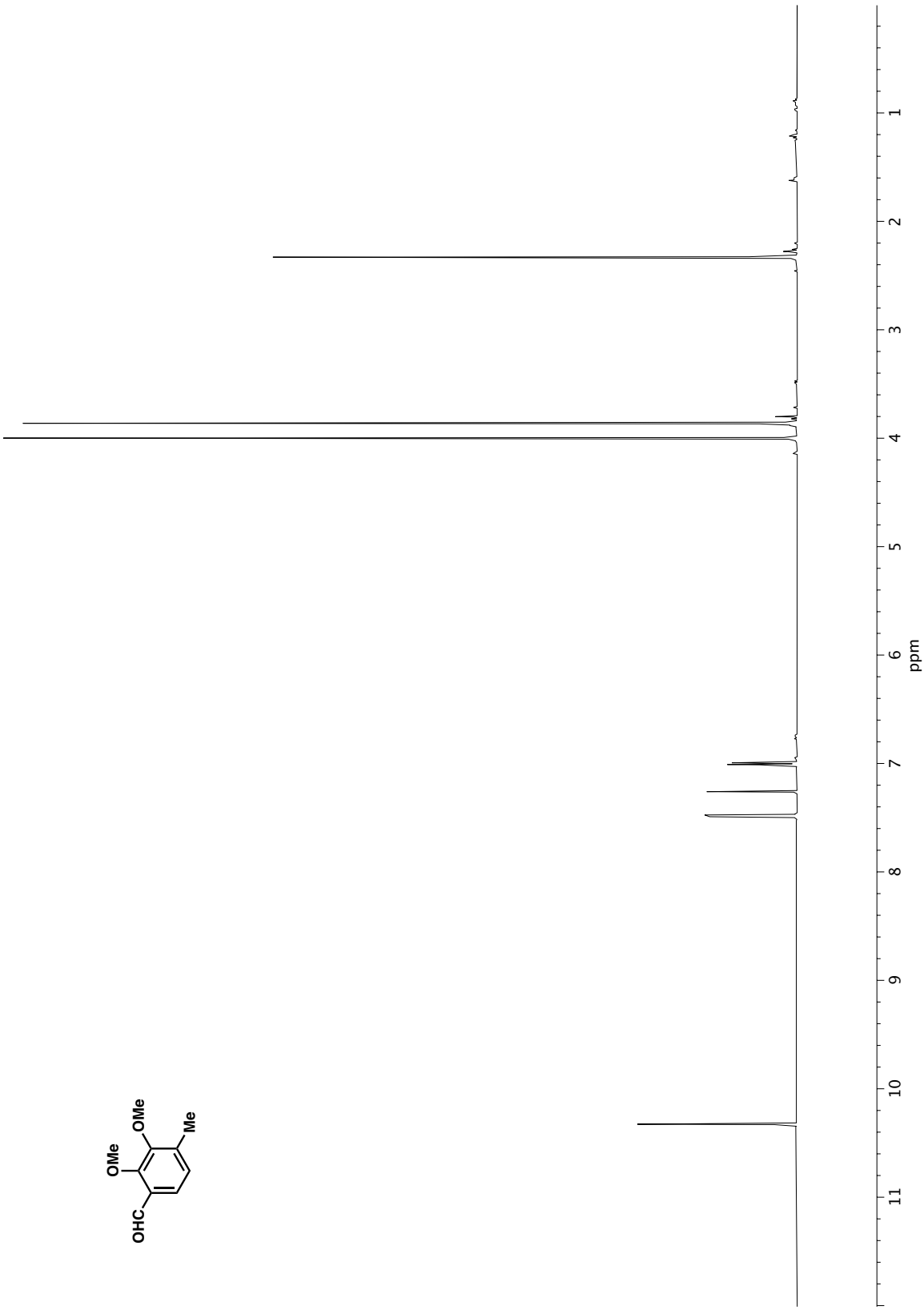


Figure A10.3 *^1H NMR (500 MHz, $CDCl_3$) of compound* ***242***.

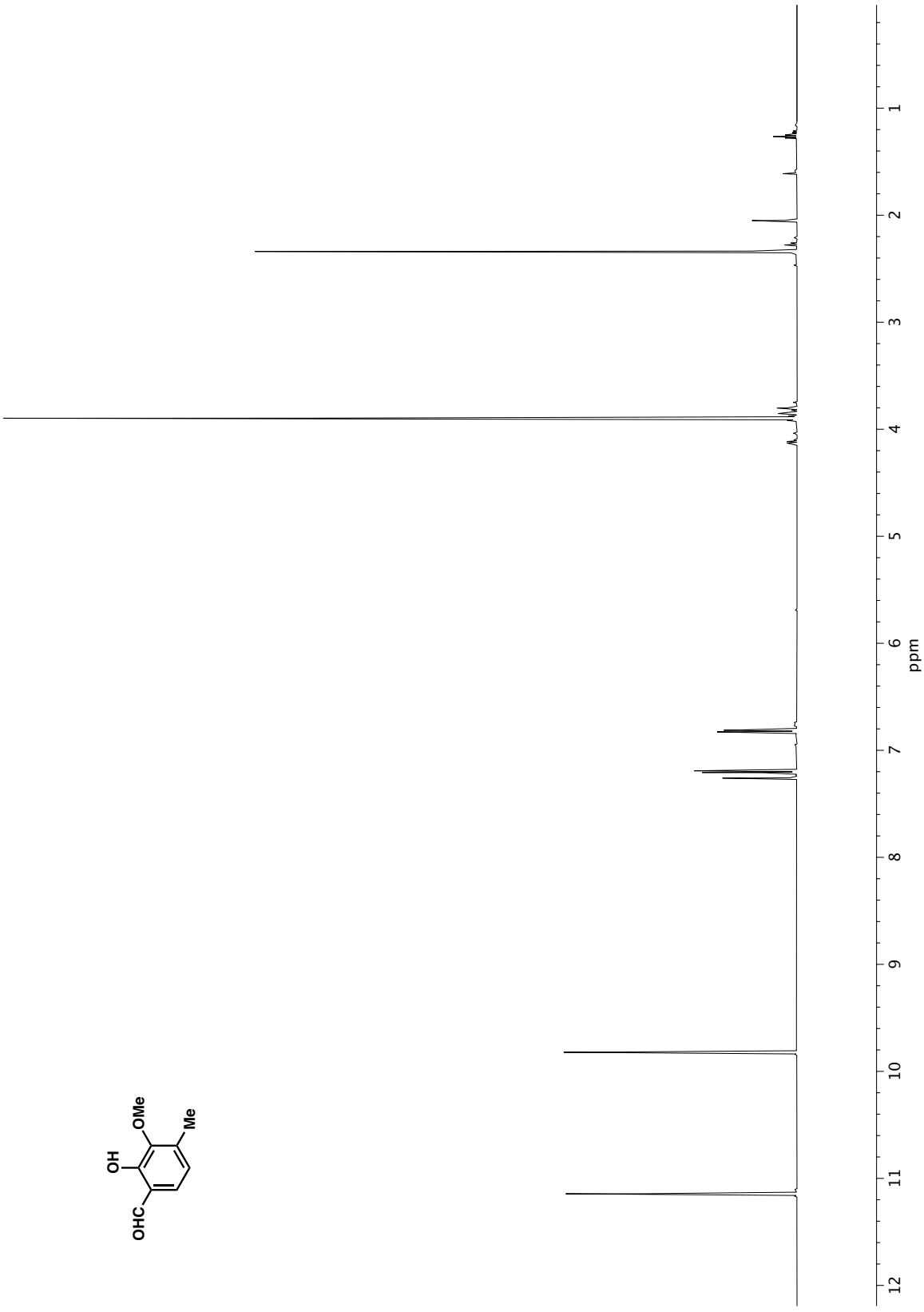


Figure A10.4 *^{1}H NMR (500 MHz, $CDCl_3$) of compound* ***243****.*

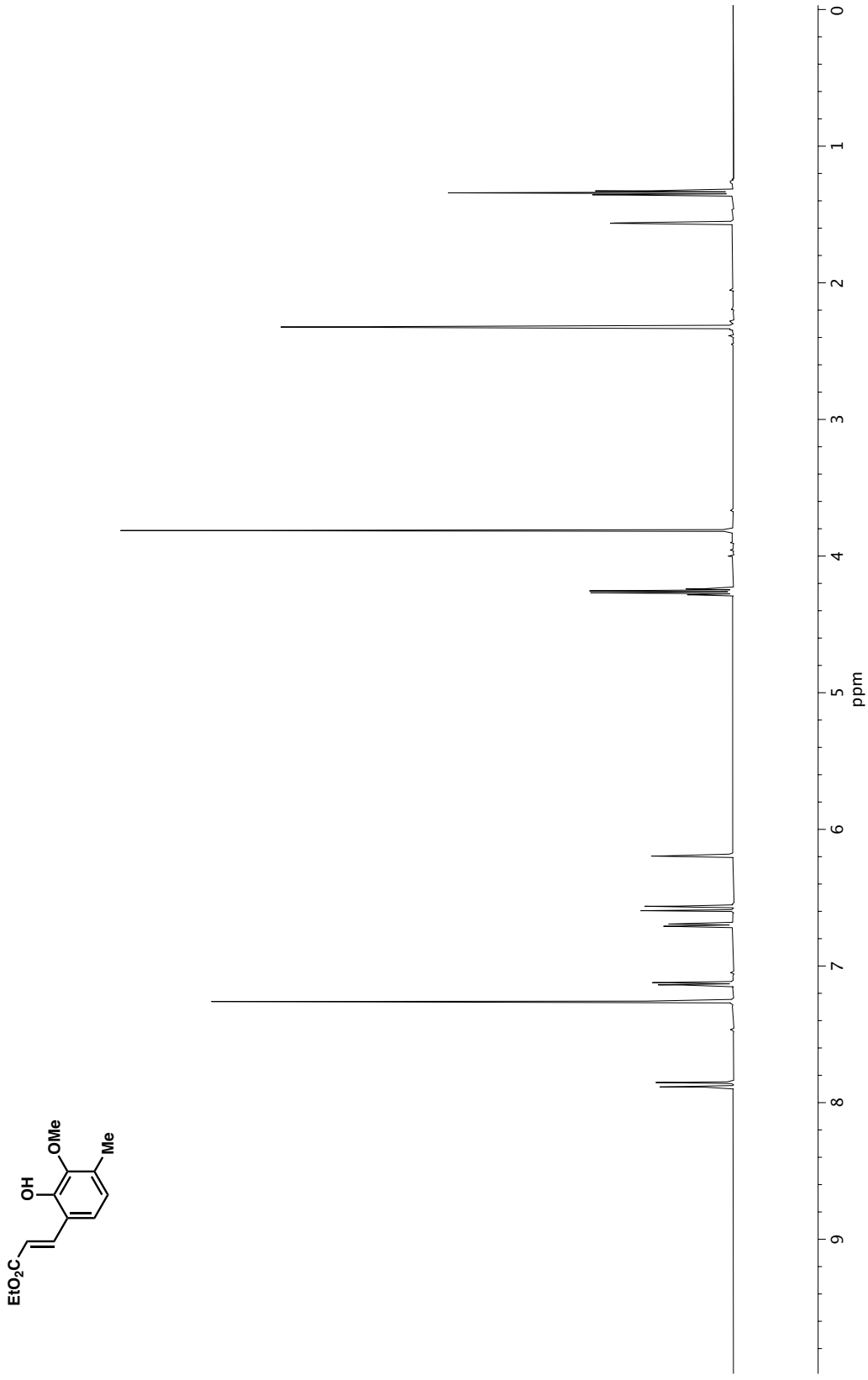


Figure A10.5 *^1H NMR (500 MHz, $CDCl_3$) of compound* ***244****.*

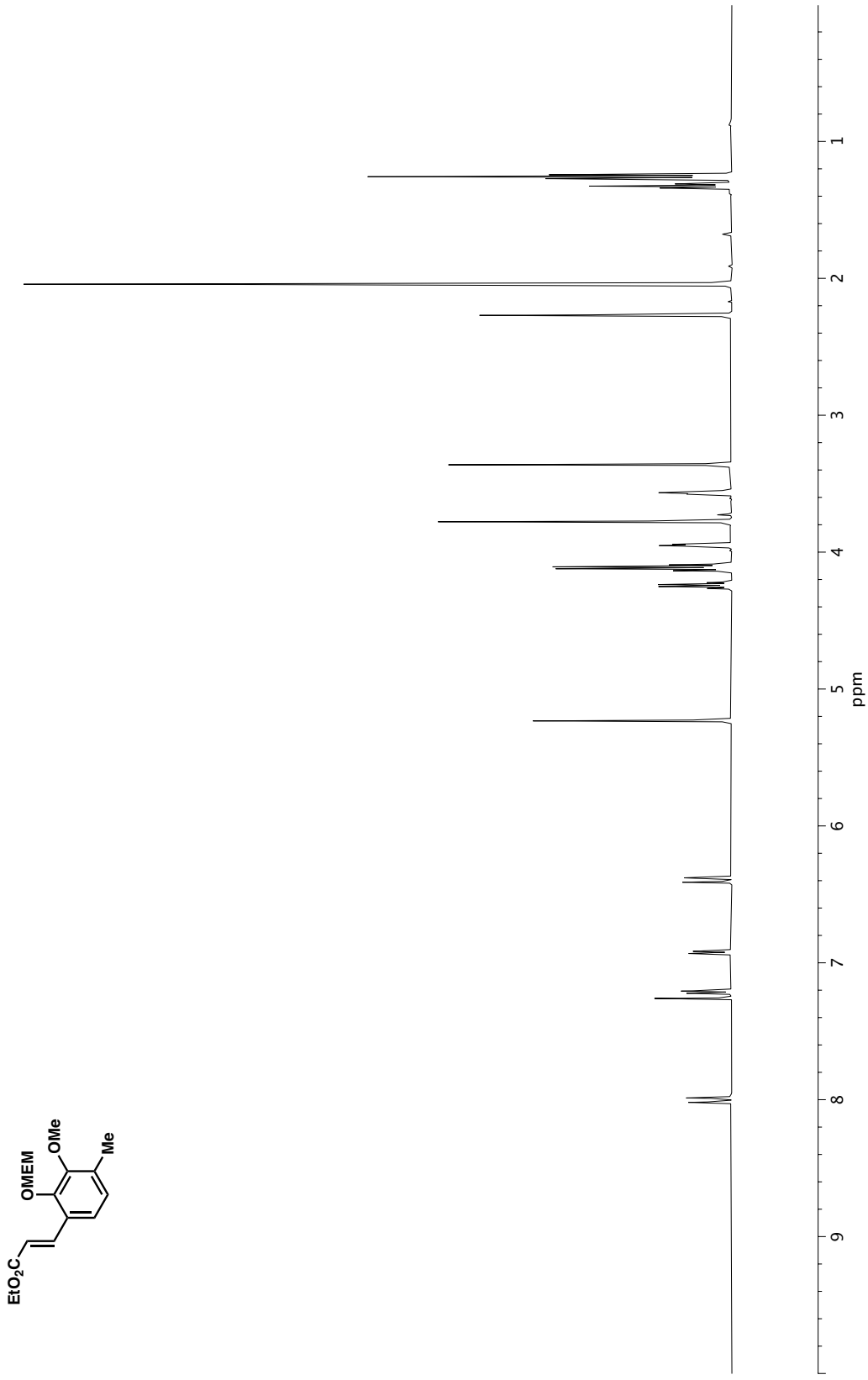


Figure A10.6 *^1H NMR (400 MHz, $CDCl_3$) of compound* ***245****.*

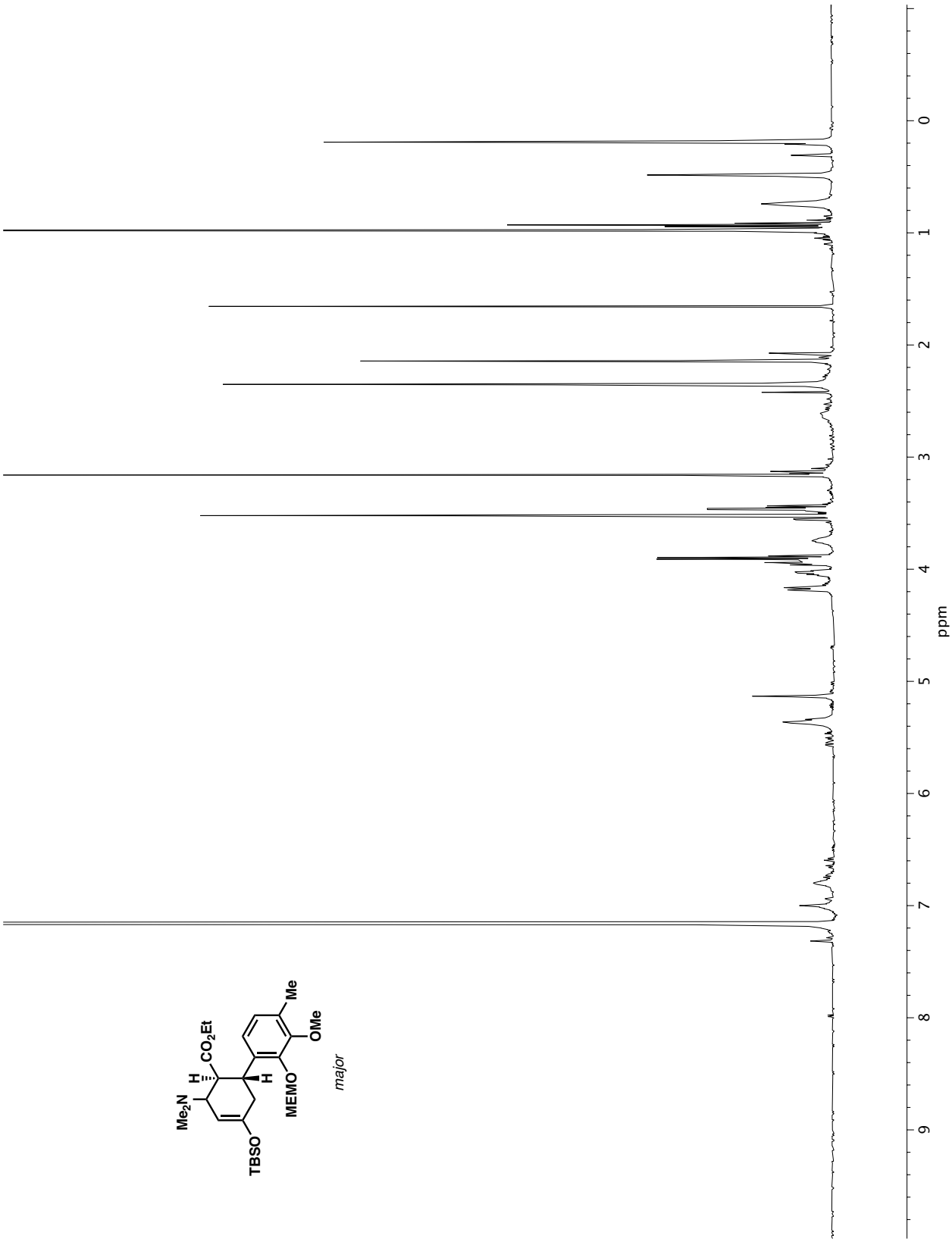


Figure A10.7 *^{1}H NMR (500 MHz, C_6D_6) of compound* ***247*** *(major).*

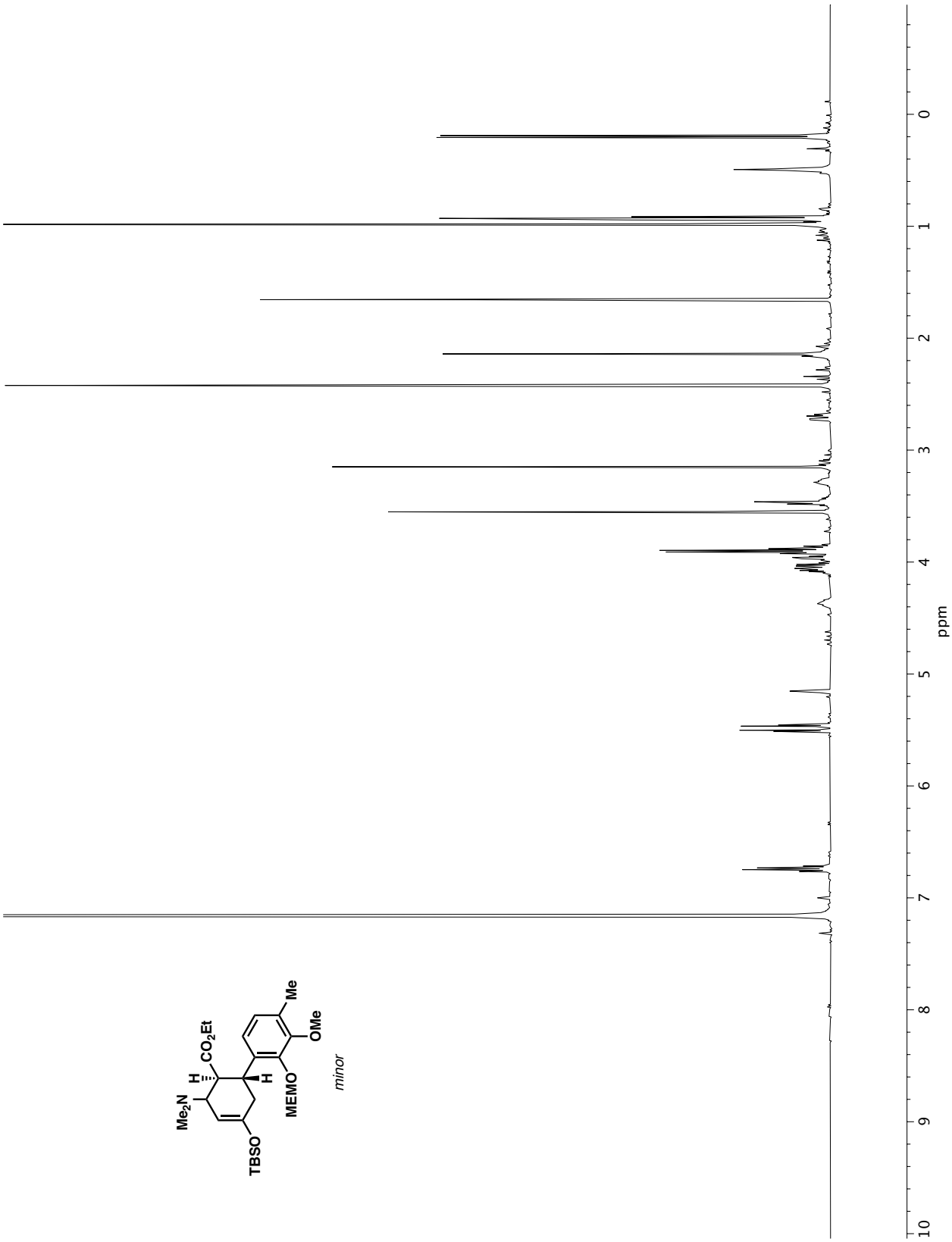


Figure A10.8 *^1H NMR (500 MHz, C_6D_6) of compound* ***247*** *(minor).*

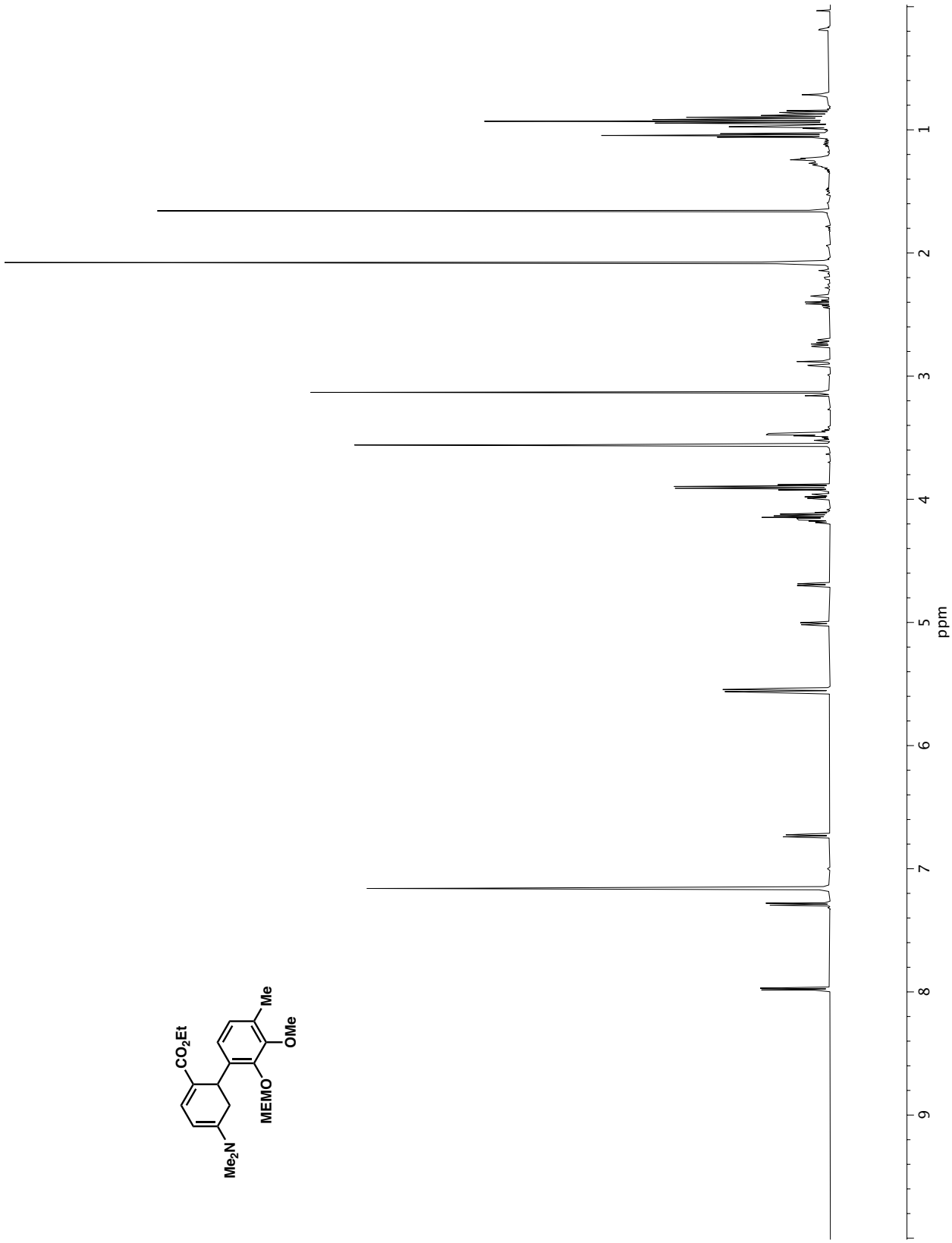


Figure A10.9 *^{1}H NMR (500 MHz, C_6D_6) of compound* ***268****.*

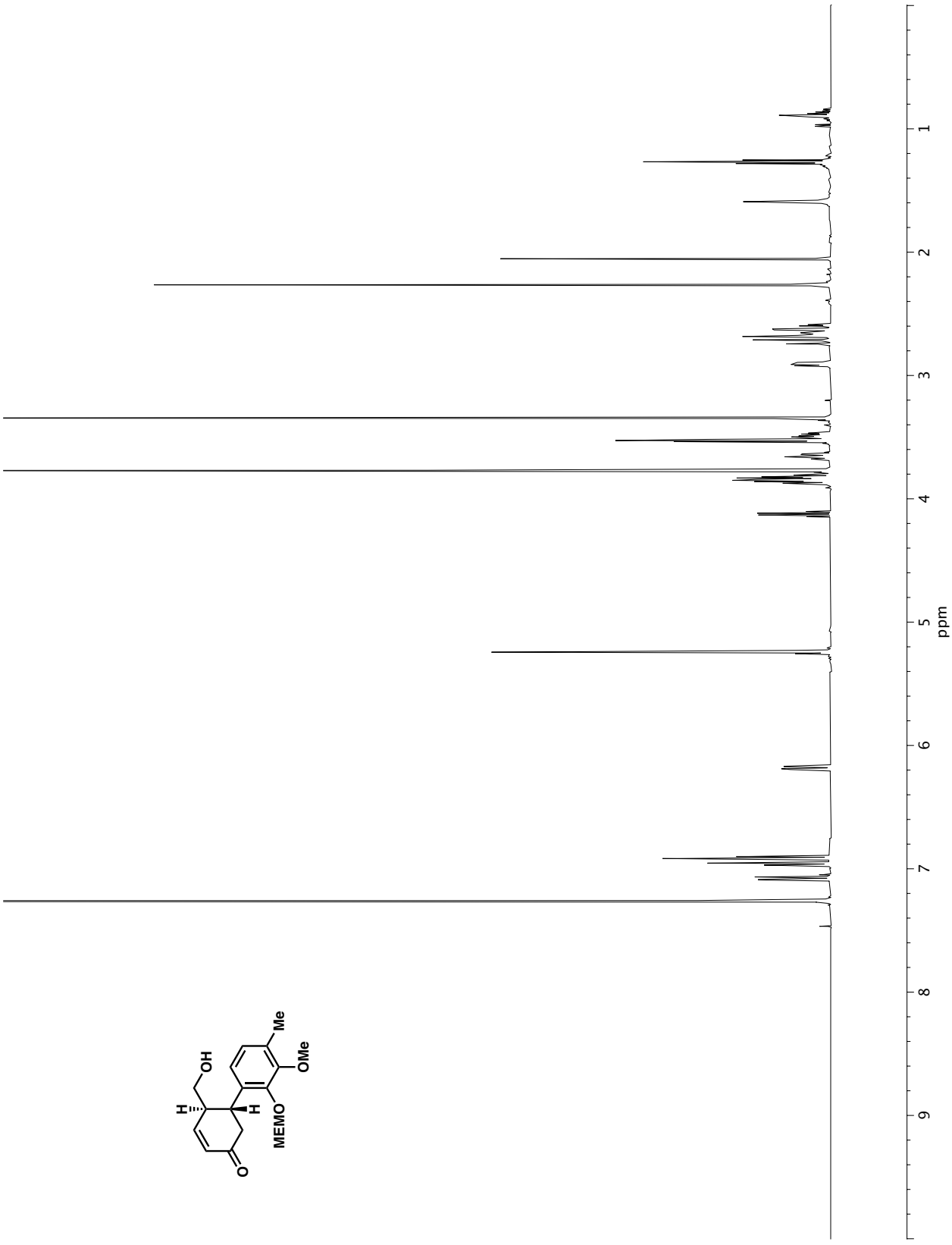


Figure A10.10 *^{1}H NMR (500 MHz, $CDCl_3$) of compound* ***248***.

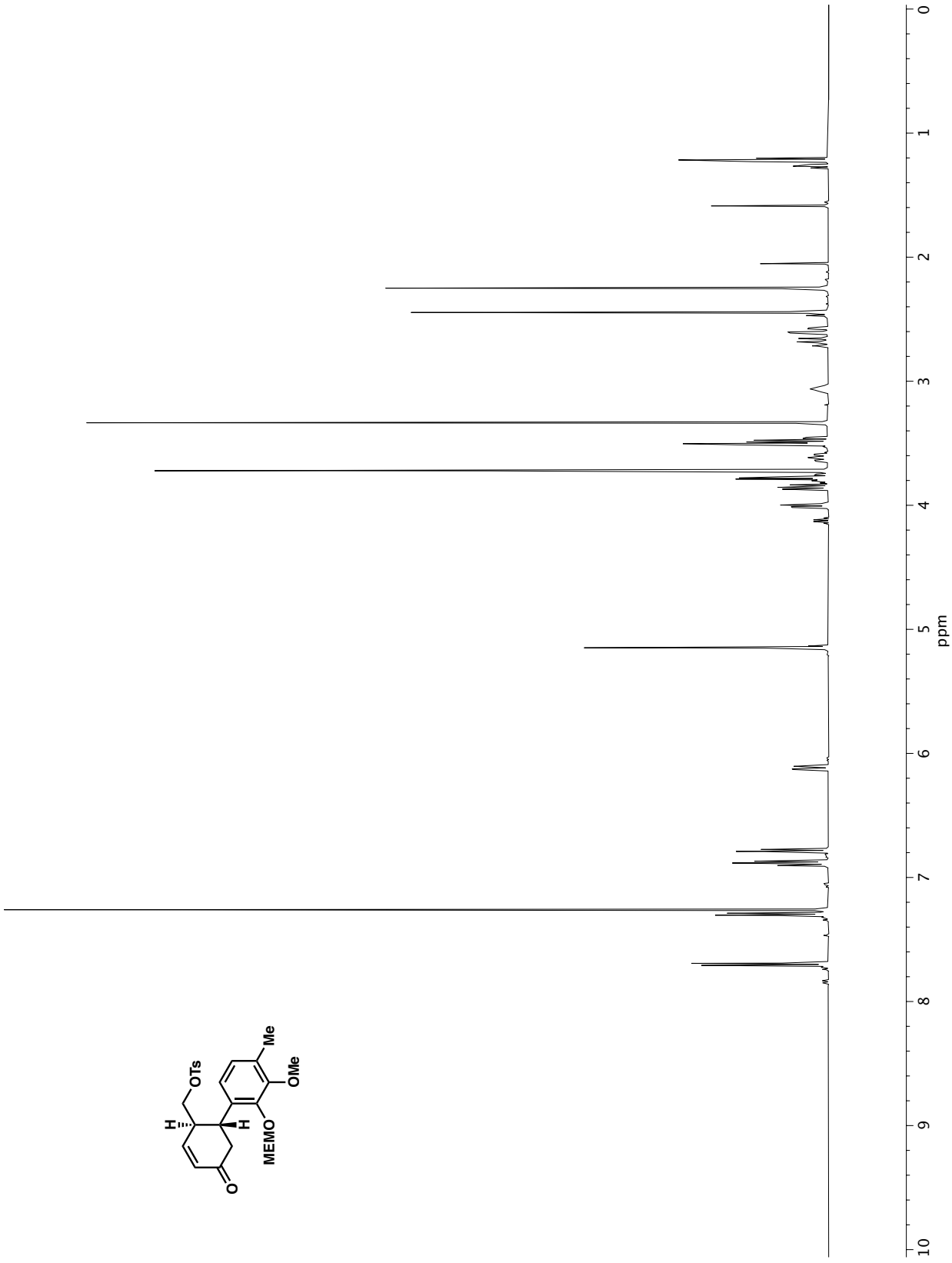


Figure A10.11 *^{1}H NMR (500 MHz, $CDCl_3$) of compound* ***249***.

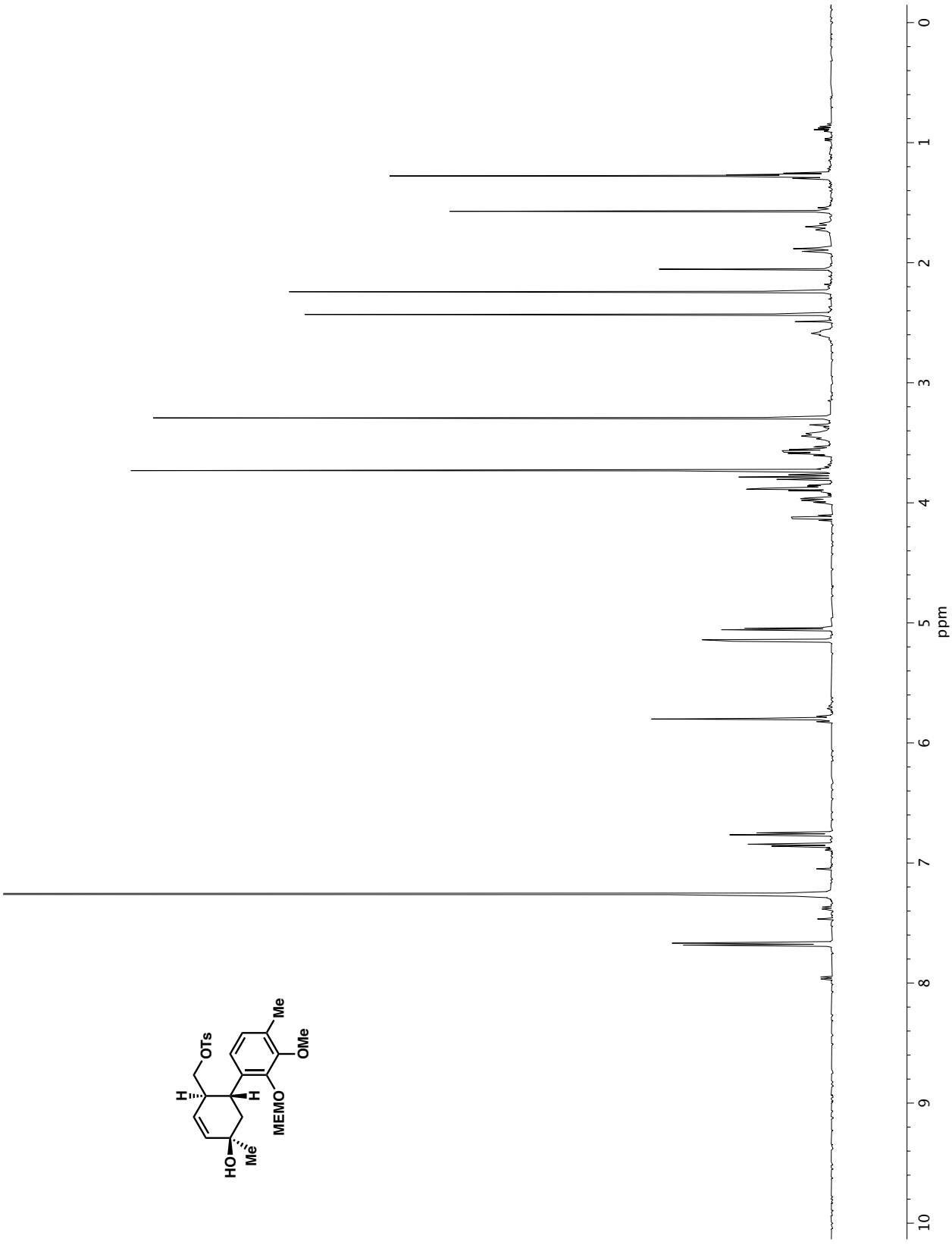


Figure A1.12 *^1H NMR (500 MHz, $CDCl_3$) of compound* ***250a***.

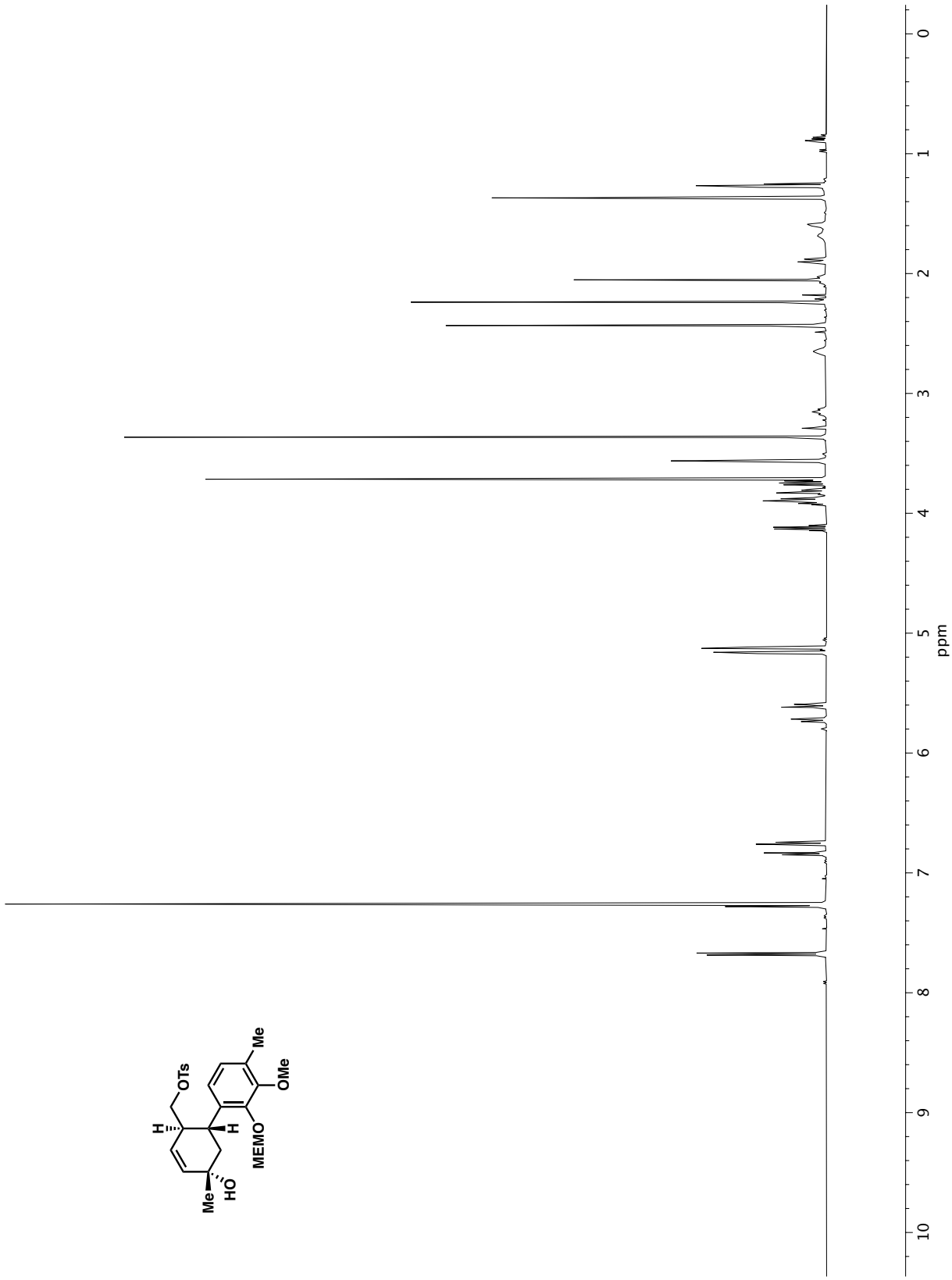


Figure A10.13 *^1H NMR (500 MHz, $CDCl_3$) of compound* ***250b***.

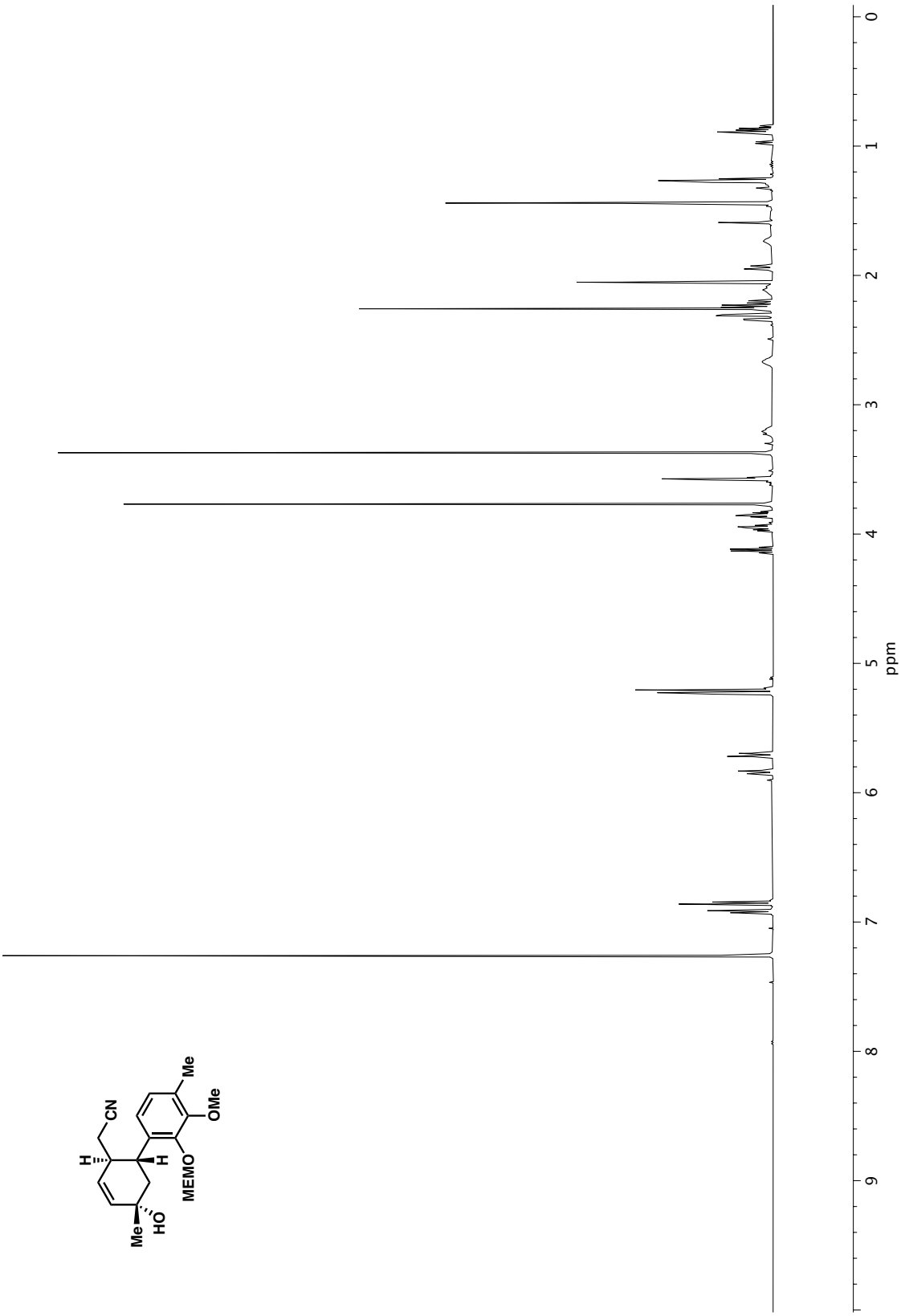


Figure A10.14 *^1H NMR (500 MHz, $CDCl_3$) of compound* ***251b****.*

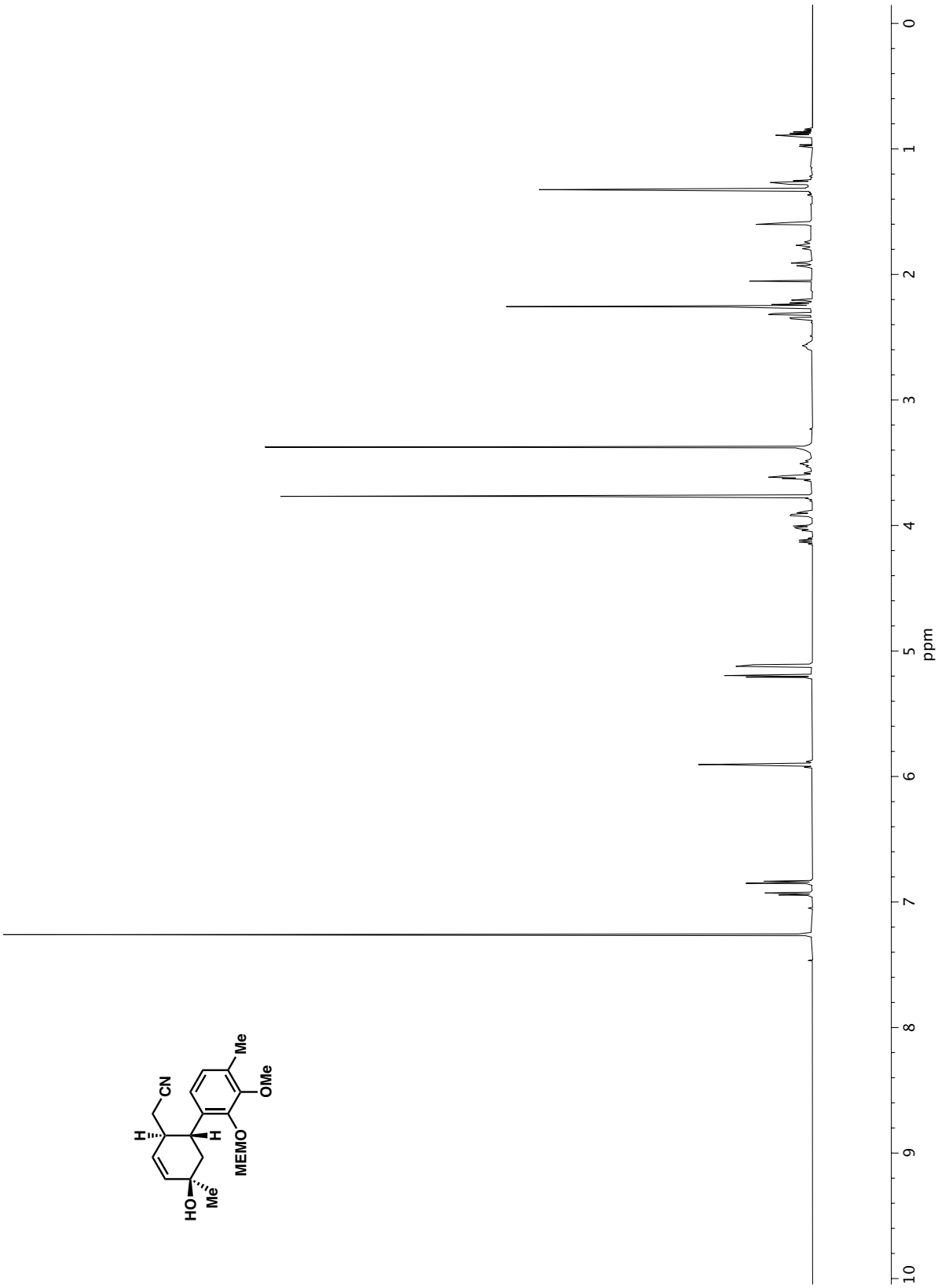


Figure A10.15 *^1H NMR (500 MHz, $CDCl_3$) of compound* ***251a***.

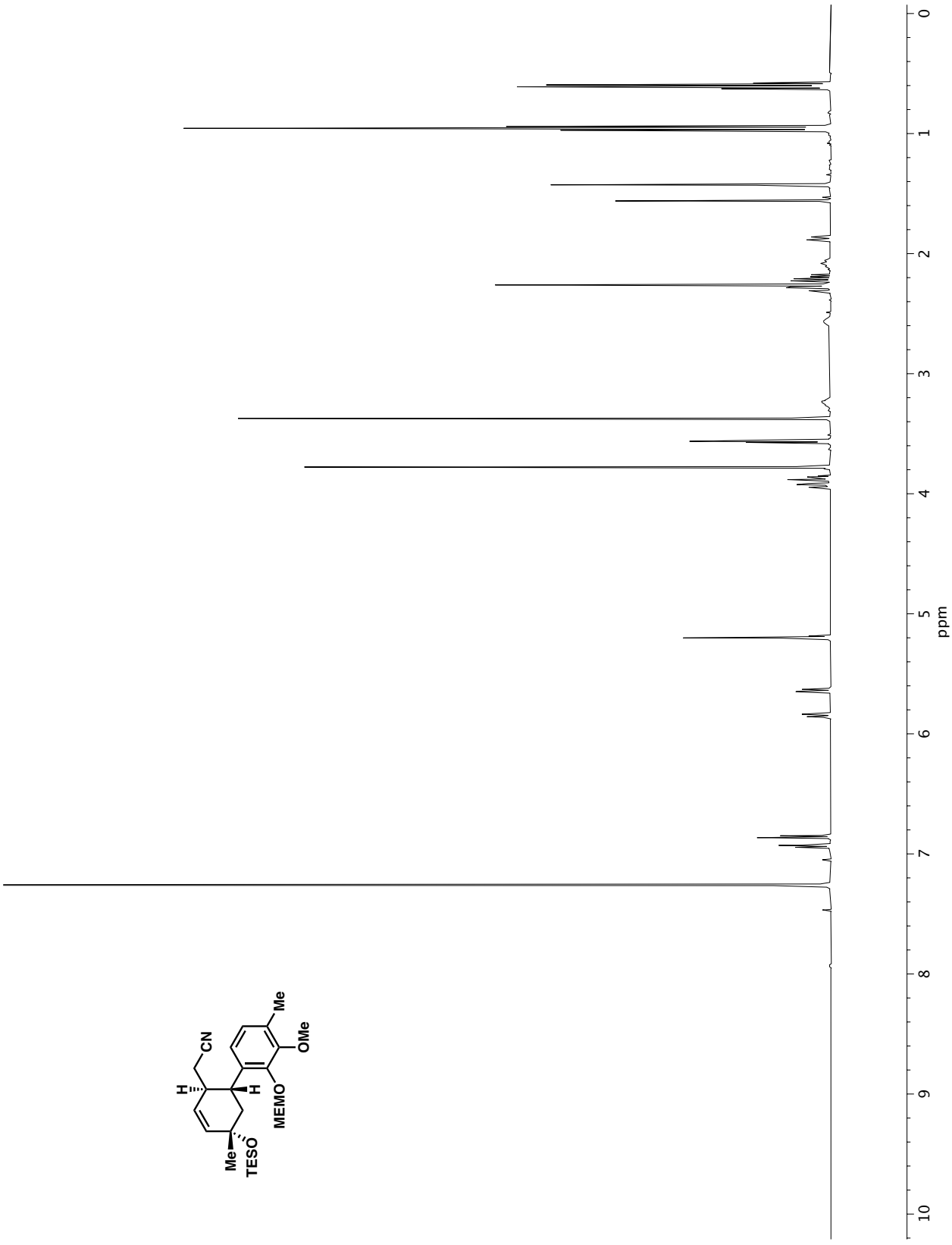


Figure A10.16 *^{1}H NMR (500 MHz, $CDCl_3$) of compound* ***252***.

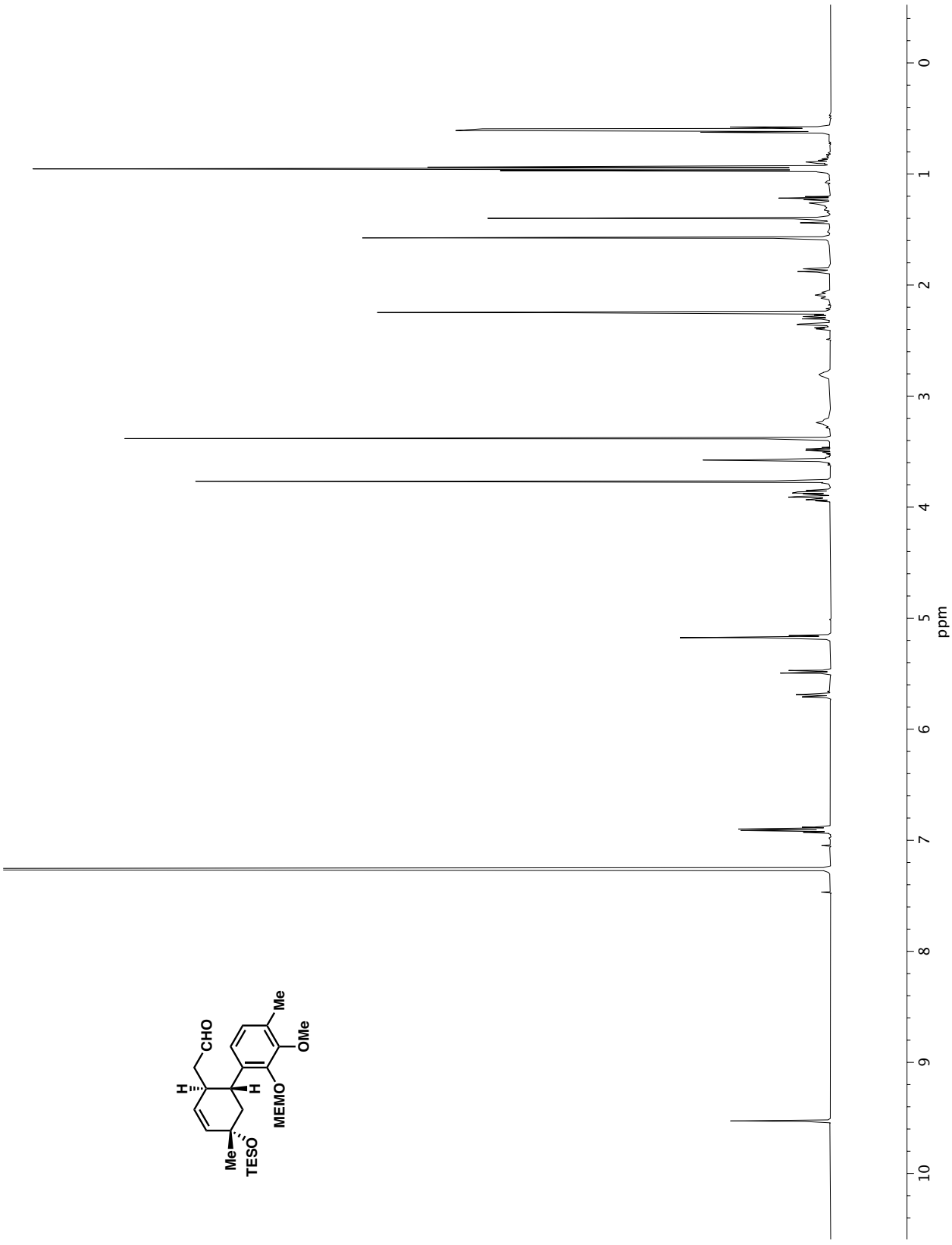


Figure A10.17 *^{1}H NMR (500 MHz, $CDCl_3$) of compound* ***253***.

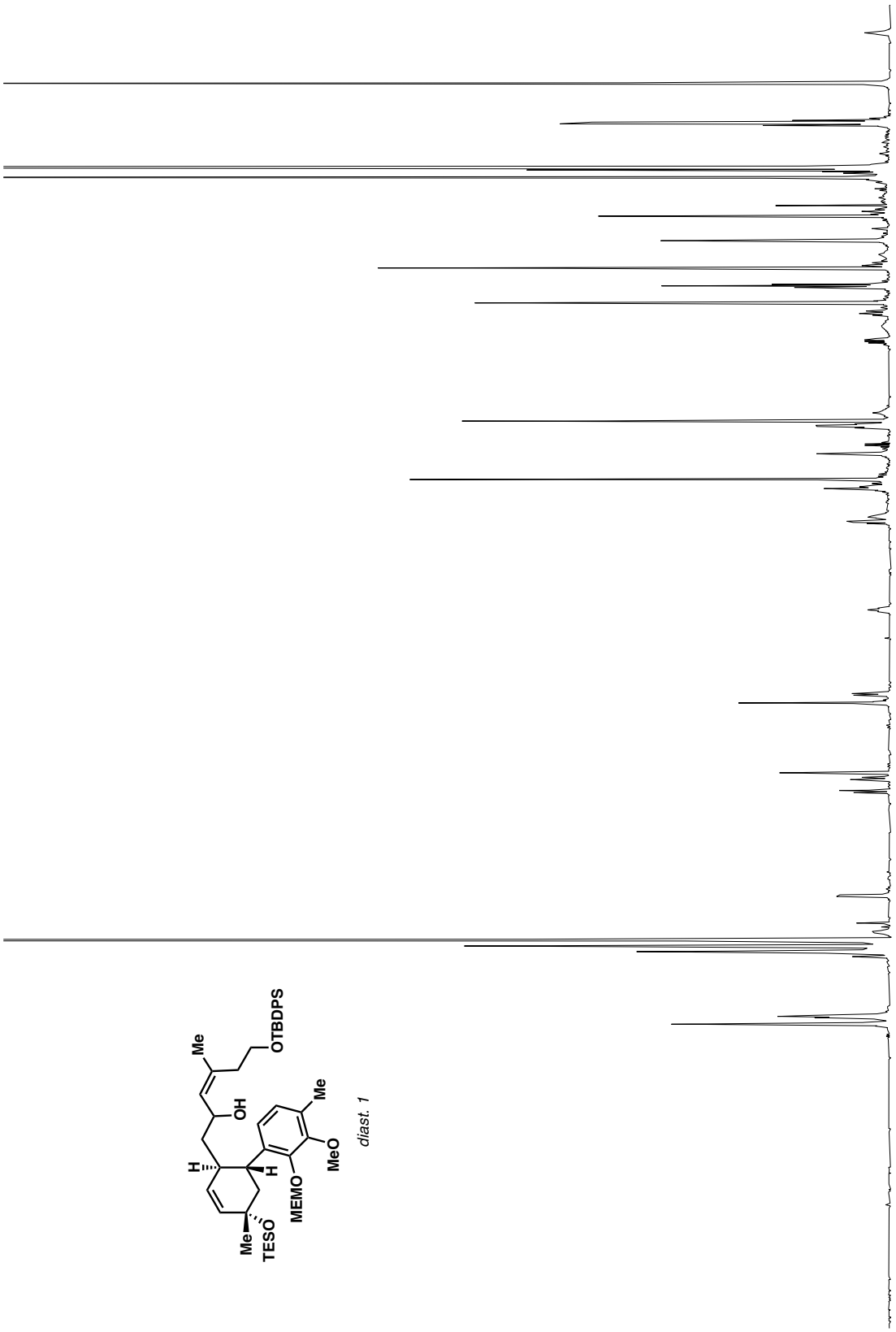


Figure A10.19 *^{1}H NMR (600 MHz, C_6D_6) of compound* ***269*** *(diast. 1).*

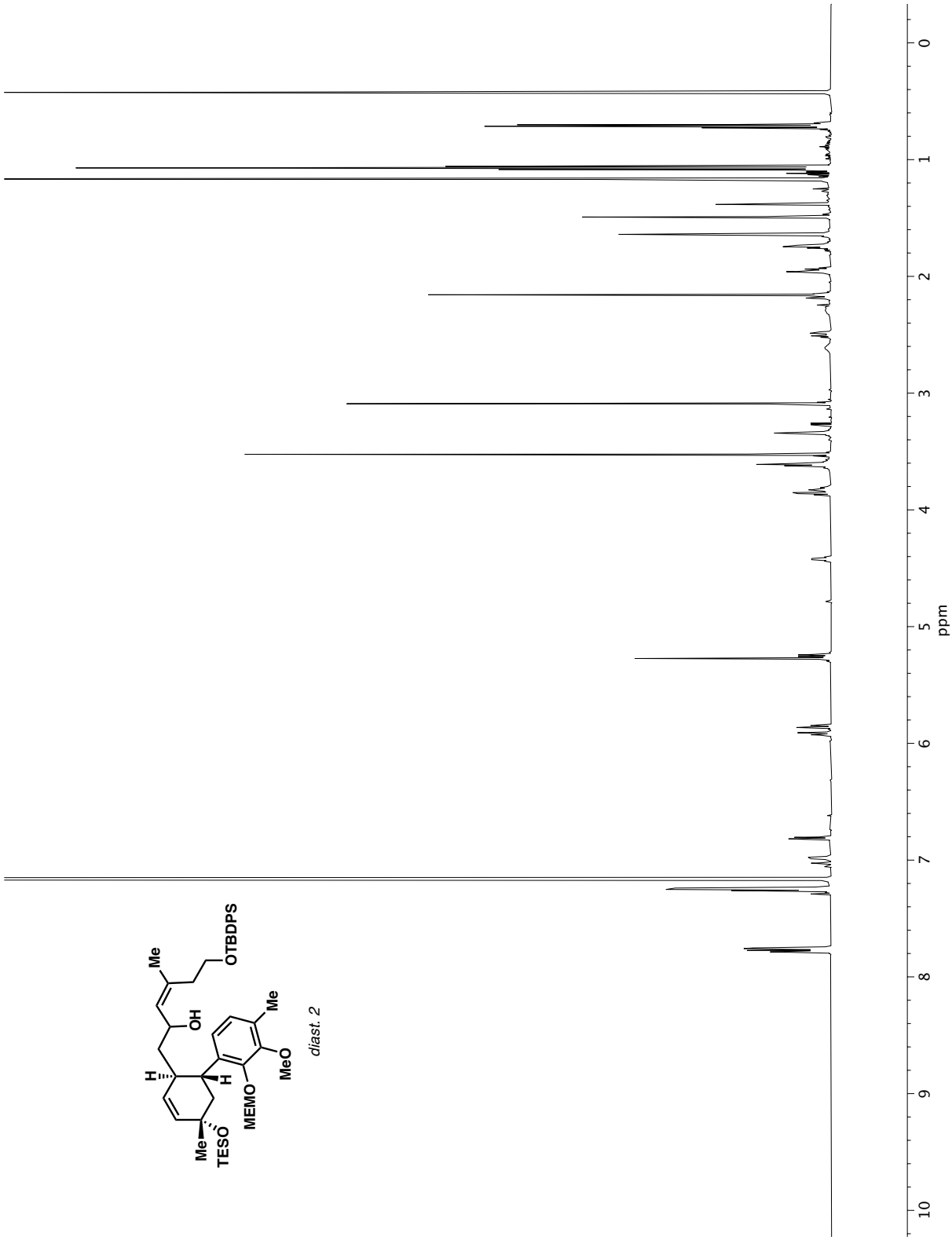


Figure A10.20 *^{1}H NMR (600 MHz, C_6D_6) of compound* ***269*** *(diast. 2).*

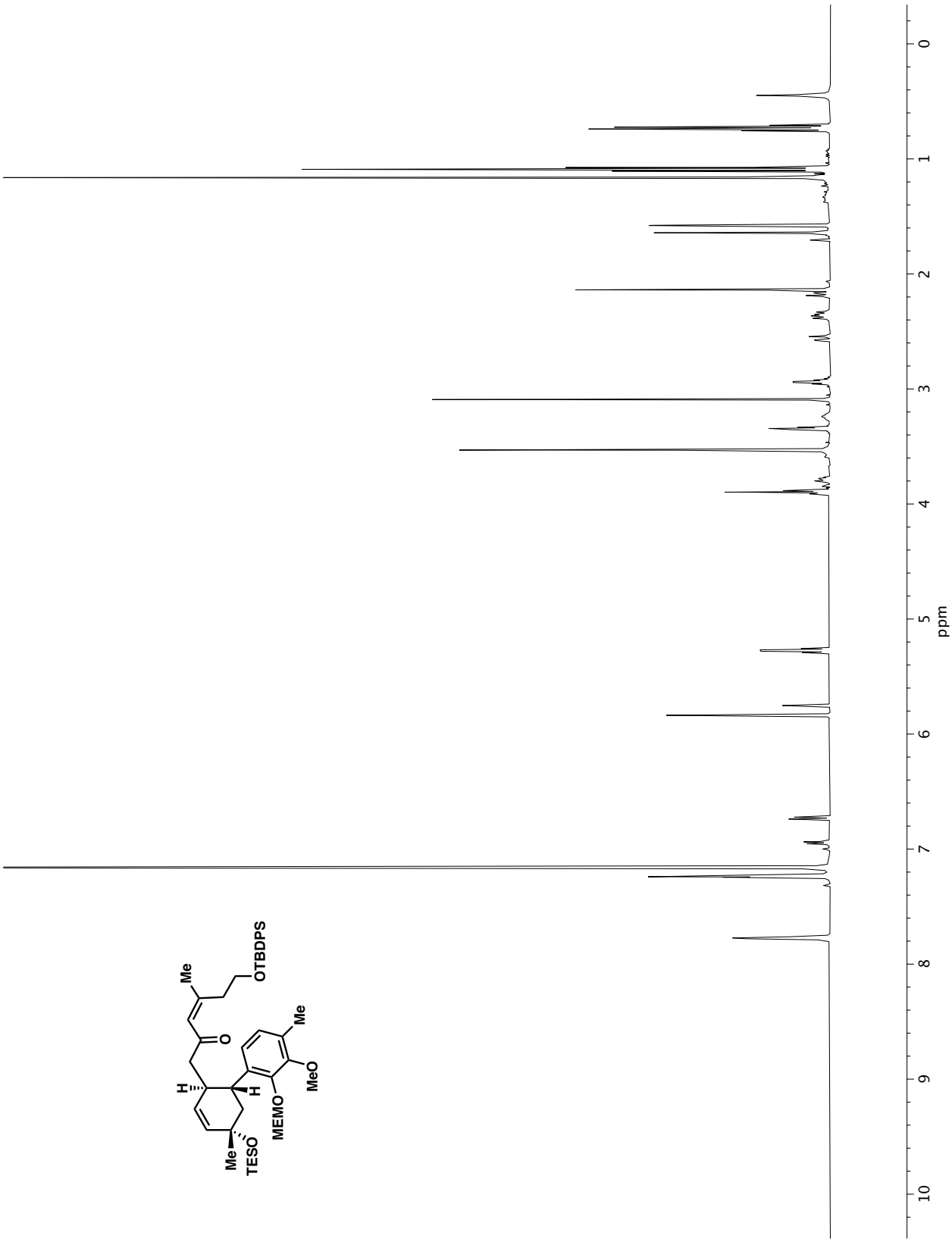


Figure A10.21 *^{1}H NMR (500 MHz, $CDCl_3$) of compound* ***254****.*

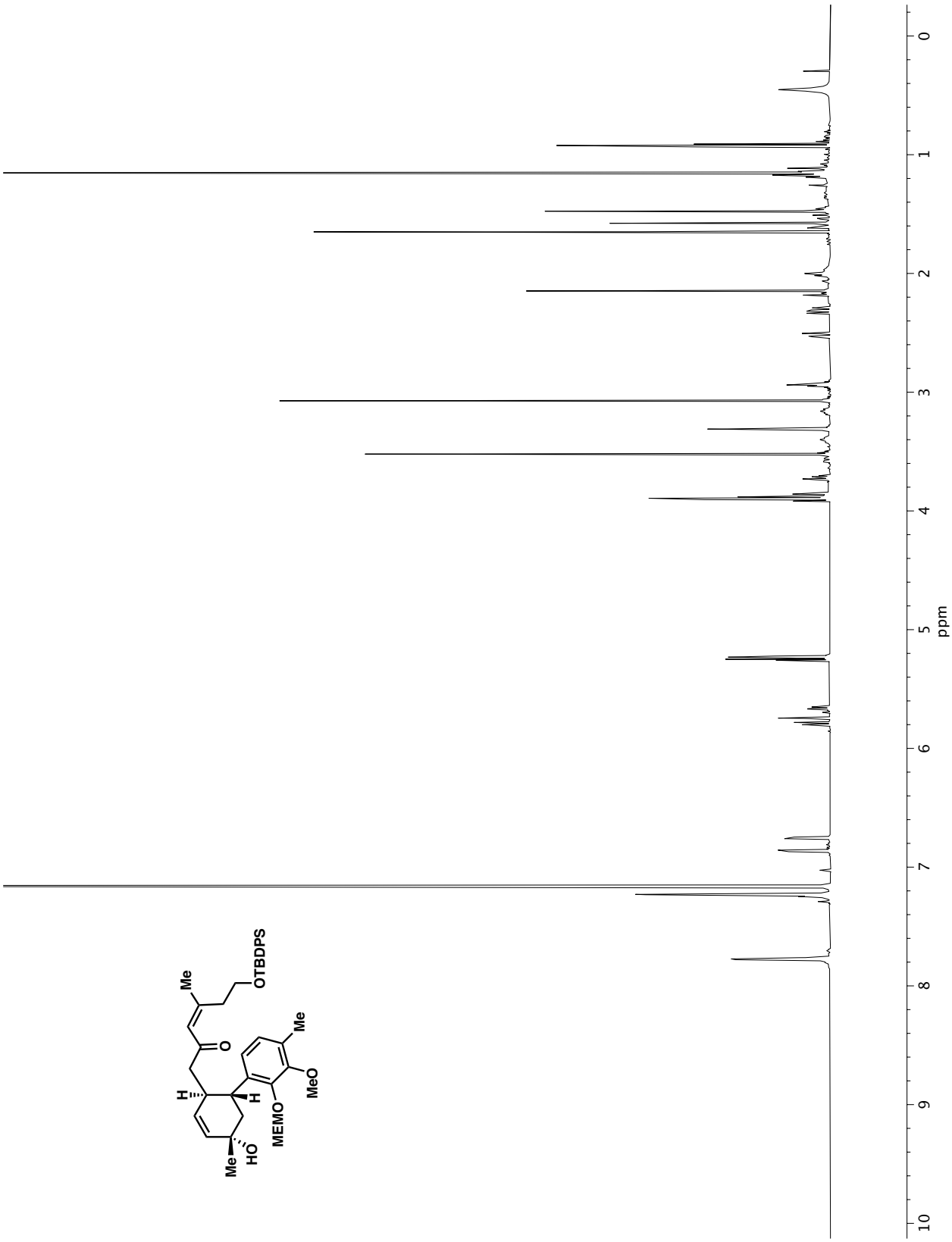


Figure A10.22 *^1H NMR (600 MHz, C_6D_6) of compound* ***256****.*

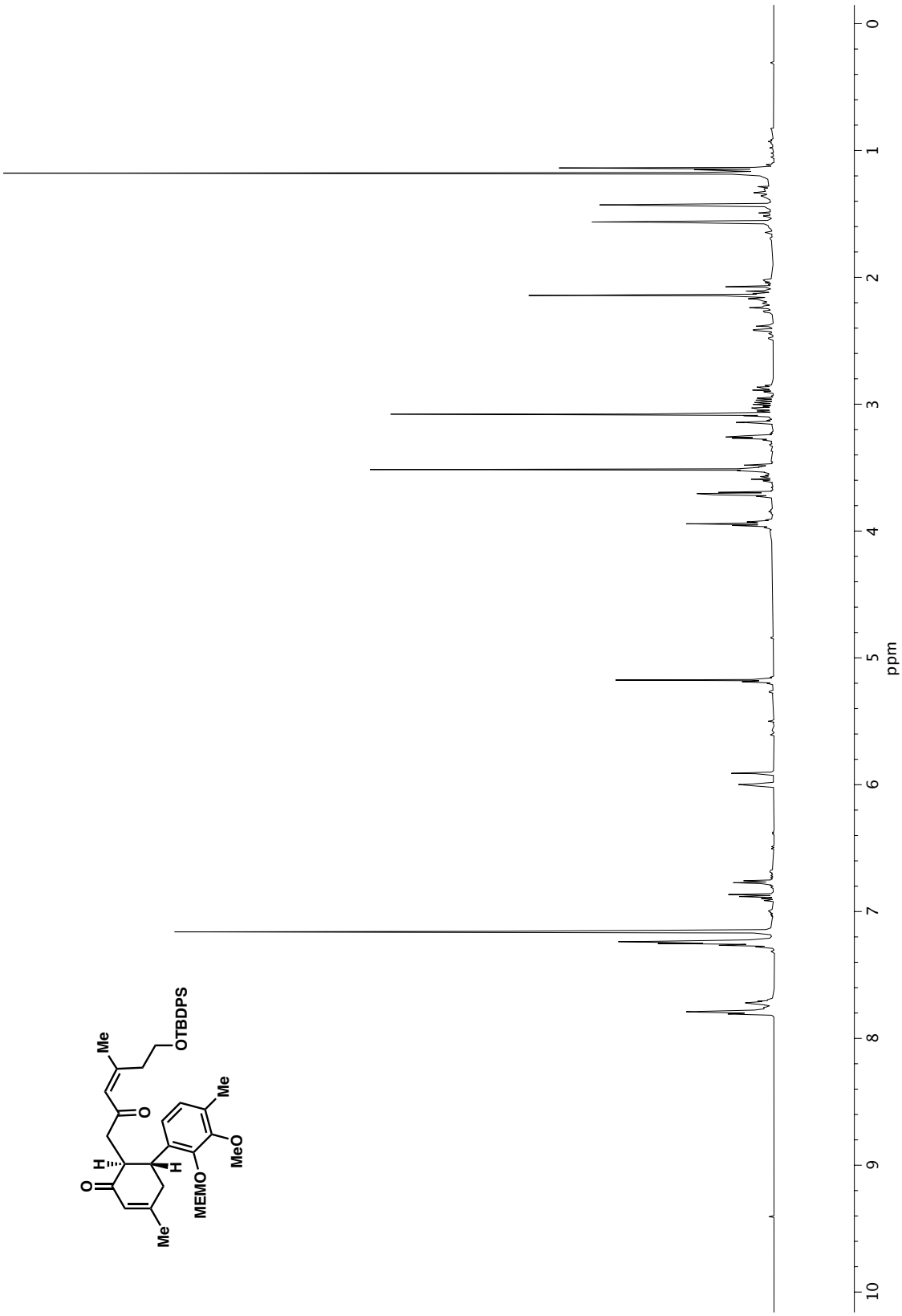


Figure A10.23 *^1H NMR (500 MHz, C_6D_6) of compound* ***257****.*

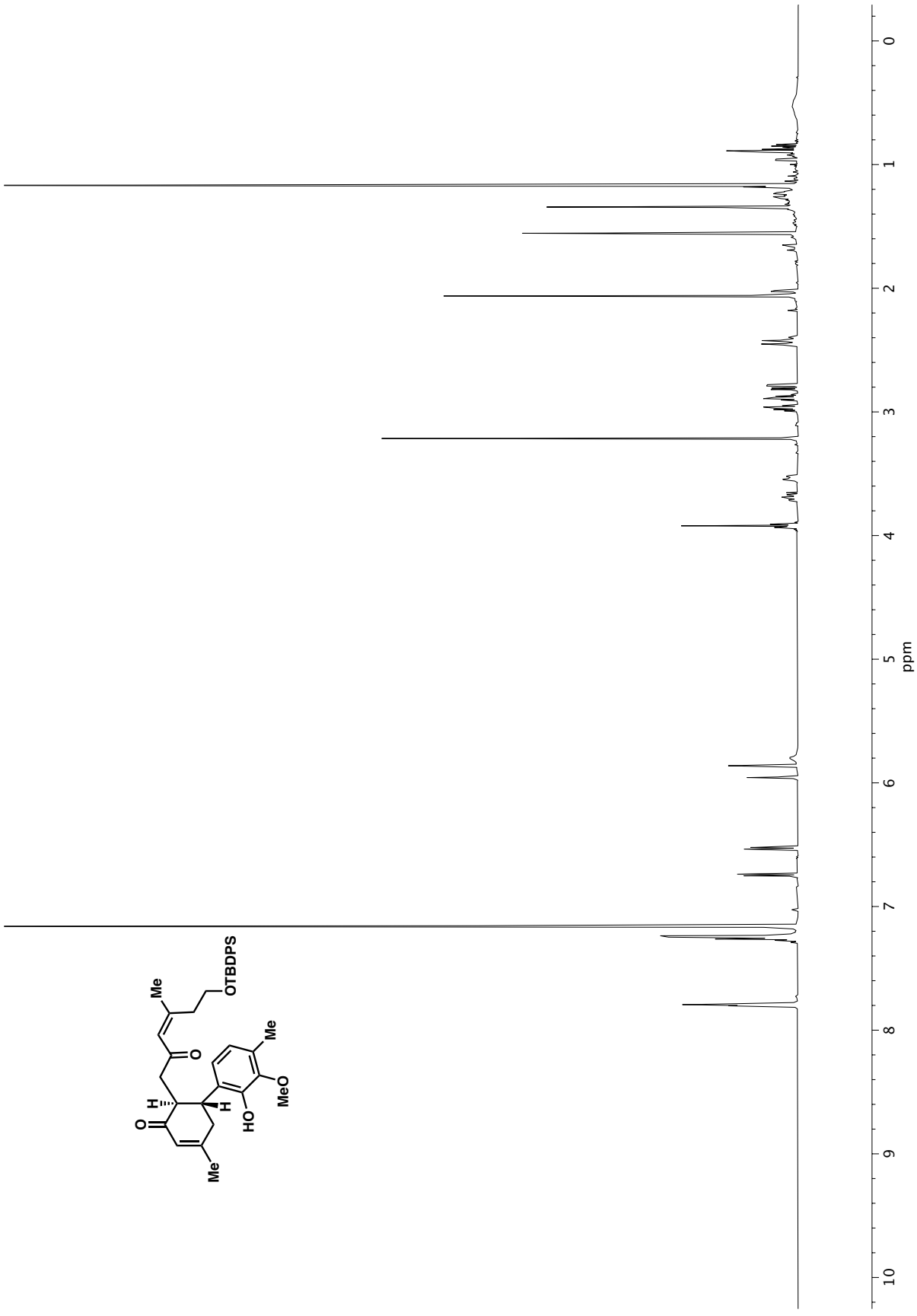


Figure A10.24 *^1H NMR (600 MHz, C_6D_6) of compound* ***258****.*

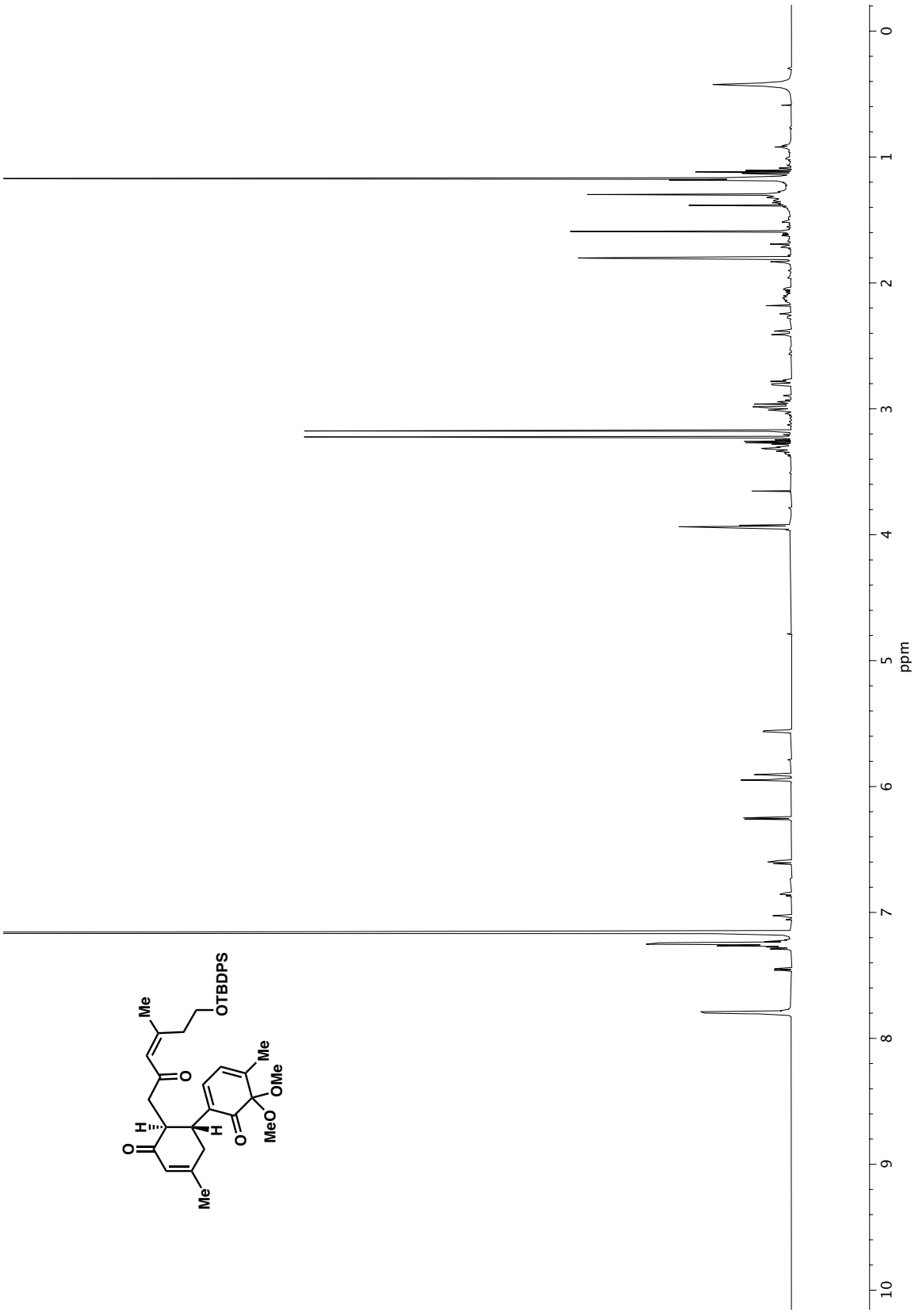


Figure A1.25 *^{1}H NMR (600 MHz, C_6D_6) of compound* ***259***.

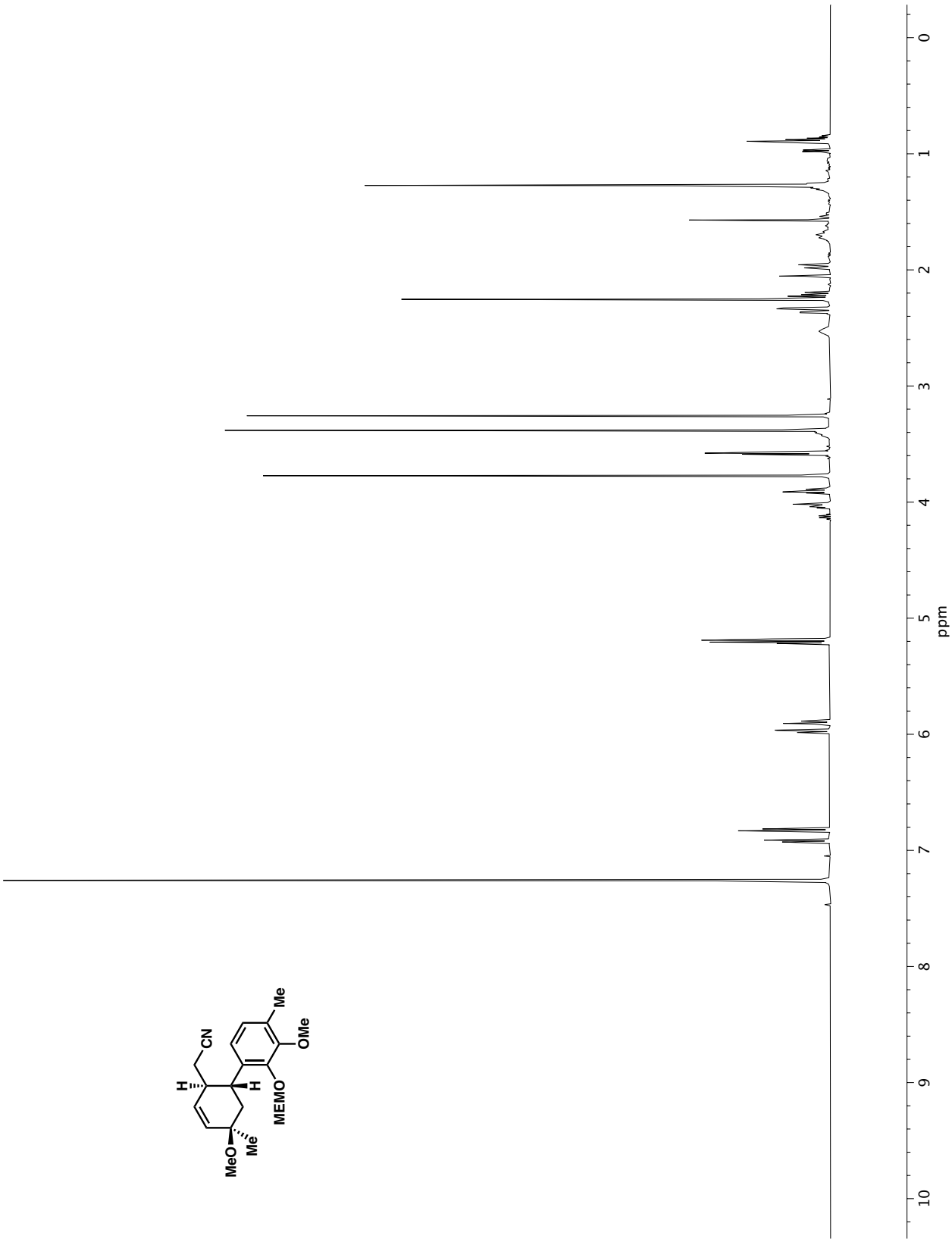


Figure A10.26 *^1H NMR (500 MHz, $CDCl_3$) of compound* ***262***.

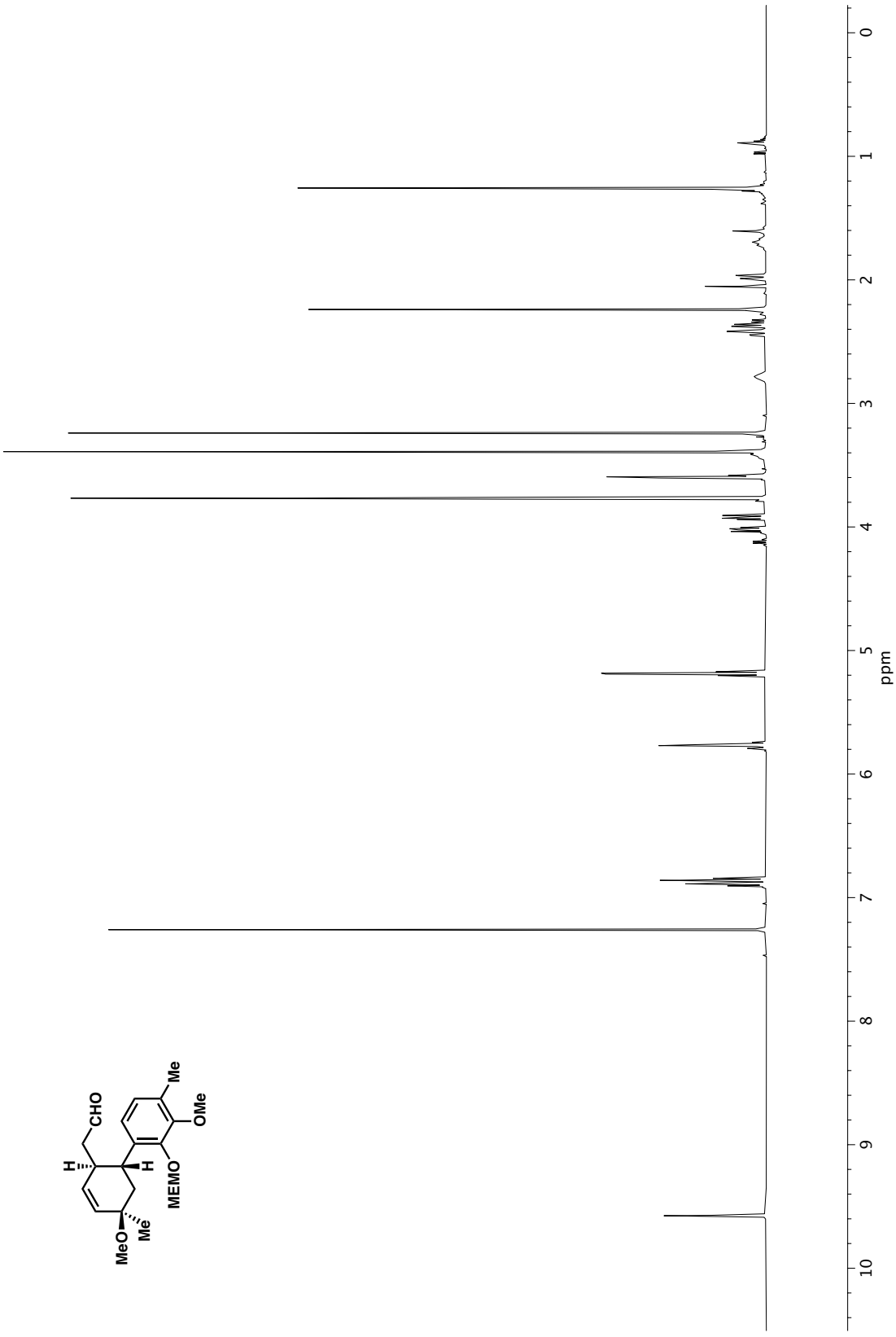


Figure A10.27 *^{1}H NMR (500 MHz, $CDCl_3$) of compound* ***270***.

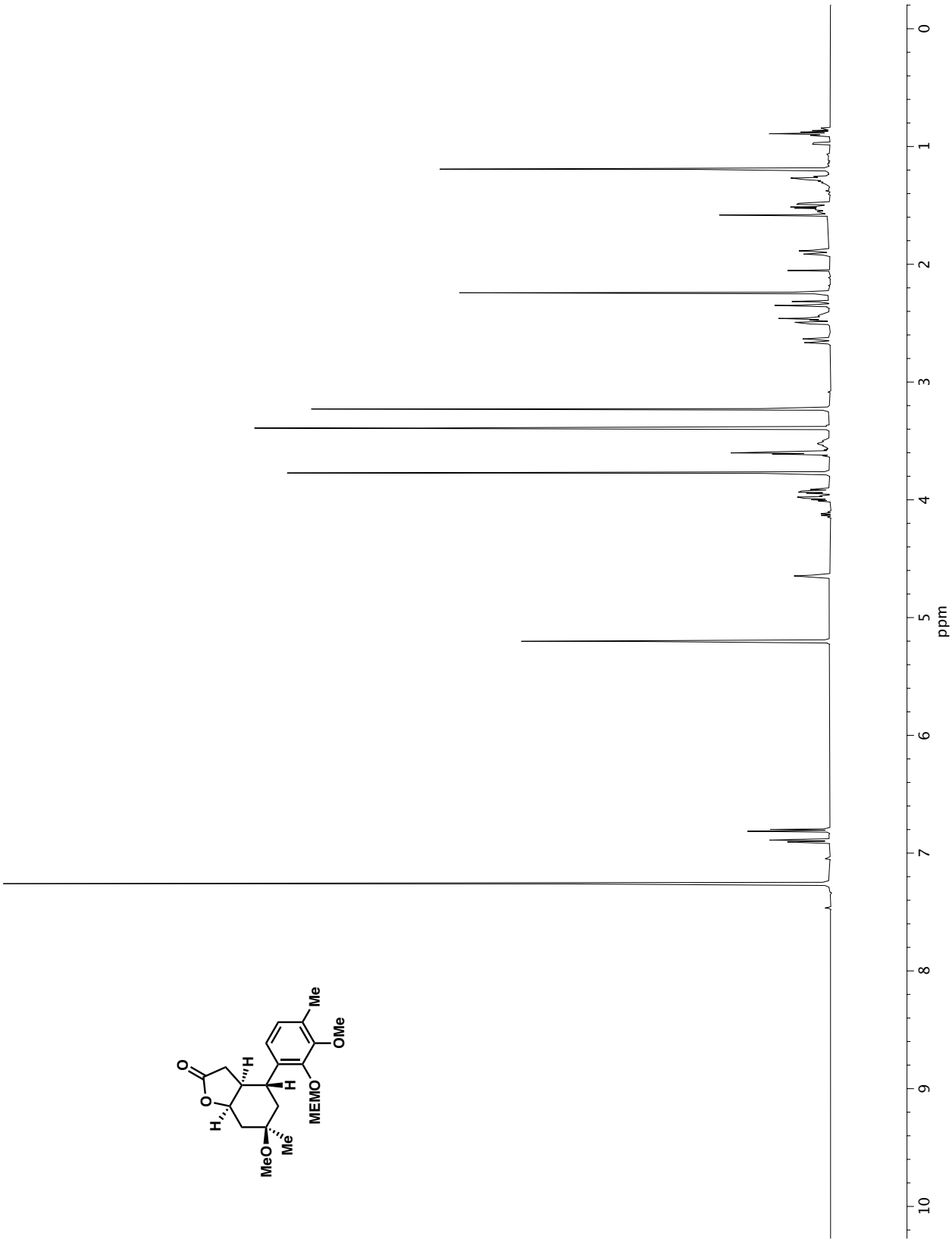


Figure A10.28 *^{1}H NMR (500 MHz, $CDCl_3$) of compound* ***264****.*

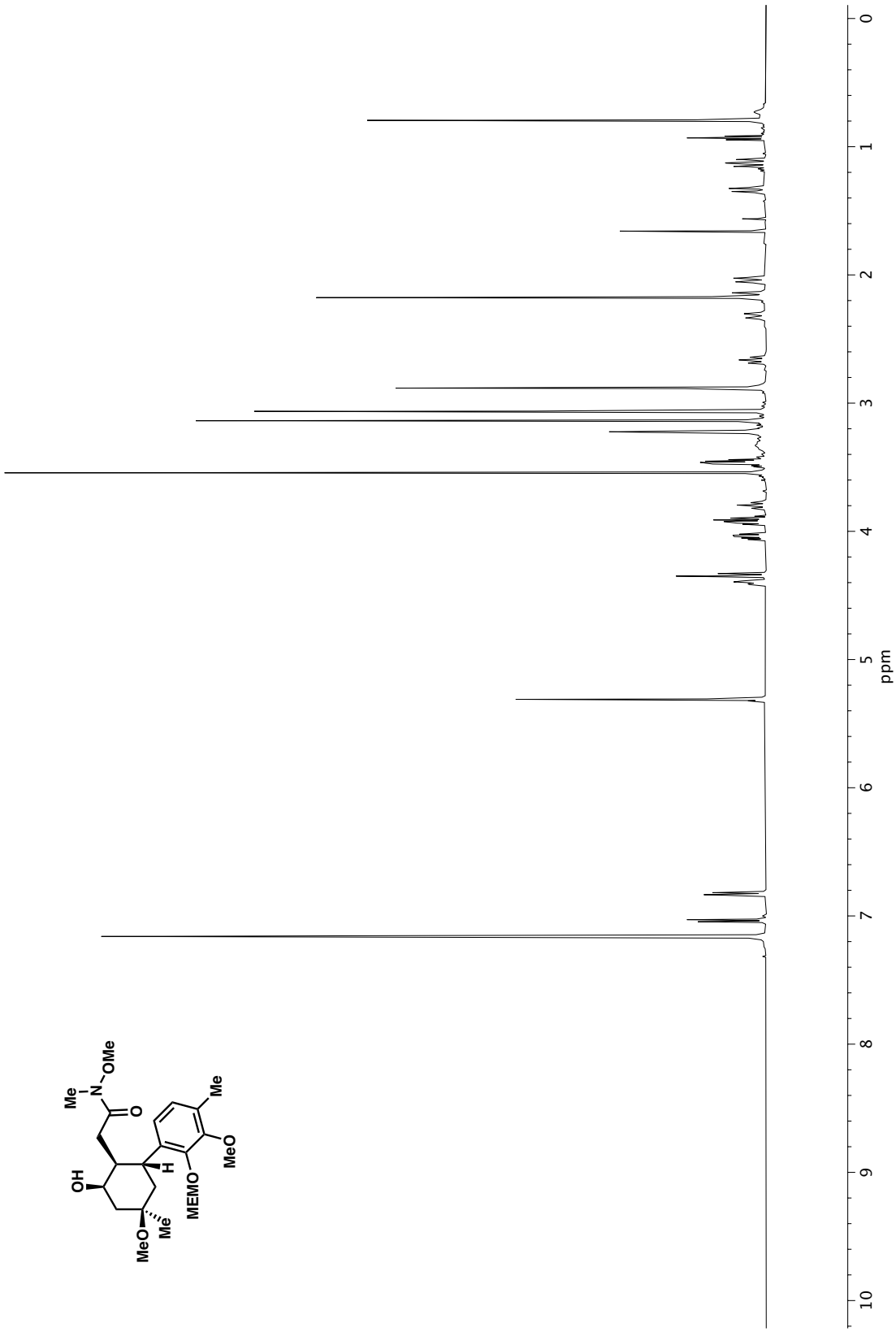


Figure A10.29 *^1H NMR (500 MHz, C_6D_6) of compound* ***266****.*

APPENDIX 11

Notebook Cross-References for New Compounds

Table A11.1 *Notebook cross-reference for Chapter 1*

Compound	^{1}H NMR (instrument)	^{13}C NMR (instrument)	Yield/Procedure
32a	FM_001_128_01_H (Florence)	FM_001_128_01_C (Florence)	FAM-I-128
33	efh-II-133-2 (Indy)	efh-II-133-2-13C (Florence)	EFH-II-133
34	efh-II-137-2 (Indy)	efh-II-137-2-13C (Florence)	EFH-II-137
35	efh-II-135-2 (Indy)	efh-II-135-2-13C (Florence)	EFH-II-135
32b	FM_001_128_05_H (Florence)	FM_001_128_05_C (Florence)	FAM-I-128
32c	FM_001_128_03_H (Florence)	FM_001_128_03_C (Florence)	FAM-I-128
32d	FM_001_128_02_H (Florence)	FM_001_128_02_C (Florence)	FAM-I-128
32e	efh-1-283B-3-1Hchar (Florence)	efh-1-283B-3-13Cchar (Florence)	EFH-II-101
32f	FM_001_146_H (Florence)	FM_001_146_C (Florence)	FAM-I-136
32g	efh-1-273B-2-1Hchar (Florence)	efh-1-273B-2-13Cchar (Florence)	EFH-II-119
32h	efh-1-275B-3-1Hchar (Florence)	efh-1-275B-3-13Cchar (Florence)	EFH-II-121
32i	efh-1-281B-3-2D (Florence)	efh-1-281B-3-13C (Florence)	EFH-II-117
32j	efh-II-123-2 (Indy)	efh-II-123-2 (Florence)	EFH-II-123
32k	efh-II-125-2 (Indy)	efh-II-125-2-13C (Florence)	EFH-II-125
32l	FM_001_130_03_H (Florence)	FM_001_130_03_H (Florence)	FAM-I-130
32m	efh-II-127-2 (Indy)	efh-II-127-2-13C (Florence)	EFH-II-127
32n	FM_001_142_02_H (Florence)	FM_001_142_02_C (Florence)	FAM-I-142
32p	efh-II-131-3 (Indy)	efh-II-131-2-13C (Florence)	EFH-II-131
32q	FM_001_128_04_H	FM_001_128_04_C	FAM-I-128
32s	FM_001_150_03_top (Florence)	FM_001_150_06_H (Florence)	FAM-I-150
32t	efh-III-phenethyl-chi-1H (Florence)	efh-III-phenethyl-chi-13C (Florence)	FAM-I-177
32u	efh-III-geranyl-chi-1H	efh-III-geranyl-chi-13C	FAM-I-177
40	efh-III-75-3 (Indy)	efh-III-75-3 (Florence)	EFH-III-75
41	efh-II-165-2 (Indy)	efh-II-165-2-13C (Florence)	EFH-II-165
42	efh-II-167-2 (Indy)	efh-II-167-2-13C (Florence)	EFH-II-167
43	FM_001_138_prepH	FM_001_138_prepC (Florence)	FAM-I-138
44	efh-II-161-2-2 (Florence)	efh-II-151-2-13C-re (Florence)	EFH-II-161
45	efh-II-179-2 (Indy)	efh-II-179-2-13C (Florence)	EFH-II-179
31g	efh-1-261-2 (Florence)	efh-1-261-2 (Florence)	EFH-I-261
31h	efh-II-111-2 (Indy)	efh-II-111-2-13C (Florence)	EFH-II-111
31k	efh-1-219-2 (Indy)	efh-1-219-2-13C (Florence)	EFH-I-219
31l	FM_001_124_02_H (Florence)	FM_001_124_02_C (Florence)	FAM-I-124
31m	FM_001_89_04_H (Florence)	FM_001_89_04_C (Florence)	FAM-I-89

Table A11.1 cont'd.

Compound	^{1}H NMR (instrument)	^{13}C NMR (instrument)	Yield/Procedure
46n	ZPS-VI-297-adapaleneKetone (Florence)	ZPS-VI-297-adapaleneKetone (Florence)	ZPS-VI-297
47n	ZPS-VI-301-adapaleneEster (Florence)	ZPS-VI-301-adapaleneEster (Florence)	ZPS-VI-301
31n	ZPS-VII-29-adapaleneCarbonate (Florence)	ZPS-VII-29-adapaleneCarbonate (Florence)	ZPS-VII-29
31p	ZPS-VI-225-TsIndoleCarbonate (Florence)	ZPS-VI-225-TsIndoleCarbonate (Florence)	ZPS-VI-225
31q	ZPS-VI-257-pyrCO2Me (Florence)	ZPS-VI-257-pyrCO2Me (Florence)	ZPS-VI-257
31s	efh-II-229-2-re (Indy)	efh-II-229-2-13C (Florence)	EFH-II-229

Table A11.2 *Notebook cross-reference for Chapter 2*

Compound	^{1}H NMR (instrument)	^{13}C NMR (instrument)	Yield/Procedure
72	efh-X-enone-off-route (Venice)	efh-X-enone-off-route (Venice)	EFH-VI-233
73	efh-X-1-4-addn-off-route (Venice)	efh-X-1-4-addn-off-route (Venice)	EFH-VI-103
76	efh-IX-143-2B-1H-char (mislabled) (Florence)	efh-IX-143-2B-13C-char (mislabled) (Florence)	EFH-IX-31
80	efh-IX-169-conj-addn-char-1H (Venice)	efh-IX-169-conj-addn-char-13C (Venice)	EFH-IX-169
68	efh-IX-171-5-5-diketone-1H-char (Venice)	efh-IX-171-5-5-diketone-13C-char (Venice)	EFH-IX-171
(±)-70	EFH-VI-241-2	–	EFH-VI-241
70	efh-IX-143-2A-1H-char-5-5-hydroxyketone (Venice)	efh-IX-143-2A-1H-char-5-5-hydroxyketone (Venice)	EFH-IX-209
81	efh-IX-143-3-pure-1H-char (Florence)	efh-IX-143-3-pure-13C-char (Florence)	EFH-IX-209
(*Z*)-82	efh-hydrazone-char (Florence)	efh-hydrazone-char-13C (Florence)	EFH-IX-163
83	efh-IX-167-2-tbs-ether-char-1H (Venice)	efh-IX-167-2-tbs-ether-char-13C (Venice)	EFH-IX-213
(*Z*)-86	efh-IX-215-2A-1H-char (Florence)	efh-IX-215-2A-13C-char (Florence)	EFH-IX-215
(*E*)-86	efh-IX-215-2B-1H-char (Florence)	efh-IX-215-2B-13C-char (Florence)	EFH-IX-215
87	efh-IX-217-2-1H-char (Florence)	efh-IX-217-2-13C-char (Florence)	EFH-IX-217
88	efh-IX-221-2-1H (Florence)	efh-IX-221-2-13C (Florence)	EFH-IX-219, 221
67	efh-IX-223-2-char-1H-again (Florence)	efh-IX-223-2-char-13C-again (Florence)	EFH-IX-223
67b	efh-VII-283-2-BOC (Fid)	efh-VII-283-2-BOC (Fid)	EFH-VII-283, 267
67c	efh-VII-281-2-TEOC (Fid)	efh-VII-281-2-TEOC (Fid)	EFH-VII-281, 273
67d	efh-VI-297-2-lactam-char (Fid)	efh-VI-297-2-lactam-char (Fid)	EFH-VI-297, 293, 289
92	efh-IX-193-1H (Florence)	efh-IX-193-13C (Florence)	EFH-VII-211, 209
93	efh-VIII-19-3-1H-char (Florence)	efh-VIII-19-3-13C-char (Florence)	EFH-VIII-19
97	efh-VIII-19-3-1H-char (Florence)	efh-VIII-19-3-13C-char (Florence)	EFH-VIII-61, EFH-VII-79
97b	–	–	EFH-VII-85
101	KI-1-113b (Venice)	efh-NTs-2-char-re (Venice)	KI-112
103	efh-VII-141-2-1H (Florence)	efh-VII-141-2-13C (Florence)	EFH-VII-141, 135
104	efh-IX-177-2-1H-char (Florence)	efh-IX-177-2-13C-char (Florence)	EFH-IX-177, 175, 173
105	efh-IX-179-2-Boc-vinyll-char (Venice)	efh-IX-179-2-Boc-vinyll-char (Venice	EFH-IX-179

Table A11.2 cont'd.

Compound	^{1}H NMR (instrument)	^{13}C NMR (instrument)	Yield/Procedure
106	efh-IX-227-2-1H-char (Florence)	efh-IX-227-2-13C-char (Florence)	EFH-X-21
107	efh-IX-237-2-1H-char (Florence)	efh-IX-237-2-13C-char (Florence)	EFH-X-27
112	efh-IX-243-2-1H-char (Florence)	efh-IX-243-2-13C-char (Florence)	EFH-X-37
64	efh-VIII-137-2-benzene (Fid)	efh-IX-281-2-char (Venice)	EFH-IX-281
116	efh-X-69-2B-1H-char (Florence)	efh-X-69-2B-13C-char (Florence)	EFH-IX-301
117	efh-X-69-2A-1H-char (Florence)	efh-X-69-2-13C-char (Florence)	EFH-IX-301
53	efh-X-61-hunterine-check (Fid)	efh-61-hunterine-13C (Florence)	EFH-X-61

Table A11.3 *Notebook cross-reference for Chapter 3*

Compound	^{1}H NMR (instrument)	^{13}C NMR (instrument)	Yield/Procedure
145	LMFR-I-57-1H (Florence)	LMFR-I-57-13C (Florence)	LMFR-I-57
146	efh-lmfr-7m-alk-re (Venice)	efh-lmfr-7m-alk-re (Venice)	LMFR-I-27
149	efh-XII-209-2-1H (Florence)	efh-XII-209-2-13C (Florence)	EFH-XII-209
150	efh-XIV-LMFR-BPin (Florence)	LMFR-I-35-13C	LMFR-I-35
151	efh-XIII-147-2-char (Venice)	efh-XIII-147-2-char (Venice)	EFH-XIII-147
152	efh-XIV-7m-aniline-re (Venice)	efh-XIV-7m-aniline-re (Venice)	EFH-XIII-225
154	LMFR-I-45(39)-1H (Florence)	LMFR-I-45(39)-13C (Florence)	LMFR-I-45
155	efh-XIII-179-2-solid-1H (Florence)	efh-XIII-179-2-solid-13C (Florence)	EFH-XIII-179
157	efh-XIII-221-2 (Florence)	efh-XIII-221-2-13C (Florence)	EFH-XIII-221
158	LMFR-I-43-1H (Florence)	LMFR-I-43-13C (Florence)	LMFR-I-49
159	LMFR-I-61-1H (Florence)	LMFR-I-61-13C (Florence)	LMFR-I-61
160	LMFR-I-69-2-CDCl3-1H (Florence)	LMFR-I-69-2-CDCl3-13C (Florence)	LMFR-I-69
161	LMFR-I-71-2A-benzene-1H (Florence)	LMFR-21-benzene-13C (Florence)	EFH-XIII-207
162	efh-XIII-193-3-1H (Florence)	efh-XIII-193-3-13C (Florence)	EFH-XIII-193
163	efh-XIII-229-2-1H (Florence)	efh-XIII-229-2-13C (Florence)	EFH-XIII-229
164	efh-XIII-231-2-1H (Florence)	efh-XIII-231-2-13C (Florence)	EFH-XIII-231
166	efh-XIII-247-2B-1H (Florence)	efh-XIII-247-2B-13C (Florence)	EFH-XII-247

Table A11.4 *Notebook cross-reference for Chapter 4*

Compound	^{1}H NMR (instrument)	^{13}C NMR (instrument)	Yield/Procedure
205	efh-X-293-2-char-1H (Florence)	efh-X-293-2-char-13C (Florence)	EFH-X-293
207	efh-XIV-75-2-char-benzene-1H (Florence)	efh-XIV-75-2-char-benzene-13C (Florence)	EFH-XIV-75-2
208	efh-XIV-79-3B-char-1H (Florence)	efh-XIV-79-3B-char-1H (Florence)	EFH-XI-71
234	efh-XIV-79-3A-1H (Florence)	efh-XIV-79-3A-13C (Florence)	EFH-XIV-79
209	efh-XIV-81-2B-char-1H (Florence)	efh-XIV-81-2B-char-13C (Florence)	EFH-XI-83
210	efh-XI-95-2-char-re-1H (Florence)	efh-XI-95-2-char-re-13C (Florence)	EFH-XI-95-2
211	efh-XI-111-char-1H (Florence)	efh-XI-111-char-13C (Florence)	EFH-XI-111
221	efh-XIV-113-2-1H (Florence)	efh-XIV-113-2-13C (Florence)	EFH-XIV-113
225	efh-XIV-135-2-1H-char (Florence)	efh-XIV-135-2-13C-char (Florence)	EFH-XIV-135
226	efh-XIV-157-2-1H (Florence)	efh-XIV-157-2-13C (Florence)	EFH-XIV-143, EFH-XIV-147
227	efh-XIV-151-re-char (Venice)	efh-XIV-151-re-char (Venice)	EFH-XIV-151
228	efh-XII-195-2 (Venice)	efh-XII-195-2 (Venice)	EFH-XII-195
230	efh-XIV-155-2-char (Venice)	efh-XIV-155-2-char (Venice)	EFH-XIV-155
231	efh-XIV-163-2A-1H (Florence)	efh-XIV-163-2A-13C (Florence)	EFH-XIV-163

Table A11.4 *Notebook cross-reference for Appendix 9*

Compound	^{1}H NMR (instrument)	Yield/Procedure
244	efh-XII-69-2 (Venice)	EFh-XII-69
245	efh-XII-79-2 (Venice)	EFH-XII-79
247	efh-XII-47-2A, efh-XII-47-2B (Venice)	EFH-XII-169
247	efh-XII-169-2B (Venice)	EFH-XII-169
248	efh-XII-177-2 (Venice)	EFH-XII-177
249	efh-XII-179-2 (Venice)	EFH-XII-179
250a	efh-XII-185-2A (Venice)	EFH-XII-185
250b	efh-XII-185-2B (Venice)	EFH-XII-185
251b	efh-XII-189-2 (Venice)	EFH-XII-189
251a	efh-XII-187-2 (Venice)	EFH-XII-187
252	efh-XII-199-2 (Venice)	EFH-XII-199
253	efh-XII-213-2 (Venice)	EFH-XII-271
269	efh-XIII-57-2A-benzene, efh-XIII-57-2B-benzene (Fid)	EFh-XIII-57
254	efh-XIII-59-2-benzene (Venice)	EFH-XIII-63
256	efh-XIII-53-2-benzene (Venice)	EFH-XIII-83
257	efh-XIII-87-2-benzene (Venice)	EFH-XIII-87
258	efh-XIII-101-2 (Fid)	EFH-XIII-101
259	efh-XIII-157-crude (Fid)	efh-XIII-125
262	efh-XIII-129-2 (Venice)	EFH-XIII-129
270	efh-XIII-135-2 (Venice)	EFH-XIII-135
263	–	EFH-XIII-143
264	efh-XIII-151-2 (Venice)	EFH-XIII-151
266	efh-XIII-163-2-benzene (Venice)	EFH-XIII-163

ABOUT THE AUTHOR

Elliot Hicks was born in Chambersburg, Pennsylvania in 1998 to Eric and Renee Hicks. He grew up in the nearby town of Mercersburg, Pennsylvania. He attended Mercersburg Academy, the school where his parents taught chemistry and biology, and developed an early interest in science. Elliot started his undergraduate studies as a biology major at Emory University in 2016 but quickly changed to a chemistry major after a freshman organic chemistry class taught by Professors Dennis Liotta and Huw Davies. In the fall of 2017, Elliot began research in Dr. Davies' lab, studying rhodium-catalyzed C–H insertion reactions into organosilanes. He spent the summer of 2019 in the laboratory of Professor Oliver Reiser in Regensburg, Germany investigating asymmetric cyclopropanation of dihydrofurans as part of a research exchange program sponsored by the Center for Selective C–H Functionalization. Elliot graduated in 2020 with a B.S. degree in chemistry and a B.A. in German studies.

Upon completion of his undergraduate education, Elliot moved to Pasadena, California to pursue a doctoral degree at the California Institute of Technology under the guidance of Professor Brian Stoltz. His research has focused on development of asymmetric methods for the synthesis of all-carbon quaternary centers and complex molecule total synthesis. Following completion of his graduate studies, Elliot will begin his professional career as a medicinal chemist at Merck in Boston, Massachusetts.